Scientific and Technical Aerospace Reports

STAR

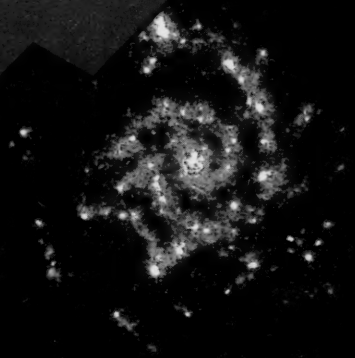

An Abstract Journal

Volume 30, Number 8
April 23, 1992
N92-16973 to N92-18005

Scientific and Technical Aerospace Reports

Scientific and Technical Aerospace Reports (STAR) is an abstract journal that provides comprehensive coverage of worldwide aerospace-related reports. It is a major product of the International Aerospace Database managed by the NASA Scientific and Technical Information (STI) Program. The coverage includes reports on aeronautics, space, and supporting disciplines. *STAR* lists current, publicly available reports entered into the NASA STI Database during the 2-week period preceding publication. A typical citation and abstract appear on page viii. They explain how to read the items that are announced in this journal.

NASA sponsors a companion journal, *International Aerospace Abstracts (IAA)* (*NOVA* for internal NASA use) that lists abstracts of the open literature on aerospace subjects available worldwide. *IAA* is available for sale through the AIAA.

Entries found in *STAR* and *IAA* are available through NASA's online service, RECON, as the International Aerospace Database and through DIALOG as the Aerospace Database.

Information on aerospace and related subjects is gathered by the NASA STI Program through national and international agreements and exchanges and is made available to the NASA community as well as to the public in many forms through various outlets. The section on NASA STI Program Products and Services contains additional information.

For further information please contact:
NASA Center for AeroSpace Information (CASI)
P.O. Box 8757
Baltimore, Maryland 21240-0757
(301) 621-0390

US ISSN 0036-8741

★ SPECIAL NOTICE ★

Beginning with this issue, *STAR* citations are in accession number order within category, as apposed to being in sequence from first page to last. Also, page number references have been added to all of the indexes including the new accession number index.

Volume 30 Number 8 / April 23, 1992

TABLE OF CONTENTS

AERONAUTICS For related information see also *Astronautics.*

01 AERONAUTICS (GENERAL) **1219**

02 AERODYNAMICS **1223**
Includes aerodynamics of bodies, combinations, wings, rotors, and control surfaces; and internal flow in ducts and turbomachinery. For related information see also *34 Fluid Mechanics and Heat Transfer.*

03 AIR TRANSPORTATION AND SAFETY **1226**
Includes passenger and cargo air transport operations; and aircraft accidents. For related information see also *16 Space Transportation* and *85 Urban Technology and Transportation.*

04 AIRCRAFT COMMUNICATIONS AND NAVIGATION **1228**
Includes digital and voice communication with aircraft; air navigation systems (satellite and ground based); and air traffic control. For related information see also *17 Space Communications, Spacecraft Communications, Command and Tracking* and *32 Communications and Radar.*

05 AIRCRAFT DESIGN, TESTING AND PERFORMANCE **1230**
Includes aircraft simulation technology. For related information see also *18 Spacecraft Design, Testing and Performance* and *39 Structural Mechanics.* For land transportation vehicles see *85 Urban Technology and Transportation.*

06 AIRCRAFT INSTRUMENTATION **1234**
Includes cockpit and cabin display devices; and flight instruments. For related information see also *19 Space craft Instrumentation* and *35 Instrumentation and Photography.*

07 AIRCRAFT PROPULSION AND POWER **1234**
Includes prime propulsion systems and systems components, e.g., gas turbine engines and compressors; and onboard auxiliary power plants for aircraft. For related information see also *20 Spacecraft Propulsion and Power, 28 Propellants and Fuels,* and *44 Energy Production and Conversion.*

08 AIRCRAFT STABILITY AND CONTROL **1236**
Includes aircraft handling qualities; piloting; flight controls; and autopilots. For related information see also *05 Aircraft Design, Testing and Performance.*

09 RESEARCH AND SUPPORT FACILITIES (AIR) **1237**
Includes airports, hangars and runways; aircraft repair and overhaul facilities; wind tunnels; shock tubes; and aircraft engine test stands. For related information see also *14 Ground Support Systems and Facilities (Space).*

ASTRONAUTICS For related information see also *Aeronautics.*

12 ASTRONAUTICS (GENERAL) ..... **N.A.**
For extraterrestrial exploration see *91 Lunar and Planetary Exploration.*

13 ASTRODYNAMICS **1239**
Includes powered and free-flight trajectories; and orbital and launching dynamics.

14 GROUND SUPPORT SYSTEMS AND FACILITIES (SPACE) **1240**
Includes launch complexes, research and production facilities; ground support equipment, e.g., mobile transporters; and simulators. For related information see also *09 Research and Support Facilities (Air).*

15 LAUNCH VEHICLES AND SPACE VEHICLES **1240**
Includes boosters; operating problems of launch/space vehicle systems; and reusable vehicles. For related information see also *20 Spacecraft Propulsion and Power.*

16 SPACE TRANSPORTATION **1240**
Includes passenger and cargo space transportation, e.g., shuttle operations; and space rescue techniques. For related information see also *03 Air Transportation and Safety* and *18 Spacecraft Design, Testing and Performance.* For space suits see *54 Man/System Technology and Life Support.*

17 SPACE COMMUNICATIONS, SPACECRAFT COMMUNICATIONS, COMMAND AND TRACKING . **1242**
Includes telemetry; space communications networks; astronavigation and guidance; and radio blackout. For related information see also *04 Aircraft Communications and Navigation* and *32 Communications and Radar.*

N.A.—no abstracts were assigned to this category for this issue.

18 SPACECRAFT DESIGN, TESTING AND PERFORMANCE **1242**
Includes satellites; space platforms; space stations; spacecraft systems and components such as thermal and environmental controls; and attitude controls. For life support systems see *54 Man/System Technology and Life Support.* For related information see also *05 Aircraft Design, Testing and Performance, 39 Structural Mechanics,* and *16 Space Transportation.*

19 SPACECRAFT INSTRUMENTATION **1252**
For related information see also *06 Aircraft Instrumentation* and *35 Instrumentation and Photography.*

20 SPACECRAFT PROPULSION AND POWER **1253**
Includes main propulsion systems and components, e.g., rocket engines; and spacecraft auxiliary power sources. For related information see also *07 Aircraft Propulsion and Power, 28 Propellants and Fuels, 44 Energy Production and Conversion,* and *15 Launch Vehicles and Space Vehicles.*

CHEMISTRY AND MATERIALS

23 CHEMISTRY AND MATERIALS (GENERAL) **1254**

24 COMPOSITE MATERIALS **1255**
Includes physical, chemical, and mechanical properties of laminates and other composite materials. For ceramic materials see *27 Nonmetallic Materials.*

25 INORGANIC AND PHYSICAL CHEMISTRY **1258**
Includes chemical analysis, e.g., chromatography; combustion theory; electrochemistry; and photochemistry. For related information see also *77 Thermodynamics and Statistical Physics.*

26 METALLIC MATERIALS **1262**
Includes physical, chemical, and mechanical properties of metals, e.g., corrosion; and metallurgy.

27 NONMETALLIC MATERIALS **1266**
Includes physical, chemical, and mechanical properties of plastics, elastomers, lubricants, polymers, textiles, adhesives, and ceramic materials. For composite materials see *24 Composite Materials.*

28 PROPELLANTS AND FUELS **1275**
Includes rocket propellants, igniters and oxidizers; their storage and handling procedures; and aircraft fuels. For related information see also *07 Aircraft Propulsion and Power, 20 Spacecraft Propulsion and Power,* and *44 Energy Production and Conversion.*

29 MATERIALS PROCESSING **1276**
Includes space-based development of products and processes for commercial application. For biological materials see *55 Space Biology.*

ENGINEERING For related information see also *Physics.*

31 ENGINEERING (GENERAL) **1276**
Includes vacuum technology; control engineering; display engineering; cryogenics; and fire prevention.

32 COMMUNICATIONS AND RADAR **1278**
Includes radar; land and global communications; communications theory; and optical communications. For related information see also *04 Aircraft Communications and Navigation* and *17 Space Communications, Spacecraft Communications, Command and Tracking.* For search and rescue see *03 Air Transportation and Safety,* and *16 Space Transportation.*

33 ELECTRONICS AND ELECTRICAL ENGINEERING **1286**
Includes test equipment and maintainability; components, e.g., tunnel diodes and transistors; microminiaturization; and integrated circuitry. For related information see also *60 Computer Operations and Hardware* and *76 Solid-State Physics.*

34 FLUID MECHANICS AND HEAT TRANSFER **1294**
Includes boundary layers; hydrodynamics; fluidics; mass transfer and ablation cooling. For related information see also *02 Aerodynamics* and *77 Thermodynamics and Statistical Physics.*

35 INSTRUMENTATION AND PHOTOGRAPHY **1300**
Includes remote sensors; measuring instruments and gauges; detectors; cameras and photographic supplies; and holography. For aerial photography see *43 Earth Resources and Remote Sensing.* For related information see also *06 Aircraft Instrumentation* and *19 Spacecraft Instrumentation.*

36 LASERS AND MASERS **1303**
Includes parametric amplifiers. For related information see also *76 Solid-State Physics.*

37 MECHANICAL ENGINEERING **1306**
Includes auxiliary systems (nonpower); machine elements and processes; and mechanical equipment.

38 QUALITY ASSURANCE AND RELIABILITY **1308**
Includes product sampling procedures and techniques; and quality control.

39 STRUCTURAL MECHANICS **1309**
Includes structural element design and weight analysis; fatigue; and thermal stress. For applications see *05 Aircraft Design, Testing and Performance* and *18 Spacecraft Design, Testing and Performance.*

GEOSCIENCES For related information see also *Space Sciences.*

42 GEOSCIENCES (GENERAL) **1311**

43 EARTH RESOURCES AND REMOTE SENSING **1312**
Includes remote sensing of earth resources by aircraft and spacecraft; photogrammetry; and aerial photography. For instrumentation see *35 Instrumentation and Photography.*

44 ENERGY PRODUCTION AND CONVERSION **1312**
Includes specific energy conversion systems, e.g., fuel cells; global sources of energy; geophysical conversion; and windpower. For related information see also *07 Aircraft Propulsion and Power, 20 Spacecraft Propulsion and Power,* and *28 Propellants and Fuels.*

45 ENVIRONMENT POLLUTION **1313**
Includes atmospheric, noise, thermal, and water pollution.

46 GEOPHYSICS **1315**
Includes aeronomy; upper and lower atmosphere studies; ionospheric and magnetospheric physics; and geomagnetism. For space radiation see *93 Space Radiation.*

47 METEOROLOGY AND CLIMATOLOGY **1317**
Includes weather forecasting and modification.

48 OCEANOGRAPHY **1323**
Includes biological, dynamic, and physical oceanography; and marine resources. For related information see also *43 Earth Resources and Remote Sensing.*

LIFE SCIENCES

51 LIFE SCIENCES (GENERAL) **1325**

52 AEROSPACE MEDICINE **1328**
Includes physiological factors; biological effects of radiation; and effects of weightlessness on man and animals.

53 BEHAVIORAL SCIENCES **1331**
Includes psychological factors; individual and group behavior; crew training and evaluation; and psychiatric research.

54 MAN/SYSTEM TECHNOLOGY AND LIFE SUPPORT **1333**
Includes human engineering; biotechnology; and space suits and protective clothing. For related information see also *16 Space Transportation.*

55 SPACE BIOLOGY ..... **N.A.**
Includes exobiology; planetary biology; and extraterrestrial life.

MATHEMATICAL AND COMPUTER SCIENCES

59 MATHEMATICAL AND COMPUTER SCIENCES (GENERAL) ..... **N.A.**

60 COMPUTER OPERATIONS AND HARDWARE **1336**
Includes hardware for computer graphics, firmware, and data processing. For components see *33 Electronics and Electrical Engineering.*

61 COMPUTER PROGRAMMING AND SOFTWARE **1337**
Includes computer programs, routines, algorithms, and specific applications, e.g., CAD/CAM.

62 COMPUTER SYSTEMS **1345**
Includes computer networks and special application computer systems.

63 CYBERNETICS **1347**
Includes feedback and control theory, artificial intelligence, robotics and expert systems. For related information see also *54 Man/System Technology and Life Support.*

64 NUMERICAL ANALYSIS **1350**
Includes iteration, difference equations, and numerical approximation.

65 STATISTICS AND PROBABILITY **1352**
Includes data sampling and smoothing; Monte Carlo method; and stochastic processes.

66 SYSTEMS ANALYSIS **1353**
Includes mathematical modeling; network analysis; and operations research.

67 THEORETICAL MATHEMATICS **1353**
Includes topology and number theory.

PHYSICS For related information see also *Engineering.*

70 PHYSICS (GENERAL) **1354**
For precision time and time interval (PTTI) see *35 Instrumentation and Photography;* for geophysics, astrophysics or solar physics see *46 Geophysics, 90 Astrophysics,* or *92 Solar Physics.*

71 ACOUSTICS **1354**
Includes sound generation, transmission, and attenuation. For noise pollution see *45 Environment Pollution.*

72 ATOMIC AND MOLECULAR PHYSICS **1356**
Includes atomic structure, electron properties, and molecular spectra.

73 NUCLEAR AND HIGH-ENERGY PHYSICS **1363**
Includes elementary and nuclear particles; and reactor theory. For space radiation see *93 Space Radiation.*

74 OPTICS **1364**
Includes light phenomena and optical devices. For lasers see *36 Lasers and Masers.*

75 PLASMA PHYSICS **1369**
Includes magnetohydrodynamics and plasma fusion. For ionospheric plasmas see *46 Geophysics.* For space plasmas see *90 Astrophysics.*

76 SOLID-STATE PHYSICS **1371**
Includes superconductivity. For related information see also *33 Electronics and Electrical Engineering* and *36 Lasers and Masers.*

77 THERMODYNAMICS AND STATISTICAL PHYSICS **1378**
Includes quantum mechanics; theoretical physics; and Bose and Fermi statistics. For related information see also *25 Inorganic and Physical Chemistry* and *34 Fluid Mechanics and Heat Transfer.*

SOCIAL SCIENCES

80 SOCIAL SCIENCES (GENERAL) ..... **N.A.**
Includes educational matters.

81 ADMINISTRATION AND MANAGEMENT **1380**
Includes management planning and research.

82 DOCUMENTATION AND INFORMATION SCIENCE **1381**
Includes information management; information storage and retrieval technology; technical writing; graphic arts; and micrography. For computer documentation see *61 Computer Programming and Software.*

83 ECONOMICS AND COST ANALYSIS ..... **N.A.**
Includes cost effectiveness studies.

84 LAW, POLITICAL SCIENCE AND SPACE POLICY **1385**
Includes NASA appropriation hearings; aviation law; space law and policy; international law; international cooperation; and patent policy.

85 URBAN TECHNOLOGY AND TRANSPORTATION **1385**
Includes applications of space technology to urban problems; technology transfer; technology assessment; and surface and mass transportation. For related information see *03 Air Transportation and Safety, 16 Space Transportation,* and *44 Energy Production and Conversion.*

SPACE SCIENCES For related information see also *Geosciences.*

88 SPACE SCIENCES (GENERAL) ..... **N.A.**

89 ASTRONOMY **1386**
Includes radio, gamma-ray, and infrared astronomy; and astrometry.

90 ASTROPHYSICS **1387**
Includes cosmology; celestial mechanics; space plasmas; and interstellar and interplanetary gases and dust. For related information see also *75 Plasma Physics.*

91 LUNAR AND PLANETARY EXPLORATION **1389**
Includes planetology; and manned and unmanned flights. For spacecraft design or space stations see *18 Spacecraft Design, Testing and Performance.*

92 SOLAR PHYSICS **1389**
Includes solar activity, solar flares, solar radiation and sunspots. For related information see *93 Space Radiation.*

93 SPACE RADIATION **1390**
Includes cosmic radiation; and inner and outer earth's radiation belts. For biological effects of radiation see *52 Aerospace Medicine.* For theory see *73 Nuclear and High-Energy Physics.*

GENERAL

Includes aeronautical, astronautical, and space science related histories, biographies, and pertinent reports too broad for categorization; histories or broad overviews of NASA programs.

99 GENERAL **1391**

SUBJECT INDEX **I-1**

PERSONAL AUTHOR INDEX **I-77**

CORPORATE SOURCE INDEX **I-85**

CONTRACT NUMBER INDEX **I-99**

REPORT NUMBER INDEX **I-103**

ACCESSION NUMBER INDEX **I-111**

APPENDIX **A-1**

TYPICAL CITATION AND ABSTRACT

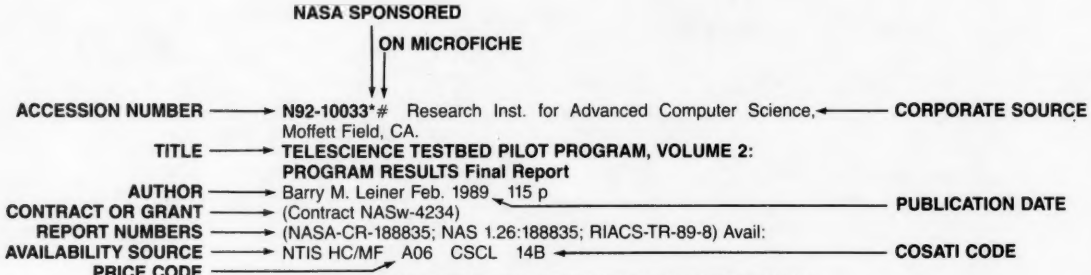

Space Station Freedom and its associated labs, coupled with the availability of new computing and communications technologies, have the potential for significantly enhancing scientific research. A Telescience Testbed Pilot Program (TTPP), aimed at developing the experience base to deal with issues in the design of the future information system of the Space Station era. The testbeds represented four scientific disciplines (astronomy and astrophysics, earth sciences, life sciences, and microgravity sciences) and studied issues in payload design, operation, and data analysis. This volume, of a 3 volume set, which all contain the results of the TTPP, contains the integrated results. Background is provided of the program and highlights of the program results. The various testbed experiments and the programmatic approach is summarized. The results are summarized on a discipline by discipline basis, highlighting the lessons learned for each discipline. Then the results are integrated across each discipline, summarizing the lessons learned overall.

Author

VOLUME 30 NUMBER 8 / APRIL 23, 1992

Scientific and Technical Aerospace Reports

A Semimonthly Publication of the National Aeronautics and Space Administration

01 AERONAUTICS (GENERAL)

N92-17346*# National Aeronautics and Space Administration. Lewis Research Center, Cleveland, OH.
VISCOUS THREE-DIMENSIONAL CALCULATIONS OF TRANSONIC FAN PERFORMANCE
Rodrick V. Chima 1991 19 p Presented at the 77th Symposium of the Propulsion and Energetics Panel entitled CFD Techniques for Propulsion Applications, San Antonio, TX, 27-31 May 1991; sponsored by AGARD Original contains color illustrations
(NASA-TM-103800; E-6088; NAS 1.15:103800) Avail: NTIS HC/MF A03; 5 functional color pages CSCL 01B

A 3-D flow analysis code was used to compute the design speed operating line of a transonic fan rotor, and the results were compared with experimental data. The code is an explicit finite difference code with an algebraic turbulence model. The transonic fan, called rotor 67, was tested experimentally at NASA-Lewis with conventional aerodynamic probes and with user anemometry and was included as one of the AGARD test cases for the computation of internal flows. The experimental data are described. Maps of total pressure ratio and adiabatic efficiency versus mass flow were computed and are compared with the experimental maps, with good agreement. Detailed comparisons between calculations and experiment are made at two operating points, one near peak efficiency and the other near stall. Blade-to-blade contour plots are used to show the shock structure. Comparisons of circumferentially integrated flow quantities downstream of the rotor show spanwise distributions of several aerodynamic parameters. Calculated Mach number distributions are compared with laser anemometer data within the blade row and the wake to quantify the accuracy of the calculations. Particle traces are used to show the nature of secondary flow. Author

N92-17477# Naval Postgraduate School, Monterey, CA.
THE V-22: CAN THE NATION AFFORD TO FORGO ITS PRODUCTION? M.S. Thesis
Michael Crouch Dec. 1991 103 p
(AD-A243158) Avail: NTIS HC/MF A06 CSCL 05/1

The V-22 was designed for the ground up to satisfy missions required by all military services. It is an airplane that represents the leading edge of tiltrotor technology. Since Secretary Cheney's decision to cancel the V-22 in 1989, lines of political competition have been drawn. Continued support for the V-22 comes from an influential group within Congress determined to advance the program based on its civil application. The V-22 no longer represents a battle between the Executive and Legislative branches over their specific defense responsibilities. This thesis addresses two questions: (1) using the V-22 as a case study, the programmatic and financial implications are examined for the Department of Defense and industry on dual-use technology and (2) the lessons of the V-22 about the process of defense budgeting. Throughout the thesis emphasis is places on the actions of the committees of Congress responsible for the defense budget, and specifically the V-22. This thesis examines the roles and relationships between the 'players' throughout the history of the V-22 program to determine if any useful analogies may be identified with respect to present and future defense budgeting and acquisition practices. GRA

N92-17731# Air Force Inst. of Tech., Wright-Patterson AFB, OH.
THE DEVELOPMENT OF MILITARY NIGHT AVIATION TO 1919 M.S. Thesis
William E. Fischer, Jr. 1991 247 p
(AD-A243350; AFIT/CI/CIA-91-068) Avail: NTIS HC/MF A11 CSCL 01/3

This study examines the development of military night aviation from its origins through the first World War. Emphasis is on the evolution of night flying in those countries which fought on the Western Front, namely France, Germany, Great Britain, and the United States. While night flying occurred in other theaters the most intense air effort was clearly in the west. There belligerents pressed aviation technology and tactics to the limits; the skies of northern France and Flanders offered the only opportunity for movement across the stagnated front. Another important consideration was the availability of a rich documentation concerning night aerial activity in the theater. A striking disparity quickly became evident during preliminary investigations of the topic. Surprisingly no single book-length study was uncovered which was dedicated exclusively to night flying along the Western Front. This thesis seeks to reduce the existing gap in scholarly knowledge. GRA

N92-17984*# National Aeronautics and Space Administration. Langley Research Center, Hampton, VA.
JOINT UNIVERSITY PROGRAM FOR AIR TRANSPORTATION RESEARCH, 1990-1991
Frederick R. Morrell, comp. Washington Dec. 1991 183 p Conference held in Athens, OH, 20-21 Jun. 1991; sponsored by NASA and FAA
(NASA-CP-3131; L-17017; NAS 1.55:3131) Avail: NTIS HC/MF A09 CSCL 01B

The goals of this program are consistent with the interests of both NASA and the FAA in furthering the safety and efficiency of the National Airspace System. Research carried out at the Massachusetts Institute of Technology (MIT), Ohio University, and Princeton University are covered. Topics studied include passive infrared ice detection for helicopters, the cockpit display of hazardous windshear information, fault detection and isolation for multisensor navigation systems, neural networks for aircraft system identification, and intelligent failure tolerant control. For individual titles, see N92-17985 through N92-18002.

N92-17985*# Massachusetts Inst. of Tech., Cambridge. Flight Transportation Lab.
AN INVESTIGATION OF AIR TRANSPORTATION TECHNOLOGY AT THE MASSACHUSETTS INSTITUTE OF TECHNOLOGY, 1990-1991 **c03**
Robert W. Simpson *In* NASA. Langley Research Center, Joint University Program for Air Transportation Research, 1990-1991 Dec. 1991 p 3-9 (For primary document see N92-17984 08-01)
Avail: NTIS HC/MF A09 CSCL 01C

Brief summaries are given of research activities at the Massachusetts Institute of Technology (MIT) under the sponsorship of the FAA/NASA Joint University Program. Topics covered include hazard assessment and cockpit presentation issues for microburst alerting systems; the situational awareness effect of automated air traffic control (ATC) datalink clearance amendments; a graphical

simulation system for adaptive, automated approach spacing; an expert system for temporal planning with application to runway configuration management; deterministic multi-zone ice accretion modeling; alert generation and cockpit presentation for an integrated microburst alerting system; and passive infrared ice detection for helicopter applications. Author

N92-17986*# Massachusetts Inst. of Tech., Cambridge. Dept. of Aeronautics and Astronautics.
EXPERIMENTAL INVESTIGATION OF PASSIVE INFRARED ICE DETECTION FOR HELICOPTER APPLICATIONS **c03**
Adam Dershowitz and R. John Hansman, Jr. *In* NASA. Langley Research Center, Joint University Program for Air Transportation Research, 1990-1991 Dec. 1991 p 11-18 Previously announced in IAA as A91-19402 (For primary document see N92-17984 08-01)
(Grant NAG3-927)
Avail: NTIS HC/MF A09 CSCL 01C

A technique is proposed to remotely detect rotor icing on helicopters. Using passive infrared (IR) thermometry, it is possible to detect the warming caused by latent heat released as supercooled water freezes. During icing, the ice accretion region on the blade leading edge will be warmer than the uniced trailing edge, resulting in a chordwise temperature profile characteristic of icing. Preliminary tests were conducted on a static model in the NASA Icing Research Tunnel for a variety of wet (glaze) and dry (rime) ice conditions. The characteristic chordwise temperature profiles were observed with an IR thermal video system and confirmed with thermocouple measurements. A prototype detector system was built consisting of a single point IR pyrometer. Experiments were run on a small scale rotor model. Again, the characteristic chordwise temperature profiles were observed during icing, and the IR system was able to remotely detect icing. Based on the static and subscale rotor tests, the passive IR technique is promising for rotor ice detection. Author

N92-17987*# Massachusetts Inst. of Tech., Cambridge. Dept. of Aeronautics and Astronautics.
DETERMINISTIC MULTI-ZONE ICE ACCRETION MODELING **c03**
K. Yamaguchi, R. John Hansman, Jr., and Michael Kazmierczak (Cincinnati Univ., OH.) *In* NASA. Langley Research Center, Joint University Program for Air Transportation Research, 1990-1991 Dec. 1991 p 19-28 Previously announced in IAA as A91-19209 Sponsored in part by NSF (For primary document see N92-17984 08-01)
(Grants NAG3-666; NGL-22-009-640)
Avail: NTIS HC/MF A09 CSCL 01C

The focus here is on a deterministic model of the surface roughness transition behavior of glaze ice. The initial smooth/rough transition location, bead formation, and the propagation of the transition location are analyzed. Based on the hypothesis that the smooth/rough transition location coincides with the laminar/turbulent boundary layer transition location, a multizone model is implemented in the LEWICE code. In order to verify the effectiveness of the model, ice accretion predictions for simple cylinders calculated by the multizone LEWICE are compared to experimental ice shapes. The glaze ice shapes are found to be sensitive to the laminar surface roughness and bead thickness parameters controlling the transition location, while the ice shapes are found to be insensitive to the turbulent surface roughness. Author

N92-17988*# Massachusetts Inst. of Tech., Cambridge. Dept. of Aeronautics and Astronautics.
ALERT GENERATION AND COCKPIT PRESENTATION FOR AN INTEGRATED MICROBURST ALERTING SYSTEM **c03**
Craig Wanke and R. John Hansman, Jr. *In* NASA. Langley Research Center, Joint University Program for Air Transportation Research, 1990-1991 Dec. 1991 p 29-39 Previously announced in IAA as A91-19207 (For primary document see N92-17984 08-01)
(Contract NGL-22-009-640; BARR-10-119)
Avail: NTIS HC/MF A09 CSCL 01C

Alert generation and cockpit presentation issues for low level wind shear (microburst) alerts are investigated. Alert generation issues center on the development of a hazard criterion which allows integration of both ground based and airborne wind shear detection systems to form an accurate picture of the aviation hazard posed by a particular wind shear situation. A methodology for the testing of a hazard criteria through flight simulation has been developed, and has been used to examine the effectiveness and feasibility of several possible criteria. Also, an experiment to evaluate candidate graphical cockpit displays for microburst alerts using a piloted simulator has been designed. Author

N92-17989*# Massachusetts Inst. of Tech., Cambridge. Dept. of Aeronautics and Astronautics.
COCKPIT DISPLAY OF HAZARDOUS WEATHER INFORMATION **c06**
R. John Hansman, Jr. and Craig Wanke *In* NASA. Langley Research Center, Joint University Program for Air Transportation Research, 1990-1991 Dec. 1991 p 41-48 Previously announced as N90-20929 Previously announced in IAA as A89-25591 (For primary document see N92-17984 08-01)
(Contract NAG1-690; NGL-22-009-640; BARR-10-119)
Avail: NTIS HC/MF A09 CSCL 01C

Information transfer and display issues associated with the dissemination of hazardous weather warnings are studied in the context of wind shear alerts. Operational and developmental wind shear detection systems are briefly reviewed. The July 11, 1988 microburst events observed as part of the Denver Terminal Doppler Weather Radar (TDWR) operational evaluation are analyzed in terms of information transfer and the effectiveness of the microburst alerts. Information transfer, message content and display issues associated with microburst alerts generated from ground based sources (Doppler Radar, Low Level Wind Shear Alert System, and Pilot Reports) are evaluated by means fo pilot opinion surveys and part task simulator studies. Author

N92-17990*# Ohio Univ., Athens. Avionics Engineering Center.
INVESTIGATION OF AIR TRANSPORTATION TECHNOLOGY AT OHIO UNIVERSITY, 1990-1991 **c03**
Robert W. Lilley *In* NASA. Langley Research Center, Joint University Program for Air Transportation Research, 1990-1991 Dec. 1991 p 51-54 (For primary document see N92-17984 08-01)
Avail: NTIS HC/MF A09 CSCL 01C

The status of the Joint University Program is given. Brief synopsis of some areas of research follow. The study of spectrum efficient methods for transmitting weather information to aircraft has resulted in definition of an improved amplitude and phase modulation process which permits reutilization of voice channels for both voice and data. The system is being implemented for testing. Multisensor navigation systems introduce increased flexibility and performance for aviation, at the expense of increased complexity. Insuring a high level of system reliability and integrity requires that faults not only be detected, but also isolated to specific elements, so that the remaining capabilities of the system may be used with confidence. An algorithm was developed. The JUP has served as a vehicle for reporting work accomplished in evoked potential vision tracking experiments to determine the engineering parameters of this input and control method. Application of GPS in an interferometric mode permits accurate measurement of differential motion; aircraft attitude may be determined using GPS only, with multiple antennas. Author

N92-17991*# Ohio Univ., Athens.
A HYBRID MODULATION FOR THE DISSEMINATION OF WEATHER DATA TO AIRCRAFT **c47**
Dennis M. Akos *In* NASA. Langley Research Center, Joint University Program for Air Transportation Research, 1990-1991 Dec. 1991 p 55-59 (For primary document see N92-17984 08-01)
Avail: NTIS HC/MF A09 CSCL 04B

Ohio University is continuing to conduct research to improve its system for weather data dissemination to aircraft. The current experimental system transmit compressed weather radar reflectivity patterns from a ground based station to aircraft. Although an effective system, the limited frequency spectrum does not provide a channel for transmission. This introduces the idea of a hybrid modulation. The hybrid technique encodes weather data using phase modulation (PM) onto an existing aeronautical channel which employs amplitude modulation (AM) for voice signal transmission. Ideally, the two modulations are independent of one another. The planned implementation and basis of the system are the reviewed. Author

N92-17992*# Ohio Univ., Athens.
FAULT DETECTION AND ISOLATION FOR MULTISENSOR NAVIGATION SYSTEMS **c04**
Paul A. Kline and Frank vanGraas *In* NASA. Langley Research Center, Joint University Program for Air Transportation Research, 1990-1991 Dec. 1991 p 61-68 (For primary document see N92-17984 08-01)
Avail: NTIS HC/MF A09 CSCL 17G

Increasing attention is being given to the problem of erroneous measurement data for multisensor navigation systems. A recursive estimator can be used in conjunction with a 'snapshot' batch estimator to provide fault detection and isolation (FDI) for these systems. A recursive estimator uses past system states to form a new state estimate and compares it to the calculated state based on a new set of measurements. A 'snapshot' batch estimator uses a set of measurements collected simultaneously and compares solutions based on subsets of measurements. The 'snapshot' approach requires redundant measurements in order to detect and isolate faults. FDI is also referred to as Receiver Autonomous Integrity Monitoring (RAIM). Author

N92-17993*# Ohio Univ., Athens.
ESTABLISHING AN EVOKED-POTENTIAL VISION-TRACKING SYSTEM **c06**
Trent A. Skidmore *In* NASA. Langley Research Center, Joint University Program for Air Transportation Research, 1990-1991 Dec. 1991 p 69-78 (For primary document see N92-17984 08-01)
(Grant NAG1-940)
Avail: NTIS HC/MF A09 CSCL 01D

This paper presents experimental evidence to support the feasibility of an evoked-potential vision-tracking system. The topics discussed are stimulator construction, verification of the photic driving response in the electroencephalogram, a method for performing frequency separation, and a transient-analysis example. The final issue considered is that of object multiplicity (concurrent visual stimuli with different flashing rates). The paper concludes by discussing several applications currently under investigation. Author

N92-17994*# Ohio Univ., Athens.
GPS INTERFEROMETRIC ATTITUDE AND HEADING DETERMINATION: INITIAL FLIGHT TEST RESULTS **c04**
Frank vanGraas and Michael Braasch *In* NASA. Langley Research Center, Joint University Program for Air Transportation Research, 1990-1991 Dec. 1991 p 79-100 (For primary document see N92-17984 08-01)
(Grant NGR-36-009-017)
Avail: NTIS HC/MF A09 CSCL 17G

Attitude and heading determination using GPS interferometry is a well-understood concept. However, efforts have been concentrated mainly in the development of robust algorithms and applications for low dynamic, rigid platforms (e.g., shipboard). This paper presents results of what is believed by the authors to be the first realtime flight test of a GPS attitude and heading determination system. The system is installed in Ohio University's Douglas DC-3 research aircraft. Signals from four antennas are processed by an Ashtech 3DF 24-channel GPS receiver. Data from the receiver are sent to a microcomputer for storage and further computations. Attitude and heading data are sent to a second computer for display on a software generated artificial horizon. Demonstration of this technique proves its candidacy for augmentation of aircraft state estimation for flight control and navigation as well as for numerous other applications. Author

N92-17995*# Princeton Univ., NJ. Dept. of Mechanical and Aerospace Engineering.
INVESTIGATION OF AIR TRANSPORTATION TECHNOLOGY AT PRINCETON UNIVERSITY, 1990-1991 **c03**
Robert F. Stengel *In* NASA. Langley Research Center, Joint University Program for Air Transportation Research, 1990-1991 Dec. 1991 p 103-112 (For primary document see N92-17984 08-01)
Avail: NTIS HC/MF A09 CSCL 01C

The Air Transportation Technology Program at Princeton University is a program that emphasizes graduate and undergraduate student research. The program proceeded along six avenues during the past year: microburst hazards to aircraft, intelligent failure tolerant control, computer-aided heuristics for piloted flight, stochastic robustness of flight control systems, neural networks for flight control, and computer-aided control system design. Author

N92-17996*# Princeton Univ., NJ. Dept. of Mechanical and Aerospace Engineering.
TARGET PITCH ANGLE FOR THE MICROBURST ESCAPE MANEUVER **c03**
Sandeep S. Mulgund *In* NASA. Langley Research Center, Joint University Program for Air Transportation Research, 1990-1991 Dec. 1991 p 113-125 (For primary document see N92-17984 08-01)
Avail: NTIS HC/MF A09 CSCL 01C

The objective of this study was to investigate the constant pitch attitude strategy as a possible non-precision maneuver for recovery from inadvertent wind shear encounters. The Wind Shear Training Aid published by the FAA recommends that upon encountering a severe wind shear, the pilot should apply maximum thrust and rotate the aircraft to an initial pitch target angle of 15 degrees. The 15 degrees target was identified through rigorous analyses using six-degree-of-freedom flight simulators and microburst models representative of actual accident cases. It was found that 15 degrees was an effective target for a wide range of shears, and was generally applicable to most jet transports. This work was undertaken to examine the issue of recovery performance in wind shear of other classes of aircraft - notably turboprop commuters and propeller-driven general aviation planes. It should be possible to postulate a target pitch angle (TPA) for such aircraft, as well. Author

N92-17997*# Princeton Univ., NJ. Dept. of Mechanical and Aerospace Engineering.
STOCHASTIC ROBUSTNESS **c08**
C. Marrison *In* NASA. Langley Research Center, Joint University Program for Air Transportation Research, 1990-1991 Dec. 1991 p 127-140 (For primary document see N92-17984 08-01)
Avail: NTIS HC/MF A09 CSCL 01C

To carry out stochastic robustness analysis, an expected probability distribution is assigned to each uncertain parameter in the system. The Monte Carlo analysis proceeds by repeatedly assigning shaped random values to each plant parameter, evaluating the stability of performance metric, and performing the binary classification (stable/unstable, etc.). If the system is stable, the state response to a unit disturbance impulse can be propagated to establish whether the response would violate settling time envelopes and whether peak actuator use would violate predetermined maximums. The final estimates of the probability of each form of unacceptable behavior are found by dividing the number of cases in which the overall system had that form of unacceptability by the number of cases run. Stability robustness can be portrayed graphically using the stochastic root locus and by using histograms of parameter values found in the unacceptable cases. Author

N92-17998*# Princeton Univ., NJ. Dept. of Mechanical and Aerospace Engineering.
NEURAL NETWORKS FOR AIRCRAFT SYSTEM IDENTIFICATION **c63**
Dennis J. Linse *In* NASA. Langley Research Center, Joint University Program for Air Transportation Research, 1990-1991 Dec. 1991 p 141-154 (For primary document see N92-17984 08-01)
Avail: NTIS HC/MF A09 CSCL 09B

Artificial neural networks offer some interesting possibilities for use in control. Our current research is on the use of neural networks on an aircraft model. The model can then be used in a nonlinear control scheme. The effectiveness of network training is demonstrated. Author

N92-17999*# Cornell Univ., Ithaca, NY.
OPTIMAL AIRCRAFT PERFORMANCE DURING MICROBURST ENCOUNTER **c03**
Mark L. Psiaki and Robert F. Stengel (Princeton Univ., NJ.) *In* NASA. Langley Research Center, Joint University Program for Air Transportation Research, 1990-1991 Dec. 1991 p 155-161 Previously announced in IAA as A91-29787 (For primary document see N92-17984 08-01)
(Grant NGL-31-001-252)
Avail: NTIS HC/MF A09 CSCL 01C

The effects of microburst characteristics on the optimal penetration performance of jet transport and general aviation aircraft are presented. The purpose is to determine the best possible performance that can be achieved in a broad range of microbursts. A secondary goal is to illustrate good strategies for dealing with a range of microbursts during takeoff and landing. Over 1100 optimal trajectories were computed for two aircraft types flying through idealized microbursts using a Successive Quadratic Programs trajectory optimization algorithm. Contours of safety metrics are plotted as functions of the length scales, magnitudes, and locations of horizontal wind shears and vertical downdrafts. These performance contours show three length-scale regimes for optimal microburst penetration. At short length scales, hazards usually associated with gustiness predominate (e.g., high normal load factor, rotational upset). At intermediate length scales, a degraded ability to maintain flight path and/or vertical velocity poses the most serious threat. At very long microburst length scales, excessive touchdown velocities may result. The ability to transit a microburst successfully also varies strongly with microburst location. The results show that both aircraft types could penetrate some very severe microbursts if optimal control histories were followed. Nevertheless, these control strategies assume perfect prior knowledge of the wind, and practical limits to successful encounter with real-time control capabilities would be lower. The optimally controlled jet transport can successfully penetrate higher intensity microbursts than can the general aviation aircraft. Author

N92-18000*# Princeton Univ., NJ. Dept. of Mechanical and Aerospace Engineering.
INTELLIGENT FAILURE-TOLERANT CONTROL **c08**
Robert F. Stengel *In* NASA. Langley Research Center, Joint University Program for Air Transportation Research, 1990-1991 Dec. 1991 p 163-172 Previously announced in IAA as A91-43931 (For primary document see N92-17984 08-01)
(Contract NGL-31-001-252; DAAL03-89-K-0092)
Avail: NTIS HC/MF A09 CSCL 01C

An overview of failure-tolerant control is presented, beginning with robust control, progressing through parallel and analytical redundancy, and ending with rule-based systems and artificial neural networks. By design or implementation, failure-tolerant control systems are 'intelligent' systems. All failure-tolerant systems require some degrees of robustness to protect against catastrophic failure; failure tolerance often can be improved by adaptivity in decision-making and control, as well as by redundancy in measurement and actuation. Reliability, maintainability, and survivability can be enhanced by failure tolerance, although each objective poses different goals for control system design. Artificial intelligence concepts are helpful for integrating and codifying failure-tolerant control systems, not as alternatives but as adjuncts to conventional design methods. Author

N92-18001*# Princeton Univ., NJ. Dept. of Mechanical and Aerospace Engineering.
SYSTEMATIC METHODS FOR KNOWLEDGE ACQUISITION AND EXPERT SYSTEM DEVELOPMENT **c54**
Brenda L. Belkin and Robert F. Stengel *In* NASA. Langley Research Center, Joint University Program for Air Transportation Research, 1990-1991 Dec. 1991 p 173-179 Previously announced in IAA as A91-43926 Sponsored in part by Natural Sciences and Research Council of Canada (For primary document see N92-17984 08-01)
(Contract NGL-31-001-252; DAAG29-84-K-0048)
Avail: NTIS HC/MF A09 CSCL 05H

Nine cooperating rule-based systems, collectively called AUTOCREW, were designed to automate functions and decisions associated with a combat aircraft's subsystem. The organization of tasks within each system is described; performance metrics were developed to evaluate the workload of each rule base, and to assess the cooperation between the rule-bases. Each AUTOCREW subsystem is composed of several expert systems that perform specific tasks. AUTOCREW's NAVIGATOR was analyzed in detail to understand the difficulties involved in designing the system and to identify tools and methodologies that ease development. The NAVIGATOR determines optimal navigation strategies from a set of available sensors. A Navigation Sensor Management (NSM) expert system was systematically designed from Kalman filter covariance data; four ground-based, a satellite-based, and two on-board INS-aiding sensors were modeled and simulated to aid an INS. The NSM Expert was developed using the Analysis of Variance (ANOVA) and the ID3 algorithm. Navigation strategy selection is based on an RSS position error decision metric, which is computed from the covariance data. Results show that the NSM Expert predicts position error correctly between 45 and 100 percent of the time for a specified navaid configuration and aircraft trajectory. The NSM Expert adapts to new situations, and provides reasonable estimates of hybrid performance. The systematic nature of the ANOVA/ID3 method makes it broadly applicable to expert system design when experimental or simulation data is available. Author

N92-18002*# Princeton Univ., NJ. Dept. of Mechanical and Aerospace Engineering.
TECHNICAL NOTES AND CORRESPONDENCE: STOCHASTIC ROBUSTNESS OF LINEAR TIME-INVARIANT CONTROL SYSTEMS **c65**
Robert F. Stengel and Laura R. Ray *In* NASA. Langley Research Center, Joint University Program for Air Transportation Research, 1990-1991 Dec. 1991 p 181-186 (For primary document see N92-17984 08-01)
(Grant NGL-31-001-252)
Avail: NTIS HC/MF A09 CSCL 12A

A simple numerical procedure for estimating the stochastic robustness of a linear time-invariant system is described. Monte Carlo evaluations of the system's eigenvalues allows the probability of instability and the related stochastic root locus to be estimated. This analysis approach treats not only Gaussian parameter uncertainties but non-Gaussian cases, including uncertain-but-bounded variation. Confidence intervals for the scalar probability of instability address computational issues inherent in Monte Carlo simulation. Trivial extensions of the procedure admit consideration of alternate discriminants; thus, the probabilities that stipulated degrees of instability will be exceeded or that closed-loop roots will leave desirable regions can also be estimated. Results are particularly amenable to graphical presentation. Author

02 AERODYNAMICS

Includes aerodynamics of bodies, combinations, wings, rotors, and control surfaces; and internal flow in ducts and turbomachinery.

For related information see also *34 Fluid Mechanics and Heat Transfer.*

N92-17114# Air Force Inst. of Tech., Wright-Patterson AFB, OH.

AN EXPERIMENTAL INVESTIGATION OF LEADING EDGE VORTICAL FLOW ABOUT A DELTA WING DURING WING ROCK M.S. Thesis

Michael D. Nelson Dec. 1991 200 p

(AD-A243363; AFIT/CI/CIA-91-066) Avail: NTIS HC/MF A09 CSCL 01/1

The primary objective of this research was to further investigate the dynamic motion of an 80 deg delta wing during wing rock in both a water and wind tunnel. Both vortical flow data and wing motion data were recorded using a video-based motion analysis system. This system provided adequate means to nonintrusively measure dynamic data. The data revealed hysteresis differences between the wind tunnel and water tunnel tests. Hysteresis in the rolling moment coefficient versus bank or roll angle, during water tunnel testing, traveled in the direction opposite to the wind tunnel results. Visualization of the water tunnel vortical flowfields provided quantified right and left vortex locations at specific roll angles during wing rock. The contribution to the rolling moment based on these vortex positions was analyzed. Results show a decrease in rolling moment before reaching the maximum roll amplitude and an increase in rolling moment after passing through the maximum roll angle. Added mass experiments were also conducted in the wind tunnel. The wind tunnel rolling moment was 15 times larger than water tunnel results, due to the difference in densities of the mediums. Although dynamic similitude was not achieved between the two fluids, a foundation for further investigation has been laid. GRA

N92-17117# Virginia Polytechnic Inst. and State Univ., Blacksburg. Dept. of Engineering Science and Mechanics.

OBSERVATION AND MEASUREMENTS OF FLOW STRUCTURES IN THE STAGNATION REGION OF A WING-BODY JUNCTION Technical Report, 1 Dec. 1988 - 31 Aug. 1991

S. Kim, D. A. Walker, and R. L. Simpson 1 Sep. 1991 277 p

(Contracts N00014-89-J-1275; N00014-90-J-1909)

(AD-A243403; VPI-E-91-20) Avail: NTIS HC/MF A13 CSCL 01/1

Behavior of a junction vortex formed around an obstacle in a boundary layer flow was studied experimentally in a water tunnel for two low speed cases. A wing consisting of a 3:2 elliptical nose and an NACA 0020 tail was used to simulate the junction vortex. A flow visualization study, using a hydrogen bubble technique, was conducted to investigate flow structures in the stagnation region of the wing. A multiple vortex system showing an acyclic flow pattern was observed. LDV measurements were performed in the plane of symmetry upstream of the wing. The general flow agrees with an earlier wind tunnel test conducted at higher speed. A low frequency, bistable flow structure was observed as in the wind tunnel measurements. The switching between two flow modes (a backflow mode and a zero flow mode) was analyzed using LDV signals in the zone of a bimodal structure. A dimensionless frequency group was found to represent the average frequency of successive switches from one mode to the other. Visual evidence of an acyclic flow pattern was consistent with LDV measurements and revealed that aperiodic stretching of the junction vortex appears responsible for the bimodal (double-peaked) structure in the velocity histograms. An attempt to measure the three-dimensional instantaneous velocity field in this region was made. A particle image displacement velocimetry technique was developed using a multiple wire hydrogen bubble method and a high speed video system. GRA

N92-17131*# National Aeronautics and Space Administration. Langley Research Center, Hampton, VA.

TWO-DIMENSIONAL STABILITY OF LAMINAR FLAMES

H. S. Mukunda and J. Philip Drummond Washington Feb. 1992 30 p

(NASA-TP-3131; L-16604; NAS 1.60:3131) Avail: NTIS HC/MF A03 CSCL 01A

The stability of laminar flames was studied numerically and the dependence of stability on finite rate chemistry with low activation energy and variable thermodynamic and transport properties was addressed. The calculations show that activation energy and details of chemistry play a minor role in altering the linear neutral stability results from asymptotic analysis. Variable specific heat makes a marginal change to the stability; variable transport properties, on the other hand, tend to substantially enhance the stability from a critical wave number of about 0.50 to 0.20. Also, the effects of variable properties tend to nullify the effects of nonunity Lewis number. When the Lewis number of a single species is different from unity, as is true in a hydrogen-air premixed flame, the stability results remain close to that of unity Lewis number. Author

N92-17222# Virginia Polytechnic Inst. and State Univ., Blacksburg. Dept. of Aerospace and Ocean Engineering.

AN EXPERIMENTAL STUDY OF A TURBULENT WING-BODY JUNCTION AND WAKE FLOW Technical Report, 1 Jun. 1989 - 31 Aug. 1991

J. L. Fleming, R. L. Simpson, and W. J. Devenport 1 Sep. 1991 198 p

(Contracts N00014-89-J-1275; N00014-90-J-1909)

(AD-A243388; VPI-AOE-179) Avail: NTIS HC/MF A09 CSCL 20/4

Extensive hot-wire measurements were conducted in incompressible turbulent flow around a wing-body junction. Measurements were performed adjacent to the body and up to 11.56 chord lengths downstream of the body. Junction wake flow entered an adverse pressure gradient region approximately 6 chord lengths downstream. This region's geometry approximated the aft portion of an aircraft fuselage or a submersible's hull. Body geometry was formed by joining a 3:2 elliptic nose to a NACA 0020 tail section at their respective maximum thickness locations. Measurements were taken with approach flow conditions of Re sub theta = 6,300, and delta/T = .513, where T is maximum body thickness. Results clearly show the characteristic horseshoe vortex flow structure, which is elliptically shaped, with del(W)/del Y forming the primary component of streamwise vorticity. Near wall measurements show a thin layer of highly concentrated vorticity, underneath and opposite in sign to the primary vortex, which is created by the wall no-slip condition. Development of flow distortions and associated vorticity distributions are highly dependent on the geometry-induced pressure gradients and resulting flow skewing directions. A quantity known as the 'distortion function' was used to separate distortive effects of secondary flow from those of the body and the local 2-D boundary layer. The distortion function revealed that adverse pressure gradient flow distortions grew primarily because of increasing boundary layer thickness. GRA

N92-17281# Aeronautical Research Labs., Melbourne (Australia).

SURFACE PRESSURE MEASUREMENTS ON THE WING OF A WIND TUNNEL MODEL DURING STEADY ROTATION

C. A. Martin and G. J. Brian Jul. 1991 84 p

(AD-A243047; ARL-FLIGHT-MECH-TM-443; DODA-AR-006-614) Avail: NTIS HC/MF A05 CSCL 01/1

Wind tunnel measurements were conducted to determine the nature of the pressure distribution over the wing of a model of a basic training aircraft for a range of angles of attack and rotation rates representative of aircraft spinning conditions. The tests were carried out as part of a collaborative program organized through The Technical Cooperation Programme and were conducted in the Spin Research Facility at the NASA Langley Research Center. Software for displaying the surface pressure distributions was

developed at the Aeronautical Research Laboratory. This report presents pressure coefficient data obtained during the program, in both numerical and graphical form. GRA

N92-17303# Old Dominion Univ., Norfolk, VA.
THE SOLUTION OF A SINGULAR INTEGRAL EQUATION ARISING FROM A LIFTING SURFACE THEORY FOR ROTATING BLADES Ph.D. Thesis
Mark H. Dunn Aug. 1991 155 p Original contains color illustrations
Avail: NTIS HC/MF A08; 11 functional color pages

A technique is presented for the solution of a linear, two dimensional, singular, Volterra integral equation of the first kind. The integral equation is derived from the basic equations of linearized acoustics and models the lifting force experienced by an infinitesimally thin surface moving tangent to itself. As a particular application, the motion of modern high speed aircraft propellers (Advanced Technology Propellers) is considered. The unknown propeller blade surface pressure distribution is approximated by a piecewise constant function and the integral equation is solved numerically by the method of collocation. Certain simplifying assumptions applied to the propeller blade model lead to a radical reduction in complexity of the solution methodology. Author

N92-17311# Messerschmitt-Boelkow-Blohm G.m.b.H., Munich (Germany, F.R.). Hubschrauber und Flugzeuge.
COMPARISON OF TWO SOLUTION METHODS FOR THE NUMERICAL CALCULATION OF HYPERSONIC FLOWS Thesis - Univ. der Bunderswehr Muenchen [VERGLEICH ZWEIER LOESUNGSVERFAHREN ZUR NUMERISCHEN BERECHNUNG VON HYPERSCHALLSTROEMUNGEN]
Christoph Mueller 31 Dec. 1990 162 p In GERMAN
(MBB-FE211-S-PUB-446; ETN-92-90617) Copyright Avail: NTIS HC/MF A08

Two methods for the numerical calculation of hypersonic flows were compared. The first solves the complete Navier-Stokes equations, and the second solves the viscous shock layer equations. The algorithms of both methods are explained. The Navier-Stokes equations were transformed for the vector notation time, application domains, and accuracy of the algorithms of both methods were compared with each other, as well as with a combined Euler boundary layer method. Good agreement between the methods is found. ESA

N92-17314# Max-Planck-Inst. fuer Stroemungsforschung, Goettingen (Germany, F.R.).
A SHORT OR A LONG CYLINDER: WHAT DIFFERENCE DOES IT MAKE TO THE KARMAN VORTEX STREET?
Holger Eisenlohr 1990 92 p In GERMAN; ENGLISH summary
(MPIS-98/1990; ISSN-0374-1257; ETN-92-90621) Avail: NTIS HC/MF A05

The difference between the behavior of the Karman vortex sheet for a short and a long circular cylinder placed perpendicular to the flow, was investigated in a wind tunnel. The complicated interaction between the vortex filaments results in a distortion of the wake profile and a change of the base pressure near the cylinder ends. This causes the vortex shedding frequency near the cylinder ends to diminish, and also leads to slanted shedding. Thus, regions of different shedding frequency appear and vortex splitting takes place. This can cause discontinuities in the smooth function normally observed. The discontinuities and slanted shedding disappear if the disturbed end regions are decoupled from the rest of the cylinder by using 'end cylinders'. ESA

N92-17315# Max-Planck-Inst. fuer Stroemungsforschung, Goettingen (Germany, F.R.).
INVESTIGATION ON THE CONTROL OF A KARMAN VORTEX STREET
Erika Roesch 1990 59 p In GERMAN; ENGLISH summary
(MPIS-99/1990; ISSN-0374-1257; ETN-92-90622) Avail: NTIS HC/MF A04

A Karman vortex street was controlled without feedback, according to the theory of Huebler, using a differential equation reconstructed by Ohle for the description of the flow in the wake of a circular cylinder. The validity of the theory was checked for its applicability to complex systems. The effectiveness of the specially calculated driving force was compared to an appropriate linear driving force. It is shown that a Van der Pol oscillator is no adequate model to control the vortex street, because the decisive terms of higher degree are absent. These terms are present in the differential equation reconstructed by Ohle, so that the prediction of the response of the vortex street to perturbations is possible. ESA

N92-17339# Naval Postgraduate School, Monterey, CA.
FLOW VISUALIZATION AND WAKE ANALYSIS FOR STANDARD AND MODIFIED CONFIGURATIONS OF THE AN/ALQ-78 ANTENNA POD M.S. Thesis
James F. Small Mar. 1991 158 p
(AD-A243552) Avail: NTIS HC/MF A08 CSCL 20/4

A low-speed wind tunnel investigation was conducted to compare the aerodynamic flow field characteristics for standard and modified configurations of a 20 percent scale model of the AN/ALQ-78 electronic support measures system antenna pod. The modification consisted of replacing the standard quasi-conically shaped radome with a cylindrical radome and adapter collar. The research was requested by the Naval Air Systems Command (NAVAIRSYSCOM) as part of a risk and feasibility assessment in preparation for possible full-scale flight tests of the modified configuration. Wake flow visualization was conducted to determine the general characteristics of the flow field. Base pressure measurements were made to assess three-dimensional effects. The presence of coherent vortex shedding in the wake was investigated using a cross-probe constant temperature hot-film anemometer and spectrum analyzer. The Reynolds number varied from 40,000 to 6 x 10(exp 5) with the upper value approximately equal to one-eighth that of the full-scale pod in flight. Asymmetric vortex shedding was visualized in the wakes of both configurations at subcritical Reynolds numbers. The modified configuration exhibited a pronounced region of quasi-two-dimensional flow during wake visualization and base pressure tests, indicating a significant increase in the aerodynamic forces acting on the pod structure. Spectral analysis of the hot-film output confirmed the presence of coherent vortex shedding in the wakes of both models at subcritical Reynolds numbers. Author (GRA)

N92-17347*# National Aeronautics and Space Administration. Lewis Research Center, Cleveland, OH.
EXPERIMENTAL ICE SHAPE AND PERFORMANCE CHARACTERISTICS FOR A MULTI-ELEMENT AIRFOIL IN THE NASA LEWIS ICING RESEARCH TUNNEL
Brian M. Berkowitz, Mark G. Potapczuk, Bahman S. Namdar, and Tammy J. Langhals (Sverdrup Technology, Inc., Brook Park, OH.)
Dec. 1991 323 p
(Contract NAS3-25266)
(NASA-TM-105380; E-6767; NAS 1.15:105380) Avail: NTIS HC/MF A14 CSCL 01A

A study of the ice accretion patterns and performance of characteristics of a multi-element airfoil was undertaken at the NASA-Lewis Icing Research Tunnel. Several configurations were examined to determine the ice shape and performance characteristics. The testing included glaze, rime, and mixed icing regimes. Tunnel cloud conditions were set to correspond to those typical of the operating environment for commercial transport aircraft. Measurements acquired included ice profile tracings and aerodynamic forces both during the accretion process and in a post-accretion evaluation over a range of angle of attack. Substantial ice accretions developed on the main wing, flaps, and slat surfaces. Force measurements indicate severe performance degradation, especially near CL max, for both light and heavy ice accretion. Frost was seen on the lower surface of the airfoil which was found to contribute significantly to the force components. Author

N92-17404# Army Natick Research and Development Command, MA.
TRAJECTORY ANALYSIS OF THE G-11 FAMILY OF CLUSTERED PARACHUTES TO DETERMINE MINIMUM ALTITUDE Final Report, Jul. 1990 - Aug. 1991
Steven Kunz Nov. 1991 25 p
(DA Proj. 1E4-64804-D-279)
(AD-A243375; NATICK/TR-92/005) Avail: NTIS HC/MF A03
CSCL 01/2

The U.S. Air Force is interested in determining the minimum altitude at which an aircraft can approach a drop zone and deploy an airdrop system to deliver cargo without its becoming damaged. Lower altitudes will reduce the exposure of aircraft to hostile fire, but being too low will result in the destruction of the cargo. The objective of this report is to determine the minimum altitude at which the cargo may be safely delivered. This was accomplished by analyzing trajectory data for airdrop systems using the G-11 parachute. It was found that the first point (time) at which cargo can be safely landed occurs when the cargo velocity reaches its first minimum total velocity, incident with the first maximum backswing orientation of the system. This criterion was used to determine the statistical mean of the altitude loss. The importance of variability is discussed as it relates to the determination of a safety factor. GRA

N92-17446# Naval Surface Warfare Center, Silver Spring, MD.
ZEUS USER MANUAL REAL GAS EFFECTS Summary Report, Aug. 1990 - Feb. 1991
F. J. Priolo and A. B. Wardlaw, Jr. 6 May 1991 97 p
(AD-A242224; NAVSWC-TR-91-86) Avail: NTIS HC/MF A05
CSCL 09/2

This report describes the extension and application of the ZEUS code to high, hypersonic Mach numbers by incorporating high temperature equilibrium air or 'real gas' effects. This approach is important for accurate aerodynamic predictions in support of atmospheric reentry vehicles with high maneuverability and future hypersonic weapons. The program employs an automatic multiple zone grid generation technique which is particularly suited to describing missile-type geometries in supersonic flight. The ZEUS code is a supersonic hypersonic space marching Euler solver which is capable of computing internal as well as external flows. The present report provides recent modifications to the program for real gas effects and user instructions for its application. The ZEUS code uses a zonal, finite volume, second order Godunov scheme to integrate the Euler equations. The computation proceeds for an initial data plane on which the flow field is specified, as shown in Figure 1, and marches in a streamwise direction until the end of the region of interest is encountered. In the case of a missile, the initial data plane is taken near the nose of the missile, and the flow field on this plane can be defined using conical flow, a blunt body solution, or uniform flow. GRA

N92-17509*# National Aeronautics and Space Administration. Langley Research Center, Hampton, VA.
STRUCTURAL DYNAMICS DIVISION RESEARCH AND TECHNOLOGY ACCOMPLISHMENTS FOR F.Y. 1991 AND PLANS FOR F.Y. 1992
Eleanor C. Wynne Jan. 1992 205 p
(NASA-TM-104188; NAS 1.15:104188) Avail: NTIS HC/MF A10
CSCL 01A

The work under each technical area is described in terms of highlights of accomplishments during the past year and highlights of plans for the current year as they relate to 5 year plans for each technical area. This information will be useful in program coordination with other government organizations and industry in areas of mutual interest. The structural dynamics division consist of the following branches: configuration aeroelasticity; unsteady aerodynamics; aeroservoelasticity; landing and impact dynamics; and spacecraft dynamics. Author

N92-17547*# National Aeronautics and Space Administration. Langley Research Center, Hampton, VA.
USER GUIDE FOR WIACX: A TRANSONIC WIND-TUNNEL WALL INTERFERENCE ASSESSMENT AND CORRECTION PROCEDURE FOR THE NTF
Javier A. Garriz and Kara J. Haigler Jan. 1992 67 p
(Contract NAS1-18585)
(NASA-TM-104168; NAS 1.15:104168) Avail: NTIS HC/MF A04
CSCL 01A

A three dimensional transonic Wind-tunnel Interference Assessment and Correction (WIAC) procedure developed specifically for use in the National Transonic Facility (NTF) at NASA Langley Research Center is discussed. This report is a user manual for the codes comprising the correction procedure. It also includes listings of sample procedures and input files for running a sample case and plotting the results. Author

N92-17681# George Washington Univ., Washington, DC.
THE EFFECT OF FREESTREAM TURBULENCE ON THE VORTICAL FLOW OVER A DELTA WING M.S. Thesis
Anthony Eugene Washburn Dec. 1990 248 p
Avail: NTIS HC/MF A11

An experimental investigation of the effect of freestream turbulence on the vortical flow over a 76 deg sharp edged delta wing at low Reynolds numbers was conducted. The investigation also considered the effect of test section type and model support system on the aerodynamic loads of the wing. The freestream turbulence intensities were increased from a baseline less than 0.1 percent to 7.5 percent by placing a grid upstream of the model. The angle of attack was varied from -6 deg to 40 deg for sideslip angles between 0 deg and 20 deg in Reynolds numbers of 0.5 x 10(exp 6) x 10(exp 6), and 1.0 x 10(exp 6), based on root chord. Off-body and surface flow visualization were used to demonstrate the turbulence effect on the vortex topology, path, and burst position as well as boundary layer transition. A non-intrusive infrared transition measurement technique was employed to support the surface flow visualization transition results. Force and moment data were taken to quantify freestream turbulence and Reynolds number effects on the aerodynamic loads. Aerodynamic load dependence on model installation was evaluated by testing the model in three closed test sections and one open test section with both sting and post mounts. Small Kelvin-Helmholtz type vortical structures in the leading edge vortex shear layer and hysteresis in burst and loads were seen with the baseline turbulence. The vortices and burst positions were unsteady in the high turbulence case and hysteresis in both burst positions and loads seemed to be eliminated. The secondary separation lines on the surface of the delta wing moved closer to the leading edge in the presence of the high turbulence indicating a turbulent boundary layer. The turbulence decreased the loads near the maximum lift angle. The aerodynamic loads are very dependent on model mounting and test section configuration with differences in maximum lift as great as 20 percent. Author

N92-17755# National Aerospace Lab., Tokyo (Japan). Aircraft Aerodynamics Div.
RESULTS OF MEASURED TEMPERATURE DISTRIBUTION ON AN ADIABATIC WING MODEL WITH RADIATION THERMOMETER [HOSHA ONDOKEI NIYORU DANNETSUYOKU MOKEIJO NO ONDO BUNPU SOKUTEI SHIKEN KEKKA]
Hideo Sawada, Akira Koike, Koichi Suzuki, Yukio Komatsu, Seigo Nakamura, and Shigeo Baba Jul. 1989 31 p In JAPANESE
(NAL-TM-610; ISSN-0452-2982; JTN-92-80246) Avail: NTIS HC/MF A03

In order to evaluate the influence of the wind tunnel difference upon the wind tunnel test result, it is necessary to evaluate the influence of the disturbance of the stream upon the boundary layer, detachment area, and disturbance area on the wind tunnel model. It is necessary to measure the transition point of boundary layer on the wing. As there is a close relationship between the boundary layer and the temperature distribution of the wing, it is effective to examine the temperature distribution on the wing in

order to study the stream on the wing. This paper describes the measurement of the temperature distribution on an adiabatic wing model by the non-contact thermometer and shows the observation results on the shockwave location, detachment area, and transition point location on the wing. Author (NASDA)

N92-17849# Manchester Univ. (England). Aeronautical Engineering Group.

BOUNDARY-LAYER TRANSITION AND HEAT TRANSFER ON SLENDER DELTA WINGS

D. I. A. Poll 1989 21 p Previously announced in IAA as A91-21194

(Aero-Rept-8904; ETN-92-90913) Avail: NTIS HC/MF A03

The problem of boundary layer transition via three different mechanisms (attachment line contamination, cross flow instability and tripping by isolated roughness elements) is considered in the context of flow over a slender delta wing. Existing knowledge of the transition mechanisms is summarized and estimates of the shape of the resulting transition fronts are made by linking the phenomena to the topography of the flow at the edge of the boundary layer. Simple relations are presented for the estimation of leading edge heating at small angles of incidence and wing center line heating at large angles of incidence. ESA

N92-17874# Midwest Research Inst., Golden, CO. National Renewable Energy Lab.

DYNAMIC STALL ON WIND TURBINE BLADES

C. P. Butterfield, D. Simms, G. Scott, and A. C. Hansen (Utah Univ., Salt Lake City.) Dec. 1991 9 p Presented at the 21st American Wind Energy Association Conference: Windpower 1991, Palm Springs, CA, 24-27 Sep. 1991

(Contract DE-AC02-83CH-10093)

(DE92-001157; NREL/TP-257-4510; CONF-9109112-7) Avail: NTIS HC/MF A02

Dynamic loads must be predicted accurately in order to estimate the fatigue life of wind turbines operating in turbulent environments. Dynamic stall contributes to increased dynamic loads during normal operation of all types of horizontal-axis wind turbine (HAWT's). This report illustrates how dynamic stall varies throughout the blade span of a 10 m HAWT during yawed and unyawed operating conditions. Lift, drag, and pitching moment coefficients during dynamics stall are discussed. Resulting dynamic loads are presented, and the effects of dynamic stall on yaw loads are demonstrated using a yaw loads dynamic analysis (YAWDYN). DOE

03 AIR TRANSPORTATION AND SAFETY

Includes passenger and cargo air transport operations; and aircraft accidents.

For related information see also *16 Space Transportation* and *85 Urban Technology and Transportation.*

N92-16986# Wichita State Univ., KS. National Inst. for Aviation Research.

WICHITA STATE UNIVERSITY 1986 AVIATION SAFETY RESEARCH PROJECTS Final Report

John J. Hutchinson Dec. 1991 28 p

(Contract DTFA03-86-C-00041)

(DOT/FAA/CT-91/4) Avail: NTIS HC/MF A03

The proposal which the National Institute for Aviation Research (NIAR) at the Wichita State University (WSU) submitted to the Federal Aviation Administration (FAA) on May 23, 1986, proposed aviation safety research efforts in four areas: crashworthiness; electro-impulse deicing; stall/spin prevention; software reliability. Specific research topics were selected on the basis of a review of FAA research interests, the specialized expertise of WSU research interests, and discussions held with FAA personnel at the FAA Technical Center in Atlantic City and at WSU. The research carried out under this contract is now complete. In addition to the research activities undertaken during the period of this contract, the NIAR has completed construction on a 74,000-square-foot building which houses the activities and laboratories of the institute. Extensive equipment has been purchased as part of this contract and is now housed in the institute building. Moreover, the FAA support for equipment has been used to match State of Kansas equipment grants and has resulted in several well equipped laboratories. This research has involved 13 faculty members and 14 students. The NIAR is now positioned for sustained research as well as advanced training of graduate students in a wide range of technical disciplines related to aviation safety. Publications resulting from their research efforts are listed by area. Summaries of research are given in the areas of crashworthiness, energy absorbing mechanisms, computational crash dynamics analysis, electro-impulse deicing, aerodynamic data on stall/spin prevention, and software reliability assessment in aviation systems. Author

N92-17133# National Transportation Safety Board, Washington, DC.

AIRCRAFT ACCIDENT REPORTS: BRIEF FORMAT. US CIVIL AND FOREIGN AVIATION ISSUE NUMBER 4 OF 1989 ACCIDENTS

18 Dec. 1990 414 p

(PB90-916904; NTSB/AAB-90/04) Avail: NTIS HC/MF A18; paper copy available on Standing Order, deposit account required (minimum deposit $100 US, Canada, and Mexico; all others $200). Single copies also available in paper copy or microfiche CSCL 01C

Presented here in brief format are selected aircraft accident reports relating to U.S. civil and foreign aviation operations during calendar year 1989. The approximately 200 general aviation and air carrier accidents contained here represent a random selection. The facts, conditions, circumstances, and probable causes for each accident are given. Author

N92-17149# Federal Aviation Administration, Atlantic City, NJ.

EFFECTIVENESS OF AN ONBOARD WATER SPRAY SYSTEM DURING AN OXYGEN ENRICHED CABIN FIRE

Timothy Marker and Bruce Downie (Rutgers Univ., New Brunswick, NJ.) Dec. 1991 33 p

(DOT/FAA/CT-TN91/51) Avail: NTIS HC/MF A03

Three full-scale fire tests were conducted in a modified DC-10 fuselage to determine the effectiveness of an onboard water spray system in reducing the hazardous effects of an oxygen enriched postcrash cabin fire. Two fuel fire tests were conducted in which pressurized oxygen was introduced into the cabin interior in the vicinity of a pool fire which was adjacent to a fuselage opening. Water was sprayed throughout the cabin during some of the two oxygen fed fire tests in order to determine the benefits of using an onboard spray system. For comparison, a third test was performed using the identical pool fire adjacent to the fuselage opening without the introduction of oxygen into the cabin in order to establish 'baseline' data. The interior of the fuselage was realistically furnished in the area adjacent to the fuel and was fully instrumented to measure the various fire hazards. Temperature profiles, smoke levels, gas concentrations and heat flux were monitored throughout the fuselage during the tests. Photographic and video recordings visually documented the progress of the fire. The results showed the water spray to be an effective method for increasing the chances of survival in the event of an oxygen enriched fire by significantly prolonging the period of time that the cabin environment remains habitable. Author

N92-17213# National Transportation Safety Board, Washington, DC.

AIRCRAFT ACCIDENT REPORT: NORTHWEST AIRLINES, INC., FLIGHTS 1482 AND 299. RUNWAY INCURSION AND COLLISION, DETROIT METROPOLITAN/WAYNE COUNTY AIRPORT, ROMULUS, MICHIGAN, DECEMBER 3, 1990

25 Jun. 1991 178 p

(PB91-910405; NTSB/AAR-91/05) Avail: NTIS HC/MF A09; paper copy also available on Standing Order, deposit account required (Minimum deposit $100 US, Canada, and Mexico; all

others $200). Single copies also available in paper copy or microfiche CSCL 01C

The runway collision of two Northwest Airlines aircraft on a runway at the Detroit Metropolitan/Wayne County Airport, Romulus, Michigan, on December 3, 1990 is explained. The safety issues discussed are airport marking and lighting, cockpit resource management, air traffic control procedures in low visibility conditions, flight attendant procedures during evacuations, and the design of the DC-9 tailcone emergency release system. Safety recommendations concerning these issues were made to the Federal Aviation Administration, the Detroit Metropolitan/Wayne County Airport, and Northwest Airlines, Inc. Author

N92-17217# Naval Postgraduate School, Monterey, CA.
ESCAPE STRATEGIES FOR TURBOPROP AIRCRAFT IN A MICROBURST WINDSHEAR M.S. Thesis
Richard B. Bobbitt Mar. 1991 247 p
(AD-A243090) Avail: NTIS HC/MF A11 CSCL 01/2

A quantitative analysis was carried out on the performance of turboprop aircraft within a microburst windshear. The objective of the analysis was to provide specific flight procedures for optimal navigation through the windshear. The microburst windshear model uses in the analysis embodied the severe characteristics of the microburst encountered by Delta Flight 191 during an approach to landing at Dallas/Ft. Worth, 2 Aug. 1985. Different escape strategies were tested using the flight performance characteristics of the U.S. Navy's P-3 'Orion' and T-44 'Pegasus' aircraft. The three flight phases investigated were approach to landing, takeoff, and the low altitude ASW mission. Results from the analysis were coupled with the pilot's view point from which conclusions were drawn. The results of the analysis support a constant-pitch-angle escape procedure. The same procedural steps can be used for both aircraft in any configuration or situation with the difference being the degree of pitch to employ. The conclusions are in a format for integrating specific microburst escape procedures within the NATOPS programs for the P-3 and T-44. GRA

N92-17259# Beltran, Inc., Brooklyn, NY.
DEVELOPMENT OF FUEL NEUTRALIZING AGENTS TO PREVENT FLASHBACK ON AIRCRAFT FIRES Final Report, Aug. 1987 - Sep. 1989
Michael R. Beltran and Constance Simo May 1991 178 p
(Contract F08635-87-C-0302)
(AD-A242828; AFESC/ESL-TR-90-60) Avail: NTIS HC/MF A09 CSCL 21/4

The object of this study was to explore chemical modification of extinguishants currently used against postcrash fuel fed fires to inhibit reignition, i.e., improve 'burnback' control, without compromising the efficacy of flame knockdown. A formulation was developed as an additive to AFFF, for delivery during fire extinguishment which succeeded in 16-inch laboratory trials, but not to the same extent in 6-foot field tests. Several causes were considered and reformulation recommended. Three other approaches, each with formulations, also showed potential for significant reduction of fuel reignition if administered subsequent to flame knockdown by AFFF. One permits resealing by AFFF, another, instant emulsification of water and JP-4, and a third, gelling of the fuel. GRA

N92-17478# Dayton Univ., OH.
EXPLICIT FINITE ELEMENT METHOD FOR TRANSPARENCY IMPACT ANALYSIS Final Technical Report, Sep. 1988 - Sep. 1990
R. A. Brockman and T. W. Held Jun. 1991 176 p
(Contract F33600-88-D-0414)
(AD-A243527; UDR-TR-90-114; WL-TR-91-3006) Avail: NTIS HC/MF A09 CSCL 01/2

This report documents new analytical methods for the solution of soft-body impact problems, including birdstrike. The approach is based on explicit finite element techniques which allow for very detailed material modeling and make efficient use of the current generation of supercomputers. The most important improvements in the present work over previous efforts are in the areas of soft-body impact loading, material modeling, and treatment of layered wall constructions. Impact loads are obtained directly by including the impacting body in the finite element model, eliminating the need for ad hoc loading models. Both the transparency and the soft body materials may be rate-sensitive, exhibit nonlinear bulk behavior, and may fail during the finite element solution. Methods have been developed to make commercial graphics software (PATRAN) deal correctly with failed elements for results output. An improved model of laminated shells is included in the plate and shell element so that each layer of a multilayered transparency need not be modeled with distinct elements, even when soft interlayers are present. The methods described have been implemented in an explicit finite element code X3D. User and programmer information are included in the report as appendices. Applications described in the report include two standard test problems and an F-16 birdstrike simulation. GRA

N92-17587# Wichita State Univ., KS. National Inst. for Aviation Research.
PROGRAM PLANS: AVIATION SAFETY RESEARCH
William H. Wentz and John J. Hutchinson Dec. 1991 40 p
(Contract DTFA03-90-C-00050)
(NIAR-91-30) Avail: NTIS HC/MF A03

In the event of an engine failure, provision for containment of moving parts is desired to prevent secondary damage of structural members and aircraft mechanical systems including possible damage to adjacent engines. This problem was addressed by large engine manufacturers to various degrees and with various analysis procedures. Currently, the wide variety of approaches in use, combined with the absence of a data base of experimental results, make the problem of developing certification standards difficult. The research collected, analyzed, and organized information on design procedures for rotor containment and the effectiveness of designs. The objective was to enable development of the most appropriate and workable standards possible. The specific elements of this study included: (1) reviewing current FAA regulations or standards addressing rotor containment; (2) reviewing existing literature on design for containment, reports of accident investigations, and test stand engine failure data; (3) contacting engine manufacturers and determining what design methods are currently employed and propulsion departments of airframe manufacturers to determine containment problems; (4) assessing effectiveness of computational codes for realistically predicting containment capabilities; and (5) presenting results of this study in a format designed to guide the development of certification standards. Author

N92-17985*# Massachusetts Inst. of Tech., Cambridge. Flight Transportation Lab.
AN INVESTIGATION OF AIR TRANSPORTATION TECHNOLOGY AT THE MASSACHUSETTS INSTITUTE OF TECHNOLOGY, 1990-1991
Robert W. Simpson *In* NASA. Langley Research Center, Joint University Program for Air Transportation Research, 1990-1991 Dec. 1991 p 3-9 (For primary document see N92-17984 08-01)
Avail: NTIS HC/MF A09 CSCL 01C

N92-17986*# Massachusetts Inst. of Tech., Cambridge. Dept. of Aeronautics and Astronautics.
EXPERIMENTAL INVESTIGATION OF PASSIVE INFRARED ICE DETECTION FOR HELICOPTER APPLICATIONS
Adam Dershowitz and R. John Hansman, Jr. *In* NASA. Langley Research Center, Joint University Program for Air Transportation Research, 1990-1991 Dec. 1991 p 11-18 Previously announced in IAA as A91-19402 (For primary document see N92-17984 08-01)
(Grant NAG3-927)
Avail: NTIS HC/MF A09 CSCL 01C

N92-17987*# Massachusetts Inst. of Tech., Cambridge. Dept. of Aeronautics and Astronautics.
DETERMINISTIC MULTI-ZONE ICE ACCRETION MODELING

K. Yamaguchi, R. John Hansman, Jr., and Michael Kazmierczak (Cincinnati Univ., OH.) *In* NASA. Langley Research Center, Joint University Program for Air Transportation Research, 1990-1991 Dec. 1991 p 19-28 Previously announced in IAA as A91-19209 Sponsored in part by NSF (For primary document see N92-17984 08-01)
(Grants NAG3-666; NGL-22-009-640)
Avail: NTIS HC/MF A09 CSCL 01C

N92-17988*# Massachusetts Inst. of Tech., Cambridge. Dept. of Aeronautics and Astronautics.
ALERT GENERATION AND COCKPIT PRESENTATION FOR AN INTEGRATED MICROBURST ALERTING SYSTEM
Craig Wanke and R. John Hansman, Jr. *In* NASA. Langley Research Center, Joint University Program for Air Transportation Research, 1990-1991 Dec. 1991 p 29-39 Previously announced in IAA as A91-19207 (For primary document see N92-17984 08-01)
(Contract NGL-22-009-640; BARR-10-119)
Avail: NTIS HC/MF A09 CSCL 01C

N92-17990*# Ohio Univ., Athens. Avionics Engineering Center.
INVESTIGATION OF AIR TRANSPORTATION TECHNOLOGY AT OHIO UNIVERSITY, 1990-1991
Robert W. Lilley *In* NASA. Langley Research Center, Joint University Program for Air Transportation Research, 1990-1991 Dec. 1991 p 51-54 (For primary document see N92-17984 08-01)
Avail: NTIS HC/MF A09 CSCL 01C

N92-17995*# Princeton Univ., NJ. Dept. of Mechanical and Aerospace Engineering.
INVESTIGATION OF AIR TRANSPORTATION TECHNOLOGY AT PRINCETON UNIVERSITY, 1990-1991
Robert F. Stengel *In* NASA. Langley Research Center, Joint University Program for Air Transportation Research, 1990-1991 Dec. 1991 p 103-112 (For primary document see N92-17984 08-01)
Avail: NTIS HC/MF A09 CSCL 01C

N92-17996*# Princeton Univ., NJ. Dept. of Mechanical and Aerospace Engineering.
TARGET PITCH ANGLE FOR THE MICROBURST ESCAPE MANEUVER
Sandeep S. Mulgund *In* NASA. Langley Research Center, Joint University Program for Air Transportation Research, 1990-1991 Dec. 1991 p 113-125 (For primary document see N92-17984 08-01)
Avail: NTIS HC/MF A09 CSCL 01C

N92-17999*# Cornell Univ., Ithaca, NY.
OPTIMAL AIRCRAFT PERFORMANCE DURING MICROBURST ENCOUNTER
Mark L. Psiaki and Robert F. Stengel (Princeton Univ., NJ.) *In* NASA. Langley Research Center, Joint University Program for Air Transportation Research, 1990-1991 Dec. 1991 p 155-161 Previously announced in IAA as A91-29787 (For primary document see N92-17984 08-01)
(Grant NGL-31-001-252)
Avail: NTIS HC/MF A09 CSCL 01C

04 AIRCRAFT COMMUNICATIONS AND NAVIGATION

Includes digital and voice communication with aircraft; air navigation systems (satellite and ground based); and air traffic control.

For related information see also *17 Space Communications, Spacecraft Communications, Command and Tracking* and *Communications and Radar.*

N92-17147# Carnegie-Mellon Univ., Pittsburgh, PA. Robotics Inst.
A SYSTEM FOR FAST NAVIGATION OF AUTONOMOUS VEHICLES
Sanjiv Singh, Dai Feng, Paul Keller, Gary Shaffer, and Wen F. Shi Sep. 1991 104 p
(AD-A243523; CMU-RI-TR-91-20) Avail: NTIS HC/MF A06 CSCL 17/7

This report describes an autonomous mobile robot designed to navigate at high speeds over featureless terrain: terrain which is not navigable by relying on features that are found on paved roads and highways. To this end, we have developed a paradigm that we call position based navigation that relies on explicit vehicle position information from inertial and satellite instruments to navigate. Specifically we have tackled four main areas: path tracking, which guides the robot vehicle over a pre-specified path; obstacle detection, which is responsible for bringing the vehicle to a stop from high speed when an obstacle is detected; obstacle avoidance, which is responsible for steering the vehicle around detected obstacles so as to rejoin the specific path; and computing architecture, which integrates all the capabilities into one system. We discuss the algorithms and the devices that were implemented on NavLab, a navigation testbed at Carnegie Mellon. The most notable of our results is the 11 m/s speed achieved by the vehicle. GRA

N92-17481# Air Force Inst. of Tech., Wright-Patterson AFB, OH. School of Engineering.
INCORPORATION OF DIFFERENTIAL GLOBAL POSITIONING SYSTEM MEASUREMENTS USING AN EXTENDED KALMAN FILTER FOR IMPROVED REFERENCE SYSTEM PERFORMANCE M.S. Thesis
William J. Negast Dec. 1991 214 p
(AD-A243742; AFIT/GE/ENG/91D-41) Avail: NTIS HC/MF A10 CSCL 17/7

To quantify the performance abilities of existing or proposed navigation systems, the US Air Force has, for the last several years, compared the performance of the system under test to the performance of a baseline navigation system known as the Completely Integrated Reference Instrumentation System (CIRIS). CIRIS obtains a highly accurate navigation solution by combining information from three major subsystems: inertial navigation system (INS) information, barometric altitude information, and range and range-rate information from ground transponders which have been precisely surveyed. Although the navigation solution produced by CIRIS is highly accurate, it will soon be inadequate as the standard against which future navigation systems can be tested. This research proposes as alternative to CIRIS - a hybrid Enhanced Navigation Reference System (ENRS) which is designed to take advantage of a newer INS (the LN-93), certain features of the current CIRIS, and certain features of differential corrections to Global Positioning System (DGPS) measurements. Analysis is conducted using a Kalman filter development package known as the Multimode Simulation for Optimal Filter Evaluation (MSOFE). Both a large order truth model for the ENRS (in which a full 24 satellite constellation is modeled) and full- and reduced-order Kalman filters are developed. Results suggest that the proposed ENRS (with DGPS aiding) provides a navigation solution one order of magnitude better than CIRIS. GRA

N92-17512*# Douglas Aircraft Co., Inc., Long Beach, CA.
ASSESSMENT OF COCKPIT INTERFACE CONCEPTS FOR DATA LINK RETROFIT Final Report

Hugh W. McCauley, William L. Miles, John P. Dwyer, and Jeffery B. Erickson Jan. 1992 107 p
(Contract NAS1-18028)
(NASA-CR-187615; NAS 1.26:187615) Avail: NTIS HC/MF A06 CSCL 01D

The problem is examined of retrofitting older generation aircraft with data link capability. The approach taken analyzes requirements for the cockpit interface, based on review of prior research and opinions obtained from subject matter experts. With this background, essential functions and constraints for a retrofit installation are defined. After an assessment of the technology available to meet the functions and constraints, candidate design concepts are developed. The most promising design concept is described in detail. Finally, needs for further research and development are identified. Author

N92-17568# National Research Council of Canada, Ottawa (Ontario). Inst. for Aerospace Research.
FLIGHT EVALUATION OF CURVED MLS PRECISION APPROACHES IN A TWIN OTTER AIRCRAFT, PHASE 2
J. B. Croll Jul. 1991 26 p
(AD-A243025; IAR-AN-73; NRC-32149) Avail: NTIS HC/MF A03 CSCL 17/7

Phase 2 flight testing of curved, segmented approaches using a Microwave Landing System (MLS) was conducted on a Twin Otter aircraft belonging to the Canadian National Research Council's Institute for Aerospace Research (IAR). Precision guidance algorithms were developed for approaches with track angle changes exceeding 180 deg. Software development flights focussed on validating these algorithms and enhancing the existing electromechanical flight director to ease the pilot workload in tracking the curved segments. A limited number of pilot evaluations confirmed that with an enhanced lateral flight director, these approaches could be flown satisfactorily regardless of the magnitude of the track angle changes. Observations were made on approach design and wind effects on curved segment tracking. GRA

N92-17639# Naval Postgraduate School, Monterey, CA.
USING THE GLOBAL POSITIONING SYSTEM (GPS) TO FULFILL THE POSITION/LOCATION REQUIREMENTS OF THE NATIONAL TRAINING CENTER (NTC) AND OTHER US ARMY INSTRUMENTED TESTING AND TRAINING RANGES M.S. Thesis
Nolan B. Young Mar. 1991 76 p
(AD-A242064) Avail: NTIS HC/MF A05 CSCL 17/7

This thesis discusses the use of the Global Positioning System (GPS) to fulfill requirements for exact position/location (P/L) of combat elements on Army testing and training ranges. These requirements include the control of the ranges, measuring effectiveness of employing new systems or doctrine, use in after action reviews (AARs) to discuss battlefield events, recording operations for later analysis, and safety. It also addresses use of GPS equipped systems by the player units while participating in simulated combat on these ranges. The National Training Center (NTC) at Fort Irwin, California, is currently the largest and most complex of the Army's instrumented ranges. It is referred to throughout this thesis for examples of P/L requirements and instrumentation capabilities. The development and fielding of GPS has added a new dimension in the Army's ability to accurately measure and record P/L. The designers of future instrumentation upgrades are incorporating GPS capabilities. This thesis will show how capabilities can be improved and money saved by using a coordinated effort when employing GPS on the Army's instrumented ranges. GRA

N92-17707# Department of the Navy, Washington, DC.
METHOD OF GUIDING AN IN-FLIGHT VEHICLE TO A DESIGNED FLIGHT PATH Patent Application
Roger L. Gray, inventor (to Navy) 27 Feb. 1991 17 p
(AD-D015061; US-Patent-Appl-SN-708991; Navy-Case-73256)
Avail: NTIS HC/MF A03 CSCL 17/7

This patent application relates generally to guidance techniques and more particularly to a method of guiding an in-flight vehicle from its initial flight path at target acquisition to a desired flight path prior to target interception. A method of using two diverts in combination to guide an in-flight vehicle from its initial flight path at target acquisition to a desired flight path prior to target interception is provided. The two diverts are of known and different magnitudes. The magnitude of an initial projected miss at a closest approach to the target is used to determine the order and timing of the two diverts. At the completion of the second divert, the vehicle is on the desired flight path which may be either a collision or offset course trajectory as required by the vehicle's terminal guidance law. GRA

N92-17844 ESDU International Ltd., London (England).
EXAMPLE OF STATISTICAL TECHNIQUES APPLIED TO AUTOLAND TOUCHDOWN DISPERSION (CONFIDENCE INTERVALS FOR NORMAL AND SKEW DISTRIBUTIONS)
Oct. 1991 11 p
(ESDU-91019; ISBN-0-85679-781-2; ISSN-0141-4054) Avail: ESDU

This data item illustrates certain aspects of statistical analysis introduced in ESDU 91017 applied to autoland touchdown dispersion. Two sets of data are analyzed, one for the standard 3 deg glide slope and one for a STOL glide slope of 7.5 deg with modified control laws. Each set consisted of 1480 points giving frequency of touchdown in various 100 ft intervals from the thresholds. The data are analyzed to establish the mean touchdown distance, the probability of touching down either short or long (200 ft before or 3000 ft beyond the threshold) and the touchdown distance three standard deviations beyond the mean touchdown point. The Chi Squared Test applied to the first set of data shows a high confidence that they are normal, and so the required results are obtained by plotting the percentage cumulative frequency data against touchdown distance using normal probability graph paper. When the Chi Squared Test is applied to the second data set, the confidence in their normality is found to be only 19 pct. A transformation of the data is therefore tried, taking the logarithm of the touchdown distance which greatly increases the confidence in normality established by the Chi Squared Test. ESDU

N92-17878# Oxford Univ. (England). Robotics Research Group.
APPLICATION OF MULTI-TARGET TRACKING TO SONAR-BASED MOBILE ROBOT NAVIGATION
John J. Leonard and Hugh F. Durrant-Whyte 1990 23 p Presented at the 29th IEEE Conference on Decision and Control, HI, Dec. 1990 Sponsored in part by Commission of the European Communities
(Contract SERC-ACME-GRE/42419)
(OUEL-1819/90; ETN-92-90904) Avail: NTIS HC/MF A03

An approach to mobile robot navigation that unifies the problems of obstacle avoidance, position estimation and map building on a common multitarget tracking framework, is described. Model based navigation is viewed as a process of tracking naturally occurring geometric targets, or beacons. Targets predicted (expected) from the environment map are tracked to provide vehicle position estimates (localization). Targets observed, but not predicted, represent unknown environment features or obstacles, and cause new tracks to be initiated, classified, and ultimately integrated into the map. A good sensor model is a crucial component of this approach, and is used both for predicting expected observations and classifying unexpected observations. This navigation framework is being implemented on a mobile robot that employs sonar as the principle navigation sensor. An implementation of model based localization that achieves robust position estimation in a known environment is presented. Preliminary results in obstacle identification and map building that lead to the belief that a complete navigation system, encompassing localization obstacle avoidance, and map building, can be implemented exclusively with sonar, are presented. ESA

N92-17992*# Ohio Univ., Athens.
FAULT DETECTION AND ISOLATION FOR MULTISENSOR NAVIGATION SYSTEMS
Paul A. Kline and Frank vanGraas *In* NASA. Langley Research Center, Joint University Program for Air Transportation Research, 1990-1991 Dec. 1991 p 61-68 (For primary document see N92-17984 08-01)
Avail: NTIS HC/MF A09 CSCL 17G

N92-17994*# Ohio Univ., Athens.
GPS INTERFEROMETRIC ATTITUDE AND HEADING DETERMINATION: INITIAL FLIGHT TEST RESULTS
Frank vanGraas and Michael Braasch *In* NASA. Langley Research Center, Joint University Program for Air Transportation Research, 1990-1991 Dec. 1991 p 79-100 (For primary document see N92-17984 08-01)
(Grant NGR-36-009-017)
Avail: NTIS HC/MF A09 CSCL 17G

05 AIRCRAFT DESIGN, TESTING AND PERFORMANCE

Includes aircraft simulation technology.

For related information see also *18 Spacecraft Design, Testing and Performance* and *39 Structural Mechanics.*For land transportation vehicles see *85 Urban Technology and Transportation.*

N92-17071*# National Aeronautics and Space Administration. Hugh L. Dryden Flight Research Facility, Edwards, CA.
AIRCRAFT GROUND TEST AND SUBSCALE MODEL RESULTS OF AXIAL THRUST LOSS CAUSED BY THRUST VECTORING USING TURNING VANES
Steven A. Johnson Washington Jan. 1992 29 p
(NASA-TM-4341; H-1743; NAS 1.15:4341) Avail: NTIS HC/MF A03 CSCL 01C

The NASA-Dryden F/A-18 high alpha research vehicle was modified to incorporate three independently controlled turning vanes located aft of the primary nozzle of each engine to vector thrust for pitch and yaw control. Ground measured axial thrust losses were compared with the results from a 14.25 pct. cold jet model for single and dual vanes inserted up to 25 degs into the engine exhaust. Data are presented for nozzle pressure ratios of 2.0 and 3.0 and nozzle exit areas of 253 and 348 sq in. The results indicate that subscale nozzle test results properly predict trends but underpredict the full scale results by approx. 1 to 4.5 pct. in thrust loss. Author

N92-17153# Advisory Group for Aerospace Research and Development, Neuilly-Sur-Seine (France). Flight Mechanics Panel.
ROTORCRAFT SYSTEM IDENTIFICATION
Oct. 1991 257 p Lecture series held in Ottobrunn, Fed. Republic of Germany, 4-5 Nov. 1991, in Rome, Italy, 7-8 Nov. 1991, and in College Park, MD, 13-14 Nov. 1991
(AGARD-LS-178; ISBN-92-835-0640-5) Copyright Avail: NTIS HC/MF A12; Non-NATO Nationals requests available only from AGARD/Scientific Publications Executive

Owing to the highly coupled flight dynamic behavior of rotorcraft configurations, long term interdisciplinary scientific knowledge combined with practical flight test experience is required to use system identification and mathematical modeling tools in the most efficient way. This lecture series is intended to establish an improved dialogue between government organizations, research institutions, and industry in order to apply these tools more routinely in rotorcraft system design, development, and evaluation. This lecture series is supported by a unique flight test data set which was specially generated and analyzed within a recent working group in the Flight Mechanics Panel of Advisory Group for Aerospace Research & Development (AGARD) on Rotorcraft System Identification (WB 18). This lecture series, sponsored by the Flight Mechanics Panel of AGARD, was implemented by the Consultant and Exchange Program. For individual titles, see N92-17154 through N92-17166.

N92-17154# Glasgow Univ. (Scotland). Dept. of Electronics and Electrical Engineering.
DESIGN OF EXPERIMENTS
David J. Murray-Smith and Gareth D. Padfield (Royal Aerospace Establishment, Bedford, England) *In* AGARD, Rotorcraft System Identification Oct. 1991 8 p (For primary document see N92-17153 08-05)
Copyright Avail: NTIS HC/MF A12; Non-NATO Nationals requests available only from AGARD/Scientific Publications Executive

The planning and conduct of flight experiments is a critically important part of the system identification process. Factors such as the choice of test input signal and the duration of the experiment can have a major influence on the quality of the identification results. Other factors such as the quality of flightcrew and groundcrew briefings and the availability of online monitoring facilities also greatly influence the effectiveness of any flight testing program. Inevitably there is a trade-off between performance and flight safety which must be taken fully into account at all stages of identification flight trials and influences the experiment design process and test matrix in a very significant way. Other important practical constraints arise in experiment design, especially when test input signals have to be applied manually by the pilot. An outline of the forms of test input most commonly used for identification is included, and an account of methods of experimental design is provided in which the value of a frequency-domain approach is emphasized. Author

N92-17155# Deutsche Forschungsanstalt fuer Luft- und Raumfahrt, Brunswick (Germany, F.R.). Inst. fuer Flugmechanik.
INSTRUMENTATION AND DATA PROCESSING
Juergen Kaletka *In* AGARD, Rotorcraft System Identification Oct. 1991 18 p (For primary document see N92-17153 08-05)
Copyright Avail: NTIS HC/MF A12; Non-NATO Nationals requests available only from AGARD/Scientific Publications Executive

The quality of measured flight test data is critically important to system identification. Inaccurate or kinematically inconsistent data can lead to identification of an incorrect model or inability to obtain convergence of the estimation solution. Therefore, this lecture concentrates on instrumentation and data processing aspects from a system identification point of view. It is mainly based on the work of the Advisory Group for Aerospace Research & Development (AGARD) Working Group WG-18 on Rotorcraft System Identification who concentrated on the identification of 6 degrees of freedom models. In addition, rotor blade instrumentation needed for the determination of extended models with explicit rotor degrees of freedom is addressed. Author

N92-17156# National Aero- and Astronautical Research Inst., Amsterdam (Netherlands). Dept. of Flight Testing and Helicopters.
FLIGHT TEST DATA QUALITY EVALUATION
Jan H. Breeman *In* AGARD, Rotorcraft System Identification Oct. 1991 8 p (For primary document see N92-17153 08-05)
Copyright Avail: NTIS HC/MF A12; Non-NATO Nationals requests available only from AGARD/Scientific Publications Executive

The quality of the measurement data determines the quality of the parameter identification results. Visual inspection of data plots is the first step in the evaluation of data quality. The measurements can be scrutinized for obvious errors such as wrong signs, excessive measurement noise, data dropouts, spikes and missing (or even exchanged) data channels. In addition, frequency domain techniques can be very useful for data quality evaluation. Any redundancy in the measured variables can be exploited to verify the data quality. Kinematic compatibility checking is explained as well as a number of solution techniques such as weighted least squares, extended Kalman filter/smoother, output error, and filter error. Some computer programs used for compatibility checking are discussed. Author

N92-17157# Toronto Univ. (Ontario). Inst. for Aerospace Studies.
IDENTIFICATION TECHNIQUES: MODEL STRUCTURE AND TIME DOMAIN METHODS
Jaap H. deLeeuw *In* AGARD, Rotorcraft System Identification Oct. 1991 9 p (For primary document see N92-17153 08-05)
Copyright Avail: NTIS HC/MF A12; Non-NATO Nationals requests available only from AGARD/Scientific Publications Executive

An overview is given of rotorcraft system identification techniques used by WG 18. The selection of model structure is considered. Here, special emphasis is given to ensuring that the model structure is appropriate to the intended model application. For example, simple decoupled first-order models that characterize the helicopter dynamics over a limited frequency range may be suitable for handling-qualities applications, while coupled 6-DoF models suitable for a broader range are needed for piloted simulation. At the other end of the complexity spectrum are models needed for use in advanced high-bandwidth rotorcraft flight control system design that must consider the coupled fuselage/rotor/airmass dynamics. Both nonparametric model structures (frequency-responses) and parametric model structures (transfer functions and state-space equations) are considered in the two sections dealing with identification techniques. The next step in the identification problem definition is the formulation of the criterion or 'cost' function. Once the model structure and cost function have been defined, the model is identified from the input/output time-history data using either time-domain or frequency-domain methods. The final step in system identification is referred to as 'model verification.' Here the extracted model is driven with flight data not used in the identification process to ensure the correctness of the identification procedure, and the utility of the model in predicting control responses rather than simply matching them. Author

N92-17158# Army Aviation Systems Command, Moffett Field, CA. Aeroflightdynamics Directorate.
IDENTIFICATION TECHNIQUES: FREQUENCY DOMAIN METHODS
Mark B. Tischler *In* AGARD, Rotorcraft System Identification Oct. 1991 4 p (For primary document see N92-17153 08-05)
Copyright Avail: NTIS HC/MF A12; Non-NATO Nationals requests available only from AGARD/Scientific Publications Executive

The starting point in frequency-domain identification methods is the conversion of time-based data to frequency-based data. This conversion, which is a batch and non-iterative process, involves a considerable amount of data conditioning not required for time-domain methods. However, once the frequency-domain data base is completed, the computational burden of the parameter nonlinear search is considerably reduced. Also, there are some important benefits of formulating the cost function in the frequency-domain. An overview of frequency-domain methods used by WG 18 members is presented. Author

N92-17159# Glasgow Univ. (Scotland). Dept. of Electronics and Electrical Engineering.
MODELLING ASPECTS AND ROBUSTNESS ISSUES IN ROTORCRAFT SYSTEM IDENTIFICATION
David J. Murray-Smith *In* AGARD, Rotorcraft System Identification Oct. 1991 9 p (For primary document see N92-17153 08-05)
Copyright Avail: NTIS HC/MF A12; Non-NATO Nationals requests available only from AGARD/Scientific Publications Executive

The concept of robustness is examined and discussed in the context of rotorcraft system identification and modeling. A classification of robustness issues is proposed involving experimental design aspects, identification techniques, model structure estimation, parameter estimation and the robustness of the complete mathematical model resulting from the application of identification processes. Associated tests of robustness are proposed and a set of special recommendations is presented for each of the aspects considered. Within these recommendations particular emphasis is placed on the need for a good user interface which fully exploits the use of computer graphics and for reliable tools for the assessment of model structure. The need for preliminary flight tests to characterize the dynamics of the system and thus guide the design of identification experiments is also emphasized. A further recommendation is that design criteria should be established for verification inputs. Author

N92-17160# McDonnell-Douglas Helicopter Co., Mesa, AZ.
ASSESSMENT OF ROTORCRAFT SYSTEM IDENTIFICATION AS APPLIED TO THE AH-64
Dev Banerjee and Jeff W. Harding *In* AGARD, Rotorcraft System Identification Oct. 1991 25 p (For primary document see N92-17153 08-05)
Copyright Avail: NTIS HC/MF A12; Non-NATO Nationals requests available only from AGARD/Scientific Publications Executive

Flight test data from the U.S. Army/McDonnell Douglas AH-64 Apache attack helicopter was provided to the AGARD FMP Working Group 18 (WG-18) on Rotorcraft System Identification. Results from the application of system identification techniques on the data by several members are compared. The data are processed by the WG members to assure consistency and remove identified measurement biases. Various time domain identification procedures ranging from linear regression to maximum likelihood are used to identify coupled six degrees of freedom rigid body models. Stability and control derivative estimates and model eigenvalues are compared. Diagonal terms in the models are consistently identified while coupling derivative estimates vary widely. Eigenvalues associated with the slower modes (phugoid and spiral) are not consistently identified due to the limited 12 second record length of the available data. Roll convergence and Dutch roll models are consistent between the models. All the models do a good job of predicting primary axis response, however, improved correlation is achieved by eliminating insensitive stability and control derivatives from the parameter sets. Author

N92-17161# Deutsche Forschungsanstalt fuer Luft- und Raumfahrt, Brunswick (Germany, F.R.). Inst. fuer Flugmechanik.
BO 105 IDENTIFICATION RESULTS
Juergen Kaletka *In* AGARD, Rotorcraft System Identification Oct. 1991 50 p (For primary document see N92-17153 08-05)
Copyright Avail: NTIS HC/MF A12; Non-NATO Nationals requests available only from AGARD/Scientific Publications Executive

BO 105 flight test data generated particularly for system identification purposes were provided to the AGARD Working Group WG-18 on Rotorcraft System Identification. The accomplishments are summarized of the WG for the data consistency analyses, and the identification and verification results for 6 degrees of freedom models. The individually applied approaches are described and representative results are presented. It is shown that the flight test data were appropriate for use of system identification. The discussion of the identification and verification results show that there are significant differences depending upon the applied identification technique. The identification is addressed of higher order models and some results are presented which were obtained for an extended model with rotor degrees of freedom. Author

N92-17162# Royal Aerospace Establishment, Bedford (England). Aerospace Div.
SA 330 PUMA IDENTIFICATION RESULTS
Gareth D. Padfield *In* AGARD, Rotorcraft System Identification Oct. 1991 38 p (For primary document see N92-17153 08-05)
Copyright Avail: NTIS HC/MF A12; Non-NATO Nationals requests available only from AGARD/Scientific Publications Executive

The SA 330 Puma test data provided by the RAE were analyzed with a variety of different identification techniques by six of the participating organizations in AGARD Flight Mechanics Panel Working Group 18. The results of this work are presented. A detailed study of the data kinematic consistency conducted by the RAE is included, highlighting some of the difficulties that can be encountered, even with high quality measurements, and ways of overcoming them. The results of the six degrees of freedom identification are discussed in terms of the conventional rigid body modes of motion. Author

N92-17163# McDonnell-Douglas Helicopter Co., Mesa, AZ.
INDUSTRY VIEW ON ROTORCRAFT SYSTEM IDENTIFICATION
Dev Banerjee and Jeff W. Harding *In* AGARD, Rotorcraft System Identification Oct. 1991 4 p (For primary document see N92-17153 08-05)
Copyright Avail: NTIS HC/MF A12; Non-NATO Nationals requests available only from AGARD/Scientific Publications Executive

An industry perspective on rotorcraft system identification is presented based on responses from eight major rotorcraft manufacturers to a questionnaire sent out by the AGARD FMP Working Group 18 on Rotorcraft System Identification. Several manufacturers are implementing system identification techniques for model validation and flight control law development. Concerns over costly data requirements and nonstandardized procedures are echoed. An example of the application of system identification for design support at McDonnell Douglas Helicopter Co. is discussed. Author

N92-17164# Royal Aerospace Establishment, Bedford (England). Aerospace Div.
APPLICATION AREAS FOR ROTORCRAFT SYSTEM IDENTIFICATION: SIMULATION MODEL VALIDATION
Gareth D. Padfield and Ronald W. DuVal (Advanced Rotorcraft Technology, Inc., Mountain View, CA.) *In* AGARD, Rotorcraft System Identification Oct. 1991 39 p (For primary document see N92-17153 08-05)
Copyright Avail: NTIS HC/MF A12; Non-NATO Nationals requests available only from AGARD/Scientific Publications Executive

The role of system identification in the validation of rotorcraft simulation models is examined in terms of the overall 'functional' fidelity and individual component 'physical' fidelity. Validation acceptance criteria are discussed in terms of modeling range and accuracy for the three fundamental flight mechanics problems - trim, stability, and response. Model development and upgrading are described as a natural part of validation, and the role that system identification can play in highlighting model deficiencies is discussed. An example from a six-degree-of-freedom analysis is presented to illustrate validation and the merits of model distortion analysis in identifying deficiencies. Results from a more detailed analysis of the SA 330 blade flapping dynamics are presented to illustrate physical validation. Author

N92-17165# Army Aviation Systems Command, Moffett Field, CA. Aeroflightdynamics Directorate.
SYSTEM IDENTIFICATION METHODS FOR HANDLING-QUALITIES EVALUATION
Mark B. Tischler *In* AGARD, Rotorcraft System Identification Oct. 1991 9 p (For primary document see N92-17153 08-05)
Copyright Avail: NTIS HC/MF A12; Non-NATO Nationals requests available only from AGARD/Scientific Publications Executive

System identification methods for rotorcraft handling-qualities studies are discussed in this paper. A key factor that is responsible for the successful application of system identification techniques in the handling-qualities community is the relative simplicity of the models which are desired for pilot-in-the-loop analyses as compared to the full 6 Degree Of Freedom (DOF) models required for most other applications. Generally, these analyses consider only the on-axis, single-input/single-output response of the pilot/vehicle system. The extracted vehicle model may be nonparametric, such as a frequency-response, or a low-order parametric model, such as a transfer function, or a simplified decoupled state-space representation. Both time- and frequency-domain methods have been widely used for these applications and are discussed in this paper. The requirements for flight testing, data analyses, and modeling for handling-qualities applications of system identification are contrasted with the requirements for extracting multi-input/multi-output state-space models for flight mechanics purposes. Typical handling qualities analysis results are illustrated using the WG 18 databases for the BO-105 and AH-64 helicopters. Author

N92-17166# Army Aviation Systems Command, Moffett Field, CA. Aeroflightdynamics Directorate.
SYSTEM IDENTIFICATION REQUIREMENTS FOR HIGH-BANDWIDTH ROTORCRAFT FLIGHT CONTROL SYSTEM DESIGN **c08**
Mark B. Tischler *In* AGARD, Rotorcraft System Identification Oct. 1991 12 p Previously announced in IAA as A90-45333 (For primary document see N92-17153 08-05)
Copyright Avail: NTIS HC/MF A12; Non-NATO Nationals requests available only from AGARD/Scientific Publications Executive

The application of system identification methods to high-bandwidth rotorcraft flight control system design is examined. Flight test and modeling requirements are illustrated using flight test data from a BO-105 hingeless rotor helicopter. The proposed approach involves the identification of nonparametric frequency-response models, followed by parametric (transfer function and state space) model identification. Results for the BO-105 show the need for including coupled body/rotor flapping and lead-lag dynamics in the identification model structure to allow the accurate prediction of control system bandwidth limitations. Lower-order models are useful for estimating nominal control system performance only when the flight data used for the identification are bandlimited to be consistent with the frequency range of applicability of the model. The flight test results presented in this paper are consistent with theoretical studies by previous researchers. Author

N92-17226*# National Aeronautics and Space Administration. Hugh L. Dryden Flight Research Facility, Edwards, CA.
FLIGHT VEHICLE THERMAL TESTING WITH INFRARED LAMPS
Roger A. Fields Washington Jan. 1992 31 p Presented at the Structural Testing Technology at High Temperature Conference, Dayton, OH, 4-6 Nov. 1991
(NASA-TM-4336; H-1779; NAS 1.15:4336) Avail: NTIS HC/MF A03 CSCL 01C

The verification and certification of new structural material concepts for advanced high speed flight vehicles relies greatly on thermal testing with infrared quartz lamps. The basic quartz heater system characteristics and design considerations are presented. Specific applications are illustrated with tests that were conducted for the X-15, the Space Shuttle, and YF-12 flight programs. Author

N92-17234# Aeronautical Research Labs., Melbourne (Australia).
MODIFICATION OF JINDIVIK AIR INTAKE DUCT WITH AN AUXILIARY INTAKE STATIC AERODYNAMIC TESTS
A. M. Abdel-Fattah Aug. 1991 37 p
(AD-A243002; ARL-PROP-TM-460; DODA-AR-006-600) Avail: NTIS HC/MF A03 CSCL 21/5

Results are presented for an R and D program to improve the take-off performance of the Jindivik target aircraft. The engine air intake duct of Jindivik is aerodynamically optimised for altitude and high subsonic cruise, and scope for its modification, for improved performance at take-off, was limited to the incorporation of an auxiliary intake system which is deployed only during take-off and is closed in flight. The auxiliary intake concept was explored experimentally with a 1/4 scale model of a Jindivik air intake duct, and involved both static testing and tests with forward speeds in the wind tunnel. This report covers the aerodynamic aspects of the static phase of the program, at which conditions substantial improvements in pressure recovery with acceptable levels of flow distortion at the engine face have been demonstrated for simple intake modifications. GRA

N92-17266# Aeronautical Research Labs., Melbourne (Australia).
WIND LOADS ON A MIRAGE III O AIRCRAFT MOUNTED ABOVE A GROUND PLANE
P. A. Hermsen Aug. 1991 21 p
(AD-A243004; ARL-FLIGHT-MECH-TM-434; DODA-AR-006-590)
Avail: NTIS HC/MF A03 CSCL 01/1

Measurements were made in ARL Salisbury's Low Speed Tunnel on a 1/72 scale model of a Mirage III O aircraft to determine steady wind loads when mounted above a ground plane. The six component data cover 360 deg in azimuth, and roll and pitch angles of -20, O, and +20 degs. GRA

N92-17300# Naval Postgraduate School, Monterey, CA.
A WING ROCK MODEL FOR THE F-14A AIRCRAFT M.S. Thesis
Steven R. Wright 1992 86 p
(AD-A243109) Avail: NTIS HC/MF A05 CSCL 01/3

An investigation of inertial coupling and its contribution to wing rock in the F-14A aircraft has been conducted. Wind tunnel data was used to obtain the stability parameters for angles of attack from zero to 25 degrees, after which linear and nonlinear analyses of the equations of motion were completed. The linearized analysis of the uncoupled longitudinal and lateral-directional equations was included to provide a baseline for comparison with the fully coupled, nonlinear equations. In both cases, the equations of motion were solved numerically and time history traces produced to illustrate aircraft response. Results indicate that a stable short period mode can feed damping energy into an unstable dutch roll mode via the coupling of the equations to produce a stable limit cycle very similar to those experienced in the aircraft. Numerous suggestions for follow-on research are presented. GRA

N92-17313# Messerschmitt-Boelkow-Blohm G.m.b.H., Munich (Germany, F.R.). Hubschrauber und Flugzeuge.
AERODYNAMIC DEVELOPMENT OF THE X-31 AIRCRAFT FOR THE HIGH ANGLE OF ATTACK REGION
Werner Kraus May 1991 38 p
(MBB-FE211-S-PUB-452; ETN-92-90620) Copyright Avail: NTIS HC/MF A03

The X-31 high agility airplane is designed to operate well at high angles of attack. The aircraft is designed to have natural aerodynamic stability about all three axes in the entire angle of attack range, except at small angles of attack, where the aircraft is unstable in pitch for performance reasons. In critical regions in which natural stability cannot be contained, the control power required to achieve stability is provided to the appropriate axis by artificial control, still leaving sufficient control for power maneuvers. The results of the wind tunnel development program are presented. Additional wind tunnel tests in a spin tunnel are presented. ESA

N92-17316*# Ohio State Univ., Columbus. ElectroScience Lab.
AUTOMATED COMPOSITE ELLIPSOID MODELLING FOR HIGH FREQUENCY GTD ANALYSIS
K. Y. Sze, R. G. Rojas, F. T. Klevenow, and J. T. Scheick Sep. 1991 188 p
(Grant NAG1-1058)
(NASA-CR-189853; NAS 1.26:189853; Rept-722792-2) Avail: NTIS HC/MF A09 CSCL 01C

The preliminary results of a scheme currently being developed to fit a composite ellipsoid to the fuselage of a helicopter in the vicinity of the antenna location are discussed under the assumption that the antenna is mounted on the fuselage. The parameters of the close-fit composite ellipsoid would then be utilized as inputs into NEWAIR3, a code programmed in FORTRAN 77 for high frequency Geometrical Theory of Diffraction (GTD) Analysis of the radiation of airborne antennas. Author

N92-17513# Northrop Corp., Hawthorne, CA. Aircraft Div.
FINITE ELEMENT ANALYSIS OF ASTOVL FIGHTER STRUCTURE Interim Report, 1 Oct. 1988 - 1 Oct. 1989
J. A. Hangen Dec. 1991 258 p
(Contract F33615-88-C-3205)
(AD-A243724; NOR-89-101; WL-TR-91-3104) Avail: NTIS HC/MF A12 CSCL 01/3

This report documents the static/dynamic and aeroelastic finite element model development and description used for the preliminary structural design and optimization of an Advanced Short Takeoff and Vertical Landing (ASTOVL) fighter structure. The model defined represents an Automated STructural Optimization System (ASTROS) compatible model initially developed from a NASTRAN finite element model. The generated data are for the purpose of enabling the repeat of the structural analysis and to independently analyze the structure in case of future structural or operational modifications to the aircraft. GRA

N92-17565# Aeronautical Research Labs., Melbourne (Australia).
GENERAL REQUIREMENTS AND TECHNIQUES FOR COMPONENT FATIGUE LIFE SUBSTANTIATION IN AUSTRALIAN SERVICE HELICOPTERS
K. F. Fraser Jun. 1991 54 p
(AD-A242881; ARL-PROP-R-187; DODA-AR-006-619) Avail: NTIS HC/MF A04 CSCL 20/11

An Australian Defense Force requirement has been defined to provide in-country capability to support component fatigue life substantiation in selected Australian fleet helicopters, with initial application to the S-70A-9 Black Hawk helicopter operated by the Australian Army. The implications of this requirement are examined, and the need to assess the severity of the spectrum of normal missions for the selected aircraft fleet is supported. Justification for a program to assess mission severity from measurements of flight regime recognition data and loads in selected components in a sample of fleet aircraft, is provided. A program to substantiate the fatigue lives of selected Black Hawk helicopter components, subject to significant in-service loads, is outlined. The general requirements of airborne and ground data systems required in support of the program are examined. GRA

N92-17843 ESDU International Ltd., London (England).
EXAMPLE OF STATISTICAL TECHNIQUES APPLIED TO CRUISE PERFORMANCE GUARANTEES (STUDENT'S t DISTRIBUTION)
Oct. 1991 5 p
(ESDU-91018; ISBN-0-85679-780-4; ISSN-0141-4054) Avail: ESDU

This data item illustrates certain aspects of statistical analysis introduced in ESDU 91017 in relation to cruise specific air range. Before issuing guarantees to a customer, flight tests were carried out around the guarantee point to verify the specific air range that could be claimed without a risk of triggering a penalty. Because the first sample of data obtained was small, it is analyzed using Student's t distribution but is found, at the chosen confidence level, to indicate an unacceptable performance. A further sample of values were therefore measured with a view to improving the prediction accuracy. Data from the two samples are first checked with the F Variance Ratio Test to establish that they may be coalesced. The samples are then combined and Student's t distribution applied again. The results are still unsatisfactory but the comment is made that one point is clearly outside the general dispersion of the data. The deviation from the pooled mean is noted but it is explained that if the result cannot be faulted on sound engineering grounds it must stand and the conclusions drawn must be accepted. ESDU

N92-17847 ESDU International Ltd., London (England).
VARIABILITY OF STANDARD AIRCRAFT PERFORMANCE PARAMETERS
Oct. 1991 8 p
(ESDU-91020; ISBN-0-85679-782-0; ISSN-0141-4054) Avail: ESDU

This data item presents data on the variability of civil aircraft and engine performance quantities drawn from a report of the ICAO Standing Committee on Performance, and also more recent information on the variability of turbo-fan engine performance quantities. These latter data are given as ranges of uncertainty and are converted to the ICAO form of a standard deviation using information from ESDU 91017. The variability data are then used to calculate the variability of takeoff climb gradient. The methods of ESDU 91017 are again used, this time to calculate the overall variability arising from the cumulative effects of the individual variabilities in drag, thrust, and weight. ESDU

06 AIRCRAFT INSTRUMENTATION

Includes cockpit and cabin display devices; and flight instruments.

For related information see also *19 Spacecraft Instrumentation* and *35 Instrumentation and Photography.*

N92-17128*# National Aeronautics and Space Administration. Hugh L. Dryden Flight Research Facility, Edwards, CA.
FAILURE DETECTION AND FAULT MANAGEMENT TECHNIQUES FOR FLUSH AIRDATA SENSING SYSTEMS
Stephen A. Whitmore, Timothy R. Moes, and Cornelius T. Leondes (Washington Univ., Seattle.) Washington Jan. 1992 22 p Presented at the Aerospace Sciences Meeting, Reno, NV, 6-9 Jan. 1992; sponsored by AIAA
(NASA-TM-4335; H-1780; NAS 1.15:4335) Avail: NTIS HC/MF A03 CSCL 01D

A high-angle-of-attack flush airdata sensing system was installed and flight tested on the F-18 High Alpha Research Vehicle at NASA-Dryden. This system uses a matrix of pressure orifices arranged in concentric circles on the nose of the vehicle to determine angles of attack, angles of sideslip, dynamic pressure, and static pressure as well as other airdata parameters. Results presented use an arrangement of 11 symmetrically distributed ports on the aircraft nose. Experience with this sensing system data indicates that the primary concern for real-time implementation is the detection and management of overall system and individual pressure sensor failures. The multiple port sensing system is more tolerant to small disturbances in the measured pressure data than conventional probe-based intrusive airdata systems. However, under adverse circumstances, large undetected failures in individual pressure ports can result in algorithm divergence and catastrophic failure of the entire system. How system and individual port failures may be detected using chi sq. analysis is shown. Once identified, the effects of failures are eliminated using weighted least squares. Author

N92-17221# Research Triangle Inst., Research Triangle Park, NC.
AGSSS: THE AIRBORNE GRAPHICS SOFTWARE SUPPORT SYSTEM; AN Ada/PHIGS-BASED DISPLAY EDITOR FOR THE RAPID DEVELOPMENT OF COCKPIT DISPLAY SOFTWARE SYSTEMS Final Report, Sep. 1987 - Sep. 1990
R. J. Montoya, Timothy L. Turner, Donna M. Jewell, James V. Aanstoos, and Ramasubramanian Suresh Sep. 1991 91 p
(Contract F33615-87-C-1531)
(AD-A243224; RTI/3966/00-01F; WL-TR-91-1042) Avail: NTIS HC/MF A05 CSCL 12/5

Over the past decade, the performance of digital graphics systems has increased several-fold. At the same time, the size of the hardware has been reduced and high performance airborne systems are now feasible. As a result, complex, three dimensional, pictorial, real time display formats can now be supported. Unfortunately, the increase in display complexity results in a significant increase in the software requirements. Additionally, dynamic displays, such as used in avionics, have a two part software problem. First, the display format and all its elements must be explicitly defined. Second, the connection must be established to the rest of the avionics. Overall, graphics software development is a truly time and labor intensive task. The goal of the AGSSS is to provide a graphics software development support environment. The AGSSS consists of four parts: the Graphics Editor for creating the format program, the Actions Editor for creating the driver software for the display dynamics, the Display Test Manager which allows the user to test the new software within the workstation, and the Display Program Integrator which creates the final software source modules tuned to the target system hardware. GRA

N92-17240# Army Engineer Waterways Experiment Station, Vicksburg, MS. Environmental Lab.
ANALYSIS OF SCENE CONDITIONS AT THE LIGHT HELICOPTER TARGET ACQUISITION SUBSYSTEM DEMONSTRATION/VALIDATION, YUMA PROVING GROUND, ARIZONA, SEPTEMBER 1990 Final Report
Bruce Sabol and Salvador Rivera, Jr. Oct. 1991 120 p
(AD-A243234; WES/TR/EL-91-15) Avail: NTIS HC/MF A06 CSCL 17/11

In support of the Light Helicopter Target Acquisition Subsystem (TAS) Demonstration/Validation conducted at Yuma Proving Grounds, Arizona, the US Army Engineer Waterways Experiment Station (WES) collected field measurements and imagery to characterize site and scene conditions. Meteorological, terrain, and target radiometric data were obtained and analyzed. Thermal and visible imagery were obtained within the field of regard during testing of the TAS. Images were processed to compute image metrics relevant to pre-detection image processing by the TAS. Image metrics included target-independent scene metrics, which measure the distribution of selected features over the entire image, and target-specific metrics, which measure specific target features and compute conspicuity of the target relative to the background. Analyses were performed to quantify temporal and spatial variations in metric values over the course of the test. GRA

N92-17989*# Massachusetts Inst. of Tech., Cambridge. Dept. of Aeronautics and Astronautics.
COCKPIT DISPLAY OF HAZARDOUS WEATHER INFORMATION
R. John Hansman, Jr. and Craig Wanke *In* NASA. Langley Research Center, Joint University Program for Air Transportation Research, 1990-1991 Dec. 1991 p 41-48 Previously announced as N90-20929 Previously announced in IAA as A89-25591 (For primary document see N92-17984 08-01)
(Contract NAG1-690; NGL-22-009-640; BARR-10-119)
Avail: NTIS HC/MF A09 CSCL 01C

N92-17993*# Ohio Univ., Athens.
ESTABLISHING AN EVOKED-POTENTIAL VISION-TRACKING SYSTEM
Trent A. Skidmore *In* NASA. Langley Research Center, Joint University Program for Air Transportation Research, 1990-1991 Dec. 1991 p 69-78 (For primary document see N92-17984 08-01)
(Grant NAG1-940)
Avail: NTIS HC/MF A09 CSCL 01D

07 AIRCRAFT PROPULSION AND POWER

Includes prime propulsion systems and systems components, e.g., gas turbine engines and compressors; and onboard auxilliary power plants for aircraft.

For related information see also *20 Spacecraft Propulsion and Power, 28 Propellants and Fuels,* and *44 Energy Production and Conversion.*

N92-17011# Deacon Research, Palo Alto, CA.
LASER BASED, NON-INTRUSIVE MEASUREMENT SYSTEM FOR ANALYSIS OF JET ENGINE FLOWS Final Technical Report, 8 Aug. 1990 - 8 Mar. 1991
A. OKeefe Oct. 1991 36 p
(Contract F33615-90-C-2077)
(AD-A242398; WL-TR-91-2108) Avail: NTIS HC/MF A03 CSCL 21/2

This document summarizes an effort to establish the feasibility of a technique which will allow the remote determination of the local flow velocity, temperature and density of selected species present in the combustion and exhaust flows of hydrocarbon fueled scram jet engine test facilities. We have developed a data acquisition system which is capable of high speed date collection (several kHZ) for time periods of many seconds before pausing

for data transfer. This program demonstrated a system prototype with a 16 millisecond capacity on a high speed combustor flow and demonstrated that the local flow speed, temperature, and density can be recovered from the data. This data was used to estimate the potential signal levels which might be attained on the test facilities and discuss how this approach might be configured and optimized on the quartz-walled test flow being developed there. GRA

N92-17061*# National Aeronautics and Space Administration. Lewis Research Center, Cleveland, OH.
SAFETY CONSIDERATIONS IN TESTING A FUEL-RICH AEROPROPULSION GAS GENERATOR
R. James Rollbuhler and David D. Hulligan (Sverdrup Technology, Inc., Brook Park, OH.) 1991 9 p Presented at the Combustion Fundamentals and Applications Meeting, Nashville, TN, 21-24 Apr. 1991; sponsored by the Combustion Inst.
(NASA-TM-105258; E-5976; NAS 1.15:105258) Avail: NTIS HC/MF A02 CSCL 21E

A catalyst containing reactor is being tested using a fuel-rich mixture of Jet A fuel and hot input air. The reactor product is a gaseous fuel that can be utilized in aeropropulsion gas turbine engines. Because the catalyst material is susceptible to damage from high temperature conditions, fuel-rich operating conditions are attained by introducing the fuel first into an inert gas stream in the reactor and then displacing the inert gas with reaction air. Once a desired fuel-to-air ratio is attained, only limited time is allowed for a catalyst induced reaction to occur; otherwise the inert gas is substituted for the air and the fuel flow is terminated. Because there presently is not a gas turbine combustor in which to burn the reactor product gas, the gas is combusted at the outlet of the test facility flare stack. This technique in operations has worked successfully in over 200 tests. Author

N92-17204# Wright Lab., Wright-Patterson AFB, OH.
PROCEEDINGS OF THE USAF STRUCTURAL INTEGRITY PROGRAM CONFERENCE Final Report, 11 - 13 Dec. 1990
Thomas D. Cooper and John W. Lincoln Aug. 1991 1064 p Conference held in San Antonio, TX, 11-13 Dec. 1990
(AF Proj. 2418)
(AD-A242943; WL-TR-91-2071) Avail: NTIS HC/MF A99 CSCL 21/5

The purpose of this 1990 Conference was to bring together technical personnel in DOD and the aerospace industry who are involved in the various technologies required to ensure the structural integrity of aircraft gas turbine engines, airframes, and other mechanical systems. It provided a forum to exchange ideas and share new information relating to the critical aspects of durability and damage tolerance technology for aircraft systems. GRA

N92-17546*# National Aeronautics and Space Administration. Lewis Research Center, Cleveland, OH.
EXPERIMENTS AND ANALYSIS CONCERNING THE USE OF EXTERNAL BURNING TO REDUCE AEROSPACE VEHICLE TRANSONIC DRAG Ph.D. Thesis - Maryland Univ., 1991
Charles J. Trefny Jan. 1992 294 p
(NASA-TM-105397; E-6789; NAS 1.15:105397) Avail: NTIS HC/MF A13 CSCL 21E

The external combustion of hydrogen to reduce transonic drag was investigated. A control volume analysis is developed and indicates that the specific impulse performance of external burning is competitive with other forms of airbreathing propulsion and depends on the fuel-air ratio, freestream Mach number, and the severity of the base drag. A method is presented for sizing fuel injectors for a desired fuel-air ratio in the unconfined stream. A two-dimensional Euler analysis is also presented which indicates that the total axial force generated by external burning depends on the total amount of energy input and is independent of the transverse and streamwise distribution of heat addition. Good agreement between the Euler and control volume analysis is demonstrated. Features of the inviscid external burning flowfield are discussed. Most notably, a strong compression forms at the sonic line within the burning stream which may induce separation of the plume and prevent realization of the full performance potential. An experimental program was conducted in a Mach 1.26 free-jet to demonstrate drag reduction on a simple expansion ramp geometry, and verify hydrogen-air stability limits at external burning conditions. Stable combustion appears feasible to Mach number of between 1.4 and 2 depending on the vehicle flight trajectory. Drag reduction is demonstrated on the expansion ramp at Mach 1.26; however, force levels showed little dependence on fuel pressure or altitude in contrast to control volume analysis predictions. Various facility interference mechanisms and scaling issues were studied and are discussed. Author

N92-17552# General Electric Co., Cincinnati, OH. Aircraft Engine Business Group.
QUALIFICATION TEST REPORT. FUEL PUMP TEST STAND 3C3965G05
J. E. Moss Oct. 1991 113 p
(Contract F33657-84-C-2011)
(AD-A242929; QTR-CDRL-29087) Avail: NTIS HC/MF A06 CSCL 13/11

The purpose of this report is to summarize the results of the qualification testing performed on the 3C3965G05 fuel pump test stand at Tinker Air Force Base. The 3C3965G05 fuel pump test stand was designed for the USAF by General Electric Aircraft Engines, Cincinnati, Ohio. It was designed to test the F101-GE-102, F110-GE-100, F108-CF-100, F118-GE-100, and F110-GE-129 fuel pumps and subassemblies. The objective of the testing program was to qualify the test stand for the F110-GE-129 main fuel pump. In so doing, the test stand was required to duplicate results obtained on the UUT manufacturer's test stand within tolerance limits established by ESO Design Engineering with concurrence from Evendale C and A Engineering. After test stand modification and prior to qualification demonstration, the stand was subjected to an engineering evaluation by the GE stand test engineer. GRA

N92-17642# Ballistic Research Labs., Aberdeen Proving Ground, MD.
ANALYSIS OF RAM ACCELERATION FOR HIGH VELOCITY APPLICATIONS Final Report, 15 Jul. 1990 - 15 Jul. 1991
David L. Kruczynski Aug. 1991 31 p
(DA Proj. 1L1-62618-AH-80)
(AD-A242338; BRL-TR-3257) Avail: NTIS HC/MF A03 CSCL 19/1

Ram acceleration is an emerging propulsion technology which appears capable of producing very high velocities with significant masses. Work at the University of Washington has demonstrated velocities in excess of 2.6 km/s in 38-mm caliber, while theory predicts that velocities in excess of 10 km/s may be obtainable. Following a brief introduction to the theory of ram acceleration, advantages and disadvantages of the technology for large caliber hypervelocity applications are examined. An empirical performance analysis of a scaled-up ram accelerator (120-mm) is presented and compared to a theoretical analysis of conventional solid propulsion. A theoretical and experimental program ongoing at the Ballistic Research Laboratory to explore scaling the technology to 120-mm is then described. GRA

N92-17644# RMA Aerospace, Inc., Mountain View, CA.
PRELIMINARY DEVELOPMENT OF A THREE-DIMENSIONAL NONLINEAR APPROXIMATION PROCEDURE FOR TURBOMACHINERY DESIGN OPTIMIZATION APPLICATIONS Final Report, Nov. 1985 - Feb. 1991
Stephen S. Stahara, Jasopin Lee, and John R. Spreiter 20 Aug. 1991 103 p
(Contract F33615-85-C-2591)
(AD-A243155; RMA-TMR-0101; WL-TR-91-2073) Avail: NTIS HC/MF A06 CSCL 01/1

A theoretical investigation was carried out involving the preliminary development of a novel three dimensional nonlinear approximation method capable of rapidly determining approximate solutions for highly nonlinear flows such as typically occur in turbomachinery applications. The ultimate goal of the study was

the preliminary demonstration of the accuracy and utility of such a method in the three dimensional turbomachinery design environment. The specific objectives of the present investigation were the theoretical development of the three-dimensional approximation procedure for highly sensitive, nonlinear flows involving: multiple shock waves; combination of the approximation method with a nonlinear three dimensional supercritical transonic flow solver; coupling of the combined approximation method and nonlinear flow solver with an optimization design procedure; and testing of the complete approximation/flow solver/optimization code on problems relevant to the turbomachinery design environment. GRA

N92-17729# Naval Postgraduate School, Monterey, CA.
AN ANALYSIS OF THE AIRCRAFT ENGINE COMPONENT IMPROVEMENT PROGRAM (CIP): A LIFE CYCLE COST APPROACH M.S. Thesis
Chris J. Borer Dec. 1990 125 p
(AD-A243346) Avail: NTIS HC/MF A06 CSCL 21/5

Increasing budgetary constraints have prompted actions to reduce the maintenance cost of current naval aircraft. This thesis examines the Aircraft Engine Component Improvement Program (CIP), its impact on these cost at the organizational and intermediate levels of maintenance, and savings from these improvements. The objectives of the research were to identify current life cycle cost (LCC) models used by the Navy and/or the other services to determine CIP benefits, to validate on-going LCC-oriented computer programs. This thesis is organized into areas covering CIP objectives and considerations, system effectiveness, reliability, LCC and related data and models, aircraft data used for LCC, CIP/LCC computer models, return on investment (ROI) analysis program of the F-14A TF30-P-414A engine improvement, conclusions and recommendations. Based on the ROI analysis and ECIFR reports, the engine improvement program has been cost effective. GRA

N92-17855# National Aerospace Lab., Tokyo (Japan). Aeroengine Div.
HYDROGEN FUELED SUBSONIC-RAM-COMBUSTOR MODEL TESTS FOR AN AIR-TURBO-RAM ENGINE
Takashi Tamaru, Kazuo Shimodaira, Takashi Saitoh, Hideshi Yamada, and Shouji Horiuchi Apr. 1990 14 p Previously announced in IAA as A90-12529
(NAL-TR-1064T; ISSN-0389-4014; JTN-92-80298) Avail: NTIS HC/MF A03

This paper deals with a basic study to facilitate the design of the hydrogen fueled subsonic ram combustor. Three types of flame holders, scaled 1/10 of the estimated actual size, were investigated to evaluate the performance for severe inlet conditions of hypersonic flight. Unidimensional analysis with total pressure at the exit and the static pressure on the duct wall gave the gas temperature and the Mach number of the combustion gas. Analysis of sampled gas at the exit gave radial profiles of equivalence ratio, combustion efficiency and so on. These results indicate that the fuel rich zone over stoichiometry must be avoided for the fuel preparation to attain the best combustion efficiencies near the stoichiometric mixture condition which is required for the engine in hypersonic flight. Author (NASDA)

08 AIRCRAFT STABILITY AND CONTROL

Includes aircraft handling qualities; piloting; flight controls; and autopilots.

For related information see also *05 Aircraft Design, Testing and Performance.*

N92-17019*# Georgia Inst. of Tech., Atlanta.
PERIODIC TRIM SOLUTIONS WITH HP-VERSION FINITE ELEMENTS IN TIME Final Report, Jul. 1989 - Dec. 1991
Dec. 1991 15 p
(Grant NAG1-1027)
(NASA-CR-189778; NAS 1.26:189778) Avail: NTIS HC/MF A03 CSCL 01C

Finite Element in Time has been proven to be a powerful alternative solving strategy for the rotor craft trim problem. Additionally, Finite Element Method in Time has been developed in various versions like time-marching framework, Galerkin framework, Rayleigh-Ritz framework, and mixed formulation. Recently, this method was applied to the rotorcraft trim problem to obtain linearized solutions. The rotorcraft trim problem consists of trying to find a period solution for period-coefficient, differential equations subject to side constraints where certain force and momentum balance equations are forced to be equal to zero. There are free (or trim) parameters that are chosen to meet these side constraints. This project aims at expanding the application, in terms of the rotorcraft trim problem, from a linearized solution to nonlinear solution. Author

N92-17096# Air Force Inst. of Tech., Wright-Patterson AFB, OH. School of Engineering.
DEVELOPMENT OF HIGH ANGLE OF ATTACK CONTROL LAWS FOR AN UNSTABLE, NON-MINIMUM PHASE AIRCRAFT USING VARIATIONS OF THE QUANTITATIVE FEEDBACK TECHNIQUE M.S. Thesis
Mark A. McClure Dec. 1991 244 p
(AD-A243698; AFIT/GE/ENG/91D-39) Avail: NTIS HC/MF A11 CSCL 01/4

This thesis discusses the application of variations of the quantitative feedback technique to a control problem with unstable, nonminimum phase plants. The X-29A research aircraft is used as the basis for developing a set of representative linearized aircraft dynamics models, which are modified to allow for the use of differential canard control inputs for enhanced maneuverability at extreme angles of attack. A specialized design approach is presented to develop frequency dependent weighting matrices, and the shortcomings of traditional methods are discussed. Four independent longitudinal compensators are developed by first designing loop transmission functions. Discussion is provided that addresses the limitations imposed on the designer by the numerous right half plane poles and zeros of the effective plants. The optimal blending method is applied in one case to achieve a marginally stable system for a virtually impossible problem. Prefilters are designed and their effects on closed-loop time responses are discussed. The singular-G method is used to improve the achievable stability characteristics of a multi-input multi-output lateral-directional controller. The optimal blending method is then applied to develop an optimal loop transmission function. Finally, the required steps for completing the MIMO design are presented to aid future research efforts. GRA

N92-17243# United Technologies Research Center, East Hartford, CT.
LOADING AND VIBRATION REDUCTION THROUGH ACTIVE AERODYNAMIC CONTROL Quarterly Progress Report, 13 Jun. - 13 Sep. 1991
John C. Simonich 13 Sep. 1991 14 p
(Contract N00014-91-C-0148)
(AD-A242321; UTRC-R91-970089-01) Avail: NTIS HC/MF A03 CSCL 20/11

The objective of this work is to provide active aerodynamic control concepts for reducing unsteady lift and moments in propulsor blades. These unsteady forces are responsible for vibration and noise during an encounter with an incident gust. This effort represents an extension of a recent UTRC breakthrough in which active aerodynamic control was used to reduce noise generated during a two dimensional (2-D) blade-gust interaction. The associated reductions in unsteady blade surface pressures responsible for the noise reduction will be evaluated under the current program. Also, an analytical effort will generate a computer code for predicting surface pressures created by an actively controlled flap system and will estimate the required flap motion to cancel the unsteady lift. This work will extend the UTRC 2-D expertise in active aerodynamic control to a three dimensional

(3-D) capability. This will be done by analytically investigating the effect of a swept gust interacting with an actively controlled, segmented flap to control the bending moment as well as the lift. Also, an exploratory experimental study on the effects of a swept gust encountering a 2-D non-segmented flap will be performed. In summary, this study will provide the Navy with concepts for active aerodynamic control for reducing unsteady blade loads responsible for structural vibration. GRA

N92-17442# Naval Postgraduate School, Monterey, CA.
MULTIPLE INPUT SLIDING MODE CONTROL FOR AUTONOMOUS DIVING AND STEERING OF UNDERWATER VEHICLES M.S. Thesis
Todd D. Hawkinson Dec. 1990 214 p
(AD-A241935) Avail: NTIS HC/MF A10 CSCL 13/10

Design and analysis of multiple input autopilots using sliding modes in order to achieve accurate horizontal and vertical plane control of an autonomous underwater vehicle over a wide variation of speeds is presented. The simulated vehicle is equipped with two (fore and aft) sets of dive planes and two sets of rudders. In addition, two vertical and two horizontal thrusters are provided for control during low speed or hovering operations. The entire range of vehicle speeds from zero speed hovering to full speed ahead is divided into regions depending on control efficiency. Thrusters are used for low speed hovering, control surfaces for transition speeds. Linear quadratic regulator optimal control techniques coupled with the robustness properties of sliding mode control are utilized to provide the necessary control reversal which occurs during the transition from cruise to hover mode. Constant disturbances arising from underwater currents are effectively compensated resulting in accurate path keeping. As a consequence of the multiple input control methodology developed in this work, it is shown that both path and orientation accuracy can be achieved in moderate cross current environments. Finally, reduced order observers are designed in order to account for sensor absence or malfunction. GRA

N92-17748# Air Force Inst. of Tech., Wright-Patterson AFB, OH. School of Engineering.
A ROBUST DIGITAL FLIGHT CONTROL SYSTEM FOR AN UNFANNED RESEARCH VEHICLE USING DISCRETE QUANTITATIVE FEEDBACK THEORY M.S. Thesis
Donald J. Lacey, Jr. Dec. 1991 190 p
(AD-A243638; AFIT/GE/ENG/91D-33) Avail: NTIS HC/MF A09 CSCL 01/3

This thesis describes application of digital multiple-input multiple-output (MIMO) Quantitative Feedback Theory (QFT) technique to the design of a three axis rate controller for the Lambda Unmanned Research Vehicle. The resulting robust controller performs well throughout the flight envelope without gain scheduling. It results from research done at the Air Force Institute of Technology. The Lambda URV was designed by the Control Systems Development Branch of the Wright Laboratory at Wright-Patterson AFB, OH for flight testing aircraft control hardware and software. The flight control system is built using a small perturbation linear model developed from flight test data. The actuators, also modelled from aircraft test data, are second order in roll and pitch and first order in yaw. Nineteen separate plants are used to represent the flight envelope of the aircraft resulting from variations in speed, altitude, center of gravity location, and weight. The sample rate is 50 Hertz. The pitch channel is decoupled from the lateral-directional resulting in a single-input single-output (SISO) system for the pitch channel and a two-by-two MIMO system for the lateral-directional channel. The design employs the Nichols Chart and is accomplished in the w'-domain. GRA

N92-17917# National Aerospace Lab., Tokyo (Japan). Flight Research Div.
IDENTIFICATION OF THE STABILITY AND CONTROL DERIVATIVES OF A DLC-FLAP SYSTEM FOR VSRA
Yukichi Tsukano, Takatsugu Ono, and Kazutoshi Ishikawa 3 Apr. 1991 18 p In JAPANESE; ENGLISH summary
(NAL-TR-1116; ISSN-0389-4010) Avail: NTIS HC/MF A03

Flight tests were conducted using the Variable Stability and Response Airplane (VSRA) in order to identify the stability and control derivatives for a Direct Lift Control (DLC) flap system. The frequency response method was selected, with a pure sinusoidal input being applied to the DLC flaps. Response from a linear system model consisting of the stability and control derivatives was compared with other flight test response data to determine general inputs. The resulting derivatives were subsequently verified. Additionally, the control capability of the DLC flaps was estimated by the control derivatives and compared with wind tunnel test data. Author

N92-17166# Army Aviation Systems Command, Moffett Field, CA. Aeroflightdynamics Directorate.
SYSTEM IDENTIFICATION REQUIREMENTS FOR HIGH-BANDWIDTH ROTORCRAFT FLIGHT CONTROL SYSTEM DESIGN
Mark B. Tischler *In* AGARD, Rotorcraft System Identification Oct. 1991 12 p Previously announced in IAA as A90-45333
(For primary document see N92-17153 08-05)
Copyright Avail: NTIS HC/MF A12; Non-NATO Nationals requests available only from AGARD/Scientific Publications Executive

N92-17997*# Princeton Univ., NJ. Dept. of Mechanical and Aerospace Engineering.
STOCHASTIC ROBUSTNESS
C. Marrison *In* NASA. Langley Research Center, Joint University Program for Air Transportation Research, 1990-1991 Dec. 1991 p 127-140 (For primary document see N92-17984 08-01)
Avail: NTIS HC/MF A09 CSCL 01C

N92-18000*# Princeton Univ., NJ. Dept. of Mechanical and Aerospace Engineering.
INTELLIGENT FAILURE-TOLERANT CONTROL
Robert F. Stengel *In* NASA. Langley Research Center, Joint University Program for Air Transportation Research, 1990-1991 Dec. 1991 p 163-172 Previously announced in IAA as A91-43931 (For primary document see N92-17984 08-01)
(Contract NGL-31-001-252; DAAL03-89-K-0092)
Avail: NTIS HC/MF A09 CSCL 01C

09 RESEARCH AND SUPPORT FACILITIES (AIR)

Includes airports, hangars and runways; aircraft repair and overhaul facilities; wind tunnels; shock tubes; and aircraft engine test stands.

For related information see also *14 Ground Support Systems and Facilities (Space).*

N92-17059*# National Aeronautics and Space Administration. Lewis Research Center, Cleveland, OH.
ADVANCED NOZZLE AND ENGINE COMPONENTS TEST FACILITY
Luis R. Beltran, Richard L. DelRoso, and Ruben DelRosario Jan. 1992 21 p
(NASA-TM-103684; E-5902; NAS 1.15:103684) Avail: NTIS HC/MF A03 CSCL 14B

A test facility for conducting scaled advanced nozzle and engine component research is described. The CE-22 test facility, located in the Engine Research Building of the NASA Lewis Research Center, contains many systems for the economical testing of advanced scale-model nozzles and engine components. The combustion air and altitude exhaust systems are described. Combustion air can be supplied to a model up to 40 psig for primary air flow, and 40, 125, and 450 psig for secondary air flow. Altitude exhaust can be simulated up to 48,000 ft, or the exhaust can be atmospheric. Descriptions of the multiaxis thrust stand, a color schlieren flow visualization system used for qualitative flow analysis, a labyrinth flow measurement system, a data acquisition system, and auxiliary systems are discussed. Model recommended

design information and temperature and pressure instrumentation recommendations are included. Author

N92-17097# Air Force Inst. of Tech., Wright-Patterson AFB, OH.
IMPLEMENTATION OF AN OBJECT-ORIENTED FLIGHT SIMULATOR D.C. ELECTRICAL SYSTEM ON A HYPERCUBE ARCHITECTURE M.S. Thesis
Guy R. Booth Dec. 1991 148 p
(AD-A243700; AFIT/GCE/ENS/91D-01) Avail: NTIS HC/MF A07 CSCL 05/9

The Software Engineering Institute developed an object-oriented paradigm for flight simulators based on the concept of mapping the behavior of physical objects from an aircraft into an object-oriented software architecture. This mapping is a semi-formal method that maps objects to a hierarchy that has three logical layers: objects, systems, and executives. The paradigm was developed with the idea of implementing the derived simulation design on a parallel or distributed computer architecture, but no explicity design features are provided for implementing the design on a parallel computer. This research addresses the issue of determining what extensions (if any) are required to implement a parallel version of the D.C. Electrical System Simulation (DESS) that the SEI developed as an example on using their paradigm. The parallel DESS design is implemented and tested using Ada on an Intel iPSC/2 Hypercube. An analysis of the performance of the simulation is presented, and some conclusions are made about implementing a parallel design based on the SEI Object-Oriented Paradigm for Flight Simulators. Author (GRA)

N92-17260# Army Engineer Waterways Experiment Station, Vicksburg, MS. Geotechnical Lab.
ALTERNATE/MODIFIED BINDERS FOR ASPHALT AIRFIELD PAVEMENTS Final Report, Jan. 1986 - Sep. 1988
Gary L. Anderton Nov. 1990 162 p
(Contracts MIPR-N-86-28; MIPR-N-87-5; MIPR-N-88-15; AF Proj. 2673)
(AD-A242829; AFESC/ESL-TR-89-40) Avail: NTIS HC/MF A08 CSCL 13/3

This report documents a laboratory research effort to determine the effects of asphalt modifiers and alternate binders on asphalt airfield pavements. The modified binders were tested to determine their potential for reducing pavement deformation distresses, improving rheological properties, reducing asphalt contents, and improving the asphalt pavement's heat resistant capabilities under jet engine blasts. An intensive literature search was performed during the first year of the study to gather all of the available information on the modifiers currently available. This information was used to choose 14 test materials, which were tested in the laboratory during the second year of the study. Data resulting from these tests were used to choose the five most promising test materials, which were evaluated further in the third and final year of the study by more detailed laboratory tests. All laboratory mix specimens were made with the same aggregate gradations and under as near identical conditions as possible. An AC-20 grade of asphalt cement was chosen as the base asphalt for all modified asphalt blends. Asphalt mix testing consisted of indirect tensile, resilient modulus and unconfined creep-rebound tests. Asphalt binder test included kinematic viscosity, Brookfield viscosity, penetration, resiliency, and chromatography. GRA

N92-17287# Army Engineer Waterways Experiment Station, Vicksburg, MS. Geotechnical Lab.
LARGE CENTRIFUGE: A CRITICAL ARMY CAPABILITY FOR THE FUTURE Final Report
Richard H. Ledbetter, Steven A. Hughes, Marian P. Rollings, Charles R. Lee, and Paul A. Gilbert May 1991 117 p
(AD-A243287; WES/MP/GL-91-12) Avail: NTIS HC/MF A06 CSCL 14/2

The purpose of this report is to present an overview of potential applications of a centrifuge for the purposes of research and development. The technical areas discussed are (1) coastal regions, (2) environmental protection, (3) geotechnical, (4) hydraulic, (5) structural, and (6) cold regions. This report discusses those areas where centrifuge testing would greatly benefit research objectives, particularly in cases where prototype data are very expensive if not impossible to acquire. Centrifuge testing offers cost effective technology to address military and civil problem areas such as: (1) Nuclear crater scaling laws; (2) Blast effects on bunkers, lined tunnels, and pile foundations from conventional munitions; (3) Stability of foundations and earth structures; (4) Vulnerability of mechanical and electrical systems to conventional threats; (5) Ground water pollution problems; (6) Projectile penetration into earth materials; (7) Pavement structure performance and materials investigations; (8) Explosive damage to underwater structures; (9) All earth works (earth and rockfill dams, levees, appurtenant structures, retaining walls, foundations, tunnels, and excavations); and (10) Frozen soil, water, and ice. GRA

N92-17297# Aeronautical Research Labs., Melbourne (Australia).
STAGNATION AND DYNAMIC PRESSURE LIMITS FOR THE S1 WIND TUNNEL
David A. Pierens Sep. 1991 30 p
(AD-A242989; ARL-FLIGHT-MECH-TM-435; DODA-AR-006-591)
Avail: NTIS HC/MF A03 CSCL 14/2

The ARL-Salisbury S1 wind tunnel is a closed circuit, continuous, variable pressure wind tunnel, with a Mach number range of 0.35 to 1.0 and 1.4 to 2.8. The nominal dimensions of the tunnel's working section are 380 mm x 380 mm. Although the tunnel has been in operation for many years, no attempt has been made to experimentally investigate and establish the operational pressure limits. Thus, it is not uncommon for new experimenters to request running conditions which the tunnel cannot achieve. This is further complicated by new temperature and current limits being adopted in 1985 after a main monitor failure. Therefore, a series of wind tunnel test runs were carried out in order to provide a reliable guide, outlining the running conditions which the S1 wind tunnel can safely achieve. This report outlines the absolute maximum pressure and the recommended maximum operating pressures for the S1 wind tunnel. The pressure limits calculated in this report were obtained from actual wind tunnel data records. GRA

N92-17756# National Aerospace Lab., Tokyo (Japan). Advanced Aircraft Research Group.
IMPROVEMENT OF DATA PROCESSING SYSTEM FOR GUST WIND TUNNEL DATA ACQUISITION PART: SYSTEM CONVERSION FROM OFF-LINE TO ON-LINE PROCESSING [TOPPU FUDO DETA SHORI SOCHI (DETA SHUSHUBU) NO KAISHU: KEISOKU SHISUTEMU NO ONRAINKA]
Toshimi Fujita, Akihito Iwasaki, and Hirotoshi Fujieda Jul. 1989 60 p In JAPANESE
(NAL-TM-611; ISSN-0452-2982; JTN-92-80247) Avail: NTIS HC/MF A04

The data acquisition part of the gust wind tunnel in National Aerospace Laboratory has been changed from the OKITAC-4300 off-line processing system to the ECLIPSE MV/7800 XP on-line processing system. At the same time, the primary data processing system has been updated with quick look display to conduct wind tunnel tests more efficiently. The new system enables the great improvement of wind tunnel test efficiency and data productivity as follows: (1) human operation errors in the wind tunnel test can be prevented; (2) repetition of the same test caused by inferior or abnormal data can be avoided; and (3) turn around time from data acquisition until data processing can be cut down from a day or hourly time scale to minutes or seconds. Author (NASDA)

N92-17967# Allied-Signal Aerospace Co., Kansas City, MO.
CLEAN ROOM WIPING LIQUIDS
W. B. Harding Dec. 1991 9 p
(Contract DE-AC04-76DP-00613)
(DE92-004793; KCP-613-4529) Avail: NTIS HC/MF A02

A water-based liquid containing isopropyl alcohol, ammonium hydroxide, and surfactants was developed to replace

1,1,2-trichlorotrifluoroethane for the dampening of clean room wiping cloths used to wipe clean benches, clean room equipment, and latex finger cots and gloves. DOE

12 ASTRONAUTICS (GENERAL)

For extraterrestrial exploration see *91 Lunar and Planetary Exploration.*

No abstracts in this category.

13 ASTRODYNAMICS

Includes powered and free-flight trajectories; and orbital and launching dynamics.

N92-17192# Naval Postgraduate School, Monterey, CA.
THE EFFECT OF TITANIUM INCLUSIONS ON HY-80 GMA WELD DEPOSITS M.S. Thesis
Dana J. Ellis Dec. 1990 78 p
(AD-A243408) Avail: NTIS HC/MF A05 CSCL 11/6

HY-80 steels are used in submarine and ship construction and it has been found that small additions of titanium to this steel during manufacture markedly improve the fracture toughness of the heat affected zone (HAZ) of Gas-Metal-Arc-Welding (GMAW) deposits made from this steel. This has been ascribed to prior austenite grain boundary pinning by titanium nitride inclusions. In the present work the weld metals, HAZ and parent metals of GMAW welds made on HY-80 steels have been studied by optical, scanning electron and transmission electron microscopy. These studies have shown that the Ti treated HY-80 has overall a lower level of non-metallic inclusions than untreated HY-80, which could certainly be responsible for improved toughness. Unfortunately, it proved difficult to correlate titanium nitride inclusions with prior-austenite-grain-boundary pinning. GRA

N92-17325# Charles River Analytics, Inc., Cambridge, MA.
AN ALTERNATIVE CONCEPT FOR AEROASSISTED ORBIT TRANSFERS
Paul G. Gonsalves, Scott M. Allen, and Alper K. Caglayan Aug. 1991 77 p
(Contract DAAH01-91-C-R061)
(AD-A243409; TR-R90222) Avail: NTIS HC/MF A05 CSCL 17/7

The primary results of this study are identification of possible new applications of aeroassisted orbital transfers to LightSat/TacSats and the feasibility evaluation of an on-line neural network implementation of an atmospheric trajectory/guidance scheme. AOT scenarios involve 2 distinct categories: on-orbit multiple-pass 'soft maneuvers' and the single-pass deep penetration into the atmosphere 'hard maneuver'. Due to propellant limitations, the soft maneuver is very conducive to address LightSac/TacSat orbital transfer requirements. Possible soft-maneuvers include inclination and perigee location stationkeeping. Hard maneuvers are more conducive to situations requiring a greater amount of maneuverability, e.g., emergency relocation of a satellite. Associated with each class of AOTs are a set of relevant vehicle and mission requirement parameters, which help define the overall feasibility of AOTs. Chief among these parameters is perigee altitude. Perigee altitude determines the amount of atmospheric density available to perform on-orbit maneuvers. Since density decreases exponentially with altitude, AOTs are not feasible beyond a perigee altitude of 200 km. Lower perigee altitudes come with detrimental effects of shorter orbital lifetimes. This can be ameliorated via more eccentric orbits. Among the relevant vehicle parameters are satellite mass, reference area, and aerodynamic efficiency. Trade-off studies were performed for two specific soft maneuvers: plane change and rotation of line of apsides. GRA

N92-17730# Air Force Inst. of Tech., Wright-Patterson AFB, OH.
CONTROL ALGORITHMS FOR AEROBRAKING IN THE MARTIAN ATMOSPHERE Ph.D. Thesis
Buford W. Shipley, Jr. Dec. 1991 187 p
(AD-A243349; AFIT/CI/CIA-91-021D) Avail: NTIS HC/MF A09 CSCL 22/1

The Analytic Predictor Corrector (APC) and Energy Controller (EC) atmospheric guidance concepts have been adapted to control an interplanetary vehicle aerobraking in the Martian atmosphere. Modifications are made to the APC to improve its robustness to density variations. These modifications include adaptation of a new exit phase algorithm, an adaptive transition velocity to initiate the exit phase, refinement of the reference dynamic pressure calculation and two hybrid density estimation techniques. The modified controller with the hybrid density estimation technique is called the Mars Hybrid Predictor Corrector (MHPC), while the modified controller with a polynomial density estimator is called the Mars Predictor Corrector (MPC). A Lyapunov Steepest Descent Controller (LSDC) is adapted to control the vehicle. The LSDC lacked robustness, so a Lyapunov tracking exit phase algorithm is developed to guide the vehicle along a reference trajectory. The equilibrium glide entry phase is employed for the first part of the trajectory. This algorithm, when using the hybrid density estimation technique to define the reference path, is called te Lyapunov Hybrid Tracking Controller (LHTC). With the polynomial density estimator used to define the reference trajectory, the algorithm is called the Lyapunov Tracking Controller (LTC). The four new controllers are tested usig a six degree of freedom computer simulation to evaluate their robustness. GRA

N92-17732# Air Force Inst. of Tech., Wright-Patterson AFB, OH.
AN ANALYTIC METHOD OF PROPAGATING A COVARIANCE MATRIX TO A MANEUVER CONDITION FOR LINEAR COVARIANCE ANALYSIS DURING RENDEZVOUS M.S. Thesis
Jesse R. Gossner Jun. 1991 96 p
(AD-A243354; AFIT/CI/CIA-91-084) Avail: NTIS HC/MF A05 CSCL 22/1

This study develops a method for analytically propagating a covariance matrix to a maneuver condition to be used in linear covariance analysis for planning the rendezvous phase of a space mission. With the generalized formulation of a condition transition matrix, an analytic method of propagating an augmented covariance matrix to any scalar terminal maneuver condition is presented. The twenty-six dimensional augmented covariance matrix used in this study includes navigation state errors, state dispersions, and time errors for both the chaser and target craft. The method is first analytically developed. The vehicles are brought to the desired rendezvous condition by linearizing motion at the maneuver condition point and allowing the time of flight to vary slightly. The analytic propagation technique is then validate by comparison to a stochastic Monte Carlo simulation for the case of several elevation angle conditions which might be used to trigger an initial rendezvous intercept burn. The validity of linearizing the motion about the terminal point is substantiated with the same situation. GRA

N92-17854# National Aerospace Lab., Tokyo (Japan). Control Systems Div.
SYSTEMATIC COMPUTATION ALGORITHM TO OBTAIN OSCULATING ORBIT ELEMENTS FROM POSITION AND VELOCITY VECTORS [ICHI SOKUDO BEKUTORU KARA SESSHOKU KIDO YOSO WO MOTOMERU HOKATSUTEKINA KEISAN ARUGORIZUMU]
Toru Shiho Sep. 1989 32 p In JAPANESE
(NAL-TM-614; ISSN-0452-2982; JTN-92-80250) Avail: NTIS HC/MF A03

This report describes calculation algorithm and its systematic procedure of osculating orbital elements computation in each case of ecliptic, parabolic, hyperbolic and rectilinear orbit. The osculating orbital elements are those elements applied only in specific timing

when position vector and velocity vector of a spacecraft or celestial body, such as comet, are input in the calculation.
Author (NASDA)

14 GROUND SUPPORT SYSTEMS AND FACILITIES (SPACE)

Includes launch complexes, research and production facilities; ground support equipment, e.g., mobile transporters; and simulators.

For related information see also *09 Research and Support Facilities (Air).*

N92-17591# Los Alamos National Lab., NM.
A DISTRIBUTED DESIGN FOR MONITORING, LOGGING, AND REPLAYING DEVICE READINGS AT LAMPF
M. Burns 1991 4 p Presented at the International Conference on Accelerator and Large Experimental Physics Control Systems, Tsukuba (Japan), 11-15 Nov. 1991
(Contract W-7405-eng-36)
(DE92-003860; LA-UR-91-3539; CONF-911116-10) Avail: NTIS HC/MF A01

As control of the Los Alamos Meson Physics linear accelerator and Proton Storage Ring moves to a more distributed system, it has been necessary to redesign the software which monitors, logs, and replays device readings throughout the facility. The new design allows devices to be monitored and their readings logged locally on a network of computers. Control of the monitoring and logging process is available throughout the network from user interfaces which communicate via remote procedure calls with server processes running on each node which monitors and records device readings. Similarly, the logged data can be replayed from anywhere on the network. Two major requirements influencing the final design were the need to reduce the load on the CPU of the control machines, and the need for much faster replay of the logged device readings. DOE

N92-17741# General Accounting Office, Washington, DC.
ROCKET TESTS IN MISSISSIPPI TO BE HEAVILY RESTRICTED
Feb. 1992 20 p
(GAO/NSIAD-92-86; B-247007) Avail: NTIS HC/MF A03

Groups representing people living near the Stennis Space Center have contested NASA's decision to test the Advanced Solid Rocket Motor (ASRM) in Mississippi because of their concerns about potential environmental consequences. They are concerned that NASA's computer modeling of ASRM tests cannot accurately predict these environmental effects and that environmental data on testing in Utah is not relevant for predicting environmental damage in Mississippi. They contend that Mississippi weather, with its high relative humidity and frequent rainfall, increases the possibility that exhaust pollutants will create acid rain and aluminum oxide fallout on the land surrounding the test site. Additionally, ASRM testing restrictions at the Stennis Space Center and environmental problems at other NASA facilities are discussed.
Author

15 LAUNCH VEHICLES AND SPACE VEHICLES

Includes boosters; operating problems of launch/space vehicle systems; and reusable vehicles.

For related information see also *20 Spacecraft Propulsion and Power.*

N92-17527# Messerschmitt-Boelkow-Blohm G.m.b.H., Munich (Germany, F.R.). Design Assurance Dept.
INTEGRATION OF RAMS ACTIVITIES DURING THE DEVELOPMENT PHASE OF ARIANE 5-COMPONENTS (EXAMPLE: VULCAIN THRUST CHAMBER)
Claudia Lex 1991 5 p Presented at the ESA Symposium on Space Product Assurance for Europe in the 1990s, Noordwijk, Netherlands, 15-19 Apr. 1991
(MBB-UK-0144-91-PUB; ETN-92-90605) Avail: NTIS HC/MF A01

The policy and methodology applied for management of Reliability, Availability, Maintainability and Safety (RAMS) information within the Vulcain thrust chamber development process are discussed. The performance of the above activities is defined by dedicated RAMS plan for Ariane propulsion projects, which meets the requirements of the relevant management specifications for RAMS established for Ariane projects. ESA

16 SPACE TRANSPORTATION

Includes passenger and cargo space transportation, e.g., shuttle operations; and space rescue techniques.

For related information see also *03 Air Transportation and Safety* and *18 Spacecraft Design, Testing and Performance.* For space suits see *54 Man/System Technology and Life Support.*

N92-16973*# National Aeronautics and Space Administration. Lyndon B. Johnson Space Center, Houston, TX.
STS-41 SPACE SHUTTLE MISSION REPORT
David W. Camp, D. M. Germany, and Leonard S. Nicholson Nov. 1990 26 p
(NASA-TM-105479; NAS 1.15:105479; NSTS-08194) Avail: NTIS HC/MF A03 CSCL 22B

The STS-41 Space Shuttle Program Mission Report contains a summary of the vehicle subsystem activities on this thirty-sixth flight of the Space Shuttle and the eleventh flight of the Orbiter vehicle, Discovery (OV-103). In addition to the Discovery vehicle, the flight vehicle consisted of an External Tank (ET) (designated as ET-39/LWT-32), three Space Shuttle main engines (SSME's) (serial numbers 2011, 2031, and 2107), and two Solid Rocket Boosters (SRB's), designated as BI-040. The primary objective of the STS-41 mission was to successfully deploy the Ulysses/inertial upper stage (IUS)/payload assist module (PAM-S) spacecraft. The secondary objectives were to perform all operations necessary to support the requirements of the Shuttle Backscatter Ultraviolet (SSBUV) Spectrometer, Solid Surface Combustion Experiment (SSCE), Space Life Sciences Training Program Chromosome and Plant Cell Division in Space (CHROMEX), Voice Command System (VCS), Physiological Systems Experiment (PSE), Radiation Monitoring Experiment - 3 (RME-3), Investigations into Polymer Membrane Processing (IPMP), Air Force Maui Optical Calibration Test (AMOS), and Intelsat Solar Array Coupon (ISAC) payloads. The sequence of events for this mission is shown in tabular form. Summarized are the significant problems that occurred in the Orbiter subsystems during the mission. The official problem tracking list is presented. In addition, each Orbiter problem is cited in the subsystem discussion. Author

N92-16974*# National Aeronautics and Space Administration. Lyndon B. Johnson Space Center, Houston, TX.
STS-36 SPACE SHUTTLE MISSION REPORT
Joseph E. Mechelay, D. M. Germany, and Leonard S. Nicholson Apr. 1990 22 p
(NASA-TM-105477; NAS 1.15:105477; NSTS-08354) Avail: NTIS HC/MF A03 CSCL 22B

The STS-36 Space Shuttle Program Mission Report contains a summary of the vehicle subsystem activities on this thirty-fourth flight of the Space Shuttle and the sixth flight of the OV-104 Orbiter vehicle, Atlantis. In addition to the Atlantis vehicle, the flight vehicle consisted of an External Tank (ET) (designated as ET-33/LWT-26), three Space Shuttle main engines (SSME's) (serial numbers 2019, 2030, and 2029), and two Solid Rocket Boosters (SRB's) (designated as BI-036). The STS-36 mission was a classified Department of Defense mission, and as such, the classified portions of the mission are not discussed. The unclassified sequence of events for this mission is shown in tabular

form. Summarized are the significant problems that occurred in the Orbiter subsystems during the mission. The official problem tracking list is presented. In addition, each of the Orbiter problems is cited in the subsystem discussion. Author

N92-16975*# National Aeronautics and Space Administration. Lyndon B. Johnson Space Center, Houston, TX.
STS-35 SPACE SHUTTLE MISSION REPORT
David W. Camp, D. M. Germany, and Leonard S. Nicholson Jan. 1991 27 p
(NASA-TM-105476; NAS 1.15:105476; NSTS-08302) Avail: NTIS HC/MF A03 CSCL 22B

The STS-35 Space Shuttle Program Mission Report contains a summary of the vehicle subsystem activities during this thirty-eighth flight of the Space Shuttle and the tenth flight of the Orbiter vehicle Columbia (OV-102). In addition to the Columbia vehicle, the flight vehicle consisted of an External Tank (ET) (designated as ET-35/LWT-28), three Space Shuttle main engines (SSME's) (serial numbers 2024, 2012, and 2028 in positions 1, 2, and 3, respectively), and two Solid Rocket Boosters (SRB's) designated as BI-038. The primary objectives of this flight were to successfully perform the planned operations of the Ultraviolet Astronomy (Astro-1) payload and the Broad-Band X-Ray Telescope (BBXRT) payload in a 190-nmi. circular orbit which had an inclination of 28.45 degrees. The sequence of events for this mission is shown in tablular form. Summarized are the significant problems that occurred in the Orbiter subsystems during the mission. The official problem tracking list is presented. In addition, each Orbiter subsystem problem is cited in the applicable subsystem discussion. Author

N92-17167*# Rockwell International Corp., Downey, CA. Space Transportation Systems Div.
RESULTS OF THE SPACE SHUTTLE VEHICLE ASCENT AIR DATA SYSTEM PROBE CALIBRATION TEST USING A 0.07-SCALE EXTERNAL TANK FOREBODY MODEL (68T) IN THE AEDC 16-FOOT TRANSONIC WIND TUNNEL (IA-310), VOLUME 1
J. G. R. Collette Nov. 1991 642 p Prepared in cooperation with Chrysler Corp., New Orleans, LA
(Contract NAS9-17840)
(NASA-CR-167696; NAS 1.26:167696; DMS-DR-2547-Vol-1)
Avail: NTIS HC/MF A99 CSCL 22B

A recalibration of the Space Shuttle Vehicle Ascent Air Data System probe was conducted in the Arnold Engineering Development Center (AEDC) transonic wind tunnel. The purpose was to improve on the accuracy of the previous calibration in order to reduce the existing uncertainties in the system. A probe tip attached to a 0.07-scale External Tank Forebody model was tested at angles of attack of -8 to +4 degrees and sideslip angles of -4 to +4 degrees. High precision instrumentation was used to acquire pressure data at discrete Mach numbers ranging from 0.6 to 1.55. Pressure coefficient uncertainties were estimated at less than 0.0020. Data is given in graphical and tabular form. Author

N92-17214*# Rockwell International Corp., Downey, CA. Space Transportation Systems Div.
RESULTS OF THE SPACE SHUTTLE VEHICLE ASCENT AIR DATA SYSTEM PROBE CALIBRATION TEST USING A 0.07-SCALE EXTERNAL TANK FOREBODY MODEL (68T) IN THE AEDC 16-FOOT TRANSONIC WIND TUNNEL (IA-310), VOLUME 2
J. G. R. Collette Nov. 1991 685 p Prepared in cooperation with Chrysler Corp., New Orleans, LA
(Contract NAS9-17840)
(NASA-CR-167697; NAS 1.26:167697; DMS-DR-2547-Vol-2)
Avail: NTIS HC/MF A99 CSCL 22B

A recalibration of the Space Shuttle Vehicle Ascent Air Data System probe was conducted in the Arnold Engineering and Development Center (AEDC) transonic wind tunnel. The purpose was to improve on the accuracy of the previous calibration in order to reduce the existing uncertainties in the system. A probe tip attached to a 0.07-scale External Tank Forebody model was tested at angles of attack of -8 to +4 degrees and sideslip angles of -4 to +4 degrees. High precision instrumentation was used to acquire pressure data at discrete Mach numbers ranging from 0.6 to 1.55. Pressure coefficient uncertainties were estimated at less than 0.0020. Additional information is given in tabular form. Author

N92-17335*# National Aeronautics and Space Administration. Langley Research Center, Hampton, VA.
LONG DURATION EXPOSURE FACILITY SOLAR ILLUMINATION DATA PACKAGE
William M. Berrios and Thomas Sampair (Lockheed Corp., Hampton, VA.) [1990] 168 p
(NASA-CR-189873; NAS 1.26:189873) Avail: NTIS HC/MF A08 CSCL 22B

A post flight solar illumination data package was created by the LDEF thermal analysis data group in support of the LDEF science office data group. The data presented was prepared with the Thermal Radiation Analysis System (TRASYS) program. Ground tracking data was used to calculate daily orbital beta angles for the calculation of resultant fluxes. This data package will be useful in calculation of solar illumination fluent for a variety of beta angle orbital conditions encountered during the LDEF mission. Author

N92-17342# Messerschmitt-Boelkow-Blohm G.m.b.H., Munich (Germany, F.R.). Design Assurance Dept.
PRODUCT ASSURANCE AND SAFETY IMPLEMENTATION IN SPACE SHUTTLE PAYLOADS: AN INDUSTRIAL PERSPECTIVE
Ian Jenkins 1991 7 p Presented at the ESA Symposium on Space Product Assurance for Europe in the 1990s, Noordwijk, Netherlands, 15-19 Apr. 1991
(MBB-UK-0143-91-PUB; ETN-92-90604) Avail: NTIS HC/MF A02

Experiences and observations gained in the Product Assurance (PA) and safety field in processing Space Shuttle payloads, are presented. These experiences and observations are called upon in plotting a direction for future European manned space programs. Experience in the management of a safety assurance program in a commercial environment is considered. An overview of PA and safety aspects in externally furnished equipment is presented. Experiences and trends within the Space Shuttle payload reviews are discussed. ESA

N92-17364*# National Aeronautics and Space Administration. Lyndon B. Johnson Space Center, Houston, TX.
STS-31 SPACE SHUTTLE MISSION REPORT
David W. Camp, D. M. Germany, and Leonard S. Nicholson May 1990 24 p
(NASA-TM-105475; NAS 1.15:105475; NSTS-08207) Avail: NTIS HC/MF A03 CSCL 22B

The STS-31 Space Shuttle Program Mission Report contains a summary of the vehicle subsystem activities on this thirty-fifth flight of the Space Shuttle and the tenth flight of the Orbiter Vehicle Discovery (OV-103). In addition to the Discovery vehicle, the flight vehicle consisted of an External Tank (ET) (designated as ET-34/LWT-27), three Space Shuttle main engines (SSME's) (serial numbers 2011, 2031, and 2107), and two Solid Rocket Booster (SRB) (designated as BI-037). The primary objective of the mission was to place the Hubble Space Telescope (HST) into a 330 nmi. circular orbit having an inclination of 28.45 degrees. The secondary objectives were to perform all operations necessary to support the requirements of the Protein Crystal Growth (PCG), Investigations into Polymer Membrane Processing (IPMP), Radiation Monitoring Equipment (RME), Ascent Particle Monitor (APM), IMAX Cargo Bay Camera (ICBC), Air Force Maui Optical Site Calibration Test (AMOS), IMAX Crew Compartment Camera, and Ion Arc payloads. In addition, 12 development test objectives (DTO's) and 10 detailed supplementary objectives (DSO's) were assigned to the flight. The sequence of events for this mission is shown. The significant problems that occurred in the Space Shuttle Orbiter subsystems during the mission are summarized, and the official problem tracking list is presented. In addition, each of the

Space Shuttle Orbiter problems is cited in the subsystem discussion. Author

N92-17534*# National Aeronautics and Space Administration. Lyndon B. Johnson Space Center, Houston, TX.
STS-38 SPACE SHUTTLE MISSION REPORT
David W. Camp, D. M. Germany, and Leonard S. Nicholson Jan. 1991 19 p
(NASA-TM-105478; NAS 1.15:105478; NSTS-08308) Avail: NTIS HC/MF A03 CSCL 22B

The STS-38 Space Shuttle Program Mission Report contains a summary of the vehicle subsystem activities on this thirty-seventh flight of the Space Shuttle and the seventh flight of the Orbiter vehicle Atlantis (OV-104). In addition to the Atlantis vehicle, the flight vehicle consisted of an External Tank (ET) (designated as ET-40/LWT-33), three Space Shuttle main engines (SSME's) (serial numbers 2019, 2022, 2027), and two Solid Rocket Boosters (SRB's), designated as BI-039. The STS-38 mission was a classified Department of Defense mission, and as much, the classified portions of the mission are not presented in this report. The sequence of events for this mission is shown. The significant problems that occurred in the Space Shuttle Orbiter subsystem during the mission are summarized and the official problem tracking list is presented. In addition, each Space Shuttle Orbiter problem is cited in the subsystem discussion. Author

N92-17104*# National Aeronautics and Space Administration, Washington, DC.
ADVANCED SPACE TRANSPORTATION SYSTEMS
Robert J. Davies *In its* Beyond the Baseline 1991: Proceedings of the Space Station Evolution Symposium. Volume 1: Space Station Freedom, Part 1 Sep. 1991 p 99-119 (For primary document see N92-17098 08-18)
Avail: NTIS HC/MF A15 CSCL 22B

17 SPACE COMM., SPACECRAFT COMM., COMMAND & TRACKING

Includes telemetry; space communications networks; astronavigation and guidance; and radio blackout.

For related information see also *04 Aircraft Communications and Navigation* and *32 Communications and Radar.*

N92-17075# Scripps Institution of Oceanography, La Jolla, CA. Satellite Oceanography Center.
DEVELOPMENT OF REAL-TIME IMAGE AND IN SITU DATA ANALYSIS AT SEA Final Report
16 Oct. 1991 11 p
(Contract N00014-90-J-1024)
(AD-A243682) Avail: NTIS HC/MF A03 CSCL 08/3

This project provided partial support for equipment upgrades of the Scripps Satellite Oceanography Center (SSOC). At the time this award was made, SSOC was using antiquated (circa 1976) computer technology to capture, archive, process, and distribute satellite data, both in near-real time and retrospectively, in support of U.S. west coast oceanographic studies. I am pleased to report that the funds provided by the Office of Naval Research through this grant, in combination with other funds, have been used to completely modernize SSOC. Because the main intent of the ONR funding was to provide for needed equipment upgrades, this final report emphasizes hardware and network infrastructure upgrades made possible by ONR funds. GRA

18 SPACECRAFT DESIGN, TESTING AND PERFORMANCE

Includes satellites; space platforms; space stations; spacecraft systems and components such as thermal and environmental controls; and attitude controls.

For life support systems see *54 Man/System Technology and Life Support.* For related information see also *05 Aircraft Design, Testing and Performance, 39 Structural Mechanics,* and *16 Space Transportation.*

N92-17045*# DYNACS Engineering Co., Inc., Palm Harbor, FL.
MODES OF INTERCONNECTED LATTICE TRUSSES USING CONTINUUM MODELS, PART 1 Interim Report
A. V. Balakrishnan Dec. 1991 49 p
(Contract NAS1-19158)
(NASA-CR-189568; NAS 1.26:189568) Avail: NTIS HC/MF A03 CSCL 22B

This represents a continuing systematic attempt to explore the use of continuum models--in contrast to the Finite Element Models currently universally in use--to develop feedback control laws for stability enhancement of structures, particularly large structures, for deployment in space. We shall show that for the control objective, continuum models do offer unique advantages. It must be admitted of course that developing continuum models for arbitrary structures is no easy task. In this paper we take advantage of the special nature of current Large Space Structures--typified by the NASA-LaRC Evolutionary Model which will be our main concern--which consists of interconnected orthogonal lattice trusses each with identical bays. Using an equivalent one-dimensional Timoshenko beam model, we develop an almost complete continuum model for the evolutionary structure. We do this in stages, beginning only with the main bus as flexible and then going on to make all the appendages also flexible-except for the antenna structure. Based on these models we proceed to develop formulas for mode frequencies and shapes. These are shown to be the roots of the determinant of a matrix of small dimension compared with mode calculations using Finite Element Models, even though the matrix involves transcendental functions. The formulas allow us to study asymptotic properties of the modes and how they evolve as we increase the number of bodies which are treated as flexible. The asymptotics, in fact, become simpler. Author

N92-17098*# National Aeronautics and Space Administration, Washington, DC.
BEYOND THE BASELINE 1991: PROCEEDINGS OF THE SPACE STATION EVOLUTION SYMPOSIUM. VOLUME 1: SPACE STATION FREEDOM, PART 1
Sep. 1991 336 p Symposium held in League City, TX, 6-8 Aug. 1991
(NASA-CP-10083-Vol-1-Pt-1; S-653-Vol-1-Pt-1; NAS 1.55:10083-Vol-1-Pt-1) Avail: NTIS HC/MF A15 CSCL 22B

Personnel responsible for Advanced Systems Studies and Advanced Development within the Space Station Freedom Program reported on the results of their work to date. The results of SSF Advanced Studies provide a road map for the evolution of Freedom in terms of user requirements, utilization and operations concepts, and growth options for distributed systems. Regarding these specific systems, special attention is given to: highlighting changes made during restructuring; description of growth paths thru the follow-on and evolution phases; identification of minimum impact provisions to allow flexibility in the baseline; and identification of enhancing and enabling technologies. Products of these tasks include: engineering fidelity demonstrations and evaluations of advanced technology; detailed requirements, performance specifications, and design accommodations for insertion of advanced technology. For individual titles, see N92-17099 through N92-17112.

N92-17099*# National Aeronautics and Space Administration, Washington, DC.
SPACE STATION FREEDOM STATUS

John Cox *In its* Beyond the Baseline 1991: Proceedings of the Space Station Evolution Symposium. Volume 1: Space Station Freedom, Part 1 Sep. 1991 p 1-19 (For primary document see N92-17098 08-18)
Avail: NTIS HC/MF A15 CSCL 22B

Several graphs are presented which illustrate the restructuring activities of the Space Station Freedom. The restructed SSF program meets the objectives including cost guidelines. The solution adopted best features from alternative concepts. The SSF program allows significantly greater utilization opportunities than other programs. It was decided that pre-integration simplifies on-orbit assembly planning and operations. The SSF permanently manned configuration is shown. E.R.

N92-17100*# European Space Agency, Paris (France).
COLUMBUS PROGRAMME (CURRENT STATUS)
In NASA, Washington, Beyond the Baseline 1991: Proceedings of the Space Station Evolution Symposium. Volume 1: Space Station Freedom, Part 1 Sep. 1991 p 21-37 (For primary document see N92-17098 08-18)
Avail: NTIS HC/MF A15 CSCL 22B

A description is presented for the Columbus Program. The Columbus program comprises a space segment, a ground segment, and operations preparation program, and a utilization preparation program. The space segment consist of three elements: an Attached Pressurized Module (APM); a Man Tended Free Flyer (MTFF); and a Polar platform (PPF). The ground segment is a program shared with other European programs such as Hermes, for communications, services, training and tracking facilities. The Operations preparation program focuses on preparing the ground segment for readiness for the launch of the space segment elements. And the Utilization preparation program includes definition of candidate payload facilities, initial payload selection and precursor flights (Eureca, Spacelab). Author

N92-17101*# National Space Development Agency, Tokyo (Japan).
STATUS OF JAPANESE EXPERIMENT MODULE (JEM) ACTIVITIES
In NASA, Washington, Beyond the Baseline 1991: Proceedings of the Space Station Evolution Symposium. Volume 1: Space Station Freedom, Part 1 Sep. 1991 p 39-57 (For primary document see N92-17098 08-18)
Avail: NTIS HC/MF A15 CSCL 22B

The current status of the JEM activities are presented in graphic form. The JEM spacecraft configuration is presented. The JEM configuration consist of the Pressurized Module, the Exposed Facility, the Experiment Logistics Module which consist of a pressurized section and an exposed section; and the Remote Manipulator System. The master schedule of the space station is given. Also the development tests of the structure and mechanism, the electrical power system, the data management system, the thermal control system, the environment control system, the experiment support system, and the remote manipulator system are listed. E.R.

N92-17102*# Canadian Space Agency, Ottawa (Ontario). Mobile Servicing System.
CANADIAN SPACE STATION PROGRAM
K. H. Doetsch *In* NASA, Washington, Beyond the Basline 1991: Proceedings of the Space Station Evolution Symposium. Volume 1: Space Station Freedom, Part 1 Sep. 1991 p 59-80 (For primary document see N92-17098 08-18)
Avail: NTIS HC/MF A15 CSCL 22B

Information on the Canadian Space Station Program is given in viewgraph form. Topics covered include the Mobile Servicing Center (MSC), Space Station Freedom assembly milestones, the MB-3 launch configuration, a new workstation configuration, strategic technology development, the User Development Program, the Space Station Program budget, and Canada's future space activities. Author

N92-17103*# National Aeronautics and Space Administration. Lyndon B. Johnson Space Center, Houston, TX.
SEI: AN UPDATE
Lewis L. Peach, Jr. *In* NASA, Washington, Beyond the Baseline 1991: Proceedings of the Space Station Evolution Symposium. Volume 1: Space Station Freedom, Part 1 Sep. 1991 p 81-98 (For primary document see N92-17098 08-18)
Avail: NTIS HC/MF A15 CSCL 22B

An update on the Space Exploration Initiative (SEI) is given in viewgraph form. Topics covered include the key prerequisites of human exploration, project planning, Mars and lunar explorations, supporting technologies, near-term strategies for SEI, human support elements, and Space Station Freedom SEI accommodations. Author

N92-17104*# National Aeronautics and Space Administration, Washington, DC.
ADVANCED SPACE TRANSPORTATION SYSTEMS c16
Robert J. Davies *In its* Beyond the Baseline 1991: Proceedings of the Space Station Evolution Symposium. Volume 1: Space Station Freedom, Part 1 Sep. 1991 p 99-119 (For primary document see N92-17098 08-18)
Avail: NTIS HC/MF A15 CSCL 22B

Information is given in viewgraph form relative to the advanced space transportation systems of the Space Station Freedom. Topics covered include heavy lift launch vehicle needs, requirements, and options; future launch vehicle concepts; modifications to the external tank; the Cargo Transfer Vehicle concept; lunar transportation options, Mars transportation options; the Assured Crew Return Vehicle (ACRV) baseline concept; Space Exploration Initiative (SEI) nodes options; and committee recommendations. Author

N92-17105*# National Aeronautics and Space Administration, Washington, DC.
SPACE STATION FREEDOM EVOLUTION SYMPOSIUM
Richard H. Ott *In its* Beyond the Baseline 1991: Proceedings of the Space Station Evolution Symposium. Volume 1: Space Station Freedom, Part 1 Sep. 1991 p 121-155 (For primary document see N92-17098 08-18)
Avail: NTIS HC/MF A15 CSCL 22B

Information on the Space Station Freedom Evolution Symposium is given in viewgraph form. Topics covered include industry development needs and the Office of Commercial Programs strategy, the three-phase program to develop commercial space, Centers for the Commercial Development of Space (CCDS), key provisions of the Joint Endeavor agreement, current commercial flight experiment requirements, the CCDS•expendable launch vehicle program, the Commercial Experiment Transporter (COMET) program, commercial launch dates, payload sponsors, the commercial roles of the Space Station Freedom, and a listing of the Office of Commercial Programs Space Station Freedom payloads. Author

N92-17106*# National Aeronautics and Space Administration, Washington, DC.
TECHNOLOGY DEVELOPMENT ON EVOLUTIONARY SPACE STATION
Judith H. Ambrus *In its* Beyond the Baseline 1991: Proceedings of the Space Station Evolution Symposium. Volume 1: Space Station Freedom, Part 1 Sep. 1991 p 157-178 (For primary document see N92-17098 08-18)
Avail: NTIS HC/MF A15 CSCL 22B

The topics covered are presented in view graph form and include a space research and technology (R&T) mission statement and a NASA action plan. With respect to an integrated technology plan for the civil space program, the following topics are also covered: (1) an R&T strategy; (2) a NASA technology maturation strategy; (3) an Office of Space Flight (OSF) technology requirements evaluation; (4) an external technology perspectives summary; (5) a work breakdown structure; (6) critical user requirements/ strategic plan element categorization; (7) technology flight experiments; (8)

proposed station paylods by thrust; and (9) an integrated traffic model K.S.

N92-17107*# National Aeronautics and Space Administration, Washington, DC.
SPACE STATION FREEDOM SCIENCE UTILIZATION: 2000 AND BEYOND
In its Beyond the Baseline 1991: Proceedings of the Space Station Evolution Symposium. Volume 1: Space Station Freedom, Part 1 Sep. 1991 p 179-201 (For primary document see N92-17098 08-18)
Avail: NTIS HC/MF A15 CSCL 22B

The Office of Space Science and Applications (OSSA) Goals are: (1) to advance scientific knowledge of the Earth, the Solar System, and the Universe; (2) to understand the effects of the space environment on biological and physical processes; and (3) to expand the human presence beyond the Earth into the Solar System. The topics covered are presented in view graph form and include the following: (1) a strategic plan; (2) evolving U.S. space science capabilities; (3) life science goals; (4) OSSA Space Station Payload Traffic Model May 1991; and (5) microgravity science and applications goals. K.S.

N92-17108*# National Aeronautics and Space Administration. Langley Research Center, Hampton, VA.
A HISTORICAL PERSPECTIVE ON SPACE STATION
W. Ray Hook *In* NASA, Washington, Beyond the Baseline 1991: Proceedings of the Space Station Evolution Symposium. Volume 1: Space Station Freedom, Part 1 Sep. 1991 p 203-23 (For primary document see N92-17098 08-18)
Avail: NTIS HC/MF A15 CSCL 22B

The historical development of space stations is presented through a series of various spacecraft configurations including: (1) Salut 6; (2) Skylab; (3) the Space Operations Center (SOC); (4) the Manned Science and Applications Space Platform; (5) Space Station Freedom; and (4) the Mir Space Station. K.S.

N92-17109*# National Aeronautics and Space Administration, Washington, DC.
ADVANCED STUDIES PROGRAM OVERVIEW
Peter R. Ahlf *In its* Beyond the Baseline 1991: Proceedings of the Space Station Evolution Symposium. Volume 1: Space Station Freedom, Part 1 Sep. 1991 p 237-253 (For primary document see N92-17098 08-18)
Avail: NTIS HC/MF A15 CSCL 22B

The topics covered are presented in view graph form and include the following: (1) Space Station Engineering; (2) level 1 engineering organization; (3) advanced studies program organization; (4) NASA Center support areas; (5) work breakdown; (6) Space Station Freedom (SSF) Program Phases; (7) distributed systems evolution; (8) Space Shuttle ET mating analogy to on-orbit tank mating; (9) reference growth concept; (10) technology assessment process; (11) SSF technology priorities; (12) accomplishments; and (13) near term direction. K.S.

N92-17110*# National Aeronautics and Space Administration, Washington, DC.
SPACE STATION FREEDOM ENGINEERING PROTOTYPE DEVELOPMENT
Alan Fernquist *In its* Beyond the Baseline 1991: Proceedings of the Space Station Evolution Symposium. Volume 1: Space Station Freedom, Part 1 Sep. 1991 p 255-292 (For primary document see N92-17098 08-18)
Avail: NTIS HC/MF A15 CSCL 22B

The content of the Advance Development Program and subsequent Engineering Prototype Development activity has been guided by a series of focused studies. These studies started with the report of the Advance Development Task Force. An outline of issues relating to Automation, Data Systems, and Telerobotics was projected for the Space Station. Subsequent studies built upon and reaffirmed a focus on development and prototyping of Automation Technology for subsystem monitoring and problem diagnosis, Data System growth to accommodate more sophisticated automation, and use of Telerobotics technology to assist in the reduction ot required ExtraVehicular Activity (EVA) and IntraVehicular Activity (IVA) task time. Author

N92-17111*# National Aeronautics and Space Administration, Washington, DC.
SPACE STATION FREEDOM PROGRAM. COMMERCIAL INFRASTRUCTURE AND TECHNOLOGY UTILIZATION
Kevin Barquinero *In its* Beyond the Baseline 1991: Proceedings of the Space Station Evolution Symposium. Volume 1: Space Station Freedom, Part 1 Sep. 1991 p 293-307 (For primary document see N92-17098 08-18)
Avail: NTIS HC/MF A15 CSCL 22B

The following topics are presented in viewgraph form: (1) the participation of the 'commercial infrastructure' in the evolution of Space Station Freedom (SSF); and (2) the commercial utilization of SSF in terms of developed technologies. Additionally, a comparison between the development of Aviation and Space flight is presented in terms of events occurring on a timeline. D.R.D.

N92-17112*# National Aeronautics and Space Administration. Langley Research Center, Hampton, VA.
EVOLUTION DESIGN REQUIREMENTS AND DESIGN STRATEGY
Donald W. Monell *In* NASA, Washington, Beyond the Baseline 1991: Proceedings of the Space Station Evolution Symposium. Volume 1: Space Station Freedom, Part 1 Sep. 1991 p 309-34 (For primary document see N92-17098 08-18)
Avail: NTIS HC/MF A15 CSCL 22B

Evolution of Space Station Freedom is justified for reasons which vary from more effectively utilizing the manned base to providing a means for incorporating new technologies as they become available. Increasing or, more importantly, balancing the resources that are provided to the users is very critical to effectively utilizing the station. At permanently manned phases of the program, there will be four crew members that will be supporting and monitoring three laboratories. Accepted user mission databases have shown a demand for more crew, power, and volume than is provided by the baseline. As the work done in space by NASA continues to expand, the station will take a more active role in the missions. New functionalities for its operation and support of other missions will be required. One important driver for growth, particularly in the area of structures, is the inability of the baseline configuration to store all the Orbital Replacement Units (ORU) spares that will be required on orbit. New technologies drive growth by providing a means of streamlining operations and possibly reducing the demand on ExtraVehicular Activity (EVA). They will also ensure that the station does not become plagued with obsolete equipment. Author

N92-17200*# Texas Univ., Austin. Dept. of Mechanical Engineering.
HYPERVELOCITY IMPACT SIMULATION FOR MICROMETEORITE AND DEBRIS SHIELD DESIGN Final Report
Eric P. Fahrenthold 27 Jan. 1992 81 p
(Grant NAG9-444)
(NASA-CR-189807; NAS 1.26:189807) Avail: NTIS HC/MF A05 CSCL 22B

A new capability has been developed for direct computer simulation of hypervelocity impacts on multi-plate orbital debris shields, for combinations of low shield thickness and wide shield spacing which place extreme demands on conventional Eulerian analysis techniques. The modeling methodology represents a novel approach to debris cloud dynamics simulation, a problem of long term interest in the design of space structures. Software implementation of the modeling methodology provides a new design tool for engineering analysis of proposed orbital debris protection systems. Author

N92-17215*# Boeing Co., Seattle, WA. Defense and Space Group.
ATOMIC OXYGEN FLUX AND FLUENCE CALCULATION FOR LONG DURATION EXPOSURE FACILITY (LDEF)
Roger J. Bourassa and James R. Gillis 18 Jan. 1991 267 p
(Contract NAS1-18224)
(NASA-CR-187418; NAS 1.26:187418) Avail: NTIS HC/MF A12 CSCL 22B

The LDEF mission was to study the effects of the space environment on various materials over an extended period of time. One of the important factors for materials degradation in low earth orbit is the atomic oxygen fluxes and fluences experienced by the materials. These fluxes and fluences are a function of orbital parameters, solar and geomagnetic activity, and material surface orientation. Calculations of atomic oxygen fluences and fluxes for the LDEF mission are summarized. Included are descriptions of LDEF orbital parameters, solar and geomagnetic data, computer code FLUXAV, which was used to perform calculations of fluxes and fluences, along with a discussion of the calculated fluxes and fluences. Author

N92-17250# General Accounting Office, Washington, DC. National Security and International Affairs Div.
EARLY WARNING SATELLITES: FUNDING FOR FOLLOW-ON SYSTEM IS PREMATURE
Nov. 1991 8 p
(AD-A242836; GAO/NSIAD-92-39) Avail: NTIS HC/MF A02 CSCL 05/1

This report examined the Department of Defense's (DOD) plans to develop a follow-on system to the Defense Support Program (DSP), including budget implications. DSP is a strategic surveillance and warning satellite system with an infrared capability to detect ballistic missile launches (intercontinental and submarine launched). It provides near real-time detection information in support of DOD's tactical warning and attack assessment (TWAA) mission. Its primary users are (1) the North American Aerospace Defense Command, which is responsible for assessing potential attacks on North America; (2) the national command authorities, who are responsible for making retaliatory decisions; and (3) other major military commands, which participate in the decision making process and are responsible for strategic offensive forces. GRA

N92-17302# Air Force Inst. of Tech., Wright-Patterson AFB, OH.
AN AEROCAPTURE ATTITUDE CONTROL SYSTEMS INCORPORATING ROBUSTNESS AND VEHICLE PARAMETER IDENTIFICATION M.S. Thesis
James R. Bell 10 May 1991 197 p
(AD-A243360; AFIT/CI/CIA-91-074) Avail: NTIS HC/MF A09 CSCL 22/3

A candidate attitude control system design is presented for an aerocapture vehicle capable of a wide range of mass properties. The control system consists of three main elements: a robust control law based on the nonlinear sliding mode control techniques, a linear programming jet selection algorithm adaptable to changing mass properties, and a mass property identification algorithm based on an extended Kalman filter design. The mass property identification algorithm is capable of accurately estimating unknown and changing vehicle mass properties. The estimated mass properties are fed back to the control law and the jet selection algorithm, extending the range of mass properties for which the control system is robust. A principal contribution of this thesis is the integration of these main elements into a viable attitude control system. The control system is demonstrated for the Aeroassist Flight Experiment (AFE) vehicle via computer simulation. GRA

N92-17334*# National Aeronautics and Space Administration. Langley Research Center, Hampton, VA.
LONG DURATION EXPOSURE FACILITY POST-FLIGHT THERMAL ANALYSIS: ORBITAL/THERMAL ENVIRONMENT DATA PACKAGE
William M. Berrios [1990] 211 p
(Contract NAS1-18224)
(NASA-CR-189872; NAS 1.26:189872) Avail: NTIS HC/MF A10 CSCL 22B

A post flight mission thermal environment for the Long Duration Exposure Facility was created as part of the thermal analysis data reduction effort. The data included herein is the thermal parameter data used in the calculation of boundary temperatures. This boundary temperature data is to be released in the near future for use by the LDEF principal investigators in the final analysis of their particular experiment temperatures. Also included is the flight temperature data as recorded by the LDEF Thermal Measurements System (THERM) for the first 90 days of flight. Author

N92-17348*# National Aeronautics and Space Administration, Washington, DC.
BEYOND THE BASELINE 1991: PROCEEDINGS OF THE SPACE STATION EVOLUTION SYMPOSIUM. VOLUME 2: SPACE STATION FREEDOM, PART 2
Sep. 1991 464 p Symposium held in League City, TX, 6-8 Aug. 1991
(NASA-CP-10083-Vol-2-Pt-2; S-653-Vol-2-Pt-2; NAS 1.55:10083-Vol-2-Pt-2) Avail: NTIS HC/MF A20 CSCL 22B

Individual presentations delivered at the Space Station Evolution Symposium in League City, Texas, on August 6, 7, and 8, 1991 are given in viewgraph form. Personnel responsible for Advanced Systems Studies and Advanced Development within the Space Station Freedom Program reported on the results of their work to date. Special attention is given to highlighting changes made during restructuring; a description of the growth paths through the follow-on and evolution stages; identification of the minimum impact provisions to allow flexibility in the baseline; and identification of enhancing and enabling technologies. For individual titles, see N92-17349 through N92-17362.

N92-17349*# National Aeronautics and Space Administration. Lyndon B. Johnson Space Center, Houston, TX.
FAILURE ENVIRONMENT ANALYSIS TOOL (FEAT)
D. G. Lawler *In* NASA, Washington, Beyond the Baseline 1991: Proceedings of the Space Station Evolution Symposium. Volume 2: Space Station Freedom, Part 2 Sep. 1991 p 1003-1019
(For primary document see N92-17348 08-18)
Avail: NTIS HC/MF A20 CSCL 22B

Information is given in viewgraph form on the Failure Environment Analysis Tool (FEAT), a tool designed to demonstrate advanced modeling and analysis techniques to better understand and capture the flow of failures within and between elements of the Space Station Freedom (SSF) and other large complex systems. Topics covered include objectives, development background, the technical approach, SSF baseline integration, and FEAT growth and evolution. Author

N92-17350*# National Aeronautics and Space Administration. Lyndon B. Johnson Space Center, Houston, TX.
ADVANCED FLIGHT SOFTWARE RECONFIGURATON
Bryan Porcher *In* NASA, Washington, Beyond the Baseline 1991: Proceedings of the Space Station Evolution Symposium. Volume 2: Space Station Freedom, Part 2 Sep. 1991 p 1021-1036 (For primary document see N92-17348 08-18)
Avail: NTIS HC/MF A20 CSCL 22B

Information is given in viewgraph form on advanced flight software reconfiguration. Reconfiguration is defined as identifying mission and configuration specific requirements, controlling mission and configuration specific data, binding this information to the flight software code to perform specific missions, and the release and distribution of the flight software. The objectives are to develop, demonstrate, and validate advanced software reconfiguration tools and techniques; to demonstrate reconfiguration approaches on Space Station Freedom (SSF) onboard systems displays; and to interactively test onboard systems displays, flight software, and flight data. Author

N92-17351*# National Aeronautics and Space Administration. Lyndon B. Johnson Space Center, Houston, TX.
SOFTWARE LIFE CYCLE METHODOLOGIES AND ENVIRONMENTS **c61**
Ernest Fridge *In* NASA, Washington, Beyond the Baseline 1991: Proceedings of the Space Station Evolution Symposium. Volume 2: Space Station Freedom, Part 2 Sep. 1991 p 1037-1103 (For primary document see N92-17348 08-18)
Avail: NTIS HC/MF A20 CSCL 09B

Products of this project will significantly improve the quality and productivity of Space Station Freedom Program software processes by: improving software reliability and safety; and broadening the range of problems that can be solved with computational solutions. Projects brings in Computer Aided Software Engineering (CASE) technology for: Environments such as Engineering Script Language/Parts Composition System (ESL/PCS) application generator, Intelligent User Interface for cost avoidance in setting up operational computer runs, Framework programmable platform for defining process and software development work flow control, Process for bringing CASE technology into an organization's culture, and CLIPS/CLIPS Ada language for developing expert systems; and methodologies such as Method for developing fault tolerant, distributed systems and a method for developing systems for common sense reasoning and for solving expert systems problems when only approximate truths are known. Author

N92-17352*# National Aeronautics and Space Administration. Lyndon B. Johnson Space Center, Houston, TX.
INTELLIGENT COMPUTER-AIDED TRAINING (ICAT) **c61**
Robert T. Savely and R. Bowen Loftin *In* NASA, Washington, Beyond the Baseline 1991: Proceedings of the Space Station Evolution Symposium. Volume 2: Space Station Freedom, Part 2 Sep. 1991 p 1105-1155 Prepared in cooperation with Houston Univ., TX (For primary document see N92-17348 08-18)
Avail: NTIS HC/MF A20 CSCL 09B

The Software Technology Branch has developed and demonstrated a number of ICAT System for a variety of complex procedural tasks in the NASA operational environment. A general ICAT architecture was developed and shown to be adaptable across this spectrum of tasks. Currently underway is the assembly of a suite of software tools that will permit the training community to rapidly develop and deploy ICAT systems for a variety of Space Station training tasks. The use of ICAT technology for selected training applications within the Space Station Freedom program can significantly reduce the costs of training system development. Once developed ICAT systems can be more readily and efficiently evolved and maintained than many conventional training systems. ICAT systems can be delivered for both ground based and on-orbit training. The availability of sophisticated on-orbit training will serve to reduce EVA time and can be especially useful in preparing crew for the performance on infrequent, mission critical tasks. ICAT systems can deliver uniform but individualized training to large numbers of personnel in a workstation environment. Author

N92-17353*# Jet Propulsion Lab., California Inst. of Tech., Pasadena.
OPERATIONS MISSION PLANNER BEYOND THE BASELINE **c61**
Eric Biefeld and Lynne Cooper *In* NASA, Washington, Beyond the Baseline 1991: Proceedings of the Space Station Evolution Symposium. Volume 2: Space Station Freedom, Part 2 Sep. 1991 p 1157-1200 (For primary document see N92-17348 08-18)
Avail: NTIS HC/MF A20 CSCL 09B

The scheduling of Space Station Freedom must satisfy four major requirements. It must ensure efficient housekeeping operations, maximize the collection of science, respond to changes in tasking and available resources, and accommodate the above changes in a manner that minimizes disruption of the ongoing operations of the station. While meeting these requirements the scheduler must cope with the complexity, scope, and flexibility of SSF operations. This requires the scheduler to deal with an astronomical number of possible schedules. The Operations Mission Planner (OMP) is centered around minimally disruptive replanning and the use of heuristics limit search in scheduling. OMP has already shown several artificial intelligence based scheduling techniques such as Interleaved Iterative Refinement and Bottleneck Identification using Process Chronologies. Author

N92-17354*# National Aeronautics and Space Administration. Lyndon B. Johnson Space Center, Houston, TX.
EMU EVOLUTION
M. Rouen *In* NASA, Washington, Beyond the Baseline 1991: Proceedings of the Space Station Evolution Symposium. Volume 2: Space Station Freedom, Part 2 Sep. 1991 p 1201-1235 (For primary document see N92-17348 08-18)
Avail: NTIS HC/MF A20 CSCL 22B

Evolution of Extravehicular Mobility Unit (EMU) technology is necessary to support the Extravehicular Activity (EVA) requirements of the Space Station Freedom Program and those of the Space Exploration Initiative (SEI). Key qualities supporting long-duration missions include technologies that are highly reliable, durable, minimize logistics requirements, and are in-flight maintainable and serviceable. While these qualities are common to SSF and SEI EVA, development paths will differ where specific mission requirements impose different constraints. Development of reusable, regenerative technologies is necessary to minimize the logistics penalties. Increased battery discharge/recharge cycle life and usable wet life, compact high current density fuel cells, reusable CO2 absorbing media, and thermal radiation coupled with venting heat rejection technologies are just some methods of reducing consumables. Development must strive for durable, reliable systems that are in-flight serviceable and maintainable, which are vital for missions where logistics capabilities are extremely constrained. Key areas include suit components (e.g., gloves, boots, and cooling garments), and life support hardware such as fans, pumps, instrumentation, and emergency O2 systems. Higher pressure suits will reduce EVA prebreathe requirements and pre-EVA operations overall. Many challenges of higher pressure suits have been addressed by on-going development. Emphasis on glove development is necessary to provide low fatigue, dexterous glove mobility at higher suit pressures. Minimum impact hooks and scars which support an advanced SSF EMU have been identified. These accommodations permit upgrades that support servicing of low volume, high pressure oxygen systems, and hydrogen technologies such as fuel cell, and venting hydrogen heat rejection systems. Author

N92-17355*# National Aeronautics and Space Administration. Marshall Space Flight Center, Huntsville, AL.
ENVIRONMENTAL CONTROL AND LIFE SUPPORT SYSTEM EVOLUTION ANALYSIS **c54**
Paul Wieland and Sandy Montgomery *In* NASA, Washington, Beyond the Baseline 1991: Proceedings of the Space Station Evolution Symposium. Volume 2: Space Station Freedom, Part 2 Sep. 1991 p 1237-1270 (For primary document see N92-17348 08-18)
Avail: NTIS HC/MF A20 CSCL 06K

The Space Station Freedom Environmental Control and Life Support System (ECLSS) will have to accommodate the changes made to Freedom as it evolves over 30 years or more. Requirements will change as pressurized modules are added, crew numbers increase, and as the tasks to be performed change. This evolution will result in different demands on the ECLSS which will have to adapt to these changes. Technologies other than the baselined ones may be better able to perform the various ECLSS functions and technological advances will result in improved life support hardware better able to meet the new requirements. Author

N92-17356*# National Aeronautics and Space Administration. Marshall Space Flight Center, Huntsville, AL.
THE ENVIRONMENTAL CONTROL AND LIFE SUPPORT SYSTEM ADVANCED AUTOMATION PROJECT **c54**

Brandon S. Dewberry *In* NASA, Washington, Beyond the Baseline 1991: Proceedings of the Space Station Evolution Symposium. Volume 2: Space Station Freedom, Part 2 Sep. 1991 p 1271-1309 (For primary document see N92-17348 08-18)
Avail: NTIS HC/MF A20 CSCL 06K

The objective of the ECLSS Advanced Automation project includes reduction of the risk associated with the integration of new, beneficial software techniques. Demonstrations of this software to baseline engineering and test personnel will show the benefits of these techniques. The advanced software will be integrated into ground testing and ground support facilities, familiarizing its usage by key personnel. Author

N92-17357*# Jet Propulsion Lab., California Inst. of Tech., Pasadena. Artificial Intelligence Group.
ECLSS PREDICTIVE MONITORING c54
Richard J. Doyle and Steve A. Chien *In* NASA, Washington, Beyond the Baseline 1991: Proceedings of the Space Station Evolution Symposium. Volume 2: Space Station Freedom, Part 2 Sep. 1991 p 1311-1351 (For primary document see N92-17348 08-18)
Avail: NTIS HC/MF A20 CSCL 06K

On Space Station Freedom (SSF), design iterations have made clear the need to keep the sensor complement small. Along with the unprecendented duration of the mission, it is imperative that decisions regarding placement of sensors be carefully examined and justified during the design phase. In the ECLSS Predictive Monitoring task, we are developing AI-based software to enable design engineers to evaluate alternate sensor configurations. Based on techniques from model-based reasoning and information theory, the software tool makes explicit the quantitative tradeoffs among competing sensor placements, and helps designers explore and justify placement decisions. This work is being applied to the Environmental Control and Life Support System (ECLSS) testbed at MSFC to assist design personnel in placing sensors for test purposes to evaluate baseline configurations and ultimately to select advanced life support system technologies for evolutionary SSF. Author

N92-17358*# Jet Propulsion Lab., California Inst. of Tech., Pasadena.
JPL SPACE STATION TELEROBOTIC ENGINEERING PROTOTYPE DEVELOPMENT: ADVANCED TELEROBOTICS SYSTEM TECHNOLOGY c37
Paul G. Backes *In* NASA, Washington, Beyond the Baseline 1991: Proceedings of the Space Station Evolution Symposium. Volume 2: Space Station Freedom, Part 2 Sep. 1991 p 1353-1374 (For primary document see N92-17348 08-18)
Avail: NTIS HC/MF A20 CSCL 13I

The objective of the Advanced Telerobotics System Technology Task is to develop/prototype advanced telerobotics supervisory and shared control to enhance Intra-Vehicular Activity (IVA) teleoperation in the Space Station. The technology provides enhanced telerobotics capabilities while operating within the expected constraints of computation limitations, time delay, and bus bandwidth. A local site operator interface has also been developed for specifying teleoperation and shared control modes as well as supervised autonomous macros for execution at the remote site. The primary objective of the task is to transfer the advanced technology to appropriate flight centers to enhance the baseline Station capabilities. Author

N92-17359*# Jet Propulsion Lab., California Inst. of Tech., Pasadena.
JPL SPACE STATION TELEROBOTIC ENGINEERING PROTOTYPE DEVELOPMENT FY 91 STATUS/ACHIEVEMENTS c37
Wayne Zimmerman *In* NASA, Washington, Beyond the Baseline 1991: Proceedings of the Space Station Evolution Symposium. Volume 2: Space Station Freedom, Part 2 Sep. 1991 p 1375-1386 (For primary document see N92-17348 08-18)
Avail: NTIS HC/MF A20 CSCL 13I

The topics covered are presented in view graph form and include: (1) streamlining intravehicular activity (IVA) teleoperation activities on the Space Station Freedom (SSF); (2) enhancing SSF utilization during the man-tended phase; (3) telerobotic ground remote operations (TGRO); and (4) advanced telerobotics system technology (shared control). Author

N92-17360*# Jet Propulsion Lab., California Inst. of Tech., Pasadena.
TELEROBOTIC GROUND-REMOTE OPERATIONS c37
Bruce Bon and Wayne Zimmerman *In* NASA, Washington, Beyond the Baseline 1991: Proceedings of the Space Station Evolution Symposium. Volume 2: Space Station Freedom, Part 2 Sep. 1991 p 1387-1404 (For primary document see N92-17348 08-18)
Avail: NTIS HC/MF A20 CSCL 13I

The Telerobotic Ground-Remote Operations task consists of development of a demonstration local-site operator control station that includes a graphical user interface (GUI) for control of a remote robot, and development of operator-assisted perception algorithms and software that will provide flexible and accurate world modeling capabilities. The topics covered are presented in view graph form and include: (1) local site development configuration; (2) system design; (3) operator control station (local site) software block diagram; (4) operator-assisted perception; and (5) program status. Author

N92-17361*# National Aeronautics and Space Administration. Goddard Space Flight Center, Greenbelt, MD.
COLLISION AVOIDANCE SENSOR SKIN
In NASA, Washington, Beyond the Baseline 1991: Proceedings of the Space Station Evolution Symposium. Volume 2: Space Station Freedom, Part 2 Sep. 1991 p 1405-1432 (For primary document see N92-17348 08-18)
Avail: NTIS HC/MF A20 CSCL 22B

The objective was to totally eliminate the possibility of a robot (or any mechanism for that matter) inducing a collision in space operations. We were particularly concerned that human beings were safe under all circumstances. This was apparently accomplished, and it is shown that GSFC has a system that is ready for space qualification and flight. However, it soon became apparent that much more could be accomplished with this technology. Payloads could be made invulnerable to collision avoidance and the blind spots behind them eliminated. This could be accomplished by a simple, non-imaging set of 'Capaciflector' sensors on each payload. It also is evident that this system could be used to align and dock the system with a wide margin of safety. Throughout, lighting problems could be ignored, and unexpected events and modeling errors taken in stride. At the same time, computational requirements would be reduced. This can be done in a simple, rugged, reliable manner that will not disturb the form factor of space systems. It will be practical for space applications. The lab experiments indicate we are well on the way to accomplishing this. Still, the research trail goes deeper. It now appears that the sensors can be extended to end effectors to provide precontact information and make robot docking (or any docking connection) very smooth, with minimal loads impacted back into the mating structures. This type of ability would be a major step forward in basic control techniques in space. There are, however, baseline and restructuring issues to be tackled. The payloads must get power and signals to them from the robot or from the astronaut servicing tool. This requires a standard electromechanical interface. Any of several could be used. The GSFC prototype shown in this presentation is a good one. Sensors with their attendant electronics must be added to the payloads, end effectors, and robot arms and integrated into the system. Author

N92-17362*# McDonnell-Douglas Space Systems Co., Huntington Beach, CA.
MARS AEROBRAKE ASSEMBLY DEMONSTRATION
John M. Garvey *In* NASA, Washington, Beyond the Baseline 1991: Proceedings of the Space Station Evolution Symposium.

Volume 2: Space Station Freedom, Part 2 Sep. 1991 p 1433-1470 (For primary document see N92-17348 08-18)
Avail: NTIS HC/MF A20 CSCL 22B

NASA has identified aerobraking as a potentially critical technology for the Space Exploration Initiative (SEI). The size of Mars aerobrakes may be beyond the capabilities of future launch vehicles to place them into orbit in one launch. On-orbit assembly using facilities and operations developed under the Space Station Freedom (SSF) Program represent one approach for realizing such large structures. the results of early testing in this subject can help influence the future evolution of the SSF. The objectives are to: (1) generate empirical data on operational procedures for on-orbit assembly of a large Mars aerobrake; (2) develop aerobrake design concepts; (3) identify critical issues and requirements associated with SSF utilization; and (4) to stimulate student participation in the SEI. Author

N92-17409*# National Aeronautics and Space Administration, Washington, DC.
BEYOND THE BASELINE 1991: PROCEEDINGS OF THE SPACE STATION EVOLUTION SYMPOSIUM. VOLUME 1: SPACE STATION FREEDOM, PART 2
Sep. 1991 369 p Symposium held in League City, TX, 6-8 Aug. 1991
(NASA-CP-10083-Vol-1-Pt-2; S-653-Vol-1-Pt-2; NAS 1.55:10083-Vol-1-Pt-2) Avail: NTIS HC/MF A16 CSCL 22B

This report contains the individual presentations delivered at the Space Station Evolution Symposium. The results of Space Station Freedom Advanced Studies provide a road map for the evolution of Freedom in terms of user requirements, utilization and operations concepts, and growth options for distributed systems. Regarding these specific systems, special attention is given to: highlighting changes made during restructuring; description of growth paths through the follow-on and evolution phases; identification of minimum impact provisions to allow flexibility in the baseline; and identification of enhancing and enabling technologies. For individual titles, see N92-17410 through N92-17422.

N92-17410*# National Aeronautics and Space Administration, Washington, DC.
SPACE STATION FREEDOM BASELINE OPERATIONS CONCEPT
Granville Paules *In its* Beyond the Baseline 1991: Proceedings of the Space Station Evolution Symposium. Volume 1: Space Station Freedom, Part 2 Sep. 1991 p 349-366 (For primary document see N92-17409 08-18)
Avail: NTIS HC/MF A16 CSCL 22B

The Baseline Operations Concept is designed to support the multiflight-multistage assembly sequence and post-Permanent Manned Configuration (PMC) era for the Space Station Freedom (SSF). Initial implementation of procedures and systems are consistent with experience gained during the operation of the Shuttle and Spacelab. Author

N92-17411*# National Aeronautics and Space Administration. Ames Research Center, Moffett Field, CA.
FACING PAGE TEST FOR THE ASTRONAUT SCIENCE ADVISOR PRESENTATION **c63**
Michael M. Compton *In* NASA, Washington, Beyond the Baseline 1991: Proceedings of the Space Statin Evolution Symposium. Volume 1: Space Station Freedom, Part 2 Sep. 1991 p 367-391 (For primary document see N92-17409 08-18)
Avail: NTIS HC/MF A16 CSCL 09B

The goal of the Astronaut Science Advisor (ASA) project is to improve the scientific return of experiments performed in space by providing astronaut experimenters with an 'intelligent assistant' that encapsulates much of the domain- and experiment-related knowledge commanded by the Principal Investigator (PI) on the ground. By using expert systems technology and the availability of flight-qualified personal computers, it is possible to encode the requisite knowledge and make it available to astronauts as they perform experiments in space. The system performs four major functions: diagnosis and troubleshooting of experiment apparatus, data collection, protocol management, and detection of interesting data. The experiment used for development of the system measures human adaptation to weightlessness in the context of the neurovestibular system. This so-called 'Rotating Dome' experiment was flown on the recent Spacelab Life Sciences One (SLS-1) Mission. This mission was used as an opportunity to test some of the system's functionality. Experiment data was downlinked from the orbiter, and the system then captured the data and analyzed it in real time. The system kept track of the time being used by the experiment, recognized occurrences of interesting data, summarized data statistically and generated potential new protocols that could be used to optimize the course of the experiment. Author

N92-17412*# National Aeronautics and Space Administration. Ames Research Center, Moffett Field, CA.
THE ASTRONAUT SCIENCE ADVISOR: GROUND TESTING DURING SLS-1 **c63**
Michael M. Compton *In* NASA, Washington, Beyond the Baseline 1991: Proceedings of the Space Station Evolution Symposium. Volume 1: Space Station Freedom, Part 2 Sep. 1991 p 393-41 (For primary document see N92-17409 08-18)
Avail: NTIS HC/MF A16 CSCL 09B

The objective of the Astronaut Science Advisor (ASA) is the improvement of the scientific return of experiments performed in space. This is accomplished through the use of expert systems technology to encode the domain and experiment knowledge commanded by the principal investigator (PI) and make it available to the astronaut experimenters. The principal functions of the ASA include the following: capture, reduce, and archive experimental data; monitor data quality and help diagnose problems with equipment when experimental data is erratic or poor; identify and permit investigation of interesting data; and suggest protocol changes that would result in better utilization of remaining time. Author

N92-17413*# National Aeronautics and Space Administration. Langley Research Center, Hampton, VA.
EVOLUTION USER REQUIREMENTS FOR THE RESTRUCTURED SPACE STATION
K. Leath, R. J. Saucillo (McDonnell-Douglas Space Systems Co., Washington, DC.), and B. D. Meredith *In* NASA, Washington, Beyond the Baseline 1991: Proceedings of the Space Station Evolution Symposium. Volume 1: Space Station Freedom, Part 2 Sep. 1991 p 417-44 (For primary document see N92-17409 08-18)
Avail: NTIS HC/MF A16 CSCL 22B

Space Station Freedom (SSF) is designed to be an Earth orbiting multidisciplinary R&D facility capable of evolving to accommodate a variety of potential uses. In order to identify SSF evolution requirement and define potential growth configurations, NASA-Langley is analyzing user resource requirements for the post-PMC time frame. The analysis goal is to define resource levels, including crew, power, and volume, which allow full utilization of SSF capabilities commensurate with minimum essential user requirements. Multiple scenarios were studied including core R&D and combined SEI plus R&D utilization. An analysis is presented of a core R&D utilization scenario. Included are discussions of resource allocation assumptions for specific R&D disciplines, user requirements trends, and growth resource projections. These preliminary results show total resource requirements of 13 crew, 150 kW power, and additional lab volume equivalent to a second U.S. lab module. Additionally, orthogonal growth structure was identified as required to support SSF systems and users. Author

N92-17414*# National Aeronautics and Space Administration. Langley Research Center, Hampton, VA.
SSF GROWTH CONCEPTS AND CONFIGURATIONS
William M. Cirillo *In* NASA, Washington, Beyond the Baseline 1991: Proceedings of the Space Station Evolution Symposium. Volume 1: Space Station Freedom, Part 2 Sep. 1991

p 449-48 (For primary document see N92-17409 08-18)
Avail: NTIS HC/MF A16 CSCL 22B

There are three primary objectives for the Space Station Freedom (SSF) Growth concepts and configuration study task. The first objective is the development of evolutionary SSF concept consistent with user requirements and program constraints. The second primary objective is to ensure the feasibility of the proposed SSF evolution concepts as the systems level. This includes an assessment of SSF evolution flight control analysis, logistics assessment, maintainability, and operational considerations. The final objective is to ensure compatibility of the baseline SSF design with the derived evolution requirements at both the system and element (habitat modules, power generation equipment, etc.) levels. Author

N92-17415*# McDonnell-Douglas Space Systems Co., Washington, DC.
STV FUELING OPTIONS
Ken Flemming *In* NASA, Washington, Beyond the Baseline 1991: Proceedings of the Space Station Evolution Symposium. Volume 1: Space Station Freedom, Part 2 Sep. 1991 p 489-53 (For primary document see N92-17409 08-18)
Avail: NTIS HC/MF A16 CSCL 22B

Lunar vehicles that will be space based and reusable will require resupply of propellants in orbit. Approximately 75 pct. of the total mass delivered to low earth orbit will be propellants. Consequently, the propellant management techniques selected for Space Exploration Initiative (SEI) orbital operations will have a major influence on the overall SEI architecture. Five proposed propellant management facility (PMF) concepts were analyzed and compared in order to determine the best method of resupplying reusable, space based Lunar Transfer Vehicles (LTVs). The processing time needed at the Space Station to prepare LTV for its next lunar mission was estimated for each of the PMF concepts. The estimated times required to assemble and maintain the different PMF concepts were also compared. The results of the maintenance analysis were similar, with co-orbiting depots needing 100 to 350 pct. more annual maintenance. The first few external tanks mating operations at KSC encountered many problems that could cause serious lunar mission schedule delays. The use of drop tanks on lunar vehicles increases by a factor of four the number of critical propellant interface disturbances. Author

N92-17416*# National Aeronautics and Space Administration. Lewis Research Center, Cleveland, OH.
SPACE STATION FREEDOM/LUNAR TRANSFER VEHICLE PROPELLANT OPERATION HAZARD ANALYSIS
Sam Dominick, Steven M. Stevenson, and Harvey Feingold (Science Applications International Corp., Schaumburg, IL.) *In* NASA, Washington, Beyond the Baseline 1991: Proceedings of the Space Station Evolution Symposium. Volume 1: Space Station Freedom, Part 2 Sep. 1991 p 533-56 (For primary document see N92-17409 08-18)
Avail: NTIS HC/MF A16 CSCL 22B

Space Station Freedom (SSF), as a transportation node for Space Exploration Initiative missions, would involve the assembly and refurbishing of lunar and Mars transfer vehicles. This includes operations involving cryogenic propellants (LH2 7 LO2) such as storing and handling of loaded propellant tanks, assembly onto the vehicle, and propellant transfer. Cryogenic propellants dictate rigorous safety precautions and impose unique requirements to ensure flight safety to both personnel and SSF elements. The objective of this study is to identify potential hazards and risks associated with cryogenic propellants. This involves identification of pertinent system design features and operational procedures. Criticality of identified risks/hazards shall be assessed and those that fall in the catastrophic and critical categories shall include mitigating solutions. Author

N92-17417*# National Aeronautics and Space Administration. Ames Research Center, Moffett Field, CA.
DATA MANAGEMENT SYSTEM ADVANCED ARCHITECTURES
Ed Chevers *In* NASA, Washington, Beyond the Baseline 1991: Proceedings of the Space Station Evolution Symposium. Volume 1: Space Station Freedom, Part 2 Sep. 1991 p 565-58 (For primary document see N92-17409 08-18)
Avail: NTIS HC/MF A16 CSCL 22B

The topics relating to the Space Station Freedom (SSF) are presented in view graph form and include: (1) the data management system (DMS) concept; (2) DMS evolution rationale; (3) the DMS advance architecture task; (4) DMS group support for Ames payloads; (5) DMS testbed development; (6) the DMS architecture task status; (7) real time multiprocessor testbed; (8) networked processor performance; (9) and the DMS advance architecture task 1992 goals. K.S.

N92-17418*# Jet Propulsion Lab., California Inst. of Tech., Pasadena. High Speed Optical Systems Group.
OPTICAL PROTOCOLS FOR ADVANCED SPACECRAFT NETWORKS **c74**
Larry A. Bergman *In* NASA, Washington, Beyond the Baseline 1991: Proceedings of the Space Station Evolution Symposium. Volume 1: Space Station Freedom, Part 2 Sep. 1991 p 583-63 (For primary document see N92-17409 08-18)
Avail: NTIS HC/MF A16 CSCL 20F

Most present day fiber optic networks are in fact extensions of copper wire networks. As a result, their speed is still limited by electronics even though optics is capable of running three orders of magnitude faster. Also, the fact that photons do not interact with one another (as electrons do) provides optical communication systems with some unique properties or new functionality that is not readily taken advantage of with conventional approaches. Some of the motivation for implementing network protocols in the optical domain, a few possible approaches including optical code-division multiple-access (CDMA), and how this class of networks can extend the technology life cycle of the Space Station Freedom (SSF) with increased performance and functionality are described. Author

N92-17419*# National Aeronautics and Space Administration. Lyndon B. Johnson Space Center, Houston, TX.
ADVANCED CREW PERSONAL SUPPORT COMPUTER (CPSC) TASK **c60**
Debra Muratore *In* NASA, Washington, Beyond the Baseline 1991: Proceedings of the Space Station Evolution Symposium. Volume 1: Space Station Freedom, Part 2 Sep. 1991 p 639-65 (For primary document see N92-17409 08-18)
Avail: NTIS HC/MF A16 CSCL 09B

The topics are presented in view graph form and include: background; objectives of task; benefits to the Space Station Freedom (SSF) Program; technical approach; baseline integration; and growth and evolution options. The objective is to: (1) introduce new computer technology into the SSF Program; (2) augment core computer capabilities to meet additional mission requirements; (3) minimize risk in upgrading technology; and (4) provide a low cost way to enhance crew and ground operations support. Author

N92-17420*# McDonnell-Douglas Space Systems Co., Washington, DC.
ISE ADVANCED TECHNOLOGY
Barry R. Fox *In* NASA, Washington, Beyond the Baseline 1991: Proceedings of the Space Station Evolution Symposium. Volume 1: Space Station Freedom, Part 2 Sep. 1991 p 651-67 (For primary document see N92-17409 08-18)
Avail: NTIS HC/MF A16 CSCL 22B

Information on Space Station Freedom scheduling problems and techniques are presented in viewgraph form. Topics covered include automated scheduling systems, user interface standards, benefits of interactive scheduling systems, incremental scheduling, software engineering, computer graphics interface, distributed resource management, and advanced applications. Author

N92-17421*# National Aeronautics and Space Administration. Lyndon B. Johnson Space Center, Houston, TX.
REAL TIME DATA SYSTEM (RTDS) **c60**
Troy A. Heindel *In* NASA, Washington, Beyond the Baseline

1991: Proceedings of the Space Station Evolution Symposium. Volume 1: Space Station Freedom, Part 2 Sep. 1991 p 681-69 (For primary document see N92-17409 08-18)
Avail: NTIS HC/MF A16 CSCL 09B

Information is given in viewgraph form on the Real Time Data System (RTDS). Topics covered include applications to the Space Station Freedom, the Space Shuttle flight controllers, the Mission Control Center workstations, and the Remote Manipulator Systems (RMS). Also covered are the technology gap, pacing factors, and lessons learned during research. Author

N92-17422*# National Aeronautics and Space Administration. John F. Kennedy Space Center, Cocoa Beach, FL.
COMPUTER SYSTEM EVOLUTION REQUIREMENTS FOR AUTONOMOUS CHECKOUT OF EXPLORATION VEHICLES
c60
Tom Davis and Mike Sklar *In* NASA, Washington, Beyond the Baseline 1991: Proceedings of the Space Station Evolution Symposium. Volume 1: Space Station Freedom, Part 2 Sep. 1991 p 697-72 (For primary document see N92-17409 08-18)
Avail: NTIS HC/MF A16 CSCL 09B

This study, now in its third year, has had the overall objective and challenge of determining the needed hooks and scars in the initial Space Station Freedom (SSF) system to assure that on-orbit assembly and refurbishment of lunar and Mars spacecraft can be accomplished with the maximum use of automation. In this study automation is all encompassing and includes physical tasks such as parts mating, tool operation, and human visual inspection, as well as non-physical tasks such as monitoring and diagnosis, planning and scheduling, and autonomous visual inspection. Potential tasks for automation include both extravehicular activity (EVA) and intravehicular activity (IVA) events. A number of specific techniques and tools have been developed to determine the ideal tasks to be automated, and the resulting timelines, changes in labor requirements and resources required. The Mars/Phobos exploratory mission developed in FY89, and the Lunar Assembly/Refurbishment mission developed in FY90 and depicted in the 90 Day Study as Option 5, have been analyzed in detailed in recent years. The complete methodology and results are presented in FY89 and FY90 final reports. Author

N92-17430# Air Force Inst. of Tech., Wright-Patterson AFB, OH.
A COMPUTER SOLUTION FOR MULTIPLE SATELLITE-SATELLITE AND SATELLITE-GROUND STATION VISIBILITY DETERMINATION M.S. Thesis
Jennifer L. Moore 31 Jul. 1991 113 p
(AD-A243490; AFIT/CI/CIA-91-098) Avail: NTIS HC/MF A06 CSCL 25/2

The purpose of this study is to examine the problem of determining rise and set times for visibility periods of multiple satellite satellite and satellite ground station communications. Additionally, the ability to maintain constant communication links is explored. This research examines three means to solve the problem: basic iteration, the Lawton Method, and an improved method involving parabolic blending and a closed form root solving technique. The greatest concentration is placed on the final solution and its application. The result of this investigation is a computer program capable of determining rise and set times for as many as four satellites and four ground stations. In addition, the program performs a check for continuous communications between the indicated satellites and earth based resources. GRA

N92-17580# TRW Systems Group, Redondo Beach, CA.
TESTING OF SPACECRAFT IN LONG-TERM STORAGE
R. J. Masterson and R. N. Miller 1991 7 p Previously announced in IAA as A73-33615
(AD-A242906) Avail: NTIS HC/MF A02 CSCL 22/2

This paper addresses the problem of developing a storage and test policy which may be applied to equipment placed in long-term storage prior to utilization. A closed-form analytic solution is developed to aid in evaluating the characteristics of a given policy in terms of test efficiency, on time delivery, and subsequent reliable operation of the equipment in its intended application. The analysis model is described in detail, a computer program based on the model is outlined, and a flow diagram of its logic included. Problems associated with estimating valid input data are treated. An example of the application of the analysis to spacecraft is presented to fully illustrate the approach. Finally, the paper closes with a discussion of some of the many situations in which such a tool could be employed in a variety of industrial, research, and sports contexts. GRA

N92-17585*# Contel Federal Systems, Inc., Chantilly, VA.
INTERIM SERVICE ISDN SATELLITE (ISIS) HARDWARE EXPERIMENT DESIGN FOR ADVANCED ISDN SATELLITE DESIGN AND EXPERIMENTS Report, 1 May 1991 - 28 Feb. 1992
Gerard R. Pepin 28 Feb. 1992 28 p
(Contract NASw-4520)
(NASA-CR-186943; NAS 1.26:186943) Avail: NTIS HC/MF A03 CSCL 22B

The Interim Service Integrated Services Digital Network (ISDN) Satellite (ISIS) Hardware Experiment Design for Advanced Satellite Designs describes the design of the ISDN Satellite Terminal Adapter (ISTA) capable of translating ISDN protocol traffic into time division multiple access (TDMA) signals for use by a communications satellite. The ISTA connects the Type 1 Network Termination (NT1) via the U-interface on the line termination side of the CPE to the V.35 interface for satellite uplink. The same ISTA converts in the opposite direction the V.35 to U-interface data with a simple switch setting. Author

N92-17602# Air Force Inst. of Tech., Wright-Patterson AFB, OH. School of Engineering.
CONTROL OF A LARGE FLEXIBLE SPACE STRUCTURE USING MULTIPLE MODEL ADAPTIVE ALGORITHMS M.S. Thesis
John A. Gustafson Dec. 1991 479 p
(AD-A243759; AFIT/GE/ENG/91D-22) Avail: NTIS HC/MF A21 CSCL 22/2

The development and performance of moving-bank multiple model adaptive estimation (MMAE) and control (MMAC) algorithms for quelling vibrations induced in the SPICE 2 space structure are analyzed in this thesis. The structure consists of a large platform and a smaller platform connected by three legs in a tripod fashion. The model supplied by Phillips Laboratory, Kirtland AFB is used to develop a truth model and multiple reduced ordered filter models. The filter models are developed from modal analysis and internally balanced techniques. Deviations of the line-of-sight vector from the center of the large platform to the center of the smaller platform are used for LQG controller performance evaluation. For use with the LQG controller, research results indicate the chosen reduced order models are of inadequate dimension and that the full ordered filter model should be implemented to quell vibrations introduced into the structure. The parameter estimator implemented the ME/I algorithm, the moving-bank logic employed parameter position monitoring and the controller used the modified MMAC method. Parameter variations of two percent caused instabilities in the single filter/controller design. The MMAE/MMAC algorithms provide an excellent method to estimate a wide range of parameter variations and to quell oscillations in the structure. GRA

N92-17728*# Boeing Co., Seattle, WA. Long Duration Exposure Facility.
SYSTEMS SPECIAL INVESTIGATION GROUP Interim Report
Jan. 1991 196 p
(Contract NAS1-18224)
(NASA-CR-187355; NAS 1.26:187355) Avail: NTIS HC/MF A09 CSCL 22B

An interim report concerning the Long Duration Exposure Facility (LDEF) is presented by a Boeing Systems special investigation group (SIG). The SIG activities were divided into five engineering disciplines: electrical, mechanical, optics, thermal, and batteries/solar cells. The responsibilities of the SIG included the following areas: support de-integration at Kennedy Space Center

(KSC); testing of hardware at Boeing; review of principal investigator (PI) test plans and test results; support of test activities at PI labs; and collation of all test results into the SIG database.

D.R.D.

N92-17754# National Aerospace Lab., Tokyo (Japan). Aerodynamics Div.

WEIGHT EVALUATION AND SENSITIVITY ANALYSIS FOR SPACE PLANE. PART 2: TSTO Report No. 1 [UCHU OHKANKI NO JURYO HYOKA TO KANDO KAISEKI (SONO 2): TSTO]

Masao Shirouzu Feb. 1989 19 p In JAPANESE
(NAL-TM-602-Pt-2; ISSN-0452-2982; JTN-92-80241) Avail: NTIS HC/MF A03

Reported here is the weight evaluation and sensitivity analysis of a two stage to orbit (TSTO) type spaceplane. The major purpose of this analysis is to get the basic data which is necessary to determine the configuration of the spaceplane. Those data are used in wind tunnel tests. As the result of weight evaluation, it is confirmed that the TSTO is more feasible than single stage to orbit (SSTO). The further analysis leads to the basic specification of TSTO as follows: total weight is 350 tons; the booster wing area is 583 square meters; and the orbiter length is 39.5 meters. As for sensitivity analysis, the following parameters are checked: orbiter lift-off weight, orbiter separation condition, lift-off wing load, and cruising range. As the result of sensitivity analysis, it is confirmed that the orbiter velocity on separation and the engines which can be used in high Mach number condition are the important factors which enable the TSTO type spaceplane.

Author (NASDA)

N92-17762# Air Force Inst. of Tech., Wright-Patterson AFB, OH.

ANALYSIS OF ORBITAL ELEMENTS AND ATMOSPHERIC ACTIVITY TO ASCERTAIN POSSIBLE PRESENCE OF AN ION PROPULSION CAPABILITY ABOARD SALYUT 7/COSMOS 1686 M.S. Thesis

Kris R. Howard Dec. 1991 126 p
(AD-A243654; AFIT/GSO/ENS/91D-09) Avail: NTIS HC/MF A07 CSCL 22/1

The purpose of this study was to analyze solar and geomagnetic activity in concert with orbital element data for the Soviet space station Salyut 7 as a means toward a determination of the possible use of an ion propulsion source aboard Salyut 7 and the Cosmos 1686 module to which it was docked. Solar activity was represented by sunspot number and 10.7 cm solar radio flux, and geomagnetic activity was represented by the general activity indices k sub p and A sub p. The effects of atmospheric activity were examined both by direct comparison with orbital data, and by using solar and geomagnetic data as inputs to an atmospheric density model. For cases where neither atmospheric activity nor known maneuvers could explain changes in an orbital parameter, the feasibility of an ion propulsion source being the cause was examined. Because the orbital element data sets were taken at inconsistent time intervals, direct comparison with the atmospheric data was difficult. However, despite this limitation, the analysis suggests that the use of ion propulsion was possible during the period 6 May to 25 June 1986. GRA

N92-17768*# National Aeronautics and Space Administration, Washington, DC.

BEYOND THE BASELINE 1991: PROCEEDINGS OF THE SPACE STATION EVOLUTION SYMPOSIUM. VOLUME 2: SPACE STATION FREEDOM, PART 1

Sep. 1991 273 p Symposium held in League City, TX, 6-8 Aug. 1991
(NASA-CP-10083-Vol-2-Pt-1; S-653-Vol-2-Pt-1; NAS 1.55:10083-Vol-2-Pt-1) Avail: NTIS HC/MF A12 CSCL 22B

The results from the Advanced Systems Study and Advanced Development within the Space Station Freedom (SSF) Program are reported. The results show the evolution of the SSF in terms of user requirements, utilization and operations concepts, and growth options for distributed systems. Special attention is given to: highlighting changes made during restructuring; description of growth paths through the follow-on and evolution phases; identification of minimum-impact provisions to allow flexibility in the baseline; and identification of enhancing and enabling technologies. Products of these tasks include: engineering fidelity demonstrations and evaluations of advanced technology; detailed requirements, performance specifications, and design accommodations for insertion of advanced technology; and mature technology, tools, applications for SSF flight, ground, and information systems. For individual titles, see N92-17769 through N92-17776.

N92-17769*# Boeing Aerospace Co., Huntsville, AL. Defense and Space Group.

TANDEM CONCENTRATOR PHOTOVOLTAIC ARRAY APPLIED TO SPACE STATION FREEDOM EVOLUTIONARY POWER REQUIREMENTS **c20**

Edward M. Fisher, Jr. *In* NASA, Washington, Beyond the Baseline 1991: Proceedings of the Space Station Evolution Symposium. Volume 2: Space Station Freedom, Part 1 Sep. 1991 p 729-76 (For primary document see N92-17768 08-18)
Avail: NTIS HC/MF A12 CSCL 10B

Additional power is required to support Space Station Freedom (SSF) evolution. Boeing Defense and Space Group, LeRC, and Entech Corporation have participated in the development of efficiency gallium arsenide and gallium antimonide solar cells make up the solar array tandem cell stacks. Entech's Mini-Dome Fresnel Lens Concentrators focus solar energy onto the active area of the solar cells at 50 times one solar energy flux. Development testing for a flight array, to be launched in Nov. 1992 is under way with support from LeRC. The tandem cells, interconnect wiring, concentrator lenses, and structure were integrated into arrays subjected to environmental testing. A tandem concentrator array can provide high mass and area specific power and can provide equal power with significantly less array area and weight than the baseline array design. Alternatively, for SSF growth, an array of twice the baseline power can be designed which still has a smaller drag area than the baseline. Author

N92-17770*# National Aeronautics and Space Administration. Lewis Research Center, Cleveland, OH.

SOLAR DYNAMIC TECHNOLOGY STATUS FOR SPACE STATION FREEDOM APPLICATION **c20**

Michael J. Zernic *In* NASA, Washington, Beyond the Baseline 1991: Proceedings of the Space Station Evolution Symposium. Volume 2: Space Station Freedom, Part 1 Sep. 1991 p 765-81 (For primary document see N92-17768 08-18)
Avail: NTIS HC/MF A12 CSCL 10B

The objectives of this presentation is to emphasize the (1) rationale to incorporate solar dynamic (SD) systems onto Space Station Freedom (SSF) as the power demand increases onboard SSF, (2) SD technical progress made through the SSF Program, (3) areas of further technology development, and (4) future plans for SD system development. The SD status summary is presented in graph form. Author

N92-17771*# National Aeronautics and Space Administration. Lewis Research Center, Cleveland, OH.

SPACE STATION FREEDOM ELECTRIC POWER SYSTEM EVOLUTION ANALYSIS STATUS **c20**

Michael J. Zernic *In* NASA, Washington, Beyond the Baseline 1991: Proceedings of the Space Station Evolution Symposium. Volume 2: Space Station Freedom, Part 1 Sep. 1991 p 813-83 (For primary document see N92-17768 08-18)
Avail: NTIS HC/MF A12 CSCL 10B

The ability is examined of the SSF baselined EPS to transition to operate at a greater system capacity beyond the SSF Permanent Manned Capability PMC) milestone. Specifically, a status of a current analysis is discussed concerning additions, modifications, changeout, or combination thereof of baseline EPS hardware and/or software needed to accomplish the power generation, distribution, operation, and use needed to meet evolving SSF mission objectives. This discussion results in several EPS

architectural options that facilitate the addition or substitution of new technologies. Author

N92-17772*# Lockheed Missiles and Space Co., Huntsville, AL.
SPACE STATION FREEDOM SOLAR ALPHA JOINT GROWTH CAPABILITY
David Snyder *In* NASA, Washington, Beyond the Baseline 1991: Proceedings of the Space Station Evolution Symposium. Volume 2: Space Station Freedom, Part 1 Sep. 1991 p 835-85 (For primary document see N92-17768 08-18)
Avail: NTIS HC/MF A12 CSCL 22B

The Solar Alpha Rotary Joint (SARJ) helps to align the power generation system, onboard the Space Station Freedom, with the sun. The SARJ is responsible for providing structural continuity and controlled rotation to the outboard transverse booms. The SARJ also provides continuous power, data, and video transfer across the joint. D.R.D.

N92-17773*# National Aeronautics and Space Administration. Lewis Research Center, Cleveland, OH.
AUTOMATED POWER MANAGEMENT AND CONTROL c20
James L. Dolce *In* NASA, Washington, Beyond the Baseline 1991: Proceedings of the Space Station Evolution Symposium. Volume 2: Space Station Freedom, Part 1 Sep. 1991 p 853-88 (For primary document see N92-17768 08-18)
Avail: NTIS HC/MF A12 CSCL 10B

A comprehensive automation design is being developed for Space Station Freedom's electric power system. A joint effort between NASA's Office of Aeronautics and Exploration Technology and NASA's Office of Space Station Freedom, it strives to increase station productivity by applying expert systems and conventional algorithms to automate power system operation. The initial station operation will use ground-based dispatches to perform the necessary command and control tasks. These tasks constitute planning and decision-making activities that strive to eliminate unplanned outages. We perceive an opportunity to help these dispatchers make fast and consistent on-line decisions by automating three key tasks: failure detection and diagnosis, resource scheduling, and security analysis. Expert systems will be used for the diagnostics and for the security analysis; conventional algorithms will be used for the resource scheduling. Author

N92-17774*# National Aeronautics and Space Administration. Marshall Space Flight Center, Huntsville, AL.
THE SSM/PMAD AUTOMATED TEST BED PROJECT c20
Louis F. Lollar *In* NASA, Washington, Beyond the Baseline 1991: Proceedings of the Space Station Evolution Symposium. Volume 2: Space Station Freedom, Part 1 Sep. 1991 p 885-91 (For primary document see N92-17768 08-18)
Avail: NTIS HC/MF A12 CSCL 10B

The Space Station Module/Power Management and Distribution (SSM/PMAD) autonomous subsystem project was initiated in 1984. The project's goal has been to design and develop an autonomous, user-supportive PMAD test bed simulating the SSF Hab/Lab module(s). An eighteen kilowatt SSM/PMAD test bed model with a high degree of automated operation has been developed. This advanced automation test bed contains three expert/knowledge based systems that interact with one another and with other more conventional software residing in up to eight distributed 386-based microcomputers to perform the necessary tasks of real-time and near real-time load scheduling, dynamic load prioritizing, and fault detection, isolation, and recovery (FDIR). Author

N92-17775*# National Aeronautics and Space Administration. Lyndon B. Johnson Space Center, Houston, TX.
ACTIVE THERMAL CONTROL SYSTEM EVOLUTION
Patricia A. Petete and Brian E. Ames *In* NASA, Washington, Beyond the Baseline 1991: Proceedings of the Space Station Evolution Symposium. Volume 2: Space Station Freedom, Part 1 Sep. 1991 p 921-96 (For primary document see N92-17768 08-18)
Avail: NTIS HC/MF A12 CSCL 22B

The 'restructured' baseline of the Space Station Freedom (SSF) has eliminated many of the growth options for the Active Thermal Control System (ATCS). Modular addition of baseline technology to increase heat rejection will be extremely difficult. The system design and the available real estate no longer accommodate this type of growth. As the station matures during its thirty years of operation, a demand of up to 165 kW of heat rejection can be expected. The baseline configuration will be able to provide 82.5 kW at Eight Manned Crew Capability (EMCC). The growth paths necessary to reach 165 kW have been identified. Doubling the heat rejection capability of SSF will require either the modification of existing radiator wings or the attachment of growth structure to the baseline truss for growth radiator wing placement. Radiator performance can be improved by enlarging the surface area or by boosting the operating temperature with a heat pump. The optimal solution will require both modifications. The addition of growth structure would permit the addition of a parallel ATCS using baseline technology. This growth system would simplify integration. The feasibility of incorporating these growth options to improve the heat rejection capacity of SSF is under evaluation. Author

N92-17776*# McDonnell-Douglas Space Systems Co., Washington, DC. Thermal Systems.
THERMAL CONTROL SYSTEM AUTOMATION PROJECT (TCSAP)
Roger L. Boyer *In* NASA, Washington, Beyond the Baseline 1991: Proceedings of the Space Station Evolution Symposium. Volume 2: Space Station Freedom, Part 1 Sep. 1991 p 971-1001 (For primary document see N92-17768 08-18)
Avail: NTIS HC/MF A12 CSCL 22B

Information is given in viewgraph form on the Space Station Freedom (SSF) Thermal Control System Automation Project (TCSAP). Topics covered include the assembly of the External Thermal Control System (ETCS); the ETCS functional schematic; the baseline Fault Detection, Isolation, and Recovery (FDIR), including the development of a knowledge based system (KBS) for application of rule based reasoning to the SSF ETCS; TCSAP software architecture; the High Fidelity Simulator architecture; the TCSAP Runtime Object Database (RODB) data flow; KBS functional architecture and logic flow; TCSAP growth and evolution; and TCSAP relationships. Author

19 SPACECRAFT INSTRUMENTATION

For related information see also *06 Aircraft Instrumentation* and *35 Instrumentation and Photography.*

N92-17150*# Catholic Univ. of America, Washington, DC. Dept. of Electrical Engineering.
ANALYSIS AND EXPERIMENTAL EVALUATION OF A STEWART PLATFORM-BASED FORCE/TORQUE SENSOR
Semiannual Progress Report, 1 Jul. 1991 - 1 Feb. 1992
Charles C. Nguyen and Sami S. Antrazi Jan. 1992 17 p (Grant NAG5-780)
(NASA-CR-189861; NAS 1.26:189861) Avail: NTIS HC/MF A03 CSCL 22B

The kinematic analysis and experimentation of a force/torque sensor whose design is based on the mechanism of the Stewart Platform are discussed. Besides being used for measurement of forces/torques, the sensor also serves as a compliant platform which provides passive compliance during a robotic assembly task. It consists of two platforms, the upper compliant platform (UCP) and the lower compliant platform (LCP), coupled together through six spring-loaded pistons whose length variations are measured by six linear voltage differential transformers (LVDT) mounted along the pistons. Solutions to the forward and inverse kinematics of the force sensor are derived. Based on the known spring constant and the piston length changes, forces/torques applied to the LCP gripper are computed using vector algebra. Results of experiments conducted to evaluate the sensing capability of the force sensor are reported and discussed. Author

20 SPACECRAFT PROPULSION AND POWER

Includes main propulsion systems and components, e.g., rocket engines; and spacecraft auxilliary power sources.

For related information see also *07 Aircraft Propulsion and Power, 28 Propellants and Fuels, 44 Energy Production and Conversion,* and *15 Launch Vehicles and Space Vehicles.*

N92-17085# Aerospace Corp., El Segundo, CA. Materials Sciences Lab.

CASE BOND LINER SYSTEMS FOR SOLID ROCKET MOTORS

Thomas W. Giants 1 Apr. 1991 21 p

(Contract F04701-88-C-0089)

(AD-A242297; TR-0090(5935-02)-1; SSD-TR-91-30) Avail: NTIS HC/MF A03 CSCL 21/8

Construction of a case bond liner system for solid rocket motors involves a series of processes designed to satisfy a variety of launch vehicle parameters. An attempt to understand the chemistry and processing variables and how they affect the interfacial bonding properties in barrier liner propellant formulations is presented. Interdiffusion rates and the cure rate of each of the layers must be considered together to minimize changes in cure stoichiometries in the interfacial zones. The control of barrier layer cure is essential, not only to reduce migration of reactants and plasticizer from liner and propellant, but also to provide an active surface for adhesion to the liner. The importance of the proper characterization of the hydroxylterminated polybutadiene binder should not be underestimated. Because the binder material is a constituent of both the liner and the propellant, variation in cure times can impact diffusion rates. The complexity of case bond liner systems has increased over time, and with it, the number of variables. As more than one variable operates near its specification limit, the potential for failure becomes statistically significant. It is recommended that, in the present system, studies be directed toward refining the process variables further with the goal of increasing the reliability of bonds at all interfaces between layers. GRA

N92-17151*# National Aeronautics and Space Administration. Lewis Research Center, Cleveland, OH.

UPPER STAGES USING LIQUID PROPULSION AND METALLIZED PROPELLANTS

Bryan A. Palaszewski Washington Feb. 1992 22 p

(NASA-TP-3191; E-6105; NAS 1.60:3191) Avail: NTIS HC/MF A03 CSCL 21H

Metallized propellants are liquid propellants with a metal additive suspended in a gelled fuel. Typically, aluminum particles are the metal additive. These propellants increase the density and/or the specific impulse of the propulsion system. Using metallized propellants for volume- and mass-constrained upper stages can deliver modest increases in performance for low Earth orbit to geosynchronous Earth orbit (LEO-GEO) and other Earth-orbital transfer missions. However, using metallized propellants for planetary missions can deliver great reductions in flight time with a single-stage, upper-stage system. Tradeoff studies comparing metallized propellant stage performance with nonmetallized upper stages and the Inertial Upper Stage (IUS) are presented. These upper stages, launched from the STS and STS-C, are both one- and two-stage vehicles that provide the added energy to send payloads to high altitude orbits and onto interplanetary trajectories that are unattainable with only the Space Transportation System (STS) and the Space Transportation System-Cargo (STS-C). The stage designs are controlled by the volume and the mass constraints of the STS and STS-C launch vehicles. The influences of the density and specific impulse increases enabled by metallized propellants are examined for a variety of different stage and propellant combinations. Author

N92-17365*# Case Western Reserve Univ., Cleveland, OH. Case Center for Electrochemical Sciences and the Chemistry Dept.

CATALYSTS FOR ULTRAHIGH CURRENT DENSITY OXYGEN CATHODES FOR SPACE FUEL CELL APPLICATIONS Final Report, 1 Feb. 1989 - 30 Apr. 1991

Donald A. Tryk and E. Yeager 13 Jan. 1992 76 p

(Grant NAG3-694)

(NASA-CR-189787; NAS 1.26:189787) Avail: NTIS HC/MF A05 CSCL 10B

The objective was to identify promising electrocatalyst/support systems for oxygen cathodes capable of operating at ultrahigh current densities in alkaline fuel cells. Such cells will require operation at relatively high temperatures and O2 pressures. A number of materials were prepared, including Pb-Ru and Pb-Ir pyrochlores, RuO2 and Pt-doped RuO2, lithiated NiO and La-Ni perovskites. Several of these materials were prepared using techniques that had not been previously used to prepare them. Particularly interesting was the use of the alkaline solution technique to prepare Pt-doped and Pb-Ru pyrochlores in high area form. Also interesting was the use of the fusion (melt) method for preparing the Pb-Ru pyrochlore. Several of the materials were also deposited with platinum. Well-crystallized Pb2Ru2O(7-y) was used to fabricate very high performance O2 cathodes with good stability in room temperature KOH. This material was also found to be stable over a useful potential range at approx. 140 C in concentrated KOH. For some of the samples, fabrication of the gas-fed electrodes could not be fully optimized during this project period. Future work may be directed at this problem. Pyrochlores that were not well-crystallized were found to be unstable in alkaline solution. Very good O2 reduction performance and stability were observed with Pb2RuO(7-y) in a carbon-based gas-fed electrode with an anion-conducting membrane placed on the electrolyte side of the electrode. The performance came within a factor of about two of that observed without carbon. High area platinum and gold supported on several conductive metal oxide supports were examined. Only small improvements in O2 reduction performance at room temperature were observed for Pb2Ru2O(7-y) as a support because of the high intrinsic activity of the pyrochlore. In contrast, a large improvement was observed for Li-doped NiO as a support for Pt. Very poor performance was observed for Au deposited on Li-NiO at approx. 150 C. Nearly reversible behavior was observed for the O2/OH(-) couple for Li-doped NiO at approx. 200 C. The temperature dependence for the O2 reduction was examined. Author

N92-17495*# Aerojet-General Corp., Sacramento, CA. Propulsion Div.

TRANSPIRATION COOLED THROAT FOR HYDROCARBON ROCKET ENGINES Final Report

Lee R. May and Wendel M. Burkhardt Dec. 1991 251 p

(Contract NAS8-36952)

(NASA-CR-184272; NAS 1.26:184272; KEE6-FR; RPT/F0175.98) Avail: NTIS HC/MF A12 CSCL 21H

The objective for the Transpiration Cooled Throat for Hydrocarbon Rocket Engines Program was to characterize the use of hydrocarbon fuels as transpiration coolants for rocket nozzle throats. The hydrocarbon fuels investigated in this program were RP-1 and methane. To adequately characterize the above transpiration coolants, a program was planned which would (1) predict engine system performance and life enhancements due to transpiration cooling of the throat region using analytical models, anchored with available data; (2) a versatile transpiration cooled subscale rocket thrust chamber was designed and fabricated; (3) the subscale thrust chamber was tested over a limited range of conditions, e.g., coolant type, chamber pressure, transpiration cooled length, and coolant flow rate; and (4) detailed data analyses were conducted to determine the relationship between the key performance and life enhancement variables. Author

N92-17510*# Toledo Univ., OH. Dept. of Electrical Engineering.

A STUDY OF IGNITION AND SIMULATION CIRCUITS FOR ARCJET THRUSTERS, PART 1 M.S. Thesis Final Report

Thomas A. Stuart, Roger J. King, and Gene P. Altenburger Dec. 1991 109 p
(Grant NAG3-1102)
(NASA-CR-189097; NAS 1.26:189097) Avail: NTIS HC/MF A06 CSCL 21H

A 1 kW electronic load was programmed to simulate the nonlinear i-v (volt-ampere) characteristics of an arcjet, both ignited and unignited. The simulator was tested and found to closely resemble an arcjet both for large transients and small perturbances up to about 40 kHz. No attempt was made to simulate the ignition process itself. The dynamic behavior of the arcjet (and the simulator) was shown to differ significantly from that of a resistor bank. Previous research led to the design and construction of a 1 kW arcjet power supply. A high voltage ignition circuit was added to this hardware, and tests on a 1 kW arcjet were performed at NASA-Lewis. All tests were successful and no ignition failures were observed. Circuit documentation and test results are included. Author

N92-17769*# Boeing Aerospace Co., Huntsville, AL. Defense and Space Group.
TANDEM CONCENTRATOR PHOTOVOLTAIC ARRAY APPLIED TO SPACE STATION FREEDOM EVOLUTIONARY POWER REQUIREMENTS
Edward M. Fisher, Jr. *In* NASA, Washington, Beyond the Baseline 1991: Proceedings of the Space Station Evolution Symposium. Volume 2: Space Station Freedom, Part 1 Sep. 1991 p 729-76 (For primary document see N92-17768 08-18)
Avail: NTIS HC/MF A12 CSCL 10B

N92-17770*# National Aeronautics and Space Administration. Lewis Research Center, Cleveland, OH.
SOLAR DYNAMIC TECHNOLOGY STATUS FOR SPACE STATION FREEDOM APPLICATION
Michael J. Zernic *In* NASA, Washington, Beyond the Baseline 1991: Proceedings of the Space Station Evolution Symposium. Volume 2: Space Station Freedom, Part 1 Sep. 1991 p 765-81 (For primary document see N92-17768 08-18)
Avail: NTIS HC/MF A12 CSCL 10B

N92-17771*# National Aeronautics and Space Administration. Lewis Research Center, Cleveland, OH.
SPACE STATION FREEDOM ELECTRIC POWER SYSTEM EVOLUTION ANALYSIS STATUS
Michael J. Zernic *In* NASA, Washington, Beyond the Baseline 1991: Proceedings of the Space Station Evolution Symposium. Volume 2: Space Station Freedom, Part 1 Sep. 1991 p 813-83 (For primary document see N92-17768 08-18)
Avail: NTIS HC/MF A12 CSCL 10B

N92-17773*# National Aeronautics and Space Administration. Lewis Research Center, Cleveland, OH.
AUTOMATED POWER MANAGEMENT AND CONTROL
James L. Dolce *In* NASA, Washington, Beyond the Baseline 1991: Proceedings of the Space Station Evolution Symposium. Volume 2: Space Station Freedom, Part 1 Sep. 1991 p 853-88 (For primary document see N92-17768 08-18)
Avail: NTIS HC/MF A12 CSCL 10B

N92-17774*# National Aeronautics and Space Administration. Marshall Space Flight Center, Huntsville, AL.
THE SSM/PMAD AUTOMATED TEST BED PROJECT
Louis F. Lollar *In* NASA, Washington, Beyond the Baseline 1991: Proceedings of the Space Station Evolution Symposium. Volume 2: Space Station Freedom, Part 1 Sep. 1991 p 885-91 (For primary document see N92-17768 08-18)
Avail: NTIS HC/MF A12 CSCL 10B

23 CHEMISTRY AND MATERIALS (GENERAL)

N92-17055# Army Cold Regions Research and Engineering Lab., Hanover, NH.
ROLE OF DONOR-ACCEPTOR INTERACTIONS IN THE SORPTION OF TNT AND OTHER NITROAROMATICS FROM SOLUTION
Daniel C. Leggett Sep. 1991 13 p
(AD-A243235; CRREL-SR-91-13) Avail: NTIS HC/MF A03 CSCL 08/7

The evidence related to sorptive interactions of nitroaromatics is reviewed. Although evidence from a variety of organic model systems suggests that sorptive interaction of nitroaromatics with organic components will occur, the statistical evidence attributes greater importance of inorganic components over organic matter in soil sorption of TNT. It was concluded that donor-acceptor interactions are more important than purely hydrophobic effects in the sorption of nitroaromatics from solution onto soils and model sorbents. Furthermore, TNT in soil-water systems may become an ultimate recipient of charge, causing its reductive transformation and subsequent covalent bonding to soil organic matter components. GRA

N92-17270# State Univ. of New York, Buffalo. Dept. of Chemistry.
LIGAND REDISTRIBUTION REACTIONS OF Me2Ga(C5H5) AND MeGa(C5H5)2
O. T. Beachley, Jr., T. L. Royster, Jr., and J. R. Arhar 2 Dec. 1991 17 p
(Contract N00014-90-J-1530)
(AD-A243264; TR-31) Avail: NTIS HC/MF A03 CSCL 07/3

The compounds Me2Ga(C5H5) and MeGa(C5H5)2 have been prepared by ligand redistribution reactions between appropriate stoichiometric quantities of Ga(C5H5)3 and GaMe3. Both compounds have been demonstrated by 1H NMR spectral studies to be unstable in solution and to form symmetrized products by ligand redistribution reactions. Thus, Me2Ga(C5H5) forms GaMe3 and MeGa(C5H5)2 as primary products whereas MeGa(C5H5)2 decomposes to Ga(C5H5)3 and Me2Ga(5H5). The compound Me2Ga(C5H5) has also been shown to serve as a cyclopentadienyl transfer reagent as it reacts with FeCl2 to form Fe(C5H5)2 and Me2GaCl. GRA

N92-17308# Colorado State Univ., Fort Collins. Dept. of Chemistry.
MOLECULAR JET STUDIES OF vdW CLUSTERS AND SOLVATION Final Report, Aug. 1988 - Sep. 1991
Elliot R. Bernstein 11 Oct. 1991 21 p LIMITED REPRODUCIBILITY: Availability: Document partially illegible
(Contract N00014-89-J-1237)
(AD-A242866) Avail: NTIS HC/MF A03 CSCL 20/5

The technique of supersonic molecular jet laser spectroscopy was used to determine the stable conformations of a series of alkylbenzenes. This study demonstrates, for the first time, the sensitivity of molecular jet spectroscopy in determining both the number of stable conformations as well as the geometry of various ethyl, propyl, and butyl substituents relative to the aromatic ring. Different rotamers with low barriers to interconversion, can be isolated in the supersonic jet expansion. Each observed conformation exhibits its own spectroscopic origin in a two-color time-of-flight mass spectrum (TOFMS). The number of stable conformations is then used to determine the minimum energy geometries of the substituent group. Previous identification of individual molecular conformations for such low barriers to interconversion has not been attainable with conventional techniques such as variable-temperature NMR. GRA

N92-17329# New Jersey Inst. of Tech., Newark. Div. of Chemistry.
THE SHAPES AND CAVITIES OF FOUR CHOLIC ACID HOST SYSTEMS
Suzanne M. Evans and Carol A. Venanzi 11 Dec. 1991 14 p
(Contract N00014-88-K-0472)
(AD-A243483; TR-12) Avail: NTIS HC/MF A03 CSCL 07/4

We have continued our efforts to correlate cholic acid host shapes and relative energies by completing the conformational analyses of the m-xylylene diamine cholic acid host. The strategy previously developed, which utilizes a combination of systematic conformational searching by energy and by distance, was employed for studying the p xylylene diamine cholic acid host (pCAH) and two derivatives degraded in the side chain, one which contains the m xylylene diamine spacer. The report compiles all of the information generated on the shapes and cavities of these four cholic acid host molecules. The cavity sizes and shapes are compared to the cavity found in arabinose binding protein and speculations on the ability of monosaccharides to bind in these cavities are made. GRA

N92-17373# NSI Technology Services Corp., Dayton, OH.
EVALUATION OF THE INITIATION/PROMOTION POTENTIAL OF CTFE TRIMER ACID Final Report, Mar. 1989 - Jul. 1990
C. S. Godin, C. D. Flemming, J. M. Drerup, and H. G. Wall Nov. 1990 42 p
(Contract F33615-85-C-0532)
(AD-A243479; AAMRL-TR-90-066) Avail: NTIS HC/MF A03 CSCL 07/2

CTFE trimer acid is a metabolite of the 6-carbon oligomer of Halocarbon 3.1 oil, a nonflammable hydraulic fluid composed of perhalogenated oligomers of varying chain length. Administration of CTFE trimer acid by oral gavage for 3 months resulted in a slight increase in the rate of peroxisomal beta-oxidation, but not relative liver weight. An increase in peroxisomal beta-oxidation has been correlated with the formation of hepatic tumors. Therefore, the present study was designed to evaluate CTFE trimer acid for both tumor initiation and promoting ability. Male Sprague-Dawley rats (4 weeks old) were partially hepatectomized. Groups of animals received a single dose of CTFE trimer acid as the initiator, followed by chronic phenobarbital administration, a known tumor promotor, for either 3 or 9 months. Diethylnitrosamine, a known tumor initiator, was administered as a single dose to separate groups of animals that were administered different doses of CTFE trimer acid as a promotor for either 3 or 9 months. Quantitative sterological analysis was performed on foci from liver sections stained for a variety of histological and histochemical markers. CTFE trimer acid does not possess tumor initiation ability. However, a significant increase in foci/sq cm and foci/cu cm in livers of treated animals over those of control after 9 months of treatment clearly indicates that CTFE trimer acid has promoting activity. Interestingly, no increase in either beta-oxidation or relative liver weight was GRA

N92-17867# Argonne National Lab., IL.
PROCESS OF CONVERTING STARCH TO GLUCOSE AND GLUCOSE TO LACTIC ACID Patent Application
TenLin Tsai, inventor (to DOE), C. Y. Sanville, inventor (to DOE), R. D. Coleman, inventor (to DOE), and W. W. Schertz, inventor (to DOE) 4 Apr. 1990 17 p
(Contract W-31-109-eng-38)
(DE92-003840; US-Patent-Appl-SN-504223; Patents-US-A7504223) Avail: NTIS HC/MF A03

This document describes a method for converting starch into lactic acid of sufficient purity for use as a substrate for biodegradable plastics. The process is designed to work on industrial food waste streams such as potato wastes or cheese whey permeate. For potato waste, (alpha)-amylase and calcium chloride are added to the starch containing waste and incubated at a pH of 4-7, a temperature of 90-130 C, and a pressure above 15 psi for not less than 15 minutes. At this point, glucoamylase is added and the mixture is incubated at a temperature of 50-70 C and a pH below 6.5 for 4 hours. This results in the conversion of more than 90 percent of the starch into glucose, which is substantially free of microbial contamination. The hydrolysate is filtered, and introduced with additional nutrients to a fermentor containing a lactose producing microorganism to form a fermentation broth. This results in the fermentation of glucose to lactose, which is filtered and subjected to electrodialysis for purification. Conversion of glucose to lactic acid or lactate occurs with an efficiency of over 95 percent. DOE

N92-17882*# National Aeronautics and Space Administration. Lewis Research Center, Cleveland, OH.
SUBSTITUTED 1,1,1-TRIARYL-2,2,2-TRIFLUOROETHANES AND PROCESSES FOR THEIR SYNTHESIS Patent Application
William B. Alston, inventor (to NASA) and Roy F. Gratz, inventor (to NASA) (Mary Washington Coll., Fredricksburg, VA.) 17 Jan. 1992 24 p
(NASA-Case-LEW-14345-6; NAS 1.71:LEW-14345-6; US-Patent-Appl-SN-822240) Avail: NTIS HC/MF A03 CSCL 07A

Synthetic procedures are given for tetraalkyl, tetraacid and dianhydrides substituted 1,1,1-triaryl-2,2,2-trifluoroethanes which comprises: (1) 1,1-bis (dialkylaryl) 1-aryl-2,2,2 trifluoroethane; (2) 1,1-bis (dicarboxyaryl) 1-aryl-2,2,2 trifluoroethane; or (3) cyclic dianhydride or diamine of 1,1-bis (dialkylaryl) 1-aryl-2,2,2 trifluoroethanes. The synthesis of (1) is accomplished by the condensation reaction of an aryltrifluoromethyl ketone with a dialkylaryl compound. The synthesis of (2) is accomplished by oxidation of (1). The synthesis dianhydride of (3) is accomplished by the conversion of (2) to its corresponding cyclic dianhydride. The synthesis of the diamine is accomplished by the similar reaction of an aryltrifluoromethyl ketone with aniline or alkyl substituted or disubstituted anilines. Also, other derivatives of the above are formed by nucleophilic displacement reactions. NASA

24 COMPOSITE MATERIALS

Includes physical, chemical, and mechanical properties of laminates and other composite materials.
For ceramic materials see *27 Nonmetallic Materials*.

N92-16992# Army Lab. Command, Watertown, MA. Material Technology Lab.
NOVEL VACUUM BAG PROCESSING APPROACHES TO VOID REDUCTION IN CARBON/EPOXY COMPOSITES Final Report
Seth R. Ghiorse Sep. 1991 25 p
(DA Proj. 1L1-621-OSAH-84)
(AD-A242396; MTL-TR-91-41) Avail: NTIS HC/MF A03 CSCL 11/4

Vacuum bag and autoclave cure methods for fabricating reproducible quality polymer composites are well established and standardized. As this field of composite processing continues to mature, the thrust of developmental work naturally shifts to areas of need. One current thrust area is an expanding effort to develop more cost effective processing methods that do not sacrifice part quality. Several novel void reduction techniques were investigated in this study. They are vibration-assisted vacuum composite processing (VAVCP), porous scrim layering (PSL), microporous membrane processing (MMP), and Narmco Materials, Inc.'s Thick Laminate Prepreg (TLP). In VAVCP, low frequency vibration was applied during the pregelation period of the cure cycle of vacuum bag processed carbon/epoxy laminates. This process affected only established gas bubbles. Decreased void content in excess of 50 pct. and increased laminate densification of 0.8 pct. were measured. Data also indicated an approx. 10 pct. increase in size of the remaining voids. The PSL process had no detectable effect on void content. MMP showed the ability to remove volatile water vapor from within the preform interior. Narmco's TLP lowered void content of vacuum bag processed laminates by 50 pct. Volatile gas and mechanically entrapped gas bubbles respond to different methods of removal from the preform interior. GRA

N92-17007*# National Aeronautics and Space Administration. Langley Research Center, Hampton, VA.
THE USE OF IMPACT FORCE AS A SCALE PARAMETER FOR THE IMPACT RESPONSE OF COMPOSITE LAMINATES
Wade C. Jackson (Army Aviation Systems Command, Hampton, VA.) and C. C. Poe, Jr. Jan. 1992 27 p Presented at the Ninth DOD/FAA Conference on Fibrous Composites in Structural Design, Lake Tahoe, NV, 4-7 Nov. 1991
(NASA-TM-104189; NAS 1.15:104189; AVSCOM-TR-92-B-001) Avail: NTIS HC/MF A03 CSCL 11D

The building block approach is currently used to design composite structures. With this approach, the data from coupon tests is scaled up to determine the design of a structure. Current standard impact tests and methods of relating test data to other structures are not generally understood and are often used improperly. A methodology is outlined for using impact force as a scale parameter for delamination damage for impacts of simple plates. Dynamic analyses were used to define ranges of plate parameters and impact parameters where quasi-static analyses are valid. These ranges include most low velocity impacts where the mass of the impacter is large and the size of the specimen is small. For large mass impacts of moderately thick (0.35 to 0.70 cm) laminates, the maximum extent of delamination damage increased with increasing impact force and decreasing specimen thickness. For large mass impact tests at a given kinetic energy, impact force and hence delamination size depends on specimen size, specimen thickness, boundary conditions, and indenter size and shape. If damage is reported in terms of impact force instead of kinetic energy, large mass test results can be applied directly to other plates of the same size. Author

N92-17053# Mission Research Corp., Costa Mesa, CA.
EFFECT OF COATINGS AND PROCESSING ON FAILURE MECHANISMS OF POLYCARBONATE MATERIAL, PHASE 1 Final Report, Dec. 1988 - Jun. 1989
R. D. Eisler, A. K. Chatterjee, G. Burghart, A. H. Koivu, and C. D. Newlander Nov. 1991 205 p
(Contract DAAK60-89-C-0011)
(AD-A243018; NATICK-TR-92/004-Phase-1) Avail: NTIS HC/MF A10 CSCL 11/3

The subject effort identified the first order damage mechanisms and governing parameters contributing to the occurrence of a ductile to brittle transition in the mechanical behavior of ballistically impacted polycarbonate materials with protective coatings. Polycarbonate embrittlement is associated with a severe reduction in impact resistance as well as extensive in-plane cracking and rear surface debris. In-plane cracking can severely block the visual surface and target debris can cause debilitating eye injury. The current effort included: (1) Definition of contact pressures associated with the impact of polycarbonate material with and without protective coatings; (2) Definition of polycarbonate substrate and coating configurations of interest; (3) Stress wave response analysis; (4) Structural and fracture mechanics analysis; and, (5) Fabrication, quasistatic penetration, and ballistic testing of polycarbonate materials with or without protective coatings. Hardening recommendations designed to mitigate the influence of damage mechanisms identified as contributing to the brittle failure of polycarbonate were also rendered. GRA

N92-17310# Messerschmitt-Boelkow-Blohm G.m.b.H., Ottobrunn (Germany, F.R.). Hubschrauber und Flugzeuge.
RAPID REPAIR OF INTEGRALLY STIFFENED CARBON FIBRE COMPOSITE STRUCTURES BY BOLTED ALUMINIUM ELEMENTS
J. Vilsmeier and G. Guenther 22 May 1991 12 p
(MBB-FE202-S-PUB-0453-A; ETN-92-90616) Copyright Avail: NTIS HC/MF A03

Integrally stiffened carbon fiber composite structures, which are representative for dominantly shear and compression loaded skins of forward fuselages of modern fighter aircraft, are repaired using bolted aluminum elements. The design criteria for the repairs and the carbon fiber skin are described. The panels are tested for static and residual strength after spectrum fatigue loading. It is shown that the goal of recovering the ultimate design strength of the structure is achieved for both static and residual strength. ESA

N92-17367# Naval Postgraduate School, Monterey, CA.
STATIC ANALYSIS OF THICK COMPOSITE PLATES USING HIGHER ORDER THREE DIMENSIONAL FINITE ELEMENTS M.S. Thesis
Yair Alon Dec. 1990 99 p
(AD-A243188) Avail: NTIS HC/MF A05 CSCL 13/13

A triquadratic isoparametric solid element is developed to study the behavior of thick isotropic and laminated composite plates. The element is a 27 noded Lagrangian element based on three dimensional elasticity. Material characteristics are accounted by either using laminate plate theory or three-dimensional anisotropic theory. Element matrices for nonlinear stability analyses are derived based on total Lagrangian formulation. Results are presented to compare with analytical solutions to validate the elements behavior. The effects of various integration schemes on the element performance are presented. Convergence studies for laminated composites for different fiber orientations are provided to illustrate applications. An analysis of thin plates is carried out and results for thick plates are compared with available higher order plate theories. One row of elements in the thickness directions gives satisfactory results for thick laminates. GRA

N92-17392# Imperial Coll. of Science and Technology, London (England).
WORKSHOP FOR FINITE ELEMENT METHODS FOR COMPOSITES
Sep. 1991 71 p Workshop held in London, England, 5-6 Sep. 1991
(Contract DAJA45-91-M-0227)
(AD-A243534; R/D-6703-MS-03) Avail: NTIS HC/MF A04 CSCL 11/4

The objective of this Workshop was to consider the current position of applying the finite element method to applications involving composite materials. It was expected that issues needing attention would be identified. Some technical conclusions were as follows: (1) The actual material must be modelled; (2) Properties must be appropriate to the scale of the analysis; (3) The system must allow for correct orientation of the material; (4) It should be possible to represent (ply) discontinuities; (5) It should be possible to incorporate through-thickness modelling; (6) Specific formulation is needed to allow for iteration; (7) It should be possible to include material and geometric nonlinearity; (8) Include relevant critical mechanical properties; (9) System must be able to identify failure mode(s); and (10) Consider using spreadsheets to interface input data with FE system users need more, and better, communication with software vendors establish a system (benchmarks) for verifying results. GRA

N92-17607# Air Force Inst. of Tech., Wright-Patterson AFB, OH. School of Engineering.
THERMO-MECHANICAL FATIGUE OF A FIBER REINFORCED TITANIUM ALUMINIDE COMPOSITE M.S. Thesis Final Report
Mark A. Bates Mar. 1991 124 p
(AD-A241988; AFIT/GAE/ENY/91S-1) Avail: NTIS HC/MF A06 CSCL 11/4

The thermomechanical fatigue behavior of a specific unidirectional fiber reinforced titanium aluminide composite was investigated. Three test specimens were subjected to in-phase thermomechanical cycling and four to out-of-phase thermomechanical cycling. The applied maximum mechanical stresses ranged from 500-800 MPa. The stress ratio of 0.1 was used for all tests. The temperature range was from 150-650 C and the resulting fatigue lives were in the 58-1487 cycles range. The out-of-phase test specimens failed sooner compared to their respective in-phase counterparts. In order to find out why, the test results were analyzed using a simple micromechanics analysis and compared. The fracture surfaces from both test conditions were investigated using the scanning electron microscope.

Additionally, the test specimens were sectioned and the fatigue damage was studied in regions away from the fracture surface using a high-power optical microscope and metallography. The stresses that occurred throughout the test cycles were analyzed and related to the observed fatigue damage. The results were compared to the existing failure model for composite materials. Additionally, the results from the in-phase and out-of-phase tests were compared to isothermal and constant load test results. GRA

N92-17611# Department of the Navy, Washington, DC.
POLYMER-REINFORCED METAL MATRIX COMPOSITE Patent Application
G. J. London, W. E. Frazier, and J. G. Williams, inventors (to Navy) 19 Feb. 1991 18 p
(AD-D015070; US-Patent-Appl-SN-660364; Navy-Case-71788)
Avail: NTIS HC/MF A03 CSCL 11/4

This patent application discloses an invention that relates to metal matrix composites (MMC) materials and to polymer-reinforced metal matrix composites. The polymer filaments are formed during processing of the MMC. MMC's incorporating a less-dense reinforcing non-metal have been developed for use in low-density applications such as for aircraft components. Other improved mechanical properties are toughness, specific strength, and specific modulus of metals such as aluminum and titanium. These can be enhanced by reinforcing them with boron, carbon, or silicon carbide filaments. It is the objective of the present invention to provide a method of producing a polymer-reinforced metal matrix composite. More particularly, it is an objective to provide a method of producing a polymer-reinforced metal matrix composite wherein polymer filaments or films are formed during processing. Another object is to provide a polymer-reinforced metal matrix composite which can be subsequently processed by a variety of methods. The invention is to provide an aluminum matrix composite material with reduced density, increased specific strength, enhanced damage tolerance, and increased mechanical damping capability compared to the corresponding properties of the aluminum material alone. GRA

N92-17816# Japan Atomic Energy Research Inst., Tokyo.
EFFECT OF THERMAL ANNEALING ON PROPERTY CHANGES OF NEUTRON-IRRADIATED NON-GRAPHITIZED CARBON MATERIALS AND NUCLEAR GRAPHITE
Hideto Matsuo (Japan Atomic Energy Research Inst., Tokai.) Jun. 1991 20 p
(DE92-704180; JAERI-M-91-090) Avail: NTIS HC/MF A03

Changes in dimension of non-graphitized carbon materials and nuclear graphite, and the bulk density, electrical resistivity, Young's modulus and thermal expansivity of nuclear graphite were studied after neutron irradiation at 1128 to 1483 K and the successive thermal annealing up to 2573 K. Carbon materials showed larger and anisotropic dimensional shrinkage than that of nuclear graphite after the irradiation. The irradiation induced dimensional shrinkage of carbon materials decreased during annealing at temperatures from 1773 to 2023 K, followed by a slight increase at higher temperatures. On the other hand, the irradiated nuclear graphite hardly showed the changes in length, density and thermal expansivity under the thermal annealing, but the electrical resistivity and Young's modulus showed a gradual decrease with annealing temperature. It has been clarified that there exists a significant difference in the effect of thermal annealing on irradiation induced dimensional shrinkage between graphitized nuclear graphite and non-graphitized carbon materials. DOE

N92-17836 Department of the Navy, Washington, DC.
THERMAL INSULATION CHEMICAL COMPOSITION AND METHOD OF MANUFACTURE Patent
Thomas F. Davidson, inventor (to Navy), Guy B. Spear, inventor (to Navy), and Timothy L. Ludlow, inventor (to Navy) 11 Jun. 1991 3 p Filed 30 Nov. 1990
(AD-D015106; US-Patent-5,023,006; US-Patent-Appl-SN-621102; US-Patent-Class-252-62) Avail: US Patent and Trademark Office CSCL 11/7

A cost effective, efficient thermal insulation composition that will have long shelf life and withstand severe high temperature and pressure conditions in high temperature solid propellant gas generators can be formed of an ethylene propylene, diene monomer (EPDM)-neoprene rubber binders containing silica powder filler and aramid fibers. The specific chemical constituents include EPDM elastomer, 2 Chlorobutadiene 1,3 elastomer, Silica hydrate, Polymerized Trimethyl Dihydroquinoline, Alkylated Diphenylamines and Diphenyl-p-Phenylendiamene, 40 percent a,a' Bis (Tert-Butylperoxy), Diisopropylbenzene, Napthenic Process Oil, Synthetic Polyterpene Resin, Aramid Fiber (0.25 inch), and Zinc Oxide, Technical. GRA

N92-17861*# National Aeronautics and Space Administration. Lewis Research Center, Cleveland, OH.
INTERCALATED HYBRID GRAPHITE FIBER COMPOSITE Patent Application
James R. Gaier, inventor (to NASA) 25 Nov. 1991 13 p
(NASA-Case-LEW-15241-1; NAS 1.71:LEW-15241-1; US-Patent-Appl-SN-798464) Avail: NTIS HC/MF A03 CSCL 11D

The invention is directed to a highly conductive lightweight hybrid material and methods of producing the same. The hybrid composite is obtained by weaving strands of a high strength carbon or graphite fiber into a fabric-like structure, depositing a layer of carbon onto the structure, heat treating the structure to graphitize the carbon layer, and intercalating the graphitic carbon layer structure. A laminate composite material useful for protection against lightning strikes comprises at least one layer of the hybrid material over at least one layer of high strength carbon or graphite fibers. The composite material of the present invention is compatible with matrix compounds, has a coefficient of thermal expansion which is the same as underlying fiber layers, and is resistant to galvanic corrosion in addition to being highly conductive. These materials are useful in the aerospace industry, in particular as lightning strike protection for airplanes. NASA

N92-17869# National Aerospace Lab., Tokyo (Japan). Airframe Div.
EXPERIMENTAL INVESTIGATION OF INTERLAMINAR FRACTURE TOUGHNESS OF CARBON FIBER/THERMOPLASTIC AND CARBON FIBER/THERMOSETTING COMPOSITES BY DCB SPECIMENS
Masamichi Matsushima, Takashi Ishikawa, Youichi Hayashi, and Shigeo Kobayashi (Tokyo Metropolitan Univ., Japan) 21 Jan. 1991 25 p In JAPANESE; ENGLISH summary Original contains color illustrations
(NAL-TR-1096; ISSN-0389-4010) Avail: NTIS HC/MF A03

Experiments were performed to measure the interlaminar fracture toughness (G sub IC) of carbon fiber (CF)/epoxy and CF/PEEK composite materials using double cantilever beam (DCB) specimens. Literature survey for extracting key points in experiments was done as the first process. Results for unidirectional CF/epoxy were obtained with a simple 'piano-hinge' type of fixture. No effect of thickness and width of specimens upon G sub IC is found if a crack length is sufficiently long. Following this, DCB tests were conducted on CF/PEEK using a specially developed loading fixture capable of withstanding high peel loads. The measured G sub IC of CF/PEEK shows 20 times higher than of unidirectional CF/epoxy. The second tests after fusion bonding exhibited similar results. A comparison of the G sub IC for the original surface, the fusion bonded surface with PEEK film and adhesion surface with epoxy adhesives demonstrated that the fusion bonding is ideal for assembling thermoplastic composite structures of complicated shape. Additionally, finite element analysis was performed to show the reliability of the present experimental method. Author

N92-17870*# National Aeronautics and Space Administration. Marshall Space Flight Center, Huntsville, AL.
PRODUCTION OF MULLITE FIBERS Patent Application
Dennis S. Tucker, inventor (to NASA) and J. Scott Sparks, inventor (to NASA) 23 Dec. 1991 15 p

(NASA-Case-MFS-28431-1; NAS 1.71:MFS-28431-1; US-Patent-Appl-SN-812084) Avail: NTIS HC/MF A03 CSCL 11D

Disclosed here is a process for making mullite fibers wherein a hydrolizable silicon compound and an aluminum compound in the form of a difunctional aluminum chelate are hydrolized to form sols using water and an alcohol with a catalytic amount of hydrochloric acid. The sols are mixed in a molar ratio of aluminum to silicon of 3 to 1 and, under polycondensation conditions, a fibrous gel is formed. From this gel the mullite fibers can be produced. NASA

N92-17881*# National Aeronautics and Space Administration. Goddard Space Flight Center, Greenbelt, MD.
ACOUSTIC EMISSION MONITORING OF LOW VELOCITY IMPACT DAMAGE IN GRAPHITE/EPOXY LAMINATES DURING TENSILE LOADING
Bradford H. Parker Feb. 1992 112 p
(NASA-TM-4339; Rept-92B00027; NAS 1.15:4339) Avail: NTIS HC/MF A06 CSCL 11F

An acoustic emission (AE) system was set up in a linear location data acquisition mode to monitor the tensile loading of eight-ply quasi-isotropic graphite/epoxy specimens containing low velocity impact damage. The impact damage was induced using an instrumented drop weight tower. During impact, specimens were supported by either an aluminum plate or a membrane configuration. Cross-sectional examinations revealed that the aluminum plate configuration resulted in primarily matrix cracking and back surface fiber failure. The membrane support resulted in only matrix cracking and delamination damage. Penetrant enhanced radiography and immersion ultrasonics were used in order to assess the amount of impact damage in each tensile specimen. During tensile loading, AE reliably detected and located the damage sites which included fiber failure. All specimens with areas of fiber breakage ultimately failed at the impact site. AE did not reliably locate damage which consisted of only delaminations and matrix cracking. Specimens with this type of damage did not ultimately fail at the impact site. In summary, AE demonstrated the ability to increase the reliability of structural proof tests; however, the successful use of this technique requires extensive baseline testing. Author

N92-17932# Air Force Inst. of Tech., Wright-Patterson AFB, OH.
THE EFFECT OF PHYSICAL AGING ON THE CREEP RESPONSE OF A THERMOPLASTIC COMPOSITE Ph.D. Thesis
Robert L. Hastie, Jr. 26 Jun. 1991 242 p
(AD-A243600; AFIT/CI/CIA-91-017D) Avail: NTIS HC/MF A11 CSCL 11/4

The effect of thermoreversible physical aging on the linear viscoelastic creep properties of a thermoplastic composite was investigated. Radel X/IM7, an amorphous composite material considered for use in the next generation high speed transport aircraft, was studied. The operating environment for the aircraft material will be near 188 C (370 F) with a service life in excess of 60,000 hours at temperature. Accurate predictions of the viscoelastic properties of the material are essential to insure that design strength and stiffness requirements are met for the entire service life. The effect of physical aging on the creep response was studied using momentary tensile creep tests conducted at increasing aging times following a rapid quench from above the glass transition temperature T(sub g) to a sub-T(sub g) aging temperature. GRA

N92-17950# Brown Univ., Providence, RI. Div. of Engineering.
DAMAGE MECHANISMS IN COMPOSITES Final Report
Aug. 1991 41 p
(Contract N00014-86-K-0125)
(AD-A242748) Avail: NTIS HC/MF A03 CSCL 20/11

Mechanically induced residual stresses are an inherent feature of permanently deformed metal-matrix composites such as aluminum/silicon carbide. The presence of hard SiC reinforcements promotes non homogeneous flow in the matrix, resulting in residual stresses when the applied loads are removed. These residual stresses are potentially important because of the effect on cavitation and other damage mechanisms leading to composite failure. We have attempted to simulate the residual stresses in the composite by solving appropriate boundary value problems using finite element method. Using this approach, we have compared predicted average residual elastic strains with those measured by neutron diffraction for Al/SiC composites subjected to different loading histories. The composite studied was a 2009 aluminum alloy reinforced with 15 percent vol SiC whiskers. Samples were subjected to various levels of plastic strain and unloaded before measuring peak shifts in neutron diffraction patterns to determine residual strains. Other research related to creep damage mechanisms in ceramic matrix composites are also discussed. GRA

25 INORGANIC AND PHYSICAL CHEMISTRY

Includes chemical analysis, e.g., chromatography; combustion theory; electrochemistry; and photochemistry.

For related information see also *77 Thermodynamics and Statistical Physics.*.

N92-16977# Columbia Univ., New York, NY.
DYNAMICS AND STABILIZATION OF MATERIALS POSSESSING HIGH ENERGY CONTENT Final Technical Report, 1 Nov. 1989 - 31 Oct. 1991
Nicholas J. Turro 31 Oct. 1991 8 p
(Grant AF-AFOSR-0049-90; AF Proj. 2303)
(AD-A243030; AFOSR-91-0919TR) Avail: NTIS HC/MF A02 CSCL 19/1

The objectives of the research supported by this AFOSR grant were to create new knowledge concerning the nature and behavior of high energy content materials adsorbed at the liquid-liquid, liquid-solid, and the solid-gas interfaces. The strategy employed was to use photochemical reactions and photophysical parameters as probes to characterize the structure and dynamics of high energy species. The reactions of radical pairs produced by photochemical excitation of ketones and the electron transfer process between a metal complex and an electron acceptor were employed as general photochemical probes of a range of interfacial regions. The techniques used were a battery of time resolved spectroscopic methods including optical absorption, optical emission, nuclear magnetic resonance and electron spin resonance. The objects achieved were the development of a framework which now allows both the chemistry of high energy species adsorbed at interfaces to be controlled and manipulated and the structure and dynamics of the interfacial region to be better understood. GRA

N92-17043# Texas Univ., Austin. Dept. of Chemistry.
NEW EXPERIMENTAL CHALLENGES IN ELEMENTAL FLUORINE CHEMISTRY: AN EMERGING TECHNOLOGY Final Report, 1 Dec. 1987 - 30 Nov. 1990
Richard J. Lagow Oct. 1991 27 p
(Grant AF-AFOSR-0084-88)
(AD-A243054; AFOSR-91-0926TR) Avail: NTIS HC/MF A03 CSCL 07/3

A controlled fluorination method using elemental fluorine has been used to synthesize a large variety of new compounds from hydrogen-containing precursors including perfluoroethers, perfluoroplyethers, perfluoro crown ethers, and perfluorocryptands. Polyesters were converted to polyethers using a combination of direct fluorination of the carbon hydrogen bonds and fluorination by SF4 of the carbonyl groups. A process was developed for partial fluorination of gas separation membranes. The selectivity of the membranes for size separation was increased significantly up to 10(exp 3). GRA

N92-17091# Air Force Inst. of Tech., Wright-Patterson AFB, OH. School of Engineering.
VIBRATIONAL ENERGY TRANSFER IN BROMINE MONOFLUORIDE M.S. Thesis
Tim L. Thompson Dec. 1991 80 p
(AD-A243690; AFIT/GEP/ENP/91D-8) Avail: NTIS HC/MF A05 CSCL 07/4

Bromine monofluoride (BrF), an interhalogen molecule, is a prospective chemical laser candidate. This study continues research begun in characterizing radiative and collisional dynamics in BrF. Vibrational energy transfer of BrF is studied using time resolved laser induced fluorescence (LIF) techniques and observing the spectrally resolved emission. First, vibrational transfer induced by the BrF production mix is determined to follow the Montroll-Shuler model and Landau-Teller scaling with a fundamental rate coefficient of k sub v (1,0) = (4.0 +/- 0.5) x 10 exp -12 cc/(molecules seconds). Also, rate coefficients for the rare gases were found to scale with the reduced mass of the collision partner, as predicted by the Schwartz, Slawsky, and Herzfeld (SSH) theory with values ranging from (3.9 +/- 0.7) x 10 exp -12 cc/(molecules x seconds) for helium to (2.2 +/- 0.3) x 10 exp -13 cc/(molecules x seconds) for xenon. GRA

N92-17210# University of Southern California, Los Angeles.
NITRATION AND NITROCOMPOUNDS Final Report, 1988 - 1991
1991 9 p
(Contract N00014-88-K-0361)
(AD-A243380) Avail: NTIS HC/MF A02 CSCL 07/3

In the course of studying new superacid system in nitration, we evaluated the nitric tetratriflatoboric acid system HNO3-HB(O3SCF3)4 for its nitrating ability of aromatics. Tetratriflatoboric acid, HB(O3SCF3)4 was conveniently prepared in situ from triflic acid (excess) and boron trichloride and could be used without any workup. Nitration of benzene, toluene, fluorobenzene, chlorobenzene, anisole and naphthalene was studied with HNO3-HB(O3SCF3)4 in methylene chloride solution at -30 C and at room temperature. the new superacidic nitration of toluene gave very low (1 percent) meta nitration both at -30 C and at room temperature. At the same time the ortholpara isomer ratio is also lower than in most studied nitronium ion nitrations, indicating ion pairing or association with bulky tetratriflatoborate anion. Similarly high regio(positional) selectivity was found in nitration of the other aromatics. GRA

N92-17246# North Carolina Univ., Chapel Hill. Dept. of Chemistry.
AN OXYGEN TRACER STUDY OF InP OXIDATION
X. Liu, M. S. Denker, and E. A. Irene Nov. 1991 19 p
(Contract N00014-89-J-1178)
(AD-A242832; TR-37) Avail: NTIS HC/MF A03 CSCL 07/4

The thermal oxidation process for InP results in a complex and process dependent oxide. From the observed self limiting behavior of the oxide growth, the rate limiting step is likely the diffusion of reaction species through the growing oxide film. O-18 marker oxidation experiments with the resulting secondary ion mass spectroscopy (SIMS) depth profiles reveal that the oxidation takes place at the oxide surface by the outward migration of In and P, rather than at the oxide substrate interface. Based on the available results possible models for the oxidation are proposed. GRA

N92-17247# North Carolina Univ., Chapel Hill. Dept. of Chemistry.
AN IN-SITU SPECTROSCOPIC ELLIPSOMETRY STUDY OF THE ELECTRON CYCLOTRON RESONANCE PLASMA OXIDATION OF SILICON AND INTERFACIAL
Y. Z. Hu, J. Joseph, and E. A. Irene Nov. 1991 15 p
(Contract N00014-89-J-1178)
(AD-A242833; TR-35) Avail: NTIS HC/MF A03 CSCL 07/4

The growth of silicon dioxide films on silicon and the evolution of interfacial damage resulting from electron cyclotron resonance plasma oxidation was studied using in situ during process spectroscopic ellipsometry. Accelerated growth under positive substrate bias indicates that negative atomic species dominate the growth above an oxide thickness of 4 nm. Below this thickness bias appears less important. The interfacial damage is different in both nature and extent from that caused by ions with higher energies. It appears that the damage layer is composed of SiO2 with alpha Si and is due to the oxidation reaction rather than the ions from the plasma. GRA

N92-17248# North Carolina Univ., Chapel Hill. Dept. of Chemistry.
INFRARED ROTATING ANALYZER ELLIPSOMETRY: CALIBRATION AND DATA PROCESSING
V. A. Yakovlev, M. Li, and E. A. Irene Nov. 1991 31 p
(Contract N00014-89-J-1178)
(AD-A242834; TR-40) Avail: NTIS HC/MF A03 CSCL 14/2

The necessary relationships and a calibration procedure is presented for a rotating analyzer infrared ellipsometer that uses wire grid polarizing optics. The wire grid polarizers contribute significant ellipticity due to relatively low extinction ratios. Jones matrices are used for the quarter-wave-plate, polarizer, sample, rotating analyzer ellipsometer configuration. Results from a calibrated infrared and visible light ellipsometer for silicon dioxide films on silicon are compared. GRA

N92-17261# North Carolina Univ., Chapel Hill. Dept. of Chemistry.
A SPECTROSCOPIC IMMERSION ELLIPSOMETRY STUDY OF THE MECHANISM OF Si/SiO2 INTERFACE ANNEALING
V. A. Yakovlev, Q. Liu, and E. A. Irene Nov. 1991 34 p
(Contract N00014-89-J-1178)
(AD-A242831; TR-41) Avail: NTIS HC/MF A03 CSCL 07/4

In this study we apply an interface sensitive ellipsometry technique to study the evolution of the Si-SiO, interface as a function of high temperature annealing (750 to 1100 C). Essentially, the ellipsometry technique embodies the use of liquids that refractive index match with the bulk film thereby removing the optical response of the overlayer and greatly enhancing sensitivity to the interface. According to both time and temperature of anneal, distinct modes of behavior are observed for the evolution of the interface. For short anneal times a rapid change in the interface is observed that correlates with the disappearance of protrusions, followed by a slower change that correlates with the disappearance of the suboxide. At high temperatures viscous relaxation dominates while at low temperatures the suboxide reduction is apparent. A model for the interface in terms of chemical and physical interface processes is proposed and model parameters are compared with literature results. GRA

N92-17323# Puerto Rico Univ., Rio Piedras. Dept. of Physics.
ESTIMATION OF THE OUTER SPHERE CONTRIBUTION TO THE ACTIVATION PARAMETERS FOR HOMOGENEOUS ELECTRON TRANSFER REACTIONS USING THE MEAN SPHERICAL APPROXIMATION Summary Report
W. R. Fawcett and L. Blum 9 Nov. 1991 19 p
(Contract N00014-90-J-1263)
(AD-A243217; TR-14) Avail: NTIS HC/MF A03 CSCL 07/4

Estimation of the outer sphere contribution to the Gibbs energy and enthalpy of activation for homogeneous electron transfer is described on the basis of the mean spherical approximation (MSA). It is shown that these quantities for spherical reactants are significantly smaller than those estimated by the Born continuum model. MSA estimates and experimental values of the activation enthalpy for the cobaltacene/cobaltacenium cation redox couple are found to agree very well with one another. The assumptions used in applying the MSA in the present paper and in earlier work are discussed. GRA

N92-17371# Puerto Rico Univ., Rio Piedras. Dept. of Physics.
APPLICATION OF THE MEAN SPHERICAL APPROXIMATION TO DESCRIBE THE GIBBS SOLVATION ENERGIES OF MONOVALENT MONOATOMIC IONS IN NON-AQUEOUS SOLVENTS

L. Blum and W. R. Fawcett 9 Nov. 1991 36 p
(Contract N00014-90-J-1263)
(AD-A243200; TR-13) Avail: NTIS HC/MF A03 CSCL 07/4

The mean spherical approximation for the ion-dipole mixture is used to study the solvation energies of monovalent monoatomic ions in polar solvents. From the structure of the analytical solution it is inferred that there are two parameters that should be used to describe the solvation: the dielectric constant and a polarization parameter which plays the role of a mean field parameter to account for nonsphericity, chemical interactions, and other effects related to failure of the hard sphere model for the system. The model was successfully fitted to data for the Gibbs solvation energy of five alkali metal cations and their halide ions in 17 different solvents including water. On the basis of this analysis, it was shown that a single value of the polarization parameter describes the data for the cations in each solvent, a quite different value being appropriate for the anions. The polarization parameters were found to be linearly correlated with empirical parameters characterizing the solvents basicity in the case of cations, and its acidity in the case of anions. GRA

N92-17389# Harvard Univ., Cambridge, MA. Dept. of Chemistry.
OMEGA-TERMINATED ALKANETHIOLATE MONOLAYERS ON SURFACES OF COPPER, SILVER AND GOLD HAVE SIMILAR WETTABILITIES
Paul E. Laibinis and George M. Whitesides Dec. 1991 51 p
(Contract N00014-86-K-0756)
(AD-A243529; TR-40) Avail: NTIS HC/MF A04 CSCL 07/3

Long chain alkanethiols (HS(CH2)nX) adsorb from solution onto the surfaces of freshly evaporated copper, silver and gold films and form oriented monolayers. Both polar and non-polar tail groups (X) can be accommodated in these adsorptions. Adsorption on all three metals generates self-assembled monolayers (SAMs) exhibiting similar wetting properties, and thus, by inference, having related oriented structures. XPS data suggest that the omega-terminated eta-alkanethiolate monolayers, like those derived from simple alkanethiols, are composed of trans-extended chains having orientations on copper and silver that are closer to the perpendicular to the surface than are those on gold. We have prepared and characterized monolayers (mixed monolayers) by exposure of all three metals to mixtures of HS(CH2)11OH and HS(CH2)11CH3. GRA

N92-17489# Case Western Reserve Univ., Cleveland, OH. Dept. of Chemistry.
STUDIES OF THE ADSORPTION OF TETRASULFONATED PHTHALOCYANINES ON GRAPHITE SUBSTRATE Technical Report, 1990 - 1991
S. Gupta, H. Huang, and E. Yeager 1991 7 p
(Contracts N00014-83-C-3043; N00014-90-J-1212)
(AD-A243443; TR-86) Avail: NTIS HC/MF A02 CSCL 07/4

The adsorption of iron and cobalt tetrasulfonated phthalocyanines (TsPcs) on ordinary pyrolytic graphite has been investigated as a function of pH and ionic strength of the adsorption solution as well as the potential. The charge corresponding to the voltammetric redox peaks of adsorbed complexes was used as a measure of the surface concentration. Adsorption of CoTsPc occurs readily from its freshly prepared aqueous solutions and is generally independent of pH. For FeTsPc, however, adsorption does strongly depend on pH. High surface coverage is achieved only from acid solutions rather than from pure water and alkaline solutions. This can be explained in terms of the form(s) of the complexes existing in the solution phase in the presence of air uv-visible spectroscopic studies coupled with the addition of CN to the macrocycle solutions provide evidence that in pure water and alkaline solutions FeTsPc exists predominantly in the u-oxo from (FeTsPc)O, which seems not to favor the adsorption process. GRA

N92-17572# Kings Coll., London (England). Dept. of Physics.
PERMITTIVITY PROBE MODELLING Final Technical Report, Sep. 1989 - Jul. 1990
Camelia Gabriel Nov. 1991 41 p
(Contract F33615-87-D-0626)
(AD-A243236; AL-TR-1991-0055) Avail: NTIS HC/MF A03 CSCL 07/4

An HP 8720 automatic network analyzer has been used with a custom made coaxial probe to measure the complex permittivity of standard limits in the frequency range 130 MHz to 20 GHz. Three equivalent circuit models were used to simulate the admittance of the probe sample interface. The expediency and limitations of these models have been studied. A critical review of these simulations is presented and illustrated by experimental evidence. Measurements were performed on high and low loss materials to test the power and versatility of the adopted technique. Its accuracy and reproducibility compare favorably with the well established, in-guide, techniques. This technique is well suited for applications in the fields of biomedicine, material studies and industrial development and control. GRA

N92-17613# North Carolina Univ., Chapel Hill. Dept. of Chemistry.
AN INTERFACE ENHANCED SPECTROSCOPIC ELLIPSOMETRY TECHNIQUE: APPLICATION TO Si-SiO2 Interim Report
V. A. Yakovlev and E. A. Irene Nov. 1991 33 p
(Contract N00014-89-J-1178)
(AD-A242867; TR-39) Avail: NTIS HC/MF A03 CSCL 09/1

In this research we demonstrate an ellipsometry technique that is sensitive to the interfacial region between a dielectric film and substrate. Essentially, a film and substrate is immersed in a liquid that index matches to the film, thereby optically removing the film from the measurement. In addition, the use of spectroscopic and multiple angles of incidence ellipsometry provides sufficient specification of the interface parameters which along with the enhanced sensitivity to the interface, enables the optical measurement of the interfacial properties. Theoretical and experimental verification is provided along with application to the Si-SiO2 interface. GRA

N92-17628# Department of the Navy, Washington, DC.
CONCENTRATION OF ISOTOPIC HYDROGEN BY TEMPERATURE GRADIENT EFFECT IN SOLUBLE METAL Patent Application
Han S. Uhm, inventor (to Navy) and Woodrow W. Lee, inventor (to Navy) 23 Aug. 1991 30 p
(AD-D015062; US-Patent-Appl-SN-749357; Navy-Case-73550)
Avail: NTIS HC/MF A03 CSCL 20/5

This invention relates to the enrichment of isotopic hydrogen in a solid-state metal by use of temperature gradient effects, and is related to the subject matter disclosed in prior copending application Serial No. 07/724,083, filed July 1, 1991. High concentration of isotopic hydrogen in the form of deuterium atoms in a soluble metal such as palladium, is very useful for various electro-chemical studies including nuclear fusion investigations. A conventional technique used for deuterium enrichment purposes involves electrolysis, where a palladium rod is immersed in heavy water as the cathode. According to the aforementioned prior copending application, deuterium density inside a palladium rod is increased by making use of plasma ion implantation. GRA

N92-17682# General Electric Co., Schenectady, NY. Engineering Systems Lab.
LOCAL EXTINCTION MECHANISMS IN NON-PREMIXED TURBULENT COMBUSTION Final Report, 1 May 1988 - 30 Jun. 1990
S. M. Correa and A. Gulati 31 Aug. 1991 78 p
(Contract F49620-88-C-0066)
(AD-A242027; AFOSR-91-0871TR) Avail: NTIS HC/MF A05 CSCL 21/2

The goal of this research was a quantitative understanding of turbulence-chemistry interactions pertinent to future aeropropulsion combustors. For example: (1) flameout and relight in turbine combustors are related to interactions of turbulence with chain-branching reactions; (2) hydrogen burnout in supersonic combustors is related to interactions with recombination reactions;

and (3) emissions of NO(x), CO, smoke, and other observables are related to nonequilibrium in the populations of intermediate species such as oxyhydrogen radicals and C(x)H(y). A bluff-body stabilized turbulent diffusion flame, time-and space-resolved laser Raman measurements of major species, and a nonequilibrium computational fluid mechanics code were applied to the problem. Principal conclusions include: (1) turbulent jet flames are being abandoned in the search for more intensely turbulent flames; (2) an axisymmetric bluff-body stabilized turbulent diffusion flame burner is a reasonable choice for combustion research at high Reynolds numbers, approaching blowoff; (3) Raman scattering for measurements of major species and temperature can be extended into the sooting/chemiluminescent environment of methane flames--space and time resolved Raman scattering measurements were made in bluff-body stabilized CO/H2/N2 and CH4 flames at conditions approaching blowoff; (4) a thermochemical submodel based on partial equilibrium in the oxyhydrogen radical pool was developed for the 27.5 percent CO/32.3 percent H2/40.2 percent N2-air system; (5) calculations compare favorably with with the Raman data; (6) work on pdf transport/Monte Carlo methods in recirculation-stabilized flames has begun; and (7) the range of turbulence-chemistry interactions in combustion has been quantified, in an attempt to gauge the universality of turbulence-chemistry models. GRA

N92-17727# Los Alamos National Lab., NM.
DIRECT SPECIATION OF METAL AND METALLOID IONS BY OPTICAL SPECTROSCOPIES
C. D. Tait, D. R. Janecky, D. L. Clark, S. A. Ekberg, P. R. Dixon, J. A. Musgrave, and P. C. Bennett (Texas Univ., Austin.) 1991 15 p Presented at the Basic Energy Sciences/Geosciences (BES) Review Workshop, Norman, OK, 18-19 Nov. 1991
(Contract W-7405-eng-36)
(DE92-003868; LA-UR-91-3498; CONF-9111114-2) Avail: NTIS HC/MF A03

Molecular level spectroscopic investigations of organic/-inorganic interactions provide important new information on sedimentary geochemistry through the identification of interactions over moderate temperature and pH ranges. Although the official title of this project indicates the use of only optical spectroscopies, a combination of Uv/Vis/IR absorption, Raman scattering, and Si-29 and C-13 nuclear magnetic resonance (NMR) experiments are actually employed. A major advantage of integrating spectroscopic results with diagenesis studies is the ability to directly examine the mechanisms of interactions, even in complex matrices and with competing processes. Furthermore, we are extending these techniques to probe fluid inclusions with micro-Raman and luminescence techniques to directly compare laboratory results with natural reservoir systems. DOE

N92-17740# Mound Lab., Miamisburg, OH.
CHROMATOGRAPHIC SEPARATION OF CALCIUM ISOTOPES
M. A. Novotny 20 Nov. 1991 16 p
(Contract DE-AC04-88DP-43495)
(DE92-004623; MLM-3716) Avail: NTIS HC/MF A03

Breakthrough chromatography was explored as a technique of separating Ca-44 and Ca-40 isotopes. The solid phase utilized polymer-bound 18-crown-6 compounds. The effect of adding dimethylsulfoxide (DMSO) to the fluid phase solution of methanol and chloroform was found to increase the separation coefficient from 0.0025 +/- 0.0003 to 0.0035 +/- 0.0003. Robotic sample preparation increased the accuracy and efficiency of the system. DOE

N92-17786# National Academy of Sciences - National Research Council, Washington, DC. Commission on Physical Sciences, Mathematics, and Applications.
CATALYSIS LOOKS TO THE FUTURE
1992 93 p Sponsored in cooperation with Air Products and Chemicals, Inc., Catalytica, Inc., Chevron Research Co., Dow Chemical USA, Exxon Research and Engineering Co., E. I. Du Pont de Nemours and Co., Inc., Mobil Research and Development Corp., and UOP, Inc. Original contains color illustrations
(Contract DE-FG05-90ER-14103; NSF CTS-89-21829; NSF CHE-89-21664)
(LC-91-66333; ISBN-0-309-04584-3) Avail: NTIS HC/MF A05

Catalysis plays a fundamental role in the economy, environment, and the public health of the nation. Specifically, two of the largest industry segments, chemicals and petroleum processing, depend on catalysis; many of the modern, cost, and energy efficient environmental technologies are catalytic; and biocatalysis offers exciting opportunities for producing a broad range of pharmaceuticals and specialty chemicals. The research opportunities and challenges are identified for catalysis in the coming decades. Chapter 1 provides an introduction to the science and technology of catalysts. Chapter 2 discusses the opportunities for developing new catalysts to meet the demands of the chemical and fuel industries, and the increasing role of catalytic technology in environmental protection. The intellectual challenges for advancing the frontiers of catalytic science are outlined in chapter 3. The human and institutional resources available in the U.S. for carrying out research on catalysis are summarized in chapter 4. The findings and recommendations for industry, academe, the national labs, and the Federal government are presented in fuller detail in chapter 5. Author

N92-17788# West Virginia Univ., Morgantown. Dept. of Chemical Engineering.
REACTION KINETICS AND TRANSPORT PROPERTIES OF THE CaO-SO2-O2 SYSTEM IN ABSENCE OF INTRA-PARTICLE DIFFUSION
Jan. 1991 35 p
(Contract DE-FC21-87MC-24207)
(DE91-002086; DOE/MC-24207/3005) Avail: NTIS HC/MF A03

This work examines the CaO-SO2-O2 chemical reaction system, with emphasis on gas diffusivity through the CaSO4 product layer. A mathematical model was developed to obtain intrinsic chemical kinetics, such as, order of reaction, reaction rate constants and SO2 gas diffusion coefficient through the CaSO2 product layer. To obtain the experimental data, equipment and procedures were developed using thermal gravimetric analysis for recording weight changes of a single CaO crystal during the reaction. For three different origins of CaO single crystals, kinetic data for the CaO-SO2-O2 reaction system, such as reaction order, rate constant, and SO2 diffusion coefficients through the product layer, were obtained experimentally without any numerical fitting technique. DOE

N92-17841# Messerschmitt-Boelkow-Blohm G.m.b.H., Munich (Germany, F.R.). Berichtsstelle.
LIGHT-CONTROLLED, ELECTROCHEMICAL, ANISOTROPIC ETCHING OF SILICON
R. Voss, Helmut Seidel, and H. Baumgaertel (Freie Univ., Berlin, Germany, F.R.) 29 Jan. 1991 5 p Presented at the Tranducers 1991 Conference, San Francisco, CA, 23-27 Jun. 1991
(MBB-Z-0368-91-PUB; ETN-92-90599) Avail: NTIS HC/MF A01

The process of electrochemical silicon etching in alkaline solutions is found to depend on illumination by light. Experiments in 30 percent KOH reveal that on p-type samples, this shift goes towards negative values. Etching can be initiated by light on p-type silicon when a potential slightly above etch stop is chosen. Etching in progress can be stopped by light on n samples when a potential slightly below etch stop is chosen. These effects are expected to open up new possibilities for micromachining such as light controlled etching of n-Si membranes or light induced anisotropy effects in p-Si. ESA

N92-17902*# National Aeronautics and Space Administration. Lewis Research Center, Cleveland, OH.
STORING FLUORINE GAS IN CARBON FIBERS AND RELEASING THE SAME Patent Application
Ching-Cheh Hung, inventor (to NASA) 26 Nov. 1991 14 p
(NASA-Case-LEW-15359-1; NAS 1.71:LEW-15359-1; US-Patent-Appl-SN-797484) Avail: NTIS HC/MF A03 CSCL 07D

Fluorine gas stored in pitch-based graphitized carbon fibers is

released by heating to a temperature between 250 C and 400 C. The fluorine is then used to conduct fluorination reactions.
NASA

N92-17925# Technische Univ., Eindhoven (Netherlands).
PROPANE AROMATIZATION OVER GALLIUM CONTAINING HZSM-5 ZEOLITES Ph.D. Thesis
Cornelis Roeland Baijense 24 Sep. 1991 194 p Sponsored by Netherlands Organization for Applied Scientific Research TNO
(ETN-92-90897) Avail: NTIS HC/MF A09

The aromatization of propane using zeolites containing gallium as catalyst, with attention paid to aspects of (mechanism of) the reaction but also regarding the properties of the catalyst, is described. The chemical properties of different forms of gallium oxide are described and the Ga/H(Al)ZSM5 system as a catalyst for hydrocarbon conversions is introduced. The synthesis and characterization of H(Ga)ZSM5 gallosilicates and H(AlZSM5) zeolites containing gallium is described. A study of the nature of the active gallium species, and its role in the separate ractions steps, gives results from which a mechanism for molecular hydrogen formation is proposed. The influence of the preparation method on the deactivation behavior of the Ga/H(Al)ZSM5 system is shown. Attempts are made for the selective removal of gallium from the H(Al+Ga)ZSM5 framework, in order to obtain a H(Al)ZSM5 zeolite with highly dispersed gallium oxide in hot pores. The Ga-71 MAS (Magic Angle Spinning) NMR (Nuclear Magnetic Resonance) framework gallium is shown to be distinguishable from extra framework gallium in steam treated samples. The main causes for the line broadening of the Ga-71 (MAS) NMR lines are shown and the quantitative aspects of this technique are described. Experiments using Zn/H(Al)ZSM5 zeolites are described for comparison with gallium. ZnAl coprecipitates are also used as co-catalysts in the reaction. The synthesis and characterization of GAPSO-11 molecular sieves and their application in hydrocarbon conversions are described. ESA

N92-17943# International Centre for Theoretical Physics, Trieste (Italy).
KINETICS OF A NEW PHASE FORMATION IN SUPERSATURATED SOLID SOLUTIONS. 1. DILUTE ONE-COMPONENT SYSTEMS
V. I. Dubinko Jul. 1991 6 p
(DE92-610065; IC-91/151) Avail: NTIS HC/MF A02

A complete set of kinetic equations describing the diffusion decay of supersaturated solutions, as well as the formation of new-phase fluctuations in equilibrium systems, is derived. A novel method of determining forward and backward reaction rates entering the master equation is proposed which does not require the use of any reference cluster size distribution, either the constrained or the true equilibrium one, employed in all modifications of the classical nucleation theory. Instead, this reference distribution can be obtained as an equilibrium solution of the present master equation. The main advantage of this method is the possibility to take into account various factors affecting the diffusion decay, such as the reaction kinetics at the precipitate surfaces and the diffusion kinetics in the mother phase with account of elastic interaction between nucleating species and their clusters. The latter is of a key importance in the irradiation environment considered in the forthcoming second part of the article. DOE

26 METALLIC MATERIALS

Includes physical, chemical, and mechanical properties of metals, e.g., corrosion; and metallurgy.

N92-16985# Puerto Rico Univ., Rio Piedras. Dept. of Physics.
IN SITU SURFACE X RAY SCATTERING OF METAL MONOLAYERS ADSORBED AT SOLID-LIQUID INTERFACES Summary Report
Michael F. Toney, Joseph G. Gordon, and Owen R. Melroy 9 Nov. 1991 15 p Prepared in cooperation with International Business Machines Corp.
(Contract N00014-90-J-1263)
(AD-A243258; TR-9) Avail: NTIS HC/MF A03 CSCL 07/4

The structure of the solid-liquid interface is of fundamental importance in chemistry, but progress in understanding this interface has been slow, due to the lack of in-situ probes that provide information at atomic scales. Recently, in-situ surface X ray scattering measurements have provided insight into the microscopic nature of solid-liquid interfaces and this paper will discuss experiments on electrochemically deposited monolayers of Pb, Tl, and Bi on Ag and Au (111) electrodes. GRA

N92-17000# Naval Postgraduate School, Monterey, CA.
A POWDER X RAY DIFFRACTION STUDY OF TWO ALUMINUM-LITHIUM BASED ALLOYS M.S. Thesis
Te-Kang Wang Mar. 1991 61 p
(AD-A243186) Avail: NTIS HC/MF A04 CSCL 11/6

The microstructures of solution treated, quenched and aged Al-2.5 wt. pct. Li and Al-2.0 wt. pct. Li-2.76 wt. pct. Mg-1.03 wt. pct. Cu alloys were studied by powder X ray diffraction. The as-quenched alloys showed extensive X ray line broadening due to particle size effects and the intensity measurements indicated a significant amount ordering in the as-quenched state. These results were interpreted using a 'spinodal ordering' model which suggests that Al-Li-based alloys order during quenching and then spinodally decompose into regions of order and disorder so that the final microstructure comprises small ordered regions (size 40 nm) in a disordered matrix. Studies on the aged Al-2.5 wt. pct. Li alloy indicated that after initial short time aging, particle growth follows Ostwald ripening kinetics in agreement with previous work. Studies on the aged quaternary alloy indicated that Tl and S phases grow in this system so that precipitates are not a dominant strengthening mechanism in this alloy. GRA

N92-17056# David Taylor Research Center, Bethesda, MD. Ship Materials Engineering Dept.
AN OPTICAL ROUGHNESS SENSOR FOR THE REAL TIME DETERMINATION OF SPRAY FORMED PREFORM QUALITY Research and Development Report, Apr. - Jul. 1991
Rochelle D. Payne, Angela L. Moran, Craig J. Madden, and Paul Kelley Jul. 1991 34 p
(AD-A243238; DTRC/SME-91/51) Avail: NTIS HC/MF A03 CSCL 11/6

The emphasis in this paper is on the application of spray forming control strategies towards the use of a laser stripe sensor for the calculation of root mean square (RMS) preform surface roughness. The objective of this study is to correlate this calculation of roughness with the preform quality. Spray forming is a relatively new processing technique in which a stream of molten metal is atomized by an inert gas, producing a spray of liquid droplets. These droplets are cooled by the atomizing gas and accelerate towards a substrate where they consolidate to form a near fully dense deposit. The spray formed product is similar to the powder metallurgy product in that it has a rapidly solidified, grain-refined microstructure with limited segregation. However, unlike powder metallurgy, spray forming is free from the time consuming and costly steps of powder production, storage and handling, sintering and hot consolidation. Recent work at David Taylor Research Center evaluated the feasibility of utilizing (Osprey) spray forming to produce a variety of alloys including nickel base alloys, steel, bronzes and copper-base alloys for military applications. An extensive study of Alloy 625 indicated that the spray formed materials had equivalent or superior properties to the conventionally and powder metallurgy processed materials at a reduced production cost. GRA

N92-17057# David Taylor Research Center, Bethesda, MD. Ship Materials Engineering Dept.
THE EFFECT OF WELD METAL STRENGTH MISMATCH ON THE DEFORMATION AND FRACTURE BEHAVIOR OF STEEL BUTT WELDMENTS Research and Development Report, Sep. 1990 - Jan. 1991

Mark T. Kirk Jan. 1991 59 p
(AD-A243239; DTRC/SME-91/06) Avail: NTIS HC/MF A04
CSCL 11/6

Considerable naval and industrial experience has indicated the engineering utility of using weld metal having strength greater than the plates being joined (over-matching). Overmatching shields the weld region, which typically has lower toughness than the plate and is often the site of defects, from the high strains that develop during an overload. This practical advantage, coupled with the ease of achieving overmatch in lower strength steel alloys (80 ksi yield strength or less) has led to codification of overmatching as a requirement in most structural design codes and fabrication specifications. However, overmatching has certain economic and technical disadvantages which undermatched (weld metal strength less than plate strength) systems might alleviate. This report reviews investigations concerning the deformation and fracture characteristics of simple mechanical test specimens containing butt welds, focusing on how the relative strength of the weld deposit and the plate influences these characteristics. All analytical and experimental evidence available indicates that plastic strain concentrates into the zone of the lowest material strength in a transversely loaded weldment. Thus, plastic strains in undermatched weldments concentrate in the weld deposit while in overmatched weldments they concentrate in the plate. GRA

N92-17264# Aeronautical Research Labs., Melbourne (Australia).
METALLOGRAPHY OF ALUMINIDE COATINGS
P. Rohan May 1991 28 p
(AD-A243000; ARL-MAT-TM-404; DODA-AR-006-602) Avail: NTIS HC/MF A03 CSCL 11/6

The Corrosion Control group at ARL has commenced a program for evaluating protective coatings for gas turbine blades currently used by the RAAF (work previously performed at MRL). To enable examination and evaluation of metallographic specimens (with particular attention given to surface features), techniques have been developed for sample preparation and microstructural etching. In developing these techniques, Allison T-56 turbine engine blades cast from a nickel based superalloy (IN 738) and coated with nickel aluminide were sectioned. The nickel aluminide coating applied by a high activity pack cementation process to the outer surface of the blades, imparts oxidation/corrosion resistance to the substrate superalloy. Metallographic procedures were developed with an aim to minimize edge rounding and highlight the detailed microstructure by selective etching. GRA

N92-17271# Puerto Rico Univ., Rio Piedras. Dept. of Physics.
AN INVESTIGATION OF UNDERPOTENTIALLY DEPOSITED THALLIUM OF SILVER (111) BY IN-SITU SURFACE X RAY SCATTERING Summary Report
Joseph G. Gordon, Michael F. Toney, Mahesh G. Samant, Gary L. Borges, and Owen R. Melroy 9 Nov. 1991 43 p
(Contract N00014-90-J-1263)
(AD-A243270; TR-10) Avail: NTIS HC/MF A03 CSCL 07/4

Using in-situ surface x ray scattering, we have investigated the atomic structure, the stability, and the dependence of the structure on electrode potential for electrochemically deposited Tl monolayers and bilayers on Ag (111). The layers were formed by underpotential deposition (UPD) at electrode potentials positive of the reversible potential for bulk Tl deposition. At potentials between -475 and -680 mV (vs. Ag/AgCl), the Tl deposit forms an incommensurate, hexagonal two dimensional (2D) monolayer that is compressed relative to bulk Tl by 1.4 to 3.0 pct. and rotated from the Ag and roll direction by omega = 4 to 5 deg. The structure of the monolayer does not change over at least 24 hours (the longest we waited). From diffraction scans of the Tl Bragg rods, we find that the in-plane and vertical' root mean square' displacement amplitudes are 0.36 + or - 0.05 lambda and 0.46 + or - 0.1 lambda, respectively. The monolayer structure is the same as that of vapor deposited Tl/Ag (111), and this shows that the interaction between the solvent molecules and the Tl adatoms does not influence the monolayer structure. Since the monolayer has a structure that is about the same as the closest packed planes of bulk Tl, we deduce that the adatom-adatom interactions are the most important structure determining forces. The compression of the monolayer (compared to bulk Tl) is explained in terms of effective medium theory. GRA

N92-17319# Miami Univ., Oxford, OH. Dept. of Physics.
MAGNETIC MULTILAYER INTERFACE ANISOTROPY
M. J. Pechan 1991 6 p
(Contract DE-FG02-86ER-45281)
(DE92-000635; DOE/ER-45281/6) Avail: NTIS HC/MF A02

Ni/Mo and Ni/V multilayer magnetic anisotropy has been investigated as a function of Ni layer thickness, frequency, and temperature. Variable frequency ferromagnetic resonance (FMR) measurements show, for the first time, significant frequency dependence associated with the multilayer magnetic anisotropy. The thickness dependence allows one to extract the interface contribution from the total anisotropy. Temperature dependent FMR (9 GHz) and room temperature magnetization indicate that strain between Ni and the non-magnetic layers if contributing significantly to the source of the interface anisotropy and the state of the interfacial magnetization. In order to examine the interface properties of other transition metal multilayer systems, investigations on Fe/Cu are underway and CoCr/Ag is being proposed. ESR measurements have been reported on Gd substituted YBaCuO superconductors and a novel quasi-equilibrium method has been developed to determine quickly and precisely the transition temperature. During the next project the P.I. proposes to: (1) extend the variable frequency FMR measurements to low temperature, where extremely large interface anisotropies are known to be obtained in Ni/Mo and Ni/V and are proposed to exist in Ni/W; (2) obtain accurate dc anisotropies via a novel, variable temperature torque magnetometer currently under construction; (3) expand upon initial findings in Fe/Cu multilayer investigations; (4) begin anisotropy investigations on Co/Ag and CoCr/Ag multilayers where the easy magnetization direction depends upon the Cr concentration; and (5) make and characterize Bi based superconductors according to resistivity, thermal conductivity, and thermoelectric power and construct YBaCuO based superconducting 'loop-gap' resonators for use in magnetic resonance work. DOE

N92-17327# SRI International Corp., Menlo Park, CA.
EVALUATION OF A DIFFUSION/TRAPPING MODEL FOR HYDROGEN INGRESS IN HIGH-STRENGTH ALLOYS Annual Report, Sep. - Nov. 1991
Bruce G. Pound 21 Nov. 1991 8 p
(Contract N00014-91-C-0263)
(AD-A243461) Avail: NTIS HC/MF A02 CSCL 11/6

A potentiostatic pulse technique was used to study the ingress of hydrogen in titanium (pure and grade 2) in an acetate buffer. Hydrogen ingress did not occur with pure titanium, indicating that the surface oxide is an effective barrier to hydrogen entry. In contrast, the data for Ti grade 2 were shown to fit a model for hydrogen diffusion and trapping, allowing values to be determined for the irreversible trapping constant (k) and the flux of hydrogen into the metal. Two values of k were obtained, depending on the level of hydrogen present in the metal. The density of irreversible traps calculated from k for low hydrogen levels suggests that the principal irreversible traps may be interstitial nitrogen, but grain boundaries are another possibility. The additional trapping constant obtained for high hydrogen levels is thought to be associated with hydride formation. The irreversible trapping constants for Ti grade 2 are consistent with its susceptibility to hydrogen embrittlement relative to that of other alloys. The results demonstrate that multiple irreversible traps can be distinguished by using the diffusion/trapping model. GRA

N92-17328# Cornell Univ., Ithaca, NY.
IN SITU STRUCTURAL STUDIES OF THE UNDERPOTENTIAL DEPOSITION OF COPPER ONTO AN IODINE COVERED PLATINUM SURFACE USING X RAY STANDING WAVES
G. M. Bommarito, D. Acevedo, J. R. Rodriguez, and H. D. Abruna

1991 16 p Sponsored in part by NSF and Navy
(AD-A243475) Avail: NTIS HC/MF A03 CSCL 07/4

We present initial results of an in situ structural investigation of the underpotential deposition of copper on an iodine platinum/carbon layered synthetic microstructure, using x ray standing waves generated by specular (total external) reflection and Bragg diffraction. We also compare the result of surface coverage isotherms derived from both electrochemical and x-ray measurements. The underpotential deposition (UPD) process has been extensively studied during the past two decades due to its theoretical and practical importance in fields such as: electrocrystallization, catalysis, and surface chemistry. In this process, submonolayer to monolayer(s) amounts of a metal can be electrodeposited on a foreign metal substrate in a quantifiable and reproducible fashion prior to bulk deposition. Numerous electrochemical and spectroscopic techniques have been utilized to probe the mechanism(s) of formation, and the structural properties of UPD layers. Conventional electrochemical methods have been used to obtain thermodynamic and kinetic information about the UPD process. Cyclic voltammetry and current transient experiments are the methods of choice in these types of studies. Structural features of the UPD layer were first derived, indirectly, from equilibrium-coverage potential isotherms using single crystal substrates. GRA

N92-17370# Puerto Rico Univ., Rio Piedras. Dept. of Physics.
A MODEL FOR VOLTAMMOGRAMS OF THE UNDERPOTENTIAL DEPOSITION OF METALS Summary Report
Dale A. Huckaby and L. Blum 9 Nov. 1991 9 p
(Contract N00014-90-J-1263)
(AD-A243199; TR-12) Avail: NTIS HC/MF A02 CSCL 11/6

A statistical mechanical model for adsorption is used to produce voltammograms with sharp spikes similar to those seen in recent studies of the underpotential deposition of metals onto single crystal electrodes. The voltammogram of the underpotential deposition of copper on the (111) surface of gold, which contains two spikes, can be reproduced by the model. GRA

N92-17376*# National Aeronautics and Space Administration. Lyndon B. Johnson Space Center, Houston, TX.
LONG-TERM CORROSION EVALUATION OF STAINLESS STEELS IN SPACE SHUTTLE IODINATED RESIN AND WATER
Douglas D. Krohn Jan. 1992 28 p
(NASA-TM-104743; S-660; NAS 1.15:104743) Avail: NTIS HC/MF A03 CSCL 11F

The effects of stainless steel exposure to iodinated water is a concern in developing the Integrated Water System (IWS) for Space Station Freedom. The IWS has a life requirement of 30 years, but the effects of general and localized corrosion over such a long period have not been determined for the candidate materials. In 1978, Umpqua Research Center immersed stainless steel 316L, 321, and 347 specimens in a solution of deionized water and the Space Shuttle microbial check valve resin. In April 1990, the solution was chemically analyzed to determine the level of corrosion formed, and the surface of each specimen was examined with scanning electron microscopy and metallography to determine the extent of general and pitting corrosion. This examination showed that the attack on the stainless steels was negligible and never penetrated past the first grain boundary layer. Of the three alloys, 316L performed the best; however, all three materials proved to be compatible with an aqueous iodine environment. In addition to the specimens exposed to aqueous iodine, a stainless steel specimen (unspecified alloy) was exposed to moist microbial check valve resin and air for a comparable period. This environment allowed contact of the metal to the resin as well as to the iodine vapor. Since the particular stainless steel alloy was not known, energy dispersive spectroscopy was used to determine that this alloy was stainless steel 301. The intergranular corrosion found on the specimen was limited to the first grain boundary layer.
Author

N92-17379# National Inst. of Standards and Technology, Boulder, CO.
ALUMINUM ALLOYS FOR ALS CRYOGENIC TANKS: COMPARATIVE MEASUREMENTS OF CRYOGENIC MECHANICAL PROPERTIES OF Al-Li ALLOYS AND ALLOY 2219 Final Report, Aug. 1989 - Mar. 1990
R. P. Reed, P. T. Purtscher, N. J. Simon, J. D. McColskey, and R. P. Walsh Oct. 1991 146 p Sponsored by Phillips Lab.
(AD-A242956; PL-TR-91-3073; AD-E200781) Avail: NTIS HC/MF A07 CSCL 11/6

Tensile and plane strain fracture toughness properties were obtained at cryogenic temperatures to compare the Al-Li alloys 8090, 2090, and WL049 and alloy 2219 in various tempers and specimen orientations. The strongest alloy at very low temperatures is WL049-T851, which is about 10 pct. stronger than 2090-T81. Both alloys are considerably stronger than 2219-T87. Alloy 2090-T81 is tougher in the in-plane orientations (about 50 pct.) than WL049-T851 at low temperatures; the higher in-plane toughness is attributed to the presence of less constituent particles and the tendency to crack out-of-plane or delaminate at low temperatures. This delamination tends to divide the moving crack, thus separating it into smaller regions where plane stress (rather than plane strain) conditions are conducive to increased toughness. Thus, a dichotomy: reduced toughness in the 'through thickness' or 'out of plane' orientations leads to increased toughness in the in-plane orientations. In service, a leak in the tank is considered failure, and a leak will be caused by a crack in the panels of the tankage growing through the panel thickness. To measure the resistance to crack growth under these conditions, surface-flawed panel tests are recommended. GRA

N92-17426# Cornell Univ., Ithaca, NY.
IN SITU X RAY STANDING WAVE STUDY OF Cu UPD ON AN IODINE COVERED PLATINUM SURFACE
G. M. Bommarito, D. Acevedo, J. F. Rodriguez, and H. D. Abruna 1991 13 p Sponsored in part by Army and Navy
(AD-A243474) Avail: NTIS HC/MF A03 CSCL 11/6

In situ structural investigations of the underpotential deposition of copper on an iodine covered platinum surface have been carried out using x ray standing waves generated by specular (total external) reflection and Bragg diffraction. Surface coverage isotherms derived from both electrochemical and x-ray measurements are also compared. The growth mode of the copper ad-layer appears to be strongly influenced by the electrode's surface morphology. The process of underpotential deposition (UPD) of metals has been extensively studied during the past two decades due to its theoretical and practical importance in fields such as electro crystallization, catalysis, and surface chemistry. Numerous electrochemical and spectroscopic techniques have been utilized to probe the mechanism(s) of formation, and the structural properties of UPD layers. Conventional electrochemical techniques have been used to obtain thermodynamic and kinetic information about the UPD process. Although electrochemical methods are invaluable in controlling and measuring thermodynamic parameters such as applied potential, charge, and coverage, any structural inferences are always indirect and often model dependent. GRA

N92-17427# Harvard Univ., Cambridge, MA. Dept. of Chemistry.
COMPARISONS OF SELF-ASSEMBLED MONOLAYERS ON SILVER AND GOLD: MIXED MONOLAYERS DERIVED FROM HS(CH2)21X AND HS(CH2)10(SUP Y) (X,Y-CH3, CH2OH) HAVE SIMILAR PROPERTIES
Paul E. Laibinis, Marye A. Fox, John P. Folkers, and George M. Whitesides Dec. 1991 53 p
(Contract N00014-86-K-0756)
(AD-A243487; TR-42) Avail: NTIS HC/MF A04 CSCL 07/4

This paper describes the preparation of self-assembled monolayers (SAMs) by adsorption of alkanethiols on evaporated silver, and compares these SAMs with analogous SAMs prepared on gold. The work concentrated on SAMs derived from mixtures of alkanethiols having long and short chains and terminating in

hydrophobic and hydrophilic tails: HS(CH2)10CH3, HS(CH2)21CH3, HS(CH2)10CH2OH, and HS(CH2)21CH2OH. The thickness and the compositions of these SAMs were established by X ray photoelectron spectroscopy (XPS). As is observed with self-assembled alkanethiolate monolayers on gold, the composition of the monolayers parallels but does not equal the solution composition. Less pronounced differences are observed between compositions in solution and on the surface of silver than have previously been reported on gold. Rates of exchange of surface thiolates with thiols in solution are similar on silver and gold. GRA

N92-17452# Department of the Navy, Washington, DC.
MICROSTRUCTURALLY TOUGHENED ARTICLES AND CASTING THEREOF Patent Application
Amarnath P. Divecha, inventor (to Navy) and Subhash D. Karmarkar, inventor (to Navy) 17 May 1991 14 p
(AD-D015065; US-Patent-Appl-SN-704563; Navy-Case-73171)
Avail: NTIS HC/MF A03 CSCL 11/4

A microstructurally toughened discontinuous composite tube and production process is provided. The tube is produced by prepositioning precast reinforcement made of a composite material inside of a centrifugal casting mold. Molten matrix metal is then introduced into the mold while being rotated about its longitudinal axis until the molten metal completely encapsulates the reinforcement. GRA

N92-17467# Naval Postgraduate School, Monterey, CA.
MICROSTRUCTURE AND MECHANICAL PROPERTIES OF HSLA-100 STEEL M.S. Thesis
Victor R. Mattes Dec. 1990 79 p
(AD-A242937) Avail: NTIS HC/MF A05 CSCL 11/6

Light microscopy, scanning electron microscopy, and transmission electron microscopy were employed to examine the microstructural basis for the mechanical properties of as-quenched and tempered HSLA-100 steel. Examination of the alloy revealed granular bainite with martensite and retained austenite in the as-quenched state which upon aging at temperatures below the lower transformation temperature, 677 C, formed tempered bainite with precipitates of copper and carbides. These results indicate the strength and toughness of HSLA-100 steel aged below 677 C is based primarily on the fine prior austenite grain size and classic copper precipitation behavior but also on the bainite dislocation substructure and carbides. After tempering at 677 C, HSLA-100 steel has a dual-phase microstructure consisting of bainitic ferrite laths, fine ferrite grain clusters and martensite with precipitates of carbides and overaged copper. The results indicate the yield strength of the overaged alloy is based on the fine ferrite grain and bainite lath sizes, the fine carbide distribution and elastic moduli strengthening while the toughness is the result of the high-angle ferrite grain boundaries, the fine intralath carbides and the ductile overaged copper precipitates. GRA

N92-17579# Los Alamos National Lab., NM.
ON SIZE SCALING IN SHOCK HYDRODYNAMICS AND THE STRESS-STRAIN BEHAVIOR OF COPPER AT EXCEEDINGLY HIGH STRAIN RATES
J. M. Walsh, G. L. Stradling, G. C. Idzorek, B. P. Shafer, and H. L. Curling, Jr. (Science Applications International Corp., Albuquerque, NM.) 1991 10 p Presented at the Workshop on Hypervelocity Impacts in Space, Canterbury, England, 1-5 Jul. 1991
(Contract W-7405-eng-36)
(DE92-003797; LA-UR-91-3495; CONF-9107182-3) Avail: NTIS HC/MF A02

In recent years, the Hypervelocity Microparticle Impact (HMI) project at Los Alamos has utilized electrostatically accelerated iron spheres of microscopic dimensions to generate hypervelocity impact experiments to about 100 x 10(exp 5) cm/sec, about an order of magnitude beyond the data range for precisely controlled impact tests with ordinary macroscopic particles. But the extreme smallness of the micro-impact events brings into question whether the usual shock-hydrodynamic size scaling can be assumed. It is to this question of the validity of size scaling (and its refinement) that the present study is directed. Hypervelocity impact craters are compared in which the two impact events are essentially identical except that the projectile masses and crater volumes differ by nearly 12 orders of magnitude -- linear dimensions and times differing by 4 orders of magnitude. Strain rates at corresponding points increase 4 orders of magnitude in the size reduction. Departures from exact scaling, by a factor of 3.7 in crater volume, are observed for copper targets -- with the microcraters being smaller than scaling would predict. This is attributed to a factor 4.7 higher effective yield stress occurring in the microcratering flow. This, in turn, is because the strain rate there is about 10(exp 8)/sec as compared to a strain rate of only 10(exp 4)/sec in the macro impact. The measurement of impact craters for very small impact events leads to the determination of metal yield stresses as strain rates more than two orders of magnitude greater than have been obtained by other methods. The determination of material strengths at these exceedingly high strain rates is of obvious fundamental importance. DOE

N92-17653# Pratt and Whitney Aircraft, West Palm Beach, FL.
FATIGUE IN SINGLE CRYSTAL NICKEL SUPERALLOYS Progress Report, 16 Sep. - 15 Nov. 1991
15 Nov. 1991 8 p
(Contract N00014-91-C-0124)
(AD-A243453; PWA-FR21998-1) Avail: NTIS HC/MF A02
CSCL 11/6

This program investigates the behavior of single crystal airfoil materials. The fatigue initiation processes in single crystal materials are significantly more complicated and involved than fatigue initiation and subsequent behavior of a (single) macrocrack in conventional, isotropic, materials. In cast single crystal nickel alloys, two basic fracture modes, crystallographic and non-crystallographic, are seen in combination. They occur in varying proportions depending upon temperature and stress state. Crystallographic orientation with respect to applied load also affects the proportion of each and influences the specific crystallographic planes and slip directions involved. Mixed mode fracture is observed under monotonic as well as cyclic conditions. GRA

N92-17703# Argonne National Lab., IL.
GROWTH RATE OF DISLOCATION LOOP IN Fe-Ni-Cr ALLOY UNDER Kr(+) ION AND ELECTRON IRRADIATION
T. Kimoto (National Research Inst. for Metals, Ibaraki, Japan), C. W. Allen, and L. E. Rehn Oct. 1991 13 p Presented at the International Conference on Fusion Reactor Materials, Clearwater, FL, 17-22 Nov. 1991
(Contract W-31-109-eng-38)
(DE92-001908; ANL/CP-74527; CONF-911111-6) Avail: NTIS HC/MF A03

In order to examine the effect of irradiating particle species on the growth rate of radiation-induced dislocation loops, a solution-annealed Fe-25Ni-15Cr-0.02C alloy was irradiated at 723 K first by 1.5 MeV Kr(+) ions for 2520 sec, then by 1.5 MeV Kr(+) ions and 1.0 MeV electrons simultaneously for 780 sec, and finally by 1.0 MeV electrons for 780 sec with the HVEM-Tandem Facility in Argonne National Laboratory. The calculated damage rate by 1.5 MeV Kr(+) ions was 5.8 x 10(exp -4) dpa/s, and that by 1.0 MeV electrons was 1 x 10(exp -4) dpa/s. The growth rate of a dislocation loop located at the center of the specimen was 7 x 10(exp -3) nm/s for the Kr(+) ion irradiation, 4 x 10(exp -2) nm/s for the simultaneous Kr(+) and electron irradiation, and 2-3 x 10(exp -2) nm/s for the electron irradiation. This implies that the electron irradiation is about 19 times more effective in the growth of radiation-induced dislocation loops than the Kr(+) ion irradiation. The dislocation loop growth rate under the simultaneous Kr(+) and electron irradiation is higher than the sum of the growth rates under the individual Kr(+) and electron irradiations. DOE

N92-17759# Naval Postgraduate School, Monterey, CA.
THE INFLUENCE OF TEMPERATURE AND COMPOSITION ON THE ACTIVATION ENERGY FOR CREEP IN BINARY

ALUMINUM LITHIUM ALLOYS M.S. Thesis
Robert L. Seaton Dec. 1990 96 p
(AD-A242299) Avail: NTIS HC/MF A05 CSCL 11/6

With the fast pace of technology in the aerospace industry, there are increasing demands for higher strength and stiffness in structural materials but with reduced weight and improved formability. Aluminum alloys have been widely used in the construction of aerospace vehicles because of their high strength to weight ratio, forming characteristics and corrosion resistance. An investigation was conducted to determine the temperature and composition dependence on the activation energy for creep of Al-0.5wt.pct.Li, Al-1.Owt.pct.Li, and Al-2.Owt.pct.Li alloys. A series of isothermal tests were conducted utilizing constant true stress creep tests, with nominal temperatures ranging from 300 to 500 C. Temperature cycling tests involved a range of 10 C for each test. Experimental results indicate all three alloys behave as a class II alloy (pure metal class) with a stress exponent, n, approximately equal to 5. In addition, subgrain formation was observed in association with the primary stage of creep. The activation energy for creep of the Al-0.5wt.pct.Li and Al-1.Owt.pct.Li alloys was observed to be essentially the same as that for pure Al. GRA

N92-17808# Joint Inst. for Nuclear Research, Dubna (USSR). Lab. of Nuclear Reactions.
DATA ACQUISITION AND MEASUREMENT SYSTEM FOR PLASTIC PARAMETERS OF RADIATION METAL RESEARCH EXPERIMENTS
Z. Illes, L. Murgash, V. A. Shchegolev (Joint Inst. for Nuclear Research, Dubna, USSR), and K. Havanczak 1990 7 p
(DE92-610350; JINR-R-10-90-299) Avail: NTIS HC/MF A02

A data acquisition system has been constructed, for investigation of a stress-strain curve measured by INSTRON. System is controlled by Commodore 64 personal computer. As a result yield-point and parameters of materials plasticity are given. DOE

N92-17858# EG and G Rocky Flats, Inc., Golden, CO.
INDUCTIVELY COUPLED PLASMA ATOMIC EMISSION SPECTROSCOPY ANALYSIS OF GOLD ELECTROPLATING SOLUTIONS
R. D. Thiel 17 Jul. 1991 15 p
(Contract DE-AC34-90DP-62349)
(DE92-004798; RFP-4387) Avail: NTIS HC/MF A03

The composition of a gold plating bath can affect adhesion, porosity, and purity of the resulting electroplate. Therefore, controlling the major components and trace impurities in gold plating baths is necessary. Bath analysis is one aspect of the process controls necessary to ensure that the resulting gold plating has the desired physical properties. The gold baths are analyzed for gold concentration. Also, concentrations are determined for 12 potentially detrimental impurity elements: arsenic, cadmium, cobalt, chromium, copper, iron, indium, manganese, nickel, lead, tin, and zinc. These analyses are performed using Inductively Coupled Plasma (ICP) Atomic Emission Spectroscopy. Using this technique, the gold level is analyzed with enough accuracy to maintain it within operating specifications. The 12 impurities are quantified at levels below the bath limits. This analysis procedure is performed in approximately two hours. DOE

27 NONMETALLIC MATERIALS

Includes physical, chemical, and mechanical properties of plastics, elastomers, lubricants, polymers, textiles, adhesives, and ceramic materials.

For composite materials see *24 Composite Materials*.

N92-16976# Texas Univ., Austin. Dept. of Chemistry.
ELECTRONIC AND IONIC TRANSPORT IN PROCESSABLE CONDUCTING POLYMERS. SYMMETRY EFFECTS ON THE PHYSICAL AND ELECTRICALLY CONDUCTING, SUBSTITUTED POLY(DI-2-THIENYLPHENYLENES) Technical Report, 1 Jun. - 30 Sep. 1991
Jose P. Ruiz, Jayesh R. Dharia, John R. Reynolds, and Leonard J. Buckley 21 Oct. 1991 55 p
(Contract N00014-90-J-1320)
(AD-A242328; TR-35) Avail: NTIS HC/MF A04 CSCL 07/6

The effect of symmetry on the physical and electronic properties of a series of conjugated polymers composed of di(2 thienyl) 2,5 phenylene repeat units, symmetrically and asymmetrically substituted with methoxy, heptoxy, dodecyloxy, hexadecyloxy, eicosinoxy and hexyl groups were studied. Polymers were prepared via an oxidative polymerization using ferric chloride and isolated after dedopping with ammonium hydroxide. Neutral polymers, soluble in common organic solvents including chloroform, methylene chloride and tetrahydrofuran, are predominantly linked at the 5 and 5' positions of the thiophene rings to result in fully conjugated main chains that are stable to 360 C under nitrogen. Molecular weight analyses indicate weight average degrees of polymerization of ca. 10-20; thus, substantial fraction of chains in each sample contains 30 to 50 aromatic rings. Differential scanning calorimetry studies revealed that melt transitions, indicative of molecular ordering, are present in the symmetrically substituted polymers. Order found in these polymers was confirmed by x ray diffraction and found to persist at elevated temperatures, yielding birefringent melts, suggestive of liquid crystalline order. Asymmetrically substituted polymers are found to be amorphous. Upon oxidation of the insulating polymers, bipolaronic charge carriers were formed with the oxidized polymers exhibiting electrical conductivities up to 4/ohms cm. GRA

N92-17004*# Old Dominion Univ., Norfolk, VA. Dept. of Civil Engineering.
POLYMER INFILTRATION STUDIES Progress Report, 16 Sep. - 31 Dec. 1991
Joseph M. Marchello Jan. 1992 23 p
(Grant NAG1-1067)
(NASA-CR-189773; NAS 1.26:189773) Avail: NTIS HC/MF A03 CSCL 11C

The preparation is reported of carbon fiber composites using advanced polymer resins. Current and ongoing research activities include: powder towpreg process; weaving, braiding and stitching dry powder prepreg; advanced tow placement; and customized ATP towpreg. The goal of these studies is to produce advanced composite materials for automated part fabrication using textile and robotics technology in the manufacture of subsonic and supersonic aircraft. Author

N92-17010# Washington State Univ., Pullman. Dept. of Chemistry.
ANOMALOUS HOLE BURNING IN POLYMERS WITH INHOMOGENEOUS BROADENING
D. L. Lin, X. Li, and Thomas F. George Oct. 1991 15 p
(Contract N00014-90-J-1193)
(AD-A242397; WSU/DC/91/TR-68) Avail: NTIS HC/MF A03 CSCL 07/6

For inhomogeneously broadened media such as polydiacetylene 4BCMU films, a phenomenological model is proposed to calculate the imaginary part of the optical susceptibility as a function of the pump field intensity. It is shown that the model can qualitatively account for the anomalous behavior of the absorption hole observed in recent experiments. Possible cause of the anomaly is discussed. Studies of transient optical effects have become important in the development of coherent optical spectroscopy

and fast response nonlinear optical materials. Many experiments have been carried out by the pump-probe technique in which the strong pump laser induces the nonlinear optical response of the sample to be examined by the weak probe laser. Spectral hole burning or bleaching accompanied by a dynamical Stark shift has been observed in such experiments on various materials such as semiconductor quantum wells and conjugated polymers. GRA

N92-17029# Gordon Research Conferences, Inc., Kingston, RI.
CERAMICS WITH SUPERELECTRICAL AND SUPERMECHANICAL PROPERTIES Final Report, period ending 15 Jul. 1991
Alexander A. Cruickshank Oct. 1991 11 p
(Grant AF-AFOSR-0311-91; AF Proj. 2306)
(AD-A243062; AFOSR-91-0920TR) Avail: NTIS HC/MF A03 CSCL 11/2

This conference was held from 29 July to 2 August, 1991, at the Holderness School in Plymouth, New Hampshire. The topics discussed included how to achieve super-responses in ceramic materials by engineering of structural instabilities, spin-glass models of relaxor ferroelectrics, engineering of super-tough ceramics in zirconias, smart materials and structures, engineering and modelling of ferroelectrics for high strain actuators, small particle size effects in ferroelectrics, ferroelectric thin films for memory and optical applications, processing and properties of nanophase ceramics, microstructure-property relationships in ceramic superconductors and fundamental aspects of phase transformations in ceramics. GRA

N92-17032*# National Aeronautics and Space Administration. Langley Research Center, Hampton, VA.
FREE VOLUME VARIATION WITH MOLECULAR WEIGHT OF POLYMERS
Jag J. Singh, Abe Eftekhari (Hampton Univ., VA.), Jeffrey A. Hinkley, Terry L. St.Clair, and Brian J. Jensen Washington Feb. 1992 10 p
(NASA-TM-4326; L-16982; NAS 1.15:4326) Avail: NTIS HC/MF A02 CSCL 11B

Free volume measurements were made in several molecular weight fractions of two different geometries of poly(arylene ether ketone)s. Free volumes were measured using positron lifetime spectroscopy. It has been observed that the free volume cell size V(sub f) varies with the molecular weight M of the test samples according to an equation of the form V(sub f) = AM(B), where A and B are constants. The molecular weights computed from the free volume cell sizes are in good agreement with the values measured by gel permeation chromatography. Author

N92-17042# Ohio State Univ., Columbus. Dept. of Materials Science and Engineering.
CODEPOSITION OF ELEMENTS IN DIFFUSION COATINGS BY THE HALIDE-ACTIVATED PACK CEMENTATION METHOD Progress Report No. 1
Robert Bianco, Mark A. Harper, and Robert A. Rapp Sep. 1991 33 p
(Contract N00014-90-J-1765)
(AD-A242860) Avail: NTIS HC/MF A03 CSCL 11/3

The codeposition of two or more elements in a halide-activated cementation pack is inherently difficult because of large differences in the thermodynamic stabilities for their volatile halides. However, through a computer-assisted analysis of the pack equilibria, combinations of suitable masteralloys and activator salts can be identified. Codeposition of chromium plus aluminum or Cr plus silicon by pack cementation has yielded diffusion coatings with excellent resistance to high-temperature oxidation/corrosion for a wide range of alloy substrates. GRA

N92-17054# Washington Univ., Seattle.
PROCESSING OF CERAMICS OF BIOPOLYMERS. ULTRASTRUCTURE-PROPERTY RELATIONSHIPS IN BIOCRYSTALS Final Report No. 3, 1 Feb. 1990 - 31 Jan. 1991
Mehmet Sarikaya, James T. Staley, and Ilahn A. Aksay 9 Oct. 1991 307 p
(Grants AF-AFOSR-0135-88; AF-AFOSR-0496-89; AF Proj. 2303)
(AD-A243061; AFOSR-91-0918TR) Avail: NTIS HC/MF A14 CSCL 07/6

Biopolymers obtained from bacterial sources were shown to be effective processing aids in the preparation of aqueous suspensions of submicron-sized ceramic powders. Potentially useful native bacterial polysaccharides was shown to be necessary to achieve suspension stability in aqueous systems. Alginates obtained from both alga and bacterial were also found to be effective processing aids. An in situ processing method was developed through the growth of alginate-producing bacteria in the presence of ceramic particles. GRA

N92-17060*# National Aeronautics and Space Administration. Lewis Research Center, Cleveland, OH.
RELIABILITY ANALYSIS OF STRUCTURAL CERAMIC COMPONENTS USING A THREE-PARAMETER WEIBULL DISTRIBUTION
Stephen F. Duffy, Lynn M. Powers (Cleveland State Univ., OH.), and Alois Starlinger 1992 12 p Proposed for presentation at the 37th International Gas Turbine and Aeroengine Congress and Exposition, Cologne, Germany, 1-4 Jun. 1992; sponsored by ASME
(Contract NCC3-81)
(NASA-TM-105370; E-6749; NAS 1.15:105370) Avail: NTIS HC/MF A03 CSCL 11C

Described here are nonlinear regression estimators for the three-Weibull distribution. Issues relating to the bias and invariance associated with these estimators are examined numerically using Monte Carlo simulation methods. The estimators were used to extract parameters from sintered silicon nitride failure data. A reliability analysis was performed on a turbopump blade utilizing the three-parameter Weibull distribution and the estimates from the sintered silicon nitride data. Author

N92-17065# North Carolina Univ., Chapel Hill. Dept. of Physics and Astronomy.
MATERIALS PROCESSING OF DIAMOND: ETCHING, DOPING BY ION IMPLANTATION AND CONTACT FORMATION Annual Technical Report, 1 Oct. 1990 - 30 Sep. 1991
Max L. Swanson 30 Sep. 1991 14 p
(Contract N00014-87-K-0243)
(AD-A243060) Avail: NTIS HC/MF A03 CSCL 20/12

Three main areas of research were pursued in this period. The first was a continued study of the ion implantation doping of natural diamond, using dual implantations of C plus B. Of special concern was the measurement of resistance versus temperature using four point probes to avoid edge effects and contact resistance. The result of these measurements was in general the elimination of the low activation energies occurring at the low temperature end of the resistance temperature plot, which were apparently due to small edge resistances. The second area was the attempt to dope natural diamond n-type by implantation with Na and Li, in collaboration with Oak Ridge National Laboratories. Linear Arrhenius plots of logR vs 1/T were obtained, with an activation energy of near 0.4 eV. However, the resistivity was high, and it increased on annealing, indicating possible effects of radiation damage. The ultimate goal of this work is the diffusion of the dopant beyond the damaged region, followed by removal of the damage by plasma etching. The third area was growth of heteroepitaxial diamond films on Cu substrates, using ion implantation of C. GRA

N92-17070*# National Aeronautics and Space Administration. Lewis Research Center, Cleveland, OH.
HIGH-TEMPERATURE DURABILITY CONSIDERATIONS FOR HSCT COMBUSTOR
Nathan S. Jacobson Washington Jan. 1992 19 p
(NASA-TP-3162; E-6343; NAS 1.60:3162) Avail: NTIS HC/MF A03 CSCL 11C

The novel combustor designs for the High Speed Civil Transport will require high temperature materials with long term environmental stability. Higher liner temperatures than in conventional combustors

and the need for reduced weight necessitates the use of advanced ceramic matrix composites. The combustor environment is defined at the current state of design, the major degradation routes are discussed for each candidate ceramic material, and where possible, the maximum use temperatures are defined for these candidate ceramics. Author

N92-17170# National Inst. of Standards and Technology, Gaithersburg, MD.
DETERMINATION OF THE OPTICAL CONSTANTS OF THIN CHEMICAL-VAPOR-DEPOSITED DIAMOND WINDOWS FROM 0.5 TO 6.5 eV
Lawrence H. Robins, Edward N. Farabaugh, and Albert Feldman 27 Sep. 1991 19 p
(Contract N00014-90-F-0011)
(AD-A243094; NIST-TR-8) Avail: NTIS HC/MF A03 CSCL 07/2

The optical constants of thin chemical vapor deposited diamond windows were determined as a function of photon energy from 0.5 to 6.5 eV by fitting experimental transmittance and reflectance data to a model that includes the effects of surface optical scatter. Root-mean-squared surface roughness values were also obtained from the analysis. The windows were fabricated by microwave plasma assisted CVD on silicon substrates, followed by partial removal of the substrates by etching. The values of the refractive index were diamonds. Substantial adsorption was found to occur in the visible to near ultraviolet region (2 to 5 eV) where single-crystal diamond is transparent. The spectrum of the low-energy absorption spectrum is diamond like amorphous carbon. There is a steep increase in absorption above the indirect bandgap of diamond (5.5 eV). GRA

N92-17171# National Inst. of Standards and Technology, Gaithersburg, MD.
CHEMICAL VAPOR DEPOSITED DIAMOND
Albert Feldman, Edward N. Farabaugh, and Lawrence H. Robins 27 Sep. 1991 50 p
(Contract N00014-90-F-0011)
(AD-A243095; NIST-TR-11) Avail: NTIS HC/MF A03 CSCL 11/3

There is considerable interest in using diamond for numerous applications because of the development of methods that allow for the deposition of diamond by chemical vapor deposition (CVD) techniques over large areas. The interest in new applications for diamond rests on combinations of superior properties that diamond possesses. These extreme properties, which are based on measurements in bulk single crystal diamond, include greatest hardness, highest elastic moduli, and highest thermal conductivity at room temperature of any material. Other important properties include optical transparency over an extensive wavelength range from the ultraviolet through the far infrared, high electrical resistivity, dopability to be a semiconductor, low permeability to diffusion, chemical inertness, and low coefficient of friction. GRA

N92-17172# National Inst. of Standards and Technology, Gaithersburg, MD.
USE OF DIAMOND AS AN OPTICAL MATERIAL
Albert Feldman 27 Sep. 1991 17 p
(Contract N00014-90-F-0011)
(AD-A243097; NIST-TR-9) Avail: NTIS HC/MF A03 CSCL 20/5

Chemical vapor deposition (CVD) processes promise inexpensive diamond optics and coatings with large dimensions. Near term optical applications include x-ray windows, membranes for x ray lithography, and infrared windows and domes. CVD diamond, which is mainly polycrystalline, shows materials problems that include scattering due to large surface roughness, absorption due to defects, non-diamond carbon phases, and impurities, and poor diamond/substrate adhesion. Free carrier absorption in CVD diamond has also been reported. While diamond films less than 3 microns thick can be made transmissive in the visible and in the ultraviolet, at these wavelengths, thicker components scatter excessively and show absorption due to defects. Continuing research is improving the optical quality of CVD diamond. New polishing methods have yielded smooth surfaces in reasonable polishing times. Recent research holds promise for large optics made from single crystal diamond. GRA

N92-17191# Rockwell International Science Center, Anaheim, CA.
DIELECTRIC PROPERTIES OF ALIGNED CONDUCTING POLYMERS Final Report, 1 Mar. 1989 - 28 Feb. 1991
H. S. Ryang and L. F. Warren Oct. 1991 30 p
(Contract N00014-89-C-0075)
(AD-A243389) Avail: NTIS HC/MF A03 CSCL 07/4

Attempts to align electrically conducting polypyrrole (PPy) were made using various electrochemical methods. Rotating cylinder anode electropolymerization was found to induce partially aligned deposits of PPy films when they were prepared in the presence of a soap supporting electrolyte or a soluble polymer additive. Degrees of dc electrical anisotropy up to 60 to 1 were observed. SEM and UV-vis results indicated that soluble pyrrole oligomers generated in the rotating anode cell result in film alignment. Electrochemically prepared PPy/poly(ethylene oxide) composites were stretchable, resulting in conductivity enhancement, but with little electrical anisotropy. Pyrrole electropolymerization in a magnetic field was also evaluated, but electrical anisotropy was not detected in any of the films. However, an unusual uniform rotational hydrodynamic motion, depending on the deposition and polarity of the electrodes, was observed with submersed electrodes in which the electric field was parallel to the magnetic field. GRA

N92-17193# Pennsylvania State Univ., University Park.
THE 5TH ANNUAL US-JAPAN SEMINAR ON DIELECTRIC AND PIEZOELECTRIC CERAMICS Final Report, 1 Jun. 1990 - 21 Oct. 1991
Joseph P. Dougherty Oct. 1991 36 p Seminar held in Kyoto, Japan, 11-14 Dec. 1990
(Contract N00014-90-J-1928)
(AD-A243465) Avail: NTIS HC/MF A03 CSCL 11/2

The Fifth United States/Japan Workshop on Dielectric and Piezoelectric Materials was held in Kyoto, Japan on December 11-14, 1990. The technical topics most discussed were: (1) thin film ferroelectrics and dielectrics, (2) relaxor ferroelectrics, and (3) piezoelectric materials and processing. Barium titanate materials for multilayer capacitors received little attention. There were no USA papers on microwave dielectrics and no Japanese papers on single crystals. There were no USA papers on piezoelectric devices, while many Japanese papers were device related. Dielectric materials for electronic packaging were few from both sides. GRA

N92-17195# International Business Machines Corp., San Jose, CA.
TWO-BEAM COUPLING MEASUREMENTS OF GRATING PHASE IN A PHOTOREFRACTIVE POLYMER Interim Technical Report
C. A. Walsh and W. E. Moerner 25 Nov. 1991 19 p
(Contract N00014-91-C-0166)
(AD-A243746; IBM-RJ8490; TR-36) Avail: NTIS HC/MF A03 CSCL 07/6

We investigate in detail the grating properties of a recently discovered organic photorefractive polymer as a function of electric field using two-beam coupling. We present measurements of index and absorption grating phase relative to the intensity interference pattern as well as the amplitude of both the absorption and index gratings. We find that in low electric fields, a weak in-phase grating (possible photochromic) and the low electro-optic coefficient prevent observation of a phase shifted photorefractive grating. However, at moderate to high electric fields, a much stronger photorefractive index grating with phase shift approaching 90 degree dominates. The field dependence of the index grating phase is discussed in terms of a standard photorefractive model. The presence of an index grating with a 90 degree phase shift at high

fields provides strong evidence that these polymers are indeed photorefractive. GRA

N92-17262# Rhode Island Univ., Kingston. Coll. of Engineering.
BLISTERING OF GRAPHITE/POLYMER COMPOSITES GALVANICALLY COUPLED WITH METALS IN SEA WATER Annual Report
Wayne C. Tucker, Richard Brown, Thomas J. Rockett, and Shravan Miriyala 1991 35 p
(Contract N00014-91-J-1328)
(AD-A242861) Avail: NTIS HC/MF A03 CSCL 11/4

The electrochemical nature of blistering in carbon vinyl ester composites in sea water and saline solution was confirmed. Carbon fiber/polyester composites also blistered. It was therefore shown that blistering is a generic degradation phenomena for many carbon containing polymer composites. The location of the fluid filled blisters in the composites was detailed. The aqueous blister liquid contains organic species and has a pH greater than 10. Blisters formed on vinyl ester/platinum composites caused degradation of the polymer which could not be duplicated in 10N sodium hydroxide solution. Absorption kinetics data for water and electrolyte in carbon fiber/vinyl ester composites is established. GRA

N92-17282# National Inst. of Standards and Technology, Gaithersburg, MD. Ceramics Div.
STRENGTH AND MICROSTRUCTURE OF CERAMICS Final Technical Report, 1 Oct. 1989 - 30 Sep. 1991
Brian R. Lawn Oct. 1991 170 p
(Grants AF-AFOSR-ISSA-90-0003; AF-AFOSR-ISSA-91-0002; AF Proj. 2306)
(AD-A243049; AFOSR-91-0892TR) Avail: NTIS HC/MF A08 CSCL 11/2

Results of a program on the toughness properties of monophase and two phase ceramics that toughen by bridging are presented. Fracture mechanics models describing this behavior, in the particular context of strength, are developed. Results of strengths tests confirming the essential predictions of the theory are presented. Innovative processing routes suggested by the models are shown to lead to two phase composites with impressive flaw insensitivity. A partial list of publications included in this report are: (1) The role of crystallization of an intergranular glassy phase in determining grain boundary residual stresses in debased aluminas; (2) In situ measurements of bridged crack interfaces in scanning electron microscopes; (3) Cyclic fatigue from frictional degradation at bridging grains in alumina; (4) Microstructure, toughness curves and mechanical properties of alumina ceramics; (5) Fabrication of flaw tolerant aluminum titanate reinforced alumina; and (6) Influence of grain size and degree of crystallization of intergranular glassy phase on the mechanical behavior of a debased alumina. GRA

N92-17397# Department of the Navy, Washington, DC.
METHOD OF JOINING DIAMOND STRUCTURES Patent Application
Lawrence T. Kabacoff, inventor (to Navy) and John Barkyoumb, inventor (to Navy) 8 Jul. 1991 11 p
(AD-D015066; US-Patent-Appl-SN-726483; Navy-Case-73416)
Avail: NTIS HC/MF A03 CSCL 07/2

A process is presented for bonding two diamond surfaces together by: (1) forming a layer of opaque nondiamond carbon material between the two diamond surfaces; (2) pressing the diamond surfaces together with the opaque nondiamond material sandwiched between the diamond surfaces; (3) using pulse lased light to quickly melt all the opaque nondiamond carbon material before a significant amount of heat is lost through the diamond surface; and (4) allowing the resulting carbon melt to cool and solidify as polycrystalline diamond which grows homoepitaxially from the diamond surfaces, bonding those surface together. GRA

N92-17448# Case Western Reserve Univ., Cleveland, OH. Dept. of Macromolecular Science.
PHASE TRANSITIONS IN NARROW MOLECULAR MASS SAMPLES OF SIDE-CHAIN LIQUID CRYSTALLINE POLYMERS: MOLECULAR MASS DEPENDENCE
U. W. Gedde, H. Johnson, A. Hult, and Virgil Percec 30 Oct. 1991 27 p
(Contract N00014-89-J-1828)
(AD-A242354; TR-51) Avail: NTIS HC/MF A03 CSCL 07/6

The molecular mass dependence of phase transitions in narrow molecular mass samples of smectic side-chain poly(vinyl ether)s is discussed in this paper with reference to earlier data by Stevens et al and Percec et al on narrow fractions of smectic side-chain polysiloxanes and polymethacrylates. The constant heat of isotropization and the proportionality between glass temperature (T sub g) and reciprocal degree of polymerization (DP) observed for polysiloxanes and polymethacrylates indicate that the order within the smectic layers and the penetration of the flexible main chains of the smectic layers was not appreciably affected by changes in DP. The poly(vinyl ether)s on the other hand exhibited a pronounced decrease in Delta h sub i with increasing DP and a more complex correlation between T sub g and DP indicative of an increasing disturbance by the flexible main chains of the smectic layers on increasing DP. These differences between polysiloxanes/polymethacrylates and poly(vinyl ethers)s were also found to have profound effects on the DP dependence of the isotropization temperature. GRA

N92-17460# Texas Univ., Arlington. Center for Advanced Polymer Research.
ELECTRONIC AND IONIC TRANSPORT IN PROCESSABLE CONDUCTING POLYMERS Quarterly Report, 1 Jun. - 30 Sep. 1991
Martin Pomerantz, John R. Reynolds, Krishnan Rajeshwar, and Dennis S. Marynick 21 Oct. 1991 6 p
(Contract N00014-90-J-1320)
(AD-A242258; TR-32) Avail: NTIS HC/MF A02 CSCL 07/6

EPR spectroscopy/electrochemical measurements have shown polaron and bipolaron states in the redox switching of poly(di-2-thienylphenylenes) substituted with alkoxy groups. The longer side chains stabilize the polaronic form of the polymers. In aqueous perchlorate and tetrafluoborate electrolytes, pyrrole electropolymerizes using only ca. 0.1 electrons per monomer. This suggests that in these cases a chain-growth polymerization is occurring rather than the more typical cation-radical coupling. Continued studies on our Pt/polypyrrole nanocomposites (a 3-dimensional array of catalytically active colloidal Pt particles in a polypyrrole matrix) has demonstrated unusual catalytic activity toward O2 and H2. A new modified extended Huckel band structure calculation method has been developed which reproduces band gaps of polyheterocycles to within 0.4 eV. A new soluble derivative of poly(thieno(3,4-b)pyrazine) with a solution band gap of 1.1 eV and which changes color from dark blue to light yellow upon doping has been prepared. GRA

N92-17461# Texas Univ., Arlington. Center for Advanced Polymer Research.
ELECTROCHEMICALLY INITIATED CHAIN POLYMERIZATION OF PYRROLE IN AQUEOUS MEDIA Technical Report, 1 Jun. - 30 Sep. 1991
Yong-Jian Qiu and John R. Reynolds 21 Oct. 1991 34 p
(Contract N00014-90-J-1320)
(AD-A242259; TR-33) Avail: NTIS HC/MF A03 CSCL 07/6

The electrochemical quartz crystal microbalance has been employed to investigate the electropolymerization of pyrrole in a variety of aqueous electrolytes. In contrast to the generally accepted cation-radical coupling process for the electropolymerization of pyrrole, an electrochemically initiated chain polymerization, featuring a high polymerization rate and involving little charge transport, was found under specific conditions in the presence of ClO4-BF4-, and PF6- electrolytes. The more typical cation-radical coupling mechanism, characterized by a constant polymerization charge to mass deposited ratio, is observed in the

presence of Cl-, NO3-, dodecyl sulfate, copper phthalocyanine tetrasulfonate, Beta-cyclodextrin tetradecasulfate, and poly(styrene sulfonate). Electrochemical characterizations of polypyrrole films prepared in aqueous ClO4- electrolytes reveal that the polymer formed via chain polymerization exhibits the ability to transport both cations and anions during electrochemical switching between redox states, while the polymer synthesized through cation-radical coupling is only capable of transporting a single ionic species. GRA

N92-17508# University of Southern California, Los Angeles. Dept. of Chemistry.
DEVELOPMENT OF PROCESSIBLE ELECTROACTIVE OLIGOMERS AND POLYMERS Final Report, 1 Jun. 1988 - 31 May 1991
Larry R. Dalton Oct. 1991 26 p
(Contract F49620-88-C-0071)
(AD-A243723; AFOSR-91-0973TR) Avail: NTIS HC/MF A03 CSCL 07/6

The objective of this research program has been the development of new materials with enhanced nonlinear optical activity and the exploration of related properties such as electrical conductivity. Initial research efforts focused upon pi-electron materials (polyenes and heteroaromatic polymers) and synthetic routes for overcoming the inherent insolubility of these materials. By steadily improving solubility and processability through utilization of derivation and precursor routes, we have been able to fabricate optical quality films of ladder-type polymers and achieve high resolution characterization of these materials both in terms of structure and electroactive properties. Electroactive molecules including fused ring (ladder oligomers) dyes, squaryl-ium-heterocyclic moieties, phenylpolyenes, thienylpolyenes, carbocyanine dyes, and tetraazaannulenes have also been synthetically incorporated into a variety of traditional polymers both as pendants and as part of the polymer backbone. GRA

N92-17541# Technische Univ., Berlin (Germany, F.R.). Fachbereich Elektrotechnik.
TEST METHOD FOR THE EVALUATION OF THE WATER TREEING BEHAVIOR OF CROSS-LINKED POLYETHYLENE MEDIUM VOLTAGE CABLES Ph.D. Thesis [PRUEFVERFAHREN ZUR BEURTEILUNG DES 'WATER TREEING'-VERHALTENS VPE-ISOLIERTER MITTELSPANNUNGSKABEL]
Detlef Fredrich 1991 164 p In GERMAN; ENGLISH summary (ETN-92-90588) Avail: NTIS HC/MF A08

Accelerated Water Treeing (WT) aging tests were carried out on 20 kV extruded cables as a contribution to the development of a WT test method optimized with regard to differentiability and test duration. The cables were isolated with water tree retardant cross linked polyethylene compounds. Extensive water supply, high bath temperature (90C), temperature gradient over the insulation, and water oxide enrichment were found to be very important WT accelerating factors. A differentiating evaluation of the WT behavior of different cables is already possible, thereby reducing the microscopic evaluation effort. The results confirm recent hypotheses that WT is mainly a field and humidity initiated, electrochemical process where oxidative degradation processes of the polymer play an essential role. ESA

N92-17576# Oak Ridge National Lab., TN.
DOE TASK FORCE MEETING ON ELECTRICAL BREAKDOWN OF INSULATING CERAMICS IN A HIGH RADIATION FIELD
P. H. Green, comp. Aug. 1991 621 p Meeting held in Vail, CO, 28 May - 2 Jun. 1991
(Contract DE-AC05-84OR-21400)
(DE92-000459; CONF-9105176) Avail: NTIS HC/MF A99

This volume contains the abstracts and presentation material from the Research Assistance Task Force Meeting, Electrical Breakdown of Insulating Ceramics in a High-Radiation Field. The meeting was jointly sponsored by the Office of Basic Energy Sciences and the Office of Fusion Energy of the U.S. Department of Energy in Vail, Colorado, May 28 to June 1, 1991. The 26 participants represented expertise in fusion, radiation damage, electrical breakdown, ceramics, and semiconductor and electronic structures. These participants came from universities, industries, national laboratories, and government. The attendees represented eight nations. The Task Force meeting was organized in response to the recent discovery that a combination of temperature, electric field, and radiation for an extended period of time has an unexplained adverse effect in ceramics, termed radiation-enhanced electrical degradation (REED). REED occurs after an incubation period and continues to accelerate with irradiation until the ceramics can no longer be regarded as insulators. It appears that REED is irreversible and the ceramic insulators cannot be readily annealed or otherwise repaired for future services. This effect poses a serious threat for fusion reactors, which require electrical insulators in diagnostic devices, in radio frequency and neutral beam systems, and in magnetic assemblies. The problem of selecting suitable electrical insulating materials is thus far more serious than previously anticipated. DOE

N92-17597# Hughes Aircraft Co., El Segundo, CA. Electro-Optical and Data Systems Group.
DETERMINATION OF THE TRIBOLOGICAL FUNDAMENTALS OF SOLID LUBRICATED CERAMICS. VOLUME 3: APPENDICES P THROUGH 2 Final Report, 9 Sep. 1985 - 16 Sep. 1989
Michael N. Gardos Sep. 1991 546 p
(Contract F33615-85-C-5087; DARPA Order 5177)
(AD-A242872; WRDC-TR-90-4096-Vol-3) Avail: NTIS HC/MF A23 CSCL 11/2

The fundamental nature of the research was exemplified by ab-initio predictions of the friction coefficient of single crystal diamond sliding against its mating diamond plane, and molecular dynamics calculations on single crystal calcium fluoride and barium fluoride interface shear forces. The test equipment developed for completing the model experiments included an Auger/ESCA tribometer capable of unidirectional and oscillatory sliding at room temperature, a scanning electron microscope tribometer designed for oscillatory sliding to 1000 C in vacuum and in partial pressures of reactive gases, an 850 C + dual-rubshoe friction and wear tester employing a rolling contact fatigue rod as one of the sliding specimens, and 850 C + friction/traction apparatus capable of operating to extraordinarily high PV limits. The fundamental nature of the research notwithstanding, the main goals were directed towards finding potential solutions and applications useful to practicing tribologists and lubrication engineers. GRA

N92-17612# Department of the Navy, Washington, DC.
CONSOLIDATION OF DIAMOND PACKED POWDERS Patent Application
Lawrence T. Kabacoff, inventor (to Navy) 8 Jul. 1991 9 p
(AD-D015071; US-Patent-Appl-SN-531488; Navy-Case-73414)
Avail: NTIS HC/MF A02 CSCL 07/2

This invention relates to diamonds and to diamond structural materials. Diamonds are the ideal material for a large number of applications. Diamonds are highly transparent to infrared radiation (IR) and radar, has the highest known heat conductivity, highest known hardness, produces little friction, does not conduct electricity, etc. However, diamond powders cannot be consolidated by currently known processes such as are used in the fabrication of ceramics (for example, sintering). Moreover, diamonds are not the thermodynamically favored structure at other than very high temperature and pressure. Complex shapes can be fabricated by deposition processes, but only at very low deposition rates. Thus, the deposition approach is very expensive. GRA

N92-17614# Hughes Aircraft Co., El Segundo, CA. Electro-Optical and Data Systems Group.
DETERMINATION OF THE TRIBOLOGICAL FUNDAMENTALS OF SOLID LUBRICATED CERAMICS. VOLUME 2: APPENDICES A THROUGH O Final Report, 9 Sep. 1985 - 16 Sep. 1989
Michael N. Gardos Sep. 1991 572 p

(Contract F33615-85-C-5087; DARPA Order 5177)
(AD-A242871; WRDC-TR-90-4096-Vol-2) Avail: NTIS HC/MF A24 CSCL 11/2

The goals, structures and highlights of a recently completed multiyear/multinational research program are described. The main driving force behind this effort was the aim to advance the technology base so engineers can design, build and operate solid lubricated ceramic tribocomponents in extreme environments. Specially designed friction and wear testers were employed to perform well-defined model experiments on single crystal and polycrystalline ceramics and solid lubricants. The research led to discoveries such as (1) a lubricious oxide with the shear strength of molybdenum disulfide in vacuum, (2) CVD diamond films with low friction and extraordinarily low wear, (3) intercalated graphites with high tribothermal resistance in vacuum and in air, and (4) a wear equation for silicon nitride ceramics. GRA

N92-17615# National Inst. of Standards and Technology, Gaithersburg, MD.
SPATIALLY AND SPECTRALLY RESOLVED CATHODOLUMINESCENCE MEASUREMENTS OF CVD-GROWN DIAMOND PARTICLES AND FILMS
Lawrence H. Robins, Edward N. Farabaugh, and Albert Feldman 27 Sep. 1991 15 p
(Contract N00014-90-F-0011)
(AD-A243220; NIST-TR-6) Avail: NTIS HC/MF A03 CSCL 20/12

Spatially and spectrally resolved cathodoluminescence (CL) was used to investigate the spatial distribution of luminescence centers in CVD-grown diamond particles and polycrystalline films. For single particles grown at a low substrate temperature (nominally 650 C), one of the two most intense CL bands, the 2.156 eV band, was found to be associated with (111) facets. The CL image of the other intense band, the 2.85 eV band, showed considerable particle-to-particle variation among the same particles. The images of the 2.156 eV and 2.85 eV CL bands were found to have a complementary relationship for some particles. A model of competing recombination centers is proposed to help explain these results. Cross-sectional measurements of the CL spectra of polycrystalline films on silicon showed that the intensity of a silicon-impurity-related CL band decreases with increasing distance from the film-substrate interface. This depth variation is interpreted as due to a silicon impurity concentration gradient. GRA

N92-17659# International Business Machines Corp., San Jose, CA.
OPTICAL SPECTRA AND KINETICS OF SINGLE IMPURITY MOLECULES IN A POLYMER: SPECTRAL DIFFUSION AND PERSISTENT SPECTRAL HOLE-BURNING Interim Technical Report
W. P. Ambrose, T. Basche, and W. E. Moerner 7 Nov. 1991 34 p
(Contract N00014-91-C-0166)
(AD-A243749; IBM-RJ8469; TR-31) Avail: NTIS HC/MF A03 CSCL 20/5

Using high efficiency fluorescence excitation techniques, optical spectra of single impurity molecules of perylene in a poly(ethylene) matrix can be obtained at 1.5 K. Analysis of such spectra show a variety of spectral diffusion effects, including fast resonance frequency changes on the 1-100 MHz scale which lead to a range of apparent linewidths, as well as discontinuous jumps in the resonance frequency of 10-1000 MHz on a longer time scale. In addition, light induced changes in resonance frequency of a single molecule (persistent spectral hole-burning) have been conclusively observed by showing that the burning time decreases with increasing laser power. Surprisingly, hole-burned single molecules often spontaneously return to the original frequency in 1-100 s. Measurements of the burning time for a large number of hole-burning events for the same simple molecule yield an exponential burn time distribution, which is the first direct measurement to our knowledge of the stochastic kinetics of a single molecule. GRA

N92-17661# International Business Machines Corp., San Jose, CA.
PHOTOREFRACTIVITY IN DOPED NONLINEAR ORGANIC POLYMERS Interim Technical Report
W. E. Moerner, C. Walsh, J. C. Scott, S. Ducharme, and D. M. Burland 7 Aug. 1991 21 p
(Contract N00014-91-C-0166)
(AD-A243751; IBM-RJ8287; TR-33) Avail: NTIS HC/MF A03 CSCL 07/6

This paper describes the properties of a new class of materials exhibiting the photorefractive effect, doped nonlinear organic polymers. Photorefraction (at 647.1 nm) was established by a combination of hologram erasability, correlation with photoconductivity and electro-optic response, and enhancement by external fields in numerous samples of two nonlinear epoxy materials doped with hole transport agents based on p-diethylaminobenzaldehyde-diphenyl hydrazone (DEH). Diffraction efficiencies up to 0.1 percent were observed at bias fields near 100 kV/cm. A useful property of these materials is that poling of the nonlinear chromophores is partially reversible, permitting partial control of the grating readout independent of the space-charge field formed. The polarization anisotropy of grating readout is consistent with the photorefractive mechanism. GRA

N92-17676*# National Aeronautics and Space Administration. Langley Research Center, Hampton, VA.
POLYIMIDES CONTAINING AMIDE AND PERFLUOROISOPROPYL CONNECTING GROUPS Patent Application
James F. Dezern, inventor (to NASA) 28 Aug. 1991 14 p
(NASA-Case-LAR-14608-1; NAS 1.71:LAR-14608-1; US-Patent-Appl-SN-752246) Avail: NTIS HC/MF A03 CSCL 11B

New, thermooxidatively stable polyimides were prepared from the reaction of aromatic dianhydrides containing isopropylidene bridging groups with aromatic diamines containing amide connecting groups between the rings. Several of these polyimides were shown to be semi-crystalline as evidenced by wide angle x ray scattering and differential scanning calorimetry. Most of the polyimides form tough, flexible films with high tensile properties. These polyimide films exhibit enhanced solubility in organic solvents. NASA

N92-17679# Texas Univ., Arlington. Center for Advanced Polymer Research.
SEPARATION OF NEUTRAL-TO-POLARON AND POLARON-TO-BIPOLARON REDOX EVENTS IN ALKOXY SUBSTITUTED DI-2-THIENYLPHENYLENE POLYMERS Technical Report, 1 Jun. - 30 Sep. 1991
Andrew D. Child and John R. Reynolds 21 Oct. 1991 9 p
(Contract N00014-90-J-1320)
(AD-A242423; TR-36) Avail: NTIS HC/MF A02 CSCL 07/4

In situ electron paramagnetic resonance (EPR)/electrochemistry methods have been used to elucidate the potential dependence of the presence of polaron and bipolaron charge carriers in poly(di-2-thienyl-2,5 diheptoxyphenylene). The identification of charge carriers in conjugated conducting polymers has recently received a great amount of attention. It is generally accepted that the electrochemical oxidation of polyheterocycles leads to the formation of delocalized radical cations (polarons) and ultimately to delocalized dications (bipolarons). Studies involving the electrochemical oxidation and reduction of conducting polyheterocycle films have suggested that the generation of polarons, and the subsequent formation of bipolarons, occurs at essentially the same potential. The potentials of these redox events appear to be too close to allow them to be distinguished by voltammetry. In situ EPR measurements carried out in an electrochemical cell have verified the presence of spin containing species (polarons) at intermediate doping levels in polypyrrole and polythiophene. The relative stability of the polaron intermediate has still not been fully elucidated; particularly in the case of polythiophene. GRA

N92-17683# Hughes Aircraft Co., El Segundo, CA. Electro-Optical and Data Systems Group.
DETERMINATION OF THE TRIBOLOGICAL FUNDAMENTALS OF SOLID LUBRICATED CERAMICS. VOLUME 1: SUMMARY Final Report, Sep. 1985 - Sep. 1989
Michael N. Gardos Nov. 1990 501 p
(Contract F33615-85-C-5087; DARPA Order 5177)
(AD-A243219; WRDC-TR-90-4096-Vol-1) Avail: NTIS HC/MF A22 CSCL 11/2

The goals, structure, and highlights of a recently completed multiyear/multinational research program are described. The main driving force behind this effort was the aim to advance the technology base so engineers can successfully and confidentially design, build, and operate solid lubricated ceramic tribocomponents in extreme environments. Specially designed friction and wear testers were employed to perform well-defined model experiment on single crystal and polycrystalline ceramics and solid lubricants. The research led to discoveries such as: (1) a lubricious oxide with the shear strength of molybdenum disulfides in vacuum; (2) CVD diamond films with low friction and extraordinarily low wear; (3) intercalated graphites with high tribothermal resistance in vacuum and in air; and (4) a wear equation for silicon nitride ceramics. The fundamental nature of the research was exemplified by ab-initio predictions of the friction coefficient of single crystal diamond sliding against its mating diamond plane, and molecular dynamics calculations on single crystal calcium fluorides and barium fluorides interface shear forces. The test equipment developed for completing the model experiments included an Auger/ESCA tribometer capable of unidirectional and oscillatory sliding at room temperature, a scanning electron microscope (SEM) tribometer designed for oscillatory sliding to 1000 C in vacuum and in partial pressures of reactive gases, an 850 C + dual-rubshoe friction and wear tester employing a rolling contact fatigue rod as one of the sliding specimens, and an 850 C + friction/traction apparatus capable of operating to extraordinarily high PV limits. GRA

N92-17693*# National Aeronautics and Space Administration. Langley Research Center, Hampton, VA.
IMIDE/ARYLENE ETHER COPOLYMERS WITH PENDENT TRIFLUOROMETHYL GROUPS
Brian J. Jensen and Stephen J. Havens (Lockheed Engineering and Sciences Co., Hampton, VA.) Jan. 1992 13 p
(NASA-TM-104195; NAS 1.15:104195) Avail: NTIS HC/MF A03 CSCL 11C

A series of imide/arylene ether block copolymers were prepared using an arylene ether block containing a hexafluoroisopropylidene group and an imide block containing a hexafluoroisopropylidene and a trifluoromethyl group in the polymer backbone. The copolymers were characterized and mechanical properties were determined and compared to the homopolymers. Author

N92-17710# Sandia National Labs., Albuquerque, NM.
ELECTRICALLY-CONTROLLED POLYMERIC GELS AS ACTIVE MATERIALS IN ADAPTIVE STRUCTURES
D. Segalman, W. Witkowski, D. Adolf, and M. Shahinpoor (New Mexico Univ., Albuquerque.) 1991 11 p Presented at the Active Materials and Adaptive Structures Conference, Alexandria, VA, 5-7 Nov. 1991
(Contract DE-AC04-76DP-00789)
(DE92-002947; SAND-91-1423C; CONF-9111130-1) Avail: NTIS HC/MF A03

This paper presents several applications of ionizable polymeric gels that are capable of undergoing substantial expansions and contractions when subjected to changing pH environments, temperature, or solvent. Conceptual designs for smart, electrically activated devices exploiting this phenomenon are discussed. These devices have the possibility of being manipulated via active computer control as large displacement actuators for use in adaptive structures. The enabling technology of these novel devices is the use of compliant containers for the gels and their solvents, removing the difficulties associated with maintaining a bath for the gels. Though most of these devices are designed using properties well discussed in the literature, some presented near the end of this paper make use of conclusions that the authors have drawn from the literature and their own experimental work. Those conclusions about the basic mechanisms of electromechanical gels are discussed in the third part of this paper and a complete set of governing equations describing these mechanisms are presented in the fourth section. This paper concludes with a discussion of some of the ramifications of the above system of equations and a discussion on gel-driven devices and on the control of such devices. DOE

N92-17745# Colorado State Univ., Fort Collins. Dept. of Chemistry.
MOLECULAR COMPOSITES FROM HIGH TEMPERATURE POLYQUINOLINES Final Report, 1 Aug. 1986 - 31 Jul. 1990
Elliot Bernstein, J. K. Stille, G. C. Berry, and D. R. Uhlmann Nov. 1991 50 p
(Contract F49620-86-C-0102)
(AD-A243634; AFOSR-91-0988TR) Avail: NTIS HC/MF A03 CSCL 07/6

The properties of blends of two polyquinolines and block copolymers of the same polymers have been studied as the basis for a molecular composite. The polyquinolines differ only in the presence or absence of an oxygen atom in the chain backbone. The chain conformation is found to be extended, with a persistence length of 20 nm without the oxygen linkage. The chain adopts a flexible conformation when the oxygen is present. Both forms, and their copolymer, were synthesized in this study. The results show that although the thermodynamically expected phase separation can be partially frustrated in the preparation of blends of the two polymers, the enhanced mobility at the elevated temperatures needed for processing the solid blend leads to substantial phase separation, with consequent deterioration of mechanical properties. GRA

N92-17749# Utah State Univ., Logan. Dept. of Chemistry and Biochemistry.
NEW FERROCENE COMPLEXES AND POLYMERS FOR NONLINEAR OPTICAL APPLICATIONS
Michael E. Wright and Edward G. Toplikar 30 Apr. 1991 10 p
(Contract N00014-91-J-1625)
(AD-A243640; TR-1) Avail: NTIS HC/MF A02 CSCL 07/6

Bis(functionalized) Ferrocene based NLO-phores were prepared. One cyclopentadienyl (Cp) ring was modified with a Beta-(alpha-cyanoacrylate) group and the other with a hydroxymethyl moiety. The ferrocene complex was placed in a poly(methyl methacrylate) matrix and subjected to corona onset poling. The polymer solutions exhibited SHG activity. The ferrocene complex was also melt cast polymerized to afford a polymer of unknown structure. The ferrocene system was modified with methacryloyl chloride and then successfully copolymerized with methyl methacrylate. A single crystal X ray diffraction study on a ferrocene NLO-phore is reported. GRA

N92-17750# Utah State Univ., Logan. Dept. of Chemistry and Biochemistry.
ORGANOMETALLIC NLO POLYMERS. LINEAR MAIN-CHAIN NLO POLYMERS OF FERROCENE
Michael E. Wright and Edward G. Toplikar 13 Dec. 1991 4 p
(Contract N00014-91-J-1625)
(AD-A243641; TR-2) Avail: NTIS HC/MF A01 CSCL 07/6

Bis(functionalized) ferrocene NLO-phore monomers were prepared. Several ferrocene NLO-phores were characterized by single-crystal molecular structures. The new ferrocene monomers were successfully polymerized using a Knoevenagel polycondensation technique. The polymers were characterized by spectroscopic and GPC data. A very recent use of ferrocene complexes has appeared in the area of nonlinear optical (NLO) materials. Based on both theory and experimental data, ferrocene compounds possess large hyperpolarizability values. These data combined with excellent thermal and photochemical stability make ferrocene systems a top organometallic candidate for use in NLO materials. Our research program has recently demonstrated that

a ferrocene complex bound to poly(methyl methacrylate) copolymer can be successfully aligned and exhibit the optical property of second harmonic generation. GRA

N92-17751# Utah State Univ., Logan. Dept. of Chemistry and Biochemistry.
ORGANOMETALLIC NLO POLYMERS. ACCORDIAN MAIN-CHAIN NLO POLYMERS OF FERROCENE
Michael E. Wright and Matthew S. Sigman 13 Dec. 1991 4 p
(Contract N00014-91-J-1625)
(AD-A243642; TR-3) Avail: NTIS HC/MF A01 CSCL 07/6

Bis(ferrocene) NLO-phore monomers were prepared. The new bis(ferrocene) monomer was successfully copolymerized with bis(cyanoacetate) comonomers using a Knoevenagel polycondensation technique. The polymers were characterized by spectroscopic, thermal analysis, and GPC data. The polymers had average molecular weights in the range of 5000 to 25,000. In the previous paper we presented the synthesis of linear organometallic main-chain NLO polymers. Our research has continued to focus on ferrocene based NLO polymers because of the outstanding results obtained by Marder and coworkers using crystalline ferrocene complexes. The ability to selectively functionalize the cyclopentadienyl rings of ferrocene has given us the ability to prepare elaborate organometallic NLO-phores. In this paper we present the synthesis and characterization of organometallic polymers with the potential of adopting the accordian macrostructure. As we saw in the previous paper, the use of the Knoevenagel condensation appears to be the most effective manner to prepare polymers of good molecular weight and tractability. GRA

N92-17752# Utah State Univ., Logan. Dept. of Chemistry and Biochemistry.
ARYL BIS(TRIFLATES) IN PALLADIUM (0) CROSS-COUPLING REACTIONS. SYNTHESIS OF POLYPHENYL-ALKYNYL, ALKENYL, AND ARYL ETHERS
Michael E. Wright 13 Dec. 1991 3 p
(Contract N00014-91-J-1625)
(AD-A243643; TR-4) Avail: NTIS HC/MF A01 CSCL 07/6

A new bis(triflate) monomer was prepared. The bis(triflate) was copolymerized with new organostannane comonomers under palladium (0) catalysis. The triflate monomer was also reacted with bis(phenol) compounds under basic conditions to afford poly(aryl ethers). The synthesis of polymers using a transition metal catalyzed cross-coupling reaction has become a growing and very productive area of polymer chemistry. Polycondensations using a transition metal catalyzed cross-coupling reaction follow polymerization rules governing stepgrowth processes, and thus, reaction efficiency and monomer purity are critical issues. As part of our polymer synthesis program we have been exploring the use of palladium (0) catalyzed polycondensation of organostannane and aryl halide partners. GRA

N92-17753# Utah State Univ., Logan. Dept. of Chemistry and Biochemistry.
ORGANIC NLO POLYMERS. LINEAR AND ACCORDIAN MAIN-CHAIN NLO POLYMERS PREPARED BY A KNOEVENAGEL POLYCONDENSATION
Michael E. Wright and Sanjoy Mullick 13 Dec. 1991 4 p
(Contract N00014-91-J-1625)
(AD-A243644; TR-5) Avail: NTIS HC/MF A01 CSCL 07/6

A new main-chain NLO polymer was prepared by transesterification and the Knoevenagel polycondensation. The latter polymer product was obtained as a higher molecular weight polymer with good solubility in organic solvents. New bis(arylcarboxaldehyde) monomers were prepared and copolymerized with bis(cyanoacetate) monomers to afford accordion main-chain NLO polymers. The polymers were characterized by spectroscopic and analytical data, thermal analysis, and GPC. GRA

N92-17777# Chicago Univ., IL.
[THE EFFECT OF MONOMER STRUCTURES AND COMPRESSIBILITY ON THE PROPERTIES OF MULTICOMPONENT POLYMER BLENDS AND SOLUTIONS] Annual Report
Karl F. Freed 6 Nov. 1991 3 p
(Contract N00014-91-J-1442)
(AD-A242863) Avail: NTIS HC/MF A01 CSCL 07/6

Our research has resulted in one paper which is in press as follows: Role of Monomer Structure and Compressibility on the Properties of Multicomponent Polymer Blends and Solutions: IV. High Molecular Weights, Temperature Dependences, and Phase Diagrams of Binary Polymer Blends. We have applied the compressible lattice cluster theory of structured polymer blends to studying how the effective interaction parameter varies with composition, monomer structure, microscopic interactions, and temperature. We consider a wide variety of different vinyl polymer structures and find that the effective interaction parameter displays a strong dependence on monomer structure. The composition dependence of the effective interaction is generally found to be a parabolic or linear function of composition, in general accord with experimental observations. Strong dependences on the microscopic interaction energies are also present. GRA

N92-17784# Washington Univ., Seattle. Dept. of Mechanical Engineering.
DYNAMIC FRACTURE CHARACTERIZATION OF Al2O3 AND SiC(w)/Al2O3
L. R. Deobald and A. S. Kobayashi Sep. 1991 19 p
(Contract N00014-87-K-0326)
(AD-A242187; UWA/DME/TR-91/7) Avail: NTIS HC/MF A03 CSCL 11/4

In spite of their many favorable properties, ceramics have severe disadvantages of brittleness and poor impact resistance due to inherently low fracture toughness. An obvious method to improve the toughness of ceramic materials is through the use of composite techniques. The possible improved toughness due to the addition of ceramic whisker fibers should allow a graceful failure rather than a catastrophic failure of a ceramic component. Several mechanisms exist by which a ceramic matrix composite can exhibit superior toughness over the toughness of the matrix material. These mechanisms include crack bridging, fiber pullout, crack deflection mechanisms, microcrack shielding, and phase transformation. In crack bridging, intact whisker fibers bridge the space between the two crack faces of the matrix. Since the fibers apply a crack closure force behind the crack tip, addition energy is required to overcome this force and propagate the crack. GRA

N92-17840# Technische Univ., Eindhoven (Netherlands).
MODELLING OF SOME EQUILIBRIUM THERMODYNAMIC PROPERTIES OF POLYMER SYSTEMS Ph.D. Thesis
Alexander Antonius M Stroeks 1991 188 p Sponsored by Netherlands Organization for Applied Scientific Research TNO
(ETN-92-90570) Avail: NTIS HC/MF A09

A study of miscibility behavior and related properties of polymer systems in the framework of the hole theories, aimed at providing more insight into the theoretical factors which govern polymer miscibility, is presented. Theoretical background of the Simha-Somcynsky theory and its relation with other equation of state theories are discussed and a theoretical modification of this theory is presented. The process of the extraction of pure component model parameters from equilibrium equation of state data is presented. A polynomial fit of the Gibbs free energy of mixing, used to compute the compositional derivatives governing phase behavior, is compared with exact and more general computations of these derivatives. Additionally, consequences for the computed phase behavior of the solution polyethylene/n-hexane are discussed. The Simha-Somcynsky theory and its modified version are confronted with detailed miscibility information of the solution polystyrene/cyclohexane. The relation between pressure influence on miscibility and thermodynamic excess functions is addressed. The phase behavior of polymer blends is addressed: phase behavior is investigated

for a hypothetical model blend; the influences of the molar mass of the constituents and pressure effects in the phase diagrams are studied; the miscibility behavior of the blend polystyrene/poly(paramethylstyrene) under atmospheric conditions is determined; and phase separation is detected by differential scanning calorimetry and phase optical microscopy techniques. ESA

N92-17842# Edgerton, Germeshausen and Grier, Inc., Idaho Falls, ID.
A METHOD FOR JOINING CERAMIC SHAPES Patent Application
B. H. Rabin, inventor (to DOE) 26 Jun. 1990 15 p
(Contract DE-AC07-76ID-01570)
(DE92-003815; US-Patent-Appl-SN-543897;
Patents-US-A7543897) Avail: NTIS HC/MF A03

The invention is a method for joining shapes of ceramic materials together to form a unitary ceramic structure. In the method of the invention, a mixture of two or more chemical components which will react exothermically is placed between the surfaces to be joined, and the joined shapes heated to a temperature sufficient to initiate the exothermic reaction forming a joining material which acts to bond the shapes together. Reaction materials are chosen which will react exothermically at temperatures below the degradation temperature of the materials to be joined. The process is particularly suited for joining composite materials of the silicon carbide-silicon carbide fiber type. DOE

N92-17935# Edgerton, Germeshausen and Grier, Inc., Idaho Falls, ID.
PHOSPHAZENE POLYMER CONTAINING COMPOSITES AND METHOD FOR MAKING PHOSPHAZENE POLYMER CONTAINING COMPOSITES Patent Application
C. A. Allen, inventor (to DOE), A. E. Grey, inventor (to DOE), R. R. McCaffrey, inventor (to DOE), B. M. Simpson, inventor (to DOE), and M. L. Stone, inventor (to DOE) 30 Jul. 1990 22 p
(Contract DE-AC07-76ID-01570)
(DE92-003826; US-Patent-Appl-SN-559234;
Patents-US-A7559234) Avail: NTIS HC/MF A03

It is the object of the invention to provide a composite material comprised of phosphazene polymer. A feature of phosphazene-containing composites is their superior stiffness, thermal stability, and hardness which is lacking in more typical composite constituents. An advantage of using phosphazene composites is a wider range of applications, including uses in harsh environments. Another object of the present invention provides a method for producing phosphazene-containing composite materials through a pultrusion process. In brief, these and other objects are achieved by a composite produced by first coating a reinforcing material with an inorganic phosphazene compound and then polymerizing the phosphazene compound so as to confer superior thermal, physical and chemical resistance qualities to the composite. DOE

N92-17938# Sandia National Labs., Albuquerque, NM.
STRUCTURE AND TOPOLOGY OF SILICA AEROGELS
D. W. Schaefer, B. J. Olivier, C. S. Ashley, D. Richter (Kernforschungsanlage, Juelich, Germany, F.R.), B. Farago, and B. Frick 1991 20 p Presented at the 3rd International Symposium on Aerogels, Wuerzburg, Fed. Repubic of Germany, 30 Sep. - 2 Oct. 1991
(Contracts DE-AC04-76DP-00789; W-7405-eng-48)
(DE92-004728; SAND-91-2509C; Conf-910960-3) Avail: NTIS HC/MF A03

Neutron spin-echo spectroscopy is used to study the topology of aerogels. Topology or connectivity is varied through precursor chemistry and thermal annealing. Topology is characterized using the concept of fractons (the vibrational excitations of a fractal network). A qualitative difference is observed in the spectrum of polymeric vs colloidal aerogels, the latter showing a peak in the density of vibrational states. For colloidal aerogels whose structure appears to arise from phase separation in the solution precursor, low-energy excitations were only observed in the lowest density material studied. Finally, a transition from fractal to colloidal microstructure was observed during the sintering of polymeric aerogels. This transformation revealed itself as a transition from a fracton-like to a peaked density of states function. DOE

N92-17942# Syracuse Univ., NY. Dept. of Chemical Engineering and Materials Science.
MECHANISMS OF GAS PERMEATION THROUGH POLYMER MEMBRANES
S. A. Stern 1991 28 p
(Contract DE-FG02-87ER-13649)
(DE92-004423; DOE/ER-13649/5) Avail: NTIS HC/MF A03

The objective of the present study is to investigate the mechanisms of gas transport in and through polymer membranes and the dependence of these mechanisms on pressure and temperature. This information is required for the development of new, energy-efficient membrane processes for the separation of industrial gas mixtures. Such processes are based on the selective permeation of the components of gas mixtures through nonporous polymer membranes. Recent work has been focused on the permeation of gases through membranes made from glassy polymers, i.e., at temperatures below the glass transition of the polymers (Tg). Glassy polymers are very useful membrane materials for gas separations because of their high selectivity toward different gases. Gases permeate through nonporous polymer membranes by a 'solution-diffusion' process. Consequently, in order to understand the characteristics of this process it is necessary to investigate also the mechanisms of gas solution and diffusion in glassy polymers. DOE GR

N92-17947# Naval Ocean Systems Center, San Diego, CA.
NOVEL CERAMIC MATRIX COMPOSITES FOR DEEP SUBMERGENCE PRESSURE VESSEL APPLICATIONS Final Report
J. D. Stachiw, T. J. Henderson, and C. A. Anderson Oct. 1991 39 p
(AD-A242740; NOSC-TD-2222) Avail: NTIS HC/MF A03
CSCL 11/4

Novel ceramic matrix composite tubes for deep submergence pressure vessel applications have been fabricated by the DIMOX directed metal oxidation process. These silicon carbides/aluminum oxides composite tubes have an eight percent lower weight to displacement ratio, approximately five times greater thermal conductivity, and more than 50 percent higher fracture toughness than a tube fabricated from alumina ceramics. Additionally, the SiC/Al2O3 composite tubes have a sixty percent lower weight to displacement ratio and a 12 times greater thermal conductivity than Ti-6Al-4V alloy tubes. Processing information, hydrostatic implosion test results, and mechanical test data are discussed. GRA

N92-17966# Utah Univ., Salt Lake City. Dept. of Physics.
PHOTOMODULATION SPECTROSCOPY OF PHOTOCARRIER DYNAMICS, ELECTRONIC DEFECTS AND MORPHOLOGY OF CONDUCTING POLYMERS
Z. V. Vardeny Oct. 1991 11 p
(Contract DE-FG02-89ER-45409)
(DE92-004687; DOE/ER-45409/2) Avail: NTIS HC/MF A03

This is a progress report on the second period of activities associated with the DOE grant to the Physics Department of the University of Utah, starting on April 1st, 1991, on photocarrier dynamics, electronic defects and morphology of conducting polymers using photomodulation spectroscopy. During the second period of this grant we have achieved impressive results and have started new studies, to be completed during the grant continuation period of the third year. We will describe our progress according to the material studied, since this is the best method to summarize our accomplishments. We have used a variety of techniques in our studies such as CW photomodulation, photomodulation in the femtosecond and picosecond time ranges, CW resonant Raman scattering, transient photoinduced Raman scattering, electro-absorption, degenerate four-wave mixing and the new

technique of spin dependent photomodulation. These techniques have been used to obtain the transient electronic response of conducing polymers. DOE

28 PROPELLANTS AND FUELS

Includes rocket propellants, igniters, and oxidizers; their storage and handling procedures; and aircraft fuels.

For related information see also *07 Aircraft Propulsion and Power, 20 Spacecraft Propulsion and Power,* and *44 Energy Production and Conversion.*

N92-17058# Materials Research Labs., Ascot Vale (Australia).
A THEORETICAL STUDY OF THE COMBUSTION OF MAGNESIUM/TEFLON/VITON PYROTECHNIC COMPOSITIONS
L. V. deYong and K. J. Smit Aug. 1991 35 p
(AD-A243244; MRL-TR-91-25; DODA-AR-006-379) Avail: NTIS HC/MF A03 CSCL 19/1

A theoretical study has been conducted using the NASA-Lewis CEC 76 computer code to model the combustion of pyrotechnic compositions based on magnesium/Teflon/Viton. The study examines the effect of formulation changes on the distribution of reaction products, the reaction temperature and the heat of reaction. The maximum temperature and heat are produced in the stoichiometric fuel concentration whilst the reaction products change significantly with the concentration of magnesium. The Teflon and Viton oxidizers generally have only a minor effect on the system thermodynamics. The major reaction products are magnesium fluoride, magnesium and solid carbon. The proportion of carbon as a combustion product remains relatively constant over a large range of fuel or oxidant concentration. The choice of the optimal MTV composition for IR decoy applications appears to be based more on burn rate and ignitability requirements than on temperature, heat output or optimization of reaction products. GRA

N92-17066# Southwest Research Inst., San Antonio, TX. Fuels and Lubricants Research Facility.
EVALUATION OF MOTOR GASOLINE STABILITY Interim Report
Leo L. Stavinoha, John N. Bowden, and Maurice E. LePera Dec. 1990 98 p
(Contract DAAK70-87-C-0043; DA Proj. 1L2-63001-D-150)
(AD-A243063; BFLRF-266) Avail: NTIS HC/MF A05 CSCL 21/4

This report covers results of a storage program whose primary goal was the development of improved methods for evaluating motor gasoline stability. Several existing and potential predictive tests were applied to individual refinery components of gasoline, selected laboratory blends, and commercial gasolines for which ASTM D 525 induction periods ranged from 75 to 5000 minutes. Darkroom storage was conducted at 43 C, 54 C, and ambient temperatures, for various time periods with ambient storage ultimately reaching 4 years for most of the samples. Results confirm the findings of earlier researchers that ASTM D 525 is not viable as a predictive device by virtue of a low coefficient of determination between induction period and gum formed in storage at 43 C for periods up to 1 year. It is recognized, however, and ASTM D 525 is not likely to be abandoned as a specification stability test. Based upon the data generated under the four phases of this storage stability of commercial/military motor gasoline (produced for long term storage) is the ASTM D 873 Method using a 6-hour aging existent gum maximum limit of 5 mg/100 mL. GRA

N92-17184# Pittsburgh Univ., PA. Dept. of Chemical and Petroleum Engineering.
CATALYTIC STUDIES ON A NOVEL SYNTHESIS OF METHANOL
V. M. Palekar, J. W. Tierney, and I. Wender 28 Jun. 1991 24 p Presented at the Summer National Meeting of the American Institute of Chemical Engineers (AIChE), Pittsburgh, PA, 20-22 Aug. 1991
(Contract DE-FG22-89PC-89786)
(DE92-002904; CONF-910852-16) Avail: NTIS HC/MF A03

Catalytic studies on a new method for methanol synthesis from CO and H2 in a slurry reactor are described. This reaction proceeds through the carbonylation of methanol to methyl formate in the liquid phase followed by hydrogenolysis of methyl formate to two molecules of methanol; the net result is the reaction of CO with H2 to give methanol. Moderate temperatures and pressures (100-160 C, 50-65 atm) are used. Reaction rates using mixed catalysts comprised of an alkali methoxide and Cu-chromite are presented. It seems likely that Cu-chromite maintains the activity of the alkali methoxide catalyst. A mixed catalyst comprised of potassium methoxide and Cu-chromite was found to be the most active under the reaction conditions used. Evidence is provided for an interaction between the alkali methoxide and Cu-chromite. DOE

N92-17399# Department of the Navy, Washington, DC.
ENERGETIC COMPOSITES OF CYCLODEXTRIN NITRATE ESTERS AND NITRATE ESTER PLASTICIZERS Patent Application
John Consaga, inventor (to Navy) 8 Jul. 1991 12 p
(AD-D015068; US-Patent-Appl-SN-728918; Navy-Case-73644)
Avail: NTIS HC/MF A03 CSCL 11/9

An energetic composite is presented that is made of a mixture of: (1) a solid nitrate ester of a cyclodextrin or a mixture of cyclodextrins; and (2) an energetic organic nitrate ester plasticizer. Author

N92-17533# Mound Lab., Miamisburg, OH.
EVALUATION OF SQUIB PERFORMANCE VARIABLES
A. C. Munger, C. M. Woods, and M. R. Phillabaum 1991 18 p Presented at the 16th International Pyrotechnic Seminar, Jonkoping (Sweden), 24-28 Jun. 1991
(Contract DE-AC04-88DP-43495)
(DE92-002034; MLM-3700(OP); CONF-9106187-3) Avail: NTIS HC/MF A03

The use of Kinetic Energy Device for measuring the output of a pyrotechnic squib or actuator was presented in the proceedings of the Thirteenth Pyrotechnic Seminar held in Grand Junction, Colorado 1988. This device was demonstrated as a valuable tool for evaluating the interface design between the squib and the next assembly. The thrust of this investigation was to evaluate the amount of containment that the interface provides and its effect on the amount of energy transmitted to a moving piston on the other side of the interface. Experiments were repeats of tests done with another test device known as the Variable Explosive Chamber. This data was presented in the proceedings of the Twelfth Pyrotechnic Seminar held in Juan-les-Pins, France 1987. A second area of investigation was to determine the effects of variation in the average compaction density and total mass of pyrotechnic powder load on the performance of the squib. The data shown here is for one specific geometry but may have implications to other geometries and even to other devices such as ignitors or matches. The equations of motion are examined for two geometries of test actuators. Pressure pulse curves are derived from the displacement versus time records for the extremes of a constant density, variable mass test series. DOE

N92-17562# Ballistic Research Labs., Aberdeen Proving Ground, MD.
PYROLYSIS GC-FTIR STUDIES OF A LOVA PROPELLANT FORMULATION SERIES Final Report, Nov. 1989 - Nov. 1990
Rose A. Pesce-Rodriguez, Frederick J. Shaw, and Robert A. Fifer Nov. 1991 56 p
(AD-A242844; BRL-TR-3288) Avail: NTIS HC/MF A04 CSCL 19/1

The primary objective of this investigation was to identify correlations between ignition times and pyrolysis product distributions. Such correlations have been found for go/no-go ignition times, but not for first light ignition times. Several trends in pyrolysis product distribution as a function of propellant

composition have been observed. Most of these trends are believed to be related to the ability of BTTN (1,2,4 Butane trinitrate) and TMETN (Trimethylolethane trinitrate) to catalyze decomposition. Pyrolysis-gas chromatography-Fourier transform infrared (P-GC-FTIR) spectroscopy was used to examine the pyrolysis product distribution for a LOVA propellant formulation series. The series was provided by the Naval Weapons Center (NWC), China Lake, and contained the oxidizers HMX and RDX, the polymers GAP, HTPB, BAMA/AMMO, and BAMO/THF, and the plasticizers BTTN and TMETN. Trends in product distribution as a function of formulation, as well as correlations between pyrolysis products and NWC performance data, were identified. The most noteworthy correlation observed was between the amount of permanent gas produced and go/no-go ignition times. In general, pyrolysis product distributions were found to be most strongly affected by the presence and type of plasticizer. The results of this investigation may serve as a basis for formulation design and bench-scale propellant screening. GRA

N92-17624# EG and G Mound Applied Technologies, Miamisburg, OH.
SENSITIVITY TESTING AND ANALYSIS
B. T. Neyer 1991 20 p Presented at the 16th International Pyrotechnic Seminar, Jonkoping (Sweden), 24-28 Jun. 1991
(Contract DE-AC04-88DP-43495)
(DE92-002033; MLM-3701(OP); CONF-9106187-4) Avail: NTIS HC/MF A03

New methods of sensitivity testing and analysis are proposed. The new test method utilizes Maximum Likelihood Estimates to pick the next test level in order to maximize knowledge of both the mean (mu) and the standard deviation (sigma) of the population. Simulation results demonstrate that this new test provides better estimators (less bias and smaller variance) of both mu and sigma than the other commonly used tests (Probit, Bruceton, Robbins-Monro, and Langlie). A new method of analyzing sensitivity tests is also proposed. It uses the Likelihood Ratio Test to compute regions of arbitrary confidence. It can calculate confidence regions, for mu, sigma, and arbitrary percentiles. Unlike presently used methods, such as the program ASENT which is based on the Cramer-Rao theorem, it can analyze the results of all sensitivity tests, and it does not significantly underestimate the size of the confidence regions. The new test and analysis methods will be explained and compared to the presently used methods. DOE

N92-17632# Army Armament Research, Development and Engineering Center, Picatinny Arsenal, NJ. Energetics and Warheads Div.
MECHANICAL AND THERMOMECHANICAL PROPERTIES OF NC BASE PROPELLANTS
D. A. Wiegand, S. Nicolaides, and J. Pinto Nov. 1991 30 p
(AD-A243045; ARAED-TR-91023) Avail: NTIS HC/MF A03
CSCL 19/1

Compressive mechanical properties have been investigated as a function of temperature and strain rate for a modified double base propellant (JA2) and comparison made with similar studies for a triple base propellant. Measurements were made at strain rates of 10 sec(-1) and 10(-3) sec(-1) and temperatures of 80 to -60 C. At the higher strain rate, the double base propellant shows ductile behavior at 20 C and brittle failure at the low temperature. However, comparison with triple base propellants indicates that this double base propellant is much less brittle at the lower temperature, and considerably less fragmentation is observed for the double base propellant. While the ductile-to-brittle transition can be related to a glass type transition temperature, the difference in fragmentation is apparently related to composition and structure. The relationship of ductile and brittle failure to abnormal burning and the related unsafe gun firing conditions is discussed. GRA

N92-17830 Department of the Navy, Washington, DC.
LAUNCHING PROJECTILES WITH HYDROGEN GAS GENERATED FROM ALUMINUM FUEL POWDER/WATER REACTIONS Patent
Woodrow W. Lee, inventor (to Navy) 1 Oct. 1991 8 p Filed 6 Aug. 1990
(AD-D015119; US-Patent-5,052,272; US-Patent-Appl-SN-564894; US-Patent-Class-89-7) Avail: US Patent and Trademark Office
CSCL 19/1

A method of propelling a projectile from a device by applying a high power pulse of electrical current to a thin metal conductor wire causing the wire to explode and disperse hot spots of molten metal throughout an aluminum fuel powder/water mixture which reacts to generate hydrogen gas at high pressure in a chamber is described. The hydrogen gas is used to push the projectile from the device. Author (GRA)

N92-17963# Oak Ridge National Lab., TN.
DETECTION OF EXPLOSIVES MATERIAL ON SINGLE MICROPARTICLES
W. B. Whitten, J. M. Dale, and J. M. Ramsey 1991 7 p Presented at the FAA Explosives Detection Symposium, Atlantic City, NJ, 13-15 Nov. 1991
(Contract DE-AC05-84OR-21400)
(DE92-004408; CONF-9111129-4) Avail: NTIS HC/MF A02

Some of the explosive materials with very low vapor pressure such as RDX or PETN are most likely to be encountered either as solids or adsorbed on solids. We are developing a new technique for the chemical characterization of explosive bearing microparticles based upon the use of electrodynamic traps. Single microparticles are analyzed by laser ablation mass spectrometry in an ion trap detector. DOE

29 MATERIALS PROCESSING

Includes space-based development of products and processes for commercial applications.
For biological materials see *55 Space Biology.*

N92-17945*# National Aeronautics and Space Administration, Washington, DC.
MICROGRAVITY SCIENCE AND APPLICATIONS PROGRAM TASKS, 1990 REVISION
May 1991 255 p
(NASA-TM-4284; NAS 1.15:4284) Avail: NTIS HC/MF A12
CSCL 22A

The active research tasks as of the end of the fiscal year 1990 sponsored by the Microgravity Science and Applications Division of the NASA Office of Space Science and Applications are compiled. The purpose is to provide an overview of the program scope for managers and scientists in industry, university, and government communities. The report includes an introductory description of the program, the strategy and overall goal; an index of principle investigators; and a description of each task. A list of recent publications is also provided. The tasks are grouped into six major categories: electronic materials; solidification of metals, alloys, and composites; fluid dynamics and transport phenomena; biotechnology; glasses and ceramics; combustion; experimental technology; facilities; and Physics And Chemistry Experiments (PACE). The tasks are divided into ground-based and flight experiments. Author

31 ENGINEERING (GENERAL)

Includes vacuum technology; control engineering; display engineering; cryogenics; and fire prevention.

N92-16989*# Martin Marietta Aerospace, Denver, CO. Astronautics Group.
EXTRAVEHICULAR MOBILITY UNIT SUBCRITICAL LIQUID OXYGEN STORAGE AND SUPPLY SYSTEM Conceptual Design Study Report, 30 Sep. 1991 - 31 Jan. 1992
John Anderson, Timothy Martin, and Ed Hodgson (Hamilton Standard Management Services, Houston, TX.) Jan. 1992 57 p

(Contract NAS9-18608)
(NASA-CR-189831; NAS 1.26:189831; MCR-92-1310; CSC-92-0141) Avail: NTIS HC/MF A04 CSCL 13B

The storage of life support oxygen in the Extravehicular Mobility Unit in the liquid state offers some advantages over the current method of storing the oxygen as a high pressure gas. Storage volume is reduced because of the increased density associated with liquid. The lower storage and operating pressures also reduce the potential for leakage or bursting of the storage tank. The potential for combustion resulting from adiabatic combustion of the gas within lines and components is substantially reduced. Design constraints on components are also relaxed due to the lower system pressures. A design study was performed to determine the requirements for a liquid storage system and prepare a conceptual design. The study involved four tasks. The first was to identify system operating requirements that influence or direct the design of the system. The second was to define candidate storage system concepts that could possibly satisfy the requirements. An evaluation and comparison of the candidate concepts was conducted in the third task. The fourth task was devoted to preparing a conceptual design of the recommended storage system and to evaluate concerns with integration of the concept into the EMU. The results are presented. Author

N92-17263# Massachusetts Inst. of Tech., Cambridge. Lab. for Computer Science.
USING MAPPINGS TO PROVE TIMING PROPERTIES
Nancy Lynch and Hagit Attiya Oct. 1991 45 p
(Contracts N00014-89-J-1988; N00014-90-J-1046; N00014-85-K-0168; N00014-87-K-0825; NSF CCR-86-11442; NSF CCR-89-15206)
(AD-A242862; MIT/LCS/TM-412-D) Avail: NTIS HC/MF A03 CSCL 12/7

A new technique for proving timing properties for timing-based algorithms is described; it is an extension of the mapping techniques previously used in proofs of safety properties for asynchronous concurrent systems. The key to the method is a way of representing a system with timing constraints as an automation whose state includes predictive timing information. Timing assumptions and timing requirements for the system are both represented in this way. A multi-valued mapping from the assumptions automation to the requirements automation is then used to show that the given system satisfies the requirements. One type of mapping is based on a collection of progress functions providing measures of progress toward timing goals. The technique is illustrated with two examples, a simple resource manager and a two-process race system. GRA

N92-17272# Department of Defense Explosives Safety Board, Alexandria, VA.
STRUCTURES TO RESIST THE EFFECTS OF ACCIDENTAL EXPLOSIONS
Nov. 1990 1783 p
(AD-A243272; DA-TM-5-1300; NAVFAC-P-397; AF-AFR-88-22) Avail: NTIS HC/MF A99 CSCL 19/1

The purpose of this manual is to present methods of design for protective construction used in facilities for development, testing, production, storage, maintenance, modification, inspection, demilitarization, and disposal of explosive materials. The primary objectives are to establish design procedures and construction techniques whereby propagation of explosion (from one structure or part of a structure to another) or mass detonation can be prevented and to provide protection for personnel and valuable equipment. The secondary objectives are to: (1) Establish the blast load parameters required for design of protective structures, (2) Provide methods for calculating the dynamic response of structural elements including reinforced concrete, and structural steel, (3) Establish construction details and procedures necessary to afford the required strength to resist the applied blast loads, and (4) Establish guidelines for siting explosive facilities to obtain maximum cost effectiveness in both the planning and structural arrangements, providing closures, and preventing damage to interior portions of structures because of structural motion, shock, and fragment perforation. GRA

N92-17535# Allied-Signal Aerospace Co., Kansas City, MO. Technical Communications.
SCALE-UP OF RECOVERY PROCESS FOR WASTE SOLVENTS Final Report
G. W. Bohnert and D. A. Carey Feb. 1991 23 p
(Contract DE-AC04-76DP-00613)
(KCP-613-4479) Avail: NTIS HC/MF A03

Recycling of spent cleaning solvents, 1,1,1 trichloroethane, trichloroethylene, and trichlorotrifluoroethane at KCP was evaluated. Gas chromatography was used to identify stabilization levels in virgin and recycled solvent. Segregation, pretreatment, and distillation processes were defined. Existing distillation equipment was modified and a solvent drying process was added. Recycled solvent quality of several production lots is also presented. Author

N92-17593# Department of Energy, Upton, NY. Engineering and Geosciences Div.
SUMMARIES OF FY 1991 ENGINEERING RESEARCH
Nov. 1991 58 p
(DE92-004708; DOE/ER-0529P) Avail: NTIS HC/MF A04

This report documents the BES Engineering Research Program for fiscal year 1991; it provides a summary for each of the program projects in addition to a brief program overview. The report is intended to provide staff of Congressional committees, other executive departments, and other DOE offices with substantive program information so as to facilitate governmental overview and coordination of Federal research programs. Of equal importance, its availability facilitates communication of program information to interested research engineers and scientists. The organizational chart for the DOE Office of Energy Research (OER) delineates the six Divisions within the OER Office of Basic Energy Sciences (BES). Each BES Division administers basic, mission oriented research programs in the area indicated by its title. The BES Engineering Research Program is one such program; it is administered by the Engineering and Geosciences Division of BES. In preparing this report we asked the principal investigators to submit summaries for their projects that were specifically applicable to fiscal year 1991. Major topics covered include fluid mechanics, fracture mechanics, chemical engineering, and mechanical engineering. DOE

N92-17674*# National Aeronautics and Space Administration. Pasadena Office, CA.
THREE-STAGE SORPTION TYPE CRYOGENIC REFRIGERATION SYSTEM AND METHOD EMPLOYING HEAT REGENERATION Patent Application
Steven Bard, inventor (to NASA) and Jack A. Jones, inventor (to NASA) (Jet Propulsion Lab., California Inst. of Tech., Pasadena.) 22 Oct. 1991 21 p
(Contract NAS7-918)
(NASA-Case-NPO-18366-1-CU; NAS 1.71:NPO-18366-1-CU; US-Patent-Appl-SN-781520) Avail: NTIS HC/MF A03 CSCL 13B

A three-stage sorption type cryogenic refrigeration system, each stage containing a fluid having a respectively different boiling point. Each stage includes a compressor in which a respective fluid is heated to be placed in a high pressure gaseous state. The compressor for that fluid which is heated to the highest temperature is enclosed by the other two compressors to permit heat to be transferred from the inner compressor to the surrounding compressors. The system may include two sets of compressors, each having the structure described above, with the interior compressors of the two sets coupled together to permit selective heat transfer therebetween, resulting in more efficient utilization of input power. NASA

N92-17757# National Aerospace Lab., Tokyo (Japan). Thermofluid Dynamics Div.
DISCUSSION FOR POSSIBILITY OF SOME AERODYNAMIC GROUND EFFECT CRAFT [ARU AERODAINAMIKKU GURAUNDO IFEKUTO KURAFUTO NO KANOSEI NIKANSURU ICHI KOSATSU]
Yoshikazu Tanabe May 1990 32 p In JAPANESE
(NAL-TM-619; ISSN-0452-2982; JTN-92-80290) Avail: NTIS HC/MF A03

Some type of pleasant, convenient, safe, and economical transportation method to supplement airplane transportation is currently required. This paper proposes an Aerodynamic Ground Effect Craft (AGEC) as this new transportation method, and studies its qualitative feasibility in comparison with present typical transportation methods such as transporter airplanes, flying boats, and linear motor cars which also have common characteristics of ultra low altitude cruising. Noteworthy points of AGEC are the effective energy consumption against transportation capacity (exergie) and the ultra low altitude cruising, which is relatively safer at the emergency landing than the subsonic airplane's body landing. Through AGEC has shorter cruising range and smaller transportation capacity, its transportation efficiency is superior to that of airplanes and linear motor cars. There is no critical difficulty in large sizing of AGEC, and AGEC is thought to be the very probable candidate which can supplement airplane transportation in the near future. Author (NASDA)

N92-17780# Los Alamos National Lab., NM.
EVALUATION OF ENVIRONMENTALLY SAFE CLEANING AGENTS FOR DIAMOND TURNED OPTICS
Lonnie A. Theye, Robert D. Day, Jeffrey Weinrach, Rudolf Schubert, and Stephen Seiffert (Benchmark Environmental Corp., Albuquerque, NM.) 1991 10 p Presented at the 1st International Congress on Environmentally Conscious Manufacturing, Santa Fe, NM, 18 Sep. 1991
(Contract W-7405-eng-36)
(DE92-002524; LA-UR-91-3437; CONF-9109259-11) Avail: NTIS HC/MF A02

Precision machining of metal surfaces using diamond turning has increased greatly in popularity at LANL in recent years. Similar techniques are used extensively to manufacture metal mirrors for use in laser applications. The diamond turned surfaces are easily damaged, making the selection of a cleaning agent very critical. These surfaces have been traditionally cleaned using Trichloroethane (TCA) to remove residual oil remaining from the machining process. The TCA was then removed with an ethanol rinse, leaving a residue free surface. Recently, however, TCA was pronounced environmentally unsafe. Consequently, we are searching for an environmentally safe cleaning agent for these diamond turned metal optics. The concern with using alternative solvents is the potential for residual surface films that produce reflectivity changes related to a combination of wavelength, surface coverage, film thickness and dielectric properties. Therefore, we have initiated a program for testing the effectiveness of a variety of environmentally safe solvents used to clean diamond turned optical surfaces. Our basic test plan consists of comparing a number of environmentally safe solvents against the TCA/ethanol cleaning system. We have identified twelve candidate solvents, but have only been able to perform a partial test on one of them to date. This paper discusses the results obtained to date using this solvent known as P F. DOE

N92-17913*# National Aeronautics and Space Administration. Lyndon B. Johnson Space Center, Houston, TX.
SHARPS CONTAINER Patent Application
Angelene M. Lee, inventor (to NASA) 7 Oct. 1991 13 p
(NASA-Case-MSC-21776-1; NAS 1.71:MSC-21776-1; US-Patent-Appl-SN-772763) Avail: NTIS HC/MF A03 CSCL 13B

This invention relates to a system for use in disposing of potentially hazardous items and more particularly a Sharps receptacle for used hypodermic needles and the like. A Sharps container is constructed from lightweight alodined nonmagnetic metal material with a cup member having an elongated tapered shape and length greater than its transverse dimensions. A magnet in the cup member provides for metal retention in the container. A nonmagnetic lid member has an opening and spring biased closure flap member. The flap member is constructed from stainless steel. A Velcro patch on the container permits selective attachment at desired locations. NASA

32 COMMUNICATIONS AND RADAR

Includes radar; land and global communications; communications theory; and optical communications.

For related information see also *04 Aircraft Communications and Navigation* and *17 Space Communications, Spacecraft Communications, Command and Tracking.* For search and rescue see *03 Air Transportation and Safety,* and *16 Space Transportation.*

N92-16980# Harry Diamond Labs., Adelphi, MD.
HEMP TEST ON FD-565 Interim Report, Jan. 1990 - Jan. 1991
Ronald J. Reyzer and Mark H. Mar Nov. 1991 33 p
(AD-A243099; HDL-SR-91-8) Avail: NTIS HC/MF A03 CSCL 20/6

This report describes the test on the FD-565 Optical Digital Transmission System against the high altitude electromagnetic pulse (HEMP). The background of this test is explained with the test objectives. The general FD-565 system configuration is described along with the test configurations. Also introduced are the facility and data acquisition and processing system. Three different kinds of data are presented: operational data, bulk current data, and field level data. For the purpose of statistical analysis, the operational data are tabulated at the end of this report. GRA

N92-16996# Delta Information Systems, Inc., Horsham, PA.
COMPARATIVE ANALYSIS OF GRAY SCALE CODING TECHNIQUES FOR GROUP 4 FACSIMILE Final Report
Aug. 1991 52 p
(Contract DCA100-87-C-0078)
(AD-A243175; NCS-TIB-90-16) Avail: NTIS HC/MF A04 CSCL 25/5

This compares bit-plane coding (BPC), differential pulse code modulation (DPCM), transform coding, and predictive vector quantization (PVQ) to determine their relative effectiveness for the addition of gray scale to Group 4 facsimile. At present, the CCITT Recommendation for Group 4 facsimile permit the transmission of only black and white imagery (black print on white paper; not photographic). Consequently, most gray scale imagery (like photographs) are usually distorted by Group 4 equipments. To correct this, the CCITT is planning to add gray scale to the Group 4 Recommendations as an option. The aforementioned coding techniques have already been studied individually, but they haven't been compared to one another, nor have they been ranked according to their suitability for Group 4 facsimile. GRA

N92-17016# Naval Postgraduate School, Monterey, CA.
A CAD MODEL FOR THE AXIAL INDUCTIVE STRIP WITH FINITE THICKNESS CENTERED IN HOMOGENEOUS FINLINE WITH W/B = 1 M.S. Thesis
Dimitris Dariotis Dec. 1990 90 p
(AD-A243553) Avail: NTIS HC/MF A05 CSCL 09/1

This thesis describes a CAD compatible circuit model for an inductive strip with finite metal thickness centered in finline with w/b = 1. Scattering coefficients predicted by the circuit model are in good agreement with those predicted by an electromagnetic model based on Maxwell's equations. Filter simulations using the circuit model predict responses which are in good agreement with laboratory measurements. Author (GRA)

N92-17031# Phillips Lab., Kirkland AFB, NM.
FREQUENCY STIRRING: AN ALTERNATE APPROACH TO MECHANICAL MODE-STIRRING FOR THE CONDUCT OF ELECTROMAGNETIC SUSCEPTIBILITY TESTING Final Report, Apr. 1990 - Apr. 1991
Thomas A. Loughry Nov. 1991 57 p
(AD-A243551; AD-E200790; PL-TR-91-1036) Avail: NTIS HC/MF A04 CSCL 20/3

This study summarizes the results of an experiment designed to determine the effectiveness of using frequency stirring to provide field homogeneity in a reverberation chamber. Frequency stirring is accomplished by up-converting band limited white Gaussian noise to microwave frequencies and thus exploits both the high mode densities achievable in a narrow bandwidth at microwave frequencies and the pseudo-statistical nature of the reverberation chamber's eigenmodes. The ultimate goal is to replace the mechanical stirring devices currently used in reverberating chambers with an equivalent electronic eigenmode stirrer. In addition, an expression for the net Q of a reverberation chamber is developed which includes the effects of antenna loading; methods for predicting the homogeneity of the resulting fields in the chamber after application of the frequency stir technique are proposed; and a theoretical basis for interpreting fringe power density levels, cross sections, and shielding effectiveness measurements is also given. GRA

N92-17036# Naval Postgraduate School, Monterey, CA.
A RING MODEL FOR LOCAL/MOBILE RADIO COMMUNICATIONS WITH VARIABLE PACKET LENGTH M.S. Thesis
Dennis V. Banh Dec. 1990 56 p
(AD-A241856) Avail: NTIS HC/MF A04 CSCL 25/2

This thesis presents an analysis of the performance of a local/mobile radio communications system utilizing the Aloha random access protocol with variable length packets. The capture phenomenon due to the near/far effect that enhances the performance of the system is investigated. A tagged packet will capture the base station if its signal-to-interference ratio exceeds a threshold gamma sub zero. Because of the near/far effect, users near the base station typically have a stronger signal than those farther away. A multiple ring model is used to alleviate this problem. Users in one ring employ a different retransmission strategy from those in other rings. A shorter retransmission delay is allocated to users in rings farther from the base station than is allocated to those closer to the base station in order to achieve approximately the same average delay throughout the network regardless of location. GRA

N92-17040# Massachusetts Inst. of Tech., Lexington. Lincoln Lab.
A COVARIANCE MODELING APPROACH TO ADAPTIVE BEAMFORMING AND DETECTION
Frank C. Robey 30 Jul. 1991 150 p
(Contract F19628-90-C-0002)
(AD-A241887; MIT-TR-918; ESD-TR-91-056) Avail: NTIS HC/MF A07 CSCL 12/1

The subject of this report is the general problem of signal processing for sensor arrays. Under certain reasonable assumptions, the model for the noise covariance matrix of the vector of array outputs is an integral involving the spatial-temporal power-spectral-density function. This report examines the application of this covariance model to problems in adaptive beamforming and detection. A constant false alarm rate detector, based on unconstrained maximum-likelihood techniques, is derived and analyzed. Techniques such as this do not fully exploit the data model and can show an appreciable loss in performance compared to optimal techniques. The space of noise covariance matrices possible from a particular array is characterized, yielding representations for the space and members of the space in terms of finite numbers of spectral points. These representations are used to derive constrained maximum-likelihood estimators that jointly estimate the parameters of the density function. Two approaches that use the constrained covariance estimates to perform beamforming are described and compared. The loss in signal-to-noise ratio and the variance of the estimators are shown to be less for these approaches than for those that do not use the covariance model. Detection methods based on the generalized likelihood ratio test and a constant false alarm rate matched-filter detector are analyzed, and simulation results are presented. GRA

N92-17046*# Dynamics Technology, Inc., Torrance, CA.
METRIWAVE FINAL REPORT
Wyman Williams Oct. 1991 223 p
(Contract NAS7-1071)
(NASA-CR-189816; NAS 1.26:189816; DTW-8944-91003) Avail: NTIS HC/MF A10 CSCL 20N

The superconductor-insulator-superconductor (SIS) mixer is a device which is being used in the construction of very sensitive receivers in the millimeter and submillimeter wavelength regions. With its potential for conversion gain and quantum-limited performance, it is becoming a device of prime importance in radio astronomy as well as earth and planetary atmospheric research. Many of the parameters of the SIS mixer cannot be readily measured in the laboratory, however, since most commercially available test instruments use test signal powers large enough to saturate or destroy SIS junctions. Detailed here is the construction of a microwave network analyzer with extremely low test signal powers. The results of a development performed by Dynamics Technology, Inc., under a Phase 2 SBIR contract from NASA (NAS7-1025) are documented. The work resulted in a network analyzer to be delivered to workers at the Jet Propulsion Laboratory, which should be capable of SIS mixer characterization in support of their ongoing work in this area. Author

N92-17047*# National Aeronautics and Space Administration. Lewis Research Center, Cleveland, OH.
ADVANCED COMMUNICATION TECHNOLOGY SATELLITE (ACTS) MULTIBEAM ANTENNA ANALYSIS AND EXPERIMENT
Roberto J. Acosta, Alan R. Lagin (Analex Corp., Brook Park, OH.), Jeffrey M. Larko, and Adabelle Narvaez 1992 5 p Proposed for presentation at the 1992 AP-S International Symposium, Chicago, IL, 18-25 Jul. 1992; sponsored by IEEE
(NASA-TM-105420; E-6835; NAS 1.15:105420) Avail: NTIS HC/MF A01 CSCL 17B

One of the most important aspects of a satellite communication system design is the accurate estimation of antenna performance degradation. Pointing error, end coverage gain, peak gain degradation, etc. are the main concerns. The thermal or dynamic distortions of a reflector antenna structural system can affect the far-field antenna power distribution in a least four ways. (1) The antenna gain is reduced; (2) the main lobe of the antenna can be mispointed thus shifting the destination of the delivered power away from the desired locations; (3) the main lobe of the antenna pattern can be broadened, thus spreading the RF power over a larger area than desired; and (4) the antenna pattern sidelobes can increase, thus increasing the chances of interference among adjacent beams of multiple beam antenna system or with antenna beams of other satellites. The in-house developed NASA Lewis Research Center thermal/structural/RF analysis program was designed to accurately simulate the ACTS in-orbit thermal environment and predict the RF antenna performance. The program combines well establish computer programs (TRASYS, SINDA and NASTAN) with a dual reflector-physical optics RF analysis program. The ACTS multibeam antenna configuration is analyzed and several thermal cases are presented and compared with measurements (pre-flight). Author

N92-17062*# National Aeronautics and Space Administration. Lewis Research Center, Cleveland, OH.
MULTIPLE-ACCESS PHASED ARRAY ANTENNA SIMULATOR FOR A DIGITAL BEAM FORMING SYSTEM INVESTIGATION
Robert J. Kerczewski, John Yu, Joanne C. Walton, Thomas D. Perl, Monty Andro, and Robert E. Alexovich (Analex Corp., Brook Park, OH.) 1992 8 p Proposed for presentation at the Ninth International Conference on Digital Satellite Communications,

Copenhagen, Denmark, 18-22 May 1992; sponsored by Intelsat and Telecom
(NASA-TM-105422; E-6838; NAS 1.15:105422) Avail: NTIS HC/MF A02 CSCL 20N

Future versions of data relay satellite systems are currently being planned by NASA. Being given consideration for implementation are on-board digital beamforming techniques which will allow multiple users to simultaneously access a single S-band phased array antenna system. To investigate the potential performance of such a system, a laboratory simulator has been developed at NASA's Lewis Research Center. This paper describes the system simulator, and in particular, the requirements, design, and performance of a key subsystem, the phased array antenna simulator, which provides realistic inputs to the digital processor including multiple signals, noise, and nonlinearities. Author

N92-17090# Air Force Inst. of Tech., Wright-Patterson AFB, OH. School of Engineering.
FACE RECOGNITION WITH THE KARHUNEN-LOEVE TRANSFORM M.S. Thesis
Pedro F. Suarez Dec. 1991 125 p
(AD-A243688; AFIT/GE/ENG/91D-54) Avail: NTIS HC/MF A06 CSCL 12/6

The major goal of this research was to investigate machine recognition of faces. The approach taken to achieve this goal was to investigate the use of Karhunen-Loe've Transform (KLT) by implementing flexible and practical code. The KLT utilizes the eigenvectors of the covariance matrix as a basis set. Faces were projected onto the eigenvectors, called eigenfaces, and the resulting projection coefficients were used as features. Face recognition accuracies for the KLT coefficients were superior to Fourier based techniques. Additionally, this thesis demonstrated the image compression and reconstruction capabilities of the KLT. This theses also developed the use of the KLT as a facial feature detector. The ability to differentiate between facial features provides a computer communications interface for non-vocal people with cerebral palsy. Lastly, this thesis developed a KLT based axis system for laser scanner data of human heads. The scanner data axis system provides the anthropometric community a more precise method of fitting custom helmets. GRA

N92-17092# Air Force Inst. of Tech., Wright-Patterson AFB, OH.
A RIGOROUS UTD ANALYSIS OF ELECTROMAGNETIC SCATTERING FROM RESISTIVE STRIPS AND RESISTIVE-LOADED CONDUCTING STRIPS M.S. Thesis
Douglas H. Casanova Dec. 1991 105 p
(AD-A243691; AFIT/GE/ENG/91D-09) Avail: NTIS HC/MF A06 CSCL 20/14

This thesis investigates electromagnetic scattering from resistive strips and resistive-loaded conducting strips using a rigorous UTD formulation. The UTD diffraction coefficients are based on the Wiener-Hopf technique and Jones' method. Scattering predictions are performed for constant resistive strips, constant resistive-loaded conducting strips, tapered resistive strips, and tapered resistive-loaded conducting strips. All strip geometries have a total width of 4 lambda. Predictions are compared to method of moments (MM) and measurements to determine the validity of the UTD prediction. Overall, there is good agreement. For TMz polarization, the only deviations that occur with MM are near edge-on when the degree of the taper increases. For TEz polarization deviations with MM occur near edge-on for all strip geometries except constant resistive strips. Comparisons with measurement are better for TMz except for constant resistive strips. Limitations are explored for tapered resistive strips and tapered resistive-loaded conducting strips based on edge-on scattering levels for TMz polarization. From these limitations, scattering characteristics of resistive-loaded conducting strips are explored. GRA

N92-17095# Air Force Inst. of Tech., Wright-Patterson AFB, OH. School of Engineering.
DETERMINATION OF BISTATIC RADAR CLUTTER POWER FROM TOPOGRAPHIC DATA M.S. Thesis
Clyde R. Heddings Dec. 1991 116 p
(AD-A243697; AFIT/GE/ENG/91D-24) Avail: NTIS HC/MF A06 CSCL 17/9

The purpose of this research was to develop a procedure for estimating the average bistatic radar clutter power from a topographic map using rough surface scattering theory. First, the terrain in the radar target area was divided into subregions having homogeneous characteristics. A joint Gaussian distribution for the surface heights was fitted from the information contained in the topographic map contour lines for each homogeneous area. From these distributions, the normalized radar cross section for each terrain area was determined. The clutter power for each range cell was then determined via a modified radar range equation. The procedure was implemented for three target areas of an existing ground based bistatic system near Hanscom AFB, MA using a U.S.G.S topographic map of the area. Scattered power from very rough surfaces was estimated. However, the accuracy of the estimates could not be verified due to a lack of actual data for comparison. It was also determined that topographic map data may not be sufficient to determine scattered power from slightly rough surfaces. GRA

N92-17139*# Notre Dame Univ., IN. Dept. of Electrical Engineering.
SUB-BAND/TRANSFORM COMPRESSION OF VIDEO SEQUENCES Final Report, 11 Jan. 1991 - 10 Jan. 1992
Ken Sauer and Peter Bauer 10 Jan. 1992 31 p
(Grant NAG3-1186)
(NASA-CR-189786; NAS 1.26:189786) Avail: NTIS HC/MF A03 CSCL 17B

The progress on compression of video sequences is discussed. The overall goal of the research was the development of data compression algorithms for high-definition television (HDTV) sequences, but most of our research is general enough to be applicable to much more general problems. We have concentrated on coding algorithms based on both sub-band and transform approaches. Two very fundamental issues arise in designing a sub-band coder. First, the form of the signal decomposition must be chosen to yield band-pass images with characteristics favorable to efficient coding. A second basic consideration, whether coding is to be done in two or three dimensions, is the form of the coders to be applied to each sub-band. Computational simplicity is of essence. We review the first portion of the year, during which we improved and extended some of the previous grant period's results. The pyramid nonrectangular sub-band coder limited to intra-frame application is discussed. Perhaps the most critical component of the sub-band structure is the design of bandsplitting filters. We apply very simple recursive filters, which operate at alternating levels on rectangularly sampled, and quincunx sampled images. We will also cover the techniques we have studied for the coding of the resulting bandpass signals. We discuss adaptive three-dimensional coding which takes advantage of the detection algorithm developed last year. To this point, all the work on this project has been done without the benefit of motion compensation (MC). Motion compensation is included in many proposed codecs, but adds significant computational burden and hardware expense. We have sought to find a lower-cost alternative featuring a simple adaptation to motion in the form of the codec. In sequences of high spatial detail and zooming or panning, it appears that MC will likely be necessary for the proposed quality and bit rates. Author

N92-17187# Mission Research Corp., Santa Barbara, CA.
INVESTIGATION OF CODING TECHNIQUES FOR MEMORY AND DELAY EFFICIENT INTERLEAVING IN SLOW RAYLEIGH FADING Technical Report, 20 Sep. 1987 - 31 Dec. 1990
Jay W. Strater 1 Nov. 1991 122 p
(Contract DNA001-87-C-0169)

(AD-A243154; MRC-R-1335; DNA-TR-91-33) Avail: NTIS HC/MF A06 CSCL 12/9

High data rate communication links operating under slow fading channel conditions may have interleaving memory requirements which are too large for practical applications. These requirements can be reduced by employing spacial diversity; however, a less costly alternative is to select coding and interleaving techniques that support memory efficient interleaving. The objective of this investigation has been to find coding and interleaving techniques with relatively small interleaving memory requirements and to accurately quantify these requirements. Toward this objective, convolutional and Ree-Solomon coding with single-stage and concatenated code configurations were evaluated with convolutional interleaving and differential phase shift keying (DPSK) modulation to determine their interleaving memory requirements. Code performance for these link selections was computed by high-fidelity link simulations and approximations over a wide range of E(sub b)/N(0) and interleaver span to scintillation decorrelation times (T(sub il)/Tau(0)) and the results of these evaluations were converted to interleaving memory requirements. Interleaving delay requirements were also determined and code selections with low interleaving memory and delay requirements were identified.

GRA

N92-17232# Naval Postgraduate School, Monterey, CA.
AN OVERVIEW OF CELLULAR TELECOMMUNICATIONS M.S. Thesis
John R. Bucher Mar. 1991 157 p
(AD-A242951) Avail: NTIS HC/MF A08 CSCL 25/2

The cellular telecommunications industry is one of the fastest growing segments in the international telecommunications domain. Many current communications systems will soon interface with cellular voice and data signals, and this interface will not be restricted to just vehicular cellular. In fact, cellular systems are now even replacing wireline telecommunications systems in certain applications. Today's communications managers and engineers should understand how cellular systems work, and how these systems might be put to work to solve communications requirements. The mobile, low-cost, tetherless characteristics of cellular systems make them ideal candidates for many military needs. This paper provides an overview of current cellular communications systems, and treats their history, theory and operation, applications, and limitations. Additionally, new experimental digital and micro-cellular systems will be introduced and described.

GRA

N92-17241# Massachusetts Inst. of Tech., Lexington. Lincoln Lab.
PERFORMANCE OF GROUND-BASED INFRARED DETECTORS FOR ACQUISITION OF SATELLITES
David R. Hearn 13 Sep. 1991 56 p
(Contract F19628-90-C-0002)
(AD-A243247; MIT-TR-919; ESD-TR-91-080) Avail: NTIS HC/MF A04 CSCL 17/5

The feasibility of acquiring satellites from the ground by using infrared focal-plane-array detectors is analyzed. The orbits of the satellites are assumed to be known to within a position uncertainty of + or - 50 km. Effects of the atmosphere have been modeled by the LOWTRAN7 code. Properties of five different available detectors have been inserted in the mathematical model. A telescope aperture of 60 cm (approx. 24 inches) is assumed in the numerical evaluations. Results are presented in graphs showing the region of space within which each candidate detector array can sense a satellite of a given infrared signature. The PtSi array can sense a medium-sized satellite in low earth orbit. A small, low-orbit satellite can be sensed at a low elevation by the HgCdTe array. That same array could also sense a medium-sized satellite at a 10,000-km altitude. Results for the InSb, Si:Ga, and IrSi arrays fall between these extremes.

GRA

N92-17244# Federal Aviation Administration, Cambridge, MA.
MULTISENSOR SIGNAL PROCESSING TECHNIQUES (HYBRID GPS/LORAN-C WITH RAIM) Final Report, Aug. 1989 - Oct. 1990
Frank VanGrass and Mark R. Kuhl Sep. 1991 95 p
(AD-A242323; DOTVNTSC-FAA-91-13; DOT/FAA/SE-91/4)
Avail: NTIS HC/MF A05 CSCL 17/7

One of the major elements in alleviating existing problems in en route airspace is to allow more aircraft to traverse a given volume of airspace. Recent developments in navigation systems will support this effort by enabling user preferred routes and by offering more precise and reliable navigational capabilities. Multisensor navigation system architectures are presented with the emphasis on signal processing techniques and receiver autonomous integrity monitoring (RAIM). This is followed by a detailed study of a hybrid navigation receiver based on the NAVSTAR Global Positioning System (GPS) and the Long Range Navigation System LORAN-C. The design, implementation and flight testing of a prototype hybrid GPS/LORAN receiver are presented, including the realtime simulation and detection of navigation signal malfunctions.

GRA

N92-17252# Naval Postgraduate School, Monterey, CA.
COMMUNICATION NETWORK SURVIVABILITY M.S. Thesis
Al-Amro Soliman Mar. 1991 77 p
(AD-A242969) Avail: NTIS HC/MF A05 CSCL 25/5

A communication network is composed of communication links and processing nodes. The effective design of a survivable communication network requires a means of determining the structural connectivity of the network both as a whole and with respect to individual resources: links and nodes. In this thesis we represent the connectivity evaluation from two perspectives. The first pertains to considerations applicable to the design schema of the network, and the second deals with an improvement of connectivity in an existing network. We then present and analyze a practical synthetic approach to a communications network's survivability profile by using the example of SACS (the Saudi Arabian Communication System). Finally, we evaluate the difference between the theoretical and practical approaches to survivability.

GRA

N92-17258# Army Lab. Command, Fort Monmouth, NJ. Electronics Technology and Devices Lab.
LOW-NOISE OSCILLATORS FOR AIRBORNE RADAR APPLICATIONS
Raymond L. Filler and John R. Vig Oct. 1991 21 p
(DA Proj. 1L1-62705-AH-94)
(AD-A242264; SLCET-TR-91-26) Avail: NTIS HC/MF A03 CSCL 17/9

Vibration induced phase noise can change the probability of detection of moving target indicator (MTI) radar from near 100 percent to zero. Oscillators that are capable of meeting the requirements of MTI radar systems in a quiet environment are readily available. In the vibrating environments of airborne platforms, however, the phase noise of oscillators degrades very significantly. For example, a 10 MHz crystal oscillator may have a phase noise of -140 dBc/Hz, 100 Hz from the carrier. Assuming a typical one part per billion per g acceleration sensitivity, this phase noise degrades to -93 dBc/Hz under a 0.1 sq g/Hz random vibration at 100 Hz away from the carrier. If there is a 1 g sinusoidal vibration at 100 Hz, there will be a pair of -86 dBc spectral lines superimposed on the signal. Of course, upon multiplication to 10 GHz, the phase noise increases by at least another 60 dB. This report reviews the causes and effects of acceleration sensitivity of bulkwave quartz crystal resonators, and the methods that reduce or compensate for that sensitivity. Most of what is discussed is equally relevant to surface acoustic wave (SAW), shallow bulk acoustic wave (SBAW), dielectric resonator oscillators (DRO), and other types of oscillators.

Author (GRA)

N92-17267# Delta Information Systems, Inc., Horsham, PA.
DEVELOPMENT OF A FEDERAL STANDARD FOR A VIDEO CODEC OPERATING AT P X 64 KBPS Final Report

Feb. 1991 218 p
(Contract DCA100-87-C-0078)
(AD-A243005; NCS-TIB-91-3) Avail: NTIS HC/MF A10 CSCL 25/5

This document is a final report under the contract entitled Development of Federal Telecommunication Standards relating to Digital Facsimile and Video Teleconferencing and Development of a Federal Standard for a Video Codec operating at P x 64 Kbps. There has been a major effort to develop a standard for a video teleconferencing/video telephone terminal. One major thrust is that the audio visual terminal be compatible with the ISDN. Since the basic building block of the ISDN is the B channel operating at 64 Kbps, the generic term P x 64 Kbps refer to operation of this audio visual terminal at integral values of P up to a maximum of 30. Author (GRA)

N92-17277# Naval Postgraduate School, Monterey, CA.
OPTIMAL CONFIGURATION OF DIGITAL COMMUNICATION NETWORK M.S. Thesis
Yong G. Hwang Dec. 1990 76 p
(AD-A243041) Avail: NTIS HC/MF A05 CSCL 25/5

As the costs for maintaining computer communication networks are rapidly rising, it is particularly important to design the network efficiently. The objective of this thesis is to model the minimum cost design of digital communications networks and propose a heuristical solution approach to the formulated model. The minimum cost design has been modeled as a zero-one integer programming problem. The Lagrangian relaxation method and subgradient optimization procedure have been used to find reasonably good feasible solutions. Although the reliability for computer communication networks is as important as the cost factor, only the cost factor is considered in the context of this thesis. Author (GRA)

N92-17279# Defence Research Establishment, Ottawa (Ontario).
A TIME-DOMAIN INCIDENT FIELD EXTRAPOLATION TECHNIQUE BASED ON THE SINGULARITY EXPANSION METHOD
J. J. Klaasen May 1991 34 p
(AD-A243044; DREO-1076) Avail: NTIS HC/MF A03 CSCL 20/15

In this report, a method presented to extrapolate measurements from Nuclear Electromagnetic Pulse (NEMP) assessments directly in the time domain. This method is based on a time domain extrapolation function which is obtained from the Singularity Expansion Method representation of the measured incident field of the NEMP simulator. Once the time domain extrapolation function is determined, the responses recorded during an assessment can be extrapolated simply by convolving them with the time domain extrapolation function. It is found that to obtain useful extrapolated responses; the incident field measurements needs to be made minimum phase; otherwise unbounded results can be obtained. Results obtained with this technique are presented, using data from actual assessments. GRA

N92-17293# Naval Postgraduate School, Monterey, CA.
TRAINING METHODOLOGIES FOR DEPENDENT SPEECH RECOGNITION (SR) SYSTEMS M.S. Thesis
Richard L. Miller Mar. 1991 32 p
(AD-A242983) Avail: NTIS HC/MF A03 CSCL 22/4

An experiment was conducted to determine whether a dependent (SR) system would perform with different accuracies given different ways in which it was trained. The experiment used an SR system (Voice Navigator) which is based on Dragon Systems, Inc. (proprietary) technology. Fifteen subjects trained three different voice patterns each and conducted four tests to compile statistics about the recognition accuracy for each pattern. The experiment was successful and demonstrated that the training method used can have significant impact on the performance of a dependent SR system. This thesis discusses the research methodology, reviews and analyzes the data collected, and states conclusions drawn about the particular dependent SR system used in the experiment. GRA

N92-17366# Naval Postgraduate School, Monterey, CA.
EFFECT OF ECONOMIC TECHNIQUES ON RADIO FREQUENCY UTILIZATION M.S. Thesis
Richard N. Fox Mar. 1991 59 p
(AD-A243187) Avail: NTIS HC/MF A04 CSCL 05/1

This thesis compares the efficacy of spectrum assignment and allocation using a market based system with the current government controlled regulatory system. In making this comparison, a brief review of the spectrum and its radio communication uses is given. An examination of the current system--historical, organizational and political--is also presented. The spectrum is then discussed as a resource in relation to its economic characteristics: supply, demand, opportunity costs, prices, externalities and property rights. Although the spectrum is a unique resource as compared to most other natural resources, this conclusion is no valid reason for not allowing the establishment of a spectrum market exists. An examination of how such a market might be established and operated, and the implications of such a market are then discussed, with an example of how this market would operate in the Land Mobile Radio Services. To better illustrate this point, a brief history of land mobile radio, its technology and applications, and current allocation and assignment mechanisms is also presented. This study concludes by discussing the importance of the frequency spectrum to economic growth, summarizes the advantages and disadvantages of both marketplace and government regulation, and proposes that a market trial be instituted to test the viability of a spectral market. GRA

N92-17383# Naval Ocean Systems Center, San Diego, CA.
EVAPORATION DUCT COMMUNICATION: TEST PLAN, PART 2 Final Report, Oct. 1990 - Sep. 1991
K. D. Anderson and L. T. Rogers Nov. 1991 27 p
(AD-A243505; NOSC-TR-1460) Avail: NTIS HC/MF A03 CSCL 25/5

This document is a continuation and expansion of an earlier study that examines the feasibility of using the evaporation duct to support an alternative high-speed communication system for Navy applications. This Evaporation Duct Communication (EDCOM) experiment is a unique opportunity to evaluate another communication channel that can alleviate Navy ship-to-ship communication problems. Therefore, it is strongly recommended to proceed with this measurement program. Author (GRA)

N92-17429# National Inst. of Standards and Technology, Boulder, CO.
SPHERICAL NEAR-FIELD SCANNING: EXPERIMENTAL AND THEORETICAL STUDIES Final Report
Ronald C. Wittmann and Carl F. Stubenrauch Apr. 1991 132 p
(Contract F30602-88-F-0021)
(AD-A243489; RL-TR-91-56) Avail: NTIS HC/MF A07 CSCL 14/2

This report documents the evaluation of spherical near-field scanning algorithms and computer code developed at the National Institute of Standards and Technology. The experimental work is primarily a comparison of probe-compensated spherical and planar near-field measurement results for a common test antenna. Theoretical work is largely supportive of the experimental effort, but some peripheral topics are developed. The peripheral topics are presented in two areas : (1) application of spherical near-field measurements to the determination of incident fields in compact ranges; and (2) spherical-wave expansions for the fields of a uniformly excited aperture (to facilitate the creation of the analytic test data). GRA

N92-17441# Naval Postgraduate School, Monterey, CA.
NATURAL RESONANCES OF SLOTTED CYLINDER CONFIGURATIONS M.S. Thesis
Keith O. Lyles Mar. 1991 110 p
(AD-A241934) Avail: NTIS HC/MF A06 CSCL 20/14

Electromagnetic sensitivity of systems from intentional apertures such as radar antennas and optical sensors are generally well studied and understood. Characteristics of electromagnetic energy that leaks into an enclosed volume through unintentional apertures such as seams at bolted, riveted, or screwed joints are not understood analytically or from a practical standpoint. Measurement of the internal electromagnetic field of axially slotted cylinders of varying slot widths provides a simple method for the analysis of internal coupled fields. Experimental results of resonance measurements and theoretical computations conducted on slotted cylinder configurations are presented. These measurements provide practical information on the resonance characteristics of different slotted cylinder configurations. Analysis of the data will provide insight into the phenomena of E-field coupling and natural resonances of slotted cylinders. GRA

N92-17464# Human Engineering Labs., Aberdeen Proving Ground, MD.
AUTOMATIC RECOGNITION OF SPEECH IN STRESSFUL ENVIRONMENTS Final Report
Mark A. Clements, John H. Hansen, Kathleen E. Cummings, and Sungjae Lim Aug. 1991 71 p
(AD-A242917; HEL-TM-14-91) Avail: NTIS HC/MF A04 CSCL 20/1

This document describes a body of research conducted for the purpose of improving the performance of automatic speech recognition (ASR) systems in noisy, stressful environments. To accomplish this, several avenues of basic research were investigated. First, novel techniques for noise reduction were developed. Second, three novel robust recognition systems were developed. One of these techniques relied on noise removal, another on linear least squares system identification, and the third on robust distance measures. Third, methods for characterizing stressed speech parametrically were developed. Among the descriptors used were various prosodic features, spectral features, and glottal excitation characteristics. Fourth, methods were developed that were shown to improve ASR performance in noisy or stressed conditions. GRA

N92-17516# Air Force Inst. of Tech., Wright-Patterson AFB, OH. School of Engineering.
COMPARISON OF AFITPAC VERSUS NOS AND A PACKET RADIO NETWORK DESIGN M.S. Thesis
Thomas A. Iannelli Dec. 1991 65 p
(AD-A243766; AFIT/GE/ENG/91D-30) Avail: NTIS HC/MF A04 CSCL 25/2

This thesis encompasses two themes: (1) A comparison of the Network Operating System (NOS) software package, developed by Phil Karn and others, and AFITPAC, written by Marsh and Geier at the Air Force Institute of Technology. The comparison is based on the Air Force Logistics Command's requirements for the development of a Packet Radio Network program. The results of the comparison are a recommendation that use of the NOS package be pursued because it can meet all twelve of the requirements and compiles with five of the Military Standard Protocols. (2) The design of a personal computer Packet Radio Network Simulator used to analyze the network performance of AFITPAC and NOS is proposed. The proposal concludes with a discussion of problems in development of the simulation which used MODSIM IITM, C++, and a 80386/25Mhz personal computer. Recommendations are made for pursuing the simulation effort on other hardware platforms and for improvements to the design. GRA

N92-17529# Gallagher Associates, Inc., West Lafayette, IN.
INTEGRATED SYSTEM FOR MISSILE DETECTION AND DISCRIMINATION
1991 84 p Prepared in cooperation with CyberOptics Corp., Minneapolis, MN
(Contract DE-AC03-87SF-16732)
(DE91-018874; DOE/SF-16732/T1) Avail: NTIS HC/MF A05

The goal of this research has been to develop a test system for simultaneously viewing a wide angle field of view as well as a high resolution zoomed image. The system is optimized for the target detection and tracking problem rather than the surveillance problem. Also, the original plan was to utilize holographic optics for certain key optical elements. In particular, by using a diffractive optical element with multiple diffraction orders to simultaneously image multiple fields of views onto a single detector array. In addition, a special signal processing scheme, which utilizes a technique known as bit reversed sampling, was proposed as a tracking algorithm. The special feature of this tracking algorithm is that it allows us to simultaneously estimate position and velocity of a moving target during the acquisition of a single frame of image data. A system with capability of simultaneous tracking targets over a wide angle and close up field of view is demonstrated. The optical system is designed to implement the bit-reversed sampling strategy which is optimum for field coverage. A second advantage of bit-reversed sampling is that it allows for the simultaneous tracking of a targets position and velocity. This can be accomplished by use of a single frame of data rather than using multiple frames. Demonstrations of the system have been performed by taking video tape of an image from a operating optical implementation and processing the video tape at a separate location by computer. DOE

N92-17563# Aeromet, Inc., Tulsa, OK.
RADIO FREQUENCY HAZARD MONITORING-USAKA Final Report, 21 Feb. - 21 Oct. 1991
David H. Brown 21 Oct. 1991 71 p
(Contract DASG60-91-C-0027)
(AD-A242873; AEROMET/TUL-9110151) Avail: NTIS HC/MF A04 CSCL 17/9

This study provides the design of a network of sensors and procedures which will allow efficient and rapid mapping of RF power density and spectral data at a large number of ground station sensors surrounding the USAKA radars as a function of antenna pointing angles, transmitter power, and time of day. The system acts as a stand alone unit, powered by solar charged batteries. The sensor network is linked to a common control center, which collects, displays and archives the data. Communication between sensor units and the control center can use telephone or VHF radio links. GRA

N92-17571# Ballistic Research Labs., Aberdeen Proving Ground, MD.
MULTIPATH INDUCED TRACKING ERRORS AT 95 AND 140 GHz Final Report, Dec. 1986 - Mar. 1987
Suzanne R. Stratton, H. B. Wallace, and Donald G. Bauerle Nov. 1991 43 p
(DA Proj. 1L1-61102-AH-43)
(AD-A243111; BRL-MR-3947) Avail: NTIS HC/MF A03 CSCL 17/9

The results of an experimental study to assess the effect of multipath propagation on the performance of low- angle tracking radars are described. Measurements of angular tracking errors at 95 and 140 GHz with a common conical scan antenna were made by tracking a trihedral reflector that was moved along a continuous range of heights between 0.4 and 3.6 m above the ground. Antenna diameters of 0.93 m (3 ft) and 0.62 m (2 ft) were used for propagation path lengths of 2,850.0 m and 838.4 m, respectively. The results indicate that angular error is substantially higher when tracking over snow and ice than when tracking over grass. Typically, for trihedral positions below 3.0 m, the errors induced by multipath at 95 GHz were between 0.13 deg. to -0.20 deg. for snow and ice and between 0.07 deg. to -12.0 deg. for grass. The maximum angular errors at 140 GHz under the same conditions were between 0.10 deg. and 0.20 deg. and between 0.04 deg. and -0.10 deg., respectively. GRA

N92-17600# SRI International Corp., Menlo Park, CA.
AURORAL-CLUTTER PREDICTIONS FOR FYLINGDALES, ENGLAND Interim Report
Roland T. Tsunoda Jul. 1991 30 p
(Contract F19628-90-K-0036)

(AD-A242957; PL-TR-91-2198; AD-E200783; SR-1) Avail: NTIS HC/MF A03 CSCL 17/9

Radar clutter produced by auroral processes in the ionospheric E layer, called auroral clutter, can have severe deleterious effects on surveillance radars that operate in the subauroral regions. Auroral clutter characteristics, however, are practically impossible to characterize with a statistical description because of the large number of controlling parameters. Recently, a predictive code called Comprehensive E-Region Auroral Clutter (CERAC) model has been written that used knowledge of the underlying physics and semiempirical data as its basis. This is a description of the predictions of the CERAC model for a surveillance radar located at Fylingdales, England. The results include predictions of occurrence, radar cross section, and Doppler velocity, all as functions of radar elevation, azimuth, range, and time. GRA

N92-17662# Air Force Inst. of Tech., Wright-Patterson AFB, OH. School of Engineering.

GABOR SEGMENTATION OF HIGH RESOLUTION SYNTHETIC APERTURE RADAR IMAGERY M.S. Thesis

Michael A. Hazlett Dec. 1991 78 p

(AD-A243753; AFIT/GE/ENG/91D-23) Avail: NTIS HC/MF A05 CSCL 17/9

This thesis investigates the use of Gabor filters and a radial basis function (RBF) network for segmentation of high resolution (1 foot by 1 foot) synthetic aperture radar (SAR) imagery. Processing involved correlation between the SAR imagery and Gabor functions. Two methods for selecting the optimal Gabor filters are presented. This research used complex Gabor functions and operated on single polarization HH complex data. Following the selection of the proper Gabor filters, correlation coefficients for each image were calculated and used as features for the RBF network. Provided are results demonstrating how Gabor processing and a RBF network provide image segmentation. GRA

N92-17689# Dayton Univ., OH. Graduate School of Engineering and Research.

THE SURFACE IMPEDANCE SYNTHESIS TECHNIQUE Final Report, Jul. 1988 - Jul. 1989

D. D. Richwine and G. A. Thiele Nov. 1991 38 p

(Contract F30602-88-D-0027)

(AD-A243731; UDR-TR-89-119; RL-TR-91-279) Avail: NTIS HC/MF A03 CSCL 20/3

A synthesis technique is discussed in the solution of inverse electromagnetic scattering problems. The technique generates possible surface profiles for a scatterer from a desired scattering pattern. Then, the surface impedance distribution of a particular surface profile can be determined to produce the desired scattering pattern. Limitations on the specifications of the scattered field are also discussed. GRA

N92-17691# Air Force Inst. of Tech., Wright-Patterson AFB, OH. School of Engineering.

WAVE PROPAGATION IN A RANDOMLY INHOMOGENEOUS MEDIUM: A STUDY OF THE PROBLEM M.S. Thesis

Kyle Hunter Dec. 1991 105 p

(AD-A243741; AFIT/GE/ENG/91D-28) Avail: NTIS HC/MF A06 CSCL 12/2

The problem of calculating the scintillation index of an atmospherically propagating spherical wave is examined. The fourth statistical moment of the complex field is obtained by using Feynman (path) integral techniques applied to the stochastic parabolic equation. The general trajectory of each Feynman integral is approximated by a truncated Fourier-sine series and the infinite-fold integration of the Feynman integral is reduced to a three-fold Riemann integral which is shown to match results derived under different assumptions. GRA

N92-17721# Air Force Inst. of Tech., Wright-Patterson AFB, OH. School of Engineering.

PARALLELIZING SERIAL CODE FOR A DISTRIBUTED PROCESSING ENVIRONMENT WITH AN APPLICATION TO HIGH FREQUENCY ELECTROMAGNETIC SCATTERING M.S. Thesis

Paul R. Work Dec. 1991 90 p

(AD-A243755; AFIT/GCS/ENG/91D-26) Avail: NTIS HC/MF A05 CSCL 12/5

This thesis investigates the parallelization of existing serial programs in computational electromagnetics for use in a parallel environment. Existing algorithms for calculating the radar cross section of an object are covered, and a ray-tracing code is chosen for implementation on a parallel machine. Current parallel architectures are introduced and a suitable parallel machine is selected for the implementation of the chosen ray-tracing algorithm. The standard techniques for the parallelization of serial codes are discussed, including load balancing and decomposition considerations, and appropriate methods for the parallelization effort are selected. A load balancing algorithm is modified to increase the efficiency of the application, and a high level design of the structure of the serial program is presented. A detailed design of the modifications for the parallel implementation is also included, with both the high level and the detailed design specified in a high level design language called UNITY. The correctness of the design is proven using UNITY and standard logic operations. The theoretical and empirical results show that it is possible to achieve an efficient parallel application for a serial computational electromagnetic program where the characteristics of the algorithm and the target architecture critically influence the development of such an implementation. GRA

N92-17722# Air Force Inst. of Tech., Wright-Patterson AFB, OH. School of Engineering.

RADAR SCATTERING FROM FOAMED PLASTIC TARGET SUPPORTS M.S. Thesis

Michael W. Chambers Dec. 1991 130 p

(AD-A243756; AFIT/GE/ENG/91D-10) Avail: NTIS HC/MF A07 CSCL 17/9

This study investigates the scattering from foamed plastic target supports. This material is often used in both indoor and outdoor ranges to support all sizes of targets for radar cross section measurements. Two common foamed plastics, styrofoam and expanded bead polystyrene (EPS), are discussed. Two types of scattering are associated with foamed plastic, coherent and incoherent. The incoherent is normally the lowest, but has not been satisfactorily quantified. Coherent scattering is related to the shape of the target, and the emphasis of this study is on the coherent return. One goal was to predict the coherent RCS of an EPS column using the Uniform Theory of Diffraction (UTD). It was found that UTD can accurately predict the backscatter of an EPS column consisting of flat and curved surfaces. The second goal was to experimentally study the effects of shaping on coherent RCS. The benefits of adding a vertical slope to circular cylindrical columns was studied. RCS reductions of approximately 20 dB were achieved. Some low RCS column shapes were also measured; sloping did not produce a measurable RCS reduction in these cases. GRA

N92-17735# Air Force Inst. of Tech., Wright-Patterson AFB, OH. School of Engineering.

A RIGOROUS UNIFORM DIFFRACTION ANALYSIS OF THE ELECTROMAGNETIC SCATTERING FROM IMPEDANCE EDGES AND JUNCTIONS M.S. Thesis

Joseph C. Fortney Dec. 1991 120 p

(AD-A243649; AFIT/GE/ENG/91D-18) Avail: NTIS HC/MF A06 CSCL 20/14

This paper investigates the scattering from impedance strips and impedance-loaded conducting strips. The impedance strips are analyzed using Senior's impedance half plane formulation. Once the primary diffraction from the impedance half plane is presented, it is used to develop multiple diffraction mechanisms on an impedance strip. The scattering from impedance-loaded strips are

analyzed using Maliuzhinets' impedance wedge formulation. The primary diffraction mechanism from an impedance wedge is used to develop the multiple diffractions on an impedance double wedge. The multiple diffractions on both types of strips are developed using the Extended Spectral Ray Method. Sample calculations are made for impedance strips and impedance-loaded strips for a large purely capacitive impedance, a large purely inductive impedance, a large real impedance, and a small real impedance. Measurements are made for impedance strips and impedance loaded strips and are used to compare against predictions. The impedance materials used are two magnetic radar absorbing materials and two resistive materials. Author (GRA)

N92-17737# Air Force Inst. of Tech., Wright-Patterson AFB, OH. School of Engineering.

VERIFICATION AND VALIDATION OF THE SIMULATED RADAR IMAGE (SRIM) CODE RADAR CROSS SECTION PREDICTIONS M.S. Thesis

Dale A. Stanley Dec. 1991 171 p

(AD-A243651; AFIT/GE/ENG/91D-51) Avail: NTIS HC/MF A08 CSCL 17/9

The objectives of this study were to verify and validate the Simulated Radar Image (SRIM) Code Version 4.0 monostatic radar cross section (RCS) predictions. SRIM, uses the theory of Physical Optics (PO) to predict backscatter for a user specified aspect angle. Target obscuration and multiple reflections are taken into account by sampling the target with ray tracing. The software verification and validation technique followed in this study entailed comparing the code predictions to closed form PO equations, other RCS prediction software packages, and measured data. The targets analyzed were a sphere, rectangular flat plate, circular flat plate, solid right circular cylinder, dihedral and trihedral corner reflectors, top hat, cone, prolate spheroid, and generic missile. SRIM RCS predictions are shown for each target as a function of frequency, aspect angle, and ray density. Also presented is an automation technique that enables the user to run SRIM sequentially over a range of azimuth angles. The FORTRAN code written by the author for the PO equations is also provided. GRA

N92-17763# Air Force Inst. of Tech., Wright-Patterson AFB, OH.

IMPROVING STOCHASTIC COMMUNICATION NETWORK PERFORMANCE: RELIABILITY VS THROUGHPUT M.S. Thesis

Leonard J. Jansen Dec. 1991 230 p

(AD-A243655; AFIT/GSO/ENS/91D-10) Avail: NTIS HC/MF A11 CSCL 12/7

This research investigated the measurement and improvement of two performance parameters, expected flow and reliability, for stochastic communication networks. There were three objectives of this research. The first was to measure the reliability of large stochastic networks. This was accomplished through an investigation into the current methodologies in the literature, with a subsequent selection and application of a factoring program developed by Page and Perry. The second objective was to develop a reliability improvement model given that a mathematical reliability expression did not exist. This was accomplished modeling a heuristic by Jain and Gopal, into a linear improvement model. Finally, the third objective was to examine the trade-off between maximizing expected flow and reliability. This was accomplished through generating bounds for the efficient frontier in a modified multicriteria optimization approach. Using the methodologies formulated in this research, the performance parameters of both expected flow and reliability can be measured and subsequent improvements made providing insight into the operational capabilities of stochastic communication networks. GRA

N92-17812# Academy of Sciences of the Ukrainian SSR, Kharkov. Fiziko-Tekhnicheskij Inst.

EFFECTS OF THE HIGH-FREQUENCY BEAM SPACE CHARGE FORCES ON THE EXCITATION OF ELECTROMAGNETIC WAVES IN RELATIVISTIC CARCINOTRON

V. A. Balakirev, A. O. Ostrovskij, and Yu. V. Tkach 1990 8 p In RUSSIAN

(DE92-610956; KFTI-90-2) Avail: NTIS HC/MF A02

Effect of a beam HF space charge force on electromagnetic wave excitation in a relativistic carcinotron is considered. Based on the general waveguide excitation theory a selfagreed equation system describing the nonlinear dynamics of relativistic electron beam interaction with the inverse corrugated waveguide wave, is derived. Solution of this system of equations is performed by numeric simulation. It is shown that HF space charge supresses the self-modulation regime of oscillation generation. Dependence of efficiency of beam energy transformation to high frequency field energy on the electron beam current value and its mean radius, is obtained. DOE

N92-17829 Department of the Navy, Washington, DC.

HIGH-SPEED BEAM SWITCHING PROCESSOR Patent

Richard A. Hills, inventor (to Navy) 3 Sep. 1991 7 p Filed 23 Oct. 1974

(AD-D015108; US-Patent-5,045,857; US-Patent-Appl-SN-517354; US-Patent-Class-342-374) Avail: US Patent and Trademark Office CSCL 09/1

A beam switching processor able to detect a microwave amplitude distribution associated with an array of receiving antenna ports and to close a single-pole, multiple-throw microwave switch to that port in a matched array of transmit antenna ports which corresponds to the receiving antenna port having the maximum signal amplitude is described. The received antenna signals are log amplified and subsequently processed in a logic section which identifies the input port having the highest energy level and energizes the corresponding microstrip switch-driver circuit. GRA

N92-17885 British Broadcasting Corp., Kingswood (England). Engineering Div.

SATELLITE LINKS FOR TELEVISION CONTRIBUTION: RECEPTION REQUIREMENTS FOR LINKS USING TRANSPORTABLE TRANSMITTING EARTH STATIONS

C. Gandy 1991 34 p

(BBC-RD-1991/5) Copyright Avail: BBC, Kingswood Warren, Tadworth, Surrey, England

The BBC operates a number of transportable satellite earth stations for linking Television and Radio Outside Broadcasts back to studio centers without the need for multiple-hop terrestrial links. There are disadvantages in this arrangement and one possible solution may be to establish a receiving earth station near to, or within BBC premises in London. While examining the requirements for such a receiving station, the item of greatest concern has been the diameter of the receiving antenna. As well as making theoretical predictions, a series of practical tests using existing earth stations with antennas of around the predicted diameter were conducted. These tests were carried out simultaneously at two earth stations in Copenhagen and Baldock during 12-14 Sep. 1989, and the methods of testing and the results are presented. Some more detailed background information is also given about the mode of operation of the satellite transponder and the factors which affect the performance of a receiving earth station. It is concluded that an antenna of about 10 m diameter will be needed to achieve a useful level of performance. Author

N92-17886 British Broadcasting Corp., Kingswood (England). Engineering Div.

IMAGE SCANNING USING A FRACTAL CURVE

J. O. Drewery 1991 51 p

(BBC-RD-1991/4) Copyright Avail: BBC, Kingswood Warren, Tadworth, Surrey, England

A novel method of scanning and displaying images based on a self similar fractal curve instead of the traditional raster is described. The Hilbert curves are introduced as a subset of the Peano curves and proposed as a means of providing a hierarchically compatible way of evolving from lower to higher definition systems. After describing the properties of the scan and the way in which the hierarchical behavior is obtained, some disadvantages of a practical system are described. The introduction of interlacing and extension to three dimensional scanning is then treated. Finally,

practical experiments are described, designed to test the hierarchical properties, noise performance, and susceptibility to timing errors. The conclusions are reached that the assumed hierarchical compatibility works and at the very least the idea could be used as a transmission technique to optimize the use of bandwidth. As a scanning technique, it would be feasible once the technology of discrete sources and display devices becomes sufficiently advanced, but would have to be introduced in the context of a completely new service. Author

N92-17931# Naval Research Lab., Washington, DC.
A STUDY OF CHANNEL-ACCESS SCHEMES FOR INTEGRATED VOICE/DATA RADIO NETWORKS Interim Report, Jul. 1989 - Jun. 1991
Jeffrey E. Wieselthier and Anthony Ephremides 29 Nov. 1991 45 p
(AD-A243584; NRL-9359) Avail: NTIS HC/MF A03 CSCL 25/2

In this report we address the major issues associated with channel access in integrated wireless networks, and we propose and analyze the Pure-Reservation Voice/Data Non-Interleaved-Frame Fixed-Length (PR-VD-NIFFL) protocol. This scheme is well suited to either satellite or terrestrial networks. A two-dimensional first-order Markov chain model for this scheme is presented, and techniques that exploit the structural properties of this chain to simplify the evaluation of the equilibrium state, without sacrificing accuracy, are described. Analytical models for the evaluation of data-packet delay for both fixed- and movable-boundary versions of this protocol and for voice-call blocking probability are presented. Computational results illustrate the dependence of performance on system parameters and demonstrate the improvement that can be achieved through the use of the movable-boundary version. GRA

33 ELECTRONICS AND ELECTRICAL ENGINEERING

Includes test equipment and maintainability; components, e.g., tunnel diodes and transistors; microminiaturization; and integrated circuitry.

For related information see also *60 Computer Operations and Hardware* and *76 Solid-State Physics*.

N92-16993# Naval Postgraduate School, Monterey, CA. Dept. of Operations Research.
A KALMAN FILTER FOR A POISSON SERIES WITH COVARIATES AND LAPLACE APPROXIMATION INTEGRATION
Donald P. Gaver and Patricia A. Jacobs Sep. 1991 57 p
(AD-A242960; NPSOR-91-030) Avail: NTIS HC/MF A04 CSCL 12/1

A hierarchical model for a Poisson time series is introduced. The model allows the mean or rate of the Poisson variables to vary slowly in time; it is modeled as the exponential of an AR/1 process. In addition the rate is influenced by a covariate. The Laplace method is used to recursively update some model parameter estimates. Frankly heuristic methods are explored to estimate other underlying parameters. The methodology is checked against simulated data with encouraging results. GRA

N92-17017# JAYCOR, San Diego, CA.
WAVEGUIDE FOUR-WAVE MIXING Final Report, May 1988 - Mar. 1991
Thomas B. Simpson and Jia-Ming Liu Oct. 1991 112 p Prepared in cooperation with California Univ., Los Angeles
(Contract F29601-88-C-0023)
(AD-A243555; J200-91-0080/7208; PL-TR-91-1045) Avail: NTIS HC/MF A06 CSCL 09/1

This program has investigated four-wave mixing (4-wm) in non-linear waveguides, with particular emphasis on waveguides with gain and a resonant enhancement. To understand the basic physical processes which determine the formation, duration, tunability, and fidelity of the scattered optical signal, a general analytical framework was developed for studying nonlinear optical processes in waveguides based on coupled-mode formalism. The influence of diffusion on those media where the nonlinearity is dominated by mobile particles, such as free carriers in a semiconductor under current injection, can be incorporated through a Lorentzian dependence on spatial and temporal frequency of the interacting modes. The theoretical analysis shows that there are strict limits on the speed and spatial fidelity of the phase conjugation process in a multimode waveguide. However, these limits can be relaxed through the use of an array of single-mode waveguides. Laser diodes are a particularly interesting nonlinear waveguide due to the simultaneous combination of strong nonlinearity, resonant gain, and a Fabry-Perot cavity. It is demonstrated that the action of a nearly-degenerate, weak signal beam is to phase modulate the output of a laser diode through 4-wm. GRA

N92-17076# Air Force Inst. of Tech., Wright-Patterson AFB, OH. School of Engineering.
DESIGN AND TESTING OF A LIGHTWEIGHT, PLANAR MICROWAVE LENS M.S. Thesis
Paul M. Proudfoot Dec. 1991 78 p
(AD-A243685; AFIT/GE/ENG/91D-43) Avail: NTIS HC/MF A05 CSCL 09/1

This thesis documents the design, fabrication, and testing of a lightweight, planar microwave lens. The lens consists of two planar arrays of lightweight printed circuit antennas interconnected by microstrip lines whose length varies as a function of position on the lens. Microwave energy is coupled from one face of the lens to the other by means of a slot etched in the ground plane. At 8.0 GHz, the lens is ten wavelengths across, is less than 1/8 inch thick, and weighs less than 4 pounds. The lens can scan a beam over a +/- 30 degree region in both the azimuth and elevation planes. The overall lens efficiency is 56 percent, a 25 percent increase over previous planar lens designs.
Author (GRA)

N92-17087# Loyola Coll., Baltimore, MD.
X RAY LITHOGRAPHY IN JAPAN Final Report
James T. Clemens, Robert W. Hill, Franco Cerrina, Gene E. Fuller, and R. F. Pease Oct. 1991 174 p
(Contract N00014-90-J-1853)
(AD-A243660) Avail: NTIS HC/MF A08 CSCL 13/8

Integrated circuits (semiconductors) are the key components of modern computers, communication systems, consumer electronics, and the new generations of smart machines and instruments. Japan's strong position and growing influence in the manufacture of semiconductors and systems based on them is well known and well documented. Microlithography is one the most critical elements of the semiconductor manufacturing process because it determines the minimum feature size and the functional capabilities of the semiconductor. Because it is used many times in the manufacturing sequence, the quality of the microlithography process (i.e., number of defects, control for feature size, etc.) is critical in determining the yield and cost of semiconductors and hence the competitiveness of the electronics industry. At present all volume semiconductor manufacturing is done with optical UV (ultraviolet) projection lithography, twenty-year-old photographic technology which has been and is still evolving. There are many issues that limit the technical capability and cost-effectiveness of UV lithography, and thus, alternate lithographic techniques are continuously being researched and developed. X-ray lithography, which was invented in the early 1970's, holds the promise of providing higher yields in manufacturing semiconductors by virtue of enhanced process latitude, process robustness, and resolution.
Author (GRA)

N92-17116# Air Force Inst. of Tech., Wright-Patterson AFB, OH.
THE ANALYSIS OF A STABILIZED 1.5 MACH-ZEHNDER INTERFEROMETRIC SENSOR WITH ENHANCED SENSITIVITY AND COMMON-MODE COMPENSATION Ph.D. Thesis

Booker H. Tyrone, Jr. Aug. 1991 113 p
(AD-A243384; AFIT/CI/CIA-91-014D) Avail: NTIS HC/MF A06 CSCL 20/6

The design and construction of an active stabilization controller and its interface to an interferometric fiber optic sensor--the enhanced sensitivity, common-mode compensated 1.5 Mach-Zehnder is reported in this dissertation. The feasibility of employing this active stabilization circuit to maintain the operation of an enhanced sensitivity, common-mode compensated 1.5 Mach-Zehnder interferometer over the narrow operating range required for common-mode compensation and high sensitivity was demonstrated. Thus, a suitable means to minimize, even eliminate, the effects of environmental disturbances (common-mode and random) and to achieve maximum sensitivity and linearity in the presence of differential phase modulation was proven. This research shows that the incorporation of a controller into the fiber optic sensor can improve the performance of the sensor with electro-optic feedback over two orders of magnitude (100 times) more than without electro-optic feedback. More importantly, the fiber optic sensor exhibited nearly a full order of magnitude (10 times) improvements in sensitivity beyond the state-of-the-art performance reported to date for the conventional Mach-Zehnder optical circuit. GRA

N92-17129 Department of the Navy, Washington, DC.
METHOD OF KALMAN FILTERING FOR ESTIMATING THE POSITION AND VELOCITY OF A TRACKED OBJECT Patent
Roger L. Gray, inventor (to Navy) 24 Sep. 1991 8 p Filed 12 Feb. 1991
(AD-D015057; US-Patent-5,051,751; US-Patent-Appl-SN-654111; US-Patent-Class-342-107) Avail: US Patent and Trademark Office CSCL 17/11

A method of Kalman filtering for estimating the position and velocity of a tracked object is provided. A Kalman filter is initialized with at least position and velocity error states in an inertial computational frame. Sensor measurements are used to develop a measured line-of-sight vector to the object. Matrix transformations are used to analytically rotate the sensor measurements into a measurement frame. The measurement frame is defined as having one axis pointing towards the estimated relative position of the object. The use of the measurement frame allows the method to be adaptable to any line-of-sight/computational frame geometry. Since statistical correlation of the measurements is not present in the measurement frame, the number of computations at each filter update is reduced. Author (GRA)

N92-17186# Royal Aircraft Establishment, Farnborough (England).
LITHIATED VANADIUM OXIDE (LVO), GAMMA-LITHIUM VANADIUM BRONZE (GAMMA-LIV2O5) AND VANADIUM DIOXIDE (VO2) AS THERMAL BATTERY CATHODE MATERIALS
A. G. Richie and K. Warner May 1991 49 p
(AD-A242948; RAE-TR-91044; DRIC-BR-305032) Avail: NTIS HC/MF A03 CSCL 10/3

Thermal batteries are high temperature reserve batteries, predominantly used in missiles. Modern designs use a lithium (or lithium alloy) anode, an immobilized molten salt electrolyte, and an iron-disulphide cathode. These batteries have many advantages: high reliability, long storage life without maintenance, wide temperature range of operation, and, sometimes, high power. However, the energy density is rather low and this could be improved if the individual cell voltage could be raised above the present 2.2 V/cell open circuit-voltage for the lithium iron-disulphide couple. A new cathode material, lithiated vanadium oxide (LVO), was invented at RAE and has the advantage of a much higher open-circuit voltage of 2.6 V/cell versus lithium. The properties of LVO have been investigated and it has been shown that LVO consists of vanadium dioxide as the major component. Some lithium bromide is also present. GRA

N92-17189# Air Force Inst. of Tech., Wright-Patterson AFB, OH.
INTEGRATION OF AN ANTI-PARALLEL PAIR OF PLANAR SCHOTTKY BARRIER DIODES FOR MILLIMETER AND SUBMILLIMETER WAVELENGTHS Ph.D. Thesis
Paul H. Ostdiek Aug. 1991 228 p
(AD-A243371; AFIT/CI/CIA-91-019D) Avail: NTIS HC/MF A11 CSCL 09/1

The focus of this work is the development of an anti-parallel pair of planar gallium arsenide Schottky barrier diodes, integrated on a monolithic chip. This chip was designed for integration into subharmonically pumped heterodyne receivers which are used to detect radiation at millimeter and submillimeter wavelengths. The advantage of such a receiver is that it uses a local oscillator source at half the frequency required by a fundamentally pumped receiver. They are therefore useful in environments that preclude the use of high frequency oscillators, such a lasers, that are bulky and have significant power requirements. Also, the use of a planar diode technology eliminates the fragile whisker contact, thus allowing the fabrication of multi-diode circuits. The combination of planar diodes and subharmonically pumped receivers is ideally suited for space applications, such as the Microwave Limb Sounder of NASA's Earth Observing System satellites which will conduct long term studies of Earth's upper atmosphere. The diode pair, which was designed and fabricated in this research, has exhibited excellent electrical characteristics. These diodes contained anodes as small as 1.2 micron. This is the first use of anodes smaller than 2.5 micron on a planar diode. Also, excellent mixing results were observed with Aerojet-General Corporation's G-band (183 GHz) subharmonically pumped receiver. This is the first successful application of a planar diode technology at a frequency significantly above 100 GHz. GRA

N92-17205# Naval Postgraduate School, Monterey, CA.
COMPUTER AIDED THERMAL ANALYSIS OF A MICROCIRCUIT STRUCTURE M.S. Thesis
Joseph A. Willhelm, Jr. Dec. 1990 65 p
(AD-A243160) Avail: NTIS HC/MF A04 CSCL 09/1

The Naval Post Graduate School has obtained software which can be used for the thermal analysis of an electronic component. This software includes two versions, one for steady state analysis and the other for transient analysis. Each version consists of two programs, a model builder and a thermal analyzer. This thesis describes a user friendly, menu driven specific model builder which may be used to rapidly generate a thermal model, containing up to 750 nodes, for a microcircuit die. This model builder is an improvement over the existing model builder in that the only pertinent input will be the physical dimensions and heat transfer data. The main feature of this model builder is the accommodation of the marked variation of silicon thermal conductivity with temperature. GRA

N92-17216# Air Force Systems Command, Brooks AFB, TX.
TESTING AND EVALUATION OF THE VANNER ELECTRICAL INVERTERS, MODELS 24-1500 AND SP 00112 Final Report, Oct. 1990 - Jan. 1991
Thomas E. Philbeck, Jr. and Philip J. Preen Oct. 1991 19 p
(AD-A241914; AL-TR-1991-0094) Avail: NTIS HC/MF A03 CSCL 10/2

The United States Air Force Military Airlift Command (MAC) provides aeromedical airlift for Department of Defense personnel. Two aircraft, the C-130 and C-141, are primarily used for the transport of cargo, but may also be configured for aeromedical use. Neither aircraft have 110-120 volt alternating current (VAC)/60 Hz power required for medical equipment items. Inverters, manufactured by Vanner Incorporated of Hilliard, OH, were selected to provide the needed power. Initially a Model 24-1500, and later a Model SP 00112 were submitted to the Armstrong Laboratory's Aeromedical Research Function at Brooks AFB, TX, for testing and evaluation. Modifications must be made to comply with MIL-STD 461, Category Ale and MIL-STD 810D. Only tested medical equipment may be operated off the Vanner. Only the 4.57 m (15 ft) 4 ga cable can be used to power the Vanner. The

Vanner was fitted with a remote switch bypass plug. At least 10.2 cm (4 in.) of clearance must be provided all around the Vanner. Tiewraps must be inspected for deterioration or displacement. Provided these requirements are met, the Vanner can be an effective device to provide 120-VAC for powering some medical equipment items on C-130 and C-141 aircraft. Author (GRA)

N92-17268# Harvard Univ., Cambridge, MA.
SUPERDIRECTIVE PROPERTIES OF CLOSED LOOPS OF PARALLEL COPLANAR DIPOLES Final Report, Mar. 1988 - Feb. 1991
Tai T. Wu, Ronald W. King, George Fikioris, and Hao-Ming Shen Sep. 1991 27 p
(Contract F19628-88-K-0024)
(AD-A243009; RL-TR-91-221) Avail: NTIS HC/MF A03 CSCL 09/1

This report describes the researches carried out under contract F19628-88-K-0024 from March 28, 1988 through February 28, 1991. After a short review of earlier work, recent progress in the theoretical analysis of resonant loops of dipoles is discussed. In particular, it is pointed out that a way has been found for relating an infinite number of integral equations to a relatively small number. An improvement in the accuracy of the analysis of a resonant circular array of electrically short elements is described and a sequence of twelve basic properties formulated. These relate to the kernel, the conductances, the susceptances, and the horizontal and vertical field patterns. An important conclusion is that any perturbation of the shape of the resonant circular array that results in only a slight change in the currents will significantly change the field pattern and possibly lead to one with superdirective properties. The report concludes with an appendix containing references to the seven published papers generated under this contract.
Author (GRA)

N92-17290# Naval Postgraduate School, Monterey, CA.
A DISCONTINUITY STUDY IN SHIELDED COPLANAR LINE M.S. Thesis
J. S. Hwang Dec. 1990 69 p
(AD-A242976) Avail: NTIS HC/MF A04 CSCL 09/1

A study of the shielded coplanar line (SCPL) is presented. The main goal of this theses is to develop an equivalent circuit model for a typical discontinuity in the SCPL. The formulation is based on Galerkin's method, using Green's function applied in the Fourier transform domain. The impedance (Z0) has been calculated by using a variational method. The propagation constant (beta/omega) and effective dielectric constant of the SCPL have been calculated by using a method of moments. The cut-off frequency of this wave guide has been obtained by a theorem of Van Bladel and Higgins. GRA

N92-17291# Materials Research Labs., Ascot Vale (Australia).
MAGNETIC FIELD DISTRIBUTION AND DESIGN OF HELMHOLTZ COILS
Julian Vrbancich Apr. 1991 62 p
(AD-A242978; MRL-TR-91-8; DODA-AR-006-355) Avail: NTIS HC/MF A04 CSCL 09/1

A uniform magnetic field is required to calibrate magnetic induction sensor coils. Two types of coil designs are considered; a single finite length solenoid and a coaxially split coil pair (Helmholtz coil). The design must be able to reliably predict the magnitude of the calibration field and its homogeneity, both radially and axially, to within certain tolerances. The experimental results of a design based on the split coil pair are given. Furthermore, it is suggested that the quasi-uniform field in the mid-plane of a split coil pair can be usefully extended by narrowing the gap of the conventional Helmholtz coil pair spacing. In such cases, the flux in a circular region in the mid-plane can approach the value that would exist for a perfectly uniform field because of the partial cancellation between fields greater than and less than the central field. The deviation of the central field from that of an infinitely long solenoid is also discussed. Author (GRA)

N92-17295# Electronics Research Lab., Adelaide (Australia).
CONSTANT MODULUS ALGORITHM TECHNIQUES FOR THE ENHANCEMENT OF SIGNAL QUALITY
Peter L. Trudinger Aug. 1991 33 p
(AD-A242986; ERL-0568-RR; DODA-AR-006-756) Avail: NTIS HC/MF A03 CSCL 09/1

The Constant Modulus Algorithm (CMA) is an adaptive algorithm, for selecting equalizer filter weights, which attempts to correct for degradation in signal quality suffered by constant envelope signals (e.g., FM) over an imperfect transmission channel. This report reviews and evaluates the standard CMA and several of its variants, which were designed to improve on its performance or extend its applicability. Two variants seem to significantly increase convergence rate and appear worthy of further study or implementation. GRA

N92-17317# Howard Univ., Washington, DC. Material Science Research Center of Excellence.
A COMPARATIVE STUDY OF THE NOISE PERFORMANCE OF ALLUMINUM GALLIUM ARSENIDE/GALLIUM ARSENIDE HIGH ELECTRON MOBILITY TRANSISTORS WITH AND WITHOUT SUPERCONDUCTING GATE ELECTRODES
Leary O. A. Myers, Michael G. Spencer, and J. A. Griffin 1992 12 p Sponsored by NSF
Avail: NTIS HC/MF A03

The noise performance of an AlGaAs high electron mobility transistor (HEMT) with a 1 micron vanadium/titanium superconducting gate electrode is compared to an otherwise identical non-superconducting titanium gate HEMT. At a frequency of 1 GHz and at a temperature below its critical temperature, the superconducting gate HEMT achieved a noise temperature of 21 K. Under these conditions the HEMT with the Ti gate electrode demonstrated a noise temperature of approximately 70 K. This factor of 3 reduction in noise temperature is due to the reduced gate resistance of the V/Ti superconducting gate. This is the first demonstration of noise reduction in a HEMT using a low-temperature superconducting gate electrode. Author

N92-17326# Harry Diamond Labs., Adelphi, MD.
PREPARATION OF FERROELECTRIC SAMPLES FOR ELECTRICAL AND RADIATION CHARACTERIZATION STUDIES Final Report, Oct. 1989 - Dec. 1990
Bernard J. Rod Dec. 1991 22 p
(AD-A243432; HDL-TM-91-14) Avail: NTIS HC/MF A03 CSCL 09/1

Procedures have been developed for preparing ferroelectric film samples for electrical and radiation characterization. The procedures discussed focus on quick turnaround of samples and the ability to handle a number of different kinds of ferroelectric materials and substrates. New methods of defining the sputtered platinum electrodes and attaching the sample die to suitable packages are also discussed. Techniques have been developed for preparing ferroelectric films for electrical characterization studies and radiation hardness assessments. In recent years, considerable interest has been rekindled in the use of these ferroelectric materials in nonvolatile memory applications. The evaluation of such characteristics as dielectric constant, coercive field, remanent polarization, fatigue, retention, and radiation hardness are especially critical to assessing the use of these materials in nonvolatile memories intended for Army advanced electronics systems. Evaluating many different samples given time is of particular importance, since no single ferroelectric material has not yet emerged as the optimum material for nonvolatile memory applications, and many different material samples must, therefore, be studied. GRA

N92-17332# Air Force Inst. of Tech., Wright-Patterson AFB, OH. School of Engineering.
APPLICATION OF SILICON MICROMACHINING TO THERMAL DISSIPATION ISSUES IN WAFER SCALE INTEGRATED CIRCUITS M.S. Thesis
Edward Cosnyka Dec. 1991 277 p

(AD-A243744; AFIT/GE/ENG/91D-12) Avail: NTIS HC/MF A13 CSCL 09/1

The purpose of this research effort was to investigate the feasibility of applying the silicon micromachining technique to thermal management as applied to integrated circuits and wafer scale integration techniques. Three silicon micromachined structures and an untextured reference wafer were compared as heat-dissipating surfaces. These four surfaces were realized using 3-inch diameter, single crystal silicon wafers. The following structures were micromachined in silicon wafers using wet chemical, anisotropic etching, and photolithographic techniques: (1) randomly spaced and sized pyramids in (100)-oriented silicon; (2) deep vertical-wall grooves in (110)-oriented silicon; and (3) micro-fluid channels in (100)-oriented silicon. The heat-dissipating silicon wafers were epoxied to silicon wafers hosting heat-producing devices to realize a silicon wafer thermal module, simulating the wafer scale integration packaging technique. Two types of heat-producing devices were compared: (1) n-diffused integrated circuit die resistors; and (2) thin-film aluminum resistors. Two configurations of the integrated circuit die were also compared: (1) a single, centered, integrated circuit die; and (2) four, centered, integrated circuit die. GRA

N92-17439# Surrey Univ., Guildford (England). Dept. of Electronic and Electrical Engineering.

TOTAL DIELECTRIC ISOLATION (TDI) OF FULLY DEPLETED DEVICE STRUCTURES Final Report, 1 Feb. 1990 - 31 Jan. 1991

Peter L. Hemment Aug. 1991 65 p

(Grant AF-AFOSR-0356-88)

(AD-A241926; EOARD-TR-91-11) Avail: NTIS HC/MF A04 CSCL 20/12

The aim of this program is to prepare, evaluate and optimize Total Dielectric Isolated (TDI) structures in order to develop the technology for the preparation of substrates for circuits which exhibit improved radiation tolerance. The work carried out during the life of this project has provided a sound base for this novel technology. Successful experiments include the preparation of device worthy substrates in variously patterned wafers, identification of the microstructure of TDI wafers by cross-sectional transmission electron microscopy (XTEM) and the successful implementation of a new predictive software package (IRIS). This SIMOX process model has been used to optimize the masking layer thicknesses and processing parameters to achieve planar TDI structures. Author (GRA)

N92-17468# Sandia National Labs., Albuquerque, NM.

PERFORMANCE OF BATTERY CHARGE CONTROLLERS: FIRST YEAR TEST REPORT

J. Dunlop, W. Bower, and S. Harrington (Ktech Corp., Albuquerque, NM.) 1991 9 p Presented at the 22nd IEEE Photovoltaic Specialists Conference, Las Vegas, NV, 7-11 Oct. 1991

(Contract DE-AC04-76DP-00789)

(DE92-002924; SAND-91-2212C; CONF-911055-9) Avail: NTIS HC/MF A02

The results of the first year of an evaluation of charge controllers for stand-alone photovoltaic (PV) systems are presented. The objectives of the test program are to positively influence the development of battery charge controllers for stand-alone PV applications and to develop design and application criteria that will improve PV system reliability and battery performance. Future goals are to expand the evaluation program to include various battery technologies and controller algorithms. Also, the information is being communicated to manufacturers to aid in the design of more effective and reliable charge controllers for PV systems. Eight different models of small (nominal 10 amp) charge controllers are being subjected to a comprehensive evaluation. These evaluations include operational tests in identical stand-alone PV systems and environmental and electrical cycling tests. Selected custom tests are also performed on the controllers to determine the response to transients, installation requirements, and system design compatibilities. Data presented in this paper include measured electrical characteristics of the controllers, temperature effects on set points, and operational performance in PV systems both in the lab and in the field. A comparison is presented for four different charge controller algorithms which include array-shunt, series-interrupting, series-linear constant-voltage, and series-linear-multistep constant-current. DOE

N92-17480# Air Force Inst. of Tech., Wright-Patterson AFB, OH. School of Engineering.

GLOBAL OPTIMIZATION OF DIGITAL CIRCUITS M.S. Thesis

Richard Flandera Dec. 1991 296 p

(AD-A243740; AFIT/GCE/ENG/91D-04) Avail: NTIS HC/MF A13 CSCL 09/1

This thesis was divided into two tasks. The first task involved developing a parser which could translate a behavioral specification in Very High-Speed Integrated Circuits (VHSIC) Hardware Description Language (VHDL) into the format used by an existing digital circuit optimization tool, Boolean Reasoning In Scheme (BORIS). Since this tool is written in Scheme, a dialect of Lisp, the parser was also written in Scheme. The parser was implemented is Artez's modification of Earley's Algorithm. Additionally, a VHDL tokenizer was implemented in Scheme and a portion of the VHDL grammar was converted into the format which the parser uses. The second task was the incorporation of intermediate functions into BORIS. The existing BORIS contains a recursive optimization system that optimizes digital circuits by using circuit outputs as inputs into other circuits. Intermediate functions provide a greater selection of functions to be used as circuits inputs. Using both intermediate functions and output functions, the costs of the circuits in the test set were reduced by 43 percent. This is a 10 percent reduction when compared to the existing recursive optimization system. Incorporating intermediate functions into BORIS required the development of an intermediate-function generator and a set of control methods to keep the computation time from increasing exponentially. GRA

N92-17490# Harvard Univ., Cambridge, MA.

X RAY DAMAGE TO CF3CO2-TERMINATED ORGANIC MONOLAYERS ON Si/Au SUPPORTS IS DUE PRIMARILY TO X RAY INDUCED ELECTRONS

Paul E. Laibinis, Robert L. Graham, Hans A. Biebuyck, and George M. Whitesides Dec. 1991 20 p

(Contract N00014-86-K-0756)

(AD-A243446; TR-44) Avail: NTIS HC/MF A03 CSCL 09/1

X rays damage organic materials. The relative importance of X rays themselves, and of both X ray generated and secondary electrons, in this damage was explored using self-assembled monolayers (SAMs) on multilayer thin film supports. The substrates were prepared by depositing thin films of Si (0, 50, 100 and 200) on thick layers of Au (2000 A); these systems were supported on chromium primed silicon wafers. Trifluoroacetyl terminated SAMs were assembled on these substrates and the samples irradiated with monochromatic Al K sub alpha X rays. The fluxes of X rays to which the different samples were exposed were the same, but the fluxes and energy distributions of the electrons generated by interactions of the X rays with the substrates differed. The loss of fluorine from the SAMs was followed by XPS and was slower on substrates emitting a lower flux of electrons. This observation indicated that the electrons, and not the X rays themselves, were largely responsible for the damage to the organic monolayer films that resulted in loss of fluorine from them. GRA

N92-17501# Air Force Inst. of Tech., Wright-Patterson AFB, OH. School of Engineering.

EVALUATION OF AN INTERDIGITATED GATE ELECTRODE FIELD-EFFECT TRANSISTOR (IGEFET) FOR IN SITU RESIN CURE MONITORING M.S. Thesis

Thomas E. Graham Dec. 1991 210 p

(AD-A243713; AFIT/GE/ENG/91D-55) Avail: NTIS HC/MF A10 CSCL 09/1

The purpose of this study was to design an Interdigitated Gate Electrode Field-Effect Transistor (IGEFET) and evaluate its performance as an in situ resin cure monitor. A commercially

available resin was selected for the research, and rheological studies were performed to identify the resin's gelation point during isothermal cures at two selected temperatures. Additional rheological studies were performed to identify the resin's glass transition temperature. The interdigitated gate electrode of the IGEFET was coated with samples of the resin, and electrical measurements were performed while the resin cured. The chemical changes which occur in the resin as a result of curing were manifested in the interdigitated gate electrode's electrical characteristics. The result reveal that the IGEFET is capable of sensing the electrical impedance changes, and hence the chemical changes, which occur during the resin's cure. In particular, the chemical changes due to gelation are evident in the IGEFET's electrical response data. In addition, the resin which was cured at the higher temperature was close to its glass transition temperature, and hence softer than the resin cured at the lower temperature, and the IGEFET was capable of detecting this difference. GRA

N92-17540# Technische Univ., Berlin (Germany, F.R.). Fachbereich Elektrotechnik.
ANALYTICAL DETERMINATION OF ARREST AND STARTING TORQUE OF A BIPOLAR DC MOTOR WITH PERMANENT MAGNETS Ph.D. Thesis [ANALYTISCHE BESTIMMUNG VON RAST- UND ANFAHRMOMENT EINER ZWEIPOLIGEN PERMANENTERREGTEN GLEICHSTROMMASCHINE]
Hans Georg Ittstein 1991 129 p In GERMAN
(ETN-92-90586) Avail: NTIS HC/MF A07

Magnetic field, arrest torque, and starting torque of a bipolar DC motor with a twelve-slot rotor, excited with permanent magnets, were analytically calculated. The magnetic field was determined as a function of the rotor position angle for some of the most common magnet schemes using a cylindrical calculation model. The arrest torque per axial unit length was obtained by integrating the tangential component of the Maxwell stress over a freely selected cylindrical air gap surface which completely comprises the rotor. It is shown that the effect of the pole coverage angle on the arrest torque is very significant. The starting moment per axial unit length for diametrically and radially magnetized systems was calculated as a function of the pole coverage angle by integrating the Maxwell stress. ESA

N92-17559# National Advisory Committee on Semiconductors, Arlington, VA.
TOWARD A NATIONAL SEMICONDUCTOR STRATEGY. REGAINING MARKETS IN HIGH-VOLUME ELECTRONICS, VOLUME 2 Annual Report No. 2
Feb. 1991 29 p
(PB91-201301) Avail: NTIS HC/MF A03; also available SOD HC $6.00 as 040-000-00556-1 CSCL 09C

Supplemental material consisting of a detailed analysis of opportunities in high-volume electronics markets and the barriers to U.S. participation are given. Author

N92-17570# Naval Postgraduate School, Monterey, CA.
COMPARISON OF ALKALI ION EMITTERS M.S. Thesis
Dean A. Gant Dec. 1991 92 p
(AD-A243105) Avail: NTIS HC/MF A05 CSCL 09/1

Lithium, Potassium, and Cesium ion sources have been studied using devices based on thermal emission from a Beta Eucryptite structure as possible ion sources for use in satellite charge control. The experiments evaluated the power requirements of the different ion emitters to produce approximately 10 microamps of current and tested the effects of using an Osmium Ruthenium coating to increase the work function of the emitter surface. Lifetime tests of the different ion emitters were also performed. Analysis of the experimental findings showed that lithium ion sources with a lifetime of 93 hours and Potassium ion sources with a lifetime of 44 hours produced acceptable current levels for use in spacecraft charge control devices. Potassium sources produced the necessary current, 10 microamps, at 140 C lower temperature than the Lithium sources. All of the coated sources produced wildly fluctuating currents at the 10 microamp level and were not acceptable for the purpose intended. GRA

N92-17573# Naval Postgraduate School, Monterey, CA.
SUSPENDED SUBSTRATE RESONATOR DESIGN M.S. Thesis
Sujiwo Dec. 1990 90 p
(AD-A243250) Avail: NTIS HC/MF A05 CSCL 09/1

The open-end resonator in a suspended substrate transmission line was analyzed in terms of two open-end discontinuities on a line segment. A procedure for computing the resonant frequency and constant of propagation was demonstrated using a full wave analysis. The fringing capacitance was computed using an equivalent length extension model and a transmission line circuit model. The characteristic equation was derived using Galerkin's method applied in the Fourier transform domain. The calculation has been carried out in two increasing orders of approximation, and the results compared. The discontinuity capacitance at the resonator open ends was calculated for a range of line dimensions and substrate dielectric constants. The dispersive propagation constant of suspended substrate line was also calculated by the Galerkin method. GRA

N92-17596# North Carolina Univ., Chapel Hill. Dept. of Chemistry.
A KINETICS STUDY OF THE ELECTRON CYCLOTRON RESONANCE PLASMA OXIDATION OF SILICON Interim Report
J. Joseph, Y. Z. Hu, and E. A. Irene Nov. 1991 38 p
(Contract N00014-89-J-1178)
(AD-A242868; TR-38) Avail: NTIS HC/MF A03 CSCL 09/1

The electron cyclotron resonance plasma oxidation of silicon was investigated using in-situ process static spectroscopic ellipsometry and dynamic real time ellipsometry at oxidation temperatures between 80 C and 400 C and at various applied biases. Successful optical modeling of the ellipsometric data was accomplished using a two layer model, in which the top layer is a pure silicon dioxide film over an interface layer. The kinetics results are compatible with the Cabrera-Mott theory for the oxidation by charged species in the limit of low electric field. The effect of applied bias suggests that the oxidizing species is O-. The energy activation is 0.18 eV, substantially lower than the thermal oxidation value. GRA

N92-17620# National Advisory Committee on Semiconductors, Arlington, VA.
TOWARD A NATIONAL SEMICONDUCTOR STRATEGY, VOLUME 1 Annual Report No. 2
Feb. 1991 62 p
(PB91-201293) Avail: NTIS HC/MF A04; also available SOD HC $6.00 as 040-000-00556-1 CSCL 09C

Updated here are key market data showing trends in the U.S. semiconductor industry's world market position. New information is given on three emerging semiconductor-based technologies: broadband communications, advanced display systems, and intelligent vehicles and highways. These are examples of important, high-volume markets that will consume significant numbers of semiconductor components and that must be addressed in a national semiconductor strategy. New recommendations and a summary of all Committee recommendations to date are given as well as a summary of comments received at a public forum held in Silicon Valley in may 1990. Author

N92-17629# Hughes Aircraft Co., El Segundo, CA. Electro-Optical and Data Systems Group.
THERMALLY REGENERATIVE FUEL CELLS Final Report
F. A. Ludwig, A. Kindler, and J. McHardy Oct. 1991 6 p
(Contract N00014-89-C-0071)
(AD-A242900) Avail: NTIS HC/MF A02 CSCL 10/3

The three phase project was undertaken to investigate solventless ionic liquids as possible working fluids for a new type of thermally regenerative fuel cell (TRFC). The heart of the new device, invented at Hughes Aircraft Company in 1983, is an electrochemical concentration cell where acid and base streams react to produce electrical energy. Thermal energy is then used to decompose the resulting salts and regenerate the cell reactants. In principle, a TRFC can be matched to any source of thermal

energy simply by selecting working fluids with the appropriate regeneration temperature. However, aqueous working fluids (the focus of previous studies) impose limitations on both the operating temperatures and the achievable energy densities. It was the need to overcome these limitations that prompted the present investigation. Specific aims were to identify possible working fluids for TRFC systems with both low and high regeneration temperatures. A major advantage of our aqueous-fluid TRFC systems has been the ability to use hydrogen electrodes. The low activation and mass transfer losses of these electrodes contribute substantially to overall system efficiency. GRA

N92-17654# Wright State Univ., Dayton, OH. Dept. of Electrical Engineering.
NEW ALGORITHMS FOR BROAD-BAND AND NARROWBAND SOURCE LOCALIZATION AND A SEPARABLE 2-D IIR FILTER REALIZATION Final Report, 1 Apr. 1989 - 30 Jun. 1991
Arnab K. Shaw 30 Sep. 1991 128 p
(Grant AF-AFOSR-0291-89; AF Proj. 2304)
(AD-A243457; AFOSR-91-0917TR) Avail: NTIS HC/MF A07 CSCL 09/1

Optimal Design of ARMA (IIR) filters with arbitrary number of poles and zeros from Impulse Response Data has been developed. The general criterion derived in this report has never been found before. Optimal synthesis of two dimensional IIR filters using one dimensional modules have been developed. Optimal design of a class of two dimensional IIR filters from spatial domain data has been developed. Optimal identification of Multivariable systems from Impulse response data is given. A Periodogram-based Maximum Likelihood estimator of Narrowband frequencies requiring only off the shelf hardware/software has been developed. A faster Simulated-Annealing method has been developed and applied to frequency estimation. A coherent one-step angles of arrival estimator of multiple broadband sources has been developed. Existing coherent techniques can not localize well separated sources in one step. An Order-Recursive approach has been given for AR-Bispectrum estimation. A Time-Delay-Neural Network has been trained with LPC coefficients for Phoneme/Vowel recognition. Parametric Non-linear prediction algorithms have been introduced for the first time for speech prediction/synthesis/coding. GRA

N92-17668# Southeastern Center for Electrical Engineering Education, Inc., Saint Cloud, FL.
ELECTROMAGNETIC PULSE-INDUCED CURRENT MEASUREMENT DEVICE Final Technical Report, Jun. 1989 - Sep. 1990
Om P. Gandhi and Jin Y. Chen Aug. 1991 17 p
(Contract F33615-87-D-0609)
(AD-A241946; AL-TR-1991-0058) Avail: NTIS HC/MF A03 CSCL 20/15

To develop safety guidelines for exposure to high fields associated with an electromagnetic pulse (EMP), it is necessary to devise techniques that would measure the peak current induced in the human body. The main focus of this project was to design, fabricate, and test a portable, self-contained stand-on device that would measure and hold the peak current and the integrated change Q. The design specifications of the EMP-Induced Current Measurement Device are as follows: rise time of the current pulse, 5 ns; peak current, 20-600 A; charge Q, 0-20 microcoulombs. The device uses a stand-on parallel-plate bilayer sensor and fast high-frequency circuit that are well-shielded against spurious responses to high incident fields. Since the polarity of the incident peak electric field of the EMP may be either positive or negative, the induced peak current can also be positive or negative. Therefore, the device is designed to respond to either of these polarities and measure and hold both the peak current and the integrated charge which are simultaneously displayed on two separate 3-1/2 digit displays. The prototype device has been preliminarily tested with the EMP's generated at the Air Force Weapons Laboratory (ALECS facility) at Kirtland AFB, New Mexico. GRA

N92-17671# Mitre Corp., Bedford, MA.
SUPERCONDUCTING MICROWAVE TRANSMISSION LINES
C. P. McClay, Steven Soares, and Peter S. Weitzman Oct. 1991 68 p
(AD-A243166; MTR-11230) Avail: NTIS HC/MF A04 CSCL 09/1

Superconducting microwave transmission lines can be designed to have lower loss, lower dispersion, and lower phase velocity than conventional metal lines. These properties make superconducting transmission lines attractive for use in many devices and systems such as filters and analog to digital converters. The problem with designing microwave circuits which utilizes these lines is that accurate circuit models do not exist. This paper present models for the microwave transmission line parameters (phase velocity, attenuation, and characteristic impedance) of superconducting lines as a function of temperature and geometry. An experiment to verify these models is also presented. GRA

N92-17672# Mitre Corp., Bedford, MA.
DESIGN AND EVALUATION OF A JOSEPHSON ARRAY OSCILLATOR
C. P. McClay, Lawrence R. DAddario, and Albert G. Montgomery Nov. 1991 50 p
(AD-A243167; MTR-11252) Avail: NTIS HC/MF A03 CSCL 09/1

This report describes the design and measured performance of a superconducting Josephson array oscillator. An array of Josephson junctions was fabricated to function as a 12 to 18-GHz frequency agile voltage controlled oscillator for application in analog-to-digital conversion. At a temperature of 4.2 K, measured peak RF power was approximately -84 dBm in a 300 kHz bandwidth. Author (GRA)

N92-17684# Rome Lab., Griffiss AFB, NY.
GATE DRAIN GEOMETRY EFFECT ON THE CURRENT VOLTAGE CHARACTERISTICS OF GaAs MESFETs Report, Jun. 1988 - Nov. 1989
Jon S. Schoenberg and Edward Cohen Jun. 1991 28 p Prepared in cooperation with Arcon Corp., Waltham, MA
(AF Proj. 2305)
(AD-A243430; RL-TR-91-181) Avail: NTIS HC/MF A03 CSCL 09/1

We investigated the effect of gate-drain distance on gallium arsenide MESFET current-voltage characteristics. DC characteristics of several GaAs MESFET's are determined and compared to results from a computer implementation of a physically based, analytical model by Chang and Day. Their model is modified to account for the effect of longer gate-drain distance, and shows excellent agreement with measured I-V curves across the full range of device geometrics tested. GRA

N92-17702 Academy of Sciences of the Ukrainian SSR, Kiev. Inst. of Physics.
ELECTRICAL AND THERMAL CONDUCTIVITY OF A VARIABLE ZONE SEMICONDUCTOR IN A LONGITUDINAL MAGNETIC FIELD [ELEKTRO I TEPLOPROVODNOST VARIZONNOGO POLUPROVODNIKA V PRODOLNOM MAGNITNOM POLE]
B. A. Martyniuk and V. A. Shenderovskii 1990 22 p In RUSSIAN
Copyright Avail: Issuing Activity

In the context of an approximation theory of effective mass an investigation is conducted into the possibility that a shift in energy extreme exists in the Brilluenza zone during the change in chemical composition of a semiconducting solid solution. It is established that the realizations related to a given characteristic of zonal structure of a semi-magnetic field leads one to anticipate a smooth-heterogeneous solid solution on the basis of an entire series of compounds A3B5:BP, AlAs, AlP and others. It is shown that the superposition of the longitudinal magnetic field can signify, in the indicated structures, a tripling in size of electro- and thermo-conductivity. Transl. by L.K.S.

N92-17708# David Sarnoff Research Center, Princeton, NJ.
INNOVATIVE SWITCHING TECHNOLOGY
A. Rosen, P. J. Stabile, A. M. Gombar, W. M. Janton, D. B. Gilbert, P. R. Herczfeld, and A. Bahasadri (Drexel Univ., Philadelphia, PA.)
29 Mar. 1991 99 p
(Contract DE-AC03-87SF-17127)
(DE92-003068; DOE/SF-17127/T1) Avail: NTIS HC/MF A05

We have developed an all-semiconductor high-power optical switch. Potential uses include both military applications, such as ultra-wide-band impulse radar and high-frequency antenna couplers, and commercial use, such as high-power switching for utility companies. Under this three-year program, we have demonstrated various switching applications from dc to GHz frequencies. The generic switches comprise a 2-D semiconductor laser diode array and Si or GaAs devices. In the Si area (linear switches - no gain) and dc-biased network, a single two-sided PIN device, activated by two 1 kW laser arrays, has yielded a holding voltage of 1.3 kV and conducted 192 A. Similar devices have later yielded a holding voltage of 3.3 kV, demonstrating the capability of switching more than 500 kW with a single two-sided PIN device. The same generic technology was also demonstrated in high-power high-frequency antenna coupler applications as well as in mm-wave (60 GHz) attenuators and phase shifters. PIN devices tested in a RF circuit between 2-30 MHz yielded an isolation value of between 28 and 49 dB in the off-state, and insertion losses as low as 0.1 dB when illuminated with 280 W (peak) optical power at 808 nm. In the area of GaAs, PIN, and bulk devices under this project, we were able to deliver devices for experiments in both opening and closing switches. We have demonstrated a compact, all-semiconductor switch system that has switched up to 8.5 MW into a 38 (omega) load. The system uses a 2-D laser diode array with a peak power of 850 W to rigger a 1.5 cm long GaAs photoconductor into a high-gain combination mode known as 'lock on'. The highest power switch was pulse-charged to 55 kV and delivered 470 A to a 38 (omega) load in 160 ns long pulse. In the area of 2-D laser arrays, a peak power density of 7 kW/cm(exp 2) was achieved. DOE

N92-17718# Air Force Inst. of Tech., Wright-Patterson AFB, OH. School of Engineering.
A WALSH-DOMAIN ADAPTIVE FILTER M.S. Thesis
Larry J. Duvall Dec. 1991 269 p
(AD-A243701; AFIT/GE/ENG/91D-15) Avail: NTIS HC/MF A12 CSCL 09/1

Two Walsh-domain dyadic convolution adaptive filters are developed using a circular convolution frequency-domain filter (FDF1) and the Fast LMS adaptive filter (FDF2): WDF1 and WDF2 respectively. General theory of time-domain adaptive filters and a theoretical analysis of the FDF1, FDF2, WDF1, and WDF2 filters are presented. WDF1 and WDF2 software implementation are shown to be error free. A time-domain filter (TDF) and a FDF2 frequency-domain filter (FDF) are implemented for comparison testing. The WDF1, WDF2, TDF, and FDF filters are tested using time-shifted sinusoidal and rectangular noisy and noiseless signals. WDF1 and WDF2 are shown to converge faster and produce less error filtering discontinuous signals, relative to the TDF and FDF performance. WDF1 and WDF2 are shown to converge slower and produce more error filtering continuous signals, relative to TDF and FDF performance. WDF1 is shown to perform better for noiseless signals, relative to WDF2 performance. WDF2 is shown to perform better for noise signals, relative to WDF1 performance. WDF1 and WDF2 filtering performance was shown to degrade with increasing time shift. A processing speed comparison showed WDF1 to be faster than the TDF, FDF, and WDF2 filters. GRA

N92-17724# Naval Postgraduate School, Monterey, CA.
HEAT TRANSFER ENHANCEMENT DUE TO BUBBLE PUMPING IN FC-72 NEAR THE SATURATION TEMPERATURE M.S. Thesis
Ali S. Eren Mar. 1991 81 p
(AD-A243558) Avail: NTIS HC/MF A05 CSCL 09/1

The use of boiling heat transfer in the liquid immersion cooling of electronic components has always been hampered by the excessive superheat necessary to initiate nucleation in the fluorinated hydrocarbons used as dielectric cooling fluids. In an attempt to overcome some of these difficulties, an experimental study of the effects of nucleate pooling boiling, on the heat transfer from surface near the boiling surface was conducted. An experimental chamber was constructed which had a column of four horizontal wires spaced 2.5 cm vertically from each other. The lowest wire was progressively heated from the natural convection region through the nucleate boiling region. A study was made of the effects of the boiling wake from the lowest wire on heat transfer from the upper wires. Under certain conditions heat transfer enhancements of up to 30 pct. were obtained. GRA

N92-17742# Auburn Univ., AL.
A STUDY OF ELECTRIC TRANSMISSION LINES FOR USE ON THE LUNAR SURFACE M.S. Thesis
Krista Lynn Gaustad 13 Dec. 1991 410 p
Avail: NTIS HC/MF A18

Analytical models have been developed to study the operating characteristics of electrical transmission lines for use on the lunar surface. Important design considerations for a transmission line operating on the lunar surface are mass, temperature, and efficiency. Transmission line parameters which impact these considerations include voltage, power loss, and waveform. The electrical and thermal models developed are used to calculate transmission line mass, temperature, and efficiency as a function of voltage, geometry, waveform, location, and line size. The analyses include ac and dc for above ground, on the surface, and below ground operation. Geometries studied include a vacuum-insulated, round two-wire transmission line, a vacuum insulated rectangular (flat) two-wire transmission line, and a solid dielectric insulated, coaxial transmission line. Author

N92-17760# Air Force Inst. of Tech., Wright-Patterson AFB, OH. School of Engineering.
ELECTRICALLY ERASABLE PROGRAMMABLE INTEGRATED CIRCUITS FOR REPLACEMENT OF OBSOLETE TTL LOGIC M.S. Thesis
Joseph V. Breen Dec. 1991 240 p
(AD-A243652; AFIT/GE/ENG/91D-06) Avail: NTIS HC/MF A11 CSCL 09/1

Two microcircuits with electrically erasable programmable logic arrays, which use Fowler-Nordheim (F-N) tunneling for both programming and erasing, were designed to demonstrate the use of programmable logic for obsolete TTL logic replacement. Each microcircuit was fabricated in the Orbit 2-micron double-poly low noise analog CMOS process through MOSIS. Software to generate VHDL structural models from a pin list was developed and the logic of both designs was verified by simulation using the Zycad VHDL simulator. The first microcircuit included a simple programmable logic circuit and test cells that allowed measurement of the programming characteristics of the floating gate transistors. Test result on this microcircuit show a wide variance of programmability even between similar transistors on the same die. Some evidence of F-N tunneling from the control gate to the floating gate was also noted. The second microcircuit was designed to emulate the logic of a group of combinational TTL circuits. VHDL simulation was successful for each emulation. Device testing provided limited results due to a design error; however, successful emulation of two sections of a 7400 quad-NAND circuit was achieved. Author (GRA)

N92-17801# Stanford Linear Accelerator Center, CA.
HIGH CURRENT TRANSISTOR PULSE GENERATOR
V. Nesterov and R. Cassel May 1991 3 p Presented at the IEEE Nuclear Science Symposium, Santa Fe, NM, 5-9 Nov. 1991
(Contract DE-AC03-76SF-00515)
(DE92-004774; SLAC-PUB-5698; CONF-911106-31) Avail: NTIS HC/MF A01

A solid state pulse generator capable of delivering high current trapezoidally shaped pulses into an inductive load has been developed at SLAC. Energy stored in the capacitor bank of the

pulse generator is switched to the load through a pair of Darlington transistors. A combination of diodes and Darlington transistors is used to obtain trapezoidal or triangular shaped current pulses into an inductive load and to recover the remaining energy in the same capacitor bank without reversing capacitor voltage. The transistors work in the switch mode, and the power losses are low. The rack mounted pulse generators presently used at SLAC contain a 660 microfarad storage capacitor bank and can deliver 400 amps at 800 volts into inductive loads up to 3 mH. The pulse generators are used in several different power systems, including pulse to pulse bipolar power supplies and in application with current pulses distributed into different inductive loads. The current amplitude and discharge time are controlled by the central computer system through a specially developed multichannel controller. Several years of operation with the pulse generators have proven their consistent performance and reliability. DOE

N92-17825# Joint Inst. for Nuclear Research, Dubna (USSR). Lab. of Nuclear Problems.
CRYOGENIC THERMORESISTOR MADE FROM p-InSb(Mn)
S. A. Obukhov (Academy of Sciences, USSR, Leningrad), B. S. Neganov, Yu. F. Kiselev, A. N. Chernikov, V. S. Vekshina, N. I. Pepik, and A. N. Popkov 1990 10 p In RUSSIAN; ENGLISH summary
(DE92-600473; JINR-R-8-90-127) Avail: NTIS HC/MF A02

Thermoresistors of InSb(Mn) for ultralow temperatures are described. Being employed below 10 mK they have higher thermosensitivity than known thermoresistors at relatively low specific resistance. They have logarithmic dependence of specific resistance on temperature. The thermometers have negative magnetic resistance. The magnetic Mn(sup +2) impurity in non-magnetic semiconductor InSb is supposed to cause a magnetic gap in the impurity zone owing to exchange interaction between manganese ions and holes. This effect increases for compensated p-InSb(Mn). DOE

N92-17831 Department of the Navy, Washington, DC.
EXPLOSIVE MAGNETIC FIELD COMPRESSION GENERATOR TRANSFORMER POWER SUPPLY FOR HIGH RESISTIVE LOADS Patent
Millard F. Rose, inventor (to Navy), Lawrence H. Luessen, inventor (to Navy), and Monty P. Villere, inventor (to Navy) 22 Oct. 1991 6 p Filed 16 May 1977
(AD-D015123; US-Patent-5,059,839; US-Patent-Appl-SN-797168; US-Patent-Class-310-10) Avail: US Patent and Trademark Office CSCL 20/3

An explosive flux compression generator is coupled to a high resistance load by a pulse transformer. Chemical energy is converted to electromagnetic energy and is transferred by means of the transformer to the high resistance load. The transformer allows coupling to a higher resistive load than is achieved with a transformerless-generator system having a current gain greater than unity. GRA

N92-17865*# National Aeronautics and Space Administration. Pasadena Office, CA.
METHOD FOR NON-DESTRUCTIVE ESTIMATION OF WAVEGUIDE DIRECTIONAL COUPLER DIMENSIONS Patent Application
Raul M. Perez, inventor (to NASA) (Jet Propulsion Lab., California Inst. of Tech., Pasadena.) 22 Oct. 1991 13 p
(Contract NAS7-918)
(NASA-Case-NPO-18454-1-CU; NAS 1.71:NPO-18454-1-CU; US-Patent-Appl-SN-781521) Avail: NTIS HC/MF A03 CSCL 09A

A method for estimating the size and location of couplings within a waveguide directional coupler is provided. The method is applied to a waveguide directional coupler having a main transmission waveguide connected to an auxiliary transmission waveguide by a number of bore hold couplings. The bore hold couplings are in the interior of the waveguide directional coupler and, therefore, are not easily measurable. The method generally includes the steps of applying a two-sided tape to a member, inserting and securing the member within the main transmission waveguide, pouring a fine particulate substance such as talc into the auxiliary transmission waveguide such that a portion of the talc enters the bore hole couplings and adheres to the two-sided tape, and withdrawing the member such that the size and location of the bore hole couplings can be determined by measuring the size and location of marks on the two-sided tape caused by the fine particular substance adhering to the two-sided tape. NASA

N92-17871 Department of the Navy, Washington, DC.
SILVER-NICKEL COMPOSITE CATHODES FOR ALKALINE SECONDARY BATTERIES Patent
William Ferrando, inventor (to Navy) 3 Sep. 1991 4 p Filed 16 Aug. 1989
(AD-D015121; US-Patent-5,045,349; US-Patent-Appl-SN-395547; US-Patent-Class-427-113) Avail: US Patent and Trademark Office CSCL 07/2

A method for producing lightweight silver-nickel composite electrodes by: (1) infiltrating a graphite fiber plaque with a suspension of finely divide nickel powder in an aqueous solution of AgNO3; (2) drying the graphite fiber plaque to produce a coating of AgNO3 crystals and nickel particles on the surfaces of the graphite fibers; (3) heating the coated graphite fiber plaque at a temperature about the melting point of AgNO3 but below the decomposition temperature of AgNO3 until the AgNO3 melts and wets the nickel particle and the surfaces of the graphite fibers; and (4) heating the molten AgNO3 coated graphite fiber plaque at a temperature from the decomposition temperature of AgNO3 to about 600 C, until the AgNO3 decomposes to form a thin uniform silver metal coating over the nickel particles and the surfaces of the graphite fibers. The silver-nickel particle coated graphite plaque is electrochemically treated to convert the silver to silver active material (Ag2O2) and the nickel to nickel active material (Ni(OH)2). GRA

N92-17907*# National Aeronautics and Space Administration. Pasadena Office, CA.
TRANSFORMERLESS DC-DC VOLTAGE AMPLIFIER WITH OPTICALLY ISOLATED SWITCHING DEVICES Patent Application
Govind Sridharan, inventor (to NASA) (Jet Propulsion Lab., California Inst. of Tech., Pasadena.) 22 Oct. 1991 13 p
(Contract NAS7-918)
(NASA-Case-NPO-17994-1-CU; NAS 1.71:NPO-17994-1-CU; US-Patent-Appl-SN-791759) Avail: NTIS HC/MF A03 CSCL 09A

A very high voltage amplifier is provided in which plural cascaded banks of capacitors are switched by optically isolated control switches so as to be charged in parallel from the preceding stage or capacitor bank and to discharge in series to the succeeding stage or capacitor bank in alternating control cycles. The optically isolated control switches are controlled by a logic controller whose power supply is virtually immune to interference from the very high voltage output of the amplifier by the optical isolation provided by the switches, so that a very high voltage amplification ratio may be attained using many capacitor banks in cascade. NASA

N92-17949# Hughes Research Labs., Malibu, CA.
HIGH TEMPERATURE SUPERCONDUCTOR THIN FILMS AND JOSEPHSON JUNCTIONS Final Report, Sep. 1988 - Aug. 1991
A. T. Hunter Oct. 1991 52 p
(Contract N00014-88-C-0667)
(AD-A242747; HAC-REF-G4663) Avail: NTIS HC/MF A04 CSCL 20/3

We have developed processes for the sputter deposition and device fabrication of Josephson tunneling structures made from YBCO materials. Very high critical current density YBCO films were used to make several different types of weak link structures. An 8-nm-diam focused ion beam was used to pattern thin YBCO films by implant damage. Procedures to fabricate trilayer devices utilizing a-axis films and non-superconducting YBCO barriers were developed. Superconducting transport through the barrier was observed, but was limited by base-electrode critical current density.

These results indicated to us that edge-junctions would be better suited to the relatively low resistance barriers than are trilayer junctions. In the final stages of the program, we developed procedures for fabricating all YBCO edge junctions. Using a post annealed base electrode and in situ counter electrode and no deposited barrier, we measured junction current densities up to 1,000,000 A/sq cm, demonstrating successful implementation of the steps required to make edge junctions, including successful annealing of the ion milling damage at the edge during counter electrode growth. This result indicates that barriers are not formed as uncontrolled artifacts of edge-junction processing, and is a crucial test of the feasibility of fabricating edge junctions with reproducible, controlled properties using deposited barriers. Edge-junction devices were fabricated with a 10-nm non-superconducting YBCO barrier under the superconducting counter-electrode layer. GRA

N92-17953# Joint Inst. for Nuclear Research, Dubna (USSR). Lab. of Nuclear Problems.
COMPARATIVE STUDY OF IRREVERSIBILITY EFFECTS IN Nb FOIL AND HIGH TEMPERATURE SUPERCONDUCTING CERAMICS BY MUON SPIN ROTATION
V. G. Grebinnik, V. N. Duginov, and V. A. Zhukov 1990 9 p Presented at the 5th International Conference on Muon Spin Rotation, Relaxation, and Resonance, Oxford, England, 9-12 Apr. 1990
(DE92-600475; JINR-E-14-90-254) Avail: NTIS HC/MF A02

We present the results of an investigation of superconducting niobium and high temperature ceramic superconductor La(1.9)Sr(0.1)CuO(4) by the (mu)SR technique. The experiments with the niobium sample have confirmed high reliability of the (mu)SR-technique in determining such characteristics of type II superconductors as T(sub c), H(sub c1), H(sub c2), the magnetic field penetration depth (lambda), and the critical current density J(sub c). The analysis of the field dependences of the distribution width and mean value of the magnetic fields on the muon when the samples are magnetized was carried out. One has revealed qualitative difference in the behavior of the magnetic field distribution width in Nb and LaSrCuO. While the niobium data are well described in the frame of the critical state model, application of the similar approach to the high-T(sub c) superconductor did not give a satisfactory description of our experimental results. DOE

N92-17971# Gosudarstvennyi Komitet po Ispolzovaniyu Atomnoi Energii, Serpukhov (USSR). Inst. Fiziki Vysokikh Ehnergij.
ANALYSIS OF POSSIBLE SCHEMES FOR TWISTING MULTIWIRE SUPERCONDUCTING CABLES AND DESIGN OF TWISTING EQUIPMENT
E. R. Borisov, Yu. V. Kuznetsov, and V. P. Oshchepkov 1991 17 p In RUSSIAN; ENGLISH summary Submitted for publication
(DE92-609667; IFVE-OEA-91-2) Avail: NTIS HC/MF A03

Possible technological schemes for obtaining superconducting twisted cables are presented. The advantages and disadvantages of the twisting schemes and deformations of the superconducting wires when being twisted are analyzed. The causes of the twist step instabilities are considered and recommendations on choosing the twisting scheme satisfying the requirements imposed on the twisted cables are presented. Brief information on the designed and used in industry equipment for superconductor twisting is given. DOE

34 FLUID MECHANICS AND HEAT TRANSFER

Includes boundary layers; hydrodynamics; fluidics; mass transfer; and ablation cooling.

For related information see also *02 Aerodynamics* and *77 Thermodynamics and Statistical Physics.*

N92-16978# David Taylor Research Center, Bethesda, MD. Ship Hydromechanics Dept.
COMPUTATION OF THE HYDRODYNAMIC FORCES AND MOMENTS ON A BODY OF REVOLUTION WITH AND WITHOUT APPENDAGES
Young S. Hong Aug. 1991 54 p
(AD-A243033; DTRC/SHD-1003-06) Avail: NTIS HC/MF A04 CSCL 20/4

An analytical method was developed to predict the hydrodynamic forces and moments developed on a body of revolution with and without appendages. The appendages included a bridge fairwater, sternplanes, and rudders. It was assumed that the body was either translating with an angle of attack of up to 20 deg or rotating with an angular velocity. Calculations were performed by using the analytical method for four different bodies of revolution and comparisons were made with available experimental data. Potential flow was used to determine the inviscid contribution to the hydrodynamic forces and moments. The viscous contribution to the hydrodynamic forces and moments was determined by assuming that there was no flow separation due to the axial flow, and that the flow separation on the leeward side of the body due to the crossflow was independent of the offsets of the body, the angle of attack, the angular velocity, and the forward speed. It was assumed that the angle at which the flow separates, as measured from the stagnation point, was 110 deg at the stern and 170 deg at the bow for the body at angle of attack and 160 deg for the body with an angular velocity. GRA

N92-16979# California Inst. of Tech., Pasadena. Graduate Aeronautical Labs.
CHEMICAL REACTIONS IN TURBULENT MIXING FLOWS Annual Report, 16 Apr. 1990 - 14 May 1991
Paul E. Dimotakis, James E. Broadwell, and Anthony Leonard 14 Sep. 1991 197 p
(Grant AF-AFOSR-0304-90; AF Proj. 2308)
(AD-A243035; AFOSR-91-0906TR) Avail: NTIS HC/MF A09 CSCL 20/4

The purpose of this research is to conduct fundamental investigations of turbulent mixing, chemical reaction and combustion processes in subsonic and supersonic flows. This program comprises experimental, analytical, computational, and modeling efforts, and a diagnostics development and data acquisition effort, the latter as dictated by specific needs of the experiments. Our approach has been to carry out a series of detailed theoretical and experimental studies primarily in two, well defined, fundamentally important flow fields: free shear layers and axisymmetric jets. To elucidate molecular transport effects, experiments and theory concern themselves with both liquids and gases, primarily in moderate to high Reynolds number flows. The computational studies are, at present, focused at fundamental issues pertaining to the computational simulation of both compressible and incompressible flows. Modeling has been focused on both shear layers and turbulent jets, with an effort to include the physics of the molecular transport processes, as well as formulation of models that permit the full chemical kinetics of the combustion process to be incorporated. GRA

N92-17002*# National Aeronautics and Space Administration. Langley Research Center, Hampton, VA.
APPLICATION OF PROGRAM LAURA TO PERFECT GAS SHOCK TUBE FLOWS: A PARAMETRIC STUDY
K. F. Mitterer, R. A. Mitcheltree, and P. A. Gnoffo Jan. 1992 23 p

(NASA-TM-104190; NAS 1.15:104190) Avail: NTIS HC/MF A03 CSCL 20D

The Langley Aerothermodynamic Upwind Relaxation Algorithm (LAURA) was originally developed to solve steady-flow problems. The desire to validate the algorithm with shock tube experimental data motivated the development of a time-accurate version of the LAURA code. The current work presents a test of the Algorithm. Computational results are compared with the exact solution for a simple shock tube case. The parameters examined are Courant number, relaxation sweeps, grid spacing, and the inviscid relaxation factor. The results of the study indicate that LAURA is capable of producing accurate solutions when appropriate values are used for each parameter. Author

N92-17012# Physical Sciences, Inc., Andover, MA.
VELOCITY MEASUREMENTS IN HIGH TEMPERATURE GASES USING LASER-INDUCED NO FLUORESCENCE Final Report, Aug. 1990 - Apr. 1991
M. G. Allen and S. J. Davis Oct. 1991 71 p
(Contract F33615-90-C-2069)
(AD-A242399; PSI-2145/TR-1108; WL-TR-91-2109) Avail: NTIS HC/MF A04 CSCL 09/3

This report describes the results of a Phase 1 SBIR program which investigated the applicability of a Laser Induced Fluorescence (LIF) velocimetry diagnostic technique based on Doppler-shifted NO fluorescence. The intent of the program was to quantitatively understand the potential accuracy of the approach in high temperature, high pressure gas flow applications when one is restricted to use only a single laser wavelength. The single laser wavelength approach greatly simplifies the experimental requirements while retaining the capability of simultaneous, multiple point velocity field measurements. The report summarizes detailed analytical studies which demonstrate that, for representative NO lineshapes and available pulse dye lasers, single shot measurements of the instantaneous velocity field are possible in essentially uncharacterized pressure and temperature fields with less than 10 percent uncertainty. When a priori information on the pressure or temperature field is available, the instantaneous measurement uncertainty is reduced to less than 5 percent. GRA

N92-17018# National Inst. of Standards and Technology, Boulder, CO. Chemical Engineering Div.
UNSTEADY LAMINAR FLOW IN A CIRCULAR TUBE: A TEST OF THE HERCOL (HERMITIAN COLLOCATION) COMPUTER CODE
James F. Welch, James A. Hurley, Michael P. Glover, Ryan D. Nassimbene, and Marilyn R. Yetzbacher May 1991 27 p
(PB91-222679; NISTIR-3963) Avail: NTIS HC/MF A03 CSCL 20D

HERCOL, a computer code for the integration of second-order differential equations in one space dimension by Hermitian collocation was used to calculate the unsteady velocity profiles for laminar flow in a circular tube. The code was tested for stability and accuracy for the problem for which an analytical solution exists prior to application to a like problem in which the initial and boundary conditions preclude the existence of analytical solutions. The test problem is one in which a pressure gradient is imposed on a fluid initially at rest in a circular tube; the fluid accelerates and at steady state has a parabolic velocity profile. A second example was constructed from the first; a pressure gradient equal but opposite in sign is imposed on the fluid with a fully developed parabolic velocity profile. At steady state, the velocity is again parabolic, but in the opposite direction to that at the initial conditions. Excellent agreement with the analytical solution was obtained in the first problem; in the second, the behavior was as expected. Author

N92-17025# Massachusetts Inst. of Tech., Cambridge. Dept. of Chemical Engineering.
GAS TRANSPORT IN POLYBUTADIENE TREATED WITH AQUEOUS BROMINE
D. H. Rein, R. F. Baddour, and R. E. Cohen 10 Oct. 1991 19 p
(Contract N00014-91-J-1045)
(AD-A241871; TR-6) Avail: NTIS HC/MF A03 CSCL 07/6

Diffusion, solubility and permeability coefficients were measured for He, CO2, Ar and CH4 in polybutadiene (PB) and in polybutadiene reacted in the solid state to various extents with aqueous bromine. Analysis of the sorption curves and x ray emission spectra showed that the bromination created a heterogeneous membrane with an outer brominated skin and an unreacted core. At relatively low extent of bromination, the diffusion and permeability coefficients for CO2, Ar and CH4 became immeasurably small after about 3 percent bromination. The ideal separation factor for gas pairs with different molecular size increased with bromination, suggesting applications in gas separation processes. Tailoring the structure of existing commodity polymers through chemical modification is an attractive approach to improving the properties of membranes for gas separation and barrier applications. Systematic alterations of the polymer structure also provide a convenient route for studying the effects of molecular architecture on the permeability. Substitutions to the backbone or side chains affect the intrasegmental mobility and intersegmental chain packing, resulting in changes in gas diffusivity, solubility and permeability coefficients. GRA

N92-17039# Washington Univ., Seattle. Dept. of Applied Mathematics.
EDDY BREAKDOWN AND STRUCTURE DEVELOPMENT Final Technical Report, 1 Jul. 1989 - 30 Jun. 1991
W. O. Criminale 17 Sep. 1991 4 p
(Grant AF-AFOSR-0404-89)
(AD-A241886; AFOSR-91-0874TR) Avail: NTIS HC/MF A01 CSCL 20/4

This research addressed a class of exact solutions for the Navier Stokes equations which are valid for basic flows with shear, can be time-dependent and non-parallel, fully three-dimensional, and offer closed-form functions for the perturbation field. Linearized initial-value problems can be completely solved by this method. Problems which were studied in the course of the research included the elliptic vortex, linear initial value problems, and exact solutions to the Navier Stokes equations. GRA

N92-17126# Naval Research Lab., Washington, DC.
EFFECTIVE VISCOSITY IN THE SIMULATION OF SPATIALLY EVOLVING SHEAR FLOWS WITH MONOTONIC FCT MODELS Memorandum Report
F. F. Grinstein and R. H. Guirguis 13 Dec. 1991 37 p
(AD-A243709; NRL-MR-6926) Avail: NTIS HC/MF A03 CSCL 20/4

The global numerical diffusion of a model for the low-Mach-number simulation of free mixing layers is investigated. The numerical model solves the inviscid time-dependent conservation equations for mass, momentum and energy, for ideal gases. The equations are solved using an explicit Flux-Corrected Transport (FCT) algorithm, directional timestep-splitting techniques on structured grids, and appropriate inflow and outflow boundary conditions. Effective measurement of the numerical diffusion of the model in uniform grids is performed by comparison of the laminar spread of the simulated mixing layers with that predicted by boundary layer theory. The results show that the residual numerical diffusion of the FCT model can emulate physical viscosity for laminar shear flows at moderately high Reynolds numbers. The global numerical diffusion is not very sensitive to changes in free-stream velocity ratio, and can be reduced in a predictable way by refining the grid spacing. GRA

N92-17168# David Taylor Research Center, Bethesda, MD. Ship Hydromechanics Dept.
USE OF NAVIER-STOKES ANALYSIS IN SECTION DESIGN Final Report, Oct. 1988 - Oct. 1990
Phuc N. Nguyen Dec. 1990 24 p
(NR Proj. RB2-3-C-22)
(AD-A242074; DTRC/SHD-1262-04) Avail: NTIS HC/MF A03 CSCL 01/1

The Navier-Stokes analysis method and a design technique based on conformal mapping are combined to develop new 2-D thick sections. The Eppler-Somers design technique allows for fast design of arbitrary section shape. The well-validated David Taylor Navier-Stokes code is used to optimize the thickness of the section. From previous experimental results, the turbulence characteristics in the near-wake region correlate with the pressure spectra on the trailing edge of a 2-D lifting surface. Therefore, the turbulent kinetic energy, and the Reynolds shear stress are used as design parameters to develop new 2-D sections. Minimizing these parameters is assumed to provide desirable boundary layer and wake characteristics. The characteristics of one new section are compared with those of a baseline section to demonstrate the new foil design method. GRA

N92-17176# Purdue Univ., West Lafayette, IN. School of Mechanical Engineering.
INJECTION OF DRAG REDUCING ADDITIVES INTO TURBULENT WATER FLOWS Final Report, 1 Mar. 1983 - 30 Nov. 1990
William G. Tiederman Nov. 1991 21 p
(Contract N00014-83-K-0183)
(AD-A243209; PME-FM-91-2) Avail: NTIS HC/MF A03 CSCL 20/4

The basic goals of this project were to determine the mechanism(s) by which drag-reducing, polymer solutions modify the turbulent momentum transport in wall bounded flows and to develop optimal methods for injecting these additives into those flows. The purpose was to learn how to control and to manipulate wall turbulence and develop faster, more energy efficient and quieter submersible vehicles. The major results from this study are presented. GRA

N92-17275# Naval Postgraduate School, Monterey, CA.
STUDY OF PLANE WAVE IMPINGEMENT ON A THIN PLATE CAPABLE OF DEFORMATION M.S. Thesis
Thomas K. Kisiel Dec. 1991 72 p
(AD-A242947) Avail: NTIS HC/MF A04 CSCL 20/4

This thesis models the effects in a fluid medium of a plane wave that has impinged upon a reinforced plate. The wave equation for pressure, and the equation of a thin plate combined with other equations are coupled at the interface between the fluid and the thin plate. The actual modeling is accomplished in a fortran computer program written to run on the Naval Postgraduate School's main frame computer. The program uses extensive finite differencing on a domain, assumed to be a small section of an infinite interface between the fluid and the plate, to simulate the deflection of the thin plate and the pressure disturbances in the fluid medium. To accomplish this, each of the above equations will be scaled or nondimensionalized. Additional finite differencing is explained which covers the special cases for the side boundaries of the fluid domain, and the artificial boundary created to model infinity. Different beam spacing is explored for its effect on the magnitude of the propagating modes of the scattered pressure wave. GRA

N92-17276# California Inst. of Tech., Pasadena. Graduate Aeronautical Labs.
AN EXPERIMENTAL INVESTIGATION OF CHEMICALLY-REACTING, GAS-PHASE TURBULENT JETS M.S. Thesis
Richard J. Gilbrech 12 Apr. 1991 97 p
(Grant AF-AFOSR-0304-90; AF Proj. 2308)
(AD-A243036; AFOSR-91-0895TR) Avail: NTIS HC/MF A05 CSCL 20/6

A new high pressure combustion facility was built to investigate mixing in axisymmetric, turbulent jets exiting into quiescent reservoirs. The facility uses fluorine and nitric oxide, diluted with nitrogen, for chemical product formation that is accompanied by heat release. The average temperature was measured by a set of long, thin, resistance wire thermometers stretched across the jet centerline at 16 downstream locations from x/do = 30 to 240. The Reynolds number was varied through density, i.e., pressure, while the jet exit velocity and exit diameter were held constant. The main result of the work is that the flame length, as estimated from the temperature measurements, varies with changes in Reynolds number, suggesting that the mixing process is not Reynolds number independent up to Re = 150,000. Additionally, the measurements revealed a 'mixing virtual origin,' defined as the far-field flame length extrapolated to phi = 0, that increases with increasing Re for Re = 20,000 and then decreases with increasing Re for Re = 20,000. The transition of the jet flow from a momentum dominated to a buoyancy dominated regime was identified in another set of experiments. GRA

N92-17307# Naval Postgraduate School, Monterey, CA.
STUDY OF TRANSITION PHENOMENA IN A STRAIGHT CHANNEL WITH 40 TO 1 ASPECT RATIO WITH AND WITHOUT IMPOSED PULSATIONS. PART TWO: REYNOLDS NUMBER SURVEYS M.S. Thesis
Bradley J. Smith Mar. 1991 111 p
(AD-A241894) Avail: NTIS HC/MF A06 CSCL 20/4

A channel with rectangular cross section, 40 to 1 aspect ratio (height is 0.0127 m) and 4.27 m test section length (336 channel lengths), is used to study the effects of imposed pulsations on laminar, transitional, and turbulent flow phenomena. Periodic velocity variations are produced in the test section using a single rotating vane located in the flow downstream of the test section. Survey data for Y/d of 0.50, 0.85, and 0.90 show how normalized average velocity and turbulence intensity data vary with Reynolds number for Reynolds numbers ranging from 1100 to 3400 at Stokes numbers of 4.08 and 5.79 and Strouhal numbers from 0.033 to 0.121. These conditions are produced from pulsations imposed at 1 Hz and 2 Hz to show how transition develops both with and without imposed pulsations. Intermittency variations increase from near zero to one as Reynolds number changes from 1450 to 2100 for Y/d=0.90, 0.85, and 0.50. Time-averaged magnitudes of the normalized longitudinal turbulence intensity increase significantly as Re changes from 1450 to 3100 at Y/d=0.90. A maxima is reached near Re=2400. Afterwards these data show a decrease and level off in the turbulent region. At Y/d=0.85, the same trend in normalized longitudinal turbulence intensity appears with a maxima appearing near Re=2300. For the center of the channel (Y/d=0.50), the maxima appears near Re=2000. The normalized longitudinal turbulence intensity level in the turbulent region increases with Y/d. GRA

N92-17309# Florida State Univ., Tallahassee. Inst. of Geophysical Fluid Dynamics.
STUDIES OF BAROCLINIC FLOW Annual Report, 1 Oct. 1990 - 30 Sep. 1991
Richard L. Pfeffer Aug. 1991 20 p
(Grants AF-AFOSR-0462-89; AF-AFOSR-0009-90; AF Proj. 2310)
(AD-A243050; AFOSR-91-0916TR) Avail: NTIS HC/MF A03 CSCL 20/4

Prof. R. Krishnamurti and Dr H. Yang have completed their investigation of finite amplitude Hele-Shaw convection with an imposed shear. Their interest was also to determine the effect of convective transport of momentum upon the mean flow. Analysis of approximate solutions of the barotropic vorticity equation subject to periodic boundary conditions continues. In another study, considerable progress has been made in solving the nonlinear steady state barotropic vorticity equation for parameters which correspond to a series of laboratory experiments involving forced flow of a rotating fluid over bottom topography. In these experiments, the fluid is contained in a rotating circular cylindrical annulus with a differentially rotating, rigid, radially sloping, lid in contact with the top surface of the fluid. The fluid is forced into motion by the rotation of the lid. In another effort, the dynamics of equilibrium states in a sheared barotropic channel flow is being investigated. This flow is relevant to meteorological flows and the object of this work is to understand the population of certain states, called free modes, and comprehend how the actual flow in phase space is attracted from one state to another. The present research effort has investigated new parallel computing techniques and fast algorithms for the efficient use of parallel computers in

solving shallow water equations. Progress has been made toward understanding the development and nonlinear behavior of traveling baroclinic waves in the atmosphere and their interaction with topographically and thermally forced planetary waves. GRA

N92-17312# Messerschmitt-Boelkow-Blohm G.m.b.H., Munich (Germany, F.R.). Hubschrauber und Flugzeuge.
NUMERICAL GRID GENERATION USING A VARIATIONAL METHOD Thesis - Univ. der Bunderswehr Muenchen [NUMERISCHE RECHENNETZGENERIERUNG MIT EINEM VERFAHREN DER VARIATIONSRECHNUNG]
Michael Euler Apr. 1991 100 p In GERMAN
(MBB-FE211-S-PUB-447; ETN-92-90618) Copyright Avail: NTIS HC/MF A05

Numerical grids were generated for the solution of partial differential equations of the thermofluid dynamics. The computational grids have to model the solid boundary, and to solve the occurring flow phenomena with sufficient accuracy. A grid generator was implemented that uses a nonlinear optimization method of the variational calculus to generate computational grids for two dimensional geometries. The solution algorithm is based on a conjugate gradient method, and was tested on several geometries. This method has advantages with a view to adaptive grid generation. ESA

N92-17337# Naval Postgraduate School, Monterey, CA.
TRANSITION PHENOMENA IN A STRAIGHT CHANNEL WITH A 40 TO 1 ASPECT RATIO WITH AND WITHOUT IMPOSED PULSATIONS. PART 1: NEAR-WALL AND CENTRAL REGION PROFILES M.S. Thesis
Darrell S. Morrow Mar. 1991 184 p
(AD-A243251) Avail: NTIS HC/MF A09 CSCL 20/4

A channel with a rectangular cross-section, 40 to 1 aspect ratio (height is 0.0127 m), and 4.27 m test section (336 channel heights) is used to study the effects of imposed pulsations on transitional flow phenomena. Periodic velocity variations are produced in the test section using a single rotating vane located in the flow downstream of the test section. Flows with Reynolds numbers (Re) ranging from 1100 to 3600 are studied at Stokes numbers of 4.08 and 5.79 and Strouhal numbers from 0.02 to 0.122 by imposing pulsations at 1 Hz and at 2 Hz. Time-averaged velocity profiles both within and outside of the Stokes layer are unaffected by the imposed pulsations at frequencies of 1 and 2 Hz for the entire range of Reynolds numbers studied. Longitudinal turbulence intensity profiles show a local maxima only at the channel centerline for Reynolds numbers from 1250 to 1550. This is evidence of a center mode of instability. Longitudinal turbulence intensity profiles show a local maxima at both the channel centerline and y/d of 0.85 to Reynolds number from 1710 to 2300. As the Reynolds number increases from 2350 to 3400 local maxima of longitudinal turbulence intensity occur only at y/d of 0.9. Normalized profiles of longitudinal turbulence intensity are the same with and without pulsations for all Reynolds number studies with the exception of Reynolds numbers 2400 and 2450. Longitudinal turbulence intensity profiles at a Reynolds number of 2400 show that magnitudes near the channel centerline are reduced at Stokes numbers of 4.08 and 5.79 (1 Hz to 2 Hz pulsations). GRA

N92-17343# Max-Planck-Inst. fuer Stroemungsforschung, Goettingen (Germany, F.R.).
THE INFLUENCE OF CAVITATION IN THE BREAKUP OF LIQUID FREE JETS Thesis [ZUM KAVITATIONSEINFLUSS AUF DEN ZERFALL VON FLUESSIGKEITSFREISTRAHLEN]
Juergen Bode Mar. 1991 112 p In GERMAN; ENGLISH summary
(MPIS-1/1991; ISSN-0436-1189; ETN-92-90623) Avail: NTIS HC/MF A06

The interaction between a diesel injection nozzle flow and the atomizing jet was investigated over a wide range of Reynolds numbers. If the pressure gradient towards the centerline of the injection nozzle, generated by the curved streamlines, becomes too large, cavitation occurs at the inlet corner. The cavitation region grows in length and boundary surface with increasing Reynolds number. The instability of the reentry flow causes unsteady fluctuations of the cavitation which influences the breakup of the liquid jet, whereby liquid films are generated which take off from the jet. Cavitation amplifies the mechanism of the atomization, based on the interaction between the jet and surrounding gas. The influence of the cavitation on the atomization is restricted to the region directly behind the nozzle exit. The injection pressure and the temperature of the gas hardly affect the atomization. The jet angle depends mainly on the density of the surrounding gas. ESA

N92-17387# Applied Research Lab., State College, PA.
BASIC HYDRODYNAMICS Final Report
G. C. Lauchle 4 Dec. 1991 10 p
(Contracts N00014-87-K-0196; N00014-91-J-1646)
(AD-A243513; PSU/ARL-TM-91-299) Avail: NTIS HC/MF A02 CSCL 20/4

Basic hydrodynamic studies in turbomachinery and hydrodynamic drag reduction have been conducted. In the turbomachinery thrust area, the overall objective is to develop an improved understanding of the complex three-dimensional flows typical of incompressible rotor and stator flows; this effort has been primarily computational in nature. The second thrust area is axisymmetric turbulent flow drag reduction through microbubble injections. The third thrust area objective is to assess experimentally the effects of wall suction of turbulent boundary layer skin friction with possible applications to drag reduction. A fourth thrust area was a combined analytical and experimental study on laminar boundary layer/particle interaction physics. GRA

N92-17398# Department of the Navy, Washington, DC.
METHOD AND APPARATUS FOR REDUCING DRAG AND NOISE ASSOCIATED WITH FLUID FLOW IN A CONDUIT Patent Application
Kam W. Ng, inventor (to Navy) 12 Jul. 1991 14 p
(AD-D015067; US-Patent-Appl-SN-729743; Navy-Case-73405)
Avail: NTIS HC/MF A03 CSCL 20/4

A method and apparatus for reducing drag and noise associated with fluid flow within a conduit is provided. The conduit has flexible walls that are shaped to form stationary waves having peaks and troughs and are repeated in the axial direction of the conduit. The stationary waves are moved along the axial direction of the conduit whereby a vortex is trapped in the fluid flow at each of the troughs. Each of the vortices forms part of an isolating layer between the conduit wall and the main stream of the fluid flow thereby reducing drag. Furthermore, the vortices push the dominant noise producing region toward the center of the fluid flow where sound coupling efficiency is lower. GRA

N92-17447# Colorado Univ., Boulder. Dept. of Mathematics
PATTERN SELECTION, WAVE FORMATION, TURBULENCE, AND VORTEX BREAKDOWN IN SPIRAL FLOWS Final Technical Report, 1 Jan. 1990 - 30 Sep. 1991
Duane P. Sather 10 Sep. 1991 4 p
(Contract N00014-90-J-1336)
(AD-A242351) Avail: NTIS HC/MF A01 CSCL 20/4

Landau type amplitude equations for the small-gap Taylor problem were derived and analyzed; the equations obtained are global and are more complete than those determined by a formal two-timing analysis. Transition solutions (i.e., heteroclinic orbits) connecting the trivial Couette flow with bifurcating steady flows were obtained by solving singular evolution equations in infinite-dimensional spaces. The existence of a continuum of periodic waves for a class of spiral flow problems was established; the general method was applied to rotating plane Couette flow to obtain an analytic description of turbulent-like flows. The usual Hopf bifurcation theory does not apply to such problems and new methods using singular evolution equations were developed. It was shown that such methods apply also to Langmuir circulations in upper-ocean mixing problems and that the use of such methods leads to a number of new results for Langmuir circulations including mixing problems where the Stokes drift has a cross-wind component. GRA

N92-17522# Technische Univ., Eindhoven (Netherlands).
MASS TRANSFER IN GAS FLUIDIZED BEDS: SCALING, MODELING, AND PARTICLE SIZE INFLUENCE Ph.D. Thesis
Cornelis Elisabeth J vanLare 1991 182 p
(ETN-92-90581) Avail: NTIS HC/MF A09

Experimental and theoretical work on the mass transfer from the bubble phase to the dense phase in a freely bubbling bed is discussed. A chemical reacting system for which the ozone decomposition was chosen as a model reaction is studied and residence time distribution measurements are performed. A numerical method for solving the equations describing the non-steady state is presented. The height of a mass transfer unit can be determined as a function of the average particle size and the superficial gas velocity, but these parameters cannot be varied completely independently of each other because larger particles require a larger flow rate. A lot of other parameters, such as maximum bubble diameter, bubbling point, and hydrodynamic behavior, are also dependent on these and other variables. Therefore, a parameter has to be found which is descriptive for all fluid bed systems with equal particle properties. This parameter can then also be used as a tool in scale up. ESA

N92-17588*# Wichita State Univ., KS. National Inst. for Aviation Research.
COMPUTATION OF THREE-DIMENSIONAL FLOWS USING TWO STREAM FUNCTIONS
Mahesh S. Greywall Oct. 1991 42 p Sponsored by NASA. Lewis Research Center
(NASA-CR-187802; NAS 1.26:187802; NIAR-91-27) Avail: NTIS HC/MF A03 CSCL 20D

An approach to compute 3-D flows using two stream functions is presented. The method generates a boundary fitted grid as part of its solution. Commonly used two steps for computing the flow fields are combined into a single step in the present approach: (1) boundary fitted grid generation; and (2) solution of Navier-Stokes equations on the generated grid. The presented method can be used to directly compute 3-D viscous flows, or the potential flow approximation of this method can be used to generate grids for other algorithms to compute 3-D viscous flows. The independent variables used are chi, a spatial coordinate, and xi and eta, values of stream functions along two sets of suitably chosen intersecting stream surfaces. The dependent variables used are the streamwise velocity, and two functions that describe the stream surfaces. Since for a 3-D flow there is no unique way to define two sets of intersecting stream surfaces to cover the given flow, different types of two sets of intersecting stream surfaces are considered. First, the metric of the (chi, xi, eta) curvilinear coordinate system associated with each type is presented. Next, equations for the steady state transport of mass, momentum, and energy are presented in terms of the metric of the (chi, xi, eta) coordinate system. Also included are the inviscid and the parabolized approximations to the general transport equations. Author

N92-17625# Lawrence Livermore National Lab., CA.
THE EFFECT OF DETONATION CURVATURE ON CYLINDRICAL WALL MOTION
D. F. Aldis, W. Quirk, and R. D. Breithaupt Jun. 1991 13 p
(Contract W-7405-eng-48)
(DE92-003110; UCRL-ID-107480) Avail: NTIS HC/MF A03

In the large scale analysis of explosive response, discrepancies have been found between the results predicted by a computer model using various sets of equation of state parameters derived from different experiments. In this report, we will present recent progress toward determining possible reasons for the differences. The system that we have modeled is the cylinder test. Numerous researchers have used this test to study the work potential of detonating explosives for the transverse expansion of metals. One of the original purposes for the development of the test was for the determination of equations of state for detonation products of explosives. The method that is used to determine the parameters for these empirical equations of state, is to iteratively simulate the detonating explosive expansion using a two dimensional hydrodynamic code, adjust the parameters, and repeat until a 'best fit' to the experimental results is obtained. We will, in this present report, explore a small part of this problem. We will concentrate on the effect of the material that is used in the all of the cylinder, the effect of detonation front curvature, and how the curvature might influence the cylindrical wall expansion. DOE

N92-17626# Edgerton, Germeshausen and Grier, Inc., Idaho Falls, ID.
DOWNFLOW HEAT TRANSFER IN A HEATED RIBBED VERTICAL ANNULUS WITH A COSINE POWER PROFILE (RESULTS FROM TEST SERIES ECS-2c)
J. L. Anderson, K. G. Condie, and T. K. Larson Oct. 1991 145 p Prepared for Westinghouse Savannah River Co., Aiken, SC
(Contracts DE-AC07-76ID-01570; DE-AC09-89SR-18035)
(DE92-003259; EGG-EAST-9348) Avail: NTIS HC/MF A07

Experiments designed to investigate downflow heat transfer in a heated, ribbed annulus test section simulating one of the annular coolant channels of a Savannah River Plant production reactor Mark 22 fuel assembly have been conducted at the Idaho National Engineering Laboratory. The inner surface of the annulus was constructed of aluminum and was electrically heated to provide an axial cosine power profile and a flat azimuthal power shape. Data presented in this report are from the ECS-2c series, which was a follow on series to the ECS-2b series, conducted specifically to provide additional data on the effect of different powers at the same test conditions, for use in evaluation of possible power effects on the aluminum temperature measurements. Electrical powers at 90, 100, and 110 percent of the power required to result in the maximum aluminum temperature at fluid saturation temperature were used at each set of test conditions previously used in the ECS-2b series. The ECS-2b series was conducted in the same test rig as the previous ECS-2b series. DOE

N92-17688# Pittsburgh Univ., PA. Dept. of Physics and Astronomy.
STUDY OF TURBULENCE BY PHOTON CORRELATION SPECTROSCOPY Final Report, 15 Jun. 1989 - 15 Dec. 1991
W. I. Goldburg 23 Oct. 1991 37 p
(Grant AF-AFOSR-0415-89; AF Proj. 2307)
(AD-A243726; AFOSR-91-0996TR) Avail: NTIS HC/MF A03 CSCL 20/4

We have studied grid-generated turbulence in a water tunnel at moderate Reynolds numbers. The method used was the standard one of Laser Doppler Velocimetry (LDV) and novel scheme, which we call photon homodyne correlation spectroscopy (HCS). With LDV, we measured the probability density function of velocity differences P(delta v(l)) on varying spatial scales l, by invoking the frozen turbulence hypothesis. The HCS technique permits measuring P without using this hypothesis. Of special interest to us was the behavior of the system at and above a Reynolds number (Re sub c) where the turbulence becomes self-similar, in that less than or = delta v(l exp 2) greater than or approx. = l to the zeta power. Above Re sub c the exponent zeta increases from 0 to 2/3 with increasing Re. GRA

N92-17699 Academy of Sciences of the Ukrainian SSR, Kiev. Inst. of Power Modelling.
CONSISTENCY AND INTEGRABILITY OF NAVIER-STOKES AND SYSTEMS OF EQUATIONS FOR INCOMPRESSIBLE FLOW MAGNETOHYDRODYNAMICS [SOVMESTNOST I INTEGRIRUEMOST URAVNENII NAVE—STOKSA I SISTEMY YRAVNENII MAGNITNOI GIDRODINAMIKI NESZHIMAEMOGO POTOKA]
A. G. Iliukhin and E. A. Bogomazova 1990 37 p In RUSSIAN
Copyright Avail: Issuing Activity

A summary is given of a number of results of geometric theory on systems of differential equations in partial derivatives which meet the criteria for compatibility and formal integration (involutiveness) of a wide class of such systems. The properties of involutiveness play a significant role in the establishment of numeric and analytic methods for solving various problems for systems of differential equations in partial derivatives. The

involutiveness criteria cited is further applied to the study of systems of differential Navier-Stokes equations for two- and three-dimensional incompressible flow, as well as the more complicated systems of magnetohydrodynamic incompressible flow. This work is recommended for specialists in the fields of mathematical physics and differential equations in partial derivatives. Transl. by L.K.H.

N92-17704# Cornell Univ., Ithaca, NY.
DEVELOPMENT AND UTILIZATION OF NEW DIAGNOSTICS FOR DENSE-PHASE PNEUMATIC TRANSPORT
1991 5 p
(Contract DE-AC22-88PC-88947)
(DE92-000337; DOE/PC-88947/T11) Avail: NTIS HC/MF A01

Dense-phase pneumatic transport is an attractive means of conveying solids. Unfortunately, because of the high solid concentrations, this transport method is a difficult regime in which to carry out detailed measurements. Hence, most details of the flow are unknown. In this context, the main objective of this work is to develop probes for local measurements of solid velocity and holdup in dense gas-solid flows. Because we anticipate the recent theories of rapid granular flows will bring insight to the dense pneumatic transport of particles, we have sought to substantiate these theories through computer simulations. There we have verified the theory of Hanes, Jenkins & Richman (1988) for the rapid, steady shear flow of identical, smooth, nearly elastic disks driven by identical, parallel, bumpy boundaries. Because granular flows depend strongly on the nature of their interaction with a boundary, we have verified the boundary conditions calculated by Jenkins (1991) for spheres interacting with a flat, frictional surface. During the previous reporting period, we began a study of the time relaxation of the second moment of velocity fluctuations for a collection of disks undergoing simple shear. In the present reporting period, we have completed this study of relaxation by comparing results of simulations with the theoretical predictions of Jenkins and Richman (1988). In addition, we have concluded a series of experiments with flour plugs in the dense-phase pneumatic setup. Finally, we have established several industrial contacts to transfer the diagnostic techniques developed under this contract. DOE

N92-17709# Illinois Inst. of Tech., Chicago. Dept. of Chemical Engineering.
DETERMINATION OF COHESIVE AND NORMAL STRESSES AND SIMULATION OF FLUIDIZATION USING KINETIC THEORY Ph.D. Thesis
R. Bezbaruah Aug. 1991 101 p
(Contract DE-FG22-89PC-89769)
(DE92-002905; DOE/PC-89769/T6) Avail: NTIS HC/MF A06

The general objective of this study is focused on the solid stresses involved in gas-solid flow. These stresses are generally included in the momentum conservation equations, essentially for stability and to prevent particles from collapsing to unreasonably low values of gas volume fraction. The first half of this work undertakes the measurement of the stresses in various powders by direct means, while the second part uses a newly developed kinetic theory constitutive equation for stress to predict the flow and also the solid's viscosity in a CFB. The cohesive or tensile stress found to exist in some classes of powders is measured using a Cohetester, based on which a cohesive force model is derived, which is sensitive to the characteristic properties of the powder material. The normal stress is measured using a Consolidometer, and the powder solid's modulus is obtained as a function of the volume fraction. The solid's modulus is seen to vary with particle size and particle type, with the smaller size particles being more compressible. The simulation of flow in the CFB using Gidaspow's (1991) extension of Ding's (1990) kinetic theory model to dilute phase flow, predicts realistic values of solids' viscosity that are comparable to viscosities obtained experimentally by Miller (1991). However, to obtain a match between the two, the value of the restitution coefficient has to be close to unity. The flow behavior showed periodic oscillations of flow (turbulence) as seen in a real system. DOE

N92-17719# Tel-Aviv Univ. (Israel). Dept. of Fluid Mechanics and Heat Transfer.
ON THE ORIGIN AND CONTROL OF LARGE COHERENT STRUCTURES IN TURBULENT SHEAR FLOW Final Technical Report, 15 Feb. 1989 - 14 Aug. 1990
A. Seifert and I. Wygnanski 31 Oct. 1991 36 p
(Grant AF-AFOSR-0307-89; AF Proj. 2307)
(AD-A243727; AFOSR-91-0995TR) Avail: NTIS HC/MF A03
CSCL 20/4

Inhibition of two-dimensional Tollmien-Schlichting waves by active mean is well known. Surface deformation, heat input, and mechanical means were used to impose disturbances on the boundary layer which have an opposite phase to the waves existing in the flow. Thus, transition might be delayed by suppressing the amplitude of these waves. Natural disturbances in boundary layers start as three-dimensional wave packets, because they originate at surface imperfections or are precipitated by temporal disturbances in the incoming stream. The possibilities of controlling such disturbances are currently being investigated. In this context, the spatial interaction among three-dimensional wave trains emanating from discrete point-sources in a Blasius boundary layer are discussed. Only a local wave attenuation is feasible by activating two harmonic, point-source disturbances anywhere in the boundary layer. This was shown theoretically for a variety of locations, separation distances, and phase delays between the two sources and proven experimentally when the disturbance sources were displaced along the span. The spanwise phase gradients of the disturbances, linked to the streamwise distance from their point-source, present a major obstacle to such a simple attenuation scheme. These difficulties cannot be foreseen by considering 3-D perturbations. Spatially distributed control mechanisms are therefore required for the purpose of delaying the amplification of concentrated three-dimensional disturbances. GRA

N92-17747# Arnold Engineering Development Center, Arnold Air Force Station, TN.
ENGINEERING MODEL OF UNSTEADY FLOW IN A CAVITY Final Report, Oct. 1989 - Sep. 1991
R. C. Bauer and R. E. Dix Dec. 1991 91 p Prepared in cooperation with Calspan Corp., Arnold AFB, TN
(AD-A243636; AEDC-TR-91-17) Avail: NTIS HC/MF A05
CSCL 20/4

A mathematical model was assembled from fundamental fluid dynamic relations and turbulent single-stream mixing zone relations to predict spectra, i.e., the frequency and amplitude, of unsteady pressures acting in a rectangular cavity exposed to an external flow parallel to the cavity opening. Characteristics of the approaching boundary layer are expected as inputs, thereby allowing computation of spectra for cases of mass-injection upstream of the cavity. The equations were compiled as a code (CAP) that can be run in less that 15 sec on a personal computer. Maximum dynamic loads acting on the contents of the cavity can be estimated, in addition to the primary frequencies of oscillation. GRA

N92-17810# Gosudarstvennyi Komitet po Ispolzovaniyu Atomnoi Energii, Obninsk (USSR). Fiziko-Ehnergeticheskij Inst.
EXPERIMENTAL STUDY OF AMPLITUDE-PHASE-FREQUENCY CHARACTERISTICS OF FLOW WHEN FOLLOWING OVER A VIBRATING PLATE
V. S. Fedotovskij, L. V. Terenik, and V. S. Spirov 1990 14 p
In RUSSIAN; ENGLISH summary
(DE92-610935; FEI-2131) Avail: NTIS HC/MF A03

Consideration is given to the technique and results of preliminary experimental study on nonstationary hydrodynamics of flow when flowing over a vibrating plate located along a rectangular channel axis. In the experiment the use was made of plate with artificial roughness in the form of ribs formed by spiral wire windings. The amplitude of flow velocity oscillation was found to grow as the plate vibration frequency increased. An occurrence of diverse phase displacements between plate displacement and flow velocity oscillations is demonstrated. DOE

N92-17850# Manchester Univ. (England). Aeronautical Engineering Group.
THE EFFECT OF ISOLATED ROUGHNESS ELEMENTS ON TRANSITION IN ATTACHMENT-LINE FLOWS
D. I. A. Poll 1989 13 p Presented at 3d IUTAM Symposium on Laminar-Turbulent Transition, Toulouse, France, Sep. 1989 Previously announced in IAA as A91-39959
(Aero-Rept-8905; ETN-92-90914) Avail: NTIS HC/MF A03

Current knowledge concerning the tripping to turbulence of an attachment line boundary layer flow under low speed conditions is summarized and compared with criteria for tripping in the incompressible, zero pressure gradient, flat plate flow. Important similarities and significant differences are illustrated and discussed. ESA

N92-17851# Manchester Univ. (England). Aeronautical Engineering Group.
FLOW BETWEEN TWO STATIONARY DISKS AND A ROTATING SHROUD
P. G. Bellamy-Knights and R. Saci 1990 28 p Previously announced in IAA as A91-50203
(Aero-Rept-9001; ETN-92-90918) Avail: NTIS HC/MF A03

The flow generated within a cylindrical container by the impulsively started constant rotation of the cylindrical part of the boundary is obtained by computationally solving the Navier-Stokes equations for Reynolds numbers up to 4000. Algorithms for both steady and unsteady flow and for three different grid sizes are appraised. Solutions for particular values of Reynolds number and aspect ratio are described. Unlike previously studied flows within cylindrical containers, the timescale for the establishment of steady flow is diffusion dominated. ESA

N92-17887*# National Aeronautics and Space Administration. Goddard Space Flight Center, Greenbelt, MD.
NUMERICAL SIMULATION OF FLUID FLOW AND HEAT TRANSFER IN A THIN LIQUID FILM OVER A STATIONARY AND ROTATING DISK AND COMPARISON WITH EXPERIMENTAL DATA
Amir Faghri (Wright State Univ., Dayton, OH.) and Theodore D. Swanson [1990] 83 p
(Grant NAG5-956)
(NASA-CR-189253; NAS 1.26:189253) Avail: NTIS HC/MF A05 CSCL 20D

In the first section, improvements in the theoretical model and computational procedure for the prediction of film height and heat-transfer coefficient of the free surface flow of a radially-spreading thin liquid film adjacent to a flat horizontal surface of finite extent are presented. Flows in the presence and absence of gravity are considered. Theoretical results are compared to available experimental data with good agreement. In the presence of gravity, a hydraulic jump is present, isolating the flow into two regimes: supercritical upstream from the jump and subcritical downstream of it. In this situation, the effects of surface tension are important near the outer edge of the disk where the fluid experiences a free fall. A region of flow separation is present just downstream of the jump. In the absence of gravity, no hydraulic jump or separated flow region is present. The variation of the heat-transfer coefficient for flows in the presence and absence of gravity are also presented. In the second section, the results of a numerical simulation of the flow field and associated heat transfer coefficients are presented for the free surface flow of a thin liquid film adjacent to a horizontal rotating disk. The computation was performed for different flow rates and rotational velocities using a 3-D boundary-fitted coordinate system. Since the geometry of the free surface is unknown and dependent on flow rate, rate of rotation, and other parameters, an iterative procedure had to be used to ascertain its location. The computed film height agreed well with existing experimental measurements. The flow is found to be dominated by inertia near the entrance and close to the free surface and dominated by centrifugal force at larger radii and adjacent to the disk. The rotation enhances the heat transfer coefficient by a significant amount. Author

N92-17888*# National Aeronautics and Space Administration. Langley Research Center, Hampton, VA.
ACTIVE CONTROL OF PRESSURE LOADS USING PASSIVE POROSITY Patent Application
Richard M. Wood, inventor (to NASA) and Steven X. S. Bauer, inventor (to NASA) 13 Aug. 1991 12 p
(NASA-Case-LAR-14594-1; NAS 1.71:LAR-14594-1; US-Patent-Appl-SN-748225) Avail: NTIS HC/MF A03 CSCL 20D

A device is provided for controlling pressure loading of a member caused by a fluid moving past the member or the member moving through a fluid. The device consists of two porous skins mounted over the solid surface of the member and separated from the solid surface by a plenum. Fluid from an area exerting high pressure on the member may enter the plenum through the pressure skins and exit into an area exerting a lower pressure on the member, thus controlling pressure loading of the member. The porous inner skin may be translated relative to the porous skin in order to achieve a porosity ranging from zero to the porosity of the porous skins. NASA

N92-17909*# National Aeronautics and Space Administration. Langley Research Center, Hampton, VA.
PASSIVE CONTROL OF PRESSURE LOADS USING POROSITY Patent Application
Richard M. Wood, inventor (to NASA) and Steven X. S. Bauer, inventor (to NASA) 13 Aug. 1991 12 p
(NASA-Case-LAR-14547-1; NAS 1.71:LAR-14547-1; US-Patent-Appl-SN-748224) Avail: NTIS HC/MF A03 CSCL 20D

A device is provided for controlling pressure loading of a member caused by a fluid moving past the member or the member moving through a fluid. The device consists of a porous skin mounted over the solid surface of the member and separated from the solid surface by a plenum. Fluid from an area exerting high pressure on the member may enter the plenum through the porous surface and exit into an area exerting a lower pressure on the member, thus controlling pressure loading of the member. NASA

N92-17974# Manchester Univ. (England). Aeronautical Engineering Group.
PHYSICAL AND COMPUTATIONAL MODELLING OF STRATIFIED SHEAR FLOWS Final Report
T. N. Stevenson and L. Y. Pao Dec. 1989 53 p
(Contract ARE-2052/70)
(Aero-Rept-8909; ETN-92-90917) Avail: NTIS HC/MF A04

Numerical computations and correlation work in stratified research are summarized. Studies on the internal waves around bodies are presented. Computations with no free surface and with a free surface using a Marker And Cell (MAC) method are described. Solutions for the stratified flow around a horizontal cylinder of square cross section under different conditions are shown. ESA

35 INSTRUMENTATION AND PHOTOGRAPHY

Includes remote sensors; measuring instruments and gages; detectors; cameras and photographic supplies; and holography.

For aerial photography see *43 Earth Resources and Remote Sensing.* For related information see also *06 Aircraft Instrumentation,* and *19 Spacecraft Instrumentation.*

N92-16983# Louisiana State Univ., Baton Rouge. Dept. of Computer Science.
A GENERAL COMPUTATIONAL FRAMEWORK FOR DISTRIBUTED SENSING AND FAULT-TOLERANT SENSOR INTEGRATION
Lakshman Prasad and S. S. Iyengar 1991 20 p

(Contract N00014-91-J-1306)
(AD-A243256) Avail: NTIS HC/MF A03 CSCL 19/5

The design of Distributed Sensor Networks has to take into consideration sensor failures that occur while functioning in the real (physical) world. This demands a technique of integration of sensor information that is fault tolerant so that the network is reliable for target recognition and tracking problems. An earlier paper proposed a computational characterization of fault tolerant integration of abstract sensors that were 1-interval estimates. This paper proposes an abstract framework to address the general problem of fault tolerant integration of sensor information in a general distributed sensor network. The essential ideas of this abstract framework stem from certain rudimentary notions in the theory of differentiable manifolds. This framework addresses a very general distributed sensor network both at the local level of sensor data integration at distributed processors as well as global exchange and assimilation of information available at various processors in the network. GRA

N92-17006*# Lockheed Aeronautical Systems Co., Burbank, CA.
HEAT FLUX SENSOR RESEARCH AND DEVELOPMENT: THE COOL FILM CALORIMETER Final Report, 25 Jan. 1990
A. Abtahi and P. Dean 30 Jun. 1990 72 p
(Contract NAS1-18570)
(NASA-CR-189789; NAS 1.26:189789; LR-31824) Avail: NTIS HC/MF A04 CSCL 14B

The goal was to meet the measurement requirement of the NASP program for a gauge capable of measuring heat flux into a 'typical' structure in a 'typical' hypersonic flight environment. A device is conceptually described that has fast response times and is small enough to fit in leading edge or cowl lip structures. The device relies heavily on thin film technology. The main conclusion is the description of the limitations of thin film technology both in the art of fabrication and in the assumption that thin films have the same material properties as the original bulk material. Three gauges were designed and fabricated. Thin film deposition processes were evaluated. The effect of different thin film materials on the performance and fabrication of the gauge was studied. The gauges were tested in an arcjet facility. Survivability and accuracy were determined under various hostile environment conditions. Author

N92-17140# David Sarnoff Research Center, Princeton, NJ.
IMPROVED 320X244-ELEMENT PtSi SCHOTTKY-BARRIER IR-CCD IMAGE SENSOR Final Report, May 1988 - Aug. 1989
F. V. Shallcross, W. F. Kosonocky, T. S. Villani, G. M. Meray, and J. M. ONeill, III Sep. 1991 41 p
(Contract F19628-88-C-0088)
(AD-A242026; RL-TR-91-199) Avail: NTIS HC/MF A03 CSCL 09/1

This report describes the design, fabrication, and performance of an improved 320 x 244-element IR-CCD imager with PtSi Schottky barrier detectors. The imager has 40 mm x 40 mm pixels, and a 44 percent fill factor. Metal silicide photodiode array technology was invented at Rome Air Development Center (RADC) Hanscom AFB, MA, and has been under development there since the early 1970's. In 1973, Shepherd and Yang proposed silicide Schottky barrier detector (SBD) arrays for infrared thermal imaging. The objectives of the work described in the present report were to design and fabricate an improved version of the 320 x 244-element PtSi array using beneficial design and process changes inferred from test results on the TA13401B device. This report describes the design, fabrication, and performance of this array (TA14804A). GRA

N92-17273# Rome Lab., Griffiss AFB, NY.
A PERFORMANCE MODEL OF THERMAL IMAGING SYSTEM (TISs) WHICH INCLUDES THE HUMAN OBSERVER'S RESPONSE TO STATE OF THE ART DISPLAYS Report, Jan. - Jun. 1991
Denise M. Blanchard Sep. 1991 32 p
(AF Proj. 4600)
(AD-A242838; RL-TR-91-307) Avail: NTIS HC/MF A03 CSCL 17/5

This paper presents a model for predicting the performance of thermal imaging systems (TISs). This model combines conventional modeling relationships and recently reported characteristics of display monitors to determine the signal-to-noise ratio (SNR) out of the TIS. Also included are the results of psychophysical experiments which evaluated the capability of a human observer to detect the presence of an object displayed on the same monitor. The model is then used to determine the noise equivalent temperature difference (NEdeltaT) based on background photon noise limited (BLIP) operating conditions of the TIS. Finally, the minimum detectable temperature difference (MDT) in the scene is determined from the maximum signal-to-noise ratio of the monitor. GRA

N92-17344# Max-Planck-Inst. fuer Stroemungsforschung, Goettingen (Germany, F.R.).
DEVELOPMENT OF AN ELECTRONIC HIGH SPEED CAMERA SYSTEM FOR THE QUANTITATIVE ANALYSIS OF UNSTEADY FLOWS
Bernward Bretthauer 1991 75 p In GERMAN; ENGLISH summary
(MPIS-100/1991; ISSN-0374-1257; ETN-92-90624) Avail: NTIS HC/MF A04

A high speed camera system, based on eight CCD cameras and the Cranz-Scharolin priciple, was developed for the quantitative analysis of unsteady flows. Light emitting diodes were used for illumination. Interferograms were taken from experiments concerned with vortex airfoil interaction, showing the generation of local stagnation points by this interaction. The camera generates high quality pictures suitable for quantitative analysis using an image processing system which was improved for this purpose. The system allows the recognition of weak compression waves. ESA

N92-17345# Max-Planck-Inst. fuer Stroemungsforschung, Goettingen (Germany, F.R.).
RECORDING OF THREE DIMENSIONAL TRAJECTORIES AND VELOCITY FIELDS BY AUTOMATIC IMAGE PROCESSING
Hans-Hermann Bartels-Lehnhoff 1991 81 p In GERMAN; ENGLISH summary
(MPIS-101/1991; ISSN-0374-1257; ETN-92-90625) Avail: NTIS HC/MF A05

An automatic system was developed to record long, (compared to geometrical lengths), three dimensional trajectories and velocity fields in a flow. With the help of video cameras two orthogonal views of a measurement volume are observed using a shadow method. The video images are digitized during the experiment and processed in a computer. The particles are recognized by the subtraction of zero images, taken prior to each experiment. Their positions in the image are calculated by computing their center of gravity. In a first step, two partial views of the particle trajectories are determined, which are then matched to three dimensional trajectories. Recording and evaluation of the images are fully automatic. The system was used to record three dimensional trajectories in a convection flow. The measured trajectories agree well with calculated trajectories. ESA

N92-17437# Technische Univ., Delft (Netherlands). Werkeenheid Fotogrammetrie en Remote Sensing.
THE CALIBRATION PROCESS OF DIGITAL CAMERAS Thesis
R. deRonde May 1991 114 p
(ETN-92-90583) Avail: NTIS HC/MF A06

The calibration process done with a CCD (Charge Coupled Device) camera, including the image acquisition, the gathering of data, and the calibration calculations, is addressed. For the image acquisition, a CCD camera and the necessary hardware is needed. A calibration method based on the self calibration is used. As ground control points, a three dimensional test field consisting of a metal frame with circular retroreflective targets is used. The coordinates of these targets are obtained with a metric camera.

In order to calibrate the camera image coordinates of the object, points are gathered. Different methods are described but special attention is paid to a method based on detection of elliptical features. The circular targets seen from under an angle are elliptical. The basic idea is to find twelve edge points and from these to extract the elliptical features. These elliptical features are the rotation, both axes, and the coordinates of the center. This method is developed and programmed. Besides the theoretical background some practical experiences are described. A calibration with a bundle adjustment program STRAAL, showing that the image coordinates can be measured with an overall precision of 0.2 pixel size, which corresponds to 2 micrometers for the camera, is given. The improvement of this result by using other targets is described. Retroreflective targets do not show a Gaussian point spread function. All routines for measuring are based on a Gaussian function. The resulting error can be up to 15 percent of the pixel size. Measurements prove the existence of this error. ESA

N92-17454# General Atomic Co., San Diego, CA.
ACTIVE HEATER CONTROL AND REGULATION FOR THE VARIAN VGT-8011 GYROTRON
T. E. Harris Oct. 1991 2 p Presented at the 14th IEEE Symposium on Fusion Engineering, San Diego, CA, 30 Sep. - 3 Oct. 1991
(Contract DE-AC03-89ER-51114)
(DE92-003638; GA-A-20645; CONF-910968-45) Avail: NTIS HC/MF A01

The Varian VGT-8011 gyrotron is currently being used in the new 110 GHz 2 MW ECH system installed on D3-D. This new ECH system augments the 60 GHz system which uses Varian VA-8060 gyrotrons. The new 110 GHz system will be used for ECH experiments on D3-D with a pulse width capability of 10 sec. In order to maintain a constant RF outpower level during long pulse operation, active filament-heater control and regulation is required to maintain a constant cathode current. On past D3-D experiments involving the use of Varian VA-8060 gyrotrons for ECH power, significant gyrotron heater-emission depletion was experienced for pulse widths greater than 300 msec. This decline in heater-emission directly results in gyrotron-cathode current droop. Since RF power from gyrotrons decreases as cathode current decreases, it is necessary to maintain a constant cathode current level during gyrotron pulses for efficient gyrotron operation. Therefore, it was determined that a filament heater control system should be developed for the Varian VGT-8011 gyrotron which will include cathode current feedback. This paper discusses the mechanisms used to regulate gyrotron filament heater voltage by using cathode current feedback. DOE

N92-17826 Department of the Navy, Washington, DC.
FIBER OPTIC ANGULAR ORIENTATION SENSOR DIGITAL SERIAL ENCODING Patent
Steven L. Garrett, inventor (to Navy), Michael R. Brininstool, inventor (to Navy), Jeffrey T. Newmaster, inventor (to Navy), and Thomas Hofler, inventor (to Navy) 27 Aug. 1991 9 p Filed 8 Aug. 1988
(AD-D015102; US-Patent-5,042,157; US-Patent-Appl-SN-230547; US-Patent-Class-33-363-K) Avail: US Patent and Trademark Office CSCL 20/6

A sensor provides remote angular orientation sensing. A rotational signal transmitted to a rotatable input shaft mounted in an encoder body causes the shaft to rotate. Light signals are transmitted through a digital code wheel mounted to the shaft. As the code wheel and shaft rotate, the light signals passing through the code wheel are superimposed with light pulses corresponding to incremental and directional changes of angular position of the code wheel with respect to the encoder body. The light signals are propagated through an optical fiber to a remote combination digital and analog circuit which converts them into a digital representation of the angular position of the code wheel. GRA

N92-17835 Department of the Navy, Washington, DC.
HIGH CONTACT BLIND HOLE THERMOCOUPLE PLUG Patent
Donald R. Burnett, inventor (to Navy) 4 Jun. 1991 4 p Filed 28 Mar. 1990
(AD-D015105; US-Patent-5,021,098; US-Patent-Appl-SN-501068; US-Patent-Class-136-201) Avail: US Patent and Trademark Office CSCL 09/1

It is useful to be able to place a thermocouple in a plug in a spacecraft heat shield without disturbing the heat flow to the thermocouple. The thermocouple wire is ceramic coated before placement in the plug and a thin metal disc is placed in the bottom of the hole. The thermocouple wire is pressed into the disc to obtain good thermal contact. Blind hole thermocouple plugs in carbon phenolic heat shields have inaccurately measured temperature due to cutting of the heat conductive fibers in the phenolic by the blind hole resulting in decreased heat flow across the hole. It is therefore a primary objective of the present invention to provide a method of forming a blind hole for a thermocouple in a heat shield which does not reduce heat flow to the thermocouple. An important advantage of the present invention is that the thin metal disc provides rapid heat conduction across the hole bottom. GRA

N92-17918 Department of the Navy, Washington, DC.
DIFFERENTIAL PRESSURE SENSOR Patent
Charles A. Rowzee, inventor (to Navy) and John D. Sherman, inventor (to Navy) 10 Sep. 1991 8 p Filed 1 Nov. 1982
(AD-D015134; US-Patent-5,046,427; US-Patent-Appl-SN-445329; US-Patent-Class-102-418) Avail: US Patent and Trademark Office CSCL 19/8

A pressure sensor for use in sea mine applications is presented. The sensor detects the presence of a passing vessel by sensing a change in ambient water pressure caused by the hydrodynamic flow induced by the vessel's motion (Bernoulli effect). The sensor emits a responsive signal which can be used alone, or with signals from other influence sensors (acoustic and magnetic), to determine when the sea mine should be exploded. The sensor provides for equal sensitivity independent of the ambient pressure of the water at various depths at which sea mines may be planted, and employs electrical filters to eliminate noise. Author (GRA)

N92-17926# Oxford Univ. (England). Robotics Research Group.
A FULLY DECENTRALIZED MULTI-SENSOR SYSTEM FOR TRACKING AND SURVEILLANCE
B. S. Y. Rao, H. F. Durrant-Whyte, and J. A. Sheen (British Aerospace Public Ltd. Co., Bristol, England) 1991 47 p Sponsored in part by Commission of the European Communities
(OUEL-1886/91; ETN-92-90910) Avail: NTIS HC/MF A03

A multisensor surveillance system that achieves a high degree of survivability by employing dencentralized sensing architecture of Durrant-Whyte, Rao, and Hu is described. Using CCD (Charge Coupled Device) cameras and optical barriers the system is able to track (in real time) people and robots as they move around a factory room. The decentralized sensing architecture takes the form of a network of transputer based sensor nodes, each with its own processing facility, which together do not require any central processor, any central communication facility, or any common clock. In this architecture, computation is performed locally and communication occurs between any two nodes as and when required. The starting point for the surveillance system is an algorithm that allows complete decentralization of the multisensor Kalman filter equations amongst a number of sensing nodes. The algorithm is developed to ensure that internodal communication is minimized and can take place without any prior synchronization between nodes. By designing a suitable track management scheme, the system is extended to cope with multitarget tracking. The specific sensors used in the implementation are interfaced to the algorithm and results of the working system are given. ESA

36 LASERS AND MASERS

Includes parametric amplifiers.
For related information see also *76 Solid-State Physics*.

N92-17080# Carnegie-Mellon Univ., Pittsburgh, PA. Robotics Inst.
CYCLONE: A LASER SCANNER FOR MOBILE ROBOT NAVIGATION
Sanjiv Singh and Jay West Sep. 1991 25 p
(AD-A243517; CMU-RI-TR-91-18) Avail: NTIS HC/MF A03
CSCL 17/7

Researchers at Carnegie Mellon's Field Robotics Center have designed and implemented a scanning laser rangefinder. The device uses a commercially available time-of-flight ranging instrument that is capable of making up to 7200 measurements per second. The laser beam is reflected by a rotating mirror, producing up to a 360 degree view. Mounted on a robot vehicle, the scanner can be used to detect obstacles in the vehicle's path or to locate the robot on a map. This report discusses the motivation, design, and some applications of the scanner. GRA

N92-17127# Naval Research Lab., Washington, DC.
THE EFFECTS OF FIELD ERRORS ON LOW-GAIN FREE ELECTRON LASERS Memorandum Report
E. Esarey, C. M. Tang, and W. Marable 18 Dec. 1991 36 p
(Contract DE-AI05-83ER-40017)
(AD-A243710; NRL-MR-6911) Avail: NTIS HC/MF A03 CSCL 20/7

The effects of random wiggler magnetic field errors on low-gain free electron lasers are examined analytically and numerically through the use of ensemble averaging techniques. Wiggler field errors perturb the electron beam as it propagates and lead to a random walk of the beam centroid delta x, variations in the axial beam energy delta gamma(z) and deviations in the relative phase of the electrons in the ponderomotive wave delta psi. In principle, the random walk may be kept as small as desired through the use of transverse focusing and beam steering. Transverse focusing of the electron beam is shown to be ineffective in reducing the phase deviation. Furthermore, it is shown that beam steering at the wiggler entrance reduces the average phase deviation at the end of the wiggler by 1/3. The effect of the field errors (via the phase deviation) on the gain in the low-gain regime is calculated. To avoid significant reduction in gain it is necessary for the phase deviation to be small compared to 2 pi. The detrimental effects of wiggler errors on low-gain free electron lasers may be reduced by arranging the magnet poles in an optimal ordering such that the magnitude of the phase deviation is minimized. GRA

N92-17137# Ballistic Research Labs., Aberdeen Proving Ground, MD.
LASER-BASED IGNITION OF H2/O2 AND D2/O2 PREMIXED GASES NEAR 243 nm: THE FIRST REPORT OF A DEUTERIUM ISOTOPE WAVELENGTH EFFECT IN LASER IGNITION Final Report, Jan. - Dec. 1990
Brad E. Forch and Andrzej W. Miziolek Dec. 1991 33 p
(AD-A243180; BRL-TR-3295) Avail: NTIS HC/MF A03 CSCL 21/2

We investigated the use of a tunable laser system which operates in the ultraviolet (UV) to ignite premixed reactive gaseous flows of H2/O2 and D2/O2 at atmospheric pressure. The amount of incident laser energy (ILE) required to ignite the premixed flows as a function of laser excitation wavelength shows two distinct minima. The spectral position of these minima correspond exactly to the location of the resonance, two-photon excitation wavelengths of atomic hydrogen and deuterium at 243.07 and 243.00 nm respectively. The relative spacing between these minima at the energy level of the 1S-2S two-photon excited transition is 22/cm which is in excellent agreement with the known value for H-D deuterium isotope shift (22.4/cm). We believe that this is both the first report of a sensitive wavelength dependence on the laser energy required to ignite these mixtures through resonant multiphoton excitation of H and D atoms (produced from H2 and D2 photolysis) and the first report of a deuterium isotope-wavelenth-effect in laser ignition. Measurement of the ILE required for ignition vs. equivalence ratio (phi) shows that the most efficient ignition occurred with approx. 0.55 mJ ILE at phi = 0.7 in the fuel lean region. GRA

N92-17152*# Johns Hopkins Univ., Baltimore, MD. Dept. of Electrical and Computer Engineering.
RECEIVER PERFORMANCE OF LASER RANGING MEASUREMENTS BETWEEN THE LUNAR OBSERVER AND A SUBSATELLITE FOR LUNAR GRAVITY STUDIES Final Report, 15 Apr. 1991 - 14 Jan. 1992
Frederic M. Davidson and Xiaoli Sun Feb. 1992 18 p
(Grant NAG5-1521)
(NASA-CR-189860; NAS 1.26:189860) Avail: NTIS HC/MF A03
CSCL 20E

The optimal receiver for a direct detection laser ranging system for slow Doppler frequency shift measurement is shown to consist of a phase tracking loop which can be implemented approximately as a phase lock loop with a 2nd or 3rd order loop filter. The laser transmitter consists of an AlGaAs laser diode at a wavelength of about 800 nm and is intensity modulated by a sinewave. The receiver performance is shown to be limited mainly by the preamplifier thermal noise when a silicon avalanche photodiode is used. A high speed microchannel plate photomultiplier tube is shown to outperform a silicon APD despite its relatively low quantum efficiency at wavelengths near 800 nm. The maximum range between the Lunar Observer and the subsatellite for lunar gravity studies is shown to be about 620 km when using a state-of-the-art silicon APD and about 1000 km when using a microchannel plate photomultiplier tube in order to achieve a relative velocity measurement accuracy of 1 millimeter per second. Other parameters such as the receiver time base jitter and drift also limit performance and have to be considered in the design of an actual system. Author

N92-17175# Gumbs (R.) Associates, East Brunswick, NJ.
ULTRAFAST PASSIVE SHIELDS FOR LASER AND BALLISTIC PROTECTION Final Report, 16 Jan. - 15 Jul. 1991
15 Jul. 1991 45 p
(Contract DAAL04-91-C-0019)
(AD-A243206) Avail: NTIS HC/MF A03 CSCL 09/3

Addressing the need for laser eye protection in the visible spectral region, the present work sought to demonstrate the applicability of a novel technology for dynamic, broad-band, ultrafast (sub-ns), passive laser shields based on conducting polymers (CP's) and inorganic semiconductor (SC) materials in a matrix to a wider range of SC's and CP's. Effective laser shielding was clearly demonstrated to occur for a number of varied systems, including Bi2S3 with poly(N-phenyl-2-naphthyl amine), poly(2-vinyl naphthalene), poly(9-vinyl carbazole), CdS with poly(2-naphthyl amine), Te with poly(N-phenyl-2-naphthyl amine), and others. The laser shielding was shown to be a cumulative effect of three complementary phenomena: the intrinsic nonlinear optical (NLO) effect in the CP; the intrinsic NLO effect in the SC, when present; and SC to CP charge transfer. Independent transient absorption (TA) studies showed switching to be broad-band, with risetimes in the sub-ns region, limited by instrumental measurement, and falltimes in the tens of ns. Laser shielding efficiency, characterized by delta OD = OD(under laser) - OD(rest), of greater than 1.0 at 532 nm were achieved for a number of systems at incident energies of ca. 0.25 mJ/pulse. Matrices of SC's and CP's in PVA and PEMA, and coatings on polycarbonate sheets and lenses and diamond-like-coated polycarbonate showed good laser shielding efficiency. The prognosis is for incorporation of the SC's and CP's exclusively into polycarbonate matrices or substrates for ballistic protection combined with laser shielding. GRA

N92-17434# Technische Univ., Eindhoven (Netherlands).
A DIFFRACTION LIMITED NITROGEN LASER FOR DETECTOR CALIBRATION IN HIGH ENERGY PHYSICS Ph.D. Thesis
Frederik Gottlieb Hartjes 1990 136 p Sponsored by Stichting voor Fundamenteel Onderzoek der Materie
(ETN-92-90567) Avail: NTIS HC/MF A07

The basic physical properties of the nitrogen laser, the design and performance characteristics, and a few examples of its application in high energy physics, are described. The theory of light emission and amplification as relevant for the nitrogren laser is given and illustrated by the properties of the type 1A laser. A more detailed description of the electrical characteristics of the nitrogen laser, and the implications of the laser design, are given. The development of the discharge is discussed. The mechanical construction and the beam optics are described. The physics process relevant for the application of the nitrogen laser for the calibration and test of drift chambers is discussed. ESA

N92-17475# Tennessee Univ. Space Inst., Tullahoma. Center for Laser Applications.
PICOSECOND LASER BREAKDOWN THRESHOLDS IN GASES Final Scientific Report, 28 Feb. 1990 - 30 Sep. 1991
Dennis Keefer 30 Sep. 1991 65 p
(Grant AF-AFOSR-0317-86; AF Proj. 2308)
(AD-A242941) Avail: NTIS HC/MF A04 CSCL 20/6

An experimental investigation of laser sustained plasmas (LSP) was begun in 1984 at the University of Tennessee Space Institute (UTSI). The objective of this research was to understand the basic physical mechanisms of the LSP and determine their influence on stability, laser power absorption, thermal radiation loss and thermal conversion efficiency. The approach used was to create the LSP in argon using a continuous wave (CW) carbon dioxide laser at moderate powers (1.5 kW) and to obtain detailed measurements of the plasma temperature field by using a modern digital image processing computer to acquire spectral images of the plasma emission. Using the measured temperature field, the laser power absorption and thermal plasma emission could be calculated at any point within the LSP to provide a detailed understanding of the energy conversion processes. These results indicate that there are no fatal flaws in the concept utilizing the LSP for laser thermal propulsion, and suggest that the internal energy conversion processes can be sufficiently well controlled through the optical and flow configurations to provide an efficient, high specific impulse propulsion system. GRA

N92-17526# Messerschmitt-Boelkow-Blohm G.m.b.H., Munich (Germany, F.R.). Zentralbereich Technik.
LDA AND PDA SYSTEMS BASED ON DIODE-PUMPED NEODYM:YAG LASERS
A. Naqwi, F. Durst, R. Mueller (Erlangen-Nuremberg Univ., Germany, F.R.), and P. Zeller 1991 16 p Presented at the SENSOR 1991, Nuernberg, Fed. Republic of Germany, 13-16 May 1991
(MBB-Z-0361-91-PUB; ETN-92-90598) Avail: NTIS HC/MF A03

Applications of diode pumped monomode neodym:YAG lasers with continuous outputs of 0.3 to 1 W are discussed. The lasers provide new opportunities for miniaturizing Laser Doppler and Phase Doppler Anemometers (LDA/PDA). Possible uses of Nd:YAG lasers for similar applications are discussed. Instruments based on either of these lasers are expected to be useful for measurements of velocity and particle size distributions in industrial environments. Peculiar aspects of Nd:YAG lasers such as large wavelength, higher absorption coefficients etc. are discussed. It is shown that these features do not impose any serious limitation in the applications of these lasers in flow measuring devices. ESA

N92-17582# Massachusetts Inst. of Tech., Cambridge. Research Lab. of Electronics.
COMPACT FREE ELECTRON LASERS FOR MEDICAL APPLICATIONS Annual Technical Report, 30 Sep. 1990 - 29 Sep. 1991
George Bekefi 12 Dec. 1991 8 p
(Contract N00014-90-J-4130)
(AD-A243497) Avail: NTIS HC/MF A02 CSCL 09/3

The MIT Microwiggler Project moved this year from the prototype and design phase through complete fabrication of all major hardware. The microwiggler system and the status of its currently ongoing integration and testing, as well as modeling efforts relating to free electron laser (FEL) research to be carried out using the MIT Microwiggler in the comming year are described. Author

N92-17627# Department of the Navy, Washington, DC.
A TUNABLE SOLID STATE LASER WITH HIGH WAVELENGTH SELECTIVITY OVER A PRESELECTED WAVELENGTH RANGE Patent Application
Leon Esterowitz, inventor (to Navy), Joseph F. Pinto, inventor (to Navy), and Gregory J. Quarles, inventor (to Navy) 12 Apr. 1991 37 p
(AD-D015055; US-Patent-Appl-SN-684091; Navy-Case-73376)
Avail: NTIS HC/MF A03 CSCL 09/3

A tunable solid state laser for producing a laser emission at any desired low or high laser gain transition in a predetermined range of wavelengths is disclosed. The tunable solid state laser comprises: a laser cavity defined by a first reflective element and an output coupler reflective element to form a reflective path therebetween; a laser crystal disposed in the laser cavity; means for optically exciting the laser crystal to produce a laser emission in the predetermined range of wavelengths; a tunable element disposed in the laser cavity between the laser crystal and one of the reflective elements for tuning the laser emission to any desired laser transition in the predetermined range of wavelengths; and a plurality of optical plates oriented at Brewster's angle in the reflective path in the laser cavity for suppressing oscillation of undesired wavelengths within the laser cavity, the optical plates being transparent to the laser emission over the predetermined range of wavelengths. GRA

N92-17649# Lawrence Livermore National Lab., CA.
X RAY LASER Patent Application
J. Nilsen, inventor (to DOE) 12 Oct. 1991 17 p
(Contract W-7405-eng-48)
(DE91-011705; US-Patent-Appl-SN-420433;
Patents-US-A7420433) Avail: NTIS HC/MF A03

An X-ray laser that lases between the K edges of carbon and oxygen, i.e., between 44 and 23 Angstroms, is provided. The laser comprises a silicon and dysprosium foil combustion that is driven by two beams of intense line focused optical laser radiation. Ground state nickel-like dysprosium ions are resonantly photo-pumped to their upper X-ray laser state by line emission from hydrogen-like silicon ions. The novel X-ray laser should prove especially useful for the microscopy of biological specimens. DOE

N92-17726# Los Alamos National Lab., NM.
DEVELOPMENT OF AN XUV-IR FREE-ELECTRON LASER USER FACILITY FOR SCIENTIFIC RESEARCH AND INDUSTRIAL APPLICATIONS
B. E. Newnam, R. W. Warren, S. D. Conradson, J. C. Goldstein, B. D. McVey, M. J. Schmitt, C. J. Elliott, M. J. Burns, B. E. Carlsten, and K. C. Chan et al 1991 21 p Presented at the Society of Photo-Optical Instrumentation Engineers (SPIE) Meeting, San Diego, CA, 21-26 Jul. 1991
(Contract W-7405-eng-36)
(DE92-003862; LA-UR-91-3532; CONF-9107115-59) Avail: NTIS HC/MF A03

Los Alamos has designed and proposes to establish an XUV-IR free electron laser (FEL) user facility for scientific research and industrial applications based on coherent radiation ranging from soft x-rays as short as 1 nm to far-infrared wavelengths as long as 100 microns. As the next-generation light source beyond low-emittance storage rings with undulator insertion devices, this proposed national FEL user facility should make available to researchers broadly tunable, picosecond-pulse, coherent radiation with 10(exp 4) to 10(exp 7) greater spectral flux and brightness. The facility design is based on two series of FEL oscillators including one regenerative amplifier. The primary series of seven FEL oscillators, driven by a single, 1-GeV RF linac, spans the short-wavelength range from 1 to 600 nm. A second 60-MeV RF linac, synchronized with the first, drives a series of three Vis/IR FEL oscillators to cover the 0.5 to 100-micron range. The motivation for such a facility arising from its inherently high power per unit

bandwidth and its potential use for an array of scientific and industrial applications is presented. The facility design, output parameters, and user laboratories are described. Comparisons with synchrotron radiation sources are made, and recent technical progress that supports the technical feasibility is summarized. DOE

N92-17795# Los Alamos National Lab., NM.
THE LOS ALAMOS FEL PHOTOINJECTOR DRIVE LASER
J. Early, J. Barton, G. Busch, R. Wenzel, and D. Remelius 1991 26 p Presented at the 13th International Free-Electron Laser (FEL) Conference, Santa Fe, NM, 25-30 Aug. 1991
(Contract W-7405-eng-36)
(DE92-003791; LA-UR-91-3825; CONF-9108118-32) Avail: NTIS HC/MF A03

The drive laser system of the photoelectric injector for the Los Alamos free electron laser (FEL) is described. The bright electron beams required for high performance FELs demand stringent specifications on drive laser output levels, beam quality, and stability. The laser system generates 7 to 15 ps (FWHM) Gaussian pulses of 527 nm light at a repetition rate of 21.67 MHz. These 'micropulses' are contained within a less than 200 microsec long 'macropulse' envelope which is emitted from the drive laser at a 1 Hz rate. Micropulse energies as large as 12 microjoules are obtained. The design specifications, laser architecture, and operating performance following the most recent round of upgrades are presented. DOE

N92-17862*# National Aeronautics and Space Administration. Pasadena Office, CA.
MULTIPERIOD-GRATING SURFACE-EMITTING LASERS Patent Application
Robert J. Lang, inventor (to NASA) (Jet Propulsion Lab., California Inst. of Tech., Pasadena.) 21 Oct. 1991 28 p
(Contract NAS7-918)
(NASA-Case-NPO-17763-1-CU; NAS 1.71:NPO-17763-1-CU; US-Patent-Appl-SN-782009) Avail: NTIS HC/MF A03 CSCL 20E

Surface-emitting distributed feedback (DFB) lasers are disclosed with hybrid gratings. A first-order grating is provided at one or both ends of the active region of the laser for retroreflection of light back into the active region, and a second-order or nonresonant grating is provided at the opposite end for coupling light out perpendicular to the surfaces of the laser or in some other selected direction. The gratings may be curved to focus light retroreflected into the active region and to focus light coupled out to a point. When so focused to a point, the DFB laser may be part of a monolithic read head for a laser recorded disk, or an optical coupler into an optical fiber. NASA

N92-17868# California Univ., Berkeley. Lawrence Berkeley Lab.
ACHROMATIC AND ISOCHRONOUS ELECTRON BEAM TRANSPORT FOR TUNABLE FREE ELECTRON LASERS
J. Bengtsson and K. J. Kim Sep. 1991 11 p Presented at the 13th International Free-Electron Laser (FEL) Conference, Santa Fe, NM, 25-30 Aug. 1991
(Contract DE-AC03-76SF-00098)
(DE92-003908; LBL-30674; ESG-133; CONF-9108118-34) Avail: NTIS HC/MF A03

We have continued the study of a suitable electron beam transport line, which is both isochronous and achromatic, for the free electron laser being designed at Lawrence Berkeley Laboratory. A refined version of the beam transport optics is discussed that accommodates two different modes of FEL wavelength tuning. For the fine tuning involving a small change of the electron beam energy, sextupoles are added to cancel the leading nonlinear dispersion. For the main tuning involving the change of the undulator gap, a practical solution of maintaining the beam matching condition is presented. Calculation of the higher order aberrations is facilitated by a newly developed code. DOE

N92-17899*# National Aeronautics and Space Administration. Pasadena Office, CA.
SELF-COLLIMATED UNSTABLE RESONATOR SEMICONDUCTOR LASER Patent Application
Robert J. Lang, inventor (to NASA) (Jet Propulsion Lab., California Inst. of Tech., Pasadena.) 28 Aug. 1991 17 p
(Contract NAS7-918)
(NASA-Case-NPO-18386-1-CU; NAS 1.71:NPO-18386-1-CU; US-Patent-Appl-SN-751440) Avail: NTIS HC/MF A03 CSCL 20E

Self-collimation of the output is achieved in an unstable resonator semiconductor laser by providing a large concave mirror (M sub 1) and a small convex mirror (M sub 2) on opposite surfaces of a semiconductor body of a material having an effective index of refraction denoted by n, where the respective mirror radii (R sub 1, R sub 2) and beam radii (r sub 1, r sub 2) are chosen to satisfy a condition (R sub 2)/(1+r sub 1) = (n-1)/n, with a value of geometric magnification 1 less than or equal to M less than or equal to (n+1)/(n-1) where r (sub 1) and r (sub 2) are the radii of counterpropagating beams at respective mirrors of radii R (sub 1) and R (sub 2). NASA

N92-17923 Department of the Navy, Washington, DC.
METHOD AND APPARATUS FOR LASING Patent
Leon Esterowitz, inventor (to Navy), Roger E. Allen, inventor (to Navy), and Gregory J. Kintz, inventor (to Navy) 6 Aug. 1991 5 p Filed 21 Feb. 1990
(AD-D015154; US-Patent-5,038,353; US-Patent-Appl-SN-488411; US-Patent-Class-372-41) Avail: US Patent and Trademark Office CSCL 09/3

A laser system employing thulium and holmium in a trivalent state. The quantum levels of interest in the thulium and holmium are coupled so that one pumping photon absorbed by the thulium results in two photons emitted by the holmium, making for an unusually efficient laser system. The lower level is sufficiently depopulated at room temperature to allow laser operation without cryogenics. In its preferred embodiment, the laser pump can be a laser diode, itself especially efficient and whose output frequency is closely matched in photon energy to the thulium quantum state of interest, thus lending additional efficiency to the overall system. The thulium and the holmium exist in an yttrium-aluminum garnet crystal as lattice replacements for yttrium. Author (GRA)

N92-17936# California Univ., Berkeley. Lawrence Berkeley Lab.
PERFORMANCE OF HOLE COUPLING RESONATOR IN THE PRESENCE OF ASYMMETRIC MODES AND FEL GAIN
Ming Xie and Kwang-Je Kim Aug. 1991 25 p Presented at the 13th International Free-Electron Laser (FEL) Conference, Santa Fe, NM, 25-30 Aug. 1991
(Contract DE-AC03-76SF-00098)
(DE92-003907; LBL-30672; CONF-9108118-33) Avail: NTIS HC/MF A03

We continue the study of the hole coupling resonator for free electron laser (FEL) application. The previous resonator code is further developed to include the effects of the azimutally asymmetric modes and the FEL gain. The implication of the additional higher order modes is that there are more degeneracies to be avoided in tuning the FEL wavelengths. The FEL interaction is modeled by constructing a transfer map in the small signal regime and incorporating it into the resonator code. The FEL gain is found to be very effective in selecting a dominant mode from the azimuthally symmetric class of modes. Schemes for broad wavelength tuning based on passive mode control via adjustable apertures are discussed. DOE

N92-17962# Range Commanders Council, White Sands Missile Range, NM.
LASER RANGE SAFETY
Oct. 1991 125 p Supersedes AD-A110634
(AD-A243606; RCC-316-91) Avail: NTIS HC/MF A06 CSCL 09/3

This document is applicable to all DoD ranges or operational

test facilities where lasers are used and all DoD laser operations conducted on non-DoD controlled ranges or test facilities. A companion document, DOD Instruction 6055.XX, is issued under the authority of DoD. Laser devices can seriously injure the unprotected eyes within the hazard zone of the laser beam. Intrabeam viewing of either the direct beam or a beam reflected from a flat mirrorlike surface may expose unprotected eyes to a potential injury and must be avoided. Every diffuse reflecting object that the laser beam strikes will reflect some energy back in all directions and toward the laser. This diffusely reflected energy will not be hazardous if the laser is located greater than a distance t from the target. The hazard of exposure to the skin is small compared to the eye; however, personnel should also avoid direct laser beam exposure to the skin within distance t from the laser. GRA

37 MECHANICAL ENGINEERING

Includes auxiliary systems (nonpower); machine elements and processes; and mechanical equipment.

N92-17024# Air Force Inst. of Tech., Wright-Patterson AFB, OH. School of Engineering.
MODEL IDENTIFICATION AND CONTROL SYSTEM DESIGN FOR THE LAMBDA UNMANNED RESEARCH VEHICLE M.S. Thesis
Gerald A. Swift Sep. 1991 245 p
(AD-A241859; AFIT/GAE/ENY/91S-4) Avail: NTIS HC/MF A11 CSCL 01/3

Research for this thesis centered on the Lambda Unmanned Research Vehicle (URV), an asset of the Flight Dynamics Directorate, Wright Laboratory Patterson AFB. The following tasks were accomplished: (1) a linear, state-space, small perturbation model was developed for both the longitudinal and lateral directional dynamics of the vehicles, and (2) pitch rate roll rate, and yaw rate flight controllers were designed using classical and multivariable feedback methods. The parameters of the linear, state space, small perturbation model were estimated from actual flight test data. Digital Datcom was first used to estimate stability and control derivatives from the vehicle's geometry. Maximum likelihood estimation was then used to adjust the Datcom derivatives so that the estimated state time histories matched the actual state time histories recorded during flight. Pitch rate, roll rate, and yaw rate controller designs were developed using classical feedback methodology characterized by single input, single output, open loop transfer function techniques. The controller designs were repeated using the Linear Quadratic Gaussian with Loop Transfer Recovery (LOG/LTR) multivariable feedback approach. GRA

N92-17183# Du Pont de Nemours (E. I.) and Co., Aiken, SC.
EXTENDABLE PIPE CRAWLER Patent Application
M. Hapstack, inventor (to DOE) 1 May 1990 23 p
(Contract DE-AC09-76SR-00001)
(DE91-011570; US-Patent-Appl-SN-461591; Patents-US-A7461591) Avail: NTIS HC/MF A03

Described here is a pipe crawler having a front leg assembly and a back leg assembly connected together by two air cylinders, each leg assembly having four extendable legs and a pair of actuators for sliding the extendable legs radically outward to increase the range of the legs when the pipe crawler enters a section of pipe having a larger diameter. The crawler crawls by inchworm-like motion, the front leg assembly and back leg assembly alternately engaging and disengaging the wall of the pipe to hold the pipe crawler as the air cylinders alternately advance the front leg assembly and bring up the rear leg assembly. The pair of actuators of each leg assembly are parallel, adjacent and opposing acting so that each slides two adjacent extendable legs radially outward. DOE

N92-17304*# Georgia Inst. of Tech., Atlanta. School of Mechanical Engineering.
ACTIVELY CONTROLLED SHAFT SEALS FOR AEROSPACE APPLICATIONS Semiannual Status Report, Jul. - Dec. 1991
Richard F. Salant Dec. 1991 143 p
(Grant NAG3-974)
(NASA-CR-189808; NAS 1.26:189808) Avail: NTIS HC/MF A07 CSCL 11A

Actively controlled mechanical seals have recently been developed for industrial use. This study investigates the feasibility of using such seals for aerospace applications. In a noncontacting mechanical seal, the film thickness depends on the geometry of the seal interface. The amount of coning, which is a measure of the radial convergence or divergence of the seal interface, has a primary effect on the film thickness. Active control of the film thickness is established by controlling the coning with a piezoelectric material. A mathematical model has been formulated to predict the performance of an actively controlled mechanical seal. Author

N92-17575# Argonne National Lab., IL.
THE SYNERGISTIC EFFECTS OF SOLID AND LIQUID LUBRICATION ON THE TRIBOLOGICAL BEHAVIOR OF TRANSFORMATION-TOUGHENED ZrO2 CERAMICS
A. Erdemir, O. O. Ajayi, G. R. Fenske, R. A. Erck, and J. H. Hsieh Feb. 1991 39 p Presented at the Society of Tribologist and Lubrication Engineers (STLE)- American Society of Mechanical Engineers (ASME) Conference on Tribology, St. Louis, MO, 14-16 Oct. 1991
(Contract W-31-109-eng-38)
(DE91-018617; ANL/CP-72505; CONF-911002-1) Avail: NTIS HC/MF A03

In this study, we investigated the synergistic effects of liquid and solid lubrication on the tribological behavior of yttria-stabilized zirconia (ZrO2) ceramics. Thin silver films 1 to 2 microns thick were produced on ZrO2 flats by ion-beam-assisted deposition (IBAD) and used as the solid lubricant. A fully formulated synthetic oil (polyolester-based) served as the liquid lubricant. Wear tests were performed on an oscillating-slider wear test machine at temperatures up to 250 C. For the specific test conditions explored, it was found that: (1) without any type of lubrication, the friction coefficients of ZrO2/ZrO2 test pairs were on the order of 0.6, and the average wear rates of pins were in the range of 5 x 10(exp -5) to 10(exp -4) mm(exp 3)/m x N exp 2, depending on the test temperature; (2) the use of solid-lubricant silver films alone reduced the friction coefficients of sliding pairs by factors of 2 to 4 and the wear rates of pins by 3 orders of magnitude; (3) the use of liquid lubricant reduced the friction coefficients of ZrO2/ZrO2 test pairs by a factor of about 5 and the wear rates of pins by 1 to 2 orders of magnitude; and (4) the concurrent use of silver films and lubricant oil resulted in virtual elimination of the wear of both the pins and the flats and in significant reduction of the friction coefficients at room temperature and at 250 C. DOE

N92-17584*# National Aeronautics and Space Administration. Marshall Space Flight Center, Huntsville, AL.
SYSTEM FOR TESTING BEARINGS Patent Application
John Gibson, inventor (to NASA) 26 Dec. 1991 8 p
(NASA-Case-MFS-28589-1; NAS 1.71:MFS-28589-1; US-Patent-Appl-SN-813628) Avail: NTIS HC/MF A02 CSCL 13I

Disclosed here is a system for testing bearings wherein a pair of spaced bearings provides support for a shaft on which is mounted a bearing to be tested, this bearing being mounted in a bearing holder spaced from and in alignment with the pair of bearings. The bearing holder is provided with an annular collar positioned in an opening in the bearing holder for holding the bearing to be tested. A screw threaded through the bearing holder into engagement with the annular collar can be turned to force the collar radially out of alignment with the pair of bearings to apply a radial load to the bearing. NASA

N92-17604# Brookhaven National Lab., Upton, NY.
WORKSHOP ON TECHNOLOGY ISSUES OF SUPERCONDUCTING MAGLEV TRANSPORTATION SYSTEMS
J. E. Wegrzyn and D. T. Shaw 27 Sep. 1991 142 p Workshop held in Upton, NY, 23-24 May 1991
(Contract DE-AC02-76CH-00016)
(DE92-002288; BNL-52302; CONF-9105133) Avail: NTIS HC/MF A07

There exists a critical need for the United States to improve its ground transportation system. One suggested system that offers many advantages over the current transportation infrastructure is Maglev. Maglev represents the latest evolution in very high speed ground transportation, where vehicles are magnetically levitated, guided, and propelled over elevated guideways at speeds of 300 miles per hour. Maglev is not a new concept but is, however, receiving renewed interest. The objective of this workshop was to further promote these interest by bringing together a small group of specialists in Maglev technology to discuss Maglev research needs and to identify key research issues to the development of a successful Maglev system. The workshop was organized into four sessions based on the following technical areas: Materials, Testing, and Shielding; Magnet Design and Cryogenic Systems; Propulsion and Levitation Systems; and, System Control and Integration. DOE

N92-17605# Cornell Univ., Ithaca, NY.
DEVELOPMENT AND UTILIZATION OF NEW DIAGNOSTICS FOR DENSE-PHASE PNEUMATIC TRANSPORT
1991 6 p
(Contract DE-AC22-88PC-88947)
(DE92-003091; DOE/PC-88947/T12) Avail: NTIS HC/MF A02

Dense-phase pneumatic transport is an attractive means of conveying solids. Unfortunately, because of the high solid concentrations, this transport method is a difficult regime in which to carry out detailed measurements. Hence most details of the flow are unknown. In this context, the main objective of this work is to develop probes for local measurements of solid velocity and holdup in dense gas-solid flows. In particular, we have designed capacitance probes to measure local, time-dependent particle concentrations, and a new optical fiber probe based on laser induced phosphorescence to measure particle velocities. DOE

N92-17677*# National Aeronautics and Space Administration. Langley Research Center, Hampton, VA.
SUBSTANTIALLY OXYGEN-FREE CONTACT TUBE Patent Application
James F. Pike, inventor (to NASA) 14 Nov. 1991 8 p
(NASA-Case-LAR-14169-1; NAS 1.71:LAR-14169-1; US-Patent-Appl-SN-791728) Avail: NTIS HC/MF A02 CSCL 13I

A device for arc welding is provided in which a continuously-fed electrode wire is in electrical contact with a contact tube. The contact tube is improved by using a substantially oxygen-free conductive alloy in order to reduce the amount of electrical erosion. NASA

N92-17678*# National Aeronautics and Space Administration. Lewis Research Center, Cleveland, OH.
THREE POINT LEAD SCREW POSITIONING APPARATUS Patent Application
Frank S. Calco, inventor (to NASA) 27 Jan. 1992 16 p
(NASA-Case-LEW-15216-1; NAS 1.71:LEW-15216-1; US-Patent-Appl-SN-826547) Avail: NTIS HC/MF A03 CSCL 13K

Three lead screws are provided for adjusting the position of a traversing plate. Each of the three lead screws is threaded through a collar that is press fitted through the center of one of three pinion gears. A sun gear meshes with all three pinion gears and transversely moves the three lead screws upon actuation of a drive gear. The drive gear meshes with the sun gear and is driven by a handle or servomotor. When the handle or servomotor rotates the drive gear, the sun gear rotates causing the three pinion gears to rotate, thus, causing transverse movement of the three lead screws and, accordingly, transverse movement of the transversing plate. When the drive gear rotates, the traversing plate is driven in and out of a microwave cavity. Thus, the length or size of the cavity can be tuned while maintaining the traversing plate in an exact parallel relationship with an opposing plate on another end of the cavity. NASA

N92-17827 Department of the Navy, Washington, DC.
LOW FREQUENCY VIBRATION ABSORBER Patent
Neil J. Dubois, inventor (to Navy) 20 Aug. 1991 6 p Filed 28 Sep. 1990
(AD-D015103; US-Patent-5,040,764; US-Patent-Appl-SN-590183; US-Patent-Class-248-635) Avail: US Patent and Trademark Office CSCL 13/9

This patent discloses a mounting assembly for absorbing low frequency vibrational energy as produced by a source and isolating a base member therefrom, the mounting assembly including a central metallic ring, non-metallic foam rings located on both sides of the central metallic ring in concentric relation with respect thereto, and inner and outer metallic ring members engaging said foam rings in concentric relation, the foam rings defining a spongy mass that effectively absorbs the low frequency vibrational energy emanating from the source. GRA

N92-17852 ESDU International Ltd., London (England).
ANALYSIS OF CAM ROLLER FOLLOWERS
Dec. 1991 46 p
(ESDU-91026; ISBN-0-85679-788-X; ISSN-0141-4046) Avail: ESDU

ESDU 91026 gives a method for estimating the life of a user-specified commercial needle-bearing roller on a translating or swinging-arm follower. The maximum static and dynamic contact forces and the maximum angular velocity of the roller are determined to compare with their respective allowable values determined from manufacturer's catalogs. A FORTRAN program is provided on disc as ESDUpac A9126 which calculates at one degree intervals through a cam rotation the force acting on the roller due to the follower system inertia, externally applied loads, and the return spring. The external load can be entered as a simple trigonometric function of cam angle, as values at each degree interval of cam rotation, or as a few key values in which case the program uses linear interpolation to obtain the force variation through a cycle. An option allows suitable values of spring rate and preload to be found that ensure cam/roller contact at all times. The roller life is determined from a standard basic rating formula, in which the determined average roller speed and root mean square contact force are used. The basic formula applies to 90 percent reliability (that is, 90 percent of rollers would survive at that level) but modification factors can be applied for higher reliabilities and to take account of shock loads. A full explanation of the mathematical model is included, and guidance is given on the input to and output from the program. Three realistic design examples illustrate its use. Author

N92-17872*# National Aeronautics and Space Administration. Lyndon B. Johnson Space Center, Houston, TX.
THRUSTER SEALING SYSTEM AND APPARATUS Patent Application
Paul A. Svejkovsky, inventor (to NASA) (Lockheed Engineering and Sciences Co., Houston, TX.) 22 Oct. 1991 20 p
(NASA-Case-MSC-21898-1; NAS 1.71:MSC-21898-1; US-Patent-Appl-SN-780512) Avail: NTIS HC/MF A03 CSCL 13I

A thruster nozzle sealing system and apparatus is provided for protection of spacecraft thruster motors. The system includes a sealing plug, a sealing plug insertion tool, an outer cover, an outer cover attachment, and a ferry flight attachment. The sealing plug prevents moisture from entering the thruster engine so as to prevent valve failure. The attachments are interchangeably connectable with the sealing plug. The ferry flight attachment is used during air transportation of the spacecraft, and the outer cover attachment is used during storage and service of the

spacecraft. The outer cover provides protection to the thruster nozzle from mechanical damage. NASA

N92-17358*# Jet Propulsion Lab., California Inst. of Tech., Pasadena.
JPL SPACE STATION TELEROBOTIC ENGINEERING PROTOTYPE DEVELOPMENT: ADVANCED TELEROBOTICS SYSTEM TECHNOLOGY
Paul G. Backes *In* NASA, Washington, Beyond the Baseline 1991: Proceedings of the Space Station Evolution Symposium. Volume 2: Space Station Freedom, Part 2 Sep. 1991 p 1353-1374 (For primary document see N92-17348 08-18)
Avail: NTIS HC/MF A20 CSCL 13I

N92-17359*# Jet Propulsion Lab., California Inst. of Tech., Pasadena.
JPL SPACE STATION TELEROBOTIC ENGINEERING PROTOTYPE DEVELOPMENT FY 91 STATUS/ACHIEVEMENTS
Wayne Zimmerman *In* NASA, Washington, Beyond the Baseline 1991: Proceedings of the Space Station Evolution Symposium. Volume 2: Space Station Freedom, Part 2 Sep. 1991 p 1375-1386 (For primary document see N92-17348 08-18)
Avail: NTIS HC/MF A20 CSCL 13I

N92-17360*# Jet Propulsion Lab., California Inst. of Tech., Pasadena.
TELEROBOTIC GROUND-REMOTE OPERATIONS
Bruce Bon and Wayne Zimmerman *In* NASA, Washington, Beyond the Baseline 1991: Proceedings of the Space Station Evolution Symposium. Volume 2: Space Station Freedom, Part 2 Sep. 1991 p 1387-1404 (For primary document see N92-17348 08-18)
Avail: NTIS HC/MF A20 CSCL 13I

38 QUALITY ASSURANCE AND RELIABILITY

Includes product sampling procedures and techniques; and quality control.

N92-16988*# National Aeronautics and Space Administration. Marshall Space Flight Center, Huntsville, AL.
PARTNERSHIP FOR CONTINUOUS IMPROVEMENT Summary Report
May 1990 170 p Presented at the 6th Annual NASA/Contractors Conference on Quality and Productivity, Huntsville, AL, 31 Oct. - 1 Nov. 1989
(NASA-TM-105464; NAS 1.15:105464; ISSN-1049-667X) Avail: NTIS HC/MF A08 CSCL 05A

The proceedings are presented of the sixth annual conference on quality control between NASA and its contractors. The emphasis is placed on a commitment to quality and excellence that guarantees mission success. A forum is provided for representatives from government, industry, and academia to exchange ideas and experiences, encouraging total quality performance that results in high quality products and services. Key points are highlighted from the presentations and activities are described that have resulted in a broad range of improvements in products and services from government, industry, and academia. Long term commitment to quality is an essential requirement that ensures future success. That commitment reinterates the dedication to excellence in space exploration and to national quality and productivity improvement. E.R.

N92-17005*# National Aeronautics and Space Administration, Washington, DC.
NASA TOTAL QUALITY MANAGEMENT 1989 ACCOMPLISHMENTS REPORT
Betty P. Tai, ed. and Lynne M. Stewart, ed. Jun. 1990 125 p
(NASA-TM-105467; NAS 1.15:105467; ISSN-1051-225X) Avail: NTIS HC/MF A06 CSCL 05A

NASA and contractor employees achieved many notable improvements in 1989. The highlights of those improvements, described in this seventh annual Accomplishments Report, demonstrate that the people who support NASA's activities are getting more involved in quality and continuous improvement efforts. Their gains solidly support NASA's and this Nation's goal to remain a leader in space exploration and in world-wide market competition, and, when communicated to others through avenues such as this report, foster improvement efforts across government and industry. The principles in practice which led to these process refinements are important cultural elements to any organization's productivity and quality efforts. The categories in this report reflect NASA principles set forth in the 1980's and are more commonly known today as Total Quality Management (TQM): top management leadership and support; strategic planning; focus on the customer; employee training and recognition; employee empowerment and teamwork; measurement and analysis; and quality assurance. Author

N92-17199*# National Aeronautics and Space Administration, Washington, DC.
NASA TOTAL QUALITY MANAGEMENT 1990 ACCOMPLISHMENTS REPORT Annual Report No. 8
Sep. 1991 200 p
(NASA-TM-105465; NAS 1.15:105465; ISSN-1051-225X) Avail: NTIS HC/MF A09 CSCL 05A

NASA's efforts in Total Quality Management are based on continuous improvement and serve as a foundation for NASA's present and future endeavors. Given here are numerous examples of quality strategies that have proven effective and efficient in a time when cost reduction is critical. These accomplishment benefit our Agency and help to achieve our primary goal, keeping American in the forefront of the aerospace industry. Author

N92-17231# George Washington Univ., Washington, DC.
RESEARCH IN SOME FUTURE DIRECTIONS IN RELIABILITY AND QUALITY CONTROL Final Report, 1 Jun. 1989 - 31 May 1991
Nozer D. Singpurwalla 25 Sep. 1991 6 p
(Grant AF-AFOSR-0381-89; AF Proj. 2304)
(AD-A242865; AFOSR-91-0879TR) Avail: NTIS HC/MF A02 CSCL 12/5

Problems emanating from the area of software engineering, especially software reliability and software testing, are researched. Bayesian acceptance sampling and life testing, accelerated life testing, and the setting of optimum warranties are areas of particular interest in terms of software development. GRA

N92-17341# Messerschmitt-Boelkow-Blohm G.m.b.H., Munich (Germany, F.R.). Design Assurance Dept.
A MANAGERIAL APPROACH FOR RELIABILITY VERIFICATION OF MECHANICAL EQUIPMENT
Gerhard Albrecht 1991 4 p Presented at the ESA Symposium on Space Product Assurance for Europe in the 1990s, Noordwijk, Netherlands, 15-19 Apr. 1991
(MBB-UK-0140-91-PUB; ETN-92-90601) Avail: NTIS HC/MF A01

Difficulties involved in the verification of the required reliability of mechanical equipment are discussed. The lack of adequate statistical failure rate data covering the specific properties of mechanical equipment is identified as being one of the major difficulties. Since a straightforward demonstration of the reliability of individual equipment through reliability testing is not feasible in most cases for cost and time reasons, an effective Reliability, Availability, Maintainability and Safety (RAMS) management system is proposed to verify the reliability using test data and other available data. ESA

N92-17431# Air Force Inst. of Tech., Wright-Patterson AFB, OH.
INCIPIENT FAULT DETECTION USING HIGHER-ORDER STATISTICS Ph.D. Thesis
Richard W. Barker Aug. 1991 191 p

(AD-A243493; AFIT/CI/CIA-91-023D) Avail: NTIS HC/MF A09 CSCL 13/8

This study balances the development of theory and its application to real and simulated incipient fault data from systems which have cyclostationary properties. The study's theoretical contribution reveals the advantages of approaching estimation of time series in a general framework where estimation of the cumulant spectrum can reveal implications for three classes of stochastic processes: stationary, cyclostationary, and nonstationary. The developed cumulant spectrum estimation capability provides for feature construction in addition to bispectrum and power spectrum estimates of stochastic process data. Actual experimental data is obtained to study the incipient wear process of manufacturing drill bits cutting through epoxy glass composite material used for construction of electronic semiconductor panels. The fluctuating vibrations caused by the drill bits cutting through the epoxy-glass composite material used for construction of electronic semiconductor panels. The fluctuating vibrations caused by the drill bits cutting through the epoxy-glass composite are not subject to precise prediction, nor are the external noise, measurement errors, and other disturbances in the transmission of the vibration signal to three accelerometers mounted on the drilling machine considered to have the same characteristic of unpredictability. GRA

N92-17544# Messerschmitt-Boelkow-Blohm G.m.b.H., Munich (Germany, F.R.). Space Communications and Propulsion Systems Div.

CONSTRAINTS AND DIFFICULTIES IN IMPLEMENTATIONS OF RAMS ASSURANCE PROGRAMMES

Miodrag Culjkovic 1991 4 p Presented at the ESA Symposium on Space Product Assurance for Europe in the 1990s, Noordwijk, Netherlands, 15-19 Apr. 1991

(MBB-UK-0141-91-PUB; ETN-92-90602) Avail: NTIS HC/MF A01

A summary of typical difficulties encountered in the implementation of Reliability, Availability, Maintainability, and Safety (RAMS) assurance programs as observed in numerous space companies is given. An attempt is made to suggest possible solutions for each listed problem in order to improve the situation and support more effective RAMS assurance management in the years to come. The external and internal difficulties which have impeded RAMS engineers in all space companies are discussed. Ways in which to overcome these difficulties are proposed. ESA

N92-17809# Gosudarstvennyi Komitet po Ispolzovaniyu Atomnoi Energii, Obninsk (USSR). Fiziko-Ehnergeticheskij Inst.

DEVELOPMENT OF A SYSTEM FOR VOID FRACTION MEASURING BY ELECTROPROBING METHOD

Eh. A. Boltenko, Yu. P. Dzhusov, A. I. Stepin, and V. L. Chernukhin 1990 15 p In RUSSIAN; ENGLISH summary

(DE92-610933; FEI-2119) Avail: NTIS HC/MF A03

An analysis of a variety of techniques to measure local values of void fractions using electric probes inserted in flow has been carried out. The main factors restricting the application of these techniques and sources of measurement errors are established. It is demonstrated that the uncertainties are primarily due to inaccurate algorithms defining the fluid phase. A description of the system developed and eliminating the elucidated shortcoming has been presented. DOE

N92-17859*# National Aeronautics and Space Administration. Langley Research Center, Hampton, VA.

A METHOD AND APPARATUS FOR INDICATING DISBONDS IN JOINT REGIONS Patent Application

Eric I. Madaras, inventor (to NASA) 29 Aug. 1991 13 p

(NASA-Case-LAR-14626-1; NAS 1.71:LAR-14626-1; US-Patent-Appl-SN-751489) Avail: NTIS HC/MF A03 CSCL 14D

A method for indicating disbonds in joint regions is discussed. A critical bondline region is located between a first material and a second material having a higher acoustic impedance than the first material. A form member having an acoustic impedance which is substantially similar to the first material has a first face which is form fitted to a surface of the first material opposite to and non-parallel with the critical bondline region. The form member has an opposite second face which is shaped to be parallel to the critical bondline region. Transducers are acoustically coupled to the second face of the form member to generate an ultrasonic tone burst through the acoustically similar form member and first material which is reflected by the critical bondline region. This reflected tone burst is received and a resulting signal is compared with a normal signal for no disbond to determine the presence of an unacceptable disbond. NASA

39 STRUCTURAL MECHANICS

Includes structural element design and weight analysis; fatigue; and thermal stress.

For applications see *05 Aircraft Design, Testing and Performance* and *18 Spacecraft Design, Testing and Performance.*

N92-17033*# National Aeronautics and Space Administration. Langley Research Center, Hampton, VA.

EXPERIENCES AT LANGLEY RESEARCH CENTER IN THE APPLICATION OF OPTIMIZATION TECHNIQUES TO HELICOPTER AIRFRAMES FOR VIBRATION REDUCTION

T. Sreekanta Murthy (Lockheed Engineering and Sciences Co., Hampton, VA.) and Raymond G. Kvaternik Dec. 1991 17 p Presented at the American Helicopter Society National Technical Specialists' Meeting on Rotorcraft Structures, Williamsburg, VA, 29-31 Oct. 1991

(NASA-TM-104193; NAS 1.15:104193) Avail: NTIS HC/MF A03 CSCL 20K

A NASA/industry rotorcraft structural dynamics program known as Design Analysis Methods for VIBrationS (DAMVIBS) was initiated at Langley Research Center in 1984 with the objective of establishing the technology base needed by the industry for developing an advanced finite-element-based vibrations design analysis capability for airframe structures. As a part of the in-house activities contributing to that program, a study was undertaken to investigate the use of formal, nonlinear programming-based, numerical optimization techniques for airframe vibrations design work. Considerable progress has been made in connection with that study since its inception in 1985. This paper presents a unified summary of the experiences and results of that study. The formulation and solution of airframe optimization problems are discussed. Particular attention is given to describing the implementation of a new computational procedure based on MSC/NASTRAN and CONstrained function MINimization (CONMIN) in a computer program system called DYNOPT for the optimization of airframes subject to strength, frequency, dynamic response, and fatigue constraints. The results from the application of the DYNOPT program to the Bell AH-1G helicopter are presented and discussed. Author

N92-17034*# National Aeronautics and Space Administration. Langley Research Center, Hampton, VA.

THE NASA/INDUSTRY DESIGN ANALYSIS METHODS FOR VIBRATIONS (DAMVIBS) PROGRAM: ACCOMPLISHMENTS AND CONTRIBUTIONS

Raymond G. Kvaternik Dec. 1991 37 p Presented at the American Helicopter Society National Technical Specialists' Meeting on Rotorcraft Structures, Williamsburg, VA, 29-31 Oct. 1991

(NASA-TM-104192; NAS 1.15:104192) Avail: NTIS HC/MF A03 CSCL 20K

A NASA Langley-sponsored rotorcraft structural dynamics program, known as Design Analysis Methods for VIBrationS (DAMVIBS), has been under development since 1984. The objective of this program was to establish the technology base needed by the industry to develop an advanced finite-element-based dynamics design analysis capability for vibrations. Under the program, teams from the four major helicopter

manufacturers have formed finite-element models, conducted ground vibration tests, made test/analysis comparisons of both metal and composite airframes, performed 'difficult components' studies on airframes to identify components which need more complete finite-element representation for improved correlation, and evaluated industry codes for computing coupled rotor-airframe vibrations. Studies aimed at establishing the role that structural optimization can play in airframe vibrations design work have also been initiated. Five government/industry meetings were held in connection with these activities during the course of the program. Because the DAMVIBS Program is coming to an end, the fifth meeting included a brief assessment of the program and its benefits to the industry. Author

N92-17230# Air Force Inst. of Tech., Wright-Patterson AFB, OH. School of Engineering.
HIGHER-ORDER THICKNESS EXPANSIONS FOR CYLINDRICAL SHELLS Ph.D. Thesis
Randy A. Smith Sep. 1991 259 p
(AD-A242017; AFIT/DS/ENY/91-1) Avail: NTIS HC/MF A12 CSCL 13/3

Eight variations of higher-order transverse shear deformation (HTSD) theory were developed for composite shells. Three attributes were varied to produce the eight variations. These attributes include the order of the thickness expansions used to approximate the shell shape factors and the assumed linear displacement field and the nonlinearity of transverse shear strain. Several cylindrical shell problems were investigated using SHELL, a finite-element code with a 36 degree of freedom cylindrical shell element. MACSYMA, a symbolic manipulation code, was used to formulate the element independent stiffness arrays for each variation of the theory. When all nonlinear strain-displacement terms for transverse shear were included for thin shallow isotropic cylindrical shells, the theory predicted a more flexible response during collapse. Higher-order thickness expansions had negligible effect upon results for shallow shell problems investigated. For deeper shells, the linear displacement assumption prohibited the use of nonlinear strain-displacement relations for transverse shear strains. Thus, for deep shells nonlinearity was limited to in-plane strain-displacement relations. GRA

N92-17254# Aeronautical Research Labs., Melbourne (Australia).
DETERMINATION OF SYMMETRIC END LOADS FROM BULK STRESSES ON A RECTANGULAR PRISM
T. Truong and J. Bennett Sep. 1991 31 p
(AD-A242973; ARL-STRUC-TM-536; DODA-AR-006-596) Avail: NTIS HC/MF A03 CSCL 20/11

The stress distribution in rectangular prisms subjected to certain normal end forces on two opposite faces is a fundamental problem in Applied Mechanics. The stress distribution near the loaded surface may be very complex, and the distribution given by elementary theory is often inaccurate. In this paper, it is assumed that the bulk stress on a lateral surface of a rectangular prism, which is being subjected to an arbitrary loading, is known. Such a measurement could be obtained using advanced thermal emission techniques. The aim of this paper is to reveal how the measured values of bulk stresses can be used to determine the actual end loads. A method for calculating the bulk stresses produced by a self-equilibrating end load is given. This will be referred to as the Direct solution. In the Inverse method we will determine the end loading from a known distribution of bulk stress values on a lateral surface. GRA

N92-17256# Metz Univ. (France). Lab. of Physics and Mechanics of Materials.
EXPERIMENTAL INVESTIGATION OF ADIABATIC SHEAR BANDING AT DIFFERENT IMPACT VELOCITIES Interim Report No. 3, 19 May - 18 Nov. 1991
J. R. Klepaczko 10 Nov. 1991 8 p
(Contract DAJA45-90-C-0052)
(AD-A243011; R/D-6148-MS-01) Avail: NTIS HC/MF A02 CSCL 14/2

During this report period the final operational stage in development of the new experimental techniques have been achieved. This technique enables the study of fast plastic deformation and development of adiabatic shear bands at differing displacement velocities. Ths technique is being tested using newly acquired measuring devices: (1) a non-contact optical extensometer/displacement gauge, and (2) an H.P. fast oscilloscope. Numerical studies of plastic zones in the double shear specimen have been started using the computer code 'ABAQUS'. Finally, some contacts with the French Army Laboratory (ETCA) have been undertaken to prepare steel specimens for a final testing. GRA

N92-17265# Aeronautical Research Labs., Melbourne (Australia).
DETERMINATION OF ANTISYMMETRIC END LOADS FROM BULK STRESSES ON A RECTANGULAR PRISM
J. Bennett Sep. 1991 44 p
(AD-A243001; ARL-STRUC-TM-539; DODA-AR-006-621) Avail: NTIS HC/MF A03 CSCL 20/11

The stress distribution in rectangular prisms subjected to certain normal end forces on its two opposite faces is a fundamental problem in Applied Mechanics. Reference supplies a method for calculating a symmetric end loading, assuming that the bulk stress on a lateral surface of the rectangular prism is known. Such a measurement could be obtained using advanced thermal emission techniques. The aim of this paper is to extend this concept to the case where an antisymmetric end loading is applied. A method for calculating the bulk stresses for a given antisymmetric end loading is presented. This will be referred to as the Direct solution. In the Inverse method the end loading will be determined from a known distribution of bulk stress values on a lateral surface. In this case, bulk stresses on the lateral surface will be simulated using the Direct solution. GRA

N92-17320# Naval Surface Warfare Center, Silver Spring, MD.
EFFECTIVE DYNAMIC MATERIAL PARAMETERS AND LOCALIZED SCATTERING Interim Report
Kurt P. Scharnhorst 20 Mar. 1991 40 p
(AD-A241957; NAVSWC-TR-91-182) Avail: NTIS HC/MF A03 CSCL 20/1

A modification of the classical effective wave vector in randomly inhomogeneous media k sub p * = k sub p + 2nnf sub p (1,0)/k sub p is discussed, which replaces the single particle far field forward scattering amplitude, f sub p (1,0), by an average pair scattering amplitude, f sub p(2,0). The Perkus-Yevick radial distribution function is used to find the average of f sub p (2,0) over radial separations extending to the first nearest neighbor maximum. The results are applied to random distributions of mass loaded polyurethane spheres in syntactic foam and to lead spheres in an epoxy resin matrix and compared with calculations based on the single particle amplitude. In the case of high concentrations of lead inclusions in epoxy, the mode conversion cross section as well as the real and imaginary parts of the effective wave vector are significantly altered by pair scattering. In the case of mass loaded polyurethane in syntactic foam, on the other hand, the effects are negligible. GRA

N92-17333*# National Aeronautics and Space Administration. Langley Research Center, Hampton, VA.
THE COMPUTATIONAL STRUCTURAL MECHANICS TESTBED PROCEDURES MANUAL
Caroline B. Stewart, comp. (Analytical Services and Materials, Inc., Hampton, VA.) Dec. 1991 557 p Revised
(NASA-TM-100646; NAS 1.15:100646) Avail: NTIS HC/MF A24 CSCL 20K

The purpose of this manual is to document the standard high level command language procedures of the Computational Structural Mechanics (CSM) Testbed software system. A description of each procedure including its function, commands, data interface, and use is presented. This manual is designed to assist users in defining and using command procedures to perform

structural analysis in the CSM Testbed User's Manual and the CSM Testbed Data Library Description. Author

N92-17511*# Maryland Univ., College Park. Dept. of Mechanical Engineering.
INELASTIC STRAIN ANALYSIS OF SOLDER JOINT IN NASA FATIGUE SPECIMEN Final Report
Abhijit Dasgupta and Chen Oyan 28 Jan. 1991 59 p
(Grant NAG5-1331)
(NASA-CR-189882; NAS 1.26:189882) Avail: NTIS HC/MF A04 CSCL 20K

The solder fatigue specimen designed by NASA-Goddard/UNISYS is analyzed in order to obtain the inelastic strain history during two different representative temperature cycles specified by UNISYS. Results are summarized from viscoplastic finite element analysis of the solder fatigue specimen for delta(T) = 113 C cycle. Large deformation continuum formulations in conjunction with a standard linear solid model is used for modeling the solder constitutive creep plasticity behavior. Relevant material properties are obtained from the literature. Strain amplitudes, mean strains, and residual strains (as well as stresses) accumulated due to a representative complete temperature cycle are obtained as a result of this analysis. The partitioning between elastic strains, time independent inelastic (plastic) strains, and time dependent (creep) strains is also explicitly obtained for two representative cycles. Detailed plots are presented for two representative temperature cycles. This information forms an important input for fatigue damage models, when predicting the fatigue life of solder joints under thermal cycling. Author

N92-17713# Westinghouse Hanford Co., Richland, WA.
FRACTURE TOUGHNESS EVALUATION FOR N REACTOR PRESSURE TUBES OF ZIRCALOY-2 USING THE ELECTRIC-POTENTIAL METHOD
F. H. Huang Nov. 1991 31 p Presented at the ASTM International Symposium on Small Specimen Test Techniques and their Applications to Nuclear Reactor Vessel Thermal Annealing and Plant Life Extension, New Orleans, LA, 29-31 Jan. 1991
(Contract DE-AC06-87RL-10930)
(DE92-003631; WHC-SA-1210; CONF-920146-1) Avail: NTIS HC/MF A03

Zircaloy is commonly used for the cladding or pressure tubes in commercial reactors because of its strength, corrosion resistance, and low absorption of thermal neutrons. Fracture toughness test techniques using small samples fabricated from archival materials from N Reactor pressure tubes of Zircaloy-2 were developed to study the factors affecting tube fracture toughness. Compact tension specimen thickness was limited by the wall thickness (7 mm) of the tubes. Specimens (5 mm thick) were prepared for fracture toughness testing and results were analyzed using the J-integral approach. To reduce the high cost of irradiated specimen testing and to more easily precrack specimens remotely, single-specimen potential drop techniques were employed to evaluate the fracture toughness of Zircaloy-2. The initiation fracture toughness was determined from J-R curves, which were constructed by plotting values of J as a function of crack extension computed from the electric-potential calibration curve. The J-R curves obtained from the calibration curve equation fit the blunting line region. The curves also fit heat-tint data well. The effects of neutron fluence and hydrogen content on the fracture toughness of N Reactor pressure tubes were evaluated. Neutron irradiation substantially degraded fracture toughness. Increasing fluence decreased the fracture toughness of the alloy. Hydrogen also decreased fracture toughness, but this effect was insignificant for the pressure tubes tested. DOE

N92-17834 ESDU International Ltd., London (England).
STRENGTH OF LUGS
Dec. 1991 33 p
(ESDU-91008; ISBN-0-85679-770-7; ISSN-0141-4097) Avail: ESDU

ESDU 91008 provides data to determine the minimum load to cause failure by rupture or by unacceptable permanent deformation of parallel sided or tapered lugs with round or square ends under axial, transverse, or oblique loading. The consideration of the effects of pin bending in a double shear joint is also included. The data on axial failure apply to any metallic material but those for transverse failure are for aluminum or steel only. The data include empirical factors that are geometry dependent and are presented as curves. However, for axial loading the semi-empirical factor is both material and geometry dependent. The theory on which its calculation is based is outlined and a FORTRAN computer program (ESDUpac A9108) is provided on disc to determine it. The program requires input of the material characteristics and an elastic stress concentration factor that may be found from ESDU 81006. A complete lug strength analysis calculation is included to illustrate the use of the program and data. ESDU

N92-17930# Army Armament Research, Development and Engineering Center, Watervliet, NY.
RESIDUAL STRESSES IN A PRESTRESSED STEEL PRESSURE VESSEL WRAPPED WITH MULTILAYERED COMPOSITES Final Report
Peter C. Chen Nov. 1991 19 p Presented at the 6th Technical Conference of the American Society for Composition, Albany, NY, 6-9 Oct. 1991
(AD-A243429; ARCCB-TR-91033) Avail: NTIS HC/MF A03 CSCL 13/10

This report presents an analytical solution for predicting residual stresses in a steel pressure vessel wrapped with a multilayered composite jacket. The numerical results for the hoop stresses before and after complete unloading are obtained for a subscale test tube. The steel liner is elastic-plastic, and the composite layup (02902)4 consists of 16 layers made of graphite bismaleimide produced by Fiberite Corporation. GRA

N92-17937# Sandia National Labs., Albuquerque, NM.
AN INVESTIGATION OF GOUGE INITIATION IN HIGH-VELOCITY SLIDING CONTACT
R. D. M. Tachau Nov. 1991 125 p
(Contract DE-AC04-76DP-00789)
(DE92-003944; SAND-91-1732) Avail: NTIS HC/MF A06

Surface damage has been observed on the rails of rocket sled tracks and on the barrels of high-velocity guns. The phenomenon is generally referred to as 'ongoing'. Damage to a stationary surface (guider) is created from the oblique impact of a high-velocity object (slider) moving over its surface. The surface damage (gouge) is typically a shallow crater in the shape of a teardrop with the leading edge characterized by the wider end and a slightly raised lip. For rocket sleds, rail gouging occurs when the sled velocity is greater than 1.5 km/sec; while in guns, barrel gouging occurs when the velocity exceeds 4 km/sec. A model is developed to describe the phenomenon of gouging. An unbalanced slider randomly causes a shallow-angle, oblique impact between the slider and the guider. At sufficiently high velocity, the impact produces a thin, but very hot, layer of soft material at the contact surface. Under the action of a moving load, the soft layer lends itself to an antisymmetric deformation and a gouge is formed when this soft material is over-run by the slider. The model is simulated numerically with a hydrodynamic (CTH) code. The results of the simulations are in good agreement with the observed phenomena. Based on the simulated temperature and pressure profiles at the contact surface, design criteria for gouge mitigation are developed in this study. DOE

42 GEOSCIENCES (GENERAL)

N92-17208# Mitre Corp., Bedford, MA.
GROUNDSCREEN CHARACTERIZATION
L. W. Parker Oct. 1991 25 p
(AD-A243164; M91-82) Avail: NTIS HC/MF A03 CSCL 17/4

The screen parameter for a Fresnel reflection coefficient model is calculated for a plane wave obliquely incident on a parallel-wire

grid of infinite extent, in proximity to and parallel to flat lossy earth. J. R. Wait has published mathematical models for this problem. The numerical results from a computer code implementing Wait's expansion models allow an assessment of the range of validity for a simplified screen parameter formula. The screen parameter developed in this paper is not applicable to grids of electrically-small extent (small compared to a wavelength) or to grids consisting of disconnected electrically-small panels of grids because diffraction and reflection at the edge of the grids causes the current distribution on the grids to differ appreciably from that on a grid of infinite extent. Author (GRA)

43 EARTH RESOURCES AND REMOTE SENSING

Includes remote sensing of earth resources by aircraft and spacecraft; photogrammetry; and aerial photography.

For instrumentation see *35 Instrumentation and Photography.*

N92-17292# Department of Defence, Canberra (Australia). Central Studies Branch.
MAP MAKER
B. K. McMillan Nov. 1991 65 p
(AD-A242980; CSB-WP-MAPS1; DODA-AR-005-791) Avail: NTIS HC/MF A04 CSCL 08/2

This report describes the application of the MAP MAKER program for PCs to produce maps of user defined areas and projections, for insertion in word processor documents. A graphics package can be used as an intermediate process, with all the advantages so implied. Options include map delimitation by latitude and longitude, level of detail, creation of reduced data set files to speed map production, some point annotation capability, and gridding. A number of data sets provided with the program are also described. GRA

N92-17436# Technische Univ., Delft (Netherlands). Sectie Fysische, Meetkundige en Ruimte Geodesie.
SPECTRAL ERROR MODELS APPLIED TO THE GEODETIC BOUNDARY VALUE PROBLEM Thesis
Kyra vanOnselen May 1991 103 p
(ETN-92-90582) Avail: NTIS HC/MF A06

Error propagation in the Geodetic Boundary Value Problem (GBVP) is addressed. The solving of overdetermined GBVP's by least squares adjustment is expounded and some properties of isotropic covariance functions and their spectra, the degree variances, are studied. Noise models for simulating a discrete noise function and correlating measurements are addressed. The use of operators, which can be represented by an isotropic kernel function, is discussed. Results on error propagation in vertical GBVP's are presented. The Gauss/Markov and the Krarup noise model are used to simulate a discrete noise function, and three types of vertical GBVP's with Stokes solution are compared. The combination of Stokes' solution with both vertical gradiometry and altimetry is examined. The GBVP gives, compared with Stokes' solution on its own, an improvement of the noise level in general, as well as improvement in the conditioning of the model. ESA

N92-17459# Environmental Research Inst. of Michigan, Ann Arbor.
SIMULTANEOUS ACTIVE AND PASSIVE MICROWAVE MEASUREMENTS OF THE OCEAN SURFACE Final Report, 1 Aug. 1989 - 30 Jun. 1991
R. G. Onstott, R. A. Shuchman, and C. L. Rufenach Jun. 1991 103 p
(Contract N00014-89-C-0117)
(AD-A242232; ERIM-218600-4-F) Avail: NTIS HC/MF A06 CSCL 17/9

This report considered both the use of an L- and X-band scatterometer to measure surface slicks on the ocean as well as the feasibility of using a dual linear polarized radiometer operating at 6 GHz in conjunction with a scatterometer to measure sea surface temperature. The scatterometer measurements show: (1) the largest peaks in fluorescence, a measure of the peak Chlorophyll A concentration, are co-located with the short wave damping at 24 and 4 cm wavelengths; (2) the maximum damping ratio, between the 24 and 4 cm waves, is at least 16 for wind speeds, 3 to 4 m/s; and (3) the radar roughness signatures at these short Bragg gravity wavelengths suggest the slicks are caused by damping rather than straining of these waves. Additional shipboard measurements are needed to further quantify these preliminary results. The active/passive microwave feasibility study indicated a + or - .12 C accuracy of SST can result if a scatterometer is used to correct the wind speed dependence of a vertically polarized radiometer operating near 6 GHz using a pencil antenna beam pointing at an incidence angle near 55 deg. GRA

N92-17715# Army Cold Regions Research and Engineering Lab., Hanover, NH.
THE ROLE OF THERMAL CONVECTION IN HEAT AND MASS TRANSPORT IN THE SUBARCTIC SNOW COVER
Matthew Sturm Oct. 1991 93 p
(DA Proj. 4A1-61101-A-91-D)
(AD-A243674; CRREL-91-19) Avail: NTIS HC/MF A05 CSCL 08/12

This study investigated the role of air convection in moving heat and water vapor in snow. To detect convection, the three-dimensional temperature field in the Fairbanks snow cover was measured hourly during three winters (1984-1987). Measurements of snow density, compaction, and grain size were made monthly to determine water vapor flux and textural changes. The snow metamorphosed into depth hoar, producing a sequence of five layers, including a basal layer with horizontal c-axes. C-axes in the overlying layers were vertical or randomly oriented. As the depth hoar developed, its air permeability increased to several times higher than previously measured for any snow, while the number of snow grains per unit volume decreased by an order of magnitude as a few select grains grew while others sublimated away. Simultaneously, there was a net transfer of mass from the base to the top of the snow due to mass flux gradients. Convection occurred sporadically in the winter of 1984-85 and continuously in the winters of 1985-86 and 1986-87. The evidence was: (1) simultaneous warming and cooling at different locations in a horizontal plane in the snow; and (2) horizontal temperature gradients of up to 16 C/m. The convection was time-dependent, with perturbations such as high wind or rapid changes in air temperature triggering periods when horizontal temperature gradients were strongest, suggesting these were also periods when the air flow was fastest. GRA

44 ENERGY PRODUCTION AND CONVERSION

Includes specific energy conversion systems, e.g., fuel cells; global sources of energy; geophysical conversion; and windpower.

For related information see also *07 Aircraft Propulsion and Power, 20 Spacecraft Propulsion and Power,* and *28 Propellants and Fuels.*

N92-17225*# Auburn Univ., AL. Space Power Inst.
LOSS TERMS IN FREE-PISTON STIRLING ENGINE MODELS Final Technical Report
Lloyd B. Gordon 25 Jan. 1992 17 p
(Grant NAG3-1161)
(NASA-CR-189840; NAS 1.26:189840) Avail: NTIS HC/MF A03 CSCL 10B

Various models for free piston Stirling engines are reviewed. Initial models were developed primarily for design purposes and to predict operating parameters, especially efficiency. More recently, however, such models have been used to predict engine stability. Free piston Stirling engines have no kinematic constraints and stability may not only be sensitive to the load, but also to various nonlinear loss and spring constraints. The present

understanding is reviewed of various loss mechanisms for free piston Stirling engines and how they have been incorporated into engine models is discussed. Author

N92-17424# Naval Postgraduate School, Monterey, CA.
OPTIMIZATION IN SOLAR HEATING/PHOTOVOLTAIC SYSTEMS M.S. Thesis
Dimitrios G. Vourazelis Dec. 1990 65 p
(AD-A242363) Avail: NTIS HC/MF A04 CSCL 13/1

This thesis is a design of an alternative system which may provide heating to the Naval Postgraduate School swimming pool. Particularly, it is a solar heating/photovoltaic system designed for a better efficiency and less cost of installation and maintenance. Principles of heat transfer, control and fluid dynamics theory are used for the determination of this heating system elements. The feasibility of its installation and use its analyzed. GRA

N92-17577# Massachusetts Univ., Amherst. Dept. of Mechanical Engineering.
PRELIMINARY DESIGN STUDY OF A CENTRAL SOLAR HEATING PLANT WITH SEASONAL STORAGE AT THE UNIVERSITY OF MASSACHUSETTS, AMHERST
D. S. Breger and J. E. Sunderland Apr. 1991 86 p
(Contract DE-FG03-88SF-17853)
(DE92-000762; DOE/SF-17853/T1) Avail: NTIS HC/MF A05

This report documents the design development and selection of the final preliminary design of a Central Solar Heating Plant with Seasonal Storage (CSHPSS) for the University of Massachusetts in Amherst (UMass). The effort has been performed by the Department of Mechanical Engineering at UMass under contract with the U.S. Department of Energy. Phase 1 of this project was directed at site selection for the CSHPSS project and was reported earlier. This report focuses on the Phase 2 development of the site conditions and analytical study of project design, performance, and cost. The UMass site presents an excellent opportunity of a CSHPSS project in terms of land availability for a large collector array, a 100 foot deep deposit of soft, saturated clay for seasonal thermal energy storage, and appropriate low temperature heating loads. The project under study represents the first implementation of this solar technology in the United States and results from the International Energy Agency collaboration on CSHPSS since 1979. The preliminary design calls for a large 10,000 m(exp 2) parabolic trough collector array, 70,000 m(exp 3) storage volume in clay with heat transfer through 900 boreholes. Design optimization is based on computer simulations using MINSUN and TRNSYS. The design is expected to provide 95 percent of the 3500 MWh heating and hot water load. A project cost of $3.12 million (plus $240,000 for HVAC load retrofit) is estimated, which provides an annualized cost of $66.2/MWh per unit solar energy delivered. The project will proceed into an engineering phase in Spring 1991. DOE

N92-17875# Midwest Research Inst., Golden, CO. National Renewable Energy Lab.
AN OVERVIEW: CHALLENGES IN WIND TECHNOLOGY DEVELOPMENT
R. W. Thresher and S. M. Hock Dec. 1991 10 p Presented at the 21st American Wind Energy Association Conference: Windpower 1991, Palm Springs, CA, 24-27 Sep. 1991
(Contract DE-AC02-83CH-10093)
(DE92-001190; NREL/TP-257-4518; CONF-9109112-8) Avail: NTIS HC/MF A02

Developing innovative wind turbine components and advanced turbine configurations is a primary focus for wind technology researchers. In their rush to bring these new components and systems to the marketplace, designers and developers should consider the lessons learned in the wind farms over the past 10 years. Experience has shown that a disciplined design approach is required that realistically accounts for the turbulence-induced loads, unsteady stall loading, and fatigue effects. This paper reviews past experiences and compares current modeling capabilities with experimental measurements in order to identify some of the knowledge gaps that challenge designers of advanced components and systems. DOE

N92-17934# Minnesota Geological Survey, Saint Paul.
UNIVERSITY OF MINNESOTA AQUIFER THERMAL ENERGY STORAGE (ATES) PROJECT REPORT ON THE FIRST LONG-TERM CYCLE
M. Walton Oct. 1991 122 p Prepared for Pacific Northwest Lab., Richalnd, WA
(Contract DE-AC06-76RL-01830)
(DE92-004699; PNL-7817) Avail: NTIS HC/MF A06

The technical feasibility of high-temperature (greater than 100 C) aquifer thermal energy storage (IOTAS) in a deep, confined aquifer was tested in a series of experimental cycles at the University of Minnesota's St. Paul field test facility (FTF). This report describes the additions to the FTF for the long-term cycles and the details of the first long-term cycle (LT1) that was conducted from November 1984 through May 1985. Heat recovery; operational experience; and thermal, chemical, hydrologic, and geologic aspects of LT1 are reported. The permits for long-term cycles required the addition of a monitoring well 30.5 m from the storage well for monitoring near the edge of the thermally affected area and allowed the addition of a cation-exchange water softener to enable continuous operation during the injection phase. Approximately 62 percent of the 9.47 GWh of energy added to the 9.21 x 10(exp 4) cu m of ground water stored in the aquifer LT1 was recovered. Ion-exchange water softening of the heated and stored ground water prevented scaling in the system heat exchangers and the storage well and changed the major-ion chemistry of the stored water. Temperatures at the storage horizons in site monitoring wells reached as high as 108 C during the injection phase of LT1. Following heat recovery, temperatures were less than 30 C at the same locations. Less permeable horizons underwent slow temperature changes. No thermal or chemical effects were observed at the remote monitoring site. DOE

45 ENVIRONMENT POLLUTION

Includes atmospheric, noise, thermal, and water pollution.

N92-17380# Army Construction Engineering Research Lab., Champaign, IL.
WORLDWIDE ENVIRONMENTAL COMPLIANCE ASSESSMENT AND MANAGEMENT PROGRAM (ECAMP): GERMAN SUPPLEMENT Final Report
Willi Ningelgen and Diane K. Mann Jan. 1991 136 p Supplement to AD-A242874
(AD-A242967; CERL-SR-N-91/35) Avail: NTIS HC/MF A07 CSCL 24/1

Because of the growing number of environmental laws and regulations worldwide, the U.S. Air Force has adopted an environmental compliance program that includes a mechanism to identify compliance problems before they become notices of violation by the U.S. Environmental Protection Agency or create non-compliance issues in host countries. In 1984, work began on the Environmental Compliance Assessment and Management Program (ECAMP). The concept was to combine Federal, Department of Defense, and Air Force environmental regulations, along with good management practices and risk management issues, into a series of checklists showing not only the legal requirements, but also what specific items or operations to review. In addition, each question or protocol would list a point of contact to help assessors review the protocols as easily as possible. ECAMP was extended worldwide to incorporate environmental legislation in host countries. The German ECAMP manual was developed using translations of existing legislation from the Federal Republic of Germany. GRA

N92-17393*# National Center for Atmospheric Research, Boulder, CO. Atmospheric Technology Div.
MEETING REVIEW: AIRBORNE AEROSOL INLET WORKSHOP

Darrel Baumgardner, Barry Huebert, and Chuck Wilson Jul. 1991 299 p Sponsored by NASA, Washington and NSF
(NASA-CR-189814; NAS 1.26:189814; PB91-233783; NCAR/TN-362+1A) Avail: NTIS HC/MF A13 CSCL 13B

Proceedings from the Airborne Aerosol Inlet Workshop are presented. The two central topics of discussion were the role of aerosols in atmospheric processes and the difficulties in characterizing aerosols. The following topics were discussed during the working sessions: airborne observations to date; identification of inlet design issues; inlet modeling needs and directions; objectives for aircraft experiments; and future laboratory and wind tunnel studies. GRA

N92-17551# Army Construction Engineering Research Lab., Champaign, IL.
WORLDWIDE ENVIRONMENTAL COMPLIANCE ASSESSMENT AND MANAGEMENT PROGRAM (ECAMP): UNITED KINGDOM SUPPLEMENT Final Report
Catherine Demeroukas and Diane K. Mann Jan. 1991 200 p
(AD-A242928; CERL-SR-N-91/11) Avail: NTIS HC/MF A09 CSCL 24/1

Because of the growing number of environmental laws and regulations worldwide, the U.S. Air Force has adopted an environmental compliance program that includes a mechanism to identify compliance problems before they become notices of violation by the U.S. Environmental Protection Agency or create non-compliance issues in host countries. The objectives of the ECAMP are to: (1) improve Air Force environmental management; (2) build supporting financial programs and budgets for environmental requirements; and (3) assure Major Commands (MAJCOMS), installation commanders, environmental protection committees, environmental coordinators, and bioenvironmental engineers that their environmental programs are effectively addressing environmental problems that could impact mission effectiveness, jeopardize the health or safety of Air Force personnel or the general public, significantly degrade the environment, and erode public confidence in the Air Force and the United States. GRA

N92-17598# Army Construction Engineering Research Lab., Champaign, IL.
WORLDWIDE ENVIRONMENTAL COMPLIANCE ASSESSMENT AND MANAGEMENT PROGRAM (ECAMP) Final Report
Diane K. Mann and Maj Roy Salomon Jan. 1991 378 p
(AD-A242874; CERL-SR-N-91/10) Avail: NTIS HC/MF A17 CSCL 24/1

Because of the growing number of environmental laws and regulations worldwide, the U.S. Air Force has adopted an environmental compliance program that includes a mechanism to identify compliance problems before they become notices of violation by the U.S. Environmental Protection Agency (USEPA). In 1984 work was begun on the Environmental Compliance Assessment and Management Program (ECAMP). The concept was to combine Federal, Department of Defense, and Air Force environmental regulations, along with good management practices and risk management issues, into a series of checklists showing not only the legal requirements, but also what specific items or operations to review. Objectives are: (1) Improve Air Force environmental management; (2) Build supporting financial programs and budgets for environmental requirements; (3) Assure Major Commands (MAJCOMS), installation commanders, environmental protection committees, environmental coordinators, and bioenvironmental engineers, that their environmental programs are effectively addressing environmental problems that could impact mission effectiveness, jeopardize the health of safety of Air Force personnel or the general public, degrade the environmental, and erode public confidence. GRA

N92-17619# Office of Technology Assessment, Washington, DC.
CHANGING BY DEGREES: STEPS TO REDUCE GREENHOUSE GASES Summary Report
1991 57 p
(PB91-205120) Avail: NTIS HC/MF A04 CSCL 13B

It is shown that major reductions of carbon dioxide and other greenhouse gases will require significant new initiatives by the Federal Government, by the private sector, and by individual citizens. Many of these initiatives will pay for themselves; for others, the economic cost may be considerable. Many of these efforts must be sustained over decades. Although many ancillary environmental benefits will accrue from the actions necessary to effect a major reduction of U.S. carbon dioxide emissions, such a decrease will not, in itself, significantly decrease the greenhouse effect. That level of reduction requires the world to wean itself from fossil fuels if it hopes to keep emissions from growing steeply under the combined pressure of economic and population growth. Steps taken now to use more efficient energy technologies would reduce emissions while buying time for the transition to nonfossil fuels. Author

N92-17665# Pacific Northwest Lab., Richland, WA.
EVOLUTION OF AN ENVIRONMENTAL AUDIT PROGRAM
J. H. Maday and T. L. Kuusinen Oct. 1991 8 p Presented at the Environmental Auditing Conference, Seattle, WA, 22-23 Oct. 1991
(Contract DE-AC06-76RL-01830)
(DE92-002681; PNL-SA-20109; CONF-9110275-2) Avail: NTIS HC/MF A02

Environmental audits are discussed. Within todays corporate culture, auditors and auditees alike, have been assigned stewardship over the environment. Audits provide a quality assurance check to contribute to the verification process, helping to ensure the management practices associated with the environmental management system are in place, functioning, and adequate. The objective of the audit is to help improve the effectiveness of that basic management system while at the same time determining compliance with the environmental requirements. Performing the audit in a well documented manner, using technique knowledgeable teams, will provide defendable benefits should the audit be challenged and will enhance the credibility of the existing environmental management system. DOE

N92-17723# Corps of Engineers, Seattle, WA.
AQUATIC PLANT MANAGEMENT PROGRAM. SUPPLEMENT Final Environmental Impact Statement, 1979 - 1991
Mar. 1991 178 p
(AD-A242420) Avail: NTIS HC/MF A09 CSCL 06/3

The purpose of this supplement to the Environmental Impact Statement (EIS, 1979) for the Aquatic Plant Management Program (APMP) is to review and update both the geographic and treatment-related programs in the treating of aquatic infestations of Eurasian Watermilfoil (Myriophyllum spicatum) and advancement of the state of the science of aquatic plant management. The purpose of the APMP is to prevent the spread of watermilfoil and to alleviate negative consequences of thick growth of the plant, such as diminished accessibility and desirability of water bodies for public recreational use, increased public costs for cleaning accumulations of plant material at dams, obstruction of drainage, restriction of natural water flows, reduced navigability, and damages to fish and wildlife habitats. GRA

N92-17982# National Academy of Sciences - National Research Council, Washington, DC.
POLICY IMPLICATIONS OF GREENHOUSE WARMING: REPORT OF THE ADAPTATION PANEL
Paul E. Waggoner, Jesse Ausubel, Clark Binkley, Mary M. Kritz, Joshua Lederberg, William Lewis, Jon C. Liebman, Jane Lubchenco, William D. Nordhaus, and Gordon H. Orians (Washington Univ., Seattle.) et al 1991 163 p Sponsored in part by EPA, NRC, Carnegie Corp. of NY, Charles E. Culpepper Foundation, William and Flora Hewlett Foundation, John D. and Catherine T. MacArthur Foundation, Andrew W. Mellon Foundation, Rockefeller Foundation, and Alfred P. Sloan Foundation, and the Academy Industry Program
Avail: NTIS HC/MF A08

The HUD-Independent Agencies Appropriations Act of 1988

called for a National Academy of Sciences (NAS) study on global climate change. This study should establish the scientific consensus on the rate and magnitude of climate change, estimate the projected impacts, and evaluate policy options for mitigating and responding to such changes. According to subsequent advice received from members of Congress, the NAS study was to focus on radiatively active trace gases from human sources, or 'greenhouse warming.' The work of the study was conducted by four panels. This is the report of the Adaptation Panel. The Adaptation Panel assessed the impacts of possible climate change on humanity and nature and the policies that could help people and nature adapt to those changes. The panel began its work by reviewing the literature in the field of impacts and adaptation, stressing studies of the U.S. Environmental Protection Agency (EPA) and the work in progress of the Intergovernmental Panel on Climate Change (IPCC). D.R.D.

46 GEOPHYSICS

Includes aeronomy; upper and lower atmosphere studies; ionospheric and magnetospheric physics; and geomagnetism.

For space radiation see *93 Space Radiation.*

N92-17008# Naval Postgraduate School, Monterey, CA.
WATER VAPOR INFLUENCE ON SATELLITE-MEASURED AEROSOL CHARACTERISTICS M.S. Thesis
Timothy P. Mahony Mar. 1991 52 p
(AD-A241918) Avail: NTIS HC/MF A04 CSCL 23/2

This study demonstrates the significance of water vapor's influence on satellite retrieved aerosol characteristics using NOAA's AVHRR. An improvement to optical depth and Aerosol Particle Size Index (S12) estimations derived from channels 1 (0.63 microns and 2 (0.86 microns), is made through knowledge of column water vapor derived from channels 4 (10.8 microns), and 5 (12.0 microns). A 2.0 gm sq cm column water vapor produces a 5 pct. increase in S12. This results in a 15 pct. error in the variable scattering phase function P and retrieved aerosol optical depth (delta-a). The error introduced by water vapor is quantified through use of the LOWTRAN7 atmospheric propagation model to be applied as a reformulated parameterization. GRA

N92-17035# Aerospace Corp., El Segundo, CA. Technology Operations.
RELAXATION PROCESSES OF VIBRATIONALLY EXCITED H2O IN THE MESOSPHERE AND THERMOSPHERE
V. I. Lang 1 Sep. 1991 39 p
(Contract F04701-88-C-0089)
(AD-A241853; TOR-0091(6078)-2) Avail: NTIS HC/MF A03 CSCL 07/4

A review of rate constants for the relaxation of vibrationally excited H2O is presented. This evaluation is the second in a series of reports intended to improve the state-of-knowledge regarding the chemical kinetics of the mesosphere and thermosphere. The vibrational levels discussed are limited to those presumably populated at altitudes greater than 50 km. The collision partners of interest are the major constituents in the upper atmosphere. The recommended rate constants have been implemented in the Strategic High Altitude Atmospheric Radiance Code (SHARC 2.0), which is used to calculate background infrared radiance. Recent laser induced fluorescence experiments have improved the temperature dependent data for the self relaxation of H2O and for the relaxation by O atoms. However, the temperature dependences of the relaxation pathways enabled by the dominant atmospheric species, N2 and O2 have not been well characterized. Ambient temperatures in the mesosphere and thermosphere typically range from 190 to 1300 K. We have compiled the available data for each relevant relaxation partner in order to obtain temperature functions. Where possible, a linear Landau Teller form was used. GRA

N92-17063 Oregon State Univ., Corvallis.
TURBULENT AND GRAVITY WAVE TRANSPORT IN THE FREE ATMOSPHERE Ph.D. Thesis
Jinwon Kim 1990 115 p
Avail: Univ. Microfilms Order No. DA9125152

Turbulent fluxes and related parameters in the free atmosphere are estimated from aircraft data obtained in the Severe Environmental Storms and Mesoscale Experiment (SESAME) and CABLE. Estimated eddy diffusivities and mixing lengths are found to increase rapidly with increasing gradient Richardson number (Ri) at small Ri, and then decrease more slowly at large Ri. The eddy Prandtl number increases with increasing Ri. This suggests that the generation of turbulent kinetic energy (TKE) by the pressure correlation term becomes more significant as the stability increases. A simple representation of the eddy diffusivities in the free atmosphere is proposed by using an asymptotic mixing length and a nondimensional function of Ri. The momentum flux by orographic gravity waves and the turbulent heat flux in the wave breaking regions are estimated from aircraft data sets in two days of the Alpine Experiment (ALPEX). The calculation of these fluxes allows the first direct comparison between gravity wave momentum transport models and observed fluxes. Toward this goal, the gravity wave stress supersaturation theory by Lindzen (1988) is generalized for application to vertically-varying mean flows. The wave momentum flux estimated from the generalized model agrees well with the observations for both the cases with and without a critical level. The wave breaking leads to convectively unstable regions of 10-20 km wide where the magnitude of the observed upward turbulent heat flux can be approximated by using the flux gradient relationship in which the mixing length and modified shear are derived from the generalized wave stress supersaturation condition. Author

N92-17094# Air Force Inst. of Tech., Wright-Patterson AFB, OH. School of Engineering.
SENSING REFRACTIVE TURBULENCE PROFILES USING WAVE FRONT SLOPE MEASUREMENTS FROM TWO REFERENCE SOURCES M.S. Thesis
Michael D. Rejack Dec. 1991 69 p
(AD-A243696; AFIT/GE/ENG/91D-46) Avail: NTIS HC/MF A04 CSCL 04/1

This thesis examines a remote sensing technique for measuring the atmospheric structure constant as a function of altitude by performing spatial correlation or wavefront sensor measurements. Two point sources are used to irradiate two wavefront sensors in the aperture plane of an optical system. The geometric relationship between the sources and the sensors gives rise to crossed optical paths. At the point where the paths cross, the correlation value of the turbulence contributions will be at a peak. The correlation is shown to be mathematically related to the structure constant in terms of an integral of the structure constant multiplied by a path weighting function. It is shown that the path weighting function can be made to have the characteristics of a sampling function and the value of the structure constant can be directly inferred from the correlation measurement. The vertical resolution and signal-to-noise ratio are calculated for a sample case of two-layer turbulence. GRA

N92-17134# Environmental Protection Agency, Research Triangle Park, NC. Atmospheric Sciences Modeling Div.
NOAA ATMOSPHERIC SCIENCES MODELING DIVISION SUPPORT TO THE US ENVIRONMENTAL PROTECTION AGENCY Summary Report, Fiscal Year 1990
Evelyn M. Poole-Kober, ed. and Herbert J. Viebrock, ed. Jul. 1991 76 p Sponsored by NOAA
(PB91-235499; NOAA-TM-ERL-ARL-188) Avail: NTIS HC/MF A05 CSCL 04A

During FY-1990, the Atmospheric Sciences Modeling Division provided meteorological research and operational support to the U.S. Environmental Protection Agency. Basic meteorological operational support consisted of applying dispersion models and conducting dispersion studies and model evaluations. The primary research effort was the development and evaluation of air quality

simulation models using numerical and physical techniques supported by field studies. Modeling emphasis was on the dispersion of photochemical oxidants and particulate matter on urban and regional scales, dispersion in complex terrain, and the transport, transformation, and deposition of acidic materials. Highlights included expansion of the Regional Acid Deposition Model/Engineering Model family to consist of the Tagged Species Engineering Model, the Non-Depleting Model, and the Sulfate Tracking Model; completion of the Acid-MODES field study; completion of the RADM2.1 evaluation; completion of the atmospheric processes section of the National Acid Precipitation Assessment Program 1990 Integrated Assessment; conduct of the first field study to examine the transport and entrainment processes of convective clouds; development of a Regional Oxidant Model-Urban Airshed Model interface program; conduct of an international sodar intercomparison experiment; incorporation of building wake dispersion in numerical models; conduct of wind-tunnel simulations of stack-tip downwash; and initiation of the publication of SCRAM NEWS. Author

N92-17202# California Univ., San Diego, La Jolla.
STUDIES OF HIGH-FREQUENCY SEISMIC WAVE PROPAGATION Final Report, 17 Oct 1988 - 17 May 1991
Jean-Bernard Minster and Jonathan Berger 29 Mar. 1991 187 p
(Contract F19628-88-K-0044)
(AD-A241938; PL-TR-91-2070) Avail: NTIS HC/MF A09 CSCL 08/11

This final report results are: (1) a study of the location of regional seismic events using a sparse network, with an application to eastern Kazakhstan; (2) an analysis of high frequency seismic observations collected in eastern Kazakhstan, including in particular calibration chemical explosions; (3) a study of the discrimination of quarry blasts from single explosions, using sonogram analysis of data collected in eastern Kazakhstan; (4) the extension of the discrimination methodology developed in the previous paper to small aperture array data, and application to the automated discrimination between earthquake and quarry blasts at NORESS; (5) the use of a new technique, labelled beam stack imaging, to map shallow crust scatterers near a small aperture array, with applications to NORESS; (6) a study of the polarization characteristics of high-frequency borehole seismograms recorded near Anza, California; and (7) an analysis of attenuation and site effects on high-frequency seismic waves, using high-frequency borehole seismograms recorded in the San Jacinto fault zone, near Anza, California. GRA

N92-17209# Northwest Research Associates, Inc., Bellevue, WA.
AN INVESTIGATION OF METHODS FOR UPDATING IONOSPHERIC SCINTILLATION MODELS USING TOPSIDE IN-SITU PLASMA DENSITY MEASUREMENTS Report, 1 May 1990 - 30 Apr. 1991
James A. Secan 15 May 1991 59 p
(Contract F19628-90-C-0072)
(AD-A243378; NWRA-CR-91-R072; PL-TR-91-2171; SR-1) Avail: NTIS HC/MF A04 CSCL 04/1

Modern military communication, navigation, and surveillance systems depend on reliable, noise-free transionospheric radio-frequency channels. They can be severely impacted by small-scale electron-density irregularities in the ionosphere, which cause both phase and amplitude scintillation. Basic tools used in planning and mitigation schemes are climatological in nature and thus may greatly over- and under-estimate the effects of scintillation in a given scenario. This report summarizes the results of the first year of a three-year investigation into the methods for updating ionospheric scintillation models using observations of ionospheric plasma-density irregularities measured by DMSP Scintillation Meter (SM) sensor. Results are reported from the analysis of data from a campaign conducted in January 1990 near Tromso, Norway, in which near coincident in-situ plasma-density and transionospheric scintillation measurements were made. Estimates for the level of intensity and phase scintillation on a transionospheric UHF radio link in the early-evening auroral zone were calculated from DMSP SM data and compared to the levels actually observed. GRA

N92-17227*# Rice Univ., Houston, TX.
A NUMERICAL CODE FOR A THREE-DIMENSIONAL MAGNETOSPHERIC MHD EQUILIBRIUM MODEL Final Technical Summary Report
G.-H. Voigt 4 Feb. 1992 10 p
(Grant NAGw-1781)
(NASA-CR-189852; NAS 1.26:189852) Avail: NTIS HC/MF A02 CSCL 04A

Two dimensional and three dimensional MHD equilibrium models were begun for Earth's magnetosphere. The original proposal was motivated by realizing that global, purely data based models of Earth's magnetosphere are inadequate for studying the underlying plasma physical principles according to which the magnetosphere evolves on the quasi-static convection time scale. Complex numerical grid generation schemes were established for a 3-D Poisson solver, and a robust Grad-Shafranov solver was coded for high beta MHD equilibria. Thus, the effects were calculated of both the magnetopause geometry and boundary conditions on the magnetotail current distribution. Author

N92-17229# Geological Survey, Denver, CO.
WORKSHOP ON GEOLOGIC APPLICATIONS OF MODERN AEROMAGNETIC SURVEYS
William F. Hanna, ed. 1990 111 p Workshop held in Lakewood, CO, 6-8 Jan. 1987
(PB91-221788; USGS-BULL-1924) Avail: NTIS HC/MF A06 CSCL 08G

A workshop entitled 'Geologic Applications of Modern Aeromagnetic Surveys,' sponsored by the U.S. Geological Survey, was conducted 6-8 Jan. 1987. The motivation for the workshop was based on the strong commitment of the U.S. Geological Survey to develop knowledge about efficient techniques for assessing mineral, fuel, and groundwater resources as well as geologic hazards. Some of the most efficient of these techniques are those which utilize airborne systems because of speed of coverage and almost unlimited accessibility. The subject workshop focused on a technique that has a proven track record and that has been extensively developed, utilized, and promoted by the U.S. Geological Survey over a 45-year period: aeromagnetic surveying. Many advances have been made since the original implementation of aeromagnetic surveys, some of which relate to the development of new instrumentation and others of which relate to the formulation of new concepts that bear on data acquisition, processing, interpretation, and display. Author

N92-17239# Mission Research Corp., Nashua, NH.
BACKGROUND ATMOSPHERE RADIANCE DAY (BARD) AND NIGHT (BARN) Technical Report, 14 Mar. 1990 - 15 Apr. 1991
R. A. Armstrong, S. B. Downer, J. P. Kennealy, R. J. Larkin, and S. P. McGowan 1 Dec. 1991 138 p
(Contract DNA001-88-C-0029)
(AD-A243153; MRC/NSH-91-0002; DNA-TR-91-97) Avail: NTIS HC/MF A07 CSCL 17/5

This document describes the format, the details, and methods used to calculate the BACKGROUND ATMOSPHERE RADIANCE DAY (BARD) and NIGHT (BARN) data bases. BARD/BARN (v4.1), in tabular ASCII form, consists of 57 bins, each 5 percent in energy, spanning 1.9 to 34 micron. BARD/BARN (v4.1) is now available and is being used within fast running codes such as IRSim, HiSEMM, and SCENARIO. ARCHON was used to determine the non-local thermodynamic equilibrium quantum state populations for tangent altitudes starting at 40 km up to 200 km. The radiation transport code NLTE was then used to determine the line-of-sight radiance within each bin for the 75 transitions occurring for CO2, H2O, CO, NO, and O3. For LTE atmosphere, MODTRAN was used for the tangent altitudes from 60 km to 0.1 km. The procedure merging the overlapped portions of the NLTE and LTE data is described. Graphical representations of the BARD/BARN data are appended for user reference. GRA

N92-17405# Lockheed Missiles and Space Co., Palo Alto, CA. Space Sciences Lab.
INVESTIGATION OF MECHANISMS FOR THE SOURCE AND LOSS OF ELECTRONS FROM THE RADIATION BELTS USING DATA FROM SEEP, SCATHA AND P78-1 SATELLITES Final Report, May 1988 - Nov. 1991
W. L. Imhof, D. W. Datlowe, H. D. Voss, and J. Mobilia 19 Nov. 1991 112 p
(Contract N00014-88-C-0033)
(AD-A243376) Avail: NTIS HC/MF A06 CSCL 04/1

Electron precipitation into the atmosphere entails ionospheric effects that have important consequences for radiowave propagation. Under this contract satellite data as well as ground based measurements have been used to evaluate the source and loss mechanisms for electrons trapped in the radiation belts. With data from the SEEP satellite payload a study was made of short duration (less than 0.6 sec) microbursts of electrons from the radiation belts. Several of the electron bursts observed at nighttime were correlated with lightning generated whistlers. A seasonal variation was found for the occurrence in precipitating inner belt electrons with peaks in the energy spectra. The fluxes of relativistic electrons precipitating into the atmosphere were found to be correlated with the fluxes of relativistic electrons at high altitudes. To investigate whether wave-particle interactions are responsible for triggering relativistic electron microbursts, an examination was made of wave data recorded at Siple Station at times when the SEEP satellite was near Siple or its conjugate point. The wave data indicate that many of the bursts may not be due to wave-particle interactions. GRA

N92-17542# Cologne Univ. (Germany, F.R.). Inst. fuer Geophysik und Meteorologie.
SPATIAL SAMPLING ERROR OF A SCANNING RADIATION BUDGET RADIOMETER Ph.D. Thesis [RAEUMLICHER STICHPROBENFEHLER EINES ABTASTENDEN STRAHLUNGSBILANZRADIOMETERS]
Petro Maria Udelhofen 1990 130 p In GERMAN; ENGLISH summary
(Contract BMFT-07-KF-1113)
(Mitt-76; ISSN-0069-5882; ETN-92-90594) Avail: NTIS HC/MF A07

Simulations of ERBE (Earth Radiation Budget Experiment) scanner measurements were performed to investigate the spatial sampling error of regional averaged radiation fluxes. Meteosat data with a spatial resolution of 0.04 deg were used for the description of the true radiation field. Regional means were calculated by weighting and arithmetically averaging the simulating ERBE scanner measurements. The optimal estimate can be derived by taking a phase shifted spatial filter as a weighting function. The phase shift of the distribution of weights varies with scan angle of the region and is related to the phase shift of the point spread function. Analyses of sampling error of the arithmetic estimates for different scene types show in most cases overestimations of short wave and underestimations of long wave fluxes. The total error of the arithmetic estimate varies between 5 and 31 W/sq m in the short wave region, and between 2 and 20 W/sq m in the long wave region. ESA

N92-17578# Lawrence Livermore National Lab., CA.
APPLICATION OF LINEAR INVERSE THEORY TO BOREHOLE GRAVITY DATA
N. R. Burkhard Sep. 1991 26 p Presented at the 6th Symposium on Containment of Underground Nuclear Explosions, Reno, NV, 24-26 Sep. 1991
(Contract W-7405-eng-48)
(DE92-002172; UCRL-JC-106782; CONF-9109114-5) Avail: NTIS HC/MF A03

Traditional borehole gravity interpretations are based upon an earth model which assumes horizontal, laterally infinite, uniformly thick, and constant density layers. I apply discrete stabilized linear inverse theory to determine the density distribution directly from borehole gravity observations that have been corrected for drift, tide, and terrain. The stabilization is the result of including a priori data about the free-air gradient and the density structure in the inversion process. The discrete generalized linear inverse approach enables one to solve for a density distribution using all of the borehole gravity data. Moreover, the data need not be free-air corrected. An important feature of the approach is that density estimates are not required to be density averages between adjacent borehole gravity observations as in the traditional method. This approach further permits the explicit incorporation of independent density information from gamma-gamma logging tools or laboratory core measurements. Finally, explicit linear constraints upon the density and/or free-air gradient can also be handled. The non-uniqueness of the density structure determined by the inversion process is represented in a resolution matrix. DOE

N92-17961# Massachusetts Inst. of Tech., Cambridge. Haystack Observatory.
RADAR-SATELLITE STUDIES OF THE HIGH-LATITUDE IONOSPHERE Annual Progress Report No. 2, Aug. 1990 - Aug. 1991
John C. Foster 9 Oct. 1991 6 p
(Grant AF-AFOSR-0454-89; AF Proj. 2310)
(AD-A243275; AFOSR-91-0914TR) Avail: NTIS HC/MF A02 CSCL 04/1

During the second year of this research program, work has continued on multi-instrument experiments investigating the effects of the large scale convection electric field in the auroral and midlatitude ionosphere. A radar satellite study of electric field latitude structure during the February 8 to 9, 1986 great magnetic storm was completed and has provided an excellent example of the application of multi-instrument techniques to the investigation of magnetosphere-ionosphere coupling problems. Studies of the high latitude boundary between auroral and polar cap latitudes have emphasized convection and ionospheric plasma structure near the dayside cusp and the transport of ionospheric plasma into the polar cap during storms. Mesoscale resolution electric field structure was addressed in a multi-instrument study involving the Canadian BARS radar facility and the Millstone Hill incoherent scatter radar. GRA

47 METEOROLOGY AND CLIMATOLOGY

Includes weather forecasting and modification.

N92-16990*# Tennessee Applied Physical Sciences, Inc., Fayetteville.
WIND PROFILER SIGNAL DETECTION IMPROVEMENTS Final Report, Aug. 1991 - Jan. 1992
G. F. Hart and Dale H. Divis Jan. 1992 78 p
(NASA Order H-08074-D)
(NASA-CR-189781; NAS 1.26:189781; TAPS-010-1992) Avail: NTIS HC/MF A05 CSCL 04B

Research is described on potential improvements to the software used with the NASA 49.25 MHz wind profiler located at Kennedy Space Center. In particular, the analysis and results are provided of a study to (1) identify preferred mathematical techniques for the detection of atmospheric signals that provide wind velocities which are obscured by natural and man-made sources, and (2) to analyze one or more preferred techniques to demonstrate proof of the capability to improve the detection of wind velocities.
Author

N92-17009# Army Field Artillery School, Fort Sill, OK.
BATTLEKING EVALUATION, BK 22-91, METEOROLOGICAL SENSOR PACKAGE (MSP) Final Report
Christine M. Johnson 24 Sep. 1991 18 p
(AD-A241919; BK-22-91) Avail: NTIS HC/MF A03 CSCL 04/2

This is a letter report covering the MSP BATTLEKING Evaluation conducted at Fort Sill, Oklahoma, 14-16 May 1991. The MSP was evaluated to determine if it could provide the data for a nine-line meteorological message and provide low level wind data for the multiple launch rocket system. The MSP produced a nine-line met message based on surface readings taken by the sensor assembly

for wind direction, wind speed, temperature, and pressure. The MSP generated messages were compared to the meteorological data systems' messages. Although the suitability of the MSP, as an alternative to the MDS system, could not be thoroughly assessed, the MSP does provide an approximation of the current met effects as contrasted to the NATO standard of no wind direction, no wind speed, and standard temperature and pressure. GRA

N92-17027# Naval Underwater Systems Center, West Palm Beach, FL.
A STATISTICAL ANALYSIS OF ELEUTHERA ISLAND WIND DATA FOR THE PERIOD 27 APRIL 1989 THROUGH 30 MARCH 1990
J. C. Park and J. J. Hinkamp 1 Jul. 1991 58 p
(AD-A241885; NUSC-TD-7016) Avail: NTIS HC/MF A04 CSCL 04/2

This document presents a statistical analysis of wind data obtained at Eleuthera Island, Bahamas, during the period between April 1989 and March 1990. The analysis is limited to empirically determined probability distribution and density functions, first- and second-moment estimators, and one-dimensional Fourier transforms, appropriately averaged for power spectral estimates. Broad conclusions are drawn about the variability of wind speed, the predominant wind direction, and the pattern of wind speed during specified intervals. GRA

N92-17028# Massachusetts Inst. of Tech., Lexington. Lincoln Lab.
TERMINAL DOPPLER WEATHER RADAR TEST BED OPERATION, ORLANDO: JANUARY-JUNE 1990 Semiannual Report, 1 Jan. - 30 Jun. 1990
David M. Bernella 4 Nov. 1991 112 p
(Contracts F19628-90-C-0001; DTFA01-L-83-4-10579)
(AD-A242890; ATC-180) Avail: NTIS HC/MF A06 CSCL 17/9

This semiannual report for the Terminal Doppler Weather Radar program, sponsored by the Federal Aviation Administration (FAA), covers the period from 1 January 1990 through 30 June 1990. The principal activity of this period was the transport and reassembly of the FL-2 weather radar test site from Kansas City, MO to Orlando, FL and the change of radar frequency from S-band used in Kansas City to C-band for Orlando operations. Site operations to prepare the FL-2C radar site for summer testing began in January and continued through May, when testing began. This report describes the RF hardware, the data collection, the computer systems at site, and the networks between Orlando, FL and Lexington, MA. Also included are discussions of the microburst and gust front algorithm development, data collection, display terminals, and training for Air Traffic Control (ATC) supervisors and controllers. GRA

N92-17050# Massachusetts Inst. of Tech., Lexington. Lincoln Lab.
ANALYSIS OF THE TERMINAL DOPPLER WEATHER RADAR ALGORITHM FOR DETECTING ROTATION ASSOCIATED WITH MICROBURSTS
Valerie C. Coel 25 Oct. 1991 81 p
(Contract DTFA01-89-Z-02033)
(AD-A242840; ATC-183; DOT/FAA/NR-91/9) Avail: NTIS HC/MF A05 CSCL 17/9

Rotating winds aloft occurring with downdrafts often are associated with microbursts, which are serious aviation hazards. The Terminal Doppler Weather Radar system detects microbursts and warns pilots of windshear events, partly by its use of rotation as precursors. The role of the rotation region detection algorithm in this system is described, and the improvements to it are analyzed using measured data and simulated rotation regions. The final results show a substantial overall decrease in the number of false detections generated by the algorithm due to adjustment of thresholds and additional logic, while still retaining a good probability of microburst rotation region detection (84 percent). Ideas for future enhancement are explored through techniques such as discriminant analysis and environmental wind filtering. GRA

N92-17072*# National Oceanic and Atmospheric Administration, Boulder, CO. Wave Propagation Lab.
RECOMMENDATIONS FOR A WIND PROFILING NETWORK TO SUPPORT SPACE SHUTTLE LAUNCHES Final Report
R. J. Zamora Washington NASA. Marshall Space Flight Center Feb. 1992 50 p
(NASA Order H-59348-B)
(NASA-CR-4421; M-678; NAS 1.26:4421) Avail: NTIS HC/MF A03 CSCL 04B

The feasibility is examined of a network of clear air radar wind profilers to forecast wind conditions before Space Shuttle launches during winter. Currently, winds are measured only in the vicinity of the shuttle launch site and wind loads on the launch vehicle are estimated using these measurements. Wind conditions upstream of the Cape are not monitored. Since large changes in the wind shear profile can be associated with weather systems moving over the Cape, it may be possible to improve wind forecasts over the launch site if wind measurements are made upstream. A radar wind profiling system is in use at the Space Shuttle launch site. This system can monitor the wind profile continuously. The existing profiler could be combined with a number of radars located upstream of the launch site. Thus, continuous wind measurements would be available upstream and at the Cape. NASA-Marshall representatives have set the requirements for radar wind profiling network. The minimum vertical resolution of the network must be set so that the wind shears over the depths greater than or = 1 km will be detected. The network should allow scientists and engineers to predict the wind profile over the Cape 6 hours before a Space Shuttle launch. Author

N92-17073# Air Force Environmental Technical Applications Center, Scott AFB, IL.
SURFACE OBSERVATION CLIMATIC SUMMARIES FOR DUKE FIELD/EGLIN AUX NO. 3, FLORIDA Data Summary, Sep. 1949 - Mar. 1991
Sep. 1991 362 p
(AD-A243310; USAFETAC/DS-91/252) Avail: NTIS HC/MF A16 CSCL 04/2

Surface observation climatic summaries (SOCS) provide statistical climatic summaries of surface weather observations taken and recorded at specified observing stations. Hourly observations are summarized from a 10-year period of record. Climatology, meteorological data, meteorological phenomena, weather, ceiling, cloud cover, snow depth, humidity, barometric pressure, atmospheric precipitation, snow, atmospheric temperature, visibility, and wind are included in this report. GRA

N92-17074# Air Force Environmental Technical Applications Center, Scott AFB, IL.
SURFACE OBSERVATION CLIMATIC SUMMARIES FOR CASTLE AFB, CALIFORNIA
Sep. 1991 366 p
(AD-A243677; USAFETAC/DS-91/253) Avail: NTIS HC/MF A16 CSCL 04/2

Surface observation climatic summaries (SOCS) provide climatic summaries of surface weather observation taken and recorded at specified observing stations. Hourly observations are summarized from a 10-year period of record. Climatology, meteorological data, meteorological phenomena, weather, ceiling, cloud cover, snow depth, humidity, barometric pressure, atmospheric precipitation, snow, atmospheric temperature, visibility, and wind are included in this report. GRA

N92-17113# Air Force Environmental Technical Applications Center, Scott AFB, IL.
RANGE REFERENCE ATMOSPHERE, FAIRBANKS
Feb. 1991 153 p
(AD-A243314; USAFETAC/PR-91/007) Avail: NTIS HC/MF A08 CSCL 04/2

This range reference atmosphere (RRA) is a statistical model

(derived from upper-air observations) of the atmosphere from 0 to 30 km over the Fairbanks range complex. The RRA provides tabulations of monthly and annual means, standard deviations, and skewness coefficients for wind speed, pressure, temperature, density, water vapor pressure, virtual temperature, and dew point temperature. It also gives means and standard deviation for the zonal and meridional wind components and hydrostatic model atmosphere. Methodology is included, along with graphic displays of wind statistics that can be derived from the wind data. GRA

N92-17138# National Oceanic and Atmospheric Administration, Miami, FL. Oceanographic and Meteorological Lab.
SURFACE METEOROLOGICAL AND NEAR SURFACE OCEANOGRAPHIC ATLAS OF THE TROPICAL INDIAN OCEAN
R. R. Rao (Naval Physical and Oceanographic Lab., Cochin, India), R. L. Molinari, and J. F. Festa Jun. 1991 65 p
(PB91-234286; NOAA-TM-ERL-AOML-69) Avail: NTIS HC/MF A04 CSCL 04B

Historical observations of surface marine meteorology (COADS: 1950-1979), near surface vertical thermal structure (MOODS: 1948-1981), and near surface ship drift (Culter and Swallow, 1984: 1854-1974) for the tropical Indian Ocean are compiled to generate mean monthly climatologies of several observed and derived parameters on a 2 degree x 2 degree grid. The derived parameters include surface heat exchanges, surface wind stress and its curl, mixed layer depth (MLS), vertical thermal gradient just beneath the mixed layer, depth of 20C isotherms, and zonal and meridional near surface flow patterns. The formulations used in the derivation of these quantities are also presented. The resultant climatological fields are machine contoured. The annual cycle of many of the fields are presented in terms of amplitude and phase of the annual and semi-annual harmonics. Author

N92-17144# Air Force Environmental Technical Applications Center, Scott AFB, IL.
SURFACE OBSERVATION CLIMATIC SUMMARIES FOR HONDO MUNICIPAL AIRPORT, TEXAS Data Summary, Oct. 1942 - Jun. 1991
Oct. 1991 355 p
(AD-A243311; USAFETAC/DS-91/255) Avail: NTIS HC/MF A16 CSCL 04/2

Surface observation climatic summaries (SOCS) provide statistical climatic summaries of surface weather observations taken and recorded at specified observing stations. Hourly observations are summarized from a 10-year period of record. Climatology, meteorological data, meteorological phenomena, weather, ceiling, cloud cover, snow depth, humidity, barometric pressure, atmospheric precipitation, snow, atmospheric temperature, visibility, and wind are included in this report. GRA

N92-17233# Phillips Lab., Hanscom AFB, MA.
A PROPOSED IMPROVED METHOD OF RADIOSONDE HUMIDITY SENSING Environmental Research Papers
James F. Morrissey 12 Apr. 1991 19 p
(AD-A242954; AD-E200776; PL-TR-91-2075; ERP-1081) Avail: NTIS HC/MF A03 CSCL 04/2

The carbon humidity element has been used in most U.S. radiosonde flights for the past twenty-five to thirty years. Although it is arguably the best radiosonde humidity sensor in use, the carbon element has physical characteristics that result in significant measurement errors as employed in today's synoptic radiosonde flights. The principal characteristics causing errors are its requirement to be in temperature equilibrium, its poor time response at low temperatures, and its poor sensitivity at low relative humidities. A proposal is made to employ the carbon element in a servo loop designed to control the temperature of the element in such a way as to maintain the measured relative humidity at 33 percent. The temperature of the element will then be used to determine either dew point or the partial pressure due to water vapor. This method will eliminate or significantly reduce the errors arising from the main error source and from some others as well. GRA

N92-17257# Air Force Environmental Technical Applications Center, Scott AFB, IL.
SURFACE OBSERVATION CLIMATIC SUMMARIES FOR BOISE AIR TERMINAL, ID Report, Jan. 1948 - Nov. 1990
May 1991 367 p
(AD-A243012; USAFETAC/DS-91/244) Avail: NTIS HC/MF A16 CSCL 04/2

Surface observation climatic summaries (SOCS) provide statistical climatic summaries of surface weather observations taken and recorded at specified observing stations. Hourly observations are summarized from a 10-year period of record. This report includes climatology, meteorological data, weather, ceiling, cloud cover, snow depth, humidity, precipitation, snow, visibility, and wind. GRA

N92-17289# ST Systems Corp., Lexington, MA.
FRONT DETECTION WITH DOPPLER RADAR
Donald Hamann 15 Feb. 1991 31 p
(Contract F19628-87-C-0124)
(AD-A242880; PL-TR-91-2034; SR-3) Avail: NTIS HC/MF A03 CSCL 17/9

A technique to detect wind discontinuities associated with gust and synoptic fronts is discussed. It first transforms the Doppler velocity and reflectivity data into gradient vector fields by applying a series of templates to the data. From these vector fields, regions with large gradient magnitudes are isolated and edges or contours extracted where both the magnitude and direction information are used. A bi-directional search orthogonal to the local gradient vector is performed to extract lines of strong gradients. A multiplicity of somewhat parallel lines are often produced, with these being reduced to a single line through the selection of the most significant of these lines. The technique utilized in this study is a fast, efficient means of detecting large gradient regions in any two-dimensional field. It has been successfully applied to both Doppler velocity and reflectivity factor fields. It is shown that individual analyses of these two fields results in only partial detection of the feature. However, when they are combined into a single product, the result is a continuous depiction. This latter product is readily amendable for the application of a variety of forecast tools. GRA

N92-17338# Naval Oceanographic and Atmospheric Research Lab., Monterey, CA.
SEVERE WEATHER GUIDE MEDITERRANEAN PORTS. PART 35: ROTA
R. E. Englebretson, R. D. Gilmore, and D. C. Perryman Jun. 1991 72 p
(AD-A243539; NOARL-TN-111) Avail: NTIS HC/MF A04 CSCL 04/2

This handbook for the port of Rota, Spain, one in a series of severe weather guides for Mediterranean ports, provides decision making guidance for ship captains whose vessels are threatened by actual or forecast strong winds, high seas, restricted visibility or thunderstorms in the port vicinity. Causes and effects of such hazardous conditions are discussed. Precautionary or evasive actions are suggested for various vessel situations. The handbook is organized in four sections for ready reference: general guidance on handbook content and use; a quick-look captain's summary; a more detailed review of general information on environmental conditions; and an appendix that provides oceanographic information. GRA

N92-17363# National Weather Service, Bohemia, NY. Scientific Services Div.
THE USE OF ADAP TO EXAMINE WARM AND QUASI-STATIONARY FRONTAL EVENTS IN THE NORTHEASTERN UNITED STATES
David R. Vallee (National Weather Service, Providence, RI.) Jul. 1991 78 p
(PB91-225037; NOAA-TM-NWS-ER-85) Avail: NTIS HC/MF A05 CSCL 04B

Some topics of discussion are labelled as follows: Approach/Methodology; Case Studies (4.1 Warm/Quasi Stationary

Front, 4.2 Slow Moving Warm Front, 4.3 Fast Moving Warm Front, 4.4 Multiple Warm and Quasi Stationary Front, 4.5 Developing Wave on a Front); and Cautions and Limitations. Author

N92-17400# Air Force Environmental Technical Applications Center, Scott AFB, IL.
SURFACE OBSERVATION CLIMATIC SUMMARIES FOR FAIRBANKS IAP, ALASKA Data Summary, Jul. 1948 - Dec. 1990
Jul. 1991 366 p
(AD-A243309; USAFETAC/DS-91/250) Avail: NTIS HC/MF A16 CSCL 04/2

Surface observation climatic summaries (SOCS) provide statistical climatic summaries of surface weather observations taken and recorded at specified observing stations. Hourly observations are summarized from a 10-year period of record. Climatology, meteorological data, meteorological phenomena, weather, ceiling, cloud cover, snow depth, humidity, barometric pressure, atmospheric precipitation, snow, atmospheric temperature, visibility, and wind are included in this report. GRA

N92-17406# Naval Oceanographic and Atmospheric Research Lab., Monterey, CA.
SEVERE WEATHER GUIDE MEDITERRANEAN PORTS. PART 38: ALEXANDRIA Final Report
R. E. Englebretson and D. C. Perryman Jun. 1991 67 p
(AD-A243451; NOARL-TN-114) Avail: NTIS HC/MF A04 CSCL 04/2

This handbook for the port of Alexandria, one in a series of severe weather guides for Mediterranean ports, provides decision making guidance for ship captains whose vessels are threatened by actual or forecast strong winds, high seas, restricted visibility or thunderstorms in the port vicinity. Causes and effects of such hazardous conditions are discussed. Precautionary or evasive actions are suggested for various vessel situations. The handbook is organized in four sections for ready reference: general guidance on handbook content and use; a quick-look captain's summary; a more detailed review of general information on environmental conditions; and an appendix that provides oceanographic information. GRA

N92-17444# Air Force Environmental Technical Applications Center, Scott AFB, IL.
SURFACE OBSERVATIONS CLIMATIC SUMMARIES FOR CAMP HUMPHREYS, KOREA Report, Mar. 1951 - Dec. 1990
Jun. 1991 375 p
(AD-A241937; USAFETAC/DS-91/248) Avail: NTIS HC/MF A16 CSCL 04/2

Surface Observation Climatic Summaries (SOCS) provide statistical climatic summaries of surface weather observations taken and recorded at specified USAF, civilian and foreign observing stations. Hourly observations are summarized from a 10-year period of record. Summary of day information is summarized from all available data in the OL-A, USAFETAC climatic database. Topics/data include: Climatology; Meteorological phenomena; Cloud cover; Snow depth; Humidity; Barometric pressure; Atmospheric precipitation; Snow temperature; Visibility. GRA

N92-17492# Naval Oceanographic and Atmospheric Research Lab., Monterey, CA.
SEVERE WEATHER GUIDE MEDITERRANEAN PORTS. PART 36: LIMASSOL
R. E. Englebretson, R. D. Gilmore, and D. C. Perryman Jun. 1991 63 p
(AD-A243448; NOARL-TN-112) Avail: NTIS HC/MF A04 CSCL 04/2

This handbook for the port of Limassol, Cyprus, one in a series of severe weather guides for Mediterranean ports, provides decision making guidance for ship captains whose vessels are threatened by actual or forecast strong winds, high seas, restricted visibility or thunderstorms in the port vicinity. Causes and effects of such hazardous conditions are discussed. Precautionary or evasive actions are suggested for various vessel situations. The handbook is organized in four sections for ready reference: general guidance on handbook content and use; a quick-look captain's summary; a more detailed review of general information on environmental conditions; and an appendix that provides oceanographic information. GRA

N92-17493# Naval Oceanographic and Atmospheric Research Lab., Monterey, CA.
SEVERE WEATHER GUIDE MEDITERRANEAN PORTS. PART 37: LARNACA
R. E. Englebretson, R. D. Gilmore, and D. C. Perryman Jun. 1991 66 p
(AD-A243449; NOARL-TN-113) Avail: NTIS HC/MF A04 CSCL 04/2

This handbook for the port of Larnaca, Cyprus, one in a series of severe weather guides for Mediterranean ports, provides decision making guidance for ship captains whose vessels are threatened by actual or forecast strong winds, high seas, restricted visibility or thunderstorms in the port vicinity. Causes and effects of such hazardous conditions are discussed. Precautionary or evasive actions are suggested for various vessel situations. The handbook is organized in four sections for ready reference: general guidance on handbook content and use; a quick-look captain's summary; a more detailed review of general information on environmental conditions; and an appendix that provides oceanographic information. GRA

N92-17494# Naval Oceanographic and Atmospheric Research Lab., Monterey, CA.
SEVERE WEATHER GUIDE MEDITERRANEAN PORTS. PART 39: PORT SAID
R. E. Englebretson and D. C. Perryman Jun. 1991 71 p
(AD-A243450; NOARL-TN-115) Avail: NTIS HC/MF A04 CSCL 04/2

This handbook for the port of Port Said, Egypt, one in a series of severe weather guides for Mediterranean ports, provides decision making guidance for ship captains whose vessels are threatened by actual or forecast strong winds, high seas, restricted visibility or thunderstorms in the port vicinity. Causes and effects of such hazardous conditions are discussed. Precautionary or evasive actions are suggested for various vessel situations. The handbook is organized in four sections for ready reference: general guidance on handbook content and use; a quick-look captain's summary; a more detailed review of general information on environmental conditions; and an appendix that provides oceanographic information. GRA

N92-17515# Naval Postgraduate School, Monterey, CA.
HIGH-FREQUENCY METEOROLOGICAL PHENOMENA OBSERVED WITH THE NAVAL POSTGRADUATE SCHOOL'S UHF DOPPLER WIND PROFILER M.S. Thesis
Daniel H. Streed Dec. 1990 134 p
(AD-A243762) Avail: NTIS HC/MF A07 CSCL 17/9

A UHF clear-air Doppler radar wind profiler was purchased by the Naval Postgraduate School and began operation in late-March of 1990. The identification of numerous meteorological phenomena using UHF Doppler radar wind profilers has been successfully documented; however, published work to-date has concentrated on interpretation of hourly-consensus data. But with the onset of improved technology, it is now possible to retrieve reliable data within the hourly period. This study examines the quality of the six-minute data through statistical analysis and determines the overall accuracy of the School's profiler. Specifically, the performance of the profiler is compared with rawinsonde data, other profiler comparison studies, as well as the contract specifications. This study also looks at overall performance of UHF Doppler radar profiler in an environment characterized by a strong marine inversion. Finally the study presents evidence that meteorological phenomena which exhibits time scales on the order of minutes can be observed using the six-minute profiler data. GRA

N92-17543# Cologne Univ. (Germany, F.R.). Inst. fuer Geophysik und Meteorologie.
NUMERICAL STUDIES OF PROCESSES IN STRATIFORM CIRRUS
Ying Zhang 1990 99 p
(Contract BMFT-KF-111)
(Mitt-78; ISSN-0069-5882; ETN-92-90595) Avail: NTIS HC/MF A05

A microphysical radiative cloud model is developed to represent the temporal evolution of stratiform ice clouds. The microphysical properties of the cloud model are evaluated based on diffusional growth and gravitational sedimentation of ice particles of inhomogenous size. Various environmental influences such as the ascending motion in air, radiation, and air moisture are considered in the model. The evolution of stratiform cirrus clouds is simulated for various ambient field cases. The results demonstrate the changes in microphysical properties and structure of the cloud as well as the changes in the ambient fields. ESA

N92-17621# National Hurricane Center, Coral Gables, FL.
DIAGNOSTIC REPORT OF THE NATIONAL HURRICANE CENTER, AUGUST AND SEPTEMBER 1990, VOLUME 3, NUMBER 2
C. J. McAdie and E. N. Rappaport 1990 90 p
(PB91-226886) Avail: NTIS HC/MF A05 CSCL 04B

An overview is given of tropical activity for August and September 1990. Information is given on mean flow patterns for the Atlantic and eastern Pacific basins; and tropical cyclone activity in the Atlantic basin. Detailed information is given for a number of named hurricanes. Author

N92-17631# Colorado State Univ., Fort Collins. Dept. of Atmospheric Science.
NUMERICAL SIMULATION OF CIRRUS CLOUDS: FIRE CASE STUDY AND SENSITIVITY ANALYSIS
Scot T. Heckman 12 Aug. 1991 142 p
(Grant AF-AFOSR-0143-88)
(AD-A242902; CSU-ATSP-483; AFOSR-91-0776TR) Avail: NTIS HC/MF A07 CSCL 04/2

The October 28, 1986 FIRE (First ISCCP Regional Experiment) case was simulated using the Regional Atmospheric Modeling System. This three dimensional, mesoscale model was applied in non-hydrostatic and nested-grid mode using explicit, bulk microphysics and radiation. The simulation resulted in very good agreement between observed and model predicted dynamic and cloud fields. We verified cloud height, thickness, areal extent, and microphysical composition against GOES satellite imagery, lidar, and aircraft measurements taken during the FIRE Cirrus IFO (Intensive Field Observation). The simulated cirrus lifecycle is examined to determine possible formation, maintenance and dissipation mechanisms. Sensitivity simulations were run to determine long and short wave radiative forcing. Also, a simulation was run with no condensate to examine cloud feedbacks on the environment. Cloud top generation zones, fallstreaks, and layering were simulated. Longwave radiation appeared to be instrumental in developing weak convective activity in the lower layer thereby increasing it's optical depth. Cloud top cooling and cloud base heating affected the flow around the cloud. Secondarily, the effects of three upper boundary conditions on cirrus clouds were studied in a synoptic setting. GRA

N92-17705# Science Applications International Corp., La Jolla, CA.
THE NATIONAL HURRICANE CENTER RISK ANALYSIS PROGRAM (HURISK)
Charles J. Neumann Aug. 1991 64 p
(Contract NOAA-50-DCNC-6-00209)
(PB91-236463; NOAA-TM-NWS-NHC-38) Avail: NTIS HC/MF A04 CSCL 04B

The National Hurricane Center (NHC) has developed a computerized model for assessing the long-term vulnerability of coastal areas to tropical cyclone events. Program output, essentially graphical, is in the form of 18 charts and diagrams. These charts depict tropical cyclone tracks, motion, intensity, and wind return periods for any coastal or near-coastal site over the Atlantic tropical cyclone basin. For input, the program accesses current NHC files of historical tropical cyclone data. Program output can therefore be updated as the need arises. The publication is intended primarily as a user's manual, describing the utility of the various charts. However, minor technical discussion, as warranted by individual chart complexity, is also given. A major technical discussion, contained in an Appendix, describes derivation of tropical cyclone return periods using a Monte-Carlo simulation procedure. Author

N92-17764# Naval Postgraduate School, Monterey, CA. Dept. of Operations Research.
PRELIMINARY RESULTS FROM THE ANALYSIS OF WIND COMPONENT ERROR
Donald P. Gaver and Patricia A. Jacobs Sep. 1991 138 p
(AD-A243772; NPSOR-91-029) Avail: NTIS HC/MF A07 CSCL 04/2

Estimation of mean square prediction error of wind components is required in the optimal interpolation (OI) process in numerical prediction of atmospheric variables. Statistical models with log-linear scale parameters which include covariates are described for the prediction error. Data from February and April of 1991 are used to fit the model parameters and to study the predictive ability of the models. This preliminary investigation indicates that observational and first guess wind components can be helpful in predicting mean square prediction error for wind components. GRA

N92-17853 ESDU International Ltd., London (England).
MEAN WIND SPEEDS OVER HILLS AND OTHER TOPOGRAPHY
Dec. 1991 41 p
(ESDU-91043; ISBN-0-85679-805-3; ISSN-0143-2702) Avail: ESDU

ESDU 91043 presents methods for estimating speed-up factors for mean wind speeds over hills, embankments, escarpments, and valleys. The methods treat all regions of a hill, including shelter regions near the foot and account for the local profile. Three-dimensional effects and wind inclination to the ridge line can be taken into account. Interference effects from other nearby topography can be assessed, and guidance is provided for the effects of flow separation on steep topography. Two methods are given: a simple graphical approach that is accurate for simple embankments but is less accurate for rounded hills because it only accounts for the overall shape, and a more precise method that accounts for the detailed shape of the hill. Irregularly-shaped hills with bulges and depressions, and multiple hills, are treated by the method of superposition, that is, each irregularity is treated as a separate isolated hill or valley and the contribution to speed up added to the other contributions for an overall solution. The methods were derived from data obtained using solutions of the Navier-Stokes equations, calibrated against both full-scale and wind-tunnel measurements. Author

N92-17975*# Illinois State Water Survey, Champaign. Office of Climate and Meteorology.
A VARIATIONAL ASSIMILATION METHOD FOR SATELLITE AND CONVENTIONAL DATA: DEVELOPMENT OF BASIC MODEL FOR DIAGNOSIS OF CYCLONE SYSTEMS Ffinal Report
Gary L. Achtemeier, Robert W. Scott, and J. Chen Jun. 1991 163 p
(Grant NAG8-59)
(NASA-CR-188236; NAS 1.26:188236) Avail: NTIS HC/MF A08 CSCL 04B

A summary is presented of the progress toward the completion of a comprehensive diagnostic objective analysis system based upon the calculus of variations. The approach was to first develop the objective analysis subject to the constraints that the final product satisfies the five basic primitive equations for a dry inviscid atmosphere: the two nonlinear horizontal momentum equations, the continuity equation, the hydrostatic equation, and the

thermodynamic equation. Then, having derived the basic model, there would be added to it the equations for moist atmospheric processes and the radiative transfer equation. For individual titles, see N92-17976 through N92-17981.

N92-17976*# Illinois State Water Survey, Champaign. Office of Climate and Meteorology.
A VARIATIONAL ASSIMILATION METHOD FOR SATELLITE AND CONVENTIONAL DATA: MODEL 2 (VERSION 1)
Gary L. Achtemeier *In its* A Variational Assimilation Method for Satellite and Conventional Data: Development of Basic Model for Diagnostics of Cyclone Systems Jun. 1991 p 11-35 (For primary document see N92-17975 08-47)
Avail: NTIS HC/MF A08 CSCL 04B

The Model II variational data assimilation model is the second of the four variational models designed to blend diverse meteorological data into a dynamically constrained data set. Model II differs from Model I in that it includes the thermodynamic equation as the fifth dynamical constraint. Thus, Model II includes all five of the primative equations that govern atmospheric flow for a dry atmosphere. Author

N92-17977*# Illinois State Water Survey, Champaign.
A VARIATIONAL ASSIMILATION METHOD FOR SATELLITE AND CONVENTIONAL DATA: A REVISED BASIC MODEL 2B
Gary L. Achtemeier, Robert W. Scott, and J. Chen *In its* A Variational Assimilation Method for Satellite and Conventional Data: Development of Basic Model for Diagnostics of Cyclone Systems Jun. 1991 p 36-122 (For primary document see N92-17975 08-47)
Avail: NTIS HC/MF A08 CSCL 04B

A variational objective analysis technique that modifies observations of temperature, height, and wind on the cyclone scale to satisfy the five 'primitive' model forecast equations is presented. This analysis method overcomes all of the problems that hindered previous versions, such as over-determination, time consistency, solution method, and constraint decoupling. A preliminary evaluation of the method shows that it converges rapidly, the divergent part of the wind is strongly coupled in the solution, fields of height and temperature are well-preserved, and derivative quantities such as vorticity and divergence are improved. Problem areas are systematic increases in the horizontal velocity components, and large magnitudes of the local tendencies of the horizontal velocity components. The preliminary evaluation makes note of these problems but detailed evaluations required to determine the origin of these problems await future research. Author

N92-17978*# Illinois State Water Survey, Champaign.
A VARIATIONAL FORMALISM FOR THE RADIATIVE TRANSFER EQUATION: PRELUDE TO MODEL 3
Gary L. Achtemeier *In its* A Variational Assimilation Method for Satellite and Conventional Data: Development of Basic Model for Diagnostics of Cyclone Systems Jun. 1991 p 123-142 (For primary document see N92-17975 08-47)
Avail: NTIS HC/MF A08 CSCL 04B

The MODEL III variational data assimilation model is the third of four general assimilation models designed to blend weather data measured from space based platforms in the meteorological data mainstream in a way that maximizes the information content of the satellite data. Because there are many different observation locations and there are many instruments with different measurement error characteristics, it is also necessary to require that the blending be done to maximize the information content of the data and simultaneously to retain a dynamically consistent and reasonably accurate description of the state of the atmosphere. This is ideally a variational problem for which the data receive relative weights that are inversely proportional to measurement error and are adjusted to satisfy a set of dynamical equations that govern atmospheric processes. The advantage of MODEL III over the previous two models is that radiance, the atmospheric variable measured by satellite, becomes a dependent variable. In the previous versions, mean layer temperatures that had been retrieved from the radiances by some method, were included in the assimilation by substituting them in place of the rawinsonde temperatures. Now both rawinsonde temperatures and satellite radiances are included independently in the assimilation. Author

N92-17979*# Illinois State Water Survey, Champaign.
A VARIATIONAL FORMALISM FOR THE RADIATIVE TRANSFER EQUATION AND A GEOSTROPHIC, HYDROSTATIC ATMOSPHERE: PRELUDE TO MODEL 3
Gary L. Achtemeier *In its* A Variational Assimilation Method for Satellite and Conventional Data: Development of Basic Model for Diagnostics of Cyclone Systems Jun. 1991 p 143-152 (For primary document see N92-17975 08-47)
Avail: NTIS HC/MF A08 CSCL 04B

The second step in development of MODEL III is summarized. It combines the four radiative transfer equations of the first step with the equations for a geostrophic and hydrostatic atmosphere. This step is intended to bring radiance into a three dimensional balance with wind, height, and temperature. The use of the geostrophic approximation in place of the full set of primitive equations allows for an easier evaluation of how the inclusion of the radiative transfer equation increases the complexity of the variational equations. Seven different variational formulations were developed for geostrophic, hydrostatic, and radiative transfer equations. The first derivation was too complex to yield solutions that were physically meaningful. For the remaining six derivations, the variational method gave the same physical interpretation (the observed brightness temperatures could provide no meaningful input to a geostrophic, hydrostatic balance) at least through the problem solving methodology used in these studies. The variational method is presented and the Euler-Lagrange equations rederived for the geostrophic, hydrostatic, and radiative transfer equations. Author

N92-17980*# Illinois State Water Survey, Champaign.
ON THE CONCEPT OF VARYING INFLUENCE RADII FOR A SUCCESSIVE CORRECTIONS OBJECTIVE ANALYSIS
Gary L. Achtemeier *In its* A Variational Assimilation Method for Satellite and Conventional Data: Development of Basic Model for Diagnostics of Cyclone Systems Jun. 1991 p 153-155 (For primary document see N92-17975 08-47)
Avail: NTIS HC/MF A08 CSCL 04B

There has been a long standing concept by those who use successive corrections objective analysis that the way to obtain the most accurate objective analysis is first, to analyze for the long wavelengths and then to build in the details of the shorter wavelengths by successively decreasing the influence of the more distant observations upon the interpolated values. Using the Barnes method, the filter characteristics were compared for families of response curves that pass through a common point at a reference wavelength. It was found that the filter cutoff is a maximum if the filter parameters that determine the influence of observations are unchanged for both the initial and corrections passes. This information was used to define and test the following hypothesis. If accuracy is defined by how well the method retains desired wavelengths and removes undesired wavelengths, then the Barnes method gives the most accurate analyses if the filter parameter on the initial and corrections passes are the same. This hypothesis does not follow the usual conceptual approach to successive corrections analysis. Author

N92-17981*# Illinois State Water Survey, Champaign.
MODIFICATION OF A SUCCESSIVE CORRECTIONS OBJECTIVE ANALYSIS FOR IMPROVED DERIVATIVE CALCULATIONS
Gary L. Achtemeier *In its* A Variational Assimilation Method for Satellite and Conventional Data: Development of Basic Model for Diagnostics of Cyclone Systems Jun. 1991 p 156-157 (For primary document see N92-17975 08-47)
Avail: NTIS HC/MF A08 CSCL 04B

The use of objectively analyzed fields of meteorological data for complex diagnostic studies and for the initialization of numerical prediction models places the requirements upon the objective

method that derivatives of the gridded fields be accurate and free from interpolation error. A modification of an objective analysis developed by Barnes provides improvements in analyses of both the field and its derivatives. Theoretical comparisons, comparisons between analyses of analytical monochromatic waves, and comparisons between analyses of actual weather data are used to show the potential of the new method. The new method restores more of the amplitudes of desired wavelengths while simultaneously filtering more of the amplitudes of undesired wavelengths. These results also hold for the first and second derivatives calculated from the gridded fields. Greatest improvements were for the Laplacian of the height field; the new method reduced the variance of undesirable very short wavelengths by 72 pct. Other improvements were found in the divergence of the gridded wind field and near the boundaries of the field data. Author

N92-17991*# Ohio Univ., Athens.
A HYBRID MODULATION FOR THE DISSEMINATION OF WEATHER DATA TO AIRCRAFT
Dennis M. Akos *In* NASA. Langley Research Center, Joint University Program for Air Transportation Research, 1990-1991 Dec. 1991 p 55-59 (For primary document see N92-17984 08-01)
Avail: NTIS HC/MF A09 CSCL 04B

48 OCEANOGRAPHY

Includes biological, dynamic, and physical oceanography; and marine resources.

For related information see also *43 Earth Resources and Remote Sensing.*

N92-17041# Naval Oceanographic and Atmospheric Research Lab., Bay Saint Louis, MS.
SEA SURFACE ENVIRONMENTAL CONDITIONS IN THE GULF OF ALASKA DURING APRIL 1990 USING SSM/I Final Report
P. M. Smith Aug. 1991 29 p
(AD-A241909; AD-E040128; NOARL-TN-136) Avail: NTIS HC/MF A03 CSCL 08/3

The Special Sensor Microwave Imager (SSM/I) is capable of mapping sea surface roughness characteristics and sea foam coverage from space in most weather conditions. The SSM/I also measures precipitation and water vapor content of atmosphere, providing a simultaneous weather analysis complementing the sea surface roughness measurements. This combination of measurements can provide input into numerical models of sound transmission in the ocean, particularly those incorporating forward scattering from the sea surface, absorption by bubbles, and the generation of noise by wind. This technical note presents a demonstration of these capabilities for the month of April 1991 Gulf of Alaska. An algorithm is applied to several SSM/I passes to produce maps of root mean square wave slope, percent sea foam coverage, precipitation, and water vapor. Two wind events are treated that were associated with the passage of low pressure systems into the gulf from the southwest. A method of driving significant wave height from wave slope variance, using independent estimates of the dominant wavelength, is also presented. GRA

N92-17051# Naval Postgraduate School, Monterey, CA.
SOURCE OF COLD WATER IN MONTEREY BAY OBSERVED BY AVHRR SATELLITE IMAGERY M.S. Thesis
Dan E. Tracy Dec. 1990 136 p
(AD-A242843) Avail: NTIS HC/MF A07 CSCL 08/3

A one year record of Advanced Very High Resolution Radiometer (AVHRR) satellite images, beginning October 1, 1988, was processed and evaluated to determine the source of cold, nutrient-rich water in Monterey Bay. Wind records indicated a strong correlation with the intensity of upwelling at Ano Nuevo and Point Sur as seen in numerous satellite images. Close quantitative agreement between satellite derived multi-channel sea surface temperature and in situ observation of sea surface temperature by oceanographic research ships support remote sensing as a valid tool for observing thermal gradients. During upwelling events in the spring and summer, offshore plumes of cold water appear at Ano Nuevo and Point Sur. In addition, southward flow at both locations is inferred from satellite images and from vertical temperature profiles. One jet of cool water, approximately 10 km wide and 30 m deep originates at Ano Nuevo and flows south across the mouth of the Monterey Bay, effectively isolating the Bay from oceanic surface circulation. Cool surface water is injected into the middle and southern Bay resulting in a generally cyclonic flow inside the Bay. Offshore, a warm core, anticyclonic eddy persists with a radius of 30 km. It is bounded on the north and south by the previously mentioned offshore plumes and on the east by the southward flow from Ano Nuevo. GRA

N92-17078# Pennsylvania State Univ., University Park. Applied Research Lab.
BOTTOM CONTOUR INFLUENCE ON RAY TRACING
Shaari M. Unger Oct. 1991 38 p
(AD-A242411; PSU/ARL-TR-91-011) Avail: NTIS HC/MF A03 CSCL 20/1

The objective of this paper is to qualitatively determine the effect changes in bottom contour will have on sound propagation using ray trace techniques. This study describes some bathymetric properties of the Nanoose Bay range. It outlines the Hamiltonian Acoustic Ray Tracing Program for the Ocean (HARPO), a ray theory based model, and discuss the relationship between ray tracing and transmission loss. HARPO ray traces are used to portray the changes in the propagation of sound as changes in bottom contour are introduced. Previously used ray trace models have assumed flat bottom boundary conditions. This qualitative study shows the impact of modeling bottom contour irregularities on the predictability of sound rays and on transmission loss. The HARPO ray trace model is presented, and qualitative results are examined between several bottom contour variations. The effects of changes in bottom contour are assessed. These irregularities caused changes in attenuation, path length, and angles of incidence. Results of a study which measured in-situ data from three equally spaced receivers are also discussed. Acoustic receive levels were comparable. Test suggestions are proposed for obtaining quantitative transmission loss values. GRA

N92-17083# Pennsylvania State Univ., University Park. Applied Research Lab.
THE EFFECTS OF SEDIMENT POROSITY ON ACOUSTIC REFLECTION AND TRANSMISSION AT THE SEAFLOOR
Charles W. Holland Oct. 1991 159 p
(Contract N00039-88-C-0051)
(AD-A241943; PSU/ARL-TR-91-012) Avail: NTIS HC/MF A08 CSCL 20/1

The Biot theory of propagation in a porous medium provides a mathematical framework for studying acoustic interaction with the seafloor. The theory considers the two-phase porous nature of marine sediments in contrast to the classical models of wave propagation in the seafloor that consider marine sediments as an extended single-phase fluid or solid. A boundary value problem is set up and solved for a line source in a fluid medium above a poro-viscoelastic halfspace. Expressions for the reflected and transmitted field are given in integral form and asymptotic expansions in the high-frequency, far-field limit. A set of simultaneous equations is solved to give plane wave reflection and transmission (Type I, Type II, and shear wave) coefficients. These equations also yield the Scholte, pseudo-Scholte, and pseudo-Rayleigh wave phase velocities and attenuations. The plane wave coefficients and the surface wave velocities and attenuations are compared with commensurate quantities from the single-phase theories. Recent experiments of high frequency transmission through a water-sand interface have indicated anomalously high transmitted energy at angles near the critical angle. The Type II wave (predicted by Biot theory but not the single-phase theories) was suspected as a possible reason for the anomalies. Calculations indicate that the contributions from the Type II wave are negligible

and not the cause of the anomalies. Much of the anomalous behavior appeared to arise simply as a result of an incorrect compressional wave attenuation in the geoacoustic model. GRA

N92-17119# Naval Postgraduate School, Monterey, CA.
A STUDY ON HYDROGRAPHIC CONDITIONS AND SALT BUDGET CALCULATION FOR THE GULF OF FARALLONES WITH THE DATA COLLECTED IN AUGUST 1990 M.S. Thesis
Erhan Gezgin Mar. 1991 92 p
(AD-A243406) Avail: NTIS HC/MF A05 CSCL 08/3

The circulation pattern observed in the Gulf of Farallones on 5-10 August 1990 was a cyclonic system of flow. Water entered the Gulf from south of the Farallon Islands and left the Gulf between Pt. Reyes and the Farallon Islands. This pattern is confirmed by a satellite image which indicates a tongue of warm water penetrating into the Gulf from offshore as well as the increasing salinity and density along a shallow salinity minimum in this area. This cyclonic flow was also observed by previous current meter moorings in and near the Gulf. Note that this circulation would provide a return flow to balance offshore flow which has been observed at Pt. Reyes. GRA

N92-17169# Naval Postgraduate School, Monterey, CA.
AN INVESTIGATION OF COLD OVERFLOW OVER THE ICELAND/FAEROES RIDGE M.S. Thesis
Peter A. Tunnicliffe Dec. 1990 107 p
(AD-A243084) Avail: NTIS HC/MF A06 CSCL 08/3

Hydrographic data were analyzed to determine spatial and temporal variability of the overflow of cold, fresh Arctic water over the Iceland/Faeroes Ridge into the Iceland Basin during both winter and summer. Regions of frequent intermittent overflow were located together with areas that remain relatively unaffected by this process. A time series of near bottom temperatures revealed a possible link between significant overflow events and local wind fields which may result in a seasonal contrast in conditions. Two overflow mechanisms were identified: an intermittent plume-like flow promoted by local wind forcing; and a continuous thin veil of mixed overflow water formed from more significantly sized eddies/filaments located on top of the ridge. Estimates were made as to the probable contribution of both mechanisms to the total transport of Norwegian Sea water into the North Atlantic Ocean. Dynamic models of overflow were reviewed and, based on hydrographic results, a probable mechanism for overflow was proposed. Sound speed profiles were constructed representing the presence/absence of overflow events and predicted sonar ranges were computed using a range-dependent parabolic equation model. Major effects on acoustic propagation are shown to be confined to regions close to the top of the rise, even during overflow events; however, large reduction in sonar ranges are predicted for areas on top of the ridge, even at low frequencies (100 Hz). Analysis of observations in the area suggest that the acoustic variability in the region can be related to small changes in sea surface temperature and consequently may lead to a prediction of acoustic conditions in the region using AVHRR imagery. GRA

N92-17177# Pacific Missile Test Center, Point Mugu, CA.
TIDAL AND LUNAR DATA FOR POINT MUGU, SAN NICOLAS ISLAND, AND THE BARKING SANDS AREA DURING 1992 Annual Technical Publication
Charles J. Fisk and Bernard C. Cohenour 31 Dec. 1991 37 p
(AD-A243210; PMTC-TP-000060) Avail: NTIS HC/MF A03 CSCL 08/3

Basic lunar and tidal data for Point Mugu, California; San Nicolas Island, California; and the Barking Sands Area, Hawaii for 1992 are provided. The data presented are: (1) tidal data; (2) times of moonrise and moonset; (3) times of lunar phases; and (4) times of sunrise and sunset. GRA

N92-17298# Army Engineer Waterways Experiment Station, Vicksburg, MS. Hydraulics Lab.
USER'S GUIDE FOR A THREE-DIMENSIONAL NUMERICAL HYDRODYNAMIC, SALINITY, AND TEMPERATURE MODEL OF CHESAPEAKE BAY Final Report
Billy H. Johnson, Keu W. Kim, Ronald E. Heath, H. L. Butler, and Bernard B. Hsieh Oct. 1991 86 p
(AD-A242993; WES/TR/HL-91-20) Avail: NTIS HC/MF A05 CSCL 08/3

A time-varying three dimensional (3D) numerical hydrodynamic model of Chesapeake Bay has been developed to provide flow fields to a 3D water quality model of the bay. The water surface, 3D velocity field, salinity, and temperature are computed. Major physical processes affecting bay circulation and vertical mixing are modeled. A particular feature of the model is the solution of transformed equations on a boundary-fitted grid in the horizontal plane. This user's guide presents a detailed discussion of theoretical aspects of the 3D model (e.g., basic equations, boundary conditions, turbulence closure, etc.), followed by a discussion of the organization of the computer code and input data requirements. Listings of portions of the various input data files for an application that simulates the hydrodynamics of the Chesapeake Bay during September 1983 are also provided. GRA

N92-17391# Stanford Univ., CA. Rockphysics Lab.
ACOUSTICAL AND OTHER PHYSICAL PROPERTIES OF MARINE SEDIMENTS Final Report
Amos Nur 1991 84 p
(Contract N00014-89-J-1316)
(AD-A243532) Avail: NTIS HC/MF A05 CSCL 08/3

This report provides the results of the research effort on the following topics: include four parts: (1) The effect of cementation on the elastic properties of granular material, and Seismic velocities in compacting sediments; (2) The mechanics of hollow grains, and Pillow basalts compaction due to grain collapse; (3) Modeling the granular structure of rocks; and (4) Anisotropic Poroelasticity and Biot's Parameters. In Part 1 a simple analytical model was developed to describe the mechanics of cemented granular material, for which a solution was obtained to model the normal and shear deformation of a cement layer with straight boundaries. In Part 2, in order to model the mechanical behavior of pillow basalts, we developed a theory for the two-dimensional deformation of hollow grains under external loading. In Part 3 the interaction of rock grains with friction and slippage is modeled using an analytical solution for plain elastic deformation of cylinders. Part 4 examines prediction of wave propagation in a submarine environment. This requires modeling the acoustic response of ocean bottom sediments which generally consists of porous granular materials partially or wholly saturated with water. GRA

N92-17539# Institute for Naval Oceanography, Bay Saint Louis, MS.
A USER'S MANUAL FOR THE PRINCETON NUMERICAL OCEAN MODEL
William P. OConnor Mar. 1991 73 p
(AD-A243773; AD-E040155; INO-SP-5) Avail: NTIS HC/MF A04 CSCL 12/5

This is a user's guide for the numerical ocean model developed at Princeton University and presently in use at the Institute for Naval Oceanography. The basic model has been applied successfully to study such diverse regions as Chesapeake Bay (Blumberg 1977), the South Atlantic Bight (Blumberg and Mellor 1983), the Mid Atlantic Bight (Blumberg and Kantha 1985), the Gulf of Mexico (Blumberg and Mellor 1985), New York Harbor (Oey et al 1985), Delaware Bay (Galperin and Mellor 1990), and the western Atlantic including Gulf Stream (Mellor and Ezer 1991). It can model regions from the size of bays and estuaries to basin scale North Atlantic domains. A good discussion of modeling bays and coastal oceans is given by Blumberg and Oey (1985). GRA

N92-17583# Woods Hole Oceanographic Inst., MA.
UPPER OCEAN DYNAMICS DURING THE LOTUS AND TROPIC HEAT EXPERIMENTS Ph.D. Thesis
Rebecca R. Schudlich Sep. 1991 159 p Prepared in cooperation with Massachusetts Inst. of Tech., Cambridge
(Contract N00014-89-J-1053)
(AD-A243730; WHOI-91-29) Avail: NTIS HC/MF A08 CSCL 08/3

The vertical structure of the upper ocean in mid-latitudes and at the equator is investigated using observations from the Long Term Upper Ocean Study (LOTUS), the Tropic Heat Experiments, and one-dimensional numerical models. When the diurnal cycle in solar heating is strong, it determines the local vertical structure of the upper ocean (in both the LOTUS and Tropic Heat Experiment observations). The Price et al. (1986) model and its extension to the equator simulate the upper ocean fairly well when the diurnal cycle is strong. During the LOTUS experiment, we found good agreement with Ekman transport by using a wind-relative averaging method. The mean current e-folds over 12 m in the summer and has a strong diurnal cycle. The mean current e-folds over 25 m in the winter, with very little diurnal cycle. An extension of the Price et al. (1986) model to the equatorial upper ocean shows that the nighttime phase of the diurnal cycle is strongly affected by the equatorial undercurrent, resulting in deep mixing and large dissipation at night consistent with observations made during the Tropic Heat Experiments. The daytime phase of the simulated diurnal cycle is unaffected by equatorial circulation and is very similar to its mid-latitude counterpart. GRA

N92-17765# Naval Oceanographic and Atmospheric Research Lab., Bay Saint Louis, MS.
MULTISPECTRAL SOFTWARE DEVELOPMENT FOR THE AIRBORNE BATHYMETRIC SURVEY SYSTEM Final Report
Maria T. Kalcic and Steve C. Lingsch May 1991 52 p
(AD-A243774; AD-E040106; NOARL-R-17) Avail: NTIS HC/MF A04 CSCL 08/3

The Mapping, Charting, and Geodesy (MC&G) Division of the Naval Oceanographic and Atmospheric Research Laboratory's Ocean Science Directorate is the primary activity within the U.S. Navy for conducting research and development in direct support of naval MC&G requirements. The Mapping Sciences Branch of the MC&G Division was tasked to develop the algorithms and software necessary to process data and to produce bathymetry from the multispectral scanner of the Airborne Bathymetric Survey system when it becomes fully functional. The software developed for this system is called the Multispectral Image Depth Analysis System, or MIDAS. The software processes multispectral data in conjunction with laser- or boat-derived soundings to produce high resolution bathymetric grids. The system is designed to estimate depths in clear, shallow coastal waters down to 20 m. The depth accuracies, derived from the system using boat soundings for control, ranged from 0.3 to 1.4 m in waters extending to 3 and 10 m respectively. The horizontal positioning accuracy of the system was in the 25 m range, as determined from a ground survey. GRA

N92-17766# Naval Oceanographic and Atmospheric Research Lab., Bay Saint Louis, MS.
OCEAN SIMULATION MODEL. VERSION 2: FIRST ORDER FRONTAL SIMULATION Final Report
K. D. Saunders and C. F. Cheng (Sverdrup Technology, Inc., Bay Saint Louis, MS.) May 1991 75 p
(AD-A243775; AD-E040096; NOARL-TN-127) Avail: NTIS HC/MF A04 CSCL 08/3

Temperature, salinity, density, and sound velocity are the properties of most interest to the physical oceanographer and acoustician. The Naval Oceanographic and Atmospheric Research Laboratory has produced a first-level numerical simulation model that can produce simulated sections of temperature, salinity, density, and sound velocity in the vicinity of an oceanic front. The user controls the front. This technical note documents the algorithms used in the simulation model and provides a users guide to the programs. Two programs are documented. The first program generates the front, and the second produces plots of the frontal properties. GRA

N92-17951# Washington Univ., Seattle. Applied Physics Lab.
PROCEEDINGS OF THE 2ND GULF OF CADIZ EXPEDITION WORKSHOP
M. D. Allison, I. Ambar, G. C. Johnson, M. A. Kennelly, and H. Koenig May 1991 64 p Workshop held in Seattle, WA, 9-11 Apr. 1991
(AD-A242749; APL-UW-TM-6-91) Avail: NTIS HC/MF A04 CSCL 08/3

The objectives of the Gulf of Cadiz Expedition were to observe the vortices shed in the wake of Ampere Seamount, to survey Meddies formed by the Mediterranean outflow near Cape St. Vincent, Portugal, and to study the structure and dynamics of the outflow plume west of the Strait of Gibraltar. During the Expedition (September 4-28, 1988), velocity, hydrographic, and dissipation measurements were made using a variety of instrument systems (XCP, XDP, XBT, XSV, CTD, and ADCP). Related work discussed includes: secondary circulation in the Faroe Bank channel outflow; turbulence and mixing in the Strait of Gibraltar; and Lagrangian observation in the Mediterranean outflow in the Iberian Basin. GRA

51 LIFE SCIENCES (GENERAL)

N92-17121# Miami Univ., Oxford, OH. Dept. of Zoology.
ASSESSMENT OF THE BEHAVIORAL AND NEUROTOXIC EFFECTS OF HEXACHLOROBENZENE (HCB) IN THE DEVELOPING RAT Final Report, May 1989 - Dec. 1990
D. H. Taylor and E. Goldey Dec. 1990 41 p Prepared for NSI Technology Services Corp., Dayton, OH
(Contract F33615-85-C-0532; AF Proj. 6302)
(AD-A243658; AAMRL-TR-90-076) Avail: NTIS HC/MF A03 CSCL 15/6

Hexachlorobenzene (HCB) is a widespread environmental contaminant. Due to its highly lipophilic nature, HCB is stored in the body adipose tissue and is released with the milk during lactation. Female Sprague-Dawley rats were given 0 (control), 10 or 100 mg HCB/kg body weight, and dosing was completed two weeks prior to breeding. We evaluated the gestational and lactational transfer of HCB from the dams to fetuses and pups and determined that HCB is present in the developing rat brain. Throughout gestation, the HCB tissue concentrations for the 10 and 100 mg HCB/kg body weight groups differed by 10 fold. The maternal body burden of HCB was quickly depleted by lactational transfer of the HCB to the suckling pups as reflected by HCB concentrations in the milk and pups. However, across treatment groups, only a 2-3 fold difference existed between tissue concentrations of HCB in both dams and pups during lactation. Subsequently, we assessed the developmental neurotoxicity of HCB using a battery of behavioral tests. The negative geotaxic response and olfactory homing were assessed in two male and two female pups from each litter between 6 and 11 days of age. GRA

N92-17142# Wellesley Coll., MA.
MELATONIN ACTION ON THE CIRCADIAN PACEMAKER IN SIBERIAN HAMSTERS Annual Report, 1 Nov. 1989 - 31 Aug. 1991
Janet M. Darrow 29 Sep. 1991 14 p
(Grant AF-AFOSR-0067-90; AF Proj. 2312)
(AD-A243057; AFOSR-91-0911TR) Avail: NTIS HC/MF A03 CSCL 06/3

This research investigates the effect of the hormone melatonin on the circadian clock of mammals, by examining daily activity rest cycles and body temperature rhythms in melatonin-infused Siberian hamsters, under a variety of environmental lighting conditions. In experiments simulating jet-lag conditions, melatonin significantly accelerated re-adjustment of sleep/wake rhythms to phase-shifted light cycles. Within days after an 8-hr phase-advance of the light/dark cycle, all melatonin-treated hamsters, but none of the saline-treated controls, had achieved the proper phase relationship with the new photoschedule. These results are consistent with reports of melatonin treatment reducing jet lag in humans. Under conditions of constant darkness, daily melatonin infusions synchronized the hamster activity/rest rhythm. In constant light, melatonin also acted as a weak entraining agent and

prevented the internal desynchronization which occurs in Siberian hamsters and in many mammals exposed to constant light. These results offer encouragement about Siberian hamsters as an appropriate model system to investigate melatonin action on the circadian clock. GRA

N92-17224# Michigan State Univ., East Lansing.
MICROBIAL DIVERSITY: COURSE REPORT 1991
John A. Breznak and Martin Dworkin 1991 32 p
(AD-A243464) Avail: NTIS HC/MF A03 CSCL 05/2

Inasmuch as the course emphasizes nature as a tremendous reservoir of microbial diversity, a special effort is made to exploit the array of terrestrial, freshwater and marine habitats in the vicinity of Woods Hole as the source of microbes to be isolated in the laboratory portion of the course. Additional samples from unusual habitats (e.g., deep sea hydrothermal vent areas; deep subsurface cores) are obtained from other investigators. Subsequent to isolation, experiments are designed to examine some of the unique biochemical and physiological properties of the organisms in pure culture and, where appropriate, when placed in defined co-culture with other microbes. To accomplish this, students are taught various techniques for cultivation of microorganisms (including the Hungate technique for strict anaerobes), as well as various methods for observing and studying the isolated microbes (phase contrast, fluorescence, and DIC microscopy; gas-liquid and high performance liquid chromatography; spectroscopy; PCR methodology and gel electrophoresis; etc.). GRA

N92-17269# Army Aeromedical Research Lab., Fort Rucker, AL.
THE EFFECT OF IMPULSE PRESENTATION ORDER ON HEARING TRAUMA IN THE CHINCHILLA
James H. Patterson, Jr., Dennis L. Curd, Ilia L. Gautier, Roger P. Hamernik, William A. Ahroon, George A. Turrentine, and C. E. Hargett, Jr. (State Univ. of New York, Plattsburgh.) Sep. 1991 70 p
(DA Proj. 3E1-62777-A-878; DA Proj. 3M1-61102-BS-15)
(AD-A243174; USAARL-91-21) Avail: NTIS HC/MF A04 CSCL 06/3

Existing criteria for exposure to impulse noise do not provide any explicit means for evaluating exposures for which the peak SPL (Sound Pressure Level) of the impulses varies in any given exposure day. Approaches to evaluating such exposures have included the application of a 'proportional dose' method such as used with continuous noise or use of an average level. Implicit in these approaches is the assumption that the order in which a sequence of variable intensity impulses is presented is not important. This same assumption is also implicit in any energy-based exposure criteria. This report presents results of a pilot experiment designed to test the validity of this assumption. Two groups of chinchillas were exposed to a sequence of 100 impulses. One group received 90 exposures at 138 dB peak SPL impulses followed by 10 exposures at 146 dB peak SPL impulses; the second group received the same series of impulses but in reverse order. Results from these two groups were compared to results of 100 exposures at 147 dB peak SPL impulses from a report by Patterson et al., (1986). The 139 dB peak SPL exposure had the same total energy as the two variable intensity exposures. Results of the three equivalent energy exposures showed that exposures having equal energies could produce statistically different levels of hearing trauma. However, while the mean data were very suggestive in showing an effect of the presentation order, this result did not hold up to statistical analysis because of a large intersubject variability. GRA

N92-17288# Georgia Tech Research Inst., Atlanta.
BIOPHYSICAL TECHNIQUES FOR EXAMINING METABOLIC, PROLIFERATIVE, AND GENETIC EFFECTS OF MICROWAVE RADIATION Final Report, 1 Oct. 1989 - 30 Aug. 1990
Martin L. Meltz Sep. 1991 37 p Prepared in cooperation with Texas Univ. Health Science Center, San Antonio
(Contract F33615-87-D-0626)
(AD-A241903; AL-TR-1991-0004) Avail: NTIS HC/MF A03 CSCL 06/5

This project was undertaken to prepare for a comprehensive research effort examining metabolic, proliferative, and genetic effects of microwave radiation. To accomplish this task, preliminary studies have been performed with 4 cells systems; Chinese hamster ovary (CHO) cells, AS52 Chinese hamster cells (heterozygous at the xanthine-guanine phosphoribosyl transferase (XGPRT) locus), 244B proliferating human lymphoblastoid cells, and freshly isolated peripheral lymphocytes. The thermal response of the 244B cells has been carefully examined, and an initial characterization of the membrane markers, membrane permeability, and cell cycle distribution of these cells undertaken. The absence of the induction of chromosome aberrations in CHO cells, after exposure to 850 MHz pulsed wave (PW), 18mW/cm2 (specific absorption rate (SAR) 14.4 W/kg) radiofrequency radiation (RFR), or after exposure to 1,200 MHz PW (220 W -300 W net forward power; SAR 24.33 W/kg RFR, is reported. The survival response of the AS52 cells, after simultaneous treatment at 37 C or 40 C, with and without mitomycin or adriamycin, is described. The survival of the AS52 cells after X-ray exposure at low and high dose rates is also described. GRA

N92-17471# Argonne National Lab., IL.
ARTIFICIAL PHOTOSYNTHESIS: PROGRESS TOWARD MOLECULAR SYSTEMS FOR PHOTOCONVERSION
M. R. Wasielewski 1991 4 p Presented at the 10th Anniversary Symposium of Japan-US Cooperative Photoconversion and Photosynthesis Research Program, Okazaki, Japan, 4-6 Dec. 1991
(Contract W-31-109-eng-38)
(DE92-003370; ANL/CP-74610; CONF-911264-1) Avail: NTIS HC/MF A01

A great deal of progress has been made in identifying the criteria necessary to design molecular systems for the efficient photochemical separation of charge over extended periods of time. Our own research in this area has focused on preparing supramolecular assemblies of electron donors and acceptors which fulfill the biomimetic criteria dictated by photosynthetic charge separation in Nature. First, it is important that the electron donors and acceptors occupy structurally well-defined spatial relationships relative to one another. A key consequence of studying well-defined structures is the simplification of mechanistic arguments that are used to describe electron transfer events in these systems. Second, the electronic coupling between the donors and acceptors must be controlled by the structure to insure that strong coupling results in rapid charge separation from the initial donor-acceptor state, and that weak coupling in the product ion pair state slows charge recombination. Considerations of electronic structure and orbital symmetry are necessary to achieve this goal. Third, the surrounding medium plays a critical role in determining the rates of electron transfer reactions. This is especially true when charges are created or annihilated in electron transfer reactions. Once again, Nature provides a high standard to be achieved. Photosynthetic reaction centers are fully competent in the solid state, even at very low temperatures, undergoing charge separation with unity quantum yield at temperatures less than 4.2 K. In order for our artificial photosynthetic systems to have general applicability as photocatalysts, it is highly desirable to have systems that are fully functional in the solid state. DOE

N92-17474# Colorado Univ., Boulder. Dept. of Electrical and Computer Engineering.
TEMPORALLY-SPECIFIC MODIFICATION OF MYELINATED AXON EXCITABILITY IN VITRO FOLLOWING A SINGLE ULTRASOUND PULSE
Richard T. Mihran, Frank S. Barnes, and Howard Wachtel 1990 26 p
(Contract N00014-87-K-0313)
(AD-A242329) Avail: NTIS HC/MF A03 CSCL 20/1

Single, short duration, low energy pulses of ultrasound were found to elicit distinct modifications of the electrical excitability of myelinated frog sciatic nerve in vitro in a window extending 40 to

50 ms after pulse termination. These modifications include both enhancement and suppression of relative excitability, the sequence of which generally follows one of two distinct temporal response patterns. The ultrasound pulses were focused, 2.7 MHz, of 500 duration, and of peak intensities of 100 to 800 W/sq cm. Total absorbed pulse energies were generally less than 100 mJ/g. corresponding to local temperature rises of the nerve trunk of no more than 0.025 C per pulse, thereby precluding bulk heating as a basis of this effect. The observed effects cannot be elicited using either a subthreshold square wave or RF electrical prestimulus, suggesting a unique form of receptivity of the nerve trunk to mechanical perturbation. We present evidence that the low-frequency radiation pressure transient accompanying the envelope of the acoustic pulse is the active parameter in this phenomenon, and postulate that it may act by the gating of stretch sensitive channels, which have been recently reported in a variety of cell membranes. These results may demonstrate that stretch sensitive channels in neural membrane could serve to functionally modulate neuro electric signals normally mediated by voltage dependent channels, a finding which could suggest new clinical applications of high peak power, low total energy pulsed ultrasound. GRA

N92-17504# Pennsylvania Univ., Philadelphia. Dept. of Computer and Information Sciences.
COMPUTATIONAL AND NEURAL NETWORK MODELS FOR THE ANALYSIS OF VISUAL TEXTURE Annual Progress Report, 1 Sep. 1990 - 31 Aug. 1991
Ruzena Bajcsy 4 Nov. 1991 5 p
(Grant AF-AFOSR-0296-88; AF Proj. 2313)
(AD-A243717; AFOSR-91-0986TR) Avail: NTIS HC/MF A01
CSCL 06/1

The detailed and biological realistic neural model of architectures that utilize Gabor filters for vision computations continues to be the focus of research. Additionally, some further testing of a three layer back propagation learning network for computing slat tilt was undertaken. A model has been developed which simulates the process of texture segmentation in the visual cortex according to the computational model of M. R. Turner et. al. using the McGregor high fidelity neural simulator. This system attempts to faithfully simulate the transfer functions of neurons using various numerical simulation methods. GRA

N92-17564# Miami Univ., FL. Div. of Marine Biology and Fisheries.
CHARACTERIZATION OF THE P. BREVIS POLYETHER NEUROTOXIN BINDING COMPONENT IN EXCITABLE MEMBRANES Final Report, 15 Aug. 1988 - 14 Aug. 1991
Daniel G. Baden 14 Sep. 1991 41 p
(Contract DAMD17-88-C-8148; DA Proj. 3M1-62787-A-871)
(AD-A242877) Avail: NTIS HC/MF A03 CSCL 06/5

The development of a functional model, and topographic picture of how and why sodium channels act in the ways in which they gate sodium ion flux is our goal. We are developing about 20 different natural toxin derivatives based on 7 divergent chemical modifications. Each type of derivative has a specific potential once synthesized. Photoaffinity probes, affinity columns, tritiated non-exchangeable toxins, and specific intermediates are in various stages of completion. These probes are being utilized to characterize the topographic relationship of sites 1, 2, and 5 associated with voltage-sensitive sodium channels. The brevetoxin binding site has already been localized on Domain IV of VSSC, and binds to an external hydrophobic peptide located between S5 and S6 of Domain IV. Antisodium channel RIA, tritiated brevetoxin photoaffinity binding, immunoprecipitation, and SDS-polyacrylamide gel electrophoresis have all made substantial contributions to brevetoxin site localization. GRA

N92-17815# International Centre for Theoretical Physics, Trieste (Italy).
MATHEMATICS AND BIOLOGY
I. A. Khan Jun. 1991 9 p
(DE92-611247; IC-91/115) Avail: NTIS HC/MF A02

In India and in so many other countries, the science students are generally separated into two main streams: one opting mathematical sciences and the other studying biological sciences. As a result, medicos and biologists have no adequate knowledge of mathematical sciences. Nowadays, this is a great drawback, because of the tremendous application of mathematics in the biosciences. The main aim of this article is to emphasize the need for mathematico-biologists in abundance for the better service of mankind. DOE

N92-17877# International Centre for Theoretical Physics, Trieste (Italy).
EVOLUTION AS A MOLECULAR COOPERATIVE PHENOMENON
J. Chela-Flores Jun. 1991 19 p
(DE92-609575; IC-91/108) Avail: NTIS HC/MF A03

We discuss an hypothesis according to which microscopic mechanisms due to cooperation, at the molecular level, may have been key factors in the evolution of life on Earth. We view our hypothesis as a natural extension to the molecular level of viewing cooperation (symbiosis) as an evolutionary driving force; this does not restrict the interpretation of the evolutionary process to be the result of slow accumulation of mutations in the DNA. Some evidence supporting this hypothesis is discussed: (1) The Salam enhancement factor. This molecular phenomenon was recently introduced in order to understand the bases of the first unifying principle of biochemistry, namely that transcription of all known genes in prokaryotes, protists, metazoan, and metaphytes are translated into L-amino acids, except for some bacterial membrane proteins. (2) The role that cooperative phenomena may have played in the origin of evolution itself, i.e., in the resolution of Sagan's ultraviolet paradox. (3) The relationship between evolution and the constraints imposed by embryonic development. This is considered from the point of view of molecular cooperative phenomena. DOE

N92-17946# International Centre for Theoretical Physics, Trieste (Italy).
GLOBAL MODELS FOR THE BIOMECHANICS OF GREEN PLANTS, PART 1
A. R. Bestman Dec. 1990 12 p
(DE91-641478; IC-90/473) Avail: NTIS HC/MF A03

The paper considers the biomechanics of green plants for Reynolds number flow in the stem. In particular, it is assumed that the stem is cylindrical and the flow fully-developed. So that if the aspect ratio is defined as the ratio of the stem radius to its length, then when the aspect ratio is small analytical solutions have been developed for the concentration, temperature and the axial velocity. The process of translocation and transpiration are discussed quantitatively. DOE

N92-17970# International Centre for Theoretical Physics, Trieste (Italy).
COMMENTS ON A NOVEL APPROACH TO THE ROLE OF CHIRALITY IN THE ORIGIN OF LIFE
J. Chela-Flores Jun. 1991 12 p
(DE92-609034; IC-91/126) Avail: NTIS HC/MF A03

We review a recent paper (Salam, 1991a) in which a specific enhancement factor (i.e., a phase transition into a condensed Bose mode) is proposed to account for the observed amplification of the ground state energies of the L- and D-amino acid enantiomers; the difference between these energies is assumed to be due to the neutral parity violating electroweak interaction. This physical effect initially shifts the enantiomer energies by about 3 x 10(exp -19)eV. The proposed phase transition is characterized by a critical temperature (T sub c), which may be studied theoretically by enlarging the standard electroweak theory to include either the top quark or supersymmetry (Salam, 1991b). Possible experimental means of finding T sub c are discussed. DOE

52 AEROSPACE MEDICINE

Includes physiological factors; biological effects of radiation; and effects of weightlessness on man and animals.

N92-17022*# National Aeronautics and Space Administration. Lyndon B. Johnson Space Center, Houston, TX.
TECHNIQUES FOR DETERMINATION OF IMPACT FORCES DURING WALKING AND RUNNING IN A ZERO-G ENVIRONMENT
Michael Greenisen, Marlei Walton, Phillip Bishop, and William Squires (Texas Lutheran Coll., Seguin.) Washington Jan. 1992 18 p
(NASA-TP-3159; S-651; NAS 1.60:3159) Avail: NTIS HC/MF A03 CSCL 06P

One of the deleterious adaptations to the microgravity conditions of space flight is the loss of bone mineral content. This loss appears to be at least partially attributable to the minimal skeletal axial loading concomitant with microgravity. The purpose of this study was to develop and fabricate the instruments and hardware necessary to quantify the vertical impact forces (Fz) imparted to users of the space shuttle passive treadmill during human locomotion in a three-dimensional zero-gravity environment. The shuttle treadmill was instrumented using a Kistler forceplate to measure vertical impact forces. To verify that the instruments and hardware were functional, they were tested both in the one-G environment and aboard the KC-135 reduced gravity aircraft. The magnitude of the impact loads generated in one-G on the shuttle treadmill for walking at 0.9 m/sec and running at 1.6 and 2.2 m/sec were 1.1, 1.7, and 1.7 G, respectively, compared with loads of 0.95, 1.2, and 1.5 G in the zero-G environment. Author

N92-17084# Army Aeromedical Research Lab., Fort Rucker, AL.
EFFECTS OF THE CHEMICAL DEFENSE ANTIDOTE ATROPINE SULFATE ON HELICOPTER PILOT PERFORMANCE: AN IN-FLIGHT STUDY
John A. Caldwell, Jr., David J. Carter, Robert L. Stephens, Lewis W. Stone, and Darcelle M. Delrie Jun. 1991 209 p
(AD-A241966; USAARL-91-17) Avail: NTIS HC/MF A10 CSCL 06/15

The effect of 2 mg and 4 mg injections of atropine sulfate on helicopter pilots was investigated using a specially instrumented UH-1H helicopter and several laboratory tests. A counterbalanced, within-subjects design was employed in which flight performance, vision, electroencephalographic activity, cognitive skill, and tracking performance were assessed on each of three different drug administration days (placebo, 2 mg, and 4 mg) separated by control days. Results indicated numerous atropine-related difficulties, seen most often with the 4 mg dose. Measurements of flight performance revealed decrements on at least one measure (i.e., heading, air speed, vertical speed) in both visual- and instrument-referenced straight and level flight, standard-rate turns, a straight climb and descent, steep turns, a climbing turn, and an instrument landing system (ILS) approach. Also, there were degradations in performance of a confined area approach and an out-of-ground-effect hover maneuver. Vision tests showed atropine-related increases in pupil diameter and double vision, concurrent with decreases in accommodation and depth perception. Cognitive tests revealed decrements in visual search, logical reasoning, quantitative ability, short-term memory, and response times. Psychomotor tracking tasks indicated atropine-induced increases in tracking errors across three levels of tracking complexity, and these sometimes were accompanied by deficits in responding to a secondary task. Various other results from this investigation are presented. GRA

N92-17089# Air Force Inst. of Tech., Wright-Patterson AFB, OH. School of Engineering.
EVALUATION OF SCALAR VALUE ESTIMATION TECHNIQUES FOR 3D MEDICAL IMAGING M.S. Thesis
Rob W. Parrott Dec. 1991 187 p
(AD-A243687; AFIT/GE/ENG/91D-17) Avail: NTIS HC/MF A09 CSCL 12/5

Scalar value estimation in 3D medical imaging increases data resolution for enhanced renditions and corrects inaccurate surface formations. Accurate estimations are vital because clinical assessment is often aided by examination of 3D medical images. This thesis explores different estimation techniques and introduces the geostatistical estimation technique called kriging to the field of 3D imaging. Kriging theory claims to be the optimal estimator--better than the standard deterministic methods commonly used. The techniques investigated are linear interpolation, trilinear interpolation, tricubic interpolation, and kriging. This research investigates scalar value estimation in the volume preprocessing operation of slice interpolation and in a surface extraction method called cell subdivision. Tricubic interpolation is shown to be most useful in artificially created volumes of smooth functions. It is also shown to produce poor results in medical volumes and in slice interpolation. More importantly, this research demonstrates that kriging subsumes the deterministic methods investigated and can estimate much better than tricubic interpolation. GRA

N92-17120# Air Force Inst. of Tech., Wright-Patterson AFB, OH.
A TOPOGRAPHICAL ANALYSIS OF THE HUMAN ELECTROENCEPHALOGRAM FOR PATTERNS IN THE DEVELOPMENT OF MOTION SICKNESS M.S. Thesis
George S. Vogen Dec. 1991 87 p
(AD-A243656; AFIT/GSO/ENG/91D-17) Avail: NTIS HC/MF A05 CSCL 06/10

A topographical analysis was performed on 12 electroencephalograms (EEG's) collected from 10 volunteers who experienced motion sickness through cross-coupled Coriolis stimulation. Seven males and three females participated in the research conducted at the Air Force Institute of Technology, Wright-Patterson AFB. Two male volunteers participated in double-blind placebo/phenytoin trials. Static brain maps and dynamic EEG's which focused on delta (below 3Hz) activity during the development of motion sickness revealed a seizure-like propagation pattern. With initial symptoms, a clear left parietal focus was seen in all records. A less dominant left fronto-temporal focus was present in 11 of the 12 records. As symptoms grew there was a contralateral spread (possibly occipitally) to the right temporal region. A steady increase in power was noticeable during the evolution of motion sickness. The 2 phenytoin trials showed less overall power when compared to their respective placebo trials. The report of this seizure-like propagation pattern during motion sickness is believed to be the first of its kind. GRA

N92-17124# Naval Medical Research Inst., Bethesda, MD.
STATISTICALLY-BASED DECOMPRESSION TABLES. 6: REPEAT DIVES ON OXYEN/NITROGEN MIXES Technical Report, Sep. 1988 - Nov. 1989
G. W. Albin and P. K. Weathersby Oct. 1991 67 p
(NMRI Proj. M00-99)
(AD-A243667; NRMI-91-84) Avail: NTIS HC/MF A04 CSCL 06/10

The risk of decompression sickness (DCS) during dives on various nitrogen/oxygen breathing mixes is analyzed using likelihood maximization. Risk is treated as cumulative, resulting from periods during which the partial pressure of dissolved N2 exceeds the hydrostatic pressure in one or more hypothetical separate tissues. Gas uptake and release are assumed to follow either mono- or bi-exponential kinetics. The database consists of 2006 well-documented wet man-dives. No statistical evidence is found to justify the use of different models or different parameter values for single dives versus repeat dives or for dives on different N2/O2 mixes. Under these models, then, the single and repeat dives in our database should be considered as belonging to the same population. However, the models do not adequately predict the probability of DCS associated with a series of 128 multilevel dives (which feature ascents to 20-30 fsw interspersed with deeper excursions) while simultaneously making a plausible prediction of the risk of any other type of dive in the database. GRA

N92-17190# Air Force Inst. of Tech., Wright-Patterson AFB, OH.

THE EFFECTS OF STORAGE ON IRRADIATED RED BLOOD CELLS: AN IN VITRO AN IN VIVO STUDY M.S. Thesis

Susan E. Knoll Aug. 1991 111 p

(AD-A243387; AFIT/CI/CIA-91-073) Avail: NTIS HC/MF A06 CSCL 06/5

Irradiation of red blood cell units has recently become a topic of special concern as the result of increasing reports of graft versus host disease in immunocompetent blood transfusion recipients. This study was designed to evaluate the potassium elevations observed in stored irradiated red blood cells and to evaluate the in vivo survival of stored irradiated red blood cells using a dog model. In the in vitro study, ten units of human CPDA-1 packed red blood cells were made into paired aliquots; one aliquot of each pair was irradiated with 3000 rads of gamma radiation and the potassium content measured at points throughout 35 days of storage. A significant increase in potassium levels in the irradiated aliquots was observed from the first day after irradiation and continued through the entire storage period. GRA

N92-17194# Air Force Inst. of Tech., Wright-Patterson AFB, OH.

INFLUENCE OF KNEE JOINT EXTENSION ON SUBMAXIMAL OXYGEN CONSUMPTION AND ANAEROBIC POWER IN CYCLISTS M.S. Thesis

Jesse Garcia 5 Jun. 1991 57 p

(AD-A243467; AFIT/CI/CIA-91-070) Avail: NTIS HC/MF A04 CSCL 06/10

This study was designed to assess the effect of alterations of maximal knee joint extension on submaximal VO2, anaerobic peak power, and the anaerobic mean power in cycling. Eleven amateur male bicycle racers between the ages of 19 and 35 years were selected for participation in this study. The subjects were randomly assigned to one of four groups. All subjects performed a five minute submaximal exercise test and a Wingate anaerobic power test at maximal knee extensions. The subjects rode an ergometer which allowed the subjects to maintain their normal riding position as saddle height was altered to position the knee at the test angles. In order to assure a random testing sequence, each group was tested with a different order of presentation of the test positions according to a 4 X 4 Latin Square design. GRA

N92-17299# Army Aeromedical Research Lab., Fort Rucker, AL.

THE HAZARD OF EXPOSURE TO 2.075 kHz CENTER FREQUENCY NARROW BAND IMPULSES

James H. Patterson, Jr., Roger P. Hamernik, William A. Ahroon, George Turrentine, and C. E. Hargett, Jr. Sep. 1991 72 p

(Contract DAMD17-86-C-6139; DA Proj. 3E1-62777-A-878; DA Proj. 3M1-61102-BS-15)

(AD-A242997; USAARL-91-20) Avail: NTIS HC/MF A04 CSCL 06/4

A previous report derived a frequency weighting function from audiometric and histological data gathered on 118 chinchillas exposed to a variety of narrow band impulses at various peak intensities. The weighting function clearly demonstrated that equivalent amounts of impulsive energy concentrated at different frequencies is not equally hazardous to the auditory system. However, on the basis of a preliminary analysis of a large amount of audiometric data obtained from chinchillas exposed to high level blast waves there appeared to be some inconsistencies between the narrow band impulse data and the blast wave data in the region of 2.0 kHz. To resolve this discrepancy, two additional groups of animals were exposed to narrow band impulses with a center frequency of 2.075 kHz and peak intensities of 134 dB and 139 dB. The results of these two additional groups confirm the shape of the original P-weighting function and indicate that changes must be made in our approach to the analysis of the blast wave data referred to above. GRA

N92-17473# Army Research Inst. of Environmental Medicine, Natick, MA.

UPPER BODY EXERCISE: PHYSIOLOGY AND TRAINING APPLICATION FOR HUMAN PRESENCE IN SPACE

Michael N. Sawka and Kent B. Pandolf Jul. 1991 21 p

(AD-A242033) Avail: NTIS HC/MF A03 CSCL 06/10

In the weightless state astronauts do a substantial amount of work with their arms and hands. Upper body exercise elicits a peak oxygen uptake approximately 70 pct. of that obtained during lower body exercise; in addition, upper body exercise requires a greater oxygen uptake at a given power output than low body exercise. Therefore, when performing exercise at a given power output, both the absolute and relative exercise intensity is greater during upper body exercise. Although cardiac output responses for a given oxygen uptake are similar, the heart rate, blood pressure and total peripheral resistance responses are greater, and the stroke volume responses are lower at a given oxygen uptake during upper than lower body exercise. Body temperature responses to both exercise type are similar, but the temperature are achieved by different heat exchange mechanisms. During upper body exercise, there is a greater reliance on torso dry heat loss for temperature regulation. Exercise training programs can improve aerobic exercise capabilities for the upper body, but there are minimal cross-training benefits between the arms and legs. Space physiologists and engineers in the manned space program should consider the unique physiology associated with upper body exercise for: (1) assuring that astronauts are prepared to perform mission related tasks; (2) developing effective exercise countermeasures programs; and (3) engineering of adequate life support systems. GRA

N92-17476# Pacific-Sierra Research Corp., Los Angeles, CA.

BIOLOGICAL EFFECTS OF PROTRACTED EXPOSURE TO IONIZING RADIATION: REVIEW, ANALYSIS, AND MODEL DEVELOPMENT Technical Report, 15 Sep. 1986 - 20 Jul. 1990

George H. Anno, Gene E. McClellan, Michael A. Dore, and Siegmund J. Baum 1 Nov. 1991 280 p

(Contracts DNA001-86-C-0307; DNA001-87-C-0104)

(AD-A242981; PSR-2040; DNA-TR-90157) Avail: NTIS HC/MF A13 CSCL 06/7

Two basic approaches are developed to mathematically model biological responses to ionizing radiation exposure, including upper gastrointestinal (UG) distress (nausea, vomiting), lower gastrointestinal (LG) distress (diarrhea, fluid loss), and GI-syndrome lethality. Models are constructed to accommodate arbitrary histories of protracted exposure. Sets of coupled differential equations are employed to simulate dynamics of the biological processes involved. The modeling approaches are guided by a comprehensive review and analysis of relevant literature, including radiation-induced symptomatology, response dynamics, physiological changes, morphological changes, cell/tissue damage and recovery mechanisms, and existing radiobiological injury and recovery models. The upper gastrointestinal distress model (UGIDM) is a two-compartment toxicokinetic model to simulate radiation-induced production and clearing of humoral substances involved in triggering UG distress. GRA

N92-17557# Ohio State Univ., Columbus. Div. of Pharmaceutics.

EVALUATION OF LIPOSOME-ENCAPSULATED HEMOGLOBIN/LR16 FORMULATIONS AS A POTENTIAL BLOOD SUBSTITUTE Performance Report No. 3, period ending 8 Nov. 1991

Thomas G. Burke 8 Nov. 1991 12 p

(Contract N00014-90-J-1648)

(AD-A243075) Avail: NTIS HC/MF A03 CSCL 06/1

Two summary sheets show the structures of several new LR16 analogues recently synthesized. Preliminary testing has shown compounds 19, 22, and 25 to be active, achieving P50 values in LEH suspensions of 29.5, 28.5, and 21.0 mm Hg, respectively, at drug concentrations of 3 mM. The two lists of structures are followed by the experimental section outlining synthetic methodologies. The final three pages summarize a synthetic

scheme and NMR data concerning our first analogue which contains a quaternary, permanently-charged nitrogen moiety (which should significantly reduce drug leakage from liposome). We are presently testing the ability of this agent to modulate the P50 value of hemoglobin. GRA

N92-17567# Vector Research, Inc., Ann Arbor, MI.
FATIGUE EFFECTS ON HUMAN PERFORMANCE IN COMBAT: A LITERATURE REVIEW, VOLUME 1 Final Report, Sep. 1986 - Oct. 1988
Susan M. Evans, Robert R. Mackie, and Dennis C. Wylie Aug. 1991 253 p
(Contract MDA903-86-C-0428)
(AD-A242887; VRI-ARI-9; FR89-1(R)-Vol-1; ARI-RN-91-90) Avail: NTIS HC/MF A12 CSCL 06/10

For this report, a literature review was conducted to assess the knowledge of the effects of fatigue and related stressors on the performance of military personnel engaged in diverse military tasks. The objective was to determine whether there are sufficient objective, quantifiable data on the effects and time-course of fatigue to justify incorporation into combat models. Both mental and physical fatigue were considered. More than 500 articles, reports, and books were reviewed for this effort. A summary table of the results of sleep deprivation studies was organized. Prediction equations for physical activity are discussed. GRA

N92-17599# Defence and Civil Inst. of Environmental Medicine, Downsview (Ontario).
ALLEVIATION OF THERMAL STRAIN IN ENGINEERING SPACE PERSONNEL ABOARD CF SHIPS WITH THE EXOTEMP PERSONAL COOLING SYSTEM
J. Frim and K. Glass Jun. 1991 54 p
(AD-A242889; DCIEM-91-62) Avail: NTIS HC/MF A04 CSCL 06/6

The engineering spaces aboard Canadian Forces (CF) ships operating in warm climate can become very hot working environments. Some of these areas, notably the boiler room, are outside the citadel, and personnel working in these areas during periods of chemical threat must wear chemical defence (CD) clothing. The extra insulation and the increased resistance to sweat evaporation of this clothing, coupled with the heat of the environment, can impose a severe heat stress on the engineering personnel. A field trial was conducted aboard the HMCS Ottawa while en route from Halifax to Puerto Rico to see if the Exotemp liquid-based personal cooling system, could alleviate thermal stress under the above simulated conditions. Twelve engine room personnel from three watches participated in the trial, conducting their normal engine-room duties while being monitored for thermal physiological strain in four clothing ensembles: normal work dress (WD); normal work dress with cooling (WC); chemical defence clothing (CD); and chemical defence clothing with cooling (CC). Heat stress conditions of 45-50 C dry-bulb temperature were created. Rectal temperatures at 90 minutes of elapsed time clearly indicated statistically significant benefits of cooling with the chemical defence clothing. Heart rates were generally above 120 bpm without cooling (condition WD and CD) while they generally remained below 120 bpm with cooling (conditions WC and CC). GRA

N92-17645*# National Aeronautics and Space Administration. Lyndon B. Johnson Space Center, Houston, TX.
ECCENTRIC AND CONCENTRIC MUSCLE PERFORMANCE FOLLOWING 7 DAYS OF SIMULATED WEIGHTLESSNESS
Judith C. Hayes, Mary L. Roper, Augustus D. Mazzocca, John J. McBrine, Linda H. Barrows (Krug Life Sciences, Inc., Houston, TX.), Bernard A. Harris, and Steven F. Siconolfi Washington Feb. 1992 13 p
(NASA-TP-3182; S-665; NAS 1.60:3182) Avail: NTIS HC/MF A03 CSCL 06P

Changes in skeletal muscle strength occur in response to chronic disuse or insufficient functional loading. The purpose of this study was to examine changes in muscle performance of the lower extremity and torso prior to and immediately after 7 days of simulated weightlessness (horizontal bed rest). A Biodex was used to determine concentric and eccentric peak torque and angle at peak torque for the back, abdomen, quadriceps, hamstring, soleus, and tibialis anterior. A reference angle of 0 degrees was set at full extension. Data were analyzed by ANOVA. Author

N92-17712# Army Environmental Hygiene Agency, Aberdeen Proving Ground, MD.
PRELIMINARY ASSESSMENT OF THE RELATIVE TOXICITY OF TETRAGLYCINE HYDROPERIODIDE, PHASE 1 Report, Jan. 1988 - Aug. 1991
Joseph A. Macko, Jr. Aug. 1991 29 p
(AD-A243334; AEHA-75-51-0742-91) Avail: NTIS HC/MF A03 CSCL 06/4

Toxicity of Technical Grade Tetraglycine Hydroperiodide (TGHP), the active ingredient in a military water purification tablet (MIL-W-283) has been completed. TGHP is moderately toxic by ingestion when prepared as a aqueous slurry. The compound has no potential for causing sensitization. However, TGHP did produce mild but reversible primary skin irritation, and the technical grade powder did cause severe and nonreversible injury to the eye. TFHP did not exhibit mutagenic activity in three of the four mutagenicity assays performed. In the Chromosome Aberration Assay, TGHP did produce a significant increase in chromosomal aberrations in CHO cells in the presence, but not in the absence, of metabolic activation. This single positive finding in the Chromosome Aberration Assay, in the presence of metabolic activation, is not considered sufficient to classify TGHP a potential human-cell mutagen. GRA

N92-17714# Lawrence Livermore National Lab., CA. Environmental Sciences Div.
THE EFFECT OF SHOWER/BATH FREQUENCY ON THE HEALTH AND OPERATIONAL EFFECTIVENESS OF SOLDIERS IN A FIELD SETTING: RECOMMENDATION OF SHOWERING FREQUENCIES FOR REDUCING PERFORMANCE-DEGRADING NONSYSTEMIC MICROBIAL SKIN INFECTIONS Final Report, Aug. 1990 - Sep. 1991
L. C. Hall, J. I. Daniels, R. Aly, H. I. Maibach, and S. A. Schaub 30 Sep. 1991 119 p Sponsored by Army
(AD-A242923; UCRL-CR-107449) Avail: NTIS HC/MF A06 CSCL 06/9

Historically, military personnel deployed in the field, particularly in hot regions or humid environments, have suffered disabling microbial infections of the skin severe enough to contribute to significant reductions in combat-troop strength. Currently, the U.S. Army makes facilities available to field personnel for showering on a weekly basis to prevent infestations of the body louse and the subsequent spread of louse-borne disease. However, a weekly showering frequency has never been evaluated for its efficacy in preventing microbial infections of the skin - a significant cause of man-days lost from combat in modern-day military conflicts. Consequently, field showers may be more important for maintaining combat effectiveness of military personnel than previously thought; however, providing such facilities requires tremendous logistical support. Therefore, we developed shower frequencies for troops in field environments that should minimize or prevent microbial skin infections. According to our calculations, the optimum showering frequency can range from as often as four times per day to as little as once every seven days, depending on skin integrity, environmental conditions, and cleansing agent. We also reviewed the scientific and regulatory information concerning the efficacy and safety of skin-cleansing products; the antimicrobial and antiseptic compounds, triclocarban and chlorhexidine, may be the most suitable for routine use by U.S. military personnel. GRA

N92-17798# Michigan Univ., Ann Arbor.
HARD-SURFACE CONTAMINATION DETECTION EXERCISE Ph.D. Thesis
S. Kawa 1991 200 p
(Contract DE-AC05-76OR-00033)
(DE92-004750; DOE/OR-00033/T455) Avail: NTIS HC/MF A09

The purpose of this thesis is to create a practical exercise which demonstrates the techniques used by Health Physicists to detect surface contamination, including both instrumentation and smear survey techniques. By understanding the basic principles of the most commonly found instruments, the intent is that a new Health Physics graduate can correctly choose and apply an instrument to their detection situation. The exercise is also intended to acquaint students with the very basic principles of smear techniques. Smear surveys are probably the most universally applied technique in this industry, however, very little literature exists on the subject. The techniques are usually taught, on-the-job and by demonstration. By their seeing and participating in this presentation, it is intended that Health Physics students can accelerate their first few weeks at their new careers, and enable them to recognize common mistakes. Health Physicists are expected to have knowledge of the basic practices of their profession. This exercise will allow Health Physics students to become familiar with the use of hand-held detection devices and the technique of smear surveys. Adequate measurement and recording of surface contamination information is necessary to: meet licensing requirements; protect the health and safety of the workers; maintain accurate records in the case of litigation or dose reconstruction; and maintain high levels of professional competency. This exercise will assist students in obtaining the skills necessary to adequately measure and record levels of surface contamination. DOE

N92-17800# Oak Ridge Associated Universities, Inc., TN.
LABOR MARKET TRENDS FOR HEALTH PHYSICISTS
Nov. 1991 18 p
(Contract DE-AC05-76OR-00033)
(DE92-004770; DOE/OR-00033/T462) Avail: NTIS HC/MF A03

Information is presented on the recent trends in enrollments, degrees and US civilian, non-medical employment for health physicists. This information is combined with other data such as salary comparisons, indicators of hiring difficulties by the Federal government, and information received from employers to assess the current labor market status for health physicists. This information indicates that for the last several years demands for new graduate health physicists have been greater than supplies. An assessment of projected enrollment and degree trends and employment trends through the mid-1990s is presented. This assessment indicates that the current labor market situation is not likely to change. The number of job openings will continue to exceed the number of new graduates available for employment. Moreover, information is presented which indicates that there are several factors at work in the general economy which will make is difficult to enhance health physics enrollments and degrees. Thus, while the recent increase in enrollments in health physics programs and the addition of two new programs in 1990 is encouraging, these are not enough to meet future employment needs. Employers will, in all likelihood, continue to have difficulties in hiring health physicists, and salaries will continue to be relatively high through the mid-1990s. DOE

N92-17802# Kyoto Univ., Kumatori (Japan). Research Reactor Inst.
PROCEEDINGS OF THE CONFERENCE ON HEALTH PHYSICS
Tadashi Tsujimoto, ed. and Mitsuo Mizuma, ed. Mar. 1991 35 p In JAPANESE; ENGLISH summary Conference held in Kumatori, Japan, 20 Mar. 1990
(DE92-704335; KURRI-TR-347; CONF-9003295) Avail: NTIS HC/MF A03

This booklet presents nine talks given at the Conference on Health Physics, which was held on March 20, 1990, at Research Reactor Institute of Kyoto University (KURRI), Japan. The first talk discusses future trends in health physics, focusing on the application of computers, development of new techniques, energy industries, and administrative regulations. The second talk discusses the importance of health physics in relation to nuclear energy. The third one addresses importance of health physics in relation to medical treatment. The fourth and fifth ones discuss the present status and future trends in education in health physics. The sixth one focuses on education in health physics, placing emphasis on grass-roots activities in this field. The seventh and eighth talks discusses various activities to be carried out in the future by the Health Physics Research Center. The ninth one describes major developments leading to the establishment of the Health Physics Research Center. Three appendices are attached which respectively summarizes major subjects at a meeting on the budget for the Health Physics Research Center, outlines some studies for radiation control in space aircraft and space bases, and describes major reasons for the necessity of the Health Physics Research Center. DOE

53 BEHAVIORAL SCIENCES

Includes psychological factors; individual and group behavior; crew training and evaluation; and psychiatric research.

N92-17052# Human Engineering Labs., Aberdeen Proving Ground, MD.
THE EFFECTS OF SPEECH INTELLIGIBILITY LEVEL ON CONCURRENT VISUAL TASK PERFORMANCE Final Report
David G. Payne, Leslie J. Peters, Deborah P. Birkmire, and Georges R. Garinther Sep. 1991 33 p
(DA Proj. 1L1-61102-B-74-A)
(AD-A243015; HEL-TM-17-91) Avail: NTIS HC/MF A03 CSCL 25/4

Two experiments were performed to determine if changes in speech intelligibility level can impact performance levels in concurrent visual tasks. The auditory task used in both experiments was the auditory memory search task in which subjects memorized a set of words and then decided whether auditorally presented probe items were members of the memorized set. Experiment 1 used an unstable tracking task as the visual task, and experiment 2 used a spatial decision-making task. Results showed that unstable tracking performance was unaffected by the level of speech intelligibility during the auditory task, whereas accuracy in the spatial decision-making task was significantly worse at low speech intelligibility levels. These results have clear implications for the design of communications systems. The findings are interpreted within the framework of multiple resource theory, and future directions for research are described. GRA

N92-17115# Air Force Inst. of Tech., Wright-Patterson AFB, OH.
NEURAL NETWORK CLASSIFICATION OF MENTAL WORKLOAD CONDITIONS BY ANALYSIS OF SPONTANEOUS ELECTROENCEPHALOGRAMS M.S. Thesis
Gretchen D. Lizza 1991 92 p
(AD-A243369; AFIT/CI/CIA-91-095) Avail: NTIS HC/MF A05 CSCL 06/1

Artificial neural networks were explored in this study to determine their capability to discriminate workload tasks on the basis of electroencephalograms (EEGs) recorded during task performance. EEG traces were recorded by placing electrodes at the occipital (Oz), parietal (Pz), central (Cz), and frontal (Fz) midline positions during workload tasks. Two conditions of workload were presented to the subjects. The first condition, an eye condition, varied whether eyes were open or closed while subjects counted or sat quietly. In the second condition, the workload conditions presented to the subjects were high and low levels of display monitoring and math processing tasks. GRA

N92-17145# Air Force Inst. of Tech., Wright-Patterson AFB, OH.
RAPID NONCONJUGATE ADAPTATION OF VERTICAL VOLUNTARY PURSUIT EYE MOVEMENTS Ph.D. Thesis
Gerald A. Gleason 1991 241 p
(AD-A243358; AFIT/CI/CIA-91-022D) Avail: NTIS HC/MF A11 CSCL 06/5

The precise yoking of the two eyes during vertical eye movements is normally preserved throughout life. This preservation

is due in part to adaptive processes that adjust the relative neural innervations sent to each eye's extraocular muscles (nonconjugate adaptation). This behavioral study investigates adaptive processes that maintain conjugacy along the vertical meridian during three types of ocular motor behavior: voluntary pursuit, saccade, and steady fixation. Binocular yoking was quantified by binocular recordings of vertical eye position (dual-Purkinje eye tracker) while vertical eye movements were monocularly stimulated. Properties of nonconjugate adaptive processes were inferred from changes in pre- and post-adaptation binocular yoking. GRA

N92-17336# Florida State Univ., Tallahassee. Dept. of Psychology.
MECHANISMS OF TEMPORAL PATTERN DISCRIMINATION BY HUMAN OBSERVERS Annual Technical Report, 1 Oct. 1990 - 30 Sep. 1991
Robert D. Sorkin 31 Oct. 1991 11 p
(Grant AF-AFOSR-0065-91; AF Proj. 2313)
(AD-A243051; AFOSR-91-0915TR) Avail: NTIS HC/MF A03 CSCL 06/4

Several studies of temporal pattern perception were conducted, using tasks where the listener discriminated whether or not two tonal sequences formed the same temporal pattern. Performance was modeled using the Pattern Correlation Model, which assumes that the listener estimates the correlation between the pattern of intervals marked by the tones in each sequence. The model was applied to experiments where the sequences were compressed or expanded in time; presented at different frequencies and to different ears; onset delayed from 1 to 1500 ms; and subject to cyclic repetitions within each sequence. Other experiments have concerned: (1) the discrimination of rhythmicity; (2) visual information processing as a function of spatial position and time stress; and (3) modeling and computer simulation of systems for group signal detection. GRA

N92-17450# Air Force Systems Command, Brooks AFB, TX. Armstrong Lab.
COMPARISON OF EXPERIMENTAL US AIR FORCE AND EURO-NATO PILOT CANDIDATE SELECTION TEST BATTERIES Interim Report, 21 May - 4 Jun. 1991
Thomas R. Carretta Oct. 1991 26 p
(AD-A242358; AL-TP-1991-0034) Avail: NTIS HC/MF A03 CSCL 05/8

Air Force personnel from several countries currently are evaluating computerized test batteries as an adjunct to current pilot candidate selection procedures. This paper describes and compares proposed U.S. Air Force (USAF) and Euro-NATO Aircrew Selection Working Group (ACSWG) pilot candidate selection test batteries. A validation strategy for the ACSWG test battery is described that focuses on test item analyses (e.g., evaluating internal consistency), evaluation of test scoring procedures, evaluation of test battery factor structure, and evaluation of test scores against training performance criteria. GRA

N92-17458# Carnegie-Mellon Univ., Pittsburgh, PA. Artificial Intelligence and Psychology Project.
ATTENTION, AUTOMATICITY AND PRIORITY LEARNING
Prahlad Gupta and Walter Schneider 1991 8 p
(Contracts N00014-86-K-0678; N00014-87-K-0397; MDA903-89-K-0174)
(AD-A242226; CMU-AIP-148) Avail: NTIS HC/MF A02 CSCL 05/8

It is widely held that there is a distinction between attentive and automatic cognitive processing. In research on attention using visual search tasks, the detection performance of human subjects in consistent mapping paradigms is generally regarded as indicating a shift, with practice, from serial, attentional, controlled processing to a parallel, automatic processing, while detection performance in varied mapping paradigms is taken to indicate that processing remains under attentional control. This paper proposes a priority learning mechanism to model the effects of practice and the development of automaticity, in visual search tasks. A connectionist simulation model implements this learning algorithm. Five prominent features of visual search practice effects are simulated. These are: (1) in consistent mapping tasks, practice reduces processing time, particularly the slope of reaction times as a function of the number of comparisons; (2) in varied mapping tasks, there is no change in the slope of the reaction time function: (3) both the consistent and varied effects can occur concurrently; (4) reversing the target and distractor sets produces strong interference effects; and (5) the benefits of practice are a function of the degree of consistency. GRA

N92-17500# Air Force Inst. of Tech., Wright-Patterson AFB, OH. School of Engineering.
ANALYSIS OF VISUAL ILLUSIONS USING MULTIRESOLUTION WAVELET DECOMPOSITION BASED MODELS M.S. Thesis
John S. Laing Dec. 1991 244 p
(AD-A243712; AFIT/GE/ENG/91D-34) Avail: NTIS HC/MF A11 CSCL 23/2

This thesis provides alternatives to the explanation that spatial filtering is responsible for the perception of illusory contours in the Kanisza Triangle illusion. Specifically, we use a Multiresolution Wavelet Decomposition to divide an image into spatial-frequency bands that are used as inputs to three biologically motivated models. The thesis includes a brief tutorial of Wavelet theory and an in-depth explanation of our implementation of recently published algorithms for Multiresolution Wavelet Analysis. The first model is based on the saccadic movements of the human eye. It demonstrates the importance of the high spatial-frequency content of an image in the formulation of the illusion. The second model is based on the serial architecture of the data transmission channel between the retina and the visual world model. The third model considers only the high spatial-frequency content of the image. It consists of lateral excitation networks that serve to simulate the local high spatial-frequency energy interactions that contribute to illusory contours. GRA

N92-17503# Yale Univ., New Haven, CT. Dept. of Psychology.
SIGNAL- AND LISTENER-BASED FACTORS IN COMPLEX AUDITORY PATTERN PERCEPTION Final Report, 1 Oct. 1990 - 30 Sep. 1991
Arthur G. Samuel 7 Oct. 1991 22 p
(Grant AF-AFOSR-0020-91; AF Proj. 2313)
(AD-A243716; AFOSR-91-0283TR) Avail: NTIS HC/MF A03 CSCL 05/8

The research conducted during the one year funding period was a subset of the original three year study of the perception of complex auditory patterns, including speech and music. One set of experiments explored two early stages in the perception of complex signals, using adaptation procedures. This research investigated effects of varying signal amplitude, and the effects of more cognitive factors: lexical knowledge, and the listener's level of attention to the adapting sound. A second set of experiments perceptual restoration effects. Those experiments investigated how knowledge of particular words influenced the perceptual restoration of deleted or degraded portions of the word. The two lines of research represent progress toward understanding the analyses conducted on complex auditory patterns by human listeners. GRA

N92-17554# Boston Univ., MA. Center for Adaptive Systems.
THE COGNITIVE, PERCEPTUAL, AND NEURAL BASES OF SKILLED PERFORMANCE Annual Technical Report, 15 Mar. 1990 - 14 Mar. 1991
Stephen B. Grossberg 14 Mar. 1991 36 p
(Grant AF-AFOSR-0175-90; AF Proj. 3484)
(AD-A243052; AFOSR-91-0913TR) Avail: NTIS HC/MF A03 CSCL 05/8

This report reviews progress from the Boston University, Northeastern University, and Harvard University/Cambridge University research groups of our AFOSR University Research Initiative grant. The report lists books and articles, summaries of research, and selected abstracts of key articles. The report also encloses the program and the abstract book of an AFOSR-supported conference that was held at the Wang Institute

of Boston University on May 11-13, 1990. The topic of the conference was Neural Networks for Automatic Target Recognition. There were fifteen invited speakers and thirty-eight contributed posters. Three-hundred scientists and students attended from twenty countries and thirty-five states of the United States. GRA

N92-17634# North Carolina Univ., Chapel Hill. Dept. of Computer Science.
ELECTRONIC EXPANSION OF HUMAN PERCEPTION
Warren Robinett 1991 7 p
(Contract N00014-86-K-0680)
(AD-A242028) Avail: NTIS HC/MF A02 CSCL 06/1

The true potential of this new field comes from the ability of a head mounted display to induce a synthetic experience in its wearer. The ability to artificially create and design experience enables possibilities and powers that were formerly impossible. If experience can be captured and transmitted, then you can 'travel' instantaneously to a distant location and see the trees, feel the wind, hear the birds, and smell the flowers. If electronic instruments can sense things that you cannot perceive, such as the inside of opaque objects, then you can be shown images of these invisible things. There are, however, things which are invisible to all of your senses. Examples of these imperceptible phenomena are X-rays, infrared radiation, radio waves, magnetic fields, radioactivity, ultrasound, electricity, the inside of opaque objects, microscopic objects, and events occurring too fast to see. Even though you cannot directly perceive these things, you can indirectly measure and observe them with various instruments and electronic sensors. GRA

N92-17648# Texas Univ. Health Science Center, San Antonio.
BRAINMAP: A DATABASE OF FUNCTIONAL NEUROANATOMY DERIVED FROM HUMAN BRAIN IMAGES Quarterly Report No. 2
14 Nov. 1991 6 p
(Contract N00014-91-J-1903)
(AD-A243161) Avail: NTIS HC/MF A02 CSCL 06/4

Our efforts during the second quarter were again primarily devoted to the Macintosh version of BrainMap. The status of the four main components of BrainMac software are: (1) Search Windows (fully conceived, fully designed and awaiting SQL interface); (2) SQL interface (mostly conceived; partly designed; not operational); (3) Review Windows (mostly conceived, mostly designed, and awaiting SQL interface), and (4) Report Generation (partly conceived, partly designed, and awaiting SQL interface). Software development is proceeding in a timely fashion, and at present we see no major problems with completing the project on time. Work on BrainMap-SQL has begun and more focus on that portion of the project will be given when BrainMap-Mac is operational. GRA

N92-17758# Dayton Univ., OH.
EFFECT OF TWO TYPES OF SCENE DETAIL ON DETECTION OF ALTITUDE CHANGE IN A FLIGHT SIMULATOR Interim Report, Jun. 1989 - Feb. 1991
James A. Kleiss and David C. Hubbard Jul. 1991 48 p
(Contract F33615-90-C-0005)
(AD-A242034; AL-TR-1991-0043) Avail: NTIS HC/MF A03 CSCL 01/2

The effect of two types of simulator scene detail on detection of change in altitude was evaluated. The first type was the density of three dimensional objects in scenes, which ranged from 11 objects per square mile to 175 objects per square mile. The second was the detail/realism of three-dimensional objects, which ranged from simple, untextured tetrahedrons (i.e., three-sided pyramids) to a mix of highly detailed and realistic appearing oak trees, pine trees, and bushes. A group of pilots and a group of non-pilots viewed short segments of flight over simulated terrains and responded by pushing one of three buttons to indicate whether they were descending, remaining level at 150 ft above ground level or ascending. Results of experiment one showed that accuracy and reaction times for both groups improved significantly with increases in object density. However, a significant effect of object type was obtained only for the non-pilot group with the accuracy dependent measures. Interestingly, the advantage favored tetrahedrons over realistic objects. In experiment two, these effects persisted even after four sessions of practice. These results suggest that available computer-image generator processing capacity may be used most effectively by maximizing object density rather than object realism. GRA

54 MAN/SYSTEM TECHNOLOGY AND LIFE SUPPORT

Includes human engineering; biotechnology; and space suits and protective clothing.

For related information see also *16 Space Transportation.*

N92-16982# Wright Lab., Wright-Patterson AFB, OH.
DUAL COLOR AND SHAPE CODING IN THE VISUAL PERIPHERY: A STUDY OF JOINT TACTICAL INFORMATION DISTRIBUTION SYSTEM (JTIDS) SYMBOLOGY Final Report, Mar. - Jul. 1991
Eileen Ancman Aug. 1991 26 p
(AD-A243253; WL-TM-91-315-FIGK) Avail: NTIS HC/MF A03 CSCL 06/4

This research looked at four different dual color and shape coded Joint Tactical Information Distribution System (JTIDS) symbols on a color CRT located in the subject's periphery. Nighttime cockpit conditions were simulated. No subject could detect the 0.5 degs. symbols in their periphery beyond 15 degs. Approximately 1/3 of the potential subject pool could not correctly identify symbol shape even at the lower end of the range under study: 5 degs. Subjects used only color to key in on the symbol's meaning; the symbol's shape did not matter at all during this recognition task, for symbol shape was harder to perceive than color in the periphery. Color and the symbol's meaning could both be perceived at approximately 12 degs. off of the fovea, while shape had to be at 8 degs before subjects could perceive it. It is recommended that additional research in this area be accomplished. If findings are confirmed, it is suggested that a careful examination of the JTIDS dual coding be undertaken. GRA

N92-17014# Navy Experimental Diving Unit, Panama City, FL.
EVALUATION OF BAUER HIGH PRESSURE BREATHING AIR P-2 PURIFICATION SYSTEM Final Report
David Sullivan Aug. 1991 19 p
(AD-A243535; NEDU-10-91) Avail: NTIS HC/MF A03 CSCL 23/5

The Navy Experimental Diving Unit (NEDU) tested the BAUER P-2 High Pressure, Breathing Air Purification System from 16 July 1991 to 19 July 1991. The purpose of this test was to determine if the P-2 Air Purification System functioned as specified and was suitable for use by the U.S. Navy. Additionally, if the system passed the test criteria a recommendation would be made to add it to the Approved for Navy Use (ANU) list. The BAUER P-2 Purification System met the manufacturer's specifications for quantity of air processed with a quality which met U.S. Navy purity standards. The design and engineering were determined to be adequate. The BAUER P-2 Air purification System is considered suitable for use with U.S. Navy divers high pressure breathing air compressors. GRA

N92-17132*# Georgia Inst. of Tech., Atlanta. School of Industrial and Systems Engineering.
ACQUISITION AND PRODUCTION OF SKILLED BEHAVIOR IN DYNAMIC DECISION-MAKING TASKS Semiannual Status Report
Alex Kirlik 31 Jan. 1992 75 p
(Grant NAG2-656)
(NASA-CR-189846; NAS 1.26:189846) Avail: NTIS HC/MF A04 CSCL 05H

Currently, two main approaches exist for improving the

human-machine interface component of a system in order to improve overall system performance - display enhancement and intelligent decision making. Discussed here are the characteristic issues of these two decision-making strategies. Differences in expert and novice decision making are described in order to help determine whether a particular strategy may be better for a particular type of user. Research is outlined to compare and contrast the two technologies, as well as to examine the interaction effects introduced by the different skill levels and the different methods for training operators. Author

N92-17143# Army Natick Research and Development Command, MA.
USER EVALUATION OF LASER BALLISTIC SUN, WIND AND DUST GOGGLE LENSES (DYE TECHNOLOGY) Final Report, Sep. 1990 - Sep. 1991
B. Jezior, C. L. Blackwell, L. L. Lesher, V. Shearer, and L. Plante Nov. 1991 93 p Prepared in cooperation with Geo-Centers, Inc., Newton, MA
(AD-A243245; NATICK/TR-92/007) Avail: NTIS HC/MF A05 CSCL 05/8

Prompted by a Product Improvement Program aimed at providing soldiers eye protection equal to that of the Ballistic Laser Protective Spectacles (BLPS), Natick Research, Development and Engineering Center recently field tested four experimental laser ballistic lenses in the Sun, Wind, and Dust Goggle. All lenses used dye absorber technology. Field testing with Armor and Infantry military personnel resulted in data collected from more than 300 soldiers on over 80 variables. The tests included typical military operational tasks. The soldiers also wore the lenses during field training exercises and were surveyed about the lenses' effects on mission performance. The Farnsworth-Munsell 100-Hue Test, a laboratory test which examines the effects of the lenses on color perception, was also conducted in both simulated daylight and reduced visibility conditions. Farnsworth-Munsell test results showed that performance was not seriously degraded by any lens in daylight illumination levels. In reduced visibility conditions there was impairment, and the degree of impairment was relatively consistent with what was expected from the respective lenses' transmittance levels and specific lines of protection. There were also some negative mission performance issues raised that were more a function of goggle wear than lens performance. GRA

N92-17278# Defence Research Establishment, Ottawa (Ontario).
HEAT STRESS CAUSED BY WEARING DIFFERENT TYPES OF CW PROTECTIVE GARMENT
S. D. Livingstone and R. W. Nolan Aug. 1991 13 p
(AD-A243043; DREO-TN-91-14) Avail: NTIS HC/MF A03 CSCL 05/8

One means of reducing the heat stress caused by wearing protective clothing is to eliminate the air layers between the skin and layers of the ensemble. In order to evaluate the effectiveness of this concept, four unacclimated males wearing either the current Canadian Forces (CF) chemical protective overgarment, and individually tailored skintight protective garment or CF combat uniform participated in a series of experiments conducted at 40 C and low relative humidity. Each was instrumented with a rectal thermistor, donned the clothing and walked on a treadmill at 5 km hr and 2 pct. grade for 90 min, until his rectal temperature reached 39 C or he requested to withdraw from the experiment. The results of this preliminary investigation indicate that there appears to be some advantage to wearing the skintight clothing under these conditions. GRA

N92-17331# Navy Experimental Diving Unit, Panama City, FL.
UNMANNED EVALUATION OF BAUER HIGH PRESSURE BREATHING AIR P-5 PURIFICATION SYSTEM Final Report
David Sullivan Aug. 1991 25 p
(AD-A243486; NEDU-12-91) Avail: NTIS HC/MF A03 CSCL 23/5

The BAUER P-5 high pressure, breathing air purification system was tested from 24 July 1991 to 12 August 1991. The purpose of this test was to determine if the P-5 air purification system functioned as specified and was suitable for use by the U.S. Navy. The BAUER P-5 air purification system met the manufacturer's specifications for quantity of air processed with a quality which met the U.S. Navy purity standards. The design and engineering were determined to be adequate. The BAUER P-5 purification system is considered suitable for use with U.S. Navy divers high pressure breathing air compressors. GRA

N92-17432# Naval Air Development Center, Warminster, PA. Air Vehicle and Crew Systems Technology Dept.
AIRCREW CRITIQUE OF HIGH-G CENTRIFUGE TRAINING: PART 3: WHAT CAN WE CHANGE TO BETTER SERVE YOU? Final Report, Oct. 1988 - May 1991
James E. Whinnery and Richard J. Hamilton 11 Jun. 1991 27 p
(AD-A243496; NADC-91071-90) Avail: NTIS HC/MF A03 CSCL 01/2

We have successfully initiated high-G centrifuge training for fighter attack aviators at the Naval Air Development Center. The response of aircrew to a post-training critique question, asking how the program could be modified to better meet operational needs, was evaluated so aircrew might have the ability to improve their training program. The recommendations could be grouped into 5 major categories: (1) no change, (2) addition of a closed loop aerial combat maneuvering (ACM) profile with bogey on a tracking task, (3) centrifuge gondola modifications, (4) training profile modifications, and (5) modifications concerning when the training is given. A number of suggestions for improvement are worth pursuing and implementing immediately. Although caution should be exercised when altering the content and goals of the proven program, we strongly concur with several of the changes. This includes providing a closed loop ACM profile with at least a moderately high-fidelity tracking task (bogey) and at least optional G-LOC training. GRA

N92-17569# David Taylor Research Center, Bethesda, MD. Ship Hydromechanics Dept.
A FREQUENCY-DOMAIN METHOD FOR ESTIMATING THE INCIDENCE AND SEVERITY OF SLIDING Final Report, 1 Jan. - 30 Aug. 1991
Ross Graham, A. E. Baitis, and William G. Meyres 30 Aug. 1991 46 p
(AD-A243077; DTRC/SHD-1361-01) Avail: NTIS HC/MF A03 CSCL 13/10

A frequency-domain method of predicting the incidence of personnel or equipment sliding is presented which includes the (linearized) forces due to roll, pitch, longitudinal, lateral and vertical accelerations, and also the effects of non-zero mean heel. The predictions of the method are compared with the results of observations of at-sea sliding incidents, and good correspondence is obtained. A simple approximation for the duration of threshold exceedance probability density is described, and used to develop a method for predicting the incidence of slides greater than a certain severity. The method applies for arbitrary lateral and vertical acceleration, but only to the case in which the longitudinal acceleration is negligible. An example of the application of the method is presented. It is argued that ship motions such as roll, pitch, lateral and longitudinal accelerations are the wrong physical parameters for expressing seakeeping criteria. These criteria become simpler when expressed in terms of the incidence of degrading events such as helicopters sliding, and are equally applicable to all vessel types. GRA

N92-17617# Air Force Inst. of Tech., Wright-Patterson AFB, OH.
VISUAL DETERMINATION OF INDUSTRIAL COLOR-DIFFERENCE TOLERANCES USING PROBIT ANALYSIS M.S. Thesis
Gregory D. Snyder Jun. 1991 112 p
(AD-A243545; AFIT/CI/CIA-91-083) Avail: NTIS HC/MF A06 CSCL 06/4

A perceptibility study was conducted to visually determine the

median tolerance values of 45 color-difference vectors in CIELAB color space using surface model viewing of paint samples. Nine different color centers, each comprising five color vectors, were employed to collect a superthreshold dataset. Fifty color normal observers made quantal judgements under simulated D65 illuminant regarding the magnitude of color difference pairs based on comparisons to a near neutral color difference anchor pair. Probit analysis was applied to the response frequencies for each vector to estimate the parameters of the distribution and the median tolerance values. Results indicated the probit adequately models the response distributions of the human observer population.
GRA

N92-17656# Marine Biological Lab., Woods Hole, MA.
THE 7TH ANNUAL WORKSHOP ON COMPUTATIONAL NEUROSCIENCE Final Report
30 Aug. 1991 7 p Workshop held in Woods Hole, MA, 24-30 Aug. 1991 Sponsored by Navy
(AD-A243462) Avail: NTIS HC/MF A02 CSCL 05/8

The Computational Neuroscience Workshop was held in Woods Hole at the Marine Biological Laboratory on August 24 to August 30, 1991, concurrently with the last week of the Computational Neuroscience Summer Course. The primary purpose of the workshop was to bring together the leading investigators interested in applying computational modeling techniques to problems in brain function. This was the seventh year in which this workshop was held at Woods Hole. There was a general feeling that the field of computational neuroscience had over this time started to live up to its early promise, and the workshop has contributed significantly to this development. The impact of the workshop was apparent in the research papers that the participants circulated, many of which grew out of discussions between participants at earlier workshops. The existence of the summer course was an encouraging indication of the hopes for the future of the field. One of the central themes of this year's workshop was learning and memory in populations of neurons. This topic was introduced in talks by Terry Sejnowski on adaption of the vestibulo-ocular reflex, by Eric Knudsen on neural and behavioral plasticity during the development of sound localization in the barn owl, by Bob Desimone on habituation of neurons in the inferior temporal cortex to complex stimuli, and by Dana Ballard on reinforcement learning in the setting of planning.
GRA

N92-17673# Mitre Corp., Bedford, MA.
USI RAPID PROTOTYPING TOOL EVALUATIONS SURVEY
Marian J. Murphy Sep. 1991 102 p
(AD-A243168; MTR-11259) Avail: NTIS HC/MF A06 CSCL 12/5

The Human Factors Engineering for User System Interface (HFE/USI) Specialty Group has conducted several evaluations of rapid prototyping tools to support the design and development of user interfaces for command and control systems. To standardize the evaluation methodology, we compiled a list of command and control criteria and rated tools against them. These ratings can be used to select a tool that will closely match the needs of a MITRE/ESD program. This paper describes the evaluation methodology and applies it to the review tools: VAPS, LUIS/SMS, SL-GMS, Data Views, TAE Plus, and SET.
GRA

N92-17866*# National Aeronautics and Space Administration. Marshall Space Flight Center, Huntsville, AL.
AUTOMATIC LOCKING ORTHOTIC KNEE DEVICE Patent Application
Bruce Weddendorf, inventor (to NASA) 26 Dec. 1991 15 p
(NASA-Case-MFS-28633-1; NAS 1.71:MFS-28633-1; US-Patent-Appl-SN-813629) Avail: NTIS HC/MF A03 CSCL 05H

An articulated tang in clevis joint for incorporation in newly manufactured conventional strap-on orthotic knee devices or for replacing such joints in conventional strap-on orthotic knee devices is discussed. The instant tang in clevis joint allows the user the freedom to extend and bend the knee normally when no load (weight) is applied to the knee and to automatically lock the knee when the user transfers weight to the knee, thus preventing a damaged knee from bending uncontrollably when weight is applied to the knee. The tang in clevis joint of the present invention includes first and second clevis plates, a tang assembly and a spacer plate secured between the clevis plates. Each clevis plate includes a bevelled serrated upper section. A bevelled shoe is secured to the tank in close proximity to the bevelled serrated upper section of the clevis plates. A coiled spring mounted within an oblong bore of the tang normally urges the shoes secured to the tang out of engagement with the serrated upper section of each clevic plate to allow rotation of the tang relative to the clevis plate. When weight is applied to the joint, the load compresses the coiled spring, the serrations on each clevis plate dig into the bevelled shoes secured to the tang to prevent relative movement between the tang and clevis plates. A shoulder is provided on the tang and the spacer plate to prevent overextension of the joint.
NASA

N92-17910*# National Aeronautics and Space Administration. Lyndon B. Johnson Space Center, Houston, TX.
TREADMILL FOR SPACE FLIGHT Patent Application
William E. Thornton, inventor (to NASA) 15 Oct. 1991 35 p
(NASA-Case-MSC-21752-1; NAS 1.71:MSC-21752-1; US-Patent-Appl-SN-775404) Avail: NTIS HC/MF A03 CSCL 05H

Method and apparatus for accurately simulating locomotion in a weightless environment, especially to prevent atrophy of a subject's musculoskeletal and cardiorespiratory systems during space travel, are disclosed. Forces, including the vertical, horizontal, and lateral force generated by an individual during locomotion on a treadmill using a rigid belt with rigid transfer elements supported by low friction bogies, are measured by strain gauges sensitive in their respective direction. The vertical forces produced by securing the subject to the treadmill via bungee cords, in conjunction with the measured velocity of the treadmill and the mode of locomotion, are used to determine the subject's equivalent weight. The other horizontal and lateral forces are used to determine the external work produced by the subject when locomotion is performed on a nonlevel surface with an effective grade angle. The measured forces are related in such a way that the grade angle is easily determined. A motor and additional circuitry can be added to the apparatus to measure and force a subject to maintain a predetermined work rate associated with a preselected grade angle and tread velocity.
NASA

N92-17355*# National Aeronautics and Space Administration. Marshall Space Flight Center, Huntsville, AL.
ENVIRONMENTAL CONTROL AND LIFE SUPPORT SYSTEM EVOLUTION ANALYSIS
Paul Wieland and Sandy Montgomery *In* NASA, Washington, Beyond the Baseline 1991: Proceedings of the Space Station Evolution Symposium. Volume 2: Space Station Freedom, Part 2 Sep. 1991 p 1237-1270 (For primary document see N92-17348 08-18)
Avail: NTIS HC/MF A20 CSCL 06K

N92-17356*# National Aeronautics and Space Administration. Marshall Space Flight Center, Huntsville, AL.
THE ENVIRONMENTAL CONTROL AND LIFE SUPPORT SYSTEM ADVANCED AUTOMATION PROJECT
Brandon S. Dewberry *In* NASA, Washington, Beyond the Baseline 1991: Proceedings of the Space Station Evolution Symposium. Volume 2: Space Station Freedom, Part 2 Sep. 1991 p 1271-1309 (For primary document see N92-17348 08-18)
Avail: NTIS HC/MF A20 CSCL 06K

N92-17357*# Jet Propulsion Lab., California Inst. of Tech., Pasadena. Artificial Intelligence Group.
ECLSS PREDICTIVE MONITORING
Richard J. Doyle and Steve A. Chien *In* NASA, Washington, Beyond the Baseline 1991: Proceedings of the Space Station Evolution Symposium. Volume 2: Space Station Freedom, Part 2

Sep. 1991 p 1311-1351 (For primary document see N92-17348 08-18)
Avail: NTIS HC/MF A20 CSCL 06K

N92-18001*# Princeton Univ., NJ. Dept. of Mechanical and Aerospace Engineering.
SYSTEMATIC METHODS FOR KNOWLEDGE ACQUISITION AND EXPERT SYSTEM DEVELOPMENT
Brenda L. Belkin and Robert F. Stengel *In* NASA. Langley Research Center, Joint University Program for Air Transportation Research, 1990-1991 Dec. 1991 p 173-179 Previously announced in IAA as A91-43926 Sponsored in part by Natural Sciences and Research Council of Canada (For primary document see N92-17984 08-01)
(Contract NGL-31-001-252; DAAG29-84-K-0048)
Avail: NTIS HC/MF A09 CSCL 05H

55 SPACE BIOLOGY

Includes exobiology; planetary biology; and extraterrestrial life.

No abstracts in this category.

59 MATHEMATICAL AND COMPUTER SCIENCES (GENERAL)

No abstracts in this category.

60 COMPUTER OPERATIONS AND HARDWARE

Includes hardware for computer graphics, firmware, and data processing.

For components see *33 Electronics and Electrical Engineering.*

N92-17466# Carnegie-Mellon Univ., Pittsburgh, PA.
PROGRAM TRANSLATION TOOLS FOR SYSTOLIC ARRAYS Final Report
Thomas Gross and H. T. King 30 Jun. 1991 5 p
(Contract N00014-87-K-0385)
(AD-A242924) Avail: NTIS HC/MF A01 CSCL 12/5

The work under this contract has concentrated on Parallel Program Generators for a systolic array (the Warp machine). A Parallel Program Generator (PPG) translates a program description for a single address space and a single thread of control into code for each of the nodes in parallel distributed memory system. We investigated three different approaches, each is discussed in more detail in a separate section: (1) Use of data parallelism to execute independent iterations on different cells; (2) Transformation of nested loops to systolic programs; and (3) Multi-model code mapping for a side-effect free program. All PPGs produce code that is then translated into Warp microcode by the W2 compiler developed with funding from ONR and DARPA. In addition, we build a debugger for Warp. Most of this work was reported on in the last interim report and is not repeated here. GRA

N92-17592# Fermi National Accelerator Lab., Batavia, IL.
RESULTS FROM A DATA ACQUISITION SYSTEM PROTOTYPE PROJECT USING A SWITCH-BASED EVENT BUILDER
D. Black, J. Andresen, E. Barsotti, A. Baumbaugh, D. Esterline, K. Knickerbocker, R. Kwarciany, G. Moore, J. Patrick, and C. Swoboda et al Nov. 1991 6 p Presented at the IEEE Nuclear Science Symposium, Santa Fe, NM, 5-9 Nov. 1991
(Contract DE-AC02-76CH-03000)
(DE92-004638; FNAL/C-91/303; CONF-911106-22) Avail: NTIS HC/MF A02

A prototype of a high bandwidth parallel event builder has been designed and tested. The architecture is based on a simple switching network and is adaptable to a wide variety of data acquisition systems. An eight channel system with a peak throughput of 160 Megabytes per second has been implemented. It is modularly expandable to 64 channels (over one Gigabyte per second). The prototype uses a number of relatively recent commercial technologies, including very high speed fiber-optic data links, high integration crossbar switches, and embedded RISC processors. It is based on an open architecture which permits the installation of new technologies with little redesign effort. DOE

N92-17720# Utah State Univ., Logan. Water Research Lab.
ENVIRONMENTAL CONTAINMENT PROPERTY ESTIMATION USING QSARs IN AN EXPERT SYSTEM Annual Report, 15 Sep. 1990 - 15 Oct. 1991
William J. Doucette, Mark S. Holt, Doug J. Denne, and Joan E. McLean 15 Oct. 1991 41 p
(Grant AF-AFOSR-0509-89; AF Proj. 2312)
(AD-A243728; AFOSR-91-0992TR) Avail: NTIS HC/MF A03 CSCL 12/4

A microcomputer program utilizing molecular connectivity indices (MCI) property, total molecular surface area (TSA) property and property-property correlations, and UNIFAC derived activity coefficients is being developed to provide a fast, economical method to estimate aqueous solubility, octanol/water partition coefficients, vapor pressures, organic carbon, normalized soil sorption coefficients, bioconcentration factors, and Henry's Law constants for use in environmental fate modeling. The structural information for the MCI and UNIFAC models can be input using Simplified Molecular Input Line Entry System (SMILES) notation or connection tables generated from a commercially available two-dimensional drawing program. The TSA module accepts 3-D cartesian coordinates entered manually or directly reads coordinate files generated by molecular modeling software. In the MCI, TSA, and Property-Property modules, the user can select from either universal or class specific regression models for each property. To aid the user in choosing the most appropriate regression model(s), the program automatically suggests the most appropriate regression model based on the structure of the compound. GRA

N92-17744# Air Force Inst. of Tech., Wright-Patterson AFB, OH. School of Engineering.
A CACHE DESIGN TO EXPLOIT STRUCTURAL LOCALITY M.S. Thesis
Curtis M. Winstead Dec. 1991 243 p
(AD-A243633; AFIT/GCS/ENG/91D-25) Avail: NTIS HC/MF A11 CSCL 12/6

A design and VHDL implementation of a content-addressable memory (CAM) to exploit structural locality is the subject of this research. The concept of structural locality is that memory locations are referenced in the same order as they were previously referenced. Therefore, if memory locations that exhibit structural locality can be made available to the CPU (Center Processing Unit) through a fast data store, an increase in speed of the computer system can be realized. The CAM's purpose is to store memory references in the order they were used by the CPU and prefetch these locations to a smaller on-chip cache. The CAM uses a FIFO circular buffer algorithm to store the memory references. When the CPU references a location that is stored in the CAM, the CAM prefetches memory locations in a FIFO manner, thus allowing the on-chip cache to capture structural locality into its memory. Basic digital logic circuits were implemented in VHDL and were the building blocks for the cache model. From these, the controller, which controls the prefetching of structural locality, was then integrated onto the chip model containing a fully associative CAM array. GRA

N92-17884*# National Aeronautics and Space Administration. Pasadena Office, CA.
NEURAL-NETWORK DEDICATED PROCESSOR FOR SOLVING COMPETITIVE ASSIGNMENT PROBLEMS Patent Application
Silvio P. Eberhardt, inventor (to NASA) (Jet Propulsion Lab., California Inst. of Tech., Pasadena.) 12 Aug. 1991 38 p
(Contract NAS7-918)
(NASA-Case-NPO-17781-1-CU; NAS 1.71:NPO-17781-1-CU; US-Patent-Appl-SN-744042) Avail: NTIS HC/MF A03 CSCL 09B

A neural-network processor for solving first-order competitive assignment problems consists of a matrix of NxM processing units, each of which corresponds to the pairing of a first number of elements of (R sub i) with a second number of elements (C sub j), wherein limits of the first number are programmed in row control superneurons, and limits of the second number are programmed in column superneurons as MIN and MAX values. The cost (weight) W sub ij of the pairings is programmed separately into each PU. For each row and column of PUs, a dedicated constraint superneuron insures that the number of active neurons within the associated row or column fall within a specified range. Annealing is provided by gradually increasing the PU gain for each row and column or increasing positive feedback to each PU, the latter being effective to increase hysteresis of each PU or by combining both of these techniques. NASA

N92-17922# Air Force Inst. of Tech., Wright-Patterson AFB, OH. School of Engineering.
EFFECT OF SPATIAL LOCALITY PREFETCHING ON STRUCTURAL LOCALITY M.S. Thesis
Dirk D. Schalch Dec. 1991 157 p
(AD-A243632; AFIT/GCS/ENG/91D-20) Avail: NTIS HC/MF A08 CSCL 12/5

The purpose of this research was to analyze the effect that spatial locality prefetching in cache memory has on the structural locality of program memory referencing behavior. To examine this, a software simulator was built to model a proposed two-level cache memory subsystem. The proposed subsystem was designed to use spatial locality prefetching to exploit the structural locality contained in executing computer workloads. New memory referencing models were developed to incorporate the combined use of structural locality and spatial locality prefetching. From these models, equations were derived to predict the hit rates for both caches. Combined with the state transition probabilities of the memory referencing models, measurements from the trace-driven simulations were used to solve the hit probability equations. This research showed that performance gains through structural locality prefetching are still possible even when spatial locality prefetching is being used in the lower level cache. GRA

N92-17419*# National Aeronautics and Space Administration. Lyndon B. Johnson Space Center, Houston, TX.
ADVANCED CREW PERSONAL SUPPORT COMPUTER (CPSC) TASK
Debra Muratore *In* NASA, Washington, Beyond the Baseline 1991: Proceedings of the Space Station Evolution Symposium. Volume 1: Space Station Freedom, Part 2 Sep. 1991 p 639-65 (For primary document see N92-17409 08-18)
Avail: NTIS HC/MF A16 CSCL 09B

N92-17421*# National Aeronautics and Space Administration. Lyndon B. Johnson Space Center, Houston, TX.
REAL TIME DATA SYSTEM (RTDS)
Troy A. Heindel *In* NASA, Washington, Beyond the Baseline 1991: Proceedings of the Space Station Evolution Symposium. Volume 1: Space Station Freedom, Part 2 Sep. 1991 p 681-69 (For primary document see N92-17409 08-18)
Avail: NTIS HC/MF A16 CSCL 09B

N92-17422*# National Aeronautics and Space Administration. John F. Kennedy Space Center, Cocoa Beach, FL.
COMPUTER SYSTEM EVOLUTION REQUIREMENTS FOR AUTONOMOUS CHECKOUT OF EXPLORATION VEHICLES
Tom Davis and Mike Sklar *In* NASA, Washington, Beyond the Baseline 1991: Proceedings of the Space Station Evolution Symposium. Volume 1: Space Station Freedom, Part 2 Sep. 1991 p 697-72 (For primary document see N92-17409 08-18)
Avail: NTIS HC/MF A16 CSCL 09B

61 COMPUTER PROGRAMMING AND SOFTWARE

Includes computer programs, routines, alogorithms, and specific applications, e.g., CAD/CAM.

N92-17023# Air Force Inst. of Tech., Wright-Patterson AFB, OH. School of Engineering.
A TOPOLOGICAL MODEL FOR PARALLEL ALGORITHM DESIGN Ph.D. Thesis
Jeffrey A. Simmers Sep. 1991 395 p
(AD-A241858; AFIT/DS/ENG/91-02) Avail: NTIS HC/MF A17 CSCL 12/5

This research demonstrates that formal, mathematical analysis in theoretical computer science can be recast in terms of the topology of complete metric spaces, and also presents a methodical technique for developing formal specifications. This effort shows that the topology of complete metric spaces provides a tool that can be used to both recreate major results about computational models and also to develop new results about these models. Using the two computational models CSP and UNITY, this effort shows that the required mathematics needed to support this alternative to the traditional analysis of computational models can be readily supported by a standard course sequence in real analysis. Since the approach of proving programs correct after being written has not been widely accepted, this effort presents an alternative approach based on the developed topological framework for the formal specification language UNITY. This approach, designed to be automated, uses a set of transformations applied to UNITY specifications that preserve desired program properties. GRA

N92-17064# TRW Space and Defense Sector, Redondo Beach, CA.
PRAGMATIC QUALITY METRICS FOR EVOLUTIONARY SOFTWARE DEVELOPMENT MODELS
Walker Royce Jan. 1991 16 p
(AD-A243022; TRW-TS-91-01) Avail: NTIS HC/MF A03 CSCL 12/5

Due to the large number of product, project and people parameters which impact large custom software development efforts, measurement of software product quality is a complex undertaking. Furthermore, the absolute perspective from which quality is measured (customer satisfaction) is intangible. While we probably can't say what the absolute quality of a software product is, we can determine the relative quality, the adequacy of this quality with respect to pragmatic considerations, and identify good and bad trends during development. While no two software engineers will ever agree on an optimum definition of software quality, they will agree that the most important perspective of software quality is its ease of change. We can call this flexibility, adaptability or some other vague term, but the critical characteristic of software is that it is soft. The easier the product is to modify, the easier it is to achieve any other software quality perspective. This paper presents objective quality metrics derived from consistent lifecycle perspectives of rework which, when used in concert with an evolutionary development approach, can provide useful insight to produce better quality per unit cost/schedule or to achieve adequate quality more efficiently. GRA

N92-17068# Institute for Defense Analyses, Alexandria, VA.
AN EXAMINATION OF SELECTED COMMERCIAL SOFTWARE TESTING TOOLS Final Report
Bill R. Brykczynski, Christine Youngblut, and Reginald N. Meeson Oct. 1991 92 p

(Contract MDA903-89-C-0003)
(AD-A243089; IDA-P-2628; IDA/HQ-91-39501) Avail: NTIS HC/MF A05 CSCL 12/5

This paper reports on the examination of ten commercial tools identified for the static and dynamic analysis of Ada code. It provides software development managers with information that may help them gain an understanding of the types of tools that are commercially available, the functionality of these tools, and how they can aid the development of Ada software. During the course of the assessment, the tools were applied to a series of Ada programs in order to assess their functionality. Each tool was then described in terms of its functionality, ease of use, and documentation and support. Problems encountered during the examination and other pertinent observations were also recorded. Significant findings from this study include the following: (1) some of the examined tools could be brought into immediate use to improve the cost-effectiveness of testing for SDI software development efforts, (2) the coverage analyzers provide reporting data that can support the management of SDI testing efforts, and (3) many of the tools can be used in conjunction to overcome the limitations of particular tools. GRA

N92-17077# Air Force Inst. of Tech., Wright-Patterson AFB, OH. School of Engineering.
FEATURE EXTRACTION FOR POSE ESTIMATION: A COMPARISON BETWEEN SYNTHETIC AND REAL IR IMAGERY M.S. Thesis
Donald J. Willis Dec. 1991 177 p
(AD-A243699; AFIT/ENG/GEO/91D-06) Avail: NTIS HC/MF A09 CSCL 17/5

This research addressed the problem of pose estimation of three-dimensional objects given their two-dimensional IR imagery and corresponding synthetic (computer-generated) IR imagery. Features and techniques were investigated to find those which may be extendable from computer models to real-world IR imagery. GTSIG and SCNGEN were used to create the synthetic imagery. Silhouette and outline shape moments were explored as optimum features for the comparison. Employing back-propagation with momentum as the training paradigm, a two-hidden-layer neural network was able to determine the base-plane orientation of the synthetic imagery to within 7.5 degrees with better than 90 percent accuracy. No conclusive results were obtained from comparison with real-world IR imagery. Additionally, the use of object hot spots relative to object height-to-width ratio is briefly discussed as an alternative feature/technique. Author (GRA)

N92-17093# Air Force Inst. of Tech., Wright-Patterson AFB, OH.
IMAGE ANALYSIS USING GABOR TRANSFORMS: CORRELATED WITH HUMAN SACCADIC MOVEMENT DATA TO IDENTIFY THE HUMAN VISUAL SEARCH STRATEGY M.S. Thesis
Ralph J. St.John Dec. 1991 111 p
(AD-A243692; AFIT/GE/ENG/91D-52) Avail: NTIS HC/MF A06 CSCL 12/6

This thesis investigated whether a relationship exists between the Gabor Correlation Coefficient (GCC) magnitudes of fixation points for a set of images viewed by six subjects and the human visual search strategy. A couple of different relationships were investigated. First, the data were analyzed to determine if the GCC magnitudes of human fixation points predicted the time ordered sequence of human fixation points during the performance of a visual search. Second, the data were analyzed to determine if there was a significant difference between the GCC magnitudes of the human fixation points and the GCC magnitudes of a random set of fixation points. Finally, the data were analyzed to ascertain whether there was a difference between the GCC magnitudes of the fixation points at the beginning of the visual search and the GCC magnitudes of the fixation points at the end of the visual search. GRA

N92-17118# Air Force Inst. of Tech., Wright-Patterson AFB, OH.
A CONVERGENT ASPIRATION BASED INTERIOR POINT METHOD (CAIN) FOR MULTIPLE OBJECTIVE LINEAR PROGRAMMING (MOLP) M.S. Thesis
M. S. Mynes Aug. 1991 89 p
(AD-A243404; AFIT/CI/CIA-91-086) Avail: NTIS HC/MF A05 CSCL 12/4

This report describes a new convergent aspiration based algorithm (CAIN--Convergent Aspiration based INterior method) for solving the multiple objective linear programming (MOLP) problem. Initial motivation for the research was provided by a recently developed methodology for the discrete multiple criteria decision making problem called AIM (Aspiration--Level Interactive model). Although CAIN uses many of the features implemented in AIM, the continuous MOLP provides for an entirely different domain of research. As part of CAIN, an innovative decision maker (DM) interaction technique called ALaRM (Aspiration Level Range Method) was concurrently developed. Using ALaRM, an interior point strategy for converging to efficient solutions is employed based upon DM levels of aspiration for the objectives. This technique, the Algorithm of Centers, has been shown to converge in polynomial time (unlike many simplex based strategies). CAIN is shown to be simple and practical from a DM standpoint, and is believed to represent an improvement over existing aspiration based MOLP techniques. GRA

N92-17122# Army Construction Engineering Research Lab., Champaign, IL.
CATHODIC PROTECTION DIAGNOSTIC COMPUTER PROGRAM FOR SACRIFICIAL AND IMPRESSED CURRENT SYSTEMS: OVERVIEW AND USER'S MANUAL Final Report
Vicki L. VanBlaricum, C. D. Page, Jr., Kim Reinke, and Ashok Kumar Sep. 1991 152 p
(AD-A243663; CERL-ADP-M-91/24) Avail: NTIS HC/MF A08 CSCL 12/5

The total of corrosion at Army facilities is a significant percentage of maintenance and repair budgets. Corrosion in underground gas piping is particularly costly because pipe damage is difficult to determine or assess until a leak occurs. Cost effective maintenance of underground gas piping and other structures requires that cathodic protection (CP) systems operate properly and that some measure of current and projected pipe condition be available. To meet this requirement, data on CP systems must be constantly monitored, and CP faults indicated by the data must be correctly recognized and interpreted. The CP Diagnostic computer program helps the recordkeeping, analysis, and maintenance requirement of sacrificial and impressed current cathodic protection systems. CP Diagnostic is a data base management program consisting of two microcomputer systems: Sacrificial CP Diagnostic and Impressed Current CP Diagnostic. The User's Manual gives an overview of the capabilities of CP Diagnostic, and step-by-step instructions for its installation and use. GRA

N92-17130*# National Aeronautics and Space Administration. Langley Research Center, Hampton, VA.
THE MULTI-ATTRIBUTE TASK BATTERY FOR HUMAN OPERATOR WORKLOAD AND STRATEGIC BEHAVIOR RESEARCH
J. Raymond Comstock, Jr. and Ruth J. Arnegard (Old Dominion Univ., Norfolk, VA.) Jan. 1992 99 p
(NASA-TM-104174; NAS 1.15:104174) Avail: NTIS HC/MF A05 CSCL 09B

The Multi-Attribute Task (MAT) Battery provides a benchmark set of tasks for use in a wide range of lab studies of operator performance and workload. The battery incorporates tasks analogous to activities that aircraft crewmembers perform in flight, while providing a high degree of experimenter control, performance data on each subtask, and freedom to use nonpilot test subjects. Features not found in existing computer based tasks include an auditory communication task (to simulate Air Traffic Control communication), a resource management task permitting many

avenues or strategies of maintaining target performance, a scheduling window which gives the operator information about future task demands, and the option of manual or automated control of tasks. Performance data are generated for each subtask. In addition, the task battery may be paused and onscreen workload rating scales presented to the subject. The MAT Battery requires a desktop computer with color graphics. The communication task requires a serial link to a second desktop computer with a voice synthesizer or digitizer card. Author

N92-17179# Wright Lab., Wright-Patterson AFB, OH.
PATTERN THEORY: AN ENGINEERING PARADIGM FOR ALGORITHM DESIGN Final Report, Oct. 1988 - Oct. 1990
Timothy D. Ross, Michael J. Noviskey, Timothy N. Taylor, and David A. Gadd 26 Jul. 1991 215 p
(AF Proj. 7629)
(AD-A243214; WL-TR-91-1060) Avail: NTIS HC/MF A10 CSCL 12/9

This report proposes Pattern Theory as a basis for an engineering theory of algorithms design. Pattern Theory (PT) begins with a general statement of the problem and then makes deliberate specializations. The problem of finding a pattern in a function is the essence of algorithm design. The key to PT is its measure of pattern-ness: Decomposed Function Cardinality (SFC). Low DFC indicates pattern-ness. The principal result is a demonstration of the generality with which DFC measures pattern-ness. This generality is supported theoretically by relating DFC to time complexity, program length, and circuit complexity. A test is developed, based on DFC, for whether or not a function will decompose. This test is used in Ada Function Decomposition (AFD) Programs. AFD produces a decomposition (i.e., an algorithm in combinational form) and DFC. The generality of DFC is also supported experimentally. The Pattern Theory approach to machine learning and data compression demonstrated greater generality than other approaches. The DFC's of over 800 nonrandom functions (numeric, symbolic, string based, graph based, images, and files) were measured. Roughly 98 percent of the nonrandom functions had low DFC versus less than 1 percent for random functions. AFD found the classical algorithms for several functions. GRA

N92-17185# Plessey Research (Caswell) Ltd., Towcester (England).
MICROSTRIP DISCONTINUITY MODELS TO 60 GHz Final Report, Sep. 1986 - Sep. 1989
R. G. Arnold, R. H. Jansen, and L. Weimer Aug. 1991 337 p
(Contract F19628-86-C-0111)
(AD-A242038; RL-TR-91-198) Avail: NTIS HC/MF A15 CSCL 09/1

A new modeling concept, in which discontinuities are coupled to package modes, has been formulated. Analytical expressions describing the electrical behavior of various gallium arsenide microstrip discontinuities for frequencies up to 60 GHz are derived. These are suitable for use in Computer Aided Design (CAD) of Monolithic Microwave and Millimeter Wave Integrated Circuits (MMIC's). The discontinuities modelled are the Open End, Gap, 90 degree Bend, and T-Junction. A physics related modeling approach was used to obtain equivalent circuits representing the microstrip and first package LSM mode and their interaction at the discontinuity. The main section explains the modeling approach undertaken and provides a description of the discontinuity models. An appendix provides details of a 3-D full wave analysis method based on a spectral operator expansion technique. This was used to check numerical results needed for the modeling.
Author (GRA)

N92-17211# Naval Ocean Systems Center, San Diego, CA.
PERFORMANCE MODELING OF THE Ada RENDEZVOUS Final Report
A. E. Sterrett and M. K. Minei Oct. 1991 32 p
(AD-A243392; NOSC/TD-2194) Avail: NTIS HC/MF A03 CSCL 12/5

The Ada Programming Language (United States Department of Defense, 1983) was designed to meet the need for a standard computer-programming language. Ada has the ability to take advantage of microprocessor environments. One feature, known as the rendezvous, allows tasks to synchronize. This very important and powerful feature is poorly understood. Rendezvous performance is a known area of concern, especially if the system is in a multiprocessor environment. In this paper, analytic techniques are developed that will predict the performance of systems using the rendezvous. In a distributed Ada system, the rendezvous provides synchronized communication between asynchronous tasks. A system of this sort would consist of at least two processors, each serving various tasks. We have analytically developed algorithms that determine the average Rendezvous Response Time for a two-processor system. Rendezvous Response Time will be defined as the amount of time one task (i.e., a client task) must wait until its rendezvous request to another task (i.e., a server task) is completed. This approach uses Mean Value Analysis (MVA), analytic extensions to MVA, and elementary queueing theory to decompose the rendezvous into interacting separate models. The notion of a software server that maintains a queue and services rendezvous requests will play an important part in the solution techniques. GRA

N92-17237# Naval Postgraduate School, Monterey, CA.
AN ANALYSIS OF MISSION CRITICAL COMPUTER SOFTWARE IN NAVAL AVIATION M.S. Thesis
Robert L. Buckley Mar. 1991 78 p
(AD-A243078) Avail: NTIS HC/MF A05 CSCL 12/5

For over 25 years, the United States Navy has been designing, developing and maintaining software for embedded computer systems. Throughout this generation of Naval aviation software development, no collective analysis of the successes and failures in software development had been accomplished. To accomplish this task, this thesis evaluated aircraft software data from the Department of the Navy against two metrics: (1) did the original software development schedule have to be changed, and (2) did the software released to the fleet contain any major defects? This research has revealed that only about half of the original software development schedules were sustained without a milestone change being made. Also, software that was released to the fleet had no major deficiencies three out of four times. To further specify this information, it has been refined into categories of software language, size of program and type of software program. The results of this study will be beneficial to aviation program managers, software developers and software maintenance technicians. GRA

N92-17280# Aeronautical Research Labs., Melbourne (Australia).
THE CONVERSION OF A FORTRAN DATA PLOTTING PROGRAM USING DI-3000 GRAPHICS TO OPERATION ON A MACINTOSH PERSONAL COMPUTER
D. M. Blunt Sep. 1991 42 p
(AD-A243046; ARL-FLIGHT-MECH-TM-446; DODA-AR-006-643)
Avail: NTIS HC/MF A03 CSCL 12/5

The planned retirement of the Elxsi 6400 mainframe computer at ARL has necessitated the conversion of the general purpose FORTRAN data plotting program TRANS to operation on a MacIntosh IIfx personal computer, where it has been renamed MacTRANS. The conversion has included the limited use of regular MacIntosh features such as pull down menus, and allowed the plots produced by MacTRANS to be edited in most commercial MacIntosh graphics programs. For most cases, the execution speed of MacTRANS on the MacIntosh IIfx has been found to be faster than that of TRANS on the Elxsi. GRA

N92-17285# Naval Postgraduate School, Monterey, CA. Dept. of Computer Science.
A GRAPHICAL DATABASE INTERFACE FOR A MULTIMEDIA DBMS Progress Report, Feb. - Mar. 1991
Daniel A. Keim and Vincent Y. Lum Jun. 1991 25 p
(AD-A243283; NPS-CS-91-013) Avail: NTIS HC/MF A03 CSCL 12/7

In this paper we describe the GRAphical Database Interface (GRADI) of a Multimedia Database Management System. As generally true, the user interface is an important part of a system which strongly determines the effectiveness of using it. In order to find a natural way of interacting with the MDBMS system we examined the query specification process used by humans. We found that incremental query specification, natural ways of expressing joins and an additional 'all'-operator are important to improve the query specification process making it considerably easier to use in comparison with query languages like SQL. The Graphical Database Interface described in this paper incorporates the mentioned capabilities as part of the MDBMS system. We think that the principles are of general use not only for multimedia systems but for any database query interface. GRA

N92-17286# North Carolina State Univ., Raleigh.
ADAPTIVE PRESORT PROCESSING Final Technical Report, Feb. 1990 - Apr. 1991
A. Vanderlugt and Reeder N. Ward Oct. 1991 118 p
(Contract F30602-88-D-0025)
(AD-A243286; RL-TR-91-253) Avail: NTIS HC/MF A06 CSCL 09/5

This report summarizes analysis and experiments of an optical signal processing architecture which excises narrow components from wideband signals using frequency plane excision. It is shown that area detection in the frequency plane is equivalent to point detection in the image plane. The design, construction, and testing of a detection system that obtains the Fourier transform of the wideband signal and adaptively searches for strong narrowband components are described. Computer simulations and experimental results of pulsed experiments are presented. GRA

N92-17296# Electronics Research Lab., Adelaide (Australia).
DECOMPILING WITH DEFINITE CLAUSE GRAMMARS
S. T. Hood Sep. 1991 34 p
(AD-A242987; ERL-0571-RR; DODA-AR-006-765) Avail: NTIS HC/MF A03 CSCL 12/5

Decompiling is the process of deriving a computer program in a high level language from one in machine-code or assembly language. Defense applications of decompiling include maintenance of obsolescent equipment, production of scientific and technical intelligence, and assessment of systems for hazards to safety or security. This paper describes an approach to the rapid generation of decompilers through the use of Definite Clause Grammars, a class of abstract grammars which can be executed as Prolog programs. The approach is illustrated using toy languages. An environment which permits the integration of diverse sources of knowledge relevant to the decompilation problem and provides a graphical interface is described. GRA

N92-17368# Naval Postgraduate School, Monterey, CA.
THE DEVELOPMENT OF USER INTERFACE TOOLS FOR THE COMPUTER AIDED PROTOTYPING SYSTEM M.S. Thesis
Mary A. Cummings Dec. 1990 343 p
(AD-A243189) Avail: NTIS HC/MF A15 CSCL 12/5

The Computer Aided Prototyping System (CAPS) was created to rapidly prototype real-time systems in order to determine if the system requirements can be met early in the development cycle. CAPS consists of several software tools that automatically generate an executable Ada model of the proposed system from a given specification. This thesis describes the development of a user interface for CAPS. The user interface supports the design, modification and execution of the software prototype throughout the entire prototyping life cycle. It makes uses of X Windows and advanced windowing techniques and allows the user to run the tools concurrently. The user interface incorporates a separate tool interface which controls the interaction between CAPS tools and the user interface. The graphic editor uses advanced graphics capabilities to give the user more flexibility in editing a graphical representation of the prototype. It automatically produces a formal representation of the prototype to be used by the other tools in CAPS. GRA

N92-17403# Naval Postgraduate School, Monterey, CA. Dept. of Computer Science.
A STOCHASTIC APPROACH TO THE WEIGHTED-REGION PROBLEM: 1. THE DESIGN OF THE PATH ANNEALING ALGORITHM Technical Report, Oct. 1990 - Sep. 1991
Mark R. Kindl, Man-Tak Shing, and Neil C. Rowe Jun. 1991 45 p
(AD-A243324; NPS-CS-91-014) Avail: NTIS HC/MF A03 CSCL 12/4

This paper presents an efficient heuristic algorithm for planning near-optimal high-level paths for a point agent through complex terrain modeled by the Weighted-Region Problem. The input to the Weighted-Region Problem is a set of non-overlapping convex homogeneous-cost regions on a two dimensional plane. Each region is associated with a cost coefficient (or weight), which indicates the relative cost per unit distance of movement in that region by the point agent. The weighted distance between two points in a convex region is the product of the corresponding cost coefficient and the Euclidean distance between them. Given a start and a goal point on the plane, the objective of the Weighted-Region Problem is to find a minimum cost path from start to goal through the weighted regions. We have designed and developed a very efficient algorithm for finding near-optimal solutions for the Weighted-Region Problem using a combination of the classical artificial intelligence heuristic search techniques and the probabilistic combinatorial optimization technique called simulated annealing. Extensive test results (to be presented in Part 2 of the paper) indicate that the new algorithm runs much faster than previous known techniques with a very minimal sacrifice in optimality. GRA

N92-17407# Air Force Inst. of Tech., Wright-Patterson AFB, OH. School of Engineering.
DESIGN OF STYLE-V: A TRANSLATOR TO CONVERT STANDARD VHDL INTO A STYLIZED FORM FOR AUTOMATED MICROCODE GENERATION M.S. Thesis
Dennis A. Rumbley Dec. 1991 232 p
(AD-A243706; AFIT/GCS/ENG/91D-19) Avail: NTIS HC/MF A11 CSCL 12/5

This thesis provides an analysis and preliminary design of Style V, a source-to-source computer language translator. Style-V converts IEEE standard VHDL into a special style of VHDL defined for a commercial tool, the Integrated Design Automation System (IDAS). Thirteen mappings between standard VHDL and the IDAS subset were identified. The mappings were analyzed using Domain Analysis and Modern Structured Analysis techniques. Four processes covering several of the mappings were completely analyzed. One mapping to convert CASE statements to IF statements was implemented. Since the IDAS restricts designs to bit logic, a method for representing multilevel logic with bit logic was devised. Unacceptable multiple process architectures were converted to multiple single process architectures which are acceptable to IDAS. The IDAS microcode generator does not recognize user-defined procedures, but in one case, mapping user-defined procedures to IDAS defined procedures was not possible. In general, this problem amounts to showing that two programs are functionally equivalent. Exhaustive testing was ruled out since proving two 32-bit adders are equivalent would take over 11 billion years at 100 procedure runs per second. The program equivalence problem was not solved by this thesis. Useful results were obtained, though IDAS failed to work. GRA

N92-17463# Princeton Univ., NJ.
CAUSAL MODELS IN THE ACQUISITION AND INSTRUCTION OF PROGRAMMING SKILLS Interim Report, Sep. 1988 - Aug. 1989
Brian J. Reiser Oct. 1991 26 p
(Contract MDA903-87-C-0652)
(AD-A242899; ARI-RN-92-04) Avail: NTIS HC/MF A03 CSCL 05/8

This report summarizes progress made on the Graphical Instruction in LISP (GIL) intelligent tutoring system and the Graphical LISP Exploratory Environment (GLEE) discovery system

for instructing programming skills. We describe the status of these computer systems and the experiments investigating the role of explanations in learning, in addition to the use of graphical representations in problem solving. We also describe the BATBook problem solving environment for the study of analogies in programming, as well as our studies of effective human tutors.
GRA

N92-17487# General Electric Co., Schenectady, NY.
CMS REVERSE ENGINEERING AND ENCORE/MODEL INTEGRATION Bimonthly Progress Report
Margaret Kelliher 31 Oct. 1991 35 p
(Contract N00014-91-C-0240)
(AD-A243438) Avail: NTIS HC/MF A03 CSCL 12/5

This document contains the high-level and low-level designs for the pass 3 phase of the CMS reverse engineering tool. It is intended both as a working document and as a starting place for future reverse engineering tools which may want to reuse parts of our approach. Our basic strategy is to divide the CMS-2 nodes into 6 basic categories, each of which will be processed in a separate package. The top level routine will determine the category to which a node belongs, and will send it to the corresponding mid-level routine. These mid-level routines are responsible for determining whether the node is to be processed, ignored, or bypassed. If it is to be processed, a low level computer routine is triggered which does the node processing required. The main package will contain the Main computer routine. The main routine will decipher the command line parameters and control the main loop which calls the parser and the node processor once for each file specified. Most of this code can be reused from JRET.
GRA

N92-17498# Advisory Group for Aerospace Research and Development, Neuilly-Sur-Seine (France). Guidance and Control Panel.
TECHNICAL EVALUATION REPORT ON THE 52ND SYMPOSIUM ON SOFTWARE FOR GUIDANCE AND CONTROL
Donald E. Dewey (Boeing Military Airplane Development, Seattle, WA.) Dec. 1991 41 p Symposium held in Thessaloniki, Greece, 7-10 May 1991
(AGARD-AR-302; ISBN-92-835-0647-2; CP-503) .Copyright
Avail: NTIS HC/MF A03; Non-NATO Nationals requests available only from AGARD/Scientific Publications Executive

A review is presented of some of the symposium sessions. The papers presented covered some of the following headings: tools and methods for a user's viewpoint; general requirements on software; integrated programs support environments; software requirements; design methods for real time software; ADA applications; and automated software generation approaches.
Author

N92-17521# Technische Univ., Eindhoven (Netherlands).
SPECIFICATION AND COMPOSITIONAL VERIFICATION OF REAL-TIME SYSTEMS Ph.D. Thesis
Jozef Johannes Maria Hooman 1991 215 p Sponsored in part by Commission of the European Communities
(ETN-92-90580) Avail: NTIS HC/MF A10

The specification and verification of real time properties of computer programs are addressed. A metric temporal logic approach and a Hoare style formalism are investigated for use in a compositional axiomatization of several versions of the programming language. The development from non-compositional proof methods towards compositional proof systems for non-real time partial correctness of parallel programs is discussed. A compositional semantics for this language is defined and proofs for the two above mentioned approaches are formulated. An example of a watchdog timer illustrates how these two proof systems can be used to verify design steps during the process of top down program development. Both formalisms are then adapted to deal with program variables. The maximal parallelism assumption is used. The model is generalized to multiprogramming where several processes can be executed on a single processor. Scheduling is based on priorities which can be assigned to statements in the program. Both proof methods can be modified to prove properties of uniprocessor implementations.
ESA

N92-17524# Technische Univ., Berlin (Germany, F.R.). Fachbereich Elektrotechnik.
A KNOWLEDGE-BASED APPROACH FOR CONFIGURING COMPUTER AIDED MEASURING SYSTEMS Ph.D. Thesis [EIN WISSENSBASIERTER ANSATZ ZUR KONFIGURIERUNG RECHNERGESTUETZTER MESSYSTEME]
Carsten Rudolf 1991 127 p In GERMAN
(ETN-92-90585) Avail: NTIS HC/MF A07

The use of knowledge based techniques for the computer aided construction of measuring systems was investigated. Starting from the general fundamentals of computer aided measuring systems and knowledge based systems, an approach for configuring such measuring systems is described. This approach integrates the development of hardware and software, and enables the interactive composition of the components as well as an abstract specification of the measurement task. A blackboard like layer model was used for the problem solving inside the software system. The representation of the technical data using hardware and software modules is made in an object oriented data base. Predefined software modules that can be parametrized were used to build the software for the measuring system. A practical realization is presented as an example.
ESA

N92-17538# Pennsylvania Univ., Philadelphia.
PROGRAMMING MECHANICAL SIMULATIONS
Joseph K. Kearney, Stuart Hansen, and James F. Cremer Sep. 1991 19 p
(Contracts N00014-88-K-0632; N00014-89-J-1946; N00014-88-K-0591; NSF IRI-88-08896; NSF IRI-90-06137)
(AD-A243767) Avail: NTIS HC/MF A03 CSCL 12/5

This paper examines the control of complex physical objects in simulation. We introduce a programming paradigm that allows a simulation to be treated as a multi-level constraint solver. The control programmer is given the ability to specify constraints on the controlled response of mechanisms and to conditionally change these constraints dependent on the state of system. The approach facilitates the development of model-based, even-driven control programs. The usefulness of the paradigm is demonstrated through the simulation of a hopping robot.
GRA

N92-17545# Messerschmitt-Boelkow-Blohm G.m.b.H., Munich (Germany, F.R.). Design Assurance Dept.
THE NEED FOR ACTIVE SOFTWARE PRODUCT ASSURANCE MANAGEMENT FOR SYSTEMS CRITICAL SOFTWARE
Richard Borcz 1991 7 p Presented at the ESA Symposium on Space Product Assurance for Europe in the 1990s, Noordwijk, Netherlands, 15-19 Apr. 1991
(MBB-UK-0142-91-PUB; ETN-92-90603) Avail: NTIS HC/MF A02

The quality, reliability, and safety impact of space systems software are discussed. Should software failure occur in a critical function, there is potential for danger to human life, systems loss, long-term environmental damage, and financial loss. It is argued that if high integrity software is needed for systems critical operation, product assurance management must move from its classical passive role to an active role. Experiences in moving product assurance software into an active mode are described.
ESA

N92-17558# Naval Postgraduate School, Monterey, CA.
MODELING CONVERGENCE ZONE GAIN ON MS-DOS BASED PERSONAL COMPUTERS M.S. Thesis
Alan K. Jenkins Dec. 1991 84 p
(AD-A243252) Avail: NTIS HC/MF A05 CSCL 20/5

The models for determining convergence zone gain (G) were developed using a linearized Sound Speed Profile (SSP) and applying ray tracing theory. The SSP was divided into three cases: bilinear, bilinear with isospeed layer, and bilinear with mixed layer. Two analytical solutions were developed using Taylor series and

binomial series expansions to determine G, one for the bilinear and bilinear with isospeed layer, and the other for the bilinear with a mixed layer. The solutions for G are exclusively a function of the SSP gradients. Each solution was compared to the solutions from ray tracing and the solutions from the Integrated Carrier Antisubmarine Warfare Prediction System (ICAPS) (which runs on mainframe computers and requires more data in addition to the SSP). When the SSP's were not too unusual, the solutions for G were fairly close when compared to ray tracing and ICAPS. GRA

N92-17561# Naval Air Development Center, Warminster, PA. Mission Avionics Technology Dept.
THE SQUARE ROOT CORDIC Final Report, Mar. - Jul. 1991
Ronald F. Gleeson, James J. Davidson, Robert M. Williams, and Robert G. Peck 26 Jul. 1991 18 p
(AD-A242318; NADC-91067-50) Avail: NTIS HC/MF A03 CSCL 12/5

The CORDIC (Coordinate Rotation Digital Computer) algorithm 1 computes certain functions such as the sine, cosine, and square root of (x squared + y squared) using only additions and bit shifting operations. We have implemented an integer math CORDIC algorithm on a high speed RISC processor. During the course of this work, we identified a convergence problem with the square root of (x squared + y squared) CORDIC. A solution to this problem is presented along with an overview of this algorithm. GRA

N92-17566# Fail-Safe Technology Corp., Los Angeles, CA.
EMBEDDED FAULT-TOLERANT COMPUTER FOR MISSION CRITICAL APPLICATIONS Final Report, Nov. 1989 - 1 Aug. 1991
Gary A. Kravetz 1 Aug. 1991 35 p
(Contract F04704-89-C-0044)
(AD-A242886; FST91-281-2; BMO-TR-91-26) Avail: NTIS HC/MF A03 CSCL 12/6

The objective of this effort is to develop an Embedded Fault-Tolerant Computer (EFTC) using a combination of off the shelf and custom hardware and software components. This prototype will then be analyzed in order to determine the concept feasibility. This report summarizes the main activities and results of the EFTC development as it has progressed through Phase II. It describes: the development of the EFTC system from evolution through hardware and software design (Section 2); brassboard implementation of hardware and software (Section 3); and the successful demonstration of generic capabilities as well as applications (Section 4). In addition, summaries of various ways in which the system can be enhanced illustrate the flexibility of the design (Section 5). GRA

N92-17581# Naval Surface Warfare Center, Dahlgren, VA.
FORTH GRAPHICS TOOLBOX (A USER'S GUIDE FOR USE WITH RFF FORTH) Final Report
Hanseok Ko 14 Jun. 1991 63 p
(AD-A242916; NAVSWC-MP-91-404) Avail: NTIS HC/MF A04 CSCL 12/5

The Forth Graphics Toolbox has a rich collection of graphics routines immediately useful for all Forth based application software running on IBM-PC clone microcomputers. The routines are built upon graphics related primitives of both video BIOS call functions and direct-video functions. The user can develop more exotic application software based on the routines listed in this package. GRA

N92-17601# Air Force Inst. of Tech., Wright-Patterson AFB, OH. School of Engineering.
SIMULATION OF FINITE-PRECISION EFFECTS IN DIGITAL FILTERS M.S. Thesis
Perry L. Choate 12 Dec. 1991 227 p
(AD-A243758; AFIT/GE/ENG/91-D-11) Avail: NTIS HC/MF A11 CSCL 12/5

This thesis develops and demonstrates software that models finite-precision effects in digital filters. Coefficient quantization and internally generated roundoff noise effects are simulated by rounding coefficients and multiplier output values to (B+1) bits. Outputs include magnitude and phase responses that may be plotted to show results of coefficient quantization. The output noise power due to roundoff is calculated. Three types of digital filter structures are examined. The first type is direct form I implementation for FIR and IIR structures, second is direct form II, and third is cascading the canonic direct form II second-order sections for higher order filter designs. Re-arrangement of the second-order sections can be done to examine the change in the roundoff power generated. One other feature converts the cascade canonic form into a direct form for analysis. The software is menu driven with help screens written in FORTRAN77. GRA

N92-17603# Air Force Inst. of Tech., Wright-Patterson AFB, OH. School of Engineering.
PARALLEL IMPLEMENTATION OF VHDL SIMULATIONS ON THE INTEL iPSC/2 HYPERCUBE M.S. Thesis
Ronald C. Comeau Dec. 1991 161 p
(AD-A243760; AFIT/GCS/ENG/91D-03) Avail: NTIS HC/MF A08 CSCL 12/5

VHDL models are executed sequentially in current commercial simulators. As chip designs grow larger and more complex, simulations must run faster. One approach to increasing simulation speed is through parallel processors. This research transforms the behavioral and structural models created by Intermetrics' sequential VHDL simulator into models for parallel execution. The models are simulated on an Intel iPSC/2 hypercube with synchronization of the nodes being achieved by utilizing the Chandy Misra paradigm for discrete-event simulations. Three eight-bit adders, the ripple carry, the carry save, and the carry-lookahead, are each run through the parallel simulator. Simulation time is cut in at least half for all three test cases over the sequential Intermetrics model. Results with regard to speedup are given to show effects of different mappings, varying workloads per node, and overhead due to output messages. GRA

N92-17636# Virginia Univ., Charlottesville. Dept. of Computer Science.
THE STARLITE PROJECT PROTOTYPING REAL-TIME SOFTWARE Annual Report, 1 Oct. 1990 - 30 Sep. 1991
R. P. Cook and S. H. Son Oct. 1991 35 p
(Contract N00014-91-J-1102)
(AD-A242032; UVA/525449/CS92/101) Avail: NTIS HC/MF A03 CSCL 12/5

The goals of the StarLite Project are twofold. First, we investigate new technologies associated with the construction of real-time, distributed operating systems, database systems, and communication networks. Secondly, the research will produce tools and experimental systems, using the StarLite software prototyping environment. The issues being addressed are priority-based scheduling, methodology for developing prototyping tools, system integration, operating system support and interface issues, and fault-tolerance in real-time computing. Our research is directed towards discovering a set of design principles and developing efficient algorithms for distributed real-time systems and database systems. In addition to theoretical study, we are also developing experimental systems and prototyping tools for performance evaluation of new technology. GRA

N92-17637# North Carolina Univ., Chapel Hill. Dept. of Computer Science.
INCREMENTAL VOLUME RENDERING ALGORITHM FOR INTERACTIVE 3D ULTRASOUND IMAGING
Ryutarou Ohbuchi and Henry Fuchs Feb. 1991 25 p
(Contract N00014-86-K-0680)
(AD-A242048; TR91-003) Avail: NTIS HC/MF A03 CSCL 20/1

This paper presents an overview of the incremental, interactive three dimensional ultrasound echography system, where two dimensional image slices are acquired along with their locations and orientations to be reconstructed and volume rendered. The system generates a new image as a new 2D slice is acquired, to maximize interactivity. The visualization algorithm works in an

incremental manner, limiting the computations to the volume where the new input has arrived. We have established the basics of the efficient incremental volume rendering algorithm, which takes advantage of the incremental nature of the input. We have designed and implemented a faster ray clipping algorithm using polygon scan conversion to clip rays to the slab where the ray should be sampled. The new ray clipping algorithm showed marked improvement over the previous method. We have proposed a new ray-caching mechanism called hierarchical ray-cache to speed up the ray-compositing further. We have also proposed an algorithm to render polygonal objects quickly in screen space composited correctly with the volume image. With this proposed algorithm, various operations on the volume image, such as cut-away of a polyhedral volume, insertion of polygons, and highlighting polyhedral volumes will be possible at an interactive rate. GRA

N92-17640# Aerospace Corp., El Segundo, CA. Space Systems Div.

CONTRACTOR SOFTWARE ENGINEERING ENVIRONMENT EVALUATIONS SUMMARY REPORT Final Report, Jan. - Dec. 1990

Ranwa Haddad and Homa Taraji May 1991 34 p

(Contract F04701-88-C-0089)

(AD-A242330; SSD-TR-91-24) Avail: NTIS HC/MF A03 CSCL 12/5

This report summarizes the results of a task to evaluate Software Engineering Environments (SEE) at defense contractors. Ten major contractors were contacted. All of them currently are involved in SEE developments, although at different levels. Some still are in the early definition phases, while others have a SEE in place. Four of them were evaluated. The SEE's were evaluated along three different dimensions: their functionality, their architecture, and their usage. All four SEE's support Ada and offer training courses. However, the SEE's are weak in their support of testing functions. The four evaluated SEE's are in a state of evolution. Although SEE's can potentially be important factors in quality and productivity improvements, and DOD-STD-2167A mandates the use of a SEE, building a SEE is a costly and lengthy process. Therefore, a methodology is needed for evaluating contractor SEE's and for determining the cost/benefit tradeoffs. This task is the first step towards defining a SEE evaluation methodology for SDD contracts. GRA

N92-17655# Washington Univ., Seattle. Dept. of Physiology and Biophysics.

NEUTRAL NETWORK MODELS OF PRIMATE MOTOR SYSTEM Final Report

Eberhard E. Fetz 4 Nov. 1991 3 p

(Contract N00014-89-J-1240)

(AD-A243460) Avail: NTIS HC/MF A01 CSCL 12/6

The primary goal of this project was to develop neural network models of the primate sensorimotor system, which succeeded beyond our original expectations. Over the two-year span of this project we acquired the requisite hardware (a SUN 3-260 and two NeXT computers), developed a unique dynamic recurrent neural network program (called NeXTNet), and derived neural network simulations for several primate sensorimotor tasks. NeXTNet is a dynamic recurrent computer network simulator based on the algorithms of Watrous (1986) and Williams and Zipser (1989); it was designed to facilitate easy set-up of networks and gradient descent (backprop) training of a wide range of spatiotemporal transforms. Being dynamic, the model can incorporate as target patterns the firing patterns of neurons and motor units previously recorded in monkeys. The network is also fully recurrent, allowing unrestricted connectivity, so the circuitry can be made to resemble anatomical pathways with feedback and collateral connections. The inputs to the network were step changes in the position of a visual target, and the outputs were the eight discharge patterns of flexor and extensor motor units. GRA

N92-17680# Naval Postgraduate School, Monterey, CA.

DESIGN IMPLEMENTATION INTO FIELD PROGRAMMABLE GATE ARRAYS M.S. Thesis

Norman C. Messa Mar. 1991 104 p

(AD-A242538) Avail: NTIS HC/MF A06 CSCL 12/6

In the past three years, a new type of programmable logic device has emerged. The programmable gate array is a new approach to an old problem of trying to implement logic designs in an efficient manner. This thesis explores the implementation of design using the Field Programmable Gate Array (FPGA). In particular, this thesis utilizes the XILINX development system tools to implement design into the XILINX Logic Cell Array (LCA). This thesis begins by defining characteristics of the LCA and then defines the characteristics of the Small Computer Systems Interface (SCSI) which is used as a design implementation example. The XILINX implementation study is conducted on the design example. Both Mentor Graphics and Futurenet schematic capture tools are used for design entry. Following design implementation, back annotated design simulation is performed to study the effect of the LCA technology on design performance. The results of showed that designs implemented using technology performed comparably to other implementation technologies. Additionally, this implementation method allows design to be completed in a significantly shorter time frame than previously possible. GRA

N92-17716# Army Construction Engineering Research Lab., Champaign, IL.

ADAPTIVE ON-LINE HELP FOR EMBEDDED INSTRUCTIONAL SYSTEMS Final Report

Doris S. Shaw, L. M. Golish, Julie L. Webster, and Der-Shung Yang Oct. 1991 40 p

(AD-A243675; CERL-TR-91/52) Avail: NTIS HC/MF A03 CSCL 12/5

The U.S. Army Corps of Engineers (USACE) has long recognized the benefits of computer-aided design (CAD) systems, and has encouraged its design architects/engineers (A/E's) to use this technology. However, traditional methods of training A/E's to use CAD have had only limited success, so USACE has investigated and developed various innovative, nontraditional methods. One such method, on-line embedded instruction, uses CAD software as the delivery medium for an on-line tutorial program. This report discusses an on-line tutorial program developed for the Corps' standard CAD system, Intergraph MicroStation. An innovative feature of the Corps' tutorial program is its adaptive on-line help function, which includes both procedural and conceptual help material, presented to the user on the basis of his or her degree of CAD experience. The effectiveness of this tutorial was investigated in a USACE Technology Transfer Test Bed (T3B) demonstration, with particular attention on the adaptive on-line help function. Findings indicate that the adaptive help function was effective for most test participants, but it could probably be modified to better address the needs of certain categories of learners. GRA

N92-17733# Air Force Inst. of Tech., Wright-Patterson AFB, OH.

IMAGE PROCESSING APPLICATIONS FOR NONLINEAR DECOMPOSITION AND SYNTHESIS M.S. Thesis

Eric W. Kelm 25 Aug. 1991 33 p

(AD-A243357; AFIT/CI/CIA-91-065) Avail: NTIS HC/MF A03 CSCL 12/6

Data representation, which is often overlooked in many image processing and analysis applications, is as critical as the algorithms applied to that data. When data is represented properly, simple algorithms can be much more powerful than sophisticated and often complex algorithms applied to an improper representation. In an image, the useful information is generally mixed in with irrelevant information or noise and often it is difficult for the computer to separate the useful information from the large volume of irrelevant data without destroying much of the useful data. To provide a solid foundation for a good solution to this problem, multiresolution decomposition and synthesis approaches have been developed which decompose raw image data into a set of partial information channels, where each channel represents a certain

modality (or aspect) of the raw image. The channels can then be processed individually or cooperatively with a wide variety of results possible. GRA

N92-17761# Air Force Inst. of Tech., Wright-Patterson AFB, OH.
VERIFICATION AND VALIDATION OF THE COMPREHENSIVE OPERATIONAL SUPPORT EVALUATION MODEL FOR SPACE M.S. Thesis
Lawrence A. Cooper Dec. 1991 138 p
(AD-A243653; AFIT/GSO/ENS/91D-05) Avail: NTIS HC/MF A07 CSCL 12/5

This study details the verification and validation (V and V) of the Comprehensive Operational Support Evaluation Model for Space (COSEMS). COSEMS is an Ada-based simulation which models spacecraft constellation support concepts such as support from the ground and on-orbit support. While the model is intended for use in analyzing Strategic Defense System concepts, it can easily evaluate non-military satellite constellations. The V&V was confined to a subset of the over 200 subprograms which comprise COSEMS. This subset covered random number generation, reliability, orbital mechanics, and mission planning functions. The study used traces and comparison to other models to perform the V&V. An input/output analysis was also performed to ascertain the ease of use of COSEMS and the utility of its output. The analysis showed that the areas under investigation performed according to the model and that the model approximated real-world behavior except for orbital motion. The part of the model governing orbital perturbations due to the non-spherical earth omitted rotation of the line-of-apsides. The analysis also revealed that the Ada code and the input/output format are highly machine dependent, which restricts the program from coming into widespread use and limits the usefulness of the output. GRA

N92-17778*# Alabama Univ., Huntsville.
KNOWLEDGE, PROGRAMMING, AND PROGRAMMING CULTURES: LISP, C, AND Ada Final Report
Daniel Rochowiak Feb. 1990 105 p
(Contract NAS8-36955)
(NASA-CR-184220; NAS 1.26:184220; JRC-RR-90-04) Avail: NTIS HC/MF A06 CSCL 09B

The results of research 'Ada as an implementation language for knowledge based systems' are presented. The purpose of the research was to compare Ada to other programming languages. The report focuses on the programming languages Ada, C, and Lisp, the programming cultures that surround them, and the programming paradigms they support. Author

N92-17822 Academy of Sciences of the Ukrainian SSR, Kiev. Inst. of Physics.
ALGORITHM AND PASCAL: A PROGRAM FOR NEURAL NET LEARNING [ALGORITM I PASKAL: PROGRAMMA OBUCHENIIA NEIROPODOBNOI SETI]
N. A. Protsenko and L. V. Taranenko 1989 21 p In RUSSIAN
Copyright Avail: Issuing Activity

An algorithm and a pascal program for neural-net learning are proposed. Examples are provided that illustrate the program's performance. Transl. by L.K.H.

N92-17860*# National Aeronautics and Space Administration. Lyndon B. Johnson Space Center, Houston, TX.
DYNAMIC PATTERN MATCHER USING INCOMPLETE DATA Patent Application
Gordon G. Johnson, inventor (to NASA) (Barrios Technology, Inc., Houston, TX.) and Iui Wang, inventor (to NASA) 26 Aug. 1991 47 p
(NASA-Case-MSC-21415-1-SB; NAS 1.71:MSC-21415-1-SB; US-Patent-Appl-SN-749819) Avail: NTIS HC/MF A03 CSCL 09B

This invention relates generally to pattern matching systems, and more particularly to a method for dynamically adapting the system to enhance the effectiveness of a pattern match. Apparatus and methods for calculating the similarity between patterns are known. There is considerable interest, however, in the storage and retrieval of data, particularly, when the search is called or initiated by incomplete information. For many search algorithms, a query initiating a data search requires exact information, and the data file is searched for an exact match. Inability to find an exact match thus results in a failure of the system or method. NASA

N92-17921# Netrologic, Inc., San Diego, CA.
FRACTAL IMAGE ENCODING Quarterly Progress Report, Aug. - Nov. 1991
1 Nov. 1991 4 p
(Contract N00014-91-C-0117)
(AD-A243620) Avail: NTIS HC/MF A01 CSCL 12/9

During the period Aug. to Nov. 1991 we concentrated our efforts in three areas, development of applications, algorithm development, and theory. Progress in algorithm development and in seeking commercial partners is encouraging. We are also continuing to evaluate hardware needs. We have selected two specific applications for our compression algorithms. These are distribution of images on CD-ROMS, and inclusion of images of structures in cartographic data bases. The eventual markets include PC-based multimedia, real estate, and civil engineering firms. We have prepared a demonstration disk for 386 and 486 machines and SUN workstations, and are currently soliciting evaluations. We have began to work with a CD-ROM distributor to adapt our software to their needs. GRA

N92-17927# Oxford Univ. (England). Robotics Research Group.
A DECENTRALIZED BAYESIAN ALGORITHM FOR IDENTIFICATION OF TRACKED TARGETS
B. S. Y. Rao and H. F. Durrant-Whyte 1991 41 p
(OUEL-1892/91; ETN-92-90911) Avail: NTIS HC/MF A03

The problem of identification of objects being tracked by a fully decentralized surveillance system is considered. A fully decentralized system is an interconnected network of intelligent sensors each with its own transducers and processing capabilities. Locally obtained results are communicated to the other sensors for further processing, allowing each sensor to achieve a global result. Such a system has many benefits in terms of modularity, speed, and survivability. In particular, this work relates to a real time multitarget surveillance system used to track targets (people and mobile robots) as they enter and move around a factory assembly room performing tasks. The sensors used on this system (CCD (Charged Coupled Device) cameras) reveal information about the targets that is sufficiently rich to allow them not only to be tracked but also identified as a person, a robot, etc. This identified information can be used as an man machine interface design and to facilitate situation assessment. The identification problem is defined and a centralized Bayesian algorithm for determining the identity of each target based on each sensor's information is developed. The algorithm is decentralized and the its performance compared to the centralized version. Results of an implementation of the algorithm working on real data from the surveillance system are presented. ESA

N92-17948# Booz-Allen and Hamilton, Inc., Bethesda, MD.
QTCM SOFTWARE DOCUMENTATION. VOLUME 2: USER'S MANUAL Final Report
Oct. 1990 40 p
(Contract DCA100-87-C-0063)
(AD-A242744; NCS-TIB-90-14) Avail: NTIS HC/MF A03 CSCL 12/5

This volume of the QTCM software manual is a user's manual for those who need to conduct QTCM analyses, but do not require an in-depth knowledge of the software model's structure and development. This manual describes the operating environment necessary to support QTCM and provides step-by-step instructions for operating the model. QTCM consists of three executable segments - the input file formatter, the network analysis segment, and the output file formatter. The input file formatter, INPFMT, allows the user to create or amend a formatted input file via a

series of user menus and prompts. NETWORK reads in the input file produced by INPFMT and performs the network analysis function of QTCM, including traffic distribution and calculation of network statistics. The output formatter, OUTFMT, then takes the output from NETWORK and allows the user to selectively display and output statistical traffic data via a series of user menus and prompts. These output data may be written to an ASCII text file if the user desires. The operation of each of these executables is described. GRA

N92-17960# Texas Univ., Austin. Center for Cybernetic Studies.
PRACTICAL ERROR BOUNDS FOR A CLASS OF QUADRATIC PROGRAMMING PROBLEMS
A. Charnes and J. Semple Mar. 1991 17 p
(Grant NSF SES-87-22504)
(AD-A243249; CCS-663) Avail: NTIS HC/MF A03 CSCL 12/4

Error bounds are developed for a class of quadratic programming problems. The absolute error between an approximate feasible solution, generated via a dual formulation, and the true optimal solution is measured. Furthermore, these error bounds involve considerably less work computationally than existing estimates. GRA

N92-17969# Edgerton, Germeshausen and Grier, Inc., Idaho Falls, ID.
SOFTWARE RELIABILITY MODELS FOR CRITICAL APPLICATIONS
H. Pham and M. Pham Dec. 1991 98 p
(Contract DE-AC07-76ID-01570)
(DE92-004797; EGG-2663) Avail: NTIS HC/MF A05

This report presents the results of the first phase of the ongoing EG&G Idaho, Inc. Software Reliability Research Program. The program is studying the existing software reliability models and proposes a state-of-the-art software reliability model that is relevant to the nuclear reactor control environment. This report consists of three parts: (1) summaries of the literature review of existing software reliability and fault tolerant software reliability models and their related issues; (2) proposed technique for software reliability enhancement; and (3) general discussion and future research. The development of this proposed state-of-the-art software reliability model will be performed in the second place. DOE

N92-17351*# National Aeronautics and Space Administration. Lyndon B. Johnson Space Center, Houston, TX.
SOFTWARE LIFE CYCLE METHODOLOGIES AND ENVIRONMENTS
Ernest Fridge *In* NASA, Washington, Beyond the Baseline 1991: Proceedings of the Space Station Evolution Symposium. Volume 2: Space Station Freedom, Part 2 Sep. 1991 p 1037-1103 (For primary document see N92-17348 08-18)
Avail: NTIS HC/MF A20 CSCL 09B

N92-17352*# National Aeronautics and Space Administration. Lyndon B. Johnson Space Center, Houston, TX.
INTELLIGENT COMPUTER-AIDED TRAINING (ICAT)
Robert T. Savely and R. Bowen Loftin *In* NASA, Washington, Beyond the Baseline 1991: Proceedings of the Space Station Evolution Symposium. Volume 2: Space Station Freedom, Part 2 Sep. 1991 p 1105-1155 Prepared in cooperation with Houston Univ., TX (For primary document see N92-17348 08-18)
Avail: NTIS HC/MF A20 CSCL 09B

N92-17353*# Jet Propulsion Lab., California Inst. of Tech., Pasadena.
OPERATIONS MISSION PLANNER BEYOND THE BASELINE
Eric Biefeld and Lynne Cooper *In* NASA, Washington, Beyond the Baseline 1991: Proceedings of the Space Station Evolution Symposium. Volume 2: Space Station Freedom, Part 2 Sep. 1991 p 1157-1200 (For primary document see N92-17348 08-18)
Avail: NTIS HC/MF A20 CSCL 09B

62 COMPUTER SYSTEMS

Includes computer networks and special application computer systems.

N92-16997# Massachusetts Inst. of Tech., Cambridge. Lab. for Computer Science.
THE REAL-TIME COST OF TIMING UNCERTAINTY: CONSENSUS AND FAILURE DETECTION
Stephen J. Ponzio Oct. 1991 71 p
(Contracts N00014-85-K-0168; N00014-91-J-1046)
(AD-A243176; MIT/LCS/TR-518) Avail: NTIS HC/MF A04 CSCL 12/7

In real distributed systems, processes may have only inexact information about the amount of real time needed for primitive operations such as process steps. This thesis studies the effect of this timing uncertainty on the real time behavior of distributed systems. We consider a semi-synchronous model in which the amount of real time between process steps is known to be in the interval (c sub 1, c sub 2) and every message is known to be delivered within time d of when it is sent. We use C = c sub 2/c sub 1 as a measure of the timing uncertainty. We first study the problem of reaching agreement in the presence of failures. A simple argument derived from the case of synchronous processes shows that at least time (f + 1) d is required to tolerate f failures, while time (f + 1) Cd is sufficient to tolerate f stopping or omission failures by directly simulating the rounds of any synchronous consensus algorithm. We narrow this gap for omission failures, building on the nearly optimal algorithm of Attiya, Dwork, Lynch, and Stockmeyer which tolerates only stopping failures. GRA

N92-17135# Naval Postgraduate School, Monterey, CA.
LOCAL AREA NETWORK STRATEGIES AND GUIDELINES FOR A PERUVIAN AIR FORCE COMPUTER CENTER M.S. Thesis
Miguel A. PalominoFonseca Mar. 1991 107 p
(AD-A242841) Avail: NTIS HC/MF A06 CSCL 12/7

This thesis examines the application of local area network (LAN) technology to the Peruvian Air Force Computer Center. The current Peruvian Air Force Computer Center communication system and its problems are discussed, along with the basic concepts of data communication, protocols, and topologies. The IEEE 802.3 and IEEE 802.5 specifications are discussed in detail. This study is primarily concerned with how to design the best local area network for the Peruvian Air Force Computer Center, and proposes a local area network implementation strategy for the Peruvian Air Force Computer Center. GRA

N92-17188# Mitre Corp., Bedford, MA.
RESOURCE ALLOCATION IN DISTRIBUTED MEMORY MULTIPROCESSING
Jonathan I. Leivent and Ann M. Wollrath Sep. 1991 29 p
(AD-A243165; MTR-11209) Avail: NTIS HC/MF A03 CSCL 09/6

The problems of load balancing and locality of reference for large distributed memory message passing multiprocessors running object-oriented applications are studied. The object-oriented nature of the applications implies that tasks must be executed on the processor containing the host object for the task (tasks are method executions; the host object is the destination of the message that invokes the method). The particular constraint for the study is that objects will not be moved between processors once allocated. The primary resource allocation problem becomes the determination of the best processor on which to allocate each new object during the execution of the application. The study uses discrete event simulation of pseudo-applications under the control of several resource allocation policies selected as limiting cases of practical solutions. Results are presented, and some general rules-of-thumb are suggested for use in real systems. GRA

N92-17395# Naval Ocean Systems Center, San Diego, CA.
PARALLEL PROCESSING APPLIED TO COMPUTATIONAL ELECTROMAGNETICS Final Report, Oct. 1990 - Sep. 1991

L. C. Russell and J. W. Rockway Oct. 1991 71 p
(Proj. RV3-6121)
(AD-A242372; NOSC/TR-1450) Avail: NTIS HC/MF A04
CSCL 20/14

This investigation applied parallel processing techniques to a computational electromagnetic code to see if high performance computing can improve the utility and efficiency of techniques used in ship electromagnetic designs. Efficient parallel matrix filling, factoring, and solving routines were developed, implemented, and evaluated. Several techniques for mapping the matrix columns onto the processors were also implemented and evaluated. This report lists several benefits that have resulted, or will result, from work done on this Independent Exploratory Development (IED) project. GRA

N92-17425# Naval Postgraduate School, Monterey, CA. Dept. of Administrative Sciences.
DELAY ANALYSIS FOR MULTIDIMENSIONAL QUEUEING PROCESS IN CSMA/CD LOCAL AREA NETWORKS
June S. Park and Keebom Kang Sep. 1991 33 p
(AD-A242364; NPS-AS-91-016) Avail: NTIS HC/MF A03
CSCL 25/5

A CSMA/CD local area network consists of single server (the channel) and multiple interacting queues of message packets. The message queueing process in a buffered, P-persistent CSMA/CD system is modeled as a multidimensional semi-markov chain. An effective approximation method to compute the mean packet delay in equilibrium is developed, based on the joint probability generating function of the queue length vector at embedded Markov epochs. We also develop a simulation model to validate approximation results. To the best of our knowledge, this work is the first in the literature that enables optimization of the control parameter P for the CSMA/CD system with more than two users. Author (GRA)

N92-17465# BDM International, Inc., McLean, VA.
ANALOG OPTICAL NEURAL NETS: A NOISE SENSITIVITY ANALYSIS Final Report, 21 Jul. 1989 - 20 Jul. 1991
Michael W. Haney, James J. Levy, and Ravindra A. Athale 11 Sep. 1991 121 p
(Contract F49620-89-C-0115)
(AD-A242920; BDM/MCL-91-0364-TR) Avail: NTIS HC/MF A06
CSCL 20/6

The development of analog optical implementations of neural networks such as the multilayer perceptron with learning by backward error propagation (BEP) requires an understanding of the noise sensitivity of such architectures. In this program computer simulations were used to study the effects of component and system noise on the performance of such optical implementations. A hybrid optical/electronic parallel architecture capable of both the forward pass and backward error propagation steps of training data presentation was conceived and modeled. The simulations showed that the most significant effects were due to the nonlinear response of the spatial light modulators used to store and update the neural weights. Another conclusion of the simulation results was that increasing the hidden layer size increases noise immunity significantly. GRA

N92-17507# Air Force Inst. of Tech., Wright-Patterson AFB, OH. School of Engineering.
IMPROVED TASK SCHEDULING FOR PARALLEL SIMULATIONS M.S. Thesis
Andrew E. McNear Dec. 1991 109 p
(AD-A243721; AFIT/GCS/ENG/91D-14) Avail: NTIS HC/MF A06 CSCL 12/6

The objective of this investigation is to design, analyze, and validate the generation of optimal schedules for simulation systems. Improved performance in simulation execution times can greatly improve the return rate of information provided by such simulations resulting in reduced development costs of future computer/electronic systems. Optimal schedule generation of precedence-constrained task systems including iterative feedback systems such as VHDL or war gaming simulations for execution on a parallel computer is known to be N P-hard. Efficiently parallelizing such problems takes full advantage of present computer technology to achieve a significant reduction in the search times required. Unfortunately, the extreme combinatoric 'explosion' of possible task assignments to processors creates an exponential search space prohibitive on any computer for search algorithms which maintain more than one branch of the search graph at any one time. This work develops various parallel modified backtracking (MBT) search algorithms for execution on an iPSC/2 hypercube that bound the space requirements and produce an optimally minimum schedule with linear speed-up. The parallel MBT search algorithm is validated using various feedback task simulation systems which are scheduled for execution on an iPSC/2 hypercube. The search time, size of the enumerated search space, and communications overhead required to ensure efficient utilization during the parallel search process are analyzed. The various applications indicate appreciable improvement in performance using this method. GRA

N92-17638# North Carolina Univ., Chapel Hill. Dept. of Computer Science.
PARALLEL RADIOSITY TECHNIQUES FOR MESH-CONNECTED SIMD COMPUTERS
Amitabh Varshney Jul. 1991 165 p
(Contract N00014-86-K-0680; NSF CCR-86-09588)
(AD-A242049; TR91-028) Avail: NTIS HC/MF A08 CSCL 12/6

This thesis investigates parallel radiosity techniques for highly-parallel, mesh-connected SIMD computers. The approaches studied differ along the two orthogonal dimensions: the method of sampling-by ray-casting or by environment-project and the method of mapping of objects to processors - by object-space-based methods or by a balanced-load method. The environment-projection approach has been observed to perform better than the ray-casting approaches. For the dataset studied, the balanced-load method appears promising. Spatially subdividing the dataset without taking the potential light interactions into account has been observed to violate the locality property of radiosity. This suggests that object-space-based methods for radiosity must take visibility into account during subdivision to achieve any speedups based on exploiting the locality property of radiosity. This thesis also investigates the reuse patterns of form-factors in perfectly diffuse environments during radiosity iterations. Results indicate that reuse is sparse even when significant convergence is achieved. GRA

N92-17670# North Carolina Univ., Chapel Hill. Dept. of Computer Science.
SCAN DIRECTED LOAD BALANCING FOR HIGHLY-PARALLEL MESH-CONNECTED COMPUTERS
Edoardo S. Biagioni and Jan F. Prins Jul. 1991 25 p
(Contract N00014-86-K-0680)
(AD-A242045) Avail: NTIS HC/MF A03 CSCL 12/6

Scan Directed Load Balancing is a new, locality-preserving, dynamic load balancing algorithm for grid based computations on mesh connected parallel computers. Scans are used to efficiently determine what areas of the machine are heavily loaded and what areas are lightly loaded, and to organize the movement of data. Data is shifted along the mesh in a regular fashion to balance the load. The Locality Property of the algorithm guarantees that all the neighbors of a data point on the grid are stored either on the same processor, or on a processor that is directly connected to it. Scan Directed Load Balancing is applicable to both SIMD and MIMD mesh-connected parallel computers, and has been implemented on the MasPar MP-1. We present some theoretical bounds achieved by the algorithm as well as the algorithm's performance on a particular image processing problem, edge-directed diffusion. Our experiments show that the algorithm is effective in improving the load distribution for real problems, while the efficiency of the original grid-based computation is preserved by the locality property. GRA

N92-17833# Center for Mathematics and Computer Science, Amsterdam (Netherlands). Dept. of Computer Science.
A PROOF THEORY FOR A SEQUENTIAL VERSION OF POOL

Pierre H. M. America and Frank S. deBoer (Philips Gloeilampenfabrieken N.V., Amsterdam, Netherlands) Mar. 1991 111 p
(CWI-CS-R9118; ETN-92-90557) Copyright Avail: NTIS HC/MF A06

A Hoare style proof theory for partial correctness of programs, written in a sequential version of the Parallel Object Oriented Language (POOL), is developed. The systems described by this language give rise to dynamically evolving process structures. One of the main objectives of the proof theory is to formalize reasoning about such structures at an abstraction level at least as high as that of the programming language. The proof system is shown to be sound and (relative) complete. ESA

63 CYBERNETICS

Includes feedback and control theory, artificial intelligence, robotics and expert systems.

For related information see also *54 Man/System Technology and Life Support.*

N92-16987*# National Aeronautics and Space Administration. Langley Research Center, Hampton, VA.
NEURAL NETWORK MODELING OF NONLINEAR SYSTEMS BASED ON VOLTERRA SERIES EXTENSION OF A LINEAR MODEL
Donald I. Soloway and Jan T. Bialasiewicz (Colorado Univ., Denver.) Jan. 1992 13 p
(NASA-TM-104177; NAS 1.15:104177) Avail: NTIS HC/MF A03 CSCL 09B

A Volterra series approach was applied to the identification of nonlinear systems which are described by a neural network model. A procedure is outlined by which a mathematical model can be developed from experimental data obtained from the network structure. Applications of the results to the control of robotic systems are discussed. Author

N92-16991# Carnegie-Mellon Univ., Pittsburgh, PA. Dept. of Psychology.
A COMPUTATIONAL MODEL OF SEMANTIC MEMORY IMPAIRMENT: MODALITY-SPECIFICITY AND EMERGENT CATEGORY-SPECIFICITY
Martha J. Farah and James L. McClelland Sep. 1991 59 p
(AD-A242377; AIP-147) Avail: NTIS HC/MF A04 CSCL 05/8

Brain damage can cause the selective loss of knowledge about living or nonliving things. This seems to imply that semantic memory is organized taxonomically, with different components specializing in representing knowledge about living and nonliving things. An alternative view of semantic memory is that it is organized by modality, with different components representing information from different sensorimotor channels. In this article we demonstrate how a modality specific semantic memory system can account for category specific impairments after brain damage. Specifically, in Experiment 1 we test and confirm the hypothesis that visual and functional knowledge play different roles in the representation of living and nonliving things. We then describe a parallel distributed processing model of semantic memory in which knowledge is subdivided by modality into visual and functional components. In Experiment 2 we lesion the model and confirm that damage to visual semantics primarily impairs knowledge of living things, and damage to functional semantics primarily impairs knowledge of nonliving things. In Experiment 3 we demonstrate that the model accounts naturally for a finding that had appeared problematic for a modality specific architecture, namely impaired retrieval of functional knowledge about living things. GRA

N92-16994# TRW, Inc., Carson City, CA. Systems Engineering and Development Div.
A SYSTEM FOR SPECIFYING AND RAPIDLY PROTOTYPING USER INTERFACES
Christopher Rouff Jun. 1991 11 p
(AD-A242963; TRW-TS-91-02) Avail: NTIS HC/MF A03 CSCL 12/5

This paper presents a system for rapidly prototyping user interfaces and a model for specifying them. The model represents the components, flow of control, constraints, and semantic feedback of an interface while the system allows the interface layout, dialogue, and application interface to be interactively defined, resulting in little or no programming to produce a prototype. As a user interface is prototyped, a model of the interface is maintained that represents its structure and functionality. This model can then be compiled into source code with calls to the X Windows and MOTIF libraries. The generated program can then be compiled and linked to application functions to produce an executable program. Other user interface builders only have interactive definitions of the interface layout and specify the dialogue in a programming language, thus requiring a programmer to learn yet another language. The system described here is based on a graph model instead of a programming language and allows complex sequencing, constraints, and the application interface to be defined interactively. This graph model representation also allows analysis of the interface to be made in terms of consistency and completeness of the specification. GRA

N92-17049# Cornell Univ., Ithaca, NY. Dept. of Computer Science.
COMPLEXITY ISSUES IN NUMERICAL OPTIMIZATION Final Report, 1 Nov. 1990 - 30 Apr. 1991
Steven A. Vavasis 17 Sep. 1991 3 p
(Grant AF-AFOSR-0878-91)
(AD-A241854; AFOSR-91-0878TR) Avail: NTIS HC/MF A01 CSCL 12/1

A conference on complexity issues in numerical optimization was held in Ithaca, NY on March 22-23, 1991. The conference featured 17 invited speakers, each of whom gave a 45 minute presentation. The conference was supported primarily by the Air Force Office of Scientific Research, with additional support from the Cornell Mathematical Sciences Institute and the Society for Industrial and Applied Mathematics (SIAM). Topics discussed included strongly polynomial algorithms for linear programs with algebraic coefficients; new results for the Steiner tree problem; complexity results for following the center of a linear inequality system as the data is parametrically deformed; continuous methods for inductive inference problems; computational complexity of inner and outer j-radii; parallel complexity of linear programming; and new iterative methods for linear inequalities. GRA

N92-17203# Defense Systems, Inc., McLean, VA.
CAUSAL SCHEMA DECISION-AIDING SYSTEM Final Report, Apr. - Oct. 1985
Gerald Hopple Oct. 1991 50 p
(Contract MDA903-85-C-0191)
(AD-A242931; ARI-RN-92-01) Avail: NTIS HC/MF A03 CSCL 23/2

This report looks at the use of causal schema to organize concepts for understanding complex decision processes. The task selected for developing a prototype causal schema decision-aiding system was to implement portions of a fire support annex for a corps operations order. A series of storyboards was developed based on an analysis of the prescribed elements of the annex; the storyboards were evaluated as a prototype 'decision aid'. It is concluded that causal schema is useful in describing tactical decision processes and may offer advantages over rule-based approaches (e.g., artificial intelligence) in developing decision aids. GRA

N92-17385# Mitre Corp., Bedford, MA.
SUMMARY OF PROFESSIONAL ACTIVITIES, CENTER FOR INTELLIGENCE AND SPECIAL PROGRAMS, 1990
Jun. 1991 41 p
(AD-A243508; M91-41) Avail: NTIS HC/MF A03 CSCL 05/1

The MITRE Corporation does not manufacture products or compete with industry. After a reorganization in 1990, MITRE expanded from three to five operating centers. Personnel from

two of the centers are located primarily at our headquarters in Bedford, Massachusetts (with one technical division located in the Washington area). These two centers are the Center for Air Force Command, Control, and Communications (C3) Systems and the Center for Intelligence and Special Programs. The remaining three operational centers are based in McLean, Virginia: the Washington C3 Center, the Center for Advanced Aviation System Development, and the Center for Civil Systems. The Center for Intelligence and Special Programs supports the Air Force Electronic Systems Division (ESD), the Army and Navy, a wide variety of intelligence agencies, and the Unified and Specified Commands. The Center provides system engineering support to components of the intelligence community, particularly in the areas of networks, information security, artificial intelligence, and workstation technologies. This publication is an overview of the professional activities of the Center for Intelligence and Special Programs for the 1990 calendar year. GRA

N92-17386# Mitre Corp., Bedford, MA.
SUMMARY OF PROFESSIONAL ACTIVITIES, CENTER FOR AIR FORCE C3 SYSTEMS
Jun. 1991 61 p
(AD-A243509; M91-42) Avail: NTIS HC/MF A04 CSCL 05/1

The MITRE Corporation does not manufacture products or compete with industry. After a reorganization in 1990, MITRE expanded from three to five operating centers. Personnel from two of the centers are located primarily at our headquarters in Bedford, Massachusetts (with one technical division located in the Washington area). These two centers and the Center for Air Force Command, Control, and Communications (C3) Systems and the Center for Intelligence and Special Programs. The remaining three operational centers are based in McLean, Virginia: the Washington C3 Center, the Center for Advanced Aviation System Development, and the Center for Civil Systems. The principal sponsor for the Center for Air Force C3 Systems is the Air Force Electronic Systems Division (ESD), which develops groundbased and airborne sensors, radios, computers, software, and displays, and integrates them into command and control systems. We also provide support to other parts of the Air Force, including Rome Laboratory, Air Force Logistics Command, Tactical Air Command, and Strategic Air Command. This publication is an overview of the professional activities of the Center for Air Force C3 Systems for the 1990 calendar year. GRA

N92-17438# BDM International, Inc., Arlington, VA.
AUTOMATED PLANNING WITH SPECIAL RELEVANCE TO ASSOCIATE SYSTEMS TECHNOLOGY AND MISSION PLANNING Final Report, May 1990 - Sep. 1991
Philip A. Merkel, Paul E. Lehner, Roger A. Geesey, and John B. Gilmer Sep. 1991 132 p
(Contract MDA072-90-C-0039; ARPA Order 6707)
(AD-A241924; BDM/VSQ-91-0742-TR) Avail: NTIS HC/MF A07 CSCL 12/6

This report describes the results of work performed to establish the technical basis for a future R and D effort in mission planning technology. One known operational need is for aircrew decision aiding for dynamic replanning during the performance of modern military air missions where information flow, knowledge and detailed reasoning can radically alter the outcome. Artificial intelligence technologies have been applied to create associate concepts with automated planning being a key construct to aid decision making in time constrained, rapidly changing situations. Basic and advanced research programs such as Pilot's Associate, Rotorcraft Pilot's Associate and the Submarine Operational Automation System have each introduced relevant advances to meet service-specific needs. This report provides an overview of automated planning techniques followed by an applications and technology map. The material is supported by information on the relationships of automated planning to the techniques of mathematical optimization, decision theory, et. al. GRA

N92-17457# Carnegie-Mellon Univ., Pittsburgh, PA. Artificial Intelligence and Psychology Project.
A CONNECTIONIST SIMULATION OF ATTENTION AND VECTOR COMPARISON: THE NEED FOR SERIAL PROCESSING IN PARALLEL HARDWARE
Judith M. Shedden and Walter Schneider 1991 8 p
(Contracts N00014-86-K-0678; N00014-87-K-0397; MDA903-89-K-0174)
(AD-A242225; CMU-AIP-149) Avail: NTIS HC/MF A02 CSCL 12/5

Given the massively parallel nature of the brain an obvious question is why are so many information processing functions serial? In particular, this paper addresses the issue of the comparison process. Behavioral data show that in perceptual matching tasks (such as memory scanning and visual search) performance is systematically affected by stimulus load, in that required processing time increases with each additional comparison item. It is arguable whether this indicates a processing system that performs serial comparisons, or a system for which comparisons are done in parallel but reaction time is affected by load because of other system limitations. In this simulation we show that in a modular connectionist system vector transmission is possible in parallel, but the comparison process within a module must be done serially unless accuracy is sacrificed. GRA

N92-17767# Air Force Inst. of Tech., Wright-Patterson AFB, OH. School of Engineering.
AN INVESTIGATION OF THE APPLICATION OF ARTIFICIAL NEURAL NETWORKS TO ADAPTIVE OPTICS IMAGING SYSTEMS M.S. Thesis
Andrew H. Suzuki Dec. 1991 89 p
(AD-A243780; AFIT/GEO/ENG/91D-04) Avail: NTIS HC/MF A05 CSCL 12/9

Recurrent and feedforward artificial neural networks are developed as wavefront reconstructors. The recurrent neural network studied is the Hopfield neural network and the feedforward neural network studied is the single layer perceptron artificial neural network. The recurrent artificial neural network input features are the wavefront sensor slope outputs and neighboring actuator feedback commands. The feedforward artificial neural network input features are just the wavefront sensor slope outputs. Both artificial neural networks use their inputs to calculate deformable mirror actuator commands. The effects of training are examined. GRA

N92-17814# Joint Inst. for Nuclear Research, Dubna (USSR). Lab. of Neutron Physics.
MICROPROCESSOR CONTROLLER IN CAMAC STANDARD FOR TEMPERATURE REGULATION AND STABILIZATION
Nguyen Nhi Dien and K. G. Rodionov 1990 11 p In RUSSIAN; ENGLISH summary
(DE92-611158; JINR-R-10-90-398) Avail: NTIS HC/MF A03

The microprocessor controller in CAMAC standard for temperature regulation and stabilization of an external object (electric furnace, thermostat) is described. The controller has two control regimes, parallel and serial, and was controlled by personal computer PC/XT/AT. The apparatus that was created and the software supply, allow the temperature of the sample to be linearly raised or lowered to: indicated value with different rates; stabilize temperature on a set level; and record a graph of current temperature both at the time of heating or cooling and at the time of stabilization with a different frequency that is set by the program. DOE

N92-17819 Academy of Sciences of the Ukrainian SSR, Kiev. Inst. of Physics.
COMPUTER MODELLING OF TWO-INPUT NEURAL-NET LEARNING [MODELIRORANIE RA EVM OBUCHENIIA DVUKHVKHODOVOI NEIROPODOBNOI SETI]
L. V. Taranenko and N. A. Protsenko 1990 38 p In RUSSIAN
Copyright Avail: Issuing Activity

A pascal program for neural-net learning having two inputs

and one output is proposed. Examples are given and are illustrated by an actual program. Transl. by L.K.H.

N92-17838# Leiden Univ. (Netherlands). Div. of Applied Mathematics.
THE MICRO-c RULE IS NOT OPTIMAL IN THE 2ND NODE OF THE TANDEM QUEUE; 2 COUNTEREXAMPLES
Arie Hordijk and Ger Koole 1991 7 p
(TW-91-05; ETN-92-90561) Avail: NTIS HC/MF A02

Two counter examples which show that the mu(c) rule is not optimal in the second node of the tandem queue are presented. These counterexamples contradict the interchange arguments for classical scheduling problems in queues and stochastic scheduling which are referenced. ESA

N92-17880# Oxford Univ. (England). Dept. of Engineering Science.
ADAPTIVE GENERALIZED PREDICTIVE CONTROL
D. W. Clarke 1991 25 p Sponsored by Science Research Council
(OUEL-1879/91; ETN-92-90906) Avail: NTIS HC/MF A03

The modern approach to self tuning and adaptive control is to couple a robust parameter estimator to a robust control algorithm. As Generalized Predictive Control (GPC) is based on long range prediction (LRP), its shares the application properties of other LRP control laws such as Dynamic Matrix Control (DMC), and shows that the simplest choice ofhorizons (giving 'mean level' control) provides dead beat disturbance rejection. GPC has useful robustness properties which are determined by the cost function parameters and a prespecified observer polynomial. The results are particularly simple for mean level and state dead beat objectives, and are extended to the case of cascade control with, say, a Proportional Integral (PI) algorithm in the inner loop. In proving convergence of adaptive algorithms, it is important to have a control law which is guaranteed to be stabilizing. Such a law was recently derived based on long range prediction yet short horizons, where the constraints are not in input increments (as in DMC and GPC), but instead are imposed on a set of future system errors. The properties of this new approach are discussed. ESA

N92-17895*# National Aeronautics and Space Administration. Pasadena Office, CA.
HIGH LEVEL LANGUAGE-BASED ROBOTIC CONTROL SYSTEM Patent Application
Guillermo Rodriguez, inventor (to NASA), Kenneth K. Kruetz, inventor (to NASA), and Abhinandan Jain, inventor (to NASA) (Jet Propulsion Lab., California Inst. of Tech., Pasadena.) 1 Nov. 1991 56 p
(Contract NAS7-918)
(NASA-Case-NPO-17918-2-CU; NAS 1.71:NPO-17918-2-CU; US-Patent-Appl-SN-786499) Avail: NTIS HC/MF A04 CSCL 09B

This invention is a robot control system based on a high level language implementing a spatial operator algebra. There are two high level languages included within the system. At the highest level, applications programs can be written in a robot-oriented applications language including broad operators such as MOVE and GRASP. The robot-oriented applications language statements are translated into statements in the spatial operator algebra language. Programming can also take place using the spatial operator algebra language. The statements in the spatial operator algebra language from either source are then translated into machine language statements for execution by a digital control computer. The system also includes the capability of executing the control code sequences in a simulation mode before actual execution to assure proper action at execution time. The robot's environment is checked as part of the process and dynamic reconfiguration is also possible. The languages and system allow the programming and control of multiple arms and the use of inward/outward spatial recursions in which every computational step can be related to a transformation from one point in the mechanical robot to another point to name two major advantages. NASA

N92-17965# Lawrence Livermore National Lab., CA.
SOFTWARE TOOLS FOR DISTRIBUTED INTELLIGENT CONTROL SYSTEMS
J. R. James and C. J. Herget Oct. 1991 7 p Presented at the 3rd International Federation of Automatic Control (IFAC) International Workshop on Artificial Intelligence in Real Time Control, Phonert Park, CA, 23-25 Sep. 1991
(Contract W-7405-eng-48)
(DE92-004656; UCRL-JC-108590; CONF-9109316-2) Avail: NTIS HC/MF A02

The future of intelligent control systems depends upon the extent to which Artificial Intelligence (AI) technology can help to control engineers deliver practical solutions to difficult control engineering problems. Conventional control design approaches have achieved notable successes in the design and implementation of robust, adaptive controllers for systems with well-defined mathematical models. However, conventional approaches have had difficulty supporting engineers in the design and implementation of control systems when an accurate mathematical model is not available. Also, verification that computer-controlled systems perform to specifications, validation of the specifications, higher-level control, operator decision aids, system diagnosis, operator alerting, and reconfiguration of systems which experience large changes over time or potentially catastrophic failures are significant challenges to control science and engineering. It is in these difficult areas where the AI technologies of knowledge representation, learning, search, diagnosis, planning, and decision are being used to aid control engineers. Algorithms for computer-controlled systems and software tools to help implement these algorithms have been a subject of research and commercialization for decades. Computer-Aided Control Engineering (CACE) tools have achieved a degree of success in the past decade based on their ability to assist in the control system design and implementation process. Specialized tools have been made available for system identification, system simulation, controller design and controller implementation. Recently, efforts have been made to build integrated CACE environments. This paper will describe the results of the workshop and subsequent efforts to use these results to shape a DARPA software development project. DOE

N92-17411*# National Aeronautics and Space Administration. Ames Research Center, Moffett Field, CA.
FACING PAGE TEST FOR THE ASTRONAUT SCIENCE ADVISOR PRESENTATION
Michael M. Compton *In* NASA, Washington, Beyond the Baseline 1991: Proceedings of the Space Statin Evolution Symposium. Volume 1: Space Station Freedom, Part 2 Sep. 1991 p 367-391 (For primary document see N92-17409 08-18)
Avail: NTIS HC/MF A16 CSCL 09B

N92-17412*# National Aeronautics and Space Administration. Ames Research Center, Moffett Field, CA.
THE ASTRONAUT SCIENCE ADVISOR: GROUND TESTING DURING SLS-1
Michael M. Compton *In* NASA, Washington, Beyond the Baseline 1991: Proceedings of the Space Station Evolution Symposium. Volume 1: Space Station Freedom, Part 2 Sep. 1991 p 393-41 (For primary document see N92-17409 08-18)
Avail: NTIS HC/MF A16 CSCL 09B

N92-17998*# Princeton Univ., NJ. Dept. of Mechanical and Aerospace Engineering.
NEURAL NETWORKS FOR AIRCRAFT SYSTEM IDENTIFICATION
Dennis J. Linse *In* NASA. Langley Research Center, Joint University Program for Air Transportation Research, 1990-1991 Dec. 1991 p 141-154 (For primary document see N92-17984 08-01)
Avail: NTIS HC/MF A09 CSCL 09B

64 NUMERICAL ANALYSIS

Includes iteration, difference equations, and numerical approximation.

N92-17081# Army Materiel Systems Analysis Activity, Aberdeen Proving Ground, MD.
THE INSTABILITY OF LINEAR HETEROGENEOUS LANCHESTER EQUATIONS
Herbert E. Cohen 20 Nov. 1991 17 p
(AD-A243519; AMSAA-TR-501) Avail: NTIS HC/MF A03
CSCL 15/6

It is shown that the structure of the linear Lanchester attrition matrix leads to invariant properties associated with the sum of the eigenvalues and to the conclusion that the linear Lanchester equations are inherently unstable. GRA

N92-17148# Columbia Univ., New York, NY. Dept. of Computer Science.
TOPOLOGICAL REPRESENTATION OF GRAPH ISOMORPHISM TYPES Final Report
Jonathan L. Gross 20 Nov. 1991 4 p
(Contract N00014-85-K-0768)
(AD-A243528) Avail: NTIS HC/MF A01 CSCL 12/2

The strategic plan of this research program was to develop the theory of imbedding distributions as a possible probabilistic approach to the graph isomorphism problem. It was projected that, although the much pursued goal of a practical polynomial-time test for graph isomorphism might not be achieved, the expected mathematical development in this novel attempt would provide a suitable return on the investment. It was hoped that 3-connected graphs would prove to be distinguishable with lower invariants in the hierarchy, since there are traceable inductive constructions of the family of all 3-connected graphs. However, algebraic methods of Rieper established that none of the well-understood lower invariants was complete for the 3-connected simple graphs. Thus, obtaining a graph isomorphism test by this avenue seems to involve either rising in the hierarchy of invariants or identifying a nearly exhaustive class of graphs for which the lower invariants are complete. GRA

N92-17206# Mitre Corp., Bedford, MA.
IMPS: AN INTERACTIVE MATHEMATICAL PROOF SYSTEM
W. M. Farmer, J. D. Guttman, and F. J. Thayer Jul. 1991 54 p
(AD-A243162; M90-19) Avail: NTIS HC/MF A04 CSCL 12/1

IMPS is an Interactive Mathematical Proof System intended as a general purpose tool for formulating and applying mathematics in a familiar fashion. The logic of IMPS is based on a version of simple type theory with partial functions and subtypes. Mathematical specification and inference are performed relative to axiomatic theories, which can be related to one another via inclusion and theory interpretation. The system supports a natural style of inference based on deduction graphs, which are akin to derivations in a sequent calculus. GRA

N92-17207# Mitre Corp., Bedford, MA.
FY92 MATHEMATICAL RESEARCH PROJECT PROPOSAL BRIEFING
R. A. Games May 1991 28 p
(AD-A243163; M91-40) Avail: NTIS HC/MF A03 CSCL 12/1

Many areas in mathematics are directly applicable to MITRE's work program. Coding theory an psuedorandom sequences are important in resolving security issues. Graph theory is an indispensable tool in the design of very large scale integrated circuits and the analysis of parallel algorithms. The use of ideas from such diverse fields as number theory and harmonic analysis is commonplace in modern signal processing. Stochastic processes play a key role in communication theory. The Mathematical Research Project was established in 1982 in response to the growing need for mathematical sophistication within the corporation's work program. Project personnel support this need by conducting research in relevant areas of mathematics and by working directly with other projects in MITRE's work program. GRA

N92-17242# Naval Surface Warfare Center, Dahlgren, VA.
SIGNIFICANT DIGIT COMPUTATION OF THE ELLIPSOIDAL COVERAGE FUNCTION AND ITS INVERSE
Armido R. Didonato Sep. 1991 81 p
(AD-A242322; NAVSWC-TR-91-487) Avail: NTIS HC/MF A05
CSCL 12/3

An algorithm is given for evaluating the cumulative trivariate normal probability distribution function, also called the ellipsoidal coverage function, over an offset sphere. A Fortran subprogram, ELLCOV, supplies the function to at least six significant digits over a large range of the input parameters when the precision is not restricted by inherent error. Also, for a given value of the function, the radius R of the sphere with given center is found by the subroutine ELINV3 to at least six significant digits. Several new procedures are used. Listings of the transportable Fortran subprograms ELLCOV and ELINV3, with supporting routines, are included. GRA

N92-17330# Dayton Univ., OH. School of Engineering.
A THEORY OF INVERSE OPERATORS FOR MULTIPLE EXCITATIONS Final Technical Report, Sep. 1988 - Sep. 1989
Krishna M. Pasala Nov. 1991 44 p
(AD-A243484; UDR-TR-89-115; RL-TR-91-278) Avail: NTIS HC/MF A03 CSCL 12/2

In this report we consider the solution to integral equations that arise in the theory of electromagnetic scattering. We develop an interactive solution valid not for just one excitation but multiple excitations. We first consider a matrix equation obtained as a projection of the integral equation to finite dimensional space. After each iteration an orthogonal vector is determined and from it a corresponding component of the inverse operator. Thus, after each iteration a best estimate to the inverse operator is determined. This may be used to obtain the estimated solution to an arbitrary number of excitations. It is shown that the outer product of the vectors needs to be computed to compute the inverse operator. Since this is an expensive operation, an alternative approach is determined whereby solution to multiple excitations is determined without computing the outer products. This theory, developed in N-dimensional space, is then generalized to infinite dimensional space. This leads to a definition and a computational procedure for inverse integral operator. The theory is illustrated by computing the induced currents on a square cylinder for several excitations. GRA

N92-17445# Texas Univ., Austin.
REGULARIZATION AND APPROXIMATION OF A CLASS OF EVOLUTION PROBLEMS IN APPLIED MATHEMATICS Final Report
Ralph E. Showalter and Graham F. Carey 1991 96 p
(Contract N00014-89-J-1002)
(AD-A242223) Avail: NTIS HC/MF A05 CSCL 12/1

The major effort of this project has been the development of the foundations for regularization techniques related to conversation equations and some possibly far-reaching contributions to this area. The approach that has been taken is a departure from the usual artificial viscosity type of strategies which are produced on a somewhat adhoc basis. The basic strategy is to regularize locally by a micro-structured parabolic system. A mathematical analysis of the regularized equations has been developed to support our approach. Supporting approximate analysis and numerical experiments have been made. The development and the mathematical foundations of these microstructure models have been primary achievements of the project. The relevant nonlinear systems of partial differential equations have also shown to provide good models of diffusion or convection of fluid or gas through a heterogeneous porous medium. Examples include flow in fissured media, problems with adsorption, heat diffusion with freezing-melting, and models for semiconductors. We have established that the problems are well posed and developed the theory of the regularity and dependence of the solutions on data. Such information will aid approximation theory and the design of algorithms to numerically simulate solutions to these types of problems. GRA

N92-17517# Leiden Univ. (Netherlands). Div. of Applied Mathematics.
A NEW INTERPOLATION PROCEDURE FOR ADAPTING RUNGE-KUTTA METHODS TO DELAY DIFFERENTIAL EQUATIONS
K. J. intHout Apr. 1991 18 p
(TW-90-09; ETN-92-90562) Avail: NTIS HC/MF A03

The adaptation of Runge-Kutta methods to differential equations with a lagging argument is addressed. A new interpolation procedure which leads to numerical processes that satisfy an important stability condition with respect to a given test equation is introduced. A numerical illustration for two of these new processes, in comparison to a standard process is given. ESA

N92-17525# Technische Univ., Berlin (Germany, F.R.). Fachbereich Mathematik.
LARGE IDEALS AND NON-REGULAR ULTRAFILTERS Ph.D. Thesis
Markus Huberich 1991 73 p
(ETN-92-90587) Avail: NTIS HC/MF A04

The relative consistency of the existence of layered and centered ideals on small cardinals is proven assuming the existence of large cardinals. How many alpha additive, 0-1 valued measures over a small cardinal are needed, such that every subset of the cardinal is measurable in at least one of them, is described along with other information about the problem. Non regular ultrafilters are constructed using a general method, extending the filter from dual to dense or layered layers. ESA

N92-17560# Naval Ocean Systems Center, San Diego, CA.
PARALLEL BLOCK METHODS FOR SPARSE SYMMETRIC LINEAR SYSTEMS OF EQUATIONS Final Report, Oct. - Dec. 1990
A. K. Kevorkian Apr. 1991 40 p
(AD-A242315; NOSC-TR-1399) Avail: NTIS HC/MF A03
CSCL 12/1

In this work, we present a new graph-theoretic algorithm for the purpose of exploiting parallelism in the sparsity structure of large symmetric matrices. The key objectives of the algorithm are to identify full blocks in a symmetric matrix M that can be factored independently of each other and also to keep the number of fill elements generated in the process of factoring the blocks as small as possible. The graph-theoretic algorithm has a running-time proportional to the number of vertices and edges in an undirected graph, making the algorithm very suitable for extremely large sparse symmetric problems. Using this graph-theoretic algorithm, we develop a block method for the solution of sparse symmetric linear systems of equations. This block method takes full advantage of the parallel capabilities of high-performance computers and makes good use of the standard routines in the quality linear algebra library LAPACK to perform the numerical computations in terms of Level 2 and Level 3 Basic Linear Algebra Subprograms (BLAS) operations. There are many defense critical applications in the Navy in the areas of signal processing, structural mechanics, and computational hydrodynamics that give rise to large sparse symmetric matrices. We strongly recommend the implementation of the presented algorithms and their application to these problems. GRA

N92-17609# Nebraska Univ., Lincoln. Dept. of Computer Science and Engineering.
STUDY OF FEATURES OF BINARY IMAGES USING ALGEBRA TECHNIQUES Final Technical Report, 1 Dec. 1989 - 30 Nov. 1990
Prabir Bhattacharya 4 Apr. 1991 11 p
(Grant AF-AFOSR-0046-90)
(AD-A242010; AFOSR-91-0827TR) Avail: NTIS HC/MF A03
CSCL 12/9

The aim of this project was to investigate features of binary images by considering a special case of the image algebra methodology obtained by representing digitized images (both monochrome and colored) by certain polynomials in two variables with coefficients from the binary field. Since polynomials can be easily manipulated and our proposed operators can be described conveniently in terms of algebraic operations on these polynomials, this approach provides a significant foundation for practical applications which would be of significant interest to AFOSR. We have developed algebraic operators in the context of the polynomial approach to determine the contour, magnification, and shrinking and a sequence of approximations (from finer to coarser) of a binary image. Furthermore, we have extended our techniques to process gray images and perform operations such as template decomposition, shape decomposition, connected component labelling. Also, we have developed an algebraic system to process colored images. Also, we have developed some fast sequential and parallel thinning algorithms. We have also extended the polynomial approach to three dimensional by developing equivalents of the standard morphological operations and by applying these to do a number of operations for the understanding of three dimensional objects. GRA

N92-17622# Instituto de Fisica Teorica, Sao Paulo (Brazil).
INEQUALITIES AMONG PARTIAL TRACES OF HERMITIAN OPERATORS AND PARTIAL SUMS OF THEIR EIGENVALUES
J. Daboul 1990 11 p
(DE91-641495; IFT-P-36/90) Avail: NTIS HC/MF A03

Two different proofs of the following inequality are given: Tr(sup k)(H) := the summation of h sub i from i = 1 to k := the summation of ((x sub i), H(x sub i)) from i = 1 to k greater than or = the summation of epsilon sub i from i = 1 to k, for k = 1, 2, N, where H is a Hermitian matrix, the (x(sub i), i = 1, 2,..., k) are any k orthonormal vectors and the e sub i are the eigenvalues of H, ordered according to increasing values. This result is a generalization of the well-known fact that the ground state of a Hamiltonian is given by its lowest eigenvalue, E (sub i). It can also be regarded as a generalization, for Hermitian operators, of the invariance of the trace under unitary transformation. A few consequences of the above result are also derived. DOE

N92-17813# Joint Inst. for Nuclear Research, Dubna (USSR). Lab. of High Energy.
USE OF THE ALGEBRAIC CODING THEORY IN NUCLEAR ELECTRONICS
N. M. Nikityuk 1990 13 p
(DE92-611125; JINR-E-10-90-184) Avail: NTIS HC/MF A03

New results of studies of the development and use of the syndrome coding method in nuclear electronics are described. Two aspects of using the syndrome coding method are considered for sequential coding devices and for the creation of fast parallel data compression devices. Specific examples of the creation of time-to-digital converters based on circular counters are described. Several time intervals can be coded very fast and with a high resolution by means of these converters. The effective coding matrix can be used for light signal coding. The rule of constructing such coding matrices for arbitrary number of channels and multiplicity n is given. The methods for solving ambiguities in silicon detectors and for creating the special-purpose processors for high-energy spectrometers are given. DOE

N92-17939# International Centre for Theoretical Physics, Trieste (Italy).
SOME RESULTS FOR EXTENDED JACOBI POLYNOMIALS
I. A. Khan Jun. 1991 8 p
(DE92-609035; IC-91/132) Avail: NTIS HC/MF A02

In this paper, some contiguous function relations and generating functions have been established for extended Jacobi polynomials. The results obtained here, are of very general nature. DOE

65 STATISTICS AND PROBABILITY

Includes data sampling and smoothing; Monte Carlo method; and stochastic processes.

N92-16998# Massachusetts Inst. of Tech., Lexington. Lincoln Lab.
PERFORMANCE MEASURES FOR ADAPTIVE DECISIONING SYSTEMS
Robert Y. Levine and Timothy S. Khuon 11 Sep. 1991 29 p
(Contract F19628-90-C-0002)
(AD-A243183; MIT-TR-927; ESD-TR-91-094) Avail: NTIS HC/MF A03 CSCL 12/3

Performance measures are derived for data-adaptive hypothesis testing by systems trained on stochastic data. The measures consist of the average performance of the systems over an ensemble of training sets. The uncertainties derivable from training sets represents an irreducible uncertainty inherent in the learning procedure. Data-adaptive system estimates are contrasted with classical hypothesis testing, in which optimum tests are based on an assumed data model. In addition, a performance estimate for the maximum a posteriori probability (MAP) N-hypothesis test is derived based on a neural-net formulation of the test. The performance of adaptive systems on a binary test of uniformly distributed data is compared with the data-adaptive and MAP estimates. The adaptive systems considered are linear extrapolation from data (LINEXT) and a back-propagation neural net (BPNN). GRA

N92-17173# Stanford Univ., CA. Dept. of Statistics.
TESTS OF FIT FOR THE CAUCHY DISTRIBUTION BASED ON THE EMPIRICAL DISTRIBUTION FUNCTION
M. A. Stephens 2 Dec. 1991 19 p
(Contract N00014-89-J-1627)
(AD-A243201) Avail: NTIS HC/MF A03 CSCL 12/3

Points are given for testing goodness of fit to the Cauchy distribution, with unknown location and/or scale parameters. The tests are based on the empirical distribution function, and the asymptotic points round off work begun by Darling (1955) on the asymptotic theory of test statistics. Monte Carlo points are given for finite n and some discussion of power is included. GRA

N92-17178# Stanford Univ., CA. Dept. of Statistics.
GIBBS SAMPLING FOR MARGINAL POSTERIOR EXPECTATIONS
Alan E. Gelfand and Adrian F. Smith 19 Nov. 1991 26 p
(Contract N00014-89-J-1627)
(AD-A243212; SU-TR-448) Avail: NTIS HC/MF A03 CSCL 12/3

In earlier work, (Gelfand and Smith, 1990 and Gelfand et al, 1989) a sampling based approach using the Gibbs sampler was offered as a means for developing marginal posterior densities for a wide range of Bayesian problems several of which were previously inaccessible. Our purpose here is two-fold. First we flesh out the implementation of this approach for calculation of arbitrary expectations of interest. Secondly we offer comparison with perhaps the most prominent approach for calculating posterior expectations: analytic approximation involving application of the LaPlace method. Several illustrative examples are discussed as well. Clear advantages for the sampling based approach emerge. GRA

N92-17223# McDonnell Aircraft Co., Saint Louis, MO.
PRODUCT DEFINITION DATA INTERFACE (PDDI) TRANSLATOR USER'S MANUAL
Jeffrey Altemueller, Rick Helldoerfer, Charles Magnuson, and John Purses Dec. 1991 56 p
(Contract F33615-82-C-5036)
(AD-A243463; WL-TR-91-8035) Avail: NTIS HC/MF A04 CSCL 12/6

This document is the Translator User's Manual for the Product Definition Data Interface (PDDI) Extensions contract. This document provides procedures for using the PDDI Translator. Users Manual UM560130001 provides procedures for use of the PDDI Access Software. This User's Manual provides a guide for the use of software developed for the Product Definition Data Interface (PDDI) Project 5601. This User's Manual is divided into six (6) main sections: Scope, References, System Operations, Post-processing Procedures, Pre-processing Procedures, and Miscellaneous Notes and Exceptions. GRA

N92-17384# Ballistic Research Labs., Aberdeen Proving Ground, MD.
DATA FUSION FOR LEAST SQUARES Final Report, Jan. 1990 - Aug. 1991
Andrew A. Thompson, III Dec. 1991 41 p
(DA Proj. 1L1-62618-AH-80)
(AD-A243507; BRL-TR-3303) Avail: NTIS HC/MF A03 CSCL 12/3

The wide array of uses for least squares estimation testifies to its effectiveness. The key to structuring a problem for a least squares solution is finding a Markov representation of the problem. This representation defines a recursive approach to estimation. When multiple estimates are available at each time step, the processing time can be decreased by using data fusion networks to reduce the information to a single estimate. Hierarchical networks, using both parallel and serial combination of data, can be devised. The cases presented herein can be used to preprocess the for any recursive least squares method. GRA

N92-17440# Naval Postgraduate School, Monterey, CA. Dept. of Operations Research.
SOME FOUNDATIONS FOR EMPIRICAL STUDY IN THE EUCLIDEAN SPATIAL MODEL OF SOCIAL CHOICE
Craig A. Tovey Aug. 1991 34 p
(AD-A241928; NPSOR-91-025) Avail: NTIS HC/MF A03 CSCL 12/2

Recent results are surveyed, and some new results are given, that contribute towards a theoretical and computational basis for empirical study in the Euclidean spatial model. The results are of two types: asymptotic statistical consistency of sample estimators, and algorithmic methods for recovering spatial locations and computing various solution concepts. The new results are: the asymptotic consistency of the sample yolk center and epsilon-core; NP-completeness of the 1-dimensional spatial location recovery system; a modification of the Poole-Rosenthal heuristic for multidimensional recovery; and fast algorithms to compute Simpson-Cramer points and supermajority win sets in fixed dimension. GRA

N92-17455# Los Alamos National Lab., NM.
PERFORMANCE OF THE RAYLEIGH TASK BASED ON THE POSTERIOR PROBABILITY OF TOMOGRAPHIC RECONSTRUCTIONS
K. M. Hanson 1991 6 p Presented at the IEEE Nuclear Science Symposium, Santa Fe, NM, 5-9 Nov. 1991
(Contract W-7405-eng-36)
(DE92-003785; LA-UR-91-3688; CONF-911106-27) Avail: NTIS HC/MF A02

We seek the best possible performance of the Rayleigh task in which one must decide whether a perceived object is a pair of Gaussian-blurred points or a blurred line. Two Bayesian reconstruction algorithms are used, the first based on a Gaussian prior-probability distribution with a nonnegativity constraint and the second based on an entropic prior. In both cases, the reconstructions are found that maximize the posterior probability. We compare the performance of the Rayleigh task obtained with two decision variables, the logarithm of the posterior probability ratio and the change in the mean-squared deviation from the reconstruction. The method of evaluation is based on the results of a numerical testing procedure in which the stated discrimination task is carried out on reconstructions of a randomly generated sequence of images. The ability to perform the Rayleigh task is summarized in terms of a discrimination index that is derived from the area under the receiver-operating characteristic (ROC) curve. We find that the use of the posterior probability does not result in

better performance of the Rayleigh task than the mean squared deviation from the reconstruction. DOE

N92-17643# Naval Postgraduate School, Monterey, CA. Dept. of Operations Research.
BAYESIAN COMPUTATIONS IN SURVIVAL MODELS VIA THE GIBBS SAMPLER
Lynn Kuo and Adrian F. Smith Jul. 1991 26 p
(AD-A242343; NPSOR-91-020) Avail: NTIS HC/MF A03
CSCL 12/3

Survival models used in biomedical and reliability contexts typically involve data censoring and may also involve constraints in the form of ordered parameters. In addition, inferential interest often focuses on nonlinear functions of natural model parameters. From a Bayesian statistical analysis perspective, these features combine to create difficult computational problems by seeming to require (multi-dimensional) numerical integrals over awkwardly defined regions. This paper illustrates how these apparent difficulties can be overcome, in both parametric and non-parametric settings, by the Gibbs sampler approach to Bayesian computation. GRA

N92-17837# Leiden Univ. (Netherlands). Div. of Applied Mathematics.
MARKED POINT PROCESSES AS LIMITS OF MARKOVIAN ARRIVAL STREAMS
Soeren Asmussen (Aalborg Univ., Denmark) and Ger Koole 1991 8 p
(TW-91-04; ETN-92-90560) Avail: NTIS HC/MF A02

A Markovian arrival stream is a marked point process generated by the state transitions of a given Markovian environmental process and Poisson arrival rates depending on the environment. It is shown that to a given marked point process N there is a sequence N(sup m) of such Markovian arrival streams with the property that N(sup m) approaches (D) towards N as m approaches infinity. Various related corollaries (involving stationarity, convergence of moments, and ergodicity) and counterexamples are discussed. ESA

N92-18002*# Princeton Univ., NJ. Dept. of Mechanical and Aerospace Engineering.
TECHNICAL NOTES AND CORRESPONDENCE: STOCHASTIC ROBUSTNESS OF LINEAR TIME-INVARIANT CONTROL SYSTEMS
Robert F. Stengel and Laura R. Ray *In* NASA. Langley Research Center, Joint University Program for Air Transportation Research, 1990-1991 Dec. 1991 p 181-186 (For primary document see N92-17984 08-01)
(Grant NGL-31-001-252)
Avail: NTIS HC/MF A09 CSCL 12A

66 SYSTEMS ANALYSIS

Includes mathematical modeling; network analysis; and operations research.

N92-17479# Air Force Inst. of Tech., Wright-Patterson AFB, OH. School of Engineering.
PRELIMINARY DESIGN OF A MODEL TO ASSESS THE EFFECT OF SPACE SURVEILLANCE NETWORK (SSN) SENSOR UPGRADES ON ORBIT PREDICTION ACCURACIES RELATIVE TO THE US ANTI-SATELLITE (ASAT) MISSION M.S. Thesis
Daniel L. OBrien Dec. 1991 81 p
(AD-A243736; AFIT/GSO/ENS/ENY/91D-14) Avail: NTIS HC/MF A05 CSCL 17/11

This study gives a basis for implementation of a model to assess the effect of proposed sensor upgrades to the Space Surveillance Network (SSN) to determine if more accurate orbital element set predictions by the Space Surveillance Center (SSC) can be obtained for US anti-satellite (ASAT) targeting. Handoff orbital element set predictions to nearby ASAT facilities for single, low-orbit satellite passes over a single radar sensor are considered. Model development began with simulation of the selected satellites passing over the selected sensors producing baseline truth observations based on the NORAD Simplified General Publications (SGP4) Model. Sensor errors, in the form of biases and standard deviations, were then factored into the model to produce representative sensor observations from the baseline truth observations. A detailed statistical analysis was performed, utilizing experimental design techniques, to allow for follow-on model development to input the representative observations into a differential correction process to produce predicted orbits. GRA

N92-17839# Technische Univ., Eindhoven (Netherlands).
MACHINE SCHEDULING AND LAGRANGIAN RELAXATION Ph.D. Thesis
Steven Leendert vandeVelde 1991 145 p
(ETN-92-90569) Avail: NTIS HC/MF A07

The application of Lagrangian relaxation and duality to machine scheduling problems is addressed. The problems discussed include those of single machine, flow shop, and parallel machine. This discussion involves different aspects of assignment, partitioning, sequencing, and scheduling problems. Scheduling has become an important area of operations research because of the practical relevance of production planning and computer scheduling problems. Lagrangian relaxation is suggested as having much to offer machine scheduling theory. Basic concepts and issues involved in its application, focusing on machine scheduling problems, are introduced. The literature on Lagrangian relaxation applied to machine scheduling problems is reviewed and objectives of the study described. The following are considered: Lagrangian relaxation and duality for single machine problems that can be formulated in terms of the job completion times in the two machine flow-shop; minimizing the makespan on unrelated parallel machines; a single machine problem where the jobs have a common due date; and the single machine scheduling problem of minimizing total inventory cost. ESA

67 THEORETICAL MATHEMATICS

Includes topology and number theory.

N92-17318# International Centre for Theoretical Physics, Trieste (Italy).
GAUGE-COVARIANT WESS-ZUMINO ACTIONS FOR SUPER p-BRANES IN SUPERSPACE
E. A. Ivanov (Joint Inst. for Nuclear Research, Dubna, USSR) and A. A. Kapustnikov Dec. 1990 20 p
(DE91-641524; IC-90/425) Avail: NTIS HC/MF A03

We present a general method of constructing manifestly world-volume supersymmetric actions of super p-branes, starting from some higher-dimensional field theories in which the partial breaking of global supersymmetry (PBGS) comes about. Our approach is based upon a substitution of the superspace coordinates which relates linear and nonlinear realizations of PBGS. As instructive examples we consider the massive $d = 2$ superparticle ($p = 0$) and $d = 4$ superstring ($p = 1$). The relevant world-line and world-sheet superfield actions naturally appear as a long-wavelength limit of the superfield actions of some two- and four-dimensional supersymmetric field theories possessing topologically nontrivial soliton solutions. The corresponding topological charges prove to enter the super p-brane actions as the coupling constants. We also give a new general Wess-Zumino-type representation of the $d = 2$ superparticle action via the world-line superfields. It respects invariances both under the target space Poincare supersymmetry and the gauge group of general reparametrizations of the world-line superspace. In one gauge it is reduced to the standard PBGS form while in another it gives rise to a very simple action which displays manifest world-line superconformal symmetry and is directly related to the familiar component action of the superparticle. The fermionic k-symmetry of the latter can be identified with the odd sector of superconformal

symmetry. This identity suggests a simple recipe for building higher-order k-invariant corrections to the minimal superparticle action. DOE

N92-17803# International Centre for Theoretical Physics, Trieste (Italy).
A GNS-TYPE THEOREM FOR A NON-INVOLUTIVE BANACH ALGEBRA
E. Desquith Feb. 1991 22 p
(DE91-641481; IC-91/19) Avail: NTIS HC/MF A03

Given an involutive Banach algebra A with a bounded approximate identity, the elegant construction by Gelfand, Naimark and Segal, associates to each positive linear functional f on A, a triple (H(sub f), pi(sub f), xi(sub f)), where H(sub f) is a Hilbert space with scalar product denoted by: /. , ./, pi(sub f) is a representation of A into L(H(sub f)), the space of bounded linear operators on H(sub f), xi(sub f) is a cyclic vector in H(sub f), such that: f(x) = /pi(sub f) (x) xi(sub f), xi(sub f)/, for all x is an element of A. In this result, the existence of a (multiplicative) involution on A, is central. The aim of this paper is to show that such a construction may be performed for a non-involutive Banach algebra, to obtain a similar triple (H, omega, xi) as above. Moreover, this procedure indeed enables us to associate to the topological dual of any Banach space, a liminary C*-subalgebra of L(H). A notion of compact Hilbert algebras will be introduced, together with a method of construction of a large collection of such spaces. DOE

N92-17804# International Centre for Theoretical Physics, Trieste (Italy).
TOPOLOGICAL DUALS OF BANACH SPACES AS BANACH ALGEBRAS AND APPLICATIONS
E. Desquith Jan. 1991 26 p
(DE91-641482; IC-91/2) Avail: NTIS HC/MF A03

Banach algebra structures on the topological dual X* of a Banach space X are defined, and some algebraic and topological properties of such Banach algebras are studied. In this paper, on the second dual space X** of a Banach space X, different products, each of which turns X** into an associative Banach algebra which satisfies similar properties are also defined. DOE

N92-17823# International Centre for Theoretical Physics, Trieste (Italy).
CHAOS CAUSED BY A TOPOLOGICALLY MIXING MAP
Jincheng Xiong and Zhongguo Yang Jan. 1991 22 p
(DE91-641486; IC-91/7) Avail: NTIS HC/MF A03

In the present paper we show that for a topologically mixing map there exists a subset consisting of considerably many points in its domain, called chaotic subset, for which orbits of all points display time dependence greatly more erratic than for a scrambled subset, i.e., if a continuous map f : X approaches X is topologically mixing, where X is a separable locally compact metric space containing at least two points, then for any increasing sequence (p(sub i)) of positive integers there exists a c-dense subset C of X satisfying the condition for any continuous map F : A approaches X, where A is a subset of C, there is a subsequence (q(sub i)) of the sequence (p(sub i)) such that limits(i approaches infinity) f(sup qi)(x) = F(x) for every x is an element of A. As an application we show that the interval maps having a chaotic (or scrambled) subset with full Lebesgue measure is dense in the space consisting of all topologically mixing (transitive, respectively) maps. DOE

70 PHYSICS (GENERAL)

For precision time and time interval (PTTI) see *35 Instrumentation and Photography;* for geophysics, astrophysics or solar physics see *46 Geophysics, 90 Astrophysics,* or *92 Solar Physics.*

N92-17548# Naval Postgraduate School, Monterey, CA.
A PROBABILISTIC DERIVATION OF STIRLING'S FORMULA
M.S. Thesis
Hsin-Yun Li Mar. 1991 48 p
(AD-A241899) Avail: NTIS HC/MF A03 CSCL 12/1

Stirling's formula is one of the most frequently used results from asymptotics. It is used in probability and statistics, algorithm analysis and physics. In this thesis, we shall give a new probabilistic derivation of Stirling's formula. Our motivation comes from sampling randomly with replacement from a group of n distinct alternatives. Usually a repetition will occur before we obtain all n distinct alternatives consecutively. We shall show that Stirling's formula can be derived and interpreted as follows: as n approaches infinity the expected total number of distinct alternatives we must sample before all n are obtained consecutively is asymptotically equal to the expected number of attempts we make to obtain all n distinct alternatives consecutively times the expected number of distinct alternatives obtained per attempt. GRA

N92-17811# Joint Inst. for Nuclear Research, Dubna (USSR). Lab. of Computing Techniques and Automation.
ON THE NONADIABATIC THEORY OF CHARGED PARTICLES MOTION IN THE MAGNETIC DIPOLE FIELD
I. V. Amirkhanov, E. P. Zhidkov, A. N. Ilina, V. D. Ilin, and B. Yu. Yushkov (Moscow State Univ., USSR) 1990 10 p In RUSSIAN; ENGLISH summary
(DE92-610951; JINR-R-9-90-154) Avail: NTIS HC/MF A02

The question of a nonadiabatic model of particle motion in the dipole field is considered. By applying the concepts of the leading line, the magnetic moment and the loss cone, an analogy to traditional ideas of the adiabatic motion theory for trapped particles of high energy is determined through numerical experiment. DOE

71 ACOUSTICS

Includes sound generation, transmission and attenuation. For noise pollution see *45 Environmental Pollution.*

N92-16999# Naval Postgraduate School, Monterey, CA.
ACOUSTIC IMPEDANCE OF MATERIALS FROM REVERBERATION TIME M.S. Thesis
Antonio J. Carocho Dec. 1991 27 p
(AD-A243184) Avail: NTIS HC/MF A03 CSCL 20/1

The design of coating materials that reduce the reflection of water borne sound is an important problem in underwater acoustics. Since it is difficult to theoretically predict the complex reflection coefficient of such a material, the reflection properties must be determined experimentally. At high frequencies it is possible to measure the reflection coefficient of a slab of material by measuring the pressure after reflection of a narrow beam of sound incident at a given angle. However, this method becomes more difficult to use as the frequency of the sound is lowered. Determining the acoustic impedance of a material by measuring the standing wave pattern in an impedance tube, while the standard procedure in air borne sound, is very difficult for water borne sound, because of the impossibility of approaching rigid conditions for the tube walls. Therefore it is attractive to investigate the possibility of determining the acoustic impedance of a material from measurements of the reverberation time in a water filled cavity with walls lined with the material. GRA

N92-17086# Washington Univ., Seattle. Applied Physics Lab.
THE APPLIED TOMOGRAPHY EXPERIMENT OF 1990 Technical Report, Mar. - Sep. 1990
28 Feb. 1991 118 p
(Contract N00039-88-C-0054)
(AD-A243525; APL-UW-TR-9106) Avail: NTIS HC/MF A06 CSCL 17/1

The feasibility of an operational tomography capability has been demonstrated. Daily inversions of acoustic travel time data produced sound speed profiles that were successfully integrated into the standard Navy operational product for the NW Atlantic. Improved estimates of the sound speed (and thus temperature)

reduced the error variance approximately 20 percent along the source-receiver vector. The resultant temperature fields, produced on a daily basis, have been reformulated as synthetic bathythermographs for input to the Optimal Thermal Interpolation System at the Fleet Numerical Oceanography Center. Sound speed fields based on tomographic results change predicted convergence zone ranges by about 10 km, corresponding changes in local acoustic intensity of 10 with dB or greater. In addition, acoustic transmissions from Bermuda through the Gulf Stream were used to estimate the position of the Gulf Stream in real time. The precision (using air-dropped expendable bathythermograph (AXBT) data as ground truth) is better than 10 km under certain circumstances. This information can be used by the Operational Oceanography Center to improve estimates of Gulf Stream frontal location, which are presently based on IR satellite images. The transmissions from Bermuda northward are continuing. The deployment of six acoustic sources south of Bermuda in 1991 will improve the horizontal resolution. GRA

N92-17236# Washington Univ., Seattle. Applied Physics Lab.
ACOUSTIC SIMULATION FOR ACOUSTICS EDUCATION Final Report
John C. Harlett 1991 1 p
(Contract N00014-90-J-4146)
(AD-A243027) Avail: NTIS HC/MF A01 CSCL 12/5

The purpose of this grant was to purchase hardware and software for computer simulation of sound transmission through the ocean. The system is to be used for class demonstrations and laboratory problem sessions in support of courses in ocean acoustics. A PESOGEN-II system and supporting software were purchased from Daubin Systems Corporation. (Approximately $7000 of APL matching funds were added to the ONR grant.) The system has been received and is mounted on a cart for portability. The system has been used for approximately two months to support the M.S. research project of LCDR Roger Rose, a student in the UW Physics Department. Current plans are for the system to be utilized in a course entitled Ocean Acoustic Tomography to be taught in Winter 1992 by Dr. Bruce Howe. GRA

N92-17381# California Univ., Irvine. Dept. of Cognitive Sciences.
CLASSIFICATION OF COMPLEX SOUNDS Annual Report, 1 Nov. 1990 - 30 Oct. 1991
Bruce G. Berg 30 Oct. 1991 10 p
(Contract N00014-91-J-1122)
(AD-A243498) Avail: NTIS HC/MF A02 CSCL 20/1

The work accomplished during the period, 11/1/90 - 10/30/91, involves the use of COSS analysis to estimate weights in various profile analysis tasks. This technique is a method for investigating how spectral information is used by listeners to discriminate complex sounds. A profile type task is essentially an empirical method for investigating how spectral information from different auditory channels is used to discriminate complex sounds. In a typical profile task, the standard consists of n tones of equal intensity and the signal consists of an increment in the intensity of a single tone complex. Since overall level is varied randomly on each stimulus presentation (over a range of 20 dB or greater), absolute intensity is not a useful cue. The first set of experiments examined listeners abilities to discriminate a flat spectrum (eight tones of equal intensity) from a 'rippled' spectra (consisting of a pattern of intensity changes across the entire spectrum). GRA

N92-17488# Sonoquest/Advanced Ultrasonics Research, Wellesley Hills, MA.
ULTRASONIC STUDIES OF TRANSIENT SEISMO-ACOUSTIC WAVES IN BOUNDED SOLIDS AND LIQUID/SOLID INTERFACES Final Report, Apr. 1990 - Oct. 1991
Jacques R. Chamuel Nov. 1991 56 p
(Contract N00014-90-C-0072)
(AD-A243441; JRC-34-91) Avail: NTIS HC/MF A04 CSCL 20/1

This report summarizes a collection of laboratory ultrasonic modeling findings on transient liquid/solid seismo-acoustic wave phenomena. The topics covered include: (1) horizontal refraction of flexural waves by trapped gas pockets underneath floating plate; (2) wide angle remote generation of broadband transient Scholte waves at liquid/solid interfaces from conversion of underwater acoustic waves by abrupt liquid discontinuities, steep topographic features, and adjacent immersed elastic solids; (3) characteristics of multiple transient leaky Rayleigh wave components in shallow water; (4) effect of water loading on edge waves along apex of immersed acute angle solid wedge; and (5) group velocity of medium frequency transient longitudinal waves in thick elastic waveguides. The findings pertain to Arctic underwater acoustics, ice mechanics, geophysical exploration, material characterization, nondestructive testing, and acoustic sensors. GRA

N92-17502# Wisconsin Univ., Milwaukee. Dept. of Psychology.
MECHANISMS MEDIATING THE PERCEPTION OF COMPLEX ACOUSTIC PATTERNS Final Report, 1 Sep. 1988 - 30 Sep. 1991
Richard M. Warren 18 Nov. 1991 21 p
(Grant AF-AFOSR-0320-88; AF Proj. 2313)
(AD-A243715; AFOSR-91-0989TR) Avail: NTIS HC/MF A03 CSCL 20/1

Many sounds of ecological importance consist of complex acoustic patterns, and the research conducted during the previous grant has dealt with some of the rules and mechanisms governing the perception of such sounds. Using randomly derived waveforms (frozen noise segments) as model long period complex sounds, a series of experiments examined aspects of the stimuli used for recognition, and tested hypotheses concerning the basic principles governing the perception of these sounds. New evidence was reported indicating that sequences of brief tones and brief vowels are perceived as global patterns or temporal compounds. Different arrangements of component sounds form distinctive compounds, so that permuted orders can be discriminated without resolution into component elements. The same basic rules govern the perception of frozen noises, sequences of tones, and sequences of vowels, with overlays of special rules for melodic and phonetic sequences. GRA

N92-17506# Army Construction Engineering Research Lab., Champaign, IL.
HUMAN RESPONSE TO HELICOPTER NOISE: A TEST OF A-WEIGHTING Final Report
Paul D. Schomer, Brian D. Hoover, and Lee R. Wagner Nov. 1991 89 p
(AD-A243719; CERL-TR-N-91/13) Avail: NTIS HC/MF A05 CSCL 01/3

Department of Defense and U.S. Army policy has long been to adjust measured helicopter noise levels upwards to account for the special character of helicopter noise in terms of human and community annoyance. In the United States, the A-weighted Day/Night Average Sound Level (DNL) descriptor is used most often for this purpose, but research has shown that it is not completely adequate. Also, many questions remain about human perception of, and response to, helicopter noise. This study is an extension of earlier research that tested human response to the noise of an Army UH-1H (Huey) helicopter flown over various indoor environments. This report documents a follow-up test using six different helicopters to replicate and expand on the earlier study. The data generally indicate that the A-weighted DNL is inadequate for assessing helicopter noise. The C-weighted scale was also tried and found inadequate. Helicopter noise measurement by either scale must be corrected to accurately correspond to human perceptions. Measuring indoors, the use of A-weighting to assess helicopter noise requires an offset that varies with helicopter A-weighted sound exposure level (ASEL), and this offset varies for different helicopters. GRA

N92-17692*# Wisconsin Univ., Madison.
PSYCHOPHYSICAL EVALUATION OF THREE-DIMENSIONAL AUDITORY DISPLAYS Semiannual Progress Report, 1 May - 1 Nov. 1991
Frederic L. Wightman 1991 25 p

(Contract NCC2-542)
(NASA-CR-189848; NAS 1.26:189848) Avail: NTIS HC/MF A03 CSCL 20A

Work during this reporting period included the completion of our research on the use of principal components analysis (PCA) to model the acoustical head related transfer functions (HRTFs) that are used to synthesize virtual sources for three dimensional auditory displays. In addition, a series of studies was initiated on the perceptual errors made by listeners when localizing free-field and virtual sources. Previous research has revealed that under certain conditions these perceptual errors, often called 'confusions' or 'reversals', are both large and frequent, thus seriously comprising the utility of a 3-D virtual auditory display. The long-range goal of our work in this area is to elucidate the sources of the confusions and to develop signal-processing strategies to reduce or eliminate them. Author

72 ATOMIC AND MOLECULAR PHYSICS

Includes atomic structure, electron properties, and molecular spectra.

N92-17026# Vanderbilt Univ., Nashville, TN. Center for Atomic and Molecular Physics at Surfaces.

ELECTRONIC INTERACTIONS OF DIRECTED PHOTON BEAMS WITH SURFACES Final Report, 1 Jun. 1988 - 31 Aug. 1990

Alan V. Barnes, Marcus Mendenhall, and Norman H. Tolk 25 Sep. 1991 17 p

(Contract F49620-88-C-0080)
(AD-A241878; Rept-4-20-630-4183) Avail: NTIS HC/MF A03 CSCL 07/4

The object of this research program is to investigate the fundamental dynamics of energy-surface interactions, with emphasis on the ways in which the energy deposited by incident UV photons and electrons lead to surface bond-breaking phenomena, to fluorescence, and to modification of surfaces and near-surface layers of bulk materials. Optical radiation may arise from electronic excitations in the near surface bulk or from excited atoms and molecules emitted from the surface. Our studies of electronically-induced desorption have shown that a significant fraction of the incident energy may be channeled into bond-breaking and desorption processes leading to ejection of excited neutral atoms and molecules from metal oxide and insulator surfaces which subsequently decay to produce optical radiation in the visible, UV or IR. Here, we report on photo-stimulated desorption of excited alkali atoms following irradiation of alkali halide crystals with ultraviolet light and on optical fluorescence arising from surfaces using an electron beam at room- and at cryo-temperatures under different gas dosing environments. GRA

N92-17038# New Orleans Univ., LA. Dept. of Chemistry.

COMPUTATIONAL STUDIES OF ENERGETIC NITRAMINES Final Report, 1 Jul. 1985 - 31 Jun. 1991

Peter Politzer 11 Sep. 1991 40 p

(Contract N00014-85-K-0217)
(AD-A241870) Avail: NTIS HC/MF A03 CSCL 21/8

This final report summarizes our computational investigations of energetic materials carried out over a six-year period. It is divided into seven main sections, describing the major themes of this project. First, factors important in designing molecules with high specific impulse values and in determining the sensitivities of energetic systems are discussed, followed by a review of our analysis of reaction energetics (carried out primarily using a local density functional approach). Next, studies aimed at providing insight into possible synthetic routes are summarized, followed by a section on fundamental molecular properties of nitramines. Surface electrostatic potentials of the four known CL-20 polymorphs show significant differences in their tendencies for intermolecular interactions. We have calculated structures and reactive properties for a variety of new energetic materials, including heterocyclic, ionic, mesoionic and zwitterionic systems. We have shown that correlations exist between key calculated properties (the electrostatic potential V(r) and the average local ionization energy I(r)) and a number of experimentally-based indices of reactivity. GRA

N92-17196# International Business Machines Corp., San Jose, CA.

DETECTION AND SPECTROSCOPY OF SINGLE PENTACENE MOLECULES IN A P-TERPHENYL CRYSTAL BY MEANS OF FLUORESCENCE EXCITATION Interim Technical Report

W. P. Ambrose, T. Basche, and W. E. Moerner 22 Jul. 1991 54 p

(Contract N00014-91-C-0166)
(AD-A243747; IBM-RJ8248; TR-35) Avail: NTIS HC/MF A04 CSCL 20/5

Recent advances in fluorescence excitation spectroscopy with high efficiency have produced greatly improved optical spectra for the first electronic transition of individual single molecules of pentacene in p-terphenyl crystals at low temperatures (1.5 to 10 K). Two classes of single molecules behavior are observed: class 1 molecules have time independent resonance frequencies, and class 2 molecules show a diffusive motion among several resonant frequencies with time, which we term spectral diffusion by analogy with a similar effect which is common in amorphous materials. The temperature dependence of the linewidth and power dependence of the fluorescence emission rate and of the linewidth are reported and analyzed. Various forms of the surprising class 2 behavior are described, including jumping among several discrete frequencies, creeping toward the center of the inhomogeneous line in many small steps, and a wandering among many possible resonance frequencies. The occurrence of class 2 behavior is restricted to the wings of the inhomogeneous line suggesting that the effect is correlated with some form of local disorder. GRA

N92-17197# International Business Machines Corp., San Jose, CA.

SINGLE MOLECULE SPECTRAL DIFFUSION IN A SOLID DETECTED VIA FLUORESCENCE SPECTROSCOPY Interim Technical Report

W. P. Ambrose, T. Basche, and W. E. Moerner 15 Oct. 1991 19 p

(Contract N00014-91-C-0166)
(AD-A243748; IBM-RJ8411; TR-34) Avail: NTIS HC/MF A03 CSCL 20/5

Recent advances in fluorescence excitation spectroscopy have produced significant increases in detection sensitivity for single performance molecules in crystals of p-terphenyl at low temperatures. With the increased signal to noise ratio, we have observed two classes of pentacene behavior. While some pentacene defects have fixed, lifetime limited Lorentzian excitation line shapes (7.8 MHz FWHM), other pentacene defects exhibit spontaneous shifts in resonance frequency of up to 100 MHz. Residence times between spectral jumps are on the order of seconds to minutes at 1.5 K. Increasing the temperature from 1.5 to 6 K appears to produce a faster-than-linear increase in jump rate with temperature; we suggest single pentacene defect spectral diffusion is due to thermally assisted structural changes in the p-terphenyl environment. GRA

N92-17305# Air Force Inst. of Tech., Wright-Patterson AFB, OH. School of Engineering.

COLLISIONAL DYNAMICS OF THE B3Pi(O+) STATE OF BROMINE OF MONOFLUORIDE Ph.D. Thesis

David W. Melton Aug. 1991 169 p

(AD-A241857; AFIT/DS/ENP/91-01) Avail: NTIS HC/MF A08 CSCL 07/4

When Bromine is combined with flourine atoms and discharged oxygen in a flow tube, BrF B3 pi(O+) is produced in a highly non-thermal distribution peaking at v'=3. The emission was linearly dependent on the concentration. The observed dependence of the BrF(B) emission on Bromine and atomic oxygen is inconsistent with a steady state prediction of a sequential excitation mechanism, where BrF(X) is excited by successive collisions with singlet oxygen.

The experimental data are consistent with a three body mechanism involving Br and F atoms. Electronic quenching of BrF(B) by a number of collision partners (Br2, CO2, O2, N2, CF4, SF6, Ar) was examined for three vibrational levels using laser induced fluorescence (LIF) techniques. Vibrational transfer in BrF(B), induced by the BrF production mix (CF4, Br2, F) was measured by observing the spectrally resolved LIF emission from each vibrational level after an initial excitation of BrF(B) v'=5. GRA

N92-17306# Naval Postgraduate School, Monterey, CA.
MEASUREMENT OF ELECTRON BEAM EMITTANCE USING OPTICAL TRANSITION RADIATION AND DEVELOPMENT OF A DIFFUSE SCREEN ELECTRON BEAM MONITOR M.S. Thesis
Carlton B. Reid, Jr. Dec. 1990 118 p
(AD-A241893) Avail: NTIS HC/MF A06 CSCL 20/7

An experimental technique for measuring electron beam emittance using Optical Transition Radiation (OTR) with the Wartski Interferometer Method has been applied to the Naval Postgraduate School linear electron accelerator. Data for obtaining the emittance of the NPS linac has been collected. A chronology of the procedure for using OTR as a beam diagnostic at the NPS Linac is described in detail. A novel OTR beam monitor consisting of a surface purposely made diffuse was also developed and proved to be an excellent profile monitor. It can be used to measure the shape of the electron beam incident on a vacuum/metal interface over a viewing angle range of +/-30 degrees. Beam current and profile measurements using the diffuse screen were compared with measurements using a front surface mirror and a fluorescent screen. The diffuse screen demonstrated a linear response to current while the fluorescent screen showed an exponential response. The OTR produced the beam incident on the diffuse screen and accurately reflected the shape of the electron beam while the secondary electron effects of the fluorescent screen distorted the image. GRA

N92-17321# Air Force Inst. of Tech., Wright-Patterson AFB, OH. School of Engineering.
QUENCHING AND ROTATIONAL ENERGY TRANSFER IN MOLECULAR BROMINE: Br2(B) M.S. Thesis
Dean A. Massman May 1991 106 p
(AD-A241987; AFIT/GEP/ENP/91J-1) Avail: NTIS HC/MF A06 CSCL 07/4

This study investigates the rotational energy transfer processes of optically excited bromine molecules in the presence of several collision partners. Resolved laser induced fluorescence spectra of collisionally populated rotational states were analyzed by means of Stern Volmer analysis. Total rotational removal rate coefficients and state-to-state rotational removal rate coefficients for the v' = 11, J' = 35 level of Br2(B) were obtained for collisions with Br2(X), He, Ar, and Xe. Rotational removal rate coefficients were also obtained for the v' = 11, J' = 26 and 47; v' = 14, J' = 36 states of Br2(B) with collisions with Ar. Total rotational removal rate for Br2 self quenching found to be 3.98 +/- 0.2 x 10 exp -10 (cc/molec-sec). Rate coefficients were scaled with respect to reduced mass of collision system and in accordance with exponential energy gap scaling law. Energy gap scaling law fit data well. Rotational removal rates displayed behavior to increase with increase in v' and J' of optically excited parent state. GRA

N92-17374# Massachusetts Inst. of Tech., Cambridge. Research Lab. of Electronics.
ATOM WAVE INTERFEROMETER Final Report, 1 Dec. 1988 - 30 Nov. 1991
David E. Pritchard 11 Dec. 1991 5 p
(Contract N00014-89-J-1207)
(AD-A243482) Avail: NTIS HC/MF A01 CSCL 20/5

The biggest accomplishment during the current grant period was the demonstration of a three grating interferometer for atoms--the first true atom interferometer reported in the literature. Our interferometer consists of three equally spaced transmission diffraction gratings which function respectively much like the beam splitter, mirrors, and beam combiner in a diamond shaped Mach-Zender interferometer. This is a well known design whose general advantages have been eloquently extolled and which has been demonstrated with light, neutrons and x rays. For atoms it can be realized either with matter (amplitude transmission) gratings or light (phase) gratings, but we elected to pursue the use of the more robust matter gratings. Our matter grating interferometer differs from most optical and neutron interferometers in that the interference is detected as a spatial variation of particle density at the third grating. GRA

N92-17394# Harry Diamond Labs., Adelphi, MD.
A PC PROGRAM TO CALCULATE THE ONE-SIDED LOWER TOLERANCE LIMIT FOR TOTAL IONIZING DOSE RADIATION DATA Final Report, Sep. 1990 - Jan. 1991
Ahmed A. Abou-Auf and Mark E. Bumbaugh Aug. 1991 60 p
(AD-A242365; HDL-TM-91-12) Avail: NTIS HC/MF A04 CSCL 18/6

The radiation level of a semiconductor part type can be found to be just above the level needed for survivability. Many times the part has to be accepted or rejected lot to lot (lot qualification) on the basis of radiation data from small a sample of the lot. One-sided lower tolerance limit statistics is used on the radiation data to determine lot acceptance or rejection. An IBM-compatible PC program, written to calculate the one-sided lower tolerance limit at 90 to 50 percent confidence for log-normally distributed radiation data (the usual distribution for semiconductor radiation data), is described in this report. The analysis results can be displayed in tabular and graphical form on the PC screen and a hard copy made on the printer. GRA

N92-17408# Joint Inst. for Nuclear Research, Dubna (USSR). Lab. of High Energy.
WHAT EXPERIMENTS SAY ABOUT POSSIBILITY OF THE NEW PARTICLE EXISTENCE WITH MASS LESS THAN THE KAON MASS
L. V. Silvestrov and G. G. Takhtamyshev 1989 22 p
(DE91-634551; JINR-R-1-89-452) Avail: NTIS HC/MF A03

Analysis of data obtained in two K(sub L)-decays experiments and five e(+)e(-) and mu(+)mu(-) (l(+)l(-) pairs) prompt production experiments indicates an anomalous l(+)l(-) pairs production which could not be explained by the known dilepton sources. The anomalous pairs masses are limited by the value M(ll) less than or = 0.38-0.42 GeV/c. The model of these pairs formation is proposed over the intermediate neutral particle k(sup 0) with the mass about 0.4 GeV/c(sup 2) and the k(sup 0) yields l(+)l(-)n(sup 0) decay where n(sup 0) is the light unregistered neutral particle. The K(sub L)-meson decays with the formation of the anomalous pairs can be written down as K(sub L) yields k(sup 0)n(sup 0). The fraction of the decay mode as the average for two experiments is equal to (3.8 +/- 1.1) x 10(exp -3). The anomalous l(+)l(-) pairs formation in hadronic collisions is possible over the inclusive h + h yields k(sup 0) + ... process. The cross section of this process is approx. = 10 (mu)b. The ratio of this value to the average inclusive production cross section of the nearest mass mesons K, eta, rho, omega is equal to (4.1 +/- 1.4) x 10(exp -3). DOE

N92-17423# Washington State Univ., Pullman. Dept. of Chemistry.
OPTICAL NONLINEARITY IN COUPLED EXCITON-PHONON SYSTEMS NEAR METAL SURFACES
X. Li, D. L. Lin, and Thomas F. George Oct. 1991 14 p
(Contract N00014-90-J-1193)
(AD-A242362; WSU/DC/91/TR-66) Avail: NTIS HC/MF A03 CSCL 20/6

Surface effects on optical bistability and pump-probe processes for coupled exciton-phonon systems are studied theoretically. When a laser beam is directed on an exciton-phonon coupling system inside an optical cavity, the cavity field intensity is investigated as a function of the driving field intensity for various distances between the sample and a metallic surface representing one of the mirrors of the cavity. It is found that the direction of switch of the optical bistability can be controlled by adjusting the distance from the surface. For a strong laser pump field and a weak probe field

directed on this system, the pump-field-induced absorption spectrum is investigated for different distances between this sample and the metal surface. It is found that the position and line shape of the spectrum are significantly changed due to the presence of the surface. GRA

N92-17428# Harvard Univ., Cambridge, MA. Dept. of Chemistry.
MOLECULAR RECOGNITION IN GELS, MONOLAYERS, AND SOLIDS
Kevin L. Prime, Yen-Ho Chu, Walther Schmid, Christopher T. Seto, and James K. Chen Dec. 1991 21 p
(Contract N00014-86-K-0756)
(AD-A243488; TR-41) Avail: NTIS HC/MF A03 CSCL 20/5

This paper describes work in four areas: affinity electrophoresis of carbonic anhydrase in cross-linked polyacrylamide derived gels containing immobilized derivatives of aryl sulfonamides; inhibition of the hemagglutination of erythrocytes induced by influenza virus using water-soluble polyacrylamides bearing sialic acid groups; the application of self-assembled monolayers (SAMs) of alkyl thiolates on gold to the study of protein adsorption on organic surfaces; and the use of networks of hydrogen bonds to generate new classes of non-covalently assembled organic materials, both in solution and in crystals. This paper summarizes research in two areas of molecular recognition: affinity polymers and molecular self assembly. We illustrate these areas by examples drawn from affinity gel electrophoresis, soluble synthetic macromolecular inhibitors of binding of influenza virus to erythrocytes protein adsorption on self assembled monolayers and self assembling hydrogen bonded molecular aggregates. GRA

N92-17433# Technische Univ., Eindhoven (Netherlands). Faculteit Natuur- en Sterrenkunde.
THE PROTON SPECTRAL FUNCTION OF Ca-40 AND Ca-48 STUDIES WITH (e, e PRIME p) REACTION: AN INVESTIGATION OF GROUND-STATE CORRELATIONS Ph.D. Thesis
Gerrit Jakob Kramer 1990 130 p Sponsored by Stichting voor Fundamenteel Onderzoek der Materie, and Netherlands Organization for the Advancement of Pure Scientific Research
(ETN-92-90566) Avail: NTIS HC/MF A07

The single particle properties of the nuclei Ca-40 and Ca-48 were studied with quasielastic knockout experiments induced with electrons. These experiments were performed with the pulsed electron beam from the Medium Energy Accelerator (MEA) and the two spectrometer setup at NIKHEF-K (nuclear physics and high energy physics section K, Netherlands). The proton-spectral functions were determined from these measurements and for the discrete transitions momentum distributions were deduced. A schematic model which effectively takes into account short range correlations in order to explain the observed low spectroscopic factors is presented. Conclusions concerning ground state correlations and the spectroscopic factors derived from (e, e'p) experiments are drawn. ESA

N92-17435# Technische Univ., Eindhoven (Netherlands).
THE ZEUS SECOND LEVEL CALORIMETER TRIGGER: PHYSICS SIMULATION, DESIGN AND IMPLEMENTATION Ph.D. Thesis
Sijbrand Jan deJong 1990 155 p Sponsored by Stichting voor Fundamenteel Onderzoek der Materie
(ETN-92-90568) Avail: NTIS HC/MF A08

The ZEUS detector for HERA (German acronym for hadron electron storage ring) is addressed. HERA parameters and physics potential are discussed. One of the main detector components of the ZEUS experiment is the high resolution depleted uranium scintillator sandwich calorimeter, which plays an important role in the (offline) reconstruction of the recorded events and in the (online) selection of the interesting events. The ZEUS detector is described with emphasis on the high resolution calorimeter and on data acquisition and triggering. The performance of the trigger algorithm implemented in a specially developed tansputer based VME module was tested using Monte Carlo events and the Monte Carlo event generators used are discussed. First level trigger studies on Monte Carlo data are discussed. The input rates for both the first and second level trigger turn out to be completely dominated by interactions of the proton beam with the rest gas in the beam pipe in a range between -60 m and + 2 m from the interaction point. Important results of the second level calorimeter trigger processor algorithm are presented. The efficiency and reliability for the recognition of electrons and jets by the second level calorimeter trigger processor were shown to be satisfactory. It is shown that with the use of the calorimeter cluster information a significant beam gas event suppression, by a factor larger than 10, can be obtained, while the interesting events are not significantly affected. ESA

N92-17453# Pacific Northwest Lab., Richland, WA.
VERIFICATION OF AN EFFECTIVE DOSE EQUIVALENT MODEL FOR NEUTRONS
J. E. Tanner, R. K. Piper, J. A. Leonowich, and L. G. Faust Oct. 1991 15 p Presented at the 7th Symposium on Neutron Dosimetry, Berlin (Germany), 14-18 Oct. 1991
(Contract DE-AC06-76RL-01830)
(DE92-002738; PNL-SA-19136; CONF-911029-2) Avail: NTIS HC/MF A03

Since the effective dose equivalent, based on the weighted sum of organ dose equivalents, is not a directly measurable quantity, it must be estimated with the assistance of computer modeling techniques and a knowledge of the radiation field. Although extreme accuracy is not necessary for radiation protection purposes, a few well chosen measurements are required to confirm the theoretical models. Neutron measurements were performed in a RANDO phantom using thermoluminescent dosemeters, track etch dosemeters, and a 1/2 in. (1.27 cm) tissue equivalent proportional counter in order to estimate neutron doses and dose equivalents within the phantom at specific locations. The phantom was exposed to bare and D2O-moderated Cf-252 neutrons at the Pacific Northwest Laboratory's Low Scatter Facility. The Monte Carlo code MCNP with the MIRD-V mathematical phantom was used to model the human body and calculate organ doses and dose equivalents. The experimental methods are described and the results of the measurements are compared to the calculations. DOE

N92-17462# Department of the Navy, Washington, DC.
STEADY-STATE, HIGH DOSE NEUTRON GENERATION AND CONCENTRATION APPARATUS AND METHOD FOR DEUTERIUM ATOMS Patent Application
Han S. Uhm, inventor (to Navy) and Woong M. Lee, inventor (to Navy) 11 Jul. 1991 39 p
(AD-D015063; US-Patent-Appl-SN-724083; Navy-Case-73297)
Avail: NTIS HC/MF A03 CSCL 20/7

A steady-state source of neutrons is produced within an electrically grounded and temperature controlled chamber confining tritium or deuterium plasma at a predetermined density to effect implantation of ions in the surface of a palladium target rod coated with diffusion barrier material and immersed in such plasma. The rod is enriched with a high concentration of deuterium atoms after a prolonged plasma ion implantation. Collision of the deuterium atoms in the target by impinging ions of the plasma initiates fusion reactions causing emission of neutrons during negative voltage pulses applied to the rod through a high power modulator. The neutrons are so generated at a relatively high dose rate under optimized process conditions. GRA

N92-17472# Purdue Univ., West Lafayette, IN. Dept. of Chemistry.
ATOMIC RELAXATION AT ORDERED ELECTROCHEMICAL SURFACES PROBED BY SCANNING TUNNELING MICROSCOPY: Au(111) IN AQUEOUS SOLUTION COMPARED WITH ULTRAHIGH-VACUUM ENVIRONMENTS
X. Gao, A. Hamelin, and M. J. Weaver 31 Oct. 1991 18 p
(Contract N00014-91-J-1409)
(AD-A242031; TR-112) Avail: NTIS HC/MF A03 CSCL 09/1

Detailed surface atomic rearrangements at the ordered

Au(111)-aqueous interface triggered by negative electrode charges are examined by in-situ scanning tunneling microscopy (STM). Not only the atomic reconstruction, but also the longer range superstructures, formed at this electrochemical interface are seen to be remarkably similar to those observed previously by STM on clean Au(111) in ultrahigh vacuum. Understanding the atomic structures formed at ordered monocrystalline metal surfaces by reconstruction, both in the absence and presence of adsorbates or other means of modifying the surface environment, constitutes a centrally important topic in surface science. Almost all the experimental information on surface reconstruction gathered so far refers to metal ultrahigh vacuum (uhv) interfaces, where electron diffraction and related techniques can be employed. Similar phenomena are anticipated at metal solution (i.e., electrochemical) interfaces, where the electrode potential offers a powerful additional means of altering the chemical and electrostatic surface state. GRA

N92-17491# Harvard Univ., Cambridge, MA. Dept. of Chemistry.
DESIGNING ORDERED MOLECULAR ARRAYS IN TWO AND THREE DIMENSIONS
John P. Folkers, Jonathan A. Zerkowski, Paul E. Laibinis, Christopher T. Seto, and George M. Whitesides Dec. 1991 38 p
(Contract N00014-86-K-0756)
(AD-A243447; TR-43) Avail: NTIS HC/MF A03 CSCL 20/5

Two and three dimensional assemblies' self assembled monolayers' (SAMs) and hydrogen-bonded co-crystals, respectively show substantial changes in their supramolecular structures with seemingly minor changes in the structure of their molecular atomic constituents. The structure of SAMs obtained by adsorption of alkanethiols onto silver and copper are indistinguishable, although the atomic radii of silver and copper are different. The structure of the SAM on silver is different from that on gold, although the atomic radii of these metals are essentially the same. A macroscopic property of the SAMs, wetting, is not affected by these structural differences. Co-crystals formed from derivatives of barbiturates and melamines form hydrogen bonded tapes in the solid state. These tapes provide a template for studying the packing forces within crystals. GRA

N92-17505# Naval Research Lab., Washington, DC.
EVIDENCE FOR MeV PARTICLE EMISSION FROM Ti CHARGED WITH LOW ENERGY DEUTERIUM IONS Final Report
George P. Chambers, Graham K. Hubler, and Kenneth S. Grabowski 18 Dec. 1991 34 p
(AD-A243718; NRL-MR-6927) Avail: NTIS HC/MF A03 CSCL 20/5

Thin titanium films have been bombarded with low energy (350 eV) deuterium ions at high current density (0.2 to 0.4 mA sq cm) to investigate the reported occurrence of nuclear reactions at ambient temperatures in deuterium charged metals. A silicon charged particle detector was used to search for charged particles produced by such reactions. Evidence is reported for the detection of hydrogen isotopes with 5 MeV energy at a rate of 10 to 16 events/deuteron pair/s. Low energy deuterium (350 eV) ions produced by an ECR microwave source impinge normally on a thin metal film in vacuum, while a Si particle detector placed directly behind the film detects particle emission. The advantages of this method are rapid and efficient deuterium charging of any material (including insulators), high particle detection efficiency and sensitivity (low background), and the ability to measure the particle energy and determine the particle type. Titanium was chosen as the target because previous work by Jones had shown neutron emission and because Ti retains more hydrogen near room temperature than does PD. GRA

N92-17514# Arcon Corp., Waltham, MA.
CALCULATIONS OF ELECTRON AND PHOTON TRANSPORT BETWEEN 1 MeV AND 1 eV Final Report, Jul. 1986 - Aug. 1989
Stanley Woolf Nov. 1991 75 p
(Contract F19628-86-C-0019)
(AD-A243725; RL-TR-91-289) Avail: NTIS HC/MF A04 CSCL 20/12

This report describes the development and implementation of numerical methods for the simulation and description of electron and photon transport in layered one-dimensional structures such as metallized semiconductors. The simulations described were used to calculate charge distributions and predict from 1 eV to 20 MeV. The scope of our work included: (1) discrete ordinates transport calculations and dose predictions for primary and secondary electrons and for bremsstrahlung photons in one-dimensional layered media; (2) Monte Carlo electron transport and dose calculations in one-, two-, and three-dimensions; (3) implementation of electron-photon scattering theory in Monte Carlo and discrete ordinates simulation of low energy 8.9 eV electron transport in SiO2. GRA

N92-17518# Technische Univ., Eindhoven (Netherlands). Faculteit der Natuur- en Sterrenkunde.
ONE-LOOP CALCULATIONS WITH MASSIVE PARTICLES Ph.D. Thesis
Geert Jan vanOldenborgh 1990 111 p
(ETN-92-90563) Avail: NTIS HC/MF A06

Techniques to evaluate one loop integrals with massive particles, which are necessary in regions of phase space where light particle masses cannot be neglected, and which can be used to do QCD (Quantum Chromodynamic) one loop calculations in four dimensions using numerical rather than analytical integration, are presented. Examples for QCD calculations are given in the form of heavy quark production in lepton-proton interactions. Numerical problems were solved using kinematical determinants and unphysical on-shell internal vectors. The resulting algorithms can be used for both analytical and numerical evaluation of the scalar and tensor n-point functions. A mass regularization scheme for the many divergences of the theory of the strong interactions was considered. This entailed the renormalization of the parton distribution functions that describe the proton in this scheme. The result for the quark distribution functions are given. Calculations concerning heavy quark production in lepton-hadron collisions are considered. For the bottom quark massless, results are that the total cross section is 1.6 times the lowest order. This is slightly more than a computation using a heavy bottom quark would indicate. The pT distribution is somewhat softer and the rapidity somewhat harder than this previous result. A user's guide to the FF package (FORTRAN routines to numerically evaluate the integrals occurring in the calculation of one loop Feynmann diagrams) is given. ESA

N92-17519# Technische Univ., Eindhoven (Netherlands).
THE DETERMINATION OF THE NUMBER OF LIGHT NEUTRINO SPECIES Ph.D. Thesis
Alphonse Alouis Rademakers 1991 115 p Sponsored by Stichting voor Fundamenteel Onderzoek der Materie
(ETN-92-90564) Avail: NTIS HC/MF A06

Data taken with DELPHI (Detector with Lepton, Photon and Hadron Identification), on measurements done at ten different center of mass energies around the Z zero peak, is analyzed. DELPHI detected about 11,000 hadronic and 600 leptonic decays of the Z zero boson, which corresponds to about 150 Z zeros per day. From this scan, the mass and width of the Z zero, the peak cross section, the partial widths, and the number of light neutrino species can be determined. The experimental setup is described, including an overview of the main features of the LEP (Large Electron-Positron) collider and a description of the DELPHI detector and its data acquisition and trigger system. The offline data analysis programs and data structures including the three dimensional interactive graphics system, are presented. The data analysis, which is used to obtain a sample of Z zero to (bar)qq events from which the experimental hadronic Z zero line shape is determined, is described. The parameters of the Z zero resonance and the number of light neutrino species are determined by fitting the experimental Z zero line shape to a theoretical model. All the

results given are in good agreement with the Standard Model with a large top quark mass and agree well with the measurements of the other LEP experiments. ESA

N92-17520# Technische Univ., Eindhoven (Netherlands).
MUONS IN UA1; THE 2ND LEVEL TRIGGER AND DIMUON RESULTS Ph.D. Thesis
Adriaan Louis vanDijk 1991 100 p Sponsored by Stichting voor Fundamenteel Onderzoek der Materie
(ETN-92-90565) Avail: NTIS HC/MF A05

The development, construction, testing and operation of the second level trigger for the UA1 experiment to measure reactions with muons are described. The muon trigger is a computer system that directly after a measurement reconstructs an event and checks for the presence of muons. The analysis of the dimuons is discussed. Physics analysis results from data collected with the muon trigger are obtained from events containing two muons. The theory is reviewed and the quality of the data and the way the selections are done are discussed. A discussion of the J/psi and Upsilon samples and the cross section of b-quark production is given. ESA

N92-17530# California Univ., Berkeley. Lawrence Berkeley Lab.
NONLINEAR SPECTROSCOPIC STUDIES OF INTERFACIAL MOLECULAR ORDERING Ph.D. Thesis
R. Superfine Jul. 1991 140 p
(Contract DE-AC03-76SF-00098)
(DE92-000864; LBL-31130) Avail: NTIS HC/MF A07

The second order nonlinear optical processes of second harmonic generation and sum frequency generation are powerful new probes of surfaces. They possess unusual surface sensitivity due to the symmetry properties of the nonlinear susceptibility. In particular, infrared-visible sum frequency generation (SFG) can obtain the vibrational spectrum of sub-monolayer coverages of molecules. In this thesis, we explore the unique information that can be obtained from SFG. We take advantage of the sensitivity of SFG to the conformation of alkane chains to study the interaction between adsorbed liquid crystal molecules and surfactant treated surfaces. The sign of the SFG susceptibility depends on the sign of the molecular polarizability and the orientation, up or down, of the molecule. We experimentally determine the sign of the susceptibility and use it to determine the absolute orientation to obtain the sign of the molecular polarizability and show that this quantity contains important information about the dynamics of molecular charge distributions. Finally, we study the vibrational spectra and the molecular orientation at the pure liquid/vapor interface of methanol and water and present the most detailed evidence yet obtained for the structure of the pure water surface. DOE

N92-17549# National Inst. of Standards and Technology, Boulder, CO.
COOLED ION FREQUENCY STANDARD Annual Report, 1 Oct. 1990 - 31 Sep. 1991
D. J. Wineland 15 Sep. 1991 8 p
(Contract N00014-90-F-0004)
(AD-A242030) Avail: NTIS HC/MF A02 CSCL 20/5

The purpose of this work is to develop techniques to overcome the fundamental limits of present frequency standards - the second-order and residual first-order Doppler shifts. To this end we study suitable frequency reference transitions in ions which are stored on electromagnetic traps and cooled by radiation pressure to less than 1K. GRA

N92-17555# New Mexico Univ., Albuquerque. Dept. of Chemical and Nuclear Engineering.
CHARACTERIZATION OF THE THERMALNESS OF A FISSILE SYSTEM WITH A 2-GROUP DIFFUSION THEORY PARAMETER Final Report M.S. Thesis
Brent B. Bredehoft Dec. 1991 159 p
(AD-A243065) Avail: NTIS HC/MF A08 CSCL 20/8

Tabulation of critical data has commonly been done using the hydrogen to fissile atom ratio H/X. This does not account for the moderating contribution of other light nuclei in the system or for the absorption characteristics important to the slowing down process. Using a two energy group diffusion theory analogy to the six-factor-formula, we define the parameter p/(eta 2 asterisk f sub 2) as an appropriate parameter for defining moderation characteristics. This parameter adequately accounts for the important details of the slowing down process - resonance absorption, total system scattering and moderation, and the effective use of thermal neutrons. This study evaluates several low to moderate enriched uranium systems with several types of moderators. It utilizes the TWODANT transport code with the Hansen Roach 16 group cross sections and group collapse theory to develop appropriate system models and two group cross sections. GRA

N92-17574# Oak Ridge National Lab., TN.
DIFFRACTION AND IMAGING THEORY OF INELASTICALLY SCATTERED ELECTRONS: A NEW APPROACH
Z. L. Wang (Tennessee Univ., Knoxville.) and J. Bentley 1991 38 p Presented at the 10th Pfefferkorn Conference on Signal and Image Processing in Microscopy and Microanalysis, Cambridge, England, 16-19 Sep. 1991
(Contract DE-AC05-84OR-21400)
(DE91-018248; CONF-9109256-1) Avail: NTIS HC/MF A03

A new dynamical theory is developed for describing inelastic electron scattering in thin crystals. Compared to existing theories, the first advantage of this new theory is that the incoherent summation of the diffracted intensities contributed by electrons after exciting vast numbers of different excited states has been evaluated before any numerical calculation. The second advantage is that only the modulus squared of the transition matrix elements are needed in the final computation. This greatly reduces the effort in searching for 'phase shifts' in inelastic scattering matrix calculations. By iterative operation of this single-inelastic scattering theory, multiple-inelastic electron scattering of phonons, single-electrons, and valence (or plasmon) excitations can be included in diffraction pattern calculations. High resolution images formed by valence excited electrons can also be calculated in this theoretical scheme for relatively thick crystals. The sharpness of thermal diffuse scattering (TDS) streaks is determined by the phonon dispersion relationships of the acoustic branches; optical branches contribute only a diffuse background. Dynamical scattering effects can change the intensity distribution of TDS electrons but have almost no effect on the sharpness of TDS streaks. To a good approximation, the TDS streaks are defined by the q(sub x) - q(sub y) curves which satisfy omega(sub j)(q) = 0, where omega(sub j)(q) is the phonon dispersion relationship determined by the 2-D atomic vibrations in the (hkl) plane perpendicular to the incident beam direction B = (hkl). This is a simplified 2-D vibration model. The directions of TDS streaks can be predicted according to a simple q x (r(iota)-r(iota sub 1)) = 0 rule, where the summation of iota(sub 1) is restricted to the first nearest neighbors of the iota(sup th) atom that are located in the same atomic plane as the iota(sup th) atom perpendicular to the incident beam direction. DOE

N92-17589# Los Alamos National Lab., NM.
RECENT DEVELOPMENTS IN NEUTRINO PHYSICS
G. T. Garvey 1991 30 p Presented at the European Physical Society Nuclear Physics Conference on Hadronic Structure and Electromagnetic Interactions, Amsterdam (Netherlands), 5-10 Aug. 1991
(Contract W-7405-eng-36)
(DE92-003855; LA-UR-91-3569; CONF-910835-1) Avail: NTIS HC/MF A03

I shall attempt to summarize recent developments in the experimental situation in neutrino physics. The paper will deal with recent results, drawing on either published work or research that has been presented in preprint form. The discussion of the theoretical implication of these experimental results will be presented in the following paper by Boris Kayser. The topics to be covered in this presentation are: direct measurements of

bar-nu(sub e) mass via beta endpoint studies; status of solar neutrino observations; status of '17 keV neutrino' reports; and the use of (nu)p elastic scattering to determine the 'strange quark' content of the proton. DOE

N92-17608# Stanford Univ., CA.
A STUDY OF GAMMA RAY GENERATION FROM CHANNELED ELECTRONS AND POSITIONS Final Report, 1 Mar. 1986 - 28 Feb. 1991
R. H. Pantell 28 Feb. 1991 3 p
(Contract F49620-86-K-0015)
(AD-A241993; AFOSR-91-0843TR) Avail: NTIS HC/MF A01 CSCL 20/7

The primary purpose of the experiments on the linac were to demonstrate that channeling radiation can be an inexpensive source of bright, hard x-rays with picosecond duration. Channeled particle trajectories are similar to the trajectories in a magnetic wiggler, but the equivalent magnetic field would have to be about ten megagauss. Indeed, a photon flux of 10 to the 19th power photons/sr-keV-sec was measured over a picosecond duration at a wavelength of 0.42 A. Our peak current levels were about 10 to the 13th power times greater than the currents used in previous channeling experiments and average currents were about 10 to the 8th power times greater. To perform these measurement, a spectrometer was developed capable of operating at high photon fluxes with several percent energy resolution at x-ray wavelengths, and in a bremsstrahlung background. This was accomplished using a graphite crystal Bragg reflector, a photomultiplier detector, and specially designed apertures. In addition to the high power channeling radiation research, we also studied channeling radiation in superlattices, both theoretically and experimentally. Superlattices offer a means for increasing the radiation, utilizing the periodicity of the layers. The Madey storage ring was to provide a bright positron current source for seeking x-ray laser action by means of channeling radiation. A current density of 10 to 100 million A/sq cm could be obtained, which would provide significant stimulated gain over a picosecond time interval. GRA

N92-17616# Harvard Univ., Cambridge, MA. Dept. of Chemistry.
MOLECULAR SELF-ASSEMBLY AND NANOCHEMISTRY: A CHEMICAL STRATEGY FOR THE SYNTHESIS OF NANOSTRUCTURES
George M. Whitesides, John P. Mathias, and Christopher T. Seto Dec. 1991 39 p
(Contract N00014-86-K-0756)
(AD-A243530; TR-45) Avail: NTIS HC/MF A03 CSCL 20/5

Molecular self assembly is the spontaneous association of molecules under equilibrium conditions into stable, structurally well-defined aggregates joined by non-covalent bonds. Molecular self-assembly is ubiquitous in biological systems, and underlies the formation of a wide variety of complex biological structures. Understanding self-assembly and the associated non-covalent interactions that connect complementary interacting molecular surfaces in biological aggregates is a central concern in structural biochemistry. Self-assembly is also emerging as a new strategy in chemical synthesis, with the potential of generating non-biological structures having dimensions of 1-10(exp 2) nanometers. Structures in the upper part of this range of sizes are presently inaccessible through chemical synthesis, and the ability to prepare them would open a route to structures comparable in size (and perhaps complementary in function) to those that can be prepared by microlithography and other techniques of microfabrication. GRA

N92-17646*# Fermi National Accelerator Lab., Batavia, IL.
AXINO-INDUCED BARYOGENESIS
Silvia Mollerach and Esteban Roulet Nov. 1991 12 p Sponsored in part by DOE and Fondazione A. dela Riccia
(Grant NAGw-2381)
(NASA-CR-189858; NAS 1.26:189858; FERMILAB-Pub-91/340-A)
Avail: NTIS HC/MF A03 CSCL 20H

We consider the possibility that the baryon asymmetry is generated at low energies as a consequence of the axino decay. We analyze models in which the axino, the superpartner of the axion, is heavy and decays into gluinos at temperatures T approx. = 1 GeV. If CP and B violating couplings for the quark superfields are included, the subsequent decay of these out of equilibrium gluinos can act as seeds for baryogenesis. The required amount of CP violation is well consistent with the bounds on the electric dipole moment of the neutron and the mechanism works even for low reheating temperatures after inflation (T sub RH greater or approx. = 10 exp 4 GeV). Author

N92-17647*# Fermi National Accelerator Lab., Batavia, IL.
FLUCTUATION DRIVEN ELECTROWEAK PHASE TRANSITION
Marcelo Gleiser and Edward W. Kolb (Chicago Univ., IL.) Nov. 1991 11 p Sponsored in part by DOE
(Grant NAGw-1340)
(NASA-CR-189859; NAS 1.26:189859; FERMILAB-Pub-91/305-A)
Avail: NTIS HC/MF A03 CSCL 20H

We examine the dynamics of the electroweak phase transition in the early Universe. For Higgs masses in the range 46 less than or = M sub H less than or = 150 GeV and top quark masses less than 200 GeV, regions of symmetric and asymmetric vacuum coexist to below the critical temperature, with thermal equilibrium between the two phases maintained by fluctuations of both phases. We propose that the transition to the asymmetric vacuum is completed by percolation of these subcritical fluctuations. Our results are relevant to scenarios of baryogenesis that invoke a weakly first-order phase transition at the electroweak scale. Author

N92-17652# Physical Sciences, Inc., Andover, MA.
RATES AND MECHANISMS OF METASTABLE DEACTIVATION OVER SURFACES Final Report, Nov. 1985 - Dec. 1988
W. T. Rawlins, W. J. Marinelli, A. M. Woodward, D. Kaufman, and B. L. Upschulte Feb. 1991 52 p
(Contract F33615-85-C-2561)
(AD-A243391; WL-TR-91-2067) Avail: NTIS HC/MF A04 CSCL 20/5

The objective of this project was to investigate mechanisms of energy disposal in the quenching of rare gas and molecular metastable species upon collisions with practical surfaces representative of plasma reactors. An apparatus was designed and constructed to generate a molecular beam of selected metastable species (He*, Ar*, N2*) and impinge the beam on clean or gas-dosed surfaces in an ultra high vacuum (UHV) chamber. The metastables were generated in a discharge-flow reactor, sampled and skimmed into a molecular beam, and directed into the UHV target chamber via two-stage differential pumping. A hemispherical, retarding potential electron energy analyzer was used to measure production rates and energy distributions of electrons ejected from the surface via the Penning ionization and Auger neutralization quenching mechanisms. The absence of significant electron ejection from metastable impingement is quite unexpected in light of previous investigations of this process for polished, high-purity, oriented single crystals. GRA

N92-17660# International Business Machines Corp., San Jose, CA.
OPTICAL MODIFICATION OF A SINGLE IMPURITY MOLECULE IN A SOLID Interim Technical Report
T. Basche and W. E. Moerner 17 Oct. 1991 15 p
(Contract N00014-91-C-0166)
(AD-A243750; IBM-RJ8420; TR-32) Avail: NTIS HC/MF A03 CSCL 20/5

The possibility of obtaining information about solids on a truly microscopic scale has stimulated several advances in the optical detection and spectroscopy of single impurity centers in solids. For the system composed of pentacene impurity molecules in the crystal terphenyl, absorption and fluorescence excitation studies at liquid helium temperatures have led to direct observations of the lifetime-limited homogeneous linewidth of a single pentacene molecule as well as surprising observation of spontaneous spectral diffusion in a crystal. Spectral diffusion, or changes in the resonance frequency of an impurity molecule with time as a result of structural

relaxation processes (two-level system (TLS) transitions) is generally expected in amorphous hosts. Using perylene impurity molecules in poly(ethylene), we have observed the optical spectra of single molecules in a polymeric host for the first time. At 1.5K, individual perylene molecules show the expected spectral diffusion; moreover, we observe light-induced changes in resonance frequency, i.e., persistent spectral hole-burning, which allows one to envision optical storage on the single-molecule level. GRA

N92-17663# Air Force Inst. of Tech., Wright-Patterson AFB, OH. School of Engineering.
STEADY-STATE PRODUCTION AND QUENCHING OF Br((2)P1/2) M.S. Thesis
Ralph F. Tate Nov. 1991 129 p
(AD-A243754; AFIT/GE/ENP/91D-01) Avail: NTIS HC/MF A07 CSCL 20/5

The spin orbit relaxation of atoms has been investigated in a steady state infrared fluorescence experiment. A CW argon ion laser operating at 488 nm was used to photodissociate gas-phase Br into equal quantities of Bromine and Bromine atoms. The resulting 2.7 micron emission was observed as a function of added quenching gas. A steady-state analysis was used to determine quenching rates for SF6, N2, O2, He, Ne, Ar, Kr, and Xe, relative to quenching by the parent molecule. Limitations in the apparatus prevented determination of the quenching rate coefficient for Br2. Recommendations are made for improvements in the apparatus and analysis for future reséarch. GRA

N92-17666# Los Alamos National Lab., NM.
MEDIUM-ENERGY NEUTRINO PHYSICS
D. H. White 22 Nov. 1991 9 p Presented at the Future of Muon Physics, Heidelberg (Germany), 7-10 May 1991
(Contract W-7405-eng-36)
(DE92-003790; LA-UR-91-3830; CONF-9105221-3) Avail: NTIS HC/MF A02

A selection of opportunities for neutrino physics from a source generated from pions that decay in flight and at rest is described. The present source at LAMPF has a duty factor of about 6 percent; improvements in opportunities that emerge from a source using a pulse 0.25 microseconds long from a proton storage ring are also described. DOE

N92-17743 Academy of Sciences of the Ukrainian SSR, Kiev. Inst. of Physics.
ION SOURCES BASED ON ELECTRON CYCLOTRON RESONANCE [IONNYE ISTOCHNIKI NA OSNOVE ELEKTRONNOGO TSIKLOTRONNOGO REZONANSA]
K. S. Golovanivskii and V. D. Dugar-Zhabon 1990 21 p In RUSSIAN
Copyright Avail: Issuing Activity

Physical principles are described and a brief summary is given of the current state of development of ion sources based on electronic cyclotron resonance (ECR) heating of plasma in a mirror-type machine. Characteristics of ECR sources are presented for positive and negative ions used chiefly in acceleration technology. Transl. by L.K.S.

N92-17789# Indiana Univ., Bloomington.
RELATIVISTIC NUCLEAR MANY-BODY THEORY
B. D. Serot and J. D. Walecka (Continuous Electron Beam Accelerator Facility, Newport New, VA.) 11 Sep. 1991 50 p Presented at the Recent Progress in Many-Body Theories, Minneapolis, MN, 26-31 Aug. 1991
(Contract DE-AC02-83ER-40105)
(DE92-003258; DOE/ER-40105/175; CEBAF-PR-91-037; IU/NTC-91-12; CONF-9108142-4) Avail: NTIS HC/MF A03

Nonrelativistic models of nuclear systems have provided important insight into nuclear physics. In future experiments, nuclear systems will be examined under extreme conditions of density and temperature, and their response will be probed at momentum and energy transfers larger than the nucleon mass. It is therefore essential to develop reliable models that go beyond the traditional nonrelativistic many-body framework. General properties of physics, such as quantum mechanics, Lorentz covariance, and microscopic causality, motivate the use of quantum field theories to describe the interacting, relativistic, nuclear many-body system. Renormalizable models based on hadronic degrees of freedom (quantum hadrodynamics) are presented, and the assumptions underlying this framework are discussed. Some applications and successes of quantum hadrodynamics are described, with an emphasis on the new features arising from relativity. Examples include the nuclear equation of state, the shell model, nucleon-nucleus scattering, and the inclusion of zero-point vacuum corrections. Current issues and problems are also considered, such as the construction of improved approximations, the full role of the quantum vacuum, and the relationship between quantum hadrodynamics and quantum chromodynamics. We also speculate on future developments. DOE

N92-17818 Academy of Sciences of the Ukrainian SSR, Kiev. Inst. of Physics.
IONIC PHYSICS AND TECHNOLOGY [IONNAIA FIZIKA I TECHNOLOGIIA]
M. D. Gabovich, M. I. Guseva, and V. E. Iurasova 1990 65 p In RUSSIAN
Copyright Avail: Issuing Activity

The area of ion physics is discussed as it applies to ion technology. Connection with the physical phenomenon which occur during the implantation of ions in metal is examined in detail, as well as the change in topography of the surface of a hard body under the influence of ion bombardment. Transl. by L.K.H.

N92-17820 Academy of Sciences of the Ukrainian SSR, Kiev. Inst. of Physics.
HIGH FREQUENCY SOURCES OF IONS FOR ION TECHNOLOGY [VYSOKOCHASTOTNYE ISTOCHNIKI IONOVDLIA IONNOI TEKHNOLOGII]
O. A. Ananev, B. A. Diachenko, and B. Ia. Pavlov 1990 34 p In RUSSIAN
Copyright Avail: Issuing Activity

The characteristics and areas of application of high frequency ion sources are examined. The physical processes in high frequency sources are summarized. The designs of the ion sources developed at the U.S.S.R. Academy of Science are described, and the characteristics and domains of their work are conveyed. Transl. by L.K.H.

N92-17954# Mohammed V Univ., Rabat (Morocco). Faculte des Sciences.
DETERMINATION OF DIFFUSION PARAMETERS OF THERMAL NEUTRONS FOR NON-MODERATOR MEDIA BY A PULSED METHOD AND A TIME INDEPENDENT METHOD Ph.D. Thesis
A. Boufraqech 21 Feb. 1991 201 p In FRENCH
(DE92-600624; INIS-mf-12963) Avail: NTIS HC/MF A10

Two methods for determining the diffusion parameters of thermal neutrons for non-moderator and non-multiplicator media have been developed. The first one, which is a pulsed method, is based on thermal neutrons relaxation coefficients measurement in a moderator, with and without the medium of interest that plays the role of reflector. For the experimental results interpretation using the diffusion theory, a corrective factor which takes into account the neutron cooling by diffusion has been introduced. Its dependence on the empirically obtained relaxation coefficients is in a good agreement with the calculations made in P3L2 approximation. The difference between linear extrapolation lengths of the moderator and the reflector has been taken into account, by developing the scalar fluxes in Bessel function series which automatically satisfy the boundary conditions at the extrapolated surfaces of the two media. The obtained results for iron are in a good agreement with those in the literature. The second method is time independent, based on the 'flux albedo' measurements interpretation (concept introduced by Amaldi and Fermi) by P3 approximation in the one group transport theory. The independent sources are introduced in the Marshak boundary conditions. An angular albedo matrix has been used to deal with multiple

reflections and to take into account the distortion of the current vector when entering a medium, after being reflected by this latter. The results obtained by this method are slightly different from those given in the literature. The analysis of the possible sources causing this discrepancy, particulary the radial distribution of flux in cylindrical geometry and the flux depression at medium-black body interface, has shown that the origin of this discrepancy is the neutron heating by diffusion. DOE

N92-17955# Joint Inst. for Nuclear Research, Dubna (USSR). Lab. of Neutron Physics.
INVESTIGATION OF HEATED ULTRACOLD NEUTRONS ON COPPER SURFACE
S. D. Kalchev, A. V. Strelkov, and G. I. Terekhov (Nauchno-Issledovatelskii Inst. Atomnykh Reaktororov, Dimitrovgrad, USSR) 1990 21 p In RUSSIAN; ENGLISH summary
(DE92-600625; JINR-R-3-90-120) Avail: NTIS HC/MF A03

Mean energies of ultracold neutrons (UCN) upscattered on a copper surface at various temperatures after different outgassing procedures were measured by transmission of heated neutrons through a gaseous adsorber (10)BF3 of variable thickness. The mean energy of UCN upscattered on a copper surface at room temperature is (23 +/- 1.5) meV before outgassing and (8.7 +/- 0.7) meV after it. DOE

N92-17956# Joint Inst. for Nuclear Research, Dubna (USSR). Lab. of Theoretical Physics.
IMPORTANCE OF THE NEUTRON-PROTON INTERACTIONS FOR THE EVEN Ra-Th NUCLEI
M. Trajdos and K. Zajac (Marie Curie-Sklodowska Univ., Lublin, Poland) 1990 13 p Submitted for publication Sponsored by Ministry of National Education
(DE92-600628; JINR-E-4-90-249) Avail: NTIS HC/MF A03

By including the most important residual interactions in the J = 0, T = 1 and J = 1, T = 0 states and treating these nucleon pairs as building blocks of a nucleus, the experimental data of even (222-226)Ra and (226-232)Th in the energy region E less than or = 1 MeV are explained. The energy values and reduced probabilities of E1 and E2 transitions together with neutron-proton and cluster structures of K(sup pi) = O+(sub 1), O+(sub 2) and O-(sub 1) band states are presented. DOE

N92-17957# Joint Inst. for Nuclear Research, Dubna (USSR). Lab. of Theoretical Physics.
ONE NUCLEON TRANSITION DENSITIES FOR 1p SHELL NUCLEI
H. R. Kissener, H. U. Jaeger, and O. Richter (Ceskoslovenska Akademie Ved, Rez.) 1990 24 p
(DE92-600629; JINR-E-4-90-57) Avail: NTIS HC/MF A03

Reduced one-body transition density matrices of the operator (c(sub alpha, sup +) c(sub beta))sub JT have been calculated for all multipole excitations (JT) between the nuclear state AJ(sub 0)T(sub 0); 0h(omega) and all final states AJ(sub f)T(sub f); (0+1)h(omega) of 1p shell nuclei, using various options for the effective two-nucleon interaction. For illustration the tables for all multipole transitions to the 1h(omega) band of the nucleus N-15 for the Millener-Kurath nuclear hamiltonian are given. DOE

N92-17958# Joint Inst. for Nuclear Research, Dubna (USSR). Lab. of Computing Techniques and Automation.
PION-NUCLEUS CROSS SECTIONS
V. S. Barashenkov 1990 12 p In RUSSIAN; ENGLISH summary
(DE92-600631; JINR-R-2-90-158) Avail: NTIS HC/MF A03

The tables of inelastic and total cross sections of pi(+-) meson interactions with nuclei He-4 - U-238 are presented. The tables are obtained by theoretical analysis of known experimental data. DOE

73 NUCLEAR AND HIGH-ENERGY PHYSICS

Includes elementary and nuclear particles; and reactor theory.

For space radiation see *93 Space Radiation.*

N92-17590# Los Alamos National Lab., NM.
BEAM POSITION MONITOR MULTIPLEXER CONTROLLER UPGRADE AT THE LAMPF PROTON STORAGE RING
W. K. Scarborough and S. Cohen 1991 3 p Presented at the International Conference on Accelerator and Large Experimental Physics Control Systems, Tsukuba (Japan), 11-15 Nov. 1991
(Contract W-7405-eng-36)
(DE92-003859; LA-UR-91-3540; CONF-911116-11) Avail: NTIS HC/MF A01

The beam position monitor (BPM) is one of the primary diagnostic tools used for the tuning of the proton storage ring (PSR) at the Clinton P. Anderson Meson Physics Facility (LAMPF). A replacement for the existing, monolithic, wire-wrapped microprocessor-based BPM multiplexer controller has been built. The controller has been redesigned as a modular system retaining the same functionality of the original system built in 1981. Individual printed circuit cards are used for each controller function to insure greater maintainability and ease of keeping a spare parts inventory. Programmable logic device technology has substantially reduced the component count of the new controller. Diagnostic software was written to support the development of the upgraded controller. The new software actually uncovered some flaws in the original CAMAC interface. DOE

N92-17738# Texas A&M Univ., College Station. Dept. of Physics.
HIGH ENERGY PHYSICS PROGRAM AT TEXAS A AND M UNIVERSITY
Oct. 1991 185 p
(Contract DE-FG05-91ER-40633)
(DE92-004426; DOE/ER-40633/1) Avail: NTIS HC/MF A09

The Texas A&M experimental high energy physics program continued to reach significant milestones in each of its research initiatives during the course of the past year. We are participating in two major operating experiments, CDF and MACRO. In CDF, the Texas A&M group has spearheaded the test beam program to recalibrate the Forward Hadron Calorimeter for the upcoming CDF data run, as well as contributing to the ongoing analysis work on jets and b-quarks. In MACRO, we have assisted in the development of the final version of the wave form digitizing system being implemented for the entire scintillator system. The construction of the first six supermodules of the detector has been completed and all six are currently taking data with streamer chambers while four have the completed scintillator counter system up and running. We have built and tested prototypes of a liquid-scintillator fiber calorimeter system, in which internally reflecting channels are imbedded in a lead matrix and filled with liquid scintillator. This approach combines the performance features of fiber calorimetry and the radiation hardness of liquid scintillator, and is being developed for forward calorimetry at the SSC. The microstrip chamber is a new technology for precision track chambers that offers the performance required for future hadron colliders. The theoretical high energy physics program has continued to develop during the past funding cycle. We have continued the study of their very successful string-derived model that unifies all known interactions, flipped SU(5), which is the leading candidate for a TOE. Work has continued on some generalizations of the symmetries of string theory, known as W algebras. These are expected to have applications in two-dimensional conformal field theory, two-dimensional extensions of gravity and topological gravity, and W-string theory. DOE

N92-17739# Sandia National Labs., Albuquerque, NM.
SOLDER EXTRUSION PRESSURE BONDING PROCESS AND BONDED PRODUCTS PRODUCED THEREBY
L. C. Beavis, inventor (to DOE), M. M. Karnowsky, inventor (to

DOE), and F. G. Yost, inventor (to DOE) 20 Apr. 1990 11 p
(Contract DE-AC04-76DP-00789)
(DE92-004603; US-Patent-Appl-SN-511684;
Patents-US-A7511684) Avail: NTIS HC/MF A03

The production of soldered joints are highly reliable and capable of surviving 10,000 thermal cycles between about -40 and 110 C. The process involves interposing a thin layer of a metal solder composition between the metal surfaces of members to be bonded and applying heat up to about 1000 psi compression pressure to the superposed members, in the presence of a reducing atmosphere, to extrude the major amount of the solder composition, contaminants including fluxing gases and air, from between the members being bonded, to form a very thin, strong intermetallic bonding layer having a thermal expansion tolerant with that of the bonded members. DOE

N92-17794# Los Alamos National Lab., NM.
PILAC: A PION LINAC FACILITY FOR 1-GeV PION PHYSICS AT LAMPF
H. A. Thiessen and D. H. White 22 Nov. 1991 6 p Presented at the Future of Muon Physics, Heidelberg (Germany), 7-10 May 1991
(Contract W-7405-eng-36)
(DE92-003789; LA-UR-91-3831; CONF-9105221-4) Avail: NTIS HC/MF A02

A design study for a Pion Linac (PILAC) at LAMPF is under way at Los Alamos. We present here a reference design for a system of pion source, linac, and high resolution beam line and spectrometer that will provide 10(exp 9) pions per second on target and 200 keV resolution for the (pi(+), K(+)) reaction at 0.92 GeV. A general purpose beam line that delivers both positive and negative pions in the energy range 0.4 to 1.1 GeV is included, thus opening up the possibility of a broad experimental program as is discussed in this report. A kicker-based beam sharing system allows delivery of beam to both beam lines simultaneously with independent sign and energy control. Because the pion linac acts like an RF particle separator, all beams produced by PILAC will be free of electron (or positron) and proton contamination. DOE

N92-17796# Los Alamos National Lab., NM.
EMITTANCE GROWTH FROM SPACE-CHARGE FORCES
T. P. Wangler 1991 21 p Presented at the Symposium on High Brightness Beams for Advanced Accelerator Applications, College Park, MD, 6-7 Jun. 1991
(Contract W-7405-eng-36)
(DE92-003804; LA-UR-91-3287; CONF-9106260-5) Avail: NTIS HC/MF A03

Space charge induced emittance growth has become a topic of much recent interest for designing the low velocity sections of high intensity, high brightness accelerators and beam transport channels. In this paper we review the properties of the space charge force, and discuss the concepts of matching, space charge and emittance-dominated beams, and equilibrium beams and their characteristics. This is followed by a survey of some of the work over the past 25 years to identify the mechanisms of this emittance growth in both ion and electron accelerators. We summarize the overall results in terms of four distinct mechanisms whose characteristics we describe. Finally, we show numerical simulation results for the evolution of initial rms-mismatched laminar beams. The examples show that for space charge dominated beams, the nonlinear space charge forces produce a highly chaotic filamentation pattern, which in projection to the 2-D phase spaces results in a 2-component beam consisting of an inner core and a diffuse outer halo. In the examples we have studied the halo contains only a few percent of the particles, but contributes about half of the emittance growth. DOE

N92-17876# Lawrence Livermore National Lab., CA.
ENERGY PRODUCTION USING FISSION FRAGMENT ROCKETS
G. Chapline and Y. Matsuda Aug. 1991 4 p Presented at the 6th International Conference on Emerging Nuclear Energy Systems, Monterey, CA, 16-21 Jun. 1991
(Contract W-7405-eng-48)
(DE92-002192; UCRL-JC-107357; CONF-910626-14) Avail: NTIS HC/MF A01

Fission fragment rockets are nuclear reactors with a core consisting of thin fibers in a vacuum, and which use magnetic fields to extract the fission fragments from the reactor core. As an alternative to ordinary nuclear reactors, fission fragment rockets would have the following advantages: approximately twice the efficiency if the fission fragment energy can be directly converted into electricity; reduction of the buildup of a fission fragment inventory in the reactor could avoid a Chernobyl type disaster; and collection of the fission fragments outside the reactor could simplify the waste disposal problem. DOE

N92-17964# Harvard Univ., Cambridge, MA.
PROTON-PROTON AND PROTON-ANTIPROTON ELASTIC SCATTERING AT HIGH ENERGIES: THEORY, PHENOMENOLOGY, AND EXPERIMENT
Tai Tsun Wu 1990 11 p Presented at the Beyond the Standard Model 2: A Critical Review of the Standard Model and the Prospects for Discovering New Physics, Norman, OK, 1-3 Nov. 1990
(Contract DE-FG02-84ER-40158)
(DE92-004414; CONF-901145-2) Avail: NTIS HC/MF A03

This is a brief review of the progress in the understanding, during the past twenty years, of hadronic elastic scattering near the forward direction at high energies. On the basis of quantum gauge field theories, the Pomeron is found to be a branch cut above 1. Using the physical picture that this result implies, phenomenology for proton-proton and antiproton-proton elastic scattering is constructed. Two noteworthy features are that, at high energies, both the total cross section and the ratio of the integrated elastic cross section to the total cross section are increasing functions of the center-of-mass energy. Detailed predictions are given for the elastic differential cross sections, Coulomb interference and the ratios of the real to imaginary parts of the forward amplitudes. These predictions have been extensively and accurately confirmed by experiments, and have also been given both for future experiments on existing accelerators and for experiments on future accelerators. DOE

N92-17973# Joint Inst. for Nuclear Research, Dubna (USSR). Lab. of Nuclear Reactions.
MULTIPLY CHARGED ION SOURCES FOR CYCLOTRONS
S. L. Bogomolov, V. B. Kutner, and Yu. P. Tretyakov 1990 13 p In RUSSIAN; ENGLISH summary
(DE92-610975; JINR-R-9-90-37) Avail: NTIS HC/MF A03

The cyclotron multiply charged ion sources are described. Data on the yields of ions of rare isotopes from the arc source with indirectly heated cathode and electron oscillations in the magnetic field are presented. The results of investigations of the laser ion source for cyclotron are presented. The problems of using the different types of ion sources, namely, arc, ECR and others, in the external injection systems for cyclotrons are discussed. Data on the yields of multiply charged ions from the ECR ion source are presented. The efficiency of consuming substances in the arc and ECR ion sources is compared. DOE

74 OPTICS

Includes light phenomena; and optical devices.
For lasers see *36 Lasers and Masers.*

N92-16981# Naval Postgraduate School, Monterey, CA.
NONCOHERENT DETECTION OF COHERENT OPTICAL HETERODYNE SIGNALS CORRUPTED BY LASER PHASE NOISE M.S. Thesis
Kent C. Varnum Mar. 1991 83 p
(AD-A243103) Avail: NTIS HC/MF A05 CSCL 12/9

An error probability analysis is performed for noncoherent detection of optical heterodyne signals corrupted by laser phase noise and additive white Gaussian noise. Two types of laser

modulation are investigated, on-off keying (OOK) and frequency shift keying (FSK). Single user OOK system performance for different linewidth-to-bit rate ratios is analyzed over a range of both signal-to-noise ratios (SNR) and normalized decision thresholds. The decision threshold analysis illustrates which noise source dominates system performance. An analytical expression representing the effect of laser phase noise on system performance is derived based on a high user bit rate assumption. The system performance obtained with the high bit rate expression is compared with the system performance obtained with currently used expressions to determine its range of validity. An error probability analysis is then performed for noncoherent detection of FSK signals corrupted by laser phase noise and additive white Gaussian receiver noise. The performance of the FSK system is compared with the performance of the OOK system. It is shown that optical FSK systems perform better than optical OOK systems. GRA

N92-17044# Michigan Univ., Ann Arbor. Dept. of Electrical Engineering and Computer Science.
TH 3-5 MODULATION AND SWITCHING DEVICES FOR OPTICAL SYSTEM APPLICATIONS Final Report, 15 Apr. 1988 - 14 Oct. 1991
Jasprit Singh 14 Oct. 1991 19 p
(Grant AF-AFOSR-0168-88; AF Proj. 2305)
(AD-A243055; AFOSR-91-0927TR) Avail: NTIS HC/MF A03 CSCL 20/6

Optical computing has been a dream of scientists for over a decade. In several areas optical processing has made great strides. These areas include optical communication, optical memory, optical scanning, etc. However, the optical computer still remains a dream. Earlier spectacular successes in very high speed optical switches based upon non-linear optical effects in III-V compound semiconductor structures have not led to useful applications. Even in optical communication, the full potential of optics remains unrealized because of lack of more tailorable devices such as wavelength selective detectors. Author (GRA)

N92-17088# Air Force Inst. of Tech., Wright-Patterson AFB, OH. School of Engineering.
DESIGN OF A FIBER OPTIC IMAGE TRANSMISSION LINK M.S. Thesis
Justin D. Redd Dec. 1991 82 p
(AD-A243686; AFIT/GE/ENG/91D-45) Avail: NTIS HC/MF A05 CSCL 20/6

An original design is presented for a fiber optic based digital image transmission link operating at a serial bit rate of 250 Mbits/Second. The link is designed as an integral part of an airborne infrared imaging system with particular emphasis on avoiding problems associated with aircraft electromagnetic interference (EMI). Unique features include simplicity (single PC board transmitter and receiver), low power, low cost (under $3,000), and use of the latest off-the-shelf components (including the Gazelle GA9011/GA9012 HOT ROD chip set). Theoretical modeling is used to predict a bit error rate of better than 10 to the minus 15th power, while actual measurements include transmission of over 10 to 13th power bits without any errors (measured bit error rate of at least 10 to the minus 13th power). Test results also show that the link is capable of transmitting 640 x 480 pixel (12 bits per pixel) images with no significant image degradation. GRA

N92-17146# Carnegie-Mellon Univ., Pittsburgh, PA. Robotics Inst.
EXTRACTING THE SHAPE AND ROUGHNESS OF SPECULAR LOBE OBJECTS USING FOUR LIGHT PHOTOMETRIC STEREO
Fredric Solomon and Katsushi Ikeuchi 31 Oct. 1991 43 p
(Contract F33615-90-C-1465; ARPA Order 7597)
(AD-A243522; CMU-RI-TR-91-17) Avail: NTIS HC/MF A03 CSCL 17/5

Two important aspects of part inspection are the measurement or surface shape and surface roughness. A noncontact method is proposed for measuring surface shape and surface roughness. The method, called 'four light photometric stereo', uses four lights which sequentially illuminate the object under inspection, and a video camera for taking images of the object. Conceptually, the problem solving has three parts: shape extraction, pixel segmentation, and roughness extraction. The shape information is produced directly by three light and four light photometric stereo methods. After one has shape information, we can apply statistical segmentation techniques to determine which pixels are specular and which are nonspecular. Then, one can use the specular pixels and shape information in conjugation with the simplified Torrance-Sparrow reflectance model to determine the surface roughness. The method has successfully been applied to a number of synthetic and real objects. GRA

N92-17180# Royal Signals and Radar Establishment, Malvern (England).
THE PHYSICAL OPTICS DESCRIPTION OF MICROWAVE SCATTERING BY THE SEA SURFACE
R. J. Tough Sep. 1991 32 p
(AD-A243216; RSRE-Memo-4529; DRIC-BR-306218) Avail: NTIS HC/MF A03 CSCL 17/9

Two problems in the calculation of sea surface microwave scattering are analyzed in detail: the evaluation of the diffraction integral by invoking a two scale separation of the surface height spectrum and the calculation of the perturbation to the surface height spectrum by an internal wave modelled by a soliton. The results obtained reveal the physical content and increase the computational efficiency of these calculations. GRA

N92-17249# North Carolina Univ., Chapel Hill. Dept. of Chemistry.
A STUDY OF NONLINEAR REFLECTION AND OPTICAL SWITCHING IN INDIUM ANTIMONIDE
S. T. Feng and E. A. Irene Nov. 1991 24 p
(Contract N00014-89-J-1178)
(AD-A242835; TR-36) Avail: NTIS HC/MF A03 CSCL 20/6

Bistability in the reflected light from an indium antimonides surface has been observed without the use of a resonance cavity, and is explained by an increasing absorption positive feedback mechanism. Relying on this mechanism, we demonstrate a novel InSb optical switch which uses only the surface reflection and operates at room temperature using a pulsed carbon dioxide laser as the pump beam. The polarity of the switched out signal, the probe beam, was found to depend on the wavelength of the probe beam in the visible and near infrared range. This novel spectral dependence was used to demonstrate several optical logic elements. GRA

N92-17284# Naval Weapons Center, China Lake, CA.
NEW OPTICAL MATERIALS FOR THE LONG-WAVE (8-12 MICRONS) REGION: DESIGN CRITERIA FOR THE SOLID-STATE CHEMIST Technical Report, Oct. 1990 - Sep. 1991
T. A. Vanderah and C. K. Lowe-Ma Oct. 1991 6 p Submitted for publication
(Contract N00014-91WX-24046)
(AD-A243280; TR-6) Avail: NTIS HC/MF A02 CSCL 20/6

Certain applications that utilize long wavelength (8 to 12 micron) infrared (LWIR) windows require environmental durability and mechanical strength in addition to infrared optical transparency; i.e., the window materials must simultaneously serve as optical and structural ceramics. The fundamental requirement of optical transparency in the long wavelength region eliminates from consideration all well known ceramic materials such as oxides, nitrides, and other light anion compounds, making this a particularly difficult materials problem. The structure property relationships and chemical rationale used to guide both the screening of known compounds and the synthesis of new compounds likely to possess the desired properties rely on factors such as atomic mass, electronic configuration, coordination number, and crystal structure-type. The resulting criteria have directed our efforts in the synthesis and characterization of a number of ternary indium sulfide phases and calcium yttrium sulfide systems. GRA

N92-17294# Weapons Systems Research Lab., Adelaide (Australia).
EVALUATION OF A COMPACT CASSEGRAIN OPTICAL SYSTEM
S. G. Garner, R. A. Joyce, and R. P. Johnson Feb. 1991 15 p
(AD-A242985; WSRL-TM-5/91; DODA-AR-006-489) Avail: NTIS HC/MF A03 CSCL 20/6

A small Cassegrain optical system, with mirrors manufactured on an in-house aspheric surface generator, has been tested using visible radiation. The optical system performance was found to be limited by the relatively poor quality of the finish on the mirrors. It was also found that the design had to be modified to reduce stray light to acceptable levels, which reduced the effective aperture and degraded the diffraction limited resolution of the design. The resulting design may be suitable for those seeker applications requiring relatively low angular resolution from a small aperture, and in which small size and light weight are of paramount importance. GRA

N92-17485# Imperial Coll. of Science and Technology, London (England).
ENHANCED BACKSCATTERING OF LIGHT FROM RANDOMLY ROUGH DIFFUSERS: APPENDIX Final Report
Andrew J. Sant Sep. 1991 119 p
(Contract DAJA45-87-C-0039)
(AD-A243436; RD-5830-EE-01-App) Avail: NTIS HC/MF A06 CSCL 20/6

An investigation into scattering of light by randomly rough diffusers is presented. Emphasis is placed on the phenomenon of enhanced backscattering, i.e., when the brightness of the incoherently scattered light peaks sharply in the direction of the illuminating source. Both experimental and theoretical aspects of the problem are addressed, comparing real measurements with numerical calculations. The experimental equipment employed for this study is able to take light measurements close to the backscatter direction enabling the backscatter peak, if present, to be observed. Measurements taken from a Lambertian reflectance standard barium sulfate exhibit strong backscatter enhancement. A method of fabricating Gaussian, randomly rough diffusers is described. Their surface profiles are characterized using a Talystep profilometer and an analysis is presented of finite-tip-size effects on the measured statistical parameters. A replication method is described which faithfully reproduces the random profile of a fabricated diffuser. A rigorous, one-dimensional analysis based on the Helmholtz-Kirchhoff integral equation is presented. Numerical calculations are critically compared with scattered light measurements from identical, metallic, and dielectric diffusers, examining the influence of the medium on the diffusers' scattering properties. The effect of changing the radiation wavelength is also investigated. GRA

N92-17486# Imperial Coll. of Science and Technology, London (England).
ENHANCED BACKSCATTERING FROM ROUGH SURFACES Final Report, Jul. 1987 - Jul. 1990
J. C. Dainty 18 Oct. 1991 41 p
(Contract DAJA45-87-C-0039)
(AD-A243437; RD-5830-EE-01) Avail: NTIS HC/MF A03 CSCL 20/6

Some areas of discussion are as follows: Polarization dependence of dynamic light scattering by disordered media; Comparison of surface scattering between identical, randomly rough metal and dielectric diffusers; Experimental study of enhanced backscattering from one and two dimensional random rough surfaces; Light transmission from a randomly rough dielectric diffuser: theoretical and experimental results; Multiple scattering from random surfaces using the Kirchhoff approximation; The opposition effect in volume and surface scattering; Enhanced backscattering and transmission of light from random surfaces on semi-infinite substrates and thin films; and Measurements of light scattering by a characterized rough surface. GRA

N92-17536# Air Force Inst. of Tech., Wright-Patterson AFB, OH.
TOWARD THE ROBUST CONTROL OF HIGH BANDWIDTH HIGH PRECISION FLEXIBLE OPTICAL SYSTEMS Ph.D. Thesis
Kenneth W. Barker 1991 195 p
(AD-A243471; AFIT/CI/CIA-91-018D) Avail: NTIS HC/MF A09 CSCL 20/6

It is well known that control structure interaction (CSI) phenomena limit the stability and performance of controlled flexible structures. Most CSI research focuses on rigid body control of flexible structures with relatively low closed loop control bandwidths. This research examines the CSI phenomena associated with high bandwidth high precision control of a reaction actuator mounted to a flexible support structure. In particular, control structure interaction using a high gain porportional integral derivative (PID) controller is examined as it relates to certain design parameters. Rapid small angle line-of-sight repositioning and precision line-of-sight stabilization against a variety of disturbances are performed using both a single and multimode model. The single flexible mode model consists of a three-mass lightly damped translating system, referred to as the modified benchmark model. The multimode model consists of a single-axis reaction steering mirror mounted to the tip of a flexible truss-like support structure. Control-structure-interaction analysis of the reaction actuator control problem is performed first on the single-mode model as a function of flexible mode location, then with the multimode model as a function of inertial and elastic coupling between the reaction steering mirror and the flexible support structure. The analysis describes the control-structure-interaction effects on both stability and performance of a high gain line-of-sight PID controller. GRA

N92-17550# Environmental Research Inst. of Michigan, Ann Arbor. Advanced Concepts Div.
HIGH RESOLUTION IMAGING USING PHASE RETRIEVAL, VOLUME 2 Final Report, Aug. 1986 - Dec. 1989
J. R. Fienup, J. D. Gorman, J. H. Seldin, and J. N. Cederquist Oct. 1991 179 p
(Contract N00014-86-C-0587)
(AD-A242925; ERIM-196800-18-F-Vol-2) Avail: NTIS HC/MF A09 CSCL 17/5

This report describes a technique for obtaining fine-resolution images, suitable for SDI midcourse discrimination, using an inexpensive, lightweight telescope that would ordinarily yield a poor image. If, instead of collecting a blurred image with the telescope, one sends the light through an amplitude interferometer, then the modulus, but not the phase, of the Fourier transform of the object can be measured, despite the aberrations. We have developed and analyzed phase retrieval algorithms that recover the unknown Fourier phase, which allows a fine-resolution image to be reconstructed despite the aberrations of the telescope. It will also correct aberrations due to atmospheric turbulence for a ground-based telescope, and can be used with several other imaging modalities. For the case of interferometry through a partially obscured aperture, an algorithm was developed that combines phase retrieval with interpolation in order to restore the information at the missing spatial frequencies while retrieving the phase at the unobscured spatial frequencies. Another new phase retrieval algorithm, based on the Ayers/Dainty blind deconvolution algorithm, was also developed. A new methodology for exploring the uniqueness of phase retrieval in a practical sense was developed and tested. It involves finding the ambiguous image which is closest to a given image by a reduced-gradient search technique. The computational requirements for the phase retrieval algorithm were quantified. Laboratory experiments to test the technique were initiated. GRA

N92-17630# Carnegie-Mellon Univ., Pittsburgh, PA. Optical Data Processing.
OPTICAL ASSOCIATIVE PROCESSORS AND DIRECTED GRAPHS Annual Report, 1 Aug. 1990 - 31 Jul. 1991
David Casasent 1 Aug. 1991 52 p
(Grant AF-AFOSR-0355-90; AF Proj. 2305)

(AD-A242901; AFOSR-91-0819TR) Avail: NTIS HC/MF A04 CSCL 09/5

The thrust of this research concerns associative processors. Many new aspects exist in this effort: large storage capacity, use of storage density as a measure of efficiency, use of new output recollection vector encoding schemes, general 1:1 and pattern recognition many:1 associative processors, new algorithms and architectures, and applications and laboratory realization. GRA

N92-17658# Air Force Inst. of Tech., Wright-Patterson AFB, OH.

TRANSMISSION OF THIN LIGHT BEAMS THROUGH TURBULENT MIXING LAYERS Ph.D. Thesis

John B. Wissler 6 Sep. 1991 122 p

(AD-A243470; AFIT/CI/CIA-91-015D) Avail: NTIS HC/MF A06 CSCL 20/6

Light transmission through incompressible gaseous turbulent mixing layers is investigated with the objective of understanding the effects of large-scale coherent structures and mixing transition on the optical quality of the mixing layer. Experiments are done in a vertically flowing mixing layer which is enclosed inside a pressure tank and fed by two banks of high-pressure gas bottles. The study considers both the unequal density (high-speed Helium and low-speed Nitrogen) and equal density (high-speed N2 and low-speed He-Ar) cases; the mixing of dissimilar gases is the source of the optical aberrations. Large-scale Reynolds numbers range between 3500 and 80000 over pressures from 2 to 6 bar. Light transmission characteristics are first studied qualitatively using a network of thin sheets of short-exposure (about 1 microsec) white light which are aberrated by the mixing layer and then image directly onto photographic film. Light transmission characteristics are then studied quantitatively using a lateral effect detector to dynamically track a thin Helium-Neon laser beam as it wanders under the influence of the passing coherent structures. The study finds that the spanwise coherent structures generate systematic deflections of the light beam in the streamwise direction; the greatest deflections occur near the trailing edges of the structures at a formation called the cusp, where the high-speed fluid and low-speed fluid are entrained into the vortex core. GRA

N92-17675*# National Aeronautics and Space Administration. Pasadena Office, CA.

REAL-TIME EDGE-ENHANCED OPTICAL CORRELATOR Patent Application

Tsuen-Hsi Liu, inventor (to NASA) and Li-Jen Cheng, inventor (to NASA) (Jet Propulsion Lab., California Inst. of Tech., Pasadena.) 25 Nov. 1991 26 p

(Contract NAS7-918)

(NASA-Case-NPO-18379-1-CU; NAS 1.71:NPO-18379-1-CU; US-Patent-Appl-SN-797569) Avail: NTIS HC/MF A03 CSCL 20F

Edge enhancement of an input image by four-wave mixing a first write beam with a second write beam in a photorefractive crystal, GaAs, achieved for VanderLugt optical correlation with an edge enhanced reference image by optimizing the power ratio of a second write beam to the first write beam (70:1) and optimizing the power ratio of a read beam, which carries the reference image to the first write beam (100:701). Liquid crystal TV panels are employed as spatial light modulators to change the input and reference images in real time. NASA

N92-17690# ERG Systems, Inc., Saint James, NY.

FULL SURFACE TESTING OF GRAZING INCIDENCE MIRRORS Quarterly Report No. 5, 12 Jun. - 11 Dec. 1991

John L. Remo 11 Dec. 1991 82 p

(Contract N00014-90-C-0246)

(AD-A243734) Avail: NTIS HC/MF A05 CSCL 20/6

The goals of this project for the first year (first four quarters) have been achieved. These include: (1) prototype design; (2) procurement and testing of components; (3) mathematics and algorithm development; (4) interferogram data reduction algorithms; (5) construction of first prototype; and (6) automated operation software development. The fifth quarter and sixth quarter goals are: (1) construction and evaluation of a modified prototype; (2) integration of automated hardware controls and software; and (3) testing of the full surface interferometer on aspheric optical surfaces. GRA

N92-17711# Space Computer Corp., Santa Monica, CA.

OBJECT ACQUISITION AND TRACKING FOR SPACE-BASED SURVEILLANCE Final Report, Dec. 1988 - May 1990

27 Nov. 1991 100 p

(Contract N00014-89-C-0015)

(AD-A243333) Avail: NTIS HC/MF A05 CSCL 17/5

This report presents the results of research carried out by Space Computer Corporation under the U.S. government's Small Business Innovation Research (SBIR) Program. The work was sponsored by the Strategic Defense Initiative Organization and managed by the Office of Naval Research under Contracts N00014-87-C-0801 (Phase 1) and N00014-89-C-0015 (Phase 2). The basic purpose of this research was to develop and demonstrate a new approach to the detection of, and initiation of track on, moving targets using data from a passive infrared or visual sensor. This approach differs in very significant ways from the traditional approach of dividing the required processing into time dependent, object dependent, and data dependent processing stages. In that approach individual targets are first detected in individual image frames, and the detections are then assembled into tracks. That requires that the signal to noise ratio in each image frame be sufficient for fairly reliable target detection. In contrast, our approach bases detection of targets on multiple image frames, and, accordingly, requires a smaller signal to noise ratio. It is sometimes referred to as track before detect, and can lead to a significant reduction in total system cost. For example, it can allow greater detection range for a single sensor, or it can allow the use of smaller sensor optics. Both the traditional and track before detect approaches are applicable to systems using scanning sensors, as well as those which use staring sensors. GRA

N92-17736# Air Force Inst. of Tech., Wright-Patterson AFB, OH. School of Engineering.

OPTICAL IMAGE SEGMENTATION USING WAVELET CORRELATION M.S. Thesis

Steven D. Pinski Dec. 1991 112 p

(AD-A243650; AFIT/GEO/ENG/91D-3) Avail: NTIS HC/MF A06 CSCL 20/6

This research introduces an optical method of segmenting potential targets using wavelet analysis. Implementation of an optical Harr wavelet is fulfilled using a magneto-optic spatial light modulator (MOSLM). Two methods of controlling wavelet dilation are explored: (1) spatial filtering of a ternary modulated MOSLM; and (2) a single aperture positioned in front of a binary modulated MOSLM. Segmentation is performed through Vander Lugt correlation of a binarized image with a binarized optical wavelet. Three different image binarization methods are investigated for use in the correlation scheme: (1) average pixel value over an entire scene; (2) localized 4 x 4 pixel average followed by an average pixel value over the remaining scene; and (3) localized 3 x 3 pixel average ANDed with an energy pixel value over the entire scene. Frequency-plane masks necessary for the correlation process are generated using thermal holography. Results show image segmentation for six possible experimental methods comprised of wavelet dilation and binarization techniques. The most successful correlation design used a single aperture to control wavelet dilation and binarization based on a localized 4 x 4 pixel average followed by an average pixel value over the remaining scene. Author (GRA)

N92-17828 Department of the Navy, Washington, DC.

PRECISION MULTI-CHANNEL FIBER OPTIC INTERFACE AND METHOD Patent

Gerald E. Holmberg, inventor (to Navy) and Roger L. Morency, inventor (to Navy) 2 Jul. 1991 7 p Filed 27 Jun. 1990

(AD-D015104; US-Patent-5,028,112; US-Patent-Appl-SN-544556; US-Patent-Class-350-96.20) Avail: US Patent and Trademark Office CSCL 20/6

Methods are disclosed for forming precision, fiber optic interfaces, and a precision, fiber optic interface is disclosed in accordance therewith. An electroformed disk is disclosed to provide fiber alignment, and electrical discharge machining (EDM) is disclosed to provide accurate angular alignment of optical fibers at a planar optical interface. In one method embodiment, a combination of EDM, an alignment bushing and an electroformed disk are used to fashion a precision multi-channel fiber optic interface, and in one interface and method embodiment, two electroformed disks are used to provide a precision, multi-channel fiber optic interface. GRA

N92-17846# Lawrence Livermore National Lab., CA.
CORRELATOR OPTICAL WAVEFRONT SENSOR COWS
Feb. 1991 43 p Prepared in cooperation with Phillips Lab., Kirtland AFB, NM; Schafer (W.J.) Associates, Inc., Albuquerque, NM
(Contract W-7405-eng-48)
(DE92-003964; UCRL-CR-108459) Avail: NTIS HC/MF A03

This report documents the significant upgrades and improvements made to the correlator optical wavefront sensor (COWS) optical bench during this phase of the program. Software for the experiment was reviewed and documented. Flowcharts showing the program flow are included as well as documentation for programs which were written to calculate and display Zernike polynomials. The system was calibrated and aligned and a series of experiments to determine the optimum settings for the input and output MOSLM polarizers were conducted. In addition, design of a simple aberration generation is included. DOE

N92-17863*# National Aeronautics and Space Administration. Lyndon B. Johnson Space Center, Houston, TX.
CLOSED-LOOP MOTOR CONTROL USING HIGH-SPEED FIBER OPTICS Patent Application
Reginald Dawson, inventor (to NASA) and Dagobert Rodriquiz, inventor (to NASA) (Lockheed Engineering and Sciences Co., Houston, TX.) 22 Oct. 1991 26 p
(NASA-Case-MSC-21806-1; NAS 1.71:MSC-21806-1; US-Patent-Appl-SN-780513) Avail: NTIS HC/MF A03 CSCL 20F

A closed-loop control system for controlling the operation of one or more servo motors or other controllable devices is described. The system employs a fiber optics link immune to electromagnetic interference, for transmission of control signals from a controller or controllers at a remote station to the power electronics located in proximity to the motors or other devices at the local station. At the remote station the electrical control signals are time-multiplexed, converted to a formatted serial bit stream, and converted to light signals for transmission over a single fiber of the fiber optics link. At the local station, the received optical signals are reconstructed as electrical control signals for the controlled motors or other devices. At the local station, an encoder sensor linked to the driven device generates encoded feedback signals which provide information as to a condition of the controlled device. The encoded signals are placed in a formatted serial bit stream, multiplexed, and transmitted as optical signals over a second fiber of the fiber optic link which closes the control loop of the closed-loop motor controller. The encoded optical signals received at the remote station are demultiplexed, reconstructed and coupled to the controller(s) as electrical feedback signals. NASA

N92-17864*# National Aeronautics and Space Administration. Pasadena Office, CA.
NEAR REAL-TIME STEREO VISION SYSTEM Patent Application
Larry H. Matthies, inventor (to NASA) and Charles H. Anderson, inventor (to NASA) (Jet Propulsion Lab., California Inst. of Tech., Pasadena.) 18 Dec. 1991 55 p
(Contract NAS7-918)
(NASA-Case-NPO-18593-1-CU; NAS 1.71:NPO-18593-1-CU; US-Patent-Appl-SN-812901) Avail: NTIS HC/MF A04 CSCL 20F

The apparatus for a near real-time stereo vision system for use with a robotic vehicle is described. The system is comprised of two cameras mounted on three-axis rotation platforms, image-processing boards, a CPU, and specialized stereo vision algorithms. Bandpass-filtered image pyramids are computed, stereo matching is performed by least-squares correlation, and confidence ranges are estimated by means of Bayes' theorem. In particular, Laplacian image pyramids are built and disparity maps are produced from the 60 x 64 level of the pyramids at rates of up to 2 seconds per image pair. The first autonomous cross-country robotic traverses (of up to 100 meters) have been achieved using the stereo vision system of the present invention with all computing done onboard the vehicle. The overall approach disclosed herein provides a unifying paradigm for practical domain-independent stereo ranging. NASA

N92-17892*# National Aeronautics and Space Administration. Pasadena Office, CA.
WIDE FIELD STRIP-IMAGING OPTICAL SYSTEM Patent Application
Arthur H. Vaughan, inventor (to NASA) (Jet Propulsion Lab., California Inst. of Tech., Pasadena.) 1 Nov. 1991 37 p
(Contract NAS7-918)
(NASA-Case-NPO-18146-1-CU; NAS 1.71:NPO-18146-1-CU; US-Patent-Appl-SN-786618) Avail: NTIS HC/MF A03 CSCL 20F

A strip imaging wide angle optical system is provided. The optical system is provided with a 'virtual' material stop to avoid aberrational effects inherent in wide angle optical systems. The optical system includes a spherical mirror section for receiving light from a 180 deg strip or arc of a target image. Light received by the spherical mirror section is reflected to a frustoconical mirror section for subsequent rereflection to a row of optical fibers. Each optical fiber transmits a portion of the received light to a detector. The optical system exploits the narrow cone of acceptance associated with optical fibers to substantially eliminate vignetting effects inherent in wide angle systems. Further, the optical system exploits the narrow cone of acceptance of the optical fibers to substantially limit spherical aberration. The optical system is ideally suited for any application wherein a 180 deg strip image need be detected, and is particularly well adapted for use in hostile environments such as in planetary exploration. NASA

N92-17959 Department of the Navy, Washington, DC.
OPTICAL FIBER MAGNETOMETER Patent
John F. Scarzello, inventor (to Navy) and Jack Finkel, inventor (to Navy) 6 Aug. 1991 5 p Filed 22 Apr. 1985
(AD-D015133; US-Patent-5,038,103; US-Patent-Appl-SN-725709; US-Patent-Class-324-244) Avail: US Patent and Trademark Office CSCL 17/6

An optical fiber magnetometer having omnidirectional capability is disclosed herein for measuring a total magnetic field independent of its physical orientation or the direction of the field or fields. A relatively long optical fiber defining a sensing arm for exposure to a magnetic field is wound in the form of a spheroid (like rubber bands on a golf ball or yarn threads on a baseball) to provide optical lengths of substantially the same total length in every direction through the spheroid winding. The plane of polarization of light transmitted through the optical fiber winding is caused to rotate (Faraday effect) when the fiber or components thereof is exposed parallel to a magnetic field. The extent of plane rotation is determined, inter alia, by the total magnetic field passing through the spheroid winding. Author (GRA)

N92-17418*# Jet Propulsion Lab., California Inst. of Tech., Pasadena. High Speed Optical Systems Group.
OPTICAL PROTOCOLS FOR ADVANCED SPACECRAFT NETWORKS
Larry A. Bergman *In* NASA, Washington, Beyond the Baseline 1991: Proceedings of the Space Station Evolution Symposium. Volume 1: Space Station Freedom, Part 2 Sep. 1991 p 583-63 (For primary document see N92-17409 08-18)
Avail: NTIS HC/MF A16 CSCL 20F

75 PLASMA PHYSICS

Includes magnetohydrodynamics and plasma fusion. For ionospheric plasmas see *46 Geophysics*. For space plasmas see *90 Astrophysics*.

N92-17030# Naval Postgraduate School, Monterey, CA.
EXPLORING PLASMA SHEATH SOLUTIONS FOR PLANAR AND CYLINDRICAL ANODES M.S. Thesis
George S. Brown Dec. 1991 100 p
(AD-A243237) Avail: NTIS HC/MF A05 CSCL 20/9

Anode sheaths impact the operation of many practical plasma devices. This complex region is explored in detail for collisional, isothermal (identical specie temperatures), low-temperature plasmas, where sheath dimensions are in the micron range. The selected approach involves postulation of a specific electric field distribution with two shape factors. Previous research regarding planar anodes is verified and expanded upon using greater parameter ranges. 'Z', a dimensionless quantity specifying plasma composition and condition, groups diverse plasmas into 'families' exhibiting similar sheath characteristics. Eta, a nondimensional ratio of electrical energy to thermal energy in the sheath, allows temperature effects to be studied. The investigation focuses on three disparate plasma families that span a range of 1.1729 to 2,1493, at eta values defined by plasma temperatures of 6000 K, 3000 K, and 3000 K. Results indicate that at lower temperatures, charge production in the outer sheath is generic to the electric field distribution, and that the sheaths themselves are nearly unaffected by substantial changes in temperature (i.e., eta). Conversely, sheath density and extent are shown to vary significantly for differing z values. Newly-derived equations governing cylindrical anodes generate sheaths that are virtually identical to corresponding planar cases. It is shown that only those anodes whose radii are comparable to the plasma's characteristic radius (gamma) must be treated with the cylindrical formulation; non-vacuous plasmas would require micron-width anodes to be thus affected. Finally, an analytical approach yields solutions that confirm the numerical results and offers an algebraic approximation for high-eta plasmas. GRA

N92-17301# Boston Coll., Chestnut Hill, MA.
EQUATION OF STATE AND CONDUCTIVITY OF HOT, DENSE MATTER Final Report, 15 Apr. 1989 - 31 Dec. 1990
Gabor J. Kalman 31 Dec. 1990 6 p
(Contract N00014-89-K-2021)
(AD-A243359) Avail: NTIS HC/MF A02 CSCL 20/9

The purpose of the research program reported here was to develop and apply a novel method to the calculation of the Equation of State (EOS), Mean Charge State (MCS) (or degree of ionization) and conductivity of dense plasmas of moderately high Z-numbers (Z less than 30). The method to be applied was the Thomas-Fermi model, modified and adapted to the dense plasma environment. The innovative elements of the approach are: (1) the plasma environment is represented by the ion-ion and ion-electron correlation functions as source densities in the TF equation; (2) the bound electron density is posited to be zero at the ion boundary - this gives a reasonably defined ion radius, separates free and bound electrons and eliminates both the unphysical extra pressure due to bound electrons (characteristic to the so-called Confined Alom model) and the infinite ion radius (characteristic to the TF-Debye model); (3) the MCS is determined by minimizing the free energy (F) of the combined TF-ion/plasma system, with the proper inclusion of all electron-electron, electron-ion, ion-ion correlations; and (4) the method can be combined with the approach of Davis and Blaha, who solved the exact Schrodinger equation for the valence electron in the TF-potential of the core electrons. GRA

N92-17456# General Atomic Co., San Diego, CA.
THE CHARGE EXCHANGE RECOMBINATION DIAGNOSTIC SYSTEM ON THE D3-D TOKAMAK
P. Gohil, K. H. Burrell, R. J. Groebner, J. Kim, W. C. Martin, E. L. McKee, and R. P. Seraydarian Nov. 1991 6 p Presented at the 14th IEEE Symposium on Fusion Engineering, San Diego, CA, 30 Sep. - 3 Oct. 1991
(Contract DE-AC03-89ER-51114)
(DE92-003805; GA-A-20652; CONF-910968-47) Avail: NTIS HC/MF A02

The charge exchange recombination (CER) diagnostic system on the DIII-D tokamak is used to make spatially and temporally resolved measurements of the ion temperature and toroidal and poloidal rotation velocities. This is performed through visible spectroscopic measurements of the Doppler broadened and Doppler shifted HE II 468.6 nm, the CVI 529.1 nm, and the BV 494.5 nm spectral lines which have been excited by charge exchange recombination interactions between the fully stripped ions and the neutral atoms from the heating beams. The plasma viewing optics comprises 32 viewing chords spanning a typical plasma minor radius of 63 cm across the midplane, of which 15 spatial chords span 4.2 cm at the plasma edge just within the separatrix and provide a chord-to-chord spatial resolution of 0.3 cm. Fast camera readout electronics can provide a temporal resolution of 260 microsec per time slice, but the effective minimum integration time, at present, is 1 ms which is limited by the detected photon flux from the plasma and the decay times of the phosphors used on the multichannel plate image intensifiers. Significant changes in the edge plasma radial electric field at the L-H transition have been observed, as determined from the CER measurements, and these results are being extensively compared to theories which consider the effects of sheared electric fields on plasma turbulence. DOE

N92-17469# Edgerton, Germeshausen and Grier, Inc., Idaho Falls, ID.
EXPERIMENTAL MEASUREMENTS OF PLASMA PROPERTIES FOR MILLER SG-100 TORCH WITH MACH I SETTING
W. L. T. Chen, J. Heberlein, and E. Pfender (Minnesota Univ., Minneapolis.) Oct. 1991 58 p
(Contract DE-AC07-76ID-01570)
(DE92-003309; EGG-SCM-9576) Avail: NTIS HC/MF A04

In this work, measurements of plasma properties, including the fields of temperature, velocity, and plasma composition have been completed for the Miller SG-100 plasma torch using argon-helium mixtures with the Mach 1 nozzle at 1 atm pressure. A computer-controlled system combining both spectroscopic and enthalpy probe diagnostics has been developed to allow temperature measurements covering a range from 2000-16000 K which includes the plasma flame region which is of interest. The experimental results expose the dominant effects in different spatial areas of argon-helium plasma jets. In the center near the nozzle exit, the temperatures exceed 10,000 K, and strong diffusion exists due to the steep radial gradients of temperature and particle number densities. In the jet tail region where the temperatures are well below 10,000 K and decay in axial and radial direction, the dominant effects in this area are strong cold gas entrainment associated with turbulence. Substantial discrepancies between temperatures evaluated from spectroscopic and enthalpy probe data are particularly severe in the jet fringes indicating that strong deviations from LTE may exist in the jet fringes. In addition, entrainment of the cold surrounding gas into the plasma jet causes severe discrepancies between spectrometric and enthalpy probe data. The validity of the two diagnostic methods will be discussed. The temperature profiles in argon-helium plasma jets are flatter and wider, and the velocities are higher than in a pure argon plasma jet. These features of argon-helium plasma jets may be beneficial for obtaining better performance in the plasma spraying process. DOE

N92-17499# Naval Research Lab., Washington, DC.
SOME ASPECTS OF NONNEUTRAL PLASMA PHYSICS Memorandum Report
Wallace M. Manheimer 18 Dec. 1991 16 p
(AD-A243711; NRL-MR-6912) Avail: NTIS HC/MF A03 CSCL 20/9

This memo considers several aspects of nonneutral plasma physics including the use of cold nonneutral plasmas as sources

for high brightness electron beams, the molecular dynamic or Monte Carlo simulation of large isolated plasmas, and the adiabatic compression of toriodal plasma clouds. GRA

N92-17556# National Academy of Sciences - National Research Council, Washington, DC. Commission on Physical Sciences, Mathematics, and Applications.
PLASMA PROCESSING OF MATERIALS: SCIENTIFIC OPPORTUNITIES AND TECHNOLOGICAL CHALLENGES
Susan Maurizi, ed. and Anne Simmons, ed. 1991 84 p Original contains color illustrations
(Contracts N00014-89-J-1728; N60921-91-M-3233; NSF ECS-89-22375; NSF PHY-88-14509)
(LC-91-66812; ISBN-0-309-04597-5) Avail: NTIS HC/MF A05

The focus is on plasma processing, a technology that impacts and is of vital importance to several of the largest manufacturing industries in the world. Characterized here are different kinds of plasmas. Emphasis is placed on the properties of man-made low-energy, highly collisional plasmas that are particularly useful in materials processing applications. A summary of the many industrial applications of plasma-based systems for processing materials is given. Plasma processing of electronic materials and, in particular, the use of plasmas in fabricating microelectronic components are discussed. The state of science that underpins plasma processing technology in the United states is outlined. The challenges and opportunities associated with providing a science education in the area of plasma processing are addressed. Author

N92-17606# California Univ., Berkeley. Dept. of Nuclear Engineering.
COOPERATIVE PROGRAM TO ANALYZE HEAT TRANSPORT AT HIGH BETA IN DIII-D
T. K. Fowler, ed. and T. K. Kurki-Suonio, ed. 1991 12 p
(Contract DE-FG03-89ER-51116)
(DE92-003545; DOE/ER-51116/1) Avail: NTIS HC/MF A03

This report discusses research in the following areas: ion temperature analysis; thermal transport in DIII-D; particle transport in DIII-D; divertor design; noncircular geometry; and TAE-mode. DOE

N92-17635# National Inst. of Standards and Technology, Boulder, CO.
LIQUID AND SOLID ION PLASMAS Annual Report, 1 Oct. 1990 - 31 Sep. 1991
D. J. Wineland and J. J. Bollinger 15 Sep. 1991 8 p
(Contract N00014-89-F-0020)
(AD-A242029) Avail: NTIS HC/MF A02 CSCL 20/9

Atomic ions which are stored in electromagnetic fields are an example of nonneutral plasmas. Laser techniques allow control of plasma angular momentum and provide plasma cooling to temperatures much less than 1K. Using imaging techniques, plasma spatial information is achieved. Laser spectroscopic techniques allow measurement of plasma velocity distribution functions. Liquid and solid behavior of ion plasmas are studied. GRA

N92-17664# MSE, Inc., Butte, MT.
MAGNETOHYDRODYNAMIC PROJECTS AT THE CDIF
1991 17 p
(Contract DE-AC07-88ID-12735)
(DE92-002636; DOE/ID-12735/T19) Avail: NTIS HC/MF A03

This quarterly technical progress report presents the tasks accomplished at the Component Development and Integration Facility during the second quarter of FY91. Areas of technical progress this quarter included: coal system development; seed system development; test train/A-Bay modifications; channel power dissipation and distribution system development; oxygen system storage upgrade; iron-core magnet thermal protection system checkout; TRW slag rejector/CDIF slag removal project; Data Acquisition System; stack gas/environmental compliance upgrade; coal-fired combustor support; 1A channels fabrication and assembly; support of Mississippi State University diagnostic testing; test operations and results; data analysis and modeling; technical papers; and projected activities. DOE

N92-17706# Department of the Navy, Washington, DC.
PLASMA CHEMICAL VAPOR DEPOSITION OF HALIDE GLASSES Patent Application
Lynda E. Busse, inventor (to Navy and Ishwar D. Aggarwal, inventor (to Navy) 27 Jun. 1991 16 p
(AD-D015060; US-Patent-Appl-SN-722447; Navy-Case-70998)
Avail: NTIS HC/MF A03 CSCL 11/2

The present invention described herein relates to the field of preparing preforms which are used to make optical fibers. More specifically, the invention relates to making preforms for halide glass fibers. The invention especially relates to making preforms for fluoride glass fibers. Simple chemical vapor deposition processes are well known in the manufacture of silica fibers. More specifically, simple chemical vapor deposition process are well known in the manufacture of fluoride glass fibers for low attenuation and good transmission beyond 2 microns, that is, in the infrared range. In such processes, organometallic precursors of BeF2 and AlF3 are volatilized and carried by an inert gas into a silicate glass tube. There the precursors break down, yielding the fluoride products which deposit on the inner wall of the tube, while the remaining products flow out the exhaust. GRA

N92-17734# Office of Naval Research, Arlington, VA.
WORKSHOP ON PLASMA EXPERIMENTS IN THE LABORATORY AND IN SPACE. ABSTRACTS
1991 59 p
(AD-A243645) Avail: NTIS HC/MF A04 CSCL 20/4

The current status of plasma experimental science is reviewed by presenting sets of laboratory configurations and measurement techniques which, when combined together, afford reasonably complete control and description of the plasma state. Examples include linear and toroidal plasma research devices; modern diagnostics, with emphasis on high resolution techniques adapted from atomic, laser and detector physics; and a selected number of new plasma processes which have been covered through their uses. GRA

N92-17792# California Univ., Los Angeles.
UCLA PROGRAM IN REACTOR STUDIES: THE ARIES TOKAMAK REACTOR STUDY
1991 9 p
(Contract DE-FG03-86ER-52126)
(DE92-003760; DOE/ER-52126/T1) Avail: NTIS HC/MF A02

The ARIES research program is a effort to develop several visions of tokamak reactors with enhanced economic, safety, and environmental features. The aims are to determine the potential economics, safety, and environmental features of a range of possible tokamak reactors, and to identify physics and technology areas with the highest leverage for achieving the best tokamak reactor. Four ARIES visions are currently planned for the ARIES program. The ARIES-1 design is a DT-burning reactor based on 'modest' extrapolations from the present tokamak physics database and relies on either existing technology or technology for which trends are already in place, often in programs outside fusion. ARIES-2 and ARIES-4 are DT-burning reactors which will employ potential advances in physics. The ARIES-2 and ARIES-4 designs employ the same plasma core but have two distinct fusion power core designs; ARIES-2 utilize the lithium as the coolant and breeder and vanadium alloys as the structural material while ARIES-4 utilizes helium is the coolant, solid tritium breeders, and SiC composite as the structural material. Lastly, the ARIES-3 is a conceptual (3)D-He reactor. During the period Dec. 1, 1990 to Nov. 31, 1991, most of the ARIES activity has been directed toward completing the technical work for the ARIES-3 design and documenting the results and findings. We have also completed the documentation for the ARIES-1 design and presented the results in various meetings and conferences. During the last quarter, we have initiated the scoping phase for ARIES-2 and ARIES-4 designs. DOE

N92-17793# Science Applications International Corp., McLean, VA.
THEORETICAL STUDIES IN TOKAMAKS: THREE-DIMENSIONAL SIMULATION OF LOWER HYBRID WAVE LAUNCHING IN TOKAMAKS
W. Grossmann 1991 4 p
(Contract DE-AC03-88ER-53270)
(DE92-003773; DOE/ER-53270/T1) Avail: NTIS HC/MF A01

Efforts during 1990 focused on two of the major issues on ICH of tokamak plasmas: 3-D numerical simulations of RF antennae, and the 2-D simulations and theory of plasma sheaths around Faraday shields. DOE

N92-17805# International Centre for Theoretical Physics, Trieste (Italy).
ON THE GENERATION OF LARGE-AMPLITUDE PLASMA WAKEFIELDS WITH LOW PHASE VELOCITIES BY AN INTENSE SHORT LASER PULSE
I. G. Murusidze and L. N. Tsintsadze Jun. 1991 7 p
(DE92-609543; IC-91/109) Avail: NTIS HC/MF A02

The problem of propagating large-amplitude laser pulses through plasmas has many unresolved issues. One of them is a group velocity of such pulses. We demonstrate that Gaussian pulses with lower amplitudes and lower group velocities are able to generate the wakefields having greater amplitudes than wakefields produced by Gaussian pulses with higher amplitudes but phase velocities close to the speed of light. DOE

N92-17806# International Centre for Theoretical Physics, Trieste (Italy).
ALFVEN WAVES IN INHOMOGENEOUS MAGNETIC FIELDS: AN INTEGRO-DIFFERENTIAL EQUATION FORMULATION
C. Uberoi and Z. Sedlacek Jun. 1991 6 p
(DE92-609544; IC-91/121) Avail: NTIS HC/MF A02

An integro-differential formulation for the equation governing the Alfven waves in inhomogeneous magnetic fields is shown to be similar to the polyvibrating equation of Mangeron. Exploiting this similarity, a time-dependent solution for smooth initial conditions is constructed. The important feature of this solution is that it separates the parts giving the Alfven wave oscillations of each layer of plasma and the interaction of these oscillations representing the phase mixing. DOE

N92-17933# Pennsylvania State Univ., University Park.
A ONE-DIMENSIONAL PLASMA AND IMPURITY TRANSPORT MODEL FOR REVERSED FIELD PINCHES Ph.D. Thesis
R. Veerasingam Nov. 1991 215 p
(Contract DE-FG02-87ER-53252)
(DE92-004691; DOE/ER-53252/28) Avail: NTIS HC/MF A10

In this thesis a one-dimensional (1-D) plasma and impurity transport model is developed to address issues related to impurity behavior in Reversed Field Pinch (RFP) fusion plasmas. A coronal non-equilibrium model is used for impurities. The impurity model is incorporated into an existing one dimensional plasma transport model creating a multi-species plasma transport model which treats the plasma and impurity evolution self-consistently. Neutral deuterium particles are treated using a one-dimensional (slab) model of neutral transport. The resulting mode, RFPBI, is then applied to existing RFP devices such as ZT-40M and MST, and also to examine steady state behavior of ZTH based on the design parameters. A parallel algorithm for the impurity transport equations is implemented and tested to determine speedup and efficiency. DOE

N92-17968# Allied-Signal Aerospace Co., Kansas City, MO.
SELECTIVE PLASMA ETCHING
G. W. Franti Dec. 1991 14 p
(Contract DE-AC04-76DP-00613)
(DE92-004794; KCP-613-4480) Avail: NTIS HC/MF A03

Plasma etching of silicon nitride glassivation layers on silicon dice using CF4 was successfully carried out with a commercial plasma etcher. The parameters of power level and partial pressure gas were downscaled from the commercial plasma etcher to a bench-top plasma etcher. Plasma etching of silicon nitride was successfully performed in the bench-top plasma etcher. DOE

76 SOLID-STATE PHYSICS

Includes superconductivity.

For related information, see also *33 Electronics and Electrical Engineering* and *36 Lasers and Masers.*

N92-16984# Cornell Univ., Ithaca, NY.
INNOVATIVE OPTOELECTRONIC MATERIALS AND STRUCTURES USING OMVPE Annual Report, 1 Jan. - 25 Nov. 1991
James R. Shealy 25 Nov. 1991 18 p
(Contract N00014-89-J-1311)
(AD-A243257) Avail: NTIS HC/MF A03 CSCL 20/12

An advanced OMVPE process is being developed for the deposition of III-V semiconductor materials and structures. There are important optoelectronic device structures which can not be realized by conventional means. These include AlGaAs semiconductor lasers with improved coherence using embedded diffraction gratings, and GaInP pseudomorphic structures on GaP substrates for short wavelength semiconductor lasers. The structure on GaP result in improved laser performance compared to the 650 nm AlGaInP devices previously developed in this program. The new OMVPE apparatus combines the multichamber reaction cell with deep UV photo-assisted growth and modulation flow epitaxial techniques. Using a combination of such processes, the growth temperature requirements for III-V alloys can be substantially reduced. Selective growth on a submicron scale will be attempted with in-situ interference holography. The materials and techniques developed in this research program will result in significant simplifications to the fabrication sequence required to realize complex integrated optoelectronic circuits. GRA

N92-16995# Harry Diamond Labs., Adelphi, MD.
THEORETICAL CRYSTAL-FIELD CALCULATIONS FOR RARE-EARTH IONS IN 3-5 SEMICONDUCTOR COMPOUNDS Summary Report, Jan. - Jul. 1991
Sally B. Stevens and Clyde A. Morrison Oct. 1991 29 p
(AD-A243098; HDL-TM-91-16) Avail: NTIS HC/MF A03 CSCL 09/1

This report presents preliminary crystal-field calculations showing the splitting of the Stark levels of three rare-earth-doped III-V semiconductor compounds: Yb3+: InP, Er+3:GaAs, and Nd3+:GaP. The crystal field parameters were obtained from a lattice-sum calculation including monopole, self-induced dipole, and self-induced quadruple contributions. The effects of varying the effective ionic charges and the ionic polarizabilities are explored. For each of the systems considered, these parameters were adjusted to match available experimental data on the ordering of the levels according to irreducible representation, the magnitude of crystal-field splitting, and intensities. A consistent set of parameters was found that gave reasonable results for all the systems considered. Refinements in the crystal field model may be necessary when more experimental data become available. GRA

N92-17015# Air Force Academy, CO.
CRITICAL TEMPERATURE DETERMINATION IN SUPERCONDUCTORS Final Report
Brian A. Doyle and Matthew G. McHarg Oct. 1991 27 p
(AD-A243537; USAFA-TR-91-17) Avail: NTIS HC/MF A03 CSCL 20/12

This project is based on a program that uses FORTRAN 77 to analyze resistance versus temperature data. The data are fit by two lines with different slopes and intercepts. A total chi-square for the fits is obtained. When the total chi-square is minimized, the critical temperature is assigned to the point where the data are broken into the intersecting two lines. The program also informs the user of the temperature at which those lines intersect. A

sensitivity study was performed to find the relationship between uncertainties in the resistance and critical temperature. This analysis showed the resistance needed to be measured with less than 5 percent error to allow the Tc to be found with an error of three Kelvins. Author (GRA)

N92-17082# Army Lab. Command, Watertown, MA. Material Technology Lab.
EXAMINING Si3N4 BASE MATERIALS WITH VARIOUS RARE EARTH ADDITIONS Final Report
George E. Gazza Dec. 1991 24 p
(DA Proj. 1L1-62105-AH-84)
(AD-A243668; MTL-TR-91-45) Avail: NTIS HC/MF A03 CSCL 20/2

Silicon nitride base compositions were prepared by using various rare earth oxide additives and hot pressing the powders to full density. Compositions were primarily explored in Si3N4-SiO2-RE2Si2O7 compatibility regions although other Si3N4-RE2O3 reactions were also investigated. Hot pressing densification data and high temperature behavior of the various silicon nitride rare earth compositional systems are examined. GRA

N92-17181# Puerto Rico Univ., Rio Piedras. Dept. of Physics.
IN SITU SURFACE X RAY CRYSTALLOGRAPHY OF ELECTROCHEMICALLY DEPOSITED Bi ON Ag(111): STRUCTURE, COMPRESSIBILITY, AND ANISOTROPY Summary Report
D. Yee, M. F. Toney, M. G. Samant, D. G. Wiesler, and L. B. Sorensen 29 Jan. 1991 14 p
(Contract N00014-90-J-1263)
(AD-A243218; TR-11) Avail: NTIS HC/MF A03 CSCL 07/4

We have performed in-situ x-ray diffraction measurements on an underpotentially deposited monolayer of Bismuth on Silver (111). The Bi forms a two-dimensional nearly centered rectangular structure that is uniaxially commensurate with the Silver (111) surface. The Bi monolayer compresses uniaxially along the incommensurate direction. Neither the Bi structure nor its compressibility is affected by the presence or absence of chloride in the electrolyte. Initial crystallographic analysis reveals that the nearly centered atom is displaced by approximately 0.35 A along the commensurate direction, and that the atomic disorder in the monolayer is anisotropic. GRA

N92-17182# Naval Weapons Center, China Lake, CA.
GROWTH OF NEAR-FREE-STANDING YBa2Cu3O7-TYPE CRYSTALS USING A SELF-DECANTING FLUX METHOD Technical Report No. 1, Oct. 1990 - Apr. 1991
T. A. Vanderah, C. K. Lowe-Ma, D. E. Bliss, M. W. Decker, and M. S. Osofsky May 1991 35 p
(AD-A243221) Avail: NTIS HC/MF A03 CSCL 20/2

Large (multi-millimeter-sized) near-free-standing platelets of YBa2Cu3O(x) have been obtained using a self-decanting flux method. The charge composition consists of 10.2 wt percent YBa2Cu3O7 in a 0.28:0.72 molar BaO:CuO flux-mixture induced to decant by a thermal gradient. After oxygen annealing, crystals display sharp Tc values near 92 K. Crystals of ten of the RBa2Cu3Ox congeners, R = Pr, Nd, Sm, Eu, Gd, Dy, Ho, Er, Tm, And Yb, were also grown using the method described. Preliminary experiments were successful in adapting the procedure to the Nd(1.85)Ce(0.15)CuO4 system and yielded small, superconducting (Tc greater than 20 K) platelets after Ar-annealing. For the YBa2Cu3O(x) system, an oxygen annealing study was conducted in order to determine the best conditions for the reliable production of crystals with optimized superconducting properties. GRA

N92-17218# Naval Weapons Center, China Lake, CA.
EVIDENCE FOR STRONG ELECTRON-PHONON COUPLING IN THERMAL CONDUCTIVITY OF YBa2Cu3O(7-DELTA) Technical Report No. 7, Oct. 1990 - Sep. 1991
Joshua L. Cohn, Stuart A. Wolf, and Terrell A. Vanderah Oct. 1991 19 p
(AD-A243192) Avail: NTIS HC/MF A03 CSCL 20/13

We have measured the ab plane thermal conductivity (k) on single crystal YBa2Cu3O(7-delta) (delta approx. = 0.08) in the temperature range 10 K less than or equal to T less than or equal to 300 K. Our main focus is an analysis of the slope change in k(T) which occurs just below the superconducting transition. The reduced temperature (t=T/T(sub c)) derivative of the normalized thermal conductivity, as determined from the data, is rather small, less than or equal to 1.1. From measurements of the electrical conductivity on the same specimens and application of the Wiedemann-Franz Law we determine the relative contributions to the heat conduction from the carriers and the lattice, and discuss the normal-state phonon scattering mechanisms. Employing these results we calculate the slope of the lattice thermal conductivity at Tc and infer that the slope of the carrier conductivity must be very large, less than or equal to 6. This result implies strong coupling for some of the carriers. GRA

N92-17219# Naval Weapons Center, China Lake, CA.
A REEXAMINATION OF F-19 NMR IN SELECTED SOLIDS, THE CONDUCTOR Ag2F AND REFERENCE INSULATORS FOR STUDIES OF YBa2Cu3O7-TYPE SUPERCONDUCTORS Technical Report No. 3, Oct. 1990 - Sep. 1991
Hongjun Pan, B. C. Gerstein, Hans R. Loeliger (Ciba-Geigy, Proprietary Ltd., Biel, Switzerland), and T. A. Vanderah Oct. 1991 30 p
(AD-A243194) Avail: NTIS HC/MF A03 CSCL 20/5

Evidence of incorporated F in the so called '1-2-3-type', YBa2Cu3O7 derived compounds has been cited. The aim was to confirm an increase in Tc as Ovshinsky claimed in 1987 by substitution of F for O. One expects for the 1-2-3-type compounds, since they display metallic conductivity at room temperature, a downfield-shifted F NMR resonance. As a guideline for judging the line positions and shapes of fluorine incorporated in the 1-2-3-type compounds, we therefore reexamined the (19)F NMR signals in a metallic inorganic conductor (Ag2F), in the insulating starting materials used to synthesize the superconductor phases (YOF, EuOF, and YF3) and in BaF2 and CuF2 which could be formed during the synthesis. AgF and KF were used as reference samples. There appear to be only two inorganic compounds containing fluorine and showing high metallic conductivity: (1) Silver subfluoride, Ag2F, with NMR results reported by Nishihara et al., and (2) Ag7O8(+) and HF2(-) reported by Hindermann. GRA

N92-17220# Naval Weapons Center, China Lake, CA.
DETERMINATION OF THE ELECTRONIC DENSITY OF STATES OF YBa2Cu3O(7-DELTA) Technical Report No. 8, Oct. 1990 - Sep. 1991
M. E. Reeves, S. A. Wolf, D. A. Ditmars, and T. A. Vanderah Oct. 1991 20 p
(AD-A243223) Avail: NTIS HC/MF A03 CSCL 20/3

We report precise measurements of the enthalpy of polycrystalline YBa2Cu3O(7-delta) at high temperatures (300 K less than T less than 700 K). From these data, we determine the lattice and electronic contributions to the specific heat. We find that anharmonicity must be included when calculating the lattice specific heat. We also find that the specific heat of the charge carriers follows the temperature dependence of a Fermi liquid with a Sommerfeld constant of 40 +/- 5 mJ/(mol)(sq K). This value is three times larger than expected from band structure calculations. GRA

N92-17238# National Inst. of Standards and Technology, Gaithersburg, MD.
HIGH RESOLUTION ELECTRON MICROSCOPY OF DIAMOND FILM GROWTH DEFECTS AND THEIR INTERACTIONS
D. Shechtman, E. N. Farabaugh, L. H. Robins, and A. Feldman 25 Sep. 1991 25 p
(Contract N00014-90-F-0011)
(AD-A243093; NIST-TR-7) Avail: NTIS HC/MF A03 CSCL 20/2

High resolution electron microscopy of plasma-assisted chemical vapor deposition (CVD) diamond films was performed. The film was fine grained with a grain size on the order of 0.1 micrometer. Several features of the microstructure were studied and their importance to the understanding of the diamond film growth was evaluated. The observations included the following: (1) twinning density rises as a function of the distance from the center of the crystal; (2) the twins have an important role in the rapid growth of this kind of film; (3) the center point of a twin quintuplet has five reentrant angles and thus serves as a preferred nucleation site for new planes as the crystal grows; and (4) misfit boundaries, being the locus of intersection points of the growing planes on two adjacent twins can serve as an indicator for the local crystal growth direction. GRA

N92-17245# Washington State Univ., Pullman. Dept. of Chemistry.
STABILITY AND STRUCTURE OF C12B24N24: A HYBRID ANALOG OF BUCKMINSTERFULLERENE
Thomas F. George, James R. Bowser, and Daniel A. Jelski (State Univ. of New York, Fredonia.) Oct. 1991 9 p
(Contract N00014-90-J-1193)
(AD-A242327; WSU/DC/91/TR-65) Avail: NTIS HC/MF A02 CSCL 20/5

The results of a study of the substituted buckminsterfullerene C12B24N24 are presented. Computational evidence is given for its stability, the molecular structure is discussed, and a possible synthetic route is proposed. The sixty-vertex, truncated icosahedral cluster system known as buckminsterfullerene has attracted increased attention following recent repairs of its laboratory-scale synthesis. Such large clusters provide a bridge between atomic and macroscopic species, and hence have considerable technological importance - for example, in electrochemistry, ferromagnetism, and superconductivity. Various efforts to add heteroatoms (especially nucleophiles) to the periphery of C60 frameworks have been successful. Smalley and co-workers doped C60 with boron and nitrogen atoms, with mass spectral evidence for C59B, C59N, C58BN, etc. having been obtained. The C58BN cluster is especially intriguing. The isoelectronic relationship between boron-nitrogen and dicarbon molecular fragments is well documented, and is manifested in a variety of ways. For example, the structural chemistry of boron nitride closely parallels that of elemental carbon-hexagonal BN is an analog of graphite, while Beta-BN is isostructural with diamond. GRA

N92-17322# National Inst. of Standards and Technology, Gaithersburg, MD.
TRANSMISSION ELECTRON MICROSCOPY OF THE CVD DIAMOND FILM/SUBSTRATE INTERFACE
D. Shechtman 27 Sep. 1991 14 p
(Contract N00014-90-F-0011)
(AD-A243096; NIST-TR-10) Avail: NTIS HC/MF A03 CSCL 20/2

The structure of grain boundaries in the diamond lattice, and twin boundaries as a special case, received considerable attention in the past thirty years. This is mainly due to the importance of defects in silicon and germanium to their usefulness as efficient semiconductors. Twin boundaries have equal importance to various properties of diamond films. Electrical and mechanical properties as well as migration mechanisms are all affected by the twin boundaries and their structure. The ever presence of twins in CVD diamond films makes their study even more important compared to semiconductors which can be grown without boundaries. The purpose of the study reported here is, therefore, to investigate the crystallography of twin boundaries which form in chemical vapor deposited (CVD) diamond films, and to compare them to the ones which were found in silicon and in germanium. GRA

N92-17375*# Texas Univ., Austin. Center for Statistical Mechanics.
THE WAVE NUMBERS OF SUPERCRITICAL SURFACE TENSION DRIVEN BENARD CONVECTION Final Report
E. L. Koschmieder and D. W. Switzer 6 Feb. 1991 34 p
(Grant NAG3-1104)
(NASA-CR-189856; NAS 1.26:189856) Avail: NTIS HC/MF A03 CSCL 20L

The cell size or the wave numbers of supercritical hexagonal convection cells in primarily surface tension driven convection on a uniformly heated plate was studied experimentally in thermal equilibrium in thin layers of silicone oil of large aspect ratio. It was found that the cell size decreases with increased temperature difference in the slightly supercritical range, and that the cell size is unique within the experimental error. It was also observed that the cell size reaches a minimum and begins to increase at larger temperature differences. This reversal of the rate of change of the wave number with temperature difference is attributed to influences of buoyancy on the fluid motion. The consequences of buoyancy were tested with three fluid layers of different depth. Author

N92-17382# Missouri Univ., Rolla. Dept. of Chemistry.
MOLECULAR MOTIONS OF THE HEAD GROUP OF SHBS IN LAMELLAR LIQUID CRYSTALS Interim Technical Report, Jan. 1990 - Nov. 1991
Joseph R. Duke, Robert B. Funchess, and Frank D. Blum 15 Nov. 1991 30 p
(Contract N00014-91-J-1274)
(AD-A243499; UMR-FDB-22) Avail: NTIS HC/MF A03 CSCL 20/2

Deuterium NMR spectra of a specifically-deuterated double-tailed surfactant sodium 4-(1'-heptylnonyl) benzenesulfonate (SHBS) both dry and in liquid crystals formed with water were obtained from -70 to 90 C. The liquid crystalline deuterium powder patterns from the phenyl-ring deuterons can be described as from motions characterized as rigid (from -70 to -30 C), two fold ring flips (from -40 to -30 C), and rotations in an anisotropic media (-20 C and higher). For the higher temperature spectra the inclusion of a single fast rotation, or even anisotropic diffusion alone did not give the best fits of the experimental spectra. The inclusion of a local ordering potential, or anisotropic viscosity, yielded good fits to the experimental spectra. The local ordering potential required local order parameters from 0.856 to 0.763 for temperatures from 10 to 90 C. The dry surfactant, in contrast to the liquid crystals at the same temperatures, undergoes both fast and slow two-fold ring flips at 25 C with the fraction of fast flippers increasing with temperature. GRA

N92-17390# North Carolina State Univ., Raleigh.
RESEARCH AND DEVELOPMENT ON ADVANCED SILICON CARBIDE THIN FILM GROWTH TECHNIQUES AND FABRICATION OF HIGH POWER AND MICROWAVE FREQUENCY SILICON CARBIDE-BASED DEVICE STRUCTURES Annual Report, 1 Jan. - 31 Dec. 1991
Robert F. Davis Dec. 1991 53 p Prepared in cooperation with Cree Research, Inc., Durham, NC
(Contract N00014-88-K-0341)
(AD-A243531) Avail: NTIS HC/MF A04 CSCL 09/1

Thin films of pure and Al doped beta-SiC have been grown on 4 off-axis Si(100) and c-axis oriented alpha(6H)-SiC in the temperature range of 1025 to 1250 C using gas source molecular beam epitaxy. Cross sectional TEM confirmed the epitaxial relationship between the films and the substrates. Double positioning boundaries have not been observed in the material grown on the 6H-SiC substrates. Platinum and Ti circular contacts were epitaxially deposited on alpha(6H)-SiC via electron beam MBE at room temperature. Leakage currents at -10V were as low as 5 x 10(exp -18) A/sq cm. The ideality factors were approximately unity. Barrier heights for the as-grown Ti and Pt contacts were determined from C-V measurements to be 0.88 and 1.02 eV, respectively. Theoretical studies of the physical limitations to the RF operation of SiC IMPATT diodes has shown that good RF output power can be obtained from these devices. However, the low magnitude of the charge carrier mobility in SiC limits the magnitude of the RF voltage that can be supported, and thereby prevents efficient dc to RF power conversion. MESFETs were

fabricated with values of ft and fmax of 4.5 GHz and 3.0 GHz, respectively. MESFETs have been fabricated with values of ft and fmax of 4.5 GHz and 3.0 GHz, respectively. GRA

N92-17449# Case Western Reserve Univ., Cleveland, OH. Dept. of Macromolecular Science.
REACTIONS AND INTERACTIONS IN LIQUID CRYSTALLINE MEDIA
V. Percec, H. Jonsson, and D. Tomazos 30 Oct. 1991 171 p
(Contract N00014-89-J-1828)
(AD-A242355; TR-55) Avail: NTIS HC/MF A08 CSCL 20/2

This chapter discusses critically the most representative examples of reactions performed both in low molar mass and polymeric liquid crystals. Examples of reactions whose pathway is affected when they are performed in low molar mass liquid crystals, as well as reactions performed on polymeric liquid crystals whose phase behavior is affected whether the reaction takes place in the isotropic or anisotropic solution or melt are discussed. Separation and transport processes in which the interaction between solute and low molar mass or polymeric liquid crystalline solvent affects the overall process are also discussed. Organization, miscibility, phase diagrams and reactions of any kind including polymerization in low molar mass and polymeric liquid crystals is an interplay of molecular chemistry (i.e., the chemistry of the covalent bond) and supramolecular chemistry (i.e., the chemistry of intermolecular bonding through specific interactions). GRA

N92-17528# Dartmouth Coll., Hanover, NH.
EXCITONS IN SEMICONDUCTING SUPERLATTICES, QUANTUM WELLS, AND TERNARY ALLOYS
M. D. Sturge, R. E. Nahory, and M. C. Tamargo (Bell Communications Research, Inc., Red Bank, NJ.) 15 Aug. 1991 13 p
(Contract DE-FG02-87ER-45330)
(DE91-018805; DOE/ER-45330/4) Avail: NTIS HC/MF A03

It is now possible to fabricate semiconducting layered structures with precisely defined layer thicknesses down to one monolayer (two atomic diameters). An example is the superlattice (SL) structure, in which two semiconductors with different band gaps are interleaved. The electronic properties of the SL are quite different from those of the constituents and offer interesting new possibilities both in device design and in basic physics. This proposal aims to improve our understanding of optically excited states (excitons and electron-hole plasmas) in a particular class of these structures: the so-called 'Type 2 indirect' SL's in which the electron and hole created by optical excitation are separated both in real and in momentum space. Time-resolved tunable laser spectroscopy, with and without external perturbations such as magnetic field, electric field, and uniaxial stress are used principally to study the following phenomena: (1) exciton states in SL's with only a few atomic layers per period, for which the familiar 'effective mass model' of semiconductor states breaks down; and (2) the electron-hole plasma which forms when the excitation density is high (this plasma may be in a liquid state at low temperatures). In the short period, superlattices are our primary concern; electrons and holes are spatially separated, leading to internal electric fields which might be expected to have a pronounced effect on the plasma properties. DOE

N92-17532# Princeton Univ., NJ. Dept. of Chemistry.
SURFACE CHEMISTRY AT THE SEMICONDUCTOR/ELECTROLYTE INTERFACE
A. B. Bocarsly 1991 12 p
(Contract DE-FG02-85ER-13438)
(DE91-018511; DOE/ER-13438/2) Avail: NTIS HC/MF A03

A critical theme over this time period has been understanding the role of intrinsic cyanometalate overlayers in modulating interfacial photoinduced charge transfer processes occurring at the cadmium chalconide/aqueous ferr-ferrocyanide interface. To accomplish this goal, detailed structural and charge transfer studies of (CdFe(CN)6)sup(2-/1-) overlayers generated either intrinsically via photoelectrochemistry at the illuminated CdX/((Fe(CN)6)sup 4-/3-) (X = S or Se) interface, or synthesized as chemical modification layers on inert metal electrodes have been undertaken. From these studies, a picture has evolved which directly links charge transfer mediated cation intercalation processes to surface overlayer crystal structure, and overlayer structure to critical charge transfer parameters. In parallel with our photoelectrochemical projects, we have also introduced work on the spatially resolved photodeposition of plantinum metal on nonconducting and semiconducting substrates. This chemistry provides new opportunities for the design of semiconductor (or insulator) metal heterostructures which have applications in solar energy conversion (i.e., Schottky barrier devices, ohmic back contacts, and MIS structure). A project has been initiated in the area of visible light, molecular, charge transfer photochemistry. A summary review of these projects is presented. DOE

N92-17553# General Electric Co., Syracuse, NY. Electronics Lab.
FAILURE MECHANISMS IN GaAs ICs: THE EFFECTS OF DEEP TRAPS Final Report
Paul A. Martin Oct. 1991 61 p
(Contract F30602-89-C-0063)
(AD-A243013; RL-TR-91-263) Avail: NTIS HC/MF A04 CSCL 20/12

GaAs FETs, 1 x 150 micron and 100 x 400 micron, were subjected to accelerated stress tests. The samples were of two types: with and without a burried p-layer. The life tests were of two types: a storage test at 250 C and a DC-biased life test at 225-235 C. The FETs were characterized prior to and during the life tests using DLTS, I-V characteristics, C-V profiling, drift mobility profiling, and backgating. Buried p devices degraded more slowly initially. There is substantial loss of carriers and significant degradation of the drift mobility. The concentration of EL2 was seen to increase near the device surface, and a new trap emerged near the end of the life tests with an energy in the 0.6 - 0.7 range. Recommendations for further work are included.
Author (GRA)

N92-17594# California Univ., Berkeley.
STUDIES OF HETERO-EPITAXY OF GaAs FILMS ON Si SUBSTRATE FOR EFFECTIVE CONTROL OF DENSITY AND INTERNAL STRESS Final Report, 15 Apr. 1988 - 14 Jul. 1991
Shyh Wang Oct. 1991 7 p
(Grant AF-AFOSR-0174-88)
(AD-A241882; AFOSR-91-0883TR) Avail: NTIS HC/MF A02 CSCL 09/3

Using various growth techniques and different buffer structures, we have been able to reduce dislocation density to below 10(exp 6) cm-2 and internal stress below 10(exp 9) dynes/sq cm. The improvements lead to the restoration of TE polarization as the dominant polarization in DH GaAs/Si lasers for the first time and bring us hope that we are close to achieving long operating life for lasers fabricated with lattice-mismatched films. However impressive these improvements are, they are still some distance away from those needed for long life lasers with dislocation density below 10 to the third power cm-2 and internal stress below 2 x 10 to the eighth power dynes/sq cm. Two possible approaches remaining unexplored for further improvements include (1) use of oxygen-free Si, especially near the surface upon which GaAs film is to grow and (2) use of quaternary quantum well as the laser-active region. The former is to smooth the transition between mechanically strong Si substrate and more ductile III-V film, thus to minimize defect generation at the interface. The purpose of the latter is three-fold. Decreasing the active layer thickness reduces the probability of intercepting dislocations. It also lowers the laser threshold and thus lessens the chance of thermal generation of dislocations. Finally, it is well known that quaternary (GaInAsP) lasers are more forgiving in terms of laser degradation and hence have much longer life than GaAs lasers. GRA

N92-17610# Department of the Navy, Washington, DC.
METHOD OF DOPING SINGLE CRYSTAL DIAMOND FOR ELECTRONIC DEVICES Patent Application

Lawrence T. Kabacoff, inventor (to Navy) 8 Jul. 1991 11 p
(AD-D015069; US-Patent-Appl-SN-726489; Navy-Case-73170)
Avail: NTIS HC/MF A03 CSCL 09/1

This invention relates to diamonds and to methods of doping diamonds. It has been widely known for many years that diamonds would be greatly superior to either silicon or GaAs as a material for integrated circuits. Reasons include the greater heat conductivity of diamonds, the higher carrier mobilities, the higher operating temperatures, and the intrinsic radiating hardness such a chip would possess. The problem has been to find a way to dope diamonds with suitable impurities to create n and p type semiconductors. The very compact structure of diamonds, coupled with the very high c-c bond energies, prevent diffusion of dopants into the material. Moreover, diamonds have an extremely high melting temperature, making the liquid hard to form. GRA

N92-17618# Air Force Inst. of Tech., Wright-Patterson AFB, OH.
OPTICAL PROPERTIES OF THERMALLY INTERMIXED QUANTUM WELLS AND SUPERLATTICES Ph.D. Thesis
Michael W. Prairie 1991 152 p
(AD-A243546; AFIT/CI/CIA-91-020D) Avail: NTIS HC/MF A08 CSCL 20/12

The optical properties of thermally intermixed GaAs/AlGaAs quantum wells and superlattices are examined using thermal annealing, photoluminescence (PL), time-resolved photoluminescence (TPL), and theoretical models. A computer model to calculate the energy structure of intermixed quantum wells is refined and used with PL and TPL techniques to characterize the properties of thin (1 monolayer (ML) to 8 ML) annealed wells. A model for intermixed superlattices is developed next which predicts the changes in energy dispersion and density of states with annealing time, and is verified using PL and TPL. Selective intermixing techniques using a gallium focused ion beam (FIB), SiNx encapsulation, and patterned GaAs grown at low substrate temperature (LT-GaAs) are then studied. The FIB technique tends to suppress layer interdiffusion in and around the implanted region. The SiNx encapsulation is most promising with an interdiffusion selectivity ratio of more than 4:1. Initial LT-GaAs experiments show a small selectivity between regions. GRA

N92-17667# Ohio Univ., Athens. Dept. of Electrical and Computer Engineering.
LUMINESCENCE AND ELECTROLUMINESCENCE PROPERTIES OF Nd, Tm, Yb DOPED GaAs II-VI COMPOUNDS Annual Report, 15 Jul. 1990 - 14 Aug. 1991
Henry J. Lozykowski 14 Aug. 1991 23 p
(Grant AF-AFOSR-90-0322A)
(AD-A242039; UT-5473-1; AFOSR-91-0817TR) Avail: NTIS HC/MF A03 CSCL 07/4

This report describes the progress accomplished during the first year of research on luminescence and electroluminescence properties of Nd, Tm, Yb doped GaAs and some II-IV compounds. The photoluminescence study of GaAs:Yb shows no 4f emission. The PL spectra of CdS:Nd were recorded and about 20 sharp emission lines were observed. This indicates that in CdS, Nd3(+) occupies different symmetry sites. The PL of CdS:Yb at 9.3 K reveals five sharp lines in the 985 nm - 990 nm range and a strong broader line at 998.3 nm. Electroluminescence of ZnS:Tm embedded in a Boric matrix was observed for the first time. Strong emission was observed at room temperature as well as at low temperature revealing only five groups of strong sharp lines which are assigned to transitions within the 4f shell of Tm3(+). EL intensity was investigated as a function of voltage, temperature and frequency. The voltage dependence of the EL intensity shows that the direct impact excitation mechanism is a dominant one. Photoluminescence spectra of InP:Yb at different temperatures consist of sharp peaks related to Yb3(+) transition. GRA

N92-17685# Naval Weapons Center, China Lake, CA.
PRESSURE DEPENDENCE OF Tc IN Tl2Ba2CaCu2O8 AT HYDROSTATIC PRESSURES TO 6 GPa Technical Report, Oct. 1990 - Sep. 1991
N. E. Moulton, S. A. Wolf, E. F. Skelton, and D. H. Liebenberg Oct. 1991 14 p
(Contract N00014-91WX-24155)
(AD-A243433; TR-6) Avail: NTIS HC/MF A03 CSCL 09/1

Studies of the pressure dependencies of the critical temperatures of hole-doped high Tc superconductors in the past have demonstrated, with very few exceptions, monotonically increasing Tc's with increasing pressure. This is thought to be due to the pressure-induced injection of holes onto the conduction planes resulting from a change in the apical Cu-O bond length: a view consistent with the drop of critical temperature with decreasing oxygen concentration and hence decreasing hole concentration. Recently, work has been performed which indicates that, for many of the thallium-based cuprates, increases in the oxygen content in as-made samples, actually decreases Tc, while decreases in oxygen content produce sharp increases in Tc, followed by decreases with further oxygen reduction. GRA

N92-17698 Academy of Sciences of the Ukrainian SSR, Kiev. Inst. of Physics.
AN ALGORITHM FOR CALCULATING THE ELECTRONIC SPECTRUM AND FUNCTION OF THE CHARGE DENSITY DISTRIBUTIONS OF CRYSTALS [ALGORITM RASCHETA ELEKTRONNOGO SPEKTRA I FUNKTSII RASPREDELENIIA PLOTNOSTI ZARIADO KRISTALLOV]
Ia. O. Dovgii, A. C. Krochuk, and N. I. Kolinko 1990 46 p In RUSSIAN
Copyright Avail: Issuing Activity

An algorithm is constructed for the calculation of an energy zone, a valence electron density chart, and functions of the electron composition of crystals by the non-local self-consistent pseudopotential method. The influence of various approximations for the cross-correlation of screening on the behavior of zones on the distribution of electron density is investigated. An analytical expression for the calculation of matrix elements is presented. The results obtained are compared to experimental data and results of calculations by other methods. Transl. by L.K.H.

N92-17700 Academy of Sciences of the Ukrainian SSR, Kiev. Inst. of Physics.
RADIATION EFFECTS IN HIGH TEMPERATURE SUPERCONDUCTORS (HTSC) OXIDES [RADIATSIONNYE EFFEKTY V VTSP-OKSIDAKH]
M. P. Krulikovskaia and G. P. Kekelidze 1990 30 p In RUSSIAN
Copyright Avail: Issuing Activity

In this summary, results of research into the effect of various types of nuclear irradiation on the superconducting characteristics of high temperature superconductors (HTSC) are cited. Data from both Soviet and foreign research concerning the role of nuclear irradiation and of the degradation of superconducting characteristics of HTSC-oxides are analyzed. The effects of the parameters of irradiation and the initial state of HTSC on this phenomenon are investigated. Transl. by L.K.H.

N92-17701 Academy of Sciences of the Ukrainian SSR, Kiev. Inst. of Physics.
THE EPR OF THE TRIPLET STATE OF ARYL CATIONS IN CRYSTALS OF DIAZONIUM SALTS [EPR TRIPLETNOGO SOSTOIANIIA APRILNYKH KATIONOV V KRISTALLAKH SOLI DIAZONIIA]
P. A. Kondratenko, E. V. Shrubovich, and S. Z. Shulga 1989 22 p In RUSSIAN
Copyright Avail: Issuing Activity

The spectra of the electron paramagnetic resonance (EPR) of aryl cations possessing a principle triplet ground-state and orientated in a monocrystal of diazonium salts is studied. It is shown that two nonequivalent paramagnetic centers, which differ in orientation are formed within the crystal. A theoretic description of experimental results is possible only when allowing for the effect of low symmetry. This symmetry is invoked by the interactivity of the paramagnetic center of symmetry C(sub 2v) with the crystal field of symmetry C(sub i). Transl. by L.K.H.

N92-17746# Air Force Inst. of Tech., Wright-Patterson AFB, OH. School of Engineering.

CHARACTERIZING THE SENSITIVITY, SELECTIVITY, AND REVERSIBILITY OF THE METAL-DOPED PHTHALOCYANINE THIN-FILMS USED WITH THE INTERDIGITATED GATE ELECTRODE FIELD-EFFECT TRANSISTOR (IGEFET) TO DETECT ORGANOPHOSPHOROUS COMPOUNDS AND NITROGEN DIOXIDE M.S. Thesis

Clayton P. Howe Dec. 1991 480 p

(AD-A243635; AFIT/GE/ENG/91D-26) Avail: NTIS HC/MF A21 CSCL 17/8

This study investigated the sensitivity, reversibility, and selectivity of the thin film coatings used on the interdigitated gate electrode field effect transistor (IGEFET) gas microsensor. These responses were quantified based on the dc resistance changes and frequency domain responses of the microsensor. The thin film materials included: copper phthalocyanine (CuPc), nickel phthalocyanine (NiPc), and cobalt phthalocyanine (CoPc). The challenge gases included: diisopropyl methylphosphonate (DIMP), dimethyl methylphosphonate (DMMP), nitrogen dioxide, ammonia, and boron trifluoride. Tests of the CuPc thin films and nitrogen dioxide challenges established the primary set of test parameters expected to maximize the selectivity, sensitivity, and reversibility of the thin film coatings. A series of experiments performed at 150 C tested the other thin film materials, on the IGEFET sensors, when challenged by listed gases. At 150 C, the nitrogen dioxide and ammonia interacted with all three film types, the boron trifluoride interacted weakly, the DIMP and DMMP show no response. GRA

N92-17779# Centro Brasileiro de Pesquisas Fisicas, Rio de Janeiro.

Y890NMR STUDY OF HYPERFINE INTERACTIONS IN (R(x)Y(1-x))Fe2

K. M. B. Alves and A. P. Guimaraes 1991 15 p

(DE91-641979; CBPF-NF-004/91) Avail: NTIS HC/MF A03

Y-89 pulsed NMR measurements have been performed at low temperatures in (R(x) Y(1-x) Fe2 compounds, where R is a heavy rare-earth (Gd, Tb, Dy, Ho, Er and Tm) in the range 0 less than or = x less than or = 0.05. The spectra were measured at 4.2 K, except for Dy (77.4 K). The spectra were analyzed in terms of direct and indirect (through common Fe neighbors) transferred hf interactions. The direct transferred hf field amounts to a few kOe per rare earth 1st neighbor; the indirect contributions of the first two shells are smaller by a factor of ten. We have found that a model that restricts the transferred hyperfine interactions to the indirect hf field or considers the first three neighbor shells in the same way is not satisfactory to explain the changes in the hyperfine field at Y nuclei. DOE

N92-17781# Los Alamos National Lab., NM.

Au AND Al SCHOTTKY BARRIER FORMATION ON GaAs (100) SURFACES PREPARED BY THERMAL DESORPTION OF A PROTECTIVE ARSENIC COATING

C. J. Spindt, M. Yamada, P. L. Meissner, K. E. Miyano, A. Herrera, W. E. Spicer, A. J. Arko, J. M. Woodall, and G. D. Pettit 1991 19 p Presented at the 18th Annual Conference on Physics and Chemistry of Semiconductor Interfaces and Topical Conferene on Silicon Based Heterostructures, Long Beach, CA, 29 Jan. - 1 Feb. 1991 Prepared in cooperation with Stanford Univ., CA

(Contract W-7405-eng-36)

(DE92-002456; LA-UR-91-3257; CONF-910115-1) Avail: NTIS HC/MF A03

Photoelectron spectroscopy has been used as a tool to investigate the initial stages of Schottky barrier formation on GaAs (100) surfaces. This is a popular technique that has been used by many researchers in the past to measure the band bending (or shift) of the valence band and conduction band (a measure of the Schottky barrier shift), while the Fermi level remains fixed at the system ground (i.e., the ground of the spectrometer). Metal deposition on a semiconductor surface can alter the Schottky barrier at the surface and pin the Fermi level near the middle of the energy gap. Extremely clean and crystallographically perfect surfaces are required in this study. Toward this end, a method of protecting the GaAs surface was employed which consists of capping the GaAs surface with a layer of As. Upon introduction into the high vacuum system the As is thermally desorbed, revealing a pure GaAs surface. Our work was motivated by a previous study (Brillson et al) on similarly capped specimens, which suggested that metal overlayers do not pin the Schottky barrier in GaAs. Barrier heights varied by as much as 0.75 eV between Al and Au overlayers. This large energy range is a striking result in view of the fact that a considerable number of prior studies on both (110) and (100) surfaces have found that all metals will pin within a narrow (0.25 eV) range at midgap. We repeated the measurements of Brillson on the identically doped samples used in their study using two extreme range metals of Au and Al as overlayers. We found that the barrier height measurements on low doped n-type samples used in this work and in the previous work are affected by photovoltaic effects, even at room temperature. This was determined from taking spectra at a number of temperatures between 20 K and room temperature and looking for shifts. DOE

N92-17782# Argonne National Lab., IL.

MICROSTRUCTURE AND COMPOSITION OF ELECTROMAGNETICALLY-CHARACTERIZED YBa2Cu3O(7-DELTA) GRAIN BOUNDARIES

S. E. Babcock, Na Zhang, Xue Yu Cai, D. C. Larbalestier (Wisconsin Univ., Madison.), Yufei Gao, K. L. Merkle, and D. L. Kaiser 1991 7 p Presented at the 2nd Tokai Univ. International Workshop on Superconductivity, Honolulu, HI, 9-12 Oct. 1991

(Contract W-31-109-eng-38)

(DE92-003520; ANL/CP-74697; CONF-9110181-1) Avail: NTIS HC/MF A02

The electrical character (flux pinning, Josephson junction, or resistive) of the grain boundaries in approx. twenty flux grown YBa2Cu3O(7-delta) bicrystals was determined in previous studies. A selection of these same bicrystals now have been thinned for study by transmission and scanning transmission electron microscopy. High spatial resolution imaging and analytical techniques reveal microstructural differences among these boundaries that are consistent with their diverse electrical characteristics. The observations offer preliminary insight into some of the feature that control the grain boundary superconducting properties and re-emphasize the very fine scale on which the grain boundary electrical character is determined. DOE

N92-17783# North Carolina State Univ., Raleigh. Dept. of Electrical and Computer Engineering.

A THEORETICAL SEARCH FOR SUPERVELOCITY SEMICONDUCTORS Annual Report

M. A. Littlejohn and K. W. Kim 21 Oct. 1991 83 p

(Contract N00014-90-J-1553)

(AD-A241981) Avail: NTIS HC/MF A05 CSCL 20/12

This document presents an annual report to the Office of Naval Research for a research program entitled 'A Theoretical Search for Supervelocity Semiconductors.' This program has been funded by ONR since 1974 in the Department of Electrical and Computer Engineering at N.C. State University. The research has resulted in more than 75 refereed publications and numerous conference presentations from its inception. Major contributions to the field of hot electron transport and semiconductor device modeling have been achieved, new computational methods have been developed (e.g., path integral Monte Carlo techniques), and the work has helped stimulate commercial ventures in the applications of quaternary semiconductor materials to electronic and optical devices. In addition, there have been twenty-six Ph.D. and M.S. students who have received degrees at N.C. State University with research support from this contract. Three visiting faculty members from Japan came to the university to work with the faculty investigators supported under this ONR contract during the 1979-1983 time period. A visiting professor from the French CNRS Microstructures and Microelectronics Laboratory in Bagneux (near Paris) spent a sabbatical year at N.C. State during 1988-89, and he devoted full-time working on this program at no cost to

ONR. During the current funding period, a visiting scholar from China is a member of our research group working on projects which directly impact this ONR program. GRA

N92-17790# Sandia National Labs., Albuquerque, NM.
CHARACTERIZATION OF PZT THIN FILMS: CRYSTALLOGRAPHIC PHASES
R. P. Goehner, M. O. Eatough, B. A. Tuttle, and T. J. Headley 1991 9 p Presented at the Pacific-International Congress on X Ray Analytical Methods, Honolulu, HI, 12-16 Aug. 1991
(Contract DE-AC04-76DP-00789)
(DE92-003514; SAND-91-0051C; CONF-910862-6) Avail: NTIS HC/MF A02

The use of grazing incident parallel beam x ray diffraction (GIXRD) in the characterization of lead zirconate titanate (PZT) films is described. This tool has enabled us to depth profile the films. The transmission electron microscopy (TEM) results obtained from a cross section of one film are shown to compliment the GIXRD results. The variation in crystallographic structure versus depth in the film was the primary focus of this study. The results from three PZT films having Zr/Ti ratios of 25/75, 48/52, and 75/25 are given. TEM results are reported from the sample with a Zr/Ti ratio of 48/52. DOE

N92-17791# California Univ., San Diego, La Jolla.
ION MIXING OF SEMICONDUCTOR LAYERED-STRUCTURES
S. S. Lau and J. W. Mayer (Cornell Univ., Ithaca, NY.) 1991 7 p
(Contract DE-FG03-84ER-45156)
(DE92-003756; DOE/ER-45156/T4) Avail: NTIS HC/MF A02

This research is a collaborative program between the University of California at San Diego and Cornell University to investigate the phenomenon of ion mixing in semiconductor layered structures. The research effort also involves interactions with Oak Ridge National Laboratory under the Surface Modification and Characterization Collaborative Research Center Program. During the current period of investigation, we investigated parameters that could affect ion-mixing rates in semiconductors. We found that the use of shallow dopants as the mixing ion did not increase the mixing rate, thus indicating that electrically active ions (or the Fermi level) do not play a significant role in ion-mixing. On the other hand, the presence of mismatch strain in Ge/Si layered structures can affect the mixing rate, especially in the temperature independent regime. Mismatch strain can also affect the solid-phase regrowth kinetics of amorphous layers of Ge-Si alloys. In summary, we found that ion mixing kinetics depend primarily on the ion and the target mass and the target temperature. Mixing rates can also be affected, to a certain extent, by thermodynamic driving forces (such as the cohesive energy and the stored strain energy of the system). Impurities do not play a significant role in mixing kinetics. DOE

N92-17797# Sandia National Labs., Albuquerque, NM.
COLLISIONAL ENERGY DEPOSITION THRESHOLD FOR EXTENDED DAMAGE DEPTHS IN ION-IMPLANTED SILICATES
G. W. Arnold, G. Battaglin, A. Boscolo-Boscoletto, and F. Caccavalle (Padua Univ., Italy) 1991 6 p Presented at the Annual Fall Meeting of the Materials Research Society, Boston, MA, 2-6 Dec. 1991
(Contract DE-AC04-76DP-00789)
(DE92-004737; SAND-91-1635C; CONF-911202-4) Avail: NTIS HC/MF A02

Many properties of implanted fused silica (e.g., surface stress, hardness) exhibit maximum implantation-induced changes for collisional energy deposition values of approx. 10(exp 20) keV/cu cm. We have observed a second critical energy deposition threshold value of about 10(exp 22) keV/cu cm in stress and hardness measurements as well as in many other experiments on silicate glasses (leaching, alkali depletion, etching rate, gaseous implant redistribution). The latter show evidence for damage depths exceeding TRIM ranges by about a factor of 2. For crystalline quartz, a similar threshold value has been found for extended damage depths (greater than TRIM) for 250 kev ions (H-Au) as measured by RBS and interference fringes. This phenomenon at high damage deposition energy may involve the large stress gradients between damaged and undamaged regions and the much increased diffusion coefficient for defect transport. DOE

N92-17799# California Univ., Berkeley. Lawrence Berkeley Lab.
QUANTUM-LIMITED DETECTION OF MILLIMETER WAVES USING SUPERCONDUCTING TUNNEL JUNCTIONS Ph.D. Thesis
C. A. Mears Sep. 1991 105 p
(Contract DE-AC03-76SF-00098)
(DE92-004757; LBL-31391) Avail: NTIS HC/MF A06

The quasiparticle tunneling current in a superconductor insulator superconductor (SIS) tunnel junction is highly nonlinear. Such a nonlinearity can be used to mix two millimeter wave signals to produce a signal at a much lower intermediate frequency. We have constructed several millimeter and submillimeter wave SIS mixers in order to study high frequency response of the quasiparticle tunneling current and the physics of high frequency mixing. We have made the first measurement of the out-of-phase tunneling currents in an SIS tunnel junction. We have developed a method that allows us to determine the parameters of the high frequency embedding circuit by studying the details of the pumped I-V curve. We have constructed a 80 to 110 GHz waveguide based mixer test apparatus that allows us to accurately measure the gain and added noise of the SIS mixer under test. Using extremely high quality tunnel junctions, we have measured an added mixer noise of 0.61 (+ or -) 0.36 quanta, which is within 25 pct of the quantum limit imposed by the Heisenberg uncertainty principle. This measured performance is in excellent agreement with that predicted by Tucker's theory of quantum mixing. We have also studied quasioptically coupled millimeter- and submillimeter-wave mixers using several types of integrated tuning elements. DOE

N92-17821 Academy of Sciences of the Ukrainian SSR, Kiev. Inst. of Physics.
OPTICAL TURBULENCE IN SECOND HARMONIC GENERATION [OPTICHESKAIA TURBULENTNOST PRI GENERATSII VTOROI GARMONIKI]
M. V. Vasnetsov and S. S. Slivsarenko 1989 16 p In RUSSIAN
Copyright Avail: Issuing Activity

An analysis is conducted of the generation of secondary harmonics in a scheme of noncolinear (vector) synchronism, where in the capacity of a secondary pumping ray, the ray of the base frequency is used after a single transmission through the crystal. A threshold of instability is created giving rise to self oscillations in the system and the appearance of chaotic oscillation.
Transl. by L.K.H.

N92-17857# Illinois Univ., Urbana.
THIN FILMS UNDER CHEMICAL STRESS
1991 29 p
(Contract DE-FG02-88ER-13949)
(DE92-004684; DOE/ER-13949/3) Avail: NTIS HC/MF A03

The goal of work on this project has been to develop a set of experimental tools to allow investigators interested in transport, binding, and segregation phenomena in composite thin film structures to study these phenomena in situ. Work to-date has focused on combining novel spatially-directed optical excitation phenomena, e.g., waveguide eigenmodes in thin dielectric slabs, surface plasmon excitations at metal-dielectric interfaces, with standard spectroscopies to understand dynamic processes in thin films and at interfaces. There have been two main scientific thrusts in the work and an additional technical project. In one thrust we have sought to develop experimental tools which will allow us to understand the chemical and physical changes which take place when thin polymer films are placed under chemical stress. In principle this stress may occur because the film is being swelled by a penetrant entrained in solvent, because interfacial reactions are occurring at one or more boundaries within the film structure, or because some component of the film is responding to an external

stimulus (e.g., pH, temperature, electric field, or radiation). However all work to-date has focused on obtaining a clearer understanding of the penetrant transport phenomena. The other thrust has addressed the kinetics of adsorption of model n-alkanoic acids from organic solvents. Both of these thrusts are important within the context of our long-term goal of understanding the behavior of composite structures, composed of thin organic polymer films interspersed with Langmuir-Blodgett (LB) and self-assembled monolayers. In addition there has been a good deal of work to develop the local technical capability to fabricate grating couplers for optical waveguide excitation. This work, which is subsidiary to the main scientific goals of the project, has been successfully completed and will be detailed as well. DOE

N92-17916# Ames Lab., IA.
STRUCTURAL, ELECTRONIC, AND MAGNETIC PROPERTIES OF La(x)Sr(1-x)VO3 (0 IS LESS THAN OR EQUAL TO x IS LESS THAN OR EQUAL TO 1.0) Ph.D. Thesis
A. Mahajan 15 Nov. 1991 107 p
(Contract W-7405-eng-82)
(DE92-003808; IS-T-1537) Avail: NTIS HC/MF A06

We report on the properties of La(x)Sr(1-x)VO3 which has a phase diagram which is similar to Sr doped La2CuO4 in that it shows a composition induced insulator to metal transition with strontium doping. In addition, the insulating compositions in the vanadium based system are antiferromagnetic and the La(x)Sr(1-x)VO3 system has a pervoskite structure. These features are reminiscent of the properties of the high T(sub c) cuprate superconductors. This makes La(x)Sr(1-x)VO3 a candidate for a detailed study of its properties in order to gain a greater insight into the mechanisms at play in the high T(sub c) cuprate superconductors. Magnetic susceptibility, X-ray powder diffraction and (51)V NMR Knight shift and relaxation rates, T1(sup -1) and T2(sup -1), are reported as functions of temperature and composition in La(x)Sr(1-x)VO3. A combined analysis of the susceptibility and the (51)V NMR data yields values of the density of states D(epsilon(f)) and for the enhancement of the uniform susceptibility. These are indicative of an exchanged enhanced narrow d-band metal for x less than 0.7. No evidence was found for antiferromagnetic spin fluctuations in the metallic phase nor for superconducting behavior, in these compounds. We have extensively investigated the properties of LaVO3. We have observed diamagnetism in this compound, which is an antiferromagnetic insulator, below the Neel temperature under field-cooled conditions. We observe hysteresis magnetization versus applied field M(2) isotherms below the Neel temperature. DOE

N92-17941# Massachusetts Inst. of Tech., Cambridge. Dept. of Materials Science and Engineering.
GRAIN BOUNDARIES
R. W. Balluffi and P. D. Bristowe 1991 14 p
(Contract DE-FG02-87ER-45310)
(DE92-004420; DOE/ER-45310/35) Avail: NTIS HC/MF A03

The present document is a progress report describing the work accomplished to date during the second year of our four-year grant (February 15, 1990 to February 14, 1994) to study grain boundaries. The research was focused on the following three major efforts: study of the atomic structure of grain boundaries by means of x-ray diffraction, transmission electron microscopy and computer modeling; study of short-circuit diffusion along grain boundaries; and development of a Thin-film Deposition/Bonding Apparatus for the manufacture of high purity bicrystals. DOE

N92-17944# Joint Inst. for Nuclear Research, Dubna (USSR). Lab. of Neutron Physics.
EXPERIMENTAL FINDINGS ON SELF-RECOVERY AND IMPROVEMENT OF REPRESENTATIVE PARAMETERS OF SOME SEMICONDUCTOR DEVICES AS IRRADIATED IN FAST NEUTRON FLUX
W. Hammer, Sl. Sterlinski, V. M. Nazarov (Joint Inst. for Nuclear Research, Dubna, USSR), and Z. Bober 1990 6 p
(DE92-611185; JINR-E-14-90-345) Avail: NTIS HC/MF A02

Semiconductor devices (Si-Li detectors, diodes, transistors and integrated circuits) were irradiated at a nuclear reactor up to 2.8 x 10(exp14)n x cm(sup -2)(E sub n greater than 0.5 MeV) anda 14 MeV neutron generator up to 10(exp 13) n x cm(sup -2). While testing radiation damage it was seen that some Si-Li detectors and integrated circuits showed the effects of self-recovery and improvement of electrical characteristics. DOE

N92-17972# International Centre for Theoretical Physics, Trieste (Italy).
LIQUID-SOLID TRANSITION IN THE BOND PARTICLE MODEL FOR ELEMENTAL SEMICONDUCTORS
Z. Badirkhan, M. P. Tosi, and M. Rovere (Trieste Univ., Italy) Jul. 1991 22 p
(DE92-610441; IC-91/153) Avail: NTIS HC/MF A03

Freezing of Silicon and Germanium involves a reconstruction of covalent tetrahedral bonds from a metallic liquid having density and coordination than the solid. We first contrast the metallic liquid structure of Germanium with that of its semiconducting amorphous state, in order to emphasize the changes in the atomic structure factor that arise from reconstruction of the interatomic bonds. We then use the density wave theory of freezing to discuss the liquid-solid transition within a pseudoclassical model, which describes the liquid structure by means of partial structure factors giving the pair correlations between atoms and bond particles. The phase transition is viewed as a freezing of the bonds driven by tetrahedrally constrained attractions between ionic cores and valence electrons and accompanied by an opening of the structure to allow long range connectivity of tetrahedral atomic units. Quantitative calculations on the bond particle model illustrate the relationship between the liquid structure and the microscopic Fourier components of the single particle densities of atoms and bonds. In further support of this picture, we also present calculations for freezing of a liquid having the density and the atomic structure of compacted amorphous Germanium. DOE

77 THERMODYNAMICS AND STATISTICAL PHYSICS

Includes quantum mechanics; theoretical physics; and Bose and Fermi statistics.

For related information see also *25 Inorganic and Physical Chemistry* and *34 Fluid Mechanics and Heat Transfer.*

N92-17324# Aspen Center for Physics, CO.
SUMMARY OF THE 1991 ACP WORKSHOP ON COHERENCE AND CHAOS IN COMPLEX DYNAMICAL SYSTEMS Final Report, 1 May - 30 Sep. 1991
J. D. Meiss, P. J. Morrison, and J. Tennyson Sep. 1991 7 p
Workshop held in Aspen, CO, 1991
(Contract N00014-91-J-1706)
(AD-A243226) Avail: NTIS HC/MF A02 CSCL 12/1

Abstracts are presented for the thirteen papers delivered at the workshop on Complex Dynamical Systems. The papers discussed the following topics: rotating fluids, trapped electrons, turbulence, and chaos theory. GRA

N92-17443# Naval Postgraduate School, Monterey, CA.
NUCLEATE POOL BOILING PERFORMANCE OF SMALL HIGH FLUX AND TURBO-B TUBE BUNDLES IN R-114/OIL MIXTURES M.S. Thesis
Hakan Eraydin Dec. 1990 121 p
(AD-A241936) Avail: NTIS HC/MF A06 CSCL 20/13

The U.S. Navy is constantly looking toward using more lightweight and compact heat exchangers. One of the areas of interest is the use of enhanced boiler tubes in the evaporator of a refrigerator plant, thereby cutting down on the number of tubes needed. The present research is a continuation of work done at NPS concentrating on the boiling characteristics from small tube bundles sitting in a pool of pure R-114, simulating the evaporator in such a heat exchanger. Two types of commercially available enhanced boiler tubes were used, namely High Flux and Turbo-B.

In addition, the effect of adding up to 6 pct. of oil to the R-114 (simulating typical amounts found in a real evaporator) during Turbo-B tube experiments was studied to see how much the heat transfer performance of the tubes decreased. All tests were conducted at 2.2 C corresponding to typical working pressures in a Navy evaporator. The results using pure R-114 indicated that the heat transfer performance for both types of tube were similar and outperformed smooth and finned tube bundles by a factor of up to 5 and 3 respectively.The effectiveness of the Turbo-B tube bundle degraded with increased amounts of oil. GRA

N92-17531# International Centre for Theoretical Physics, Trieste (Italy).
LIE-ISOTOPIC GENERALIZATION OF THE POINCARE SYMMETRY: CLASSICAL FORMULATION
R. M. Santilli Mar. 1991 47 p
(DE91-642825; IC-91/45) Avail: NTIS HC/MF A03

This paper is devoted to the origin and methodology of the several phenomenological predictions of deviations from Einstein's Special Relativity and related Lorentz symmetry in the behavior of the lifetime of unstable hadrons at different speeds, that exist in the literature since the early 1960's. After reviewing the background phenomenological literature, we outline the Lie-isotopic symmetry of the emerging deformations of the Minkowski metric introduced in a preceding paper, and extend the results to the construction of the full Poincare-isotopic symmetry. The local isomorphism of the Poincare-isotopic symmetry with the conventional symmetry is proved for all possible topology-preserving deformations of the Minkowski metric. In this way, we establish that the phenomenological predictions of deviations recalled earlier must be specifically referred to Einstein's Special Relativity, but they cannot be referred to the Lorentz (or to the Poincare) symmetry which remains exact. Particular attention is devoted to the proof of the compatibility of the exact validity of the Special Relativity for the center-of-mass trajectory of a hadron in a particle accelerator, with conceivable deviations from the same relativity in the interior structural problem. For completeness, the analysis is complemented with a few remarks on the gravitational profile. First, we review the pioneering Lie-isotopic generalization of Einstein's Gravitation worked out by Gasperini, which possesses precisely a locally Lorentz-isotopic structure. We then restrict this theory to the interior gravitational problem in order to achieve compatibility with the particle setting. DOE

N92-17537# Navy Clothing and Textile Research Facility, Natick, MA.
THERMAL ENERGY TEST APPARATUS Technical Report, period ending 1974
N. F. Audet Oct. 1991 33 p
(AD-A243526; NCTRF-187) Avail: NTIS HC/MF A03 CSCL 20/13

The Navy Clothing and Textile Research Facility (NCTRF) designed and fabricated a thermal energy test apparatus to permit evaluation of the heat protection provided by crash crew firefighter's proximity clothing materials against radiant and convective heat loads, similar to those found outside the flame zone of aircraft fuel fires. The apparatus employs electrically operated quartz lamp radiant heaters and a hot air convective heater assembly to produce the heat load conditions the materials to be subjected to, and is equipped with heat flux sensors of different sensitivities to measure the incident heat flux on the sample material as well as the heat flux transmitted by the sample. Tests of the apparatus have shown that it can produce radiant heat flux levels equivalent to those estimated to be possible in close proximity to large aircraft fuel fires, and can produce convective heat fluxes equivalent to those measured in close proximity to aircraft fuel fires at upwind and sidewind locations. Work was performed in 1974. GRA

N92-17686# Naval Postgraduate School, Monterey, CA.
EFFECTS OF POWER PULSATIONS ON HEAT TRANSFER FROM DISCRETE HEAT SOURCES M.S. Thesis
Erhan M. Akdeniz Mar. 1991 111 p
(AD-A243434) Avail: NTIS HC/MF A06 CSCL 13/1

The natural convection heat transfer from an array of heaters flush mounted on a vertical test surface in response to both step and periodic input power has been investigated. Baseline surface temperature measurements in water were obtained for several steady power inputs, ranging from 0.2 W to 1.0 W for the vertical test surface. Also, the effects of the presence of a parallel shroud near the test surface on measured temperature values were studied. The effects of periodic variations in input power on the heater element temperatures were then examined at selected locations. The resulting transient heater temperatures were measured for various amplitudes, frequencies, and average levels of the periodic input power. These transient measurements are compared with a two-dimensional numerical simulation of the relevant fluid flow and heat transfer processes. The computed heater surface temperatures supported the trends of the measurements and were within the expected range. GRA

N92-17807# International Centre for Theoretical Physics, Trieste (Italy).
TEMPERATURE DEPENDENT ANOMALOUS STATISTICS
A. Das and S. Panda Jul. 1991 6 p
(DE92-609665; IC-91/145; UR-1214; ER-13065-666) Avail: NTIS HC/MF A02

We show that the anomalous statistics which arises in 2 + 1 dimensional Chern-Simons gauge theories can become temperature dependent in the most natural way. We analyze and show that a statistic's changing phase transition can happen in these theories only as T yields infinity. DOE

N92-17817# Tokyo Univ., Tanashi (Japan). Inst. for Nuclear Study.
FUTURE PROSPECTS OF PREGEOMETRY
Hidezumi Terazawa Jun. 1991 19 p
(DE92-704278; INS-879) Avail: NTIS HC/MF A03

Pregeometry is a theory, first suggested by Sakharov in 1967, in which gravity is taken as a quantum effect of matter fields and in which Einstein's theory of general relativity for gravity appears as an approximate and effective theory at long distances. It is shown by reviewing the extensive developments of pregeometric theories of gravity for the last more than a decade that the original idea by Sakharov is really working. Many future prospects of the theories are discussed in some detail. DOE

N92-17824# International Centre for Theoretical Physics, Trieste (Italy).
STATE VECTOR REDUCTION. PART 1: DYNAMICAL REDUCTION THEORIES; CHANGING QUANTUM THEORY SO THE STATEVECTOR REPRESENTS REALITY
G. C. Ghirardi and P. Pearle (Hamilton Coll., Clinton, NY.) Feb. 1991 19 p
(DE91-641488; IC-91/22) Avail: NTIS HC/MF A03

The propositions, that what we see around us is real and that reality should be represented by the statevector, conflict with quantum theory. In quantum theory, the statevector can readily become a sum of states of comparable norm, each state representing a different reality. In this paper we present the Continuous Spontaneous Localization (CSL) theory, in which a modified Schroedinger equation, while scarcely affecting the dynamics of a microscopic system, rapidly 'reduces' the statevector of a macroscopic system to a state appropriate for representing individual reality. DOE

N92-17848# European Space Agency, Paris (France).
THEORETICAL INVESTIGATION OF THE INJECTION AND EVAPORATION OF WATER IN A HYDROGEN/OXYGEN STEAM GENERATOR
Stefan Beer (Deutsche Forschungsanstalt fuer Luft- und Raumfahrt, Lampoldshausen, Germany, F.R.) Jul. 1991 68 p Transl. into ENGLISH of Theoretische Untersuchung ueber das Einspritzen und Verdampfen von Wasser beim Wasserstoff/-Sauerstoff Dampferzeuger (Lampoldshausen, Fed. Republic of Germany, DLR), May 1990 68 p Original language document was announced as N91-21938

(ESA-TT-1252; DLR-FB-90-20; ETN-92-90747) Avail: NTIS HC/MF A04; original German version available from DLR Wissenschaftliches Bertichtswesen, VB-PL-DO, Postfach 90 60 58, 5000 Cologne, Fed. Republic of Germany, HC 25.50 DM

Water is injected into the gas stream for the purpose of cooling the reaction products resulting from the stochiometric combustion of hydrogen with oxygen. The penetration of the jet decisively influences the temperature profile across the flow cross section in the water vapor. The penetration of the water jet into the stream is calculated using the jet shedding model and compared with the garden hose model. Models for the evaporation of water droplets in superheated steam are developed for calculating the evaporation paths. The parameters which influence the injection and evaporation process are subjected to variation and their effects in the evaporation paths are analyzed. ESA

N92-17879# Oxford Univ. (England). Dept. of Engineering Science.

WALL TEMPERATURE PATTERNS IN NUCLEATE BOILING

D. B. R. Kenning 1991 24 p

(OUEL-1876/91; ETN-92-90905) Avail: NTIS HC/MF A03

Temperature patterns on the back of a thin stainless steel heated plate during pool nucleate boiling of water are measured with thermocromic liquid crystal. It is shown that spatial variations which are large fractions of the mean wall superheat are to be expected in many experimental and industrial applications of boiling. They can cause errors on the measurement of the mean wall superheat by some conventional methods. Established mechanistic models which assume uniformity of wall superheat cannot represent correctly the processes controlling the density and intermittent activity of the bubble nucleation sites on walls of finite thermal conductivity. The essential features of a realistic model are described. ESA

80 SOCIAL SCIENCES (GENERAL)

Includes educational matters.

No abstracts in this category.

81 ADMINISTRATION AND MANAGEMENT

Includes management planning and research.

N92-17198# Advisory Group for Aerospace Research and Development, Neuilly-Sur-Seine (France). Groupe Consultatif pour la Recherche.

CALENDAR OF SELECTED AERONAUTICAL AND SPACE MEETINGS, JULY 1990 ONWARDS

10 Sep. 1990 136 p In ENGLISH and FRENCH

(AGARD-CAL-90/2; ISBN-92-835-0575-1) Copyright Avail: NTIS HC/MF A07; Non-NATO Nationals requests available only from AGARD/Scientific Publications Executive

A listing is presented of selected meetings which will assist members of the aeronautical and space community by informing them about many scheduled International Scientific and Technical meetings and help is provided in avoiding the need to consult several sources in order to find out what meetings have been planned, their dates, and locations. The AGARD calendar is published every six months, in June and December of each year. Author

N92-17212# Advisory Group for Aerospace Research and Development, Neuilly-Sur-Seine (France).

CALENDAR OF SELECTED AERONAUTICAL AND SPACE MEETINGS, JANUARY 1992 AND ONWARDS

1992 121 p In ENGLISH and FRENCH

(AGARD-CAL-92/1; ISBN-92-835-0651-O) Copyright Avail: NTIS HC/MF A06; Non-NATO Nationals requests available only from AGARD/Scientific Publications Executive

A listing is presented of scheduled International Scientific and Technical meetings and helps in avoiding the need to consult several sources in order to find out what meetings have been planned, their dates and locations. Details concerning the meetings listed in this issue of the calendar were obtained from National and International Organizations which sponsor Aeronautical and Space meetings and from other sources. Author

N92-17388# Naval Postgraduate School, Monterey, CA.

A MANAGEMENT CASE ANALYSIS OF THE DEPARTMENT OF DEFENSE CONTRACTOR RISK ASSESSMENT GUIDE PROGRAM M.S. Thesis

David M. Harp Dec. 1990 82 p

(AD-A243515) Avail: NTIS HC/MF A05 CSCL 05/9

This thesis investigates the extent to which the Contractor Risk Assessment Guide (CRAG) Program at General Dynamics in San Diego, California, is achieving the goal of improved Department of Defense oversight processes and more effective contractor internal control systems. The study describes the development, reviews the basic audit procedures, and examines the five chapters of the CRAG Program. The research demonstrates that reduced duplication of effort was attained at General Dynamics' San Diego divisions through coordinated statistical sampling and audit planning. The environment created by the CRAG Program has resulted in an improved relationship between General Dynamics and government oversight personnel. The study concludes that the CRAG Program is an effective method to promote self-governance in the defense industry and recommends continued support from both industry and the Department of Defense. GRA

N92-17451# Naval Postgraduate School, Monterey, CA.

FEEDBACK IN DYNAMIC DECISION MAKING: AN EXPERIMENT IN SOFTWARE PROJECT MANAGEMENT M.S. Thesis

Robert D. Goodwin, Jr. Mar. 1991 70 p

(AD-A242361) Avail: NTIS HC/MF A04 CSCL 12/5

Software project development has been plagued with an infamous for cost overruns, late deliveries, poor reliability and users' dissatisfaction. Much of this blame has been placed on the manner in which software development projects are managed. The System Dynamics Model of Software Project Management is a quantitative model of software project dynamics that is attempting to gain some valuable insight into the managerial side of developing software systems. The objective of this thesis is to use the System Dynamics Model's gaming interface to investigate the effects of feedback on software project managers. Specifically, subjects were provided with either feedforward, outcome feedback, or cognitive feedback to determine which feedback form, if any, improved the subjects' performance when confronted with a complex dynamic task, such as software project management. The results show that subjects in the cognitive feedback condition achieve a higher level of performance than those in either the feedforward or outcome feedback conditions. GRA

N92-17651# North Carolina Univ., Chapel Hill. Dept. of Computer Science.

THE UNC GRAPH SERVER: A DISTRIBUTED HYPERMEDIA DATA MANAGEMENT SYSTEM

Douglas E. Shackelford, John B. Smith, Joan Boone, and Barry Elledge Apr. 1991 14 p

(Contract N00014-86-K-0680; NSF IRI-90-15443)

(AD-A242041; TR91-019) Avail: NTIS HC/MF A03 CSCL 12/7

Our project is studying the process by which groups of individuals work together to build large, complex structures of ideas and is building a distributed hypermedia system to support that process. This description focuses on the hypermedia data management system, which we call a graph server, we are developing to support groups of collaborators working on individual

workstations within a distributed computing environment. The discussion covers the graph-based data model provided by the server to client hypermedia programs as well as the architecture of the system. A number of research issues are raised and discussed in context including: partitioning the hypermedia graph; an open, extensible architecture for applications; composite objects; anchored links; and the integrity, consistency, and completeness of the artifact as a whole. GRA

N92-17669# North Carolina Univ., Chapel Hill. Dept. of Computer Science.
MATHEMATICAL BASIS FOR A SYSTEM TO MANAGE AUTOMATED PROTOCOL ANALYSIS
Richard M. Hawkes Apr. 1991 28 p
(Contract N00014-86-K-0680; NSF IRI-85-19517; NSF IRI-88-17305)
(AD-A242042; TR91-024) Avail: NTIS HC/MF A03 CSCL 12/6

The TextLab Research Group has developed a number of tools and techniques for automatically recording users' interactions with computer systems in machine readable form, for replaying sessions, for analyzing protocol data using cognitive grammars, for filtering analyzed data and interfacing with statistical packages, and for displaying results in visual forms that facilitate interpretation. The methodology they are developing encourages the collection of large numbers of protocols that must be stored, retrieved, divided into meaningful groups, etc., before they can be analyzed. Thus, managing protocol data becomes increasingly important. Our long-term goal is to develop an integrated environment from which to control and monitor all stages of the process; the goal of this paper is to provide a conceptual foundation for that system. It discusses issues concerned with sorting and selecting protocols according to associated attributes and with criteria for the proper application of particular statistical or other analytic functions to particular forms of protocols or data derived from them. The mathematical model presented is general and can be applied to other applications in which matching analytic program requirements with data type or organization is important. GRA

N92-17687# Naval Postgraduate School, Monterey, CA.
DEVELOPMENT OF A KNOWLEDGE BASE FOR USE IN AN EXPERT SYSTEM ADVISOR FOR AIRCRAFT MAINTENANCE SCHEDULING (ESAAMS) M.S. Thesis
Mark H. Stone, Jr. Mar. 1991 100 p
(AD-A243435) Avail: NTIS HC/MF A05 CSCL 12/5

The Expert System Advisor for Aircraft Maintenance Scheduling (ESAAMS) was originally proposed to assist in the scheduling of discrepancies in a naval aviation squadron maintenance department. The development of a knowledge base for ESAAMS which will support the stated goals of the system is addressed. An overview of expert systems in general and specifically the ESAAMS system is presented as background information to the reader. A specific approach to acquiring, documenting, and storing the knowledge is suggested which will facilitate further development of the system prototype. Based on interviews with experienced maintenance controllers, an initial knowledge base is provided for use in the prototype system. Recommendations for further study based upon the findings discovered during this research are presented. GRA

N92-17940 Department of the Navy, Washington, DC.
MAGNETIC MULTILAYER STRAIN GAGE Patent Application
M. Wun-Fogle, inventor (to Navy), A. K. Clark, inventor (to Navy), and K. B. Hathaway, inventor (to Navy) 1 Nov. 1991 10 p
(AD-D015163; US-Patent-Appl-SN-786641; Navy-Case-73415)
Avail: NTIS HC/MF A02 CSCL 14/2

A strain gauge comprised of a magnetic multilayer assembly exhibiting spin-valve effect with individual ferromagnetic layers possessing magnetostrictive properties is described. A magnetic field source is used to bias the magnetic moments of the ferromagnetic layers in a given direction whereby stress applied causes previously antiferromagnetically coupled moments to be angularly realigned toward a ferromagnetic arrangement. Such realignment causes a corresponding resistance change of unexpectedly high magnitude thereby providing a highly sensitive strain gauge. Author (GRA)

N92-17952# Columbia Univ., New York, NY. Dept. of Electrical Engineering.
MANAGEMENT, CONTROL AND PERFORMANCE OF BROADBAND INTEGRATED NETWORKS Final Report, 1 Jan. 1990 - 30 Sep. 1991
Mischa Schwartz, Thomas E. Stern, and Aurel Lazar 30 Sep. 1991 7 p
(Contract N00014-90-J-1289)
(AD-A242750) Avail: NTIS HC/MF A02 CSCL 25/2

This research summary covers the following areas of activity: (1) network management and control, and (2) asynchronous network performance evaluation and design. The network management and control research covered two topics: Access control in broadband integrated networks, with particular focus on video traffic streams; and fault management. The work on asynchronous network performance evaluation focused on integrated networks (for example, asynchronous transfer mode) carrying bursty, heterogenous traffic from large numbers of sources. Three aspects of the problem were considered: performance analysis and control using Markov-modulated rate process (MMRP) models; analysis and design of fast packet switches; and performance of full motion coded video sources in asynchronous networks. GRA

82 DOCUMENTATION AND INFORMATION SCIENCE

Includes information management; information storage and retrieval technology; technical writing; graphic arts; and micrography.

For computer documentation see *61 Computer Programming and Software.*

N92-17001*# National Aeronautics and Space Administration. Langley Research Center, Hampton, VA.
NASA/DOD AEROSPACE KNOWLEDGE DIFFUSION RESEARCH PROJECT: CHRONOLOGY OF SELECTED LITERATURE, REPORTS, POLICY INSTRUMENTS, AND SIGNIFICANT EVENTS AFFECTING FEDERAL SCIENTIFIC AND TECHNICAL INFORMATION (STI) IN THE US
Thomas E. Pinelli, Madeline Henderson, Ann P. Bishop, and Philip Doty (Texas Univ., Austin.) Jan. 1992 131 p
(NASA-TM-101662; Rept-11; NAS 1.15:101662) Avail: NTIS HC/MF A07 CSCL 05B

The chronology is a comprehensive bibliography. It contains 512 entries covering a variety of selected literature, reports, policy instruments, and significant events affecting Federal Scientific and Technical Information (STI) from 1945 to 1990. It includes some publications and events of historic interest which relate to the evaluation of aerospace and aerospace knowledge diffusion. Each entry has been given an item number and items are arranged by columns. To provide an overview of Federal STI developments, the entries are generally arranged by date of publication and event. Author

N92-17013# Air Force Occupational Measurement Center, Randolph AFB, TX.
INFORMATION MANAGEMENT 70XX CIVILIAN EQUIVALENT
Jun. 1991 170 p
(AD-A242875; AFPT-90-70X-877) Avail: NTIS HC/MF A08 CSCL 05/9

Information Management civilian personnel in paygrades GS-7 and above in selected occupational series were surveyed to obtain current data to assist Air Staff in future Civilian Information Management Career Program (IMCP) and training decisions. Three clusters and four independent jobs were identified. Although the Information Management personnel perform diverse functions, the majority of the personnel perform many similar tasks which have

an administrative orientation, such as general administrative, management, and supervisory tasks. Those personnel in technically oriented positions also spend a substantial amount of their job time performing general administrative functions. The analysis of the occupational series, paygrade groups, and selected background data indicates both the diversity of the various series and the similarity of some of the tasks performed among the survey respondents. Data comparisons pinpoint clearly the differences and similarities of the tasks performed, as well as the usual paygrade progression relationships between and within the respective occupational series. GRA

N92-17037# Georgia Inst. of Tech., Atlanta. School of Electrical Engineering.
OPTICAL CONTENT-ADDRESSABLE MEMORIES FOR DATA/KNOWLEDGE BASE PROCESSING Report, Dec. 1987 - Dec. 1988
Thomas K. Gaylord Aug. 1991 100 p
(Contract F30602-81-C-0185)
(AD-A241866; RL-TR-91-192) Avail: NTIS HC/MF A05 CSCL 20/6

This project studied the potential of managing a data/knowledge base using an optical content-addressable memory (OCAM) as opposed to an electronic location-addressable memory. In an optical content-addressable memory, inputs are compared with the stored data, and detected matches found in parallel. In a holographic OCAM, the number of reference patterns represents the number of holograms that need to be stored in the system. Using thick holographic recording media, such as photo-refractive lithium niobate, holograms may be multiplexed together in a common volume. This project completed work on applying OCAMs to the operations of addition and multiplication by using residue-coded numbers and other operations such as discrete matched filtering. These operations can be used to perform data searching or truth-table look-up processing. GRA

N92-17067# Naval Postgraduate School, Monterey, CA.
ECONOMIC ANALYSIS OF INFORMATION SYSTEM M.S. Thesis
Charles G. Walker, Jr. Mar. 1991 124 p
(AD-A243079) Avail: NTIS HC/MF A06 CSCL 05/3

This paper examines the utilities of present value analysis, discounted payback analysis, uniform annual cost, benefit-cost ratio, savings investment ratio, internal rate or return, and break even analysis, as economic analysis techniques. These techniques are analyzed using comparative four-way data sets that have front-loaded and back-loaded costs and front-loaded and back-loaded benefits. The findings of this analysis are then summarized in a matrix that scores the category of utility for each technique. An expert system (COSTEX) is then developed using the Intelligence Compiler expert system shell. The system directs MIS managers in the selection of appropriate techniques of analysis for a given set of economic analysis contingencies. The Basic Economic Analysis Decision Support framework and a tutorial on the methodologies and virtues of each of the economic analysis techniques. GRA

N92-17125# Naval Postgraduate School, Monterey, CA.
BENEFIT ANALYSIS OF PROPOSED INFORMATION SYSTEMS M.S. Thesis
Mark H. Besore Mar. 1991 90 p
(AD-A243707) Avail: NTIS HC/MF A05 CSCL 05/3

This thesis reviews two different approaches to benefit analysis, benefit comparison and user satisfaction, that could be applied to the evaluation of proposed information systems which are under consideration for acquisition by the Federal government. Currently the General Services Administration only recommends that present value analysis methods be used in the analysis of alternatives even though the GSA specifies that non-cost factors should be evaluated in such an analysis. Different benefit comparison and user satisfaction methods are reviewed for their particular advantages and disadvantages. A discussion is given on how selected methods of each approach may be used within the Federal government for the evaluation of alternatives. Suggestions are made for ways of conducting a more complete analysis of alternatives through incorporating present value analysis, benefit comparison of non-cost factors, and analysis of user satisfaction, into one comprehensive analysis. GRA

N92-17136# Naval Postgraduate School, Monterey, CA.
ELECTRONIC DATA INTERCHANGE M.S. Thesis
Jae Du Chung Mar. 1991 85 p
(AD-A242959) Avail: NTIS HC/MF A05 CSCL 12/7

Electronic data interchange (EDI) is the intercompany, computer-to-computer exchange of business documents in standard formats. The direct benefits of EDI consist of cost savings, operational accuracy, and speedy processing of transactions. This thesis provides guidelines to develop an EDI system. It discusses the basic concepts, standards, data mapping, hardware and software requirements, and networking requirements. Also discussed are some auditing and security issues in implementing EDI. Electronic data interchange is fast becoming the standard way of exchanging business documents, not only in this country but also in the rest of the world. EDI provides a faster, more accurate, less costly method of communication than do traditional methods of business communications such as mail, telephone, and personal delivery. However, EDI is doing more than just changing how businesses communicate; it is changing the way businesses operate. Electronic data interchange is changing industry. Trading relationships are changing, management philosophies are changing, and production techniques are changing. GRA

N92-17174# IIT Research Inst., Rome, NY.
CALS DATABASE USAGE AND ANALYSIS TOOL STUDY Final Report
James H. Cook and Edward J. Szwedo Sep. 1991 71 p
(Contract MDA903-90-D-0022)
(AD-A243205) Avail: NTIS HC/MF A04 CSCL 05/2

The computer Assisted Acquisition and Logistics Support (CALS) effort will involve large and geographically dispersed databases of proprietary technical information pertaining to weapons systems and parts. These databases will be combined to form the CALS Integrated Weapons Systems Database (IWSDB). While a goal of the CALS effort is to openly exchange information in a standardized format, it is recognized that unlimited access to large amounts of weapons systems data will pose a security risk. These databases will be shared by government and industry personnel and by their very nature will contain data that when aggregated could increase in sensitivity or classification. The purpose of this study was to develop a conceptual design for a tool that will monitor CALS database usage in real-time to prevent unauthorized access to potentially sensitive and propriety data. GRA

N92-17228# Executive Office of the President, Washington, DC. Office of Administration.
PUBLICATIONS OF THE EXECUTIVE OFFICE OF THE PRESIDENT, JANUARY 20, 1989 TO JUNE 30, 1991
Jun. 1991 11 p
(PB91-202762) Avail: NTIS HC/MF A03 CSCL 05B

The report lists publications of the Executive Office of the President for the Bush Administration for the Period 20 Jan. 1989 through 30 Jun. 1991. Listed are publications released by the following groups: Council of Economic Advisers (CEA), Council on Environmental Quality (CEQ), Office of Administration (OA), Office of Management and Budget (OMB), President's Council on Integrity and Efficiency (PCIE), Statistical Policy Working Paper Series, Office of National Drug Control Policy (ONDCP), Office of Science and Technology Policy (OSTP), Office of the United States Trade Representative (USTR), Office of the Vice President (OVP), National Space Council (NSPC), and White House Office (WHO). Author

N92-17255# Naval Postgraduate School, Monterey, CA.
THE TOP TEN CRITICAL MIS ISSUES IN THE DEPARTMENT

OF DEFENSE M.S. Thesis
Rafael A. Gacel Mar. 1991 115 p
(AD-A242975) Avail: NTIS HC/MF A06 CSCL 05/1

Information systems (IS) professionals in the Department of the Navy (DON), face a multitude of IS management problems. Unfortunately, the U.S. Navy and Marine Corps do not have the financial, managerial, or technical resources to tackle every one of these problems. Therefore, it is helpful to determine which are the most critical issues facing IS officers in the Navy and Marine Corps, and how much agreement there is among IS officers in the Navy and Marine Corps regarding the importance of these critical issues. It is also helpful to determine how those critical issues identified by Navy IS officers compare with those identified by Marine Corps IS officers, and how their critical issues compare with those identified by civilian corporate IS executives. GRA

N92-17274# Army Natick Labs., MA.
BIBLIOGRAPHY OF TECHNICAL PUBLICATIONS, PAPERS, AND LIST OF PATENTS, OCTOBER 1988 - SEPTEMBER 1989 Final Report, Oct. 1988 - Sep. 1989
Patricia E. Bremner and M. E. Collins Sep. 1991 23 p
(AD-A242839; NATICK/TR-90/001) Avail: NTIS HC/MF A03 CSCL 05/2

This report contains a bibliographic listing of technical publications and papers presented by personnel of the U.S. Army Natick Research, Development and Engineering Center and its contractors for the period October 1988 to September 1989. This report also lists patents issued to Natick personnel during the same period. GRA

N92-17340# Naval Postgraduate School, Monterey, CA.
COST MODELS AND THE CORPORATE INFORMATION MANAGEMENT (CIM) INITIATIVE M.S. Thesis
David P. Faulk Mar. 1991 73 p
(AD-A243554) Avail: NTIS HC/MF A04 CSCL 05/3

This thesis provides a brief history of the Corporate Information Management (CIM) initiative, and includes a summary of the methodology being employed to complete the initiative. The focus of this thesis is on the alternative cost models that are available to the Department of Defense (DoD), and the information requirements for each of them. The cost models reviewed include actual, normal, standard, variable, cost-volume-profit analysis, and job order. Advantages and disadvantages of each of these models is discussed. In addition, the current DoD implementation of unit costing is also discussed and compared and contrasted to the alternative models that exist. GRA

N92-17369# Naval Ocean Systems Center, San Diego, CA.
INFORMATION MANAGEMENT ENGINEERING (IME) LABORATORY: A DATABASE DEVELOPMENT FACILITY Final Report, FY 1985 - FY 1991
Marion G. Ceruti and Richard A. Auclair Aug. 1991 21 p
(AD-A243191; NOSC-TD-2174) Avail: NTIS HC/MF A03 CSCL 12/7

An Information Management Engineering (IME) database development laboratory is described that features a VAX/Macintosh hardware suite and a menu driven user interface. The software system was created for, and is used by, database developers and database administrators who work with the Digital Equipment Corporation Virtual Memory Operating System (VMS) and the Oracle Database Management System. It was designed to accomplish a variety of database related tasks, including data input from magnetic tape, disk file management, database fill, data entry, data dictionary report generation, data quality analysis and validation, data reference inventory management, and user communications. This system was used to develop and enhance several command and control databases for the following projects: the OSIS Baseline Upgrade (OBU); the Maritime Defense Zone (MDZ); the Operations Support Group Prototype (OSGP); the Fleet Command Center Battle Management Program (FCCBMP) for CINCPACFLT at Pearl Harbor, HI; CINCPACAF Integrated Decision Support System (CIDSS) testing for CINCPACAF at Hicham Air Force Base, HI; the Mobile Systems Tactical Data Facility (MSTDF); and the Operational Support System (OSS). GRA

N92-17378# Woods Hole Oceanographic Inst., MA.
BIBLIOGRAPHY OF TECHNICAL REPORTS 1990
Susan S. Putnum Jun. 1991 17 p
(AD-A242376; WHOI-91-16) Avail: NTIS HC/MF A03 CSCL 05/2

The technical reports prepared by the Woods Hole Oceanographic Institution in 1990 are listed in this bibliography. Inquiries about availability of extra copies will be handled on an individual basis. Initial distribution of the reports is controlled by the funding agencies. NTIS order numbers are included with each report listed or can be obtained from the Document Library. The Document Library provides Interlibrary Loan service for all Institution reports and will assist with problems of identification. GRA

N92-17396# CSA Engineering, Inc., Palo Alto, CA.
FEM-X USER'S GUIDE Final Report, Mar. 1989 - Dec. 1990
Warren C. Gibson 23 Aug. 1991 40 p
(Contract F33615-89-C-3205)
(AD-A242374; CSA-91-01-03; WL-TR-91-3056) Avail: NTIS HC/MF A03 CSCL 12/7

This document is a User's Guide for FEM-X, a database management system for finite element models. The Guide describes the organization of finite element model data and descriptive text in FEM-X, and describes briefly the operations of model data entry and text data entry, and extraction and translation of model data. FEM-X is a window based product designed to run on engineering workstations under the X Window System. The graphical interface makes operation of FEM-X intuitive, with on-line help available at each stage. Discussions of CADDB, the database system used for FEM-X, and its query software, ICE, are also provided. GRA

N92-17401# Air Force Environmental Technical Applications Center, Scott AFB, IL.
COMPARISON OF TWO EIGHTH-MESH TERRAIN DATABASES
Richard W. Hartman Sep. 1991 26 p
(AD-A243315; USAFETAC/PR-91/019) Avail: NTIS HC/MF A03 CSCL 08/2

An accurate geographical and terrain database is important to providing surface characteristics, such as the locations of ice, water, or land. It is also important in calculating terrain elevations for a grid of evenly spaced points around the world and in providing critical input information for the meteorological computer models used by the Air Force Global Weather Central (AFGWC) and the USAF Environmental Technical Applications Center. This report compares the accuracy of the new Phillips Laboratory Geophysics Directorate (GD) eighth-mesh terrain database with an older eighth-mesh terrain database developed and used by the AFGWC. Most of the eighth-mesh grid points located over major land masses were examined by comparing the point values for each database with the elevation of nearby Air Weather Service Master Station Catalog (AWSMSC) stations. By subtracting the point values of each database from the AWSMSC, two sets of difference values were created and summarized with the root mean square error and mean of the absolute error. The comparison showed that there was little difference between databases in the northern hemisphere, but that the GD database was much better than the AFGWC database in the Southern Hemisphere. GRA

N92-17402# Naval Postgraduate School, Monterey, CA. Dept. of Computer Science.
TOWARDS INTELLIGENT DATA RETRIEVAL IN MULTIMEDIA DATABASES
Kyung-Chang Kim and Vincent Y. Lum Feb. 1991 26 p
(AD-A243323; NPS-CS-91-009) Avail: NTIS HC/MF A03 CSCL 12/7

Manipulation of multimedia data in multimedia databases is not straightforward as in conventional databases because of the complex structure of the multimedia data such as image or sound. The issue in the retrieval of multimedia data from the database is

the matching of the contents of multimedia data to a user query. The common solution is to use either keywords or natural language descriptions to describe both the contents of multimedia data and user queries. The major problem is that different users, or the same user at different times, describe the same thing differently, which results in the descriptions of the contents of multimedia data to rarely exactly match the descriptions of the user queries. Hence, partial or approximate match between descriptions of multimedia data and user queries is often required during multimedia data retrieval. In this paper, we propose an intelligent approach to approximate match by integrating both object-oriented and natural language understanding techniques. GRA

N92-17470# Edgerton, Germeshausen and Grier, Inc., Idaho Falls, ID.
VERSATILE DATA ACQUISITION SYSTEM MODEL II USER'S MANUAL
R. A. Richardson and R. G. Berg Sep. 1991 261 p
(Contract DE-AC07-76ID-01570)
(DE92-003311; EGG-EP-9846) Avail: NTIS HC/MF A12

This document details the installation, use, and operation of a portable data acquisition system. The system provides a means of acquiring detailed test data in applications where limited space is available, the operating environment is harsh, and unattended operation is desirable. It combines the design of hardware and menu driven software for data acquisition in a variety of applications. The system was designed for electric vehicle performance testing but has the versatility to be used in many applications. Performance parameters can be measured during over the road driving with data stored on an IBM-PC compatible disk. Data may then be reduced and analyzed using any of several commercially available software programs. This data acquisition system was designed to meet the following objectives: (1) light compact construction for easy installation in space limited applications; (2) ruggedized construction; (3) powdered by a 12 volt battery; (4) sufficient data storage for several days of unattended data acquisition; (5) versatility with respect to the types of measurement sensors that can be utilized; and (6) ease of system setup and operation using menu driven software. In the preferred form, the system consists of a battery powered data acquisition logging and processing unit (the actual Versatile Data Acquisition System enclosure) and a number of remote sensors. A keyboard and portable monitor can be connected to the system for on-line monitoring of data or modifications to the software setup procedures. DOE

N92-17482# Air Force Inst. of Tech., Wright-Patterson AFB, OH. School of Engineering.
AN OBJECT-ORIENTED DATABASE IMPLEMENTATION OF THE MAGIC VLSI LAYOUT DESIGN SYSTEM M.S. Thesis
Timothy M. Jacobs Dec. 1991 73 p
(AD-A243743; AFIT/GCS/ENG/91D-09) Avail: NTIS HC/MF A04 CSCL 05/2

This thesis attempts to prove that the commercially available ObjectStore data management system provide the performance and functionality necessary to support a complex engineering design system. This is accomplished by modifying the Magic VLSI Circuit Layout Design System to eliminate its current Unix file data management system and replace it with ObjectStore. The approach to this research effort includes a design recovery of the Magic System and identification of its key data management functions. These functions are then modified to take advantage of the database management facilities of ObjectStore. Additional code is added to instrument performance measurement of both the original and the ObjectStore versions of the Magic System. Testing is accomplished using existing Magic commands to test key database performance criteria. The ObjectStore version of Magic performed better than the original version for some performance criteria and significantly slower than the original version for other criteria. The conversion effort was difficult and time consuming due to the complexity of the original Magic software and the ObjectStore database management system. A more specific implementation of ObjectStore capabilities for conclusive results. GRA

N92-17586*# National Aeronautics and Space Administration. Marshall Space Flight Center, Huntsville, AL.
FY 1991 SCIENTIFIC AND TECHNICAL REPORTS, ARTICLES, PAPERS, AND PRESENTATIONS
Joyce E. Turner, comp. Oct. 1991 69 p
(NASA-TM-103567; NAS 1.15:103567) Avail: NTIS HC/MF A04 CSCL 05B

Formal NASA technical reports, papers published in technical journals, and presentations by MSFC personnel in FY 1991 are presented. Papers of MSFC contractors are also included. The information in this report may be of value to the scientific and engineering community in determining what information has been published and what is available. Author

N92-17633# Naval Postgraduate School, Monterey, CA.
A COMPARISON OF DATA INTEGRITY MODELS M.S. Thesis
Thomas R. Ivan Mar. 1991 88 p
(AD-A243770) Avail: NTIS HC/MF A05 CSCL 05/2

Data integrity in computer based information systems is a concern because of the damage that can be done by unauthorized manipulation or modification of data. While a standard exists for data security, there currently is not an acceptable standard for integrity. There is a need for incorporation of a data integrity policy into the standard concerning data security in order to produce a complete protection policy. There are several existing models which address data integrity. The Biba, Goguen and Meseguer, and Clark/Wilson data integrity models each offer a definition of data integrity and introduce their own mechanisms for preserving integrity. Acceptance of one of these models as a standard for data integrity will create a complete protection policy which addresses both security and integrity. GRA

N92-17641# Carnegie-Mellon Univ., Pittsburgh, PA. Software Engineering Inst.
SERPENT: DIALOGUE EDITOR USER'S GUIDE. SYSTEM FOR USER INTERFACE DEVELOPMENT, VERSION 1 Final Report
Sep. 1991 71 p
(Contract F19628-90-C-0003)
(AD-A242331; CMU/SEI-91-UG-4) Avail: NTIS HC/MF A04 CSCL 12/5

This guide introduces the Serpent dialogue editor, which is used to communicate the dialogue between the end user and the functional, or application, portion of a system. This dialogue specifies both the presentation of application information and end-user interactions. Put differently, the dialogue editor provides an environment in which to develop and maintain Slang dialogue specifications. Most of what is built in the editor translates directly into Slang, the Serpent dialogue specification language. That is, the Slang code generated from the dialogue editor can be compiled and run to produce the user interface for an application. Although the dialogue editor hides much Slang syntax, users of the editor should understand the conceptual model of Slang, as well as the syntax of code snippets and expressions that are used to define much of the interactive behavior. GRA

N92-17785# Pennsylvania Univ., Philadelphia.
THE DYNAMICS OF VISUAL REPRESENTATION, ATTENTION, ENCODING, AND RETRIEVAL PROCESSES Annual Report, 1 Oct. 1990 - 30 Sep. 1991
Saul Sternberg 31 Oct. 1991 5 p
(Grant AF-AFOSR-0015-91; AF Proj. 2313)
(AD-A243031; AFOSR-91-0905TR) Avail: NTIS HC/MF A01 CSCL 05/8

This is the Annual Technical Report of work supported by a grant entitled, The dynamics of visual representation: Attention, encoding, and retrieval processes. After a section describing the objectives of the work, the report provides a synopsis of the principal accomplishments thus far, under the following headings: Relations between the transformation revealed by two paradigms; Influence of reciting direction on location probe performance in

the probed reciting/location probe mixture; Improvements in the timing of spoken responses; Representation of location information; Initial results from a 'double location probe' procedure; Completion of analyses and publication supporting stages in mental operations; Effects of two kinds of degradation on encoding arrays of characters; and Effects of legibility on order of processing. GRA

N92-17787# National Aerospace Lab., Tokyo (Japan). Kakuda Research Center.
MAKING OF FUNCTIONALLY GRADIENT MATERIALS DATA BASE [KEISHA KINO ZAIRYO DETA BESU NO SAKUSEI]
Takayuki Sudo, Katsuto Kisara, Akio Moro, Masayuki Niino, and Yoshitsugu Ishibashi (Nippon Kokan Co. Ltd., Tokyo, Japan) Jun. 1990 39 p In JAPANESE
(NAL-TM-621; ISSN-0452-2982; JTN-92-80292) Avail: NTIS HC/MF A03

In order to satisfy the severe requirements for super heat resistant materials to be used in spaceplanes or nuclear fusion reactors, the functionally gradient materials (FGM), which use ceramics on the high temperature side and metals on the low temperature side, have been developed. The FGM database has been developed for the use of designers, material control teams, and evaluation team of the material. The features and structures of this database are shown in this report. Author (NASDA)

N92-17845# Lawrence Livermore National Lab., CA.
DEVELOPING A BROADER BASIS FOR SCIENTIFIC DATA ANALYSIS INTERFACES
R. R. Springmeyer, M. M. Blattner, and N. L. Max 1991 8 p Presented at the CHI '92, Monterey, CA, 3-7 May 1991
(Contract W-7405-eng-48)
(DE92-003963; UCRL-JC-108648; CONF-9105285-2) Avail: NTIS HC/MF A02

Typical interfaces for recent scientific data analysis tools have emphasized visualization. Their focus on images can obscure the goal of the scientific data analysis process, which is an understanding of some physical phenomenon. We present the results of a two-phase study of this process, undertaken to inform the design of analysis tools with a broader basis. In the first phase, scientists from several disciplines were interviewed and observed while analyzing their own data. The observations exposed elements of scientific data analysis such as quantitative queries and comparisons, simple calculations, data culling, and record keeping. These elements form the basis of a scientific data analysis description which extends beyond image viewing. The second phase demonstrates how this broader understanding can be applied, with the design and implementation of a tool for culling regions of interest from large, complex data sets. Observations of the prototype tool in use reveal the effectiveness of a quantitative approach to culling complex data sets. The results of this study are three-fold: a method for studying a single-person process, a description of the fundamental elements of scientific data analysis, and a successful demonstration of applying this broader knowledge with a prototype implementation. DOE

N92-17856# Linus Pauling Inst. of Science and Medicine, Palo Alto, CA.
EFFICIENT IDENTIFICATION AND ANALYSIS OF LOW AND MEDIUM FREQUENCY REPEATS
J. Jurka 28 Aug. 1991 23 p
(Contract DE-FG03-91ER-61152)
(DE92-003758; DOE/ER-61152/T1) Avail: NTIS HC/MF A03

The effective starting date of this grant was May 15. In the first three months of this project we focused primarily on organizational and technical aspects of our research which included organization of the database of repeats in primates; preparation of software for rapid and sensitive search of novel repetitive elements in GenBank; purchase and installation of the Sun workstation; and research on the mammal-specific MAR1 family of repetitive elements (to be communicated in October). DOE

83 ECONOMICS AND COST ANALYSIS

Includes cost effectiveness studies.

No abstracts in this category.

84 LAW, POLITICAL SCIENCE AND SPACE POLICY

Includes NASA appropriation hearings; aviation law; space law and policy; international law; international cooperation; and patent policy.

N92-17283# National Academy of Sciences - National Research Council, Washington, DC. Office of Japan Affairs.
SCIENTIFIC AND TECHNOLOGICAL RELATIONS BETWEEN THE UNITED STATES AND JAPAN: ISSUES AND RECOMMENDATIONS
Frank Press and Martha C. Harris Nov. 1990 39 p Sponsored by Commission on United States-Japan relations for the Twenty First Century
(PB91-219170) Avail: NTIS HC/MF A03 CSCL 05D

Discussed here are issues and recommendations relating to Japanese investment in small, high technology corporations, treatment of multinational companies, foreign funding for U.S. university research, asymmetry in training, U.S.-Japan cooperation in science and technology, and asymmetries in science and technology. Author

85 URBAN TECHNOLOGY AND TRANSPORTATION

Includes applications of space technology to urban problems; technology transfer; technology assessment; and surface and mass transportation.

For related information see also *03 Air Transportation and Safety, 16 Space Transportation,* and *44 Energy Production and Conversion.*

N92-17141# David Taylor Research Center, Bethesda, MD.
VALUABLE PATENTS FOR US BUSINESSES: A CATALOG OF DTRC PATENTS AVAILABLE FOR LICENSING BY THE PRIVATE SECTOR Final Report, 1977 - 1991
Basil V. Nakonechny Oct. 1991 47 p
(AD-A242071; DTRC-91/CT07) Avail: NTIS HC/MF A03 CSCL 05/2

The Stevenson-Wydler Technology Innovations Act of 1980 and the Federal Technology Transfer Act of 1986 encourage the transfer of technology derived from Federally sponsored research and development (R and D) to both the public and private sectors. The acts require each Federal agency conducting R and D and its major laboratories to identify and encourage transfer of technologies having potential commercial or practical application. Under new regulations, exclusive licensing is offered as an incentive to transfer Federal technology to U.S. industry and to encourage venture capital investment in improving the nation's technology base. The mission of the David Taylor Research Center (DTRC) is to serve as the principal Navy RDT and E Center for naval vehicles and logistics and to provide RDT and E support for the U.S. Maritime Administration and the maritime industry. DTRC is an active participant in various domestic technology transfer activities sponsored by the U.S. Navy. These include the Navy Potential Contractor Program (NPCP), Cooperative Research and Development Agreements (CRDAs), the Federal Laboratory Consortium (FLC) for technology transfer, and the National Technology Transfer Center (NTTC). The present document provides examples of Center inventions having potential for commercial use. This document contains a list of patents issued

to DTRC employees from June 1977 through June 1991. These selected patents have been examined by the Center's Patent Review Committee and are considered to have possible commercial application. GRA

88 SPACE SCIENCES (GENERAL)

No abstracts in this category.

89 ASTRONOMY

Includes radio, gamma-ray, and infrared astronomy, and astrometry.

N92-17003*# Lockheed Missiles and Space Co., Palo Alto, CA. Research Lab.
ARIES X RAY OBJECTIVE GRATING SPECTROGRAPH Final Report
R. C. Catura 15 Jun. 1991 54 p
(Contract NAS5-27900)
(NASA-CR-189245; NAS 1.26:189245) Avail: NTIS HC/MF A04 CSCL 03A

This investigation was initiated in June of 1983. An Aries payload involving a single Wolter 1 telescope was developed and flown under a previous contract and the objective of this work was to add two additional mirrors, nested inside of the then existing mirror and add 12 objective reflection gratings to convert the telescope into a spectrograph. A summary of major milestones in the investigation are given. Results of efforts under this contract prior to 1987 are presented in the form of four reprints of published papers attached to this report. Results of the gamma-ray research are also included in the form of an attached reprint. A summary of other work under the contract since 1987 is given. Author

N92-17020*# Space Telescope Science Inst., Baltimore, MD.
HUBBLE SPACE TELESCOPE: FINE GUIDANCE SENSORS INSTRUMENT HANDBOOK. VERSION 2.1
Larry Taff, ed. May 1990 48 p Revised
(Contract NAS5-26555)
(NASA-CR-189745; NAS 1.26:189745) Avail: NTIS HC/MF A03 CSCL 03A

The Fine Guidance Sensors (FGS) are a system of photomultiplier tubes and white light amplitude interferometers (Koester's prism) which are used for the fine guidance of the Hubble Space Telescope (HST). The purpose of the handbook is to provide information to a potential user of the FGS so that he may explore the feasibility of performing various observations. A brief overview is given of how the FGS works, along with an explanation of the instrument in some detail. The procedure for estimating exposure times is explained. The observing modes are described. Some details needed to specify the exposures and observation requirements on the proposal forms are explained. Data reduction procedures are outlined. Author

N92-17021*# Space Telescope Science Inst., Baltimore, MD.
HUBBLE SPACE TELESCOPE: FAINT OBJECT CAMERA INSTRUMENT HANDBOOK. VERSION 2.0
Francesco Paresce, ed. May 1990 114 p Revised
(Contract NAS5-26555)
(NASA-CR-189746; NAS 1.26:189746) Avail: NTIS HC/MF A06 CSCL 03A

The Faint Object Camera (FOC) is a long focal ratio, photon counting device designed to take high resolution two dimensional images of areas of the sky up to 44 by 44 arcseconds squared in size, with pixel dimensions as small as 0.0007 by 0.0007 arcseconds squared in the 1150 to 6500 A wavelength range. The basic aim of the handbook is to make relevant information about the FOC available to a wide range of astronomers, many of whom may wish to apply for HST observing time. The FOC, as presently configured, is briefly described, and some basic performance parameters are summarized. Also included are detailed performance parameters and instructions on how to derive approximate FOC exposure times for the proposed targets. Author

N92-17483*# Space Telescope Science Inst., Baltimore, MD.
HUBBLE SPACE TELESCOPE: OPTICAL TELESCOPE ASSEMBLY HANDBOOK. VERSION 1.0
Chris Burrows May 1990 67 p Revised
(Contract NAS5-26555)
(NASA-CR-189751; NAS 1.26:189751) Avail: NTIS HC/MF A04 CSCL 03A

The Hubble Space Telescope is described along with how its design affects the images produced at the Science Instruments. An overview is presented of the hardware. Details are presented of the focal plane, throughput of the telescope, and the point spread function (image of an unresolved point source). Some detailed simulations are available of this, which might be useful to observers in planning their observations and in reducing their data. Author

N92-17484*# Space Telescope Science Inst., Baltimore, MD.
HUBBLE SPACE TELESCOPE: WIDE FIELD AND PLANETARY CAMERA INSTRUMENT HANDBOOK. VERSION 2.1
Richard Griffiths, ed. May 1990 85 p Revised
(Contract NAS5-26555)
(NASA-CR-189753; NAS 1.26:189753) Avail: NTIS HC/MF A05 CSCL 03A

An overview is presented of the development and construction of the Wide Field and Planetary Camera (WF/PC). The WF/PC is a duel two dimensional spectrophotometer with rudimentary polarimetric and transmission grating capabilities. The instrument operates from 1150 to 11000 A with a resolution of 0.1 arcsec per pixel or 0.043 arcsec per pixel. Data products and standard calibration methods are briefly summarized. Author

N92-17497*# Space Telescope Science Inst., Baltimore, MD.
HUBBLE SPACE TELESCOPE: HIGH SPEED PHOTOMETER INSTRUMENT HANDBOOK. VERSION 2.0
Richard L. White, ed. May 1990 48 p Revised
(Contract NAS5-26555)
(NASA-CR-189750; NAS 1.26:189750) Avail: NTIS HC/MF A03 CSCL 03A

This manual is a guide for astronomers who intend to use the High Speed Photometer (HSP), one of the scientific instruments onboard the Hubble Space Telescope (HST). All the information needed for ordinary uses of the HSP is presented, including: (1) an overview of the instrument; (2) a detailed description of some details of the HSP-ST system that may be important for some observations; (3) tables and figures describing the sensitivity and limitations of the HSP; (4) how to go about planning an observation with the HSP; and (5) a description of the standard calibration to be applied to HSP data and the resulting data products. Author

N92-17523# Technische Univ., Berlin (Germany, F.R.). Fachbereich Physik.
GEOMETRICAL METHODS FOR THE ANALYSIS OF COSMOLOGICAL OBSERVATIONS Ph.D. Thesis [GEOMETRISCHE AUSWERTUNGSMETHODEN FUER KOSMOLOGISCHE BEOBACHTUNGEN]
Wolfgang Hasse 1991 240 p In GERMAN; ENGLISH summary
(ETN-92-90584) Avail: NTIS HC/MF A11

Methods were analyzed with which the cosmologically significant content of cosmological observations can be exploited for the establishment of cosmological models. The studies, based on the invariant calculus of differential geometry, were performed in the framework of the general relativity theory, with real shift, angular diameter, and apparent luminosity as observable quantities. The ascertainment procedure for the cosmological parameters (Hubble

constant and deceleration parameter) are transferred from kinematical Robertson-Walker models to universal space-time models, leading to several generalizations of these parameters. Then idealized observation results are analyzed with a view to the circumscription of the world model to be constructed. ESA

N92-17650*# Space Telescope Science Inst., Baltimore, MD.
HUBBLE SPACE TELESCOPE: THE GO AND GTO OBSERVING PROGRAMS. VERSION 1.0
Abhijit Saha May 1990 622 p
(Contract NAS5-26555)
(NASA-CR-189815; NAS 1.26:189815) Avail: NTIS HC/MF A99 CSCL 03A

Selected information from the current Hubble Space Telescope (HST) science programs for the Guaranteed Time Observers (GTO's) and General Observers (GO's) is presented. Included are program abstracts, detailed listings of specific targets, and exposure information. Author

N92-17694*# National Aeronautics and Space Administration. Goddard Space Flight Center, Greenbelt, MD.
RADIO SKY MAPPING FROM SATELLITES AT VERY LOW FREQUENCIES
L. R. O. Storey Nov. 1991 21 p Presented at the URSI Commission E Symposium, Tokyo, Japan, 4-6 Sep. 1989 Submitted for publication
(Grant NSF ATM-83-18186)
(NASA-TM-105452; NAS 1.15:105452; NSSDC/WDC-A-R/S-91-25) Avail: NTIS HC/MF A03 CSCL 03A

Wave Distribution Function (WDF) analysis is a procedure for making sky maps of the sources of natural electromagnetic waves in space plasmas, given local measurements of some or all of the three magnetic and three electric field components. The work that still needs to be done on this subject includes solving basic methodological problems, translating the solution into efficient algorithms, and embodying the algorithms in computer software. One important scientific use of WDF analysis is to identify the mode of origin of plasmaspheric hiss. Some of the data from the Japanese satellite Akebono (EXOS D) are likely to be suitable for this purpose. Author

N92-17695*# Boston Univ., MA. Dept. of Astronomy.
IRAS AND THE BOSTON UNIVERSITY ARECIBO GALACTIC H I SURVEY: A CATALOG OF CLOUD PROPERTIES Final Report
Thomas M. Bania 28 Jan. 1992 8 p
(Grant NAG5-1193)
(NASA-CR-189806; NAS 1.26:189806) Avail: NTIS HC/MF A02 CSCL 03A

The Infrared Astronomy Satellite (IRAS) Galactic Plane Surface Brightness Images were used to identify infrared emission associated with cool, diffuse H I clouds detected by the Boston University-Arecibo Galactic H I Survey. These clouds are associated with galactic star clusters, H II regions, and molecular clouds. Using emission-absorption experiments toward galactic H II regions, we determined the H I properties of cool H I clouds seen in absorption against the thermal continuum, including their kinematic distances. Correlations were then made between IRAS sources and these H II regions, thus some of the spatial confusion associated with the IRAS fields near the galactic plane was resolved since the distances to these sources was known. Because we can also correlate the BU-Arecibo clouds with existing CO surveys, these results will allow us to determine the intrinsic properties of the gas (neutral and ionized atomic as well as molecular) and dust for interstellar clouds in the inner galaxy. For the IRAS-identified H II region sample, we have established the far infrared (FIR) luminosities and galactic distribution of these sources. Author

N92-17873*# National Aeronautics and Space Administration, Washington, DC.
HUBBLE SPACE TELESCOPE: SRM/QA OBSERVATIONS AND LESSONS LEARNED
George A. Rodney 1990 27 p
(NASA-TM-105505; NAS 1.15:105505) Avail: NTIS HC/MF A03 CSCL 03A

The Hubble Space Telescope (HST) Optical Systems Board of Investigation was established on July 2, 1990 to review, analyze, and evaluate the facts and circumstances regarding the manufacture, development, and testing of the HST Optical Telescope Assembly (OTA). Specifically, the board was tasked to ascertain what caused the spherical aberration and how it escaped notice until on-orbit operation. The error that caused the on-orbit spherical aberration in the primary mirror was traced to the assembly process of the Reflective Null Corrector, one of the three Null Correctors developed as special test equipment (STE) to measure and test the primary mirror. Therefore, the safety, reliability, maintainability, and quality assurance (SRM&QA) investigation covers the events and the overall product assurance environment during the manufacturing phase of the primary mirror and Null Correctors (from 1978 through 1981). The SRM&QA issues that were identified during the HST investigation are summarized. The crucial product assurance requirements (including nonconformance processing) for the HST are examined. The history of Quality Assurance (QA) practices at Perkin-Elmer (P-E) for the period under investigation are reviewed. The importance of the information management function is discussed relative to data retention/control issues. Metrology and other critical technical issues also are discussed. The SRM&QA lessons learned from the investigation are presented along with specific recommendations. Appendix A provides the MSFC SRM&QA report. Appendix B provides supplemental reference materials. Appendix C presents the findings of the independent optical consultants, Optical Research Associates (ORA). Appendix D provides further details of the fault-tree analysis portion of the investigation process. Author

N92-17920# Air Force Inst. of Tech., Wright-Patterson AFB, OH.
EVALUATION OF LOWTRAN AND MODTRAN FOR USE OVER HIGH ZENITH ANGLE/LONG PATH LENGTH VIEWING M.S. Thesis
Jonathan C. Wright May 1991 187 p
(AD-A243599; AFIT/CI/CIA-91-075) Avail: NTIS HC/MF A09 CSCL 12/5

LOWTRAN and MODTRAN were evaluated in the 2.0-5.5 micron region against field collection data at high zenith angle/long path lengths to determine the degree of uncertainty associated with these models under these conditions. Matching data sets were developed using data from the Air Force Geophysics Laboratory Flying Infrared Signatures Technology Aircraft (FISTA) as the field reference. The Kolmogorov-Smirnov test was applied to determine the degree to which the outputs of LOWTRAN and MODTRAN follow the same distribution as the field data. The percent difference between the model and field data was also studied. Agreement between the model and field data was found to be better than 97 percent for most cases. Median percent difference was within 10 percent for zenith angles less than 90 deg. GRA

90 ASTROPHYSICS

Includes cosmology; celestial mechanics; space plasmas; and interstellar and interplanetary gases and dust.

For related information see also *75 Plasma Physics*.

N92-17251# National Geophysical Data Center, Boulder, CO.
SOLAR-GEOPHYSICAL DATA NUMBER 562, JUNE 1991. PART 2: (COMPREHENSIVE REPORTS). DATA FOR DECEMBER 1990 AND MISCELLANEOUS
Helen E. Coffey Jun. 1991 103 p
(PB91-230219; SGD-562-Pt-2) Avail: NTIS HC/MF A06 CSCL 03B

A detailed index data for 1990-1991 is given. Data for December 1990 is given on solar flares, solar radio bursts at fixed frequencies,

solar x-ray radiation from GOES satellites, mass ejections from the sun, active prominences, and filaments. Author

N92-17253# Naval Postgraduate School, Monterey, CA.
STELLAR SPECTRAL LINE SYNTHESIS FROM AN INDIVIDUAL PHOTON-FOLLOWING SIMULATION M.S. Thesis
Gregory F. DeVogel Dec. 1990 65 p
(AD-A242970) Avail: NTIS HC/MF A04 CSCL 04/1

A stochastic stellar atmosphere model which simulates the behavior of photons in the atmospheres of stars by following individual photons is described and tested. The model accounts for stellar turbulence, atmospheric curvature, stellar rotation, collisional excitation, collisional de-excitation, and stellar winds. Testing shows that this new method of stellar radiative transfer is successful in simulating all of the processes. Particular results of interest include simulation of solar limb darkening and spectral synthesis of three different solar absorption lines. GRA

N92-17377*# Fermi National Accelerator Lab., Batavia, IL.
BLACK HOLES IN MAGNETIC MONOPOLES
Kimyeong Lee, V. P. Nair, and Erick J. Weinberg (Columbia Univ., New York, NY.) Nov. 1991 34 p Sponsored in part by DOE and NSF
(Grant NAGw-2381)
(NASA-CR-189842; NAS 1.26:189842;
FERMILAB-Pub-91/312-A/T; CU-TP-539) Avail: NTIS HC/MF A03 CSCL 03B

We study magnetically charged classical solutions of a spontaneously broken gauge theory interacting with gravity. We show that nonsingular monopole solutions exist only if the Higgs field vacuum expectation value v is less than or equal to a critical value v sub cr, which is of the order of the Planck mass. In the limiting case, the monopole becomes a black hole, with the region outside the horizon described by the critical Reissner-Nordstrom solution. For v less than v sub cr, we find additional solutions which are singular at f = 0, but which have this singularity hidden within a horizon. These have nontrivial matter fields outside the horizon, and may be interpreted as small black holes lying within a magnetic monopole. The nature of these solutions as a function of v and of the total mass M and their relation to the Reissner-Nordstrom solutions is discussed. Author

N92-17595# Air Force Academy, CO.
COMPARISON OF STATION-KEEPING ALGORITHMS FOR AN INTERIOR LIBRATION POINT ORBIT IN THE SUN-EARTH+MOON ELLIPTIC RESTRICTED THREE-BODY PROBLEM Final Report
Steven C. Gordon 10 Oct. 1991 106 p
(AD-A241896; USAFA-TR-91-13) Avail: NTIS HC/MF A06 CSCL 22/3

A spacecraft near a Lagrange (libration) point orbit between the Earth and the Sun can study the important interaction of the Sun's corona with the terrestrial environment. However, the spacecraft will drift from the nominal (unstable) path. The accumulated error in the spacecraft's position and velocity relative to the nominal path after a predetermined period of range and range-rate tracking can be computed. This error, or uncertainty, in the spacecraft state is measured through simulations, commonly referred to as orbit determination error analysis, and is presented as either variances or standard deviations of the state vector elements. The state uncertainty computed in the error analysis can then be input to a station-keeping algorithm. The algorithm computes control maneuvers that return the spacecraft to the vicinity of the nominal path. Variations in orbital shapes and sizes may, however, have some effect on the station-keeping costs. Several algorithms are derived and are used to test differences in station-keeping costs for orbits of different size and shape. Statistical hypothesis tests for equality of means are used in the comparisons. GRA

N92-17696*# Fermi National Accelerator Lab., Batavia, IL.
LATE TIME COSMOLOGICAL PHASE TRANSITIONS 1: PARTICLE PHYSICS MODELS AND COSMIC EVOLUTION
Joshua A. Frieman, Christopher T. Hill, and Richard Watkins (Chicago Univ., IL.) Nov. 1991 42 p Sponsored in part by DOE
(Grant NAGw-1340)
(NASA-CR-189857; NAS 1.26:189857; FERMILAB-PUB-91/324-A) Avail: NTIS HC/MF A03 CSCL 03B

We described a natural particle physics basis for late-time phase transitions in the universe. Such a transition can seed the formation of large-scale structure while leaving a minimal imprint upon the microwave background anisotropy. The key ingredient is an ultra-light pseudo-Nambu-Goldstone boson with an astronomically large (O(kpc-Mpc)) Compton wavelength. We analyze the cosmological signatures of and constraints upon a wide class of scenarios which do not involve domain walls. In addition to seeding structure, coherent ultra-light bosons may also provide unclustered dark matter in a spatially flat universe, omega sub phi approx. = 1. Author

N92-17697*# Fermi National Accelerator Lab., Batavia, IL.
A CLASSICAL INSTABILITY OF REISSNER-NORDSTROM SOLUTIONS AND THE FATE OF MAGNETICALLY CHARGED BLACK HOLES
Kimyeong Lee, V. P. Nair, and Erick J. Weinberg (Columbia Univ., New York, NY.) Nov. 1991 10 p Sponsored in part by DOE and NSF
(Grant NAGw-2381)
(NASA-CR-189843; NAS 1.26:189843;
FERMILAB-Pub-91/326-A/T; CU-TP-540) Avail: NTIS HC/MF A02 CSCL 03B

Working in the context of spontaneously broken gauge theories, we show that the magnetically charged Reissner-Nordstrom solution develops a classical instability if the horizon is sufficiently small. This instability has significant implications for the evolution of a magnetically charged black hole. In particular, it leads to the possibility that such a hole could evaporate completely, leaving in its place a nonsingular magnetic monopole. Author

N92-17717# McDonnell-Douglas Space Systems Co., Huntington Beach, CA. Advanced Product Development and Technology.
MAGNETOSPHERIC RESPONSE TO VARIATIONS IN THE INTERPLANETARY MAGNETIC FIELD Final Report
K. A. Pfitzer Nov. 1991 51 p
(Contract N00014-89-C-0122)
(AD-A243683) Avail: NTIS HC/MF A04 CSCL 04/1

Models of the disturbance wave propagating within the tail of the magnetosphere are the first of a series of steps necessary to develop a comprehensive understanding of magnetotail dynamics. This work, in conjunction with work on particle entry into the magnetosphere, provides a detailed understanding of magnetosphere particle energization. The magnetic field model of the disturbance magnetic field when combined with the existing dynamic magnetic field model provides a tool for evaluating the response of the plasma to the magnetic stimulus of the IMF (Interplanetary Magnetic Fields). This effort will ultimately permit us to understand the role of the IMF in controlling and/or triggering processes within the magnetosphere. The equation on wave propagation and wave penetration into the magnetosphere are based on Maxwell's equation. They present a novel new method for studying the interaction magnetic variations in the solar wind with the plasma inside the magnetosphere. The dynamic model of the plasma sheet magnetic field developed as a part of this effort includes variations in the IMF and can be used to study the response of the tail to external stimuli. Much additional work needs to be done. The above described model is not completely self-consistent. GRA

N92-17832# Lawrence Livermore National Lab., CA.
COLLABORATIVE RESEARCH ON EXPERIMENTAL ASTROPHYSICS
17 Sep. 1991 2 p
(Contract W-7405-eng-48)
(DE92-003970; UCRL-CR-108433) Avail: NTIS HC/MF A01

In association with the above subcontract, the Space Sciences

Laboratory of the University of California at Berkeley (UCB) has pursued a program of experimental astrophysics research in collaboration with scientists at the Laboratory for Experimental Astrophysics of the Lawrence Livermore National Laboratory. This research program encompassed a number of disparate areas: design and development of the GRATIS balloon payload; the multi-object spectrograph; investigation of the use of cryogenic detectors for non-dispersive X-ray spectroscopy; laboratory astrophysics investigations; and astronomical data analysis. DOE

91 LUNAR AND PLANETARY EXPLORATION

Includes planetology; and manned and unmanned flights.
For spacecraft design or space stations see *18 Spacecraft Design, Testing and Performance.*

N92-17069*# National Aeronautics and Space Administration. Lewis Research Center, Cleveland, OH.
ENVIRONMENTAL INTERACTIONS IN SPACE EXPLORATION: ANNOUNCEMENT OF THE FORMATION OF AN ENVIRONMENTAL INTERACTIONS WORKING GROUP
Joseph C. Kolecki and G. Barry Hillard Nov. 1991 10 p
(NASA-TM-105294; E-6633; NAS 1.15:105294) Avail: NTIS HC/MF A02 CSCL 03B

With the advent of the Space Exploration Initiative, the possibility of designing and using systems on scales not heretofore attempted presents exciting new challenges in systems design and space science. The environments addressed by the Space Exploration Initiative include the surfaces of the Moon and Mars, as well as the varied plasma and field environments which will be encountered by humans and cargo enroute to these destinations. Systems designers will need to understand environmental interactions and be able to model these mechanisms from the earliest conceptual design stages through design completion. To the end of understanding environmental interactions and establishing robotic precursor mission requirements, an Environmental Interactions Working Group has been established as part of the Robotic Missions Working Group. The current paper describes the working group and gives an update of its current activities. Working group charter and operation are reviewed, background information on the environmental interactions and their characteristics is offered, and the current status of the group's activities is presented along with anticipations for the future.
Author

N92-17123# Army Construction Engineering Research Lab., Champaign, IL.
CONSTRUCTION EQUIPMENT FOR LUNAR SURFACE OPERATIONS Final Report
James W. Brazell and Alvin Smith Sep. 1991 43 p
(AD-A243665; CERL-TR-M-91/25) Avail: NTIS HC/MF A03 CSCL 13/3

Future endeavors in space will be shaped by the concept of extraterrestrial surface bases. The lunar environment presents an extraordinary challenge in designing equipment and machinery to operate during lunar exploration missions and to construct a lunar base or early outpost. Because familiar terrestrial machines are so large, it is prohibitively expensive to move them to the moon. Also, they could not accomplish all the required work tasks. The objective of this study was to create conceptual models of equipment and machines suitable for operation on the surface of the moon. This report presents the design concepts for five machine vibrations and eight implements for mobility, lifting, digging, etc. The implements may be regarded as somewhat universal since they may be used with most of the machine concepts described. It is recommended that information in this report be integrated into mission planning documents. GRA

92 SOLAR PHYSICS

Includes solar activity, solar flares, solar radiation and sunspots.
For related information see *93 Space Radiation.*

N92-17048*# National Aeronautics and Space Administration. Goddard Space Flight Center, Greenbelt, MD.
THE COMPLETE HARD X RAY BURST SPECTROMETER EVENT LIST, 1980-1989
Ken Frost, B. R. Dennis, L. E. Orwig, G. S. Kennard, G. J. Labow, R. A. Schwartz, A. R. Shaver, and A. K. Tolbert (ST Systems Corp., Lanham, MD.) Washington Dec. 1991 222 p
(NASA-TM-4332; Rept-92B00009; NAS 1.15:4332) Avail: NTIS HC/MF A10 CSCL 03B

This event list is a comprehensive reference for all Hard X-Ray bursts detected with the Hard X-Ray Burst Spectrometer on the Solar Maximum Mission from the time of launch on 14 Feb. 1980 to the end of the mission in Dec. 1989. Over 12,500 events were detected in the energy range 30 to 600 keV with the vast majority being solar flares. This list includes the start time, peak time, duration, and peak rate of each event.
Author

N92-17201# Los Alamos National Lab., NM.
SOLAR NEUTRINOS: PROBING THE SUN OR NEUTRINOS?
J. F. Wilkerson 1991 15 p Presented at the 3rd Annual Symposium on Frontiers of Science, Irvine, CA, 7-9 Nov. 1991
(Contract W-7405-eng-36)
(DE92-003849; LA-UR-91-3616; CONF-9111136-1) Avail: NTIS HC/MF A03

The decade of the 1990's should prove to be a landmark period for the study of solar neutrino physics. Current observations show 2-3 times fewer neutrinos coming from the sun than are theoretically expected. As we enter the decade, new experiments are poised to attempt and discover whether this deficit is a problem with our understanding of how the sun works, is a hint of new neutrino properties beyond those predicted by the standard model of particle physics, or perhaps a combination of both. A review of the current status of the field is presented, and how future measurements should help solve this interesting puzzle is shown.
DOE

N92-17235# Kansas Univ., Lawrence. Dept. of Physics and Astronomy.
EVALUATION OF SOLAR FLARES AND ELECTRON PRECIPITATION BY NITRATE DISTRIBUTION IN ANTARCTICA Annual Report, 1 Nov. 1990 - 31 Oct. 1991
Gisela A. Dreschhoff and Edward J. Zeller 31 Oct. 1991 47 p
(Grant AF-AFOSR-0065-88; AF Proj. 2311)
(AD-A243026; AFOSR-91-0912TR) Avail: NTIS HC/MF A03 CSCL 04/1

Most of the time devoted to project research was spent in Antarctica. A firm core was drilled by hand to a depth of 29 meters at Windless Bight on the Ross Ice Shelf. The main result is that all of the major peaks identified as resulting from ionization caused by SPEs that were found in the 1988-89 core could also be identified in the analytical sequence from the 1990-91 core. Following the Antarctic field season, a set of snow samples were obtained that had been collected by the International Trans-Antarctica Expedition. The analysis of these samples showed nitrate flux that correlates closely with known spatial distribution of electron precipitation in the south polar region. A new apparatus has been build for field analysis on a continuous basis of nitrate and conductivity in a melt derived from the vertical melting of ice cores.
GRA

N92-17725# Los Alamos National Lab., NM.
IN SITU OBSERVATIONS OF CORONAL MASS EJECTIONS IN INTERPLANETARY SPACE
J. T. Gosling 1991 11 p Presented at the 133rd International Astronomical Union (IAU) Colloquium, Iguazu (Argentina), 2-6 Aug. 1991
(Contract W-7405-eng-36)

(DE92-003857; LA-UR-91-3546; CONF-9108182-1) Avail: NTIS HC/MF A03

Coronal mass ejections, CME's, in the solar wind at 1 AU generally have distinct plasma and field signatures by which they can be distinguished from the ordinary solar wind. These include one or more of the following: helium abundance enhancements, ion and electron temperature depressions, unusual ionization states, strong magnetic fields, low plasma beta, low magnetic field variance, coherent field rotations, counterstreaming (along the field) energetic protons, and counterstreaming suprathermal electrons. The most reliable of these appears to be counterstreaming electrons, which indicates that CME's at 1 AU typically are closed field structures either rooted at both ends in the Sun or entirely disconnected from it as plasmoids. About 1/3 of all CME's have sufficiently high speeds to produce transient interplanetary shock disturbances at 1 AU; the remainder simply ride along with the solar wind. The frequency of occurrence of CME's in the ecliptic plane, as distinguished by the counterstreaming electron signature, varies roughly in phase and amplitude with the 11-yr solar activity cycle. Near solar maximum they account for (approximately) 15 percent of all solar wind measurements, while near solar minimum they account for less than 1 percent of all the measurements. All but one of the 37 largest geomagnetic storms near the last solar maximum were associated with Earth-passage of interplanetary disturbances driven by fast CME's; that is, CME's are the prime link between solar and geomagnetic activity. However, more than half of all earthward directed CME's are relatively ineffective in a geomagnetic sense. DOE

N92-17883# Los Alamos National Lab., NM.
SOLAR NEUTRINO PHYSICS IN THE NINETIES
J. F. Wilkerson 1990 8 p Presented at the 1990 DPF Summer Study on High Energy Physics, Snowmass, CO, 25 Jun. - 13 Jul. 1990
(Contract W-7405-eng-36)
(DE92-003848; LA-UR-91-3617; CONF-9006267-35) Avail: NTIS HC/MF A02

The decade of the 1990's should prove to be a landmark period for the study of solar neutrino physics. Current observations show 2-3 times fewer neutrinos coming from the sun than are theoretically expected. As we enter the decade, new experiments are poised to investigate whether this deficit is a problem with our understanding of how the sun works, is a hint of new neutrino properties beyond those predicted by the standard model of particle physics, or is perhaps a combination of both. This paper will briefly review the current status of the field and point out how future measurements should help solve this interesting puzzle. DOE

93 SPACE RADIATION

Includes cosmic radiation; and inner and outer earth's radiation belts.

For biological effects of radiation see *52 Aerospace Medicine*. For theory see *73 Nuclear and High-Energy Physics*.

N92-18003*# Cornell Univ., Ithaca, NY. Dept. of Astronomy.
CONSTRAINTS ON COSMIC RAY PROPAGATION IN THE GALAXY Final Report
James M. Cordes 1992 32 p
(Grant NAGw-1646)
(NASA-CR-189779; NAS 1.26:189779) Avail: NTIS HC/MF A03 CSCL 03B

The goal was to derive a more detailed picture of magnetohydrodynamic turbulence in the interstellar medium and its effects on cosmic ray propagation. To do so, radio astronomical observations (scattering and Faraday rotation) were combined with knowledge of solar system spacecraft observations of MHD turbulence, simulations of wave propagation, and modeling of the galactic distribution to improve the knowledge. A more sophisticated model was developed for the galactic distribution of electron density turbulence. Faraday rotation measure data was analyzed to constrain magnetic field fluctuations in the ISM. VLBI observations were acquired of compact sources behind the supernova remnant CTA1. Simple calculations were made about the energies of the turbulence assuming a direct link between electron density and magnetic field variations. A simulation is outlined of cosmic ray propagation through the galaxy using the above results. For individual titles, see N92-18004 through N92-18005.

N92-18004*# Cornell Univ., Ithaca, NY. Dept. of Astronomy.
INTERSTELLAR SCATTERING TOWARDS THE GALACTIC CENTER AS PROBED BY OH/IR STARS
Huib Jan vanLangevelde, Dale A. Frail, James M. Cordes, and Philip J. Diamond (National Radio Astronomy Observatory, Socorro, NM.) *In* Constraints on Cosmic Ray Propagation in the Galaxy 1992 20 p Sponsored in part by Natural Sciences and Engineering Research Council of Canada; by National Radio Astronomy Observatory; and by National Astronomy and Ionosphere Center (For primary document see N92-18003 08-93)
(Grant NAGw-1646)
Avail: NTIS HC/MF A03 CSCL 03B

Angular broadening measurements are reported of 20 OH/IR stars near the galactic center. This class of sources is known to have bright, intrinsically compact (less than or equal to 20 mas) maser components within their circumstellar shells. VLBA antennas and the VLA were used to perform a MKII spectral line VLBI experiment. The rapid drop in correlated flux with increasing baseline, especially for sources closest to the galactic center, is attributed to interstellar scattering. Angular diameters were measured for 13 of our sources. Lower limits were obtained for the remaining seven. With the data, together with additional data taken from the literature, the distribution was determined of interstellar scattering toward the galactic center. A region was found of pronounced scattering nearly centered on SgrA*. Two interpretations are considered for the enhanced scattering. One hypothesis is that the scattering is due to a clump of enhanced turbulence, such as those that lie along lines of sight to other known objects, that has no physical relationship to the galactic center. The other model considers the location of the enhanced scattering to arise in the galactic center itself. The physical implications of the models yield information on the nature of interstellar scattering. Author

N92-18005*# Cornell Univ., Ithaca, NY. Dept. of Astronomy.
LOW FREQUENCY INTERSTELLAR SCATTERING AND PULSAR OBSERVATIONS
James M. Cordes *In* Contraints on Cosmic Ray Propagation in the Galaxy 1992 10 p Previously announced in IAA as A91-57047 (For primary document see N92-18003 08-93)
(Grant NAGw-1646)
Avail: NTIS HC/MF A03 CSCL 03B

Radio astronomy at frequencies from 2 to 30 MHz challenges time tested methods for extracting usable information from observations. One fundamental reason for this is that propagation effects due to the magnetoionic ionosphere, interplanetary medium, and interstellar matter (ISM) increase strongly with wavelength. The problems associated with interstellar scattering off of small scale irregularities in the electron density are addressed. What is known about interstellar scattering is summarized on the basis of high frequency observations, including scintillation and temporal broadening of pulsars and angular broadening of various galactic and extragalactic radio sources. Then those high frequency phenomena are addressed that are important or detectable at low frequencies. The radio sky becomes much simpler at low frequencies, most pulsars will not be seen as time varying sources, intensity variations will be quenched or will occur on time scales much longer than a human lifetime, and many sources will be angularly broadened and/or absorbed into the noise. Angular broadening measurements will help delineate the galactic distribution and power spectrum of small scale electron density irregularities. Author

99 GENERAL

N92-17079# Systran Corp., Dayton, OH.
CONTRIBUTIVE RESEARCH AND DEVELOPMENT Final Technical Report, 22 Jan. 1988 - 31 Dec. 1990
Milton Zellmer 25 Sep. 1991 194 p
(Contract F33615-88-C-5402)
(AD-A243331; WL-TR-91-4044) Avail: NTIS HC/MF A09 CSCL 11/4

This technical report gives a summary of the research performed in the materials and physical sciences. The report contains abstracts covering the nature of the research and the results for each of 208 tasks completed under the contract. Topics include morphology, microstructure, mechanical properties, optical properties, laser hardening, powder metallurgy, epitaxy, crystallization, and other subjects related to the behavior and application of advanced materials. Manufacturing processes such as annealing and forging are also presented. GRA

N92-17372# Naval Training Systems Center, Orlando, FL.
RESEARCH AND DEVELOPMENT PROJECT SUMMARIES, OCTOBER 1991 Annual Report
Robbie Petersen Oct. 1991 74 p
(AD-A243477; NTSC-91-01) Avail: NTIS HC/MF A04 CSCL 13/10

This brochure presents brief summaries of the FY92 research efforts at the Naval Training Systems Center (NAVTRASYSCEN) in Orlando, FL. NAVTRASYSCEN has comprehensive simulation and training systems responsibilities ranging from research and technology base development through system acquisition and life cycle support. The NAVTRASYSCEN is unique in this integrated role because it performs research, specifies the training device's engineering, instructional, and operational requirements, selects the contractor, evaluates the trainer as it is being built, and ensures the trainer can be properly operated and maintained in the field. In addition to the Navy, NAVTRASYSCEN provides services for the Marine Corps, Army, Air Force, and foreign governments. The NAVTRASYSCEN's research mission is to plan and perform a full range of directed research and development in support of Naval training systems for all warfare areas and platforms, to maintain an expanding technology base, and to transition research results to the fleet. R and D program emphasis is on fleet and training command requirements, rapid transition of products, industry/university coordination, improved planning, coordination with other services, and improved quality and cost effectiveness of products. GRA

N92-17623# Kyoto Univ., Kumatori (Japan). Research Reactor Inst.
SUMMARY REPORTS OF ACTIVITIES UNDER VISITING RESEARCH PROGRAM
Feb. 1991 69 p In JAPANESE
(DE91-522477; KURRI-TR-341) Avail: NTIS HC/MF A04

The book carries a large number of summary studies made by using the Research Reactor (KUR) or the Critical Assembly (KUCA). These studies include: low temperature irradiation effect on iron-alloy and ceramics; the influence of the neutron irradiation on the low temperature strength of various welded joint of dissimilar materials; effects of neutron irradiation on superconducting properties under stress in superconducting wires; neutron activation analysis and photo-emission phenomena from gamma-ray irradiated rock-forming minerals; irradiation effects in nonmetallic conductors, distribution, and mobility of ions of metal elements in stem; activation analysis of high purity metals; Moessbauer spectroscopic studies of superionic conductor; neutron spectrometry with CR-39 track detector; geochemical study on trace element abundances in island arc igneous rocks; reactor rate distribution measurement of tight pitch lattice core with internal blanket; measurement of the foil reaction rates in a critical core; and many more. DOE

N92-17657# Army Communications-Electronics Command, Fort Monmouth, NJ.
C3 SYSTEMS TECHNOLOGY SYMPOSIUM ON ADVANCE PLANNING BRIEFINGS FOR INDUSTRY
8 Oct. 1991 102 p Symposium held in Fort Monmouth, NJ, 8 Oct. 1991
(AD-A243466) Avail: NTIS HC/MF A06 CSCL 25/5

Information is given in viewgraph form on the Speakeasy program, a multiphased effort at developing a software reprogrammable radio system; the antenna subsystem of the Speakeasy program; the Vehicular Conformal Antenna; UHF electronic counter measure countermeasure (ECCM) techniques; survivable adaptive system technology; adaptive network planning and management for the localized network environment; the Soldier's Computer; user interface technology; lower echelon command and control; a tactical multinet gateway for the localized network environment; fiber optic technology; information security; and modeling simulation. GRA

N92-17928# Manchester Univ. (England). Aeronautical Engineering Group.
SYDNEY GOLDSTEIN FRS HON FRAeS: AN APPRECIATION
J. A. D. Ackroyd 1989 18 p
(Aero-Rept-8903; ETN-92-90912) Avail: NTIS HC/MF A03

The contribution of Goldstein to aeronautical technology in Britain is reviewed. The history of the boundary layer concept is described, with reference to theories of Prandtl, Kutta, and Zhukonskii. A biography of Goldstein with emphasis on his research activities is presented. ESA

SUBJECT INDEX

SCIENTIFIC AND TECHNICAL AEROSPACE REPORTS VOLUME 30 NUMBER 8

Typical Subject Index Listing

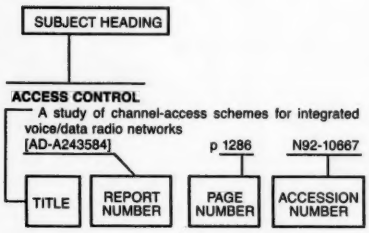

The subject heading is a key to the subject content of the document. Titles, report numbers, and accession numbers of pertinent documents are provided under each subject heading. When the title is insufficiently descriptive of the document content, a title extension has been added, separated from the title by three hyphens. The report number helps to indicate the type of document cited (e.g., NASA report, NASA translation, NASA contractor report). The accession number is the number by which the document abstracts are arranged in this journal and by which the document is sold or requested. The page number helps you locate the the citation in the abstract section. The titles, with title extensions if present, are arranged under each subject heading in ascending accession number order. The subject headings have been selected from the latest revision of the *NASA Thesaurus*.

A

ABERRATION
Hubble Space Telescope: SRM/QA observations and lessons learned
| NASA-TM-105505 | p 1387 N92-17873

ABRASION
An investigation of gouge initiation in high-velocity sliding contact
| DE92-003944 | p 1311 N92-17937

ABSORBENTS
Propane aromatization over gallium containing HZSM-5 zeolites
| ETN-92-90897 | p 1262 N92-17925

ABSORPTION SPECTROSCOPY
Direct speciation of metal and metalloid ions by optical spectroscopies
| DE92-003868 | p 1261 N92-17727

ABSTRACTS
The cognitive, perceptual, and neural bases of skilled performance
| AD-A243052 | p 1332 N92-17554
Summaries of FY 1991 engineering research
| DE92-004708 | p 1277 N92-17593

ACCELERATED LIFE TESTS
Research in some future directions in reliability and quality control
| AD-A242865 | p 1308 N92-17231
Test method for the evaluation of the water treeing behavior of cross-linked polyethylene medium voltage cables
| ETN-92-90588 | p 1270 N92-17541
Failure mechanisms in GaAs ICs: The effects of deep traps
| AD-A243013 | p 1374 N92-17553

ACCELERATION (PHYSICS)
Low-noise oscillators for airborne radar applications
| AD-A242264 | p 1281 N92-17258
A frequency-domain method for estimating the incidence and severity of sliding
| AD-A243077 | p 1334 N92-17569
Analysis of ram acceleration for high velocity applications
| AD-A242338 | p 1235 N92-17642

ACCELERATION STRESSES (PHYSIOLOGY)
Aircrew critique of high-G centrifuge training: Part 3: What can we change to better serve you?
| AD-A243496 | p 1334 N92-17432

ACCELERATORS
Analysis of ram acceleration for high velocity applications
| AD-A242338 | p 1235 N92-17642

ACCEPTABILITY
Qualification test report. Fuel pump test stand 3C3965G05
| AD-A242929 | p 1235 N92-17552

ACCESS CONTROL
A study of channel-access schemes for integrated voice/data radio networks
| AD-A243584 | p 1286 N92-17931
Management, control and performance of broadband integrated networks
| AD-A242750 | p 1381 N92-17952

ACCUMULATORS
Preliminary design study of a central solar heating plant with seasonal storage at the University of Massachusetts, Amherst
| DE92-000762 | p 1313 N92-17577

ACETATES
Evaluation of a diffusion/trapping model for hydrogen ingress in high-strength alloys
| AD-A243461 | p 1263 N92-17327

ACID RAIN
Rocket tests in Mississippi to be heavily restricted
| GAO/NSIAD-92-86 | p 1240 N92-17741

ACIDS
The shapes and cavities of four cholic acid host systems
| AD-A243483 | p 1255 N92-17329

ACOUSTIC EMISSION
Acoustic emission monitoring of low velocity impact damage in graphite/epoxy laminates during tensile loading
| NASA-TM-4339 | p 1258 N92-17881

ACOUSTIC EXCITATION
A method and apparatus for indicating disbonds in joint regions
| NASA-CASE-LAR-14626-1 | p 1309 N92-17859

ACOUSTIC IMPEDANCE
Acoustic impedance of materials from reverberation time
| AD-A243184 | p 1354 N92-16999
A method and apparatus for indicating disbonds in joint regions
| NASA-CASE-LAR-14626-1 | p 1309 N92-17859

ACOUSTIC MEASUREMENT
Bottom contour influence on ray tracing
| AD-A242411 | p 1323 N92-17078
Human response to helicopter noise: A test of A-weighting
| AD-A243719 | p 1355 N92-17506

ACOUSTIC PROPAGATION
The effects of sediment porosity on acoustic reflection and transmission at the seafloor
| AD-A241943 | p 1323 N92-17083

ACOUSTIC PROPERTIES
Acoustical and other physical properties of marine sediments
| AD-A243532 | p 1324 N92-17391

ACOUSTIC SIMULATION
Acoustic simulation for acoustics education
| AD-A243027 | p 1355 N92-17236

ACOUSTIC VELOCITY
The applied tomography experiment of 1990
| AD-A243525 | p 1354 N92-17086
An investigation of cold overflow over the Iceland/Faeroes Ridge
| AD-A243084 | p 1324 N92-17169
Modeling convergence zone gain on MS-DOS based personal computers
| AD-A243252 | p 1341 N92-17558
Ocean simulation model. Version 2: First order frontal simulation
| AD-A243775 | p 1325 N92-17766

ACOUSTICS
An investigation of cold overflow over the Iceland/Faeroes Ridge
| AD-A243084 | p 1324 N92-17169

ACQUISITION
Benefit analysis of proposed information systems
| AD-A243707 | p 1382 N92-17125
Performance of ground-based infrared detectors for acquisition of satellites
| AD-A243247 | p 1281 N92-17241

ACRYLIC RESINS
New ferrocene complexes and polymers for nonlinear optical applications
| AD-A243640 | p 1272 N92-17749

ACTIVATION
Estimation of the outer sphere contribution to the activation parameters for homogeneous electron transfer reactions using the mean spherical approximation
| AD-A243217 | p 1259 N92-17323

ACTIVATION ENERGY
Two-dimensional stability of laminar flames
| NASA-TP-3131 | p 1223 N92-17131
The influence of temperature and composition on the activation energy for creep in binary aluminum lithium alloys
| AD-A242299 | p 1265 N92-17759

ACTIVE CONTROL
Loading and vibration reduction through active aerodynamic control
| AD-A242321 | p 1236 N92-17243
Actively controlled shaft seals for aerospace applications
| NASA-CR-189808 | p 1306 N92-17304
Electrically-controlled polymeric gels as active materials in adaptive structures
| DE92-002947 | p 1272 N92-17710
Active thermal control system evolution
p 1252 N92-17775
Active control of pressure loads using passive porosity
| NASA-CASE-LAR-14594-1 | p 1300 N92-17888
Software tools for distributed intelligent control systems
| DE92-004656 | p 1349 N92-17965

ACTIVITY (BIOLOGY)
Artificial photosynthesis: Progress toward molecular systems for photoconversion
| DE92-003370 | p 1326 N92-17471

ACTS
Advanced Communication Technology Satellite (ACTS) multibeam antenna analysis and experiment
| NASA-TM-105420 | p 1279 N92-17047

ACTUATORS
Evaluation of squib performance variables
| DE92-002034 | p 1275 N92-17533
Toward the robust control of high bandwidth high precision flexible optical systems
| AD-A243471 | p 1366 N92-17536
Electrically-controlled polymeric gels as active materials in adaptive structures
| DE92-002947 | p 1272 N92-17710

ADA (PROGRAMMING LANGUAGE)
An examination of selected commercial software testing tools
| AD-A243089 | p 1337 N92-17068
Pattern Theory: An engineering paradigm for algorithm design
| AD-A243214 | p 1339 N92-17179
Performance modeling of the Ada rendezvous
| AD-A243392 | p 1339 N92-17211
Technical evaluation report on the 52nd Symposium on Software for Guidance and Control
| AGARD-AR-302 | p 1341 N92-17498
Contractor software engineering environment evaluations summary report
| AD-A242330 | p 1343 N92-17640

Verification and validation of the Comprehensive Operational Support Evaluation Model for space
[AD-A243653] p 1344 N92-17761
Knowledge, programming, and programming cultures: LISP, C, and Ada
[NASA-CR-184220] p 1344 N92-17778

ADAPTATION
A covariance modeling approach to adaptive beamforming and detection
[AD-A241887] p 1279 N92-17040
Pragmatic quality metrics for evolutionary software development models
[AD-A243022] p 1337 N92-17064
Rapid nonconjugate adaptation of vertical voluntary pursuit eye movements
[AD-A243358] p 1331 N92-17145
Control of a large flexible space structure using multiple model adaptive algorithms
[AD-A243759] p 1250 N92-17602

ADAPTIVE CONTROL
Adaptive generalized predictive control
[OUEL-1879/91] p 1349 N92-17880

ADAPTIVE FILTERS
Constant modulus algorithm techniques for the enhancement of signal quality
[AD-A242986] p 1288 N92-17295
A Walsh-domain adaptive filter
[AD-A243701] p 1292 N92-17718

ADAPTIVE OPTICS
An investigation of the application of artificial neural networks to adaptive optics imaging systems
[AD-A243780] p 1348 N92-17767

ADDING CIRCUITS
Design of Style-V: A translator to convert standard VHDL into a stylized form for automated microcode generation
[AD-A243706] p 1340 N92-17407

ADDITIVES
Materials processing of diamond: Etching, doping by ion implantation and contact formation
[AD-A243060] p 1267 N92-17065
Examining Si3N4 base materials with various rare earth additions
[AD-A243668] p 1372 N92-17082
Injection of drag reducing additives into turbulent water flows
[AD-A243209] p 1296 N92-17176
Method of doping single crystal diamond for electronic devices
[AD-D015069] p 1374 N92-17610
Photorefractivity in doped nonlinear organic polymers
[AD-A243751] p 1271 N92-17661

ADHESIVE BONDING
Case bond liner systems for solid rocket motors
[AD-A242297] p 1253 N92-17085

ADHESIVES
Method for non-destructive estimation of waveguide directional coupler dimensions
[NASA-CASE-NPO-18454-1-CU] p 1293 N92-17865

ADIABATIC CONDITIONS
Experimental investigation of adiabatic shear banding at different impact velocities
[AD-A243011] p 1310 N92-17256
Some aspects of nonneutral plasma physics
[AD-A243711] p 1369 N92-17499

ADIABATIC EQUATIONS
On the nonadiabatic theory of charged particles motion in the magnetic dipole field
[DE92-610951] p 1354 N92-17811

ADSORPTION
In situ surface x ray scattering of metal monolayers adsorbed at solid-liquid interfaces
[AD-A243258] p 1262 N92-16985
Omega-terminated alkanethiolate monolayers on surfaces of copper, silver and gold have similar wettabilities
[AD-A243529] p 1260 N92-17389
Comparisons of self-assembled monolayers on silver and gold: Mixed monolayers derived from HS(CH2)21X and HS(CH2)10(sup Y) (X,Y-CH3, CH2OH) have similar properties
[AD-A243487] p 1264 N92-17427
Molecular recognition in gels, monolayers, and solids
[AD-A243488] p 1358 N92-17428
Studies of the adsorption of tetrasulfonated phthalocyanines on graphite substrate
[AD-A243443] p 1260 N92-17489
Designing ordered molecular arrays in two and three dimensions
[AD-A243447] p 1359 N92-17491
Thin films under chemical stress
[DE92-004684] p 1377 N92-17857

ADVANCED VERY HIGH RESOLUTION RADIOMETER
Source of cold water in Monterey Bay observed by AVHRR satellite imagery
[AD-A242843] p 1323 N92-17051

AERIAL RECONNAISSANCE
Multispectral software development for the Airborne Bathymetric Survey System
[AD-A243774] p 1325 N92-17765

AEROASSIST
An alternative concept for aeroassisted orbit transfers
[AD-A243409] p 1239 N92-17325

AEROBRAKING
Mars aerobrake assembly demonstration
p 1247 N92-17362
Control algorithms for aerobraking in the Martian atmosphere
[AD-A243349] p 1239 N92-17730

AEROCAPTURE
An aerocapture attitude control systems incorporating robustness and vehicle parameter identification
[AD-A243360] p 1245 N92-17302

AERODYNAMIC BRAKES
Mars aerobrake assembly demonstration
p 1247 N92-17362

AERODYNAMIC CHARACTERISTICS
Aerodynamic development of the X-31 aircraft for the high angle of attack region
[MBB-FE211-S-PUB-452] p 1233 N92-17313

AERODYNAMIC COEFFICIENTS
Dynamic stall on wind turbine blades
[DE92-001157] p 1226 N92-17874

AERODYNAMIC DRAG
Experiments and analysis concerning the use of external burning to reduce aerospace vehicle transonic drag
[NASA-TM-105397] p 1235 N92-17546
Dynamic stall on wind turbine blades
[DE92-001157] p 1226 N92-17874

AERODYNAMIC FORCES
Experimental ice shape and performance characteristics for a multi-element airfoil in the NASA Lewis Icing Research Tunnel
[NASA-TM-105380] p 1224 N92-17347

AERODYNAMIC INTERFERENCE
User guide for WIACX: A transonic wind-tunnel wall interference assessment and correction procedure for the NTF
[NASA-TM-104168] p 1225 N92-17547

AERODYNAMIC LOADS
Wind loads on a mirage III O aircraft mounted above a ground plane
[AD-A243004] p 1232 N92-17266
Dynamic stall on wind turbine blades
[DE92-001157] p 1226 N92-17874
An overview: Challenges in wind technology development
[DE92-001190] p 1313 N92-17875

AERODYNAMIC STABILITY
Periodic trim solutions with HP-version finite elements in time
[NASA-CR-189778] p 1236 N92-17019
Assessment of rotorcraft system identification as applied to the AH-64 p 1231 N92-17160
Aerodynamic development of the X-31 aircraft for the high angle of attack region
[MBB-FE211-S-PUB-452] p 1233 N92-17313

AERODYNAMIC STALLING
Wichita State University 1986 aviation safety research projects
[DOT/FAA/CT-91/4] p 1226 N92-16986
Dynamic stall on wind turbine blades
[DE92-001157] p 1226 N92-17874
An overview: Challenges in wind technology development
[DE92-001190] p 1313 N92-17875

AERODYNAMICS
Wichita State University 1986 aviation safety research projects
[DOT/FAA/CT-91/4] p 1226 N92-16986
Identification techniques: Frequency domain methods
p 1231 N92-17158
Modification of Jindivik air intake duct with an auxiliary intake static aerodynamic tests
[AD-A243002] p 1232 N92-17234
An alternative concept for aeroassisted orbit transfers
[AD-A243409] p 1239 N92-17325
Flow visualization and wake analysis for standard and modified configurations of the AN/ALQ-78 antenna pod
[AD-A243552] p 1224 N92-17339

AEROELASTICITY
Structural dynamics division research and technology accomplishments for F.Y. 1991 and plans for F.Y. 1992
[NASA-TM-104188] p 1225 N92-17509

AEROGELS
Structure and topology of silica aerogels
[DE92-004728] p 1274 N92-17938

AEROMAGNETISM
Workshop on Geologic Applications of Modern Aeromagnetic Surveys
[PB91-221788] p 1316 N92-17229

AERONAUTICAL ENGINEERING
Sydney Goldstein FRS Hon FRAeS: An appreciation
[AERO-REPT-8903] p 1391 N92-17928

AEROSOLS
Water vapor influence on satellite-measured aerosol characteristics
[AD-A241918] p 1315 N92-17008
Meeting Review: Airborne Aerosol Inlet Workshop
[NASA-CR-189814] p 1313 N92-17393

AEROSPACE ENGINEERING
NASA/DoD aerospace knowledge diffusion research project: Chronology of selected literature, reports, policy instruments, and significant events affecting Federal Scientific and Technical Information (STI) in the US
[NASA-TM-101662] p 1381 N92-17001
Proceedings of the USAF Structural Integrity Program Conference
[AD-A242943] p 1235 N92-17204
FY 1991 scientific and technical reports, articles, papers, and presentations
[NASA-TM-103567] p 1384 N92-17586
Beyond the Baseline 1991: Proceedings of the Space Station Evolution Symposium. Volume 2: Space Station Freedom, part 1
[NASA-CP-10083-VOL-2-PT-1] p 1251 N92-17768

AEROSPACE ENVIRONMENTS
Atomic oxygen flux and fluence calculation for Long Duration Exposure Facility (LDEF)
[NASA-CR-187418] p 1245 N92-17215

AEROSPACE INDUSTRY
NASA total quality management 1990 accomplishments report
[NASA-TM-105465] p 1308 N92-17199
Proceedings of the USAF Structural Integrity Program Conference
[AD-A242943] p 1235 N92-17204

AEROSPACE MEDICINE
Testing and evaluation of the Vanner electrical inverters, models 24-1500 and SP 00112
[AD-A241914] p 1287 N92-17216
Proceedings of the Conference on Health Physics
[DE92-704335] p 1331 N92-17802

AEROSPACE PLANES
Weight evaluation and sensitivity analysis for space plane. Part 2: TSTO
[NAL-TM-602-PT-2] p 1251 N92-17754

AEROSPACE SAFETY
Collision avoidance sensor skin p 1247 N92-17361

AEROSPACE SCIENCES
NASA/DoD aerospace knowledge diffusion research project: Chronology of selected literature, reports, policy instruments, and significant events affecting Federal Scientific and Technical Information (STI) in the US
[NASA-TM-101662] p 1381 N92-17001
Space Station Freedom science utilization: 2000 and beyond p 1244 N92-17107

AEROSPACE SYSTEMS
Collision avoidance sensor skin p 1247 N92-17361

AEROSPACE TECHNOLOGY TRANSFER
NASA/DoD aerospace knowledge diffusion research project: Chronology of selected literature, reports, policy instruments, and significant events affecting Federal Scientific and Technical Information (STI) in the US
[NASA-TM-101662] p 1381 N92-17001
Proceedings of the USAF Structural Integrity Program Conference
[AD-A242943] p 1235 N92-17204

AEROSPACE VEHICLES
An aerocapture attitude control systems incorporating robustness and vehicle parameter identification
[AD-A243360] p 1245 N92-17302
Experiments and analysis concerning the use of external burning to reduce aerospace vehicle transonic drag
[NASA-TM-105397] p 1235 N92-17546

AEROTHERMODYNAMICS
Application of program LAURA to perfect gas shock tube flows: A parametric study
[NASA-TM-104190] p 1294 N92-17002

AGING (MATERIALS)
A powder x ray diffraction study of two aluminum-lithium based alloys
[AD-A243186] p 1262 N92-17000
Microstructure and mechanical properties of HSLA-100 steel
[AD-A242937] p 1265 N92-17467
Test method for the evaluation of the water treeing behavior of cross-linked polyethylene medium voltage cables
[ETN-92-90588] p 1270 N92-17541

AH-64 HELICOPTER
Assessment of rotorcraft system identification as applied to the AH-64 p 1231 N92-17160

AIR BREATHING ENGINES
Experiments and analysis concerning the use of external burning to reduce aerospace vehicle transonic drag
[NASA-TM-105397] p 1235 N92-17546

AIR CURRENTS
The role of thermal convection in heat and mass transport in the subarctic snow cover
| AD-A243674 | p 1312 N92-17715
AIR DATA SYSTEMS
Results of the space shuttle vehicle ascent air data system probe calibration test using a 0.07-scale external tank forebody model (68T) in the AEDC 16-foot transonic wind tunnel (IA-310), volume 1
| NASA-CR-167696 | p 1241 N92-17167
Results of the space shuttle vehicle ascent air data system probe calibration test using a 0.07-scale external tank forebody model (68T) in the AEDC 16-foot transonic wind tunnel (IA-310), volume 2
| NASA-CR-167697 | p 1241 N92-17214
AIR DROP OPERATIONS
Trajectory analysis of the G-11 family of clustered parachutes to determine minimum altitude
| AD-A243375 | p 1225 N92-17404
AIR DUCTS
Modification of Jindivik air intake duct with an auxiliary intake static aerodynamic tests
| AD-A243002 | p 1232 N92-17234
AIR FLOW
A variational assimilation method for satellite and conventional data: Model 2 (version 1)
p 1322 N92-17976
AIR INTAKES
Meeting Review: Airborne Aerosol Inlet Workshop
| NASA-CR-189814 | p 1313 N92-17393
AIR NAVIGATION
Multisensor signal processing techniques (hybrid GPS/LORAN-C with RAIM)
| AD-A242323 | p 1281 N92-17244
Fault detection and isolation for multisensor navigation systems p 1221 N92-17992
Systematic methods for knowledge acquisition and expert system development p 1222 N92-18001
AIR PURIFICATION
Evaluation of BAUER high pressure breathing air P-2 purification system
| AD-A243535 | p 1333 N92-17014
Unmanned evaluation of BAUER high pressure breathing air P-5 purification system
| AD-A243486 | p 1334 N92-17331
AIR QUALITY
NOAA Atmospheric Sciences Modeling Division support to the US Environmental Protection Agency
| PB91-235499 | p 1315 N92-17134
AIR TRAFFIC CONTROL
Terminal Doppler weather radar test bed operation, Orlando: January-June 1990
| AD-A242890 | p 1318 N92-17028
An investigation of air transportation technology at the Massachusetts Institute of Technology, 1990-1991
p 1219 N92-17985
AIR TRANSPORTATION
Aircraft accident reports: Brief format. US civil and foreign aviation issue number 4 of 1989 accidents
| PB90-916904 | p 1226 N92-17133
Discussion for possibility of some aerodynamic ground effect craft
| NAL-TM-619 | p 1278 N92-17757
Joint University Program for Air Transportation Research, 1990-1991
| NASA-CP-3131 | p 1219 N92-17984
An investigation of air transportation technology at the Massachusetts Institute of Technology, 1990-1991
p 1219 N92-17985
Investigation of air transportation technology at Ohio University, 1990-1991 p 1220 N92-17990
Investigation of air transportation technology at Princeton University, 1990-1991 p 1221 N92-17995
AIR WATER INTERACTIONS
Surface meteorological and near surface oceanographic atlas of the tropical Indian Ocean
| PB91-234286 | p 1319 N92-17138
AIRBORNE/SPACEBORNE COMPUTERS
An analysis of mission critical computer software in Naval aviation
| AD-A243078 | p 1339 N92-17237
Advanced Crew Personal Support Computer (CPSC) task p 1249 N92-17419
Computer system evolution requirements for autonomous checkout of exploration vehicles
p 1250 N92-17422
AIRCRAFT ACCIDENT INVESTIGATION
Aircraft accident reports: Brief format. US civil and foreign aviation issue number 4 of 1989 accidents
| PB90-916904 | p 1226 N92-17133
Aircraft accident report: Northwest Airlines, Inc., Flights 1482 and 299. Runway incursion and collision, Detroit Metropolitan/Wayne County Airport, Romulus, Michigan, December 3, 1990
| PB91-910405 | p 1226 N92-17213
AIRCRAFT ACCIDENTS
Aircraft accident reports: Brief format. US civil and foreign aviation issue number 4 of 1989 accidents
| PB90-916904 | p 1226 N92-17133
Aircraft accident report: Northwest Airlines, Inc., Flights 1482 and 299. Runway incursion and collision, Detroit Metropolitan/Wayne County Airport, Romulus, Michigan, December 3, 1990
| PB91-910405 | p 1226 N92-17213
AIRCRAFT ANTENNAS
Automated composite ellipsoid modelling for high frequency GTD analysis
| NASA-CR-189853 | p 1233 N92-17316
AIRCRAFT CONFIGURATIONS
Rotorcraft System Identification
| AGARD-LS-178 | p 1230 N92-17153
Finite element analysis of ASTOVL fighter structure
| AD-A243724 | p 1233 N92-17513
AIRCRAFT CONSTRUCTION MATERIALS
Rapid repair of integrally stiffened carbon fibre composite structures by bolted aluminium elements
| MBB-FE202-S-PUB-0453-A | p 1256 N92-17310
AIRCRAFT CONTROL
Aircraft ground test and subscale model results of axial thrust loss caused by thrust vectoring using turning vanes
| NASA-TM-4341 | p 1230 N92-17071
Development of high angle of attack control laws for an unstable, non-minimum phase aircraft using variations of the quantitative feedback technique
| AD-A243698 | p 1236 N92-17096
Loading and vibration reduction through active aerodynamic control
| AD-A242321 | p 1236 N92-17243
A robust digital flight control system for an unfanned research vehicle using discrete quantitative feedback theory
| AD-A243638 | p 1237 N92-17748
Identification of the stability and control derivatives of a DLC-flap system for VSRA
| NAL-TR-1116 | p 1237 N92-17917
Investigation of air transportation technology at Princeton University, 1990-1991 p 1221 N92-17995
Neural networks for aircraft system identification
p 1222 N92-17998
Optimal aircraft performance during microburst encounter p 1222 N92-17999
AIRCRAFT DESIGN
Finite element analysis of ASTOVL fighter structure
| AD-A243724 | p 1233 N92-17513
AIRCRAFT ENGINES
Safety considerations in testing a fuel-rich aeropropulsion gas generator
| NASA-TM-105258 | p 1235 N92-17061
Proceedings of the USAF Structural Integrity Program Conference
| AD-A242943 | p 1235 N92-17204
Qualification test report. Fuel pump test stand 3C3965G05
| AD-A242929 | p 1235 N92-17552
Local extinction mechanisms in non-premixed turbulent combustion
| AD-A242027 | p 1260 N92-17682
An analysis of the aircraft engine Component Improvement Program (CIP): A life cycle cost approach
| AD-A243346 | p 1236 N92-17729
Hydrogen fueled subsonic-ram-combustor model tests for an air-turbo-ram engine
| NAL-TR-1064T | p 1236 N92-17855
AIRCRAFT EQUIPMENT
Design of a fiber optic image transmission link
| AD-A243686 | p 1365 N92-17088
AIRCRAFT GUIDANCE
Method of guiding an in-flight vehicle to a designed flight path
| AD-D015061 | p 1229 N92-17707
AIRCRAFT HAZARDS
Thermal energy test apparatus
| AD-A243526 | p 1379 N92-17537
AIRCRAFT ICING
Experimental ice shape and performance characteristics for a multi-element airfoil in the NASA Lewis Icing Research Tunnel
| NASA-TM-105380 | p 1224 N92-17347
AIRCRAFT INSTRUMENTS
Instrumentation and data processing
p 1230 N92-17155
Systematic methods for knowledge acquisition and expert system development p 1222 N92-18001
AIRCRAFT MAINTENANCE
Rapid repair of integrally stiffened carbon fibre composite structures by bolted aluminium elements
| MBB-FE202-S-PUB-0453-A | p 1256 N92-17310
Development of a knowledge base for use in an Expert System Advisor for Aircraft Maintenance Scheduling (ESAAMS)
| AD-A243435 | p 1381 N92-17687
An analysis of the aircraft engine Component Improvement Program (CIP): A life cycle cost approach
| AD-A243346 | p 1236 N92-17729
AIRCRAFT MANEUVERS
Target pitch angle for the microburst escape maneuver p 1221 N92-17996
AIRCRAFT MODELS
Development of high angle of attack control laws for an unstable, non-minimum phase aircraft using variations of the quantitative feedback technique
| AD-A243698 | p 1236 N92-17096
Rotorcraft System Identification
| AGARD-LS-178 | p 1230 N92-17153
Instrumentation and data processing
p 1230 N92-17155
Neural networks for aircraft system identification
p 1222 N92-17998
AIRCRAFT NOISE
Human response to helicopter noise: A test of A-weighting
| AD-A243719 | p 1355 N92-17506
AIRCRAFT PERFORMANCE
System identification methods for handling-qualities evaluation p 1232 N92-17165
Discussion for possibility of some aerodynamic ground effect craft
| NAL-TM-619 | p 1278 N92-17757
Example of statistical techniques applied to cruise performance guarantees (Student's t distribution)
| ESDU-91018 | p 1233 N92-17843
Example of statistical techniques applied to autoland touchdown dispersion (confidence intervals for normal and skew distributions)
| ESDU-91019 | p 1229 N92-17844
Variability of standard aircraft performance parameters
| ESDU-91020 | p 1233 N92-17847
Optimal aircraft performance during microburst encounter p 1222 N92-17999
AIRCRAFT PILOTS
Effects of the chemical defense antidote atropine sulfate on helicopter pilot performance: An in-flight study
| AD-A241966 | p 1328 N92-17084
Aircrew critique of high-G centrifuge training: Part 3: What can we change to better serve you?
| AD-A243496 | p 1334 N92-17432
AIRCRAFT SAFETY
Wichita State University 1986 aviation safety research projects
| DOT/FAA/CT-91/4 | p 1226 N92-16986
Program plans: Aviation safety research
| NIAR-91-30 | p 1227 N92-17587
Discussion for possibility of some aerodynamic ground effect craft
| NAL-TM-619 | p 1278 N92-17757
Joint University Program for Air Transportation Research, 1990-1991
| NASA-CP-3131 | p 1219 N92-17984
An investigation of air transportation technology at the Massachusetts Institute of Technology, 1990-1991
p 1219 N92-17985
AIRCRAFT SPIN
Wichita State University 1986 aviation safety research projects
| DOT/FAA/CT-91/4 | p 1226 N92-16986
Surface pressure measurements on the wing of a wind tunnel model during steady rotation
| AD-A243047 | p 1223 N92-17281
AIRCRAFT STABILITY
Identification of the stability and control derivatives of a DLC-flap system for VSRA
| NAL-TR-1116 | p 1237 N92-17917
AIRCRAFT STRUCTURES
Rapid repair of integrally stiffened carbon fibre composite structures by bolted aluminium elements
| MBB-FE202-S-PUB-0453-A | p 1256 N92-17310
Explicit finite element method for transparency impact analysis
| AD-A243527 | p 1227 N92-17478
AIRCRAFT WAKES
An experimental study of a turbulent wing-body junction and wake flow
| AD-A243388 | p 1223 N92-17222
AIRFOILS
Use of Navier-Stokes analysis in section design
| AD-A242074 | p 1295 N92-17168
Experimental ice shape and performance characteristics for a multi-element airfoil in the NASA Lewis Icing Research Tunnel
| NASA-TM-105380 | p 1224 N92-17347

AIRFRAMES
Experiences at Langley Research Center in the application of optimization techniques to helicopter airframes for vibration reduction
| NASA-TM-104193 | p 1309 N92-17033
The NASA/industry design analysis methods for vibrations (DAMVIBS) program: Accomplishments and contributions
| NASA-TM-104192 | p 1309 N92-17034
Proceedings of the USAF Structural Integrity Program Conference
| AD-A242943 | p 1235 N92-17204
AIRLINE OPERATIONS
Aircraft accident report: Northwest Airlines, Inc., Flights 1482 and 299. Runway incursion and collision, Detroit Metropolitan/Wayne County Airport, Romulus, Michigan, December 3, 1990
| PB91-910405 | p 1226 N92-17213
AIRPORTS
Surface observation climatic summaries for Hondo Municipal Airport, Texas
| AD-A243311 | p 1319 N92-17144
ALASKA
Surface observation climatic summaries for Fairbanks IAP, Alaska
| AD-A243309 | p 1320 N92-17400
ALGEBRA
Complexity issues in numerical optimization
| AD-A241854 | p 1347 N92-17049
Study of features of binary images using algebra techniques
| AD-A242010 | p 1351 N92-17609
A GNS-type theorem for a non-involutive Banach algebra
| DE91-641481 | p 1354 N92-17803
Topological duals of Banach spaces as Banach algebras and applications
| DE91-641482 | p 1354 N92-17804
Use of the algebraic coding theory in nuclear electronics
| DE92-611125 | p 1351 N92-17813
High level language-based robotic control system
| NASA-CASE-NPO-17918-2-CU | p 1349 N92-17895
ALGORITHMS
Wind profiler signal detection improvements
| NASA-CR-189781 | p 1317 N92-16990
The real-time cost of timing uncertainty: Consensus and failure detection
| AD-A243176 | p 1345 N92-16997
A topological model for parallel algorithm design
| AD-A241858 | p 1337 N92-17023
A convergent aspiration based interior point method (CAIN) for Multiple Objective Linear Programming (MOLP)
| AD-A243404 | p 1338 N92-17118
Effective viscosity in the simulation of spatially evolving shear flows with monotonic FCT models
| AD-A243709 | p 1295 N92-17126
Failure detection and fault management techniques for flush airdata sensing systems
| NASA-TM-4335 | p 1234 N92-17128
Sub-band/transform compression of video sequences
| NASA-CR-189786 | p 1280 N92-17139
A system for fast navigation of autonomous vehicles
| AD-A243523 | p 1228 N92-17147
Pattern Theory: An engineering paradigm for algorithm design
| AD-A243214 | p 1339 N92-17179
Performance modeling of the Ada rendezvous
| AD-A243392 | p 1339 N92-17211
Using mappings to prove timing properties
| AD-A242862 | p 1277 N92-17263
Constant modulus algorithm techniques for the enhancement of signal quality
| AD-A242986 | p 1288 N92-17295
Telerobotic ground-remote operations
p 1247 N92-17360
A stochastic approach to the weighted-region problem: 1. The design of the path annealing algorithm
| AD-A243324 | p 1340 N92-17403
The ZEUS second level calorimeter trigger: Physics simulation, design and implementation
| ETN-92-90568 | p 1358 N92-17435
Some foundations for empirical study in the euclidean spatial model of social choice
| AD-A241928 | p 1352 N92-17440
Regularization and approximation of a class of evolution problems in applied mathematics
| AD-A242223 | p 1350 N92-17445
Performance of the Rayleigh task based on the posterior probability of tomographic reconstructions
| DE92-003785 | p 1352 N92-17455
Attention, automaticity and priority learning
| AD-A242226 | p 1332 N92-17458
Improved task scheduling for parallel simulations
| AD-A243721 | p 1346 N92-17507
Muons in UA1; the 2nd level trigger and dimuon results
| ETN-92-90565 | p 1360 N92-17520
Parallel block methods for sparse symmetric linear systems of equations
| AD-A242315 | p 1351 N92-17560
The square root cordic
| AD-A242318 | p 1342 N92-17561
Computation of three-dimensional flows using two stream functions
| NASA-CR-187802 | p 1298 N92-17588
Comparison of station-keeping algorithms for an interior libration point orbit in the Sun-Earth + Moon elliptic restricted three-body problem
| AD-A241896 | p 1388 N92-17595
Control of a large flexible space structure using multiple model adaptive algorithms
| AD-A243759 | p 1250 N92-17602
Study of features of binary images using algebra techniques
| AD-A242010 | p 1351 N92-17609
Incremental volume rendering algorithm for interactive 3D ultrasound imaging
| AD-A242048 | p 1342 N92-17637
New algorithms for broad-band and narrowband source localization and a separable 2-D IIR filter realization
| AD-A243457 | p 1291 N92-17654
Neutral network models of primate motor system
| AD-A243460 | p 1343 N92-17655
Scan directed load balancing for highly-parallel mesh-connected computers
| AD-A242045 | p 1346 N92-17670
Full surface testing of grazing incidence mirrors
| AD-A243734 | p 1367 N92-17690
An algorithm for calculating the electronic spectrum and function of the charge density distributions of crystals
p 1375 N92-17698
Object acquisition and tracking for space-based surveillance
| AD-A243333 | p 1367 N92-17711
Parallelizing serial code for a distributed processing environment with an application to high frequency electromagnetic scattering
| AD-A243755 | p 1284 N92-17721
Control algorithms for aerobraking in the Martian atmosphere
| AD-A243349 | p 1239 N92-17730
Image processing applications for nonlinear decomposition and synthesis
| AD-A243357 | p 1343 N92-17733
A cache design to exploit structural locality
| AD-A243633 | p 1336 N92-17744
Multispectral software development for the Airborne Bathymetric Survey System
| AD-A243774 | p 1325 N92-17765
Ocean simulation model. Version 2: First order frontal simulation
| AD-A243775 | p 1325 N92-17766
Development of a system for void fraction measuring by electroprobing method
| DE92-610933 | p 1309 N92-17809
On the nonadiabatic theory of charged particles motion in the magnetic dipole field
| DE92-610951 | p 1354 N92-17811
Algorithm and Pascal: A program for neural net learning p 1344 N92-17822
Flow between two stationary disks and a rotating shroud
| AERO-REPT-9001 | p 1300 N92-17851
Systematic computation algorithm to obtain osculating orbit elements from position and velocity vectors
| NAL-TM-614 | p 1239 N92-17854
A fully decentralized multi-sensor system for tracking and surveillance
| OUEL-1886/91 | p 1302 N92-17926
A decentralized Bayesian algorithm for identification of tracked targets
| OUEL-1892/91 | p 1344 N92-17927
A one-dimensional plasma and impurity transport model for reversed field pinches
| DE92-004691 | p 1371 N92-17933
Fault detection and isolation for multisensor navigation systems p 1221 N92-17992
ALIGNMENT
Dielectric properties of aligned conducting polymers
| AD-A243389 | p 1268 N92-17191
Precision multi-channel fiber optic interface and method
| AD-D015104 | p 1367 N92-17828
Correlator optical wavefront sensor COWS
| DE92-003964 | p 1368 N92-17846
ALKALIES
Comparison of alkali ion emitters
| AD-A243105 | p 1290 N92-17570
ALKALINE BATTERIES
Catalysts for ultrahigh current density oxygen cathodes for space fuel cell applications
| NASA-CR-189787 | p 1253 N92-17365
Silver-nickel composite cathodes for alkaline secondary batteries
| AD-D015121 | p 1293 N92-17871
ALKYL COMPOUNDS
Molecular jet studies of vdW clusters and solvation
| AD-A242866 | p 1254 N92-17308
Molecular recognition in gels, monolayers, and solids
| AD-A243488 | p 1358 N92-17428
ALLOYS
The effect of weld metal strength mismatch on the deformation and fracture behavior of steel butt weldments
| AD-A243239 | p 1262 N92-17057
ALTERNATIVES
Benefit analysis of proposed information systems
| AD-A243707 | p 1382 N92-17125
ALTITUDE SIMULATION
Effect of two types of scene detail on detection of altitude change in a flight simulator
| AD-A242034 | p 1333 N92-17758
ALUMINIDES
Metallography of aluminide coatings
| AD-A243000 | p 1263 N92-17264
Thermo-mechanical fatigue of a fiber reinforced titanium aluminide composite
| AD-A241988 | p 1256 N92-17607
ALUMINUM
Optical properties of thermally intermixed quantum wells and superlattices
| AD-A243546 | p 1375 N92-17618
Launching projectiles with hydrogen gas generated from aluminum fuel powder/water reactions
| AD-D015119 | p 1276 N92-17830
Production of mullite fibers
| NASA-CASE-MFS-28431-1 | p 1257 N92-17870
ALUMINUM BORON COMPOSITES
Polymer-reinforced metal matrix composite
| AD-D015070 | p 1257 N92-17611
ALUMINUM COMPOUNDS
Production of mullite fibers
| NASA-CASE-MFS-28431-1 | p 1257 N92-17870
ALUMINUM GALLIUM ARSENIDES
Innovative optoelectronic materials and structures using OMVPE
| AD-A243257 | p 1371 N92-16984
A comparative study of the noise performance of Alluminum Gallium Arsenide/Gallium Arsenide high electron mobility transistors with and without superconducting gate electrodes p 1288 N92-17317
ALUMINUM OXIDES
Strength and microstructure of ceramics
| AD-A243049 | p 1269 N92-17282
Rocket tests in Mississippi to be heavily restricted
| GAO/NSIAD-92-86 | p 1240 N92-17741
Dynamic fracture characterization of Al2O3 and SiC(w)/Al2O3
| AD-A242187 | p 1273 N92-17784
ALUMINUM-LITHIUM ALLOYS
A powder x ray diffraction study of two aluminum-lithium based alloys
| AD-A243186 | p 1262 N92-17000
Aluminum alloys for ALS cryogenic tanks: Comparative measurements of cryogenic mechanical properties of Al-Li alloys and alloy 2219
| AD-A242956 | p 1264 N92-17379
The influence of temperature and composition on the activation energy for creep in binary aluminum lithium alloys
| AD-A242299 | p 1265 N92-17759
AMINO ACIDS
Comments on a novel approach to the role of chirality in the origin of life
| DE92-609034 | p 1327 N92-17970
AMMONIUM COMPOUNDS
Clean room wiping liquids
| DE92-004793 | p 1238 N92-17967
AMMUNITION
Pyrolysis GC-FTIR studies of a LOVA propellant formulation series
| AD-A242844 | p 1275 N92-17562
AMORPHOUS MATERIALS
The effect of physical aging on the creep response of a thermoplastic composite
| AD-A243600 | p 1258 N92-17932
AMORPHOUS SILICON
Liquid-solid transition in the bond particle model for elemental semiconductors
| DE92-610441 | p 1378 N92-17972
AMPLIFICATION
Modeling convergence zone gain on MS-DOS based personal computers
| AD-A243252 | p 1341 N92-17558

Performance of hole coupling resonator in the presence of asymmetric modes and FEL gain
| DE92-003907 | p 1305 N92-17936

AMPLITUDE MODULATION
A hybrid modulation for the dissemination of weather data to aircraft p 1220 N92-17991

AMPLITUDES
High-speed beam switching processor
| AD-D015108 | p 1285 N92-17829

ANAEROBES
Microbial diversity: Course report 1991
| AD-A243464 | p 1326 N92-17224

ANALOG TO DIGITAL CONVERTERS
Design and evaluation of a Josephson array oscillator
| AD-A243167 | p 1291 N92-17672

ANALYSIS (MATHEMATICS)
A wing rock model for the F-14A aircraft
| AD-A243109 | p 1233 N92-17300

ANALYTIC FUNCTIONS
Mathematical basis for a system to manage automated protocol analysis
| AD-A242042 | p 1381 N92-17669

ANALYZERS
Permittivity probe modelling
| AD-A243236 | p 1260 N92-17572

ANATOMY
BrainMap: A database of functional neuroanatomy derived from human brain images
| AD-A243161 | p 1333 N92-17648

ANECHOIC CHAMBERS
Frequency stirring: An alternate approach to mechanical mode-stirring for the conduct of electromagnetic susceptibility testing
| AD-A243551 | p 1279 N92-17031

ANGLE OF ATTACK
Development of high angle of attack control laws for an unstable, non-minimum phase aircraft using variations of the quantitative feedback technique
| AD-A243698 | p 1236 N92-17096
A wing rock model for the F-14A aircraft
| AD-A243109 | p 1233 N92-17300
Aerodynamic development of the X-31 aircraft for the high angle of attack region
| MBB-FE211-S-PUB-452 | p 1233 N92-17313

ANGLES (GEOMETRY)
Fiber optic angular orientation sensor digital serial encoding
| AD-D015102 | p 1302 N92-17826

ANGULAR VELOCITY
Computation of the hydrodynamic forces and moments on a body of revolution with and without appendages
| AD-A243033 | p 1294 N92-16978

ANHYDRIDES
Substituted 1,1,1-triaryl-2,2,2-trifluoroethanes and processes for their synthesis
| NASA-CASE-LEW-14345-6 | p 1255 N92-17882

ANISOTROPY
In situ surface x ray crystallography of electrochemically deposited Bi on Ag(111): Structure, compressibility, and anisotropy
| AD-A243218 | p 1372 N92-17181
Magnetic multilayer interface anisotropy
| DE92-000635 | p 1263 N92-17319
Late time cosmological phase transitions 1: Particle physics models and cosmic evolution
| NASA-CR-189857 | p 1388 N92-17696
Light-controlled, electrochemical, anisotropic etching of silicon
| MBB-Z-0368-91-PUB | p 1261 N92-17841

ANNEALING
Materials processing of diamond: Etching, doping by ion implantation and contact formation
| AD-A243060 | p 1267 N92-17065
A spectroscopic immersion ellipsometry study of the mechanism of Si/SiO2 interface annealing
| AD-A242831 | p 1259 N92-17261
Optical properties of thermally intermixed quantum wells and superlattices
| AD-A243546 | p 1375 N92-17618
Effect of thermal annealing on property changes of neutron-irradiated non-graphitized carbon materials and nuclear graphite
| DE92-704180 | p 1257 N92-17816
Structure and topology of silica aerogels
| DE92-004728 | p 1274 N92-17938

ANODES
Exploring plasma sheath solutions for planar and cylindrical anodes
| AD-A243237 | p 1369 N92-17030

ANTARCTIC REGIONS
Evaluation of solar flares and electron precipitation by nitrate distribution in Antarctica
| AD-A243026 | p 1389 N92-17235

ANTENNA ARRAYS
Multiple-access phased array antenna simulator for a digital beam forming system investigation
| NASA-TM-105422 | p 1279 N92-17062
Design and testing of a lightweight, planar microwave lens
| AD-A243685 | p 1286 N92-17076
High-speed beam switching processor
| AD-D015108 | p 1285 N92-17829

ANTENNA DESIGN
Advanced Communication Technology Satellite (ACTS) multibeam antenna analysis and experiment
| NASA-TM-105420 | p 1279 N92-17047
Multiple-access phased array antenna simulator for a digital beam forming system investigation
| NASA-TM-105422 | p 1279 N92-17062
Multipath induced tracking errors at 95 and 140 GHz
| AD-A243111 | p 1283 N92-17571

ANTENNA RADIATION PATTERNS
Advanced Communication Technology Satellite (ACTS) multibeam antenna analysis and experiment
| NASA-TM-105420 | p 1279 N92-17047
Spherical near-field scanning: Experimental and theoretical studies
| AD-A243489 | p 1282 N92-17429

ANTENNAS
Flow visualization and wake analysis for standard and modified configurations of the AN/ALQ-78 antenna pod
| AD-A243552 | p 1224 N92-17339
Theoretical studies in tokamaks: Three-dimensional simulation of lower hybrid wave launching in tokamaks
| DE92-003773 | p 1371 N92-17793

ANTHROPOMETRY
Face recognition with the Karhunen-Loeve transform
| AD-A243688 | p 1280 N92-17090

ANTICYCLONES
Source of cold water in Monterey Bay observed by AVHRR satellite imagery
| AD-A242843 | p 1323 N92-17051

ANTIDOTES
Effects of the chemical defense antidote atropine sulfate on helicopter pilot performance: An in-flight study
| AD-A241966 | p 1328 N92-17084

ANTIFERROMAGNETISM
Structural, electronic, and magnetic properties of La(x)Sr(1-x)VO3 (0 is less than or equal to x is less than or equal to 1.0)
| DE92-003808 | p 1378 N92-17916

ANTIINFECTIVES AND ANTIBACTERIALS
The effect of shower/bath frequency on the health and operational effectiveness of soldiers in a field setting: Recommendation of showering frequencies for reducing performance-degrading nonsystemic microbial skin infections
| AD-A242923 | p 1330 N92-17714

ANTIMISSILE DEFENSE
High resolution imaging using phase retrieval, volume 2
| AD-A242925 | p 1366 N92-17550
Verification and validation of the Comprehensive Operational Support Evaluation Model for space
| AD-A243653 | p 1344 N92-17761

ANTIMONY COMPOUNDS
Cryogenic thermoresistor made from p-InSb(Mn)
| DE92-600473 | p 1293 N92-17825

ANTIPROTONS
Proton-proton and proton-antiproton elastic scattering at high energies: Theory, phenomenology, and experiment
| DE92-004414 | p 1364 N92-17964

ANTISEPTICS
The effect of shower/bath frequency on the health and operational effectiveness of soldiers in a field setting: Recommendation of showering frequencies for reducing performance-degrading nonsystemic microbial skin infections
| AD-A242923 | p 1330 N92-17714

APERTURES
Evaluation of a compact Cassegrain optical system
| AD-A242985 | p 1366 N92-17294
Spherical near-field scanning: Experimental and theoretical studies
| AD-A243489 | p 1282 N92-17429
Performance of hole coupling resonator in the presence of asymmetric modes and FEL gain
| DE92-003907 | p 1305 N92-17936

APPLICATIONS PROGRAMS (COMPUTERS)
Background Atmosphere Radiance Day (BARD) and Night (BARN)
| AD-A243153 | p 1316 N92-17239
Map maker
| AD-A242980 | p 1312 N92-17292
Advanced flight software reconfiguraton p 1245 N92-17350
The effect of detonation curvature on cylindrical wall motion
| DE92-003110 | p 1298 N92-17625
Environmental containment property estimation using QSARs in an expert system
| AD-A243728 | p 1336 N92-17720
Analysis of cam roller followers
| ESDU-91026 | p 1307 N92-17852
High level language-based robotic control system
| NASA-CASE-NPO-17918-2-CU | p 1349 N92-17895

APPROACH
Flight evaluation of curved MLS precision approaches in a twin otter aircraft, phase 2
| AD-A243025 | p 1229 N92-17568

APPROXIMATION
A Kalman filter for a Poisson series with covariates and Laplace approximation integration
| AD-A242960 | p 1286 N92-16993
Estimation of the outer sphere contribution to the activation parameters for homogeneous electron transfer reactions using the mean spherical approximation
| AD-A243217 | p 1259 N92-17323
Regularization and approximation of a class of evolution problems in applied mathematics
| AD-A242223 | p 1350 N92-17445
Preliminary development of a three-dimensional nonlinear approximation procedure for turbomachinery design optimization applications
| AD-A243155 | p 1235 N92-17644

AQUATIC PLANTS
Aquatic plant management program. Supplement
| AD-A242420 | p 1314 N92-17723

AQUEOUS SOLUTIONS
Atomic relaxation at ordered electrochemical surfaces probed by scanning tunneling microscopy: Au(111) in aqueous solution compared with ultrahigh-vacuum environments
| AD-A242031 | p 1358 N92-17472

AQUIFERS
University of Minnesota Aquifer Thermal Energy Storage (ATES) project report on the first long-term cycle
| DE92-004699 | p 1313 N92-17934

ARC JET ENGINES
A study of ignition and simulation circuits for arcjet thrusters, part 1
| NASA-CR-189097 | p 1253 N92-17510

ARC WELDING
The effect of titanium inclusions on HY-80 GMA weld deposits
| AD-A243408 | p 1239 N92-17192
Substantially oxygen-free contact tube
| NASA-CASE-LAR-14169-1 | p 1307 N92-17677

ARCHITECTURE (COMPUTERS)
An examination of selected commercial software testing tools
| AD-A243089 | p 1337 N92-17068
Implementation of an object-oriented flight simulator D.C. electrical system on a hypercube architecture
| AD-A243700 | p 1238 N92-17097
Adaptive presort processing
| AD-A243286 | p 1340 N92-17286
Design of Style-V: A translator to convert standard VHDL into a stylized form for automated microcode generation
| AD-A243706 | p 1340 N92-17407
Data management system advanced architectures p 1249 N92-17417
Program translation tools for systolic arrays
| AD-A242924 | p 1336 N92-17466
Parallel radiosity techniques for mesh-connected SIMD computers
| AD-A242049 | p 1346 N92-17638
The UNC graph server: A distributed hypermedia data management system
| AD-A242041 | p 1380 N92-17651
Object acquisition and tracking for space-based surveillance
| AD-A243333 | p 1367 N92-17711
Parallelizing serial code for a distributed processing environment with an application to high frequency electromagnetic scattering
| AD-A243755 | p 1284 N92-17721

ARCTIC REGIONS
An investigation of cold overflow over the Iceland/Faeroes Ridge
| AD-A243084 | p 1324 N92-17169

ARGON LASERS
Steady-state production and quenching of Br((2)P1/2)
| AD-A243754 | p 1362 N92-17663

ARGON PLASMA
Experimental measurements of plasma properties for Miller SG-100 torch with Mach I setting
| DE92-003309 | p 1369 N92-17469
Picosecond laser breakdown thresholds in gases
| AD-A242941 | p 1304 N92-17475

ARIANE LAUNCH VEHICLE
Integration of RAMS activities during the development phase of Ariane 5-components (example: Vulcain thrust chamber)
| MBB-UK-0144-91-PUB | p 1240 N92-17527

ARIES SOUNDING ROCKET
Aries x ray objective grating spectrograph
| NASA-CR-189245 | p 1386 N92-17003

ARMED FORCES (FOREIGN)
Local area network strategies and guidelines for a Peruvian Air Force Computer Center
| AD-A242841 | p 1345 N92-17135

ARMED FORCES (UNITED STATES)
Cathodic protection diagnostic computer program for sacrificial and impressed current systems: Overview and user's manual
| AD-A243663 | p 1338 N92-17122
Summary of professional activities, center for Air Force C3 systems
| AD-A243509 | p 1348 N92-17386
Worldwide Environmental Compliance Assessment and Management Program (ECAMP): United Kingdom supplement
| AD-A242928 | p 1314 N92-17551
Worldwide Environmental Compliance Assessment and Management Program (ECAMP)
| AD-A242874 | p 1314 N92-17598
The effect of shower/bath frequency on the health and operational effectiveness of soldiers in a field setting: Recommendation of showering frequencies for reducing performance-degrading nonsystemic microbial skin infections
| AD-A242923 | p 1330 N92-17714

AROMATIC COMPOUNDS
The EPR of the triplet state of aryl cations in crystals of diazonium salts p 1375 N92-17701

ARRAYS
A covariance modeling approach to adaptive beamforming and detection
| AD-A241887 | p 1279 N92-17040
Design implementation into field programmable gate arrays
| AD-A242538 | p 1343 N92-17680

ARSENIC
Au and Al Schottky barrier formation on GaAs (100) surfaces prepared by thermal desorption of a protective arsenic coating
| DE92-002456 | p 1376 N92-17781

ARTIFICIAL INTELLIGENCE
Causal schema decision-aiding system
| AD-A242931 | p 1347 N92-17203
Operations mission planner beyond the baseline p 1246 N92-17353
Summary of professional activities, center for intelligence and special programs, 1990
| AD-A243508 | p 1347 N92-17385
Computer system evolution requirements for autonomous checkout of exploration vehicles p 1250 N92-17422
Automated planning with special relevance to associate systems technology and mission planning
| AD-A241924 | p 1348 N92-17438
An investigation of the application of artificial neural networks to adaptive optics imaging systems
| AD-A243780 | p 1348 N92-17767
Software tools for distributed intelligent control systems
| DE92-004656 | p 1349 N92-17965
Intelligent failure-tolerant control p 1222 N92-18000

ARTIFICIAL SATELLITES
Early warning satellites: Funding for follow-on system is premature
| AD-A242836 | p 1245 N92-17250
Radar-satellite studies of the high-latitude ionosphere
| AD-A243275 | p 1317 N92-17961

ASCENT
Results of the space shuttle vehicle ascent air data system probe calibration test using a 0.07-scale external tank forebody model (68T) in the AEDC 16-foot transonic wind tunnel (IA-310), volume 1
| NASA-CR-167696 | p 1241 N92-17167
Results of the space shuttle vehicle ascent air data system probe calibration test using a 0.07-scale external tank forebody model (68T) in the AEDC 16-foot transonic wind tunnel (IA-310), volume 2
| NASA-CR-167697 | p 1241 N92-17214

ASPECT RATIO
Study of transition phenomena in a straight channel with 40 to 1 aspect ratio with and without imposed pulsations. Part two: Reynolds number surveys
| AD-A241894 | p 1296 N92-17307

ASPHALT
Alternate/modified binders for asphalt airfield pavements
| AD-A242829 | p 1238 N92-17260

ASPHERICITY
Evaluation of a compact Cassegrain optical system
| AD-A242985 | p 1366 N92-17294

ASSEMBLY LANGUAGE
Decompiling with definite clause grammars
| AD-A242987 | p 1340 N92-17296

ASSOCIATIVE PROCESSING (COMPUTERS)
Optical associative processors and directed graphs
| AD-A242901 | p 1366 N92-17630

ASTRONAUT TRAINING
Upper body exercise: Physiology and training application for human presence in space
| AD-A242033 | p 1329 N92-17473

ASTRONOMICAL CATALOGS
IRAS and the Boston University Arecibo Galactic H I Survey: A catalog of cloud properties
| NASA-CR-189806 | p 1387 N92-17695

ASTRONOMICAL MAPS
Radio sky mapping from satellites at very low frequencies
| NASA-TM-105452 | p 1387 N92-17694

ASTRONOMICAL MODELS
Geometrical methods for the analysis of cosmological observations
| ETN-92-90584 | p 1386 N92-17523
Late time cosmological phase transitions 1: Particle physics models and cosmic evolution
| NASA-CR-189857 | p 1388 N92-17696

ASTRONOMY
Hubble Space Telescope: Fine guidance sensors instrument handbook. Version 2.1
| NASA-CR-189745 | p 1386 N92-17020
Hubble Space Telescope: Faint object camera instrument handbook. Version 2.0
| NASA-CR-189746 | p 1386 N92-17021

ASTROPHYSICS
Collaborative research on experimental astrophysics
| DE92-003970 | p 1388 N92-17832

ASYMMETRY
Axino-induced baryogenesis
| NASA-CR-189858 | p 1361 N92-17646
Fluctuation driven electroweak phase transition
| NASA-CR-189859 | p 1361 N92-17647

ASYMPTOTIC METHODS
Tests of fit for the Cauchy distribution based on the empirical distribution function
| AD-A243201 | p 1352 N92-17173

ATLANTIC OCEAN
An investigation of cold overflow over the Iceland/Faeroes Ridge
| AD-A243084 | p 1324 N92-17169
A user's manual for the Princeton Numerical Ocean Model
| AD-A243773 | p 1324 N92-17539

ATLANTIS (ORBITER)
STS-38 Space Shuttle mission report
| NASA-TM-105478 | p 1242 N92-17534

ATMOSPHERIC CHEMISTRY
NOAA Atmospheric Sciences Modeling Division support to the US Environmental Protection Agency
| PB91-235499 | p 1315 N92-17134

ATMOSPHERIC CIRCULATION
Studies of baroclinic flow
| AD-A243050 | p 1296 N92-17309

ATMOSPHERIC COMPOSITION
Meeting Review: Airborne Aerosol Inlet Workshop
| NASA-CR-189814 | p 1313 N92-17393

ATMOSPHERIC DENSITY
Control algorithms for aerobraking in the Martian atmosphere
| AD-A243349 | p 1239 N92-17730

ATMOSPHERIC MODELS
An investigation of methods for updating ionospheric scintillation models using topside in-situ plasma density measurements
| AD-A243378 | p 1316 N92-17209
Stellar spectral line synthesis from an individual photon-following simulation
| AD-A242970 | p 1388 N92-17253
Meeting Review: Airborne Aerosol Inlet Workshop
| NASA-CR-189814 | p 1313 N92-17393
Numerical simulation of cirrus clouds: Fire case study and sensitivity analysis
| AD-A242902 | p 1321 N92-17631
Evaluation of LOWTRAN and MODTRAN for use over high zenith angle/long path length viewing
| AD-A243599 | p 1387 N92-17920
A variational assimilation method for satellite and conventional data: A revised basic model 2B p 1322 N92-17977
A variational formalism for the radiative transfer equation: Prelude to model 3 p 1322 N92-17978
A variational formalism for the radiative transfer equation and a geostrophic, hydrostatic atmosphere: Prelude to model 3 p 1322 N92-17979

ATMOSPHERIC OPTICS
Evaluation of LOWTRAN and MODTRAN for use over high zenith angle/long path length viewing
| AD-A243599 | p 1387 N92-17920

ATMOSPHERIC PHYSICS
NOAA Atmospheric Sciences Modeling Division support to the US Environmental Protection Agency
| PB91-235499 | p 1315 N92-17134

ATMOSPHERIC PRESSURE
Surface observation climatic summaries for Fairbanks IAP, Alaska
| AD-A243309 | p 1320 N92-17400

ATMOSPHERIC TEMPERATURE
Surface observation climatic summaries for Fairbanks IAP, Alaska
| AD-A243309 | p 1320 N92-17400
A variational assimilation method for satellite and conventional data: A revised basic model 2B p 1322 N92-17977
A variational formalism for the radiative transfer equation and a geostrophic, hydrostatic atmosphere: Prelude to model 3 p 1322 N92-17979

ATOMIC COLLISIONS
Collisional dynamics of the B3Pi(O+) state of bromine of monofluoride
| AD-A241857 | p 1356 N92-17305
Steady-state, high dose neutron generation and concentration apparatus and method for deuterium atoms
| AD-D015063 | p 1358 N92-17462

ATOMIC SPECTRA
An algorithm for calculating the electronic spectrum and function of the charge density distributions of crystals p 1375 N92-17698
Inductively coupled plasma atomic emission spectroscopy analysis of gold electroplating solutions
| DE92-004798 | p 1266 N92-17858

ATOMIC STRUCTURE
Laser-based ignition of H2/O2 and D2/O2 premixed gases near 243 nm: The first report of a deuterium isotope wavelength effect in laser ignition
| AD-A243180 | p 1303 N92-17137
An investigation of underpotentially deposited thallium of silver (111) by in-situ surface x ray scattering
| AD-A243270 | p 1263 N92-17271
Atomic relaxation at ordered electrochemical surfaces probed by scanning tunneling microscopy: Au(111) in aqueous solution compared with ultrahigh-vacuum environments
| AD-A242031 | p 1358 N92-17472
Designing ordered molecular arrays in two and three dimensions
| AD-A243447 | p 1359 N92-17491
Structural, electronic, and magnetic properties of La(x)Sr(1-x)VO3 (0 is less than or equal to x is less than or equal to 1.0)
| DE92-003808 | p 1378 N92-17916
Grain boundaries
| DE92-004420 | p 1378 N92-17941
Liquid-solid transition in the bond particle model for elemental semiconductors
| DE92-610441 | p 1378 N92-17972

ATOMS
Relaxation processes of vibrationally excited H2O in the mesosphere and thermosphere
| AD-A241853 | p 1315 N92-17035
Atom wave interferometer
| AD-A243482 | p 1357 N92-17374

ATROPINE
Effects of the chemical defense antidote atropine sulfate on helicopter pilot performance: An in-flight study
| AD-A241966 | p 1328 N92-17084

ATTENTION
A connectionist simulation of attention and vector comparison: The need for serial processing in parallel hardware
| AD-A242225 | p 1348 N92-17457
Attention, automaticity and priority learning
| AD-A242226 | p 1332 N92-17458
The dynamics of visual representation, attention, encoding, and retrieval processes
| AD-A243031 | p 1384 N92-17785

ATTITUDE (INCLINATION)
Target pitch angle for the microburst escape maneuver p 1221 N92-17996

ATTITUDE CONTROL
An aerocapture attitude control systems incorporating robustness and vehicle parameter identification
| AD-A243360 | p 1245 N92-17302

ATTITUDE INDICATORS
GPS interferometric attitude and heading determination: Initial flight test results p 1221 N92-17994

AUDIO EQUIPMENT
Development of a Federal standard for a video codec operating at P x 64 KBPS
| AD-A243005 | p 1281 N92-17267

AUDIO FREQUENCIES
Mechanisms of temporal pattern discrimination by human observers
| AD-A243051 | p 1332 N92-17336
Classification of complex sounds
| AD-A243498 | p 1355 N92-17381
Mechanisms mediating the perception of complex acoustic patterns
| AD-A243715 | p 1355 N92-17502

AUDIOMETRY
The effect of impulse presentation order on hearing trauma in the chinchilla
| AD-A243174 | p 1326 N92-17269
The hazard of exposure to 2.075 kHz center frequency narrow band impulses
| AD-A242997 | p 1329 N92-17299

AUDITORY PERCEPTION
Mechanisms mediating the perception of complex acoustic patterns
| AD-A243715 | p 1355 N92-17502
Signal- and listener-based factors in complex auditory pattern perception
| AD-A243716 | p 1332 N92-17503
Human response to helicopter noise: A test of A-weighting
| AD-A243719 | p 1355 N92-17506
Psychophysical evaluation of three-dimensional auditory displays
| NASA-CR-189848 | p 1355 N92-17692

AUDITORY SIGNALS
Signal- and listener-based factors in complex auditory pattern perception
| AD-A243716 | p 1332 N92-17503
Psychophysical evaluation of three-dimensional auditory displays
| NASA-CR-189848 | p 1355 N92-17692

AUTOMATIC CONTROL
Space Station Freedom engineering prototype development p 1244 N92-17110
A system for fast navigation of autonomous vehicles
| AD-A243523 | p 1228 N92-17147
Using mappings to prove timing properties
| AD-A242862 | p 1277 N92-17263
The environmental control and life support system advanced automation project p 1246 N92-17356
Computer system evolution requirements for autonomous checkout of exploration vehicles p 1250 N92-17422
Automated planning with special relevance to associate systems technology and mission planning
| AD-A241924 | p 1348 N92-17438
Attention, automaticity and priority learning
| AD-A242226 | p 1332 N92-17458
Automatic recognition of speech in stressful environments
| AD-A242917 | p 1283 N92-17464
Automated power management and control p 1252 N92-17773
The SSM/PMAD automated test bed project p 1252 N92-17774

AUTOMATIC PILOTS
Multiple input sliding mode control for autonomous diving and steering of underwater vehicles
| AD-A241935 | p 1237 N92-17442

AUTONOMOUS NAVIGATION
Multisensor signal processing techniques (hybrid GPS/LORAN-C with RAIM)
| AD-A242323 | p 1281 N92-17244

AUTONOMY
JPL space station telerobotic engineering prototype development: Advanced telerobotics system technology p 1247 N92-17358

AVALANCHE DIODES
Research and development on advanced silicon carbide thin film growth techniques and fabrication of high power and microwave frequency silicon carbide-based device structures
| AD-A243531 | p 1373 N92-17390

AVIATION METEOROLOGY
Alert generation and cockpit presentation for an integrated microburst alerting system p 1220 N92-17988

AVIONICS
AGSSS: The Airborne Graphics Software Support System; an Ada/PHIGS-based display editor for the rapid development of cockpit display software systems
| AD-A243224 | p 1234 N92-17221

AXIAL LOADS
Strength of lugs
| ESDU-91008 | p 1311 N92-17834

AXONS
Temporally-specific modification of myelinated axon excitability in vitro following a single ultrasound pulse
| AD-A242329 | p 1326 N92-17474

AZO COMPOUNDS
The EPR of the triplet state of aryl cations in crystals of diazonium salts p 1375 N92-17701

B

BACKGROUND NOISE
A performance model of Thermal Imaging System (TISs) which includes the human observer's response to state of the art displays
| AD-A242838 | p 1301 N92-17273

BACKGROUND RADIATION
Late time cosmological phase transitions 1: Particle physics models and cosmic evolution
| NASA-CR-189857 | p 1388 N92-17696
Evaluation of LOWTRAN and MODTRAN for use over high zenith angle/long path length viewing
| AD-A243599 | p 1387 N92-17920

BACKSCATTERING
Enhanced backscattering of light from randomly rough diffusers: Appendix
| AD-A243436 | p 1366 N92-17485
Enhanced backscattering from rough surfaces
| AD-A243437 | p 1366 N92-17486
Auroral-clutter predictions for Fylingdales, England
| AD-A242957 | p 1283 N92-17600
Verification and validation of the simulated radar image (SRIM) code radar cross section predictions
| AD-A243651 | p 1285 N92-17737

BACTERIA
Processing of ceramics of biopolymers. Ultrastructure-property relationships in biocrystals
| AD-A243061 | p 1267 N92-17054

BAHAMAS
A statistical analysis of Eleuthera Island wind data for the period 27 April 1989 through 30 March 1990
| AD-A241885 | p 1318 N92-17027

BAINITE
Microstructure and mechanical properties of HSLA-100 steel
| AD-A242937 | p 1265 N92-17467

BALLISTICS
Effect of coatings and processing on failure mechanisms of polycarbonate material, phase 1
| AD-A243018 | p 1256 N92-17053
User evaluation of laser ballistic sun, wind and dust goggle lenses (dye technology)
| AD-A243245 | p 1334 N92-17143
Ultrafast passive shields for laser and ballistic protection
| AD-A243206 | p 1303 N92-17175

BANACH SPACE
A GNS-type theorem for a non-involutive Banach algebra
| DE91-641481 | p 1354 N92-17803
Topological duals of Banach spaces as Banach algebras and applications
| DE91-641482 | p 1354 N92-17804

BANDWIDTH
Frequency stirring: An alternate approach to mechanical mode-stirring for the conduct of electromagnetic susceptibility testing
| AD-A243551 | p 1279 N92-17031

BARIUM OXIDES
Growth of near-free-standing YBa2Cu3O7-type crystals using a self-decanting flux method
| AD-A243221 | p 1372 N92-17182
High temperature superconductor thin films and Josephson junctions
| AD-A242747 | p 1293 N92-17949

BAROCLINIC WAVES
Studies of baroclinic flow
| AD-A243050 | p 1296 N92-17309

BAROTROPIC FLOW
Studies of baroclinic flow
| AD-A243050 | p 1296 N92-17309

BARYONS
Axino-induced baryogenesis
| NASA-CR-189858 | p 1361 N92-17646
Fluctuation driven electroweak phase transition
| NASA-CR-189859 | p 1361 N92-17647

BATHYMETERS
Bottom contour influence on ray tracing
| AD-A242411 | p 1323 N92-17078
Multispectral software development for the Airborne Bathymetric Survey System
| AD-A243774 | p 1325 N92-17765

BATHYTHERMOGRAPHS
The applied tomography experiment of 1990
| AD-A243525 | p 1354 N92-17086

BAYES THEOREM
Gibbs sampling for marginal posterior expectations
| AD-A243212 | p 1352 N92-17178
Research in some future directions in reliability and quality control
| AD-A242865 | p 1308 N92-17231
Bayesian computations in survival models via the Gibbs sampler
| AD-A242343 | p 1353 N92-17643
A decentralized Bayesian algorithm for identification of tracked targets
| OUEL-1892/91 | p 1344 N92-17927

BEAM CURRENTS
Effects of the high-frequency beam space charge forces on the excitation of electromagnetic waves in relativistic carcinotron
| DE92-610956 | p 1285 N92-17812

BEAM INJECTION
The Los Alamos FEL photoinjector drive laser
| DE92-003791 | p 1305 N92-17795
Multiply charged ion sources for cyclotrons
| DE92-610975 | p 1364 N92-17973

BEAM INTERACTIONS
Effects of the high-frequency beam space charge forces on the excitation of electromagnetic waves in relativistic carcinotron
| DE92-610956 | p 1285 N92-17812

BEAM SWITCHING
High-speed beam switching processor
| AD-D015108 | p 1285 N92-17829

BEAMS (RADIATION)
Two-beam coupling measurements of grating phase in a photorefractive polymer
| AD-A243746 | p 1268 N92-17195
Beam position monitor multiplexer controller upgrade at the LAMPF proton storage ring
| DE92-003859 | p 1363 N92-17590

BEARING (DIRECTION)
Fiber optic angular orientation sensor digital serial encoding
| AD-D015102 | p 1302 N92-17826
Optical fiber magnetometer
| AD-D015133 | p 1368 N92-17959

BEARINGS
System for testing bearings
| NASA-CASE-MFS-28589-1 | p 1306 N92-17584

BED REST
Eccentric and concentric muscle performance following 7 days of simulated weightlessness
| NASA-TP-3182 | p 1330 N92-17645

BEHAVIOR
The 7th Annual Workshop on Computational Neuroscience
| AD-A243462 | p 1335 N92-17656

BENARD CELLS
The wave numbers of supercritical surface tension driven Benard convection
| NASA-CR-189856 | p 1373 N92-17375

BENDING
Strength of lugs
| ESDU-91008 | p 1311 N92-17834
Automatic locking orthotic knee device
| NASA-CASE-MFS-28633-1 | p 1335 N92-17866

BENDING MOMENTS
Loading and vibration reduction through active aerodynamic control
| AD-A242321 | p 1236 N92-17243

BENZENE
Molecular jet studies of vdW clusters and solvation
| AD-A242866 | p 1254 N92-17308

BIBLIOGRAPHIES
NASA/DoD aerospace knowledge diffusion research project: Chronology of selected literature, reports, policy instruments, and significant events affecting Federal Scientific and Technical Information (STI) in the US
| NASA-TM-101662 | p 1381 N92-17001
Bibliography of technical publications, papers, and list of patents, October 1988 - September 1989
| AD-A242839 | p 1383 N92-17274
Bibliography of technical reports 1990
| AD-A242376 | p 1383 N92-17378

BICRYSTALS
Microstructure and composition of electromagnetically-characterized YBa2Cu3O(7-delta) grain boundaries
| DE92-003520 | p 1376 N92-17782
Grain boundaries
| DE92-004420 | p 1378 N92-17941

BINARY ALLOYS
The influence of temperature and composition on the activation energy for creep in binary aluminum lithium alloys
| AD-A242299 | p 1265 N92-17759

BINARY DATA
Study of features of binary images using algebra techniques
| AD-A242010 | p 1351 N92-17609

BINDERS (MATERIALS)
Alternate/modified binders for asphalt airfield pavements
[AD-A242829] p 1238 N92-17260
BIOCHEMISTRY
Microbial diversity: Course report 1991
[AD-A243464] p 1326 N92-17224
Molecular self-assembly and nanochemistry: A chemical strategy for the synthesis of nanostructures
[AD-A243530] p 1361 N92-17616
Evolution as a molecular cooperative phenomenon
[DE92-609575] p 1327 N92-17877
Comments on a novel approach to the role of chirality in the origin of life
[DE92-609034] p 1327 N92-17970
BIOCONVERSION
Artificial photosynthesis: Progress toward molecular systems for photoconversion
[DE92-003370] p 1326 N92-17471
Process of converting starch to glucose and glucose to lactic acid
[DE92-003840] p 1255 N92-17867
BIODYNAMICS
Global models for the biomechanics of green plants, part 1
[DE91-641478] p 1327 N92-17946
BIOELECTRIC POTENTIAL
Establishing an evoked-potential vision-tracking system p 1234 N92-17993
BIOELECTRICITY
Electromagnetic pulse-induced current measurement device
[AD-A241946] p 1291 N92-17668
BIOENGINEERING
Worldwide Environmental Compliance Assessment and Management Program (ECAMP): United Kingdom supplement
[AD-A242928] p 1314 N92-17551
Worldwide Environmental Compliance Assessment and Management Program (ECAMP)
[AD-A242874] p 1314 N92-17598
BIOLOGICAL EFFECTS
The hazard of exposure to 2.075 kHz center frequency narrow band impulses
[AD-A242997] p 1329 N92-17299
Biological effects of protracted exposure to ionizing radiation: Review, analysis, and model development
[AD-A242981] p 1329 N92-17476
BIOLOGICAL EVOLUTION
Evolution as a molecular cooperative phenomenon
[DE92-609575] p 1327 N92-17877
Comments on a novel approach to the role of chirality in the origin of life
[DE92-609034] p 1327 N92-17970
BIOPHYSICS
Biophysical techniques for examining metabolic, proliferative, and genetic effects of microwave radiation
[AD-A241903] p 1326 N92-17288
BIOPOLYMERS
Processing of ceramics of biopolymers. Ultrastructure-property relationships in biocrystals
[AD-A243061] p 1267 N92-17054
BIOREACTORS
Process of converting starch to glucose and glucose to lactic acid
[DE92-003840] p 1255 N92-17867
BIRD-AIRCRAFT COLLISIONS
Explicit finite element method for transparency impact analysis
[AD-A243527] p 1227 N92-17478
BISMUTH
In situ surface x ray crystallography of electrochemically deposited Bi on Ag(111): Structure, compressibility, and anisotropy
[AD-A243218] p 1372 N92-17181
BLACK HOLES (ASTRONOMY)
Black holes in magnetic monopoles
[NASA-CR-189842] p 1388 N92-17377
A classical instability of Reissner-Nordstrom solutions and the fate of magnetically charged black holes
[NASA-CR-189843] p 1388 N92-17697
BLAST LOADS
Structures to resist the effects of accidental explosions
[AD-A243272] p 1277 N92-17272
BLEACHING
Anomalous hole burning in polymers with inhomogeneous broadening
[AD-A242397] p 1266 N92-17010
BLOCK COPOLYMERS
Imide/arylene ether copolymers with pendent trifluoromethyl groups
[NASA-TM-104195] p 1272 N92-17693
Molecular composites from high temperature polyquinolines
[AD-A243634] p 1272 N92-17745
BLOOD
Evaluation of liposome-encapsulated Hemoglobin/LR16 formulations as a potential blood substitute
[AD-A243075] p 1329 N92-17557
BODIES OF REVOLUTION
Computation of the hydrodynamic forces and moments on a body of revolution with and without appendages
[AD-A243033] p 1294 N92-16978
BODY TEMPERATURE
Heat stress caused by wearing different types of CW protective garment
[AD-A243043] p 1334 N92-17278
BODY-WING CONFIGURATIONS
Observation and measurements of flow structures in the stagnation region of a wing-body junction
[AD-A243403] p 1223 N92-17117
An experimental study of a turbulent wing-body junciion and wake flow
[AD-A243388] p 1223 N92-17222
BOILERS
Nucleate pool boiling performance of small high flux and turbo-B tube bundles in R-114/oil mixtures
[AD-A241936] p 1379 N92-17443
Theoretical investigation of the injection and evaporation of water in a hydrogen/oxygen steam generator
[ESA-TT-1252] p 1380 N92-17848
BOILING
Nucleate pool boiling performance of small high flux and turbo-B tube bundles in R-114/oil mixtures
[AD-A241936] p 1379 N92-17443
BOLTED JOINTS
Rapid repair of integrally stiffened carbon fibre composite structures by bolted aluminium elements
[MBB-FE202-S-PUB-0453-A] p 1256 N92-17310
BONDING
Method of joining diamond structures
[AD-D015066] p 1269 N92-17397
A method for joining ceramic shapes
[DE92-003815] p 1274 N92-17842
A method and apparatus for indicating disbonds in joint regions
[NASA-CASE-LAR-14626-1] p 1309 N92-17859
BONE DEMINERALIZATION
Techniques for determination of impact forces during walking and running in a zero-G environment
[NASA-TP-3159] p 1328 N92-17022
BOREHOLES
Application of linear inverse theory to borehole gravity data
[DE92-002172] p 1317 N92-17578
BORON
Nitration and nitrocompounds
[AD-A243380] p 1259 N92-17210
BOSONS
The determination of the number of light neutrino species
[ETN-92-90564] p 1360 N92-17519
Late time cosmological phase transitions 1: Particle physics models and cosmic evolution
[NASA-CR-189857] p 1388 N92-17696
BOUNDARIES
Effective viscosity in the simulation of spatially evolving shear flows with monotonic FCT models
[AD-A243709] p 1295 N92-17126
BOUNDARY CONDITIONS
Unsteady laminar flow in a circular tube: A test of the HERCOL (Hermitian collocation) computer code
[PB91-222679] p 1295 N92-17018
BOUNDARY LAYER CONTROL
Frequency stirring: An alternate approach to mechanical mode-stirring for the conduct of electromagnetic susceptibility testing
[AD-A243551] p 1279 N92-17031
BOUNDARY LAYER EQUATIONS
Comparison of two solution methods for the numerical calculation of hypersonic flows
[MBB-FE211-S-PUB-446] p 1224 N92-17311
BOUNDARY LAYER FLOW
Observation and measurements of flow structures in the stagnation region of a wing-body junction
[AD-A243403] p 1223 N92-17117
Results of measured temperature distribution on an adiabatic wing model with radiation thermometer
[NAL-TM-610] p 1225 N92-17755
The effect of isolated roughness elements on transition in attachment-line flows
[AERO-REPT-8905] p 1300 N92-17850
BOUNDARY LAYER SEPARATION
On the origin and control of large coherent structures in turbulent shear flow
[AD-A243727] p 1299 N92-17719
BOUNDARY LAYER TRANSITION
The effect of freestream turbulence on the vortical flow over a delta wing p 1225 N92-17681
Results of measured temperature distribution on an adiabatic wing model with radiation thermometer
[NAL-TM-610] p 1225 N92-17755
Boundary-layer transition and heat transfer on slender delta wings
[AERO-REPT-8904] p 1226 N92-17849
The effect of isolated roughness elements on transition in attachment-line flows
[AERO-REPT-8905] p 1300 N92-17850
Deterministic multi-zone ice accretion modeling p 1227 N92-17987
BOUNDARY LAYERS
On the origin and control of large coherent structures in turbulent shear flow
[AD-A243727] p 1299 N92-17719
Sydney Goldstein FRS Hon FRAeS: An appreciation
[AERO-REPT-8903] p 1391 N92-17928
BOUNDARY VALUE PROBLEMS
Eddy breakdown and structure development
[AD-A241886] p 1295 N92-17039
Spectral error models applied to the geodetic boundary value problem
[ETN-92-90582] p 1312 N92-17436
Damage mechanisms in composites
[AD-A242748] p 1258 N92-17950
BRAGG ANGLE
In situ structural studies of the underpotential deposition of copper onto an iodine covered platinum surface using x ray standing waves
[AD-A243475] p 1263 N92-17328
In situ x ray standing wave study of Cu UPD on an iodine covered platinum surface
[AD-A243474] p 1264 N92-17426
BRAIN
A topographical analysis of the human electroencephalogram for patterns in the development of motion sickness
[AD-A243656] p 1328 N92-17120
Assessment of the behavioral and neurotoxic effects of hexachlorobenzene (HCB) in the developing rat
[AD-A243658] p 1325 N92-17121
BrainMap: A database of functional neuroanatomy derived from human brain images
[AD-A243161] p 1333 N92-17648
The 7th Annual Workshop on Computational Neuroscience
[AD-A243462] p 1335 N92-17656
BRAIN DAMAGE
A computational model of semantic memory impairment: Modality-specificity and emergent category-specificity
[AD-A242377] p 1347 N92-16991
BREATHING APPARATUS
Evaluation of BAUER high pressure breathing air P-2 purification system
[AD-A243535] p 1333 N92-17014
Unmanned evaluation of BAUER high pressure breathing air P-5 purification system
[AD-A243486] p 1334 N92-17331
BRIGHTNESS TEMPERATURE
A variational formalism for the radiative transfer equation and a geostrophic, hydrostatic atmosphere: Prelude to model 3 p 1322 N92-17979
BRITTLE MATERIALS
Effect of coatings and processing on failure mechanisms of polycarbonate material, phase 1
[AD-A243018] p 1256 N92-17053
BRITTLENESS
Effect of coatings and processing on failure mechanisms of polycarbonate material, phase 1
[AD-A243018] p 1256 N92-17053
Mechanical and thermomechanical properties of NC base propellants
[AD-A243045] p 1276 N92-17632
Dynamic fracture characterization of Al2O3 and SiC(w)/Al2O3
[AD-A242187] p 1273 N92-17784
BROADBAND
Adaptive presort processing
[AD-A243286] p 1340 N92-17286
Toward a national semiconductor strategy, volume 1
[PB91-201293] p 1290 N92-17620
New algorithms for broad-band and narrowband source localization and a separable 2-D IIR filter realization
[AD-A243457] p 1291 N92-17654
Management, control and performance of broadband integrated networks
[AD-A242750] p 1381 N92-17952
BROMINATION
Gas transport in polybutadiene treated with aqueous bromine
[AD-A241871] p 1295 N92-17025
BROMINE
Gas transport in polybutadiene treated with aqueous bromine
[AD-A241871] p 1295 N92-17025

Collisional dynamics of the B3Pi(O 1) state of bromine of monofluoride
| AD-A241857 | p 1356 N92-17305
Quenching and rotational energy transfer in molecular bromine: Br2(B)
| AD-A241987 | p 1357 N92-17321
Steady-state production and quenching of Br((2)P1/2)
| AD-A243754 | p 1362 N92-17663

BROMINE COMPOUNDS
Vibrational energy transfer in bromine monofluoride
| AD-A243690 | p 1259 N92-17091

BUBBLES
Mass transfer in gas fluidized beds: Scaling, modeling, and particle size influence
| ETN-92-90581 | p 1298 N92-17522
Heat transfer enhancement due to bubble pumping in FC-72 near the saturation temperature
| AD-A243558 | p 1292 N92-17724

BUCKMINSTERFULLERENE
Stability and structure of C12B24N24: A hybrid analog of buckminsterfullerene
| AD-A242327 | p 1373 N92-17245

BUOYANCY
The wave numbers of supercritical surface tension driven Benard convection
| NASA-CR-189856 | p 1373 N92-17375

BURNING RATE
A theoretical study of the combustion of magnesium/teflon/viton pyrotechnic compositions
| AD-A243244 | p 1275 N92-17058
Optical spectra and kinetics of single impurity molecules in a polymer: Spectral diffusion and persistent spectral hole-burning
| AD-A243749 | p 1271 N92-17659

BURSTS
The complete hard x ray burst spectrometer event list, 1980-1989
| NASA-TM-4332 | p 1389 N92-17048

BUTT JOINTS
The effect of weld metal strength mismatch on the deformation and fracture behavior of steel butt weldments
| AD-A243239 | p 1262 N92-17057

C

C (PROGRAMMING LANGUAGE)
Knowledge, programming, and programming cultures: LISP, C, and Ada
| NASA-CR-184220 | p 1344 N92-17778

C BAND
Terminal Doppler weather radar test bed operation, Orlando: January-June 1990
| AD-A242890 | p 1318 N92-17028

C-130 AIRCRAFT
Testing and evaluation of the Vanner electrical inverters, models 24-1500 and SP 00112
| AD-A241914 | p 1287 N92-17216

C-141 AIRCRAFT
Testing and evaluation of the Vanner electrical inverters, models 24-1500 and SP 00112
| AD-A241914 | p 1287 N92-17216

CABIN ATMOSPHERES
Effectiveness of an onboard water spray system during an oxygen enriched cabin fire
| DOT/FAA/CT-TN91/51 | p 1226 N92-17149

CALCIUM ISOTOPES
The proton spectral function of Ca-40 and Ca-48 studies with (e, e prime p) reaction: An investigation of ground-state correlations
| ETN-92-90566 | p 1358 N92-17433
Chromatographic separation of calcium isotopes
| DE92-004623 | p 1261 N92-17740

CALCIUM OXIDES
Reaction kinetics and transport properties of the CaO-SO2-O2 system in absence of intra-particle diffusion
| DE91-002086 | p 1261 N92-17788

CALCULUS
IMPS: An Interactive Mathematical Proof System
| AD-A243162 | p 1350 N92-17206
Geometrical methods for the analysis of cosmological observations
| ETN-92-90584 | p 1386 N92-17523
A probabilistic derivation of Stirling's formula
| AD-A241899 | p 1354 N92-17548

CALCULUS OF VARIATIONS
Numerical grid generation using a variational method
| MBB-FE211-S-PUB-447 | p 1297 N92-17312
A variational assimilation method for satellite and conventional data: Development of basic model for diagnosis of cyclone systems
| NASA-CR-188236 | p 1321 N92-17975
A variational assimilation method for satellite and conventional data: Model 2 (version 1)
p 1322 N92-17976
On the concept of varying influence radii for a successive corrections objective analysis p 1322 N92-17980

CALENDARS
Calendar of selected aeronautical and space meetings, July 1990 onwards
| AGARD-CAL-90/2 | p 1380 N92-17198
Calendar of selected aeronautical and space meetings, January 1992 and onwards
| AGARD-CAL-92/1 | p 1380 N92-17212

CALIBRATING
Results of the space shuttle vehicle ascent air data system probe calibration test using a 0.07-scale external tank forebody model (68T) in the AEDC 16-foot transonic wind tunnel (IA-310), volume 1
| NASA-CR-167696 | p 1241 N92-17167
Results of the space shuttle vehicle ascent air data system probe calibration test using a 0.07-scale external tank forebody model (68T) in the AEDC 16-foot transonic wind tunnel (IA-310), volume 2
| NASA-CR-167697 | p 1241 N92-17214
The calibration process of digital cameras
| ETN-92-90583 | p 1301 N92-17437
High energy physics program at Texas A and M University
| DE92-004426 | p 1363 N92-17738
Correlator optical wavefront sensor COWS
| DE92-003964 | p 1368 N92-17846
Mean wind speeds over hills and other topography
| ESDU-91043 | p 1321 N92-17853

CALIFORNIA
Source of cold water in Monterey Bay observed by AVHRR satellite imagery
| AD-A242843 | p 1323 N92-17051
Surface observation climatic summaries for Castle AFB, California
| AD-A243677 | p 1318 N92-17074

CALIFORNIUM ISOTOPES
Verification of an effective dose equivalent model for neutrons
| DE92-002738 | p 1358 N92-17453

CALORIMETERS
Heat flux sensor research and development: The cool film calorimeter
| NASA-CR-189789 | p 1301 N92-17006
The ZEUS second level calorimeter trigger: Physics simulation, design and implementation
| ETN-92-90568 | p 1358 N92-17435
Muons in UA1; the 2nd level trigger and dimuon results
| ETN-92-90565 | p 1360 N92-17520
High energy physics program at Texas A and M University
| DE92-004426 | p 1363 N92-17738

CAMERAS
Extracting the shape and roughness of specular lobe objects using four light photometric stereo
| AD-A243522 | p 1365 N92-17146
The calibration process of digital cameras
| ETN-92-90583 | p 1301 N92-17437
Hubble Space Telescope: Wide field and planetary camera instrument handbook. Version 2.1
| NASA-CR-189753 | p 1386 N92-17484
Near real-time stereo vision system
| NASA-CASE-NPO-18593-1-CU | p 1368 N92-17864

CAMS
Analysis of cam roller followers
| ESDU-91026 | p 1307 N92-17852

CANADIAN SPACE PROGRAM
Canadian Space Station program
p 1243 N92-17102

CANTILEVER BEAMS
Experimental investigation of interlaminar fracture toughness of carbon fiber/thermoplastic and carbon fiber/thermosetting composites by DCB specimens
| NAL-TR-1096 | p 1257 N92-17869

CAPACITANCE
Suspended substrate resonator design
| AD-A243250 | p 1290 N92-17573

CAPACITORS
Transformerless DC-DC voltage amplifier with optically isolated switching devices
| NASA-CASE-NPO-17994-1-CU | p 1293 N92-17907

CARBON
Stability and structure of C12B24N24: A hybrid analog of buckminsterfullerene
| AD-A242327 | p 1373 N92-17245
In situ structural studies of the underpotential deposition of copper onto an iodine covered platinum surface using x ray standing waves
| AD-A243475 | p 1263 N92-17328
Method of joining diamond structures
| AD-D015066 | p 1269 N92-17397
Effect of thermal annealing on property changes of neutron-irradiated non-graphitized carbon materials and nuclear graphite
| DE92-704180 | p 1257 N92-17816

CARBON DIOXIDE
EMU evolution p 1246 N92-17354
Changing by degrees: Steps to reduce greenhouse gases
| PB91-205120 | p 1314 N92-17619

CARBON DIOXIDE LASERS
A study of nonlinear reflection and optical switching in indium antimonide
| AD-A242835 | p 1365 N92-17249
Picosecond laser breakdown thresholds in gases
| AD-A242941 | p 1304 N92-17475

CARBON FIBER REINFORCED PLASTICS
Rapid repair of integrally stiffened carbon fibre composite structures by bolted aluminium elements
| MBB-FE202-S-PUB-0453-A | p 1256 N92-17310
Experimental investigation of interlaminar fracture toughness of carbon fiber/thermoplastic and carbon fiber/thermosetting composites by DCB specimens
| NAL-TR-1096 | p 1257 N92-17869

CARBON FIBERS
Polymer infiltration studies
| NASA-CR-189773 | p 1266 N92-17004
Blistering of graphite/polymer composites galvanically coupled with metals in sea water
| AD-A242861 | p 1269 N92-17262
Intercalated hybrid graphite fiber composite
| NASA-CASE-LEW-15241-1 | p 1257 N92-17861
Experimental investigation of interlaminar fracture toughness of carbon fiber/thermoplastic and carbon fiber/thermosetting composites by DCB specimens
| NAL-TR-1096 | p 1257 N92-17869
Energy production using fission fragment rockets
| DE92-002192 | p 1364 N92-17876
Storing fluorine gas in carbon fibers and releasing the same
| NASA-CASE-LEW-15359-1 | p 1261 N92-17902

CARBON MONOXIDE
Catalytic studies on a novel synthesis of methanol
| DE92-002904 | p 1275 N92-17184

CARBON TETRAFLUORIDE
Selective plasma etching
| DE92-004794 | p 1371 N92-17968

CARBONIC ANHYDRASE
Molecular recognition in gels, monolayers, and solids
| AD-A243488 | p 1358 N92-17428

CARCINOGENS
Evaluation of the initiation/promotion potential of CTFE trimer acid
| AD-A243479 | p 1255 N92-17373

CARCINOTRONS
Effects of the high-frequency beam space charge forces on the excitation of electromagnetic waves in relativistic carcinotron
| DE92-610956 | p 1285 N92-17812

CARGO
Trajectory analysis of the G-11 family of clustered parachutes to determine minimum altitude
| AD-A243375 | p 1225 N92-17404

CARIBBEAN SEA
A study on hydrographic conditions and salt budget calculation for the Gulf of Farallones with the data collected in August 1990
| AD-A243406 | p 1324 N92-17119

CARRIER MOBILITY
Method of doping single crystal diamond for electronic devices
| AD-D015069 | p 1374 N92-17610

CASE BONDED PROPELLANTS
Case bond liner systems for solid rocket motors
| AD-A242297 | p 1253 N92-17085

CASSEGRAIN OPTICS
Evaluation of a compact Cassegrain optical system
| AD-A242985 | p 1366 N92-17294

CATALOGS (PUBLICATIONS)
Valuable patents for US businesses: A catalog of DTRC patents available for licensing by the private sector
| AD-A242071 | p 1385 N92-17141

CATALYSIS
Catalytic studies on a novel synthesis of methanol
| DE92-002904 | p 1275 N92-17184
Aryl bis(triflates) in palladium (0) cross-coupling reactions. Synthesis of polyphenyl-alkynyl, alkenyl, and aryl ethers
| AD-A243643 | p 1273 N92-17752
Catalysis looks to the future
| LC-91-66333 | p 1261 N92-17786

CATALYSTS
Safety considerations in testing a fuel-rich aeropropulsion gas generator
| NASA-TM-105258 | p 1235 N92-17061
Catalytic studies on a novel synthesis of methanol
| DE92-002904 | p 1275 N92-17184

Catalysts for ultrahigh current density oxygen cathodes for space fuel cell applications
| NASA-CR-189787 | p 1253 N92-17365
Catalysis looks to the future
| LC-91-66333 | p 1261 N92-17786
Propane aromatization over gallium containing HZSM-5 zeolites
| ETN-92-90897 | p 1262 N92-17925

CATHODE RAY TUBES
Dual color and shape coding in the visual periphery: A study of Joint Tactical Information Distribution System (JTIDS) symbology
| AD-A243253 | p 1333 N92-16982

CATHODES
Lithiated Vanadium Oxide (LVO), gamma-lithium vanadium bronze (Gamma-LIV2O5) and vanadium dioxide (VO2) as thermal battery cathode materials
| AD-A242948 | p 1287 N92-17186
Silver-nickel composite cathodes for alkaline secondary batteries
| AD-D015121 | p 1293 N92-17871

CATHODIC COATINGS
Cathodic protection diagnostic computer program for sacrificial and impressed current systems: Overview and user's manual
| AD-A243663 | p 1338 N92-17122
Lithiated Vanadium Oxide (LVO), gamma-lithium vanadium bronze (Gamma-LIV2O5) and vanadium dioxide (VO2) as thermal battery cathode materials
| AD-A242948 | p 1287 N92-17186

CATHODOLUMINESCENCE
Spatially and spectrally resolved cathodoluminescence measurements of CVD-grown diamond particles and films
| AD-A243220 | p 1271 N92-17615

CATIONS
The EPR of the triplet state of aryl cations in crystals of diazonium salts p 1375 N92-17701
Growth rate of dislocation loop in Fe-Ni-Cr alloy under Kr(+) ion and electron irradiation
| DE92-001908 | p 1265 N92-17703

CAUCHY PROBLEM
Tests of fit for the Cauchy distribution based on the empirical distribution function
| AD-A243201 | p 1352 N92-17173

CAVITATION FLOW
The influence of cavitation in the breakup of liquid free jets
| MPIS-1/1991 | p 1297 N92-17343

CAVITIES
Superdirective properties of closed loops of parallel coplanar dipoles
| AD-A243009 | p 1288 N92-17268
The shapes and cavities of four cholic acid host systems
| AD-A243483 | p 1255 N92-17329
Engineering model of unsteady flow in a cavity
| AD-A243636 | p 1299 N92-17747

CAVITY RESONATORS
A study of nonlinear reflection and optical switching in indium antimonide
| AD-A242835 | p 1365 N92-17249
Three point lead screw positioning apparatus
| NASA-CASE-LEW-15216-1 | p 1307 N92-17678
Performance of hole coupling resonator in the presence of asymmetric modes and FEL gain
| DE92-003907 | p 1305 N92-17936

CEILINGS (METEOROLOGY)
Surface observation climatic summaries for Fairbanks IAP, Alaska
| AD-A243309 | p 1320 N92-17400

CELL ANODES
Dielectric properties of aligned conducting polymers
| AD-A243389 | p 1268 N92-17191

CELL CATHODES
Catalysts for ultrahigh current density oxygen cathodes for space fuel cell applications
| NASA-CR-189787 | p 1253 N92-17365

CELLS (BIOLOGY)
Biophysical techniques for examining metabolic, proliferative, and genetic effects of microwave radiation
| AD-A241903 | p 1326 N92-17288

CEMENTATION
Codeposition of elements in diffusion coatings by the halide-activated pack cementation method
| AD-A242860 | p 1267 N92-17042

CENTRIFUGAL CASTING
Microstructurally toughened articles and casting thereof
| AD-D015065 | p 1265 N92-17452

CENTRIFUGES
Large centrifuge: A critical Army capability for the future
| AD-A243287 | p 1238 N92-17287

CERAMIC FIBERS
Dynamic fracture characterization of Al2O3 and SiC(w)/Al2O3
| AD-A242187 | p 1273 N92-17784
A method for joining ceramic shapes
| DE92-003815 | p 1274 N92-17842

CERAMIC MATRIX COMPOSITES
High-temperature durability considerations for HSCT combustor
| NASA-TP-3162 | p 1267 N92-17070
Novel ceramic matrix composites for deep submergence pressure vessel applications
| AD-A242740 | p 1274 N92-17947
Damage mechanisms in composites
| AD-A242748 | p 1258 N92-17950

CERAMICS
Ceramics with superelectrical and supermechanical properties
| AD-A243062 | p 1267 N92-17029
Processing of ceramics of biopolymers. Ultrastructure-property relationships in biocrystals
| AD-A243061 | p 1267 N92-17054
Reliability analysis of structural ceramic components using a three-parameter Weibull distribution
| NASA-TM-105370 | p 1267 N92-17060
Strength and microstructure of ceramics
| AD-A243049 | p 1269 N92-17282
New optical materials for the long-wave (8-12 microns) region: Design criteria for the solid-state chemist
| AD-A243280 | p 1365 N92-17284
The synergistic effects of solid and liquid lubrication on the tribological behavior of transformation-toughened ZrO2 ceramics
| DE91-018617 | p 1306 N92-17575
DOE Task Force Meeting on Electrical Breakdown of Insulating Ceramics in a High Radiation Field
| DE92-000459 | p 1270 N92-17576
Determination of the tribological fundamentals of solid lubricated ceramics. Volume 3: Appendices P through 2
| AD-A242872 | p 1270 N92-17597
Determination of the tribological fundamentals of solid lubricated ceramics. Volume 2: Appendices A through O
| AD-A242871 | p 1270 N92-17614
Determination of the tribological fundamentals of solid lubricated ceramics. Volume 1: Summary
| AD-A243219 | p 1272 N92-17683
Dynamic fracture characterization of Al2O3 and SiC(w)/Al2O3
| AD-A242187 | p 1273 N92-17784
Making of functionally gradient materials data base
| NAL-TM-621 | p 1385 N92-17787
High contact blind hole thermocouple plug
| AD-D015105 | p 1302 N92-17835
A method for joining ceramic shapes
| DE92-003815 | p 1274 N92-17842
Comparative study of irreversibility effects in Nb foil and high temperature superconducting ceramics by muon spin rotation
| DE92-600475 | p 1294 N92-17953

CESIUM IONS
Comparison of alkali ion emitters
| AD-A243105 | p 1290 N92-17570

CHAINS
Comparisons of self-assembled monolayers on silver and gold: Mixed monolayers derived from HS(CH2)21X and HS(CH2)10(sup Y) (X,Y-CH3, CH2OH) have similar properties
| AD-A243487 | p 1264 N92-17427

CHANNEL FLOW
Study of transition phenomena in a straight channel with 40 to 1 aspect ratio with and without imposed pulsations. Part two: Reynolds number surveys
| AD-A241894 | p 1296 N92-17307
Studies of baroclinic flow
| AD-A243050 | p 1296 N92-17309
Transition phenomena in a straight channel with a 40 to 1 aspect ratio with and without imposed pulsations. Part 1: Near-wall and central region profiles
| AD-A243251 | p 1297 N92-17337
Downflow heat transfer in a heated ribbed vertical annulus with a cosine power profile (results from test series ECS-2c)
| DE92-003259 | p 1298 N92-17626

CHANNELS (DATA TRANSMISSION)
Evaporation duct communication: Test plan, part 2
| AD-A243505 | p 1282 N92-17383
A study of channel-access schemes for integrated voice/data radio networks
| AD-A243584 | p 1286 N92-17931

CHAOS
Summary of the 1991 ACP Workshop on Coherence and Chaos in Complex Dynamical Systems
| AD-A243226 | p 1378 N92-17324
Chaos caused by a topologically mixing map
| DE91-641486 | p 1354 N92-17823

CHARACTERIZATION
Groundscreen characterization
| AD-A243164 | p 1311 N92-17208

CHARGE CARRIERS
Research and development on advanced silicon carbide thin film growth techniques and fabrication of high power and microwave frequency silicon carbide-based device structures
| AD-A243531 | p 1373 N92-17390
Separation of neutral-to-polaron and polaron-to-bipolaron redox events in alkoxy substituted di-2-thienylphenylene polymers
| AD-A242423 | p 1271 N92-17679

CHARGE COUPLED DEVICES
Improved 320x244-element PtSi Schottky-barrier IR-CCD image sensor
| AD-A242026 | p 1301 N92-17140
Development of an electronic high speed camera system for the quantitative analysis of unsteady flows
| MPIS-100/1991 | p 1301 N92-17344
The calibration process of digital cameras
| ETN-92-90583 | p 1301 N92-17437

CHARGE DISTRIBUTION
Calculations of electron and photon transport between 1 MeV and 1 eV
| AD-A243725 | p 1359 N92-17514
Nonlinear spectroscopic studies of interfacial molecular ordering
| DE92-000864 | p 1360 N92-17530
An algorithm for calculating the electronic spectrum and function of the charge density distributions of crystals p 1375 N92-17698

CHARGE EXCHANGE
The charge exchange recombination diagnostic system on the D3-D tokamak
| DE92-003805 | p 1369 N92-17456

CHARTS
The National Hurricane Center Risk Analysis Program (HURISK)
| PB91-236463 | p 1321 N92-17705

CHECKOUT
Computer system evolution requirements for autonomous checkout of exploration vehicles p 1250 N92-17422

CHELATES
Production of mullite fibers
| NASA-CASE-MFS-28431-1 | p 1257 N92-17870

CHEMICAL BONDS
The shapes and cavities of four cholic acid host systems
| AD-A243483 | p 1255 N92-17329
Omega-terminated alkanethiolate monolayers on surfaces of copper, silver and gold have similar wettabilities
| AD-A243529 | p 1260 N92-17389
Electronic and ionic transport in processable conducting polymers
| AD-A242258 | p 1269 N92-17460
Electrochemically initiated chain polymerization of pyrrole in aqueous media
| AD-A242259 | p 1269 N92-17461
Polyimides containing amide and perfluoroisopropyl connecting groups
| NASA-CASE-LAR-14608-1 | p 1271 N92-17676
Liquid-solid transition in the bond particle model for elemental semiconductors
| DE92-610441 | p 1378 N92-17972

CHEMICAL COMPOSITION
Evaluation of liposome-encapsulated Hemoglobin/LR16 formulations as a potential blood substitute
| AD-A243075 | p 1329 N92-17557
Concentration of isotopic hydrogen by temperature gradient effect in soluble metal
| AD-D015062 | p 1260 N92-17628
The influence of temperature and composition on the activation energy for creep in binary aluminum lithium alloys
| AD-A242299 | p 1265 N92-17759
Microstructure and composition of electromagnetically-characterized YBa2Cu3O(7-delta) grain boundaries
| DE92-003520 | p 1376 N92-17782
Thermal insulation chemical composition and method of manufacture
| AD-D015106 | p 1257 N92-17836

CHEMICAL DEFENSE
Effects of the chemical defense antidote atropine sulfate on helicopter pilot performance: An in-flight study
| AD-A241966 | p 1328 N92-17084

CHEMICAL ENERGY
Application of the mean spherical approximation to describe the Gibbs solvation energies of monovalent monoatomic ions in non-aqueous solvents
| AD-A243200 | p 1259 N92-17371

Explosive magnetic field compression generator transformer power supply for high resistive loads
[AD-D015123] p 1293 N92-17831

CHEMICAL EXPLOSIONS
Studies of high-frequency seismic wave propagation
[AD-A241938] p 1316 N92-17202
The effect of detonation curvature on cylindrical wall motion
[DE92-003110] p 1298 N92-17625

CHEMICAL LASERS
Vibrational energy transfer in bromine monofluoride
[AD-A243690] p 1259 N92-17091

CHEMICAL PROPERTIES
Environmental containment property estimation using QSARs in an expert system
[AD-A243728] p 1336 N92-17720
Propane aromatization over gallium containing HZSM-5 zeolites
[ETN-92-90897] p 1262 N92-17925

CHEMICAL REACTIONS
Chemical reactions in turbulent mixing flows
[AD-A243035] p 1294 N92-16979
Examining Si3N4 base materials with various rare earth additions
[AD-A243668] p 1372 N92-17082
Ligand redistribution reactions of Me2Ga(C5H5) and MeGa(C5H5)2
[AD-A243264] p 1254 N92-17270
An experimental investigation of chemically-reacting, gas-phase turbulent jets
[AD-A243C36] p 1296 N92-17276
Substituted 1,1,1-triaryl-2,2,2-trifluoroethanes and processes for their synthesis
[NASA-CASE-LEW-14345-6] p 1255 N92-17882
Propane aromatization over gallium containing HZSM-5 zeolites
[ETN-92-90897] p 1262 N92-17925

CHEMICAL REACTORS
Catalytic studies on a novel synthesis of methanol
[DE92-002904] p 1275 N92-17184

CHEMICAL WARFARE
Alleviation of thermal strain in engineering space personnel aboard CF ships with the exotemp personal cooling system
[AD-A242889] p 1330 N92-17599

CHESAPEAKE BAY (US)
User's guide for a three-dimensional numerical hydrodynamic, salinity, and temperature model of Chesapeake Bay
[AD-A242993] p 1324 N92-17298
A user's manual for the Princeton Numerical Ocean Model
[AD-A243773] p 1324 N92-17539

CHIPS (ELECTRONICS)
Integration of an anti-parallel pair of planar Schottky barrier diodes for millimeter and submillimeter wavelengths
[AD-A243371] p 1287 N92-17189

CHIPS (MEMORY DEVICES)
A cache design to exploit structural locality
[AD-A243633] p 1336 N92-17744

CHLOROBENZENES
Assessment of the behavioral and neurotoxic effects of hexachlorobenzene (HCB) in the developing rat
[AD-A243658] p 1325 N92-17121
Nitration and nitrocompounds
[AD-A243380] p 1259 N92-17210

CHLOROCARBONS
Scale-up of recovery process for waste solvents
[KCP-613-4479] p 1277 N92-17535

CHLOROFLUOROCARBONS
Scale-up of recovery process for waste solvents
[KCP-613-4479] p 1277 N92-17535

CHLOROPRENE RESINS
Thermal insulation chemical composition and method of manufacture
[AD-D015106] p 1257 N92-17836

CHROMATOGRAPHY
Chromatographic separation of calcium isotopes
[DE92-004623] p 1261 N92-17740

CHROMIUM ALLOYS
Growth rate of dislocation loop in Fe-Ni-Cr alloy under Kr(+) ion and electron irradiation
[DE92-001908] p 1265 N92-17703

CHROMOSOMES
Biophysical techniques for examining metabolic, proliferative, and genetic effects of microwave radiation
[AD-A241903] p 1326 N92-17288

CIRCADIAN RHYTHMS
Melatonin action on the circadian pacemaker in Siberian hamsters
[AD-A243057] p 1325 N92-17142

CIRCUITS
The analysis of a stabilized 1.5 Mach-Zehnder interferometric sensor with enhanced sensitivity and common-mode compensation
[AD-A243384] p 1286 N92-17116
High-speed beam switching processor
[AD-D015108] p 1285 N92-17829

CIRCULAR CYLINDERS
A short or a long cylinder: What difference does it make to the Karman vortex street?
[MPIS-98/1990] p 1224 N92-17314
Investigation on the control of a Karman vortex street
[MPIS-99/1990] p 1224 N92-17315

CIRCULAR TUBES
Unsteady laminar flow in a circular tube: A test of the HERCOL (Hermitian collocation) computer code
[PB91-222679] p 1295 N92-17018
Substantially oxygen-free contact tube
[NASA-CASE-LAR-14169-1] p 1307 N92-17677

CIRRUS CLOUDS
Numerical studies of processes in stratiform cirrus
[MITT-78] p 1321 N92-17543
Numerical simulation of cirrus clouds: Fire case study and sensitivity analysis
[AD-A242902] p 1321 N92-17631

CIVIL AVIATION
Aircraft accident report: Northwest Airlines, Inc., Flights 1482 and 299. Runway incursion and collision, Detroit Metropolitan/Wayne County Airport, Romulus, Michigan, December 3, 1990
[PB91-910405] p 1226 N92-17213
Variability of standard aircraft performance parameters
[ESDU-91020] p 1233 N92-17847

CLASSIFICATIONS
Neural network classification of mental workload conditions by analysis of spontaneous electroencephalograms
[AD-A243369] p 1331 N92-17115
Modelling aspects and robustness issues in rotorcraft system identification p 1231 N92-17159

CLEAN ROOMS
Clean room wiping liquids
[DE92-004793] p 1238 N92-17967

CLEANERS
Evaluation of environmentally safe cleaning agents for diamond turned optics
[DE92-002524] p 1278 N92-17780

CLEANING
Evaluation of environmentally safe cleaning agents for diamond turned optics
[DE92-002524] p 1278 N92-17780
Clean room wiping liquids
[DE92-004793] p 1238 N92-17967

CLEAR AIR TURBULENCE
High-frequency meteorological phenomena observed with the Naval Postgraduate School's UHF Doppler wind profiler
[AD-A243762] p 1320 N92-17515

CLIMATE
Surface observation climatic summaries for Castle AFB, California
[AD-A243677] p 1318 N92-17074
Surface observation climatic summaries for Fairbanks IAP, Alaska
[AD-A243309] p 1320 N92-17400
Surface observations climatic summaries for Camp Humphreys, Korea
[AD-A241937] p 1320 N92-17444

CLIMATE CHANGE
Policy implications of greenhouse warming: Report of the adaptation panel p 1314 N92-17982

CLIMATOLOGY
Surface observation climatic summaries for Duke Field/Eglin aux no. 3, Florida
[AD-A243310] p 1318 N92-17073
Surface observation climatic summaries for Castle AFB, California
[AD-A243677] p 1318 N92-17074
Surface meteorological and near surface oceanographic atlas of the tropical Indian Ocean
[PB91-234286] p 1319 N92-17138
Surface observation climatic summaries for Hondo Municipal Airport, Texas
[AD-A243311] p 1319 N92-17144
Surface observation climatic summaries for Boise Air Terminal, ID
[AD-A243012] p 1319 N92-17257
Meeting Review: Airborne Aerosol Inlet Workshop
[NASA-CR-189814] p 1313 N92-17393
Surface observation climatic summaries for Fairbanks IAP, Alaska
[AD-A243309] p 1320 N92-17400
Surface observations climatic summaries for Camp Humphreys, Korea
[AD-A241937] p 1320 N92-17444

CLIMBING FLIGHT
Variability of standard aircraft performance parameters
[ESDU-91020] p 1233 N92-17847

CLINICAL MEDICINE
Evaluation of scalar value estimation techniques for 3D medical imaging
[AD-A243687] p 1328 N92-17089
Proceedings of the Conference on Health Physics
[DE92-704335] p 1331 N92-17802

CLOTHING
Heat stress caused by wearing different types of CW protective garment
[AD-A243043] p 1334 N92-17278

CLOUD COVER
Surface observation climatic summaries for Fairbanks IAP, Alaska
[AD-A243309] p 1320 N92-17400
Numerical simulation of cirrus clouds: Fire case study and sensitivity analysis
[AD-A242902] p 1321 N92-17631

CLOUD PHYSICS
IRAS and the Boston University Arecibo Galactic H I Survey: A catalog of cloud properties
[NASA-CR-189806] p 1387 N92-17695

CLUTTER
Determination of bistatic radar clutter power from topographic data
[AD-A243697] p 1280 N92-17095
Auroral-clutter predictions for Fylingdales, England
[AD-A242957] p 1283 N92-17600

COASTS
A user's manual for the Princeton Numerical Ocean Model
[AD-A243773] p 1324 N92-17539
The National Hurricane Center Risk Analysis Program (HURISK)
[PB91-236463] p 1321 N92-17705

COATING
Silver-nickel composite cathodes for alkaline secondary batteries
[AD-D015121] p 1293 N92-17871

COATINGS
Acoustic impedance of materials from reverberation time
[AD-A243184] p 1354 N92-16999
Codeposition of elements in diffusion coatings by the halide-activated pack cementation method
[AD-A242860] p 1267 N92-17042
Effect of coatings and processing on failure mechanisms of polycarbonate material, phase 1
[AD-A243018] p 1256 N92-17053
Au and Al Schottky barrier formation on GaAs (100) surfaces prepared by thermal desorption of a protective arsenic coating
[DE92-002456] p 1376 N92-17781
Phosphazene polymer containing composites and method for making phosphazene polymer containing composites
[DE92-003826] p 1274 N92-17935

COAXIAL CABLES
Test method for the evaluation of the water treeing behavior of cross-linked polyethylene medium voltage cables
[ETN-92-90588] p 1270 N92-17541
A study of electric transmission lines for use on the lunar surface p 1292 N92-17742

COBALT
Studies of the adsorption of tetrasulfonated phthalocyanines on graphite substrate
[AD-A243443] p 1260 N92-17489

COCKPITS
AGSSS: The Airborne Graphics Software Support System; an Ada/PHIGS-based display editor for the rapid development of cockpit display software systems
[AD-A243224] p 1234 N92-17221
Assessment of cockpit interface concepts for data link retrofit
[NASA-CR-187615] p 1228 N92-17512
Alert generation and cockpit presentation for an integrated microburst alerting system p 1220 N92-17988

CODERS
Sub-band/transform compression of video sequences
[NASA-CR-189786] p 1280 N92-17139
Fiber optic angular orientation sensor digital serial encoding
[AD-D015102] p 1302 N92-17826

CODING
Comparative analysis of gray scale coding techniques for group 4 facsimile
[AD-A243175] p 1278 N92-16996
Sub-band/transform compression of video sequences
[NASA-CR-189786] p 1280 N92-17139
Investigation of coding techniques for memory and delay efficient interleaving in slow Rayleigh fading
[AD-A243154] p 1280 N92-17187

FY92 mathematical research project proposal briefing
[AD-A243163] p 1350 N92-17207
New algorithms for broad-band and narrowband source localization and a separable 2-D IIR filter realization
[AD-A243457] p 1291 N92-17654
Parallelizing serial code for a distributed processing environment with an application to high frequency electromagnetic scattering
[AD-A243755] p 1284 N92-17721
The dynamics of visual representation, attention, encoding, and retrieval processes
[AD-A243031] p 1384 N92-17785
Use of the algebraic coding theory in nuclear electronics
[DE92-611125] p 1351 N92-17813
Fiber optic angular orientation sensor digital serial encoding
[AD-D015102] p 1302 N92-17826
Fractal image encoding
[AD-A243620] p 1344 N92-17921

COEFFICIENTS
Quenching and rotational energy transfer in molecular bromine: Br2(B)
[AD-A241987] p 1357 N92-17321

COGNITION
Feedback in dynamic decision making: An experiment in software project management
[AD-A242361] p 1380 N92-17451
Attention, automaticity and priority learning
[AD-A242226] p 1332 N92-17458
Signal- and listener-based factors in complex auditory pattern perception
[AD-A243716] p 1332 N92-17503
The cognitive, perceptual, and neural bases of skilled performance
[AD-A243052] p 1332 N92-17554

COHERENT RADIATION
Development of an XUV-IR free-electron laser user facility for scientific research and industrial applications
[DE92-003862] p 1304 N92-17726

COHESION
Determination of cohesive and normal stresses and simulation of fluidization using kinetic theory
[DE92-002905] p 1299 N92-17709

COLD NEUTRONS
Investigation of heated ultracold neutrons on copper surface
[DE92-600625] p 1383 N92-17955

COLD PLASMAS
Exploring plasma sheath solutions for planar and cylindrical anodes
[AD-A243237] p 1369 N92-17030
Materials processing of diamond: Etching, doping by ion implantation and contact formation
[AD-A243060] p 1267 N92-17065
Some aspects of nonneutral plasma physics
[AD-A243711] p 1369 N92-17499

COLD STRENGTH
Microstructure and mechanical properties of HSLA-100 steel
[AD-A242937] p 1265 N92-17467

COLD WATER
Source of cold water in Monterey Bay observed by AVHRR satellite imagery
[AD-A242843] p 1323 N92-17051

COLLAPSE
Characterization of the thermalness of a fissile system with a 2-group diffusion theory parameter
[AD-A243065] p 1360 N92-17555

COLLIMATION
A covariance modeling approach to adaptive beamforming and detection
[AD-A241887] p 1279 N92-17040
Multiple-access phased array antenna simulator for a digital beam forming system investigation
[NASA-TM-105422] p 1279 N92-17062
Self-collimated unstable resonator semiconductor laser
[NASA-CASE-NPO-18386-1-CU] p 1305 N92-17899

COLLISION AVOIDANCE
Collision avoidance sensor skin p 1247 N92-17361

COLLISIONAL PLASMAS
Plasma processing of materials: Scientific opportunities and technological challenges
[LC-91-66812] p 1370 N92-17556

COLLISIONS
Aircraft accident report: Northwest Airlines, Inc., Flights 1482 and 299. Runway incursion and collision, Detroit Metropolitan/Wayne County Airport, Romulus, Michigan, December 3, 1990
[PB91-910405] p 1226 N92-17213
Collisional dynamics of the B3Pi(O+) state of bromine of monofluoride
[AD-A241857] p 1356 N92-17305

COLLOCATION
Unsteady laminar flow in a circular tube: A test of the HERCOL (Hermitian collocation) computer code
[PB91-222679] p 1295 N92-17018

COLLOIDS
Structure and topology of silica aerogels
[DE92-004728] p 1274 N92-17938

COLOR
Visual determination of industrial color-difference tolerances using probit analysis
[AD-A243545] p 1334 N92-17617

COLOR CENTERS
Visual determination of industrial color-difference tolerances using probit analysis
[AD-A243545] p 1334 N92-17617

COLOR CODING
Dual color and shape coding in the visual periphery: A study of Joint Tactical Information Distribution System (JTIDS) symbology
[AD-A243253] p 1333 N92-16982

COLOR VISION
Dual color and shape coding in the visual periphery: A study of Joint Tactical Information Distribution System (JTIDS) symbology
[AD-A243253] p 1333 N92-16982
User evaluation of laser ballistic sun, wind and dust goggle lenses (dye technology)
[AD-A243245] p 1334 N92-17143

COLUMBUS SPACE STATION
Columbus Programme (current status)
p 1243 N92-17100

COMBAT
Causal schema decision-aiding system
[AD-A242931] p 1347 N92-17203
Fatigue effects on human performance in combat: A literature review, volume 1
[AD-A242887] p 1330 N92-17567
Using the Global Positioning System (GPS) to fulfill the position/location requirements of the National Training Center (NTC) and other US Army instrumented testing and training ranges
[AD-A242064] p 1229 N92-17639
The development of military night aviation to 1919
[AD-A243350] p 1219 N92-17731

COMBINATORIAL ANALYSIS
A stochastic approach to the weighted-region problem: 1. The design of the path annealing algorithm
[AD-A243324] p 1340 N92-17403
A probabilistic derivation of Stirling's formula
[AD-A241899] p 1354 N92-17548

COMBUSTIBLE FLOW
Chemical reactions in turbulent mixing flows
[AD-A243035] p 1294 N92-16979
Laser based, non-intrusive measurement system for analysis of jet engine flows
[AD-A242398] p 1234 N92-17011
Local extinction mechanisms in non-premixed turbulent combustion
[AD-A242027] p 1260 N92-17682

COMBUSTION
Extravehicular mobility unit subcritical liquid oxygen storage and supply system
[NASA-CR-189831] p 1276 N92-16989
Advanced nozzle and engine components test facility
[NASA-TM-103684] p 1237 N92-17059

COMBUSTION CHAMBERS
Safety considerations in testing a fuel-rich aeropropulsion gas generator
[NASA-TM-105258] p 1235 N92-17061
High-temperature durability considerations for HSCT combustor
[NASA-TP-3162] p 1267 N92-17070
Magnetohydrodynamic projects at the CDIF
[DE92-002636] p 1370 N92-17664
Local extinction mechanisms in non-premixed turbulent combustion
[AD-A242027] p 1260 N92-17682
Hydrogen fueled subsonic-ram-combustor model tests for an air-turbo-ram engine
[NAL-TR-1064T] p 1236 N92-17855

COMBUSTION CHEMISTRY
Two-dimensional stability of laminar flames
[NASA-TP-3131] p 1223 N92-17131

COMBUSTION EFFICIENCY
Hydrogen fueled subsonic-ram-combustor model tests for an air-turbo-ram engine
[NAL-TR-1064T] p 1236 N92-17855

COMBUSTION PHYSICS
Local extinction mechanisms in non-premixed turbulent combustion
[AD-A242027] p 1260 N92-17682

COMBUSTION PRODUCTS
A theoretical study of the combustion of magnesium/teflon/viton pyrotechnic compositions
[AD-A243244] p 1275 N92-17058

COMBUSTION TEMPERATURE
Hydrogen fueled subsonic-ram-combustor model tests for an air-turbo-ram engine
[NAL-TR-1064T] p 1236 N92-17855

COMMAND AND CONTROL
Causal schema decision-aiding system
[AD-A242931] p 1347 N92-17203
Information Management Engineering (IME) laboratory: A database development facility
[AD-A243191] p 1383 N92-17369
Summary of professional activities, center for Air Force C3 systems
[AD-A243509] p 1348 N92-17386
C3 Systems Technology Symposium on Advance Planning Briefings for Industry
[AD-A243466] p 1391 N92-17657
USI rapid prototyping tool evaluations survey
[AD-A243168] p 1335 N92-17673

COMMAND LANGUAGES
The computational structural mechanics testbed procedures manual
[NASA-TM-100646] p 1310 N92-17333

COMMERCIAL AIRCRAFT
Aircraft accident report: Northwest Airlines, Inc., Flights 1482 and 299. Runway incursion and collision, Detroit Metropolitan/Wayne County Airport, Romulus, Michigan, December 3, 1990
[PB91-910405] p 1226 N92-17213
Discussion for possibility of some aerodynamic ground effect craft
[NAL-TM-619] p 1278 N92-17757

COMMUNICATION
Evaporation duct communication: Test plan, part 2
[AD-A243505] p 1282 N92-17383

COMMUNICATION NETWORKS
Investigation of coding techniques for memory and delay efficient interleaving in slow Rayleigh fading
[AD-A243154] p 1280 N92-17187
Communication network survivability
[AD-A242969] p 1281 N92-17252
Optimal configuration of digital communication network
[AD-A243041] p 1282 N92-17277
Optical protocols for advanced spacecraft networks
p 1249 N92-17418
A computer solution for multiple satellite-satellite and satellite-ground station visibility determination
[AD-A243490] p 1250 N92-17430
Comparison of AFITPAC versus NOS and a packet radio network design
[AD-A243766] p 1283 N92-17516
Interim Service ISDN Satellite (ISIS) hardware experiment design for advanced ISDN satellite design and experiments
[NASA-CR-186943] p 1250 N92-17585
The StarLite Project prototyping real-time software
[AD-A242032] p 1342 N92-17636
Improving stochastic communication network performance: Reliability vs throughput
[AD-A243655] p 1285 N92-17763
A study of channel-access schemes for integrated voice/data radio networks
[AD-A243584] p 1286 N92-17931
QTCM software documentation. Volume 2: User's manual
[AD-A242744] p 1344 N92-17948
Management, control and performance of broadband integrated networks
[AD-A242750] p 1381 N92-17952

COMMUNICATION SATELLITES
A computer solution for multiple satellite-satellite and satellite-ground station visibility determination
[AD-A243490] p 1250 N92-17430

COMMUNICATION THEORY
The effects of speech intelligibility level on concurrent visual task performance
[AD-A243015] p 1331 N92-17052
FY92 mathematical research project proposal briefing
[AD-A243163] p 1350 N92-17207

COMPATIBILITY
Flight test data quality evaluation
p 1230 N92-17156

COMPILERS
Decompiling with definite clause grammars
[AD-A242987] p 1340 N92-17296

COMPLETENESS
A proof theory for a sequential version of POOL
[CWI-CS-R9118] p 1346 N92-17833

COMPLEX SYSTEMS
Summary of the 1991 ACP Workshop on Coherence and Chaos in Complex Dynamical Systems
[AD-A243226] p 1378 N92-17324
Failure Environment Analysis Tool (FEAT)
p 1245 N92-17349

COMPOSITE MATERIALS
Blistering of graphite/polymer composites galvanically coupled with metals in sea water
|AD-A242861| p 1269 N92-17262
Workshop for Finite Element Methods for Composites
|AD-A243534| p 1256 N92-17392
Molecular composites from high temperature polyquinolines
|AD-A243634| p 1272 N92-17745
A method for joining ceramic shapes
|DE92-003815| p 1274 N92-17842
Residual stresses in a prestressed steel pressure vessel wrapped with multilayered composites
|AD-A243429| p 1311 N92-17930
The effect of physical aging on the creep response of a thermoplastic composite
|AD-A243600| p 1258 N92-17932
Phosphazene polymer containing composites and method for making phosphazene polymer containing composites
|DE92-003826| p 1274 N92-17935

COMPOSITE PROPELLANTS
Energetic composites of cyclodextrin nitrate esters and nitrate ester plasticizers
|AD-D015068| p 1275 N92-17399

COMPOSITE STRUCTURES
The use of impact force as a scale parameter for the impact response of composite laminates
|NASA-TM-104189| p 1256 N92-17007
Higher-order thickness expansions for cylindrical shells
|AD-A242017| p 1310 N92-17230
Rapid repair of integrally stiffened carbon fibre composite structures by bolted aluminium elements
|MBB-FE202-S-PUB-0453-A| p 1256 N92-17310
Static analysis of thick composite plates using higher order three dimensional finite elements
|AD-A243188| p 1256 N92-17367
Microstructurally toughened articles and casting thereof
|AD-D015065| p 1265 N92-17452
Novel ceramic matrix composites for deep submergence pressure vessel applications
|AD-A242740| p 1274 N92-17947

COMPRESSIBILITY
In situ surface x ray crystallography of electrochemically deposited Bi on Ag(111): Structure, compressibility, and anisotropy
|AD-A243218| p 1372 N92-17181
The effect of monomer structures and compressibility on the properties of multicomponent polymer blends and solutions
|AD-A242863| p 1273 N92-17777

COMPRESSION LOADS
Solder extrusion pressure bonding process and bonded products produced thereby
|DE92-004603| p 1363 N92-17739

COMPRESSIVE STRENGTH
Mechanical and thermomechanical properties of NC base propellants
|AD-A243045| p 1276 N92-17632
Novel ceramic matrix composites for deep submergence pressure vessel applications
|AD-A242740| p 1274 N92-17947

COMPUTATION
A topological model for parallel algorithm design
|AD-A241858| p 1337 N92-17023
Computational studies of energetic nitramines
|AD-A241870| p 1356 N92-17038
Method of Kalman filtering for estimating the position and velocity of a tracked object
|AD-D015057| p 1287 N92-17129
One-loop calculations with massive particles
|ETN-92-90563| p 1359 N92-17518
Parallel block methods for sparse symmetric linear systems of equations
|AD-A242315| p 1351 N92-17560

COMPUTATIONAL FLUID DYNAMICS
Numerical grid generation using a variational method
|MBB-FE211-S-PUB-447| p 1297 N92-17312
Program plans: Aviation safety research
|NIAR-91-30| p 1227 N92-17587
Physical and computational modelling of stratified shear flows
|AERO-REPT-8909| p 1300 N92-17974

COMPUTATIONAL GRIDS
A numerical code for a three-dimensional magnetospheric MHD equilibrium model
|NASA-CR-189852| p 1316 N92-17227
Numerical grid generation using a variational method
|MBB-FE211-S-PUB-447| p 1297 N92-17312
Scan directed load balancing for highly-parallel mesh-connected computers
|AD-A242045| p 1346 N92-17670

COMPUTER AIDED DESIGN
A CAD model for the axial inductive strip with finite thickness centered in homogeneous finline with w/b = 1
|AD-A243553| p 1278 N92-17016
Microstrip discontinuity models to 60 GHz
|AD-A242038| p 1339 N92-17185
Computer aided thermal analysis of a microcircuit structure
|AD-A243160| p 1287 N92-17205
Parallel processing applied to computational electromagnetics
|AD-A242372| p 1345 N92-17395
FEM-X user's guide
|AD-A242374| p 1383 N92-17396
A knowledge-based approach for configuring computer aided measuring systems
|ETN-92-90585| p 1341 N92-17524
Adaptive on-line help for embedded instructional systems
|AD-A243675| p 1343 N92-17716
Investigation of air transportation technology at Princeton University, 1990-1991 p 1221 N92-17995

COMPUTER ASSISTED INSTRUCTION
Adaptive on-line help for embedded instructional systems
|AD-A243675| p 1343 N92-17716

COMPUTER GRAPHICS
Evaluation of scalar value estimation techniques for 3D medical imaging
|AD-A243687| p 1328 N92-17089
The multi-attribute task battery for human operator workload and strategic behavior research
|NASA-TM-104174| p 1338 N92-17130
The conversion of a FORTRAN data plotting program using DI-3000 graphics to operation on a Macintosh Personal Computer
|AD-A243046| p 1339 N92-17280
A graphical database interface for a multimedia DBMS
|AD-A243283| p 1339 N92-17285
Map maker
|AD-A242980| p 1312 N92-17292
Telerobotic ground-remote operations p 1247 N92-17360
The development of user interface tools for the computer aided prototyping system
|AD-A243189| p 1340 N92-17368
ISE advanced technology p 1249 N92-17420
Causal models in the acquisition and instruction of programming skills
|AD-A242899| p 1340 N92-17463
Programming mechanical simulations
|AD-A243767| p 1341 N92-17538
Forth Graphics Toolbox (A user's guide for use with RFF FORTH)
|AD-A242916| p 1342 N92-17581
BrainMap: A database of functional neuroanatomy derived from human brain images
|AD-A243161| p 1333 N92-17648
Developing a broader basis for scientific data analysis interfaces
|DE92-003963| p 1385 N92-17845

COMPUTER INFORMATION SECURITY
CALS database usage and analysis tool study
|AD-A243205| p 1382 N92-17174
FY92 mathematical research project proposal briefing
|AD-A243163| p 1350 N92-17207
Decompiling with definite clause grammars
|AD-A242987| p 1340 N92-17296
Summary of professional activities, center for intelligence and special programs, 1990
|AD-A243508| p 1347 N92-17385
A comparison of data integrity models
|AD-A243770| p 1384 N92-17633

COMPUTER NETWORKS
Development of real-time image and in situ data analysis at sea
|AD-A243682| p 1242 N92-17075
Optimal configuration of digital communication network
|AD-A243041| p 1282 N92-17277
Summary of professional activities, center for intelligence and special programs, 1990
|AD-A243508| p 1347 N92-17385
A distributed design for monitoring, logging, and replaying device readings at LAMPF
|DE92-003860| p 1240 N92-17591
Software tools for distributed intelligent control systems
|DE92-004656| p 1349 N92-17965

COMPUTER PROGRAMMING
A system for specifying and rapidly prototyping user interfaces
|AD-A242963| p 1347 N92-16994
Pragmatic quality metrics for evolutionary software development models
|AD-A243022| p 1337 N92-17064
An examination of selected commercial software testing tools
|AD-A243089| p 1337 N92-17068
Using mappings to prove timing properties
|AD-A242862| p 1277 N92-17263
Operations mission planner beyond the baseline p 1246 N92-17353
Causal models in the acquisition and instruction of programming skills
|AD-A242899| p 1340 N92-17463
CMS reverse engineering and encore/model integration
|AD-A243438| p 1341 N92-17487
Technical evaluation report on the 52nd Symposium on Software for Guidance and Control
|AGARD-AR-302| p 1341 N92-17498
Specification and compositional verification of real-time systems
|ETN-92-90580| p 1341 N92-17521
Programming mechanical simulations
|AD-A243767| p 1341 N92-17538
BrainMap: A database of functional neuroanatomy derived from human brain images
|AD-A243161| p 1333 N92-17648
Design implementation into field programmable gate arrays
|AD-A242538| p 1343 N92-17680
Full surface testing of grazing incidence mirrors
|AD-A243734| p 1367 N92-17690
Electrically erasable programmable integrated circuits for replacement of obsolete TTL logic
|AD-A243652| p 1292 N92-17760
Machine scheduling and Lagrangian relaxation
|ETN-92-90569| p 1353 N92-17839
Neural-network dedicated processor for solving competitive assignment problems
|NASA-CASE-NPO-17781-1-CU| p 1337 N92-17884

COMPUTER PROGRAMS
Critical temperature determination in superconductors
|AD-A243537| p 1371 N92-17015
Unsteady laminar flow in a circular tube: A test of the HERCOL (Hermitian collocation) computer code
|PB91-222679| p 1295 N92-17018
Pragmatic quality metrics for evolutionary software development models
|AD-A243022| p 1337 N92-17064
Cathodic protection diagnostic computer program for sacrificial and impressed current systems: Overview and user's manual
|AD-A243663| p 1338 N92-17122
Electronic data interchange
|AD-A242959| p 1382 N92-17136
Computer aided thermal analysis of a microcircuit structure
|AD-A243160| p 1287 N92-17205
Groundscreen characterization
|AD-A243164| p 1311 N92-17208
Performance modeling of the Ada rendezvous
|AD-A243392| p 1339 N92-17211
Atomic oxygen flux and fluence calculation for Long Duration Exposure Facility (LDEF)
|NASA-CR-187418| p 1245 N92-17215
Product Definition Data Interface (PDDI) translator user's manual
|AD-A243463| p 1352 N92-17223
An analysis of mission critical computer software in Naval aviation
|AD-A243078| p 1339 N92-17237
Study of plane wave impingement on a thin plate capable of deformation
|AD-A242947| p 1296 N92-17275
The conversion of a FORTRAN data plotting program using DI-3000 graphics to operation on a Macintosh Personal Computer
|AD-A243046| p 1339 N92-17280
Automated composite ellipsoid modelling for high frequency GTD analysis
|NASA-CR-189853| p 1233 N92-17316
Viscous three-dimensional calculations of transonic fan performance
|NASA-TM-103800| p 1219 N92-17346
Software life cycle methodologies and environments p 1246 N92-17351
Information Management Engineering (IME) laboratory: A database development facility
|AD-A243191| p 1383 N92-17369
Summary of professional activities, center for Air Force C3 systems
|AD-A243509| p 1348 N92-17386
Workshop for Finite Element Methods for Composites
|AD-A243534| p 1256 N92-17392

A PC program to calculate the one-sided lower tolerance limit for total ionizing dose radiation data
| AD-A242365 | p 1357 N92-17394
Parallel processing applied to computational electromagnetics
| AD-A242372 | p 1345 N92-17395
Design of Style-V: A translator to convert standard VHDL into a stylized form for automated microcode generation
| AD-A243706 | p 1340 N92-17407
Total Dielectric Isolation (TDI) of fully depleted device structures
| AD-A241926 | p 1289 N92-17439
ZEUS user manual real gas effects
| AD-A242224 | p 1225 N92-17446
Feedback in dynamic decision making: An experiment in software project management
| AD-A242361 | p 1380 N92-17451
Verification of an effective dose equivalent model for neutrons
| DE92-002738 | p 1358 N92-17453
Versatile Data Acquisition System Model II user's manual
| DE92-003311 | p 1384 N92-17470
Comparison of AFITPAC versus NOS and a packet radio network design
| AD-A243766 | p 1283 N92-17516
Specification and compositional verification of real-time systems
| ETN-92-90580 | p 1341 N92-17521
Testing of spacecraft in long-term storage
| AD-A242906 | p 1250 N92-17580
Forth Graphics Toolbox (A user's guide for use with RFF FORTH)
| AD-A242916 | p 1342 N92-17581
Program plans: Aviation safety research
| NIAR-91-30 | p 1227 N92-17587
Auroral-clutter predictions for Fylingdales, England
| AD-A242957 | p 1283 N92-17600
Simulation of finite-precision effects in digital filters
| AD-A243758 | p 1342 N92-17601
BrainMap: A database of functional neuroanatomy derived from human brain images
| AD-A243161 | p 1333 N92-17648
New algorithms for broad-band and narrowband source localization and a separable 2-D IIR filter realization
| AD-A243457 | p 1291 N92-17654
Full surface testing of grazing incidence mirrors
| AD-A243734 | p 1367 N92-17690
Adaptive on-line help for embedded instructional systems
| AD-A243675 | p 1343 N92-17716
An analysis of the aircraft engine Component Improvement Program (CIP): A life cycle cost approach
| AD-A243346 | p 1236 N92-17729
Control algorithms for aerobraking in the Martian atmosphere
| AD-A243349 | p 1239 N92-17730
A robust digital flight control system for an unfanned research vehicle using discrete quantitative feedback theory
| AD-A243638 | p 1237 N92-17748
Verification and validation of the Comprehensive Operational Support Evaluation Model for space
| AD-A243653 | p 1344 N92-17761
Multispectral software development for the Airborne Bathymetric Survey System
| AD-A243774 | p 1325 N92-17765
Microprocessor controller in CAMAC standard for temperature regulation and stabilization
| DE92-611158 | p 1348 N92-17814
Algorithm and Pascal: A program for neural net learning p 1344 N92-17822
Achromatic and isochronous electron beam transport for tunable free electron lasers
| DE92-003908 | p 1305 N92-17868
QTCM software documentation. Volume 2: User's manual
| AD-A242744 | p 1344 N92-17948
Software reliability models for critical applications
| DE92-004797 | p 1345 N92-17969

COMPUTER STORAGE DEVICES
Resource allocation in distributed memory multiprocessing
| AD-A243165 | p 1345 N92-17188
Program translation tools for systolic arrays
| AD-A242924 | p 1336 N92-17466
Optical associative processors and directed graphs
| AD-A242901 | p 1366 N92-17630
Effect of spatial locality prefetching on structural locality
| AD-A243632 | p 1337 N92-17922

COMPUTER SYSTEMS DESIGN
Causal schema decision-aiding system
| AD-A242931 | p 1347 N92-17203
Advanced Crew Personal Support Computer (CPSC) task p 1249 N92-17419
An object-oriented database implementation of the Magic VLSI Layout Design System
| AD-A243743 | p 1384 N92-17482
The StarLite Project prototyping real-time software
| AD-A242032 | p 1342 N92-17636
Mathematical basis for a system to manage automated protocol analysis
| AD-A242042 | p 1381 N92-17669
Design implementation into field programmable gate arrays
| AD-A242538 | p 1343 N92-17680
Improvement of data processing system for gust wind tunnel data acquisition part: System conversion from off-line to on-line processing
| NAL-TM-611 | p 1238 N92-17756
Neural-network dedicated processor for solving competitive assignment problems
| NASA-CASE-NPO-17781-1-CU | p 1337 N92-17884

COMPUTER SYSTEMS PERFORMANCE
The real-time cost of timing uncertainty: Consensus and failure detection
| AD-A243176 | p 1345 N92-16997
Using mappings to prove timing properties
| AD-A242862 | p 1277 N92-17263
The conversion of a FORTRAN data plotting program using DI-3000 graphics to operation on a Macintosh Personal Computer
| AD-A243046 | p 1339 N92-17280
A graphical database interface for a multimedia DBMS
| AD-A243283 | p 1339 N92-17285
CMS reverse engineering and encore/model integration
| AD-A243438 | p 1341 N92-17487
Improved task scheduling for parallel simulations
| AD-A243721 | p 1346 N92-17507
A cache design to exploit structural locality
| AD-A243633 | p 1336 N92-17744
Improvement of data processing system for gust wind tunnel data acquisition part: System conversion from off-line to on-line processing
| NAL-TM-611 | p 1238 N92-17756

COMPUTER SYSTEMS PROGRAMS
ISE advanced technology p 1249 N92-17420

COMPUTER SYSTEMS SIMULATION
Design implementation into field programmable gate arrays
| AD-A242538 | p 1343 N92-17680
Computer modelling of two-input neural-net learning p 1348 N92-17819

COMPUTER TECHNIQUES
CALS database usage and analysis tool study
| AD-A243205 | p 1382 N92-17174
Intelligent Computer-Aided Training (ICAT) p 1246 N92-17352
Comparison of experimental US Air Force and Euro-NATO pilot candidate selection test batteries
| AD-A242358 | p 1332 N92-17450
Embedded fault-tolerant computer for mission critical applications
| AD-A242886 | p 1342 N92-17566
Investigation of air transportation technology at Princeton University, 1990-1991 p 1221 N92-17995

COMPUTER VISION
Extracting the shape and roughness of specular lobe objects using four light photometric stereo
| AD-A243522 | p 1365 N92-17146
Near real-time stereo vision system
| NASA-CASE-NPO-18593-1-CU | p 1368 N92-17864

COMPUTERIZED SIMULATION
Feature extraction for pose estimation: A comparison between synthetic and real IR imagery
| AD-A243699 | p 1338 N92-17077
Implementation of an object-oriented flight simulator D.C. electrical system on a hypercube architecture
| AD-A243700 | p 1238 N92-17097
Hypervelocity impact simulation for micrometeorite and debris shield design
| NASA-CR-189807 | p 1244 N92-17200
Acoustic simulation for acoustics education
| AD-A243027 | p 1355 N92-17236
Adaptive presort processing
| AD-A243286 | p 1340 N92-17286
An aerocapture attitude control systems incorporating robustness and vehicle parameter identification
| AD-A243360 | p 1245 N92-17302
Comparison of two eighth-mesh terrain databases
| AD-A243315 | p 1383 N92-17401
Analog optical neural nets: A noise sensitivity analysis
| AD-A242920 | p 1346 N92-17465
Comparison of AFITPAC versus NOS and a packet radio network design
| AD-A243766 | p 1283 N92-17516
Programming mechanical simulations
| AD-A243767 | p 1341 N92-17538
Neutral network models of primate motor system
| AD-A243460 | p 1343 N92-17655
Weight evaluation and sensitivity analysis for space plane. Part 2: TSTO
| NAL-TM-602-PT-2 | p 1251 N92-17754
Electrically erasable programmable integrated circuits for replacement of obsolete TTL logic
| AD-A243652 | p 1292 N92-17760
Ocean simulation model. Version 2: First order frontal simulation
| AD-A243775 | p 1325 N92-17766
An investigation of gouge initiation in high-velocity sliding contact
| DE92-003944 | p 1311 N92-17937

COMPUTERS
Pattern Theory: An engineering paradigm for algorithm design
| AD-A243214 | p 1339 N92-17179
Versatile Data Acquisition System Model II user's manual
| DE92-003311 | p 1384 N92-17470

CONCATENATED CODES
Investigation of coding techniques for memory and delay efficient interleaving in slow Rayleigh fading
| AD-A243154 | p 1280 N92-17187

CONCENTRATION (COMPOSITION)
Concentration of isotopic hydrogen by temperature gradient effect in soluble metal
| AD-D015062 | p 1260 N92-17628

CONCENTRATORS
Tandem concentrator photovoltaic array applied to Space Station Freedom evolutionary power requirements p 1251 N92-17769

CONDENSERS
Active thermal control system evolution p 1252 N92-17775

CONDENSING
Organometallic NLO polymers. Accordian main-chain NLO polymers of ferrocene
| AD-A243642 | p 1273 N92-17751
Aryl bis(triflates) in palladium (0) cross-coupling reactions. Synthesis of polyphenyl-alkynyl, alkenyl, and aryl ethers
| AD-A243643 | p 1273 N92-17752
Organic NLO polymers. Linear and accordian main-chain NLO polymers prepared by a Knoevenagel polycondensation
| AD-A243644 | p 1273 N92-17753

CONDUCTING POLYMERS
Electronic and ionic transport in processable conducting polymers. Symmetry effects on the physical and electrically conducting, substituted poly(di-2-thienylphenylenes)
| AD-A242328 | p 1266 N92-16976
Ultrafast passive shields for laser and ballistic protection
| AD-A243206 | p 1303 N92-17175
Dielectric properties of aligned conducting polymers
| AD-A243389 | p 1268 N92-17191
Electronic and ionic transport in processable conducting polymers
| AD-A242258 | p 1269 N92-17460
Development of processible electroactive oligomers and polymers
| AD-A243723 | p 1270 N92-17508
Separation of neutral-to-polaron and polaron-to-bipolaron redox events in alkoxy substituted di-2-thienylphenylene polymers
| AD-A242423 | p 1271 N92-17679
Photomodulation spectroscopy of photocarrier dynamics, electronic defects and morphology of conducting polymers
| DE92-004687 | p 1274 N92-17966

CONDUCTION ELECTRONS
Evidence for strong electron-phonon coupling in thermal conductivity of YBa2Cu3O(7-delta)
| AD-A243192 | p 1372 N92-17218

CONDUCTORS
A reexamination of F-19 NMR in selected solids, the conductor Ag2F and reference insulators for studies of YBa2Cu3O7-type superconductors
| AD-A243194 | p 1372 N92-17219

CONFERENCES
Complexity issues in numerical optimization
| AD-A241854 | p 1347 N92-17049
Space Station Freedom Evolution Symposium p 1243 N92-17105
The 5th Annual US-Japan Seminar on Dielectric and Piezoelectric Ceramics
| AD-A243465 | p 1268 N92-17193
Calendar of selected aeronautical and space meetings, July 1990 onwards
| AGARD-CAL-90/2 | p 1380 N92-17198
Proceedings of the USAF Structural Integrity Program Conference
| AD-A242943 | p 1235 N92-17204
Calendar of selected aeronautical and space meetings, January 1992 and onwards
| AGARD-CAL-92/1 | p 1380 N92-17212

Beyond the Baseline 1991: Proceedings of the Space Station Evolution Symposium. Volume 2: Space Station Freedom, part 2
| NASA-CP-10083-VOL-2-PT-2 | p 1245 N92-17348
Meeting Review: Airborne Aerosol Inlet Workshop
| NASA-CR-189814 | p 1313 N92-17393
Beyond the Baseline 1991: Proceedings of the Space Station Evolution Symposium. Volume 1: Space Station Freedom, part 2
| NASA-CP-10083-VOL-1-PT-2 | p 1248 N92-17409
DOE Task Force Meeting on Electrical Breakdown of Insulating Ceramics in a High Radiation Field
| DE92-000459 | p 1270 N92-17576
The 7th Annual Workshop on Computational Neuroscience
| AD-A243462 | p 1335 N92-17656
C3 Systems Technology Symposium on Advance Planning Briefings for Industry
| AD-A243466 | p 1391 N92-17657
Beyond the Baseline 1991: Proceedings of the Space Station Evolution Symposium. Volume 2: Space Station Freedom, part 1
| NASA-CP-10083-VOL-2-PT-1 | p 1251 N92-17768

CONFIDENCE LIMITS
Sensitivity testing and analysis
| DE92-002033 | p 1276 N92-17624

CONFIGURATION MANAGEMENT
An investigation of air transportation technology at the Massachusetts Institute of Technology, 1990-1991 p 1219 N92-17985

CONFORMAL MAPPING
Use of Navier-Stokes analysis in section design
| AD-A242074 | p 1295 N92-17168
Gauge-covariant Wess-Zumino actions for super p-branes in superspace
| DE91-641524 | p 1353 N92-17318

CONICAL SCANNING
Multipath induced tracking errors at 95 and 140 GHz
| AD-A243111 | p 1283 N92-17571

CONJUGATE GRADIENT METHOD
Numerical grid generation using a variational method
| MBB-FE211-S-PUB-447 | p 1297 N92-17312

CONSOLIDATION
Consolidation of diamond packed powders
| AD-D015071 | p 1270 N92-17612

CONTAINERS
Sharps container
| NASA-CASE-MSC-21776-1 | p 1278 N92-17913

CONTAINMENT
Environmental containment property estimation using QSARs in an expert system
| AD-A243728 | p 1336 N92-17720

CONTAMINATION
Hard-surface contamination detection exercise
| DE92-004750 | p 1330 N92-17798

CONTINUOUS WAVE LASERS
Steady-state production and quenching of Br((2)P1/2)
| AD-A243754 | p 1362 N92-17663

CONTINUUM MODELING
Modes of interconnected lattice trusses using continuum models, part 1
| NASA-CR-189568 | p 1242 N92-17045

CONTOURS
Bottom contour influence on ray tracing
| AD-A242411 | p 1323 N92-17078

CONTRACTORS
Valuable patents for US businesses: A catalog of DTRC patents available for licensing by the private sector
| AD-A242071 | p 1385 N92-17141
A management case analysis of the Department of Defense contractor risk assessment guide program
| AD-A243515 | p 1380 N92-17388
Contractor software engineering environment evaluations summary report
| AD-A242330 | p 1343 N92-17640

CONTROL EQUIPMENT
Cyclone: A laser scanner for mobile robot navigation
| AD-A243517 | p 1303 N92-17080
Performance of battery charge controllers: First year test report
| DE92-002924 | p 1269 N92-17468
On the origin and control of large coherent structures in turbulent shear flow
| AD-A243727 | p 1299 N92-17719

CONTROL SIMULATION
Programming mechanical simulations
| AD-A243767 | p 1341 N92-17538
Electrically erasable programmable integrated circuits for replacement of obsolete TTL logic
| AD-A243652 | p 1292 N92-17760

CONTROL SURFACES
Loading and vibration reduction through active aerodynamic control
| AD-A242321 | p 1236 N92-17243

CONTROL SYSTEMS DESIGN
Model identification and control system design for the lambda unmanned research vehicle
| AD-A241859 | p 1306 N92-17024
Identification techniques: Model structure and time domain methods p 1231 N92-17157
System identification requirements for high-bandwidth rotorcraft flight control system design p 1232 N92-17166
An aerocapture attitude control systems incorporating robustness and vehicle parameter identification
| AD-A243360 | p 1245 N92-17302
Active heater control and regulation for the Varian VGT-8011 gyrotron
| DE92-003638 | p 1302 N92-17454
Control of a large flexible space structure using multiple model adaptive algorithms
| AD-A243759 | p 1250 N92-17602
Microprocessor controller in CAMAC standard for temperature regulation and stabilization
| DE92-611158 | p 1348 N92-17814
High level language-based robotic control system
| NASA-CASE-NPO-17918-2-CU | p 1349 N92-17895
Passive control of pressure loads using porosity
| NASA-CASE-LAR-14547-1 | p 1300 N92-17909
Software tools for distributed intelligent control systems
| DE92-004656 | p 1349 N92-17965
Investigation of air transportation technology at Princeton University, 1990-1991 p 1221 N92-17995
Neural networks for aircraft system identification p 1222 N92-17998
Intelligent failure-tolerant control p 1222 N92-18000
Technical notes and correspondence: Stochastic robustness of linear time-invariant control systems p 1222 N92-18002

CONTROL THEORY
Modes of interconnected lattice trusses using continuum models, part 1
| NASA-CR-189568 | p 1242 N92-17045
Development of high angle of attack control laws for an unstable, non-minimum phase aircraft using variations of the quantitative feedback technique
| AD-A243698 | p 1236 N92-17096
An aerocapture attitude control systems incorporating robustness and vehicle parameter identification
| AD-A243360 | p 1245 N92-17302
Adaptive generalized predictive control
| OUEL-1879/91 | p 1349 N92-17880
Software tools for distributed intelligent control systems
| DE92-004656 | p 1349 N92-17965

CONTROLLABILITY
System identification methods for handling-qualities evaluation p 1232 N92-17165

CONTROLLERS
Neural network modeling of nonlinear systems based on Volterra series extension of a linear model
| NASA-TM-104177 | p 1347 N92-16987
The analysis of a stabilized 1.5 Mach-Zehnder interferometric sensor with enhanced sensitivity and common-mode compensation
| AD-A243384 | p 1286 N92-17116
Toward the robust control of high bandwidth high precision flexible optical systems
| AD-A243471 | p 1366 N92-17536
Comparison of alkali ion emitters
| AD-A243105 | p 1290 N92-17570
Beam position monitor multiplexer controller upgrade at the LAMPF proton storage ring
| DE92-003859 | p 1363 N92-17590
Control of a large flexible space structure using multiple model adaptive algorithms
| AD-A243759 | p 1250 N92-17602
Microprocessor controller in CAMAC standard for temperature regulation and stabilization
| DE92-611158 | p 1348 N92-17814
Closed-loop motor control using high-speed fiber optics
| NASA-CASE-MSC-21806-1 | p 1368 N92-17863
Transformerless DC-DC voltage amplifier with optically isolated switching devices
| NASA-CASE-NPO-17994-1-CU | p 1293 N92-17907

CONVECTION CELLS
The wave numbers of supercritical surface tension driven Benard convection
| NASA-CR-189856 | p 1373 N92-17375

CONVECTION CURRENTS
The role of thermal convection in heat and mass transport in the subarctic snow cover
| AD-A243674 | p 1312 N92-17715

CONVECTIVE FLOW
Studies of baroclinic flow
| AD-A243050 | p 1296 N92-17309

CONVECTIVE HEAT TRANSFER
Effects of power pulsations on heat transfer from discrete heat sources
| AD-A243434 | p 1379 N92-17686
The role of thermal convection in heat and mass transport in the subarctic snow cover
| AD-A243674 | p 1312 N92-17715

CONVERGENCE
A convergent aspiration based interior point method (CAIN) for Multiple Objective Linear Programming (MOLP)
| AD-A243404 | p 1338 N92-17118
Parallel radiosity techniques for mesh-connected SIMD computers
| AD-A242049 | p 1346 N92-17638

CONVEXITY
Self-collimated unstable resonator semiconductor laser
| NASA-CASE-NPO-18386-1-CU | p 1305 N92-17899

COOLANTS
Transpiration cooled throat for hydrocarbon rocket engines
| NASA-CR-184272 | p 1253 N92-17495

COOLING
Application of silicon micromachining to thermal dissipation issues in wafer scale integrated circuits
| AD-A243744 | p 1288 N92-17332
Cooled ion frequency standard
| AD-A242030 | p 1360 N92-17549
Alleviation of thermal strain in engineering space personnel aboard CF ships with the exotemp personal cooling system
| AD-A242889 | p 1330 N92-17599

COOLING SYSTEMS
Alleviation of thermal strain in engineering space personnel aboard CF ships with the exotemp personal cooling system
| AD-A242889 | p 1330 N92-17599
Downflow heat transfer in a heated ribbed vertical annulus with a cosine power profile (results from test series ECS-2c)
| DE92-003259 | p 1298 N92-17626

COORDINATES
The square root cordic
| AD-A242318 | p 1342 N92-17561

COPOLYMERIZATION
Molecular composites from high temperature polyquinolines
| AD-A243634 | p 1272 N92-17745
New ferrocene complexes and polymers for nonlinear optical applications
| AD-A243640 | p 1272 N92-17749
Organometallic NLO polymers. Accordian main-chain NLO polymers of ferrocene
| AD-A243642 | p 1273 N92-17751
Aryl bis(triflates) in palladium (0) cross-coupling reactions. Synthesis of polyphenyl-alkynyl, alkenyl, and aryl ethers
| AD-A243643 | p 1273 N92-17752
Organic NLO polymers. Linear and accordian main-chain NLO polymers prepared by a Knoevenagel polycondensation
| AD-A243644 | p 1273 N92-17753

COPOLYMERS
Organic NLO polymers. Linear and accordian main-chain NLO polymers prepared by a Knoevenagel polycondensation
| AD-A243644 | p 1273 N92-17753

COPPER
In situ structural studies of the underpotential deposition of copper onto an iodine covered platinum surface using x ray standing waves
| AD-A243475 | p 1263 N92-17328
Designing ordered molecular arrays in two and three dimensions
| AD-A243447 | p 1359 N92-17491
On size scaling in shock hydrodynamics and the stress-strain behavior of copper at exceedingly high strain rates
| DE92-003797 | p 1265 N92-17579
Investigation of heated ultracold neutrons on copper surface
| DE92-600625 | p 1363 N92-17955

COPPER OXIDES
Growth of near-free-standing YBa2Cu3O7-type crystals using a self-decanting flux method
| AD-A243221 | p 1372 N92-17182
Microstructure and composition of electromagnetically-characterized YBa2Cu3O(7-delta) grain boundaries
| DE92-003520 | p 1376 N92-17782
High temperature superconductor thin films and Josephson junctions
| AD-A242747 | p 1293 N92-17949

CORRECTION
User guide for WIACX: A transonic wind-tunnel wall interference assessment and correction procedure for the NTF
| NASA-TM-104168 | p 1225 N92-17547
CORRELATION DETECTION
Sensing refractive turbulence profiles using wave front slope measurements from two reference sources
| AD-A243696 | p 1315 N92-17094
CORRELATORS
Correlator optical wavefront sensor COWS
| DE92-003964 | p 1368 N92-17846
CORROSION
Codeposition of elements in diffusion coatings by the halide-activated pack cementation method
| AD-A242860 | p 1267 N92-17042
Cathodic protection diagnostic computer program for sacrificial and impressed current systems: Overview and user's manual
| AD-A243663 | p 1338 N92-17122
CORROSION RESISTANCE
Metallography of aluminide coatings
| AD-A243000 | p 1263 N92-17264
CORROSION TESTS
Long-term corrosion evaluation of stainless steels in Space Shuttle iodinated resin and water
| NASA-TM-104743 | p 1264 N92-17376
COSMIC RAYS
Collaborative research on experimental astrophysics
| DE92-003970 | p 1388 N92-17832
Constraints on cosmic ray propagation in the galaxy
| NASA-CR-189779 | p 1390 N92-18003
COSMOLOGY
Geometrical methods for the analysis of cosmological observations
| ETN-92-90584 | p 1386 N92-17523
Axino-induced baryogenesis
| NASA-CR-189858 | p 1361 N92-17646
Fluctuation driven electroweak phase transition
| NASA-CR-189859 | p 1361 N92-17647
Late time cosmological phase transitions 1: Particle physics models and cosmic evolution
| NASA-CR-189857 | p 1388 N92-17696
Future prospects of pregeometry
| DE92-704278 | p 1379 N92-17817
COST ANALYSIS
Optimal configuration of digital communication network
| AD-A243041 | p 1282 N92-17277
Cost models and the Corporate Information Management (CIM) initiative
| AD-A243554 | p 1383 N92-17340
COST EFFECTIVENESS
Economic analysis of information system
| AD-A243079 | p 1382 N92-17067
Structures to resist the effects of accidental explosions
| AD-A243272 | p 1277 N92-17272
Large centrifuge: A critical Army capability for the future
| AD-A243287 | p 1238 N92-17287
COST REDUCTION
NASA total quality management 1990 accomplishments report
| NASA-TM-105465 | p 1308 N92-17199
COUETTE FLOW
Pattern selection, wave formation, turbulence, and vortex breakdown in spiral flows
| AD-A242351 | p 1297 N92-17447
COUPLINGS
Method for non-destructive estimation of waveguide directional coupler dimensions
| NASA-CASE-NPO-18454-1-CU | p 1293 N92-17865
COVALENT BONDS
Role of donor-acceptor interactions in the sorption of TNT and other nitroaromatics from solution
| AD-A243235 | p 1254 N92-17055
Reactions and interactions in liquid crystalline media
| AD-A242355 | p 1374 N92-17449
COVARIANCE
A covariance modeling approach to adaptive beamforming and detection
| AD-A241887 | p 1279 N92-17040
Face recognition with the Karhunen-Loeve transform
| AD-A243688 | p 1280 N92-17090
Gauge-covariant Wess-Zumino actions for super p-branes in superspace
| DE91-641524 | p 1353 N92-17318
An analytic method of propagating a covariance matrix to a maneuver condition for linear covariance analysis during rendezvous
| AD-A243354 | p 1239 N92-17732
Systematic methods for knowledge acquisition and expert system development p 1222 N92-18001
CRACK CLOSURE
Dynamic fracture characterization of Al2O3 and SiC(w)/Al2O3
| AD-A242187 | p 1273 N92-17784
CRACK PROPAGATION
Aluminum alloys for ALS cryogenic tanks: Comparative measurements of cryogenic mechanical properties of Al-Li alloys and alloy 2219
| AD-A242956 | p 1264 N92-17379
Fracture toughness evaluation for N Reactor pressure tubes of Zircaloy-2 using the electric-potential method
| DE92-003631 | p 1311 N92-17713
CRASHES
Wichita State University 1986 aviation safety research projects
| DOT/FAA/CT-91/4 | p 1226 N92-16986
CRASHWORTHINESS
Wichita State University 1986 aviation safety research projects
| DOT/FAA/CT-91/4 | p 1226 N92-16986
CRATERS
On size scaling in shock hydrodynamics and the stress-strain behavior of copper at exceedingly high strain rates
| DE92-003797 | p 1265 N92-17579
CREEP PROPERTIES
The influence of temperature and composition on the activation energy for creep in binary aluminum lithium alloys
| AD-A242299 | p 1265 N92-17759
The effect of physical aging on the creep response of a thermoplastic composite
| AD-A243600 | p 1258 N92-17932
Damage mechanisms in composites
| AD-A242748 | p 1258 N92-17950
CREEP TESTS
The effect of physical aging on the creep response of a thermoplastic composite
| AD-A243600 | p 1258 N92-17932
CREW WORKSTATIONS
AGSSS: The Airborne Graphics Software Support System; an Ada/PHIGS-based display editor for the rapid development of cockpit display software systems
| AD-A243224 | p 1234 N92-17221
CRITICAL TEMPERATURE
Critical temperature determination in superconductors
| AD-A243537 | p 1371 N92-17015
Pressure dependence of Tc in Tl2Ba2CaCu2O8 at hydrostatic pressures to 6 GPa
| AD-A243433 | p 1375 N92-17685
CROSS CORRELATION
Sensing refractive turbulence profiles using wave front slope measurements from two reference sources
| AD-A243696 | p 1315 N92-17094
CROSS SECTIONS
Recent developments in neutrino physics
| DE92-003855 | p 1360 N92-17589
CROSSLINKING
Molecular recognition in gels, monolayers, and solids
| AD-A243488 | p 1358 N92-17428
CRUDE OIL
Catalysis looks to the future
| LC-91-66333 | p 1261 N92-17786
CRUISING FLIGHT
Example of statistical techniques applied to cruise performance guarantees (Student's t distribution)
| ESDU-91018 | p 1233 N92-17843
CRYOGENIC COOLING
Three-stage sorption type cryogenic refrigeration system and method employing heat regeneration
| NASA-CASE-NPO-18366-1-CU | p 1277 N92-17674
CRYOGENIC EQUIPMENT
Cryogenic thermoresistor made from p-InSb(Mn)
| DE92-600473 | p 1293 N92-17825
CRYOGENIC FLUID STORAGE
Extravehicular mobility unit subcritical liquid oxygen storage and supply system
| NASA-CR-189831 | p 1276 N92-16989
CRYOGENIC ROCKET PROPELLANTS
Space Station Freedom/lunar transfer vehicle propellant operation hazard analysis p 1249 N92-17416
CRYOGENIC TEMPERATURE
Aluminum alloys for ALS cryogenic tanks: Comparative measurements of cryogenic mechanical properties of Al-Li alloys and alloy 2219
| AD-A242956 | p 1264 N92-17379
CRYSTAL DEFECTS
Collisional energy deposition threshold for extended damage depths in ion-implanted silicates
| DE92-004737 | p 1377 N92-17797
CRYSTAL DISLOCATIONS
Growth rate of dislocation loop in Fe-Ni-Cr alloy under Kr(+) ion and electron irradiation
| DE92-001908 | p 1265 N92-17703
CRYSTAL GROWTH
Growth of near-free-standing YBa2Cu3O7-type crystals using a self-decanting flux method
| AD-A243221 | p 1372 N92-17182
Consolidation of diamond packed powders
| AD-D015071 | p 1270 N92-17612
Spatially and spectrally resolved cathodoluminescence measurements of CVD-grown diamond particles and films
| AD-A243220 | p 1271 N92-17615
Growth rate of dislocation loop in Fe-Ni-Cr alloy under Kr(+) ion and electron irradiation
| DE92-001908 | p 1265 N92-17703
CRYSTAL STRUCTURE
Theoretical crystal-field calculations for rare-earth ions in 3-5 semiconductor compounds
| AD-A243098 | p 1371 N92-16995
Designing ordered molecular arrays in two and three dimensions
| AD-A243447 | p 1359 N92-17491
Y890NMR study of hyperfine interactions in (R(x)Y(1-x))Fe2
| DE91-641979 | p 1376 N92-17779
Characterization of PZT thin films: Crystallographic phases
| DE92-003514 | p 1377 N92-17790
CRYSTAL SURFACES
Electronic interactions of directed photon beams with surfaces
| AD-A241878 | p 1356 N92-17026
CRYSTALLIZATION
Contributive research and development
| AD-A243331 | p 1391 N92-17079
CRYSTALLOGRAPHY
In situ surface x ray crystallography of electrochemically deposited Bi on Ag(111): Structure, compressibility, and anisotropy
| AD-A243218 | p 1372 N92-17181
Transmission electron microscopy of the CVD diamond film/substrate interface
| AD-A243096 | p 1373 N92-17322
Fatigue in single crystal nickel superalloys
| AD-A243453 | p 1265 N92-17653
CRYSTALS
Processing of ceramics of biopolymers. Ultrastructure-property relationships in biocrystals
| AD-A243061 | p 1267 N92-17054
Single molecule spectral diffusion in a solid detected via fluorescence spectroscopy
| AD-A243748 | p 1356 N92-17197
Diffraction and imaging theory of inelastically scattered electrons: A new approach
| DE91-018248 | p 1360 N92-17574
An algorithm for calculating the electronic spectrum and function of the charge density distributions of crystals p 1375 N92-17698
The EPR of the triplet state of aryl cations in crystals of diazonium salts p 1375 N92-17701
CUBIC LATTICES
Characterization of PZT thin films: Crystallographic phases
| DE92-003514 | p 1377 N92-17790
CURING
Novel vacuum bag processing approaches to void reduction in carbon/epoxy composites
| AD-A242396 | p 1255 N92-16992
Case bond liner systems for solid rocket motors
| AD-A242297 | p 1253 N92-17085
Evaluation of an Interdigitated Gate Electrode Field-Effect Transistor (IGEFET) for in situ resin cure monitoring
| AD-A243713 | p 1289 N92-17501
CURRENT DENSITY
Catalysts for ultrahigh current density oxygen cathodes for space fuel cell applications
| NASA-CR-189787 | p 1253 N92-17365
Microstructure and composition of electromagnetically-characterized YBa2Cu3O(7-delta) grain boundaries
| DE92-003520 | p 1376 N92-17782
CURVATURE
The effect of detonation curvature on cylindrical wall motion
| DE92-003110 | p 1298 N92-17625
CURVE FITTING
Critical temperature determination in superconductors
| AD-A243537 | p 1371 N92-17015
CYCLONES
A variational assimilation method for satellite and conventional data: Development of basic model for diagnosis of cyclone systems
| NASA-CR-188236 | p 1321 N92-17975
A variational assimilation method for satellite and conventional data: A revised basic model 2B p 1322 N92-17977

CYCLOTRON RESONANCE
An in-situ spectroscopic ellipsometry study of the electron cyclotron resonance plasma oxidation of silicon and interfacial
[AD-A242833] p 1259 N92-17247
A kinetics study of the electron cyclotron resonance plasma oxidation of silicon
[AD-A242868] p 1290 N92-17596
Ion sources based on electron cyclotron resonance
p 1362 N92-17743
CYCLOTRON RESONANCE DEVICES
Active heater control and regulation for the Varian VGT-8011 gyrotron
[DE92-003638] p 1302 N92-17454
CYCLOTRONS
Multiply charged ion sources for cyclotrons
[DE92-610975] p 1364 N92-17973
CYLINDRICAL BODIES
Exploring plasma sheath solutions for planar and cylindrical anodes
[AD-A243237] p 1369 N92-17030
A theory of inverse operators for multiple excitations
[AD-A243484] p 1350 N92-17330
Flow visualization and wake analysis for standard and modified configurations of the AN/ALQ-78 antenna pod
[AD-A243552] p 1224 N92-17339
Natural resonances of slotted cylinder configurations
[AD-A241934] p 1282 N92-17441
The effect of detonation curvature on cylindrical wall motion
[DE92-003110] p 1298 N92-17625
Physical and computational modelling of stratified shear flows
[AERO-REPT-8909] p 1300 N92-17974
CYLINDRICAL CHAMBERS
Flow between two stationary disks and a rotating shroud
[AERO-REPT-9001] p 1300 N92-17851
CYLINDRICAL SHELLS
Higher-order thickness expansions for cylindrical shells
[AD-A242017] p 1310 N92-17230
CYPRUS
Severe weather guide Mediterranean ports. Part 36: Limassol
[AD-A243448] p 1320 N92-17492
Severe weather guide Mediterranean ports. Part 37: Larnaca
[AD-A243449] p 1320 N92-17493

D

DAMAGE
An investigation of gouge initiation in high-velocity sliding contact
[DE92-003944] p 1311 N92-17937
DARK MATTER
Late time cosmological phase transitions 1: Particle physics models and cosmic evolution
[NASA-CR-189857] p 1388 N92-17696
DARKNESS
Melatonin action on the circadian pacemaker in Siberian hamsters
[AD-A243057] p 1325 N92-17142
DATA ACQUISITION
HEMP test on FD-565
[AD-A243099] p 1278 N92-16980
Advanced nozzle and engine components test facility
[NASA-TM-103684] p 1237 N92-17059
The ZEUS second level calorimeter trigger: Physics simulation, design and implementation
[ETN-92-90568] p 1358 N92-17435
Versatile Data Acquisition System Model II user's manual
[DE92-003311] p 1384 N92-17470
The determination of the number of light neutrino species
[ETN-92-90564] p 1359 N92-17519
Muons in UA1; the 2nd level trigger and dimuon results
[ETN-92-90565] p 1360 N92-17520
Results from a data acquisition system prototype project using a switch-based event builder
[DE92-004638] p 1336 N92-17592
Magnetohydrodynamic projects at the CDIF
[DE92-002636] p 1370 N92-17664
Improvement of data processing system for gust wind tunnel data acquisition part: System conversion from off-line to on-line processing
[NAL-TM-611] p 1238 N92-17756
Data acquisition and measurement system for plastic parameters of radiation metal research experiments
[DE92-610350] p 1266 N92-17808
DATA BASE MANAGEMENT SYSTEMS
Cathodic protection diagnostic computer program for sacrificial and impressed current systems: Overview and user's manual
[AD-A243663] p 1338 N92-17122
A graphical database interface for a multimedia DBMS
[AD-A243283] p 1339 N92-17285
Information Management Engineering (IME) laboratory: A database development facility
[AD-A243191] p 1383 N92-17369
FEM-X user's guide
[AD-A242374] p 1383 N92-17396
Towards intelligent data retrieval in multimedia databases
[AD-A243323] p 1383 N92-17402
An object-oriented database implementation of the Magic VLSI Layout Design System
[AD-A243743] p 1384 N92-17482
The UNC graph server: A distributed hypermedia data management system
[AD-A242041] p 1380 N92-17651
Efficient identification and analysis of low and medium frequency repeats
[DE92-003758] p 1385 N92-17856
DATA BASES
Optical content-addressable memories for data/knowledge base processing
[AD-A241866] p 1382 N92-17037
Evolution design requirements and design strategy
p 1244 N92-17112
Statistically-based decompression tables. 6: Repeat dives on oxyen/nitrogen mixes
[AD-A243667] p 1328 N92-17124
Identification techniques: Frequency domain methods
p 1231 N92-17158
CALS database usage and analysis tool study
[AD-A243205] p 1382 N92-17174
Map maker
[AD-A242980] p 1312 N92-17292
Comparison of two eighth-mesh terrain databases
[AD-A243315] p 1383 N92-17401
Towards intelligent data retrieval in multimedia databases
[AD-A243323] p 1383 N92-17402
Surface observations climatic summaries for Camp Humphreys, Korea
[AD-A241937] p 1320 N92-17444
An object-oriented database implementation of the Magic VLSI Layout Design System
[AD-A243743] p 1384 N92-17482
A knowledge-based approach for configuring computer aided measuring systems
[ETN-92-90585] p 1341 N92-17524
The StarLite Project prototyping real-time software
[AD-A242032] p 1342 N92-17636
BrainMap: A database of functional neuroanatomy derived from human brain images
[AD-A243161] p 1333 N92-17648
The UNC graph server: A distributed hypermedia data management system
[AD-A242041] p 1380 N92-17651
Thermal Control System Automation Project (TCSAP)
p 1252 N92-17776
Making of functionally gradient materials data base
[NAL-TM-621] p 1385 N92-17787
Fractal image encoding
[AD-A243620] p 1344 N92-17921
DATA COMPRESSION
Sub-band/transform compression of video sequences
[NASA-CR-189786] p 1280 N92-17139
Pattern Theory: An engineering paradigm for algorithm design
[AD-A243214] p 1339 N92-17179
Image processing applications for nonlinear decomposition and synthesis
[AD-A243357] p 1343 N92-17733
Use of the algebraic coding theory in nuclear electronics
[DE92-611125] p 1351 N92-17813
Image scanning using a fractal curve
[BBC-RD-1991/4] p 1285 N92-17886
DATA CONVERTERS
Use of the algebraic coding theory in nuclear electronics
[DE92-611125] p 1351 N92-17813
DATA LINKS
Multiple-access phased array antenna simulator for a digital beam forming system investigation
[NASA-TM-105422] p 1279 N92-17062
Design of a fiber optic image transmission link
[AD-A243686] p 1365 N92-17088
Investigation of coding techniques for memory and delay efficient interleaving in slow Rayleigh fading
[AD-A243154] p 1280 N92-17187
Communication network survivability
[AD-A242969] p 1281 N92-17252
Assessment of cockpit interface concepts for data link retrofit
[NASA-CR-187615] p 1228 N92-17512
Satellite links for television contribution: Reception requirements for links using transportable transmitting earth stations
[BBC-RD-1991/5] p 1285 N92-17885
DATA MANAGEMENT
Performance measures for adaptive decisioning systems
[AD-A243183] p 1352 N92-16998
Electronic data interchange
[AD-A242959] p 1382 N92-17136
Cost models and the Corporate Information Management (CIM) initiative
[AD-A243554] p 1383 N92-17340
Data management system advanced architectures
p 1249 N92-17417
A comparison of data integrity models
[AD-A243770] p 1384 N92-17633
DATA PROCESSING
Optical content-addressable memories for data/knowledge base processing
[AD-A241866] p 1382 N92-17037
Development of real-time image and in situ data analysis at sea
[AD-A243682] p 1242 N92-17075
Instrumentation and data processing
p 1230 N92-17155
Flight test data quality evaluation
p 1230 N92-17156
Identification techniques: Frequency domain methods
p 1231 N92-17158
Product Definition Data Interface (PDDI) translator user's manual
[AD-A243463] p 1352 N92-17223
Versatile Data Acquisition System Model II user's manual
[DE92-003311] p 1384 N92-17470
The determination of the number of light neutrino species
[ETN-92-90564] p 1359 N92-17519
A distributed design for monitoring, logging, and replaying device readings at LAMPF
[DE92-003860] p 1240 N92-17591
Developing a broader basis for scientific data analysis interfaces
[DE92-003963] p 1385 N92-17845
DATA REDUCTION
Long duration exposure facility post-flight thermal analysis: Orbital/thermal environment data package
[NASA-CR-189872] p 1245 N92-17334
Full surface testing of grazing incidence mirrors
[AD-A243734] p 1367 N92-17690
Developing a broader basis for scientific data analysis interfaces
[DE92-003963] p 1385 N92-17845
Efficient identification and analysis of low and medium frequency repeats
[DE92-003758] p 1385 N92-17856
DATA RETRIEVAL
Towards intelligent data retrieval in multimedia databases
[AD-A243323] p 1383 N92-17402
DATA SAMPLING
Bayesian computations in survival models via the Gibbs sampler
[AD-A242343] p 1353 N92-17643
DATA STORAGE
Optical content-addressable memories for data/knowledge base processing
[AD-A241866] p 1382 N92-17037
Effect of spatial locality prefetching on structural locality
[AD-A243632] p 1337 N92-17922
DATA SYSTEMS
Space Station Freedom engineering prototype development p 1244 N92-17110
Real Time Data System (RTDS) p 1249 N92-17421
Improvement of data processing system for gust wind tunnel data acquisition part: System conversion from off-line to on-line processing
[NAL-TM-611] p 1238 N92-17756
Making of functionally gradient materials data base
[NAL-TM-621] p 1385 N92-17787
DATA TRANSMISSION
HEMP test on FD-565
[AD-A243099] p 1278 N92-16980
Comparative analysis of gray scale coding techniques for group 4 facsimile
[AD-A243175] p 1278 N92-16996
NASA/DoD aerospace knowledge diffusion research project: Chronology of selected literature, reports, policy instruments, and significant events affecting Federal Scientific and Technical Information (STI) in the US
[NASA-TM-101662] p 1381 N92-17001

Design of a fiber optic image transmission link
| AD-A243686 | p 1365 N92-17088
Local area network strategies and guidelines for a Peruvian Air Force Computer Center
| AD-A242841 | p 1345 N92-17135
An overview of cellular telecommunications
| AD-A242951 | p 1281 N92-17232
Data fusion for least squares
| AD-A243507 | p 1352 N92-17384
Results from a data acquisition system prototype project using a switch-based event builder
| DE92-004638 | p 1336 N92-17592

DAYTIME
Background Atmosphere Radiance Day (BARD) and Night (BARN)
| AD-A243153 | p 1316 N92-17239

DEACTIVATION
Rates and mechanisms of metastable deactivation over surfaces
| AD-A243391 | p 1361 N92-17652

DEBRIS
Effect of coatings and processing on failure mechanisms of polycarbonate material, phase 1
| AD-A243018 | p 1256 N92-17053

DECELERATION
Geometrical methods for the analysis of cosmological observations
| ETN-92-90584 | p 1386 N92-17523

DECISION MAKING
The effects of speech intelligibility level on concurrent visual task performance
| AD-A243015 | p 1331 N92-17052
Acquisition and production of skilled behavior in dynamic decision-making tasks
| NASA-CR-189846 | p 1333 N92-17132
Causal schema decision-aiding system
| AD-A242931 | p 1347 N92-17203
Automated planning with special relevance to associate systems technology and mission planning
| AD-A241924 | p 1348 N92-17438
Feedback in dynamic decision making: An experiment in software project management
| AD-A242361 | p 1380 N92-17451
Severe weather guide Mediterranean ports. Part 36: Limassol
| AD-A243448 | p 1320 N92-17492
Severe weather guide Mediterranean ports. Part 37: Larnaca
| AD-A243449 | p 1320 N92-17493
Severe weather guide Mediterranean ports. Part 39: Port Said
| AD-A243450 | p 1320 N92-17494
Automated power management and control p 1252 N92-17773

DECOMPOSITION
Mass transfer in gas fluidized beds: Scaling, modeling, and particle size influence
| ETN-92-90581 | p 1298 N92-17522
Image processing applications for nonlinear decomposition and synthesis
| AD-A243357 | p 1343 N92-17733

DECOMPRESSION SICKNESS
Statistically-based decompression tables. 6: Repeat dives on oxyen/nitrogen mixes
| AD-A243667 | p 1328 N92-17124

DEDUCTION
IMPS: An Interactive Mathematical Proof System
| AD-A243162 | p 1350 N92-17206

DEFECTS
The effect of weld metal strength mismatch on the deformation and fracture behavior of steel butt weldments
| AD-A243239 | p 1262 N92-17057
High resolution electron microscopy of diamond film growth defects and their interactions
| AD-A243093 | p 1372 N92-17238
Photomodulation spectroscopy of photocarrier dynamics, electronic defects and morphology of conducting polymers
| DE92-004687 | p 1274 N92-17966

DEFENSE COMMUNICATIONS SYSTEM (DCS)
Communication network survivability
| AD-A242969 | p 1281 N92-17252

DEFENSE INDUSTRY
The V-22: Can the nation afford to forgo its production?
| AD-A243158 | p 1219 N92-17477

DEFENSE PROGRAM
Early warning satellites: Funding for follow-on system is premature
| AD-A242836 | p 1245 N92-17250
Worldwide Environmental Compliance Assessment and Management Program (ECAMP): German supplement
| AD-A242967 | p 1313 N92-17380
A management case analysis of the Department of Defense contractor risk assessment guide program
| AD-A243515 | p 1380 N92-17388
The V-22: Can the nation afford to forgo its production?
| AD-A243158 | p 1219 N92-17477
Worldwide Environmental Compliance Assessment and Management Program (ECAMP)
| AD-A242874 | p 1314 N92-17598

DEFORMATION
The effect of weld metal strength mismatch on the deformation and fracture behavior of steel butt weldments
| AD-A243239 | p 1262 N92-17057
Inelastic strain analysis of solder joint in NASA fatigue specimen
| NASA-CR-189882 | p 1311 N92-17511
On the origin and control of large coherent structures in turbulent shear flow
| AD-A243727 | p 1299 N92-17719
Strength of lugs
| ESDU-91008 | p 1311 N92-17834

DEGRADATION
Constant modulus algorithm techniques for the enhancement of signal quality
| AD-A242986 | p 1288 N92-17295
Failure mechanisms in GaAs ICs: The effects of deep traps
| AD-A243013 | p 1374 N92-17553
Studies of hetero-epitaxy of GaAs films on Si substrate for effective control of density and internal stress
| AD-A241882 | p 1374 N92-17594

DEICING
Wichita State University 1986 aviation safety research projects
| DOT/FAA/CT-91/4 | p 1226 N92-16986

DEIONIZATION
Long-term corrosion evaluation of stainless steels in Space Shuttle iodinated resin and water
| NASA-TM-104743 | p 1264 N92-17376

DELAMINATING
The use of impact force as a scale parameter for the impact response of composite laminates
| NASA-TM-104189 | p 1256 N92-17007

DELAWARE BAY (US)
A user's manual for the Princeton Numerical Ocean Model
| AD-A243773 | p 1324 N92-17539

DELTA WINGS
An experimental investigation of leading edge vortical flow about a delta wing during wing rock
| AD-A243363 | p 1223 N92-17114
The effect of freestream turbulence on the vortical flow over a delta wing p 1225 N92-17681
Boundary-layer transition and heat transfer on slender delta wings
| AERO-REPT-8904 | p 1226 N92-17849

DEMAND (ECONOMICS)
Labor market trends for health physicists
| DE92-004770 | p 1331 N92-17800

DENSE PLASMAS
Equation of state and conductivity of hot, dense matter
| AD-A243359 | p 1369 N92-17301

DENSITY DISTRIBUTION
Application of linear inverse theory to borehole gravity data
| DE92-002172 | p 1317 N92-17578

DENSITY MEASUREMENT
An investigation of methods for updating ionospheric scintillation models using topside in-situ plasma density measurements
| AD-A243378 | p 1316 N92-17209

DEPENDENT VARIABLES
A variational formalism for the radiative transfer equation: Prelude to model 3 p 1322 N92-17978

DEPOSITION
Codeposition of elements in diffusion coatings by the halide-activated pack cementation method
| AD-A242860 | p 1267 N92-17042
An investigation of underpotentially deposited thallium of silver (111) by in-situ surface x ray scattering
| AD-A243270 | p 1263 N92-17271
A model for voltammograms of the underpotential deposition of metals
| AD-A243199 | p 1264 N92-17370
Au and Al Schottky barrier formation on GaAs (100) surfaces prepared by thermal desorption of a protective arsenic coating
| DE92-002456 | p 1376 N92-17781

DEPOSITS
An optical roughness sensor for the real time determination of spray formed preform quality
| AD-A243238 | p 1262 N92-17056
The effect of weld metal strength mismatch on the deformation and fracture behavior of steel butt weldments
| AD-A243239 | p 1262 N92-17057
The effect of titanium inclusions on HY-80 GMA weld deposits
| AD-A243408 | p 1239 N92-17192

DESIGN ANALYSIS
The NASA/industry design analysis methods for vibrations (DAMVIBS) program: Accomplishments and contributions
| NASA-TM-104192 | p 1309 N92-17034
Construction equipment for lunar surface operations
| AD-A243665 | p 1389 N92-17123
Use of Navier-Stokes analysis in section design
| AD-A242074 | p 1295 N92-17168
Environmental control and life support system evolution analysis p 1246 N92-17355
Suspended substrate resonator design
| AD-A243250 | p 1290 N92-17573
Preliminary design study of a central solar heating plant with seasonal storage at the University of Massachusetts, Amherst
| DE92-000762 | p 1313 N92-17577
The StarLite Project prototyping real-time software
| AD-A242032 | p 1342 N92-17636
Preliminary development of a three-dimensional nonlinear approximation procedure for turbomachinery design optimization applications
| AD-A243155 | p 1235 N92-17644

DETECTION
A covariance modeling approach to adaptive beamforming and detection
| AD-A241887 | p 1279 N92-17040
Analysis of the terminal Doppler weather radar algorithm for detecting rotation associated with microbursts
| AD-A242840 | p 1318 N92-17050
An optical roughness sensor for the real time determination of spray formed preform quality
| AD-A243238 | p 1262 N92-17056
Detection and spectroscopy of single pentacene molecules in a p-terphenyl crystal by means of fluorescence excitation
| AD-A243747 | p 1356 N92-17196
Single molecule spectral diffusion in a solid detected via fluorescence spectroscopy
| AD-A243748 | p 1356 N92-17197
Incipient fault detection using higher-order statistics
| AD-A243493 | p 1308 N92-17431
High-speed beam switching processor
| AD-D015108 | p 1285 N92-17829
Solar neutrino physics in the nineties
| DE92-003848 | p 1390 N92-17883
Differential pressure sensor
| AD-D015134 | p 1302 N92-17918
Detection of explosives material on single microparticles
| DE92-004408 | p 1276 N92-17963

DETERMINANTS
One-loop calculations with massive particles
| ETN-92-90563 | p 1359 N92-17518

DETONATION
Structures to resist the effects of accidental explosions
| AD-A243272 | p 1277 N92-17272

DETONATION WAVES
The effect of detonation curvature on cylindrical wall motion
| DE92-003110 | p 1298 N92-17625

DEUTERIUM
Laser-based ignition of H2/O2 and D2/O2 premixed gases near 243 nm: The first report of a deuterium isotope wavelength effect in laser ignition
| AD-A243180 | p 1303 N92-17137
Molecular motions of the head group of SHBS in lamellar liquid crystals
| AD-A243499 | p 1373 N92-17382
Steady-state, high dose neutron generation and concentration apparatus and method for deuterium atoms
| AD-D015063 | p 1358 N92-17462
Evidence for MeV particle emission from Ti charged with low energy deuterium ions
| AD-A243718 | p 1359 N92-17505
Concentration of isotopic hydrogen by temperature gradient effect in soluble metal
| AD-D015062 | p 1260 N92-17628

DEUTERIUM PLASMA
Steady-state, high dose neutron generation and concentration apparatus and method for deuterium atoms
| AD-D015063 | p 1358 N92-17462

DEW POINT
A proposed improved method of radiosonde humidity sensing
| AD-A242954 | p 1319 N92-17233

DIAGNOSIS
Facing page test for the astronaut science advisor presentation p 1248 N92-17411
DIAMINES
Substituted 1,1,1-triaryl-2,2,2-trifluoroethanes and processes for their synthesis
| NASA-CASE-LEW-14345-6 | p 1255 N92-17882
DIAMOND FILMS
Determination of the optical constants of thin Chemical-Vapor-Deposited diamond windows from 0.5 to 6.5 eV
| AD-A243094 | p 1268 N92-17170
Use of diamond as an optical material
| AD-A243097 | p 1268 N92-17172
High resolution electron microscopy of diamond film growth defects and their interactions
| AD-A243093 | p 1372 N92-17238
Spatially and spectrally resolved cathodoluminescence measurements of CVD-grown diamond particles and films
| AD-A243220 | p 1271 N92-17615
DIAMONDS
Materials processing of diamond: Etching, doping by ion implantation and contact formation
| AD-A243060 | p 1267 N92-17065
Chemical vapor deposited diamond
| AD-A243095 | p 1268 N92-17171
Use of diamond as an optical material
| AD-A243097 | p 1268 N92-17172
Transmission electron microscopy of the CVD diamond film/substrate interface
| AD-A243096 | p 1373 N92-17322
Method of joining diamond structures
| AD-D015066 | p 1269 N92-17397
Determination of the tribological fundamentals of solid lubricated ceramics. Volume 3: Appendices P through 2
| AD-A242872 | p 1270 N92-17597
Method of doping single crystal diamond for electronic devices
| AD-D015069 | p 1374 N92-17610
Consolidation of diamond packed powders
| AD-D015071 | p 1270 N92-17612
Evaluation of environmentally safe cleaning agents for diamond turned optics
| DE92-002524 | p 1278 N92-17780
DIELECTRIC PROPERTIES
Dielectric properties of aligned conducting polymers
| AD-A243389 | p 1268 N92-17191
Permittivity probe modelling
| AD-A243236 | p 1260 N92-17572
DIELECTRICS
The 5th Annual US-Japan Seminar on Dielectric and Piezoelectric Ceramics
| AD-A243465 | p 1268 N92-17193
Total Dielectric Isolation (TDI) of fully depleted device structures
| AD-A241926 | p 1289 N92-17439
Heat transfer enhancement due to bubble pumping in FC-72 near the saturation temperature
| AD-A243558 | p 1292 N92-17724
A study of electric transmission lines for use on the lunar surface p 1292 N92-17742
Thin films under chemical stress
| DE92-004684 | p 1377 N92-17857
DIENES
Thermal insulation chemical composition and method of manufacture
| AD-D015106 | p 1257 N92-17836
DIFFERENTIAL EQUATIONS
The instability of linear heterogeneous Lanchester equations
| AD-A243519 | p 1350 N92-17081
A new interpolation procedure for adapting Runge-Kutta methods to delay differential equations
| TW-90-09 | p 1351 N92-17517
Alfven waves in inhomogeneous magnetic fields: An integro-differential equation formulation
| DE92-609544 | p 1371 N92-17806
DIFFERENTIAL GEOMETRY
Geometrical methods for the analysis of cosmological observations
| ETN-92-90584 | p 1386 N92-17523
DIFFERENTIAL PRESSURE
Differential pressure sensor
| AD-D015134 | p 1302 N92-17918
DIFFERENTIAL PULSE CODE MODULATION
Comparative analysis of gray scale coding techniques for group 4 facsimile
| AD-A243175 | p 1278 N92-16996
DIFFRACTION
Photorefractivity in doped nonlinear organic polymers
| AD-A243751 | p 1271 N92-17661
A rigorous uniform diffraction analysis of the electromagnetic scattering from impedance edges and junctions
| AD-A243649 | p 1284 N92-17735
DIFFRACTION PATTERNS
Diffraction and imaging theory of inelastically scattered electrons: A new approach
| DE91-018248 | p 1360 N92-17574
DIFFUSE RADIATION
Laser range safety
| AD-A243606 | p 1305 N92-17962
DIFFUSION
Codeposition of elements in diffusion coatings by the halide-activated pack cementation method
| AD-A242860 | p 1267 N92-17042
Effective viscosity in the simulation of spatially evolving shear flows with monotonic FCT models
| AD-A243709 | p 1295 N92-17126
Reaction kinetics and transport properties of the CaO-SO2-O2 system in absence of intra-particle diffusion
| DE91-002086 | p 1261 N92-17788
Kinetics of a new phase formation in supersaturated solid solutions. 1. Dilute one-component systems
| DE92-610065 | p 1262 N92-17943
DIFFUSION FLAMES
Local extinction mechanisms in non-premixed turbulent combustion
| AD-A242027 | p 1260 N92-17682
DIFFUSION THEORY
Characterization of the thermalness of a fissile system with a 2-group diffusion theory parameter
| AD-A243065 | p 1360 N92-17555
DIFFUSIVITY
Gas transport in polybutadiene treated with aqueous bromine
| AD-A241871 | p 1295 N92-17025
DIGITAL COMPUTERS
The square root cordic
| AD-A242318 | p 1342 N92-17561
Improvement of data processing system for gust wind tunnel data acquisition part: System conversion from off-line to on-line processing
| NAL-TM-611 | p 1238 N92-17756
DIGITAL DATA
HEMP test on FD-565
| AD-A243099 | p 1278 N92-16980
Study of features of binary images using algebra techniques
| AD-A242010 | p 1351 N92-17609
DIGITAL ELECTRONICS
Global optimization of digital circuits
| AD-A243740 | p 1289 N92-17480
Use of the algebraic coding theory in nuclear electronics
| DE92-611125 | p 1351 N92-17813
DIGITAL FILTERS
Simulation of finite-precision effects in digital filters
| AD-A243758 | p 1342 N92-17601
New algorithms for broad-band and narrowband source localization and a separable 2-D IIR filter realization
| AD-A243457 | p 1291 N92-17654
DIGITAL SYSTEMS
An overview of cellular telecommunications
| AD-A242951 | p 1281 N92-17232
The calibration process of digital cameras
| ETN-92-90583 | p 1301 N92-17437
Assessment of cockpit interface concepts for data link retrofit
| NASA-CR-187615 | p 1228 N92-17512
Interim Service ISDN Satellite (ISIS) hardware experiment design for advanced ISDN satellite design and experiments
| NASA-CR-186943 | p 1250 N92-17585
A robust digital flight control system for an unfanned research vehicle using discrete quantitative feedback theory
| AD-A243638 | p 1237 N92-17748
Fiber optic angular orientation sensor digital serial encoding
| AD-D015102 | p 1302 N92-17826
DIGITS
Significant digit computation of the ellipsoidal coverage function and its inverse
| AD-A242322 | p 1350 N92-17242
DIODES
Waveguide four-wave mixing
| AD-A243555 | p 1286 N92-17017
DIPOLE ANTENNAS
Superdirective properties of closed loops of parallel coplanar dipoles
| AD-A243009 | p 1288 N92-17268
DIRECT CURRENT
Implementation of an object-oriented flight simulator D.C. electrical system on a hypercube architecture
| AD-A243700 | p 1238 N92-17097
Analytical determination of arrest and starting torque of a bipolar DC motor with permanent magnets
| ETN-92-90586 | p 1290 N92-17540
Gate drain geometry effect on the current voltage characteristics of GaAs MESFETs
| AD-A243430 | p 1291 N92-17684
Transformerless DC-DC voltage amplifier with optically isolated switching devices
| NASA-CASE-NPO-17994-1-CU | p 1293 N92-17907
DIRECT LIFT CONTROLS
Identification of the stability and control derivatives of a DLC-flap system for VSRA
| NAL-TR-1116 | p 1237 N92-17917
DIRECTION FINDING
Radio sky mapping from satellites at very low frequencies
| NASA-TM-105452 | p 1387 N92-17694
DIRECTIONAL CONTROL
Model identification and control system design for the lambda unmanned research vehicle
| AD-A241859 | p 1306 N92-17024
DISCONTINUITY
Microstrip discontinuity models to 60 GHz
| AD-A242038 | p 1339 N92-17185
A discontinuity study in shielded coplanar line
| AD-A242976 | p 1288 N92-17290
DISCOVERY (ORBITER)
STS-41 Space Shuttle mission report
| NASA-TM-105479 | p 1240 N92-16973
STS-31 Space Shuttle mission report
| NASA-TM-105475 | p 1241 N92-17364
DISEASES
The effects of storage on irradiated red blood cells: An in vitro an in vivo study
| AD-A243387 | p 1329 N92-17190
DISK OPERATING SYSTEM (DOS)
Modeling convergence zone gain on MS-DOS based personal computers
| AD-A243252 | p 1341 N92-17558
DISPLACEMENT
Experimental investigation of adiabatic shear banding at different impact velocities
| AD-A243011 | p 1310 N92-17256
An investigation of underpotentially deposited thallium of silver (111) by in-situ surface x ray scattering
| AD-A243270 | p 1263 N92-17271
DISPLAY DEVICES
Neural network classification of mental workload conditions by analysis of spontaneous electroencephalograms
| AD-A243369 | p 1331 N92-17115
Acquisition and production of skilled behavior in dynamic decision-making tasks
| NASA-CR-189846 | p 1333 N92-17132
AGSSS: The Airborne Graphics Software Support System; an Ada/PHIGS-based display editor for the rapid development of cockpit display software systems
| AD-A243224 | p 1234 N92-17221
Development of a Federal standard for a video codec operating at P x 64 KBPS
| AD-A243005 | p 1281 N92-17267
A performance model of Thermal Imaging System (TISs) which includes the human observer's response to state of the art displays
| AD-A242838 | p 1301 N92-17273
Psychophysical evaluation of three-dimensional auditory displays
| NASA-CR-189848 | p 1355 N92-17692
Image scanning using a fractal curve
| BBC-RD-1991/4 | p 1285 N92-17886
Cockpit display of hazardous weather information p 1220 N92-17989
DISPOSAL
Rates and mechanisms of metastable deactivation over surfaces
| AD-A243391 | p 1361 N92-17652
Sharps container
| NASA-CASE-MSC-21776-1 | p 1278 N92-17913
DISTILLATION
Scale-up of recovery process for waste solvents
| KCP-613-4479 | p 1277 N92-17535
DISTILLATION EQUIPMENT
Scale-up of recovery process for waste solvents
| KCP-613-4479 | p 1277 N92-17535
DISTORTION
High resolution imaging using phase retrieval, volume 2
| AD-A242925 | p 1366 N92-17550
Transmission of thin light beams through turbulent mixing layers
| AD-A243470 | p 1367 N92-17658
DISTRIBUTED FEEDBACK LASERS
Multiperiod-grating surface-emitting lasers
| NASA-CASE-NPO-17763-1-CU | p 1305 N92-17862
DISTRIBUTED PARAMETER SYSTEMS
A general computational framework for distributed sensing and fault-tolerant sensor integration
| AD-A243256 | p 1300 N92-16983

Beyond the Baseline 1991: Proceedings of the Space Station Evolution Symposium. Volume 2: Space Station Freedom, part 1
| NASA-CP-10083-VOL-2-PT-1 | p 1251 N92-17768
DISTRIBUTED PROCESSING
Performance measures for adaptive decisioning systems
| AD-A243183 | p 1352 N92-16998
Resource allocation in distributed memory multiprocessing
| AD-A243165 | p 1345 N92-17188
A distributed design for monitoring, logging, and replaying device readings at LAMPF
| DE92-003860 | p 1240 N92-17591
The StarLite Project prototyping real-time software
| AD-A242032 | p 1342 N92-17636
The UNC graph server: A distributed hypermedia data management system
| AD-A242041 | p 1380 N92-17651
Parallelizing serial code for a distributed processing environment with an application to high frequency electromagnetic scattering
| AD-A243755 | p 1284 N92-17721
Software tools for distributed intelligent control systems
| DE92-004656 | p 1349 N92-17965
DISTRIBUTION (PROPERTY)
Evaluation of solar flares and electron precipitation by nitrate distribution in Antarctica
| AD-A243026 | p 1389 N92-17235
DISTRIBUTION FUNCTIONS
Tests of fit for the Cauchy distribution based on the empirical distribution function
| AD-A243201 | p 1352 N92-17173
The proton spectral function of Ca-40 and Ca-48 studies with (e, e prime p) reaction: An investigation of ground-state correlations
| ETN-92-90566 | p 1358 N92-17433
One-loop calculations with massive particles
| ETN-92-90563 | p 1359 N92-17518
DISTRIBUTION MOMENTS
Wave propagation in a randomly inhomogeneous medium: A study of the problem
| AD-A243741 | p 1284 N92-17691
DIURNAL VARIATIONS
Upper ocean dynamics during the LOTUS and Tropic Heat Experiments
| AD-A243730 | p 1324 N92-17583
DIVING (UNDERWATER)
Evaluation of BAUER high pressure breathing air P-2 purification system
| AD-A243535 | p 1333 N92-17014
Statistically-based decompression tables. 6: Repeat dives on oxyen/nitrogen mixes
| AD-A243667 | p 1328 N92-17124
Multiple input sliding mode control for autonomous diving and steering of underwater vehicles
| AD-A241935 | p 1237 N92-17442
DOCUMENTS
FY 1991 scientific and technical reports, articles, papers, and presentations
| NASA-TM-103567 | p 1384 N92-17586
DOPED CRYSTALS
Stability and structure of C12B24N24: A hybrid analog of buckminsterfullerene
| AD-A242327 | p 1373 N92-17245
Luminescence and electroluminescence properties of Nd, Tm, Yb doped GaAs II-VI compounds
| AD-A242039 | p 1375 N92-17667
Structural, electronic, and magnetic properties of La(x)Sr(1-x)VO3 (0 is less than or equal to x is less than or equal to 1.0)
| DE92-003808 | p 1378 N92-17916
DOPPLER EFFECT
Wind profiler signal detection improvements
| NASA-CR-189781 | p 1317 N92-16990
DOPPLER RADAR
Terminal Doppler weather radar test bed operation, Orlando: January-June 1990
| AD-A242890 | p 1318 N92-17028
Analysis of the terminal Doppler weather radar algorithm for detecting rotation associated with microbursts
| AD-A242840 | p 1318 N92-17050
Front detection with Doppler radar
| AD-A242880 | p 1319 N92-17289
High-frequency meteorological phenomena observed with the Naval Postgraduate School's UHF Doppler wind profiler
| AD-A243762 | p 1320 N92-17515
Cockpit display of hazardous weather information p 1220 N92-17989
DOUBLE BASE PROPELLANTS
Mechanical and thermomechanical properties of NC base propellants
| AD-A243045 | p 1276 N92-17632
DRAG REDUCTION
Injection of drag reducing additives into turbulent water flows
| AD-A243209 | p 1296 N92-17176
Basic hydrodynamics
| AD-A243513 | p 1297 N92-17387
Method and apparatus for reducing drag and noise associated with fluid flow in a conduit
| AD-D015067 | p 1297 N92-17398
Experiments and analysis concerning the use of external burning to reduce aerospace vehicle transonic drag
| NASA-TM-105397 | p 1235 N92-17546
DRILL BITS
Incipient fault detection using higher-order statistics
| AD-A243493 | p 1308 N92-17431
DROP TESTS
Acoustic emission monitoring of low velocity impact damage in graphite/epoxy laminates during tensile loading
| NASA-TM-4339 | p 1258 N92-17881
DROPS (LIQUIDS)
An optical roughness sensor for the real time determination of spray formed preform quality
| AD-A243238 | p 1262 N92-17056
DRUGS
Effects of the chemical defense antidote atropine sulfate on helicopter pilot performance: An in-flight study
| AD-A241966 | p 1328 N92-17084
Evaluation of liposome-encapsulated Hemoglobin/LR16 formulations as a potential blood substitute
| AD-A243075 | p 1329 N92-17557
DRYING
Scale-up of recovery process for waste solvents
| KCP-613-4479 | p 1277 N92-17535
DUALITY PRINCIPLE
Machine scheduling and Lagrangian relaxation
| ETN-92-90569 | p 1353 N92-17839
DUCTILITY
Mechanical and thermomechanical properties of NC base propellants
| AD-A243045 | p 1276 N92-17632
DUCTS
Evaporation duct communication: Test plan, part 2
| AD-A243505 | p 1282 N92-17383
DUST
User evaluation of laser ballistic sun, wind and dust goggle lenses (dye technology)
| AD-A243245 | p 1334 N92-17143
DYNAMIC CHARACTERISTICS
Effective dynamic material parameters and localized scattering
| AD-A241957 | p 1310 N92-17320
DYNAMIC CONTROL
Dynamic pattern matcher using incomplete data
| NASA-CASE-MSC-21415-1-SB | p 1344 N92-17860
Neural networks for aircraft system identification p 1222 N92-17998
DYNAMIC LOADS
Engineering model of unsteady flow in a cavity
| AD-A243636 | p 1299 N92-17747
The SSM/PMAD automated test bed project p 1252 N92-17774
DYNAMIC MODELS
Model identification and control system design for the lambda unmanned research vehicle
| AD-A241859 | p 1306 N92-17024
Feedback in dynamic decision making: An experiment in software project management
| AD-A242361 | p 1380 N92-17451
Magnetospheric response to variations in the interplanetary magnetic field
| AD-A243683 | p 1388 N92-17717
DYNAMIC PRESSURE
Stagnation and dynamic pressure limits for the S1 wind tunnel
| AD-A242989 | p 1238 N92-17297
DYNAMIC RESPONSE
Identification techniques: Frequency domain methods p 1231 N92-17158
A wing rock model for the F-14A aircraft
| AD-A243109 | p 1233 N92-17300
Structural dynamics division research and technology accomplishments for F.Y. 1991 and plans for F.Y. 1992
| NASA-TM-104188 | p 1225 N92-17509
Weight evaluation and sensitivity analysis for space plane. Part 2: TSTO
| NAL-TM-602-PT-2 | p 1251 N92-17754
DYNAMIC STABILITY
Loss terms in free-piston Stirling engine models
| NASA-CR-189840 | p 1312 N92-17225
DYNAMIC STRUCTURAL ANALYSIS
Experiences at Langley Research Center in the application of optimization techniques to helicopter airframes for vibration reduction
| NASA-TM-104193 | p 1309 N92-17033
The NASA/industry design analysis methods for vibrations (DAMVIBS) program: Accomplishments and contributions
| NASA-TM-104192 | p 1309 N92-17034
Structural dynamics division research and technology accomplishments for F.Y. 1991 and plans for F.Y. 1992
| NASA-TM-104188 | p 1225 N92-17509
Program plans: Aviation safety research
| NIAR-91-30 | p 1227 N92-17587
DYNAMICAL SYSTEMS
Summary of the 1991 ACP Workshop on Coherence and Chaos in Complex Dynamical Systems
| AD-A243226 | p 1378 N92-17324

E

E REGION
Auroral-clutter predictions for Fylingdales, England
| AD-A242957 | p 1283 N92-17600
EARLY WARNING SYSTEMS
Early warning satellites: Funding for follow-on system is premature
| AD-A242836 | p 1245 N92-17250
EARTH ATMOSPHERE
A variational assimilation method for satellite and conventional data: Model 2 (version 1) p 1322 N92-17976
EARTH IONOSPHERE
An investigation of methods for updating ionospheric scintillation models using topside in-situ plasma density measurements
| AD-A243378 | p 1316 N92-17209
Investigation of mechanisms for the source and loss of electrons from the radiation belts using data from SEEP, SCATHA and P78-1 satellites
| AD-A243376 | p 1317 N92-17405
EARTH MAGNETOSPHERE
A numerical code for a three-dimensional magnetospheric MHD equilibrium model
| NASA-CR-189852 | p 1316 N92-17227
Magnetospheric response to variations in the interplanetary magnetic field
| AD-A243683 | p 1388 N92-17717
EARTH ORBITAL ENVIRONMENTS
Systems special investigation group
| NASA-CR-187355 | p 1250 N92-17728
EARTH ORBITS
Evolution user requirements for the restructured space station p 1248 N92-17413
EARTH RADIATION BUDGET EXPERIMENT
Spatial sampling error of a scanning radiation budget radiometer
| MITT-76 | p 1317 N92-17542
EARTH TIDES
Tidal and lunar data for Point Mugu, San Nicolas Island, and the Barking Sands area during 1992
| AD-A243210 | p 1324 N92-17177
EARTHQUAKES
Studies of high-frequency seismic wave propagation
| AD-A241938 | p 1316 N92-17202
ECHO SOUNDING
Incremental volume rendering algorithm for interactive 3D ultrasound imaging
| AD-A242048 | p 1342 N92-17637
ECONOMIC ANALYSIS
Economic analysis of information system
| AD-A243079 | p 1382 N92-17067
ECONOMICS
Changing by degrees: Steps to reduce greenhouse gases
| PB91-205120 | p 1314 N92-17619
EDGES
A rigorous uniform diffraction analysis of the electromagnetic scattering from impedance edges and junctions
| AD-A243649 | p 1284 N92-17735
EDITING ROUTINES (COMPUTERS)
Serpent: Dialogue editor user's guide. System for user interface development, version 1
| AD-A242331 | p 1384 N92-17641
EDUCATION
Acoustic simulation for acoustics education
| AD-A243027 | p 1355 N92-17236
Intelligent Computer-Aided Training (ICAT) p 1246 N92-17352
Research and development project summaries, October 1991
| AD-A243477 | p 1391 N92-17372
Comparison of experimental US Air Force and Euro-NATO pilot candidate selection test batteries
| AD-A242358 | p 1332 N92-17450
Causal models in the acquisition and instruction of programming skills
| AD-A242899 | p 1340 N92-17463

Proceedings of the Conference on Health Physics
| DE92-704335 | p 1331 N92-17802
Mathematics and biology
| DE92-611247 | p 1327 N92-17815
Investigation of air transportation technology at Princeton University, 1990-1991 p 1221 N92-17995
Target pitch angle for the microburst escape maneuver p 1221 N92-17996

EFFECTIVE PERCEIVED NOISE LEVELS
Human response to helicopter noise: A test of A-weighting
| AD-A243719 | p 1355 N92-17506

EIGENVALUES
The instability of linear heterogeneous Lanchester equations
| AD-A243519 | p 1350 N92-17081
Inequalities among partial traces of Hermitian operators and partial sums of their Eigenvalues
| DE91-641495 | p 1351 N92-17622

ELASTIC DEFORMATION
Alternate/modified binders for asphalt airfield pavements
| AD-A242829 | p 1238 N92-17260
Acoustical and other physical properties of marine sediments
| AD-A243532 | p 1324 N92-17391
Damage mechanisms in composites
| AD-A242748 | p 1258 N92-17950

ELASTIC PLATES
Static analysis of thick composite plates using higher order three dimensional finite elements
| AD-A243188 | p 1256 N92-17367

ELASTIC PROPERTIES
Toward the robust control of high bandwidth high precision flexible optical systems
| AD-A243471 | p 1366 N92-17536

ELASTIC SCATTERING
Recent developments in neutrino physics
| DE92-003855 | p 1360 N92-17589
Proton-proton and proton-antiproton elastic scattering at high energies: Theory, phenomenology, and experiment
| DE92-004414 | p 1364 N92-17964

ELASTOMERS
Thermal insulation chemical composition and method of manufacture
| AD-D015106 | p 1257 N92-17836

ELECTRIC BATTERIES
EMU evolution p 1246 N92-17354
Performance of battery charge controllers: First year test report
| DE92-002924 | p 1289 N92-17468

ELECTRIC CHARGE
Performance of battery charge controllers: First year test report
| DE92-002924 | p 1289 N92-17468
An algorithm for calculating the electronic spectrum and function of the charge density distributions of crystals p 1375 N92-17698

ELECTRIC CONDUCTORS
A rigorous UTD analysis of electromagnetic scattering from resistive strips and resistive-loaded conducting strips
| AD-A243691 | p 1280 N92-17092

ELECTRIC CONTACTS
Substantially oxygen-free contact tube
| NASA-CASE-LAR-14169-1 | p 1307 N92-17677

ELECTRIC CONTROL
Electrically-controlled polymeric gels as active materials in adaptive structures
| DE92-002947 | p 1272 N92-17710

ELECTRIC CURRENT
Electromagnetic pulse-induced current measurement device
| AD-A241946 | p 1291 N92-17668

ELECTRIC DISCHARGES
Precision multi-channel fiber optic interface and method
| AD-D015104 | p 1367 N92-17828

ELECTRIC FIELDS
Exploring plasma sheath solutions for planar and cylindrical anodes
| AD-A243237 | p 1369 N92-17030
Two-beam coupling measurements of grating phase in a photorefractive polymer
| AD-A243746 | p 1268 N92-17195
Natural resonances of slotted cylinder configurations
| AD-A241934 | p 1282 N92-17441
Radar-satellite studies of the high-latitude ionosphere
| AD-A243275 | p 1317 N92-17961

ELECTRIC GENERATORS
Space Station Freedom electric power system evolution analysis status p 1251 N92-17771
Explosive magnetic field compression generator transformer power supply for high resistive loads
| AD-D015123 | p 1293 N92-17831

ELECTRIC MOTOR VEHICLES
Versatile Data Acquisition System Model II user's manual
| DE92-003311 | p 1384 N92-17470

ELECTRIC POTENTIAL
A model for voltammograms of the underpotential deposition of metals
| AD-A243199 | p 1264 N92-17370
Temporally-specific modification of myelinated axon excitability in vitro following a single ultrasound pulse
| AD-A242329 | p 1326 N92-17474
Gate drain geometry effect on the current voltage characteristics of GaAs MESFETs
| AD-A243430 | p 1291 N92-17684
Fracture toughness evaluation for N Reactor pressure tubes of Zircaloy-2 using the electric-potential method
| DE92-003631 | p 1311 N92-17713
A study of electric transmission lines for use on the lunar surface p 1292 N92-17742

ELECTRIC POWER TRANSMISSION
Space Station Freedom electric power system evolution analysis status p 1251 N92-17771

ELECTRIC SWITCHES
Innovative switching technology
| DE92-003068 | p 1292 N92-17708

ELECTRICAL ENGINEERING
A diffraction limited nitrogen laser for detector calibration in high energy physics
| ETN-92-90567 | p 1303 N92-17434

ELECTRICAL FAULTS
DOE Task Force Meeting on Electrical Breakdown of Insulating Ceramics in a High Radiation Field
| DE92-000459 | p 1270 N92-17576

ELECTRICAL IMPEDANCE
A rigorous UTD analysis of electromagnetic scattering from resistive strips and resistive-loaded conducting strips
| AD-A243691 | p 1280 N92-17092
Evaluation of an Interdigitated Gate Electrode Field-Effect Transistor (IGEFET) for in situ resin cure monitoring
| AD-A243713 | p 1289 N92-17501
Permittivity probe modelling
| AD-A243236 | p 1260 N92-17572
The surface impedance synthesis technique
| AD-A243731 | p 1284 N92-17689

ELECTRICAL INSULATION
DOE Task Force Meeting on Electrical Breakdown of Insulating Ceramics in a High Radiation Field
| DE92-000459 | p 1270 N92-17576

ELECTRICAL MEASUREMENT
Preparation of ferroelectric samples for electrical and radiation characterization studies
| AD-A243432 | p 1288 N92-17326
Development of a system for void fraction measuring by electroprobing method
| DE92-610933 | p 1309 N92-17809

ELECTRICAL PROPERTIES
Testing and evaluation of the Vanner electrical inverters, models 24-1500 and SP 00112
| AD-A241914 | p 1287 N92-17216
Preparation of ferroelectric samples for electrical and radiation characterization studies
| AD-A243432 | p 1288 N92-17326
Structural, electronic, and magnetic properties of La(x)Sr(1-x)VO3 (0 is less than or equal to x is less than or equal to 1.0)
| DE92-003808 | p 1378 N92-17916

ELECTRICAL RESISTIVITY
Electronic and ionic transport in processable conducting polymers. Symmetry effects on the physical and electrically conducting, substituted poly(di-2-thienylphenylenes)
| AD-A242328 | p 1266 N92-16976
Critical temperature determination in superconductors
| AD-A243537 | p 1371 N92-17015
Evidence for strong electron-phonon coupling in thermal conductivity of YBa2Cu3O(7-delta)
| AD-A243192 | p 1372 N92-17218
Development of processible electroactive oligomers and polymers
| AD-A243723 | p 1270 N92-17508
Electrical and thermal conductivity of a variable zone semiconductor in a longitudinal magnetic field p 1291 N92-17702
Explosive magnetic field compression generator transformer power supply for high resistive loads
| AD-D015123 | p 1293 N92-17831

ELECTRICITY
Thermally regenerative fuel cells
| AD-A242900 | p 1290 N92-17629

ELECTRO-OPTICS
Innovative optoelectronic materials and structures using OMVPE
| AD-A243257 | p 1371 N92-16984
The analysis of a stabilized 1.5 Mach-Zehnder interferometric sensor with enhanced sensitivity and common-mode compensation
| AD-A243384 | p 1286 N92-17116
Two-beam coupling measurements of grating phase in a photorefractive polymer
| AD-A243746 | p 1268 N92-17195
Photorefractivity in doped nonlinear organic polymers
| AD-A243751 | p 1271 N92-17661

ELECTROCHEMICAL OXIDATION
Separation of neutral-to-polaron and polaron-to-bipolaron redox events in alkoxy substituted di-2-thienylphenylene polymers
| AD-A242423 | p 1271 N92-17679
Light-controlled, electrochemical, anisotropic etching of silicon
| MBB-Z-0368-91-PUB | p 1261 N92-17841

ELECTROCHEMISTRY
Electronic and ionic transport in processable conducting polymers
| AD-A242258 | p 1269 N92-17460
Electrochemically initiated chain polymerization of pyrrole in aqueous media
| AD-A242259 | p 1269 N92-17461
Thermally regenerative fuel cells
| AD-A242900 | p 1290 N92-17629
Separation of neutral-to-polaron and polaron-to-bipolaron redox events in alkoxy substituted di-2-thienylphenylene polymers
| AD-A242423 | p 1271 N92-17679

ELECTRODEPOSITION
In situ surface x ray crystallography of electrochemically deposited Bi on Ag(111): Structure, compressibility, and anisotropy
| AD-A243218 | p 1372 N92-17181
In situ structural studies of the underpotential deposition of copper onto an iodine covered platinum surface using x ray standing waves
| AD-A243475 | p 1263 N92-17328

ELECTRODES
Dielectric properties of aligned conducting polymers
| AD-A243389 | p 1268 N92-17191
A model for voltammograms of the underpotential deposition of metals
| AD-A243199 | p 1264 N92-17370
Substantially oxygen-free contact tube
| NASA-CASE-LAR-14169-1 | p 1307 N92-17677

ELECTROENCEPHALOGRAPHY
Neural network classification of mental workload conditions by analysis of spontaneous electroencephalograms
| AD-A243369 | p 1331 N92-17115
A topographical analysis of the human electroencephalogram for patterns in the development of motion sickness
| AD-A243656 | p 1328 N92-17120

ELECTROFORMING
Precision multi-channel fiber optic interface and method
| AD-D015104 | p 1367 N92-17828

ELECTROLUMINESCENCE
Luminescence and electroluminescence properties of Nd, Tm, Yb doped GaAs II-VI compounds
| AD-A242039 | p 1375 N92-17667

ELECTROLYTES
Electronic and ionic transport in processable conducting polymers
| AD-A242258 | p 1269 N92-17460
Surface chemistry at the semiconductor/electrolyte interface
| DE91-018511 | p 1374 N92-17532

ELECTROLYTIC CELLS
Lithiated Vanadium Oxide (LVO), gamma-lithium vanadium bronze (Gamma-LIV2O5) and vanadium dioxide (VO2) as thermal battery cathode materials
| AD-A242948 | p 1287 N92-17186
Dielectric properties of aligned conducting polymers
| AD-A243389 | p 1268 N92-17191

ELECTROMAGNETIC ABSORPTION
Determination of the optical constants of thin Chemical-Vapor-Deposited diamond windows from 0.5 to 6.5 eV
| AD-A243094 | p 1268 N92-17170
A study of nonlinear reflection and optical switching in indium antimonide
| AD-A242835 | p 1365 N92-17249

ELECTROMAGNETIC INTERACTIONS
Electronic interactions of directed photon beams with surfaces
| AD-A241878 | p 1356 N92-17026
Natural resonances of slotted cylinder configurations
| AD-A241934 | p 1282 N92-17441

ELECTROMAGNETIC INTERFERENCE
Design of a fiber optic image transmission link
| AD-A243686 | p 1365 N92-17088

Constant modulus algorithm techniques for the enhancement of signal quality
| AD-A242986 | p 1288 N92-17295

ELECTROMAGNETIC MEASUREMENT
Electromagnetic pulse-induced current measurement device
| AD-A241946 | p 1291 N92-17668

ELECTROMAGNETIC NOISE
Spectral error models applied to the geodetic boundary value problem
| ETN-92-90582 | p 1312 N92-17436
Analog optical neural nets: A noise sensitivity analysis
| AD-A242920 | p 1346 N92-17465

ELECTROMAGNETIC PULSES
HEMP test on FD-565
| AD-A243099 | p 1278 N92-16980
Electromagnetic pulse-induced current measurement device
| AD-A241946 | p 1291 N92-17668

ELECTROMAGNETIC RADIATION
A CAD model for the axial inductive strip with finite thickness centered in homogeneous finline with w/b = 1
| AD-A243553 | p 1278 N92-17016
Frequency stirring: An alternate approach to mechanical mode-stirring for the conduct of electromagnetic susceptibility testing
| AD-A243551 | p 1279 N92-17031
Natural resonances of slotted cylinder configurations
| AD-A241934 | p 1282 N92-17441
Radio sky mapping from satellites at very low frequencies
| NASA-TM-105452 | p 1387 N92-17694
Explosive magnetic field compression generator transformer power supply for high resistive loads
| AD-D015123 | p 1293 N92-17831

ELECTROMAGNETIC SCATTERING
A rigorous UTD analysis of electromagnetic scattering from resistive strips and resistive-loaded conducting strips
| AD-A243691 | p 1280 N92-17092
A theory of inverse operators for multiple excitations
| AD-A243484 | p 1350 N92-17330
The surface impedance synthesis technique
| AD-A243731 | p 1284 N92-17689
Parallelizing serial code for a distributed processing environment with an application to high frequency electromagnetic scattering
| AD-A243755 | p 1284 N92-17721
A rigorous uniform diffraction analysis of the electromagnetic scattering from impedance edges and junctions
| AD-A243649 | p 1284 N92-17735

ELECTROMAGNETISM
Parallel processing applied to computational electromagnetics
| AD-A242372 | p 1345 N92-17395
Cooled ion frequency standard
| AD-A242030 | p 1360 N92-17549

ELECTROMAGNETS
Magnetic field distribution and design of Helmholtz coils
| AD-A242978 | p 1288 N92-17291

ELECTROMECHANICS
Electrically-controlled polymeric gels as active materials in adaptive structures
| DE92-002947 | p 1272 N92-17710

ELECTRON ACCELERATORS
The proton spectral function of Ca-40 and Ca-48 studies with (e, e prime p) reaction: An investigation of ground-state correlations
| ETN-92-90566 | p 1358 N92-17433
The determination of the number of light neutrino species
| ETN-92-90564 | p 1359 N92-17519
Emittance growth from space-charge forces
| DE92-003804 | p 1364 N92-17796

ELECTRON BEAMS
Electronic interactions of directed photon beams with surfaces
| AD-A241878 | p 1356 N92-17026
The effects of field errors on low-gain free electron lasers
| AD-A243710 | p 1303 N92-17127
Measurement of electron beam emittance using optical transition radiation and development of a diffuse screen electron beam monitor
| AD-A241893 | p 1357 N92-17306
Some aspects of nonneutral plasma physics
| AD-A243711 | p 1369 N92-17499
Diffraction and imaging theory of inelastically scattered electrons: A new approach
| DE91-018248 | p 1360 N92-17574
The Los Alamos FEL photoinjector drive laser
| DE92-003791 | p 1305 N92-17795
Emittance growth from space-charge forces
| DE92-003804 | p 1364 N92-17796
Effects of the high-frequency beam space charge forces on the excitation of electromagnetic waves in relativistic carcinotron
| DE92-610956 | p 1285 N92-17812
Achromatic and isochronous electron beam transport for tunable free electron lasers
| DE92-003908 | p 1305 N92-17868

ELECTRON CYCLOTRON HEATING
Active heater control and regulation for the Varian VGT-8011 gyrotron
| DE92-003638 | p 1302 N92-17454
Ion sources based on electron cyclotron resonance p 1362 N92-17743

ELECTRON DENSITY (CONCENTRATION)
Equation of state and conductivity of hot, dense matter
| AD-A243359 | p 1369 N92-17301
Constraints on cosmic ray propagation in the galaxy
| NASA-CR-189779 | p 1390 N92-18003
Low frequency interstellar scattering and pulsar observations p 1390 N92-18005

ELECTRON DIFFRACTION
Diffraction and imaging theory of inelastically scattered electrons: A new approach
| DE91-018248 | p 1360 N92-17574

ELECTRON DISTRIBUTION
Evaluation of solar flares and electron precipitation by nitrate distribution in Antarctica
| AD-A243026 | p 1389 N92-17235
X ray damage to CF3CO2-Terminated organic monolayers on Si/Au supports is due primarily to x ray induced electrons
| AD-A243446 | p 1289 N92-17490
Rates and mechanisms of metastable deactivation over surfaces
| AD-A243391 | p 1361 N92-17652

ELECTRON IRRADIATION
Growth rate of dislocation loop in Fe-Ni-Cr alloy under Kr(+) ion and electron irradiation
| DE92-001908 | p 1265 N92-17703

ELECTRON MICROSCOPY
High resolution electron microscopy of diamond film growth defects and their interactions
| AD-A243093 | p 1372 N92-17238
Long-term corrosion evaluation of stainless steels in Space Shuttle iodinated resin and water
| NASA-TM-104743 | p 1264 N92-17376
Microstructure and composition of electromagnetically-characterized YBa2Cu3O(7-delta) grain boundaries
| DE92-003520 | p 1376 N92-17782
Grain boundaries
| DE92-004420 | p 1378 N92-17941

ELECTRON PARAMAGNETIC RESONANCE
Separation of neutral-to-polaron and polaron-to-bipolaron redox events in alkoxy substituted di-2-thienylphenylene polymers
| AD-A242423 | p 1271 N92-17679
The EPR of the triplet state of aryl cations in crystals of diazonium salts p 1375 N92-17701

ELECTRON PLASMA
Excitons in semiconducting superlattices, quantum wells, and ternary alloys
| DE91-018805 | p 1374 N92-17528

ELECTRON PRECIPITATION
Evaluation of solar flares and electron precipitation by nitrate distribution in Antarctica
| AD-A243026 | p 1389 N92-17235

ELECTRON SCATTERING
Diffraction and imaging theory of inelastically scattered electrons: A new approach
| DE91-018248 | p 1360 N92-17574

ELECTRON SOURCES
Equation of state and conductivity of hot, dense matter
| AD-A243359 | p 1369 N92-17301

ELECTRON STATES
Determination of the electronic density of states of YBa2Cu3O(7-delta)
| AD-A243223 | p 1372 N92-17220
One nucleon transition densities for 1p shell nuclei
| DE92-600629 | p 1363 N92-17957

ELECTRON TRANSFER
Dynamics and stabilization of materials possessing high energy content
| AD-A243030 | p 1258 N92-16977
Estimation of the outer sphere contribution to the activation parameters for homogeneous electron transfer reactions using the mean spherical approximation
| AD-A243217 | p 1259 N92-17323
Artificial photosynthesis: Progress toward molecular systems for photoconversion
| DE92-003370 | p 1326 N92-17471
Calculations of electron and photon transport between 1 MeV and 1 eV
| AD-A243725 | p 1359 N92-17514
A theoretical search for supervelocity semiconductors
| AD-A241981 | p 1376 N92-17783

ELECTRON TUNNELING
Atomic relaxation at ordered electrochemical surfaces probed by scanning tunneling microscopy: Au(111) in aqueous solution compared with ultrahigh-vacuum environments
| AD-A242031 | p 1358 N92-17472

ELECTRONIC COUNTERMEASURES
C3 Systems Technology Symposium on Advance Planning Briefings for Industry
| AD-A243466 | p 1391 N92-17657

ELECTRONIC EQUIPMENT
X ray lithography in Japan
| AD-A243660 | p 1286 N92-17087
Implementation of an object-oriented flight simulator D.C. electrical system on a hypercube architecture
| AD-A243700 | p 1238 N92-17097
Electronic expansion of human perception
| AD-A242028 | p 1333 N92-17634

ELECTRONIC EQUIPMENT TESTS
A study of ignition and simulation circuits for arcjet thrusters, part 1
| NASA-CR-189097 | p 1253 N92-17510

ELECTRONIC MAIL
Electronic data interchange
| AD-A242959 | p 1382 N92-17136

ELECTRONIC PACKAGING
The 5th Annual US-Japan Seminar on Dielectric and Piezoelectric Ceramics
| AD-A243465 | p 1268 N92-17193

ELECTRONS
Electronic interactions of directed photon beams with surfaces
| AD-A241878 | p 1356 N92-17026
Investigation of mechanisms for the source and loss of electrons from the radiation belts using data from SEEP, SCATHA and P78-1 satellites
| AD-A243376 | p 1317 N92-17405
Medium-energy neutrino physics
| DE92-003790 | p 1362 N92-17666

ELECTROPHORESIS
Molecular recognition in gels, monolayers, and solids
| AD-A243488 | p 1358 N92-17428

ELECTROPLATING
Inductively coupled plasma atomic emission spectroscopy analysis of gold electroplating solutions
| DE92-004798 | p 1266 N92-17858

ELECTROSTATIC CHARGE
Computational studies of energetic nitramines
| AD-A241870 | p 1356 N92-17038

ELECTROSTATICS
Atomic relaxation at ordered electrochemical surfaces probed by scanning tunneling microscopy: Au(111) in aqueous solution compared with ultrahigh-vacuum environments
| AD-A242031 | p 1358 N92-17472

ELEVATION
Comparison of two eighth-mesh terrain databases
| AD-A243315 | p 1383 N92-17401

ELLIPSOIDS
Automated composite ellipsoid modelling for high frequency GTD analysis
| NASA-CR-189853 | p 1233 N92-17316

ELLIPSOMETERS
An interface enhanced spectroscopic ellipsometry technique: Application to Si-SiO2
| AD-A242867 | p 1260 N92-17613

ELLIPSOMETRY
An in-situ spectroscopic ellipsometry study of the electron cyclotron resonance plasma oxidation of silicon and interfacial
| AD-A242833 | p 1259 N92-17247
Infrared rotating analyzer ellipsometry: Calibration and data processing
| AD-A242834 | p 1259 N92-17248
A spectroscopic immersion ellipsometry study of the mechanism of Si/SiO2 interface annealing
| AD-A242831 | p 1259 N92-17261
An interface enhanced spectroscopic ellipsometry technique: Application to Si-SiO2
| AD-A242867 | p 1260 N92-17613

ELLIPTIC FUNCTIONS
Eddy breakdown and structure development
| AD-A241886 | p 1295 N92-17039

ELLIPTICAL ORBITS
An alternative concept for aeroassisted orbit transfers
| AD-A243409 | p 1239 N92-17325

EMBEDDED COMPUTER SYSTEMS
An analysis of mission critical computer software in Naval aviation
| AD-A243078 | p 1339 N92-17237

Embedded fault-tolerant computer for mission critical applications
| AD-A242886 | p 1342 N92-17566
Adaptive on-line help for embedded instructional systems
| AD-A243675 | p 1343 N92-17716

EMBRITTLEMENT
Effect of coatings and processing on failure mechanisms of polycarbonate material, phase 1
| AD-A243018 | p 1256 N92-17053

EMISSION SPECTRA
Luminescence and electroluminescence properties of Nd, Tm, Yb doped GaAs II-VI compounds
| AD-A242039 | p 1375 N92-17667
Inductively coupled plasma atomic emission spectroscopy analysis of gold electroplating solutions
| DE92-004798 | p 1266 N92-17858

EMITTANCE
Measurement of electron beam emittance using optical transition radiation and development of a diffuse screen electron beam monitor
| AD-A241893 | p 1357 N92-17306
Emittance growth from space-charge forces
| DE92-003804 | p 1364 N92-17796

EMITTERS
Comparison of alkali ion emitters
| AD-A243105 | p 1290 N92-17570

EMULSIONS
Development of fuel neutralizing agents to prevent flashback on aircraft fires
| AD-A242828 | p 1227 N92-17259

END EFFECTORS
Collision avoidance sensor skin p 1247 N92-17361

ENERGY CONVERSION
Explosive magnetic field compression generator transformer power supply for high resistive loads
| AD-D015123 | p 1293 N92-17831

ENERGY CONVERSION EFFICIENCY
Picosecond laser breakdown thresholds in gases
| AD-A242941 | p 1304 N92-17475

ENERGY DISSIPATION
Application of silicon micromachining to thermal dissipation issues in wafer scale integrated circuits
| AD-A243744 | p 1288 N92-17332
X ray damage to CF3CO2-Terminated organic monolayers on Si/Au supports is due primarily to x ray induced electrons
| AD-A243446 | p 1289 N92-17490

ENERGY LEVELS
High-speed beam switching processor
| AD-D015108 | p 1285 N92-17829
One nucleon transition densities for 1p shell nuclei
| DE92-600629 | p 1363 N92-17957

ENERGY SPECTRA
Laser-based ignition of H2/O2 and D2/O2 premixed gases near 243 nm: The first report of a deuterium isotope wavelength effect in laser ignition
| AD-A243180 | p 1303 N92-17137

ENERGY STORAGE
High current transistor pulse generator
| DE92-004774 | p 1292 N92-17801

ENERGY TECHNOLOGY
Summaries of FY 1991 engineering research
| DE92-004708 | p 1277 N92-17593
Changing by degrees: Steps to reduce greenhouse gases
| PB91-205120 | p 1314 N92-17619

ENERGY TRANSFER
Vibrational energy transfer in bromine monofluoride
| AD-A243690 | p 1259 N92-17091
Quenching and rotational energy transfer in molecular bromine: Br2(B)
| AD-A241987 | p 1357 N92-17321
Calculations of electron and photon transport between 1 MeV and 1 eV
| AD-A243725 | p 1359 N92-17514
Collisional energy deposition threshold for extended damage depths in ion-implanted silicates
| DE92-004737 | p 1377 N92-17797

ENGINE DESIGN
Program plans: Aviation safety research
| NIAR-91-30 | p 1227 N92-17587

ENGINE FAILURE
Program plans: Aviation safety research
| NIAR-91-30 | p 1227 N92-17587

ENGINE INLETS
Modification of Jindivik air intake duct with an auxiliary intake static aerodynamic tests
| AD-A243002 | p 1232 N92-17234

ENGINE PARTS
Advanced nozzle and engine components test facility
| NASA-TM-103684 | p 1237 N92-17059
An analysis of the aircraft engine Component Improvement Program (CIP): A life cycle cost approach
| AD-A243346 | p 1236 N92-17729

ENTHALPY
Determination of the electronic density of states of YBa2Cu3O(7-delta)
| AD-A243223 | p 1372 N92-17220
Estimation of the outer sphere contribution to the activation parameters for homogeneous electron transfer reactions using the mean spherical approximation
| AD-A243217 | p 1259 N92-17323

ENVIRONMENT EFFECTS
Worldwide Environmental Compliance Assessment and Management Program (ECAMP): German supplement
| AD-A242967 | p 1313 N92-17380
Worldwide Environmental Compliance Assessment and Management Program (ECAMP): United Kingdom supplement
| AD-A242928 | p 1314 N92-17551
Rocket tests in Mississippi to be heavily restricted
| GAO/NSIAD-92-86 | p 1240 N92-17741
Evaluation of environmentally safe cleaning agents for diamond turned optics
| DE92-002524 | p 1278 N92-17780

ENVIRONMENT MANAGEMENT
Worldwide Environmental Compliance Assessment and Management Program (ECAMP): German supplement
| AD-A242967 | p 1313 N92-17380
Worldwide Environmental Compliance Assessment and Management Program (ECAMP): United Kingdom supplement
| AD-A242928 | p 1314 N92-17551
Worldwide Environmental Compliance Assessment and Management Program (ECAMP)
| AD-A242874 | p 1314 N92-17598
Evolution of an environmental audit program
| DE92-002681 | p 1314 N92-17665

ENVIRONMENT MODELS
NOAA Atmospheric Sciences Modeling Division support to the US Environmental Protection Agency
| PB91-235499 | p 1315 N92-17134
Environmental containment property estimation using QSARs in an expert system
| AD-A243728 | p 1336 N92-17720
Rocket tests in Mississippi to be heavily restricted
| GAO/NSIAD-92-86 | p 1240 N92-17741

ENVIRONMENT PROTECTION
NOAA Atmospheric Sciences Modeling Division support to the US Environmental Protection Agency
| PB91-235499 | p 1315 N92-17134
Large centrifuge: A critical Army capability for the future
| AD-A243287 | p 1238 N92-17287
Worldwide Environmental Compliance Assessment and Management Program (ECAMP): United Kingdom supplement
| AD-A242928 | p 1314 N92-17551
Worldwide Environmental Compliance Assessment and Management Program (ECAMP)
| AD-A242874 | p 1314 N92-17598

ENVIRONMENT SIMULATION
Numerical studies of processes in stratiform cirrus
| MITT-78 | p 1321 N92-17543
Treadmill for space flight
| NASA-CASE-MSC-21752-1 | p 1335 N92-17910

ENVIRONMENTAL CONTROL
Environmental control and life support system evolution analysis p 1246 N92-17355
The environmental control and life support system advanced automation project p 1246 N92-17356
ECLSS predictive monitoring p 1247 N92-17357

ENVIRONMENTAL ENGINEERING
Worldwide Environmental Compliance Assessment and Management Program (ECAMP): United Kingdom supplement
| AD-A242928 | p 1314 N92-17551
Worldwide Environmental Compliance Assessment and Management Program (ECAMP)
| AD-A242874 | p 1314 N92-17598

ENVIRONMENTAL MONITORING
Worldwide Environmental Compliance Assessment and Management Program (ECAMP): German supplement
| AD-A242967 | p 1313 N92-17380

ENVIRONMENTAL SURVEYS
Aquatic plant management program. Supplement
| AD-A242420 | p 1314 N92-17723

ENZYMES
Process of converting starch to glucose and glucose to lactic acid
| DE92-003840 | p 1255 N92-17867

EPITAXY
Contributive research and development
| AD-A243331 | p 1391 N92-17079
Method of joining diamond structures
| AD-D015066 | p 1269 N92-17397
Studies of hetero-epitaxy of GaAs films on Si substrate for effective control of density and internal stress
| AD-A241882 | p 1374 N92-17594

EPOXY MATRIX COMPOSITES
Novel vacuum bag processing approaches to void reduction in carbon/epoxy composites
| AD-A242396 | p 1255 N92-16992
Effective dynamic material parameters and localized scattering
| AD-A241957 | p 1310 N92-17320

EPOXY RESINS
Novel vacuum bag processing approaches to void reduction in carbon/epoxy composites
| AD-A242396 | p 1255 N92-16992
Experimental investigation of interlaminar fracture toughness of carbon fiber/thermoplastic and carbon fiber/thermosetting composites by DCB specimens
| NAL-TR-1096 | p 1257 N92-17869

EQUATIONS OF MOTION
A wing rock model for the F-14A aircraft
| AD-A243109 | p 1233 N92-17300
Evaluation of squib performance variables
| DE92-002034 | p 1275 N92-17533

EQUATIONS OF STATE
Equation of state and conductivity of hot, dense matter
| AD-A243359 | p 1369 N92-17301
The effect of detonation curvature on cylindrical wall motion
| DE92-003110 | p 1298 N92-17625
Relativistic nuclear many-body theory
| DE92-003258 | p 1362 N92-17789
Modelling of some equilibrium thermodynamic properties of polymer systems
| ETN-92-90570 | p 1273 N92-17840

EQUATORIAL REGIONS
Upper ocean dynamics during the LOTUS and Tropic Heat Experiments
| AD-A243730 | p 1324 N92-17583

EQUILIBRIUM FLOW
ZEUS user manual real gas effects
| AD-A242224 | p 1225 N92-17446

EQUIPMENT SPECIFICATIONS
Construction equipment for lunar surface operations
| AD-A243665 | p 1389 N92-17123

EQUIVALENT CIRCUITS
Microstrip discontinuity models to 60 GHz
| AD-A242038 | p 1339 N92-17185
A discontinuity study in shielded coplanar line
| AD-A242976 | p 1288 N92-17290
Permittivity probe modelling
| AD-A243236 | p 1260 N92-17572

ERGOMETERS
Influence of knee joint extension on submaximal oxygen consumption and anaerobic power in cyclists
| AD-A243467 | p 1329 N92-17194

ERROR ANALYSIS
Spectral error models applied to the geodetic boundary value problem
| ETN-92-90582 | p 1312 N92-17436
Spatial sampling error of a scanning radiation budget radiometer
| MITT-76 | p 1317 N92-17542
Comparison of station-keeping algorithms for an interior libration point orbit in the Sun-Earth + Moon elliptic restricted three-body problem
| AD-A241896 | p 1388 N92-17595
Preliminary results from the analysis of wind component error
| AD-A243772 | p 1321 N92-17764
Hubble Space Telescope: SRM/QA observations and lessons learned
| NASA-TM-105505 | p 1387 N92-17873
Modification of a successive corrections objective analysis for improved derivative calculations p 1322 N92-17981

ERROR SIGNALS
A Walsh-domain adaptive filter
| AD-A243701 | p 1292 N92-17718

ERRORS
Advanced Communication Technology Satellite (ACTS) multibeam antenna analysis and experiment
| NASA-TM-105420 | p 1279 N92-17047
The effects of field errors on low-gain free electron lasers
| AD-A243710 | p 1303 N92-17127
Flight test data quality evaluation p 1230 N92-17156
Identification techniques: Frequency domain methods p 1231 N92-17158
Incipient fault detection using higher-order statistics
| AD-A243493 | p 1308 N92-17431
Spectral error models applied to the geodetic boundary value problem
| ETN-92-90582 | p 1312 N92-17436
Multipath induced tracking errors at 95 and 140 GHz
| AD-A243111 | p 1283 N92-17571

Practical error bounds for a class of quadratic programming problems
| AD-A243249 | p 1345 N92-17960

ERYTHROCYTES
The effects of storage on irradiated red blood cells: An in vitro an in vivo study
| AD-A243387 | p 1329 N92-17190

ESTERS
Blistering of graphite/polymer composites galvanically coupled with metals in sea water
| AD-A242861 | p 1269 N92-17262

ESTIMATING
Estimation of the outer sphere contribution to the activation parameters for homogeneous electron transfer reactions using the mean spherical approximation
| AD-A243217 | p 1259 N92-17323
A frequency-domain method for estimating the incidence and severity of sliding
| AD-A243077 | p 1334 N92-17569
Analysis of cam roller followers
| ESDU-91026 | p 1307 N92-17852
Mean wind speeds over hills and other topography
| ESDU-91043 | p 1321 N92-17853
Method for non-destructive estimation of waveguide directional coupler dimensions
| NASA-CASE-NPO-18454-1-CU | p 1293 N92-17865

ESTUARIES
A user's manual for the Princeton Numerical Ocean Model
| AD-A243773 | p 1324 N92-17539

ETCHING
Materials processing of diamond: Etching, doping by ion implantation and contact formation
| AD-A243060 | p 1267 N92-17065
Metallography of aluminide coatings
| AD-A243000 | p 1263 N92-17264
Light-controlled, electrochemical, anisotropic etching of silicon
| MBB-Z-0368-91-PUB | p 1261 N92-17841

ETHANE
Substituted 1,1,1-triaryl-2,2,2-trifluoroethanes and processes for their synthesis
| NASA-CASE-LEW-14345-6 | p 1255 N92-17882

ETHERS
New experimental challenges in elemental fluorine chemistry: An emerging technology
| AD-A243054 | p 1258 N92-17043
Phase transitions in narrow molecular mass samples of side-chain liquid crystalline polymers: Molecular mass dependence
| AD-A242354 | p 1269 N92-17448
Imide/arylene ether copolymers with pendent trifluoromethyl groups
| NASA-TM-104195 | p 1272 N92-17693

ETHYLENE
Thermal insulation chemical composition and method of manufacture
| AD-D015106 | p 1257 N92-17836

EUCLIDEAN GEOMETRY
Some foundations for empirical study in the euclidean spatial model of social choice
| AD-A241928 | p 1352 N92-17440

EUROPEAN SPACE PROGRAMS
Product assurance and safety implementation in Space Shuttle payloads: An industrial perspective
| MBB-UK-0143-91-PUB | p 1241 N92-17342

EVALUATION
Benefit analysis of proposed information systems
| AD-A243707 | p 1382 N92-17125
An analysis of mission critical computer software in Naval aviation
| AD-A243078 | p 1339 N92-17237

EVAPORATION
Evaporation duct communication: Test plan, part 2
| AD-A243505 | p 1282 N92-17383
Theoretical investigation of the injection and evaporation of water in a hydrogen/oxygen steam generator
| ESA-TT-1252 | p 1379 N92-17848

EVAPORATORS
Active thermal control system evolution
p 1252 N92-17775

EVEN-EVEN NUCLEI
Importance of the neutron-proton interactions for the even Ra-Th nuclei
| DE92-600628 | p 1363 N92-17956

EVOKED RESPONSE (PSYCHOPHYSIOLOGY)
Establishing an evoked-potential vision-tracking system p 1221 N92-17993

EVOLUTION (DEVELOPMENT)
Beyond the Baseline 1991: Proceedings of the Space Station Evolution Symposium. Volume 2: Space Station Freedom, part 2
| NASA-CP-10083-VOL-2-PT-2 | p 1245 N92-17348

EXCITATION
Detection and spectroscopy of single pentacene molecules in a p-terphenyl crystal by means of fluorescence excitation
| AD-A243747 | p 1356 N92-17196
Collisional dynamics of the B3Pi(O+) state of bromine of monofluoride
| AD-A241857 | p 1356 N92-17305
Characterization of the P. brevis polyether neurotoxin binding component in excitable membranes
| AD-A242877 | p 1327 N92-17564

EXCITONS
Optical nonlinearity in coupled exciton-phonon systems near metal surfaces
| AD-A242362 | p 1357 N92-17423
Excitons in semiconducting superlattices, quantum wells, and ternary alloys
| DE91-018805 | p 1374 N92-17528

EXERCISE PHYSIOLOGY
Influence of knee joint extension on submaximal oxygen consumption and anaerobic power in cyclists
| AD-A243467 | p 1329 N92-17194
Upper body exercise: Physiology and training application for human presence in space
| AD-A242033 | p 1329 N92-17473

EXHAUST SYSTEMS
Advanced nozzle and engine components test facility
| NASA-TM-103684 | p 1237 N92-17059

EXOTHERMIC REACTIONS
A method for joining ceramic shapes
| DE92-003815 | p 1274 N92-17842

EXPEDITIONS
Proceedings of the 2nd Gulf of Cadiz Expedition Workshop
| AD-A242749 | p 1325 N92-17951

EXPERIMENT DESIGN
Design of experiments p 1230 N92-17154
Interim Service ISDN Satellite (ISIS) hardware experiment design for advanced ISDN satellite design and experiments
| NASA-CR-186943 | p 1250 N92-17585

EXPERT SYSTEMS
Optical content-addressable memories for data/knowledge base processing
| AD-A241866 | p 1382 N92-17037
Economic analysis of information system
| AD-A243079 | p 1382 N92-17067
Acquisition and production of skilled behavior in dynamic decision-making tasks
| NASA-CR-189846 | p 1333 N92-17132
Software life cycle methodologies and environments
p 1246 N92-17351
Beyond the Baseline 1991: Proceedings of the Space Station Evolution Symposium. Volume 1: Space Station Freedom, part 2
| NASA-CP-10083-VOL-1-PT-2 | p 1248 N92-17409
Facing page test for the astronaut science advisor presentation p 1248 N92-17411
The astronaut science advisor: Ground testing during SLS-1 p 1248 N92-17412
Technical evaluation report on the 52nd Symposium on Software for Guidance and Control
| AGARD-AR-302 | p 1341 N92-17498
A knowledge-based approach for configuring computer aided measuring systems
| ETN-92-90585 | p 1341 N92-17524
Development of a knowledge base for use in an Expert System Advisor for Aircraft Maintenance Scheduling (ESAAMS)
| AD-A243435 | p 1381 N92-17687
Environmental containment property estimation using QSARs in an expert system
| AD-A243728 | p 1336 N92-17720
Automated power management and control
p 1252 N92-17773
The SSM/PMAD automated test bed project
p 1252 N92-17774
Thermal Control System Automation Project (TCSAP)
p 1252 N92-17776
Software tools for distributed intelligent control systems
| DE92-004656 | p 1349 N92-17965
An investigation of air transportation technology at the Massachusetts Institute of Technology, 1990-1991
p 1219 N92-17985
Systematic methods for knowledge acquisition and expert system development p 1222 N92-18001

EXPLOSIONS
Structures to resist the effects of accidental explosions
| AD-A243272 | p 1277 N92-17272
Large centrifuge: A critical Army capability for the future
| AD-A243287 | p 1238 N92-17287

EXPLOSIVES
Energetic composites of cyclodextrin nitrate esters and nitrate ester plasticizers
| AD-D015068 | p 1275 N92-17399

EXPONENTIAL FUNCTIONS
The micro-c rule is not optimal in the 2nd node of the tandem queue; 2 counterexamples
| TW-91-05 | p 1349 N92-17838

EXPOSURE
Biological effects of protracted exposure to ionizing radiation: Review, analysis, and model development
| AD-A242981 | p 1329 N92-17476

EXTERNAL COMBUSTION ENGINES
Experiments and analysis concerning the use of external burning to reduce aerospace vehicle transonic drag
| NASA-TM-105397 | p 1235 N92-17546

EXTERNAL TANKS
Results of the space shuttle vehicle ascent air data system probe calibration test using a 0.07-scale external tank forebody model (68T) in the AEDC 16-foot transonic wind tunnel (IA-310), volume 1
| NASA-CR-167696 | p 1241 N92-17167
Results of the space shuttle vehicle ascent air data system probe calibration test using a 0.07-scale external tank forebody model (68T) in the AEDC 16-foot transonic wind tunnel (IA-310), volume 2
| NASA-CR-167697 | p 1241 N92-17214
STV fueling options p 1249 N92-17415

EXTINCTION
Infrared rotating analyzer ellipsometry: Calibration and data processing
| AD-A242834 | p 1259 N92-17248

EXTINGUISHING
Development of fuel neutralizing agents to prevent flashback on aircraft fires
| AD-A242828 | p 1227 N92-17259

EXTRAPOLATION
Performance measures for adaptive decisioning systems
| AD-A243183 | p 1352 N92-16998

EXTRAVEHICULAR ACTIVITY
EMU evolution p 1246 N92-17354
Computer system evolution requirements for autonomous checkout of exploration vehicles
p 1250 N92-17422

EXTRAVEHICULAR MOBILITY UNITS
Extravehicular mobility unit subcritical liquid oxygen storage and supply system
| NASA-CR-189831 | p 1276 N92-16989
EMU evolution p 1246 N92-17354

EXTREME ULTRAVIOLET RADIATION
Development of an XUV-IR free-electron laser user facility for scientific research and industrial applications
| DE92-003862 | p 1304 N92-17726

EXTRUDING
Solder extrusion pressure bonding process and bonded products produced thereby
| DE92-004603 | p 1363 N92-17739

EYE (ANATOMY)
Neural network classification of mental workload conditions by analysis of spontaneous electroencephalograms
| AD-A243369 | p 1331 N92-17115
Rapid nonconjugate adaptation of vertical voluntary pursuit eye movements
| AD-A243358 | p 1331 N92-17145
Preliminary assessment of the relative toxicity of tetraglycine hydroperiodide, phase 1
| AD-A243334 | p 1330 N92-17712

EYE MOVEMENTS
Rapid nonconjugate adaptation of vertical voluntary pursuit eye movements
| AD-A243358 | p 1331 N92-17145

EYE PROTECTION
User evaluation of laser ballistic sun, wind and dust goggle lenses (dye technology)
| AD-A243245 | p 1334 N92-17143
Ultrafast passive shields for laser and ballistic protection
| AD-A243206 | p 1303 N92-17175

F

F-14 AIRCRAFT
A wing rock model for the F-14A aircraft
| AD-A243109 | p 1233 N92-17300

FABRICATION
Consolidation of diamond packed powders
| AD-D015071 | p 1270 N92-17612
Molecular self-assembly and nanochemistry: A chemical strategy for the synthesis of nanostructures
| AD-A243530 | p 1361 N92-17616
High temperature superconductor thin films and Josephson junctions
| AD-A242747 | p 1293 N92-17949

FACE (ANATOMY)
Face recognition with the Karhunen-Loeve transform
| AD-A243688 | p 1280 N92-17090
FACILITIES
Cathodic protection diagnostic computer program for sacrificial and impressed current systems: Overview and user's manual
| AD-A243663 | p 1338 N92-17122
FACTOR ANALYSIS
Visual determination of industrial color-difference tolerances using probit analysis
| AD-A243545 | p 1334 N92-17617
FAILURE
Effect of coatings and processing on failure mechanisms of polycarbonate material, phase 1
| AD-A243018 | p 1256 N92-17053
Dynamic fracture characterization of Al2O3 and SiC(w)/Al2O3
| AD-A242187 | p 1273 N92-17784
Strength of lugs
| ESDU-91008 | p 1311 N92-17834
FAILURE ANALYSIS
Rapid repair of integrally stiffened carbon fibre composite structures by bolted aluminium elements
| MBB-FE202-S-PUB-0453-A | p 1256 N92-17310
Failure Environment Analysis Tool (FEAT)
p 1245 N92-17349
Explicit finite element method for transparency impact analysis
| AD-A243527 | p 1227 N92-17478
Program plans: Aviation safety research
| NIAR-91-30 | p 1227 N92-17587
Thermo-mechanical fatigue of a fiber reinforced titanium aluminide composite
| AD-A241988 | p 1256 N92-17607
Acoustic emission monitoring of low velocity impact damage in graphite/epoxy laminates during tensile loading
| NASA-TM-4339 | p 1258 N92-17881
FAINT OBJECT CAMERA
Hubble Space Telescope: Faint object camera instrument handbook. Version 2.0
| NASA-CR-189746 | p 1386 N92-17021
FAR FIELDS
Advanced Communication Technology Satellite (ACTS) multibeam antenna analysis and experiment
| NASA-TM-105420 | p 1279 N92-17047
Automated composite ellipsoid modelling for high frequency GTD analysis
| NASA-CR-189853 | p 1233 N92-17316
Effective dynamic material parameters and localized scattering
| AD-A241957 | p 1310 N92-17320
FAR INFRARED RADIATION
Simulation of finite-precision effects in digital filters
| AD-A243758 | p 1342 N92-17601
FARADAY EFFECT
Optical fiber magnetometer
| AD-D015133 | p 1368 N92-17959
FAST NEUTRONS
Experimental findings on self-recovery and improvement of representative parameters of some semiconductor devices as irradiated in fast neutron flux
| DE92-611185 | p 1378 N92-17944
FATIGUE (BIOLOGY)
Fatigue effects on human performance in combat: A literature review, volume 1
| AD-A242887 | p 1330 N92-17567
FATIGUE (MATERIALS)
Fatigue in single crystal nickel superalloys
| AD-A243453 | p 1265 N92-17653
FATIGUE LIFE
Inelastic strain analysis of solder joint in NASA fatigue specimen
| NASA-CR-189882 | p 1311 N92-17511
General requirements and techniques for component fatigue life substantiation in Australian service helicopters
| AD-A242881 | p 1233 N92-17565
Dynamic stall on wind turbine blades
| DE92-001157 | p 1226 N92-17874
FATIGUE TESTS
Rapid repair of integrally stiffened carbon fibre composite structures by bolted aluminium elements
| MBB-FE202-S-PUB-0453-A | p 1256 N92-17310
Thermo-mechanical fatigue of a fiber reinforced titanium aluminide composite
| AD-A241988 | p 1256 N92-17607
FATTY ACIDS
Evaluation of the initiation/promotion potential of CTFE trimer acid
| AD-A243479 | p 1255 N92-17373
FAULT TOLERANCE
A general computational framework for distributed sensing and fault-tolerant sensor integration
| AD-A243256 | p 1300 N92-16983
Failure detection and fault management techniques for flush airdata sensing systems
| NASA-TM-4335 | p 1234 N92-17128
Embedded fault-tolerant computer for mission critical applications
| AD-A242886 | p 1342 N92-17566
Fault detection and isolation for multisensor navigation systems p 1221 N92-17992
Intelligent failure-tolerant control p 1222 N92-18000
FEASIBILITY ANALYSIS
The applied tomography experiment of 1990
| AD-A243525 | p 1354 N92-17086
Weight evaluation and sensitivity analysis for space plane. Part 2: TSTO
| NAL-TM-602-PT-2 | p 1251 N92-17754
FEDERAL BUDGETS
The V-22: Can the nation afford to forgo its production?
| AD-A243158 | p 1219 N92-17477
FEEDBACK
Feedback in dynamic decision making: An experiment in software project management
| AD-A242361 | p 1380 N92-17451
FEEDBACK CIRCUITS
The analysis of a stabilized 1.5 Mach-Zehnder interferometric sensor with enhanced sensitivity and common-mode compensation
| AD-A243384 | p 1286 N92-17116
FEEDBACK CONTROL
Modes of interconnected lattice trusses using continuum models, part 1
| NASA-CR-189568 | p 1242 N92-17045
Development of high angle of attack control laws for an unstable, non-minimum phase aircraft using variations of the quantitative feedback technique
| AD-A243698 | p 1236 N92-17096
A robust digital flight control system for an unfanned research vehicle using discrete quantitative feedback theory
| AD-A243638 | p 1237 N92-17748
Closed-loop motor control using high-speed fiber optics
| NASA-CASE-MSC-21806-1 | p 1368 N92-17863
Adaptive generalized predictive control
| OUEL-1879/91 | p 1349 N92-17880
Technical notes and correspondence: Stochastic robustness of linear time-invariant control systems
p 1222 N92-18002
FEMALES
Assessment of the behavioral and neurotoxic effects of hexachlorobenzene (HCB) in the developing rat
| AD-A243658 | p 1325 N92-17121
FERMENTATION
Process of converting starch to glucose and glucose to lactic acid
| DE92-003840 | p 1255 N92-17867
FERMI LIQUIDS
Determination of the electronic density of states of YBa2Cu3O(7-delta)
| AD-A243223 | p 1372 N92-17220
FERRITES
Microstructure and mechanical properties of HSLA-100 steel
| AD-A242937 | p 1265 N92-17467
FERROCENES
New ferrocene complexes and polymers for nonlinear optical applications
| AD-A243640 | p 1272 N92-17749
Organometallic NLO polymers. Linear main-chain NLO polymers of ferrocene
| AD-A243641 | p 1272 N92-17750
Organometallic NLO polymers. Accordian main-chain NLO polymers of ferrocene
| AD-A243642 | p 1273 N92-17751
FERROELECTRICITY
Ceramics with superelectrical and supermechanical properties
| AD-A243062 | p 1267 N92-17029
The 5th Annual US-Japan Seminar on Dielectric and Piezoelectric Ceramics
| AD-A243465 | p 1268 N92-17193
Preparation of ferroelectric samples for electrical and radiation characterization studies
| AD-A243432 | p 1288 N92-17326
FERROMAGNETIC MATERIALS
Magnetic multilayer strain gage
| AD-D015163 | p 1381 N92-17940
FETUSES
Assessment of the behavioral and neurotoxic effects of hexachlorobenzene (HCB) in the developing rat
| AD-A243658 | p 1325 N92-17121
FIBER COMPOSITES
Polymer infiltration studies
| NASA-CR-189773 | p 1266 N92-17004
Thermo-mechanical fatigue of a fiber reinforced titanium aluminide composite
| AD-A241988 | p 1256 N92-17607
Intercalated hybrid graphite fiber composite
| NASA-CASE-LEW-15241-1 | p 1257 N92-17861
Experimental investigation of interlaminar fracture toughness of carbon fiber/thermoplastic and carbon fiber/thermosetting composites by DCB specimens
| NAL-TR-1096 | p 1257 N92-17869
Silver-nickel composite cathodes for alkaline secondary batteries
| AD-D015121 | p 1293 N92-17871
Damage mechanisms in composites
| AD-A242748 | p 1258 N92-17950
FIBER OPTICS
Design of a fiber optic image transmission link
| AD-A243686 | p 1365 N92-17088
The analysis of a stabilized 1.5 Mach-Zehnder interferometric sensor with enhanced sensitivity and common-mode compensation
| AD-A243384 | p 1286 N92-17116
Optical protocols for advanced spacecraft networks
p 1249 N92-17418
C3 Systems Technology Symposium on Advance Planning Briefings for Industry
| AD-A243466 | p 1391 N92-17657
Fiber optic angular orientation sensor digital serial encoding
| AD-D015102 | p 1302 N92-17826
Precision multi-channel fiber optic interface and method
| AD-D015104 | p 1367 N92-17828
Closed-loop motor control using high-speed fiber optics
| NASA-CASE-MSC-21806-1 | p 1368 N92-17863
Wide field strip-imaging optical system
| NASA-CASE-NPO-18146-1-CU | p 1368 N92-17892
Optical fiber magnetometer
| AD-D015133 | p 1368 N92-17959
FIBER ORIENTATION
Static analysis of thick composite plates using higher order three dimensional finite elements
| AD-A243188 | p 1256 N92-17367
FIBERS
Dynamic fracture characterization of Al2O3 and SiC(w)/Al2O3
| AD-A242187 | p 1273 N92-17784
Production of mullite fibers
| NASA-CASE-MFS-28431-1 | p 1257 N92-17870
FIELD EFFECT TRANSISTORS
Research and development on advanced silicon carbide thin film growth techniques and fabrication of high power and microwave frequency silicon carbide-based device structures
| AD-A243531 | p 1373 N92-17390
Evaluation of an Interdigitated Gate Electrode Field-Effect Transistor (IGEFET) for in situ resin cure monitoring
| AD-A243713 | p 1289 N92-17501
Failure mechanisms in GaAs ICs: The effects of deep traps
| AD-A243013 | p 1374 N92-17553
Gate drain geometry effect on the current voltage characteristics of GaAs MESFETs
| AD-A243430 | p 1291 N92-17684
Characterizing the sensitivity, selectivity, and reversibility of the metal-doped phthalocyanine thin-films used with the Interdigitated Gate Electrode Field-Effect Transistor (IGEFET) to detect organophosphorous compounds and nitrogen dioxide
| AD-A243635 | p 1376 N92-17746
FIELD STRENGTH
Optical nonlinearity in coupled exciton-phonon systems near metal surfaces
| AD-A242362 | p 1357 N92-17423
FIELD THEORY (PHYSICS)
Gauge-covariant Wess-Zumino actions for super p-branes in superspace
| DE91-641524 | p 1353 N92-17318
Axino-induced baryogenesis
| NASA-CR-189858 | p 1361 N92-17646
Future prospects of pregeometry
| DE92-704278 | p 1379 N92-17817
FIGHTER AIRCRAFT
Aerodynamic development of the X-31 aircraft for the high angle of attack region
| MBB-FE211-S-PUB-452 | p 1233 N92-17313
The development of military night aviation to 1919
| AD-A243350 | p 1219 N92-17731
FILLERS
Thermal insulation chemical composition and method of manufacture
| AD-D015106 | p 1257 N92-17836

FILM THICKNESS
Actively controlled shaft seals for aerospace applications
| NASA-CR-189808 | p 1306 N92-17304
Characterization of PZT thin films: Crystallographic phases
| DE92-003514 | p 1377 N92-17790
FILTRATION
Process of converting starch to glucose and glucose to lactic acid
| DE92-003840 | p 1255 N92-17867
FINITE DIFFERENCE THEORY
The effect of detonation curvature on cylindrical wall motion
| DE92-003110 | p 1298 N92-17625
FINITE ELEMENT METHOD
Periodic trim solutions with HP-version finite elements in time
| NASA-CR-189778 | p 1236 N92-17019
Modes of interconnected lattice trusses using continuum models, part 1
| NASA-CR-189568 | p 1242 N92-17045
Static analysis of thick composite plates using higher order three dimensional finite elements
| AD-A243188 | p 1256 N92-17367
Workshop for Finite Element Methods for Composites
| AD-A243534 | p 1256 N92-17392
FEM-X user's guide
| AD-A242374 | p 1383 N92-17396
Explicit finite element method for transparency impact analysis
| AD-A243527 | p 1227 N92-17478
Finite element analysis of ASTOVL fighter structure
| AD-A243724 | p 1233 N92-17513
An overview: Challenges in wind technology development
| DE92-001190 | p 1313 N92-17875
FIRE (CLIMATOLOGY)
Numerical simulation of cirrus clouds: Fire case study and sensitivity analysis
| AD-A242902 | p 1321 N92-17631
FIRE EXTINGUISHERS
Effectiveness of an onboard water spray system during an oxygen enriched cabin fire
| DOT/FAA/CT-TN91/51 | p 1226 N92-17149
Development of fuel neutralizing agents to prevent flashback on aircraft fires
| AD-A242828 | p 1227 N92-17259
FIRE FIGHTING
Thermal energy test apparatus
| AD-A243526 | p 1379 N92-17537
FIRES
Effectiveness of an onboard water spray system during an oxygen enriched cabin fire
| DOT/FAA/CT-TN91/51 | p 1226 N92-17149
Thermal energy test apparatus
| AD-A243526 | p 1379 N92-17537
FISSION
Energy production using fission fragment rockets
| DE92-002192 | p 1364 N92-17876
FISSION PRODUCTS
Energy production using fission fragment rockets
| DE92-002192 | p 1364 N92-17876
FISSIONABLE MATERIALS
Characterization of the thermalness of a fissile system with a 2-group diffusion theory parameter
| AD-A243065 | p 1360 N92-17555
Energy production using fission fragment rockets
| DE92-002192 | p 1364 N92-17876
FLAME STABILITY
Two-dimensional stability of laminar flames
| NASA-TP-3131 | p 1223 N92-17131
FLAME TEMPERATURE
An experimental investigation of chemically-reacting, gas-phase turbulent jets
| AD-A243036 | p 1296 N92-17276
FLAPPING
Application areas for rotorcraft system identification: Simulation model validation p 1232 N92-17164
FLAPS (CONTROL SURFACES)
Identification of the stability and control derivatives of a DLC-flap system for VSRA
| NAL-TR-1116 | p 1237 N92-17917
FLAT SURFACES
Laser range safety
| AD-A243606 | p 1305 N92-17962
FLEXIBLE BODIES
Method and apparatus for reducing drag and noise associated with fluid flow in a conduit
| AD-D015067 | p 1297 N92-17398
Toward the robust control of high bandwidth high precision flexible optical systems
| AD-A243471 | p 1366 N92-17536
Control of a large flexible space structure using multiple model adaptive algorithms
| AD-A243759 | p 1250 N92-17602
FLIGHT CHARACTERISTICS
Rotorcraft System Identification
| AGARD-LS-178 | p 1230 N92-17153
Escape strategies for turboprop aircraft in a microburst windshear
| AD-A243090 | p 1227 N92-17217
Discussion for possibility of some aerodynamic ground effect craft
| NAL-TM-619 | p 1278 N92-17757
FLIGHT CONTROL
Model identification and control system design for the lambda unmanned research vehicle
| AD-A241859 | p 1306 N92-17024
Identification techniques: Model structure and time domain methods p 1231 N92-17157
Industry view on rotorcraft system identification p 1232 N92-17163
System identification requirements for high-bandwidth rotorcraft flight control system design p 1232 N92-17166
Advanced flight software reconfiguraton p 1245 N92-17350
SSF growth concepts and configurations p 1248 N92-17414
Flight evaluation of curved MLS precision approaches in a twin otter aircraft, phase 2
| AD-A243025 | p 1229 N92-17568
A robust digital flight control system for an unfanned research vehicle using discrete quantitative feedback theory
| AD-A243638 | p 1237 N92-17748
GPS interferometric attitude and heading determination: Initial flight test results p 1221 N92-17994
Investigation of air transportation technology at Princeton University, 1990-1991 p 1221 N92-17995
Technical notes and correspondence: Stochastic robustness of linear time-invariant control systems p 1222 N92-18002
FLIGHT CREWS
The multi-attribute task battery for human operator workload and strategic behavior research
| NASA-TM-104174 | p 1338 N92-17130
Aircrew critique of high-G centrifuge training: Part 3: What can we change to better serve you?
| AD-A243496 | p 1334 N92-17432
FLIGHT HAZARDS
Cockpit display of hazardous weather information p 1220 N92-17989
Optimal aircraft performance during microburst encounter p 1222 N92-17999
FLIGHT MECHANICS
Rotorcraft System Identification
| AGARD-LS-178 | p 1230 N92-17153
SA 330 Puma identification results p 1231 N92-17162
Application areas for rotorcraft system identification: Simulation model validation p 1232 N92-17164
System identification methods for handling-qualities evaluation p 1232 N92-17165
FLIGHT PATHS
Method of guiding an in-flight vehicle to a designed flight path
| AD-D015061 | p 1229 N92-17707
Optimal aircraft performance during microburst encounter p 1222 N92-17999
FLIGHT SAFETY
Design of experiments p 1230 N92-17154
Space Station Freedom/lunar transfer vehicle propellant operation hazard analysis p 1249 N92-17416
Alert generation and cockpit presentation for an integrated microburst alerting system p 1220 N92-17988
FLIGHT SIMULATION
Weight evaluation and sensitivity analysis for space plane. Part 2: TSTO
| NAL-TM-602-PT-2 | p 1251 N92-17754
FLIGHT SIMULATORS
Implementation of an object-oriented flight simulator D.C. electrical system on a hypercube architecture
| AD-A243700 | p 1238 N92-17097
Effect of two types of scene detail on detection of altitude change in a flight simulator
| AD-A242034 | p 1333 N92-17758
FLIGHT TESTS
Model identification and control system design for the lambda unmanned research vehicle
| AD-A241859 | p 1306 N92-17024
Design of experiments p 1230 N92-17154
Instrumentation and data processing p 1230 N92-17155
Flight test data quality evaluation p 1230 N92-17156
Assessment of rotorcraft system identification as applied to the AH-64 p 1231 N92-17160
BO 105 identification results p 1231 N92-17161
System identification methods for handling-qualities evaluation p 1232 N92-17165
Flight evaluation of curved MLS precision approaches in a twin otter aircraft, phase 2
| AD-A243025 | p 1229 N92-17568
Example of statistical techniques applied to cruise performance guarantees (Student's t distribution)
| ESDU-91018 | p 1233 N92-17843
Identification of the stability and control derivatives of a DLC-flap system for VSRA
| NAL-TR-1116 | p 1237 N92-17917
FLORIDA
Surface observation climatic summaries for Duke Field/Eglin aux no. 3, Florida
| AD-A243310 | p 1318 N92-17073
FLOW DISTORTION
An experimental study of a turbulent wing-body junction and wake flow
| AD-A243388 | p 1223 N92-17222
Modification of Jindivik air intake duct with an auxiliary intake static aerodynamic tests
| AD-A243002 | p 1232 N92-17234
FLOW DISTRIBUTION
Computation of the hydrodynamic forces and moments on a body of revolution with and without appendages
| AD-A243033 | p 1294 N92-16978
Chemical reactions in turbulent mixing flows
| AD-A243035 | p 1294 N92-16979
An experimental investigation of leading edge vortical flow about a delta wing during wing rock
| AD-A243363 | p 1223 N92-17114
A study on hydrographic conditions and salt budget calculation for the Gulf of Farallones with the data collected in August 1990
| AD-A243406 | p 1324 N92-17119
An experimental study of a turbulent wing-body junction and wake flow
| AD-A243388 | p 1223 N92-17222
Wind loads on a mirage III O aircraft mounted above a ground plane
| AD-A243004 | p 1232 N92-17266
Flow visualization and wake analysis for standard and modified configurations of the AN/ALQ-78 antenna pod
| AD-A243552 | p 1224 N92-17339
Viscous three-dimensional calculations of transonic fan performance
| NASA-TM-103800 | p 1219 N92-17346
ZEUS user manual real gas effects
| AD-A242224 | p 1225 N92-17446
Pattern selection, wave formation, turbulence, and vortex breakdown in spiral flows
| AD-A242351 | p 1297 N92-17447
Computation of three-dimensional flows using two stream functions
| NASA-CR-187802 | p 1298 N92-17588
Diagnostic report of the National Hurricane Center, August and September 1990, volume 3, number 2
| PB91-226886 | p 1321 N92-17621
Results of measured temperature distribution on an adiabatic wing model with radiation thermometer
| NAL-TM-610 | p 1225 N92-17755
Boundary-layer transition and heat transfer on slender delta wings
| AERO-REPT-8904 | p 1226 N92-17849
Flow between two stationary disks and a rotating shroud
| AERO-REPT-9001 | p 1300 N92-17851
Numerical simulation of fluid flow and heat transfer in a thin liquid film over a stationary and rotating disk and comparison with experimental data
| NASA-CR-189253 | p 1300 N92-17887
FLOW EQUATIONS
Effective viscosity in the simulation of spatially evolving shear flows with monotonic FCT models
| AD-A243709 | p 1295 N92-17126
Studies of baroclinic flow
| AD-A243050 | p 1296 N92-17309
Pattern selection, wave formation, turbulence, and vortex breakdown in spiral flows
| AD-A242351 | p 1297 N92-17447
FLOW GEOMETRY
An experimental study of a turbulent wing-body junction and wake flow
| AD-A243388 | p 1223 N92-17222
FLOW MEASUREMENT
Advanced nozzle and engine components test facility
| NASA-TM-103684 | p 1237 N92-17059
An experimental investigation of leading edge vortical flow about a delta wing during wing rock
| AD-A243363 | p 1223 N92-17114
Observation and measurements of flow structures in the stagnation region of a wing-body junction
| AD-A243403 | p 1223 N92-17117
LDA and PDA systems based on diode-pumped Neodym:YAG lasers
| MBB-Z-0361-91-PUB | p 1304 N92-17526

Development and utilization of new diagnostics for dense-phase pneumatic transport
| DE92-003091 | p 1307 N92-17605
Development and utilization of new diagnostics for dense-phase pneumatic transport
| DE92-000337 | p 1299 N92-17704

FLOW VELOCITY
Application of program LAURA to perfect gas shock tube flows: A parametric study
| NASA-TM-104190 | p 1294 N92-17002
Laser based, non-intrusive measurement system for analysis of jet engine flows
| AD-A242398 | p 1234 N92-17011
An experimental investigation of chemically-reacting, gas-phase turbulent jets
| AD-A243036 | p 1296 N92-17276
Recording of three dimensional trajectories and velocity fields by automatic image processing
| MPIS-101/1991 | p 1301 N92-17345
Mass transfer in gas fluidized beds: Scaling, modeling, and particle size influence
| ETN-92-90581 | p 1298 N92-17522
Development and utilization of new diagnostics for dense-phase pneumatic transport
| DE92-003091 | p 1307 N92-17605
Development and utilization of new diagnostics for dense-phase pneumatic transport
| DE92-000337 | p 1299 N92-17704
Experimental study of amplitude-phase-frequency characteristics of flow when following over a vibrating plate
| DE92-610935 | p 1299 N92-17810

FLOW VISUALIZATION
Advanced nozzle and engine components test facility
| NASA-TM-103684 | p 1237 N92-17059
Observation and measurements of flow structures in the stagnation region of a wing-body junction
| AD-A243403 | p 1223 N92-17117
Flow visualization and wake analysis for standard and modified configurations of the AN/ALQ-78 antenna pod
| AD-A243552 | p 1224 N92-17339
The effect of freestream turbulence on the vortical flow over a delta wing p 1225 N92-17681
Results of measured temperature distribution on an adiabatic wing model with radiation thermometer
| NAL-TM-610 | p 1225 N92-17755

FLUENCE
Atomic oxygen flux and fluence calculation for Long Duration Exposure Facility (LDEF)
| NASA-CR-187418 | p 1245 N92-17215

FLUID BOUNDARIES
Studies of baroclinic flow
| AD-A243050 | p 1296 N92-17309

FLUID DYNAMICS
Effective viscosity in the simulation of spatially evolving shear flows with monotonic FCT models
| AD-A243709 | p 1295 N92-17126
Study of transition phenomena in a straight channel with 40 to 1 aspect ratio with and without imposed pulsations. Part two: Reynolds number surveys
| AD-A241894 | p 1296 N92-17307
Transition phenomena in a straight channel with a 40 to 1 aspect ratio with and without imposed pulsations. Part 1: Near-wall and central region profiles
| AD-A243251 | p 1297 N92-17337

FLUID FILMS
Numerical simulation of fluid flow and heat transfer in a thin liquid film over a stationary and rotating disk and comparison with experimental data
| NASA-CR-189253 | p 1300 N92-17887

FLUID FLOW
Method and apparatus for reducing drag and noise associated with fluid flow in a conduit
| AD-D015067 | p 1297 N92-17398
Effects of power pulsations on heat transfer from discrete heat sources
| AD-A243434 | p 1379 N92-17686
Numerical simulation of fluid flow and heat transfer in a thin liquid film over a stationary and rotating disk and comparison with experimental data
| NASA-CR-189253 | p 1300 N92-17887
Global models for the biomechanics of green plants, part 1
| DE91-641478 | p 1327 N92-17946

FLUID JETS
The influence of cavitation in the breakup of liquid free jets
| MPIS-1/1991 | p 1297 N92-17343

FLUID MECHANICS
Global models for the biomechanics of green plants, part 1
| DE91-641478 | p 1327 N92-17946

FLUID PRESSURE
Study of plane wave impingement on a thin plate capable of deformation
| AD-A242947 | p 1296 N92-17275
Active control of pressure loads using passive porosity
| NASA-CASE-LAR-14594-1 | p 1300 N92-17888
Passive control of pressure loads using porosity
| NASA-CASE-LAR-14547-1 | p 1300 N92-17909

FLUIDIZED BED PROCESSORS
Determination of cohesive and normal stresses and simulation of fluidization using kinetic theory
| DE92-002905 | p 1299 N92-17709

FLUORESCENCE
Electronic interactions of directed photon beams with surfaces
| AD-A241878 | p 1356 N92-17026
Detection and spectroscopy of single pentacene molecules in a p-terphenyl crystal by means of fluorescence excitation
| AD-A243747 | p 1356 N92-17196
Single molecule spectral diffusion in a solid detected via fluorescence spectroscopy
| AD-A243748 | p 1356 N92-17197
Microbial diversity: Course report 1991
| AD-A243464 | p 1326 N92-17224
Measurement of electron beam emittance using optical transition radiation and development of a diffuse screen electron beam monitor
| AD-A241893 | p 1357 N92-17306
Simultaneous active and passive microwave measurements of the ocean surface
| AD-A242232 | p 1312 N92-17459
Optical modification of a single impurity molecule in a solid
| AD-A243750 | p 1361 N92-17660
Steady-state production and quenching of Br((2)P1/2)
| AD-A243754 | p 1362 N92-17663

FLUORIDES
Vibrational energy transfer in bromine monofluoride
| AD-A243690 | p 1259 N92-17091
Plasma chemical vapor deposition of halide glasses
| AD-D015060 | p 1370 N92-17706

FLUORINATION
New experimental challenges in elemental fluorine chemistry: An emerging technology
| AD-A243054 | p 1258 N92-17043
Storing fluorine gas in carbon fibers and releasing the same
| NASA-CASE-LEW-15359-1 | p 1261 N92-17902

FLUORINE
New experimental challenges in elemental fluorine chemistry: An emerging technology
| AD-A243054 | p 1258 N92-17043
A reexamination of F-19 NMR in selected solids, the conductor Ag2F and reference insulators for studies of YBa2Cu3O7-type superconductors
| AD-A243194 | p 1372 N92-17219
Storing fluorine gas in carbon fibers and releasing the same
| NASA-CASE-LEW-15359-1 | p 1261 N92-17902

FLUORINE COMPOUNDS
Imide/arylene ether copolymers with pendent trifluoromethyl groups
| NASA-TM-104195 | p 1272 N92-17693

FLUORO COMPOUNDS
Substituted 1,1,1-triaryl-2,2,2-trifluoroethanes and processes for their synthesis
| NASA-CASE-LEW-14345-6 | p 1255 N92-17882

FLUOROHYDROCARBONS
Heat transfer enhancement due to bubble pumping in FC-72 near the saturation temperature
| AD-A243558 | p 1292 N92-17724

FLUOROPOLYMERS
A theoretical study of the combustion of magnesium/teflon/viton pyrotechnic compositions
| AD-A243244 | p 1275 N92-17058

FLUX (RATE)
Evaluation of solar flares and electron precipitation by nitrate distribution in Antarctica
| AD-A243026 | p 1389 N92-17235

FOAMS
Radar scattering from foamed plastic target supports
| AD-A243756 | p 1284 N92-17722

FOCAL PLANE DEVICES
Performance of ground-based infrared detectors for acquisition of satellites
| AD-A243247 | p 1281 N92-17241
Hubble Space Telescope: Optical telescope assembly handbook. Version 1.0
| NASA-CR-189751 | p 1386 N92-17483

FOILS (MATERIALS)
Comparative study of irreversibility effects in Nb foil and high temperature superconducting ceramics by muon spin rotation
| DE92-600475 | p 1294 N92-17953

FOREBODIES
Results of the space shuttle vehicle ascent air data system probe calibration test using a 0.07-scale external tank forebody model (68T) in the AEDC 16-foot transonic wind tunnel (IA-310), volume 1
| NASA-CR-167696 | p 1241 N92-17167
Results of the space shuttle vehicle ascent air data system probe calibration test using a 0.07-scale external tank forebody model (68T) in the AEDC 16-foot transonic wind tunnel (IA-310), volume 2
| NASA-CR-167697 | p 1241 N92-17214

FORMALISM
A variational formalism for the radiative transfer equation: Prelude to model 3 p 1322 N92-17978

FORMULATIONS
Exploring plasma sheath solutions for planar and cylindrical anodes
| AD-A243237 | p 1369 N92-17030

FORWARD SCATTERING
Effective dynamic material parameters and localized scattering
| AD-A241957 | p 1310 N92-17320

FOSSIL FUELS
Changing by degrees: Steps to reduce greenhouse gases
| PB91-205120 | p 1314 N92-17619

FOURIER ANALYSIS
High resolution imaging using phase retrieval, volume 2
| AD-A242925 | p 1366 N92-17550
Wave propagation in a randomly inhomogeneous medium: A study of the problem
| AD-A243741 | p 1284 N92-17691

FRACTALS
Image scanning using a fractal curve
| BBC-RD-1991/4 | p 1285 N92-17886
Fractal image encoding
| AD-A243620 | p 1344 N92-17921

FRACTURE MECHANICS
The effect of weld metal strength mismatch on the deformation and fracture behavior of steel butt weldments
| AD-A243239 | p 1262 N92-17057
The effect of titanium inclusions on HY-80 GMA weld deposits
| AD-A243408 | p 1239 N92-17192
Thermo-mechanical fatigue of a fiber reinforced titanium aluminide composite
| AD-A241988 | p 1256 N92-17607
Dynamic fracture characterization of Al2O3 and SiC(w)/Al2O3
| AD-A242187 | p 1273 N92-17784

FRACTURE STRENGTH
Strength and microstructure of ceramics
| AD-A243049 | p 1269 N92-17282
Aluminum alloys for ALS cryogenic tanks: Comparative measurements of cryogenic mechanical properties of Al-Li alloys and alloy 2219
| AD-A242956 | p 1264 N92-17379
Fracture toughness evaluation for N Reactor pressure tubes of Zircaloy-2 using the electric-potential method
| DE92-003631 | p 1311 N92-17713
Dynamic fracture characterization of Al2O3 and SiC(w)/Al2O3
| AD-A242187 | p 1273 N92-17784
Experimental investigation of interlaminar fracture toughness of carbon fiber/thermoplastic and carbon fiber/thermosetting composites by DCB specimens
| NAL-TR-1096 | p 1257 N92-17869
Novel ceramic matrix composites for deep submergence pressure vessel applications
| AD-A242740 | p 1274 N92-17947

FRACTURES (MATERIALS)
Effect of coatings and processing on failure mechanisms of polycarbonate material, phase 1
| AD-A243018 | p 1256 N92-17053
The effect of weld metal strength mismatch on the deformation and fracture behavior of steel butt weldments
| AD-A243239 | p 1262 N92-17057
Fatigue in single crystal nickel superalloys
| AD-A243453 | p 1265 N92-17653

FRACTURING
Dynamic fracture characterization of Al2O3 and SiC(w)/Al2O3
| AD-A242187 | p 1273 N92-17784

FRAGMENTS
Stability and structure of C12B24N24: A hybrid analog of buckminsterfullerene
| AD-A242327 | p 1373 N92-17245

FREE ATMOSPHERE
Turbulent and gravity wave transport in the free atmosphere p 1315 N92-17063

FREE CONVECTION
Effects of power pulsations on heat transfer from discrete heat sources
| AD-A243434 | p 1379 N92-17686
The role of thermal convection in heat and mass transport in the subarctic snow cover
| AD-A243674 | p 1312 N92-17715
FREE ELECTRON LASERS
The effects of field errors on low-gain free electron lasers
| AD-A243710 | p 1303 N92-17127
Compact free electron lasers for medical applications
| AD-A243497 | p 1304 N92-17582
Development of an XUV-IR free-electron laser user facility for scientific research and industrial applications
| DE92-003862 | p 1304 N92-17726
The Los Alamos FEL photoinjector drive laser
| DE92-003791 | p 1305 N92-17795
Achromatic and isochronous electron beam transport for tunable free electron lasers
| DE92-003908 | p 1305 N92-17868
Performance of hole coupling resonator in the presence of asymmetric modes and FEL gain
| DE92-003907 | p 1305 N92-17936
FREE ELECTRONS
Equation of state and conductivity of hot, dense matter
| AD-A243359 | p 1369 N92-17301
FREE FLOW
Effective viscosity in the simulation of spatially evolving shear flows with monotonic FCT models
| AD-A243709 | p 1295 N92-17126
The effect of freestream turbulence on the vortical flow over a delta wing p 1225 N92-17681
FREE-PISTON ENGINES
Loss terms in free-piston Stirling engine models
| NASA-CR-189840 | p 1312 N92-17225
FREEZING
Liquid-solid transition in the bond particle model for elemental semiconductors
| DE92-610441 | p 1378 N92-17972
FREQUENCIES
Frequency stirring: An alternate approach to mechanical mode-stirring for the conduct of electromagnetic susceptibility testing
| AD-A243551 | p 1279 N92-17031
Identification techniques: Frequency domain methods p 1231 N92-17158
Cooled ion frequency standard
| AD-A242030 | p 1360 N92-17549
A frequency-domain method for estimating the incidence and severity of sliding
| AD-A243077 | p 1334 N92-17569
FREQUENCY ASSIGNMENT
Effect of economic techniques on radio frequency utilization
| AD-A243187 | p 1282 N92-17366
FREQUENCY CONTROL
Effect of economic techniques on radio frequency utilization
| AD-A243187 | p 1282 N92-17366
FREQUENCY DISTRIBUTION
A hybrid modulation for the dissemination of weather data to aircraft p 1220 N92-17991
FREQUENCY RESPONSE
System identification requirements for high-bandwidth rotorcraft flight control system design p 1232 N92-17166
FREQUENCY SHIFT KEYING
Noncoherent detection of coherent optical heterodyne signals corrupted by laser phase noise
| AD-A243103 | p 1364 N92-16981
FREQUENCY STANDARDS
Cooled ion frequency standard
| AD-A242030 | p 1360 N92-17549
FRESNEL LENSES
Tandem concentrator photovoltaic array applied to Space Station Freedom evolutionary power requirements p 1251 N92-17769
FRICTION
Determination of the tribological fundamentals of solid lubricated ceramics. Volume 2: Appendices A through O
| AD-A242871 | p 1270 N92-17614
Determination of the tribological fundamentals of solid lubricated ceramics. Volume 1: Summary
| AD-A243219 | p 1272 N92-17683
FRONTS (METEOROLOGY)
Front detection with Doppler radar
| AD-A242880 | p 1319 N92-17289
Ocean simulation model. Version 2: First order frontal simulation
| AD-A243775 | p 1325 N92-17766
FUEL CELLS
EMU evolution p 1246 N92-17354
Catalysts for ultrahigh current density oxygen cathodes for space fuel cell applications
| NASA-CR-189787 | p 1253 N92-17365
FUEL COMBUSTION
A theoretical study of the combustion of magnesium/teflon/viton pyrotechnic compositions
| AD-A243244 | p 1275 N92-17058
FUEL FLOW
Safety considerations in testing a fuel-rich aeropropulsion gas generator
| NASA-TM-105258 | p 1235 N92-17061
FUEL PUMPS
Qualification test report. Fuel pump test stand 3C3965G05
| AD-A242929 | p 1235 N92-17552
FUEL-AIR RATIO
Experiments and analysis concerning the use of external burning to reduce aerospace vehicle transonic drag
| NASA-TM-105397 | p 1235 N92-17546
FULL SCALE TESTS
Mean wind speeds over hills and other topography
| ESDU-91043 | p 1321 N92-17853
FUNCTION SPACE
Chaos caused by a topologically mixing map
| DE91-641486 | p 1354 N92-17823
FUNCTIONAL ANALYSIS
Radio sky mapping from satellites at very low frequencies
| NASA-TM-105452 | p 1387 N92-17694
FUNCTIONAL DESIGN SPECIFICATIONS
Beyond the Baseline 1991: Proceedings of the Space Station Evolution Symposium. Volume 2: Space Station Freedom, part 1
| NASA-CP-10083-VOL-2-PT-1 | p 1251 N92-17768
FUSELAGES
An experimental study of a turbulent wing-body junction and wake flow
| AD-A243388 | p 1223 N92-17222
Rapid repair of integrally stiffened carbon fibre composite structures by bolted aluminium elements
| MBB-FE202-S-PUB-0453-A | p 1256 N92-17310

G

GALACTIC EVOLUTION
Late time cosmological phase transitions 1: Particle physics models and cosmic evolution
| NASA-CR-189857 | p 1388 N92-17696
GALACTIC NUCLEI
Interstellar scattering towards the galactic center as probed by OH/IR stars p 1390 N92-18004
GALAXIES
Constraints on cosmic ray propagation in the galaxy
| NASA-CR-189779 | p 1390 N92-18003
GALLIUM
Propane aromatization over gallium containing HZSM-5 zeolites
| ETN-92-90897 | p 1262 N92-17925
GALLIUM ANTIMONIDES
Tandem concentrator photovoltaic array applied to Space Station Freedom evolutionary power requirements p 1251 N92-17769
GALLIUM ARSENIDE LASERS
Studies of hetero-epitaxy of GaAs films on Si substrate for effective control of density and internal stress
| AD-A241882 | p 1374 N92-17594
GALLIUM ARSENIDES
Microstrip discontinuity models to 60 GHz
| AD-A242038 | p 1339 N92-17185
Failure mechanisms in GaAs ICs: The effects of deep traps
| AD-A243013 | p 1374 N92-17553
Studies of hetero-epitaxy of GaAs films on Si substrate for effective control of density and internal stress
| AD-A241882 | p 1374 N92-17594
Optical properties of thermally intermixed quantum wells and superlattices
| AD-A243546 | p 1375 N92-17618
Real-time edge-enhanced optical correlator
| NASA-CASE-NPO-18379-1-CU | p 1367 N92-17675
Gate drain geometry effect on the current voltage characteristics of GaAs MESFETs
| AD-A243430 | p 1291 N92-17684
Innovative switching technology
| DE92-003068 | p 1292 N92-17708
Tandem concentrator photovoltaic array applied to Space Station Freedom evolutionary power requirements p 1251 N92-17769
Au and Al Schottky barrier formation on GaAs (100) surfaces prepared by thermal desorption of a protective arsenic coating
| DE92-002456 | p 1376 N92-17781
GALLIUM COMPOUNDS
Ligand redistribution reactions of Me2Ga(C5H5) and MeGa(C5H5)2
| AD-A243264 | p 1254 N92-17270
GAMMA RAYS
The effects of storage on irradiated red blood cells: An in vitro an in vivo study
| AD-A243387 | p 1329 N92-17190
A study of gamma ray generation from channeled electrons and positions
| AD-A241993 | p 1361 N92-17608
GAS DENSITY
Transmission of thin light beams through turbulent mixing layers
| AD-A243470 | p 1367 N92-17658
GAS DYNAMICS
Statistically-based decompression tables. 6: Repeat dives on oxyen/nitrogen mixes
| AD-A243667 | p 1328 N92-17124
GAS FLOW
Velocity measurements in high temperature gases using laser-induced no fluorescence
| AD-A242399 | p 1295 N92-17012
Mass transfer in gas fluidized beds: Scaling, modeling, and particle size influence
| ETN-92-90581 | p 1298 N92-17522
Development and utilization of new diagnostics for dense-phase pneumatic transport
| DE92-003091 | p 1307 N92-17605
Determination of cohesive and normal stresses and simulation of fluidization using kinetic theory
| DE92-002905 | p 1299 N92-17709
Experimental study of amplitude-phase-frequency characteristics of flow when following over a vibrating plate
| DE92-610935 | p 1299 N92-17810
GAS GENERATORS
Safety considerations in testing a fuel-rich aeropropulsion gas generator
| NASA-TM-105258 | p 1235 N92-17061
Thermal insulation chemical composition and method of manufacture
| AD-D015106 | p 1257 N92-17836
GAS MIXTURES
Statistically-based decompression tables. 6: Repeat dives on oxyen/nitrogen mixes
| AD-A243667 | p 1328 N92-17124
Laser-based ignition of H2/O2 and D2/O2 premixed gases near 243 nm: The first report of a deuterium isotope wavelength effect in laser ignition
| AD-A243180 | p 1303 N92-17137
GAS TRANSPORT
Gas transport in polybutadiene treated with aqueous bromine
| AD-A241871 | p 1295 N92-17025
Mechanisms of gas permeation through polymer membranes
| DE92-004423 | p 1274 N92-17942
GAS TURBINE ENGINES
Safety considerations in testing a fuel-rich aeropropulsion gas generator
| NASA-TM-105258 | p 1235 N92-17061
Proceedings of the USAF Structural Integrity Program Conference
| AD-A242943 | p 1235 N92-17204
Local extinction mechanisms in non-premixed turbulent combustion
| AD-A242027 | p 1260 N92-17682
GAS-SOLID INTERFACES
Dynamics and stabilization of materials possessing high energy content
| AD-A243030 | p 1258 N92-16977
GASEOUS DIFFUSION
Mechanisms of gas permeation through polymer membranes
| DE92-004423 | p 1274 N92-17942
GASEOUS FUELS
Safety considerations in testing a fuel-rich aeropropulsion gas generator
| NASA-TM-105258 | p 1235 N92-17061
GASES
Launching projectiles with hydrogen gas generated from aluminum fuel powder/water reactions
| AD-D015119 | p 1276 N92-17830
GASOLINE
Evaluation of motor gasoline stability
| AD-A243063 | p 1275 N92-17066
GASTROINTESTINAL SYSTEM
Biological effects of protracted exposure to ionizing radiation: Review, analysis, and model development
| AD-A242981 | p 1329 N92-17476
GATES (CIRCUITS)
A comparative study of the noise performance of Alluminum Gallium Arsenide/Gallium Arsenide high electron mobility transistors with and without superconducting gate electrodes p 1288 N92-17317

Evaluation of an Interdigitated Gate Electrode Field-Effect Transistor (IGEFET) for in situ resin cure monitoring
| AD-A243713 | p 1289 N92-17501
Design implementation into field programmable gate arrays
| AD-A242538 | p 1343 N92-17680
Gate drain geometry effect on the current voltage characteristics of GaAs MESFETs
| AD-A243430 | p 1291 N92-17684
Characterizing the sensitivity, selectivity, and reversibility of the metal-doped phthalocyanine thin-films used with the Interdigitated Gate Electrode Field-Effect Transistor (IGEFET) to detect organophosphorous compounds and nitrogen dioxide
| AD-A243635 | p 1376 N92-17746

GAUGE INVARIANCE
Gauge-covariant Wess-Zumino actions for super p-branes in superspace
| DE91-641524 | p 1353 N92-17318

GAUGE THEORY
Gauge-covariant Wess-Zumino actions for super p-branes in superspace
| DE91-641524 | p 1353 N92-17318
Black holes in magnetic monopoles
| NASA-CR-189842 | p 1388 N92-17377
A classical instability of Reissner-Nordstrom solutions and the fate of magnetically charged black holes
| NASA-CR-189843 | p 1388 N92-17697
Temperature dependent anomalous statistics
| DE92-609665 | p 1379 N92-17807

GELLED PROPELLANTS
Upper stages using liquid propulsion and metallized propellants
| NASA-TP-3191 | p 1253 N92-17151

GELS
Molecular recognition in gels, monolayers, and solids
| AD-A243488 | p 1358 N92-17428
Electrically-controlled polymeric gels as active materials in adaptive structures
| DE92-002947 | p 1272 N92-17710
Production of mullite fibers
| NASA-CASE-MFS-28431-1 | p 1257 N92-17870

GENETICS
Biophysical techniques for examining metabolic, proliferative, and genetic effects of microwave radiation
| AD-A241903 | p 1326 N92-17288
Efficient identification and analysis of low and medium frequency repeats
| DE92-003758 | p 1385 N92-17856

GEOCHEMISTRY
Direct speciation of metal and metalloid ions by optical spectroscopies
| DE92-003868 | p 1261 N92-17727

GEODETIC ACCURACY
Spectral error models applied to the geodetic boundary value problem
| ETN-92-90582 | p 1312 N92-17436

GEOLOGICAL FAULTS
Studies of high-frequency seismic wave propagation
| AD-A241938 | p 1316 N92-17202

GEOLOGICAL SURVEYS
Workshop on Geologic Applications of Modern Aeromagnetic Surveys
| PB91-221788 | p 1316 N92-17229

GEOMAGNETISM
Atomic oxygen flux and fluence calculation for Long Duration Exposure Facility (LDEF)
| NASA-CR-187418 | p 1245 N92-17215
Workshop on Geologic Applications of Modern Aeromagnetic Surveys
| PB91-221788 | p 1316 N92-17229
Analysis of orbital elements and atmospheric activity to ascertain possible presence of an ion propulsion capability aboard Salyut 7/Cosmos 1686
| AD-A243654 | p 1251 N92-17762

GEOMETRICAL THEORY OF DIFFRACTION
A rigorous UTD analysis of electromagnetic scattering from resistive strips and resistive-loaded conducting strips
| AD-A243691 | p 1280 N92-17092
Automated composite ellipsoid modelling for high frequency GTD analysis
| NASA-CR-189853 | p 1233 N92-17316
A rigorous uniform diffraction analysis of the electromagnetic scattering from impedance edges and junctions
| AD-A243649 | p 1284 N92-17735

GEOPHYSICS
Solar-geophysical data number 562, June 1991. Part 2: (Comprehensive reports). Data for December 1990 and miscellaneous
| PB91-230219 | p 1387 N92-17251
Comparison of two eighth-mesh terrain databases
| AD-A243315 | p 1383 N92-17401

GEOPOTENTIAL HEIGHT
Modification of a successive corrections objective analysis for improved derivative calculations
p 1322 N92-17981

GEOSTROPHIC WIND
A variational formalism for the radiative transfer equation and a geostrophic, hydrostatic atmosphere: Prelude to model 3
p 1322 N92-17979

GERMANIUM
Transmission electron microscopy of the CVD diamond film/substrate interface
| AD-A243096 | p 1373 N92-17322
Liquid-solid transition in the bond particle model for elemental semiconductors
| DE92-610441 | p 1378 N92-17972

GERMANY
Worldwide Environmental Compliance Assessment and Management Program (ECAMP): German supplement
| AD-A242967 | p 1313 N92-17380

GIBBS FREE ENERGY
Application of the mean spherical approximation to describe the Gibbs solvation energies of monovalent monoatomic ions in non-aqueous solvents
| AD-A243200 | p 1259 N92-17371
Modelling of some equilibrium thermodynamic properties of polymer systems
| ETN-92-90570 | p 1273 N92-17840

GLASS ELECTRODES
Evaluation of an Interdigitated Gate Electrode Field-Effect Transistor (IGEFET) for in situ resin cure monitoring
| AD-A243713 | p 1289 N92-17501

GLASS FIBERS
Plasma chemical vapor deposition of halide glasses
| AD-D015060 | p 1370 N92-17706

GLASS TRANSITION TEMPERATURE
Phase transitions in narrow molecular mass samples of side-chain liquid crystalline polymers: Molecular mass dependence
| AD-A242354 | p 1269 N92-17448
Evaluation of an Interdigitated Gate Electrode Field-Effect Transistor (IGEFET) for in situ resin cure monitoring
| AD-A243713 | p 1289 N92-17501
Mechanical and thermomechanical properties of NC base propellants
| AD-A243045 | p 1276 N92-17632
The effect of physical aging on the creep response of a thermoplastic composite
| AD-A243600 | p 1258 N92-17932

GLAZES
Experimental ice shape and performance characteristics for a multi-element airfoil in the NASA Lewis Icing Research Tunnel
| NASA-TM-105380 | p 1224 N92-17347

GLOBAL POSITIONING SYSTEM
Multisensor signal processing techniques (hybrid GPS/LORAN-C with RAIM)
| AD-A242323 | p 1281 N92-17244
Incorporation of differential global positioning system measurements using an extended Kalman filter for improved reference system performance
| AD-A243742 | p 1228 N92-17481
Using the Global Positioning System (GPS) to fulfill the position/location requirements of the National Training Center (NTC) and other US Army instrumented testing and training ranges
| AD-A242064 | p 1229 N92-17639
Investigation of air transportation technology at Ohio University, 1990-1991 p 1220 N92-17990
GPS interferometric attitude and heading determination: Initial flight test results p 1221 N92-17994

GLUCOSE
Process of converting starch to glucose and glucose to lactic acid
| DE92-003840 | p 1255 N92-17867

GLYCINE
Preliminary assessment of the relative toxicity of tetraglycine hydroperiodide, phase 1
| AD-A243334 | p 1330 N92-17712

GOGGLES
User evaluation of laser ballistic sun, wind and dust goggle lenses (dye technology)
| AD-A243245 | p 1334 N92-17143

GOLD
Comparisons of self-assembled monolayers on silver and gold: Mixed monolayers derived from HS(CH2)21X and HS(CH2)10(sup Y) (X,Y-CH3, CH2OH) have similar properties
| AD-A243487 | p 1264 N92-17427
Inductively coupled plasma atomic emission spectroscopy analysis of gold electroplating solutions
| DE92-004798 | p 1266 N92-17858

GONDOLAS
Aircrew critique of high-G centrifuge training: Part 3: What can we change to better serve you?
| AD-A243496 | p 1334 N92-17432

GOODNESS OF FIT
Tests of fit for the Cauchy distribution based on the empirical distribution function
| AD-A243201 | p 1352 N92-17173

GOVERNMENT/INDUSTRY RELATIONS
The NASA/industry design analysis methods for vibrations (DAMVIBS) program: Accomplishments and contributions
| NASA-TM-104192 | p 1309 N92-17034
Space Station Freedom program. Commercial infrastructure and technology utilization
p 1244 N92-17111
Valuable patents for US businesses: A catalog of DTRC patents available for licensing by the private sector
| AD-A242071 | p 1385 N92-17141

GOVERNMENTS
Publications of the Executive Office of the President, January 20, 1989 to June 30, 1991
| PB91-202762 | p 1382 N92-17228

GRAIN BOUNDARIES
The effect of titanium inclusions on HY-80 GMA weld deposits
| AD-A243408 | p 1239 N92-17192
Strength and microstructure of ceramics
| AD-A243049 | p 1269 N92-17282
Transmission electron microscopy of the CVD diamond film/substrate interface
| AD-A243096 | p 1373 N92-17322
Microstructure and mechanical properties of HSLA-100 steel
| AD-A242937 | p 1265 N92-17467
Microstructure and composition of electromagnetically-characterized YBa2Cu3O(7-delta) grain boundaries
| DE92-003520 | p 1376 N92-17782
Grain boundaries
| DE92-004420 | p 1378 N92-17941

GRAIN SIZE
High resolution electron microscopy of diamond film growth defects and their interactions
| AD-A243093 | p 1372 N92-17238
Microstructure and mechanical properties of HSLA-100 steel
| AD-A242937 | p 1265 N92-17467

GRAMMARS
Decompiling with definite clause grammars
| AD-A242987 | p 1340 N92-17296
Mathematical basis for a system to manage automated protocol analysis
| AD-A242042 | p 1381 N92-17669

GRANULAR MATERIALS
Development and utilization of new diagnostics for dense-phase pneumatic transport
| DE92-000337 | p 1299 N92-17704

GRAPH THEORY
Topological representation of graph isomorphism types
| AD-A243528 | p 1350 N92-17148
IMPS: An Interactive Mathematical Proof System
| AD-A243162 | p 1350 N92-17206
FY92 mathematical research project proposal briefing
| AD-A243163 | p 1350 N92-17207

GRAPHITE
Determination of the tribological fundamentals of solid lubricated ceramics. Volume 2: Appendices A through O
| AD-A242871 | p 1270 N92-17614
Intercalated hybrid graphite fiber composite
| NASA-CASE-LEW-15241-1 | p 1257 N92-17861

GRAPHITE-EPOXY COMPOSITES
Acoustic emission monitoring of low velocity impact damage in graphite/epoxy laminates during tensile loading
| NASA-TM-4339 | p 1258 N92-17881

GRAPHITIZATION
Effect of thermal annealing on properly changes of neutron-irradiated non-graphitized carbon materials and nuclear graphite
| DE92-704180 | p 1257 N92-17816
Storing fluorine gas in carbon fibers and releasing the same
| NASA-CASE-LEW-15359-1 | p 1261 N92-17902

GRAPHS (CHARTS)
Topological representation of graph isomorphism types
| AD-A243528 | p 1350 N92-17148
Diagnostic report of the National Hurricane Center, August and September 1990, volume 3, number 2
| PB91-226886 | p 1321 N92-17621

GRATINGS (SPECTRA)
Aries x ray objective grating spectrograph
| NASA-CR-189245 | p 1386 N92-17003

Two-beam coupling measurements of grating phase in a photorefractive polymer
| AD-A243746 | p 1268 N92-17195
Atom wave interferometer
| AD-A243482 | p 1357 N92-17374
Photorefractivity in doped nonlinear organic polymers
| AD-A243751 | p 1271 N92-17661

GRAVITATION
Black holes in magnetic monopoles
| NASA-CR-189842 | p 1388 N92-17377
Lie-isotopic generalization of the Poincare symmetry: Classical formulation
| DE91-642825 | p 1379 N92-17531
Application of linear inverse theory to borehole gravity data
| DE92-002172 | p 1317 N92-17578
Future prospects of pregeometry
| DE92-704278 | p 1379 N92-17817

GRAVITATIONAL PHYSIOLOGY
Techniques for determination of impact forces during walking and running in a zero-G environment
| NASA-TP-3159 | p 1328 N92-17022

GRAVITY WAVES
Turbulent and gravity wave transport in the free atmosphere p 1315 N92-17063

GRAY SCALE
Comparative analysis of gray scale coding techniques for group 4 facsimile
| AD-A243175 | p 1278 N92-16996

GRAZING INCIDENCE
Full surface testing of grazing incidence mirrors
| AD-A243734 | p 1367 N92-17690

GREENHOUSE EFFECT
Changing by degrees: Steps to reduce greenhouse gases
| PB91-205120 | p 1314 N92-17619
Policy implications of greenhouse warming: Report of the adaptation panel p 1314 N92-17982

GRID GENERATION (MATHEMATICS)
Numerical grid generation using a variational method
| MBB-FE211-S-PUB-447 | p 1297 N92-17312
Computation of three-dimensional flows using two stream functions
| NASA-CR-187802 | p 1298 N92-17588
Study of turbulence by photon correlation spectroscopy
| AD-A243726 | p 1298 N92-17688

GRIDS
Groundscreen characterization
| AD-A243164 | p 1311 N92-17208

GROUND EFFECT MACHINES
Discussion for possibility of some aerodynamic ground effect craft
| NAL-TM-619 | p 1278 N92-17757

GROUND OPERATIONAL SUPPORT SYSTEM
Columbus Programme (current status) p 1243 N92-17100
JPL space station telerobotic engineering prototype development FY 91 status/achievements p 1247 N92-17359
Telerobotic ground-remote operations p 1247 N92-17360
Advanced Crew Personal Support Computer (CPSC) task p 1249 N92-17419

GROUND STATE
The EPR of the triplet state of aryl cations in crystals of diazonium salts p 1375 N92-17701

GROUND STATIONS
A computer solution for multiple satellite-satellite and satellite-ground station visibility determination
| AD-A243490 | p 1250 N92-17430
Radio frequency hazard monitoring-USAKA
| AD-A242873 | p 1283 N92-17563
Satellite links for television contribution: Reception requirements for links using transportable transmitting earth stations
| BBC-RD-1991/5 | p 1285 N92-17885

GROUND TESTS
Aircraft ground test and subscale model results of axial thrust loss caused by thrust vectoring using turning vanes
| NASA-TM-4341 | p 1230 N92-17071
The astronaut science advisor: Ground testing during SLS-1 p 1248 N92-17412

GROUND WATER
University of Minnesota Aquifer Thermal Energy Storage (ATES) project report on the first long-term cycle
| DE92-004699 | p 1313 N92-17934

GROUND WIND
Surface meteorological and near surface oceanographic atlas of the tropical Indian Ocean
| PB91-234286 | p 1319 N92-17138

GROUP THEORY
Characterization of the thermalness of a fissile system with a 2-group diffusion theory parameter
| AD-A243065 | p 1360 N92-17555

GROUP VELOCITY
On the generation of large-amplitude plasma wakefields with low phase velocities by an intense short laser pulse
| DE92-609543 | p 1371 N92-17805

GUIDANCE (MOTION)
Severe weather guide Mediterranean ports. Part 36: Limassol
| AD-A243448 | p 1320 N92-17492
Severe weather guide Mediterranean ports. Part 37: Larnaca
| AD-A243449 | p 1320 N92-17493
Flight evaluation of curved MLS precision approaches in a twin otter aircraft, phase 2
| AD-A243025 | p 1229 N92-17568

GUIDANCE SENSORS
Hubble Space Telescope: Fine guidance sensors instrument handbook. Version 2.1
| NASA-CR-189745 | p 1386 N92-17020

GULF OF ALASKA
Sea surface environmental conditions in the Gulf of Alaska during April 1990 using SSM/I
| AD-A241909 | p 1323 N92-17041

GULFS
A study on hydrographic conditions and salt budget calculation for the Gulf of Farallones with the data collected in August 1990
| AD-A243406 | p 1324 N92-17119
Proceedings of the 2nd Gulf of Cadiz Expedition Workshop
| AD-A242749 | p 1325 N92-17951

GUN PROPELLANTS
Energetic composites of cyclodextrin nitrate esters and nitrate ester plasticizers
| AD-D015068 | p 1275 N92-17399

GUSTS
Loading and vibration reduction through active aerodynamic control
| AD-A242321 | p 1236 N92-17243

H

H I REGIONS
IRAS and the Boston University Arecibo Galactic H I Survey: A catalog of cloud properties
| NASA-CR-189806 | p 1387 N92-17695

H II REGIONS
IRAS and the Boston University Arecibo Galactic H I Survey: A catalog of cloud properties
| NASA-CR-189806 | p 1387 N92-17695

HABITATS
Microbial diversity: Course report 1991
| AD-A243464 | p 1326 N92-17224

HABITUATION (LEARNING)
The 7th Annual Workshop on Computational Neuroscience
| AD-A243462 | p 1335 N92-17656

HADRONS
What experiments say about possibility of the new particle existence with mass less than the kaon mass
| DE91-634551 | p 1357 N92-17408
The determination of the number of light neutrino species
| ETN-92-90564 | p 1359 N92-17519
Muons in UA1; the 2nd level trigger and dimuon results
| ETN-92-90565 | p 1360 N92-17520
Lie-isotopic generalization of the Poincare symmetry: Classical formulation
| DE91-642825 | p 1379 N92-17531
High energy physics program at Texas A and M University
| DE92-004426 | p 1363 N92-17738
Relativistic nuclear many-body theory
| DE92-003258 | p 1362 N92-17789

HALIDES
Codeposition of elements in diffusion coatings by the halide-activated pack cementation method
| AD-A242860 | p 1267 N92-17042
Plasma chemical vapor deposition of halide glasses
| AD-D015060 | p 1370 N92-17706

HAMILTONIAN FUNCTIONS
Bottom contour influence on ray tracing
| AD-A242411 | p 1323 N92-17078
Inequalities among partial traces of Hermitian operators and partial sums of their Eigenvalues
| DE91-641495 | p 1351 N92-17622

HAMSTERS
Melatonin action on the circadian pacemaker in Siberian hamsters
| AD-A243057 | p 1325 N92-17142

HANDBOOKS
Hubble Space Telescope: Fine guidance sensors instrument handbook. Version 2.1
| NASA-CR-189745 | p 1386 N92-17020
Hubble Space Telescope: Faint object camera instrument handbook. Version 2.0
| NASA-CR-189746 | p 1386 N92-17021
Severe weather guide mediterranean ports. Part 35: Rota
| AD-A243539 | p 1319 N92-17338
Severe weather guide Mediterranean ports. Part 38: Alexandria
| AD-A243451 | p 1320 N92-17406
Hubble Space Telescope: Optical telescope assembly handbook. Version 1.0
| NASA-CR-189751 | p 1386 N92-17483
Hubble Space Telescope: Wide field and planetary camera instrument handbook. Version 2.1
| NASA-CR-189753 | p 1386 N92-17484
Hubble Space Telescope: High speed photometer instrument handbook. Version 2.0
| NASA-CR-189750 | p 1386 N92-17497

HARBORS
A user's manual for the Princeton Numerical Ocean Model
| AD-A243773 | p 1324 N92-17539

HARDENING (MATERIALS)
Effect of coatings and processing on failure mechanisms of polycarbonate material, phase 1
| AD-A243018 | p 1256 N92-17053

HARDNESS
Collisional energy deposition threshold for extended damage depths in ion-implanted silicates
| DE92-004737 | p 1377 N92-17797
Phosphazene polymer containing composites and method for making phosphazene polymer containing composites
| DE92-003826 | p 1274 N92-17935

HARDWARE
Muons in UA1; the 2nd level trigger and dimuon results
| ETN-92-90565 | p 1360 N92-17520
Interim Service ISDN Satellite (ISIS) hardware experiment design for advanced ISDN satellite design and experiments
| NASA-CR-186943 | p 1250 N92-17585
Effect of spatial locality prefetching on structural locality
| AD-A243632 | p 1337 N92-17922

HARMONIC GENERATIONS
Nonlinear spectroscopic studies of interfacial molecular ordering
| DE92-000864 | p 1360 N92-17530
Optical turbulence in second harmonic generation p 1377 N92-17821

HAZARDS
The hazard of exposure to 2.075 kHz center frequency narrow band impulses
| AD-A242997 | p 1329 N92-17299
Severe weather guide mediterranean ports. Part 35: Rota
| AD-A243539 | p 1319 N92-17338
Severe weather guide Mediterranean ports. Part 38: Alexandria
| AD-A243451 | p 1320 N92-17406
Radio frequency hazard monitoring-USAKA
| AD-A242873 | p 1283 N92-17563
Laser range safety
| AD-A243606 | p 1305 N92-17962
Alert generation and cockpit presentation for an integrated microburst alerting system p 1220 N92-17988

HEALTH
The effect of shower/bath frequency on the health and operational effectiveness of soldiers in a field setting: Recommendation of showering frequencies for reducing performance-degrading nonsystemic microbial skin infections
| AD-A242923 | p 1330 N92-17714

HEALTH PHYSICS
Hard-surface contamination detection exercise
| DE92-004750 | p 1330 N92-17798
Labor market trends for health physicists
| DE92-004770 | p 1331 N92-17800
Proceedings of the Conference on Health Physics
| DE92-704335 | p 1331 N92-17802

HEARING
The effects of speech intelligibility level on concurrent visual task performance
| AD-A243015 | p 1331 N92-17052
The effect of impulse presentation order on hearing trauma in the chinchilla
| AD-A243174 | p 1326 N92-17269

HEAT
Heat stress caused by wearing different types of CW protective garment
| AD-A243043 | p 1334 N92-17278

Alleviation of thermal strain in engineering space personnel aboard CF ships with the exotemp personal cooling system
| AD-A242889 | p 1330 N92-17599

HEAT EXCHANGERS
Nucleate pool boiling performance of small high flux and turbo-B tube bundles in R-114/oil mixtures
| AD-A241936 | p 1378 N92-17443

HEAT FLUX
Heat flux sensor research and development: The cool film calorimeter
| NASA-CR-189789 | p 1301 N92-17006
Thermal energy test apparatus
| AD-A243526 | p 1379 N92-17537

HEAT OF FORMATION
An experimental investigation of chemically-reacting, gas-phase turbulent jets
| AD-A243036 | p 1296 N92-17276

HEAT RESISTANT ALLOYS
Codeposition of elements in diffusion coatings by the halide-activated pack cementation method
| AD-A242860 | p 1267 N92-17042

HEAT SHIELDING
High contact blind hole thermocouple plug
| AD-D015105 | p 1302 N92-17835

HEAT STORAGE
Preliminary design study of a central solar heating plant with seasonal storage at the University of Massachusetts, Amherst
| DE92-000762 | p 1313 N92-17577
University of Minnesota Aquifer Thermal Energy Storage (ATES) project report on the first long-term cycle
| DE92-004699 | p 1313 N92-17934

HEAT TOLERANCE
Heat stress caused by wearing different types of CW protective garment
| AD-A243043 | p 1334 N92-17278

HEAT TRANSFER
Optimization in solar heating/photovoltaic systems
| AD-A242363 | p 1313 N92-17424
Nucleate pool boiling performance of small high flux and turbo-B tube bundles in R-114/oil mixtures
| AD-A241936 | p 1378 N92-17443
Preliminary design study of a central solar heating plant with seasonal storage at the University of Massachusetts, Amherst
| DE92-000762 | p 1313 N92-17577
Cooperative program to analyze heat transport at high beta in DIII-D
| DE92-003545 | p 1370 N92-17606
Downflow heat transfer in a heated ribbed vertical annulus with a cosine power profile (results from test series ECS-2c)
| DE92-003259 | p 1298 N92-17626
Heat transfer enhancement due to bubble pumping in FC-72 near the saturation temperature
| AD-A243558 | p 1292 N92-17724
Active thermal control system evolution
p 1252 N92-17775
Boundary-layer transition and heat transfer on slender delta wings
| AERO-REPT-8904 | p 1226 N92-17849
Wall temperature patterns in nucleate boiling
| OUEL-1876/91 | p 1380 N92-17879
Numerical simulation of fluid flow and heat transfer in a thin liquid film over a stationary and rotating disk and comparison with experimental data
| NASA-CR-189253 | p 1300 N92-17887

HEAT TRANSFER COEFFICIENTS
Numerical simulation of fluid flow and heat transfer in a thin liquid film over a stationary and rotating disk and comparison with experimental data
| NASA-CR-189253 | p 1300 N92-17887

HEAT TREATMENT
Solder extrusion pressure bonding process and bonded products produced thereby
| DE92-004603 | p 1363 N92-17739

HEATERS
Flight vehicle thermal testing with infrared lamps
| NASA-TM-4336 | p 1232 N92-17226
Active heater control and regulation for the Varian VGT-8011 gyrotron
| DE92-003638 | p 1302 N92-17454
Effects of power pulsations on heat transfer from discrete heat sources
| AD-A243434 | p 1379 N92-17686

HEATING
Storing fluorine gas in carbon fibers and releasing the same
| NASA-CASE-LEW-15359-1 | p 1261 N92-17902

HEATING EQUIPMENT
Optimization in solar heating/photovoltaic systems
| AD-A242363 | p 1313 N92-17424

HEAVY LIFT LAUNCH VEHICLES
Advanced space transportation systems
p 1242 N92-17104

HELICOPTER CONTROL
Instrumentation and data processing
p 1230 N92-17155
System identification requirements for high-bandwidth rotorcraft flight control system design
p 1232 N92-17166

HELICOPTER DESIGN
Design of experiments p 1230 N92-17154
BO 105 identification results p 1231 N92-17161
Industry view on rotorcraft system identification
p 1232 N92-17163

HELICOPTER PERFORMANCE
BO 105 identification results p 1231 N92-17161
SA 330 Puma identification results
p 1231 N92-17162
Industry view on rotorcraft system identification
p 1232 N92-17163

HELICOPTERS
Experiences at Langley Research Center in the application of optimization techniques to helicopter airframes for vibration reduction
| NASA-TM-104193 | p 1309 N92-17033
The NASA/industry design analysis methods for vibrations (DAMVIBS) program: Accomplishments and contributions
| NASA-TM-104192 | p 1309 N92-17034
Effects of the chemical defense antidote atropine sulfate on helicopter pilot performance: An in-flight study
| AD-A241966 | p 1328 N92-17084
Design of experiments p 1230 N92-17154
Instrumentation and data processing
p 1230 N92-17155
Identification techniques: Model structure and time domain methods p 1231 N92-17157
Automated composite ellipsoid modelling for high frequency GTD analysis
| NASA-CR-189853 | p 1233 N92-17316
Human response to helicopter noise: A test of A-weighting
| AD-A243719 | p 1355 N92-17506
General requirements and techniques for component fatigue life substantiation in Australian service helicopters
| AD-A242881 | p 1233 N92-17565
A frequency-domain method for estimating the incidence and severity of sliding
| AD-A243077 | p 1334 N92-17569
An investigation of air transportation technology at the Massachusetts Institute of Technology, 1990-1991
p 1219 N92-17985
Experimental investigation of passive infrared ice detection for helicopter applications
p 1220 N92-17986

HELIUM PLASMA
Experimental measurements of plasma properties for Miller SG-100 torch with Mach I setting
| DE92-003309 | p 1369 N92-17469

HELIUM-NEON LASERS
Transmission of thin light beams through turbulent mixing layers
| AD-A243470 | p 1367 N92-17658

HELMET MOUNTED DISPLAYS
Electronic expansion of human perception
| AD-A242028 | p 1333 N92-17634

HERMITIAN POLYNOMIAL
Inequalities among partial traces of Hermitian operators and partial sums of their Eigenvalues
| DE91-641495 | p 1351 N92-17622

HETERODYNING
Noncoherent detection of coherent optical heterodyne signals corrupted by laser phase noise
| AD-A243103 | p 1364 N92-16981

HETEROGENEITY
The instability of linear heterogeneous Lanchester equations
| AD-A243519 | p 1350 N92-17081

HEURISTIC METHODS
A Kalman filter for a Poisson series with covariates and Laplace approximation integration
| AD-A242960 | p 1286 N92-16993
Operations mission planner beyond the baseline
p 1246 N92-17353
A stochastic approach to the weighted-region problem: 1. The design of the path annealing algorithm
| AD-A243324 | p 1340 N92-17403

HEXAGONAL CELLS
The wave numbers of supercritical surface tension driven Benard convection
| NASA-CR-189856 | p 1373 N92-17375

HIERARCHIES
Topological representation of graph isomorphism types
| AD-A243528 | p 1350 N92-17148

HIGH DEFINITION TELEVISION
Sub-band/transform compression of video sequences
| NASA-CR-189786 | p 1280 N92-17139
Image scanning using a fractal curve
| BBC-RD-1991/4 | p 1285 N92-17886

HIGH ELECTRON MOBILITY TRANSISTORS
A comparative study of the noise performance of Alluminum Gallium Arsenide/Gallium Arsenide high electron mobility transistors with and without superconducting gate electrodes p 1288 N92-17317

HIGH ENERGY ELECTRONS
Dynamics and stabilization of materials possessing high energy content
| AD-A243030 | p 1258 N92-16977

HIGH ENERGY INTERACTIONS
High energy physics program at Texas A and M University
| DE92-004426 | p 1363 N92-17738

HIGH FREQUENCIES
Studies of high-frequency seismic wave propagation
| AD-A241938 | p 1316 N92-17202
Parallelizing serial code for a distributed processing environment with an application to high frequency electromagnetic scattering
| AD-A243755 | p 1284 N92-17721

HIGH GRAVITY ENVIRONMENTS
Aircrew critique of high-G centrifuge training: Part 3: What can we change to better serve you?
| AD-A243496 | p 1334 N92-17432

HIGH LEVEL LANGUAGES
Decompiling with definite clause grammars
| AD-A242987 | p 1340 N92-17296
The computational structural mechanics testbed procedures manual
| NASA-TM-100646 | p 1310 N92-17333
Parallelizing serial code for a distributed processing environment with an application to high frequency electromagnetic scattering
| AD-A243755 | p 1284 N92-17721
High level language-based robotic control system
| NASA-CASE-NPO-17918-2-CU | p 1349 N92-17895

HIGH PRESSURE
Evaluation of BAUER high pressure breathing air P-2 purification system
| AD-A243535 | p 1333 N92-17014
Launching projectiles with hydrogen gas generated from aluminum fuel powder/water reactions
| AD-D015119 | p 1276 N92-17830

HIGH RESOLUTION
High resolution electron microscopy of diamond film growth defects and their interactions
| AD-A243093 | p 1372 N92-17238
The ZEUS second level calorimeter trigger: Physics simulation, design and implementation
| ETN-92-90568 | p 1358 N92-17435
High resolution imaging using phase retrieval, volume 2
| AD-A242925 | p 1366 N92-17550
Gabor segmentation of high resolution synthetic aperture radar imagery
| AD-A243753 | p 1284 N92-17662

HIGH SPEED CAMERAS
Development of an electronic high speed camera system for the quantitative analysis of unsteady flows
| MPIS-100/1991 | p 1301 N92-17344

HIGH STRENGTH ALLOYS
Evaluation of a diffusion/trapping model for hydrogen ingress in high-strength alloys
| AD-A243461 | p 1263 N92-17327

HIGH TEMPERATURE AIR
ZEUS user manual real gas effects
| AD-A242224 | p 1225 N92-17446

HIGH TEMPERATURE ENVIRONMENTS
Making of functionally gradient materials data base
| NAL-TM-621 | p 1385 N92-17787

HIGH TEMPERATURE FLUIDS
Thermally regenerative fuel cells
| AD-A242900 | p 1290 N92-17629

HIGH TEMPERATURE GASES
Velocity measurements in high temperature gases using laser-induced no fluorescence
| AD-A242399 | p 1295 N92-17012

HIGH TEMPERATURE SUPERCONDUCTORS
Growth of near-free-standing YBa2Cu3O7-type crystals using a self-decanting flux method
| AD-A243221 | p 1372 N92-17182
Evidence for strong electron-phonon coupling in thermal conductivity of YBa2Cu3O(7-delta)
| AD-A243192 | p 1372 N92-17218
A reexamination of F-19 NMR in selected solids, the conductor Ag2F and reference insulators for studies of YBa2Cu3O7-type superconductors
| AD-A243194 | p 1372 N92-17219
Determination of the electronic density of states of YBa2Cu3O(7-delta)
| AD-A243223 | p 1372 N92-17220
Magnetic multilayer interface anisotropy
| DE92-000635 | p 1263 N92-17319

Pressure dependence of Tc in Tl2Ba2CaCu2O8 at hydrostatic pressures to 6 GPa
| AD-A243433 | p 1375 N92-17685
Radiation effects in High Temperature Superconductors (HTSC) oxides p 1375 N92-17700
Microstructure and composition of electromagnetically-characterized YBa2Cu3O(7-delta) grain boundaries
| DE92-003520 | p 1376 N92-17782
High temperature superconductor thin films and Josephson junctions
| AD-A242747 | p 1293 N92-17949
Comparative study of irreversibility effects in Nb foil and high temperature superconducting ceramics by muon spin rotation
| DE92-600475 | p 1294 N92-17953

HIGH TEMPERATURE TESTS
High-temperature durability considerations for HSCT combustor
| NASA-TP-3162 | p 1267 N92-17070
Flight vehicle thermal testing with infrared lamps
| NASA-TM-4336 | p 1232 N92-17226
A spectroscopic immersion ellipsometry study of the mechanism of Si/SiO2 interface annealing
| AD-A242831 | p 1259 N92-17261

HIGHLY MANEUVERABLE AIRCRAFT
Aerodynamic development of the X-31 aircraft for the high angle of attack region
| MBB-FE211-S-PUB-452 | p 1233 N92-17313

HISS
Radio sky mapping from satellites at very low frequencies
| NASA-TM-105452 | p 1387 N92-17694

HISTOCHEMICAL ANALYSIS
Evaluation of the initiation/promotion potential of CTFE trimer acid
| AD-A243479 | p 1255 N92-17373

HMX
Pyrolysis GC-FTIR studies of a LOVA propellant formulation series
| AD-A242844 | p 1275 N92-17562

HOLDERS
System for testing bearings
| NASA-CASE-MFS-28589-1 | p 1306 N92-17584

HOLE BURNING
Anomalous hole burning in polymers with inhomogeneous broadening
| AD-A242397 | p 1266 N92-17010

HOLES
High contact blind hole thermocouple plug
| AD-D015105 | p 1302 N92-17835

HOLES (ELECTRON DEFICIENCIES)
Excitons in semiconducting superlattices, quantum wells, and ternary alloys
| DE91-018805 | p 1374 N92-17528

HOLMIUM
Method and apparatus for lasing
| AD-D015154 | p 1305 N92-17923

HOLOGRAPHY
Optical content-addressable memories for data/knowledge base processing
| AD-A241866 | p 1382 N92-17037

HOMING DEVICES
Evaluation of a compact Cassegrain optical system
| AD-A242985 | p 1366 N92-17294

HOMODYNE RECEPTION
Study of turbulence by photon correlation spectroscopy
| AD-A243726 | p 1298 N92-17688

HOMOGENEITY
Frequency stirring: An alternate approach to mechanical mode-stirring for the conduct of electromagnetic susceptibility testing
| AD-A243551 | p 1279 N92-17031

HOOKS
Computer system evolution requirements for autonomous checkout of exploration vehicles p 1250 N92-17422

HORMONES
Melatonin action on the circadian pacemaker in Siberian hamsters
| AD-A243057 | p 1325 N92-17142

HOT ELECTRONS
A theoretical search for supervelocity semiconductors
| AD-A241981 | p 1376 N92-17783

HOT PRESSING
Examining Si3N4 base materials with various rare earth additions
| AD-A243668 | p 1372 N92-17082

HUBBLE CONSTANT
Geometrical methods for the analysis of cosmological observations
| ETN-92-90584 | p 1386 N92-17523

HUBBLE SPACE TELESCOPE
Hubble Space Telescope: Fine guidance sensors instrument handbook. Version 2.1
| NASA-CR-189745 | p 1386 N92-17020
Hubble Space Telescope: Faint object camera instrument handbook. Version 2.0
| NASA-CR-189746 | p 1386 N92-17021
STS-31 Space Shuttle mission report
| NASA-TM-105475 | p 1241 N92-17364
Hubble Space Telescope: Optical telescope assembly handbook. Version 1.0
| NASA-CR-189751 | p 1386 N92-17483
Hubble Space Telescope: Wide field and planetary camera instrument handbook. Version 2.1
| NASA-CR-189753 | p 1386 N92-17484
Hubble Space Telescope: The GO and GTO Observing Programs. Version 1.0
| NASA-CR-189815 | p 1387 N92-17650
Hubble Space Telescope: SRM/QA observations and lessons learned
| NASA-TM-105505 | p 1387 N92-17873

HUMAN BEINGS
A topographical analysis of the human electroencephalogram for patterns in the development of motion sickness
| AD-A243656 | p 1328 N92-17120
Melatonin action on the circadian pacemaker in Siberian hamsters
| AD-A243057 | p 1325 N92-17142
Mechanisms of temporal pattern discrimination by human observers
| AD-A243051 | p 1332 N92-17336
BrainMap: A database of functional neuroanatomy derived from human brain images
| AD-A243161 | p 1333 N92-17648

HUMAN BODY
Electromagnetic pulse-induced current measurement device
| AD-A241946 | p 1291 N92-17668

HUMAN CENTRIFUGES
Aircrew critique of high-G centrifuge training: Part 3: What can we change to better serve you?
| AD-A243496 | p 1334 N92-17432

HUMAN FACTORS ENGINEERING
USI rapid prototyping tool evaluations survey
| AD-A243168 | p 1335 N92-17673
Developing a broader basis for scientific data analysis interfaces
| DE92-003963 | p 1385 N92-17845

HUMAN PERFORMANCE
The effects of speech intelligibility level on concurrent visual task performance
| AD-A243015 | p 1331 N92-17052
Image analysis using Gabor transforms: Correlated with human saccadic movement data to identify the human visual search strategy
| AD-A243692 | p 1338 N92-17093
Neural network classification of mental workload conditions by analysis of spontaneous electroencephalograms
| AD-A243369 | p 1331 N92-17115
A performance model of Thermal Imaging System (TISs) which includes the human observer's response to state of the art displays
| AD-A242838 | p 1301 N92-17273
Intelligent Computer-Aided Training (ICAT) p 1246 N92-17352
Fatigue effects on human performance in combat: A literature review, volume 1
| AD-A242887 | p 1330 N92-17567
Eccentric and concentric muscle performance following 7 days of simulated weightlessness
| NASA-TP-3182 | p 1330 N92-17645

HUMAN REACTIONS
Rapid nonconjugate adaptation of vertical voluntary pursuit eye movements
| AD-A243358 | p 1331 N92-17145

HUMIDITY
Heat stress caused by wearing different types of CW protective garment
| AD-A243043 | p 1334 N92-17278
Upper body exercise: Physiology and training application for human presence in space
| AD-A242033 | p 1329 N92-17473

HUMIDITY MEASUREMENT
A proposed improved method of radiosonde humidity sensing
| AD-A242954 | p 1319 N92-17233

HURRICANES
Diagnostic report of the National Hurricane Center, August and September 1990, volume 3, number 2
| PB91-226886 | p 1321 N92-17621
The National Hurricane Center Risk Analysis Program (HURISK)
| PB91-236463 | p 1321 N92-17705

HYBRID NAVIGATION SYSTEMS
Incorporation of differential global positioning system measurements using an extended Kalman filter for improved reference system performance
| AD-A243742 | p 1228 N92-17481

HYDRAULICS
Downflow heat transfer in a heated ribbed vertical annulus with a cosine power profile (results from test series ECS-2c)
| DE92-003259 | p 1298 N92-17626

HYDRODYNAMIC EQUATIONS
Parallel block methods for sparse symmetric linear systems of equations
| AD-A242315 | p 1351 N92-17560

HYDRODYNAMICS
Computation of the hydrodynamic forces and moments on a body of revolution with and without appendages
| AD-A243033 | p 1294 N92-16978
Dielectric properties of aligned conducting polymers
| AD-A243389 | p 1268 N92-17191
User's guide for a three-dimensional numerical hydrodynamic, salinity, and temperature model of Chesapeake Bay
| AD-A242993 | p 1324 N92-17298
Basic hydrodynamics
| AD-A243513 | p 1297 N92-17387
On size scaling in shock hydrodynamics and the stress-strain behavior of copper at exceedingly high strain rates
| DE92-003797 | p 1265 N92-17579
The effect of detonation curvature on cylindrical wall motion
| DE92-003110 | p 1298 N92-17625
Differential pressure sensor
| AD-D015134 | p 1302 N92-17918
An investigation of gouge initiation in high-velocity sliding contact
| DE92-003944 | p 1311 N92-17937

HYDROGEN
Experiments and analysis concerning the use of external burning to reduce aerospace vehicle transonic drag
| NASA-TM-105397 | p 1235 N92-17546

HYDROGEN ATOMS
Laser-based ignition of H2/O2 and D2/O2 premixed gases near 243 nm: The first report of a deuterium isotope wavelength effect in laser ignition
| AD-A243180 | p 1303 N92-17137

HYDROGEN BONDS
Designing ordered molecular arrays in two and three dimensions
| AD-A243447 | p 1359 N92-17491

HYDROGEN EMBRITTLEMENT
Evaluation of a diffusion/trapping model for hydrogen ingress in high-strength alloys
| AD-A243461 | p 1263 N92-17327

HYDROGEN FUELS
Launching projectiles with hydrogen gas generated from aluminum fuel powder/water reactions
| AD-D015119 | p 1276 N92-17830

HYDROGEN ISOTOPES
Concentration of isotopic hydrogen by temperature gradient effect in soluble metal
| AD-D015062 | p 1260 N92-17628

HYDROGEN PRODUCTION
Catalytic studies on a novel synthesis of methanol
| DE92-002904 | p 1275 N92-17184

HYDROGRAPHY
A study on hydrographic conditions and salt budget calculation for the Gulf of Farallones with the data collected in August 1990
| AD-A243406 | p 1324 N92-17119
An investigation of cold overflow over the Iceland/Faeroes Ridge
| AD-A243084 | p 1324 N92-17169
Proceedings of the 2nd Gulf of Cadiz Expedition Workshop
| AD-A242749 | p 1325 N92-17951

HYDROSTATIC PRESSURE
Pressure dependence of Tc in Tl2Ba2CaCu2O8 at hydrostatic pressures to 6 GPa
| AD-A243433 | p 1375 N92-17685

HYDROSTATICS
A variational assimilation method for satellite and conventional data: Development of basic model for diagnosis of cyclone systems
| NASA-CR-188236 | p 1321 N92-17975
A variational formalism for the radiative transfer equation and a geostrophic, hydrostatic atmosphere: Prelude to model 3 p 1322 N92-17979

HYDROXIDES
Clean room wiping liquids
| DE92-004793 | p 1238 N92-17967

HYDROXYL EMISSION
Interstellar scattering towards the galactic center as probed by OH/IR stars p 1390 N92-18004

HYGIENE
The effect of shower/bath frequency on the health and operational effectiveness of soldiers in a field setting: Recommendation of showering frequencies for reducing performance-degrading nonsystemic microbial skin infections
| AD-A242923 | p 1330 N92-17714
HYPERCUBE MULTIPROCESSORS
Implementation of an object-oriented flight simulator D.C. electrical system on a hypercube architecture
| AD-A243700 | p 1238 N92-17097
Improved task scheduling for parallel simulations
| AD-A243721 | p 1346 N92-17507
Parallel implementation of VHDL simulations on the Intel iPSC/2 hypercube
| AD-A243760 | p 1342 N92-17603
HYPERFINE STRUCTURE
Y89ONMR study of hyperfine interactions in (R(x)Y(1-x))Fe2
| DE91-641979 | p 1376 N92-17779
HYPERGEOMETRIC FUNCTIONS
Some results for extended Jacobi polynomials
| DE92-609035 | p 1351 N92-17939
HYPERSONIC FLOW
Comparison of two solution methods for the numerical calculation of hypersonic flows
| MBB-FE211-S-PUB-446 | p 1224 N92-17311
HYPERVELOCITY IMPACT
Hypervelocity impact simulation for micrometeorite and debris shield design
| NASA-CR-189807 | p 1244 N92-17200
On size scaling in shock hydrodynamics and the stress-strain behavior of copper at exceedingly high strain rates
| DE92-003797 | p 1265 N92-17579
HYPERVELOCITY LAUNCHERS
Analysis of ram acceleration for high velocity applications
| AD-A242338 | p 1235 N92-17642
HYPERVELOCITY PROJECTILES
Analysis of ram acceleration for high velocity applications
| AD-A242338 | p 1235 N92-17642
HYSTERESIS
An experimental investigation of leading edge vortical flow about a delta wing during wing rock
| AD-A243363 | p 1223 N92-17114

I

ICE
Evaluation of solar flares and electron precipitation by nitrate distribution in Antarctica
| AD-A243026 | p 1389 N92-17235
Experimental ice shape and performance characteristics for a multi-element airfoil in the NASA Lewis Icing Research Tunnel
| NASA-TM-105380 | p 1224 N92-17347
Deterministic multi-zone ice accretion modeling
p 1220 N92-17987
ICE FORMATION
An investigation of air transportation technology at the Massachusetts Institute of Technology, 1990-1991
p 1219 N92-17985
Experimental investigation of passive infrared ice detection for helicopter applications
p 1220 N92-17986
Deterministic multi-zone ice accretion modeling
p 1220 N92-17987
ICE REPORTING
Experimental investigation of passive infrared ice detection for helicopter applications
p 1220 N92-17986
ICELAND
An investigation of cold overflow over the Iceland/Faeroes Ridge
| AD-A243084 | p 1324 N92-17169
IDEAL GAS
Application of program LAURA to perfect gas shock tube flows: A parametric study
| NASA-TM-104190 | p 1294 N92-17002
IDENTIFYING
New algorithms for broad-band and narrowband source localization and a separable 2-D IIR filter realization
| AD-A243457 | p 1291 N92-17654
IGNITION
Development of fuel neutralizing agents to prevent flashback on aircraft fires
| AD-A242828 | p 1227 N92-17259
A study of ignition and simulation circuits for arcjet thrusters, part 1
| NASA-CR-189097 | p 1253 N92-17510
Pyrolysis GC-FTIR studies of a LOVA propellant formulation series
| AD-A242844 | p 1275 N92-17562
ILLUMINANCE
Transmission of thin light beams through turbulent mixing layers
| AD-A243470 | p 1367 N92-17658
ILLUSIONS
Analysis of visual illusions using multiresolution wavelet decomposition based models
| AD-A243712 | p 1332 N92-17500
IMAGE ANALYSIS
Development of real-time image and in situ data analysis at sea
| AD-A243682 | p 1242 N92-17075
Feature extraction for pose estimation: A comparison between synthetic and real IR imagery
| AD-A243699 | p 1338 N92-17077
Image analysis using Gabor transforms: Correlated with human saccadic movement data to identify the human visual search strategy
| AD-A243692 | p 1338 N92-17093
Analysis of scene conditions at the light helicopter target acquisition subsystem demonstration/validation, Yuma Proving Ground, Arizona, September 1990
| AD-A243234 | p 1234 N92-17240
IMAGE ENHANCEMENT
Real-time edge-enhanced optical correlator
| NASA-CASE-NPO-18379-1-CU | p 1367 N92-17675
IMAGE PROCESSING
Design of a fiber optic image transmission link
| AD-A243686 | p 1365 N92-17088
Evaluation of scalar value estimation techniques for 3D medical imaging
| AD-A243687 | p 1328 N92-17089
Face recognition with the Karhunen-Loeve transform
| AD-A243688 | p 1280 N92-17090
Analysis of scene conditions at the light helicopter target acquisition subsystem demonstration/validation, Yuma Proving Ground, Arizona, September 1990
| AD-A243234 | p 1234 N92-17240
Development of an electronic high speed camera system for the quantitative analysis of unsteady flows
| MPIS-100/1991 | p 1301 N92-17344
Recording of three dimensional trajectories and velocity fields by automatic image processing
| MPIS-101/1991 | p 1301 N92-17345
Integrated system for missile detection and discrimination
| DE91-018874 | p 1283 N92-17529
Study of features of binary images using algebra techniques
| AD-A242010 | p 1351 N92-17609
Electronic expansion of human perception
| AD-A242028 | p 1333 N92-17634
Gabor segmentation of high resolution synthetic aperture radar imagery
| AD-A243753 | p 1284 N92-17662
Image processing applications for nonlinear decomposition and synthesis
| AD-A243357 | p 1343 N92-17733
Optical image segmentation using wavelet correlation
| AD-A243650 | p 1367 N92-17736
Effect of two types of scene detail on detection of altitude change in a flight simulator
| AD-A242034 | p 1333 N92-17758
Developing a broader basis for scientific data analysis interfaces
| DE92-003963 | p 1385 N92-17845
Image scanning using a fractal curve
| BBC-RD-1991/4 | p 1285 N92-17886
IMAGE RECONSTRUCTION
Face recognition with the Karhunen-Loeve transform
| AD-A243688 | p 1280 N92-17090
Performance of the Rayleigh task based on the posterior probability of tomographic reconstructions
| DE92-003785 | p 1352 N92-17455
IMAGE RESOLUTION
Analysis of visual illusions using multiresolution wavelet decomposition based models
| AD-A243712 | p 1332 N92-17500
IMAGES
High resolution imaging using phase retrieval, volume 2
| AD-A242925 | p 1366 N92-17550
The cognitive, perceptual, and neural bases of skilled performance
| AD-A243052 | p 1332 N92-17554
IMAGING TECHNIQUES
Evaluation of scalar value estimation techniques for 3D medical imaging
| AD-A243687 | p 1328 N92-17089
Extracting the shape and roughness of specular lobe objects using four light photometric stereo
| AD-A243522 | p 1365 N92-17146
Studies of high-frequency seismic wave propagation
| AD-A241938 | p 1316 N92-17202
Integrated system for missile detection and discrimination
| DE91-018874 | p 1283 N92-17529
High resolution imaging using phase retrieval, volume 2
| AD-A242925 | p 1366 N92-17550
Diffraction and imaging theory of inelastically scattered electrons: A new approach
| DE91-018248 | p 1360 N92-17574
Liquid and solid ion plasmas
| AD-A242029 | p 1370 N92-17635
Incremental volume rendering algorithm for interactive 3D ultrasound imaging
| AD-A242048 | p 1342 N92-17637
An investigation of the application of artificial neural networks to adaptive optics imaging systems
| AD-A243780 | p 1348 N92-17767
Wide field strip-imaging optical system
| NASA-CASE-NPO-18146-1-CU | p 1368 N92-17892
IMIDES
Imide/arylene ether copolymers with pendent trifluoromethyl groups
| NASA-TM-104195 | p 1272 N92-17693
IMMUNOASSAY
Characterization of the P. brevis polyether neurotoxin binding component in excitable membranes
| AD-A242877 | p 1327 N92-17564
IMPACT DAMAGE
Effect of coatings and processing on failure mechanisms of polycarbonate material, phase 1
| AD-A243018 | p 1256 N92-17053
On size scaling in shock hydrodynamics and the stress-strain behavior of copper at exceedingly high strain rates
| DE92-003797 | p 1265 N92-17579
Acoustic emission monitoring of low velocity impact damage in graphite/epoxy laminates during tensile loading
| NASA-TM-4339 | p 1258 N92-17881
IMPACT LOADS
Techniques for determination of impact forces during walking and running in a zero-G environment
| NASA-TP-3159 | p 1328 N92-17022
Explicit finite element method for transparency impact analysis
| AD-A243527 | p 1227 N92-17478
Structural dynamics division research and technology accomplishments for F.Y. 1991 and plans for F.Y. 1992
| NASA-TM-104188 | p 1225 N92-17509
IMPACT STRENGTH
The use of impact force as a scale parameter for the impact response of composite laminates
| NASA-TM-104189 | p 1256 N92-17007
IMPACT TESTS
The use of impact force as a scale parameter for the impact response of composite laminates
| NASA-TM-104189 | p 1256 N92-17007
On size scaling in shock hydrodynamics and the stress-strain behavior of copper at exceedingly high strain rates
| DE92-003797 | p 1265 N92-17579
IMPEDANCE
A discontinuity study in shielded coplanar line
| AD-A242976 | p 1288 N92-17290
A rigorous uniform diffraction analysis of the electromagnetic scattering from impedance edges and junctions
| AD-A243649 | p 1284 N92-17735
IMPINGEMENT
Study of plane wave impingement on a thin plate capable of deformation
| AD-A242947 | p 1296 N92-17275
IMPLANTATION
Optical properties of thermally intermixed quantum wells and superlattices
| AD-A243546 | p 1375 N92-17618
IMPULSES
The hazard of exposure to 2.075 kHz center frequency narrow band impulses
| AD-A242997 | p 1329 N92-17299
IMPURITIES
Optical spectra and kinetics of single impurity molecules in a polymer: Spectral diffusion and persistent spectral hole-burning
| AD-A243749 | p 1271 N92-17659
Optical modification of a single impurity molecule in a solid
| AD-A243750 | p 1361 N92-17660
A one-dimensional plasma and impurity transport model for reversed field pinches
| DE92-004691 | p 1371 N92-17933
INCLUSIONS
The effect of titanium inclusions on HY-80 GMA weld deposits
| AD-A243408 | p 1239 N92-17192

INCOHERENT SCATTER RADAR
Radar-satellite studies of the high-latitude ionosphere
| AD-A243275 | p 1317 N92-17961
INCOMPRESSIBLE FLOW
An experimental study of a turbulent wing-body junction and wake flow
| AD-A243388 | p 1223 N92-17222
Consistency and integrability of Navier-Stokes and systems of equations for incompressible flow magnetohydrodynamics p 1298 N92-17699
The effect of isolated roughness elements on transition in attachment-line flows
| AERO-REPT-8905 | p 1300 N92-17850
INDIAN OCEAN
Surface meteorological and near surface oceanographic atlas of the tropical Indian Ocean
| PB91-234286 | p 1319 N92-17138
INDIUM ANTIMONIDES
A study of nonlinear reflection and optical switching in indium antimonide
| AD-A242835 | p 1365 N92-17249
INDIUM COMPOUNDS
Cryogenic thermoresistor made from p-InSb(Mn)
| DE92-600473 | p 1293 N92-17825
INDIUM PHOSPHIDES
Innovative optoelectronic materials and structures using OMVPE
| AD-A243257 | p 1371 N92-16984
INDUCTION MOTORS
Analytical determination of arrest and starting torque of a bipolar DC motor with permanent magnets
| ETN-92-90586 | p 1290 N92-17540
INDUSTRIAL MANAGEMENT
A management case analysis of the Department of Defense contractor risk assessment guide program
| AD-A243515 | p 1380 N92-17388
INDUSTRIAL WASTES
Scale-up of recovery process for waste solvents
| KCP-613-4479 | p 1277 N92-17535
INDUSTRIES
Valuable patents for US businesses: A catalog of DTRC patents available for licensing by the private sector
| AD-A242071 | p 1385 N92-17141
Plasma processing of materials: Scientific opportunities and technological challenges
| LC-91-66812 | p 1370 N92-17556
INELASTIC SCATTERING
Diffraction and imaging theory of inelastically scattered electrons: A new approach
| DE91-018248 | p 1360 N92-17574
Pion-nucleus cross sections
| DE92-600631 | p 1363 N92-17958
INEQUALITIES
Inequalities among partial traces of Hermitian operators and partial sums of their Eigenvalues
| DE91-641495 | p 1351 N92-17622
INERTIAL NAVIGATION
Incorporation of differential global positioning system measurements using an extended Kalman filter for improved reference system performance
| AD-A243742 | p 1228 N92-17481
Investigation of air transportation technology at Ohio University, 1990-1991 p 1220 N92-17990
INERTIAL UPPER STAGE
Upper stages using liquid propulsion and metallized propellants
| NASA-TP-3191 | p 1253 N92-17151
INFECTIOUS DISEASES
The effect of shower/bath frequency on the health and operational effectiveness of soldiers in a field setting: Recommendation of showering frequencies for reducing performance-degrading nonsystemic microbial skin infections
| AD-A242923 | p 1330 N92-17714
INFERENCE
IMPS: An Interactive Mathematical Proof System
| AD-A243162 | p 1350 N92-17206
INFILTRATION
Polymer infiltration studies
| NASA-CR-189773 | p 1266 N92-17004
INFORMATION
Acquisition and production of skilled behavior in dynamic decision-making tasks
| NASA-CR-189846 | p 1333 N92-17132
INFORMATION DISSEMINATION
Bibliography of technical reports 1990
| AD-A242376 | p 1383 N92-17378
INFORMATION FLOW
Thermal Control System Automation Project (TCSAP) p 1252 N92-17776
INFORMATION MANAGEMENT
Information management 70XX civilian equivalent
| AD-A242875 | p 1381 N92-17013
The top ten critical MIS issues in the Department of Defense
| AD-A242975 | p 1382 N92-17255
Bibliography of technical publications, papers, and list of patents, October 1988 - September 1989
| AD-A242839 | p 1383 N92-17274
Cost models and the Corporate Information Management (CIM) initiative
| AD-A243554 | p 1383 N92-17340
Information Management Engineering (IME) laboratory: A database development facility
| AD-A243191 | p 1383 N92-17369
INFORMATION PROCESSING (BIOLOGY)
A computational model of semantic memory impairment: Modality-specificity and emergent category-specificity
| AD-A242377 | p 1347 N92-16991
A connectionist simulation of attention and vector comparison: The need for serial processing in parallel hardware
| AD-A242225 | p 1348 N92-17457
Attention, automaticity and priority learning
| AD-A242226 | p 1332 N92-17458
INFORMATION RETRIEVAL
Towards intelligent data retrieval in multimedia databases
| AD-A243323 | p 1383 N92-17402
The dynamics of visual representation, attention, encoding, and retrieval processes
| AD-A243031 | p 1384 N92-17785
Dynamic pattern matcher using incomplete data
| NASA-CASE-MSC-21415-1-SB | p 1344 N92-17860
INFORMATION SYSTEMS
BATTLEKING evaluation, BK 22-91, Meteorological Sensor Package (MSP)
| AD-A241919 | p 1317 N92-17009
Information management 70XX civilian equivalent
| AD-A242875 | p 1381 N92-17013
Economic analysis of information system
| AD-A243079 | p 1382 N92-17067
Benefit analysis of proposed information systems
| AD-A243707 | p 1382 N92-17125
CALS database usage and analysis tool study
| AD-A243205 | p 1382 N92-17174
The top ten critical MIS issues in the Department of Defense
| AD-A242975 | p 1382 N92-17255
Cost models and the Corporate Information Management (CIM) initiative
| AD-A243554 | p 1383 N92-17340
A comparison of data integrity models
| AD-A243770 | p 1384 N92-17633
Dynamic pattern matcher using incomplete data
| NASA-CASE-MSC-21415-1-SB | p 1344 N92-17860
INFORMATION THEORY
ECLSS predictive monitoring p 1247 N92-17357
Dynamic pattern matcher using incomplete data
| NASA-CASE-MSC-21415-1-SB | p 1344 N92-17860
INFORMATION TRANSFER
Cockpit display of hazardous weather information p 1220 N92-17989
INFRARED ASTRONOMY
IRAS and the Boston University Arecibo Galactic H I Survey: A catalog of cloud properties
| NASA-CR-189806 | p 1387 N92-17695
INFRARED ASTRONOMY SATELLITE
IRAS and the Boston University Arecibo Galactic H I Survey: A catalog of cloud properties
| NASA-CR-189806 | p 1387 N92-17695
INFRARED DETECTORS
Performance of ground-based infrared detectors for acquisition of satellites
| AD-A243247 | p 1281 N92-17241
An investigation of air transportation technology at the Massachusetts Institute of Technology, 1990-1991 p 1219 N92-17985
Experimental investigation of passive infrared ice detection for helicopter applications p 1220 N92-17986
INFRARED IMAGERY
Feature extraction for pose estimation: A comparison between synthetic and real IR imagery
| AD-A243699 | p 1338 N92-17077
Design of a fiber optic image transmission link
| AD-A243686 | p 1365 N92-17088
Improved 320x244-element PtSi Schottky-barrier IR-CCD image sensor
| AD-A242026 | p 1301 N92-17140
A performance model of Thermal Imaging System (TISs) which includes the human observer's response to state of the art displays
| AD-A242838 | p 1301 N92-17273
INFRARED LASERS
Development of an XUV-IR free-electron laser user facility for scientific research and industrial applications
| DE92-003862 | p 1304 N92-17726
INFRARED RADIATION
Flight vehicle thermal testing with infrared lamps
| NASA-TM-4336 | p 1232 N92-17226
Infrared rotating analyzer ellipsometry: Calibration and data processing
| AD-A242834 | p 1259 N92-17248
Steady-state production and quenching of Br((2)P1/2)
| AD-A243754 | p 1362 N92-17663
INFRARED SIGNATURES
Performance of ground-based infrared detectors for acquisition of satellites
| AD-A243247 | p 1281 N92-17241
Evaluation of LOWTRAN and MODTRAN for use over high zenith angle/long path length viewing
| AD-A243599 | p 1387 N92-17920
INFRARED STARS
Interstellar scattering towards the galactic center as probed by OH/IR stars p 1390 N92-18004
INFRARED WINDOWS
New optical materials for the long-wave (8-12 microns) region: Design criteria for the solid-state chemist
| AD-A243280 | p 1365 N92-17284
INGESTION (BIOLOGY)
Preliminary assessment of the relative toxicity of tetraglycine hydroperiodide, phase 1
| AD-A243334 | p 1330 N92-17712
INHOMOGENEITY
Large ideals and non-regular ultrafilters
| ETN-92-90587 | p 1351 N92-17525
Wave propagation in a randomly inhomogeneous medium: A study of the problem
| AD-A243741 | p 1284 N92-17691
INJECTION
Injection of drag reducing additives into turbulent water flows
| AD-A243209 | p 1296 N92-17176
INLET NOZZLES
The influence of cavitation in the breakup of liquid free jets
| MPIS-1/1991 | p 1297 N92-17343
INLET PRESSURE
Modification of Jindivik air intake duct with an auxiliary intake static aerodynamic tests
| AD-A243002 | p 1232 N92-17234
INPUT/OUTPUT ROUTINES
Verification and validation of the Comprehensive Operational Support Evaluation Model for space
| AD-A243653 | p 1344 N92-17761
INSPECTION
Extendable pipe crawler
| DE91-011570 | p 1306 N92-17183
INSULATORS
A reexamination of F-19 NMR in selected solids, the conductor Ag2F and reference insulators for studies of YBa2Cu3O7-type superconductors
| AD-A243194 | p 1372 N92-17219
Structural, electronic, and magnetic properties of La(x)Sr(1-x)VO3 (0 is less than or equal to x is less than or equal to 1.0)
| DE92-003808 | p 1378 N92-17916
INTEGRAL EQUATIONS
A theory of inverse operators for multiple excitations
| AD-A243484 | p 1350 N92-17330
Alfven waves in inhomogeneous magnetic fields: An integro-differential equation formulation
| DE92-609544 | p 1371 N92-17806
INTEGRALS
One-loop calculations with massive particles
| ETN-92-90563 | p 1359 N92-17518
INTEGRATED CIRCUITS
Innovative optoelectronic materials and structures using OMVPE
| AD-A243257 | p 1371 N92-16984
X ray lithography in Japan
| AD-A243660 | p 1286 N92-17087
Microstrip discontinuity models to 60 GHz
| AD-A242038 | p 1339 N92-17185
Integration of an anti-parallel pair of planar Schottky barrier diodes for millimeter and submillimeter wavelengths
| AD-A243371 | p 1287 N92-17189
Application of silicon micromachining to thermal dissipation issues in wafer scale integrated circuits
| AD-A243744 | p 1288 N92-17332
Toward a national semiconductor strategy. Regaining markets in high-volume electronics, volume 2
| PB91-201301 | p 1290 N92-17559
Method of doping single crystal diamond for electronic devices
| AD-D015069 | p 1374 N92-17610
Electrically erasable programmable integrated circuits for replacement of obsolete TTL logic
| AD-A243652 | p 1292 N92-17760
INTELLIGIBILITY
The effects of speech intelligibility level on concurrent visual task performance
| AD-A243015 | p 1331 N92-17052

INTERFACES
A spectroscopic immersion ellipsometry study of the mechanism of Si/SiO2 interface annealing
| AD-A242831 | p 1259 N92-17261
Transmission electron microscopy of the CVD diamond film/substrate interface
| AD-A243096 | p 1373 N92-17322
Precision multi-channel fiber optic interface and method
| AD-D015104 | p 1367 N92-17828
INTERFACIAL TENSION
The wave numbers of supercritical surface tension driven Benard convection
| NASA-CR-189856 | p 1373 N92-17375
INTERFERENCE GRATING
Innovative optoelectronic materials and structures using OMVPE
| AD-A243257 | p 1371 N92-16984
Two-beam coupling measurements of grating phase in a photorefractive polymer
| AD-A243746 | p 1268 N92-17195
INTERFERENCE IMMUNITY
Analog optical neural nets: A noise sensitivity analysis
| AD-A242920 | p 1346 N92-17465
INTERFEROMETERS
Hubble Space Telescope: Fine guidance sensors instrument handbook, Version 2.1
| NASA-CR-189745 | p 1386 N92-17020
Measurement of electron beam emittance using optical transition radiation and development of a diffuse screen electron beam monitor
| AD-A241893 | p 1357 N92-17306
Atom wave interferometer
| AD-A243482 | p 1357 N92-17374
Full surface testing of grazing incidence mirrors
| AD-A243734 | p 1367 N92-17690
INTERFEROMETRY
The analysis of a stabilized 1.5 Mach-Zehnder interferometric sensor with enhanced sensitivity and common-mode compensation
| AD-A243384 | p 1286 N92-17116
Full surface testing of grazing incidence mirrors
| AD-A243734 | p 1367 N92-17690
GPS interferometric attitude and heading determination: Initial flight test results p 1221 N92-17994
INTERLAYERS
Solder extrusion pressure bonding process and bonded products produced thereby
| DE92-004603 | p 1363 N92-17739
INTERMETALLICS
Solder extrusion pressure bonding process and bonded products produced thereby
| DE92-004603 | p 1363 N92-17739
INTERNAL WAVES
The physical optics description of microwave scattering by the sea surface
| AD-A243216 | p 1365 N92-17180
Physical and computational modelling of stratified shear flows
| AERO-REPT-8909 | p 1300 N92-17974
INTERNATIONAL RELATIONS
Scientific and technological relations between the United States and Japan: Issues and recommendations
| PB91-219170 | p 1385 N92-17283
INTERNATIONAL TRADE
Toward a national semiconductor strategy. Regaining markets in high-volume electronics, volume 2
| PB91-201301 | p 1290 N92-17559
INTERPLANETARY MAGNETIC FIELDS
Magnetospheric response to variations in the interplanetary magnetic field
| AD-A243683 | p 1388 N92-17717
INTERPLANETARY SPACE
In situ observations of coronal mass ejections in interplanetary space
| DE92-003857 | p 1389 N92-17725
INTERPOLATION
The applied tomography experiment of 1990
| AD-A243525 | p 1354 N92-17086
Evaluation of scalar value estimation techniques for 3D medical imaging
| AD-A243687 | p 1328 N92-17089
A new interpolation procedure for adapting Runge-Kutta methods to delay differential equations
| TW-90-09 | p 1351 N92-17517
High resolution imaging using phase retrieval, volume 2
| AD-A242925 | p 1366 N92-17550
Preliminary results from the analysis of wind component error
| AD-A243772 | p 1321 N92-17764
On the concept of varying influence radii for a successive corrections objective analysis p 1322 N92-17980
Modification of a successive corrections objective analysis for improved derivative calculations p 1322 N92-17981
INTERPROCESSOR COMMUNICATION
Electronic data interchange
| AD-A242959 | p 1382 N92-17136
Optimal configuration of digital communication network
| AD-A243041 | p 1282 N92-17277
Parallel radiosity techniques for mesh-connected SIMD computers
| AD-A242049 | p 1346 N92-17638
INTERSTELLAR MASERS
Interstellar scattering towards the galactic center as probed by OH/IR stars p 1390 N92-18004
INTERSTELLAR MATTER
Constraints on cosmic ray propagation in the galaxy
| NASA-CR-189779 | p 1390 N92-18003
Low frequency interstellar scattering and pulsar observations p 1390 N92-18005
INTERSTITIALS
Evaluation of a diffusion/trapping model for hydrogen ingress in high-strength alloys
| AD-A243461 | p 1263 N92-17327
INTERVALS
Mechanisms of temporal pattern discrimination by human observers
| AD-A243051 | p 1332 N92-17336
INTRAVEHICULAR ACTIVITY
JPL space station telerobotic engineering prototype development FY 91 status/achievements p 1247 N92-17359
INVARIANCE
The instability of linear heterogeneous Lanchester equations
| AD-A243519 | p 1350 N92-17081
Geometrical methods for the analysis of cosmological observations
| ETN-92-90584 | p 1386 N92-17523
INVERSE KINEMATICS
Analysis and experimental evaluation of a Stewart platform-based force/torque sensor
| NASA-CR-189861 | p 1252 N92-17150
INVERSE SCATTERING
The surface impedance synthesis technique
| AD-A243731 | p 1284 N92-17689
INVERSIONS
Application of linear inverse theory to borehole gravity data
| DE92-002172 | p 1317 N92-17578
INVERTED CONVERTERS (DC TO AC)
Testing and evaluation of the Vanner electrical inverters, models 24-1500 and SP 00112
| AD-A241914 | p 1287 N92-17216
INVISCID FLOW
Application of program LAURA to perfect gas shock tube flows: A parametric study
| NASA-TM-104190 | p 1294 N92-17002
Effective viscosity in the simulation of spatially evolving shear flows with monotonic FCT models
| AD-A243709 | p 1295 N92-17126
A variational assimilation method for satellite and conventional data: Development of basic model for diagnosis of cyclone systems
| NASA-CR-188236 | p 1321 N92-17975
IODIDES
Preliminary assessment of the relative toxicity of tetraglycine hydroperiodide, phase 1
| AD-A243334 | p 1330 N92-17712
IODINE
In situ structural studies of the underpotential deposition of copper onto an iodine covered platinum surface using x ray standing waves
| AD-A243475 | p 1263 N92-17328
Long-term corrosion evaluation of stainless steels in Space Shuttle iodinated resin and water
| NASA-TM-104743 | p 1264 N92-17376
In situ x ray standing wave study of Cu UPD on an iodine covered platinum surface
| AD-A243474 | p 1264 N92-17426
ION ACCELERATORS
Emittance growth from space-charge forces
| DE92-003804 | p 1364 N92-17796
ION BEAMS
Ion mixing of semiconductor layered-structures
| DE92-003756 | p 1377 N92-17791
Emittance growth from space-charge forces
| DE92-003804 | p 1364 N92-17796
ION EMISSION
Evidence for MeV particle emission from Ti charged with low energy deuterium ions
| AD-A243718 | p 1359 N92-17505
Comparison of alkali ion emitters
| AD-A243105 | p 1290 N92-17570
ION IMPLANTATION
Materials processing of diamond: Etching, doping by ion implantation and contact formation
| AD-A243060 | p 1267 N92-17065
Steady-state, high dose neutron generation and concentration apparatus and method for deuterium atoms
| AD-D015063 | p 1358 N92-17462
Concentration of isotopic hydrogen by temperature gradient effect in soluble metal
| AD-D015062 | p 1260 N92-17628
Growth rate of dislocation loop in Fe-Ni-Cr alloy under Kr(+) ion and electron irradiation
| DE92-001908 | p 1265 N92-17703
Collisional energy deposition threshold for extended damage depths in ion-implanted silicates
| DE92-004737 | p 1377 N92-17797
Ionic physics and technology p 1362 N92-17818
High frequency sources of ions for ion technology p 1362 N92-17820
ION IRRADIATION
Ionic physics and technology p 1362 N92-17818
High frequency sources of ions for ion technology p 1362 N92-17820
ION PRODUCTION RATES
Rates and mechanisms of metastable deactivation over surfaces
| AD-A243391 | p 1361 N92-17652
ION PROPULSION
Analysis of orbital elements and atmospheric activity to ascertain possible presence of an ion propulsion capability aboard Salyut 7/Cosmos 1686
| AD-A243654 | p 1251 N92-17762
ION SOURCES
Comparison of alkali ion emitters
| AD-A243105 | p 1290 N92-17570
Ion sources based on electron cyclotron resonance p 1362 N92-17743
Analysis of orbital elements and atmospheric activity to ascertain possible presence of an ion propulsion capability aboard Salyut 7/Cosmos 1686
| AD-A243654 | p 1251 N92-17762
High frequency sources of ions for ion technology p 1362 N92-17820
Multiply charged ion sources for cyclotrons
| DE92-610975 | p 1364 N92-17973
ION TEMPERATURE
The charge exchange recombination diagnostic system on the D3-D tokamak
| DE92-003805 | p 1369 N92-17456
Cooperative program to analyze heat transport at high beta in DIII-D
| DE92-003545 | p 1370 N92-17606
IONIZATION
Studies of the adsorption of tetrasulfonated phthalocyanines on graphite substrate
| AD-A243443 | p 1260 N92-17489
IONIZING RADIATION
A PC program to calculate the one-sided lower tolerance limit for total ionizing dose radiation data
| AD-A242365 | p 1357 N92-17394
Biological effects of protracted exposure to ionizing radiation: Review, analysis, and model development
| AD-A242981 | p 1329 N92-17476
IONOSPHERIC DISTURBANCES
Auroral-clutter predictions for Fylingdales, England
| AD-A242957 | p 1283 N92-17600
IONOSPHERIC STORMS
Radar-satellite studies of the high-latitude ionosphere
| AD-A243275 | p 1317 N92-17961
IONS
Cooled ion frequency standard
| AD-A242030 | p 1360 N92-17549
Ion mixing of semiconductor layered-structures
| DE92-003756 | p 1377 N92-17791
IRON
Studies of the adsorption of tetrasulfonated phthalocyanines on graphite substrate
| AD-A243443 | p 1260 N92-17489
IRON ALLOYS
Growth rate of dislocation loop in Fe-Ni-Cr alloy under Kr(+) ion and electron irradiation
| DE92-001908 | p 1265 N92-17703
IRRADIATION
The effects of storage on irradiated red blood cells: An in vitro an in vivo study
| AD-A243387 | p 1329 N92-17190
Radiation effects in High Temperature Superconductors (HTSC) oxides p 1375 N92-17700
Experimental findings on self-recovery and improvement of representative parameters of some semiconductor devices as irradiated in fast neutron flux
| DE92-611185 | p 1378 N92-17944
ISOELECTRONIC SEQUENCE
Stability and structure of C12B24N24: A hybrid analog of buckminsterfullerene
| AD-A242327 | p 1373 N92-17245

ISOLATION
Total Dielectric Isolation (TDI) of fully depleted device structures
| AD-A241926 | p 1289 N92-17439
ISOMORPHISM
Topological representation of graph isomorphism types
| AD-A243528 | p 1350 N92-17148
ISOPROPYL ALCOHOL
Clean room wiping liquids
| DE92-004793 | p 1238 N92-17967
ISOPROPYL COMPOUNDS
Polyimides containing amide and perfluoroisopropyl connecting groups
| NASA-CASE-LAR-14608-1 | p 1271 N92-17676
ISOTOPE EFFECT
Laser-based ignition of H2/O2 and D2/O2 premixed gases near 243 nm: The first report of a deuterium isotope wavelength effect in laser ignition
| AD-A243180 | p 1303 N92-17137
ISOTOPE SEPARATION
Chromatographic separation of calcium isotopes
| DE92-004623 | p 1261 N92-17740
ISOTOPES
Lie-isotopic generalization of the Poincare symmetry: Classical formulation
| DE91-642825 | p 1379 N92-17531
ISOTOPIC ENRICHMENT
Concentration of isotopic hydrogen by temperature gradient effect in soluble metal
| AD-D015062 | p 1260 N92-17628
ISOTOPIC LABELING
An oxygen tracer study of InP oxidation
| AD-A242832 | p 1259 N92-17246
ISOTROPY
Higher-order thickness expansions for cylindrical shells
| AD-A242017 | p 1310 N92-17230
ITERATION
Complexity issues in numerical optimization
| AD-A241854 | p 1347 N92-17049
Program translation tools for systolic arrays
| AD-A242924 | p 1336 N92-17466
Improved task scheduling for parallel simulations
| AD-A243721 | p 1346 N92-17507

J

JAPAN
X ray lithography in Japan
| AD-A243660 | p 1286 N92-17087
Scientific and technological relations between the United States and Japan: Issues and recommendations
| PB91-219170 | p 1385 N92-17283
JAPANESE SPACE PROGRAM
Status of Japanese Experiment Module (JEM) activities p 1243 N92-17101
JET ENGINE FUELS
Safety considerations in testing a fuel-rich aeropropulsion gas generator
| NASA-TM-105258 | p 1235 N92-17061
JET ENGINES
Laser based, non-intrusive measurement system for analysis of jet engine flows
| AD-A242398 | p 1234 N92-17011
JET FLOW
Laser based, non-intrusive measurement system for analysis of jet engine flows
| AD-A242398 | p 1234 N92-17011
The influence of cavitation in the breakup of liquid free jets
| MPIS-1/1991 | p 1297 N92-17343
JINDIVIK TARGET AIRCRAFT
Modification of Jindivik air intake duct with an auxiliary intake static aerodynamic tests
| AD-A243002 | p 1232 N92-17234
JOINING
Method of joining diamond structures
| AD-D015066 | p 1269 N92-17397
JOINTS (ANATOMY)
Automatic locking orthotic knee device
| NASA-CASE-MFS-28633-1 | p 1335 N92-17866
JOINTS (JUNCTIONS)
Space Station Freedom solar alpha joint growth capability p 1252 N92-17772
A method for joining ceramic shapes
| DE92-003815 | p 1274 N92-17842
A method and apparatus for indicating disbonds in joint regions
| NASA-CASE-LAR-14626-1 | p 1309 N92-17859
JOSEPHSON JUNCTIONS
Design and evaluation of a Josephson array oscillator
| AD-A243167 | p 1291 N92-17672
Quantum-limited detection of millimeter waves using superconducting tunnel junctions
| DE92-004757 | p 1377 N92-17799
High temperature superconductor thin films and Josephson junctions
| AD-A242747 | p 1293 N92-17949

K

K LINES
Luminescence and electroluminescence properties of Nd, Tm, Yb doped GaAs II-VI compounds
| AD-A242039 | p 1375 N92-17667
KALMAN FILTERS
A Kalman filter for a Poisson series with covariates and Laplace approximation integration
| AD-A242960 | p 1286 N92-16993
Method of Kalman filtering for estimating the position and velocity of a tracked object
| AD-D015057 | p 1287 N92-17129
Incorporation of differential global positioning system measurements using an extended Kalman filter for improved reference system performance
| AD-A243742 | p 1228 N92-17481
A fully decentralized multi-sensor system for tracking and surveillance
| OUEL-1886/91 | p 1302 N92-17926
Systematic methods for knowledge acquisition and expert system development p 1222 N92-18001
KAONS
What experiments say about possibility of the new particle existence with mass less than the kaon mass
| DE91-634551 | p 1357 N92-17408
KARMAN VORTEX STREET
A short or a long cylinder: What difference does it make to the Karman vortex street?
| MPIS-98/1990 | p 1224 N92-17314
Investigation on the control of a Karman vortex street
| MPIS-99/1990 | p 1224 N92-17315
KINEMATICS
Analysis and experimental evaluation of a Stewart platform-based force/torque sensor
| NASA-CR-189861 | p 1252 N92-17150
Flight test data quality evaluation p 1230 N92-17156
SA 330 Puma identification results p 1231 N92-17162
One-loop calculations with massive particles
| ETN-92-90563 | p 1359 N92-17518
KINETIC ENERGY
Evaluation of squib performance variables
| DE92-002034 | p 1275 N92-17533
KINETIC EQUATIONS
Kinetics of a new phase formation in supersaturated solid solutions. 1. Dilute one-component systems
| DE92-610065 | p 1262 N92-17943
KINETIC THEORY
Determination of cohesive and normal stresses and simulation of fluidization using kinetic theory
| DE92-002905 | p 1299 N92-17709
KINETICS
A kinetics study of the electron cyclotron resonance plasma oxidation of silicon
| AD-A242868 | p 1290 N92-17596
Optical spectra and kinetics of single impurity molecules in a polymer: Spectral diffusion and persistent spectral hole-burning
| AD-A243749 | p 1271 N92-17659
KNEE (ANATOMY)
Influence of knee joint extension on submaximal oxygen consumption and anaerobic power in cyclists
| AD-A243467 | p 1329 N92-17194
Automatic locking orthotic knee device
| NASA-CASE-MFS-28633-1 | p 1335 N92-17866
KNOWLEDGE BASES (ARTIFICIAL INTELLIGENCE)
Optical content-addressable memories for data/knowledge base processing
| AD-A241866 | p 1382 N92-17037
Development of a knowledge base for use in an Expert System Advisor for Aircraft Maintenance Scheduling (ESAAMS)
| AD-A243435 | p 1381 N92-17687
Knowledge, programming, and programming cultures: LISP, C, and Ada
| NASA-CR-184220 | p 1344 N92-17778
KNOWLEDGE REPRESENTATION
Image processing applications for nonlinear decomposition and synthesis
| AD-A243357 | p 1343 N92-17733
KOREA
Surface observations climatic summaries for Camp Humphreys, Korea
| AD-A241937 | p 1320 N92-17444
KRIGING
Evaluation of scalar value estimation techniques for 3D medical imaging
| AD-A243687 | p 1328 N92-17089
KRYPTON
Growth rate of dislocation loop in Fe-Ni-Cr alloy under Kr(+) ion and electron irradiation
| DE92-001908 | p 1265 N92-17703

L

LABOR
Labor market trends for health physicists
| DE92-004770 | p 1331 N92-17800
LABORATORIES
Acoustic simulation for acoustics education
| AD-A243027 | p 1355 N92-17236
LACTIC ACID
Process of converting starch to glucose and glucose to lactic acid
| DE92-003840 | p 1255 N92-17867
LAGRANGE MULTIPLIERS
Machine scheduling and Lagrangian relaxation
| ETN-92-90569 | p 1353 N92-17839
LAMBERT SURFACE
Enhanced backscattering of light from randomly rough diffusers: Appendix
| AD-A243436 | p 1366 N92-17485
LAMINAR BOUNDARY LAYER
Basic hydrodynamics
| AD-A243513 | p 1297 N92-17387
LAMINAR FLOW
Unsteady laminar flow in a circular tube: A test of the HERCOL (Hermitian collocation) computer code
| PB91-222679 | p 1295 N92-17018
Two-dimensional stability of laminar flames
| NASA-TP-3131 | p 1223 N92-17131
Study of transition phenomena in a straight channel with 40 to 1 aspect ratio with and without imposed pulsations. Part two: Reynolds number surveys
| AD-A241894 | p 1296 N92-17307
Deterministic multi-zone ice accretion modeling p 1220 N92-17987
LAMINAR MIXING
Effective viscosity in the simulation of spatially evolving shear flows with monotonic FCT models
| AD-A243709 | p 1295 N92-17126
LAMINATES
Novel vacuum bag processing approaches to void reduction in carbon/epoxy composites
| AD-A242396 | p 1255 N92-16992
The use of impact force as a scale parameter for the impact response of composite laminates
| NASA-TM-104189 | p 1256 N92-17007
Static analysis of thick composite plates using higher order three dimensional finite elements
| AD-A243188 | p 1256 N92-17367
Explicit finite element method for transparency impact analysis
| AD-A243527 | p 1227 N92-17478
Intercalated hybrid graphite fiber composite
| NASA-CASE-LEW-15241-1 | p 1257 N92-17861
Experimental investigation of interlaminar fracture toughness of carbon fiber/thermoplastic and carbon fiber/thermosetting composites by DCB specimens
| NAL-TR-1096 | p 1257 N92-17869
Acoustic emission monitoring of low velocity impact damage in graphite/epoxy laminates during tensile loading
| NASA-TM-4339 | p 1258 N92-17881
LAND MOBILE SATELLITE SERVICE
Effect of economic techniques on radio frequency utilization
| AD-A243187 | p 1282 N92-17366
LANDFORMS
University of Minnesota Aquifer Thermal Energy Storage (ATES) project report on the first long-term cycle
| DE92-004699 | p 1313 N92-17934
LANDING LOADS
Structural dynamics division research and technology accomplishments for F.Y. 1991 and plans for F.Y. 1992
| NASA-TM-104188 | p 1225 N92-17509
LANGUAGES
Decompiling with definite clause grammars
| AD-A242987 | p 1340 N92-17296
LARGE SPACE STRUCTURES
Modes of interconnected lattice trusses using continuum models, part 1
| NASA-CR-189568 | p 1242 N92-17045
Hypervelocity impact simulation for micrometeorite and debris shield design
| NASA-CR-189807 | p 1244 N92-17200
Control of a large flexible space structure using multiple model adaptive algorithms
| AD-A243759 | p 1250 N92-17602

LASER ANEMOMETERS
LDA and PDA systems based on diode-pumped Neodym:YAG lasers
| MBB-Z-0361-91-PUB | p 1304 N92-17526
LASER APPLICATIONS
Noncoherent detection of coherent optical heterodyne signals corrupted by laser phase noise
| AD-A243103 | p 1364 N92-16981
Laser based, non-intrusive measurement system for analysis of jet engine flows
| AD-A242398 | p 1234 N92-17011
Contributive research and development
| AD-A243331 | p 1391 N92-17079
Laser-based ignition of H2/O2 and D2/O2 premixed gases near 243 nm: The first report of a deuterium isotope wavelength effect in laser ignition
| AD-A243180 | p 1303 N92-17137
Development of an XUV-IR free-electron laser user facility for scientific research and industrial applications
| DE92-003862 | p 1304 N92-17726
Multiperiod-grating surface-emitting lasers
| NASA-CASE-NPO-17763-1-CU | p 1305 N92-17862
LASER ARRAYS
Innovative switching technology
| DE92-003068 | p 1292 N92-17708
LASER BEAMS
Waveguide four-wave mixing
| AD-A243555 | p 1286 N92-17017
Transmission of thin light beams through turbulent mixing layers
| AD-A243470 | p 1367 N92-17658
Laser range safety
| AD-A243606 | p 1305 N92-17962
LASER CAVITIES
A tunable solid state laser with high wavelength selectivity over a preselected wavelength range
| AD-D015055 | p 1304 N92-17627
Optical turbulence in second harmonic generation
p 1377 N92-17821
LASER DAMAGE
Ultrafast passive shields for laser and ballistic protection
| AD-A243206 | p 1303 N92-17175
LASER DOPPLER VELOCIMETERS
LDA and PDA systems based on diode-pumped Neodym:YAG lasers
| MBB-Z-0361-91-PUB | p 1304 N92-17526
Study of turbulence by photon correlation spectroscopy
| AD-A243726 | p 1298 N92-17688
LASER INDUCED FLUORESCENCE
Velocity measurements in high temperature gases using laser-induced no fluorescence
| AD-A242399 | p 1295 N92-17012
Vibrational energy transfer in bromine monofluoride
| AD-A243690 | p 1259 N92-17091
Collisional dynamics of the B3Pi(O+) state of bromine of monofluoride
| AD-A241857 | p 1356 N92-17305
Quenching and rotational energy transfer in molecular bromine: Br2(B)
| AD-A241987 | p 1357 N92-17321
LASER MATERIALS
Vibrational energy transfer in bromine monofluoride
| AD-A243690 | p 1259 N92-17091
LASER OUTPUTS
A tunable solid state laser with high wavelength selectivity over a preselected wavelength range
| AD-D015055 | p 1304 N92-17627
Multiperiod-grating surface-emitting lasers
| NASA-CASE-NPO-17763-1-CU | p 1305 N92-17862
Method and apparatus for lasing
| AD-D015154 | p 1305 N92-17923
LASER PLASMA INTERACTIONS
On the generation of large-amplitude plasma wakefields with low phase velocities by an intense short laser pulse
| DE92-609543 | p 1371 N92-17805
LASER PLASMAS
Picosecond laser breakdown thresholds in gases
| AD-A242941 | p 1304 N92-17475
Liquid and solid ion plasmas
| AD-A242029 | p 1370 N92-17635
Workshop on Plasma Experiments in the Laboratory and in Space. Abstracts
| AD-A243645 | p 1370 N92-17734
Multiply charged ion sources for cyclotrons
| DE92-610975 | p 1364 N92-17973
LASER PUMPING
Anomalous hole burning in polymers with inhomogeneous broadening
| AD-A242397 | p 1266 N92-17010
Method and apparatus for lasing
| AD-D015154 | p 1305 N92-17923
LASER RANGE FINDERS
Cyclone: A laser scanner for mobile robot navigation
| AD-A243517 | p 1303 N92-17080
Receiver performance of laser ranging measurements between the Lunar Observer and a subsatellite for lunar gravity studies
| NASA-CR-189860 | p 1303 N92-17152
LASER SPECTROSCOPY
Molecular jet studies of vdW clusters and solvation
| AD-A242866 | p 1254 N92-17308
Liquid and solid ion plasmas
| AD-A242029 | p 1370 N92-17635
LASERS
An optical roughness sensor for the real time determination of spray formed preform quality
| AD-A243238 | p 1262 N92-17056
User evaluation of laser ballistic sun, wind and dust goggle lenses (dye technology)
| AD-A243245 | p 1334 N92-17143
Optical spectra and kinetics of single impurity molecules in a polymer: Spectral diffusion and persistent spectral hole-burning
| AD-A243749 | p 1271 N92-17659
Laser range safety
| AD-A243606 | p 1305 N92-17962
LAUNCH VEHICLES
Case bond liner systems for solid rocket motors
| AD-A242297 | p 1253 N92-17085
Upper stages using liquid propulsion and metallized propellants
| NASA-TP-3191 | p 1253 N92-17151
Mars aerobrake assembly demonstration
p 1247 N92-17362
LAUNCHING
Launching projectiles with hydrogen gas generated from aluminum fuel powder/water reactions
| AD-D015119 | p 1276 N92-17830
LAW (JURISPRUDENCE)
Worldwide Environmental Compliance Assessment and Management Program (ECAMP): German supplement
| AD-A242967 | p 1313 N92-17380
Worldwide Environmental Compliance Assessment and Management Program (ECAMP)
| AD-A242874 | p 1314 N92-17598
LEAD ZIRCONATE TITANATES
Characterization of PZT thin films: Crystallographic phases
| DE92-003514 | p 1377 N92-17790
LEADERSHIP
NASA total quality management 1990 accomplishments report
| NASA-TM-105465 | p 1308 N92-17199
LEADING EDGES
Heat flux sensor research and development: The cool film calorimeter
| NASA-CR-189789 | p 1301 N92-17006
An experimental investigation of leading edge vortical flow about a delta wing during wing rock
| AD-A243363 | p 1223 N92-17114
LEARNING
Attention, automaticity and priority learning
| AD-A242226 | p 1332 N92-17458
Causal models in the acquisition and instruction of programming skills
| AD-A242899 | p 1340 N92-17463
The 7th Annual Workshop on Computational Neuroscience
| AD-A243462 | p 1335 N92-17656
LEAST SQUARES METHOD
Critical temperature determination in superconductors
| AD-A243537 | p 1371 N92-17015
Data fusion for least squares
| AD-A243507 | p 1352 N92-17384
Spectral error models applied to the geodetic boundary value problem
| ETN-92-90582 | p 1312 N92-17436
Near real-time stereo vision system
| NASA-CASE-NPO-18593-1-CU | p 1368 N92-17864
LENS ANTENNAS
Design and testing of a lightweight, planar microwave lens
| AD-A243685 | p 1286 N92-17076
LENS DESIGN
Design and testing of a lightweight, planar microwave lens
| AD-A243685 | p 1286 N92-17076
LENSES
User evaluation of laser ballistic sun, wind and dust goggle lenses (dye technology)
| AD-A243245 | p 1334 N92-17143
Ultrafast passive shields for laser and ballistic protection
| AD-A243206 | p 1303 N92-17175
LEWIS NUMBERS
Two-dimensional stability of laminar flames
| NASA-TP-3131 | p 1223 N92-17131
LIAPUNOV FUNCTIONS
Control algorithms for aerobraking in the Martian atmosphere
| AD-A243349 | p 1239 N92-17730
LIBRARIES
Bibliography of technical reports 1990
| AD-A242376 | p 1383 N92-17378
LICENSING
Valuable patents for US businesses: A catalog of DTRC patents available for licensing by the private sector
| AD-A242071 | p 1385 N92-17141
LIE GROUPS
Lie-isotopic generalization of the Poincare symmetry: Classical formulation
| DE91-642825 | p 1379 N92-17531
LIFE (DURABILITY)
Analysis of cam roller followers
| ESDU-91026 | p 1307 N92-17852
LIFE CYCLE COSTS
An analysis of the aircraft engine Component Improvement Program (CIP): A life cycle cost approach
| AD-A243346 | p 1236 N92-17729
LIFE SCIENCES
Space Station Freedom science utilization: 2000 and beyond p 1244 N92-17107
Mathematics and biology
| DE92-611247 | p 1327 N92-17815
LIFE SUPPORT SYSTEMS
EMU evolution p 1246 N92-17354
Environmental control and life support system evolution analysis p 1246 N92-17355
The environmental control and life support system advanced automation project p 1246 N92-17356
ECLSS predictive monitoring p 1247 N92-17357
LIFTING REENTRY VEHICLES
Weight evaluation and sensitivity analysis for space plane. Part 2: TSTO
| NAL-TM-602-PT-2 | p 1251 N92-17754
LIGANDS
Ligand redistribution reactions of Me2Ga(C5H5) and MeGa(C5H5)2
| AD-A243264 | p 1254 N92-17270
LIGHT (VISIBLE RADIATION)
Melatonin action on the circadian pacemaker in Siberian hamsters
| AD-A243057 | p 1325 N92-17142
Fiber optic angular orientation sensor digital serial encoding
| AD-D015102 | p 1302 N92-17826
LIGHT BEAMS
Achromatic and isochronous electron beam transport for tunable free electron lasers
| DE92-003908 | p 1305 N92-17868
LIGHT EMISSION
A diffraction limited nitrogen laser for detector calibration in high energy physics
| ETN-92-90567 | p 1303 N92-17434
LIGHT HELICOPTERS
Analysis of scene conditions at the light helicopter target acquisition subsystem demonstration/validation, Yuma Proving Ground, Arizona, September 1990
| AD-A243234 | p 1234 N92-17240
LIGHT MODULATION
Real-time edge-enhanced optical correlator
| NASA-CASE-NPO-18379-1-CU | p 1367 N92-17675
Optical image segmentation using wavelet correlation
| AD-A243650 | p 1367 N92-17736
Correlator optical wavefront sensor COWS
| DE92-003964 | p 1368 N92-17846
LIGHT SCATTERING
Enhanced backscattering of light from randomly rough diffusers: Appendix
| AD-A243436 | p 1366 N92-17485
Enhanced backscattering from rough surfaces
| AD-A243437 | p 1366 N92-17486
Study of turbulence by photon correlation spectroscopy
| AD-A243726 | p 1298 N92-17688
LIGHT SOURCES
Development of an XUV-IR free-electron laser user facility for scientific research and industrial applications
| DE92-003862 | p 1304 N92-17726
LIGHT TRANSMISSION
Transmission of thin light beams through turbulent mixing layers
| AD-A243470 | p 1367 N92-17658
LIKELIHOOD RATIO
Sensitivity testing and analysis
| DE92-002033 | p 1276 N92-17624
LINE OF SIGHT
Toward the robust control of high bandwidth high precision flexible optical systems
| AD-A243471 | p 1366 N92-17536

LINE SHAPE
Optical nonlinearity in coupled exciton-phonon systems near metal surfaces
| AD-A242362 | p 1357 N92-17423
LINE SPECTRA
Stellar spectral line synthesis from an individual photon-following simulation
| AD-A242970 | p 1388 N92-17253
Interstellar scattering towards the galactic center as probed by OH/IR stars p 1390 N92-18004
LINEAR ACCELERATORS
A study of gamma ray generation from channeled electrons and positions
| AD-A241993 | p 1361 N92-17608
PILAC: A Pion Linac facility for 1-GeV pion physics at LAMPF
| DE92-003789 | p 1364 N92-17794
High current transistor pulse generator
| DE92-004774 | p 1292 N92-17801
LINEAR EQUATIONS
The instability of linear heterogeneous Lanchester equations
| AD-A243519 | p 1350 N92-17081
Parallel block methods for sparse symmetric linear systems of equations
| AD-A242315 | p 1351 N92-17560
LINEAR PROGRAMMING
Complexity issues in numerical optimization
| AD-A241854 | p 1347 N92-17049
A convergent aspiration based interior point method (CAIN) for Multiple Objective Linear Programming (MOLP)
| AD-A243404 | p 1338 N92-17118
LINEAR QUADRATIC GAUSSIAN CONTROL
Control of a large flexible space structure using multiple model adaptive algorithms
| AD-A243759 | p 1250 N92-17602
LINEAR QUADRATIC REGULATOR
Multiple input sliding mode control for autonomous diving and steering of underwater vehicles
| AD-A241935 | p 1237 N92-17442
LINEAR SYSTEMS
Complexity issues in numerical optimization
| AD-A241854 | p 1347 N92-17049
Parallel block methods for sparse symmetric linear systems of equations
| AD-A242315 | p 1351 N92-17560
Application of linear inverse theory to borehole gravity data
| DE92-002172 | p 1317 N92-17578
Technical notes and correspondence: Stochastic robustness of linear time-invariant control systems p 1222 N92-18002
LININGS
High-temperature durability considerations for HSCT combustor
| NASA-TP-3162 | p 1267 N92-17070
LIQUID ALLOYS
An optical roughness sensor for the real time determination of spray formed preform quality
| AD-A243238 | p 1262 N92-17056
LIQUID COOLING
Heat transfer enhancement due to bubble pumping in FC-72 near the saturation temperature
| AD-A243558 | p 1292 N92-17724
LIQUID CRYSTALS
Electronic and ionic transport in processable conducting polymers. Symmetry effects on the physical and electrically conducting, substituted poly(di-2-thienylphenylenes)
| AD-A242328 | p 1266 N92-16976
Molecular motions of the head group of SHBS in lamellar liquid crystals
| AD-A243499 | p 1373 N92-17382
Phase transitions in narrow molecular mass samples of side-chain liquid crystalline polymers: Molecular mass dependence
| AD-A242354 | p 1269 N92-17448
Reactions and interactions in liquid crystalline media
| AD-A242355 | p 1374 N92-17449
Real-time edge-enhanced optical correlator
| NASA-CASE-NPO-18379-1-CU | p 1367 N92-17675
LIQUID METALS
Launching projectiles with hydrogen gas generated from aluminum fuel powder/water reactions
| AD-D015119 | p 1276 N92-17830
LIQUID OXYGEN
Extravehicular mobility unit subcritical liquid oxygen storage and supply system
| NASA-CR-189831 | p 1276 N92-16989
LIQUID-LIQUID INTERFACES
Dynamics and stabilization of materials possessing high energy content
| AD-A243030 | p 1258 N92-16977
LIQUID-SOLID INTERFACES
Dynamics and stabilization of materials possessing high energy content
| AD-A243030 | p 1258 N92-16977
In situ surface x ray scattering of metal monolayers adsorbed at solid-liquid interfaces
| AD-A243258 | p 1262 N92-16985
Ultrasonic studies of transient seismo-acoustic waves in bounded solids and Liquid/Solid interfaces
| AD-A243441 | p 1355 N92-17488
Surface chemistry at the semiconductor/electrolyte interface
| DE91-018511 | p 1374 N92-17532
Liquid-solid transition in the bond particle model for elemental semiconductors
| DE92-010441 | p 1378 N92-17972
LISP (PROGRAMMING LANGUAGE)
Causal models in the acquisition and instruction of programming skills
| AD-A242899 | p 1340 N92-17463
Knowledge, programming, and programming cultures: LISP, C, and Ada
| NASA-CR-184220 | p 1344 N92-17778
LITHIUM ALLOYS
Lithiated Vanadium Oxide (LVO), gamma-lithium vanadium bronze (Gamma-LIV2O5) and vanadium dioxide (VO2) as thermal battery cathode materials
| AD-A242948 | p 1287 N92-17186
LOAD TESTING MACHINES
System for testing bearings
| NASA-CASE-MFS-28589-1 | p 1306 N92-17584
LOAD TESTS
Thermo-mechanical fatigue of a fiber reinforced titanium aluminide composite
| AD-A241988 | p 1256 N92-17607
Experimental investigation of interlaminar fracture toughness of carbon fiber/thermoplastic and carbon fiber/thermosetting composites by DCB specimens
| NAL-TR-1096 | p 1257 N92-17869
Dynamic stall on wind turbine blades
| DE92-001157 | p 1226 N92-17874
Acoustic emission monitoring of low velocity impact damage in graphite/epoxy laminates during tensile loading
| NASA-TM-4339 | p 1258 N92-17881
LOADS (FORCES)
Loss terms in free-piston Stirling engine models
| NASA-CR-189840 | p 1312 N92-17225
Determination of antisymmetric end loads from bulk stresses on a rectangular prism
| AD-A243001 | p 1310 N92-17265
Explosive magnetic field compression generator transformer power supply for high resistive loads
| AD-D015123 | p 1293 N92-17831
Automatic locking orthotic knee device
| NASA-CASE-MFS-28633-1 | p 1335 N92-17866
LOCAL AREA NETWORKS
Local area network strategies and guidelines for a Peruvian Air Force Computer Center
| AD-A242841 | p 1345 N92-17135
Delay analysis for multidimensional queueing process in CSMA/CD local area networks
| AD-A242364 | p 1346 N92-17425
LOCAL THERMODYNAMIC EQUILIBRIUM
Background Atmosphere Radiance Day (BARD) and Night (BARN)
| AD-A243153 | p 1316 N92-17239
LOCKING
Automatic locking orthotic knee device
| NASA-CASE-MFS-28633-1 | p 1335 N92-17866
LOCOMOTION
Treadmill for space flight
| NASA-CASE-MSC-21752-1 | p 1335 N92-17910
LOGIC CIRCUITS
Global optimization of digital circuits
| AD-A243740 | p 1289 N92-17480
Design implementation into field programmable gate arrays
| AD-A242538 | p 1343 N92-17680
A cache design to exploit structural locality
| AD-A243633 | p 1336 N92-17744
Electrically erasable programmable integrated circuits for replacement of obsolete TTL logic
| AD-A243652 | p 1292 N92-17760
LOGIC DESIGN
Design implementation into field programmable gate arrays
| AD-A242538 | p 1343 N92-17680
LOGISTICS
CALS database usage and analysis tool study
| AD-A243205 | p 1382 N92-17174
EMU evolution p 1246 N92-17354
LOGISTICS MANAGEMENT
Summary of professional activities, center for Air Force C3 systems
| AD-A243509 | p 1348 N92-17386
Space Station Freedom baseline operations concept p 1248 N92-17410
LONG DURATION EXPOSURE FACILITY
Atomic oxygen flux and fluence calculation for Long Duration Exposure Facility (LDEF)
| NASA-CR-187418 | p 1245 N92-17215
Long duration exposure facility post-flight thermal analysis: Orbital/thermal environment data package
| NASA-CR-189872 | p 1245 N92-17334
Long duration exposure facility solar illumination data package
| NASA-CR-189873 | p 1241 N92-17335
Systems special investigation group
| NASA-CR-187355 | p 1250 N92-17728
LONGITUDINAL WAVES
Effective dynamic material parameters and localized scattering
| AD-A241957 | p 1310 N92-17320
LOOPS
Superdirective properties of closed loops of parallel coplanar dipoles
| AD-A243009 | p 1288 N92-17268
LORAN C
Multisensor signal processing techniques (hybrid GPS/LORAN-C with RAIM)
| AD-A242323 | p 1281 N92-17244
LOSSES
Investigation of mechanisms for the source and loss of electrons from the radiation belts using data from SEEP, SCATHA and P78-1 satellites
| AD-A243376 | p 1317 N92-17405
LOW ALTITUDE
Trajectory analysis of the G-11 family of clustered parachutes to determine minimum altitude
| AD-A243375 | p 1225 N92-17404
LOW FREQUENCIES
Observation and measurements of flow structures in the stagnation region of a wing-body junction
| AD-A243403 | p 1223 N92-17117
Low frequency interstellar scattering and pulsar observations p 1390 N92-18005
LOW PASS FILTERS
Image processing applications for nonlinear decomposition and synthesis
| AD-A243357 | p 1343 N92-17733
LOW SPEED
Observation and measurements of flow structures in the stagnation region of a wing-body junction
| AD-A243403 | p 1223 N92-17117
Acoustic emission monitoring of low velocity impact damage in graphite/epoxy laminates during tensile loading
| NASA-TM-4339 | p 1258 N92-17881
LOW TEMPERATURE
A proposed improved method of radiosonde humidity sensing
| AD-A242954 | p 1319 N92-17233
LUBRICANTS
The synergistic effects of solid and liquid lubrication on the tribological behavior of transformation-toughened ZrO2 ceramics
| DE91-018617 | p 1306 N92-17575
LUBRICATION
The synergistic effects of solid and liquid lubrication on the tribological behavior of transformation-toughened ZrO2 ceramics
| DE91-018617 | p 1306 N92-17575
Determination of the tribological fundamentals of solid lubricated ceramics. Volume 3: Appendices P through 2
| AD-A242872 | p 1270 N92-17597
LUGS
Strength of lugs
| ESDU-91008 | p 1311 N92-17834
LUMINAIRES
Extracting the shape and roughness of specular lobe objects using four light photometric stereo
| AD-A243522 | p 1365 N92-17146
Fiber optic angular orientation sensor digital serial encoding
| AD-D015102 | p 1302 N92-17826
LUMINESCENCE
Luminescence and electroluminescence properties of Nd, Tm, Yb doped GaAs II-VI compounds
| AD-A242039 | p 1375 N92-17667
LUMINOUS INTENSITY
Luminescence and electroluminescence properties of Nd, Tm, Yb doped GaAs II-VI compounds
| AD-A242039 | p 1375 N92-17667
Light-controlled, electrochemical, anisotropic etching of silicon
| MBB-Z-0368-91-PUB | p 1261 N92-17841
LUNAR BASES
Construction equipment for lunar surface operations
| AD-A243665 | p 1389 N92-17123

LUNAR CONSTRUCTION EQUIPMENT
Construction equipment for lunar surface operations
| AD-A243665 | p 1389 N92-17123
LUNAR ENVIRONMENT
Environmental interactions in Space Exploration: Announcement of the formation of an Environmental Interactions Working Group
| NASA-TM-105294 | p 1389 N92-17069
LUNAR EXCAVATION EQUIPMENT
Construction equipment for lunar surface operations
| AD-A243665 | p 1389 N92-17123
LUNAR GRAVITATION
Receiver performance of laser ranging measurements between the Lunar Observer and a subsatellite for lunar gravity studies
| NASA-CR-189860 | p 1303 N92-17152
LUNAR OBSERVATORIES
Receiver performance of laser ranging measurements between the Lunar Observer and a subsatellite for lunar gravity studies
| NASA-CR-189860 | p 1303 N92-17152
LUNAR PHASES
Tidal and lunar data for Point Mugu, San Nicolas Island, and the Barking Sands area during 1992
| AD-A243210 | p 1324 N92-17177
LUNAR SPACECRAFT
Computer system evolution requirements for autonomous checkout of exploration vehicles
p 1250 N92-17422
LUNAR SURFACE
Construction equipment for lunar surface operations
| AD-A243665 | p 1389 N92-17123
A study of electric transmission lines for use on the lunar surface p 1292 N92-17742
LUNAR TIDES
Tidal and lunar data for Point Mugu, San Nicolas Island, and the Barking Sands area during 1992
| AD-A243210 | p 1324 N92-17177
LYMPHOCYTES
Biophysical techniques for examining metabolic, proliferative, and genetic effects of microwave radiation
| AD-A241903 | p 1326 N92-17288

M

MACH NUMBER
Experimental measurements of plasma properties for Miller SG-100 torch with Mach I setting
| DE92-003309 | p 1369 N92-17469
Hydrogen fueled subsonic-ram-combustor model tests for an air-turbo-ram engine
| NAL-TR-1064T | p 1236 N92-17855
MACHINE LEARNING
Pattern Theory: An engineering paradigm for algorithm design
| AD-A243214 | p 1339 N92-17179
Computer modelling of two-input neural-net learning p 1348 N92-17819
Algorithm and Pascal: A program for neural net learning p 1344 N92-17822
Neural networks for aircraft system identification p 1222 N92-17998
MACHINING
Application of silicon micromachining to thermal dissipation issues in wafer scale integrated circuits
| AD-A243744 | p 1288 N92-17332
Precision multi-channel fiber optic interface and method
| AD-D015104 | p 1367 N92-17828
MAGNESIUM
A theoretical study of the combustion of magnesium/teflon/viton pyrotechnic compositions
| AD-A243244 | p 1275 N92-17058
MAGNESIUM FLUORIDES
A theoretical study of the combustion of magnesium/teflon/viton pyrotechnic compositions
| AD-A243244 | p 1275 N92-17058
MAGNET COILS
Magnetic field distribution and design of Helmholtz coils
| AD-A242978 | p 1288 N92-17291
MAGNETIC COMPRESSION
Explosive magnetic field compression generator transformer power supply for high resistive loads
| AD-D015123 | p 1293 N92-17831
MAGNETIC DIPOLES
On the nonadiabatic theory of charged particles motion in the magnetic dipole field
| DE92-610951 | p 1354 N92-17811
MAGNETIC FIELD CONFIGURATIONS
Magnetic field distribution and design of Helmholtz coils
| AD-A242978 | p 1288 N92-17291
MAGNETIC FIELDS
The effects of field errors on low-gain free electron lasers
| AD-A243710 | p 1303 N92-17127
Magnetic field distribution and design of Helmholtz coils
| AD-A242978 | p 1288 N92-17291
Explosive magnetic field compression generator transformer power supply for high resistive loads
| AD-D015123 | p 1293 N92-17831
Magnetic multilayer strain gage
| AD-D015163 | p 1381 N92-17940
Comparative study of irreversibility effects in Nb foil and high temperature superconducting ceramics by muon spin rotation
| DE92-600475 | p 1294 N92-17953
Optical fiber magnetometer
| AD-D015133 | p 1368 N92-17959
Multiply charged ion sources for cyclotrons
| DE92-610975 | p 1364 N92-17973
Constraints on cosmic ray propagation in the galaxy
| NASA-CR-189779 | p 1390 N92-18003
MAGNETIC LEVITATION VEHICLES
Workshop on Technology Issues of Superconducting MAGLEV Transportation Systems
| DE92-002288 | p 1307 N92-17604
MAGNETIC MEASUREMENT
Workshop on Geologic Applications of Modern Aeromagnetic Surveys
| PB91-221788 | p 1316 N92-17229
MAGNETIC MOMENTS
On the nonadiabatic theory of charged particles motion in the magnetic dipole field
| DE92-610951 | p 1354 N92-17811
Magnetic multilayer strain gage
| AD-D015163 | p 1381 N92-17940
MAGNETIC MONOPOLES
Black holes in magnetic monopoles
| NASA-CR-189842 | p 1388 N92-17377
A classical instability of Reissner-Nordstrom solutions and the fate of magnetically charged black holes
| NASA-CR-189843 | p 1388 N92-17697
MAGNETIC PERMEABILITY
Structural, electronic, and magnetic properties of La(x)Sr(1-x)VO3 (0 is less than or equal to x is less than or equal to 1.0)
| DE92-003808 | p 1378 N92-17916
MAGNETIC PROPERTIES
Magnetic multilayer interface anisotropy
| DE92-000635 | p 1263 N92-17319
Structural, electronic, and magnetic properties of La(x)Sr(1-x)VO3 (0 is less than or equal to x is less than or equal to 1.0)
| DE92-003808 | p 1378 N92-17916
MAGNETIC SURVEYS
Workshop on Geologic Applications of Modern Aeromagnetic Surveys
| PB91-221788 | p 1316 N92-17229
MAGNETIC VARIATIONS
Magnetospheric response to variations in the interplanetary magnetic field
| AD-A243683 | p 1388 N92-17717
MAGNETO-OPTICS
Optical image segmentation using wavelet correlation
| AD-A243650 | p 1367 N92-17736
Correlator optical wavefront sensor COWS
| DE92-003964 | p 1368 N92-17846
MAGNETOHYDRODYNAMIC GENERATORS
Magnetohydrodynamic projects at the CDIF
| DE92-002636 | p 1370 N92-17664
MAGNETOHYDRODYNAMIC TURBULENCE
Constraints on cosmic ray propagation in the galaxy
| NASA-CR-189779 | p 1390 N92-18003
MAGNETOHYDRODYNAMIC WAVES
Alfven waves in inhomogeneous magnetic fields: An integro-differential equation formulation
| DE92-609544 | p 1371 N92-17806
MAGNETOHYDRODYNAMICS
A numerical code for a three-dimensional magnetospheric MHD equilibrium model
| NASA-CR-189852 | p 1316 N92-17227
Magnetohydrodynamic projects at the CDIF
| DE92-002636 | p 1370 N92-17664
Consistency and integrability of Navier-Stokes and systems of equations for incompressible flow magnetohydrodynamics p 1298 N92-17699
MAGNETOIONICS
Low frequency interstellar scattering and pulsar observations p 1390 N92-18005
MAGNETOMETERS
Optical fiber magnetometer
| AD-D015133 | p 1368 N92-17959
MAGNETOPAUSE
A numerical code for a three-dimensional magnetospheric MHD equilibrium model
| NASA-CR-189852 | p 1316 N92-17227
MAGNETOSPHERE-IONOSPHERE COUPLING
Radar-satellite studies of the high-latitude ionosphere
| AD-A243275 | p 1317 N92-17961
MAGNETOSTRICTION
Magnetic multilayer strain gage
| AD-D015163 | p 1381 N92-17940
MAGNETOTAILS
Magnetospheric response to variations in the interplanetary magnetic field
| AD-A243683 | p 1388 N92-17717
MAINTAINABILITY
Integration of RAMS activities during the development phase of Ariane 5-components (example: Vulcain thrust chamber)
| MBB-UK-0144-91-PUB | p 1240 N92-17527
MAINTENANCE
Cathodic protection diagnostic computer program for sacrificial and impressed current systems: Overview and user's manual
| AD-A243663 | p 1338 N92-17122
Extendable pipe crawler
| DE91-011570 | p 1306 N92-17183
Facing page test for the astronaut science advisor presentation p 1248 N92-17411
MAN MACHINE SYSTEMS
Acquisition and production of skilled behavior in dynamic decision-making tasks
| NASA-CR-189846 | p 1333 N92-17132
Training methodologies for dependent Speech Recognition (SR) systems
| AD-A242983 | p 1282 N92-17293
USI rapid prototyping tool evaluations survey
| AD-A243168 | p 1335 N92-17673
MAN TENDED FREE FLYERS
Columbus Programme (current status)
p 1243 N92-17100
MAN-COMPUTER INTERFACE
A system for specifying and rapidly prototyping user interfaces
| AD-A242963 | p 1347 N92-16994
Acquisition and production of skilled behavior in dynamic decision-making tasks
| NASA-CR-189846 | p 1333 N92-17132
IMPS: An Interactive Mathematical Proof System
| AD-A243162 | p 1350 N92-17206
AGSSS: The Airborne Graphics Software Support System; an Ada/PHIGS-based display editor for the rapid development of cockpit display software systems
| AD-A243224 | p 1234 N92-17221
A graphical database interface for a multimedia DBMS
| AD-A243283 | p 1339 N92-17285
The development of user interface tools for the computer aided prototyping system
| AD-A243189 | p 1340 N92-17368
Information Management Engineering (IME) laboratory: A database development facility
| AD-A243191 | p 1383 N92-17369
USI rapid prototyping tool evaluations survey
| AD-A243168 | p 1335 N92-17673
Developing a broader basis for scientific data analysis interfaces
| DE92-003963 | p 1385 N92-17845
MANAGEMENT ANALYSIS
A management case analysis of the Department of Defense contractor risk assessment guide program
| AD-A243515 | p 1380 N92-17388
MANAGEMENT INFORMATION SYSTEMS
The top ten critical MIS issues in the Department of Defense
| AD-A242975 | p 1382 N92-17255
An object-oriented database implementation of the Magic VLSI Layout Design System
| AD-A243743 | p 1384 N92-17482
MANAGEMENT METHODS
NASA total quality management 1989 accomplishments report
| NASA-TM-105467 | p 1308 N92-17005
A managerial approach for reliability verification of mechanical equipment
| MBB-UK-0140-91-PUB | p 1308 N92-17341
MANAGEMENT PLANNING
NASA total quality management 1989 accomplishments report
| NASA-TM-105467 | p 1308 N92-17005
Information Management Engineering (IME) laboratory: A database development facility
| AD-A243191 | p 1383 N92-17369
MANAGEMENT SYSTEMS
Data management system advanced architectures
p 1249 N92-17417
Serpent: Dialogue editor user's guide. System for user interface development, version 1
| AD-A242331 | p 1384 N92-17641
Evolution of an environmental audit program
| DE92-002681 | p 1314 N92-17665

Automated power management and control
p 1252 N92-17773
Systematic methods for knowledge acquisition and expert system development p 1222 N92-18001

MANEUVERABILITY
Industry view on rotorcraft system identification
p 1232 N92-17163

MANIFOLDS (MATHEMATICS)
A general computational framework for distributed sensing and fault-tolerant sensor integration
| AD-A243256 | p 1300 N92-16983

MANNED SPACE FLIGHT
Upper body exercise: Physiology and training application for human presence in space
| AD-A242033 | p 1329 N92-17473

MANUFACTURING
X ray lithography in Japan
| AD-A243660 | p 1286 N92-17087
Plasma processing of materials: Scientific opportunities and technological challenges
| LC-91-66812 | p 1370 N92-17556
Hubble Space Telescope: SRM/QA observations and lessons learned
| NASA-TM-105505 | p 1387 N92-17873

MANY BODY PROBLEM
Relativistic nuclear many-body theory
| DE92-003258 | p 1362 N92-17789

MAPPING
Using mappings to prove timing properties
| AD-A242862 | p 1277 N92-17263
Map maker
| AD-A242980 | p 1312 N92-17292
Radio frequency hazard monitoring-USAKA
| AD-A242873 | p 1283 N92-17563

MARINE BIOLOGY
The 7th Annual Workshop on Computational Neuroscience
| AD-A243462 | p 1335 N92-17656

MARINE ENVIRONMENTS
Acoustical and other physical properties of marine sediments
| AD-A243532 | p 1324 N92-17391

MARINE METEOROLOGY
Surface meteorological and near surface oceanographic atlas of the tropical Indian Ocean
| PB91-234286 | p 1319 N92-17138

MARINE RESOURCES
Aquatic plant management program. Supplement
| AD-A242420 | p 1314 N92-17723

MARKET RESEARCH
Toward a national semiconductor strategy. Regaining markets in high-volume electronics, volume 2
| PB91-201301 | p 1290 N92-17559
Toward a national semiconductor strategy, volume 1
| PB91-201293 | p 1290 N92-17620

MARKETING
Effect of economic techniques on radio frequency utilization
| AD-A243187 | p 1282 N92-17366
Toward a national semiconductor strategy. Regaining markets in high-volume electronics, volume 2
| PB91-201301 | p 1290 N92-17559

MARKOV PROCESSES
Data fusion for least squares
| AD-A243507 | p 1352 N92-17384
Delay analysis for multidimensional queueing process in CSMA/CD local area networks
| AD-A242364 | p 1346 N92-17425
Marked point processes as limits of Markovian arrival streams
| TW-91-04 | p 1353 N92-17837

MARS (PLANET)
Mars aerobrake assembly demonstration
p 1247 N92-17362

MARS ATMOSPHERE
Environmental interactions in Space Exploration: Announcement of the formation of an Environmental Interactions Working Group
| NASA-TM-105294 | p 1389 N92-17069
Control algorithms for aerobraking in the Martian atmosphere
| AD-A243349 | p 1239 N92-17730

MARTENSITIC TRANSFORMATION
Microstructure and mechanical properties of HSLA-100 steel
| AD-A242937 | p 1265 N92-17467

MASS SPECTRA
Molecular jet studies of vdW clusters and solvation
| AD-A242866 | p 1254 N92-17308

MASS SPECTROSCOPY
Detection of explosives material on single microparticles
| DE92-004408 | p 1276 N92-17963

MASS TRANSFER
Mass transfer in gas fluidized beds: Scaling, modeling, and particle size influence
| ETN-92-90581 | p 1298 N92-17522
The role of thermal convection in heat and mass transport in the subarctic snow cover
| AD-A243674 | p 1312 N92-17715

MASSIVELY PARALLEL PROCESSORS
Scan directed load balancing for highly-parallel mesh-connected computers
| AD-A242045 | p 1346 N92-17670

MATERIALS RECOVERY
Scale-up of recovery process for waste solvents
| KCP-613-4479 | p 1277 N92-17535

MATERIALS SCIENCE
Contributive research and development
| AD-A243331 | p 1391 N92-17079

MATHEMATICAL LOGIC
IMPS: An Interactive Mathematical Proof System
| AD-A243162 | p 1350 N92-17206
Specification and compositional verification of real-time systems
| ETN-92-90580 | p 1341 N92-17521

MATHEMATICAL MODELS
A computational model of semantic memory impairment: Modality-specificity and emergent category-specificity
| AD-A242377 | p 1347 N92-16991
A topological model for parallel algorithm design
| AD-A241858 | p 1337 N92-17023
Feature extraction for pose estimation: A comparison between synthetic and real IR imagery
| AD-A243699 | p 1338 N92-17077
Development of high angle of attack control laws for an unstable, non-minimum phase aircraft using variations of the quantitative feedback technique
| AD-A243698 | p 1236 N92-17096
Statistically-based decompression tables. 6: Repeat dives on oxyen/nitrogen mixes
| AD-A243667 | p 1328 N92-17124
Rotorcraft System Identification
| AGARD-LS-178 | p 1230 N92-17153
Instrumentation and data processing
p 1230 N92-17155
Modelling aspects and robustness issues in rotorcraft system identification p 1231 N92-17159
Gibbs sampling for marginal posterior expectations
| AD-A243212 | p 1352 N92-17178
Groundscreen characterization
| AD-A243164 | p 1311 N92-17208
Loss terms in free-piston Stirling engine models
| NASA-CR-189840 | p 1312 N92-17225
Automated composite ellipsoid modelling for high frequency GTD analysis
| NASA-CR-189853 | p 1233 N92-17316
Cost models and the Corporate Information Management (CIM) initiative
| AD-A243554 | p 1383 N92-17340
A model for voltammograms of the underpotential deposition of metals
| AD-A243199 | p 1264 N92-17370
Acoustical and other physical properties of marine sediments
| AD-A243532 | p 1324 N92-17391
FEM-X user's guide
| AD-A242374 | p 1383 N92-17396
Spectral error models applied to the geodetic boundary value problem
| ETN-92-90582 | p 1312 N92-17436
Some foundations for empirical study in the euclidean spatial model of social choice
| AD-A241928 | p 1352 N92-17440
Verification of an effective dose equivalent model for neutrons
| DE92-002738 | p 1358 N92-17453
Computational and neural network models for the analysis of visual texture
| AD-A243717 | p 1327 N92-17504
Mass transfer in gas fluidized beds: Scaling, modeling, and particle size influence
| ETN-92-90581 | p 1298 N92-17522
Large ideals and non-regular ultrafilters
| ETN-92-90587 | p 1351 N92-17525
Numerical studies of processes in stratiform cirrus
| MITT-78 | p 1321 N92-17543
Testing of spacecraft in long-term storage
| AD-A242906 | p 1250 N92-17580
Upper ocean dynamics during the LOTUS and Tropic Heat Experiments
| AD-A243730 | p 1324 N92-17583
Bayesian computations in survival models via the Gibbs sampler
| AD-A242343 | p 1353 N92-17643
Axino-induced baryogenesis
| NASA-CR-189858 | p 1361 N92-17646
Gate drain geometry effect on the current voltage characteristics of GaAs MESFETs
| AD-A243430 | p 1291 N92-17684
Environmental containment property estimation using QSARs in an expert system
| AD-A243728 | p 1336 N92-17720
Engineering model of unsteady flow in a cavity
| AD-A243636 | p 1299 N92-17747
Improving stochastic communication network performance: Reliability vs throughput
| AD-A243655 | p 1285 N92-17763
Preliminary results from the analysis of wind component error
| AD-A243772 | p 1321 N92-17764
A theoretical search for supervelocity semiconductors
| AD-A241981 | p 1376 N92-17783
Analysis of cam roller followers
| ESDU-91026 | p 1307 N92-17852
Numerical simulation of fluid flow and heat transfer in a thin liquid film over a stationary and rotating disk and comparison with experimental data
| NASA-CR-189253 | p 1300 N92-17887
Global models for the biomechanics of green plants, part 1
| DE91-641478 | p 1327 N92-17946
Software reliability models for critical applications
| DE92-004797 | p 1345 N92-17969
Physical and computational modelling of stratified shear flows
| AERO-REPT-8909 | p 1300 N92-17974
A variational assimilation method for satellite and conventional data: Development of basic model for diagnosis of cyclone systems
| NASA-CR-188236 | p 1321 N92-17975
A variational assimilation method for satellite and conventional data: Model 2 (version 1)
p 1322 N92-17976
Modification of a successive corrections objective analysis for improved derivative calculations
p 1322 N92-17981

MATHEMATICS
Mathematics and biology
| DE92-611247 | p 1327 N92-17815

MATRICES (MATHEMATICS)
The instability of linear heterogeneous Lanchester equations
| AD-A243519 | p 1350 N92-17081
Face recognition with the Karhunen-Loeve transform
| AD-A243688 | p 1280 N92-17090
Inequalities among partial traces of Hermitian operators and partial sums of their Eigenvalues
| DE91-641495 | p 1351 N92-17622
An analytic method of propagating a covariance matrix to a maneuver condition for linear covariance analysis during rendezvous
| AD-A243354 | p 1239 N92-17732
Neural-network dedicated processor for solving competitive assignment problems
| NASA-CASE-NPO-17781-1-CU | p 1337 N92-17884

MATRIX MATERIALS
Dynamic fracture characterization of Al2O3 and SiC(w)/Al2O3
| AD-A242187 | p 1273 N92-17784

MATTER (PHYSICS)
Equation of state and conductivity of hot, dense matter
| AD-A243359 | p 1369 N92-17301

MAXIMUM LIKELIHOOD ESTIMATES
Statistically-based decompression tables. 6: Repeat dives on oxyen/nitrogen mixes
| AD-A243667 | p 1328 N92-17124
Sensitivity testing and analysis
| DE92-002033 | p 1276 N92-17624

MEAN
Sensitivity testing and analysis
| DE92-002033 | p 1276 N92-17624

MEASURING INSTRUMENTS
A knowledge-based approach for configuring computer aided measuring systems
| ETN-92-90585 | p 1341 N92-17524
Development and utilization of new diagnostics for dense-phase pneumatic transport
| DE92-003091 | p 1307 N92-17605
Electromagnetic pulse-induced current measurement device
| AD-A241946 | p 1291 N92-17668
Development and utilization of new diagnostics for dense-phase pneumatic transport
| DE92-000337 | p 1299 N92-17704

MECHANICAL DEVICES
A managerial approach for reliability verification of mechanical equipment
| MBB-UK-0140-91-PUB | p 1308 N92-17341
Electrically-controlled polymeric gels as active materials in adaptive structures
| DE92-002947 | p 1272 N92-17710

MECHANICAL DRIVES
Space Station Freedom solar alpha joint growth capability p 1252 N92-17772
MECHANICAL PROPERTIES
Ceramics with superelectrical and supermechanical properties
| AD-A243062 | p 1267 N92-17029
Contributive research and development
| AD-A243331 | p 1391 N92-17079
A diffraction limited nitrogen laser for detector calibration in high energy physics
| ETN-92-90567 | p 1303 N92-17434
Polymer-reinforced metal matrix composite
| AD-D015070 | p 1257 N92-17611
MEDICAL EQUIPMENT
Evaluation of scalar value estimation techniques for 3D medical imaging
| AD-A243687 | p 1328 N92-17089
Testing and evaluation of the Vanner electrical inverters, models 24-1500 and SP 00112
| AD-A241914 | p 1287 N92-17216
Compact free electron lasers for medical applications
| AD-A243497 | p 1304 N92-17582
MEDICAL PERSONNEL
Testing and evaluation of the Vanner electrical inverters, models 24-1500 and SP 00112
| AD-A241914 | p 1287 N92-17216
Labor market trends for health physicists
| DE92-004770 | p 1331 N92-17800
MEDITERRANEAN SEA
Severe weather guide mediterranean ports. Part 35: Rota
| AD-A243539 | p 1319 N92-17338
Severe weather guide Mediterranean ports. Part 38: Alexandria
| AD-A243451 | p 1320 N92-17406
Severe weather guide Mediterranean ports. Part 36: Limassol
| AD-A243448 | p 1320 N92-17492
Severe weather guide Mediterranean ports. Part 37: Larnaca
| AD-A243449 | p 1320 N92-17493
Severe weather guide Mediterranean ports. Part 39: Port Said
| AD-A243450 | p 1320 N92-17494
Proceedings of the 2nd Gulf of Cadiz Expedition Workshop
| AD-A242749 | p 1325 N92-17951
MEMBRANES
New experimental challenges in elemental fluorine chemistry: An emerging technology
| AD-A243054 | p 1258 N92-17043
Biophysical techniques for examining metabolic, proliferative, and genetic effects of microwave radiation
| AD-A241903 | p 1326 N92-17288
Characterization of the P. brevis polyether neurotoxin binding component in excitable membranes
| AD-A242877 | p 1327 N92-17564
Mechanisms of gas permeation through polymer membranes
| DE92-004423 | p 1274 N92-17942
MEMORY
A computational model of semantic memory impairment: Modality-specificity and emergent category-specificity
| AD-A242377 | p 1347 N92-16991
The effects of speech intelligibility level on concurrent visual task performance
| AD-A243015 | p 1331 N92-17052
MEMORY (COMPUTERS)
Resource allocation in distributed memory multiprocessing
| AD-A243165 | p 1345 N92-17188
Effect of spatial locality prefetching on structural locality
| AD-A243632 | p 1337 N92-17922
MENTAL PERFORMANCE
Neural network classification of mental workload conditions by analysis of spontaneous electroencephalograms
| AD-A243369 | p 1331 N92-17115
Automated planning with special relevance to associate systems technology and mission planning
| AD-A241924 | p 1348 N92-17438
The cognitive, perceptual, and neural bases of skilled performance
| AD-A243052 | p 1332 N92-17554
MESONS
What experiments say about possibility of the new particle existence with mass less than the kaon mass
| DE91-634551 | p 1357 N92-17408
MESOSCALE PHENOMENA
Turbulent and gravity wave transport in the free atmosphere p 1315 N92-17063
Numerical simulation of cirrus clouds: Fire case study and sensitivity analysis
| AD-A242902 | p 1321 N92-17631
MESOSPHERE
Relaxation processes of vibrationally excited H2O in the mesosphere and thermosphere
| AD-A241853 | p 1315 N92-17035
MESSAGE PROCESSING
BATTLEKING evaluation, BK 22-91, Meteorological Sensor Package (MSP)
| AD-A241919 | p 1317 N92-17009
Resource allocation in distributed memory multiprocessing
| AD-A243165 | p 1345 N92-17188
Delay analysis for multidimensional queueing process in CSMA/CD local area networks
| AD-A242364 | p 1346 N92-17425
METABOLISM
Preliminary assessment of the relative toxicity of tetraglycine hydroperiodide, phase 1
| AD-A243334 | p 1330 N92-17712
METAL COATINGS
An optical roughness sensor for the real time determination of spray formed preform quality
| AD-A243238 | p 1262 N92-17056
Silver-nickel composite cathodes for alkaline secondary batteries
| AD-D015121 | p 1293 N92-17871
METAL FATIGUE
Fatigue in single crystal nickel superalloys
| AD-A243453 | p 1265 N92-17653
METAL FILMS
Evidence for MeV particle emission from Ti charged with low energy deuterium ions
| AD-A243718 | p 1359 N92-17505
METAL FINISHING
Evaluation of environmentally safe cleaning agents for diamond turned optics
| DE92-002524 | p 1278 N92-17780
METAL FOAMS
Low frequency vibration absorber
| AD-D015103 | p 1307 N92-17827
METAL FUELS
Launching projectiles with hydrogen gas generated from aluminum fuel powder/water reactions
| AD-D015119 | p 1276 N92-17830
METAL IONS
Theoretical crystal-field calculations for rare-earth ions in 3-5 semiconductor compounds
| AD-A243098 | p 1371 N92-16995
Evidence for MeV particle emission from Ti charged with low energy deuterium ions
| AD-A243718 | p 1359 N92-17505
Direct speciation of metal and metalloid ions by optical spectroscopies
| DE92-003868 | p 1261 N92-17727
METAL MATRIX COMPOSITES
Microstructurally toughened articles and casting thereof
| AD-D015065 | p 1265 N92-17452
Polymer-reinforced metal matrix composite
| AD-D015070 | p 1257 N92-17611
Damage mechanisms in composites
| AD-A242748 | p 1258 N92-17950
METAL OXIDES
Electronic interactions of directed photon beams with surfaces
| AD-A241878 | p 1356 N92-17026
METAL PROPELLANTS
Upper stages using liquid propulsion and metallized propellants
| NASA-TP-3191 | p 1253 N92-17151
METAL SURFACES
In situ surface x ray crystallography of electrochemically deposited Bi on Ag(111): Structure, compressibility, and anisotropy
| AD-A243218 | p 1372 N92-17181
Omega-terminated alkanethiolate monolayers on surfaces of copper, silver and gold have similar wettabilities
| AD-A243529 | p 1260 N92-17389
Optical nonlinearity in coupled exciton-phonon systems near metal surfaces
| AD-A242362 | p 1357 N92-17423
Enhanced backscattering from rough surfaces
| AD-A243437 | p 1366 N92-17486
Evaluation of environmentally safe cleaning agents for diamond turned optics
| DE92-002524 | p 1278 N92-17780
Ionic physics and technology p 1362 N92-17818
Investigation of heated ultracold neutrons on copper surface
| DE92-600625 | p 1363 N92-17955
METAL-GAS SYSTEMS
Evaluation of a diffusion/trapping model for hydrogen ingress in high-strength alloys
| AD-A243461 | p 1263 N92-17327
METAL-METAL BONDING
Solder extrusion pressure bonding process and bonded products produced thereby
| DE92-004603 | p 1363 N92-17739
METAL-WATER REACTIONS
Blistering of graphite/polymer composites galvanically coupled with metals in sea water
| AD-A242861 | p 1269 N92-17262
METALLIZING
A model for voltammograms of the underpotential deposition of metals
| AD-A243199 | p 1264 N92-17370
METALLOGRAPHY
Metallography of aluminide coatings
| AD-A243000 | p 1263 N92-17264
Long-term corrosion evaluation of stainless steels in Space Shuttle iodinated resin and water
| NASA-TM-104743 | p 1264 N92-17376
METALLOIDS
Direct speciation of metal and metalloid ions by optical spectroscopies
| DE92-003868 | p 1261 N92-17727
METALS
A CAD model for the axial inductive strip with finite thickness centered in homogeneous finline with w/b = 1
| AD-A243553 | p 1278 N92-17016
Making of functionally gradient materials data base
| NAL-TM-621 | p 1385 N92-17787
METASTABLE STATE
Rates and mechanisms of metastable deactivation over surfaces
| AD-A243391 | p 1361 N92-17652
METEOROLOGICAL INSTRUMENTS
BATTLEKING evaluation, BK 22-91, Meteorological Sensor Package (MSP)
| AD-A241919 | p 1317 N92-17009
METEOROLOGICAL PARAMETERS
Surface observation climatic summaries for Duke Field/Eglin aux no. 3, Florida
| AD-A243310 | p 1318 N92-17073
Surface observation climatic summaries for Castle AFB, California
| AD-A243677 | p 1318 N92-17074
Surface observation climatic summaries for Hondo Municipal Airport, Texas
| AD-A243311 | p 1319 N92-17144
Surface observation climatic summaries for Boise Air Terminal, ID
| AD-A243012 | p 1319 N92-17257
Surface observations climatic summaries for Camp Humphreys, Korea
| AD-A241937 | p 1320 N92-17444
Severe weather guide Mediterranean ports. Part 37: Larnaca
| AD-A243449 | p 1320 N92-17493
Severe weather guide Mediterranean ports. Part 39: Port Said
| AD-A243450 | p 1320 N92-17494
High-frequency meteorological phenomena observed with the Naval Postgraduate School's UHF Doppler wind profiler
| AD-A243762 | p 1320 N92-17515
A variational assimilation method for satellite and conventional data: Model 2 (version 1) p 1322 N92-17976
A variational formalism for the radiative transfer equation: Prelude to model 3 p 1322 N92-17978
On the concept of varying influence radii for a successive corrections objective analysis p 1322 N92-17980
Modification of a successive corrections objective analysis for improved derivative calculations p 1322 N92-17981
METEOROLOGICAL RADAR
Terminal Doppler weather radar test bed operation, Orlando: January-June 1990
| AD-A242890 | p 1318 N92-17028
Analysis of the terminal Doppler weather radar algorithm for detecting rotation associated with microbursts
| AD-A242840 | p 1318 N92-17050
Recommendations for a wind profiling network to support Space Shuttle launches
| NASA-CR-4421 | p 1318 N92-17072
METEOROLOGICAL SATELLITES
Evaluation of LOWTRAN and MODTRAN for use over high zenith angle/long path length viewing
| AD-A243599 | p 1387 N92-17920
A variational formalism for the radiative transfer equation: Prelude to model 3 p 1322 N92-17978
METEOROLOGICAL SERVICES
NOAA Atmospheric Sciences Modeling Division support to the US Environmental Protection Agency
| PB91-235499 | p 1315 N92-17134

METEOROLOGY
NOAA Atmospheric Sciences Modeling Division support to the US Environmental Protection Agency
| PB91-235499 | p 1315 N92-17134
Studies of baroclinic flow
| AD-A243050 | p 1296 N92-17309
Comparison of two eighth-mesh terrain databases
| AD-A243315 | p 1383 N92-17401

METHANE
Transpiration cooled throat for hydrocarbon rocket engines
| NASA-CR-184272 | p 1253 N92-17495

METHOD OF MOMENTS
A rigorous UTD analysis of electromagnetic scattering from resistive strips and resistive-loaded conducting strips
| AD-A243691 | p 1280 N92-17092

METHYL ALCOHOL
Catalytic studies on a novel synthesis of methanol
| DE92-002904 | p 1275 N92-17184

METHYL COMPOUNDS
Imide/arylene ether copolymers with pendent trifluoromethyl groups
| NASA-TM-104195 | p 1272 N92-17693

METHYLENE
Nitration and nitrocompounds
| AD-A243380 | p 1259 N92-17210

METRIC PHOTOGRAPHY
The calibration process of digital cameras
| ETN-92-90583 | p 1301 N92-17437

METRIC SPACE
A topological model for parallel algorithm design
| AD-A241858 | p 1337 N92-17023
Lie-isotopic generalization of the Poincare symmetry: Classical formulation
| DE91-642825 | p 1379 N92-17531

MICROANALYSIS
Detection of explosives material on single microparticles
| DE92-004408 | p 1276 N92-17963

MICROBURSTS (METEOROLOGY)
Analysis of the terminal Doppler weather radar algorithm for detecting rotation associated with microbursts
| AD-A242840 | p 1318 N92-17050
Escape strategies for turboprop aircraft in a microburst windshear
| AD-A243090 | p 1227 N92-17217
An investigation of air transportation technology at the Massachusetts Institute of Technology, 1990-1991
p 1219 N92-17985
Alert generation and cockpit presentation for an integrated microburst alerting system
p 1220 N92-17988
Cockpit display of hazardous weather information
p 1220 N92-17989
Target pitch angle for the microburst escape maneuver p 1221 N92-17996
Optimal aircraft performance during microburst encounter p 1222 N92-17999

MICROCOMPUTERS
The conversion of a FORTRAN data plotting program using DI-3000 graphics to operation on a Macintosh Personal Computer
| AD-A243046 | p 1339 N92-17280

MICROELECTRONICS
Integration of an anti-parallel pair of planar Schottky barrier diodes for millimeter and submillimeter wavelengths
| AD-A243371 | p 1287 N92-17189
Computer aided thermal analysis of a microcircuit structure
| AD-A243160 | p 1287 N92-17205
Application of silicon micromachining to thermal dissipation issues in wafer scale integrated circuits
| AD-A243744 | p 1288 N92-17332
Plasma processing of materials: Scientific opportunities and technological challenges
| LC-91-66812 | p 1370 N92-17556

MICROGRAVITY APPLICATIONS
Space Station Freedom science utilization: 2000 and beyond p 1244 N92-17107
Microgravity Science and Applications Program tasks, 1990 revision
| NASA-TM-4284 | p 1276 N92-17945

MICROMECHANICS
Light-controlled, electrochemical, anisotropic etching of silicon
| MBB-Z-0368-91-PUB | p 1261 N92-17841

MICROMETEORITES
Hypervelocity impact simulation for micrometeorite and debris shield design
| NASA-CR-189807 | p 1244 N92-17200

MICROMETEOROLOGY
Numerical studies of processes in stratiform cirrus
| MITT-78 | p 1321 N92-17543

MICROMINIATURIZATION
Molecular self-assembly and nanochemistry: A chemical strategy for the synthesis of nanostructures
| AD-A243530 | p 1361 N92-17616

MICROORGANISMS
The effect of shower/bath frequency on the health and operational effectiveness of soldiers in a field setting: Recommendation of showering frequencies for reducing performance-degrading nonsystemic microbial skin infections
| AD-A242923 | p 1330 N92-17714
Evolution as a molecular cooperative phenomenon
| DE92-609575 | p 1327 N92-17877

MICROPARTICLES
On size scaling in shock hydrodynamics and the stress-strain behavior of copper at exceedingly high strain rates
| DE92-003797 | p 1265 N92-17579
Detection of explosives material on single microparticles
| DE92-004408 | p 1276 N92-17963

MICROPROCESSORS
Performance modeling of the Ada rendezvous
| AD-A243392 | p 1339 N92-17211
Beam position monitor multiplexer controller upgrade at the LAMPF proton storage ring
| DE92-003859 | p 1363 N92-17590
Microprocessor controller in CAMAC standard for temperature regulation and stabilization
| DE92-611158 | p 1348 N92-17814

MICROPROGRAMMING
Design of Style-V: A translator to convert standard VHDL into a stylized form for automated microcode generation
| AD-A243706 | p 1340 N92-17407

MICROSCOPY
X ray laser
| DE91-011705 | p 1304 N92-17649
Optical modification of a single impurity molecule in a solid
| AD-A243750 | p 1361 N92-17660

MICROSTRIP DEVICES
A CAD model for the axial inductive strip with finite thickness centered in homogeneous finline with w/b = 1
| AD-A243553 | p 1278 N92-17016
Microstrip discontinuity models to 60 GHz
| AD-A242038 | p 1339 N92-17185

MICROSTRIP TRANSMISSION LINES
Design and testing of a lightweight, planar microwave lens
| AD-A243685 | p 1286 N92-17076

MICROSTRUCTURE
A powder x ray diffraction study of two aluminum-lithium based alloys
| AD-A243186 | p 1262 N92-17000
Contributive research and development
| AD-A243331 | p 1391 N92-17079
High resolution electron microscopy of diamond film growth defects and their interactions
| AD-A243093 | p 1372 N92-17238
Metallography of aluminide coatings
| AD-A243000 | p 1263 N92-17264
Strength and microstructure of ceramics
| AD-A243049 | p 1269 N92-17282
In situ structural studies of the underpotential deposition of copper onto an iodine covered platinum surface using x ray standing waves
| AD-A243475 | p 1263 N92-17328
Microstructure and mechanical properties of HSLA-100 steel
| AD-A242937 | p 1265 N92-17467
Microstructure and composition of electromagnetically-characterized YBa2Cu3O(7-delta) grain boundaries
| DE92-003520 | p 1376 N92-17782

MICROWAVE ANTENNAS
Multiple-access phased array antenna simulator for a digital beam forming system investigation
| NASA-TM-105422 | p 1279 N92-17062
Design and testing of a lightweight, planar microwave lens
| AD-A243685 | p 1286 N92-17076

MICROWAVE CIRCUITS
A CAD model for the axial inductive strip with finite thickness centered in homogeneous finline with w/b = 1
| AD-A243553 | p 1278 N92-17016
Microstrip discontinuity models to 60 GHz
| AD-A242038 | p 1339 N92-17185
Superconducting microwave transmission lines
| AD-A243166 | p 1291 N92-17671

MICROWAVE COUPLING
Microstrip discontinuity models to 60 GHz
| AD-A242038 | p 1339 N92-17185

MICROWAVE EQUIPMENT
Sea surface environmental conditions in the Gulf of Alaska during April 1990 using SSM/I
| AD-A241909 | p 1323 N92-17041
Three point lead screw positioning apparatus
| NASA-CASE-LEW-15216-1 | p 1307 N92-17678

MICROWAVE FREQUENCIES
Research and development on advanced silicon carbide thin film growth techniques and fabrication of high power and microwave frequency silicon carbide-based device structures
| AD-A243531 | p 1373 N92-17390
Innovative switching technology
| DE92-003068 | p 1292 N92-17708

MICROWAVE IMAGERY
Sea surface environmental conditions in the Gulf of Alaska during April 1990 using SSM/I
| AD-A241909 | p 1323 N92-17041

MICROWAVE LANDING SYSTEMS
Flight evaluation of curved MLS precision approaches in a twin otter aircraft, phase 2
| AD-A243025 | p 1229 N92-17568

MICROWAVE SCATTERING
The physical optics description of microwave scattering by the sea surface
| AD-A243216 | p 1365 N92-17180

MICROWAVE TRANSMISSION
Superconducting microwave transmission lines
| AD-A243166 | p 1291 N92-17671

MICROWAVES
Biophysical techniques for examining metabolic, proliferative, and genetic effects of microwave radiation
| AD-A241903 | p 1326 N92-17288
Simultaneous active and passive microwave measurements of the ocean surface
| AD-A242232 | p 1312 N92-17459
Late time cosmological phase transitions 1: Particle physics models and cosmic evolution
| NASA-CR-189857 | p 1388 N92-17696
High-speed beam switching processor
| AD-D015108 | p 1285 N92-17829

MILITARY AIR FACILITIES
Surface observation climatic summaries for Castle AFB, California
| AD-A243677 | p 1318 N92-17074

MILITARY AIRCRAFT
Development of a knowledge base for use in an Expert System Advisor for Aircraft Maintenance Scheduling (ESAAMS)
| AD-A243435 | p 1381 N92-17687

MILITARY OPERATIONS
Causal schema decision-aiding system
| AD-A242931 | p 1347 N92-17203
Early warning satellites: Funding for follow-on system is premature
| AD-A242836 | p 1245 N92-17250

MILITARY TECHNOLOGY
Early warning satellites: Funding for follow-on system is premature
| AD-A242836 | p 1245 N92-17250
Communication network survivability
| AD-A242969 | p 1281 N92-17252
Using the Global Positioning System (GPS) to fulfill the position/location requirements of the National Training Center (NTC) and other US Army instrumented testing and training ranges
| AD-A242064 | p 1229 N92-17639

MILK
Assessment of the behavioral and neurotoxic effects of hexachlorobenzene (HCB) in the developing rat
| AD-A243658 | p 1325 N92-17121

MILLIMETER WAVES
Microstrip discontinuity models to 60 GHz
| AD-A242038 | p 1339 N92-17185
Integration of an anti-parallel pair of planar Schottky barrier diodes for millimeter and submillimeter wavelengths
| AD-A243371 | p 1287 N92-17189
Quantum-limited detection of millimeter waves using superconducting tunnel junctions
| DE92-004757 | p 1377 N92-17799

MIMO (CONTROL SYSTEMS)
A robust digital flight control system for an unfanned research vehicle using discrete quantitative feedback theory
| AD-A243638 | p 1237 N92-17748

MINES (ORDNANCE)
Differential pressure sensor
| AD-D015134 | p 1302 N92-17918

MINIATURIZATION
LDA and PDA systems based on diode-pumped Neodym:YAG lasers
| MBB-Z-0361-91-PUB | p 1304 N92-17526

MINKOWSKI SPACE
Lie-isotopic generalization of the Poincare symmetry: Classical formulation
| DE91-642825 | p 1379 N92-17531
MIRAGE AIRCRAFT
Wind loads on a mirage III O aircraft mounted above a ground plane
| AD-A243004 | p 1232 N92-17266
MIRRORS
Aries x ray objective grating spectrograph
| NASA-CR-189245 | p 1386 N92-17003
Evaluation of a compact Cassegrain optical system
| AD-A242985 | p 1366 N92-17294
Optical nonlinearity in coupled exciton-phonon systems near metal surfaces
| AD-A242362 | p 1357 N92-17423
Full surface testing of grazing incidence mirrors
| AD-A243734 | p 1367 N92-17690
Evaluation of environmentally safe cleaning agents for diamond turned optics
| DE92-002524 | p 1278 N92-17780
Hubble Space Telescope: SRM/QA observations and lessons learned
| NASA-TM-105505 | p 1387 N92-17873
Wide field strip-imaging optical system
| NASA-CASE-NPO-18146-1-CU | p 1368 N92-17892
Self-collimated unstable resonator semiconductor laser
| NASA-CASE-NPO-18386-1-CU | p 1305 N92-17899
MISSILE DETECTION
Integrated system for missile detection and discrimination
| DE91-018874 | p 1283 N92-17529
MISSILES
Early warning satellites: Funding for follow-on system is premature
| AD-A242836 | p 1245 N92-17250
MISSION PLANNING
Environmental interactions in Space Exploration: Announcement of the formation of an Environmental Interactions Working Group
| NASA-TM-105294 | p 1389 N92-17069
Evolution design requirements and design strategy
p 1244 N92-17112
Construction equipment for lunar surface operations
| AD-A243665 | p 1389 N92-17123
Advanced flight software reconfiguraton
p 1245 N92-17350
Operations mission planner beyond the baseline
p 1246 N92-17353
Environmental control and life support system evolution analysis p 1246 N92-17355
Space Station Freedom baseline operations concept
p 1248 N92-17410
Advanced Crew Personal Support Computer (CPSC) task p 1249 N92-17419
Automated planning with special relevance to associate systems technology and mission planning
| AD-A241924 | p 1348 N92-17438
Hubble Space Telescope: The GO and GTO Observing Programs. Version 1.0
| NASA-CR-189815 | p 1387 N92-17650
Verification and validation of the Comprehensive Operational Support Evaluation Model for space
| AD-A243653 | p 1344 N92-17761
Beyond the Baseline 1991: Proceedings of the Space Station Evolution Symposium. Volume 2: Space Station Freedom, part 1
| NASA-CP-10083-VOL-2-PT-1 | p 1251 N92-17768
MIXED OXIDES
Growth of near-free-standing YBa2Cu3O7-type crystals using a self-decanting flux method
| AD-A243221 | p 1372 N92-17182
MIXERS
Quantum-limited detection of millimeter waves using superconducting tunnel junctions
| DE92-004757 | p 1377 N92-17799
MIXING
Waveguide four-wave mixing
| AD-A243555 | p 1286 N92-17017
Ion mixing of semiconductor layered-structures
| DE92-003756 | p 1377 N92-17791
MIXING CIRCUITS
Metriwave final report
| NASA-CR-189816 | p 1279 N92-17046
MIXING LENGTH FLOW THEORY
An experimental investigation of chemically-reacting, gas-phase turbulent jets
| AD-A243036 | p 1296 N92-17276
MOBILE COMMUNICATION SYSTEMS
A ring model for local/mobile radio communications with variable packet length
| AD-A241856 | p 1279 N92-17036
An overview of cellular telecommunications
| AD-A242951 | p 1281 N92-17232
MODELS
A CAD model for the axial inductive strip with finite thickness centered in homogeneous finline with w/b = 1
| AD-A243553 | p 1278 N92-17016
Melatonin action on the circadian pacemaker in Siberian hamsters
| AD-A243057 | p 1325 N92-17142
Neutral network models of primate motor system
| AD-A243460 | p 1343 N92-17655
MODULATORS
Correlator optical wavefront sensor COWS
| DE92-003964 | p 1368 N92-17846
MOLECULAR BEAM EPITAXY
Research and development on advanced silicon carbide thin film growth techniques and fabrication of high power and microwave frequency silicon carbide-based device structures
| AD-A243531 | p 1373 N92-17390
MOLECULAR BEAMS
Rates and mechanisms of metastable deactivation over surfaces
| AD-A243391 | p 1361 N92-17652
MOLECULAR BIOLOGY
Efficient identification and analysis of low and medium frequency repeats
| DE92-003758 | p 1385 N92-17856
Evolution as a molecular cooperative phenomenon
| DE92-609575 | p 1327 N92-17877
Comments on a novel approach to the role of chirality in the origin of life
| DE92-609034 | p 1327 N92-17970
MOLECULAR CHAINS
Gas transport in polybutadiene treated with aqueous bromine
| AD-A241871 | p 1295 N92-17025
MOLECULAR CLOUDS
IRAS and the Boston University Arecibo Galactic H I Survey: A catalog of cloud properties
| NASA-CR-189806 | p 1387 N92-17695
MOLECULAR COLLISIONS
Vibrational energy transfer in bromine monofluoride
| AD-A243690 | p 1259 N92-17091
Quenching and rotational energy transfer in molecular bromine: Br2(B)
| AD-A241987 | p 1357 N92-17321
MOLECULAR DIFFUSION
Detection and spectroscopy of single pentacene molecules in a p-terphenyl crystal by means of fluorescence excitation
| AD-A243747 | p 1356 N92-17196
Single molecule spectral diffusion in a solid detected via fluorescence spectroscopy
| AD-A243748 | p 1356 N92-17197
Molecular motions of the head group of SHBS in lamellar liquid crystals
| AD-A243499 | p 1373 N92-17382
Optical spectra and kinetics of single impurity molecules in a polymer: Spectral diffusion and persistent spectral hole-burning
| AD-A243749 | p 1271 N92-17659
Optical modification of a single impurity molecule in a solid
| AD-A243750 | p 1361 N92-17660
MOLECULAR EXCITATION
Detection and spectroscopy of single pentacene molecules in a p-terphenyl crystal by means of fluorescence excitation
| AD-A243747 | p 1356 N92-17196
Single molecule spectral diffusion in a solid detected via fluorescence spectroscopy
| AD-A243748 | p 1356 N92-17197
Optical modification of a single impurity molecule in a solid
| AD-A243750 | p 1361 N92-17660
MOLECULAR GASES
Gas transport in polybutadiene treated with aqueous bromine
| AD-A241871 | p 1295 N92-17025
MOLECULAR INTERACTIONS
Reactions and interactions in liquid crystalline media
| AD-A242355 | p 1374 N92-17449
Direct speciation of metal and metalloid ions by optical spectroscopies
| DE92-003868 | p 1261 N92-17727
MOLECULAR RELAXATION
Relaxation processes of vibrationally excited H2O in the mesosphere and thermosphere
| AD-A241853 | p 1315 N92-17035
MOLECULAR ROTATION
Quenching and rotational energy transfer in molecular bromine: Br2(B)
| AD-A241987 | p 1357 N92-17321
MOLECULAR SPECTROSCOPY
Molecular jet studies of vdW clusters and solvation
| AD-A242866 | p 1254 N92-17308
MOLECULAR STRUCTURE
Stability and structure of C12B24N24: A hybrid analog of buckminsterfullerene
| AD-A242327 | p 1373 N92-17245
New optical materials for the long-wave (8-12 microns) region: Design criteria for the solid-state chemist
| AD-A243280 | p 1365 N92-17284
Designing ordered molecular arrays in two and three dimensions
| AD-A243447 | p 1359 N92-17491
Nonlinear spectroscopic studies of interfacial molecular ordering
| DE92-000864 | p 1360 N92-17530
Organometallic NLO polymers. Linear main-chain NLO polymers of ferrocene
| AD-A243641 | p 1272 N92-17750
MOLECULAR WEIGHT
Free volume variation with molecular weight of polymers
| NASA-TM-4326 | p 1267 N92-17032
The effect of monomer structures and compressibility on the properties of multicomponent polymer blends and solutions
| AD-A242863 | p 1273 N92-17777
MOLECULES
Detection and spectroscopy of single pentacene molecules in a p-terphenyl crystal by means of fluorescence excitation
| AD-A243747 | p 1356 N92-17196
The shapes and cavities of four cholic acid host systems
| AD-A243483 | p 1255 N92-17329
Rates and mechanisms of metastable deactivation over surfaces
| AD-A243391 | p 1361 N92-17652
Optical spectra and kinetics of single impurity molecules in a polymer: Spectral diffusion and persistent spectral hole-burning
| AD-A243749 | p 1271 N92-17659
MOLTEN SALT ELECTROLYTES
Lithiated Vanadium Oxide (LVO), gamma-lithium vanadium bronze (Gamma-LiV2O5) and vanadium dioxide (VO2) as thermal battery cathode materials
| AD-A242948 | p 1287 N92-17186
MOMENTS
Computation of the hydrodynamic forces and moments on a body of revolution with and without appendages
| AD-A243033 | p 1294 N92-16978
MONITORS
Measurement of electron beam emittance using optical transition radiation and development of a diffuse screen electron beam monitor
| AD-A241893 | p 1357 N92-17306
Radio frequency hazard monitoring-USAKA
| AD-A242873 | p 1283 N92-17563
Beam position monitor multiplexer controller upgrade at the LAMPF proton storage ring
| DE92-003859 | p 1363 N92-17590
A distributed design for monitoring, logging, and replaying device readings at LAMPF
| DE92-003860 | p 1240 N92-17591
MONKEYS
Neutral network models of primate motor system
| AD-A243460 | p 1343 N92-17655
MONOMERS
Organometallic NLO polymers. Linear main-chain NLO polymers of ferrocene
| AD-A243641 | p 1272 N92-17750
Organometallic NLO polymers. Accordian main-chain NLO polymers of ferrocene
| AD-A243642 | p 1273 N92-17751
Aryl bis(triflates) in palladium (0) cross-coupling reactions. Synthesis of polyphenyl-alkynyl, alkenyl, and aryl ethers
| AD-A243643 | p 1273 N92-17752
Organic NLO polymers. Linear and accordian main-chain NLO polymers prepared by a Knoevenagel polycondensation
| AD-A243644 | p 1273 N92-17753
The effect of monomer structures and compressibility on the properties of multicomponent polymer blends and solutions
| AD-A242863 | p 1273 N92-17777
MONOSACCHARIDES
The shapes and cavities of four cholic acid host systems
| AD-A243483 | p 1255 N92-17329
MONTE CARLO METHOD
Tests of fit for the Cauchy distribution based on the empirical distribution function
| AD-A243201 | p 1352 N92-17173
The ZEUS second level calorimeter trigger: Physics simulation, design and implementation
| ETN-92-90568 | p 1358 N92-17435

Performance of the Rayleigh task based on the posterior probability of tomographic reconstructions
| DE92-003785 | p 1352 N92-17455
A theoretical search for supervelocity semiconductors
| AD-A241981 | p 1376 N92-17783
Stochastic robustness p 1221 N92-17997
Technical notes and correspondence: Stochastic robustness of linear time-invariant control systems p 1222 N92-18002

MONTEREY BAY (CA)
Source of cold water in Monterey Bay observed by AVHRR satellite imagery
| AD-A242843 | p 1323 N92-17051

MOON
Environmental interactions in Space Exploration: Announcement of the formation of an Environmental Interactions Working Group
| NASA-TM-105294 | p 1389 N92-17069

MOTION PERCEPTION
The cognitive, perceptual, and neural bases of skilled performance
| AD-A243052 | p 1332 N92-17554

MOTION SICKNESS
A topographical analysis of the human electroencephalogram for patterns in the development of motion sickness
| AD-A243656 | p 1328 N92-17120

MOTION SICKNESS DRUGS
A topographical analysis of the human electroencephalogram for patterns in the development of motion sickness
| AD-A243656 | p 1328 N92-17120

MOVING TARGET INDICATORS
Low-noise oscillators for airborne radar applications
| AD-A242264 | p 1281 N92-17258
Establishing an evoked-potential vision-tracking system p 1221 N92-17993

MULLITES
Production of mullite fibers
| NASA-CASE-MFS-28431-1 | p 1257 N92-17870

MULTIBEAM ANTENNAS
Advanced Communication Technology Satellite (ACTS) multibeam antenna analysis and experiment
| NASA-TM-105420 | p 1279 N92-17047

MULTIPATH TRANSMISSION
Constant modulus algorithm techniques for the enhancement of signal quality
| AD-A242986 | p 1288 N92-17295
Multipath induced tracking errors at 95 and 140 GHz
| AD-A243111 | p 1283 N92-17571

MULTIPLE ACCESS
Multiple-access phased array antenna simulator for a digital beam forming system investigation
| NASA-TM-105422 | p 1279 N92-17062

MULTIPLEXING
Beam position monitor multiplexer controller upgrade at the LAMPF proton storage ring
| DE92-003859 | p 1363 N92-17590
Closed-loop motor control using high-speed fiber optics
| NASA-CASE-MSC-21806-1 | p 1368 N92-17863

MULTIPROCESSING (COMPUTERS)
Resource allocation in distributed memory multiprocessing
| AD-A243165 | p 1345 N92-17188
Performance modeling of the Ada rendezvous
| AD-A243392 | p 1339 N92-17211
Data management system advanced architectures p 1249 N92-17417

MULTISENSOR APPLICATIONS
Multisensor signal processing techniques (hybrid GPS/LORAN-C with RAIM)
| AD-A242323 | p 1281 N92-17244
A fully decentralized multi-sensor system for tracking and surveillance
| OUEL-1886/91 | p 1302 N92-17926

MULTISPECTRAL BAND SCANNERS
Multispectral software development for the Airborne Bathymetric Survey System
| AD-A243774 | p 1325 N92-17765

MULTISTATIC RADAR
Determination of bistatic radar clutter power from topographic data
| AD-A243697 | p 1280 N92-17095

MULTIVARIATE STATISTICAL ANALYSIS
New algorithms for broad-band and narrowband source localization and a separable 2-D IIR filter realization
| AD-A243457 | p 1291 N92-17654
A variational assimilation method for satellite and conventional data: A revised basic model 2B p 1322 N92-17977

MUON SPIN ROTATION
Comparative study of irreversibility effects in Nb foil and high temperature superconducting ceramics by muon spin rotation
| DE92-600475 | p 1294 N92-17953

MUONS
Muons in UA1; the 2nd level trigger and dimuon results
| ETN-92-90565 | p 1360 N92-17520

MUSCLES
Eccentric and concentric muscle performance following 7 days of simulated weightlessness
| NASA-TP-3182 | p 1330 N92-17645

MUSCULAR FUNCTION
Eccentric and concentric muscle performance following 7 days of simulated weightlessness
| NASA-TP-3182 | p 1330 N92-17645

MUSCULOSKELETAL SYSTEM
Techniques for determination of impact forces during walking and running in a zero-G environment
| NASA-TP-3159 | p 1328 N92-17022
Eccentric and concentric muscle performance following 7 days of simulated weightlessness
| NASA-TP-3182 | p 1330 N92-17645

MUTAGENS
Preliminary assessment of the relative toxicity of tetraglycine hydroperiodide, phase 1
| AD-A243334 | p 1330 N92-17712

MUTATIONS
Biophysical techniques for examining metabolic, proliferative, and genetic effects of microwave radiation
| AD-A241903 | p 1326 N92-17288

N

NAPHTHALENE
Nitration and nitrocompounds
| AD-A243380 | p 1259 N92-17210

NARROWBAND
New algorithms for broad-band and narrowband source localization and a separable 2-D IIR filter realization
| AD-A243457 | p 1291 N92-17654

NASA PROGRAMS
NASA total quality management 1989 accomplishments report
| NASA-TM-105467 | p 1308 N92-17005
NASA total quality management 1990 accomplishments report
| NASA-TM-105465 | p 1308 N92-17199
Space Station Freedom baseline operations concept p 1248 N92-17410
FY 1991 scientific and technical reports, articles, papers, and presentations
| NASA-TM-103567 | p 1384 N92-17586

NASA SPACE PROGRAMS
Technology development on evolutionary space station p 1243 N92-17106
Advanced studies program overview p 1244 N92-17109

NATIONAL AIRSPACE SYSTEM
Joint University Program for Air Transportation Research, 1990-1991
| NASA-CP-3131 | p 1219 N92-17984

NATURAL LANGUAGE (COMPUTERS)
Towards intelligent data retrieval in multimedia databases
| AD-A243323 | p 1383 N92-17402

NAVIER-STOKES EQUATION
Eddy breakdown and structure development
| AD-A241886 | p 1295 N92-17039
Use of Navier-Stokes analysis in section design
| AD-A242074 | p 1295 N92-17168
Comparison of two solution methods for the numerical calculation of hypersonic flows
| MBB-FE211-S-PUB-446 | p 1224 N92-17311
Computation of three-dimensional flows using two stream functions
| NASA-CR-187802 | p 1298 N92-17588
Consistency and integrability of Navier-Stokes and systems of equations for incompressible flow magnetohydrodynamics p 1298 N92-17699
Flow between two stationary disks and a rotating shroud
| AERO-REPT-9001 | p 1300 N92-17851
Mean wind speeds over hills and other topography
| ESDU-91043 | p 1321 N92-17853

NAVIGATION
An investigation of methods for updating ionospheric scintillation models using topside in-situ plasma density measurements
| AD-A243378 | p 1316 N92-17209
Application of multi-target tracking to sonar-based mobile robot navigation
| OUEL-1819/90 | p 1229 N92-17878
Joint University Program for Air Transportation Research, 1990-1991
| NASA-CP-3131 | p 1219 N92-17984

NAVIGATION AIDS
Cyclone: A laser scanner for mobile robot navigation
| AD-A243517 | p 1303 N92-17080
A system for fast navigation of autonomous vehicles
| AD-A243523 | p 1228 N92-17147
Application of multi-target tracking to sonar-based mobile robot navigation
| OUEL-1819/90 | p 1229 N92-17878
Systematic methods for knowledge acquisition and expert system development p 1222 N92-18001

NAVIGATION INSTRUMENTS
GPS interferometric attitude and heading determination: Initial flight test results p 1221 N92-17994
Systematic methods for knowledge acquisition and expert system development p 1222 N92-18001

NEAR FIELDS
Spherical near-field scanning: Experimental and theoretical studies
| AD-A243489 | p 1282 N92-17429

NEAR WAKES
Use of Navier-Stokes analysis in section design
| AD-A242074 | p 1295 N92-17168

NEARSHORE WATER
Source of cold water in Monterey Bay observed by AVHRR satellite imagery
| AD-A242843 | p 1323 N92-17051

NEEDLE BEARINGS
Analysis of cam roller followers
| ESDU-91026 | p 1307 N92-17852

NEEDLES
Sharps container
| NASA-CASE-MSC-21776-1 | p 1278 N92-17913

NEOPLASMS
Evaluation of the initiation/promotion potential of CTFE trimer acid
| AD-A243479 | p 1255 N92-17373

NERVOUS SYSTEM
Temporally-specific modification of myelinated axon excitability in vitro following a single ultrasound pulse
| AD-A242329 | p 1326 N92-17474
Computational and neural network models for the analysis of visual texture
| AD-A243717 | p 1327 N92-17504

NETWORK ANALYSIS
A general computational framework for distributed sensing and fault-tolerant sensor integration
| AD-A243256 | p 1300 N92-16983
Neural network classification of mental workload conditions by analysis of spontaneous electroencephalograms
| AD-A243369 | p 1331 N92-17115
Optimal configuration of digital communication network
| AD-A243041 | p 1282 N92-17277
Computational and neural network models for the analysis of visual texture
| AD-A243717 | p 1327 N92-17504
Permittivity probe modelling
| AD-A243236 | p 1260 N92-17572
Improving stochastic communication network performance: Reliability vs throughput
| AD-A243655 | p 1285 N92-17763
QTCM software documentation. Volume 2: User's manual
| AD-A242744 | p 1344 N92-17948
Management, control and performance of broadband integrated networks
| AD-A242750 | p 1381 N92-17952

NETWORK CONTROL
A study of channel-access schemes for integrated voice/data radio networks
| AD-A243584 | p 1286 N92-17931
Management, control and performance of broadband integrated networks
| AD-A242750 | p 1381 N92-17952

NETWORK SYNTHESIS
Results from a data acquisition system prototype project using a switch-based event builder
| DE92-004638 | p 1336 N92-17592

NEURAL NETS
Neural network modeling of nonlinear systems based on Volterra series extension of a linear model
| NASA-TM-104177 | p 1347 N92-16987
Feature extraction for pose estimation: A comparison between synthetic and real IR imagery
| AD-A243699 | p 1338 N92-17077
Neural network classification of mental workload conditions by analysis of spontaneous electroencephalograms
| AD-A243369 | p 1331 N92-17115
Analog optical neural nets: A noise sensitivity analysis
| AD-A242920 | p 1346 N92-17465
The cognitive, perceptual, and neural bases of skilled performance
| AD-A243052 | p 1332 N92-17554
Neutral network models of primate motor system
| AD-A243460 | p 1343 N92-17655

An investigation of the application of artificial neural networks to adaptive optics imaging systems
| AD-A243780 | p 1348 N92-17767
Computer modelling of two-input neural-net learning
p 1348 N92-17819
Algorithm and Pascal: A program for neural net learning p 1344 N92-17822
Neural-network dedicated processor for solving competitive assignment problems
| NASA-CASE-NPO-17781-1-CU | p 1337 N92-17884
Neural networks for aircraft system identification
p 1222 N92-17998
Intelligent failure-tolerant control p 1222 N92-18000

NEUROLOGY
Assessment of the behavioral and neurotoxic effects of hexachlorobenzene (HCB) in the developing rat
| AD-A243658 | p 1325 N92-17121
BrainMap: A database of functional neuroanatomy derived from human brain images
| AD-A243161 | p 1333 N92-17648
The 7th Annual Workshop on Computational Neuroscience
| AD-A243462 | p 1335 N92-17656

NEURONS
Neutral network models of primate motor system
| AD-A243460 | p 1343 N92-17655
The 7th Annual Workshop on Computational Neuroscience
| AD-A243462 | p 1335 N92-17656

NEUTRINO BEAMS
The determination of the number of light neutrino species
| ETN-92-90564 | p 1359 N92-17519

NEUTRINOS
Recent developments in neutrino physics
| DE92-003855 | p 1360 N92-17589
Medium-energy neutrino physics
| DE92-003790 | p 1362 N92-17666

NEUTRON FLUX DENSITY
Experimental findings on self-recovery and improvement of representative parameters of some semiconductor devices as irradiated in fast neutron flux
| DE92-611185 | p 1378 N92-17944

NEUTRON IRRADIATION
Fracture toughness evaluation for N Reactor pressure tubes of Zircaloy-2 using the electric-potential method
| DE92-003631 | p 1311 N92-17713

NEUTRON PHYSICS
Determination of diffusion parameters of thermal neutrons for non-moderator media by a pulsed method and a time independent method
| DE92-600624 | p 1362 N92-17954

NEUTRON SOURCES
Steady-state, high dose neutron generation and concentration apparatus and method for deuterium atoms
| AD-D015063 | p 1358 N92-17462
Evidence for MeV particle emission from Ti charged with low energy deuterium ions
| AD-A243718 | p 1359 N92-17505

NEUTRONS
Atom wave interferometer
| AD-A243482 | p 1357 N92-17374
Verification of an effective dose equivalent model for neutrons
| DE92-002738 | p 1358 N92-17453
Axino-induced baryogenesis
| NASA-CR-189858 | p 1361 N92-17646
Effect of thermal annealing on property changes of neutron-irradiated non-graphitized carbon materials and nuclear graphite
| DE92-704180 | p 1257 N92-17816
Structure and topology of silica aerogels
| DE92-004728 | p 1274 N92-17938

NICKEL
Silver-nickel composite cathodes for alkaline secondary batteries
| AD-D015121 | p 1293 N92-17871

NICKEL ALLOYS
Fatigue in single crystal nickel superalloys
| AD-A243453 | p 1265 N92-17653
Growth rate of dislocation loop in Fe-Ni-Cr alloy under Kr(+) ion and electron irradiation
| DE92-001908 | p 1265 N92-17703

NICKEL COATINGS
Metallography of aluminide coatings
| AD-A243000 | p 1263 N92-17264
Characterizing the sensitivity, selectivity, and reversibility of the metal-doped phthalocyanine thin-films used with the Interdigitated Gate Electrode Field-Effect Transistor (IGEFET) to detect organophosphorous compounds and nitrogen dioxide
| AD-A243635 | p 1376 N92-17746

NIGHT
Background Atmosphere Radiance Day (BARD) and Night (BARN)
| AD-A243153 | p 1316 N92-17239

NIGHT FLIGHTS (AIRCRAFT)
The development of military night aviation to 1919
| AD-A243350 | p 1219 N92-17731

NITRAMINE PROPELLANTS
Computational studies of energetic nitramines
| AD-A241870 | p 1356 N92-17038

NITRATE ESTERS
Energetic composites of cyclodextrin nitrate esters and nitrate ester plasticizers
| AD-D015068 | p 1275 N92-17399

NITRATES
Evaluation of solar flares and electron precipitation by nitrate distribution in Antarctica
| AD-A243026 | p 1389 N92-17235

NITRATION
Nitration and nitrocompounds
| AD-A243380 | p 1259 N92-17210

NITROGEN
Statistically-based decompression tables. 6: Repeat dives on oxyen/nitrogen mixes
| AD-A243667 | p 1328 N92-17124
Steady-state production and quenching of Br((2)P1/2)
| AD-A243754 | p 1362 N92-17663

NITROGEN DIOXIDE
Characterizing the sensitivity, selectivity, and reversibility of the metal-doped phthalocyanine thin-films used with the Interdigitated Gate Electrode Field-Effect Transistor (IGEFET) to detect organophosphorous compounds and nitrogen dioxide
| AD-A243635 | p 1376 N92-17746

NITROGEN HYDRIDES
Evaluation of a diffusion/trapping model for hydrogen ingress in high-strength alloys
| AD-A243461 | p 1263 N92-17327

NITROGEN IONS
Electronic and ionic transport in processable conducting polymers. Symmetry effects on the physical and electrically conducting, substituted poly(di-2-thienylphenylenes)
| AD-A242328 | p 1266 N92-16976

NITROGEN LASERS
A diffraction limited nitrogen laser for detector calibration in high energy physics
| ETN-92-90567 | p 1303 N92-17434

NITROGEN OXIDES
Nitration and nitrocompounds
| AD-A243380 | p 1259 N92-17210

NITROGEN POLYMERS
Electronic and ionic transport in processable conducting polymers. Symmetry effects on the physical and electrically conducting, substituted poly(di-2-thienylphenylenes)
| AD-A242328 | p 1266 N92-16976

NITROGEN 15
One nucleon transition densities for 1p shell nuclei
| DE92-600629 | p 1363 N92-17957

NOISE INTENSITY
The effect of impulse presentation order on hearing trauma in the chinchilla
| AD-A243174 | p 1326 N92-17269
The hazard of exposure to 2.075 kHz center frequency narrow band impulses
| AD-A242997 | p 1329 N92-17299

NOISE MEASUREMENT
Incipient fault detection using higher-order statistics
| AD-A243493 | p 1308 N92-17431

NOISE PREDICTION (AIRCRAFT)
The solution of a singular integral equation arising from a lifting surface theory for rotating blades
p 1224 N92-17303

NOISE REDUCTION
A comparative study of the noise performance of Alluminum Gallium Arsenide/Gallium Arsenide high electron mobility transistors with and without superconducting gate electrodes p 1288 N92-17317
Method and apparatus for reducing drag and noise associated with fluid flow in a conduit
| AD-D015067 | p 1297 N92-17398
Automatic recognition of speech in stressful environments
| AD-A242917 | p 1283 N92-17464

NOISE SPECTRA
Classification of complex sounds
| AD-A243498 | p 1355 N92-17381
Spectral error models applied to the geodetic boundary value problem
| ETN-92-90582 | p 1312 N92-17436

NOISE TEMPERATURE
A comparative study of the noise performance of Alluminum Gallium Arsenide/Gallium Arsenide high electron mobility transistors with and without superconducting gate electrodes p 1288 N92-17317

NOISE THRESHOLD
Noncoherent detection of coherent optical heterodyne signals corrupted by laser phase noise
| AD-A243103 | p 1364 N92-16981

NOISE TOLERANCE
Human response to helicopter noise: A test of A-weighting
| AD-A243719 | p 1355 N92-17506

NONAQUEOUS ELECTROLYTES
Application of the mean spherical approximation to describe the Gibbs solvation energies of monovalent monoatomic ions in non-aqueous solvents
| AD-A243200 | p 1259 N92-17371

NONDESTRUCTIVE TESTS
Laser based, non-intrusive measurement system for analysis of jet engine flows
| AD-A242398 | p 1234 N92-17011
Extracting the shape and roughness of specular lobe objects using four light photometric stereo
| AD-A243522 | p 1365 N92-17146
A method and apparatus for indicating disbonds in joint regions
| NASA-CASE-LAR-14626-1 | p 1309 N92-17859
Method for non-destructive estimation of waveguide directional coupler dimensions
| NASA-CASE-NPO-18454-1-CU | p 1293 N92-17865

NONLINEAR EQUATIONS
Periodic trim solutions with HP-version finite elements in time
| NASA-CR-189778 | p 1236 N92-17019

NONLINEAR FEEDBACK
A study of nonlinear reflection and optical switching in indium antimonide
| AD-A242835 | p 1365 N92-17249

NONLINEAR OPTICS
Waveguide four-wave mixing
| AD-A243555 | p 1286 N92-17017
New ferrocene complexes and polymers for nonlinear optical applications
| AD-A243640 | p 1272 N92-17749
Organometallic NLO polymers. Linear main-chain NLO polymers of ferrocene
| AD-A243641 | p 1272 N92-17750
Organometallic NLO polymers. Accordian main-chain NLO polymers of ferrocene
| AD-A243642 | p 1273 N92-17751
Organic NLO polymers. Linear and accordian main-chain NLO polymers prepared by a Knoevenagel polycondensation
| AD-A243644 | p 1273 N92-17753

NONLINEAR SYSTEMS
Neural network modeling of nonlinear systems based on Volterra series extension of a linear model
| NASA-TM-104177 | p 1347 N92-16987
Regularization and approximation of a class of evolution problems in applied mathematics
| AD-A242223 | p 1350 N92-17445
Preliminary development of a three-dimensional nonlinear approximation procedure for turbomachinery design optimization applications
| AD-A243155 | p 1235 N92-17644
New algorithms for broad-band and narrowband source localization and a separable 2-D IIR filter realization
| AD-A243457 | p 1291 N92-17654

NONLINEARITY
Identification techniques: Frequency domain methods
p 1231 N92-17158
Higher-order thickness expansions for cylindrical shells
| AD-A242017 | p 1310 N92-17230
Nonlinear spectroscopic studies of interfacial molecular ordering
| DE92-000864 | p 1360 N92-17530

NONUNIFORM MAGNETIC FIELDS
Alfven waves in inhomogeneous magnetic fields: An integro-differential equation formulation
| DE92-609544 | p 1371 N92-17806

NONUNIFORMITY
Large ideals and non-regular ultrafilters
| ETN-92-90587 | p 1351 N92-17525

NORMAL DENSITY FUNCTIONS
Significant digit computation of the ellipsoidal coverage function and its inverse
| AD-A242322 | p 1350 N92-17242
The calibration process of digital cameras
| ETN-92-90583 | p 1301 N92-17437
Example of statistical techniques applied to autoland touchdown dispersion (confidence intervals for normal and skew distributions)
| ESDU-91019 | p 1229 N92-17844

NORTHERN SKY
The development of military night aviation to 1919
| AD-A243350 | p 1219 N92-17731

NOSES (FOREBODIES)
Failure detection and fault management techniques for flush airdata sensing systems
| NASA-TM-4335 | p 1234 N92-17128
NOZZLE FLOW
Aircraft ground test and subscale model results of axial thrust loss caused by thrust vectoring using turning vanes
| NASA-TM-4341 | p 1230 N92-17071
The influence of cavitation in the breakup of liquid free jets
| MPIS-1/1991 | p 1297 N92-17343
NUCLEAR DEFORMATION
Relativistic nuclear many-body theory
| DE92-003258 | p 1362 N92-17789
NUCLEAR DEVICES
Steady-state, high dose neutron generation and concentration apparatus and method for deuterium atoms
| AD-D015063 | p 1358 N92-17462
NUCLEAR ELECTRIC POWER GENERATION
Energy production using fission fragment rockets
| DE92-002192 | p 1364 N92-17876
NUCLEAR FUEL ELEMENTS
Downflow heat transfer in a heated ribbed vertical annulus with a cosine power profile (results from test series ECS-2c)
| DE92-003259 | p 1298 N92-17626
NUCLEAR FUSION
Characterization of the thermalness of a fissile system with a 2-group diffusion theory parameter
| AD-A243065 | p 1360 N92-17555
NUCLEAR INTERACTIONS
Pion-nucleus cross sections
| DE92-600631 | p 1363 N92-17958
NUCLEAR MAGNETIC RESONANCE
A reexamination of F-19 NMR in selected solids, the conductor Ag2F and reference insulators for studies of YBa2Cu3O7-type superconductors
| AD-A243194 | p 1372 N92-17219
Y890NMR study of hyperfine interactions in (R(x)Y(1-x))Fe2
| DE91-641979 | p 1376 N92-17779
Structure and topology of silica aerogels
| DE92-004728 | p 1274 N92-17938
NUCLEAR MODELS
Importance of the neutron-proton interactions for the even Ra-Th nuclei
| DE92-600628 | p 1363 N92-17956
One nucleon transition densities for 1p shell nuclei
| DE92-600629 | p 1363 N92-17957
NUCLEAR POWER PLANTS
Energy production using fission fragment rockets
| DE92-002192 | p 1364 N92-17876
Software reliability models for critical applications
| DE92-004797 | p 1345 N92-17969
NUCLEAR POWER REACTORS
Fracture toughness evaluation for N Reactor pressure tubes of Zircaloy-2 using the electric-potential method
| DE92-003631 | p 1311 N92-17713
NUCLEAR PROPULSION
Energy production using fission fragment rockets
| DE92-002192 | p 1364 N92-17876
NUCLEAR REACTOR CONTROL
Software reliability models for critical applications
| DE92-004797 | p 1345 N92-17969
NUCLEAR REACTORS
Summary reports of activities under visiting research program
| DE91-522477 | p 1391 N92-17623
Downflow heat transfer in a heated ribbed vertical annulus with a cosine power profile (results from test series ECS-2c)
| DE92-003259 | p 1298 N92-17626
UCLA program in reactor studies: The ARIES tokamak reactor study
| DE92-003760 | p 1370 N92-17792
Energy production using fission fragment rockets
| DE92-002192 | p 1364 N92-17876
NUCLEATE BOILING
Nucleate pool boiling performance of small high flux and turbo-B tube bundles in R-114/oil mixtures
| AD-A241936 | p 1378 N92-17443
Heat transfer enhancement due to bubble pumping in FC-72 near the saturation temperature
| AD-A243558 | p 1292 N92-17724
Wall temperature patterns in nucleate boiling
| OUEL-1876/91 | p 1380 N92-17879
NUCLEON-NUCLEON INTERACTIONS
Relativistic nuclear many-body theory
| DE92-003258 | p 1362 N92-17789
Importance of the neutron-proton interactions for the even Ra-Th nuclei
| DE92-600628 | p 1363 N92-17956
NUCLEONS
One nucleon transition densities for 1p shell nuclei
| DE92-600629 | p 1363 N92-17957
NUMERICAL ANALYSIS
Complexity issues in numerical optimization
| AD-A241854 | p 1347 N92-17049
Large ideals and non-regular ultrafilters
| ETN-92-90587 | p 1351 N92-17525
NUMERICAL CONTROL
Performance of battery charge controllers: First year test report
| DE92-002924 | p 1289 N92-17468
Beam position monitor multiplexer controller upgrade at the LAMPF proton storage ring
| DE92-003859 | p 1363 N92-17590
A distributed design for monitoring, logging, and replaying device readings at LAMPF
| DE92-003860 | p 1240 N92-17591
Electrically-controlled polymeric gels as active materials in adaptive structures
| DE92-002947 | p 1272 N92-17710
Microprocessor controller in CAMAC standard for temperature regulation and stabilization
| DE92-611158 | p 1348 N92-17814
NUMERICAL DATA BASES
Making of functionally gradient materials data base
| NAL-TM-621 | p 1385 N92-17787
NUMERICAL INTEGRATION
Wave propagation in a randomly inhomogeneous medium: A study of the problem
| AD-A243741 | p 1284 N92-17691
NUMERICAL STABILITY
The instability of linear heterogeneous Lanchester equations
| AD-A243519 | p 1350 N92-17081

O

OBJECT-ORIENTED PROGRAMMING
Implementation of an object-oriented flight simulator D.C. electrical system on a hypercube architecture
| AD-A243700 | p 1238 N92-17097
An object-oriented database implementation of the Magic VLSI Layout Design System
| AD-A243743 | p 1384 N92-17482
A knowledge-based approach for configuring computer aided measuring systems
| ETN-92-90585 | p 1341 N92-17524
A proof theory for a sequential version of POOL
| CWI-CS-R9118 | p 1346 N92-17833
OBSERVATION
Surface observation climatic summaries for Boise Air Terminal, ID
| AD-A243012 | p 1319 N92-17257
Surface observation climatic summaries for Fairbanks IAP, Alaska
| AD-A243309 | p 1320 N92-17400
OBSTACLE AVOIDANCE
Cyclone: A laser scanner for mobile robot navigation
| AD-A243517 | p 1303 N92-17080
A system for fast navigation of autonomous vehicles
| AD-A243523 | p 1228 N92-17147
Application of multi-target tracking to sonar-based mobile robot navigation
| OUEL-1819/90 | p 1229 N92-17878
OCEAN BOTTOM
Bottom contour influence on ray tracing
| AD-A242411 | p 1323 N92-17078
The effects of sediment porosity on acoustic reflection and transmission at the seafloor
| AD-A241943 | p 1323 N92-17083
Acoustical and other physical properties of marine sediments
| AD-A243532 | p 1324 N92-17391
OCEAN CURRENTS
An investigation of cold overflow over the Iceland/Faeroes Ridge
| AD-A243084 | p 1324 N92-17169
Upper ocean dynamics during the LOTUS and Tropic Heat Experiments
| AD-A243730 | p 1324 N92-17583
Proceedings of the 2nd Gulf of Cadiz Expedition Workshop
| AD-A242749 | p 1325 N92-17951
OCEAN DYNAMICS
Upper ocean dynamics during the LOTUS and Tropic Heat Experiments
| AD-A243730 | p 1324 N92-17583
OCEAN MODELS
A user's manual for the Princeton Numerical Ocean Model
| AD-A243773 | p 1324 N92-17539
Ocean simulation model. Version 2: First order frontal simulation
| AD-A243775 | p 1325 N92-17766
OCEAN SURFACE
Sea surface environmental conditions in the Gulf of Alaska during April 1990 using SSM/I
| AD-A241909 | p 1323 N92-17041
Surface meteorological and near surface oceanographic atlas of the tropical Indian Ocean
| PB91-234286 | p 1319 N92-17138
An investigation of cold overflow over the Iceland/Faeroes Ridge
| AD-A243084 | p 1324 N92-17169
The physical optics description of microwave scattering by the sea surface
| AD-A243216 | p 1365 N92-17180
Simultaneous active and passive microwave measurements of the ocean surface
| AD-A242232 | p 1312 N92-17459
OCEAN TEMPERATURE
Source of cold water in Monterey Bay observed by AVHRR satellite imagery
| AD-A242843 | p 1323 N92-17051
Surface meteorological and near surface oceanographic atlas of the tropical Indian Ocean
| PB91-234286 | p 1319 N92-17138
OCEANOGRAPHIC PARAMETERS
Severe weather guide mediterranean ports. Part 35: Rota
| AD-A243539 | p 1319 N92-17338
Severe weather guide Mediterranean ports. Part 38: Alexandria
| AD-A243451 | p 1320 N92-17406
OCEANOGRAPHY
Development of real-time image and in situ data analysis at sea
| AD-A243682 | p 1242 N92-17075
The applied tomography experiment of 1990
| AD-A243525 | p 1354 N92-17086
Surface meteorological and near surface oceanographic atlas of the tropical Indian Ocean
| PB91-234286 | p 1319 N92-17138
A user's manual for the Princeton Numerical Ocean Model
| AD-A243773 | p 1324 N92-17539
OCEANS
Acoustic simulation for acoustics education
| AD-A243027 | p 1355 N92-17236
OILS
The wave numbers of supercritical surface tension driven Benard convection
| NASA-CR-189856 | p 1373 N92-17375
Nucleate pool boiling performance of small high flux and turbo-B tube bundles in R-114/oil mixtures
| AD-A241936 | p 1378 N92-17443
OLIGOMERS
Evaluation of the initiation/promotion potential of CTFE trimer acid
| AD-A243479 | p 1255 N92-17373
Development of processible electroactive oligomers and polymers
| AD-A243723 | p 1270 N92-17508
ON-LINE SYSTEMS
FEM-X user's guide
| AD-A242374 | p 1383 N92-17396
Adaptive on-line help for embedded instructional systems
| AD-A243675 | p 1343 N92-17716
Improvement of data processing system for gust wind tunnel data acquisition part: System conversion from off-line to on-line processing
| NAL-TM-611 | p 1238 N92-17756
Automated power management and control
p 1252 N92-17773
OPERATING SYSTEMS (COMPUTERS)
Comparison of AFITPAC versus NOS and a packet radio network design
| AD-A243766 | p 1283 N92-17516
The StarLite Project prototyping real-time software
| AD-A242032 | p 1342 N92-17636
OPERATING TEMPERATURE
Method of doping single crystal diamond for electronic devices
| AD-D015069 | p 1374 N92-17610
OPERATIONS RESEARCH
Machine scheduling and Lagrangian relaxation
| ETN-92-90569 | p 1353 N92-17839
OPERATOR PERFORMANCE
The multi-attribute task battery for human operator workload and strategic behavior research
| NASA-TM-104174 | p 1338 N92-17130
USI rapid prototyping tool evaluations survey
| AD-A243168 | p 1335 N92-17673
OPERATORS (MATHEMATICS)
A theory of inverse operators for multiple excitations
| AD-A243484 | p 1350 N92-17330
Study of features of binary images using algebra techniques
| AD-A242010 | p 1351 N92-17609

Inequalities among partial traces of Hermitian operators and partial sums of their Eigenvalues
| DE91-641495 | p 1351 N92-17622

OPTICAL BISTABILITY
Optical nonlinearity in coupled exciton-phonon systems near metal surfaces
| AD-A242362 | p 1357 N92-17423

OPTICAL COMMUNICATION
Th 3-5 modulation and switching devices for optical system applications
| AD-A243055 | p 1365 N92-17044
Optical protocols for advanced spacecraft networks p 1249 N92-17418
Closed-loop motor control using high-speed fiber optics
| NASA-CASE-MSC-21806-1 | p 1368 N92-17863

OPTICAL COMPUTERS
Optical associative processors and directed graphs
| AD-A242901 | p 1366 N92-17630

OPTICAL CORRELATORS
Real-time edge-enhanced optical correlator
| NASA-CASE-NPO-18379-1-CU | p 1367 N92-17675
Optical image segmentation using wavelet correlation
| AD-A243650 | p 1367 N92-17736

OPTICAL COUPLING
Optical nonlinearity in coupled exciton-phonon systems near metal surfaces
| AD-A242362 | p 1357 N92-17423

OPTICAL DATA PROCESSING
Th 3-5 modulation and switching devices for optical system applications
| AD-A243055 | p 1365 N92-17044

OPTICAL EQUIPMENT
An optical roughness sensor for the real time determination of spray formed preform quality
| AD-A243238 | p 1262 N92-17056
Toward the robust control of high bandwidth high precision flexible optical systems
| AD-A243471 | p 1366 N92-17536
Evaluation of environmentally safe cleaning agents for diamond turned optics
| DE92-002524 | p 1278 N92-17780

OPTICAL FIBERS
Plasma chemical vapor deposition of halide glasses
| AD-D015060 | p 1370 N92-17706
Wide field strip-imaging optical system
| NASA-CASE-NPO-18146-1-CU | p 1368 N92-17892

OPTICAL MATERIALS
Determination of the optical constants of thin Chemical-Vapor-Deposited diamond windows from 0.5 to 6.5 eV
| AD-A243094 | p 1268 N92-17170
Use of diamond as an optical material
| AD-A243097 | p 1268 N92-17172

OPTICAL MEASUREMENT
Sensing refractive turbulence profiles using wave front slope measurements from two reference sources
| AD-A243696 | p 1315 N92-17094
Measurement of electron beam emittance using optical transition radiation and development of a diffuse screen electron beam monitor
| AD-A241893 | p 1357 N92-17306

OPTICAL MEASURING INSTRUMENTS
Correlator optical wavefront sensor COWS
| DE92-003964 | p 1368 N92-17846

OPTICAL MEMORY (DATA STORAGE)
Optical content-addressable memories for data/knowledge base processing
| AD-A241866 | p 1382 N92-17037
Th 3-5 modulation and switching devices for optical system applications
| AD-A243055 | p 1365 N92-17044
Optical associative processors and directed graphs
| AD-A242901 | p 1366 N92-17630
Fractal image encoding
| AD-A243620 | p 1344 N92-17921

OPTICAL PROPERTIES
Anomalous hole burning in polymers with inhomogeneous broadening
| AD-A242397 | p 1266 N92-17010
Electronic interactions of directed photon beams with surfaces
| AD-A241878 | p 1356 N92-17026
Ceramics with superelectrical and supermechanical properties
| AD-A243062 | p 1267 N92-17029
Contributive research and development
| AD-A243331 | p 1391 N92-17079
Determination of the optical constants of thin Chemical-Vapor-Deposited diamond windows from 0.5 to 6.5 eV
| AD-A243094 | p 1268 N92-17170
Use of diamond as an optical material
| AD-A243097 | p 1268 N92-17172
A diffraction limited nitrogen laser for detector calibration in high energy physics
| ETN-92-90567 | p 1303 N92-17434
Development of processible electroactive oligomers and polymers
| AD-A243723 | p 1270 N92-17508
An interface enhanced spectroscopic ellipsometry technique: Application to Si-SiO2
| AD-A242867 | p 1260 N92-17613
Optical properties of thermally intermixed quantum wells and superlattices
| AD-A243546 | p 1375 N92-17618
Optical modification of a single impurity molecule in a solid
| AD-A243750 | p 1361 N92-17660
Evaluation of environmentally safe cleaning agents for diamond turned optics
| DE92-002524 | p 1278 N92-17780

OPTICAL PUMPING
X ray laser
| DE91-011705 | p 1304 N92-17649

OPTICAL REFLECTION
Groundscreen characterization
| AD-A243164 | p 1311 N92-17208
A tunable solid state laser with high wavelength selectivity over a preselected wavelength range
| AD-D015055 | p 1304 N92-17627

OPTICAL SCANNERS
Cyclone: A laser scanner for mobile robot navigation
| AD-A243517 | p 1303 N92-17080

OPTICAL SWITCHING
Innovative switching technology
| DE92-003068 | p 1292 N92-17708

OPTICAL THICKNESS
Water vapor influence on satellite-measured aerosol characteristics
| AD-A241918 | p 1315 N92-17008

OPTICAL TRACKING
Integrated system for missile detection and discrimination
| DE91-018874 | p 1283 N92-17529
Establishing an evoked-potential vision-tracking system p 1221 N92-17993

OPTICAL WAVEGUIDES
Waveguide four-wave mixing
| AD-A243555 | p 1286 N92-17017

OPTIMAL CONTROL
Optimal aircraft performance during microburst encounter p 1222 N92-17999

OPTIMIZATION
The real-time cost of timing uncertainty: Consensus and failure detection
| AD-A243176 | p 1345 N92-16997
Performance measures for adaptive decisioning systems
| AD-A243183 | p 1352 N92-16998
Experiences at Langley Research Center in the application of optimization techniques to helicopter airframes for vibration reduction
| NASA-TM-104193 | p 1309 N92-17033
Complexity issues in numerical optimization
| AD-A241854 | p 1347 N92-17049
A stochastic approach to the weighted-region problem: 1. The design of the path annealing algorithm
| AD-A243324 | p 1340 N92-17403
Optimization in solar heating/photovoltaic systems
| AD-A242363 | p 1313 N92-17424
Global optimization of digital circuits
| AD-A243740 | p 1289 N92-17480
Preliminary design study of a central solar heating plant with seasonal storage at the University of Massachusetts, Amherst
| DE92-000762 | p 1313 N92-17577
Preliminary development of a three-dimensional nonlinear approximation procedure for turbomachinery design optimization applications
| AD-A243155 | p 1235 N92-17644
The micro-c rule is not optimal in the 2nd node of the tandem queue; 2 counterexamples
| TW-91-05 | p 1349 N92-17838
Machine scheduling and Lagrangian relaxation
| ETN-92-90569 | p 1353 N92-17839
Practical error bounds for a class of quadratic programming problems
| AD-A243249 | p 1345 N92-17960

ORBIT CALCULATION
Systematic computation algorithm to obtain osculating orbit elements from position and velocity vectors
| NAL-TM-614 | p 1239 N92-17854

ORBIT TRANSFER VEHICLES
Space Station Freedom/lunar transfer vehicle propellant operation hazard analysis p 1249 N92-17416

ORBITAL ASSEMBLY
Mars aerobrake assembly demonstration p 1247 N92-17362
Computer system evolution requirements for autonomous checkout of exploration vehicles p 1250 N92-17422

ORBITAL ELEMENTS
Preliminary design of a model to assess the effect of Space Surveillance Network (SSN) sensor upgrades on orbit prediction accuracies relative to the US Anti-Satellite (ASAT) mission
| AD-A243736 | p 1353 N92-17479
Analysis of orbital elements and atmospheric activity to ascertain possible presence of an ion propulsion capability aboard Salyut 7/Cosmos 1686
| AD-A243654 | p 1251 N92-17762
Systematic computation algorithm to obtain osculating orbit elements from position and velocity vectors
| NAL-TM-614 | p 1239 N92-17854

ORBITAL MANEUVERS
An alternative concept for aeroassisted orbit transfers
| AD-A243409 | p 1239 N92-17325
Comparison of station-keeping algorithms for an interior libration point orbit in the Sun-Earth + Moon elliptic restricted three-body problem
| AD-A241896 | p 1388 N92-17595

ORBITAL MECHANICS
Systematic computation algorithm to obtain osculating orbit elements from position and velocity vectors
| NAL-TM-614 | p 1239 N92-17854

ORBITAL POSITION ESTIMATION
Systematic computation algorithm to obtain osculating orbit elements from position and velocity vectors
| NAL-TM-614 | p 1239 N92-17854

ORBITAL VELOCITY
Systematic computation algorithm to obtain osculating orbit elements from position and velocity vectors
| NAL-TM-614 | p 1239 N92-17854

ORDER-DISORDER TRANSFORMATIONS
A powder x ray diffraction study of two aluminum-lithium based alloys
| AD-A243186 | p 1262 N92-17000
Enhanced backscattering from rough surfaces
| AD-A243437 | p 1366 N92-17486

ORGANIC COMPOUNDS
Photorefractivity in doped nonlinear organic polymers
| AD-A243751 | p 1271 N92-17661

ORGANIC MATERIALS
Role of donor-acceptor interactions in the sorption of TNT and other nitroaromatics from solution
| AD-A243235 | p 1254 N92-17055
X ray damage to CF3CO2-Terminated organic monolayers on Si/Au supports is due primarily to x ray induced electrons
| AD-A243446 | p 1289 N92-17490

ORGANIC NITRATES
Energetic composites of cyclodextrin nitrate esters and nitrate ester plasticizers
| AD-D015068 | p 1275 N92-17399

ORGANIC PHOSPHORUS COMPOUNDS
Characterizing the sensitivity, selectivity, and reversibility of the metal-doped phthalocyanine thin-films used with the Interdigitated Gate Electrode Field-Effect Transistor (IGEFET) to detect organophosphorous compounds and nitrogen dioxide
| AD-A243635 | p 1376 N92-17746

ORGANOMETALLIC POLYMERS
Organometallic NLO polymers. Linear main-chain NLO polymers of ferrocene
| AD-A243641 | p 1272 N92-17750
Organometallic NLO polymers. Accordian main-chain NLO polymers of ferrocene
| AD-A243642 | p 1273 N92-17751

OROGRAPHY
Turbulent and gravity wave transport in the free atmosphere p 1315 N92-17063

OSCILLATING FLOW
Engineering model of unsteady flow in a cavity
| AD-A243636 | p 1299 N92-17747

OSCILLATION DAMPERS
A wing rock model for the F-14A aircraft
| AD-A243109 | p 1233 N92-17300

OSCILLATIONS
An experimental investigation of leading edge vortical flow about a delta wing during wing rock
| AD-A243363 | p 1223 N92-17114
Experimental study of amplitude-phase-frequency characteristics of flow when following over a vibrating plate
| DE92-610935 | p 1299 N92-17810

OSCILLATORS
Low-noise oscillators for airborne radar applications
| AD-A242264 | p 1281 N92-17258
Design and evaluation of a Josephson array oscillator
| AD-A243167 | p 1291 N92-17672

OUTLET FLOW
Hydrogen fueled subsonic-ram-combustor model tests for an air-turbo-ram engine
| NAL-TR-1064T | p 1236 N92-17855

OVARIES
Biophysical techniques for examining metabolic, proliferative, and genetic effects of microwave radiation
| AD-A241903 | p 1326 N92-17288
OXIDATION
An oxygen tracer study of InP oxidation
| AD-A242832 | p 1259 N92-17246
An in-situ spectroscopic ellipsometry study of the electron cyclotron resonance plasma oxidation of silicon and interfacial
| AD-A242833 | p 1259 N92-17247
A kinetics study of the electron cyclotron resonance plasma oxidation of silicon
| AD-A242868 | p 1290 N92-17596
Substituted 1,1,1-triaryl-2,2,2-trifluoroethanes and processes for their synthesis
| NASA-CASE-LEW-14345-6 | p 1255 N92-17882
OXIDATION RESISTANCE
Polyimides containing amide and perfluoroisopropyl connecting groups
| NASA-CASE-LAR-14608-1 | p 1271 N92-17676
OXIDATION-REDUCTION REACTIONS
Electrochemically initiated chain polymerization of pyrrole in aqueous media
| AD-A242259 | p 1269 N92-17461
Separation of neutral-to-polaron and polaron-to-bipolaron redox events in alkoxy substituted di-2-thienylphenylene polymers
| AD-A242423 | p 1271 N92-17679
OXIDE FILMS
An oxygen tracer study of InP oxidation
| AD-A242832 | p 1259 N92-17246
OXIDES
Examining Si3N4 base materials with various rare earth additions
| AD-A243668 | p 1372 N92-17082
Evaluation of a diffusion/trapping model for hydrogen ingress in high-strength alloys
| AD-A243461 | p 1263 N92-17327
OXIDIZERS
A theoretical study of the combustion of magnesium/teflon/viton pyrotechnic compositions
| AD-A243244 | p 1275 N92-17058
OXYGEN
Statistically-based decompression tables. 6: Repeat dives on oxyen/nitrogen mixes
| AD-A243667 | p 1328 N92-17124
Effectiveness of an onboard water spray system during an oxygen enriched cabin fire
| DOT/FAA/CT-TN91/51 | p 1226 N92-17149
Catalysts for ultrahigh current density oxygen cathodes for space fuel cell applications
| NASA-CR-189787 | p 1253 N92-17365
Steady-state production and quenching of Br((2)P1/2)
| AD-A243754 | p 1362 N92-17663
Reaction kinetics and transport properties of the CaO-SO2-O2 system in absence of intra-particle diffusion
| DE91-002086 | p 1261 N92-17788
OXYGEN ATOMS
Atomic oxygen flux and fluence calculation for Long Duration Exposure Facility (LDEF)
| NASA-CR-187418 | p 1245 N92-17215
Collisional dynamics of the B3Pi(O +) state of bromine of monofluoride
| AD-A241857 | p 1356 N92-17305
Molecular composites from high temperature polyquinolines
| AD-A243634 | p 1272 N92-17745
OXYGEN CONSUMPTION
Influence of knee joint extension on submaximal oxygen consumption and anaerobic power in cyclists
| AD-A243467 | p 1329 N92-17194
OXYGEN ISOTOPES
An oxygen tracer study of InP oxidation
| AD-A242832 | p 1259 N92-17246
OXYGEN PLASMA
An in-situ spectroscopic ellipsometry study of the electron cyclotron resonance plasma oxidation of silicon and interfacial
| AD-A242833 | p 1259 N92-17247
OXYGEN PRODUCTION
Collisional dynamics of the B3Pi(O +) state of bromine of monofluoride
| AD-A241857 | p 1356 N92-17305
OXYGEN SUPPLY EQUIPMENT
EMU evolution p 1246 N92-17354
Magnetohydrodynamic projects at the CDIF
| DE92-002636 | p 1370 N92-17664
OZONE
Mass transfer in gas fluidized beds: Scaling, modeling, and particle size influence
| ETN-92-90581 | p 1298 N92-17522

P

PACKET SWITCHING
Delay analysis for multidimensional queueing process in CSMA/CD local area networks
| AD-A242364 | p 1346 N92-17425
PACKET TRANSMISSION
Comparison of AFITPAC versus NOS and a packet radio network design
| AD-A243766 | p 1283 N92-17516
PACKING DENSITY
Designing ordered molecular arrays in two and three dimensions
| AD-A243447 | p 1359 N92-17491
PALLADIUM
Concentration of isotopic hydrogen by temperature gradient effect in soluble metal
| AD-D015062 | p 1260 N92-17628
PANEL METHOD (FLUID DYNAMICS)
Use of Navier-Stokes analysis in section design
| AD-A242074 | p 1295 N92-17168
PANELS
Rapid repair of integrally stiffened carbon fibre composite structures by bolted aluminium elements
| MBB-FE202-S-PUB-0453-A | p 1256 N92-17310
Real-time edge-enhanced optical correlator
| NASA-CASE-NPO-18379-1-CU | p 1367 N92-17675
PARABOLIC DIFFERENTIAL EQUATIONS
Wave propagation in a randomly inhomogeneous medium: A study of the problem
| AD-A243741 | p 1284 N92-17691
PARABOLIC REFLECTORS
Preliminary design study of a central solar heating plant with seasonal storage at the University of Massachusetts, Amherst
| DE92-000762 | p 1313 N92-17577
PARACHUTES
Trajectory analysis of the G-11 family of clustered parachutes to determine minimum altitude
| AD-A243375 | p 1225 N92-17404
PARALLEL COMPUTERS
Implementation of an object-oriented flight simulator D.C. electrical system on a hypercube architecture
| AD-A243700 | p 1238 N92-17097
A connectionist simulation of attention and vector comparison: The need for serial processing in parallel hardware
| AD-A242225 | p 1348 N92-17457
Improved task scheduling for parallel simulations
| AD-A243721 | p 1346 N92-17507
Parallel radiosity techniques for mesh-connected SIMD computers
| AD-A242049 | p 1346 N92-17638
Scan directed load balancing for highly-parallel mesh-connected computers
| AD-A242045 | p 1346 N92-17670
PARALLEL PROCESSING (COMPUTERS)
FY92 mathematical research project proposal briefing
| AD-A243163 | p 1350 N92-17207
Parallel processing applied to computational electromagnetics
| AD-A242372 | p 1345 N92-17395
Analog optical neural nets: A noise sensitivity analysis
| AD-A242920 | p 1346 N92-17465
Parallel implementation of VHDL simulations on the Intel iPSC/2 hypercube
| AD-A243760 | p 1342 N92-17603
Use of the algebraic coding theory in nuclear electronics
| DE92-611125 | p 1351 N92-17813
PARALLEL PROGRAMMING
Parallelizing serial code for a distributed processing environment with an application to high frequency electromagnetic scattering
| AD-A243755 | p 1284 N92-17721
A proof theory for a sequential version of POOL
| CWI-CS-R9118 | p 1346 N92-17833
PARAMETER IDENTIFICATION
Flight test data quality evaluation
p 1230 N92-17156
An aerocapture attitude control systems incorporating robustness and vehicle parameter identification
| AD-A243360 | p 1245 N92-17302
PARSING ALGORITHMS
Global optimization of digital circuits
| AD-A243740 | p 1289 N92-17480
CMS reverse engineering and encore/model integration
| AD-A243438 | p 1341 N92-17487
PARTIAL DIFFERENTIAL EQUATIONS
Numerical grid generation using a variational method
| MBB-FE211-S-PUB-447 | p 1297 N92-17312
Regularization and approximation of a class of evolution problems in applied mathematics
| AD-A242223 | p 1350 N92-17445
Consistency and integrability of Navier-Stokes and systems of equations for incompressible flow magnetohydrodynamics p 1298 N92-17699
PARTIAL PRESSURE
A proposed improved method of radiosonde humidity sensing
| AD-A242954 | p 1319 N92-17233
PARTICLE ACCELERATOR TARGETS
PILAC: A Pion Linac facility for 1-GeV pion physics at LAMPF
| DE92-003789 | p 1364 N92-17794
PARTICLE COLLISIONS
What experiments say about possibility of the new particle existence with mass less than the kaon mass
| DE91-634551 | p 1357 N92-17408
The ZEUS second level calorimeter trigger: Physics simulation, design and implementation
| ETN-92-90568 | p 1358 N92-17435
One-loop calculations with massive particles
| ETN-92-90563 | p 1359 N92-17518
Muons in UA1; the 2nd level trigger and dimuon results
| ETN-92-90565 | p 1360 N92-17520
High energy physics program at Texas A and M University
| DE92-004426 | p 1363 N92-17738
PARTICLE DIFFUSION
Determination of diffusion parameters of thermal neutrons for non-moderator media by a pulsed method and a time independent method
| DE92-600624 | p 1362 N92-17954
PARTICLE EMISSION
Evidence for MeV particle emission from Ti charged with low energy deuterium ions
| AD-A243718 | p 1359 N92-17505
PARTICLE ENERGY
Evidence for MeV particle emission from Ti charged with low energy deuterium ions
| AD-A243718 | p 1359 N92-17505
Investigation of heated ultracold neutrons on copper surface
| DE92-600625 | p 1363 N92-17955
One nucleon transition densities for 1p shell nuclei
| DE92-600629 | p 1363 N92-17957
PARTICLE INTERACTIONS
Equation of state and conductivity of hot, dense matter
| AD-A243359 | p 1369 N92-17301
What experiments say about possibility of the new particle existence with mass less than the kaon mass
| DE91-634551 | p 1357 N92-17408
Recent developments in neutrino physics
| DE92-003855 | p 1360 N92-17589
Medium-energy neutrino physics
| DE92-003790 | p 1362 N92-17666
Proton-proton and proton-antiproton elastic scattering at high energies: Theory, phenomenology, and experiment
| DE92-004414 | p 1364 N92-17964
PARTICLE MASS
What experiments say about possibility of the new particle existence with mass less than the kaon mass
| DE91-634551 | p 1357 N92-17408
PARTICLE MOTION
On the nonadiabatic theory of charged particles motion in the magnetic dipole field
| DE92-610951 | p 1354 N92-17811
PARTICLE PRODUCTION
What experiments say about possibility of the new particle existence with mass less than the kaon mass
| DE91-634551 | p 1357 N92-17408
Axino-induced baryogenesis
| NASA-CR-189858 | p 1361 N92-17646
Fluctuation driven electroweak phase transition
| NASA-CR-189859 | p 1361 N92-17647
PARTICLE SIZE DISTRIBUTION
A powder x ray diffraction study of two aluminum-lithium based alloys
| AD-A243186 | p 1262 N92-17000
Water vapor influence on satellite-measured aerosol characteristics
| AD-A241918 | p 1315 N92-17008
Mass transfer in gas fluidized beds: Scaling, modeling, and particle size influence
| ETN-92-90581 | p 1298 N92-17522
PARTICLE THEORY
Gauge-covariant Wess-Zumino actions for super p-branes in superspace
| DE91-641524 | p 1353 N92-17318
PARTICLE TRAJECTORIES
Recording of three dimensional trajectories and velocity fields by automatic image processing
| MPIS-101/1991 | p 1301 N92-17345
Lie-isotopic generalization of the Poincare symmetry: Classical formulation
| DE91-642825 | p 1379 N92-17531

A study of gamma ray generation from channeled electrons and positions
| AD-A241993 | p 1361 N92-17608

PARTICULATE REINFORCED COMPOSITES
Novel ceramic matrix composites for deep submergence pressure vessel applications
| AD-A242740 | p 1274 N92-17947

PATENTS
Valuable patents for US businesses: A catalog of DTRC patents available for licensing by the private sector
| AD-A242071 | p 1385 N92-17141
Bibliography of technical publications, papers, and list of patents, October 1988 - September 1989
| AD-A242839 | p 1383 N92-17274

PATTERN RECOGNITION
Feature extraction for pose estimation: A comparison between synthetic and real IR imagery
| AD-A243699 | p 1338 N92-17077
Face recognition with the Karhunen-Loeve transform
| AD-A243688 | p 1280 N92-17090
Pattern Theory: An engineering paradigm for algorithm design
| AD-A243214 | p 1339 N92-17179
A connectionist simulation of attention and vector comparison: The need for serial processing in parallel hardware
| AD-A242225 | p 1348 N92-17457
Optical associative processors and directed graphs
| AD-A242901 | p 1366 N92-17630

PAVEMENTS
Alternate/modified binders for asphalt airfield pavements
| AD-A242829 | p 1238 N92-17260

PAYLOAD CONTROL
Collision avoidance sensor skin p 1247 N92-17361

PAYLOADS
Space Station Freedom Evolution Symposium
p 1243 N92-17105

PEEK
Experimental investigation of interlaminar fracture toughness of carbon fiber/thermoplastic and carbon fiber/thermosetting composites by DCB specimens
| NAL-TR-1096 | p 1257 N92-17869

PENETRANTS
Thin films under chemical stress
| DE92-004684 | p 1377 N92-17857

PENTOSE
The shapes and cavities of four cholic acid host systems
| AD-A243483 | p 1255 N92-17329

PEPTIDES
Characterization of the P. brevis polyether neurotoxin binding component in excitable membranes
| AD-A242877 | p 1327 N92-17564

PERCEPTION
Mechanisms of temporal pattern discrimination by human observers
| AD-A243051 | p 1332 N92-17336

PERCOLATION
Fluctuation driven electroweak phase transition
| NASA-CR-189859 | p 1361 N92-17647

PERFLUORO COMPOUNDS
Polyimides containing amide and perfluoroisopropyl connecting groups
| NASA-CASE-LAR-14608-1 | p 1271 N92-17676

PERFORMANCE PREDICTION
Discussion for possibility of some aerodynamic ground effect craft
| NAL-TM-619 | p 1278 N92-17757

PERFORMANCE TESTS
User evaluation of laser ballistic sun, wind and dust goggle lenses (dye technology)
| AD-A243245 | p 1334 N92-17143
Performance of battery charge controllers: First year test report
| DE92-002924 | p 1289 N92-17468
Versatile Data Acquisition System Model II user's manual
| DE92-003311 | p 1384 N92-17470
Evaluation of squib performance variables
| DE92-002034 | p 1275 N92-17533
Test method for the evaluation of the water treeing behavior of cross-linked polyethylene medium voltage cables
| ETN-92-90588 | p 1270 N92-17541
Qualification test report. Fuel pump test stand 3C3965G05
| AD-A242929 | p 1235 N92-17552
Flight evaluation of curved MLS precision approaches in a twin otter aircraft, phase 2
| AD-A243025 | p 1229 N92-17568
Full surface testing of grazing incidence mirrors
| AD-A243734 | p 1367 N92-17690
A Walsh-domain adaptive filter
| AD-A243701 | p 1292 N92-17718

PERIPHERAL VISION
Dual color and shape coding in the visual periphery: A study of Joint Tactical Information Distribution System (JTIDS) symbology
| AD-A243253 | p 1333 N92-16982

PERMANENT MAGNETS
Analytical determination of arrest and starting torque of a bipolar DC motor with permanent magnets
| ETN-92-90586 | p 1290 N92-17540

PERMEABILITY
Gas transport in polybutadiene treated with aqueous bromine
| AD-A241871 | p 1295 N92-17025
Mechanisms of gas permeation through polymer membranes
| DE92-004423 | p 1274 N92-17942

PERMITTIVITY
A discontinuity study in shielded coplanar line
| AD-A242976 | p 1288 N92-17290
Application of the mean spherical approximation to describe the Gibbs solvation energies of monovalent monoatomic ions in non-aqueous solvents
| AD-A243200 | p 1259 N92-17371
Permittivity probe modelling
| AD-A243236 | p 1260 N92-17572
Suspended substrate resonator design
| AD-A243250 | p 1290 N92-17573

PERSONAL COMPUTERS
Map maker
| AD-A242980 | p 1312 N92-17292
Facing page test for the astronaut science advisor presentation p 1248 N92-17411
Advanced Crew Personal Support Computer (CPSC) task p 1249 N92-17419
Versatile Data Acquisition System Model II user's manual
| DE92-003311 | p 1384 N92-17470
Modeling convergence zone gain on MS-DOS based personal computers
| AD-A243252 | p 1341 N92-17558
Microprocessor controller in CAMAC standard for temperature regulation and stabilization
| DE92-611158 | p 1348 N92-17814

PERSONNEL
Information management 70XX civilian equivalent
| AD-A242875 | p 1381 N92-17013
Alleviation of thermal strain in engineering space personnel aboard CF ships with the exotemp personal cooling system
| AD-A242889 | p 1330 N92-17599
The effect of shower/bath frequency on the health and operational effectiveness of soldiers in a field setting: Recommendation of showering frequencies for reducing performance-degrading nonsystemic microbial skin infections
| AD-A242923 | p 1330 N92-17714

PERSONNEL MANAGEMENT
NASA total quality management 1989 accomplishments report
| NASA-TM-105467 | p 1308 N92-17005

PERTURBATION
Eddy breakdown and structure development
| AD-A241886 | p 1295 N92-17039

PERU
Local area network strategies and guidelines for a Peruvian Air Force Computer Center
| AD-A242841 | p 1345 N92-17135

PETN
Detection of explosives material on single microparticles
| DE92-004408 | p 1276 N92-17963

PH FACTOR
Studies of the adsorption of tetrasulfonated phthalocyanines on graphite substrate
| AD-A243443 | p 1260 N92-17489
Direct speciation of metal and metalloid ions by optical spectroscopies
| DE92-003868 | p 1261 N92-17727

PHARMACOLOGY
A topographical analysis of the human electroencephalogram for patterns in the development of motion sickness
| AD-A243656 | p 1328 N92-17120

PHASE DIAGRAMS
The effect of monomer structures and compressibility on the properties of multicomponent polymer blends and solutions
| AD-A242863 | p 1273 N92-17777

PHASE MODULATION
A hybrid modulation for the dissemination of weather data to aircraft p 1220 N92-17991

PHASE SHIFT CIRCUITS
A study of ignition and simulation circuits for arcjet thrusters, part 1
| NASA-CR-189097 | p 1253 N92-17510

PHASE SHIFT KEYING
Investigation of coding techniques for memory and delay efficient interleaving in slow Rayleigh fading
| AD-A243154 | p 1280 N92-17187

PHASE TRANSFORMATIONS
Ceramics with superelectrical and supermechanical properties
| AD-A243062 | p 1267 N92-17029
Phase transitions in narrow molecular mass samples of side-chain liquid crystalline polymers: Molecular mass dependence
| AD-A242354 | p 1269 N92-17448
Fluctuation driven electroweak phase transition
| NASA-CR-189859 | p 1361 N92-17647
Late time cosmological phase transitions 1: Particle physics models and cosmic evolution
| NASA-CR-189857 | p 1388 N92-17696
Temperature dependent anomalous statistics
| DE92-609665 | p 1379 N92-17807
Modelling of some equilibrium thermodynamic properties of polymer systems
| ETN-92-90570 | p 1273 N92-17840
Comments on a novel approach to the role of chirality in the origin of life
| DE92-609034 | p 1327 N92-17970

PHASE VELOCITY
On the generation of large-amplitude plasma wakefields with low phase velocities by an intense short laser pulse
| DE92-609543 | p 1371 N92-17805

PHASE-SPACE INTEGRAL
One-loop calculations with massive particles
| ETN-92-90563 | p 1359 N92-17518

PHASED ARRAYS
Multiple-access phased array antenna simulator for a digital beam forming system investigation
| NASA-TM-105422 | p 1279 N92-17062

PHENYLS
Single molecule spectral diffusion in a solid detected via fluorescence spectroscopy
| AD-A243748 | p 1356 N92-17197

PHONEMES
New algorithms for broad-band and narrowband source localization and a separable 2-D IIR filter realization
| AD-A243457 | p 1291 N92-17654

PHONETICS
Mechanisms mediating the perception of complex acoustic patterns
| AD-A243715 | p 1355 N92-17502

PHONONS
Evidence for strong electron-phonon coupling in thermal conductivity of YBa2Cu3O(7-delta)
| AD-A243192 | p 1372 N92-17218
Optical nonlinearity in coupled exciton-phonon systems near metal surfaces
| AD-A242362 | p 1357 N92-17423

PHOSPHAZENE
Phosphazene polymer containing composites and method for making phosphazene polymer containing composites
| DE92-003826 | p 1274 N92-17935

PHOTICS
Establishing an evoked-potential vision-tracking system p 1221 N92-17993

PHOTOCHEMICAL REACTIONS
Dynamics and stabilization of materials possessing high energy content
| AD-A243030 | p 1258 N92-16977
Surface chemistry at the semiconductor/electrolyte interface
| DE91-018511 | p 1374 N92-17532

PHOTOCONDUCTIVITY
Photorefractivity in doped nonlinear organic polymers
| AD-A243751 | p 1271 N92-17661

PHOTODIODES
Improved 320x244-element PtSi Schottky-barrier IR-CCD image sensor
| AD-A242026 | p 1301 N92-17140
Receiver performance of laser ranging measurements between the Lunar Observer and a subsatellite for lunar gravity studies
| NASA-CR-189860 | p 1303 N92-17152

PHOTOELECTRIC EFFECT
The Los Alamos FEL photoinjector drive laser
| DE92-003791 | p 1305 N92-17795

PHOTOELECTROCHEMISTRY
Surface chemistry at the semiconductor/electrolyte interface
| DE91-018511 | p 1374 N92-17532

PHOTOELECTRON SPECTROSCOPY
Au and Al Schottky barrier formation on GaAs (100) surfaces prepared by thermal desorption of a protective arsenic coating
| DE92-002456 | p 1376 N92-17781

PHOTOGRAPHIC FILM
Transmission of thin light beams through turbulent mixing layers
| AD-A243470 | p 1367 N92-17658
PHOTOLITHOGRAPHY
X ray lithography in Japan
| AD-A243660 | p 1286 N92-17087
Molecular self-assembly and nanochemistry: A chemical strategy for the synthesis of nanostructures
| AD-A243530 | p 1361 N92-17616
PHOTOLUMINESCENCE
Optical properties of thermally intermixed quantum wells and superlattices
| AD-A243546 | p 1375 N92-17618
Luminescence and electroluminescence properties of Nd, Tm, Yb doped GaAs II-VI compounds
| AD-A242039 | p 1375 N92-17667
PHOTOLYSIS
Artificial photosynthesis: Progress toward molecular systems for photoconversion
| DE92-003370 | p 1326 N92-17471
PHOTOMETERS
Hubble Space Telescope: High speed photometer instrument handbook. Version 2.0
| NASA-CR-189750 | p 1386 N92-17497
PHOTOMETRY
Extracting the shape and roughness of specular lobe objects using four light photometric stereo
| AD-A243522 | p 1365 N92-17146
PHOTOMULTIPLIER TUBES
Hubble Space Telescope: Fine guidance sensors instrument handbook. Version 2.1
| NASA-CR-189745 | p 1386 N92-17020
PHOTON BEAMS
Electronic interactions of directed photon beams with surfaces
| AD-A241878 | p 1356 N92-17026
PHOTONS
Stellar spectral line synthesis from an individual photon-following simulation
| AD-A242970 | p 1388 N92-17253
A performance model of Thermal Imaging System (TISs) which includes the human observer's response to state of the art displays
| AD-A242838 | p 1301 N92-17273
Calculations of electron and photon transport between 1 MeV and 1 eV
| AD-A243725 | p 1359 N92-17514
Study of turbulence by photon correlation spectroscopy
| AD-A243726 | p 1298 N92-17688
Collaborative research on experimental astrophysics
| DE92-003970 | p 1388 N92-17832
Method and apparatus for lasing
| AD-D015154 | p 1305 N92-17923
PHOTOSYNTHESIS
Artificial photosynthesis: Progress toward molecular systems for photoconversion
| DE92-003370 | p 1326 N92-17471
PHOTOVOLTAIC CELLS
Performance of battery charge controllers: First year test report
| DE92-002924 | p 1289 N92-17468
PHOTOVOLTAIC EFFECT
Optimization in solar heating/photovoltaic systems
| AD-A242363 | p 1313 N92-17424
Au and Al Schottky barrier formation on GaAs (100) surfaces prepared by thermal desorption of a protective arsenic coating
| DE92-002456 | p 1376 N92-17781
PHTHALOCYANIN
Studies of the adsorption of tetrasulfonated phthalocyanines on graphite substrate
| AD-A243443 | p 1260 N92-17489
Characterizing the sensitivity, selectivity, and reversibility of the metal-doped phthalocyanine thin-films used with the Interdigitated Gate Electrode Field-Effect Transistor (IGEFET) to detect organophosphorous compounds and nitrogen dioxide
| AD-A243635 | p 1376 N92-17746
PHYSICAL OPTICS
The physical optics description of microwave scattering by the sea surface
| AD-A243216 | p 1365 N92-17180
Verification and validation of the simulated radar image (SRIM) code radar cross section predictions
| AD-A243651 | p 1285 N92-17737
Achromatic and isochronous electron beam transport for tunable free electron lasers
| DE92-003908 | p 1305 N92-17868
PHYSICAL WORK
Treadmill for space flight
| NASA-CASE-MSC-21752-1 | p 1335 N92-17910
PHYSIOLOGICAL EFFECTS
Alleviation of thermal strain in engineering space personnel aboard CF ships with the exotemp personal cooling system
| AD-A242889 | p 1330 N92-17599
PHYSIOLOGICAL RESPONSES
Rapid nonconjugate adaptation of vertical voluntary pursuit eye movements
| AD-A243358 | p 1331 N92-17145
Biological effects of protracted exposure to ionizing radiation: Review, analysis, and model development
| AD-A242981 | p 1329 N92-17476
PICOSECOND PULSES
A study of gamma ray generation from channeled electrons and positions
| AD-A241993 | p 1361 N92-17608
PIEZOELECTRIC CERAMICS
The 5th Annual US-Japan Seminar on Dielectric and Piezoelectric Ceramics
| AD-A243465 | p 1268 N92-17193
PIEZOELECTRICITY
Actively controlled shaft seals for aerospace applications
| NASA-CR-189808 | p 1306 N92-17304
PILOT PERFORMANCE
Effects of the chemical defense antidote atropine sulfate on helicopter pilot performance: An in-flight study
| AD-A241966 | p 1328 N92-17084
System identification methods for handling-qualities evaluation p 1232 N92-17165
Comparison of experimental US Air Force and Euro-NATO pilot candidate selection test batteries
| AD-A242358 | p 1332 N92-17450
Effect of two types of scene detail on detection of altitude change in a flight simulator
| AD-A242034 | p 1333 N92-17758
PILOT SELECTION
Comparison of experimental US Air Force and Euro-NATO pilot candidate selection test batteries
| AD-A242358 | p 1332 N92-17450
PILOT TRAINING
Aircrew critique of high-G centrifuge training: Part 3: What can we change to better serve you?
| AD-A243496 | p 1334 N92-17432
PINS
Strength of lugs
| ESDU-91008 | p 1311 N92-17834
PIONS
Medium-energy neutrino physics
| DE92-003790 | p 1362 N92-17666
PILAC: A Pion Linac facility for 1-GeV pion physics at LAMPF
| DE92-003789 | p 1364 N92-17794
Pion-nucleus cross sections
| DE92-600631 | p 1363 N92-17958
PIPE FLOW
Method and apparatus for reducing drag and noise associated with fluid flow in a conduit
| AD-D015067 | p 1297 N92-17398
PIPES (TUBES)
Cathodic protection diagnostic computer program for sacrificial and impressed current systems: Overview and user's manual
| AD-A243663 | p 1338 N92-17122
Extendable pipe crawler
| DE91-011570 | p 1306 N92-17183
Method and apparatus for reducing drag and noise associated with fluid flow in a conduit
| AD-D015067 | p 1297 N92-17398
Microstructurally toughened articles and casting thereof
| AD-D015065 | p 1265 N92-17452
Fracture toughness evaluation for N Reactor pressure tubes of Zircaloy-2 using the electric-potential method
| DE92-003631 | p 1311 N92-17713
PITCH (INCLINATION)
Target pitch angle for the microburst escape maneuver p 1221 N92-17996
PITCHING MOMENTS
Dynamic stall on wind turbine blades
| DE92-001157 | p 1226 N92-17874
PITTING
Long-term corrosion evaluation of stainless steels in Space Shuttle iodinated resin and water
| NASA-TM-104743 | p 1264 N92-17376
PIXELS
Improved 320x244-element PtSi Schottky-barrier IR-CCD image sensor
| AD-A242026 | p 1301 N92-17140
PLANAR STRUCTURES
Exploring plasma sheath solutions for planar and cylindrical anodes
| AD-A243237 | p 1369 N92-17030
Integration of an anti-parallel pair of planar Schottky barrier diodes for millimeter and submillimeter wavelengths
| AD-A243371 | p 1287 N92-17189
Superdirective properties of closed loops of parallel coplanar dipoles
| AD-A243009 | p 1288 N92-17268
A discontinuity study in shielded coplanar line
| AD-A242976 | p 1288 N92-17290
PLANE STRAIN
Aluminum alloys for ALS cryogenic tanks: Comparative measurements of cryogenic mechanical properties of Al-Li alloys and alloy 2219
| AD-A242956 | p 1264 N92-17379
PLANE WAVES
Groundscreen characterization
| AD-A243164 | p 1311 N92-17208
Study of plane wave impingement on a thin plate capable of deformation
| AD-A242947 | p 1296 N92-17275
PLANNING
Causal schema decision-aiding system
| AD-A242931 | p 1347 N92-17203
PLANT DESIGN
Development of an XUV-IR free-electron laser user facility for scientific research and industrial applications
| DE92-003862 | p 1304 N92-17726
PLANTS (BOTANY)
Global models for the biomechanics of green plants, part 1
| DE91-641478 | p 1327 N92-17946
PLASMA COMPOSITION
Experimental measurements of plasma properties for Miller SG-100 torch with Mach I setting
| DE92-003309 | p 1369 N92-17469
A one-dimensional plasma and impurity transport model for reversed field pinches
| DE92-004691 | p 1371 N92-17933
PLASMA CONDUCTIVITY
Equation of state and conductivity of hot, dense matter
| AD-A243359 | p 1369 N92-17301
PLASMA CONTROL
Liquid and solid ion plasmas
| AD-A242029 | p 1370 N92-17635
Workshop on Plasma Experiments in the Laboratory and in Space. Abstracts
| AD-A243645 | p 1370 N92-17734
PLASMA COOLING
Liquid and solid ion plasmas
| AD-A242029 | p 1370 N92-17635
PLASMA DENSITY
An investigation of methods for updating ionospheric scintillation models using topside in-situ plasma density measurements
| AD-A243378 | p 1316 N92-17209
Equation of state and conductivity of hot, dense matter
| AD-A243359 | p 1369 N92-17301
Steady-state, high dose neutron generation and concentration apparatus and method for deuterium atoms
| AD-D015063 | p 1358 N92-17462
PLASMA DIAGNOSTICS
The charge exchange recombination diagnostic system on the D3-D tokamak
| DE92-003805 | p 1369 N92-17456
Experimental measurements of plasma properties for Miller SG-100 torch with Mach I setting
| DE92-003309 | p 1369 N92-17469
Liquid and solid ion plasmas
| AD-A242029 | p 1370 N92-17635
PLASMA DIFFUSION
Steady-state, high dose neutron generation and concentration apparatus and method for deuterium atoms
| AD-D015063 | p 1358 N92-17462
PLASMA EQUILIBRIUM
A numerical code for a three-dimensional magnetospheric MHD equilibrium model
| NASA-CR-189852 | p 1316 N92-17227
PLASMA ETCHING
Materials processing of diamond: Etching, doping by ion implantation and contact formation
| AD-A243060 | p 1267 N92-17065
Selective plasma etching
| DE92-004794 | p 1371 N92-17968
PLASMA GENERATORS
High frequency sources of ions for ion technology p 1362 N92-17820
PLASMA HEATING
Ion sources based on electron cyclotron resonance p 1362 N92-17743
Theoretical studies in tokamaks: Three-dimensional simulation of lower hybrid wave launching in tokamaks
| DE92-003773 | p 1371 N92-17793

PLASMA INTERACTIONS
Environmental interactions in Space Exploration: Announcement of the formation of an Environmental Interactions Working Group
[NASA-TM-105294] p 1389 N92-17069
PLASMA JETS
Experimental measurements of plasma properties for Miller SG-100 torch with Mach I setting
[DE92-003309] p 1369 N92-17469
PLASMA LAYERS
Magnetospheric response to variations in the interplanetary magnetic field
[AD-A243683] p 1389 N92-17717
Alfven waves in inhomogeneous magnetic fields: An integro-differential equation formulation
[DE92-609544] p 1371 N92-17806
PLASMA OSCILLATIONS
Alfven waves in inhomogeneous magnetic fields: An integro-differential equation formulation
[DE92-609544] p 1371 N92-17806
PLASMA PHYSICS
Some aspects of nonneutral plasma physics
[AD-A243711] p 1370 N92-17499
PLASMA PINCH
A one-dimensional plasma and impurity transport model for reversed field pinches
[DE92-004691] p 1371 N92-17933
PLASMA PROBES
Materials processing of diamond: Etching, doping by ion implantation and contact formation
[AD-A243060] p 1267 N92-17065
Experimental measurements of plasma properties for Miller SG-100 torch with Mach I setting
[DE92-003309] p 1369 N92-17469
PLASMA RADIATION
Inductively coupled plasma atomic emission spectroscopy analysis of gold electroplating solutions
[DE92-004798] p 1266 N92-17858
PLASMA SHEATHS
Exploring plasma sheath solutions for planar and cylindrical anodes
[AD-A243237] p 1369 N92-17030
Theoretical studies in tokamaks: Three-dimensional simulation of lower hybrid wave launching in tokamaks
[DE92-003773] p 1371 N92-17793
PLASMA SPECTRA
Picosecond laser breakdown thresholds in gases
[AD-A242941] p 1304 N92-17475
PLASMA TEMPERATURE
Exploring plasma sheath solutions for planar and cylindrical anodes
[AD-A243237] p 1369 N92-17030
Experimental measurements of plasma properties for Miller SG-100 torch with Mach I setting
[DE92-003309] p 1369 N92-17469
PLASMA TORCHES
Experimental measurements of plasma properties for Miller SG-100 torch with Mach I setting
[DE92-003309] p 1369 N92-17469
PLASMA TURBULENCE
The charge exchange recombination diagnostic system on the D3-D tokamak
[DE92-003805] p 1369 N92-17456
PLASMA WAVES
On the generation of large-amplitude plasma wakefields with low phase velocities by an intense short laser pulse
[DE92-609543] p 1371 N92-17805
PLASMAS (PHYSICS)
Environmental interactions in Space Exploration: Announcement of the formation of an Environmental Interactions Working Group
[NASA-TM-105294] p 1389 N92-17069
A kinetics study of the electron cyclotron resonance plasma oxidation of silicon
[AD-A242868] p 1290 N92-17596
A one-dimensional plasma and impurity transport model for reversed field pinches
[DE92-004691] p 1371 N92-17933
PLASMONS
Diffraction and imaging theory of inelastically scattered electrons: A new approach
[DE91-018248] p 1360 N92-17574
PLASTIC DEFORMATION
Experimental investigation of adiabatic shear banding at different impact velocities
[AD-A243011] p 1310 N92-17256
PLASTIC PROPERTIES
Data acquisition and measurement system for plastic parameters of radiation metal research experiments
[DE92-610350] p 1266 N92-17808
An investigation of gouge initiation in high-velocity sliding contact
[DE92-003944] p 1311 N92-17937
PLASTICIZERS
Energetic composites of cyclodextrin nitrate esters and nitrate ester plasticizers
[AD-D015068] p 1275 N92-17399
Pyrolysis GC-FTIR studies of a LOVA propellant formulation series
[AD-A242844] p 1275 N92-17562
PLASTICS
Mechanisms of gas permeation through polymer membranes
[DE92-004423] p 1274 N92-17942
PLATES (STRUCTURAL MEMBERS)
Three point lead screw positioning apparatus
[NASA-CASE-LEW-15216-1] p 1307 N92-17678
Experimental study of amplitude-phase-frequency characteristics of flow when following over a vibrating plate
[DE92-610935] p 1299 N92-17810
PLATINUM
Blistering of graphite/polymer composites galvanically coupled with metals in sea water
[AD-A242861] p 1269 N92-17262
In situ structural studies of the underpotential deposition of copper onto an iodine covered platinum surface using x ray standing waves
[AD-A243475] p 1263 N92-17328
In situ x ray standing wave study of Cu UPD on an iodine covered platinum surface
[AD-A243474] p 1264 N92-17426
PLOTTING
The conversion of a FORTRAN data plotting program using DI-3000 graphics to operation on a Macintosh Personal Computer
[AD-A243046] p 1339 N92-17280
PLUGS
High contact blind hole thermocouple plug
[AD-D015105] p 1302 N92-17835
Thruster sealing system and apparatus
[NASA-CASE-MSC-21898-1] p 1308 N92-17872
PLY ORIENTATION
Workshop for Finite Element Methods for Composites
[AD-A243534] p 1256 N92-17392
PNEUMATICS
Development and utilization of new diagnostics for dense-phase pneumatic transport
[DE92-003091] p 1307 N92-17605
Development and utilization of new diagnostics for dense-phase pneumatic transport
[DE92-000337] p 1299 N92-17704
PODS (EXTERNAL STORES)
Flow visualization and wake analysis for standard and modified configurations of the AN/ALQ-78 antenna pod
[AD-A243552] p 1224 N92-17339
POINT SOURCES
Hubble Space Telescope: Optical telescope assembly handbook. Version 1.0
[NASA-CR-189751] p 1386 N92-17483
POISSON DENSITY FUNCTIONS
A Kalman filter for a Poisson series with covariates and Laplace approximation integration
[AD-A242960] p 1286 N92-16993
Marked point processes as limits of Markovian arrival streams
[TW-91-04] p 1353 N92-17837
POLAR CAPS
Radar-satellite studies of the high-latitude ionosphere
[AD-A243275] p 1317 N92-17961
POLARIZED LIGHT
Infrared rotating analyzer ellipsometry: Calibration and data processing
[AD-A242834] p 1259 N92-17248
POLARONS
Electronic and ionic transport in processable conducting polymers
[AD-A242258] p 1269 N92-17460
Separation of neutral-to-polaron and polaron-to-bipolaron redox events in alkoxy substituted di-2-thienylphenylene polymers
[AD-A242423] p 1271 N92-17679
POLICIES
Publications of the Executive Office of the President, January 20, 1989 to June 30, 1991
[PB91-202762] p 1383 N92-17228
Policy implications of greenhouse warming: Report of the adaptation panel p 1314 N92-17982
POLLUTION CONTROL
Policy implications of greenhouse warming: Report of the adaptation panel p 1314 N92-17982
POLYACETYLENE
Anomalous hole burning in polymers with inhomogeneous broadening
[AD-A242397] p 1266 N92-17010
POLYBUTADIENE
Gas transport in polybutadiene treated with aqueous bromine
[AD-A241871] p 1295 N92-17025
Pyrolysis GC-FTIR studies of a LOVA propellant formulation series
[AD-A242844] p 1275 N92-17562
POLYCARBONATES
Effect of coatings and processing on failure mechanisms of polycarbonate material, phase 1
[AD-A243018] p 1256 N92-17053
POLYCRYSTALS
Determination of the electronic density of states of YBa2Cu3O(7-delta)
[AD-A243223] p 1373 N92-17220
Method of joining diamond structures
[AD-D015066] p 1269 N92-17397
Determination of the tribological fundamentals of solid lubricated ceramics. Volume 2: Appendices A through O
[AD-A242871] p 1270 N92-17614
Spatially and spectrally resolved cathodoluminescence measurements of CVD-grown diamond particles and films
[AD-A243220] p 1271 N92-17615
Determination of the tribological fundamentals of solid lubricated ceramics. Volume 1: Summary
[AD-A243219] p 1272 N92-17683
POLYESTER RESINS
Blistering of graphite/polymer composites galvanically coupled with metals in sea water
[AD-A242861] p 1269 N92-17262
POLYESTERS
New experimental challenges in elemental fluorine chemistry: An emerging technology
[AD-A243054] p 1258 N92-17043
Organic NLO polymers. Linear and accordian main-chain NLO polymers prepared by a Knoevenagel polycondensation
[AD-A243644] p 1273 N92-17753
Mechanisms of gas permeation through polymer membranes
[DE92-004423] p 1274 N92-17942
POLYETHYLENES
Dielectric properties of aligned conducting polymers
[AD-A243389] p 1268 N92-17191
Optical spectra and kinetics of single impurity molecules in a polymer: Spectral diffusion and persistent spectral hole-burning
[AD-A243749] p 1271 N92-17659
POLYIMIDES
Polyimides containing amide and perfluoroisopropyl connecting groups
[NASA-CASE-LAR-14608-1] p 1271 N92-17676
POLYMER BLENDS
The effect of monomer structures and compressibility on the properties of multicomponent polymer blends and solutions
[AD-A242863] p 1273 N92-17777
Modelling of some equilibrium thermodynamic properties of polymer systems
[ETN-92-90570] p 1273 N92-17840
POLYMER CHEMISTRY
Reactions and interactions in liquid crystalline media
[AD-A242355] p 1374 N92-17449
Imide/arylene ether copolymers with pendent trifluoromethyl groups
[NASA-TM-104195] p 1272 N92-17693
Chromatographic separation of calcium isotopes
[DE92-004623] p 1261 N92-17740
Molecular composites from high temperature polyquinolines
[AD-A243634] p 1272 N92-17745
Aryl bis(triflates) in palladium (0) cross-coupling reactions. Synthesis of polyphenyl-alkynyl, alkenyl, and aryl ethers
[AD-A243643] p 1273 N92-17752
Organic NLO polymers. Linear and accordian main-chain NLO polymers prepared by a Knoevenagel polycondensation
[AD-A243644] p 1273 N92-17753
Substituted 1,1,1-triaryl-2,2,2-trifluoroethanes and processes for their synthesis
[NASA-CASE-LEW-14345-6] p 1255 N92-17882
POLYMER MATRIX COMPOSITES
Novel vacuum bag processing approaches to void reduction in carbon/epoxy composites
[AD-A242396] p 1255 N92-16992
POLYMERIC FILMS
Free volume variation with molecular weight of polymers
[NASA-TM-4326] p 1267 N92-17032
Electrochemically initiated chain polymerization of pyrrole in aqueous media
[AD-A242259] p 1269 N92-17461
Separation of neutral-to-polaron and polaron-to-bipolaron redox events in alkoxy substituted di-2-thienylphenylene polymers
[AD-A242423] p 1271 N92-17679

POLYMERIZATION
Electronic and ionic transport in processable conducting polymers. Symmetry effects on the physical and electrically conducting, substituted poly(di-2-thienylphenylenes)
| AD-A242328 | p 1266 N92-16976
Dielectric properties of aligned conducting polymers
| AD-A243389 | p 1268 N92-17191
Phase transitions in narrow molecular mass samples of side-chain liquid crystalline polymers: Molecular mass dependence
| AD-A242354 | p 1269 N92-17448
Reactions and interactions in liquid crystalline media
| AD-A242355 | p 1374 N92-17449
Electrochemically initiated chain polymerization of pyrrole in aqueous media
| AD-A242259 | p 1269 N92-17461
Development of processible electroactive oligomers and polymers
| AD-A243723 | p 1270 N92-17508
Polymer-reinforced metal matrix composite
| AD-D015070 | p 1257 N92-17611
Organometallic NLO polymers. Linear main-chain NLO polymers of ferrocene
| AD-A243641 | p 1272 N92-17750
Substituted 1,1,1-triaryl-2,2,2-trifluoroethanes and processes for their synthesis
| NASA-CASE-LEW-14345-6 | p 1255 N92-17882
Phosphazene polymer containing composites and method for making phosphazene polymer containing composites
| DE92-003826 | p 1274 N92-17935

POLYMERS
Two-beam coupling measurements of grating phase in a photorefractive polymer
| AD-A243746 | p 1268 N92-17195
Photorefractivity in doped nonlinear organic polymers
| AD-A243751 | p 1271 N92-17661
Electrically-controlled polymeric gels as active materials in adaptive structures
| DE92-002947 | p 1272 N92-17710

POLYMETHYL METHACRYLATE
Phase transitions in narrow molecular mass samples of side-chain liquid crystalline polymers: Molecular mass dependence
| AD-A242354 | p 1269 N92-17448
New ferrocene complexes and polymers for nonlinear optical applications
| AD-A243640 | p 1272 N92-17749
Organometallic NLO polymers. Linear main-chain NLO polymers of ferrocene
| AD-A243641 | p 1272 N92-17750

POLYNOMIALS
Complexity issues in numerical optimization
| AD-A241854 | p 1347 N92-17049
A convergent aspiration based interior point method (CAIN) for Multiple Objective Linear Programming (MOLP)
| AD-A243404 | p 1338 N92-17118
Study of features of binary images using algebra techniques
| AD-A242010 | p 1351 N92-17609
Some results for extended Jacobi polynomials
| DE92-609035 | p 1351 N92-17939

POLYSILOXANES
Phase transitions in narrow molecular mass samples of side-chain liquid crystalline polymers: Molecular mass dependence
| AD-A242354 | p 1269 N92-17448

POLYSTYRENE
Radar scattering from foamed plastic target supports
| AD-A243756 | p 1284 N92-17722

POLYURETHANE FOAM
Effective dynamic material parameters and localized scattering
| AD-A241957 | p 1310 N92-17320

POPULATIONS
Sensitivity testing and analysis
| DE92-002033 | p 1276 N92-17624

POROSITY
The effects of sediment porosity on acoustic reflection and transmission at the seafloor
| AD-A241943 | p 1323 N92-17083
Active control of pressure loads using passive porosity
| NASA-CASE-LAR-14594-1 | p 1300 N92-17888
Passive control of pressure loads using porosity
| NASA-CASE-LAR-14547-1 | p 1300 N92-17909

POSITION (LOCATION)
Method of Kalman filtering for estimating the position and velocity of a tracked object
| AD-D015057 | p 1287 N92-17129
Performance of ground-based infrared detectors for acquisition of satellites
| AD-A243247 | p 1281 N92-17241
Using the Global Positioning System (GPS) to fulfill the position/location requirements of the National Training Center (NTC) and other US Army instrumented testing and training ranges
| AD-A242064 | p 1229 N92-17639
Fiber optic angular orientation sensor digital serial encoding
| AD-D015102 | p 1302 N92-17826
Systematic computation algorithm to obtain osculating orbit elements from position and velocity vectors
| NAL-TM-614 | p 1239 N92-17854
Method for non-destructive estimation of waveguide directional coupler dimensions
| NASA-CASE-NPO-18454-1-CU | p 1293 N92-17865

POSITION ERRORS
Fault detection and isolation for multisensor navigation systems p 1221 N92-17992

POSITION SENSING
Application of multi-target tracking to sonar-based mobile robot navigation
| OUEL-1819/90 | p 1229 N92-17878

POSITIONING
Rapid nonconjugate adaptation of vertical voluntary pursuit eye movements
| AD-A243358 | p 1331 N92-17145
Space Station Freedom solar alpha joint growth capability p 1252 N92-17772

POSITIONING DEVICES (MACHINERY)
Three point lead screw positioning apparatus
| NASA-CASE-LEW-15216-1 | p 1307 N92-17678

POSITRONS
Free volume variation with molecular weight of polymers
| NASA-TM-4326 | p 1267 N92-17032

POSTFLIGHT ANALYSIS
Long duration exposure facility post-flight thermal analysis: Orbital/thermal environment data package
| NASA-CR-189872 | p 1245 N92-17334
Systems special investigation group
| NASA-CR-187355 | p 1250 N92-17728

POWDER (PARTICLES)
Examining Si3N4 base materials with various rare earth additions
| AD-A243668 | p 1372 N92-17082
Consolidation of diamond packed powders
| AD-D015071 | p 1270 N92-17612
Determination of cohesive and normal stresses and simulation of fluidization using kinetic theory
| DE92-002905 | p 1299 N92-17709

POWDER METALLURGY
Contributive research and development
| AD-A243331 | p 1391 N92-17079

POWER CONVERTERS
Transformerless DC-DC voltage amplifier with optically isolated switching devices
| NASA-CASE-NPO-17994-1-CU | p 1293 N92-17907

POWER EFFICIENCY
Radio frequency hazard monitoring-USAKA
| AD-A242873 | p 1283 N92-17563

POWER LINES
Analysis of possible schemes for twisting multiwire superconducting cables and design of twisting equipment
| DE92-609667 | p 1294 N92-17971

POWER SPECTRA
Simulation of finite-precision effects in digital filters
| AD-A243758 | p 1342 N92-17601

POWER SUPPLIES
Explosive magnetic field compression generator transformer power supply for high resistive loads
| AD-D015123 | p 1293 N92-17831

POWER TRANSMISSION
Analysis of possible schemes for twisting multiwire superconducting cables and design of twisting equipment
| DE92-609667 | p 1294 N92-17971

PRECIPITATION (METEOROLOGY)
Surface observation climatic summaries for Boise Air Terminal, ID
| AD-A243012 | p 1319 N92-17257
Surface observation climatic summaries for Fairbanks IAP, Alaska
| AD-A243309 | p 1320 N92-17400

PRECISION
Simulation of finite-precision effects in digital filters
| AD-A243758 | p 1342 N92-17601

PREDICTION ANALYSIS TECHNIQUES
Design of a fiber optic image transmission link
| AD-A243686 | p 1365 N92-17088
Preliminary design of a model to assess the effect of Space Surveillance Network (SSN) sensor upgrades on orbit prediction accuracies relative to the US Anti-Satellite (ASAT) mission
| AD-A243736 | p 1353 N92-17479
Program plans: Aviation safety research
| NIAR-91-30 | p 1227 N92-17587
Preliminary results from the analysis of wind component error
| AD-A243772 | p 1321 N92-17764

PREDICTIONS
ECLSS predictive monitoring p 1247 N92-17357
Auroral-clutter predictions for Fylingdales, England
| AD-A242957 | p 1283 N92-17600
Adaptive generalized predictive control
| OUEL-1879/91 | p 1349 N92-17880

PREFORMS
An optical roughness sensor for the real time determination of spray formed preform quality
| AD-A243238 | p 1262 N92-17056
Plasma chemical vapor deposition of halide glasses
| AD-D015060 | p 1370 N92-17706

PREMIXED FLAMES
Two-dimensional stability of laminar flames
| NASA-TP-3131 | p 1223 N92-17131

PRESIDENTIAL REPORTS
Publications of the Executive Office of the President, January 20, 1989 to June 30, 1991
| PB91-202762 | p 1382 N92-17228

PRESSURE BREATHING
Evaluation of BAUER high pressure breathing air P-2 purification system
| AD-A243535 | p 1333 N92-17014
Unmanned evaluation of BAUER high pressure breathing air P-5 purification system
| AD-A243486 | p 1334 N92-17331

PRESSURE DEPENDENCE
Pressure dependence of Tc in Tl2Ba2CaCu2O8 at hydrostatic pressures to 6 GPa
| AD-A243433 | p 1375 N92-17685
Mechanisms of gas permeation through polymer membranes
| DE92-004423 | p 1274 N92-17942

PRESSURE DISTRIBUTION
Failure detection and fault management techniques for flush airdata sensing systems
| NASA-TM-4335 | p 1234 N92-17128
Surface pressure measurements on the wing of a wind tunnel model during steady rotation
| AD-A243047 | p 1223 N92-17281
Engineering model of unsteady flow in a cavity
| AD-A243636 | p 1299 N92-17747
Active control of pressure loads using passive porosity
| NASA-CASE-LAR-14594-1 | p 1300 N92-17888
Passive control of pressure loads using porosity
| NASA-CASE-LAR-14547-1 | p 1300 N92-17909

PRESSURE MEASUREMENT
Stagnation and dynamic pressure limits for the S1 wind tunnel
| AD-A242989 | p 1238 N92-17297
Flow visualization and wake analysis for standard and modified configurations of the AN/ALQ-78 antenna pod
| AD-A243552 | p 1224 N92-17339

PRESSURE RATIO
Aircraft ground test and subscale model results of axial thrust loss caused by thrust vectoring using turning vanes
| NASA-TM-4341 | p 1230 N92-17071
Viscous three-dimensional calculations of transonic fan performance
| NASA-TM-103800 | p 1219 N92-17346

PRESSURE REGULATORS
Active control of pressure loads using passive porosity
| NASA-CASE-LAR-14594-1 | p 1300 N92-17888
Passive control of pressure loads using porosity
| NASA-CASE-LAR-14547-1 | p 1300 N92-17909

PRESSURE SENSORS
Advanced nozzle and engine components test facility
| NASA-TM-103684 | p 1237 N92-17059
Failure detection and fault management techniques for flush airdata sensing systems
| NASA-TM-4335 | p 1234 N92-17128
Differential pressure sensor
| AD-D015134 | p 1302 N92-17918

PRESSURE VESSELS
Fracture toughness evaluation for N Reactor pressure tubes of Zircaloy-2 using the electric-potential method
| DE92-003631 | p 1311 N92-17713
Residual stresses in a prestressed steel pressure vessel wrapped with multilayered composites
| AD-A243429 | p 1311 N92-17930
Novel ceramic matrix composites for deep submergence pressure vessel applications
| AD-A242740 | p 1274 N92-17947

PRESTRESSING
Residual stresses in a prestressed steel pressure vessel wrapped with multilayered composites
| AD-A243429 | p 1311 N92-17930

PRIMATES
Efficient identification and analysis of low and medium frequency repeats
| DE92-003758 | p 1385 N92-17856

PRIMITIVE EQUATIONS
A variational assimilation method for satellite and conventional data: A revised basic model 2B
p 1322 N92-17977
PRINCIPAL COMPONENTS ANALYSIS
Psychophysical evaluation of three-dimensional auditory displays
| NASA-CR-189848 | p 1355 N92-17692
PRINTED CIRCUITS
Design and testing of a lightweight, planar microwave lens
| AD-A243685 | p 1286 N92-17076
PRIORITIES
Attention, automaticity and priority learning
| AD-A242226 | p 1332 N92-17458
PRISMS
Determination of symmetric end loads from bulk stresses on a rectangular prism
| AD-A242973 | p 1310 N92-17254
Determination of antisymmetric end loads from bulk stresses on a rectangular prism
| AD-A243001 | p 1310 N92-17265
PROBABILITY DENSITY FUNCTIONS
A frequency-domain method for estimating the incidence and severity of sliding
| AD-A243077 | p 1334 N92-17569
PROBABILITY DISTRIBUTION FUNCTIONS
A statistical analysis of Eleuthera Island wind data for the period 27 April 1989 through 30 March 1990
| AD-A241885 | p 1318 N92-17027
Significant digit computation of the ellipsoidal coverage function and its inverse
| AD-A242322 | p 1350 N92-17242
PROBABILITY THEORY
Topological representation of graph isomorphism types
| AD-A243528 | p 1350 N92-17148
Significant digit computation of the ellipsoidal coverage function and its inverse
| AD-A242322 | p 1350 N92-17242
A stochastic approach to the weighted-region problem: 1. The design of the path annealing algorithm
| AD-A243324 | p 1340 N92-17403
Performance of the Rayleigh task based on the posterior probability of tomographic reconstructions
| DE92-003785 | p 1352 N92-17455
A probabilistic derivation of Stirling's formula
| AD-A241899 | p 1354 N92-17548
Example of statistical techniques applied to autoland touchdown dispersion (confidence intervals for normal and skew distributions)
| ESDU-91019 | p 1229 N92-17844
A study of channel-access schemes for integrated voice/data radio networks
| AD-A243584 | p 1286 N92-17931
Stochastic robustness p 1221 N92-17997
PROBLEM SOLVING
A theory of inverse operators for multiple excitations
| AD-A243484 | p 1350 N92-17330
PROCESS CONTROL (INDUSTRY)
Processing of ceramics of biopolymers. Ultrastructure-property relationships in biocrystals
| AD-A243061 | p 1267 N92-17054
Thermal insulation chemical composition and method of manufacture
| AD-D015106 | p 1257 N92-17836
Process of converting starch to glucose and glucose to lactic acid
| DE92-003840 | p 1255 N92-17867
PRODUCTIVITY
Partnership for Continuous Improvement
| NASA-TM-105464 | p 1308 N92-16988
NASA total quality management 1989 accomplishments report
| NASA-TM-105467 | p 1308 N92-17005
NASA total quality management 1990 accomplishments report
| NASA-TM-105465 | p 1308 N92-17199
Software life cycle methodologies and environments
p 1246 N92-17351
PROGRAM VERIFICATION (COMPUTERS)
An examination of selected commercial software testing tools
| AD-A243089 | p 1337 N92-17068
Research in some future directions in reliability and quality control
| AD-A242865 | p 1308 N92-17231
Specification and compositional verification of real-time systems
| ETN-92-90580 | p 1341 N92-17521
Verification and validation of the simulated radar image (SRIM) code radar cross section predictions
| AD-A243651 | p 1285 N92-17737
Verification and validation of the Comprehensive Operational Support Evaluation Model for space
| AD-A243653 | p 1344 N92-17761
PROGRAMMING LANGUAGES
A system for specifying and rapidly prototyping user interfaces
| AD-A242963 | p 1347 N92-16994
Design of Style-V: A translator to convert standard VHDL into a stylized form for automated microcode generation
| AD-A243706 | p 1340 N92-17407
PROGRAMS
Summaries of FY 1991 engineering research
| DE92-004708 | p 1277 N92-17593
PROGRESS
NASA total quality management 1989 accomplishments report
| NASA-TM-105467 | p 1308 N92-17005
PROJECT MANAGEMENT
Advanced studies program overview
p 1244 N92-17109
NASA total quality management 1990 accomplishments report
| NASA-TM-105465 | p 1308 N92-17199
Summary of professional activities, center for intelligence and special programs, 1990
| AD-A243508 | p 1347 N92-17385
Feedback in dynamic decision making: An experiment in software project management
| AD-A242361 | p 1380 N92-17451
PROJECT PLANNING
SEI: An update p 1243 N92-17103
Advanced studies program overview
p 1244 N92-17109
Beyond the Baseline 1991: Proceedings of the Space Station Evolution Symposium. Volume 2: Space Station Freedom, part 2
| NASA-CP-10083-VOL-2-PT-2 | p 1245 N92-17348
Beyond the Baseline 1991: Proceedings of the Space Station Evolution Symposium. Volume 2: Space Station Freedom, part 1
| NASA-CP-10083-VOL-2-PT-1 | p 1251 N92-17768
PROJECTILES
Launching projectiles with hydrogen gas generated from aluminum fuel powder/water reactions
| AD-D015119 | p 1276 N92-17830
PROPANE
Propane aromatization over gallium containing HZSM-5 zeolites
| ETN-92-90897 | p 1262 N92-17925
PROPELLANT ADDITIVES
Upper stages using liquid propulsion and metallized propellants
| NASA-TP-3191 | p 1253 N92-17151
PROPELLANT BINDERS
Case bond liner systems for solid rocket motors
| AD-A242297 | p 1253 N92-17085
PROPELLANT CHEMISTRY
Case bond liner systems for solid rocket motors
| AD-A242297 | p 1253 N92-17085
PROPELLANT COMBUSTION
Experiments and analysis concerning the use of external burning to reduce aerospace vehicle transonic drag
| NASA-TM-105397 | p 1235 N92-17546
PROPELLANT DECOMPOSITION
Pyrolysis GC-FTIR studies of a LOVA propellant formulation series
| AD-A242844 | p 1275 N92-17562
PROPELLANT TRANSFER
STV fueling options p 1249 N92-17415
Space Station Freedom/lunar transfer vehicle propellant operation hazard analysis p 1249 N92-17416
PROPELLER BLADES
The solution of a singular integral equation arising from a lifting surface theory for rotating blades
p 1224 N92-17303
PROPELLERS
The solution of a singular integral equation arising from a lifting surface theory for rotating blades
p 1224 N92-17303
PROPULSION SYSTEM CONFIGURATIONS
Workshop on Technology Issues of Superconducting MAGLEV Transportation Systems
| DE92-002288 | p 1307 N92-17604
Analysis of ram acceleration for high velocity applications
| AD-A242338 | p 1235 N92-17642
PROPULSION SYSTEM PERFORMANCE
Analysis of ram acceleration for high velocity applications
| AD-A242338 | p 1235 N92-17642
PROPYLENE
Thermal insulation chemical composition and method of manufacture
| AD-D015106 | p 1257 N92-17836
PROSTHETIC DEVICES
Automatic locking orthotic knee device
| NASA-CASE-MFS-28633-1 | p 1335 N92-17866
PROTECTIVE CLOTHING
Thermal energy test apparatus
| AD-A243526 | p 1379 N92-17537
Alleviation of thermal strain in engineering space personnel aboard CF ships with the exotemp personal cooling system
| AD-A242889 | p 1330 N92-17599
PROTECTIVE COATINGS
Effect of coatings and processing on failure mechanisms of polycarbonate material, phase 1
| AD-A243018 | p 1256 N92-17053
Au and Al Schottky barrier formation on GaAs (100) surfaces prepared by thermal desorption of a protective arsenic coating
| DE92-002456 | p 1376 N92-17781
PROTEIN CRYSTAL GROWTH
STS-31 Space Shuttle mission report
| NASA-TM-105475 | p 1241 N92-17364
PROTOCOL (COMPUTERS)
Local area network strategies and guidelines for a Peruvian Air Force Computer Center
| AD-A242841 | p 1345 N92-17135
Optical protocols for advanced spacecraft networks
p 1249 N92-17418
Mathematical basis for a system to manage automated protocol analysis
| AD-A242042 | p 1381 N92-17669
A study of channel-access schemes for integrated voice/data radio networks
| AD-A243584 | p 1286 N92-17931
PROTONS
The proton spectral function of Ca-40 and Ca-48 studies with (e, e prime p) reaction: An investigation of ground-state correlations
| ETN-92-90566 | p 1358 N92-17433
Medium-energy neutrino physics
| DE92-003790 | p 1362 N92-17666
Proton-proton and proton-antiproton elastic scattering at high energies: Theory, phenomenology, and experiment
| DE92-004414 | p 1364 N92-17964
PROTOTYPES
Space Station Freedom engineering prototype development p 1244 N92-17110
JPL space station telerobotic engineering prototype development: Advanced telerobotics system technology
p 1247 N92-17358
JPL space station telerobotic engineering prototype development FY 91 status/achievements
p 1247 N92-17359
The development of user interface tools for the computer aided prototyping system
| AD-A243189 | p 1340 N92-17368
Results from a data acquisition system prototype project using a switch-based event builder
| DE92-004638 | p 1336 N92-17592
The StarLite Project prototyping real-time software
| AD-A242032 | p 1342 N92-17636
USI rapid prototyping tool evaluations survey
| AD-A243168 | p 1335 N92-17673
PSYCHOACOUSTICS
Psychophysical evaluation of three-dimensional auditory displays
| NASA-CR-189848 | p 1355 N92-17692
PSYCHOPHYSIOLOGY
A computational model of semantic memory impairment: Modality-specificity and emergent category-specificity
| AD-A242377 | p 1347 N92-16991
PULSE GENERATORS
High current transistor pulse generator
| DE92-004774 | p 1292 N92-17801
PULSE HEATING
Temporally-specific modification of myelinated axon excitability in vitro following a single ultrasound pulse
| AD-A242329 | p 1326 N92-17474
PULSED LASERS
Velocity measurements in high temperature gases using laser-induced no fluorescence
| AD-A242399 | p 1295 N92-17012
On the generation of large-amplitude plasma wakefields with low phase velocities by an intense short laser pulse
| DE92-609543 | p 1371 N92-17805
PULSES
Transition phenomena in a straight channel with a 40 to 1 aspect ratio with and without imposed pulsations. Part 1: Near-wall and central region profiles
| AD-A243251 | p 1297 N92-17337
Launching projectiles with hydrogen gas generated from aluminum fuel powder/water reactions
| AD-D015119 | p 1276 N92-17830
PURITY
Evaluation of BAUER high pressure breathing air P-2 purification system
| AD-A243535 | p 1333 N92-17014

Unmanned evaluation of BAUER high pressure breathing air P-5 purification system
| AD-A243486 | p 1334 N92-17331

PYRAMIDS
Near real-time stereo vision system
| NASA-CASE-NPO-18593-1-CU | p 1368 N92-17864

PYROLYTIC GRAPHITE
Studies of the adsorption of tetrasulfonated phthalocyanines on graphite substrate
| AD-A243443 | p 1260 N92-17489

PYROTECHNICS
A theoretical study of the combustion of magnesium/teflon/viton pyrotechnic compositions
| AD-A243244 | p 1275 N92-17058
Evaluation of squib performance variables
| DE92-002034 | p 1275 N92-17533

PYRROLES
Electronic and ionic transport in processable conducting polymers
| AD-A242258 | p 1269 N92-17460
Electrochemically initiated chain polymerization of pyrrole in aqueous media
| AD-A242259 | p 1269 N92-17461

Q

QUADRATIC PROGRAMMING
Practical error bounds for a class of quadratic programming problems
| AD-A243249 | p 1345 N92-17960

QUALITATIVE ANALYSIS
Advanced nozzle and engine components test facility
| NASA-TM-103684 | p 1237 N92-17059

QUALITY
Pragmatic quality metrics for evolutionary software development models
| AD-A243022 | p 1337 N92-17064

QUALITY CONTROL
Partnership for Continuous Improvement
| NASA-TM-105464 | p 1308 N92-16988
NASA total quality management 1989 accomplishments report
| NASA-TM-105467 | p 1308 N92-17005
NASA total quality management 1990 accomplishments report
| NASA-TM-105465 | p 1308 N92-17199
Research in some future directions in reliability and quality control
| AD-A242865 | p 1308 N92-17231
A managerial approach for reliability verification of mechanical equipment
| MBB-UK-0140-91-PUB | p 1308 N92-17341
Product assurance and safety implementation in Space Shuttle payloads: An industrial perspective
| MBB-UK-0143-91-PUB | p 1241 N92-17342
Constraints and difficulties in implementations of RAMS assurance programmes
| MBB-UK-0141-91-PUB | p 1309 N92-17544
The need for active software product assurance management for systems critical software
| MBB-UK-0142-91-PUB | p 1341 N92-17545
Evolution of an environmental audit program
| DE92-002681 | p 1314 N92-17665
Hubble Space Telescope: SRM/QA observations and lessons learned
| NASA-TM-105505 | p 1387 N92-17873

QUANTITATIVE ANALYSIS
Escape strategies for turboprop aircraft in a microburst windshear
| AD-A243090 | p 1227 N92-17217
Inductively coupled plasma atomic emission spectroscopy analysis of gold electroplating solutions
| DE92-004798 | p 1266 N92-17858

QUANTUM CHROMODYNAMICS
One-loop calculations with massive particles
| ETN-92-90563 | p 1359 N92-17518
High energy physics program at Texas A and M University
| DE92-004426 | p 1363 N92-17738
Relativistic nuclear many-body theory
| DE92-003258 | p 1362 N92-17789

QUANTUM ELECTRONICS
Optical properties of thermally intermixed quantum wells and superlattices
| AD-A243546 | p 1375 N92-17618
Optical turbulence in second harmonic generation
p 1377 N92-17821

QUANTUM MECHANICS
Temperature dependent anomalous statistics
| DE92-609665 | p 1379 N92-17807

QUANTUM STATISTICS
Temperature dependent anomalous statistics
| DE92-609665 | p 1379 N92-17807

QUANTUM THEORY
Future prospects of pregeometry
| DE92-704278 | p 1379 N92-17817
State vector reduction. Part 1: Dynamical reduction theories; changing quantum theory so the statevector represents reality
| DE91-641488 | p 1379 N92-17824

QUANTUM WELLS
Anomalous hole burning in polymers with inhomogeneous broadening
| AD-A242397 | p 1266 N92-17010
Excitons in semiconducting superlattices, quantum wells, and ternary alloys
| DE91-018805 | p 1374 N92-17528
Optical properties of thermally intermixed quantum wells and superlattices
| AD-A243546 | p 1375 N92-17618

QUARKS
Axino-induced baryogenesis
| NASA-CR-189858 | p 1361 N92-17646

QUARTZ CRYSTALS
Electrochemically initiated chain polymerization of pyrrole in aqueous media
| AD-A242259 | p 1269 N92-17461

QUARTZ LAMPS
Flight vehicle thermal testing with infrared lamps
| NASA-TM-4336 | p 1232 N92-17226

QUEUEING THEORY
Performance modeling of the Ada rendezvous
| AD-A243392 | p 1339 N92-17211
Delay analysis for multidimensional queueing process in CSMA/CD local area networks
| AD-A242364 | p 1346 N92-17425
Marked point processes as limits of Markovian arrival streams
| TW-91-04 | p 1353 N92-17837
The micro-c rule is not optimal in the 2nd node of the tandem queue; 2 counterexamples
| TW-91-05 | p 1349 N92-17838
Neural-network dedicated processor for solving competitive assignment problems
| NASA-CASE-NPO-17781-1-CU | p 1337 N92-17884

QUINOLINE
Molecular composites from high temperature polyquinolines
| AD-A243634 | p 1272 N92-17745

R

RADAR
Terminal Doppler weather radar test bed operation, Orlando: January-June 1990
| AD-A242890 | p 1318 N92-17028

RADAR ANTENNAS
Multipath induced tracking errors at 95 and 140 GHz
| AD-A243111 | p 1283 N92-17571

RADAR CROSS SECTIONS
Determination of bistatic radar clutter power from topographic data
| AD-A243697 | p 1280 N92-17095
Auroral-clutter predictions for Fylingdales, England
| AD-A242957 | p 1283 N92-17600
Parallelizing serial code for a distributed processing environment with an application to high frequency electromagnetic scattering
| AD-A243755 | p 1284 N92-17721
Radar scattering from foamed plastic target supports
| AD-A243756 | p 1284 N92-17722
A rigorous uniform diffraction analysis of the electromagnetic scattering from impedance edges and junctions
| AD-A243649 | p 1284 N92-17735
Verification and validation of the simulated radar image (SRIM) code radar cross section predictions
| AD-A243651 | p 1285 N92-17737

RADAR DETECTION
Front detection with Doppler radar
| AD-A242880 | p 1319 N92-17289

RADAR ECHOES
Radar scattering from foamed plastic target supports
| AD-A243756 | p 1284 N92-17722

RADAR EQUIPMENT
Low-noise oscillators for airborne radar applications
| AD-A242264 | p 1281 N92-17258

RADAR IMAGERY
Low-noise oscillators for airborne radar applications
| AD-A242264 | p 1281 N92-17258
Gabor segmentation of high resolution synthetic aperture radar imagery
| AD-A243753 | p 1284 N92-17662
Verification and validation of the simulated radar image (SRIM) code radar cross section predictions
| AD-A243651 | p 1285 N92-17737

RADAR NETWORKS
Radio frequency hazard monitoring-USAKA
| AD-A242873 | p 1283 N92-17563

RADAR RANGE
Determination of bistatic radar clutter power from topographic data
| AD-A243697 | p 1280 N92-17095

RADAR SCATTERING
Determination of bistatic radar clutter power from topographic data
| AD-A243697 | p 1280 N92-17095
Radar scattering from foamed plastic target supports
| AD-A243756 | p 1284 N92-17722

RADAR TARGETS
Determination of bistatic radar clutter power from topographic data
| AD-A243697 | p 1280 N92-17095

RADAR TRACKING
Multipath induced tracking errors at 95 and 140 GHz
| AD-A243111 | p 1283 N92-17571

RADIANCE
Relaxation processes of vibrationally excited H2O in the mesosphere and thermosphere
| AD-A241853 | p 1315 N92-17035
Background Atmosphere Radiance Day (BARD) and Night (BARN)
| AD-A243153 | p 1316 N92-17239

RADIATION BELTS
Investigation of mechanisms for the source and loss of electrons from the radiation belts using data from SEEP, SCATHA and P78-1 satellites
| AD-A243376 | p 1317 N92-17405

RADIATION COUNTERS
The determination of the number of light neutrino species
| ETN-92-90564 | p 1359 N92-17519
Use of the algebraic coding theory in nuclear electronics
| DE92-611125 | p 1351 N92-17813
Solar neutrino physics in the nineties
| DE92-003848 | p 1390 N92-17883

RADIATION DAMAGE
X ray damage to CF3CO2-Terminated organic monolayers on Si/Au supports is due primarily to x ray induced electrons
| AD-A243446 | p 1289 N92-17490
DOE Task Force Meeting on Electrical Breakdown of Insulating Ceramics in a High Radiation Field
| DE92-000459 | p 1270 N92-17576
Growth rate of dislocation loop in Fe-Ni-Cr alloy under Kr(+) ion and electron irradiation
| DE92-001908 | p 1265 N92-17703

RADIATION DETECTORS
Electronic expansion of human perception
| AD-A242028 | p 1333 N92-17634
Hard-surface contamination detection exercise
| DE92-004750 | p 1330 N92-17798
Quantum-limited detection of millimeter waves using superconducting tunnel junctions
| DE92-004757 | p 1377 N92-17799
Collaborative research on experimental astrophysics
| DE92-003970 | p 1388 N92-17832
Experimental findings on self-recovery and improvement of representative parameters of some semiconductor devices as irradiated in fast neutron flux
| DE92-611185 | p 1378 N92-17944

RADIATION DISTRIBUTION
Verification of an effective dose equivalent model for neutrons
| DE92-002738 | p 1358 N92-17453
DOE Task Force Meeting on Electrical Breakdown of Insulating Ceramics in a High Radiation Field
| DE92-000459 | p 1270 N92-17576

RADIATION DOSAGE
Biophysical techniques for examining metabolic, proliferative, and genetic effects of microwave radiation
| AD-A241903 | p 1326 N92-17288
A PC program to calculate the one-sided lower tolerance limit for total ionizing dose radiation data
| AD-A242365 | p 1357 N92-17394
Verification of an effective dose equivalent model for neutrons
| DE92-002738 | p 1358 N92-17453
Biological effects of protracted exposure to ionizing radiation: Review, analysis, and model development
| AD-A242981 | p 1329 N92-17476
Calculations of electron and photon transport between 1 MeV and 1 eV
| AD-A243725 | p 1359 N92-17514

RADIATION EFFECTS
Atomic oxygen flux and fluence calculation for Long Duration Exposure Facility (LDEF)
| NASA-CR-187418 | p 1245 N92-17215
DOE Task Force Meeting on Electrical Breakdown of Insulating Ceramics in a High Radiation Field
| DE92-000459 | p 1270 N92-17576

Radiation effects in High Temperature Superconductors (HTSC) oxides p 1375 N92-17700
Data acquisition and measurement system for plastic parameters of radiation metal research experiments
|DE92-610350| p 1266 N92-17808
Effect of thermal annealing on property changes of neutron-irradiated non-graphitized carbon materials and nuclear graphite
|DE92-704180| p 1257 N92-17816
Experimental findings on self-recovery and improvement of representative parameters of some semiconductor devices as irradiated in fast neutron flux
|DE92-611185| p 1378 N92-17944

RADIATION HARDENING
Preparation of ferroelectric samples for electrical and radiation characterization studies
|AD-A243432| p 1288 N92-17326

RADIATION HAZARDS
Hard-surface contamination detection exercise
|DE92-004750| p 1330 N92-17798

RADIATION MEASUREMENT
Solar neutrinos: Probing the sun or neutrinos?
|DE92-003849| p 1389 N92-17201
Preparation of ferroelectric samples for electrical and radiation characterization studies
|AD-A243432| p 1288 N92-17326
Recent developments in neutrino physics
|DE92-003855| p 1360 N92-17589
A study of gamma ray generation from channeled electrons and positions
|AD-A241993| p 1361 N92-17608
Hard-surface contamination detection exercise
|DE92-004750| p 1330 N92-17798

RADIATION PRESSURE
Temporally-specific modification of myelinated axon excitability in vitro following a single ultrasound pulse
|AD-A242329| p 1326 N92-17474
Cooled ion frequency standard
|AD-A242030| p 1360 N92-17549

RADIATION PROTECTION
Ultrafast passive shields for laser and ballistic protection
|AD-A243206| p 1303 N92-17175

RADIATION PYROMETERS
Results of measured temperature distribution on an adiabatic wing model with radiation thermometer
|NAL-TM-610| p 1225 N92-17755

RADIATION SHIELDING
Ultrafast passive shields for laser and ballistic protection
|AD-A243206| p 1303 N92-17175

RADIATION SOURCES
PILAC: A Pion Linac facility for 1-GeV pion physics at LAMPF
|DE92-003789| p 1364 N92-17794

RADIATION TOLERANCE
A PC program to calculate the one-sided lower tolerance limit for total ionizing dose radiation data
|AD-A242365| p 1357 N92-17394
Total Dielectric Isolation (TDI) of fully depleted device structures
|AD-A241926| p 1289 N92-17439

RADIATION TRANSPORT
Background Atmosphere Radiance Day (BARD) and Night (BARN)
|AD-A243153| p 1316 N92-17239

RADIATIVE TRANSFER
A variational assimilation method for satellite and conventional data: Development of basic model for diagnosis of cyclone systems
|NASA-CR-188236| p 1321 N92-17975
A variational formalism for the radiative transfer equation: Prelude to model 3 p 1322 N92-17978
A variational formalism for the radiative transfer equation and a geostrophic, hydrostatic atmosphere: Prelude to model 3 p 1322 N92-17979

RADII
Significant digit computation of the ellipsoidal coverage function and its inverse
|AD-A242322| p 1350 N92-17242
On the concept of varying influence radii for a successive corrections objective analysis p 1322 N92-17980

RADIO ANTENNAS
Radio frequency hazard monitoring-USAKA
|AD-A242873| p 1283 N92-17563

RADIO ASTRONOMY
Metriwave final report
|NASA-CR-189816| p 1279 N92-17046

RADIO COMMUNICATION
A ring model for local/mobile radio communications with variable packet length
|AD-A241856| p 1279 N92-17036
Effect of economic techniques on radio frequency utilization
|AD-A243187| p 1282 N92-17366
Radio frequency hazard monitoring-USAKA
|AD-A242873| p 1283 N92-17563
C3 Systems Technology Symposium on Advance Planning Briefings for Industry
|AD-A243466| p 1391 N92-17657
QTCM software documentation. Volume 2: User's manual
|AD-A242744| p 1344 N92-17948

RADIO DIRECTION FINDERS
Radio sky mapping from satellites at very low frequencies
|NASA-TM-105452| p 1387 N92-17694

RADIO EQUIPMENT
A ring model for local/mobile radio communications with variable packet length
|AD-A241856| p 1279 N92-17036

RADIO FREQUENCIES
Terminal Doppler weather radar test bed operation, Orlando: January-June 1990
|AD-A242890| p 1318 N92-17028
Effect of economic techniques on radio frequency utilization
|AD-A243187| p 1282 N92-17366
Evaporation duct communication: Test plan, part 2
|AD-A243505| p 1282 N92-17383

RADIO RECEIVERS
Multisensor signal processing techniques (hybrid GPS/LORAN-C with RAIM)
|AD-A242323| p 1281 N92-17244

RADIO TRANSMISSION
Investigation of mechanisms for the source and loss of electrons from the radiation belts using data from SEEP, SCATHA and P78-1 satellites
|AD-A243376| p 1317 N92-17405

RADIO WAVES
An investigation of methods for updating ionospheric scintillation models using topside in-situ plasma density measurements
|AD-A243378| p 1316 N92-17209

RADIOACTIVE DECAY
What experiments say about possibility of the new particle existence with mass less than the kaon mass
|DE91-634551| p 1357 N92-17408
The determination of the number of light neutrino species
|ETN-92-90564| p 1359 N92-17519

RADIOBIOLOGY
Biological effects of protracted exposure to ionizing radiation: Review, analysis, and model development
|AD-A242981| p 1329 N92-17476

RADIOMETERS
Sea surface environmental conditions in the Gulf of Alaska during April 1990 using SSM/I
|AD-A241909| p 1323 N92-17041
Spatial sampling error of a scanning radiation budget radiometer
|MITT-76| p 1317 N92-17542

RADIOSONDES
A proposed improved method of radiosonde humidity sensing
|AD-A242954| p 1319 N92-17233

RADIUM ISOTOPES
Importance of the neutron-proton interactions for the even Ra-Th nuclei
|DE92-600628| p 1363 N92-17956

RADOMES
Flow visualization and wake analysis for standard and modified configurations of the AN/ALQ-78 antenna pod
|AD-A243552| p 1224 N92-17339

RAIL TRANSPORTATION
Workshop on Technology Issues of Superconducting MAGLEV Transportation Systems
|DE92-002288| p 1307 N92-17604

RAILS
An investigation of gouge initiation in high-velocity sliding contact
|DE92-003944| p 1311 N92-17937

RAMAN SPECTRA
Direct speciation of metal and metalloid ions by optical spectroscopies
|DE92-003868| p 1261 N92-17727

RAMJET ENGINES
Hydrogen fueled subsonic-ram-combustor model tests for an air-turbo-ram engine
|NAL-TR-1064T| p 1236 N92-17855

RANDOM ACCESS MEMORY
A ring model for local/mobile radio communications with variable packet length
|AD-A241856| p 1279 N92-17036

RANDOM WALK
The effects of field errors on low-gain free electron lasers
|AD-A243710| p 1303 N92-17127

RANGE SAFETY
Laser range safety
|AD-A243606| p 1305 N92-17962

RANGES (FACILITIES)
Laser range safety
|AD-A243606| p 1305 N92-17962

RAPID TRANSIT SYSTEMS
Workshop on Technology Issues of Superconducting MAGLEV Transportation Systems
|DE92-002288| p 1307 N92-17604

RARE EARTH COMPOUNDS
Examining Si3N4 base materials with various rare earth additions
|AD-A243668| p 1372 N92-17082

RARE EARTH ELEMENTS
Theoretical crystal-field calculations for rare-earth ions in 3-5 semiconductor compounds
|AD-A243098| p 1371 N92-16995
Examining Si3N4 base materials with various rare earth additions
|AD-A243668| p 1372 N92-17082

RARE GASES
Rates and mechanisms of metastable deactivation over surfaces
|AD-A243391| p 1361 N92-17652

RATES (PER TIME)
Quenching and rotational energy transfer in molecular bromine: Br2(B)
|AD-A241987| p 1357 N92-17321

RATS
Assessment of the behavioral and neurotoxic effects of hexachlorobenzene (HCB) in the developing rat
|AD-A243658| p 1325 N92-17121

RAWINSONDES
A variational formalism for the radiative transfer equation: Prelude to model 3 p 1322 N92-17978

RAY TRACING
Bottom contour influence on ray tracing
|AD-A242411| p 1323 N92-17078
Modeling convergence zone gain on MS-DOS based personal computers
|AD-A243252| p 1341 N92-17558
Parallelizing serial code for a distributed processing environment with an application to high frequency electromagnetic scattering
|AD-A243755| p 1284 N92-17721
Verification and validation of the simulated radar image (SRIM) code radar cross section predictions
|AD-A243651| p 1285 N92-17737

RDX
Pyrolysis GC-FTIR studies of a LOVA propellant formulation series
|AD-A242844| p 1275 N92-17562
Detection of explosives material on single microparticles
|DE92-004408| p 1276 N92-17963

REACTION KINETICS
Relaxation processes of vibrationally excited H2O in the mesosphere and thermosphere
|AD-A241853| p 1315 N92-17035
A theoretical study of the combustion of magnesium/teflon/viton pyrotechnic compositions
|AD-A243244| p 1275 N92-17058
Catalytic studies on a novel synthesis of methanol
|DE92-002904| p 1275 N92-17184
An oxygen tracer study of InP oxidation
|AD-A242832| p 1259 N92-17246
Artificial photosynthesis: Progress toward molecular systems for photoconversion
|DE92-003370| p 1326 N92-17471
Reaction kinetics and transport properties of the CaO-SO2-O2 system in absence of intra-particle diffusion
|DE91-002086| p 1261 N92-17788
Ion mixing of semiconductor layered-structures
|DE92-003756| p 1377 N92-17791
Process of converting starch to glucose and glucose to lactic acid
|DE92-003840| p 1255 N92-17867
Kinetics of a new phase formation in supersaturated solid solutions. 1. Dilute one-component systems
|DE92-610065| p 1262 N92-17943

REACTIVITY
Computational studies of energetic nitramines
|AD-A241870| p 1356 N92-17038
Propane aromatization over gallium containing HZSM-5 zeolites
|ETN-92-90897| p 1262 N92-17925

REACTOR DESIGN
Cooperative program to analyze heat transport at high beta in DIII-D
|DE92-003545| p 1370 N92-17606
UCLA program in reactor studies: The ARIES tokamak reactor study
|DE92-003760| p 1370 N92-17792

REACTOR MATERIALS
Fracture toughness evaluation for N Reactor pressure tubes of Zircaloy-2 using the electric-potential method
|DE92-003631| p 1311 N92-17713

REACTOR SAFETY
UCLA program in reactor studies: The ARIES tokamak reactor study
| DE92-003760 | p 1370 N92-17792
Energy production using fission fragment rockets
| DE92-002192 | p 1364 N92-17876
REACTOR TECHNOLOGY
Summary reports of activities under visiting research program
| DE91-522477 | p 1391 N92-17623
UCLA program in reactor studies: The ARIES tokamak reactor study
| DE92-003760 | p 1370 N92-17792
READ-ONLY MEMORY DEVICES
Fractal image encoding
| AD-A243620 | p 1344 N92-17921
REAL GASES
ZEUS user manual real gas effects
| AD-A242224 | p 1225 N92-17446
REAL TIME OPERATION
The real-time cost of timing uncertainty: Consensus and failure detection
| AD-A243176 | p 1345 N92-16997
Development of real-time image and in situ data analysis at sea
| AD-A243682 | p 1242 N92-17075
The applied tomography experiment of 1990
| AD-A243525 | p 1354 N92-17086
CALS database usage and analysis tool study
| AD-A243205 | p 1382 N92-17174
Using mappings to prove timing properties
| AD-A242862 | p 1277 N92-17263
Facing page test for the astronaut science advisor presentation p 1248 N92-17411
Real Time Data System (RTDS) p 1249 N92-17421
Technical evaluation report on the 52nd Symposium on Software for Guidance and Control
| AGARD-AR-302 | p 1341 N92-17498
Specification and compositional verification of real-time systems
| ETN-92-90580 | p 1341 N92-17521
The StarLite Project prototyping real-time software
| AD-A242032 | p 1342 N92-17636
Real-time edge-enhanced optical correlator
| NASA-CASE-NPO-18379-1-CU | p 1367 N92-17675
Near real-time stereo vision system
| NASA-CASE-NPO-18593-1-CU | p 1368 N92-17864
RECEIVERS
Metriwave final report
| NASA-CR-189816 | p 1279 N92-17046
Receiver performance of laser ranging measurements between the Lunar Observer and a subsatellite for lunar gravity studies
| NASA-CR-189860 | p 1303 N92-17152
GPS interferometric attitude and heading determination: Initial flight test results p 1221 N92-17994
RECOGNITION
New algorithms for broad-band and narrowband source localization and a separable 2-D IIR filter realization
| AD-A243457 | p 1291 N92-17654
RECOMBINATION REACTIONS
The charge exchange recombination diagnostic system on the D3-D tokamak
| DE92-003805 | p 1369 N92-17456
RECTANGULAR BEAMS
Determination of symmetric end loads from bulk stresses on a rectangular prism
| AD-A242973 | p 1310 N92-17254
RECURSIVE FUNCTIONS
Data fusion for least squares
| AD-A243507 | p 1352 N92-17384
RECYCLING
Scale-up of recovery process for waste solvents
| KCP-613-4479 | p 1277 N92-17535
REDUCED GRAVITY
Techniques for determination of impact forces during walking and running in a zero-G environment
| NASA-TP-3159 | p 1328 N92-17022
Space Station Freedom science utilization: 2000 and beyond p 1244 N92-17107
Microgravity Science and Applications Program tasks, 1990 revision
| NASA-TM-4284 | p 1276 N92-17945
REFERENCE ATMOSPHERES
Range reference atmosphere, Fairbanks
| AD-A243314 | p 1318 N92-17113
REFLECTANCE
Acoustic impedance of materials from reverberation time
| AD-A243184 | p 1354 N92-16999
Groundscreen characterization
| AD-A243164 | p 1311 N92-17208
Enhanced backscattering of light from randomly rough diffusers: Appendix
| AD-A243436 | p 1366 N92-17485
A tunable solid state laser with high wavelength selectivity over a preselected wavelength range
| AD-D015055 | p 1304 N92-17627
A hybrid modulation for the dissemination of weather data to aircraft p 1220 N92-17991
REFLECTION
A study of nonlinear reflection and optical switching in indium antimonide
| AD-A242835 | p 1365 N92-17249
Laser range safety
| AD-A243606 | p 1305 N92-17962
REFLECTOR ANTENNAS
Advanced Communication Technology Satellite (ACTS) multibeam antenna analysis and experiment
| NASA-TM-105420 | p 1279 N92-17047
REFRACTIVITY
Sensing refractive turbulence profiles using wave front slope measurements from two reference sources
| AD-A243696 | p 1315 N92-17094
Two-beam coupling measurements of grating phase in a photorefractive polymer
| AD-A243746 | p 1268 N92-17195
Self-collimated unstable resonator semiconductor laser
| NASA-CASE-NPO-18386-1-CU | p 1305 N92-17899
REFRACTORY MATERIALS
High-temperature durability considerations for HSCT combustor
| NASA-TP-3162 | p 1267 N92-17070
Alternate/modified binders for asphalt airfield pavements
| AD-A242829 | p 1238 N92-17260
Making of functionally gradient materials data base
| NAL-TM-621 | p 1385 N92-17787
REFRIGERATORS
Three-stage sorption type cryogenic refrigeration system and method employing heat regeneration
| NASA-CASE-NPO-18366-1-CU | p 1277 N92-17674
REFUELING
STV fueling options p 1249 N92-17415
REGENERATIVE COOLING
Three-stage sorption type cryogenic refrigeration system and method employing heat regeneration
| NASA-CASE-NPO-18366-1-CU | p 1277 N92-17674
REGENERATIVE FUEL CELLS
Thermally regenerative fuel cells
| AD-A242900 | p 1290 N92-17629
REGIONS
Experimental investigation of adiabatic shear banding at different impact velocities
| AD-A243011 | p 1310 N92-17256
REGRESSION ANALYSIS
Environmental containment property estimation using QSARs in an expert system
| AD-A243728 | p 1336 N92-17720
REGULATIONS
Worldwide Environmental Compliance Assessment and Management Program (ECAMP)
| AD-A242874 | p 1314 N92-17598
Proceedings of the Conference on Health Physics
| DE92-704335 | p 1331 N92-17802
REINFORCEMENT (STRUCTURES)
Structures to resist the effects of accidental explosions
| AD-A243272 | p 1277 N92-17272
REISSNER-NORDSTROM SOLUTION
A classical instability of Reissner-Nordstrom solutions and the fate of magnetically charged black holes
| NASA-CR-189843 | p 1388 N92-17697
RELATIVISTIC PARTICLES
Investigation of mechanisms for the source and loss of electrons from the radiation belts using data from SEEP, SCATHA and P78-1 satellites
| AD-A243376 | p 1317 N92-17405
RELATIVISTIC THEORY
Geometrical methods for the analysis of cosmological observations
| ETN-92-90584 | p 1386 N92-17523
Relativistic nuclear many-body theory
| DE92-003258 | p 1362 N92-17789
RELATIVITY
Lie-isotopic generalization of the Poincare symmetry: Classical formulation
| DE91-642825 | p 1379 N92-17531
Future prospects of pregeometry
| DE92-704278 | p 1379 N92-17817
RELAXATION METHOD (MATHEMATICS)
Machine scheduling and Lagrangian relaxation
| ETN-92-90569 | p 1353 N92-17839
RELAY SATELLITES
Multiple-access phased array antenna simulator for a digital beam forming system investigation
| NASA-TM-105422 | p 1279 N92-17062
RELIABILITY
A managerial approach for reliability verification of mechanical equipment
| MBB-UK-0140-91-PUB | p 1308 N92-17341
Integration of RAMS activities during the development phase of Ariane 5-components (example: Vulcain thrust chamber)
| MBB-UK-0144-91-PUB | p 1240 N92-17527
Constraints and difficulties in implementations of RAMS assurance programmes
| MBB-UK-0141-91-PUB | p 1309 N92-17544
The need for active software product assurance management for systems critical software
| MBB-UK-0142-91-PUB | p 1341 N92-17545
RELIABILITY ANALYSIS
Reliability analysis of structural ceramic components using a three-parameter Weibull distribution
| NASA-TM-105370 | p 1267 N92-17060
Testing of spacecraft in long-term storage
| AD-A242906 | p 1250 N92-17580
Software reliability models for critical applications
| DE92-004797 | p 1345 N92-17969
RELIABILITY ENGINEERING
Research in some future directions in reliability and quality control
| AD-A242865 | p 1308 N92-17231
Intelligent failure-tolerant control p 1222 N92-18000
RELIEF MAPS
Determination of bistatic radar clutter power from topographic data
| AD-A243697 | p 1280 N92-17095
REMOTE CONTROL
Telerobotic ground-remote operations p 1247 N92-17360
Closed-loop motor control using high-speed fiber optics
| NASA-CASE-MSC-21806-1 | p 1368 N92-17863
Experimental investigation of passive infrared ice detection for helicopter applications p 1220 N92-17986
REMOTE MANIPULATOR SYSTEM
Status of Japanese Experiment Module (JEM) activities p 1243 N92-17101
REMOTE SENSING
Sensing refractive turbulence profiles using wave front slope measurements from two reference sources
| AD-A243696 | p 1315 N92-17094
REQUIREMENTS
General requirements and techniques for component fatigue life substantiation in Australian service helicopters
| AD-A242881 | p 1233 N92-17565
RESEARCH
Investigation of air transportation technology at Princeton University, 1990-1991 p 1221 N92-17995
RESEARCH AIRCRAFT
Aerodynamic development of the X-31 aircraft for the high angle of attack region
| MBB-FE211-S-PUB-452 | p 1233 N92-17313
RESEARCH AND DEVELOPMENT
Contributive research and development
| AD-A243331 | p 1391 N92-17079
Technology development on evolutionary space station p 1243 N92-17106
Scientific and technological relations between the United States and Japan: Issues and recommendations
| PB91-219170 | p 1385 N92-17283
Catalysis looks to the future
| LC-91-66333 | p 1261 N92-17786
Microgravity Science and Applications Program tasks, 1990 revision
| NASA-TM-4284 | p 1276 N92-17945
RESEARCH FACILITIES
Development of an XUV-IR free-electron laser user facility for scientific research and industrial applications
| DE92-003862 | p 1304 N92-17726
RESEARCH MANAGEMENT
Summaries of FY 1991 engineering research
| DE92-004708 | p 1277 N92-17593
RESEARCH PROJECTS
FY92 mathematical research project proposal briefing
| AD-A243163 | p 1350 N92-17207
FY 1991 scientific and technical reports, articles, papers, and presentations
| NASA-TM-103567 | p 1384 N92-17586
Summary reports of activities under visiting research program
| DE91-522477 | p 1391 N92-17623
Magnetohydrodynamic projects at the CDIF
| DE92-002636 | p 1370 N92-17664
RESEARCH VEHICLES
Model identification and control system design for the lambda unmanned research vehicle
| AD-A241859 | p 1306 N92-17024

A robust digital flight control system for an unfanned research vehicle using discrete quantitative feedback theory
| AD-A243638 | p 1237 N92-17748

RESIDUAL STRESS
Studies of hetero-epitaxy of GaAs films on Si substrate for effective control of density and internal stress
| AD-A241882 | p 1374 N92-17594
Residual stresses in a prestressed steel pressure vessel wrapped with multilayered composites
| AD-A243429 | p 1311 N92-17930
Damage mechanisms in composites
| AD-A242748 | p 1258 N92-17950

RESIN BONDING
Reactions and interactions in liquid crystalline media
| AD-A242355 | p 1374 N92-17449

RESIN MATRIX COMPOSITES
Effective dynamic material parameters and localized scattering
| AD-A241957 | p 1310 N92-17320

RESINS
Polymer infiltration studies
| NASA-CR-189773 | p 1266 N92-17004
A theoretical study of the combustion of magnesium/teflon/viton pyrotechnic compositions
| AD-A243244 | p 1275 N92-17058
Long-term corrosion evaluation of stainless steels in Space Shuttle iodinated resin and water
| NASA-TM-104743 | p 1264 N92-17376
Evaluation of an Interdigitated Gate Electrode Field-Effect Transistor (IGEFET) for in situ resin cure monitoring
| AD-A243713 | p 1289 N92-17501

RESONANCE
Waveguide four-wave mixing
| AD-A243555 | p 1286 N92-17017
Superdirective properties of closed loops of parallel coplanar dipoles
| AD-A243009 | p 1288 N92-17268
Natural resonances of slotted cylinder configurations
| AD-A241934 | p 1282 N92-17441

RESONANT FREQUENCIES
Detection and spectroscopy of single pentacene molecules in a p-terphenyl crystal by means of fluorescence excitation
| AD-A243747 | p 1356 N92-17196
Single molecule spectral diffusion in a solid detected via fluorescence spectroscopy
| AD-A243748 | p 1356 N92-17197
Suspended substrate resonator design
| AD-A243250 | p 1290 N92-17573

RESONATORS
A discontinuity study in shielded coplanar line
| AD-A242976 | p 1288 N92-17290
Suspended substrate resonator design
| AD-A243250 | p 1290 N92-17573
Self-collimated unstable resonator semiconductor laser
| NASA-CASE-NPO-18386-1-CU | p 1305 N92-17899
Performance of hole coupling resonator in the presence of asymmetric modes and FEL gain
| DE92-003907 | p 1305 N92-17936

RESOURCE ALLOCATION
Resource allocation in distributed memory multiprocessing
| AD-A243165 | p 1345 N92-17188

RESOURCES MANAGEMENT
NASA total quality management 1990 accomplishments report
| NASA-TM-105465 | p 1308 N92-17199
ISE advanced technology p 1249 N92-17420
Aquatic plant management program. Supplement
| AD-A242420 | p 1314 N92-17723

RESPONSES
Visual determination of industrial color-difference tolerances using probit analysis
| AD-A243545 | p 1334 N92-17617

RETINA
Analysis of visual illusions using multiresolution wavelet decomposition based models
| AD-A243712 | p 1332 N92-17500

RETROFITTING
Assessment of cockpit interface concepts for data link retrofit
| NASA-CR-187615 | p 1228 N92-17512

RETROREFLECTION
The calibration process of digital cameras
| ETN-92-90583 | p 1301 N92-17437
Multiperiod-grating surface-emitting lasers
| NASA-CASE-NPO-17763-1-CU | p 1305 N92-17862

REVERBERATION
Acoustic impedance of materials from reverberation time
| AD-A243184 | p 1354 N92-16999

REVERBERATION CHAMBERS
Frequency stirring: An alternate approach to mechanical mode-stirring for the conduct of electromagnetic susceptibility testing
| AD-A243551 | p 1279 N92-17031

REVERSE FIELD PINCH
A one-dimensional plasma and impurity transport model for reversed field pinches
| DE92-004691 | p 1371 N92-17933

REYNOLDS NUMBER
An experimental investigation of chemically-reacting, gas-phase turbulent jets
| AD-A243036 | p 1296 N92-17276
Flow between two stationary disks and a rotating shroud
| AERO-REPT-9001 | p 1300 N92-17851

RISK
A management case analysis of the Department of Defense contractor risk assessment guide program
| AD-A243515 | p 1380 N92-17388
The National Hurricane Center Risk Analysis Program (HURISK)
| PB91-236463 | p 1321 N92-17705

ROBOT ARMS
High level language-based robotic control system
| NASA-CASE-NPO-17918-2-CU | p 1349 N92-17895

ROBOT CONTROL
Cyclone: A laser scanner for mobile robot navigation
| AD-A243517 | p 1303 N92-17080
A system for fast navigation of autonomous vehicles
| AD-A243523 | p 1228 N92-17147
Telerobotic ground-remote operations p 1247 N92-17360
Application of multi-target tracking to sonar-based mobile robot navigation
| OUEL-1819/90 | p 1229 N92-17878
High level language-based robotic control system
| NASA-CASE-NPO-17918-2-CU | p 1349 N92-17895

ROBOT DYNAMICS
Cyclone: A laser scanner for mobile robot navigation
| AD-A243517 | p 1303 N92-17080
A system for fast navigation of autonomous vehicles
| AD-A243523 | p 1228 N92-17147
Application of multi-target tracking to sonar-based mobile robot navigation
| OUEL-1819/90 | p 1229 N92-17878

ROBOT SENSORS
Analysis and experimental evaluation of a Stewart platform-based force/torque sensor
| NASA-CR-189861 | p 1252 N92-17150
Collision avoidance sensor skin p 1247 N92-17361

ROBOTICS
Cyclone: A laser scanner for mobile robot navigation
| AD-A243517 | p 1303 N92-17080
Analysis and experimental evaluation of a Stewart platform-based force/torque sensor
| NASA-CR-189861 | p 1252 N92-17150
Near real-time stereo vision system
| NASA-CASE-NPO-18593-1-CU | p 1368 N92-17864
High level language-based robotic control system
| NASA-CASE-NPO-17918-2-CU | p 1349 N92-17895

ROBOTS
Cyclone: A laser scanner for mobile robot navigation
| AD-A243517 | p 1303 N92-17080
Analysis and experimental evaluation of a Stewart platform-based force/torque sensor
| NASA-CR-189861 | p 1252 N92-17150
Extendable pipe crawler
| DE91-011570 | p 1306 N92-17183
High level language-based robotic control system
| NASA-CASE-NPO-17918-2-CU | p 1349 N92-17895

ROBUSTNESS (MATHEMATICS)
Modelling aspects and robustness issues in rotorcraft system identification p 1231 N92-17159
An aerocapture attitude control systems incorporating robustness and vehicle parameter identification
| AD-A243360 | p 1245 N92-17302
Control algorithms for aerobraking in the Martian atmosphere
| AD-A243349 | p 1239 N92-17730
Stochastic robustness p 1221 N92-17997
Intelligent failure-tolerant control p 1222 N92-18000
Technical notes and correspondence: Stochastic robustness of linear time-invariant control systems p 1222 N92-18002

ROCKET LININGS
Case bond liner systems for solid rocket motors
| AD-A242297 | p 1253 N92-17085

ROCKET NOZZLES
Transpiration cooled throat for hydrocarbon rocket engines
| NASA-CR-184272 | p 1253 N92-17495
Thruster sealing system and apparatus
| NASA-CASE-MSC-21898-1 | p 1307 N92-17872

ROCKET OXIDIZERS
Pyrolysis GC-FTIR studies of a LOVA propellant formulation series
| AD-A242844 | p 1275 N92-17562

ROCKET PROPELLED SLEDS
An investigation of gouge initiation in high-velocity sliding contact
| DE92-003944 | p 1311 N92-17937

ROCKET TEST FACILITIES
Rocket tests in Mississippi to be heavily restricted
| GAO/NSIAD-92-86 | p 1240 N92-17741

ROCKET-BORNE INSTRUMENTS
Aries x ray objective grating spectrograph
| NASA-CR-189245 | p 1386 N92-17003

ROLL
Model identification and control system design for the lambda unmanned research vehicle
| AD-A241859 | p 1306 N92-17024

ROLLERS
Analysis of cam roller followers
| ESDU-91026 | p 1307 N92-17852

ROLLING CONTACT LOADS
Analysis of cam roller followers
| ESDU-91026 | p 1307 N92-17852

ROLLING MOMENTS
An experimental investigation of leading edge vortical flow about a delta wing during wing rock
| AD-A243363 | p 1223 N92-17114

ROOM TEMPERATURE
A reexamination of F-19 NMR in selected solids, the conductor Ag2F and reference insulators for studies of YBa2Cu3O7-type superconductors
| AD-A243194 | p 1372 N92-17219

ROSS ICE SHELF
Evaluation of solar flares and electron precipitation by nitrate distribution in Antarctica
| AD-A243026 | p 1389 N92-17235

ROTARY STABILITY
Application areas for rotorcraft system identification: Simulation model validation p 1232 N92-17164

ROTARY WING AIRCRAFT
Rotorcraft System Identification
| AGARD-LS-178 | p 1230 N92-17153
Modelling aspects and robustness issues in rotorcraft system identification p 1231 N92-17159
Assessment of rotorcraft system identification as applied to the AH-64 p 1231 N92-17160
BO 105 identification results p 1231 N92-17161
Industry view on rotorcraft system identification p 1232 N92-17163
Application areas for rotorcraft system identification: Simulation model validation p 1232 N92-17164
System identification methods for handling-qualities evaluation p 1232 N92-17165

ROTARY WINGS
Periodic trim solutions with HP-version finite elements in time
| NASA-CR-189778 | p 1236 N92-17019
The solution of a singular integral equation arising from a lifting surface theory for rotating blades p 1224 N92-17303

ROTATING CYLINDERS
Flow between two stationary disks and a rotating shroud
| AERO-REPT-9001 | p 1300 N92-17851

ROTATING DISKS
Numerical simulation of fluid flow and heat transfer in a thin liquid film over a stationary and rotating disk and comparison with experimental data
| NASA-CR-189253 | p 1300 N92-17887

ROTATING FLUIDS
Studies of baroclinic flow
| AD-A243050 | p 1296 N92-17309

ROTATING SHAFTS
Actively controlled shaft seals for aerospace applications
| NASA-CR-189808 | p 1306 N92-17304

ROTATION
Analysis of the terminal Doppler weather radar algorithm for detecting rotation associated with microbursts
| AD-A242840 | p 1318 N92-17050
Surface pressure measurements on the wing of a wind tunnel model during steady rotation
| AD-A243047 | p 1223 N92-17281
Space Station Freedom solar alpha joint growth capability p 1252 N92-17772
Fiber optic angular orientation sensor digital serial encoding
| AD-D015102 | p 1302 N92-17826

ROTOR AERODYNAMICS
Rotorcraft System Identification
| AGARD-LS-178 | p 1230 N92-17153
Application areas for rotorcraft system identification: Simulation model validation p 1232 N92-17164

ROTOR BODY INTERACTIONS
Rotorcraft System Identification
| AGARD-LS-178 | p 1230 N92-17153
ROTORCRAFT AIRCRAFT
SA 330 Puma identification results
p 1231 N92-17162
ROTORS
Viscous three-dimensional calculations of transonic fan performance
| NASA-TM-103800 | p 1219 N92-17346
RP-1 ROCKET PROPELLANTS
Transpiration cooled throat for hydrocarbon rocket engines
| NASA-CR-184272 | p 1253 N92-17495
RUBBER
Thermal insulation chemical composition and method of manufacture
| AD-D015106 | p 1257 N92-17836
RUNGE-KUTTA METHOD
A new interpolation procedure for adapting Runge-Kutta methods to delay differential equations
| TW-90-09 | p 1351 N92-17517

S

SACCADIC EYE MOVEMENTS
Image analysis using Gabor transforms: Correlated with human saccadic movement data to identify the human visual search strategy
| AD-A243692 | p 1338 N92-17093
Analysis of visual illusions using multiresolution wavelet decomposition based models
| AD-A243712 | p 1332 N92-17500
SAFETY FACTORS
Discussion for possibility of some aerodynamic ground effect craft
| NAL-TM-619 | p 1278 N92-17757
SAFETY MANAGEMENT
Constraints and difficulties in implementations of RAMS assurance programmes
| MBB-UK-0141-91-PUB | p 1309 N92-17544
The need for active software product assurance management for systems critical software
| MBB-UK-0142-91-PUB | p 1341 N92-17545
SALINITY
A study on hydrographic conditions and salt budget calculation for the Gulf of Farallones with the data collected in August 1990
| AD-A243406 | p 1324 N92-17119
User's guide for a three-dimensional numerical hydrodynamic, salinity, and temperature model of Chesapeake Bay
| AD-A242993 | p 1324 N92-17298
SALYUT SPACE STATION
Analysis of orbital elements and atmospheric activity to ascertain possible presence of an ion propulsion capability aboard Salyut 7/Cosmos 1686
| AD-A243654 | p 1251 N92-17762
SAMPLERS
Gibbs sampling for marginal posterior expectations
| AD-A243212 | p 1352 N92-17178
Bayesian computations in survival models via the Gibbs sampler
| AD-A242343 | p 1353 N92-17643
SAMPLING
Gibbs sampling for marginal posterior expectations
| AD-A243212 | p 1352 N92-17178
Research in some future directions in reliability and quality control
| AD-A242865 | p 1308 N92-17231
Spatial sampling error of a scanning radiation budget radiometer
| MITT-76 | p 1317 N92-17542
A probabilistic derivation of Stirling's formula
| AD-A241899 | p 1354 N92-17548
SATELLITE ANTENNAS
Advanced Communication Technology Satellite (ACTS) multibeam antenna analysis and experiment
| NASA-TM-105420 | p 1279 N92-17047
SATELLITE COMMUNICATION
Advanced Communication Technology Satellite (ACTS) multibeam antenna analysis and experiment
| NASA-TM-105420 | p 1279 N92-17047
A computer solution for multiple satellite-satellite and satellite-ground station visibility determination
| AD-A243490 | p 1250 N92-17430
Interim Service ISDN Satellite (ISIS) hardware experiment design for advanced ISDN satellite design and experiments
| NASA-CR-186943 | p 1250 N92-17585
SATELLITE DESIGN
Interim Service ISDN Satellite (ISIS) hardware experiment design for advanced ISDN satellite design and experiments
| NASA-CR-186943 | p 1250 N92-17585
SATELLITE IMAGERY
Source of cold water in Monterey Bay observed by AVHRR satellite imagery
| AD-A242843 | p 1323 N92-17051
Development of real-time image and in situ data analysis at sea
| AD-A243682 | p 1242 N92-17075
The applied tomography experiment of 1990
| AD-A243525 | p 1354 N92-17086
Numerical simulation of cirrus clouds: Fire case study and sensitivity analysis
| AD-A242902 | p 1321 N92-17631
SATELLITE INSTRUMENTS
Development of real-time image and in situ data analysis at sea
| AD-A243682 | p 1242 N92-17075
Receiver performance of laser ranging measurements between the Lunar Observer and a subsatellite for lunar gravity studies
| NASA-CR-189860 | p 1303 N92-17152
Preliminary design of a model to assess the effect of Space Surveillance Network (SSN) sensor upgrades on orbit prediction accuracies relative to the US Anti-Satellite (ASAT) mission
| AD-A243736 | p 1353 N92-17479
SATELLITE NETWORKS
Development of real-time image and in situ data analysis at sea
| AD-A243682 | p 1242 N92-17075
A computer solution for multiple satellite-satellite and satellite-ground station visibility determination
| AD-A243490 | p 1250 N92-17430
Preliminary design of a model to assess the effect of Space Surveillance Network (SSN) sensor upgrades on orbit prediction accuracies relative to the US Anti-Satellite (ASAT) mission
| AD-A243736 | p 1353 N92-17479
Interim Service ISDN Satellite (ISIS) hardware experiment design for advanced ISDN satellite design and experiments
| NASA-CR-186943 | p 1250 N92-17585
Satellite links for television contribution: Reception requirements for links using transportable transmitting earth stations
| BBC-RD-1991/5 | p 1285 N92-17885
SATELLITE OBSERVATION
Radio sky mapping from satellites at very low frequencies
| NASA-TM-105452 | p 1387 N92-17694
On the concept of varying influence radii for a successive corrections objective analysis p 1322 N92-17980
SATELLITE ORBITS
Preliminary design of a model to assess the effect of Space Surveillance Network (SSN) sensor upgrades on orbit prediction accuracies relative to the US Anti-Satellite (ASAT) mission
| AD-A243736 | p 1353 N92-17479
SATELLITE SOUNDING
Integration of an anti-parallel pair of planar Schottky barrier diodes for millimeter and submillimeter wavelengths
| AD-A243371 | p 1287 N92-17189
SATELLITE TRACKING
Preliminary design of a model to assess the effect of Space Surveillance Network (SSN) sensor upgrades on orbit prediction accuracies relative to the US Anti-Satellite (ASAT) mission
| AD-A243736 | p 1353 N92-17479
SATELLITE TRANSMISSION
Satellite links for television contribution: Reception requirements for links using transportable transmitting earth stations
| BBC-RD-1991/5 | p 1285 N92-17885
SATELLITE-BORNE PHOTOGRAPHY
Source of cold water in Monterey Bay observed by AVHRR satellite imagery
| AD-A242843 | p 1323 N92-17051
SCALARS
Evaluation of scalar value estimation techniques for 3D medical imaging
| AD-A243687 | p 1328 N92-17089
SCANNING
Image scanning using a fractal curve
| BBC-RD-1991/4 | p 1285 N92-17886
SCATTERING
Characterization of the thermalness of a fissile system with a 2-group diffusion theory parameter
| AD-A243065 | p 1360 N92-17555
Interstellar scattering towards the galactic center as probed by OH/IR stars p 1390 N92-18004
SCATTERING AMPLITUDE
Proton-proton and proton-antiproton elastic scattering at high energies: Theory, phenomenology, and experiment
| DE92-004414 | p 1364 N92-17964
SCATTERING COEFFICIENTS
A CAD model for the axial inductive strip with finite thickness centered in homogeneous finline with w/b 1
| AD-A243553 | p 1278 N92-17016
SCATTERING CROSS SECTIONS
Pion-nucleus cross sections
| DE92-600631 | p 1363 N92-17958
SCENE ANALYSIS
Optical image segmentation using wavelet correlation
| AD-A243650 | p 1367 N92-17736
Effect of two types of scene detail on detection of altitude change in a flight simulator
| AD-A242034 | p 1333 N92-17758
SCHEDULES
Operations mission planner beyond the baseline
p 1246 N92-17353
SCHEDULING
Operations mission planner beyond the baseline
p 1246 N92-17353
ISE advanced technology p 1249 N92-17420
Improved task scheduling for parallel simulations
| AD-A243721 | p 1346 N92-17507
Development of a knowledge base for use in an Expert System Advisor for Aircraft Maintenance Scheduling (ESAAMS)
| AD-A243435 | p 1381 N92-17687
Machine scheduling and Lagrangian relaxation
| ETN-92-90569 | p 1353 N92-17839
SCHOTTKY DIODES
Improved 320x244-element PtSi Schottky-barrier IR-CCD image sensor
| AD-A242026 | p 1301 N92-17140
Integration of an anti-parallel pair of planar Schottky barrier diodes for millimeter and submillimeter wavelengths
| AD-A243371 | p 1287 N92-17189
Au and Al Schottky barrier formation on GaAs (100) surfaces prepared by thermal desorption of a protective arsenic coating
| DE92-002456 | p 1376 N92-17781
SCHROEDINGER EQUATION
State vector reduction. Part 1: Dynamical reduction theories; changing quantum theory so the statevector represents reality
| DE91-641488 | p 1379 N92-17824
SCINTILLATION
An investigation of methods for updating ionospheric scintillation models using topside in-situ plasma density measurements
| AD-A243378 | p 1316 N92-17209
Wave propagation in a randomly inhomogeneous medium: A study of the problem
| AD-A243741 | p 1284 N92-17691
SCINTILLATION COUNTERS
High energy physics program at Texas A and M University
| DE92-004426 | p 1363 N92-17738
SCORING
An investigation of gouge initiation in high-velocity sliding contact
| DE92-003944 | p 1311 N92-17937
SCREWS
Three point lead screw positioning apparatus
| NASA-CASE-LEW-15216-1 | p 1307 N92-17678
SEA STATES
Sea surface environmental conditions in the Gulf of Alaska during April 1990 using SSM/I
| AD-A241909 | p 1323 N92-17041
SEA SURFACE TEMPERATURE
Simultaneous active and passive microwave measurements of the ocean surface
| AD-A242232 | p 1312 N92-17459
SEA WATER
An investigation of cold overflow over the Iceland/Faeroes Ridge
| AD-A243084 | p 1324 N92-17169
Blistering of graphite/polymer composites galvanically coupled with metals in sea water
| AD-A242861 | p 1269 N92-17262
SEALING
Thruster sealing system and apparatus
| NASA-CASE-MSC-21898-1 | p 1307 N92-17872
SEALS (STOPPERS)
Actively controlled shaft seals for aerospace applications
| NASA-CR-189808 | p 1306 N92-17304
Thruster sealing system and apparatus
| NASA-CASE-MSC-21898-1 | p 1307 N92-17872
SEARCH PROFILES
Improved task scheduling for parallel simulations
| AD-A243721 | p 1346 N92-17507
SEARCHING
Dynamic pattern matcher using incomplete data
| NASA-CASE-MSC-21415-1-SB | p 1344 N92-17860

SECONDARY EMISSION
Measurement of electron beam emittance using optical transition radiation and development of a diffuse screen electron beam monitor
| AD-A241893 | p 1357 N92-17306
SECONDARY FLOW
An experimental study of a turbulent wing-body junction and wake flow
| AD-A243388 | p 1223 N92-17222
SEDIMENTS
The effects of sediment porosity on acoustic reflection and transmission at the seafloor
| AD-A241943 | p 1323 N92-17083
Acoustical and other physical properties of marine sediments
| AD-A243532 | p 1324 N92-17391
SEGMENTS
Optical image segmentation using wavelet correlation
| AD-A243650 | p 1367 N92-17736
SEISMIC WAVES
Studies of high-frequency seismic wave propagation
| AD-A241938 | p 1316 N92-17202
Ultrasonic studies of transient seismo-acoustic waves in bounded solids and Liquid/Solid interfaces
| AD-A243441 | p 1355 N92-17488
SEISMOGRAMS
Studies of high-frequency seismic wave propagation
| AD-A241938 | p 1316 N92-17202
SEMANTICS
A computational model of semantic memory impairment: Modality-specificity and emergent category-specificity
| AD-A242377 | p 1347 N92-16991
A system for specifying and rapidly prototyping user interfaces
| AD-A242963 | p 1347 N92-16994
SEMICONDUCTOR DEVICES
A PC program to calculate the one-sided lower tolerance limit for total ionizing dose radiation data
| AD-A242365 | p 1357 N92-17394
Toward a national semiconductor strategy. Regaining markets in high-volume electronics, volume 2
| PB91-201301 | p 1290 N92-17559
DOE Task Force Meeting on Electrical Breakdown of Insulating Ceramics in a High Radiation Field
| DE92-000459 | p 1270 N92-17576
Toward a national semiconductor strategy, volume 1
| PB91-201293 | p 1290 N92-17620
A theoretical search for supervelocity semiconductors
| AD-A241981 | p 1376 N92-17783
Cryogenic thermoresistor made from p-InSb(Mn)
| DE92-600473 | p 1293 N92-17825
SEMICONDUCTOR DIODES
Innovative switching technology
| DE92-003068 | p 1292 N92-17708
SEMICONDUCTOR LASERS
Innovative optoelectronic materials and structures using OMVPE
| AD-A243257 | p 1371 N92-16984
Receiver performance of laser ranging measurements between the Lunar Observer and a subsatellite for lunar gravity studies
| NASA-CR-189860 | p 1303 N92-17152
Innovative switching technology
| DE92-003068 | p 1292 N92-17708
Self-collimated unstable resonator semiconductor laser
| NASA-CASE-NPO-18386-1-CU | p 1305 N92-17899
SEMICONDUCTOR PLASMAS
Excitons in semiconducting superlattices, quantum wells, and ternary alloys
| DE91-018805 | p 1374 N92-17528
SEMICONDUCTORS (MATERIALS)
Innovative optoelectronic materials and structures using OMVPE
| AD-A243257 | p 1371 N92-16984
Theoretical crystal-field calculations for rare-earth ions in 3-5 semiconductor compounds
| AD-A243098 | p 1371 N92-16995
Waveguide four-wave mixing
| AD-A243555 | p 1286 N92-17017
Th 3-5 modulation and switching devices for optical system applications
| AD-A243055 | p 1365 N92-17044
X ray lithography in Japan
| AD-A243660 | p 1286 N92-17087
Ultrafast passive shields for laser and ballistic protection
| AD-A243206 | p 1303 N92-17175
Transmission electron microscopy of the CVD diamond film/substrate interface
| AD-A243096 | p 1373 N92-17322
Calculations of electron and photon transport between 1 MeV and 1 eV
| AD-A243725 | p 1359 N92-17514
Excitons in semiconducting superlattices, quantum wells, and ternary alloys
| DE91-018805 | p 1374 N92-17528
Surface chemistry at the semiconductor/electrolyte interface
| DE91-018511 | p 1374 N92-17532
Toward a national semiconductor strategy. Regaining markets in high-volume electronics, volume 2
| PB91-201301 | p 1290 N92-17559
Toward a national semiconductor strategy, volume 1
| PB91-201293 | p 1290 N92-17620
Electrical and thermal conductivity of a variable zone semiconductor in a longitudinal magnetic field
p 1291 N92-17702
A theoretical search for supervelocity semiconductors
| AD-A241981 | p 1376 N92-17783
Ion mixing of semiconductor layered-structures
| DE92-003756 | p 1377 N92-17791
Self-collimated unstable resonator semiconductor laser
| NASA-CASE-NPO-18386-1-CU | p 1305 N92-17899
SENSITIVITY
A proposed improved method of radiosonde humidity sensing
| AD-A242954 | p 1319 N92-17233
Sensitivity testing and analysis
| DE92-002033 | p 1276 N92-17624
SENSORS
ECLSS predictive monitoring p 1247 N92-17357
Collision avoidance sensor skin p 1247 N92-17361
SENSORY PERCEPTION
Electronic expansion of human perception
| AD-A242028 | p 1333 N92-17634
SEPARATED FLOW
Computation of the hydrodynamic forces and moments on a body of revolution with and without appendages
| AD-A243033 | p 1294 N92-16978
Mean wind speeds over hills and other topography
| ESDU-91043 | p 1321 N92-17853
SEQUENCING
Marked point processes as limits of Markovian arrival streams
| TW-91-04 | p 1353 N92-17837
SEQUENTIAL CONTROL
High level language-based robotic control system
| NASA-CASE-NPO-17918-2-CU | p 1349 N92-17895
SERIES (MATHEMATICS)
Neural network modeling of nonlinear systems based on Volterra series extension of a linear model
| NASA-TM-104177 | p 1347 N92-16987
SERIES EXPANSION
A time-domain incident field extrapolation technique based on the singularity expansion method
| AD-A243044 | p 1282 N92-17279
Modeling convergence zone gain on MS-DOS based personal computers
| AD-A243252 | p 1341 N92-17558
SERVOMECHANISMS
Closed-loop motor control using high-speed fiber optics
| NASA-CASE-MSC-21806-1 | p 1368 N92-17863
SHAFTS (MACHINE ELEMENTS)
Actively controlled shaft seals for aerospace applications
| NASA-CR-189808 | p 1306 N92-17304
System for testing bearings
| NASA-CASE-MFS-28589-1 | p 1306 N92-17584
Fiber optic angular orientation sensor digital serial encoding
| AD-D015102 | p 1302 N92-17826
SHALLOW SHELLS
Higher-order thickness expansions for cylindrical shells
| AD-A242017 | p 1310 N92-17230
SHALLOW WATER
Studies of baroclinic flow
| AD-A243050 | p 1296 N92-17309
SHAPES
Dual color and shape coding in the visual periphery: A study of Joint Tactical Information Distribution System (JTIDS) symbology
| AD-A243253 | p 1333 N92-16982
Extracting the shape and roughness of specular lobe objects using four light photometric stereo
| AD-A243522 | p 1365 N92-17146
Experimental ice shape and performance characteristics for a multi-element airfoil in the NASA Lewis Icing Research Tunnel
| NASA-TM-105380 | p 1224 N92-17347
SHEAR FLOW
Eddy breakdown and structure development
| AD-A241886 | p 1295 N92-17039
Effective viscosity in the simulation of spatially evolving shear flows with monotonic FCT models
| AD-A243709 | p 1295 N92-17126
Development and utilization of new diagnostics for dense-phase pneumatic transport
| DE92-000337 | p 1299 N92-17704
On the origin and control of large coherent structures in turbulent shear flow
| AD-A243727 | p 1299 N92-17719
Physical and computational modelling of stratified shear flows
| AERO-REPT-8909 | p 1300 N92-17974
SHEAR LAYERS
Effective viscosity in the simulation of spatially evolving shear flows with monotonic FCT models
| AD-A243709 | p 1295 N92-17126
Acoustical and other physical properties of marine sediments
| AD-A243532 | p 1324 N92-17391
SHEAR PROPERTIES
Experimental investigation of adiabatic shear banding at different impact velocities
| AD-A243011 | p 1310 N92-17256
SHEAR STRAIN
Experimental investigation of adiabatic shear banding at different impact velocities
| AD-A243011 | p 1310 N92-17256
SHELL THEORY
Y890NMR study of hyperfine interactions in (R(x)Y(1-x))Fe2
| DE91-641979 | p 1376 N92-17779
SHELLS (STRUCTURAL FORMS)
Explicit finite element method for transparency impact analysis
| AD-A243527 | p 1227 N92-17478
SHIPS
Severe weather guide mediterranean ports. Part 35: Rota
| AD-A243539 | p 1319 N92-17338
Severe weather guide Mediterranean ports. Part 36: Limassol
| AD-A243448 | p 1320 N92-17492
Severe weather guide Mediterranean ports. Part 37: Larnaca
| AD-A243449 | p 1320 N92-17493
A frequency-domain method for estimating the incidence and severity of sliding
| AD-A243077 | p 1334 N92-17569
SHOCK LAYERS
Comparison of two solution methods for the numerical calculation of hypersonic flows
| MBB-FE211-S-PUB-446 | p 1224 N92-17311
SHOCK LOADS
Analysis of cam roller followers
| ESDU-91026 | p 1307 N92-17852
SHOCK TESTS
On size scaling in shock hydrodynamics and the stress-strain behavior of copper at exceedingly high strain rates
| DE92-003797 | p 1265 N92-17579
SHOCK TUBES
Application of program LAURA to perfect gas shock tube flows: A parametric study
| NASA-TM-104190 | p 1294 N92-17002
SHOCK WAVES
The hazard of exposure to 2.075 kHz center frequency narrow band impulses
| AD-A242997 | p 1329 N92-17299
SHORT TAKEOFF AIRCRAFT
Finite element analysis of ASTOVL fighter structure
| AD-A243724 | p 1233 N92-17513
SIDESLIP
Failure detection and fault management techniques for flush airdata sensing systems
| NASA-TM-4335 | p 1234 N92-17128
SIGNAL DETECTION
Noncoherent detection of coherent optical heterodyne signals corrupted by laser phase noise
| AD-A243103 | p 1364 N92-16981
Wind profiler signal detection improvements
| NASA-CR-189781 | p 1317 N92-16990
Mechanisms of temporal pattern discrimination by human observers
| AD-A243051 | p 1332 N92-17336
Psychophysical evaluation of three-dimensional auditory displays
| NASA-CR-189848 | p 1355 N92-17692
Object acquisition and tracking for space-based surveillance
| AD-A243333 | p 1367 N92-17711
SIGNAL DETECTORS
Ultrasonic studies of transient seismo-acoustic waves in bounded solids and Liquid/Solid interfaces
| AD-A243441 | p 1355 N92-17488
SIGNAL ENCODING
Fiber optic angular orientation sensor digital serial encoding
| AD-D015102 | p 1302 N92-17826

SIGNAL FADING
Investigation of coding techniques for memory and delay efficient interleaving in slow Rayleigh fading
| AD-A243154 | p 1280 N92-17187
SIGNAL PROCESSING
A covariance modeling approach to adaptive beamforming and detection
| AD-A241887 | p 1279 N92-17040
FY92 mathematical research project proposal briefing
| AD-A243163 | p 1350 N92-17207
Multisensor signal processing techniques (hybrid GPS/LORAN-C with RAIM)
| AD-A242323 | p 1281 N92-17244
Adaptive presort processing
| AD-A243286 | p 1340 N92-17286
Integrated system for missile detection and discrimination
| DE91-018874 | p 1283 N92-17529
A Walsh-domain adaptive filter
| AD-A243701 | p 1292 N92-17718
SIGNAL TO NOISE RATIOS
Noncoherent detection of coherent optical heterodyne signals corrupted by laser phase noise
| AD-A243103 | p 1364 N92-16981
A covariance modeling approach to adaptive beamforming and detection
| AD-A241887 | p 1279 N92-17040
A performance model of Thermal Imaging System (TISs) which includes the human observer's response to state of the art displays
| AD-A242838 | p 1301 N92-17273
Constant modulus algorithm techniques for the enhancement of signal quality
| AD-A242986 | p 1288 N92-17295
Object acquisition and tracking for space-based surveillance
| AD-A243333 | p 1367 N92-17711
SIGNAL TRANSMISSION
A hybrid modulation for the dissemination of weather data to aircraft p 1220 N92-17991
SIGNS AND SYMPTOMS
A topographical analysis of the human electroencephalogram for patterns in the development of motion sickness
| AD-A243656 | p 1328 N92-17120
SILICATES
Collisional energy deposition threshold for extended damage depths in ion-implanted silicates
| DE92-004737 | p 1377 N92-17797
SILICIDES
Improved 320x244-element PtSi Schottky-barrier IR-CCD image sensor
| AD-A242026 | p 1301 N92-17140
SILICON
An in-situ spectroscopic ellipsometry study of the electron cyclotron resonance plasma oxidation of silicon and interfacial
| AD-A242833 | p 1259 N92-17247
Application of silicon micromachining to thermal dissipation issues in wafer scale integrated circuits
| AD-A243744 | p 1288 N92-17332
Light-controlled, electrochemical, anisotropic etching of silicon
| MBB-Z-0368-91-PUB | p 1261 N92-17841
SILICON CARBIDES
Research and development on advanced silicon carbide thin film growth techniques and fabrication of high power and microwave frequency silicon carbide-based device structures
| AD-A243531 | p 1373 N92-17390
Dynamic fracture characterization of Al2O3 and SiC(w)/Al2O3
| AD-A242187 | p 1273 N92-17784
A method for joining ceramic shapes
| DE92-003815 | p 1274 N92-17842
SILICON COMPOUNDS
Production of mullite fibers
| NASA-CASE-MFS-28431-1 | p 1257 N92-17870
SILICON DIOXIDE
Infrared rotating analyzer ellipsometry: Calibration and data processing
| AD-A242834 | p 1259 N92-17248
A kinetics study of the electron cyclotron resonance plasma oxidation of silicon
| AD-A242868 | p 1290 N92-17596
Structure and topology of silica aerogels
| DE92-004728 | p 1274 N92-17938
SILICON FILMS
Infrared rotating analyzer ellipsometry: Calibration and data processing
| AD-A242834 | p 1259 N92-17248
Transmission electron microscopy of the CVD diamond film/substrate interface
| AD-A243096 | p 1373 N92-17322
A kinetics study of the electron cyclotron resonance plasma oxidation of silicon
| AD-A242868 | p 1290 N92-17596
SILICON NITRIDES
Reliability analysis of structural ceramic components using a three-parameter Weibull distribution
| NASA-TM-105370 | p 1267 N92-17060
Examining Si3N4 base materials with various rare earth additions
| AD-A243668 | p 1372 N92-17082
Determination of the tribological fundamentals of solid lubricated ceramics. Volume 2: Appendices A through O
| AD-A242871 | p 1270 N92-17614
Selective plasma etching
| DE92-004794 | p 1371 N92-17968
SILICON OXIDES
An interface enhanced spectroscopic ellipsometry technique: Application to Si-SiO2
| AD-A242867 | p 1260 N92-17613
SILICONES
The wave numbers of supercritical surface tension driven Benard convection
| NASA-CR-189856 | p 1373 N92-17375
SILVER
in situ surface x ray crystallography of electrochemically deposited Bi on Ag(111): Structure, compressibility, and anisotropy
| AD-A243218 | p 1372 N92-17181
An investigation of underpotentially deposited thallium of silver (111) by in-situ surface x ray scattering
| AD-A243270 | p 1263 N92-17271
Comparisons of self-assembled monolayers on silver and gold: Mixed monolayers derived from HS(CH2)21X and HS(CH2)10(sup Y) (X,Y-CH3, CH2OH) have similar properties
| AD-A243487 | p 1264 N92-17427
Silver-nickel composite cathodes for alkaline secondary batteries
| AD-D015121 | p 1293 N92-17871
SIMD (COMPUTERS)
Parallel radiosity techniques for mesh-connected SIMD computers
| AD-A242049 | p 1346 N92-17638
SIMULATION
A CAD model for the axial inductive strip with finite thickness centered in homogeneous finline with w/b = 1
| AD-A243553 | p 1278 N92-17016
Effective viscosity in the simulation of spatially evolving shear flows with monotonic FCT models
| AD-A243709 | p 1295 N92-17126
A stochastic approach to the weighted-region problem: 1. The design of the path annealing algorithm
| AD-A243324 | p 1340 N92-17403
Simulation of finite-precision effects in digital filters
| AD-A243758 | p 1342 N92-17601
Parallel implementation of VHDL simulations on the Intel iPSC/2 hypercube
| AD-A243760 | p 1342 N92-17603
Downflow heat transfer in a heated ribbed vertical annulus with a cosine power profile (results from test series ECS-2c)
| DE92-003259 | p 1298 N92-17626
SIMULATORS
Multiple-access phased array antenna simulator for a digital beam forming system investigation
| NASA-TM-105422 | p 1279 N92-17062
Parallel implementation of VHDL simulations on the Intel iPSC/2 hypercube
| AD-A243760 | p 1342 N92-17603
Effect of spatial locality prefetching on structural locality
| AD-A243632 | p 1337 N92-17922
SINGLE CRYSTALS
Chemical vapor deposited diamond
| AD-A243095 | p 1268 N92-17171
The 5th Annual US-Japan Seminar on Dielectric and Piezoelectric Ceramics
| AD-A243465 | p 1268 N92-17193
Detection and spectroscopy of single pentacene molecules in a p-terphenyl crystal by means of fluorescence excitation
| AD-A243747 | p 1356 N92-17196
Evidence for strong electron-phonon coupling in thermal conductivity of YBa2Cu3O(7-delta)
| AD-A243192 | p 1372 N92-17218
Determination of the tribological fundamentals of solid lubricated ceramics. Volume 3: Appendices P through 2
| AD-A242872 | p 1270 N92-17597
Method of doping single crystal diamond for electronic devices
| AD-D015069 | p 1374 N92-17610
Rates and mechanisms of metastable deactivation over surfaces
| AD-A243391 | p 1361 N92-17652
Fatigue in single crystal nickel superalloys
| AD-A243453 | p 1265 N92-17653
Determination of the tribological fundamentals of solid lubricated ceramics. Volume 1: Summary
| AD-A243219 | p 1272 N92-17683
The EPR of the triplet state of aryl cations in crystals of diazonium salts p 1375 N92-17701
SINGULAR INTEGRAL EQUATIONS
The solution of a singular integral equation arising from a lifting surface theory for rotating blades
p 1224 N92-17303
SINGULARITY (MATHEMATICS)
A time-domain incident field extrapolation technique based on the singularity expansion method
| AD-A243044 | p 1282 N92-17279
SINTERING
Reliability analysis of structural ceramic components using a three-parameter Weibull distribution
| NASA-TM-105370 | p 1267 N92-17060
Structure and topology of silica aerogels
| DE92-004728 | p 1274 N92-17938
SIS (SUPERCONDUCTORS)
Metriwave final report
| NASA-CR-189816 | p 1279 N92-17046
SISO (CONTROL SYSTEMS)
A robust digital flight control system for an unfanned research vehicle using discrete quantitative feedback theory
| AD-A243638 | p 1237 N92-17748
SIZE SEPARATION
New experimental challenges in elemental fluorine chemistry: An emerging technology
| AD-A243054 | p 1258 N92-17043
SKIN (ANATOMY)
Preliminary assessment of the relative toxicity of tetraglycine hydroperiodide, phase 1
| AD-A243334 | p 1330 N92-17712
SKIN (STRUCTURAL MEMBER)
Collision avoidance sensor skin p 1247 N92-17361
Active control of pressure loads using passive porosity
| NASA-CASE-LAR-14594-1 | p 1300 N92-17888
SLEEP DEPRIVATION
Fatigue effects on human performance in combat: A literature review, volume 1
| AD-A242887 | p 1330 N92-17567
SLENDER WINGS
Boundary-layer transition and heat transfer on slender delta wings
| AERO-REPT-8904 | p 1226 N92-17849
SLIDING
Multiple input sliding mode control for autonomous diving and steering of underwater vehicles
| AD-A241935 | p 1237 N92-17442
A frequency-domain method for estimating the incidence and severity of sliding
| AD-A243077 | p 1334 N92-17569
Determination of the tribological fundamentals of solid lubricated ceramics. Volume 3: Appendices P through 2
| AD-A242872 | p 1270 N92-17597
SLIDING CONTACT
An investigation of gouge initiation in high-velocity sliding contact
| DE92-003944 | p 1311 N92-17937
SLIDING FRICTION
The synergistic effects of solid and liquid lubrication on the tribological behavior of transformation-toughened ZrO2 ceramics
| DE91-018617 | p 1306 N92-17575
SLOPES
Sensing refractive turbulence profiles using wave front slope measurements from two reference sources
| AD-A243696 | p 1315 N92-17094
SLOT ANTENNAS
Design and testing of a lightweight, planar microwave lens
| AD-A243685 | p 1286 N92-17076
SLOTS
Natural resonances of slotted cylinder configurations
| AD-A241934 | p 1282 N92-17441
SLURRIES
Catalytic studies on a novel synthesis of methanol
| DE92-002904 | p 1275 N92-17184
SMART STRUCTURES
Electrically-controlled polymeric gels as active materials in adaptive structures
| DE92-002947 | p 1272 N92-17710
SNOW
Evaluation of solar flares and electron precipitation by nitrate distribution in Antarctica
| AD-A243026 | p 1389 N92-17235
Surface observation climatic summaries for Fairbanks IAP, Alaska
| AD-A243309 | p 1320 N92-17400
The role of thermal convection in heat and mass transport in the subarctic snow cover
| AD-A243674 | p 1312 N92-17715

SNOW COVER
The role of thermal convection in heat and mass transport in the subarctic snow cover
| AD-A243674 | p 1312 N92-17715
SODIUM
Characterization of the P. brevis polyether neurotoxin binding component in excitable membranes
| AD-A242877 | p 1327 N92-17564
SOFTWARE ENGINEERING
Pragmatic quality metrics for evolutionary software development models
| AD-A243022 | p 1337 N92-17064
An examination of selected commercial software testing tools
| AD-A243089 | p 1337 N92-17068
An analysis of mission critical computer software in Naval aviation
| AD-A243078 | p 1339 N92-17237
Beyond the Baseline 1991: Proceedings of the Space Station Evolution Symposium. Volume 2: Space Station Freedom, part 2
| NASA-CP-10083-VOL-2-PT-2 | p 1245 N92-17348
Advanced flight software reconfiguraton p 1245 N92-17350
Software life cycle methodologies and environments p 1246 N92-17351
Intelligent Computer-Aided Training (ICAT) p 1246 N92-17352
The environmental control and life support system advanced automation project p 1246 N92-17356
A distributed design for monitoring, logging, and replaying device readings at LAMPF
| DE92-003860 | p 1240 N92-17591
Contractor software engineering environment evaluations summary report
| AD-A242330 | p 1343 N92-17640
SOFTWARE TOOLS
Intelligent Computer-Aided Training (ICAT) p 1246 N92-17352
The development of user interface tools for the computer aided prototyping system
| AD-A243189 | p 1340 N92-17368
CMS reverse engineering and encore/model integration
| AD-A243438 | p 1341 N92-17487
Forth Graphics Toolbox (A user's guide for use with RFF FORTH)
| AD-A242916 | p 1342 N92-17581
The UNC graph server: A distributed hypermedia data management system
| AD-A242041 | p 1380 N92-17651
Mathematical basis for a system to manage automated protocol analysis
| AD-A242042 | p 1381 N92-17669
Developing a broader basis for scientific data analysis interfaces
| DE92-003963 | p 1385 N92-17845
Software tools for distributed intelligent control systems
| DE92-004656 | p 1349 N92-17965
SOILS
Role of donor-acceptor interactions in the sorption of TNT and other nitroaromatics from solution
| AD-A243235 | p 1254 N92-17055
SOLAR ACTIVITY
Analysis of orbital elements and atmospheric activity to ascertain possible presence of an ion propulsion capability aboard Salyut 7/Cosmos 1686
| AD-A243654 | p 1251 N92-17762
SOLAR ACTIVITY EFFECTS
Evaluation of solar flares and electron precipitation by nitrate distribution in Antarctica
| AD-A243026 | p 1389 N92-17235
In situ observations of coronal mass ejections in interplanetary space
| DE92-003857 | p 1389 N92-17725
SOLAR ARRAYS
Tandem concentrator photovoltaic array applied to Space Station Freedom evolutionary power requirements p 1251 N92-17769
SOLAR CELLS
Tandem concentrator photovoltaic array applied to Space Station Freedom evolutionary power requirements p 1251 N92-17769
SOLAR COLLECTORS
Preliminary design study of a central solar heating plant with seasonal storage at the University of Massachusetts, Amherst
| DE92-000762 | p 1313 N92-17577
SOLAR CORONA
In situ observations of coronal mass ejections in interplanetary space
| DE92-003857 | p 1389 N92-17725
SOLAR DYNAMIC POWER SYSTEMS
Solar dynamic technology status for Space Station Freedom application p 1251 N92-17770
SOLAR ENERGY
Preliminary design study of a central solar heating plant with seasonal storage at the University of Massachusetts, Amherst
| DE92-000762 | p 1313 N92-17577
SOLAR FLARES
Evaluation of solar flares and electron precipitation by nitrate distribution in Antarctica
| AD-A243026 | p 1389 N92-17235
Solar-geophysical data number 562, June 1991. Part 2: (Comprehensive reports). Data for December 1990 and miscellaneous
| PB91-230219 | p 1387 N92-17251
SOLAR HEATING
Optimization in solar heating/photovoltaic systems
| AD-A242363 | p 1313 N92-17424
Preliminary design study of a central solar heating plant with seasonal storage at the University of Massachusetts, Amherst
| DE92-000762 | p 1313 N92-17577
SOLAR MAXIMUM MISSION
The complete hard x ray burst spectrometer event list, 1980-1989
| NASA-TM-4332 | p 1389 N92-17048
SOLAR NEUTRINOS
Solar neutrinos: Probing the sun or neutrinos?
| DE92-003849 | p 1389 N92-17201
Solar neutrino physics in the nineties
| DE92-003848 | p 1390 N92-17883
SOLAR PHYSICS
Solar neutrinos: Probing the sun or neutrinos?
| DE92-003849 | p 1389 N92-17201
Solar-geophysical data number 562, June 1991. Part 2: (Comprehensive reports). Data for December 1990 and miscellaneous
| PB91-230219 | p 1387 N92-17251
Solar neutrino physics in the nineties
| DE92-003848 | p 1390 N92-17883
SOLAR PROMINENCES
Solar-geophysical data number 562, June 1991. Part 2: (Comprehensive reports). Data for December 1990 and miscellaneous
| PB91-230219 | p 1387 N92-17251
SOLAR PROTONS
Evaluation of solar flares and electron precipitation by nitrate distribution in Antarctica
| AD-A243026 | p 1389 N92-17235
SOLAR RADIATION
Long duration exposure facility solar illumination data package
| NASA-CR-189873 | p 1241 N92-17335
SOLAR RADIO BURSTS
Solar-geophysical data number 562, June 1991. Part 2: (Comprehensive reports). Data for December 1990 and miscellaneous
| PB91-230219 | p 1387 N92-17251
SOLAR SENSORS
Space Station Freedom solar alpha joint growth capability p 1252 N92-17772
SOLAR SPECTRA
Stellar spectral line synthesis from an individual photon-following simulation
| AD-A242970 | p 1388 N92-17253
SOLAR WIND
Magnetospheric response to variations in the interplanetary magnetic field
| AD-A243683 | p 1388 N92-17717
In situ observations of coronal mass ejections in interplanetary space
| DE92-003857 | p 1389 N92-17725
SOLAR X-RAYS
The complete hard x ray burst spectrometer event list, 1980-1989
| NASA-TM-4332 | p 1389 N92-17048
SOLDERED JOINTS
Solder extrusion pressure bonding process and bonded products produced thereby
| DE92-004603 | p 1363 N92-17739
SOLDERING
Inelastic strain analysis of solder joint in NASA fatigue specimen
| NASA-CR-189882 | p 1311 N92-17511
Solder extrusion pressure bonding process and bonded products produced thereby
| DE92-004603 | p 1363 N92-17739
SOLENOIDS
Magnetic field distribution and design of Helmholtz coils
| AD-A242978 | p 1288 N92-17291
SOLID ELECTRODES
In situ surface x ray scattering of metal monolayers adsorbed at solid-liquid interfaces
| AD-A243258 | p 1262 N92-16985
SOLID LUBRICANTS
The synergistic effects of solid and liquid lubrication on the tribological behavior of transformation-toughened ZrO2 ceramics
| DE91-018617 | p 1306 N92-17575
Determination of the tribological fundamentals of solid lubricated ceramics. Volume 3: Appendices P through 2
| AD-A242872 | p 1270 N92-17597
Determination of the tribological fundamentals of solid lubricated ceramics. Volume 2: Appendices A through O
| AD-A242871 | p 1270 N92-17614
Determination of the tribological fundamentals of solid lubricated ceramics. Volume 1: Summary
| AD-A243219 | p 1272 N92-17683
SOLID PROPELLANT ROCKET ENGINES
Case bond liner systems for solid rocket motors
| AD-A242297 | p 1253 N92-17085
Rocket tests in Mississippi to be heavily restricted
| GAO/NSIAD-92-86 | p 1240 N92-17741
Thermal insulation chemical composition and method of manufacture
| AD-D015106 | p 1257 N92-17836
SOLID SOLUTIONS
Electrical and thermal conductivity of a variable zone semiconductor in a longitudinal magnetic field p 1291 N92-17702
Kinetics of a new phase formation in supersaturated solid solutions. 1. Dilute one-component systems
| DE92-610065 | p 1262 N92-17943
SOLID STATE
New optical materials for the long-wave (8-12 microns) region: Design criteria for the solid-state chemist
| AD-A243280 | p 1365 N92-17284
Concentration of isotopic hydrogen by temperature gradient effect in soluble metal
| AD-D015062 | p 1260 N92-17628
SOLID STATE LASERS
A tunable solid state laser with high wavelength selectivity over a preselected wavelength range
| AD-D015055 | p 1304 N92-17627
SOLID-SOLID INTERFACES
Magnetic multilayer interface anisotropy
| DE92-000635 | p 1263 N92-17319
Method of joining diamond structures
| AD-D015066 | p 1269 N92-17397
SOLIDS
Molecular recognition in gels, monolayers, and solids
| AD-A243488 | p 1358 N92-17428
Ultrasonic studies of transient seismo-acoustic waves in bounded solids and Liquid/Solid interfaces
| AD-A243441 | p 1355 N92-17488
Optical modification of a single impurity molecule in a solid
| AD-A243750 | p 1361 N92-17660
SOLIDS FLOW
Development and utilization of new diagnostics for dense-phase pneumatic transport
| DE92-003091 | p 1307 N92-17605
Development and utilization of new diagnostics for dense-phase pneumatic transport
| DE92-000337 | p 1299 N92-17704
Determination of cohesive and normal stresses and simulation of fluidization using kinetic theory
| DE92-002905 | p 1299 N92-17709
SOLITARY WAVES
The physical optics description of microwave scattering by the sea surface
| AD-A243216 | p 1365 N92-17180
SOLUBILITY
Gas transport in polybutadiene treated with aqueous bromine
| AD-A241871 | p 1295 N92-17025
Modelling of some equilibrium thermodynamic properties of polymer systems
| ETN-92-90570 | p 1273 N92-17840
SOLUTIONS
Studies of baroclinic flow
| AD-A243050 | p 1296 N92-17309
SOLVATION
Molecular jet studies of vdW clusters and solvation
| AD-A242866 | p 1254 N92-17308
Application of the mean spherical approximation to describe the Gibbs solvation energies of monovalent monoatomic ions in non-aqueous solvents
| AD-A243200 | p 1259 N92-17371
SOLVENTS
Scale-up of recovery process for waste solvents
| KCP-613-4479 | p 1277 N92-17535
Evaluation of environmentally safe cleaning agents for diamond turned optics
| DE92-002524 | p 1278 N92-17780
Thin films under chemical stress
| DE92-004684 | p 1377 N92-17857

SONAR
An investigation of cold overflow over the Iceland/Faeroes Ridge
[AD-A243084] p 1324 N92-17169
Application of multi-target tracking to sonar-based mobile robot navigation
[OUEL-1819/90] p 1229 N92-17878
SONOGRAMS
Studies of high-frequency seismic wave propagation
[AD-A241938] p 1316 N92-17202
SORBENTS
Role of donor-acceptor interactions in the sorption of TNT and other nitroaromatics from solution
[AD-A243235] p 1254 N92-17055
SORPTION
Role of donor-acceptor interactions in the sorption of TNT and other nitroaromatics from solution
[AD-A243235] p 1254 N92-17055
Three-stage sorption type cryogenic refrigeration system and method employing heat regeneration
[NASA-CASE-NPO-18366-1-CU] p 1277 N92-17674
SOUND FIELDS
Mechanisms mediating the perception of complex acoustic patterns
[AD-A243715] p 1355 N92-17502
Signal- and listener-based factors in complex auditory pattern perception
[AD-A243716] p 1332 N92-17503
SOUND INTENSITY
Classification of complex sounds
[AD-A243498] p 1355 N92-17381
SOUND LOCALIZATION
Psychophysical evaluation of three-dimensional auditory displays
[NASA-CR-189848] p 1355 N92-17692
SOUND PRESSURE
The effect of impulse presentation order on hearing trauma in the chinchilla
[AD-A243174] p 1326 N92-17269
Classification of complex sounds
[AD-A243498] p 1355 N92-17381
SOUND PROPAGATION
Bottom contour influence on ray tracing
[AD-A242411] p 1323 N92-17078
The effects of sediment porosity on acoustic reflection and transmission at the seafloor
[AD-A241943] p 1323 N92-17083
SOUND TRANSMISSION
Acoustic impedance of materials from reverberation time
[AD-A243184] p 1354 N92-16999
Bottom contour influence on ray tracing
[AD-A242411] p 1323 N92-17078
The effects of sediment porosity on acoustic reflection and transmission at the seafloor
[AD-A241943] p 1323 N92-17083
Acoustic simulation for acoustics education
[AD-A243027] p 1355 N92-17236
SOUND WAVES
Bottom contour influence on ray tracing
[AD-A242411] p 1323 N92-17078
The effects of sediment porosity on acoustic reflection and transmission at the seafloor
[AD-A241943] p 1323 N92-17083
Temporally-specific modification of myelinated axon excitability in vitro following a single ultrasound pulse
[AD-A242329] p 1326 N92-17474
Ultrasonic studies of transient seismo-acoustic waves in bounded solids and Liquid/Solid interfaces
[AD-A243441] p 1355 N92-17488
SPACE CHARGE
Emittance growth from space-charge forces
[DE92-003804] p 1364 N92-17796
Effects of the high-frequency beam space charge forces on the excitation of electromagnetic waves in relativistic carcinotron
[DE92-610956] p 1285 N92-17812
SPACE COMMERCIALIZATION
Space Station Freedom Evolution Symposium
p 1243 N92-17105
Space Station Freedom program. Commercial infrastructure and technology utilization
p 1244 N92-17111
SPACE DEBRIS
Hypervelocity impact simulation for micrometeorite and debris shield design
[NASA-CR-189807] p 1244 N92-17200
SPACE EXPLORATION
Partnership for Continuous Improvement
[NASA-TM-105464] p 1308 N92-16988
Environmental interactions in Space Exploration: Announcement of the formation of an Environmental Interactions Working Group
[NASA-TM-105294] p 1389 N92-17069
SEI: An update p 1243 N92-17103
Advanced space transportation systems
p 1242 N92-17104
Mars aerobrake assembly demonstration
p 1247 N92-17362
Space Station Freedom/lunar transfer vehicle propellant operation hazard analysis p 1249 N92-17416
SPACE INDUSTRIALIZATION
Product assurance and safety implementation in Space Shuttle payloads: An industrial perspective
[MBB-UK-0143-91-PUB] p 1241 N92-17342
SPACE LABORATORIES
The astronaut science advisor: Ground testing during SLS-1 p 1248 N92-17412
SPACE LOGISTICS
Space Station Freedom baseline operations concept
p 1248 N92-17410
SPACE MAINTENANCE
Canadian Space Station program
p 1243 N92-17102
SPACE MISSIONS
STS-41 Space Shuttle mission report
[NASA-TM-105479] p 1240 N92-16973
STS-36 Space Shuttle mission report
[NASA-TM-105477] p 1240 N92-16974
STS-35 Space Shuttle mission report
[NASA-TM-105476] p 1241 N92-16975
Upper stages using liquid propulsion and metallized propellants
[NASA-TP-3191] p 1253 N92-17151
STS-31 Space Shuttle mission report
[NASA-TM-105475] p 1241 N92-17364
STS-38 Space Shuttle mission report
[NASA-TM-105478] p 1242 N92-17534
An analytic method of propagating a covariance matrix to a maneuver condition for linear covariance analysis during rendezvous
[AD-A243354] p 1239 N92-17732
SPACE NAVIGATION
An analytic method of propagating a covariance matrix to a maneuver condition for linear covariance analysis during rendezvous
[AD-A243354] p 1239 N92-17732
SPACE PLASMAS
Radio sky mapping from satellites at very low frequencies
[NASA-TM-105452] p 1387 N92-17694
SPACE POWER REACTORS
Energy production using fission fragment rockets
[DE92-002192] p 1364 N92-17876
SPACE PROCESSING
Microgravity Science and Applications Program tasks, 1990 revision
[NASA-TM-4284] p 1276 N92-17945
SPACE PROGRAMS
Technology development on evolutionary space station p 1243 N92-17106
Constraints and difficulties in implementations of RAMS assurance programmes
[MBB-UK-0141-91-PUB] p 1309 N92-17544
SPACE RENDEZVOUS
An analytic method of propagating a covariance matrix to a maneuver condition for linear covariance analysis during rendezvous
[AD-A243354] p 1239 N92-17732
SPACE SHUTTLE BOOSTERS
STS-36 Space Shuttle mission report
[NASA-TM-105477] p 1240 N92-16974
SPACE SHUTTLE PAYLOADS
Product assurance and safety implementation in Space Shuttle payloads: An industrial perspective
[MBB-UK-0143-91-PUB] p 1241 N92-17342
STS-31 Space Shuttle mission report
[NASA-TM-105475] p 1241 N92-17364
SPACE SHUTTLES
STS-36 Space Shuttle mission report
[NASA-TM-105477] p 1240 N92-16974
STS-35 Space Shuttle mission report
[NASA-TM-105476] p 1241 N92-16975
Results of the space shuttle vehicle ascent air data system probe calibration test using a 0.07-scale external tank forebody model (68T) in the AEDC 16-foot transonic wind tunnel (IA-310), volume 1
[NASA-CR-167696] p 1241 N92-17167
Results of the space shuttle vehicle ascent air data system probe calibration test using a 0.07-scale external tank forebody model (68T) in the AEDC 16-foot transonic wind tunnel (IA-310), volume 2
[NASA-CR-167697] p 1241 N92-17214
STS-31 Space Shuttle mission report
[NASA-TM-105475] p 1241 N92-17364
Real Time Data System (RTDS) p 1249 N92-17421
STS-38 Space Shuttle mission report
[NASA-TM-105478] p 1242 N92-17534
SPACE STATION FREEDOM
Beyond the Baseline 1991: Proceedings of the Space Station Evolution Symposium. Volume 1: Space Station Freedom, part 1
[NASA-CP-10083-VOL-1-PT-1] p 1242 N92-17098
Space Station Freedom status p 1242 N92-17099
Canadian Space Station program
p 1243 N92-17102
SEI: An update p 1243 N92-17103
Advanced space transportation systems
p 1242 N92-17104
Space Station Freedom Evolution Symposium
p 1243 N92-17105
Technology development on evolutionary space station p 1243 N92-17106
Space Station Freedom science utilization: 2000 and beyond p 1244 N92-17107
A historical perspective on space station
p 1244 N92-17108
Advanced studies program overview
p 1244 N92-17109
Space Station Freedom engineering prototype development p 1244 N92-17110
Space Station Freedom program. Commercial infrastructure and technology utilization
p 1244 N92-17111
Evolution design requirements and design strategy
p 1244 N92-17112
Beyond the Baseline 1991: Proceedings of the Space Station Evolution Symposium. Volume 2: Space Station Freedom, part 2
[NASA-CP-10083-VOL-2-PT-2] p 1245 N92-17348
Failure Environment Analysis Tool (FEAT)
p 1245 N92-17349
Advanced flight software reconfiguraton
p 1245 N92-17350
Software life cycle methodologies and environments
p 1246 N92-17351
Operations mission planner beyond the baseline
p 1246 N92-17353
EMU evolution p 1246 N92-17354
Environmental control and life support system evolution analysis p 1246 N92-17355
The environmental control and life support system advanced automation project p 1246 N92-17356
ECLSS predictive monitoring p 1247 N92-17357
JPL space station telerobotic engineering prototype development FY 91 status/achievements
p 1247 N92-17359
Beyond the Baseline 1991: Proceedings of the Space Station Evolution Symposium. Volume 1: Space Station Freedom, part 2
[NASA-CP-10083-VOL-1-PT-2] p 1248 N92-17409
Space Station Freedom baseline operations concept
p 1248 N92-17410
The astronaut science advisor: Ground testing during SLS-1 p 1248 N92-17412
Evolution user requirements for the restructured space station p 1248 N92-17413
SSF growth concepts and configurations
p 1248 N92-17414
STV fueling options p 1249 N92-17415
Data management system advanced architectures
p 1249 N92-17417
Optical protocols for advanced spacecraft networks
p 1249 N92-17418
Advanced Crew Personal Support Computer (CPSC) task p 1249 N92-17419
ISE advanced technology p 1249 N92-17420
Real Time Data System (RTDS) p 1249 N92-17421
Computer system evolution requirements for autonomous checkout of exploration vehicles
p 1250 N92-17422
Beyond the Baseline 1991: Proceedings of the Space Station Evolution Symposium. Volume 2: Space Station Freedom, part 1
[NASA-CP-10083-VOL-2-PT-1] p 1251 N92-17768
Tandem concentrator photovoltaic array applied to Space Station Freedom evolutionary power requirements
p 1251 N92-17769
Solar dynamic technology status for Space Station Freedom application p 1251 N92-17770
Space Station Freedom electric power system evolution analysis status p 1251 N92-17771
Space Station Freedom solar alpha joint growth capability p 1252 N92-17772
Automated power management and control
p 1252 N92-17773
Active thermal control system evolution
p 1252 N92-17775
Thermal Control System Automation Project (TCSAP)
p 1252 N92-17776
SPACE STATION PAYLOADS
Space Station Freedom science utilization: 2000 and beyond p 1244 N92-17107

SPACE STATION POWER SUPPLIES
Solar dynamic technology status for Space Station Freedom application p 1251 N92-17770
Space Station Freedom electric power system evolution analysis status p 1251 N92-17771
Automated power management and control p 1252 N92-17773
The SSM/PMAD automated test bed project p 1252 N92-17774

SPACE STATIONS
Status of Japanese Experiment Module (JEM) activities p 1243 N92-17101
A historical perspective on space station p 1244 N92-17108
JPL space station telerobotic engineering prototype development: Advanced telerobotics system technology p 1247 N92-17358
The SSM/PMAD automated test bed project p 1252 N92-17774

SPACE SUITS
EMU evolution p 1246 N92-17354

SPACE SURVEILLANCE (SPACEBORNE)
Preliminary design of a model to assess the effect of Space Surveillance Network (SSN) sensor upgrades on orbit prediction accuracies relative to the US Anti-Satellite (ASAT) mission
|AD-A243736| p 1353 N92-17479

SPACE TRANSPORTATION
Advanced space transportation systems p 1242 N92-17104
Upper stages using liquid propulsion and metallized propellants
|NASA-TP-3191| p 1253 N92-17151

SPACE TRANSPORTATION SYSTEM
Advanced space transportation systems p 1242 N92-17104
Upper stages using liquid propulsion and metallized propellants
|NASA-TP-3191| p 1253 N92-17151

SPACE TRANSPORTATION SYSTEM FLIGHTS
STS-41 Space Shuttle mission report
|NASA-TM-105479| p 1240 N92-16973
STS-36 Space Shuttle mission report
|NASA-TM-105477| p 1240 N92-16974
STS-35 Space Shuttle mission report
|NASA-TM-105476| p 1241 N92-16975
STS-31 Space Shuttle mission report
|NASA-TM-105475| p 1241 N92-17364
STS-38 Space Shuttle mission report
|NASA-TM-105478| p 1242 N92-17534

SPACE WEAPONS
Preliminary design of a model to assess the effect of Space Surveillance Network (SSN) sensor upgrades on orbit prediction accuracies relative to the US Anti-Satellite (ASAT) mission
|AD-A243736| p 1353 N92-17479

SPACEBORNE ASTRONOMY
Hubble Space Telescope: High speed photometer instrument handbook. Version 2.0
|NASA-CR-189750| p 1386 N92-17497
Hubble Space Telescope: The GO and GTO Observing Programs. Version 1.0
|NASA-CR-189815| p 1387 N92-17650

SPACEBORNE EXPERIMENTS
Space Station Freedom science utilization: 2000 and beyond p 1244 N92-17107
The astronaut science advisor: Ground testing during SLS-1 p 1248 N92-17412
Microgravity Science and Applications Program tasks, 1990 revision
|NASA-TM-4284| p 1276 N92-17945

SPACECRAFT CHARGING
Comparison of alkali ion emitters
|AD-A243105| p 1290 N92-17570

SPACECRAFT COMMUNICATION
Optical protocols for advanced spacecraft networks p 1249 N92-17418

SPACECRAFT COMPONENTS
The need for active software product assurance management for systems critical software
|MBB-UK-0142-91-PUB| p 1341 N92-17545

SPACECRAFT CONFIGURATIONS
Beyond the Baseline 1991: Proceedings of the Space Station Evolution Symposium. Volume 1: Space Station Freedom, part 1
|NASA-CP-10083-VOL-1-PT-1| p 1242 N92-17098
Space Station Freedom status p 1242 N92-17099
Status of Japanese Experiment Module (JEM) activities p 1243 N92-17101
A historical perspective on space station p 1244 N92-17108
SSF growth concepts and configurations p 1248 N92-17414
Verification and validation of the Comprehensive Operational Support Evaluation Model for space
|AD-A243653| p 1344 N92-17761

SPACECRAFT CONSTRUCTION MATERIALS
Flight vehicle thermal testing with infrared lamps
|NASA-TM-4336| p 1232 N92-17226
The influence of temperature and composition on the activation energy for creep in binary aluminum lithium alloys
|AD-A242299| p 1265 N92-17759

SPACECRAFT CONTROL
Advanced flight software reconfiguraton p 1245 N92-17350
Comparison of station-keeping algorithms for an interior libration point orbit in the Sun-Earth + Moon elliptic restricted three-body problem
|AD-A241896| p 1388 N92-17595
Technical notes and correspondence: Stochastic robustness of linear time-invariant control systems p 1222 N92-18002

SPACECRAFT DESIGN
Beyond the Baseline 1991: Proceedings of the Space Station Evolution Symposium. Volume 1: Space Station Freedom, part 1
|NASA-CP-10083-VOL-1-PT-1| p 1242 N92-17098
Space Station Freedom status p 1242 N92-17099
Evolution design requirements and design strategy p 1244 N92-17112
SSF growth concepts and configurations p 1248 N92-17414
Beyond the Baseline 1991: Proceedings of the Space Station Evolution Symposium. Volume 2: Space Station Freedom, part 1
|NASA-CP-10083-VOL-2-PT-1| p 1251 N92-17768

SPACECRAFT DOCKING
Collision avoidance sensor skin p 1247 N92-17361

SPACECRAFT ENVIRONMENTS
The environmental control and life support system advanced automation project p 1246 N92-17356

SPACECRAFT INSTRUMENTS
Systems special investigation group
|NASA-CR-187355| p 1250 N92-17728

SPACECRAFT LAUNCHING
Recommendations for a wind profiling network to support Space Shuttle launches
|NASA-CR-4421| p 1318 N92-17072
Columbus Programme (current status) p 1243 N92-17100
Mars aerobrake assembly demonstration p 1247 N92-17362

SPACECRAFT MANEUVERS
An alternative concept for aeroassisted orbit transfers
|AD-A243409| p 1239 N92-17325
An analytic method of propagating a covariance matrix to a maneuver condition for linear covariance analysis during rendezvous
|AD-A243354| p 1239 N92-17732

SPACECRAFT ORBITS
Comparison of station-keeping algorithms for an interior libration point orbit in the Sun-Earth + Moon elliptic restricted three-body problem
|AD-A241896| p 1388 N92-17595

SPACECRAFT POWER SUPPLIES
Catalysts for ultrahigh current density oxygen cathodes for space fuel cell applications
|NASA-CR-189787| p 1253 N92-17365
Tandem concentrator photovoltaic array applied to Space Station Freedom evolutionary power requirements p 1251 N92-17769

SPACECRAFT PROPULSION
Upper stages using liquid propulsion and metallized propellants
|NASA-TP-3191| p 1253 N92-17151
Energy production using fission fragment rockets
|DE92-002192| p 1364 N92-17876

SPACECRAFT RELIABILITY
Testing of spacecraft in long-term storage
|AD-A242906| p 1250 N92-17580

SPACECRAFT SHIELDING
Hypervelocity impact simulation for micrometeorite and debris shield design
|NASA-CR-189807| p 1244 N92-17200

SPACECRAFT STRUCTURES
Control of a large flexible space structure using multiple model adaptive algorithms
|AD-A243759| p 1250 N92-17602

SPACECRAFT TEMPERATURE
Active thermal control system evolution p 1252 N92-17775
Thermal Control System Automation Project (TCSAP) p 1252 N92-17776

SPACECRAFT TRACKING
Comparison of station-keeping algorithms for an interior libration point orbit in the Sun-Earth + Moon elliptic restricted three-body problem
|AD-A241896| p 1388 N92-17595

SPACECREWS
Intelligent Computer-Aided Training (ICAT) p 1246 N92-17352
Upper body exercise: Physiology and training application for human presence in space
|AD-A242033| p 1329 N92-17473

SPACELAB
Facing page test for the astronaut science advisor presentation p 1248 N92-17411

SPATIAL DISTRIBUTION
Sensing refractive turbulence profiles using wave front slope measurements from two reference sources
|AD-A243696| p 1315 N92-17094
Some foundations for empirical study in the euclidean spatial model of social choice
|AD-A241928| p 1352 N92-17440
Spatially and spectrally resolved cathodoluminescence measurements of CVD-grown diamond particles and films
|AD-A243220| p 1271 N92-17615

SPATIAL RESOLUTION
Analysis of visual illusions using multiresolution wavelet decomposition based models
|AD-A243712| p 1332 N92-17500

SPECIFIC IMPULSE
Computational studies of energetic nitramines
|AD-A241870| p 1356 N92-17038
Experiments and analysis concerning the use of external burning to reduce aerospace vehicle transonic drag
|NASA-TM-105397| p 1235 N92-17546

SPECIFICATIONS
Evaluation of motor gasoline stability
|AD-A243063| p 1275 N92-17066
Unmanned evaluation of BAUER high pressure breathing air P-5 purification system
|AD-A243486| p 1334 N92-17331
Specification and compositional verification of real-time systems
|ETN-92-90580| p 1341 N92-17521

SPECTRA
Optical spectra and kinetics of single impurity molecules in a polymer: Spectral diffusion and persistent spectral hole-burning
|AD-A243749| p 1271 N92-17659
Optical modification of a single impurity molecule in a solid
|AD-A243750| p 1361 N92-17660

SPECTRAL CORRELATION
Study of turbulence by photon correlation spectroscopy
|AD-A243726| p 1298 N92-17688

SPECTROGRAPHS
Aries x ray objective grating spectrograph
|NASA-CR-189245| p 1386 N92-17003

SPECTROMETERS
The proton spectral function of Ca-40 and Ca-48 studies with (e, e prime p) reaction: An investigation of ground-state correlations
|ETN-92-90566| p 1358 N92-17433
A study of gamma ray generation from channeled electrons and positions
|AD-A241993| p 1361 N92-17608
Use of the algebraic coding theory in nuclear electronics
|DE92-611125| p 1351 N92-17813

SPECTROPHOTOMETERS
Hubble Space Telescope: Wide field and planetary camera instrument handbook. Version 2.1
|NASA-CR-189753| p 1386 N92-17484

SPECTROSCOPIC ANALYSIS
Nonlinear spectroscopic studies of interfacial molecular ordering
|DE92-000864| p 1360 N92-17530
An interface enhanced spectroscopic ellipsometry technique: Application to Si-SiO2
|AD-A242867| p 1260 N92-17613
Direct speciation of metal and metalloid ions by optical spectroscopies
|DE92-003868| p 1261 N92-17727

SPECTROSCOPY
Free volume variation with molecular weight of polymers
|NASA-TM-4326| p 1267 N92-17032
Detection and spectroscopy of single pentacene molecules in a p-terphenyl crystal by means of fluorescence excitation
|AD-A243747| p 1356 N92-17196
Single molecule spectral diffusion in a solid detected via fluorescence spectroscopy
|AD-A243748| p 1356 N92-17197
Optical modification of a single impurity molecule in a solid
|AD-A243750| p 1361 N92-17660
Study of turbulence by photon correlation spectroscopy
|AD-A243726| p 1298 N92-17688
Thin films under chemical stress
|DE92-004684| p 1377 N92-17857

Inductively coupled plasma atomic emission spectroscopy analysis of gold electroplating solutions
| DE92-004798 | p 1266 N92-17858
Structure and topology of silica aerogels
| DE92-004728 | p 1274 N92-17938
Photomodulation spectroscopy of photocarrier dynamics, electronic defects and morphology of conducting polymers
| DE92-004687 | p 1274 N92-17966

SPECTRUM ANALYSIS
The proton spectral function of Ca-40 and Ca-48 studies with (e, e prime p) reaction: An investigation of ground-state correlations
| ETN-92-90566 | p 1358 N92-17433
Spectral error models applied to the geodetic boundary value problem
| ETN-92-90582 | p 1312 N92-17436

SPECULAR REFLECTION
In situ structural studies of the underpotential deposition of copper onto an iodine covered platinum surface using x ray standing waves
| AD-A243475 | p 1263 N92-17328
In situ x ray standing wave study of Cu UPD on an iodine covered platinum surface
| AD-A243474 | p 1264 N92-17426

SPEECH
The effects of speech intelligibility level on concurrent visual task performance
| AD-A243015 | p 1331 N92-17052
Automatic recognition of speech in stressful environments
| AD-A242917 | p 1283 N92-17464
New algorithms for broad-band and narrowband source localization and a separable 2-D IIR filter realization
| AD-A243457 | p 1291 N92-17654

SPEECH RECOGNITION
Training methodologies for dependent Speech Recognition (SR) systems
| AD-A242983 | p 1282 N92-17293
Automatic recognition of speech in stressful environments
| AD-A242917 | p 1283 N92-17464

SPHERES
Significant digit computation of the ellipsoidal coverage function and its inverse
| AD-A242322 | p 1350 N92-17242
Effective dynamic material parameters and localized scattering
| AD-A241957 | p 1310 N92-17320
Estimation of the outer sphere contribution to the activation parameters for homogeneous electron transfer reactions using the mean spherical approximation
| AD-A243217 | p 1259 N92-17323
Application of the mean spherical approximation to describe the Gibbs solvation energies of monovalent monoatomic ions in non-aqueous solvents
| AD-A243200 | p 1259 N92-17371

SPHERICAL ANTENNAS
Spherical near-field scanning: Experimental and theoretical studies
| AD-A243489 | p 1282 N92-17429

SPHERICAL WAVES
Spherical near-field scanning: Experimental and theoretical studies
| AD-A243489 | p 1282 N92-17429
Wave propagation in a randomly inhomogeneous medium: A study of the problem
| AD-A243741 | p 1284 N92-17691

SPRAYERS
An optical roughness sensor for the real time determination of spray formed preform quality
| AD-A243238 | p 1262 N92-17056
Effectiveness of an onboard water spray system during an oxygen enriched cabin fire
| DOT/FAA/CT-TN91/51 | p 1226 N92-17149

SPUTTERING
High temperature superconductor thin films and Josephson junctions
| AD-A242747 | p 1293 N92-17949

SQUIBS
Evaluation of squib performance variables
| DE92-002034 | p 1275 N92-17533

STABILITY
Modes of interconnected lattice trusses using continuum models, part 1
| NASA-CR-189568 | p 1242 N92-17045
Stability and structure of C12B24N24: A hybrid analog of buckminsterfullerene
| AD-A242327 | p 1373 N92-17245
Stochastic robustness p 1221 N92-17997

STABILITY DERIVATIVES
Identification of the stability and control derivatives of a DLC-flap system for VSRA
| NAL-TR-1116 | p 1237 N92-17917

STABILIZATION
The analysis of a stabilized 1.5 Mach-Zehnder interferometric sensor with enhanced sensitivity and common-mode compensation
| AD-A243384 | p 1286 N92-17116
Toward the robust control of high bandwidth high precision flexible optical systems
| AD-A243471 | p 1366 N92-17536

STABLE OSCILLATIONS
A wing rock model for the F-14A aircraft
| AD-A243109 | p 1233 N92-17300

STAGNATION FLOW
Observation and measurements of flow structures in the stagnation region of a wing-body junction
| AD-A243403 | p 1223 N92-17117

STAGNATION POINT
Observation and measurements of flow structures in the stagnation region of a wing-body junction
| AD-A243403 | p 1223 N92-17117

STAGNATION PRESSURE
Stagnation and dynamic pressure limits for the S1 wind tunnel
| AD-A242989 | p 1238 N92-17297

STAINLESS STEELS
Long-term corrosion evaluation of stainless steels in Space Shuttle iodinated resin and water
| NASA-TM-104743 | p 1264 N92-17376
Sharps container
| NASA-CASE-MSC-21776-1 | p 1278 N92-17913

STANDARD DEVIATION
Range reference atmosphere, Fairbanks
| AD-A243314 | p 1318 N92-17113
Preliminary design of a model to assess the effect of Space Surveillance Network (SSN) sensor upgrades on orbit prediction accuracies relative to the US Anti-Satellite (ASAT) mission
| AD-A243736 | p 1353 N92-17479
Comparison of station-keeping algorithms for an interior libration point orbit in the Sun-Earth + Moon elliptic restricted three-body problem
| AD-A241896 | p 1388 N92-17595
Sensitivity testing and analysis
| DE92-002033 | p 1276 N92-17624
Example of statistical techniques applied to autoland touchdown dispersion (confidence intervals for normal and skew distributions)
| ESDU-91019 | p 1229 N92-17844
Variability of standard aircraft performance parameters
| ESDU-91020 | p 1233 N92-17847

STANDARDS
Development of a Federal standard for a video codec operating at P x 64 KBPS
| AD-A243005 | p 1281 N92-17267

STANDING WAVES
In situ structural studies of the underpotential deposition of copper onto an iodine covered platinum surface using x ray standing waves
| AD-A243475 | p 1263 N92-17328
Method and apparatus for reducing drag and noise associated with fluid flow in a conduit
| AD-D015067 | p 1297 N92-17398
In situ x ray standing wave study of Cu UPD on an iodine covered platinum surface
| AD-A243474 | p 1264 N92-17426

STAR CLUSTERS
IRAS and the Boston University Arecibo Galactic H I Survey: A catalog of cloud properties
| NASA-CR-189806 | p 1387 N92-17695

STARCHES
Process of converting starch to glucose and glucose to lactic acid
| DE92-003840 | p 1255 N92-17867

STARK EFFECT
Anomalous hole burning in polymers with inhomogeneous broadening
| AD-A242397 | p 1266 N92-17010

STATE ESTIMATION
Fault detection and isolation for multisensor navigation systems p 1221 N92-17992

STATE VECTORS
State vector reduction. Part 1: Dynamical reduction theories; changing quantum theory so the statevector represents reality
| DE91-641488 | p 1379 N92-17824

STATIC TESTS
Modification of Jindivik air intake duct with an auxiliary intake static aerodynamic tests
| AD-A243002 | p 1232 N92-17234
Numerical simulation of fluid flow and heat transfer in a thin liquid film over a stationary and rotating disk and comparison with experimental data
| NASA-CR-189253 | p 1300 N92-17887

STATISTICAL ANALYSIS
Surface observation climatic summaries for Duke Field/Eglin aux no. 3, Florida
| AD-A243310 | p 1318 N92-17073
Surface observation climatic summaries for Castle AFB, California
| AD-A243677 | p 1318 N92-17074
Range reference atmosphere, Fairbanks
| AD-A243314 | p 1318 N92-17113
Method of Kalman filtering for estimating the position and velocity of a tracked object
| AD-D015057 | p 1287 N92-17129
Surface observation climatic summaries for Hondo Municipal Airport, Texas
| AD-A243311 | p 1319 N92-17144
Extracting the shape and roughness of specular lobe objects using four light photometric stereo
| AD-A243522 | p 1365 N92-17146
Gibbs sampling for marginal posterior expectations
| AD-A243212 | p 1352 N92-17178
A model for voltammograms of the underpotential deposition of metals
| AD-A243199 | p 1264 N92-17370
Bayesian computations in survival models via the Gibbs sampler
| AD-A242343 | p 1353 N92-17643
Preliminary results from the analysis of wind component error
| AD-A243772 | p 1321 N92-17764
Example of statistical techniques applied to cruise performance guarantees (Student's t distribution)
| ESDU-91018 | p 1233 N92-17843
Example of statistical techniques applied to autoland touchdown dispersion (confidence intervals for normal and skew distributions)
| ESDU-91019 | p 1229 N92-17844
Fault detection and isolation for multisensor navigation systems p 1221 N92-17992

STATISTICAL DISTRIBUTIONS
Example of statistical techniques applied to cruise performance guarantees (Student's t distribution)
| ESDU-91018 | p 1233 N92-17843

STATISTICAL TESTS
Tests of fit for the Cauchy distribution based on the empirical distribution function
| AD-A243201 | p 1352 N92-17173
Example of statistical techniques applied to autoland touchdown dispersion (confidence intervals for normal and skew distributions)
| ESDU-91019 | p 1229 N92-17844

STATISTICAL WEATHER FORECASTING
A variational assimilation method for satellite and conventional data: A revised basic model 2B p 1322 N92-17977

STEADY FLOW
Application of program LAURA to perfect gas shock tube flows: A parametric study
| NASA-TM-104190 | p 1294 N92-17002
Pattern selection, wave formation, turbulence, and vortex breakdown in spiral flows
| AD-A242351 | p 1297 N92-17447
Development and utilization of new diagnostics for dense-phase pneumatic transport
| DE92-000337 | p 1299 N92-17704

STEADY STATE
Steady-state, high dose neutron generation and concentration apparatus and method for deuterium atoms
| AD-D015063 | p 1358 N92-17462

STEAM
Theoretical investigation of the injection and evaporation of water in a hydrogen/oxygen steam generator
| ESA-TT-1252 | p 1379 N92-17848

STEELS
The effect of weld metal strength mismatch on the deformation and fracture behavior of steel butt weldments
| AD-A243239 | p 1262 N92-17057
Residual stresses in a prestressed steel pressure vessel wrapped with multilayered composites
| AD-A243429 | p 1311 N92-17930
An investigation of gouge initiation in high-velocity sliding contact
| DE92-003944 | p 1311 N92-17937

STEERING
Multiple input sliding mode control for autonomous diving and steering of underwater vehicles
| AD-A241935 | p 1237 N92-17442
Toward the robust control of high bandwidth high precision flexible optical systems
| AD-A243471 | p 1366 N92-17536

STELLAR ATMOSPHERES
Stellar spectral line synthesis from an individual photon-following simulation
| AD-A242970 | p 1388 N92-17253

STELLAR ENVELOPES
Interstellar scattering towards the galactic center as probed by OH/IR stars p 1390 N92-18004

STELLAR MASS EJECTION
In situ observations of coronal mass ejections in interplanetary space
[DE92-003857] p 1390 N92-17725
STEMS
Global models for the biomechanics of green plants, part 1
[DE91-641478] p 1327 N92-17946
STEREOPHOTOGRAPHY
Extracting the shape and roughness of specular lobe objects using four light photometric stereo
[AD-A243522] p 1365 N92-17146
STEREOSCOPIC VISION
Near real-time stereo vision system
[NASA-CASE-NPO-18593-1-CU] p 1368 N92-17864
STIRLING ENGINES
Loss terms in free-piston Stirling engine models
[NASA-CR-189840] p 1312 N92-17225
STIRRING
Frequency stirring: An alternate approach to mechanical mode-stirring for the conduct of electromagnetic susceptibility testing
[AD-A243551] p 1279 N92-17031
STOCHASTIC PROCESSES
Performance measures for adaptive decisioning systems
[AD-A243183] p 1352 N92-16998
Stellar spectral line synthesis from an individual photon-following simulation
[AD-A242970] p 1388 N92-17253
A stochastic approach to the weighted-region problem: 1. The design of the path annealing algorithm
[AD-A243324] p 1340 N92-17403
Incipient fault detection using higher-order statistics
[AD-A243493] p 1308 N92-17431
Optical spectra and kinetics of single impurity molecules in a polymer: Spectral diffusion and persistent spectral hole-burning
[AD-A243749] p 1271 N92-17659
Wave propagation in a randomly inhomogeneous medium: A study of the problem
[AD-A243741] p 1284 N92-17691
Improving stochastic communication network performance: Reliability vs throughput
[AD-A243655] p 1285 N92-17763
The micro-c rule is not optimal in the 2nd node of the tandem queue; 2 counterexamples
[TW-91-05] p 1349 N92-17838
Stochastic robustness p 1237 N92-17997
Technical notes and correspondence: Stochastic robustness of linear time-invariant control systems p 1353 N92-18002
STOICHIOMETRY
A theoretical study of the combustion of magnesium/teflon/viton pyrotechnic compositions
[AD-A243244] p 1275 N92-17058
Ligand redistribution reactions of Me2Ga(C5H5) and MeGa(C5H5)2
[AD-A243264] p 1254 N92-17270
STORAGE BATTERIES
Silver-nickel composite cathodes for alkaline secondary batteries
[AD-D015121] p 1293 N92-17871
STORAGE RINGS (PARTICLE ACCELERATORS)
A study of gamma ray generation from channeled electrons and positions
[AD-A241993] p 1361 N92-17608
Medium-energy neutrino physics
[DE92-003790] p 1362 N92-17666
STORAGE STABILITY
Extravehicular mobility unit subcritical liquid oxygen storage and supply system
[NASA-CR-189831] p 1276 N92-16989
Evaluation of motor gasoline stability
[AD-A243063] p 1275 N92-17066
Testing of spacecraft in long-term storage
[AD-A242906] p 1250 N92-17580
STORAGE TANKS
Extravehicular mobility unit subcritical liquid oxygen storage and supply system
[NASA-CR-189831] p 1276 N92-16989
Aluminum alloys for ALS cryogenic tanks: Comparative measurements of cryogenic mechanical properties of Al-Li alloys and alloy 2219
[AD-A242956] p 1264 N92-17379
STORMS (METEOROLOGY)
Turbulent and gravity wave transport in the free atmosphere p 1315 N92-17063
The use of ADAP to examine warm and quasi-stationary frontal events in the northeastern United States
[PB91-225037] p 1319 N92-17363
STRAIN GAGES
Treadmill for space flight
[NASA-CASE-MSC-21752-1] p 1335 N92-17910
Magnetic multilayer strain gage
[AD-D015163] p 1381 N92-17940
STRAIN RATE
Mechanical and thermomechanical properties of NC base propellants
[AD-A243045] p 1276 N92-17632
STRATIFIED FLOW
Physical and computational modelling of stratified shear flows
[AERO-REPT-8909] p 1300 N92-17974
STREAM FUNCTIONS (FLUIDS)
Computation of three-dimensional flows using two stream functions
[NASA-CR-187802] p 1298 N92-17588
STRESS (PHYSIOLOGY)
Heat stress caused by wearing different types of CW protective garment
[AD-A243043] p 1334 N92-17278
Alleviation of thermal strain in engineering space personnel aboard CF ships with the exotemp personal cooling system
[AD-A242889] p 1330 N92-17599
STRESS ANALYSIS
Determination of symmetric end loads from bulk stresses on a rectangular prism
[AD-A242973] p 1310 N92-17254
Inelastic strain analysis of solder joint in NASA fatigue specimen
[NASA-CR-189882] p 1311 N92-17511
Strength of lugs
[ESDU-91008] p 1311 N92-17834
STRESS CONCENTRATION
Determination of antisymmetric end loads from bulk stresses on a rectangular prism
[AD-A243001] p 1310 N92-17265
STRESS DISTRIBUTION
Determination of symmetric end loads from bulk stresses on a rectangular prism
[AD-A242973] p 1310 N92-17254
Determination of antisymmetric end loads from bulk stresses on a rectangular prism
[AD-A243001] p 1310 N92-17265
Collisional energy deposition threshold for extended damage depths in ion-implanted silicates
[DE92-004737] p 1377 N92-17797
Residual stresses in a prestressed steel pressure vessel wrapped with multilayered composites
[AD-A243429] p 1311 N92-17930
STRESS MEASUREMENT
Determination of cohesive and normal stresses and simulation of fluidization using kinetic theory
[DE92-002905] p 1299 N92-17709
STRESS-STRAIN RELATIONSHIPS
Experimental investigation of adiabatic shear banding at different impact velocities
[AD-A243011] p 1310 N92-17256
On size scaling in shock hydrodynamics and the stress-strain behavior of copper at exceedingly high strain rates
[DE92-003797] p 1265 N92-17579
Data acquisition and measurement system for plastic parameters of radiation metal research experiments
[DE92-610350] p 1266 N92-17808
STRESSES
Thin films under chemical stress
[DE92-004684] p 1378 N92-17857
STRING THEORY
Gauge-covariant Wess-Zumino actions for super p-branes in superspace
[DE91-641524] p 1353 N92-17318
High energy physics program at Texas A and M University
[DE92-004426] p 1363 N92-17738
STRIP
A rigorous UTD analysis of electromagnetic scattering from resistive strips and resistive-loaded conducting strips
[AD-A243691] p 1280 N92-17092
STRIP TRANSMISSION LINES
A discontinuity study in shielded coplanar line
[AD-A242976] p 1288 N92-17290
STRUCTURAL ANALYSIS
Effect of coatings and processing on failure mechanisms of polycarbonate material, phase 1
[AD-A243018] p 1256 N92-17053
Structures to resist the effects of accidental explosions
[AD-A243272] p 1277 N92-17272
The computational structural mechanics testbed procedures manual
[NASA-TM-100646] p 1310 N92-17333
Finite element analysis of ASTOVL fighter structure
[AD-A243724] p 1233 N92-17513
Parallel block methods for sparse symmetric linear systems of equations
[AD-A242315] p 1351 N92-17560
Molecular self-assembly and nanochemistry: A chemical strategy for the synthesis of nanostructures
[AD-A243530] p 1361 N92-17616
Optical modification of a single impurity molecule in a solid
[AD-A243750] p 1362 N92-17660
STRUCTURAL DESIGN
Reliability analysis of structural ceramic components using a three-parameter Weibull distribution
[NASA-TM-105370] p 1267 N92-17060
STRUCTURAL ENGINEERING
Parallel block methods for sparse symmetric linear systems of equations
[AD-A242315] p 1351 N92-17560
STRUCTURAL FAILURE
Proceedings of the USAF Structural Integrity Program Conference
[AD-A242943] p 1235 N92-17204
STRUCTURAL RELIABILITY
Proceedings of the USAF Structural Integrity Program Conference
[AD-A242943] p 1235 N92-17204
STRUCTURAL VIBRATION
The NASA/industry design analysis methods for vibrations (DAMVIBS) program: Accomplishments and contributions
[NASA-TM-104192] p 1309 N92-17034
Loading and vibration reduction through active aerodynamic control
[AD-A242321] p 1236 N92-17243
Control of a large flexible space structure using multiple model adaptive algorithms
[AD-A243759] p 1250 N92-17602
STUDENTS
Mathematics and biology
[DE92-611247] p 1327 N92-17815
SUBDIVISIONS
Summaries of FY 1991 engineering research
[DE92-004708] p 1277 N92-17593
SUBMILLIMETER WAVES
Integration of an anti-parallel pair of planar Schottky barrier diodes for millimeter and submillimeter wavelengths
[AD-A243371] p 1287 N92-17189
SUBSONIC FLOW
Chemical reactions in turbulent mixing flows
[AD-A243035] p 1294 N92-16979
SUBSTITUTES
A reexamination of F-19 NMR in selected solids, the conductor Ag2F and reference insulators for studies of YBa2Cu3O7-type superconductors
[AD-A243194] p 1372 N92-17219
Evaluation of liposome-encapsulated Hemoglobin/LR16 formulations as a potential blood substitute
[AD-A243075] p 1329 N92-17557
Propane aromatization over gallium containing HZSM-5 zeolites
[ETN-92-90897] p 1262 N92-17925
SUBSTRATES
Transmission electron microscopy of the CVD diamond film/substrate interface
[AD-A243096] p 1373 N92-17322
Total Dielectric Isolation (TDI) of fully depleted device structures
[AD-A241926] p 1289 N92-17439
Suspended substrate resonator design
[AD-A243250] p 1290 N92-17573
Studies of hetero-epitaxy of GaAs films on Si substrate for effective control of density and internal stress
[AD-A241882] p 1374 N92-17594
SULFATES
Effects of the chemical defense antidote atropine sulfate on helicopter pilot performance: An in-flight study
[AD-A241966] p 1328 N92-17084
SULFONATES
Molecular motions of the head group of SHBS in lamellar liquid crystals
[AD-A243499] p 1373 N92-17382
Studies of the adsorption of tetrasulfonated phthalocyanines on graphite substrate
[AD-A243443] p 1260 N92-17489
SULFUR DIOXIDES
Reaction kinetics and transport properties of the CaO-SO2-O2 system in absence of intra-particle diffusion
[DE91-002086] p 1261 N92-17788
SUMMARIES
Summary reports of activities under visiting research program
[DE91-522477] p 1391 N92-17623
SUMS
Inequalities among partial traces of Hermitian operators and partial sums of their Eigenvalues
[DE91-641495] p 1351 N92-17622

SUN
Solar-geophysical data number 562, June 1991. Part 2: (Comprehensive reports). Data for December 1990 and miscellaneous
| PB91-230219 | p 1387 N92-17251
SUNLIGHT
User evaluation of laser ballistic sun, wind and dust goggle lenses (dye technology)
| AD-A243245 | p 1334 N92-17143
SUNRISE
Tidal and lunar data for Point Mugu, San Nicolas Island, and the Barking Sands area during 1992
| AD-A243210 | p 1324 N92-17177
SUNSET
Tidal and lunar data for Point Mugu, San Nicolas Island, and the Barking Sands area during 1992
| AD-A243210 | p 1324 N92-17177
SUPERCONDUCTING FILMS
High temperature superconductor thin films and Josephson junctions
| AD-A242747 | p 1293 N92-17949
Comparative study of irreversibility effects in Nb foil and high temperature superconducting ceramics by muon spin rotation
| DE92-600475 | p 1294 N92-17953
SUPERCONDUCTING MAGNETS
Workshop on Technology Issues of Superconducting MAGLEV Transportation Systems
| DE92-002288 | p 1307 N92-17604
SUPERCONDUCTING SUPER COLLIDER
High energy physics program at Texas A and M University
| DE92-004426 | p 1363 N92-17738
SUPERCONDUCTIVITY
Growth of near-free-standing YBa2Cu3O7-type crystals using a self-decanting flux method
| AD-A243221 | p 1372 N92-17182
Evidence for strong electron-phonon coupling in thermal conductivity of YBa2Cu3O(7-delta)
| AD-A243192 | p 1372 N92-17218
A comparative study of the noise performance of Alluminum Gallium Arsenide/Gallium Arsenide high electron mobility transistors with and without superconducting gate electrodes p 1288 N92-17317
Superconducting microwave transmission lines
| AD-A243166 | p 1291 N92-17671
Design and evaluation of a Josephson array oscillator
| AD-A243167 | p 1291 N92-17672
Radiation effects in High Temperature Superconductors (HTSC) oxides p 1375 N92-17700
Comparative study of irreversibility effects in Nb foil and high temperature superconducting ceramics by muon spin rotation
| DE92-600475 | p 1294 N92-17953
SUPERCONDUCTORS
Critical temperature determination in superconductors
| AD-A243537 | p 1371 N92-17015
Ceramics with superelectrical and supermechanical properties
| AD-A243062 | p 1267 N92-17029
Superdirective properties of closed loops of parallel coplanar dipoles
| AD-A243009 | p 1288 N92-17268
Analysis of possible schemes for twisting multiwire superconducting cables and design of twisting equipment
| DE92-609667 | p 1294 N92-17971
SUPERHEATING
Wall temperature patterns in nucleate boiling
| OUEL-1876/91 | p 1380 N92-17879
SUPERHIGH FREQUENCIES
Simultaneous active and passive microwave measurements of the ocean surface
| AD-A242232 | p 1312 N92-17459
SUPERLATTICES
Excitons in semiconducting superlattices, quantum wells, and ternary alloys
| DE91-018805 | p 1374 N92-17528
A study of gamma ray generation from channeled electrons and positions
| AD-A241993 | p 1361 N92-17608
Optical properties of thermally intermixed quantum wells and superlattices
| AD-A243546 | p 1375 N92-17618
SUPERNOVA REMNANTS
Constraints on cosmic ray propagation in the galaxy
| NASA-CR-189779 | p 1390 N92-18003
SUPERSATURATION
Kinetics of a new phase formation in supersaturated solid solutions. 1. Dilute one-component systems
| DE92-610065 | p 1262 N92-17943
SUPERSONIC JET FLOW
Chemical reactions in turbulent mixing flows
| AD-A243035 | p 1294 N92-16979
SUPERSYMMETRY
Gauge-covariant Wess-Zumino actions for super p-branes in superspace
| DE91-641524 | p 1353 N92-17318
SUPPORT SYSTEMS
AGSSS: The Airborne Graphics Software Support System; an Ada/PHIGS-based display editor for the rapid development of cockpit display software systems
| AD-A243224 | p 1234 N92-17221
SUPPORTS
Radar scattering from foamed plastic target supports
| AD-A243756 | p 1284 N92-17722
Low frequency vibration absorber
| AD-D015103 | p 1307 N92-17827
SURFACE CRACKS
Effect of coatings and processing on failure mechanisms of polycarbonate material, phase 1
| AD-A243018 | p 1256 N92-17053
SURFACE DIFFUSION
Evaluation of a diffusion/trapping model for hydrogen ingress in high-strength alloys
| AD-A243461 | p 1263 N92-17327
SURFACE LAYERS
In situ surface x ray scattering of metal monolayers adsorbed at solid-liquid interfaces
| AD-A243258 | p 1262 N92-16985
Electronic interactions of directed photon beams with surfaces
| AD-A241878 | p 1356 N92-17026
An investigation of underpotentially deposited thallium of silver (111) by in-situ surface x ray scattering
| AD-A243270 | p 1263 N92-17271
SURFACE NAVIGATION
Severe weather guide Mediterranean ports. Part 38: Alexandria
| AD-A243451 | p 1320 N92-17406
SURFACE PROPERTIES
Surface observation climatic summaries for Duke Field/Eglin aux no. 3, Florida
| AD-A243310 | p 1318 N92-17073
Surface observation climatic summaries for Castle AFB, California
| AD-A243677 | p 1318 N92-17074
Extracting the shape and roughness of specular lobe objects using four light photometric stereo
| AD-A243522 | p 1365 N92-17146
Comparison of two eighth-mesh terrain databases
| AD-A243315 | p 1383 N92-17401
Atomic relaxation at ordered electrochemical surfaces probed by scanning tunneling microscopy: Au(111) in aqueous solution compared with ultrahigh-vacuum environments
| AD-A242031 | p 1358 N92-17472
Nonlinear spectroscopic studies of interfacial molecular ordering
| DE92-000864 | p 1360 N92-17530
The surface impedance synthesis technique
| AD-A243731 | p 1284 N92-17689
Environmental containment property estimation using QSARs in an expert system
| AD-A243728 | p 1336 N92-17720
SURFACE REACTIONS
In situ x ray standing wave study of Cu UPD on an iodine covered platinum surface
| AD-A243474 | p 1264 N92-17426
Comparisons of self-assembled monolayers on silver and gold: Mixed monolayers derived from HS(CH2)21X and HS(CH2)10(sup Y) (X,Y-CH3, CH2OH) have similar properties
| AD-A243487 | p 1264 N92-17427
Surface chemistry at the semiconductor/electrolyte interface
| DE91-018511 | p 1374 N92-17532
Ionic physics and technology p 1362 N92-17818
SURFACE ROUGHNESS
Sea surface environmental conditions in the Gulf of Alaska during April 1990 using SSM/I
| AD-A241909 | p 1323 N92-17041
An optical roughness sensor for the real time determination of spray formed preform quality
| AD-A243238 | p 1262 N92-17056
Extracting the shape and roughness of specular lobe objects using four light photometric stereo
| AD-A243522 | p 1365 N92-17146
Enhanced backscattering of light from randomly rough diffusers: Appendix
| AD-A243436 | p 1366 N92-17485
Enhanced backscattering from rough surfaces
| AD-A243437 | p 1366 N92-17486
Deterministic multi-zone ice accretion modeling p 1220 N92-17987
SURFACE TEMPERATURE
Effects of power pulsations on heat transfer from discrete heat sources
| AD-A243434 | p 1379 N92-17686
SURFACE VEHICLES
Workshop on Technology Issues of Superconducting MAGLEV Transportation Systems
| DE92-002288 | p 1307 N92-17604
Discussion for possibility of some aerodynamic ground effect craft
| NAL-TM-619 | p 1278 N92-17757
SURFACTANTS
Molecular motions of the head group of SHBS in lamellar liquid crystals
| AD-A243499 | p 1373 N92-17382
Clean room wiping liquids
| DE92-004793 | p 1238 N92-17967
SURVEILLANCE
Early warning satellites: Funding for follow-on system is premature
| AD-A242836 | p 1245 N92-17250
A fully decentralized multi-sensor system for tracking and surveillance
| OUEL-1886/91 | p 1302 N92-17926
SURVEYS
Information management 70XX civilian equivalent
| AD-A242875 | p 1381 N92-17013
USI rapid prototyping tool evaluations survey
| AD-A243168 | p 1335 N92-17673
IRAS and the Boston University Arecibo Galactic H I Survey: A catalog of cloud properties
| NASA-CR-189806 | p 1387 N92-17695
SURVIVAL
Bayesian computations in survival models via the Gibbs sampler
| AD-A242343 | p 1353 N92-17643
SWEAT COOLING
Transpiration cooled throat for hydrocarbon rocket engines
| NASA-CR-184272 | p 1253 N92-17495
SWELLING
Thin films under chemical stress
| DE92-004684 | p 1377 N92-17857
SWITCHES
Th 3-5 modulation and switching devices for optical system applications
| AD-A243055 | p 1365 N92-17044
Transformerless DC-DC voltage amplifier with optically isolated switching devices
| NASA-CASE-NPO-17994-1-CU | p 1293 N92-17907
SWITCHING
Th 3-5 modulation and switching devices for optical system applications
| AD-A243055 | p 1365 N92-17044
A study of nonlinear reflection and optical switching in indium antimonide
| AD-A242835 | p 1365 N92-17249
SWITCHING CIRCUITS
Results from a data acquisition system prototype project using a switch-based event builder
| DE92-004638 | p 1336 N92-17592
SYMBIOSIS
Evolution as a molecular cooperative phenomenon
| DE92-609575 | p 1327 N92-17877
SYMMETRY
Lie-isotopic generalization of the Poincare symmetry: Classical formulation
| DE91-642825 | p 1379 N92-17531
SYNCHRONISM
Performance modeling of the Ada rendezvous
| AD-A243392 | p 1339 N92-17211
SYNOPTIC METEOROLOGY
Surface observation climatic summaries for Boise Air Terminal, ID
| AD-A243012 | p 1319 N92-17257
SYNTHESIS (CHEMISTRY)
Catalytic studies on a novel synthesis of methanol
| DE92-002904 | p 1275 N92-17184
Ligand redistribution reactions of Me2Ga(C5H5) and MeGa(C5H5)2
| AD-A243264 | p 1254 N92-17270
Molecular self-assembly and nanochemistry: A chemical strategy for the synthesis of nanostructures
| AD-A243530 | p 1361 N92-17616
SYNTHETIC APERTURE RADAR
Gabor segmentation of high resolution synthetic aperture radar imagery
| AD-A243753 | p 1284 N92-17662
SYSTEM EFFECTIVENESS
Dynamic pattern matcher using incomplete data
| NASA-CASE-MSC-21415-1-SB | p 1344 N92-17860
SYSTEM FAILURES
Communication network survivability
| AD-A242969 | p 1281 N92-17252
SYSTEM IDENTIFICATION
Neural network modeling of nonlinear systems based on Volterra series extension of a linear model
| NASA-TM-104177 | p 1347 N92-16987
Rotorcraft System Identification
| AGARD-LS-178 | p 1230 N92-17153

Design of experiments p 1230 N92-17154
Instrumentation and data processing p 1230 N92-17155
Identification techniques: Model structure and time domain methods p 1231 N92-17157
Identification techniques: Frequency domain methods p 1231 N92-17158
Modelling aspects and robustness issues in rotorcraft system identification p 1231 N92-17159
Assessment of rotorcraft system identification as applied to the AH-64 p 1231 N92-17160
BO 105 identification results p 1231 N92-17161
SA 330 Puma identification results p 1231 N92-17162
Industry view on rotorcraft system identification p 1232 N92-17163
Application areas for rotorcraft system identification: Simulation model validation p 1232 N92-17164
System identification methods for handling-qualities evaluation p 1232 N92-17165
System identification requirements for high-bandwidth rotorcraft flight control system design p 1232 N92-17166
Neural networks for aircraft system identification p 1222 N92-17998

SYSTEMS ANALYSIS
Benefit analysis of proposed information systems
| AD-A243707 | p 1382 N92-17125
Systems special investigation group
| NASA-CR-187355 | p 1250 N92-17728

SYSTEMS ENGINEERING
Environmental interactions in Space Exploration: Announcement of the formation of an Environmental Interactions Working Group
| NASA-TM-105294 | p 1389 N92-17069
Beyond the Baseline 1991: Proceedings of the Space Station Evolution Symposium. Volume 2: Space Station Freedom, part 2
| NASA-CP-10083-VOL-2-PT-2 | p 1245 N92-17348
Failure Environment Analysis Tool (FEAT) p 1245 N92-17349
Muons in UA1; the 2nd level trigger and dimuon results
| ETN-92-90565 | p 1360 N92-17520
Magnetohydrodynamic projects at the CDIF
| DE92-002636 | p 1370 N92-17664
Active thermal control system evolution p 1252 N92-17775

SYSTEMS MANAGEMENT
The top ten critical MIS issues in the Department of Defense
| AD-A242975 | p 1382 N92-17255

SYSTOLIC ARRAYS
Program translation tools for systolic arrays
| AD-A242924 | p 1336 N92-17466

T

TABLES (DATA)
The complete hard x ray burst spectrometer event list, 1980-1989
| NASA-TM-4332 | p 1389 N92-17048
Surface observation climatic summaries for Duke Field/Eglin aux no. 3, Florida
| AD-A243310 | p 1318 N92-17073
Surface observation climatic summaries for Castle AFB, California
| AD-A243677 | p 1318 N92-17074
Surface observation climatic summaries for Hondo Municipal Airport, Texas
| AD-A243311 | p 1319 N92-17144

TAKEOFF
Variability of standard aircraft performance parameters
| ESDU-91020 | p 1233 N92-17847

TAPES
Method for non-destructive estimation of waveguide directional coupler dimensions
| NASA-CASE-NPO-18454-1-CU | p 1293 N92-17865

TARGET ACQUISITION
Analysis of scene conditions at the light helicopter target acquisition subsystem demonstration/validation, Yuma Proving Ground, Arizona, September 1990
| AD-A243234 | p 1234 N92-17240
Integrated system for missile detection and discrimination
| DE91-018874 | p 1283 N92-17529
Method of guiding an in-flight vehicle to a designed flight path
| AD-D015061 | p 1229 N92-17707
Object acquisition and tracking for space-based surveillance
| AD-A243333 | p 1367 N92-17711
A decentralized Bayesian algorithm for identification of tracked targets
| OUEL-1892/91 | p 1344 N92-17927

TARGET RECOGNITION
A general computational framework for distributed sensing and fault-tolerant sensor integration
| AD-A243256 | p 1300 N92-16983
Object acquisition and tracking for space-based surveillance
| AD-A243333 | p 1367 N92-17711
A decentralized Bayesian algorithm for identification of tracked targets
| OUEL-1892/91 | p 1344 N92-17927

TARGETS
Radar scattering from foamed plastic target supports
| AD-A243756 | p 1284 N92-17722

TASK COMPLEXITY
The multi-attribute task battery for human operator workload and strategic behavior research
| NASA-TM-104174 | p 1338 N92-17130

TASKS
The effects of speech intelligibility level on concurrent visual task performance
| AD-A243015 | p 1331 N92-17052
Neural network classification of mental workload conditions by analysis of spontaneous electroencephalograms
| AD-A243369 | p 1331 N92-17115

TAYLOR SERIES
Modeling convergence zone gain on MS-DOS based personal computers
| AD-A243252 | p 1341 N92-17558

TECHNOLOGICAL FORECASTING
Automated planning with special relevance to associate systems technology and mission planning
| AD-A241924 | p 1348 N92-17438

TECHNOLOGIES
Scientific and technological relations between the United States and Japan: Issues and recommendations
| PB91-219170 | p 1385 N92-17283

TECHNOLOGY TRANSFER
Valuable patents for US businesses: A catalog of DTRC patents available for licensing by the private sector
| AD-A242071 | p 1385 N92-17141

TECHNOLOGY UTILIZATION
Space Station Freedom program. Commercial infrastructure and technology utilization p 1244 N92-17111
Collision avoidance sensor skin p 1247 N92-17361
Catalysts for ultrahigh current density oxygen cathodes for space fuel cell applications
| NASA-CR-189787 | p 1253 N92-17365

TEFLON (TRADEMARK)
A theoretical study of the combustion of magnesium/teflon/viton pyrotechnic compositions
| AD-A243244 | p 1275 N92-17058

TELECOMMUNICATION
An overview of cellular telecommunications
| AD-A242951 | p 1281 N92-17232
Toward a national semiconductor strategy, volume 1
| PB91-201293 | p 1290 N92-17620

TELECONFERENCING
Development of a Federal standard for a video codec operating at P x 64 KBPS
| AD-A243005 | p 1281 N92-17267

TELEMETRY
Investigation of mechanisms for the source and loss of electrons from the radiation belts using data from SEEP, SCATHA and P78-1 satellites
| AD-A243376 | p 1317 N92-17405

TELEOPERATORS
JPL space station telerobotic engineering prototype development: Advanced telerobotics system technology p 1247 N92-17358
JPL space station telerobotic engineering prototype development FY 91 status/achievements p 1247 N92-17359

TELEROBOTICS
Space Station Freedom engineering prototype development p 1244 N92-17110
JPL space station telerobotic engineering prototype development: Advanced telerobotics system technology p 1247 N92-17358
JPL space station telerobotic engineering prototype development FY 91 status/achievements p 1247 N92-17359
Telerobotic ground-remote operations p 1247 N92-17360

TELESCOPES
High resolution imaging using phase retrieval, volume 2
| AD-A242925 | p 1366 N92-17550

TELEVISION SYSTEMS
Real-time edge-enhanced optical correlator
| NASA-CASE-NPO-18379-1-CU | p 1367 N92-17675

TEMPERATURE CONTROL
Application of silicon micromachining to thermal dissipation issues in wafer scale integrated circuits
| AD-A243744 | p 1288 N92-17332
Upper body exercise: Physiology and training application for human presence in space
| AD-A242033 | p 1329 N92-17473
Active thermal control system evolution p 1252 N92-17775
Thermal Control System Automation Project (TCSAP) p 1252 N92-17776
Microprocessor controller in CAMAC standard for temperature regulation and stabilization
| DE92-611158 | p 1348 N92-17814

TEMPERATURE DEPENDENCE
Determination of the electronic density of states of YBa2Cu3O(7-delta)
| AD-A243223 | p 1372 N92-17220
The effect of monomer structures and compressibility on the properties of multicomponent polymer blends and solutions
| AD-A242863 | p 1273 N92-17777
Temperature dependent anomalous statistics
| DE92-609665 | p 1379 N92-17807
Mechanisms of gas permeation through polymer membranes
| DE92-004423 | p 1274 N92-17942

TEMPERATURE DISTRIBUTION
Surface meteorological and near surface oceanographic atlas of the tropical Indian Ocean
| PB91-234286 | p 1319 N92-17138
The charge exchange recombination diagnostic system on the D3-D tokamak
| DE92-003805 | p 1369 N92-17456
A study of electric transmission lines for use on the lunar surface p 1292 N92-17742
Results of measured temperature distribution on an adiabatic wing model with radiation thermometer
| NAL-TM-610 | p 1225 N92-17755
Wall temperature patterns in nucleate boiling
| OUEL-1876/91 | p 1380 N92-17879

TEMPERATURE EFFECTS
Examining Si3N4 base materials with various rare earth additions
| AD-A243668 | p 1372 N92-17082
Flight vehicle thermal testing with infrared lamps
| NASA-TM-4336 | p 1232 N92-17226
A spectroscopic immersion ellipsometry study of the mechanism of Si/SiO2 interface annealing
| AD-A242831 | p 1259 N92-17261
The wave numbers of supercritical surface tension driven Benard convection
| NASA-CR-189856 | p 1373 N92-17375
Molecular motions of the head group of SHBS in lamellar liquid crystals
| AD-A243499 | p 1373 N92-17382
Inelastic strain analysis of solder joint in NASA fatigue specimen
| NASA-CR-189882 | p 1311 N92-17511
Concentration of isotopic hydrogen by temperature gradient effect in soluble metal
| AD-D015062 | p 1260 N92-17628
Direct speciation of metal and metalloid ions by optical spectroscopies
| DE92-003868 | p 1261 N92-17727
The influence of temperature and composition on the activation energy for creep in binary aluminum lithium alloys
| AD-A242299 | p 1265 N92-17759
Effect of thermal annealing on property changes of neutron-irradiated non-graphitized carbon materials and nuclear graphite
| DE92-704180 | p 1257 N92-17816

TEMPERATURE GRADIENTS
Source of cold water in Monterey Bay observed by AVHRR satellite imagery
| AD-A242843 | p 1323 N92-17051
Surface meteorological and near surface oceanographic atlas of the tropical Indian Ocean
| PB91-234286 | p 1319 N92-17138
Concentration of isotopic hydrogen by temperature gradient effect in soluble metal
| AD-D015062 | p 1260 N92-17628

TEMPERATURE MEASUREMENT
Velocity measurements in high temperature gases using laser-induced no fluorescence
| AD-A242399 | p 1295 N92-17012
Experimental measurements of plasma properties for Miller SG-100 torch with Mach I setting
| DE92-003309 | p 1369 N92-17469
Effects of power pulsations on heat transfer from discrete heat sources
| AD-A243434 | p 1379 N92-17686
Results of measured temperature distribution on an adiabatic wing model with radiation thermometer
| NAL-TM-610 | p 1225 N92-17755
Experimental investigation of passive infrared ice detection for helicopter applications p 1220 N92-17986

TEMPERATURE PROFILES
Source of cold water in Monterey Bay observed by AVHRR satellite imagery
| AD-A242843 | p 1323 N92-17051
An investigation of cold overflow over the Iceland/Faeroes Ridge
| AD-A243084 | p 1324 N92-17169
TENSILE PROPERTIES
Aluminum alloys for ALS cryogenic tanks: Comparative measurements of cryogenic mechanical properties of Al-Li alloys and alloy 2219
| AD-A242956 | p 1264 N92-17379
TENSILE TESTS
Acoustic emission monitoring of low velocity impact damage in graphite/epoxy laminates during tensile loading
| NASA-TM-4339 | p 1258 N92-17881
TERMINAL BALLISTICS
Large centrifuge: A critical Army capability for the future
| AD-A243287 | p 1238 N92-17287
TERMINAL GUIDANCE
Method of guiding an in-flight vehicle to a designed flight path
| AD-D015061 | p 1229 N92-17707
TERNARY ALLOYS
Excitons in semiconducting superlattices, quantum wells, and ternary alloys
| DE91-018805 | p 1374 N92-17528
TERNARY SYSTEMS
New optical materials for the long-wave (8-12 microns) region: Design criteria for the solid-state chemist
| AD-A243280 | p 1365 N92-17284
TERRAIN
Comparison of two eighth-mesh terrain databases
| AD-A243315 | p 1383 N92-17401
A stochastic approach to the weighted-region problem: 1. The design of the path annealing algorithm
| AD-A243324 | p 1340 N92-17403
Effect of two types of scene detail on detection of altitude change in a flight simulator
| AD-A242034 | p 1333 N92-17758
TEST CHAMBERS
Downflow heat transfer in a heated ribbed vertical annulus with a cosine power profile (results from test series ECS-2c)
| DE92-003259 | p 1298 N92-17626
TEST EQUIPMENT
Thermal energy test apparatus
| AD-A243526 | p 1379 N92-17537
Determination of the tribological fundamentals of solid lubricated ceramics. Volume 1: Summary
| AD-A243219 | p 1272 N92-17683
TEST FACILITIES
Advanced nozzle and engine components test facility
| NASA-TM-103684 | p 1237 N92-17059
Safety considerations in testing a fuel-rich aeropropulsion gas generator
| NASA-TM-105258 | p 1235 N92-17061
Spherical near-field scanning: Experimental and theoretical studies
| AD-A243489 | p 1282 N92-17429
Using the Global Positioning System (GPS) to fulfill the position/location requirements of the National Training Center (NTC) and other US Army instrumented testing and training ranges
| AD-A242064 | p 1229 N92-17639
Laser range safety
| AD-A243606 | p 1305 N92-17962
TEST STANDS
Qualification test report. Fuel pump test stand 3C3965G05
| AD-A242929 | p 1235 N92-17552
TEXAS
Surface observation climatic summaries for Hondo Municipal Airport, Texas
| AD-A243311 | p 1319 N92-17144
TEXTILES
Polymer infiltration studies
| NASA-CR-189773 | p 1266 N92-17004
THALLIUM
An investigation of underpotentially deposited thallium of silver (111) by in-situ surface x ray scattering
| AD-A243270 | p 1263 N92-17271
THEOREM PROVING
A proof theory for a sequential version of POOL
| CWI-CS-R9118 | p 1346 N92-17833
THEOREMS
A GNS-type theorem for a non-involutive Banach algebra
| DE91-641481 | p 1354 N92-17803
A proof theory for a sequential version of POOL
| CWI-CS-R9118 | p 1346 N92-17833
Sydney Goldstein FRS Hon FRAeS: An appreciation
| AERO-REPT-8903 | p 1391 N92-17928
THEORETICAL PHYSICS
Axino-induced baryogenesis
| NASA-CR-189858 | p 1361 N92-17646
Medium-energy neutrino physics
| DE92-003790 | p 1362 N92-17666
THERMAL ABSORPTION
Biophysical techniques for examining metabolic, proliferative, and genetic effects of microwave radiation
| AD-A241903 | p 1326 N92-17288
Picosecond laser breakdown thresholds in gases
| AD-A242941 | p 1304 N92-17475
THERMAL ANALYSIS
Computer aided thermal analysis of a microcircuit structure
| AD-A243160 | p 1287 N92-17205
Long duration exposure facility post-flight thermal analysis: Orbital/thermal environment data package
| NASA-CR-189872 | p 1245 N92-17334
Long duration exposure facility solar illumination data package
| NASA-CR-189873 | p 1241 N92-17335
THERMAL BATTERIES
Lithiated Vanadium Oxide (LVO), gamma-lithium vanadium bronze (Gamma-LiV2O5) and vanadium dioxide (VO2) as thermal battery cathode materials
| AD-A242948 | p 1287 N92-17186
THERMAL CONDUCTIVITY
Evidence for strong electron-phonon coupling in thermal conductivity of YBa2Cu3O(7-delta)
| AD-A243192 | p 1372 N92-17218
Method of doping single crystal diamond for electronic devices
| AD-D015069 | p 1374 N92-17610
Electrical and thermal conductivity of a variable zone semiconductor in a longitudinal magnetic field
p 1291 N92-17702
High contact blind hole thermocouple plug
| AD-D015105 | p 1302 N92-17835
THERMAL CYCLING TESTS
Thermo-mechanical fatigue of a fiber reinforced titanium aluminide composite
| AD-A241988 | p 1256 N92-17607
THERMAL EMISSION
Determination of antisymmetric end loads from bulk stresses on a rectangular prism
| AD-A243001 | p 1310 N92-17265
THERMAL ENERGY
University of Minnesota Aquifer Thermal Energy Storage (ATES) project report on the first long-term cycle
| DE92-004699 | p 1313 N92-17934
THERMAL ENVIRONMENTS
Long duration exposure facility post-flight thermal analysis: Orbital/thermal environment data package
| NASA-CR-189872 | p 1245 N92-17334
Alleviation of thermal strain in engineering space personnel aboard CF ships with the exotemp personal cooling system
| AD-A242889 | p 1330 N92-17599
THERMAL FATIGUE
Thermo-mechanical fatigue of a fiber reinforced titanium aluminide composite
| AD-A241988 | p 1256 N92-17607
THERMAL INSULATION
Thermal insulation chemical composition and method of manufacture
| AD-D015106 | p 1257 N92-17836
THERMAL MAPPING
Analysis of scene conditions at the light helicopter target acquisition subsystem demonstration/validation, Yuma Proving Ground, Arizona, September 1990
| AD-A243234 | p 1234 N92-17240
THERMAL NEUTRONS
Characterization of the thermalness of a fissile system with a 2-group diffusion theory parameter
| AD-A243065 | p 1360 N92-17555
Determination of diffusion parameters of thermal neutrons for non-moderator media by a pulsed method and a time independent method
| DE92-600624 | p 1362 N92-17954
THERMAL PROTECTION
Thermal energy test apparatus
| AD-A243526 | p 1379 N92-17537
Magnetohydrodynamic projects at the CDIF
| DE92-002636 | p 1370 N92-17664
THERMAL RADIATION
Exploring plasma sheath solutions for planar and cylindrical anodes
| AD-A243237 | p 1369 N92-17030
Long duration exposure facility solar illumination data package
| NASA-CR-189873 | p 1241 N92-17335
EMU evolution p 1246 N92-17354
Picosecond laser breakdown thresholds in gases
| AD-A242941 | p 1304 N92-17475
Optical properties of thermally intermixed quantum wells and superlattices
| AD-A243546 | p 1375 N92-17618
THERMAL RESISTANCE
Solder extrusion pressure bonding process and bonded products produced thereby
| DE92-004603 | p 1363 N92-17739
THERMAL STABILITY
High-temperature durability considerations for HSCT combustor
| NASA-TP-3162 | p 1267 N92-17070
Polyimides containing amide and perfluoroisopropyl connecting groups
| NASA-CASE-LAR-14608-1 | p 1271 N92-17676
THERMAL STRESSES
Alleviation of thermal strain in engineering space personnel aboard CF ships with the exotemp personal cooling system
| AD-A242889 | p 1330 N92-17599
THERMISTORS
Cryogenic thermoresistor made from p-InSb(Mn)
| DE92-600473 | p 1293 N92-17825
THERMOCOUPLES
High contact blind hole thermocouple plug
| AD-D015105 | p 1302 N92-17835
THERMODYNAMIC EQUILIBRIUM
The wave numbers of supercritical surface tension driven Benard convection
| NASA-CR-189856 | p 1373 N92-17375
THERMODYNAMIC PROPERTIES
Collisional dynamics of the B3Pi(O+) state of bromine of monofluoride
| AD-A241857 | p 1356 N92-17305
Numerical grid generation using a variational method
| MBB-FE211-S-PUB-447 | p 1297 N92-17312
Modelling of some equilibrium thermodynamic properties of polymer systems
| ETN-92-90570 | p 1273 N92-17840
THERMODYNAMICS
Codeposition of elements in diffusion coatings by the halide-activated pack cementation method
| AD-A242860 | p 1267 N92-17042
A variational assimilation method for satellite and conventional data: Development of basic model for diagnosis of cyclone systems
| NASA-CR-188236 | p 1321 N92-17975
A variational assimilation method for satellite and conventional data: Model 2 (version 1)
p 1322 N92-17976
THERMOELECTRIC POWER GENERATION
Thermally regenerative fuel cells
| AD-A242900 | p 1290 N92-17629
THERMOPLASTICITY
The effect of physical aging on the creep response of a thermoplastic composite
| AD-A243600 | p 1258 N92-17932
THERMOSPHERE
Relaxation processes of vibrationally excited H2O in the mesosphere and thermosphere
| AD-A241853 | p 1315 N92-17035
THICK PLATES
Static analysis of thick composite plates using higher order three dimensional finite elements
| AD-A243188 | p 1256 N92-17367
THICKNESS
Higher-order thickness expansions for cylindrical shells
| AD-A242017 | p 1310 N92-17230
Magnetic multilayer interface anisotropy
| DE92-000635 | p 1263 N92-17319
THIN FILMS
Heat flux sensor research and development: The cool film calorimeter
| NASA-CR-189789 | p 1301 N92-17006
Preparation of ferroelectric samples for electrical and radiation characterization studies
| AD-A243432 | p 1288 N92-17326
Research and development on advanced silicon carbide thin film growth techniques and fabrication of high power and microwave frequency silicon carbide-based device structures
| AD-A243531 | p 1373 N92-17390
Enhanced backscattering from rough surfaces
| AD-A243437 | p 1366 N92-17486
X ray damage to CF3CO2-Terminated organic monolayers on Si/Au supports is due primarily to x ray induced electrons
| AD-A243446 | p 1289 N92-17490
An interface enhanced spectroscopic ellipsometry technique: Application to Si-SiO2
| AD-A242867 | p 1260 N92-17613
Spatially and spectrally resolved cathodoluminescence measurements of CVD-grown diamond particles and films
| AD-A243220 | p 1271 N92-17615

Polyimides containing amide and perfluoroisopropyl connecting groups
| NASA-CASE-LAR-14608-1 | p 1271 N92-17676
Characterizing the sensitivity, selectivity, and reversibility of the metal-doped phthalocyanine thin-films used with the Interdigitated Gate Electrode Field-Effect Transistor (IGEFET) to detect organophosphorous compounds and nitrogen dioxide
| AD-A243635 | p 1376 N92-17746
Characterization of PZT thin films: Crystallographic phases
| DE92-003514 | p 1377 N92-17790
Thin films under chemical stress
| DE92-004684 | p 1377 N92-17857
Numerical simulation of fluid flow and heat transfer in a thin liquid film over a stationary and rotating disk and comparison with experimental data
| NASA-CR-189253 | p 1300 N92-17887
High temperature superconductor thin films and Josephson junctions
| AD-A242747 | p 1293 N92-17949

THIN PLATES
Study of plane wave impingement on a thin plate capable of deformation
| AD-A242947 | p 1296 N92-17275

THIN WALLED SHELLS
Higher-order thickness expansions for cylindrical shells
| AD-A242017 | p 1310 N92-17230

THIOLS
Omega-terminated alkanethiolate monolayers on surfaces of copper, silver and gold have similar wettabilities
| AD-A243529 | p 1260 N92-17389
Comparisons of self-assembled monolayers on silver and gold: Mixed monolayers derived from HS(CH2)21X and HS(CH2)10(sup Y) (X,Y-CH3, CH2OH) have similar properties
| AD-A243487 | p 1264 N92-17427

THORIUM ISOTOPES
Importance of the neutron-proton interactions for the even Ra-Th nuclei
| DE92-600628 | p 1363 N92-17956

THREE BODY PROBLEM
Comparison of station-keeping algorithms for an interior libration point orbit in the Sun-Earth + Moon elliptic restricted three-body problem
| AD-A241896 | p 1388 N92-17595

THREE DIMENSIONAL FLOW
Recording of three dimensional trajectories and velocity fields by automatic image processing
| MPIS-101/1991 | p 1301 N92-17345
Viscous three-dimensional calculations of transonic fan performance
| NASA-TM-103800 | p 1219 N92-17346
Basic hydrodynamics
| AD-A243513 | p 1297 N92-17387
Computation of three-dimensional flows using two stream functions
| NASA-CR-187802 | p 1298 N92-17588
Preliminary development of a three-dimensional nonlinear approximation procedure for turbomachinery design optimization applications
| AD-A243155 | p 1235 N92-17644

THREE DIMENSIONAL MODELS
A numerical code for a three-dimensional magnetospheric MHD equilibrium model
| NASA-CR-189852 | p 1316 N92-17227
User's guide for a three-dimensional numerical hydrodynamic, salinity, and temperature model of Chesapeake Bay
| AD-A242993 | p 1324 N92-17298
Numerical simulation of cirrus clouds: Fire case study and sensitivity analysis
| AD-A242902 | p 1321 N92-17631
Theoretical studies in tokamaks: Three-dimensional simulation of lower hybrid wave launching in tokamaks
| DE92-003773 | p 1371 N92-17793

THROATS
Transpiration cooled throat for hydrocarbon rocket engines
| NASA-CR-184272 | p 1253 N92-17495

THRUST CHAMBERS
Integration of RAMS activities during the development phase of Ariane 5-components (example: Vulcain thrust chamber)
| MBB-UK-0144-91-PUB | p 1240 N92-17527

THRUST VECTOR CONTROL
Aircraft ground test and subscale model results of axial thrust loss caused by thrust vectoring using turning vanes
| NASA-TM-4341 | p 1230 N92-17071

THULIUM
Method and apparatus for lasing
| AD-D015154 | p 1305 N92-17923

THUNDERSTORMS
Severe weather guide mediterranean ports. Part 35: Rota
| AD-A243539 | p 1319 N92-17338
Severe weather guide Mediterranean ports. Part 38: Alexandria
| AD-A243451 | p 1320 N92-17406
Severe weather guide Mediterranean ports. Part 39: Port Said
| AD-A243450 | p 1320 N92-17494

TILTING ROTORS
The V-22: Can the nation afford to forgo its production?
| AD-A243158 | p 1219 N92-17477

TIME
Using mappings to prove timing properties
| AD-A242862 | p 1277 N92-17263
Mechanisms of temporal pattern discrimination by human observers
| AD-A243051 | p 1332 N92-17336

TIME DEPENDENCE
Inelastic strain analysis of solder joint in NASA fatigue specimen
| NASA-CR-189882 | p 1311 N92-17511

TIME DIVISION MULTIPLE ACCESS
Interim Service ISDN Satellite (ISIS) hardware experiment design for advanced ISDN satellite design and experiments
| NASA-CR-186943 | p 1250 N92-17585

TIME DIVISION MULTIPLEXING
Results from a data acquisition system prototype project using a switch-based event builder
| DE92-004638 | p 1336 N92-17592

TIME MARCHING
Periodic trim solutions with HP-version finite elements in time
| NASA-CR-189778 | p 1236 N92-17019

TIME OF FLIGHT SPECTROMETERS
Molecular jet studies of vdW clusters and solvation
| AD-A242866 | p 1254 N92-17308

TIME OPTIMAL CONTROL
Global optimization of digital circuits
| AD-A243740 | p 1289 N92-17480

TIME SERIES ANALYSIS
A Kalman filter for a Poisson series with covariates and Laplace approximation integration
| AD-A242960 | p 1286 N92-16993
An investigation of cold overflow over the Iceland/Faeroes Ridge
| AD-A243084 | p 1324 N92-17169
Incipient fault detection using higher-order statistics
| AD-A243493 | p 1308 N92-17431

TIMING DEVICES
Specification and compositional verification of real-time systems
| ETN-92-90580 | p 1341 N92-17521

TISSUES (BIOLOGY)
Characterization of the P. brevis polyether neurotoxin binding component in excitable membranes
| AD-A242877 | p 1327 N92-17564

TITANIUM
The effect of titanium inclusions on HY-80 GMA weld deposits
| AD-A243408 | p 1239 N92-17192
Evaluation of a diffusion/trapping model for hydrogen ingress in high-strength alloys
| AD-A243461 | p 1263 N92-17327
Evidence for MeV particle emission from Ti charged with low energy deuterium ions
| AD-A243718 | p 1359 N92-17505

TITANIUM ALLOYS
Thermo-mechanical fatigue of a fiber reinforced titanium aluminide composite
| AD-A241988 | p 1256 N92-17607

TITANIUM NITRIDES
The effect of titanium inclusions on HY-80 GMA weld deposits
| AD-A243408 | p 1239 N92-17192

TOKAMAK DEVICES
Active heater control and regulation for the Varian VGT-8011 gyrotron
| DE92-003638 | p 1302 N92-17454
The charge exchange recombination diagnostic system on the D3-D tokamak
| DE92-003805 | p 1369 N92-17456
Cooperative program to analyze heat transport at high beta in DIII-D
| DE92-003545 | p 1370 N92-17606
UCLA program in reactor studies: The ARIES tokamak reactor study
| DE92-003760 | p 1370 N92-17792
Theoretical studies in tokamaks: Three-dimensional simulation of lower hybrid wave launching in tokamaks
| DE92-003773 | p 1371 N92-17793

TOLERANCES (MECHANICS)
Polymer-reinforced metal matrix composite
| AD-D015070 | p 1257 N92-17611

TOLLMIEN-SCHLICHTING WAVES
On the origin and control of large coherent structures in turbulent shear flow
| AD-A243727 | p 1299 N92-17719

TOMOGRAPHY
The applied tomography experiment of 1990
| AD-A243525 | p 1354 N92-17086
Acoustic simulation for acoustics education
| AD-A243027 | p 1355 N92-17236
Performance of the Rayleigh task based on the posterior probability of tomographic reconstructions
| DE92-003785 | p 1352 N92-17455

TOPOGRAPHY
Mean wind speeds over hills and other topography
| ESDU-91043 | p 1321 N92-17853

TOPOLOGY
A topological model for parallel algorithm design
| AD-A241858 | p 1337 N92-17023
A GNS-type theorem for a non-involutive Banach algebra
| DE91-641481 | p 1354 N92-17803
Topological duals of Banach spaces as Banach algebras and applications
| DE91-641482 | p 1354 N92-17804
Chaos caused by a topologically mixing map
| DE91-641486 | p 1354 N92-17823
Structure and topology of silica aerogels
| DE92-004728 | p 1274 N92-17938

TOROIDAL PLASMAS
Some aspects of nonneutral plasma physics
| AD-A243711 | p 1369 N92-17499
Workshop on Plasma Experiments in the Laboratory and in Space. Abstracts
| AD-A243645 | p 1370 N92-17734

TORQUE
Analytical determination of arrest and starting torque of a bipolar DC motor with permanent magnets
| ETN-92-90586 | p 1290 N92-17540

TORQUE SENSORS (ROBOTICS)
Analysis and experimental evaluation of a Stewart platform-based force/torque sensor
| NASA-CR-189861 | p 1252 N92-17150

TOUCHDOWN
Example of statistical techniques applied to autoland touchdown dispersion (confidence intervals for normal and skew distributions)
| ESDU-91019 | p 1229 N92-17844

TOUGHNESS
Polymer-reinforced metal matrix composite
| AD-D015070 | p 1257 N92-17611

TOXIC HAZARDS
Assessment of the behavioral and neurotoxic effects of hexachlorobenzene (HCB) in the developing rat
| AD-A243658 | p 1325 N92-17121

TOXICITY
Assessment of the behavioral and neurotoxic effects of hexachlorobenzene (HCB) in the developing rat
| AD-A243658 | p 1325 N92-17121
Preliminary assessment of the relative toxicity of tetraglycine hydroperiodide, phase 1
| AD-A243334 | p 1330 N92-17712

TOXINS AND ANTITOXINS
Characterization of the P. brevis polyether neurotoxin binding component in excitable membranes
| AD-A242877 | p 1327 N92-17564

TRACE CONTAMINANTS
Policy implications of greenhouse warming: Report of the adaptation panel p 1314 N92-17982

TRACKING (POSITION)
The effects of speech intelligibility level on concurrent visual task performance
| AD-A243015 | p 1331 N92-17052
A system for fast navigation of autonomous vehicles
| AD-A243523 | p 1228 N92-17147
Flight evaluation of curved MLS precision approaches in a twin otter aircraft, phase 2
| AD-A243025 | p 1229 N92-17568
Application of multi-target tracking to sonar-based mobile robot navigation
| OUEL-1819/90 | p 1229 N92-17878
A fully decentralized multi-sensor system for tracking and surveillance
| OUEL-1886/91 | p 1302 N92-17926
A decentralized Bayesian algorithm for identification of tracked targets
| OUEL-1892/91 | p 1344 N92-17927

TRACKING NETWORKS
A fully decentralized multi-sensor system for tracking and surveillance
| OUEL-1886/91 | p 1302 N92-17926
A decentralized Bayesian algorithm for identification of tracked targets
| OUEL-1892/91 | p 1344 N92-17927

TRACKING PROBLEM
Integrated system for missile detection and discrimination
| DE91-018874 | p 1283 N92-17529
TRADEOFFS
ECLSS predictive monitoring p 1247 N92-17357
TRAILING EDGES
Use of Navier-Stokes analysis in section design
| AD-A242074 | p 1295 N92-17168
TRAINING ANALYSIS
Acquisition and production of skilled behavior in dynamic decision-making tasks
| NASA-CR-189846 | p 1333 N92-17132
TRAINING DEVICES
Training methodologies for dependent Speech Recognition (SR) systems
| AD-A242983 | p 1282 N92-17293
Research and development project summaries, October 1991
| AD-A243477 | p 1391 N92-17372
Adaptive on-line help for embedded instructional systems
| AD-A243675 | p 1343 N92-17716
TRAINING EVALUATION
The multi-attribute task battery for human operator workload and strategic behavior research
| NASA-TM-104174 | p 1338 N92-17130
Training methodologies for dependent Speech Recognition (SR) systems
| AD-A242983 | p 1282 N92-17293
Research and development project summaries, October 1991
| AD-A243477 | p 1391 N92-17372
TRAJECTORIES
An alternative concept for aeroassisted orbit transfers
| AD-A243409 | p 1239 N92-17325
Trajectory analysis of the G-11 family of clustered parachutes to determine minimum altitude
| AD-A243375 | p 1225 N92-17404
TRAJECTORY ANALYSIS
Trajectory analysis of the G-11 family of clustered parachutes to determine minimum altitude
| AD-A243375 | p 1225 N92-17404
TRAJECTORY CONTROL
Control algorithms for aerobraking in the Martian atmosphere
| AD-A243349 | p 1239 N92-17730
TRAJECTORY OPTIMIZATION
Optimal aircraft performance during microburst encounter p 1222 N92-17999
TRANSDUCERS
A method and apparatus for indicating disbonds in joint regions
| NASA-CASE-LAR-14626-1 | p 1309 N92-17859
TRANSFER FUNCTIONS
Computational and neural network models for the analysis of visual texture
| AD-A243717 | p 1327 N92-17504
TRANSFER ORBITS
An alternative concept for aeroassisted orbit transfers
| AD-A243409 | p 1239 N92-17325
TRANSFORMATIONS (MATHEMATICS)
Face recognition with the Karhunen-Loeve transform
| AD-A243688 | p 1280 N92-17090
Image analysis using Gabor transforms: Correlated with human saccadic movement data to identify the human visual search strategy
| AD-A243692 | p 1338 N92-17093
TRANSFORMERS
Explosive magnetic field compression generator transformer power supply for high resistive loads
| AD-D015123 | p 1293 N92-17831
TRANSISTORS
High current transistor pulse generator
| DE92-004774 | p 1292 N92-17801
TRANSITION FLOW
Transition phenomena in a straight channel with a 40 to 1 aspect ratio with and without imposed pulsations. Part 1: Near-wall and central region profiles
| AD-A243251 | p 1297 N92-17337
TRANSITION LAYERS
Transition phenomena in a straight channel with a 40 to 1 aspect ratio with and without imposed pulsations. Part 1: Near-wall and central region profiles
| AD-A243251 | p 1297 N92-17337
TRANSITION METALS
Magnetic multilayer interface anisotropy
| DE92-000635 | p 1263 N92-17319
TRANSITION POINTS
Results of measured temperature distribution on an adiabatic wing model with radiation thermometer
| NAL-TM-610 | p 1225 N92-17755
TRANSITION PROBABILITIES
Effect of spatial locality prefetching on structural locality
| AD-A243632 | p 1337 N92-17922
One nucleon transition densities for 1p shell nuclei
| DE92-600629 | p 1363 N92-17957
TRANSLATING
Design of Style-V: A translator to convert standard VHDL into a stylized form for automated microcode generation
| AD-A243706 | p 1340 N92-17407
Program translation tools for systolic arrays
| AD-A242924 | p 1336 N92-17466
TRANSMISSION CIRCUITS
Suspended substrate resonator design
| AD-A243250 | p 1290 N92-17573
TRANSMISSION LINES
Superconducting microwave transmission lines
| AD-A243166 | p 1291 N92-17671
A study of electric transmission lines for use on the lunar surface p 1292 N92-17742
TRANSMITTANCE
User evaluation of laser ballistic sun, wind and dust goggle lenses (dye technology)
| AD-A243245 | p 1334 N92-17143
Evaluation of LOWTRAN and MODTRAN for use over high zenith angle/long path length viewing
| AD-A243599 | p 1387 N92-17920
TRANSMITTER RECEIVERS
Satellite links for television contribution: Reception requirements for links using transportable transmitting earth stations
| BBC-RD-1991/5 | p 1285 N92-17885
TRANSMITTERS
Receiver performance of laser ranging measurements between the Lunar Observer and a subsatellite for lunar gravity studies
| NASA-CR-189860 | p 1303 N92-17152
Radio frequency hazard monitoring-USAKA
| AD-A242873 | p 1283 N92-17563
TRANSONIC FLOW
Experiments and analysis concerning the use of external burning to reduce aerospace vehicle transonic drag
| NASA-TM-105397 | p 1235 N92-17546
Results of measured temperature distribution on an adiabatic wing model with radiation thermometer
| NAL-TM-610 | p 1225 N92-17755
TRANSONIC WIND TUNNELS
Results of the space shuttle vehicle ascent air data system probe calibration test using a 0.07-scale external tank forebody model (68T) in the AEDC 16-foot transonic wind tunnel (IA-310), volume 1
| NASA-CR-167696 | p 1241 N92-17167
Stagnation and dynamic pressure limits for the S1 wind tunnel
| AD-A242989 | p 1238 N92-17297
User guide for WIACX: A transonic wind-tunnel wall interference assessment and correction procedure for the NTF
| NASA-TM-104168 | p 1225 N92-17547
Results of measured temperature distribution on an adiabatic wing model with radiation thermometer
| NAL-TM-610 | p 1225 N92-17755
TRANSPIRATION
Transpiration cooled throat for hydrocarbon rocket engines
| NASA-CR-184272 | p 1253 N92-17495
Global models for the biomechanics of green plants, part 1
| DE91-641478 | p 1327 N92-17946
TRANSPORT PROPERTIES
Electronic and ionic transport in processable conducting polymers. Symmetry effects on the physical and electrically conducting, substituted poly(di-2-thienylphenylenes)
| AD-A242328 | p 1266 N92-16976
Electronic and ionic transport in processable conducting polymers
| AD-A242258 | p 1269 N92-17460
Cooperative program to analyze heat transport at high beta in DIII-D
| DE92-003545 | p 1370 N92-17606
Reaction kinetics and transport properties of the CaO-SO2-O2 system in absence of intra-particle diffusion
| DE91-002086 | p 1261 N92-17788
Thin films under chemical stress
| DE92-004684 | p 1377 N92-17857
Investigation of heated ultracold neutrons on copper surface
| DE92-600625 | p 1363 N92-17955
TRANSPORT THEORY
A one-dimensional plasma and impurity transport model for reversed field pinches
| DE92-004691 | p 1371 N92-17933
Determination of diffusion parameters of thermal neutrons for non-moderator media by a pulsed method and a time independent method
| DE92-600624 | p 1362 N92-17954
TRANSPUTERS
A fully decentralized multi-sensor system for tracking and surveillance
| OUEL-1886/91 | p 1302 N92-17926
TRAPPED VORTICES
Method and apparatus for reducing drag and noise associated with fluid flow in a conduit
| AD-D015067 | p 1297 N92-17398
TRAPS
Failure mechanisms in GaAs ICs: The effects of deep traps
| AD-A243013 | p 1374 N92-17553
TREADMILLS
Treadmill for space flight
| NASA-CASE-MSC-21752-1 | p 1335 N92-17910
TRENDS
Toward a national semiconductor strategy, volume 1
| PB91-201293 | p 1290 N92-17620
TRIBOLOGY
The synergistic effects of solid and liquid lubrication on the tribological behavior of transformation-toughened ZrO2 ceramics
| DE91-018617 | p 1306 N92-17575
Determination of the tribological fundamentals of solid lubricated ceramics. Volume 3: Appendices P through 2
| AD-A242872 | p 1270 N92-17597
Determination of the tribological fundamentals of solid lubricated ceramics. Volume 2: Appendices A through O
| AD-A242871 | p 1270 N92-17614
Determination of the tribological fundamentals of solid lubricated ceramics. Volume 1: Summary
| AD-A243219 | p 1272 N92-17683
TRIMERS
Evaluation of the initiation/promotion potential of CTFE trimer acid
| AD-A243479 | p 1255 N92-17373
TRINITROTOLUENE
Role of donor-acceptor interactions in the sorption of TNT and other nitroaromatics from solution
| AD-A243235 | p 1254 N92-17055
TRITIUM
Steady-state, high dose neutron generation and concentration apparatus and method for deuterium atoms
| AD-D015063 | p 1358 N92-17462
TROPICAL METEOROLOGY
The National Hurricane Center Risk Analysis Program (HURISK)
| PB91-236463 | p 1321 N92-17705
TROPICAL REGIONS
Upper ocean dynamics during the LOTUS and Tropic Heat Experiments
| AD-A243730 | p 1324 N92-17583
Diagnostic report of the National Hurricane Center, August and September 1990, volume 3, number 2
| PB91-226886 | p 1321 N92-17621
The National Hurricane Center Risk Analysis Program (HURISK)
| PB91-236463 | p 1321 N92-17705
TRUSSES
Modes of interconnected lattice trusses using continuum models, part 1
| NASA-CR-189568 | p 1242 N92-17045
TUNABLE LASERS
A tunable solid state laser with high wavelength selectivity over a preselected wavelength range
| AD-D015055 | p 1304 N92-17627
Achromatic and isochronous electron beam transport for tunable free electron lasers
| DE92-003908 | p 1305 N92-17868
TUNING
Beam position monitor multiplexer controller upgrade at the LAMPF proton storage ring
| DE92-003859 | p 1363 N92-17590
TURBINE BLADES
Dynamic stall on wind turbine blades
| DE92-001157 | p 1226 N92-17874
TURBINE PUMPS
Reliability analysis of structural ceramic components using a three-parameter Weibull distribution
| NASA-TM-105370 | p 1267 N92-17060
Actively controlled shaft seals for aerospace applications
| NASA-CR-189808 | p 1306 N92-17304
TURBOMACHINERY
Basic hydrodynamics
| AD-A243513 | p 1297 N92-17387
Preliminary development of a three-dimensional nonlinear approximation procedure for turbomachinery design optimization applications
| AD-A243155 | p 1235 N92-17644
TURBOPROP AIRCRAFT
Escape strategies for turboprop aircraft in a microburst windshear
| AD-A243090 | p 1227 N92-17217

TURBULENCE
Turbulent and gravity wave transport in the free atmosphere p 1315 N92-17063
Sensing refractive turbulence profiles using wave front slope measurements from two reference sources
| AD-A243696 | p 1315 N92-17094
Study of transition phenomena in a straight channel with 40 to 1 aspect ratio with and without imposed pulsations. Part two: Reynolds number surveys
| AD-A241894 | p 1296 N92-17307
Transition phenomena in a straight channel with a 40 to 1 aspect ratio with and without imposed pulsations. Part 1: Near-wall and central region profiles
| AD-A243251 | p 1297 N92-17337
Pattern selection, wave formation, turbulence, and vortex breakdown in spiral flows
| AD-A242351 | p 1297 N92-17447
Study of turbulence by photon correlation spectroscopy
| AD-A243726 | p 1298 N92-17688
Optical turbulence in second harmonic generation p 1377 N92-17821
The effect of isolated roughness elements on transition in attachment-line flows
| AERO-REPT-8905 | p 1300 N92-17850
An overview: Challenges in wind technology development
| DE92-001190 | p 1313 N92-17875

TURBULENCE EFFECTS
The effect of freestream turbulence on the vortical flow over a delta wing p 1225 N92-17681

TURBULENCE MODELS
Viscous three-dimensional calculations of transonic fan performance
| NASA-TM-103800 | p 1219 N92-17346

TURBULENT BOUNDARY LAYER
An experimental study of a turbulent wing-body junction and wake flow
| AD-A243388 | p 1223 N92-17222
Basic hydrodynamics
| AD-A243513 | p 1297 N92-17387
The effect of freestream turbulence on the vortical flow over a delta wing p 1225 N92-17681
Deterministic multi-zone ice accretion modeling p 1220 N92-17987

TURBULENT DIFFUSION
Local extinction mechanisms in non-premixed turbulent combustion
| AD-A242027 | p 1260 N92-17682

TURBULENT FLOW
Use of Navier-Stokes analysis in section design
| AD-A242074 | p 1295 N92-17168
Injection of drag reducing additives into turbulent water flows
| AD-A243209 | p 1296 N92-17176
An experimental study of a turbulent wing-body junction and wake flow
| AD-A243388 | p 1223 N92-17222
Study of transition phenomena in a straight channel with 40 to 1 aspect ratio with and without imposed pulsations. Part two: Reynolds number surveys
| AD-A241894 | p 1296 N92-17307
Transmission of thin light beams through turbulent mixing layers
| AD-A243470 | p 1367 N92-17658
Local extinction mechanisms in non-premixed turbulent combustion
| AD-A242027 | p 1260 N92-17682
On the origin and control of large coherent structures in turbulent shear flow
| AD-A243727 | p 1299 N92-17719
Deterministic multi-zone ice accretion modeling p 1220 N92-17987

TURBULENT HEAT TRANSFER
Turbulent and gravity wave transport in the free atmosphere p 1315 N92-17063

TURBULENT JETS
An experimental investigation of chemically-reacting, gas-phase turbulent jets
| AD-A243036 | p 1296 N92-17276

TURBULENT MIXING
Chemical reactions in turbulent mixing flows
| AD-A243035 | p 1294 N92-16979
Transmission of thin light beams through turbulent mixing layers
| AD-A243470 | p 1367 N92-17658

TURBULENT WAKES
Use of Navier-Stokes analysis in section design
| AD-A242074 | p 1295 N92-17168
An experimental study of a turbulent wing-body junction and wake flow
| AD-A243388 | p 1223 N92-17222
Investigation on the control of a Karman vortex street
| MPIS-99/1990 | p 1224 N92-17315

TWISTING
Analysis of possible schemes for twisting multiwire superconducting cables and design of twisting equipment
| DE92-609667 | p 1294 N92-17971

TWO DIMENSIONAL MODELS
A numerical code for a three-dimensional magnetospheric MHD equilibrium model
| NASA-CR-189852 | p 1316 N92-17227

TWO PHASE FLOW
Development and utilization of new diagnostics for dense-phase pneumatic transport
| DE92-003091 | p 1307 N92-17605
Development and utilization of new diagnostics for dense-phase pneumatic transport
| DE92-000337 | p 1299 N92-17704
Determination of cohesive and normal stresses and simulation of fluidization using kinetic theory
| DE92-002905 | p 1299 N92-17709
Development of a system for void fraction measuring by electroprobing method
| DE92-610933 | p 1309 N92-17809

U

ULTRAHIGH FREQUENCIES
An investigation of methods for updating ionospheric scintillation models using topside in-situ plasma density measurements
| AD-A243378 | p 1316 N92-17209
Simultaneous active and passive microwave measurements of the ocean surface
| AD-A242232 | p 1312 N92-17459
C3 Systems Technology Symposium on Advance Planning Briefings for Industry
| AD-A243466 | p 1391 N92-17657

ULTRAHIGH VACUUM
Atomic relaxation at ordered electrochemical surfaces probed by scanning tunneling microscopy: Au(111) in aqueous solution compared with ultrahigh-vacuum environments
| AD-A242031 | p 1358 N92-17472

ULTRASONICS
Temporally-specific modification of myelinated axon excitability in vitro following a single ultrasound pulse
| AD-A242329 | p 1326 N92-17474
Ultrasonic studies of transient seismo-acoustic waves in bounded solids and Liquid/Solid interfaces
| AD-A243441 | p 1355 N92-17488
Incremental volume rendering algorithm for interactive 3D ultrasound imaging
| AD-A242048 | p 1342 N92-17637

ULTRAVIOLET LASERS
Development of an XUV-IR free-electron laser user facility for scientific research and industrial applications
| DE92-003862 | p 1304 N92-17726

ULTRAVIOLET MICROSCOPY
X ray lithography in Japan
| AD-A243660 | p 1286 N92-17087

UNDERWATER ACOUSTICS
Acoustic impedance of materials from reverberation time
| AD-A243184 | p 1354 N92-16999
The effects of sediment porosity on acoustic reflection and transmission at the seafloor
| AD-A241943 | p 1323 N92-17083
The applied tomography experiment of 1990
| AD-A243525 | p 1354 N92-17086
Acoustic simulation for acoustics education
| AD-A243027 | p 1355 N92-17236
Ultrasonic studies of transient seismo-acoustic waves in bounded solids and Liquid/Solid interfaces
| AD-A243441 | p 1355 N92-17488

UNDERWATER STRUCTURES
Novel ceramic matrix composites for deep submergence pressure vessel applications
| AD-A242740 | p 1274 N92-17947

UNDERWATER VEHICLES
Multiple input sliding mode control for autonomous diving and steering of underwater vehicles
| AD-A241935 | p 1237 N92-17442

UNITED STATES
Publications of the Executive Office of the President, January 20, 1989 to June 30, 1991
| PB91-202762 | p 1382 N92-17228
Scientific and technological relations between the United States and Japan: Issues and recommendations
| PB91-219170 | p 1385 N92-17283

UNIVERSE
Fluctuation driven electroweak phase transition
| NASA-CR-189859 | p 1361 N92-17647
Late time cosmological phase transitions 1: Particle physics models and cosmic evolution
| NASA-CR-189857 | p 1388 N92-17696

UNIVERSITY PROGRAM
A theoretical search for supervelocity semiconductors
| AD-A241981 | p 1376 N92-17783
Joint University Program for Air Transportation Research, 1990-1991
| NASA-CP-3131 | p 1219 N92-17984
An investigation of air transportation technology at the Massachusetts Institute of Technology, 1990-1991 p 1219 N92-17985
Investigation of air transportation technology at Ohio University, 1990-1991 p 1220 N92-17990

UNLOADING
Residual stresses in a prestressed steel pressure vessel wrapped with multilayered composites
| AD-A243429 | p 1311 N92-17930

UNSTEADY AERODYNAMICS
Structural dynamics division research and technology accomplishments for F.Y. 1991 and plans for F.Y. 1992
| NASA-TM-104188 | p 1225 N92-17509

UNSTEADY FLOW
Unsteady laminar flow in a circular tube: A test of the HERCOL (Hermitian collocation) computer code
| PB91-222679 | p 1295 N92-17018
Study of transition phenomena in a straight channel with 40 to 1 aspect ratio with and without imposed pulsations. Part two: Reynolds number surveys
| AD-A241894 | p 1296 N92-17307
Transition phenomena in a straight channel with a 40 to 1 aspect ratio with and without imposed pulsations. Part 1: Near-wall and central region profiles
| AD-A243251 | p 1297 N92-17337
Development of an electronic high speed camera system for the quantitative analysis of unsteady flows
| MPIS-100/1991 | p 1301 N92-17344
Effects of power pulsations on heat transfer from discrete heat sources
| AD-A243434 | p 1379 N92-17686
Engineering model of unsteady flow in a cavity
| AD-A243636 | p 1299 N92-17747

UPPER ATMOSPHERE
Relaxation processes of vibrationally excited H2O in the mesosphere and thermosphere
| AD-A241853 | p 1315 N92-17035
Range reference atmosphere, Fairbanks
| AD-A243314 | p 1318 N92-17113

UPWELLING WATER
Source of cold water in Monterey Bay observed by AVHRR satellite imagery
| AD-A242843 | p 1323 N92-17051

URANIUM
Characterization of the thermalness of a fissile system with a 2-group diffusion theory parameter
| AD-A243065 | p 1360 N92-17555

USER MANUALS (COMPUTER PROGRAMS)
Cathodic protection diagnostic computer program for sacrificial and impressed current systems: Overview and user's manual
| AD-A243663 | p 1338 N92-17122
Product Definition Data Interface (PDDI) translator user's manual
| AD-A243463 | p 1352 N92-17223
User's guide for a three-dimensional numerical hydrodynamic, salinity, and temperature model of Chesapeake Bay
| AD-A242993 | p 1324 N92-17298
The computational structural mechanics testbed procedures manual
| NASA-TM-100646 | p 1310 N92-17333
ZEUS user manual real gas effects
| AD-A242224 | p 1225 N92-17446
Versatile Data Acquisition System Model II user's manual
| DE92-003311 | p 1384 N92-17470
A user's manual for the Princeton Numerical Ocean Model
| AD-A243773 | p 1324 N92-17539
User guide for WIACX: A transonic wind-tunnel wall interference assessment and correction procedure for the NTF
| NASA-TM-104168 | p 1225 N92-17547
Forth Graphics Toolbox (A user's guide for use with RFF FORTH)
| AD-A242916 | p 1342 N92-17581
Serpent: Dialogue editor user's guide. System for user interface development, version 1
| AD-A242331 | p 1384 N92-17641
QTCM software documentation. Volume 2: User's manual
| AD-A242744 | p 1344 N92-17948

USER REQUIREMENTS
Beyond the Baseline 1991: Proceedings of the Space Station Evolution Symposium. Volume 1: Space Station Freedom, part 1
| NASA-CP-10083-VOL-1-PT-1 | p 1242 N92-17098

The development of user interface tools for the computer aided prototyping system
| AD-A243189 | p 1340 N92-17368
Information Management Engineering (IME) laboratory: A database development facility
| AD-A243191 | p 1383 N92-17369
Space Station Freedom baseline operations concept p 1248 N92-17410
Evolution user requirements for the restructured space station p 1248 N92-17413
SSF growth concepts and configurations p 1248 N92-17414
Hubble Space Telescope: High speed photometer instrument handbook. Version 2.0
| NASA-CR-189750 | p 1386 N92-17497
Beyond the Baseline 1991: Proceedings of the Space Station Evolution Symposium. Volume 2: Space Station Freedom, part 1
| NASA-CP-10083-VOL-2-PT-1 | p 1251 N92-17768

V

V-22 AIRCRAFT
The V-22: Can the nation afford to forgo its production?
| AD-A243158 | p 1219 N92-17477
V/STOL AIRCRAFT
Finite element analysis of ASTOVL fighter structure
| AD-A243724 | p 1233 N92-17513
VACUUM
Fluctuation driven electroweak phase transition
| NASA-CR-189859 | p 1361 N92-17647
VALVES
Thruster sealing system and apparatus
| NASA-CASE-MSC-21898-1 | p 1307 N92-17872
VANADIUM
A comparative study of the noise performance of Alluminum Gallium Arsenide/Gallium Arsenide high electron mobility transistors with and without superconducting gate electrodes p 1288 N92-17317
VANADIUM OXIDES
Lithiated Vanadium Oxide (LVO), gamma-lithium vanadium bronze (Gamma-LIV2O5) and vanadium dioxide (VO2) as thermal battery cathode materials
| AD-A242948 | p 1287 N92-17186
VANES
Aircraft ground test and subscale model results of axial thrust loss caused by thrust vectoring using turning vanes
| NASA-TM-4341 | p 1230 N92-17071
VAPOR DEPOSITION
Determination of the optical constants of thin Chemical-Vapor-Deposited diamond windows from 0.5 to 6.5 eV
| AD-A243094 | p 1268 N92-17170
Chemical vapor deposited diamond
| AD-A243095 | p 1268 N92-17171
Use of diamond as an optical material
| AD-A243097 | p 1268 N92-17172
Transmission electron microscopy of the CVD diamond film/substrate interface
| AD-A243096 | p 1373 N92-17322
Spatially and spectrally resolved cathodoluminescence measurements of CVD-grown diamond particles and films
| AD-A243220 | p 1271 N92-17615
Plasma chemical vapor deposition of halide glasses
| AD-D015060 | p 1370 N92-17706
VAPOR PHASE EPITAXY
Innovative optoelectronic materials and structures using OMVPE
| AD-A243257 | p 1371 N92-16984
VARIANCE (STATISTICS)
The applied tomography experiment of 1990
| AD-A243525 | p 1354 N92-17086
VECTOR ANALYSIS
Front detection with Doppler radar
| AD-A242880 | p 1319 N92-17289
VECTOR PROCESSING (COMPUTERS)
A connectionist simulation of attention and vector comparison: The need for serial processing in parallel hardware
| AD-A242225 | p 1348 N92-17457
VECTORS (MATHEMATICS)
Effective dynamic material parameters and localized scattering
| AD-A241957 | p 1310 N92-17320
VEGETATION GROWTH
Aquatic plant management program. Supplement
| AD-A242420 | p 1314 N92-17723
VELOCITY
Front detection with Doppler radar
| AD-A242880 | p 1319 N92-17289
VELOCITY DISTRIBUTION
Velocity measurements in high temperature gases using laser-induced no fluorescence
| AD-A242399 | p 1295 N92-17012
Recording of three dimensional trajectories and velocity fields by automatic image processing
| MPIS-101/1991 | p 1301 N92-17345
Mass transfer in gas fluidized beds: Scaling, modeling, and particle size influence
| ETN-92-90581 | p 1298 N92-17522
VELOCITY MEASUREMENT
Observation and measurements of flow structures in the stagnation region of a wing-body junction
| AD-A243403 | p 1223 N92-17117
Viscous three-dimensional calculations of transonic fan performance
| NASA-TM-103800 | p 1219 N92-17346
Development and utilization of new diagnostics for dense-phase pneumatic transport
| DE92-003091 | p 1307 N92-17605
VERTICAL DISTRIBUTION
Upper ocean dynamics during the LOTUS and Tropic Heat Experiments
| AD-A243730 | p 1324 N92-17583
VERTICAL ORIENTATION
Rapid nonconjugate adaptation of vertical voluntary pursuit eye movements
| AD-A243358 | p 1331 N92-17145
VERY LARGE SCALE INTEGRATION
FY92 mathematical research project proposal briefing
| AD-A243163 | p 1350 N92-17207
An object-oriented database implementation of the Magic VLSI Layout Design System
| AD-A243743 | p 1384 N92-17482
VERY LOW FREQUENCIES
Radio sky mapping from satellites at very low frequencies
| NASA-TM-105452 | p 1387 N92-17694
VHSIC (CIRCUITS)
Global optimization of digital circuits
| AD-A243740 | p 1289 N92-17480
Parallel implementation of VHDL simulations on the Intel iPSC/2 hypercube
| AD-A243760 | p 1342 N92-17603
VIBRATION
Low frequency vibration absorber
| AD-D015103 | p 1307 N92-17827
VIBRATION DAMPING
Experiences at Langley Research Center in the application of optimization techniques to helicopter airframes for vibration reduction
| NASA-TM-104193 | p 1309 N92-17033
Loss terms in free-piston Stirling engine models
| NASA-CR-189840 | p 1312 N92-17225
Loading and vibration reduction through active aerodynamic control
| AD-A242321 | p 1236 N92-17243
Low frequency vibration absorber
| AD-D015103 | p 1307 N92-17827
VIBRATION EFFECTS
Low-noise oscillators for airborne radar applications
| AD-A242264 | p 1281 N92-17258
Experimental study of amplitude-phase-frequency characteristics of flow when following over a vibrating plate
| DE92-610935 | p 1299 N92-17810
VIBRATION MODE
Modes of interconnected lattice trusses using continuum models, part 1
| NASA-CR-189568 | p 1242 N92-17045
VIBRATIONAL SPECTRA
Vibrational energy transfer in bromine monofluoride
| AD-A243690 | p 1259 N92-17091
Nonlinear spectroscopic studies of interfacial molecular ordering
| DE92-000864 | p 1360 N92-17530
VIDEO COMMUNICATION
Management, control and performance of broadband integrated networks
| AD-A242750 | p 1381 N92-17952
VIDEO DATA
Integrated system for missile detection and discrimination
| DE91-018874 | p 1283 N92-17529
VINYL POLYMERS
The effect of monomer structures and compressibility on the properties of multicomponent polymer blends and solutions
| AD-A242863 | p 1273 N92-17777
VISCOELASTICITY
The effect of physical aging on the creep response of a thermoplastic composite
| AD-A243600 | p 1258 N92-17932
VISCOPLASTICITY
Inelastic strain analysis of solder joint in NASA fatigue specimen
| NASA-CR-189882 | p 1311 N92-17511
VISCOSITY
Effective viscosity in the simulation of spatially evolving shear flows with monotonic FCT models
| AD-A243709 | p 1295 N92-17126
VISCOUS FLOW
Comparison of two solution methods for the numerical calculation of hypersonic flows
| MBB-FE211-S-PUB-446 | p 1224 N92-17311
Viscous three-dimensional calculations of transonic fan performance
| NASA-TM-103800 | p 1219 N92-17346
VISIBILITY
User evaluation of laser ballistic sun, wind and dust goggle lenses (dye technology)
| AD-A243245 | p 1334 N92-17143
Surface observation climatic summaries for Fairbanks IAP, Alaska
| AD-A243309 | p 1320 N92-17400
A computer solution for multiple satellite-satellite and satellite-ground station visibility determination
| AD-A243490 | p 1250 N92-17430
Severe weather guide Mediterranean ports. Part 39: Port Said
| AD-A243450 | p 1320 N92-17494
VISION
Computational and neural network models for the analysis of visual texture
| AD-A243717 | p 1327 N92-17504
VISUAL DISCRIMINATION
The dynamics of visual representation, attention, encoding, and retrieval processes
| AD-A243031 | p 1384 N92-17785
Investigation of air transportation technology at Ohio University, 1990-1991 p 1220 N92-17990
VISUAL PERCEPTION
Dual color and shape coding in the visual periphery: A study of Joint Tactical Information Distribution System (JTIDS) symbology
| AD-A243253 | p 1333 N92-16982
The effects of speech intelligibility level on concurrent visual task performance
| AD-A243015 | p 1331 N92-17052
Analysis of visual illusions using multiresolution wavelet decomposition based models
| AD-A243712 | p 1332 N92-17500
Visual determination of industrial color-difference tolerances using probit analysis
| AD-A243545 | p 1334 N92-17617
VISUAL STIMULI
Establishing an evoked-potential vision-tracking system p 1221 N92-17993
VISUAL TASKS
The effects of speech intelligibility level on concurrent visual task performance
| AD-A243015 | p 1331 N92-17052
VOICE COMMUNICATION
An overview of cellular telecommunications
| AD-A242951 | p 1281 N92-17232
A study of channel-access schemes for integrated voice/data radio networks
| AD-A243584 | p 1286 N92-17931
VOID RATIO
Development of a system for void fraction measuring by electroprobing method
| DE92-610933 | p 1309 N92-17809
VOIDS
Novel vacuum bag processing approaches to void reduction in carbon/epoxy composites
| AD-A242396 | p 1255 N92-16992
VOLT-AMPERE CHARACTERISTICS
A study of ignition and simulation circuits for arcjet thrusters, part 1
| NASA-CR-189097 | p 1253 N92-17510
Gate drain geometry effect on the current voltage characteristics of GaAs MESFETs
| AD-A243430 | p 1291 N92-17684
VOLTAGE AMPLIFIERS
Transformerless DC-DC voltage amplifier with optically isolated switching devices
| NASA-CASE-NPO-17994-1-CU | p 1293 N92-17907
VOLTAGE CONTROLLED OSCILLATORS
Design and evaluation of a Josephson array oscillator
| AD-A243167 | p 1291 N92-17672
VOLTERRA EQUATIONS
The solution of a singular integral equation arising from a lifting surface theory for rotating blades p 1224 N92-17303
VORTEX BREAKDOWN
Pattern selection, wave formation, turbulence, and vortex breakdown in spiral flows
| AD-A242351 | p 1297 N92-17447

VORTEX FILAMENTS
A short or a long cylinder: What difference does it make to the Karman vortex street?
|MPIS-98/1990| p 1224 N92-17314
VORTEX SHEDDING
A short or a long cylinder: What difference does it make to the Karman vortex street?
|MPIS-98/1990| p 1224 N92-17314
Flow visualization and wake analysis for standard and modified configurations of the AN/ALQ-78 antenna pod
|AD-A243552| p 1224 N92-17339
VORTICES
Eddy breakdown and structure development
|AD-A241886| p 1295 N92-17039
An experimental investigation of leading edge vortical flow about a delta wing during wing rock
|AD-A243363| p 1223 N92-17114
Observation and measurements of flow structures in the stagnation region of a wing-body junction
|AD-A243403| p 1223 N92-17117
Studies of baroclinic flow
|AD-A243050| p 1296 N92-17309
A short or a long cylinder: What difference does it make to the Karman vortex street?
|MPIS-98/1990| p 1224 N92-17314
Investigation on the control of a Karman vortex street
|MPIS-99/1990| p 1224 N92-17315
The effect of freestream turbulence on the vortical flow over a delta wing p 1225 N92-17681
Proceedings of the 2nd Gulf of Cadiz Expedition Workshop
|AD-A242749| p 1325 N92-17951
VORTICITY
A variational assimilation method for satellite and conventional data: A revised basic model 2B p 1322 N92-17977
VULNERABILITY
Large centrifuge: A critical Army capability for the future
|AD-A243287| p 1238 N92-17287

W

WAFERS
Application of silicon micromachining to thermal dissipation issues in wafer scale integrated circuits
|AD-A243744| p 1288 N92-17332
Total Dielectric Isolation (TDI) of fully depleted device structures
|AD-A241926| p 1289 N92-17439
WAKES
Flow visualization and wake analysis for standard and modified configurations of the AN/ALQ-78 antenna pod
|AD-A243552| p 1224 N92-17339
WALKING
Techniques for determination of impact forces during walking and running in a zero-G environment
|NASA-TP-3159| p 1328 N92-17022
WALKING MACHINES
Extendable pipe crawler
|DE91-011570| p 1306 N92-17183
WALL FLOW
Injection of drag reducing additives into turbulent water flows
|AD-A243209| p 1296 N92-17176
User guide for WIACX: A transonic wind-tunnel wall interference assessment and correction procedure for the NTF
|NASA-TM-104168| p 1225 N92-17547
WALL TEMPERATURE
Wall temperature patterns in nucleate boiling
|OUEL-1876/91| p 1380 N92-17879
WALLS
Method and apparatus for reducing drag and noise associated with fluid flow in a conduit
|AD-D015067| p 1297 N92-17398
The effect of detonation curvature on cylindrical wall motion
|DE92-003110| p 1298 N92-17625
WARM FRONTS
The use of ADAP to examine warm and quasi-stationary frontal events in the northeastern United States
|PB91-225037| p 1319 N92-17363
WARNING SYSTEMS
An investigation of air transportation technology at the Massachusetts Institute of Technology, 1990-1991 p 1219 N92-17985
Cockpit display of hazardous weather information p 1220 N92-17989
WATER
Relaxation processes of vibrationally excited H2O in the mesosphere and thermosphere
|AD-A241853| p 1315 N92-17035
Effectiveness of an onboard water spray system during an oxygen enriched cabin fire
|DOT/FAA/CT-TN91/51| p 1226 N92-17149
Long-term corrosion evaluation of stainless steels in Space Shuttle iodinated resin and water
|NASA-TM-104743| p 1264 N92-17376
WATER CIRCULATION
Source of cold water in Monterey Bay observed by AVHRR satellite imagery
|AD-A242843| p 1323 N92-17051
WATER COOLED REACTORS
Fracture toughness evaluation for N Reactor pressure tubes of Zircaloy-2 using the electric-potential method
|DE92-003631| p 1311 N92-17713
WATER CURRENTS
A study on hydrographic conditions and salt budget calculation for the Gulf of Farallones with the data collected in August 1990
|AD-A243406| p 1324 N92-17119
WATER DEPTH
Multispectral software development for the Airborne Bathymetric Survey System
|AD-A243774| p 1325 N92-17765
WATER FLOW
Injection of drag reducing additives into turbulent water flows
|AD-A243209| p 1296 N92-17176
WATER INJECTION
Theoretical investigation of the injection and evaporation of water in a hydrogen/oxygen steam generator
|ESA-TT-1252| p 1379 N92-17848
WATER PRESSURE
Differential pressure sensor
|AD-D015134| p 1302 N92-17918
WATER QUALITY
User's guide for a three-dimensional numerical hydrodynamic, salinity, and temperature model of Chesapeake Bay
|AD-A242993| p 1324 N92-17298
WATER TEMPERATURE
Effects of power pulsations on heat transfer from discrete heat sources
|AD-A243434| p 1379 N92-17686
WATER TUNNEL TESTS
Study of turbulence by photon correlation spectroscopy
|AD-A243726| p 1298 N92-17688
WATER VAPOR
Water vapor influence on satellite-measured aerosol characteristics
|AD-A241918| p 1315 N92-17008
Sea surface environmental conditions in the Gulf of Alaska during April 1990 using SSM/I
|AD-A241909| p 1323 N92-17041
The role of thermal convection in heat and mass transport in the subarctic snow cover
|AD-A243674| p 1312 N92-17715
WAVE ATTENUATION
Studies of high-frequency seismic wave propagation
|AD-A241938| p 1316 N92-17202
On the origin and control of large coherent structures in turbulent shear flow
|AD-A243727| p 1299 N92-17719
WAVE DIFFRACTION
Groundscreen characterization
|AD-A243164| p 1311 N92-17208
WAVE EQUATIONS
Study of plane wave impingement on a thin plate capable of deformation
|AD-A242947| p 1296 N92-17275
Effective dynamic material parameters and localized scattering
|AD-A241957| p 1310 N92-17320
WAVE FRONTS
Sensing refractive turbulence profiles using wave front slope measurements from two reference sources
|AD-A243696| p 1315 N92-17094
Correlator optical wavefront sensor COWS
|DE92-003964| p 1368 N92-17846
WAVE FUNCTIONS
Radio sky mapping from satellites at very low frequencies
|NASA-TM-105452| p 1387 N92-17694
State vector reduction. Part 1: Dynamical reduction theories; changing quantum theory so the statevector represents reality
|DE91-641488| p 1379 N92-17824
WAVE PACKETS
On the origin and control of large coherent structures in turbulent shear flow
|AD-A243727| p 1299 N92-17719
WAVE PROPAGATION
Studies of high-frequency seismic wave propagation
|AD-A241938| p 1316 N92-17202
Evaporation duct communication: Test plan, part 2
|AD-A243505| p 1282 N92-17383
Acoustical and other physical properties of marine sediments
|AD-A243532| p 1324 N92-17391
Mechanisms mediating the perception of complex acoustic patterns
|AD-A243715| p 1355 N92-17502
Signal- and listener-based factors in complex auditory pattern perception
|AD-A243716| p 1332 N92-17503
The effect of detonation curvature on cylindrical wall motion
|DE92-003110| p 1298 N92-17625
Wave propagation in a randomly inhomogeneous medium: A study of the problem
|AD-A243741| p 1284 N92-17691
Magnetospheric response to variations in the interplanetary magnetic field
|AD-A243683| p 1388 N92-17717
On the generation of large-amplitude plasma wakefields with low phase velocities by an intense short laser pulse
|DE92-609543| p 1371 N92-17805
Performance of hole coupling resonator in the presence of asymmetric modes and FEL gain
|DE92-003907| p 1305 N92-17936
Constraints on cosmic ray propagation in the galaxy
|NASA-CR-189779| p 1390 N92-18003
WAVE REFLECTION
The effects of sediment porosity on acoustic reflection and transmission at the seafloor
|AD-A241943| p 1323 N92-17083
WAVE SCATTERING
Low frequency interstellar scattering and pulsar observations p 1390 N92-18005
WAVEGUIDES
Waveguide four-wave mixing
|AD-A243555| p 1286 N92-17017
Method for non-destructive estimation of waveguide directional coupler dimensions
|NASA-CASE-NPO-18454-1-CU| p 1293 N92-17865
WAVELENGTHS
New optical materials for the long-wave (8-12 microns) region: Design criteria for the solid-state chemist
|AD-A243280| p 1365 N92-17284
WEAK INTERACTIONS (FIELD THEORY)
Fluctuation driven electroweak phase transition
|NASA-CR-189859| p 1361 N92-17647
WEAPON SYSTEMS
CALS database usage and analysis tool study
|AD-A243205| p 1382 N92-17174
WEAR
Incipient fault detection using higher-order statistics
|AD-A243493| p 1308 N92-17431
An investigation of gouge initiation in high-velocity sliding contact
|DE92-003944| p 1311 N92-17937
WEAR TESTS
The synergistic effects of solid and liquid lubrication on the tribological behavior of transformation-toughened ZrO2 ceramics
|DE91-018617| p 1306 N92-17575
Determination of the tribological fundamentals of solid lubricated ceramics. Volume 1: Summary
|AD-A243219| p 1272 N92-17683
WEATHER
Sea surface environmental conditions in the Gulf of Alaska during April 1990 using SSM/I
|AD-A241909| p 1323 N92-17041
Surface observation climatic summaries for Duke Field/Eglin aux no. 3, Florida
|AD-A243310| p 1318 N92-17073
Surface observation climatic summaries for Castle AFB, California
|AD-A243677| p 1318 N92-17074
Surface observation climatic summaries for Hondo Municipal Airport, Texas
|AD-A243311| p 1319 N92-17144
Surface observation climatic summaries for Boise Air Terminal, ID
|AD-A243012| p 1319 N92-17257
Severe weather guide mediterranean ports. Part 35: Rota
|AD-A243539| p 1319 N92-17338
Severe weather guide Mediterranean ports. Part 38: Alexandria
|AD-A243451| p 1320 N92-17406
WEATHER FORECASTING
Front detection with Doppler radar
|AD-A242880| p 1319 N92-17289
The use of ADAP to examine warm and quasi-stationary frontal events in the northeastern United States
|PB91-225037| p 1319 N92-17363
WEIBULL DENSITY FUNCTIONS
Reliability analysis of structural ceramic components using a three-parameter Weibull distribution
|NASA-TM-105370| p 1267 N92-17060

WEIGHT ANALYSIS
Weight evaluation and sensitivity analysis for space plane. Part 2: TSTO
| NAL-TM-602-PT-2 | p 1251 N92-17754
WEIGHTING FUNCTIONS
The hazard of exposure to 2.075 kHz center frequency narrow band impulses
| AD-A242997 | p 1329 N92-17299
WEIGHTLESSNESS
Treadmill for space flight
| NASA-CASE-MSC-21752-1 | p 1335 N92-17910
WEIGHTLESSNESS SIMULATION
Techniques for determination of impact forces during walking and running in a zero-G environment
| NASA-TP-3159 | p 1328 N92-17022
Eccentric and concentric muscle performance following 7 days of simulated weightlessness
| NASA-TP-3182 | p 1330 N92-17645
WELD STRENGTH
The effect of weld metal strength mismatch on the deformation and fracture behavior of steel butt weldments
| AD-A243239 | p 1262 N92-17057
WELDED JOINTS
The effect of weld metal strength mismatch on the deformation and fracture behavior of steel butt weldments
| AD-A243239 | p 1262 N92-17057
The effect of titanium inclusions on HY-80 GMA weld deposits
| AD-A243408 | p 1239 N92-17192
WELDED STRUCTURES
The effect of weld metal strength mismatch on the deformation and fracture behavior of steel butt weldments
| AD-A243239 | p 1262 N92-17057
WELDING
The effect of weld metal strength mismatch on the deformation and fracture behavior of steel butt weldments
| AD-A243239 | p 1262 N92-17057
WETTABILITY
Omega-terminated alkanethiolate monolayers on surfaces of copper, silver and gold have similar wettabilities
| AD-A243529 | p 1260 N92-17389
WHISTLERS
Investigation of mechanisms for the source and loss of electrons from the radiation belts using data from SEEP, SCATHA and P78-1 satellites
| AD-A243376 | p 1317 N92-17405
WHITE NOISE
Noncoherent detection of coherent optical heterodyne signals corrupted by laser phase noise
| AD-A243103 | p 1364 N92-16981
WIDE ANGLE LENSES
Hubble Space Telescope: Wide field and planetary camera instrument handbook. Version 2.1
| NASA-CR-189753 | p 1386 N92-17484
Wide field strip-imaging optical system
| NASA-CASE-NPO-18146-1-CU | p 1368 N92-17892
WIENER HOPF EQUATIONS
A rigorous UTD analysis of electromagnetic scattering from resistive strips and resistive-loaded conducting strips
| AD-A243691 | p 1280 N92-17092
WIGGLER MAGNETS
The effects of field errors on low-gain free electron lasers
| AD-A243710 | p 1303 N92-17127
Compact free electron lasers for medical applications
| AD-A243497 | p 1304 N92-17582
WIND (METEOROLOGY)
A statistical analysis of Eleuthera Island wind data for the period 27 April 1989 through 30 March 1990
| AD-A241885 | p 1318 N92-17027
Analysis of the terminal Doppler weather radar algorithm for detecting rotation associated with microbursts
| AD-A242840 | p 1318 N92-17050
User evaluation of laser ballistic sun, wind and dust goggle lenses (dye technology)
| AD-A243245 | p 1334 N92-17143
The use of ADAP to examine warm and quasi-stationary frontal events in the northeastern United States
| PB91-225037 | p 1319 N92-17363
Flight evaluation of curved MLS precision approaches in a twin otter aircraft, phase 2
| AD-A243025 | p 1229 N92-17568
The National Hurricane Center Risk Analysis Program (HURISK)
| PB91-236463 | p 1321 N92-17705
Preliminary results from the analysis of wind component error
| AD-A243772 | p 1321 N92-17764
A variational assimilation method for satellite and conventional data: A revised basic model 2B
p 1322 N92-17977
WIND DIRECTION
BATTLEKING evaluation, BK 22-91, Meteorological Sensor Package (MSP)
| AD-A241919 | p 1317 N92-17009
A statistical analysis of Eleuthera Island wind data for the period 27 April 1989 through 30 March 1990
| AD-A241885 | p 1318 N92-17027
Recommendations for a wind profiling network to support Space Shuttle launches
| NASA-CR-4421 | p 1318 N92-17072
WIND EFFECTS
Wind loads on a mirage III O aircraft mounted above a ground plane
| AD-A243004 | p 1232 N92-17266
WIND MEASUREMENT
A statistical analysis of Eleuthera Island wind data for the period 27 April 1989 through 30 March 1990
| AD-A241885 | p 1318 N92-17027
WIND PROFILES
Wind profiler signal detection improvements
| NASA-CR-189781 | p 1317 N92-16990
Recommendations for a wind profiling network to support Space Shuttle launches
| NASA-CR-4421 | p 1318 N92-17072
High-frequency meteorological phenomena observed with the Naval Postgraduate School's UHF Doppler wind profiler
| AD-A243762 | p 1320 N92-17515
WIND SHEAR
Recommendations for a wind profiling network to support Space Shuttle launches
| NASA-CR-4421 | p 1318 N92-17072
Surface meteorological and near surface oceanographic atlas of the tropical Indian Ocean
| PB91-234286 | p 1319 N92-17138
Escape strategies for turboprop aircraft in a microburst windshear
| AD-A243090 | p 1227 N92-17217
High-frequency meteorological phenomena observed with the Naval Postgraduate School's UHF Doppler wind profiler
| AD-A243762 | p 1320 N92-17515
Alert generation and cockpit presentation for an integrated microburst alerting system
p 1220 N92-17988
Cockpit display of hazardous weather information
p 1220 N92-17989
Target pitch angle for the microburst escape maneuver p 1221 N92-17996
Optimal aircraft performance during microburst encounter p 1222 N92-17999
WIND TUNNEL APPARATUS
Improvement of data processing system for gust wind tunnel data acquisition part: System conversion from off-line to on-line processing
| NAL-TM-611 | p 1238 N92-17756
WIND TUNNEL CALIBRATION
Results of measured temperature distribution on an adiabatic wing model with radiation thermometer
| NAL-TM-610 | p 1225 N92-17755
WIND TUNNEL MODELS
Surface pressure measurements on the wing of a wind tunnel model during steady rotation
| AD-A243047 | p 1223 N92-17281
WIND TUNNEL STABILITY TESTS
A wing rock model for the F-14A aircraft
| AD-A243109 | p 1233 N92-17300
WIND TUNNEL TESTS
Results of the space shuttle vehicle ascent air data system probe calibration test using a 0.07-scale external tank forebody model (68T) in the AEDC 16-foot transonic wind tunnel (IA-310), volume 2
| NASA-CR-167697 | p 1241 N92-17214
Surface pressure measurements on the wing of a wind tunnel model during steady rotation
| AD-A243047 | p 1223 N92-17281
Stagnation and dynamic pressure limits for the S1 wind tunnel
| AD-A242989 | p 1238 N92-17297
Aerodynamic development of the X-31 aircraft for the high angle of attack region
| MBB-FE211-S-PUB-452 | p 1233 N92-17313
A short or a long cylinder: What difference does it make to the Karman vortex street?
| MPIS-98/1990 | p 1224 N92-17314
Flow visualization and wake analysis for standard and modified configurations of the AN/ALQ-78 antenna pod
| AD-A243552 | p 1224 N92-17339
Mean wind speeds over hills and other topography
| ESDU-91043 | p 1321 N92-17853
WIND TUNNEL WALLS
User guide for WIACX: A transonic wind-tunnel wall interference assessment and correction procedure for the NTF
| NASA-TM-104168 | p 1225 N92-17547
WIND TUNNELS
An experimental investigation of leading edge vortical flow about a delta wing during wing rock
| AD-A243363 | p 1223 N92-17114
WIND TURBINES
Dynamic stall on wind turbine blades
| DE92-001157 | p 1226 N92-17874
An overview: Challenges in wind technology development
| DE92-001190 | p 1313 N92-17875
WIND VARIATIONS
Sea surface environmental conditions in the Gulf of Alaska during April 1990 using SSM/I
| AD-A241909 | p 1323 N92-17041
An investigation of cold overflow over the Iceland/Faeroes Ridge
| AD-A243084 | p 1324 N92-17169
WIND VELOCITY
Wind profiler signal detection improvements
| NASA-CR-189781 | p 1317 N92-16990
BATTLEKING evaluation, BK 22-91, Meteorological Sensor Package (MSP)
| AD-A241919 | p 1317 N92-17009
Recommendations for a wind profiling network to support Space Shuttle launches
| NASA-CR-4421 | p 1318 N92-17072
Wind loads on a mirage III O aircraft mounted above a ground plane
| AD-A243004 | p 1232 N92-17266
Simultaneous active and passive microwave measurements of the ocean surface
| AD-A242232 | p 1312 N92-17459
Mean wind speeds over hills and other topography
| ESDU-91043 | p 1321 N92-17853
Modification of a successive corrections objective analysis for improved derivative calculations
p 1322 N92-17981
WINDOWS
Determination of the optical constants of thin Chemical-Vapor-Deposited diamond windows from 0.5 to 6.5 eV
| AD-A243094 | p 1268 N92-17170
WINDPOWERED GENERATORS
An overview: Challenges in wind technology development
| DE92-001190 | p 1313 N92-17875
WING FLAPS
Experimental ice shape and performance characteristics for a multi-element airfoil in the NASA Lewis Icing Research Tunnel
| NASA-TM-105380 | p 1224 N92-17347
WING PROFILES
Surface pressure measurements on the wing of a wind tunnel model during steady rotation
| AD-A243047 | p 1223 N92-17281
WINGS
A wing rock model for the F-14A aircraft
| AD-A243109 | p 1233 N92-17300
Results of measured temperature distribution on an adiabatic wing model with radiation thermometer
| NAL-TM-610 | p 1225 N92-17755
WINTER
Recommendations for a wind profiling network to support Space Shuttle launches
| NASA-CR-4421 | p 1318 N92-17072
WORKING FLUIDS
Thermally regenerative fuel cells
| AD-A242900 | p 1290 N92-17629
WORKLOADS (PSYCHOPHYSIOLOGY)
Neural network classification of mental workload conditions by analysis of spontaneous electroencephalograms
| AD-A243369 | p 1331 N92-17115
The multi-attribute task battery for human operator workload and strategic behavior research
| NASA-TM-104174 | p 1338 N92-17130

X

X RAY DIFFRACTION
A powder x ray diffraction study of two aluminum-lithium based alloys
| AD-A243186 | p 1262 N92-17000
In situ surface x ray crystallography of electrochemically deposited Bi on Ag(111): Structure, compressibility, and anisotropy
| AD-A243218 | p 1372 N92-17181
Grain boundaries
| DE92-004420 | p 1378 N92-17941

X RAY LASERS
X ray laser
| DE91-011705 | p 1304 N92-17649
X RAY SCATTERING
In situ surface x ray scattering of metal monolayers adsorbed at solid-liquid interfaces
| AD-A243258 | p 1262 N92-16985
X RAY SOURCES
A study of gamma ray generation from channeled electrons and positions
| AD-A241993 | p 1361 N92-17608
X RAY SPECTROSCOPY
The complete hard x ray burst spectrometer event list, 1980-1989
| NASA-TM-4332 | p 1389 N92-17048
Collaborative research on experimental astrophysics
| DE92-003970 | p 1388 N92-17832
X RAY TELESCOPES
Aries x ray objective grating spectrograph
| NASA-CR-189245 | p 1386 N92-17003
X RAYS
X ray lithography in Japan
| AD-A243660 | p 1286 N92-17087
In situ structural studies of the underpotential deposition of copper onto an iodine covered platinum surface using x ray standing waves
| AD-A243475 | p 1263 N92-17328
In situ x ray standing wave study of Cu UPD on an iodine covered platinum surface
| AD-A243474 | p 1264 N92-17426
X ray damage to CF3CO2-Terminated organic monolayers on Si/Au supports is due primarily to x ray induced electrons
| AD-A243446 | p 1289 N92-17490
X-29 AIRCRAFT
Development of high angle of attack control laws for an unstable, non-minimum phase aircraft using variations of the quantitative feedback technique
| AD-A243698 | p 1236 N92-17096

Y

YAG LASERS
LDA and PDA systems based on diode-pumped Neodym:YAG lasers
| MBB-Z-0361-91-PUB | p 1304 N92-17526
YAGI ANTENNAS
Superdirective properties of closed loops of parallel coplanar dipoles
| AD-A243009 | p 1288 N92-17268
YAWING MOMENTS
Dynamic stall on wind turbine blades
| DE92-001157 | p 1226 N92-17874
YIELD POINT
Data acquisition and measurement system for plastic parameters of radiation metal research experiments
| DE92-610350 | p 1266 N92-17808
YIELD STRENGTH
Microstructure and mechanical properties of HSLA-100 steel
| AD-A242937 | p 1265 N92-17467
YTTRIUM ISOTOPES
Y890NMR study of hyperfine interactions in (R(x)Y(1-x))Fe2
| DE91-641979 | p 1376 N92-17779
YTTRIUM OXIDES
Growth of near-free-standing YBa2Cu3O7-type crystals using a self-decanting flux method
| AD-A243221 | p 1372 N92-17182
High temperature superconductor thin films and Josephson junctions
| AD-A242747 | p 1293 N92-17949

Z

ZENITH
Evaluation of LOWTRAN and MODTRAN for use over high zenith angle/long path length viewing
| AD-A243599 | p 1387 N92-17920
ZEOLITES
Propane aromatization over gallium containing HZSM-5 zeolites
| ETN-92-90897 | p 1262 N92-17925
ZIRCALOY 2 (TRADEMARK)
Fracture toughness evaluation for N Reactor pressure tubes of Zircaloy-2 using the electric-potential method
| DE92-003631 | p 1311 N92-17713
ZIRCONIUM OXIDES
The synergistic effects of solid and liquid lubrication on the tribological behavior of transformation-toughened ZrO2 ceramics
| DE91-018617 | p 1306 N92-17575

PERSONAL AUTHOR INDEX

Typical Personal Author Index Listing

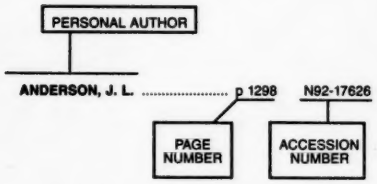

Listings in this index are arranged alphabetically by personal author. The page number helps you locate the citation in the abstract section. The accession number denotes the number by which the citation is identified.

A

AANSTOOS, JAMES V. ..... p 1234 N92-17221
ABDEL-FATTAH, A. M. ..... p 1232 N92-17234
ABOU-AUF, AHMED A. ..... p 1357 N92-17394
ABRUNA, H. D. ..... p 1263 N92-17328
p 1264 N92-17426
ABTAHI, A. ..... p 1301 N92-17006
ACEVEDO, D. ..... p 1263 N92-17328
p 1264 N92-17426
ACHTEMEIER, GARY L. ..... p 1321 N92-17975
p 1322 N92-17976
p 1322 N92-17977
p 1322 N92-17978
p 1322 N92-17979
p 1322 N92-17980
p 1322 N92-17981
ACKROYD, J. A. D. ..... p 1391 N92-17928
ACOSTA, ROBERTO J. ..... p 1279 N92-17047
ADOLF, D. ..... p 1272 N92-17710
AGGARWAL, ISHWAR D. ..... p 1370 N92-17706
AHLF, PETER R. ..... p 1244 N92-17109
AHROON, WILLIAM A. ..... p 1326 N92-17269
p 1329 N92-17299
AJAYI, O. O. ..... p 1306 N92-17575
AKDENIZ, ERHAN M. ..... p 1379 N92-17686
AKOS, DENNIS M. ..... p 1220 N92-17991
AKSAY, ILHAN A. ..... p 1267 N92-17054
ALBIN, G. W. ..... p 1328 N92-17124
ALBRECHT, GERHARD ..... p 1308 N92-17341
ALDIS, D. F. ..... p 1298 N92-17625
ALEXOVICH, ROBERT E. ..... p 1279 N92-17062
ALLEN, C. A. ..... p 1274 N92-17935
ALLEN, C. W. ..... p 1265 N92-17703
ALLEN, M. G. ..... p 1295 N92-17012
ALLEN, ROGER E. ..... p 1305 N92-17923
ALLEN, SCOTT M. ..... p 1239 N92-17325
ALLISON, M. D. ..... p 1325 N92-17951
ALON, YAIR ..... p 1256 N92-17367
ALSTON, WILLIAM B. ..... p 1255 N92-17882
ALTEMUELLER, JEFFREY ..... p 1352 N92-17223
ALTENBURGER, GENE P. ..... p 1253 N92-17510
ALVES, K. M. B. ..... p 1376 N92-17779
ALY, R. ..... p 1330 N92-17714
AMBAR, I. ..... p 1325 N92-17951
AMBROSE, W. P. ..... p 1356 N92-17196
p 1356 N92-17197
p 1271 N92-17659
AMBRUS, JUDITH H. ..... p 1243 N92-17106
AMERICA, PIERRE H. M. ..... p 1346 N92-17833
AMES, BRIAN E. ..... p 1252 N92-17775
AMIRKHANOV, I. V. ..... p 1354 N92-17811
ANANEV, O. A. ..... p 1362 N92-17820
ANCMAN, EILEEN ..... p 1333 N92-16982
ANDERSON, C. A. ..... p 1274 N92-17947
ANDERSON, CHARLES H. ..... p 1368 N92-17864
ANDERSON, J. L. ..... p 1298 N92-17626
ANDERSON, JOHN ..... p 1276 N92-16989
ANDERSON, K. D. ..... p 1282 N92-17383
ANDERTON, GARY L. ..... p 1238 N92-17260
ANDRESEN, J. ..... p 1336 N92-17592
ANDRO, MONTY ..... p 1279 N92-17062
ANNO, GEORGE H. ..... p 1329 N92-17476
ANTRAZI, SAMI S. ..... p 1252 N92-17150
ARHAR, J. R. ..... p 1254 N92-17270
ARKO, A. J. ..... p 1376 N92-17781
ARMSTRONG, R. A. ..... p 1316 N92-17239
ARNEGARD, RUTH J. ..... p 1338 N92-17130
ARNOLD, G. W. ..... p 1377 N92-17797
ARNOLD, R. G. ..... p 1339 N92-17185
ASHLEY, C. S. ..... p 1274 N92-17938
ASMUSSEN, SOEREN ..... p 1353 N92-17837
ATHALE, RAVINDRA A. ..... p 1346 N92-17465
ATTIYA, HAGIT ..... p 1277 N92-17263
AUCLAIR, RICHARD A. ..... p 1383 N92-17369
AUDET, N. F. ..... p 1379 N92-17537
AUSUBEL, JESSE ..... p 1314 N92-17982

B

BABA, SHIGEO ..... p 1225 N92-17755
BABCOCK, S. E. ..... p 1376 N92-17782
BACKES, PAUL G. ..... p 1247 N92-17358
BADDOUR, R. F. ..... p 1295 N92-17025
BADEN, DANIEL G. ..... p 1327 N92-17564
BADIRKHAN, Z. ..... p 1378 N92-17972
BAHASADRI, A. ..... p 1292 N92-17708
BAIJENSE, CORNELIS ROELAND
p 1262 N92-17925
BAITIS, A. E. ..... p 1334 N92-17569
BAJCSY, RUZENA ..... p 1327 N92-17504
BALAKIREV, V. A. ..... p 1285 N92-17812
BALAKRISHNAN, A. V. ..... p 1242 N92-17045
BALLUFFI, R. W. ..... p 1378 N92-17941
BANERJEE, DEV ..... p 1231 N92-17160
p 1232 N92-17163
BANH, DENNIS V. ..... p 1279 N92-17036
BANIA, THOMAS M. ..... p 1387 N92-17695
BARASHENKOV, V. S. ..... p 1363 N92-17958
BARD, STEVEN ..... p 1277 N92-17674
BARKER, KENNETH W. ..... p 1366 N92-17536
BARKER, RICHARD W. ..... p 1308 N92-17431
BARKYOUMB, JOHN ..... p 1269 N92-17397
BARNES, ALAN V. ..... p 1356 N92-17026
BARNES, FRANK S. ..... p 1326 N92-17474
BARQUINERO, KEVIN ..... p 1244 N92-17111
BARROWS, LINDA H. ..... p 1330 N92-17645
BARSOTTI, E. ..... p 1336 N92-17592
BARTELS-LEHNHOFF, HANS-HERMANN
p 1301 N92-17345
BARTON, J. ..... p 1305 N92-17795
BASCHE, T. ..... p 1356 N92-17196
p 1356 N92-17197
p 1271 N92-17659
p 1361 N92-17660
BATES, MARK A. ..... p 1256 N92-17607
BATTAGLIN, G. ..... p 1377 N92-17797
BAUER, PETER ..... p 1280 N92-17139
BAUER, R. C. ..... p 1299 N92-17747
BAUER, STEVEN X. S. ..... p 1300 N92-17888
p 1300 N92-17909
BAUERLE, DONALD G. ..... p 1283 N92-17571
BAUM, SIEGMUND J. ..... p 1329 N92-17476
BAUMBAUGH, A. ..... p 1336 N92-17592
BAUMGAERTEL, H. ..... p 1261 N92-17841
BAUMGARDNER, DARREL ..... p 1313 N92-17393
BEACHLEY, O. T., JR. ..... p 1254 N92-17270
BEAVIS, L. C. ..... p 1363 N92-17739
BEER, STEFAN ..... p 1379 N92-17848
BEKEFI, GEORGE ..... p 1304 N92-17582
BELKIN, BRENDA L. ..... p 1222 N92-18001
BELL, JAMES R. ..... p 1245 N92-17302
BELLAMY-KNIGHTS, P. G. ..... p 1300 N92-17851
BELTRAN, LUIS R. ..... p 1237 N92-17059
BELTRAN, MICHAEL R. ..... p 1227 N92-17259
BENGTSSON, J. ..... p 1305 N92-17868
BENNETT, J. ..... p 1310 N92-17254
p 1310 N92-17265
BENNETT, P. C. ..... p 1261 N92-17727
BENTLEY, J. ..... p 1360 N92-17574
BERG, BRUCE G. ..... p 1355 N92-17381
BERG, R. G. ..... p 1384 N92-17470
BERGER, JONATHAN ..... p 1316 N92-17202
BERGMAN, LARRY A. ..... p 1249 N92-17418
BERKOWITZ, BRIAN M. ..... p 1224 N92-17347
BERNELLA, DAVID M. ..... p 1318 N92-17028
BERNSTEIN, ELLIOT ..... p 1272 N92-17745
BERNSTEIN, ELLIOT R. ..... p 1254 N92-17308
BERRIOS, WILLIAM M. ..... p 1245 N92-17334
p 1241 N92-17335
BERRY, G. C. ..... p 1272 N92-17745
BESORE, MARK H. ..... p 1382 N92-17125
BESTMAN, A. R. ..... p 1327 N92-17946
BEZBARUAH, R. ..... p 1299 N92-17709
BHATTACHARYA, PRABIR ..... p 1351 N92-17609
BIAGIONI, EDOARDO S. ..... p 1346 N92-17670
BIALASIEWICZ, JAN T. ..... p 1347 N92-16987
BIANCO, ROBERT ..... p 1267 N92-17042
BIEBUYCK, HANS A. ..... p 1289 N92-17490
BIEFELD, ERIC ..... p 1246 N92-17353
BINKLEY, CLARK ..... p 1314 N92-17982
BIRKMIRE, DEBORAH P. ..... p 1331 N92-17052
BISHOP, ANN P. ..... p 1381 N92-17001
BISHOP, PHILLIP ..... p 1328 N92-17022
BLACK, D. ..... p 1336 N92-17592
BLACKWELL, C. L. ..... p 1334 N92-17143
BLANCHARD, DENISE M. ..... p 1301 N92-17273
BLATTNER, M. M. ..... p 1385 N92-17845
BLISS, D. E. ..... p 1372 N92-17182
BLUM, FRANK D. ..... p 1373 N92-17382
BLUM, L. ..... p 1259 N92-17323
p 1264 N92-17370
p 1259 N92-17371
BLUNT, D. M. ..... p 1339 N92-17280
BOBBITT, RICHARD B. ..... p 1227 N92-17217
BOBER, Z. ..... p 1378 N92-17944
BOCARSLY, A. B. ..... p 1374 N92-17532
BODE, JUERGEN ..... p 1297 N92-17343
BOGOMAZOVA, E. A. ..... p 1298 N92-17699
BOGOMOLOV, S. L. ..... p 1364 N92-17973
BOHNERT, G. W. ..... p 1277 N92-17535
BOLLINGER, J. J. ..... p 1370 N92-17635
BOLTENKO, EH. A. ..... p 1309 N92-17809
BOMMARITO, G. M. ..... p 1263 N92-17328
p 1264 N92-17426
BON, BRUCE ..... p 1247 N92-17360
BOONE, JOAN ..... p 1380 N92-17651
BOOTH, GUY R. ..... p 1238 N92-17097
BORCZ, RICHARD ..... p 1341 N92-17545
BORER, CHRIS J. ..... p 1236 N92-17729
BORGES, GARY L. ..... p 1263 N92-17271
BORISOV, E. R. ..... p 1294 N92-17971
BOSCOLO-BOSCOLETTO, A. ..... p 1377 N92-17797
BOUFRAQECH, A. ..... p 1362 N92-17954
BOURASSA, ROGER J. ..... p 1245 N92-17215
BOWDEN, JOHN N. ..... p 1275 N92-17066
BOWER, W. ..... p 1289 N92-17468
BOWSER, JAMES R. ..... p 1373 N92-17245
BOYER, ROGER L. ..... p 1252 N92-17776
BRAASCH, MICHAEL ..... p 1221 N92-17994
BRAZELL, JAMES W. ..... p 1389 N92-17123
BREDEHOFT, BRENT B. ..... p 1360 N92-17555
BREEMAN, JAN H. ..... p 1230 N92-17156
BREEN, JOSEPH V. ..... p 1292 N92-17760
BREGER, D. S. ..... p 1313 N92-17577
BREITHAUPT, R. D. ..... p 1298 N92-17625
BREMNER, PATRICIA E. ..... p 1383 N92-17274
BRETTHAUER, BERNWARD ..... p 1301 N92-17344
BREZNAK, JOHN A. ..... p 1326 N92-17224
BRIAN, G. J. ..... p 1223 N92-17281
BRININSTOOL, MICHAEL R. ..... p 1302 N92-17826
BRISTOWE, P. D. ..... p 1378 N92-17941
BROADWELL, JAMES E. ..... p 1294 N92-16979
BROCKMAN, R. A. ..... p 1227 N92-17478
BROWN, DAVID H. ..... p 1283 N92-17563
BROWN, GEORGE S. ..... p 1369 N92-17030
BROWN, RICHARD ..... p 1269 N92-17262
BRYKCZYNSKI, BILL R. ..... p 1337 N92-17068
BUCHER, JOHN R. ..... p 1281 N92-17232
BUCKLEY, LEONARD J. ..... p 1266 N92-16976
BUCKLEY, ROBERT L. ..... p 1339 N92-17237
BUMBAUGH, MARK E. ..... p 1357 N92-17394
BURGHART, G. ..... p 1256 N92-17053

BURKE, THOMAS G. ..... p 1329 N92-17557
BURKHARD, N. R. ..... p 1317 N92-17578
BURKHARDT, WENDEL M. ..... p 1253 N92-17495
BURLAND, D. M. ..... p 1271 N92-17661
BURNETT, DONALD R. ..... p 1302 N92-17835
BURNS, M. ..... p 1240 N92-17591
BURNS, M. J. ..... p 1304 N92-17726
BURRELL, K. H. ..... p 1369 N92-17456
BURROWS, CHRIS ..... p 1386 N92-17483
BUSCH, G. ..... p 1305 N92-17795
BUSSE, LYNDA E. ..... p 1370 N92-17706
BUTLER, H. L. ..... p 1324 N92-17298
BUTTERFIELD, C. P. ..... p 1226 N92-17874

C

CACCAVALLE, F. ..... p 1377 N92-17797
CAGLAYAN, ALPER K. ..... p 1239 N92-17325
CAI, XUE YU ..... p 1376 N92-17782
CALCO, FRANK S. ..... p 1307 N92-17678
CALDWELL, JOHN A., JR. ..... p 1328 N92-17084
CAMP, DAVID W. ..... p 1240 N92-16973
p 1241 N92-16975
p 1241 N92-17364
p 1242 N92-17534
CAREY, D. A. ..... p 1277 N92-17535
CAREY, GRAHAM F. ..... p 1350 N92-17445
CARLSTEN, B. E. ..... p 1304 N92-17726
CAROCHO, ANTONIO J. ..... p 1354 N92-16999
CARRETTA, THOMAS R. ..... p 1332 N92-17450
CARTER, DAVID J. ..... p 1328 N92-17084
CASANOVA, DOUGLAS H. ..... p 1280 N92-17092
CASASENT, DAVID ..... p 1366 N92-17630
CASSEL, R. ..... p 1292 N92-17801
CATURA, R. C. ..... p 1386 N92-17003
CEDERQUIST, J. N. ..... p 1366 N92-17550
CERRINA, FRANCO ..... p 1286 N92-17087
CERUTI, MARION G. ..... p 1383 N92-17369
CHAMBERS, GEORGE P. ..... p 1359 N92-17505
CHAMBERS, MICHAEL W. ..... p 1284 N92-17722
CHAMUEL, JACQUES R. ..... p 1355 N92-17488
CHAN, K. C. ..... p 1304 N92-17726
CHAPLINE, G. ..... p 1364 N92-17876
CHARNES, A. ..... p 1345 N92-17960
CHATTERJEE, A. K. ..... p 1256 N92-17053
CHELA-FLORES, J. ..... p 1327 N92-17877
p 1327 N92-17970
CHEN, J. ..... p 1321 N92-17975
p 1322 N92-17977
CHEN, JAMES K. ..... p 1358 N92-17428
CHEN, JIN Y. ..... p 1291 N92-17668
CHEN, PETER C. ..... p 1311 N92-17930
CHEN, W. L. T. ..... p 1369 N92-17469
CHENG, C. F. ..... p 1325 N92-17766
CHENG, LI-JEN ..... p 1367 N92-17675
CHERNIKOV, A. N. ..... p 1293 N92-17825
CHERNUKHIN, V. L. ..... p 1309 N92-17809
CHEVERS, ED ..... p 1249 N92-17417
CHIEN, STEVE A. ..... p 1247 N92-17357
CHILD, ANDREW D. ..... p 1271 N92-17679
CHIMA, RODRICK V. ..... p 1219 N92-17346
CHOATE, PERRY L. ..... p 1342 N92-17601
CHU, YEN-HO ..... p 1358 N92-17428
CHUNG, JAE DU ..... p 1382 N92-17136
CIRILLO, WILLIAM M. ..... p 1248 N92-17414
CLARK, A. K. ..... p 1381 N92-17940
CLARK, D. L. ..... p 1261 N92-17727
CLARKE, D. W. ..... p 1349 N92-17880
CLEMENS, JAMES T. ..... p 1286 N92-17087
CLEMENTS, MARK A. ..... p 1283 N92-17464
COEL, VALERIE C. ..... p 1318 N92-17050
COFFEY, HELEN E. ..... p 1387 N92-17251
COHEN, EDWARD ..... p 1291 N92-17684
COHEN, HERBERT E. ..... p 1350 N92-17081
COHEN, R. E. ..... p 1295 N92-17025
COHEN, S. ..... p 1363 N92-17590
COHENOUR, BERNARD C. ..... p 1324 N92-17177
COHN, JOSHUA L. ..... p 1372 N92-17218
COLEMAN, R. D. ..... p 1255 N92-17867
COLLETTE, J. G. R. ..... p 1241 N92-17167
p 1241 N92-17214
COLLINS, M. E. ..... p 1383 N92-17274
COMEAU, RONALD C. ..... p 1342 N92-17603
COMPTON, MICHAEL M. ..... p 1248 N92-17411
p 1248 N92-17412
COMSTOCK, J. RAYMOND, JR. .. p 1338 N92-17130
CONDIE, K. G. ..... p 1298 N92-17626
CONRADSON, S. D. ..... p 1304 N92-17726
CONSAGA, JOHN ..... p 1275 N92-17399
COOK, JAMES H. ..... p 1382 N92-17174
COOK, R. P. ..... p 1342 N92-17636
COOPER, LAWRENCE A. ..... p 1344 N92-17761
COOPER, LYNNE ..... p 1246 N92-17353
COOPER, THOMAS D. ..... p 1235 N92-17204
CORDES, JAMES M. ..... p 1390 N92-18003
p 1390 N92-18004
p 1390 N92-18005
CORREA, S. M. ..... p 1260 N92-17682
COSNYKA, EDWARD ..... p 1288 N92-17332
COX, JOHN ..... p 1242 N92-17099
CREMER, JAMES F. ..... p 1341 N92-17538
CRIMINALE, W. O. ..... p 1295 N92-17039
CROLL, J. B. ..... p 1229 N92-17568
CROUCH, MICHAEL ..... p 1219 N92-17477
CRUICKSHANK, ALEXANDER A. p 1267 N92-17029
CULJKOVIC, MIODRAG ..... p 1309 N92-17544
CUMMINGS, KATHLEEN E. ..... p 1283 N92-17464
CUMMINGS, MARY A. ..... p 1340 N92-17368
CURD, DENNIS L. ..... p 1326 N92-17269
CURLING, H. L., JR. ..... p 1265 N92-17579

D

DABOUL, J. ..... p 1351 N92-17622
DADDARIO, LAWRENCE R. ..... p 1291 N92-17672
DAINTY, J. C. ..... p 1366 N92-17486
DALE, J. M. ..... p 1276 N92-17963
DALTON, LARRY R. ..... p 1270 N92-17508
DANIELS, J. I. ..... p 1330 N92-17714
DARIOTIS, DIMITRIS ..... p 1278 N92-17016
DARROW, JANET M. ..... p 1325 N92-17142
DAS, A. ..... p 1379 N92-17807
DASGUPTA, ABHIJIT ..... p 1311 N92-17511
DATLOWE, D. W. ..... p 1317 N92-17405
DAVIDSON, FREDERIC M. ..... p 1303 N92-17152
DAVIDSON, JAMES J. ..... p 1342 N92-17561
DAVIDSON, THOMAS F. ..... p 1257 N92-17836
DAVIES, ROBERT J. ..... p 1242 N92-17104
DAVIS, ROBERT F. ..... p 1373 N92-17390
DAVIS, S. J. ..... p 1295 N92-17012
DAVIS, TOM ..... p 1250 N92-17422
DAWSON, REGINALD ..... p 1368 N92-17863
DAY, ROBERT D. ..... p 1278 N92-17780
DEAN, P. ..... p 1301 N92-17006
DEBOER, FRANK S. ..... p 1346 N92-17833
DECKER, M. W. ..... p 1372 N92-17182
DEJONG, SIJBRAND JAN ..... p 1358 N92-17435
DELEEUW, JAAP H. ..... p 1231 N92-17157
DELRIE, DARCELLE M. ..... p 1328 N92-17084
DELROSARIO, RUBEN ..... p 1237 N92-17059
DELROSO, RICHARD L. ..... p 1237 N92-17059
DEMEROUKAS, CATHERINE ..... p 1314 N92-17551
DENKER, M. S. ..... p 1259 N92-17246
DENNE, DOUG J. ..... p 1336 N92-17720
DENNIS, B. R. ..... p 1389 N92-17048
DEOBALD, L. R. ..... p 1273 N92-17784
DERONDE, R. ..... p 1301 N92-17437
DERSHOWITZ, ADAM ..... p 1220 N92-17986
DESQUITH, E. ..... p 1354 N92-17803
p 1354 N92-17804
DEVENPORT, W. J. ..... p 1223 N92-17222
DEVOGEL, GREGORY F. ..... p 1388 N92-17253
DEWBERRY, BRANDON S. ..... p 1246 N92-17356
DEWEY, DONALD E. ..... p 1341 N92-17498
DEYONG, L. V. ..... p 1275 N92-17058
DEZERN, JAMES F. ..... p 1271 N92-17676
DHARIA, JAYESH R. ..... p 1266 N92-16976
DIACHENKO, B. A. ..... p 1362 N92-17820
DIAMOND, PHILIP J. ..... p 1390 N92-18004
DIDONATO, ARMIDO R. ..... p 1350 N92-17242
DIEN, NGUYEN NHI ..... p 1348 N92-17814
DIMOTAKIS, PAUL E. ..... p 1294 N92-16979
DITMARS, D. A. ..... p 1372 N92-17220
DIVECHA, AMARNATH P. ..... p 1265 N92-17452
DIVIS, DALE H. ..... p 1317 N92-16990
DIX, R. E. ..... p 1299 N92-17747
DIXON, P. R. ..... p 1261 N92-17727
DOETSCH, K. H. ..... p 1243 N92-17102
DOLCE, JAMES L. ..... p 1252 N92-17773
DOMINICK, SAM ..... p 1249 N92-17416
DORE, MICHAEL A. ..... p 1329 N92-17476
DOTY, PHILIP ..... p 1381 N92-17001
DOUCETTE, WILLIAM J. ..... p 1336 N92-17720
DOUGHERTY, JOSEPH P. ..... p 1268 N92-17193
DOVGII, IA. O. ..... p 1375 N92-17698
DOWNER, S. B. ..... p 1316 N92-17239
DOWNIE, BRUCE ..... p 1226 N92-17149
DOYLE, BRIAN A. ..... p 1371 N92-17015
DOYLE, RICHARD J. ..... p 1247 N92-17357
DRERUP, J. M. ..... p 1255 N92-17373
DRESCHHOFF, GISELA A. ..... p 1389 N92-17235
DREWERY, J. O. ..... p 1285 N92-17886
DRUMMOND, J. PHILIP ..... p 1223 N92-17131
DUBINKO, V. I. ..... p 1262 N92-17943
DUBOIS, NEIL J. ..... p 1307 N92-17827
DUCHARME, S. ..... p 1271 N92-17661
DUFFY, STEPHEN F. ..... p 1267 N92-17060
DUGAR-ZHABON, V. D. ..... p 1362 N92-17743
DUGINOV, V. N. ..... p 1294 N92-17953
DUKE, JOSEPH R. ..... p 1373 N92-17382
DUNLOP, J. ..... p 1289 N92-17468
DUNN, MARK H. ..... p 1224 N92-17303
DURRANT-WHYTE, H. F. ..... p 1302 N92-17926
p 1344 N92-17927
DURRANT-WHYTE, HUGH F. ..... p 1229 N92-17878
DURST, F. ..... p 1304 N92-17526
DUVAL, RONALD W. ..... p 1232 N92-17164
DUVALL, LARRY J. ..... p 1292 N92-17718
DWORKIN, MARTIN ..... p 1326 N92-17224
DWYER, JOHN P. ..... p 1228 N92-17512
DZHUSOV, YU. P. ..... p 1309 N92-17809

E

EARLY, J. ..... p 1305 N92-17795
EATOUGH, M. O. ..... p 1377 N92-17790
EBERHARDT, SILVIO P. ..... p 1337 N92-17884
EFTEKHARI, ABE ..... p 1267 N92-17032
EISENLOHR, HOLGER ..... p 1224 N92-17314
EISLER, R. D. ..... p 1256 N92-17053
EKBERG, S. A. ..... p 1261 N92-17727
ELLEDGE, BARRY ..... p 1380 N92-17651
ELLIOTT, C. J. ..... p 1304 N92-17726
ELLIS, DANA J. ..... p 1239 N92-17192
ENGLEBRETSON, R. E. ..... p 1319 N92-17338
p 1320 N92-17406
p 1320 N92-17492
p 1320 N92-17493
p 1320 N92-17494
EPHREMIDES, ANTHONY ..... p 1286 N92-17931
ERAYDIN, HAKAN ..... p 1378 N92-17443
ERCK, R. A. ..... p 1306 N92-17575
ERDEMIR, A. ..... p 1306 N92-17575
EREN, ALI S. ..... p 1292 N92-17724
ERICKSON, JEFFERY B. ..... p 1228 N92-17512
ESAREY, E. ..... p 1303 N92-17127
ESTERLINE, D. ..... p 1336 N92-17592
ESTEROWITZ, LEON ..... p 1304 N92-17627
p 1305 N92-17923
p 1297 N92-17312
EULER, MICHAEL ..... p 1330 N92-17567
EVANS, SUSAN M. ..... p 1255 N92-17329
EVANS, SUZANNE M.

F

FAGHRI, AMIR ..... p 1300 N92-17887
FAHRENTHOLD, ERIC P. ..... p 1244 N92-17200
FARABAUGH, E. N. ..... p 1372 N92-17238
FARABAUGH, EDWARD N. ..... p 1268 N92-17170
p 1268 N92-17171
p 1271 N92-17615
FARAGO, B. ..... p 1274 N92-17938
FARAH, MARTHA J. ..... p 1347 N92-16991
FARMER, W. M. ..... p 1350 N92-17206
FAULK, DAVID P. ..... p 1383 N92-17340
FAUST, L. G. ..... p 1358 N92-17453
FAWCETT, W. R. ..... p 1259 N92-17323
p 1259 N92-17371
FEDOTOVSKIJ, V. S. ..... p 1299 N92-17810
FEINGOLD, HARVEY ..... p 1249 N92-17416
FELDMAN, A. ..... p 1372 N92-17238
FELDMAN, ALBERT ..... p 1268 N92-17170
p 1268 N92-17171
p 1268 N92-17172
p 1271 N92-17615
FENG, DAI ..... p 1228 N92-17147
FENG, S. T. ..... p 1365 N92-17249
FENSKE, G. R. ..... p 1306 N92-17575
FERNQUIST, ALAN ..... p 1244 N92-17110
FERRANDO, WILLIAM ..... p 1293 N92-17871
FESTA, J. F. ..... p 1319 N92-17138
FETZ, EBERHARD E. ..... p 1343 N92-17655
FIELDS, ROGER A. ..... p 1232 N92-17226
FIENUP, J. R. ..... p 1366 N92-17550
FIFER, ROBERT A. ..... p 1275 N92-17562
FIKIORIS, GEORGE ..... p 1288 N92-17268
FILLER, RAYMOND L. ..... p 1281 N92-17258
FINKEL, JACK ..... p 1368 N92-17959
FISCHER, WILLIAM E., JR. ..... p 1219 N92-17731
FISHER, EDWARD M., JR. ..... p 1251 N92-17769
FISK, CHARLES J. ..... p 1324 N92-17177
FLANDERA, RICHARD ..... p 1289 N92-17480
FLEMING, J. L. ..... p 1223 N92-17222
FLEMMING, C. D. ..... p 1255 N92-17373
FLEMMING, KEN ..... p 1249 N92-17415
FOLKERS, JOHN P. ..... p 1264 N92-17427
p 1359 N92-17491
FORCH, BRAD E. ..... p 1303 N92-17137
FORTNEY, JOSEPH C. ..... p 1284 N92-17735
FOSTER, JOHN C. ..... p 1317 N92-17961
FOWLER, T. K. ..... p 1370 N92-17606
FOX, BARRY R. ..... p 1249 N92-17420
FOX, MARYE A. ..... p 1264 N92-17427
FOX, RICHARD N. ..... p 1282 N92-17366
FRAIL, DALE A. ..... p 1390 N92-18004

FRANTI, G. W. p 1371 N92-17968
FRASER, K. F. p 1233 N92-17565
FRAZIER, W. E. p 1257 N92-17611
FREDRICH, DETLEF p 1270 N92-17541
FREED, KARL F. p 1273 N92-17777
FRICK, B. p 1274 N92-17938
FRIDGE, ERNEST p 1246 N92-17351
FRIEMAN, JOSHUA A. p 1388 N92-17696
FRIM, J. p 1330 N92-17599
FROST, KEN p 1389 N92-17048
FUCHS, HENRY p 1342 N92-17637
FUJIEDA, HIROTOSHI p 1238 N92-17756
FUJITA, TOSHIMI p 1238 N92-17756
FULLER, GENE E. p 1286 N92-17087
FUNCHESS, ROBERT B. p 1373 N92-17382

G

GABOVICH, M. D. p 1362 N92-17818
GABRIEL, CAMELIA p 1260 N92-17572
GACEL, RAFAEL A. p 1382 N92-17255
GADD, DAVID A. p 1339 N92-17179
GAIER, JAMES R. p 1257 N92-17861
GAMES, R. A. p 1350 N92-17207
GANDHI, OM P. p 1291 N92-17668
GANDY, C. p 1285 N92-17885
GANT, DEAN A. p 1290 N92-17570
GAO, X. p 1358 N92-17472
GAO, YUFEI p 1376 N92-17782
GARCIA, JESSE p 1329 N92-17194
GARDOS, MICHAEL N. p 1270 N92-17597
p 1270 N92-17614
p 1272 N92-17683
GARINTHER, GEORGES R. p 1331 N92-17052
GARNER, S. G. p 1366 N92-17294
GARRETT, STEVEN L. p 1302 N92-17826
GARRIZ, JAVIER A. p 1225 N92-17547
GARVEY, G. T. p 1360 N92-17589
GARVEY, JOHN M. p 1247 N92-17362
GAUSTAD, KRISTA LYNN p 1292 N92-17742
GAUTIER, ILIA L. p 1326 N92-17269
GAVER, DONALD P. p 1286 N92-16993
p 1321 N92-17764
GAYLORD, THOMAS K. p 1382 N92-17037
GAZZA, GEORGE E. p 1372 N92-17082
GEDDE, U. W. p 1269 N92-17448
GEESEY, ROGER A. p 1348 N92-17438
GELFAND, ALAN E. p 1352 N92-17178
GEORGE, THOMAS F. p 1266 N92-17010
p 1373 N92-17245
p 1357 N92-17423
GERMANY, D. M. p 1240 N92-16973
p 1240 N92-16974
p 1241 N92-16975
p 1241 N92-17364
p 1242 N92-17534
GERSTEIN, B. C. p 1372 N92-17219
GEZGIN, ERHAN p 1324 N92-17119
GHIORSE, SETH R. p 1255 N92-16992
GHIRARDI, G. C. p 1379 N92-17824
GIANTS, THOMAS W. p 1253 N92-17085
GIBSON, JOHN p 1306 N92-17584
GIBSON, WARREN C. p 1383 N92-17396
GILBERT, D. B. p 1292 N92-17708
GILBERT, PAUL A. p 1238 N92-17287
GILBRECH, RICHARD J. p 1296 N92-17276
GILLIS, JAMES R. p 1245 N92-17215
GILMER, JOHN B. p 1348 N92-17438
GILMORE, R. D. p 1319 N92-17338
p 1320 N92-17492
p 1320 N92-17493
GLASS, K. p 1330 N92-17599
GLEASON, GERALD A. p 1331 N92-17145
GLEESON, RONALD F. p 1342 N92-17561
GLEISER, MARCELO p 1361 N92-17647
GLOVER, MICHAEL P. p 1295 N92-17018
GNOFFO, P. A. p 1294 N92-17002
GODIN, C. S. p 1255 N92-17373
GOEHNER, R. P. p 1377 N92-17790
GOHIL, P. p 1369 N92-17456
GOLDBURG, W. I. p 1298 N92-17688
GOLDEY, E. p 1325 N92-17121
GOLDSTEIN, J. C. p 1304 N92-17726
GOLISH, L. M. p 1343 N92-17716
GOLOVANIVSKII, K. S. p 1362 N92-17743
GOMBAR, A. M. p 1292 N92-17708
GONSALVES, PAUL G. p 1239 N92-17325
GOODWIN, ROBERT D., JR. p 1380 N92-17451
GORDON, JOSEPH G. p 1262 N92-16985
p 1263 N92-17271
GORDON, LLOYD B. p 1312 N92-17225
GORDON, STEVEN C. p 1388 N92-17595
GORMAN, J. D. p 1366 N92-17550
GOSLING, J. T. p 1389 N92-17725
GOSSNER, JESSE R. p 1239 N92-17732
GRABOWSKI, KENNETH S. p 1359 N92-17505
GRAHAM, ROBERT L. p 1289 N92-17490
GRAHAM, ROSS p 1334 N92-17569
GRAHAM, THOMAS E. p 1289 N92-17501
GRATZ, ROY F. p 1255 N92-17882
GRAY, ROGER L. p 1287 N92-17129
p 1229 N92-17707
GREBINNIK, V. G. p 1294 N92-17953
GREEN, P. H. p 1270 N92-17576
GREENISEN, MICHAEL p 1328 N92-17022
GREY, A. E. p 1274 N92-17935
GREYWALL, MAHESH S. p 1298 N92-17588
GRIFFIN, J. A. p 1288 N92-17317
GRIFFITHS, RICHARD p 1386 N92-17484
GRINSTEIN, F. F. p 1295 N92-17126
GROEBNER, R. J. p 1369 N92-17456
GROSS, JONATHAN L. p 1350 N92-17148
GROSS, THOMAS p 1336 N92-17466
GROSSBERG, STEPHEN B. p 1332 N92-17554
GROSSMANN, W. p 1371 N92-17793
GUENTHER, G. p 1256 N92-17310
GUIMARAES, A. P. p 1376 N92-17779
GUIRGUIS, R. H. p 1295 N92-17126
GULATI, A. p 1260 N92-17682
GUPTA, PRAHLAD p 1332 N92-17458
GUPTA, S. p 1260 N92-17489
GUSEVA, M. I. p 1362 N92-17818
GUSTAFSON, JOHN A. p 1250 N92-17602
GUTTMAN, J. D. p 1350 N92-17206

H

HADDAD, RANWA p 1343 N92-17640
HAIGLER, KARA J. p 1225 N92-17547
HALL, L. C. p 1330 N92-17714
HAMANN, DONALD p 1319 N92-17289
HAMELIN, A. p 1358 N92-17472
HAMERNIK, ROGER P. p 1326 N92-17269
p 1329 N92-17299
HAMILTON, RICHARD J. p 1334 N92-17432
HAMMER, W. p 1378 N92-17944
HANEY, MICHAEL W. p 1346 N92-17465
HANGEN, J. A. p 1233 N92-17513
HANNA, WILLIAM F. p 1316 N92-17229
HANSEN, A. C. p 1226 N92-17874
HANSEN, JOHN H. p 1283 N92-17464
HANSEN, STUART p 1341 N92-17538
HANSMAN, R. JOHN, JR. p 1220 N92-17986
p 1220 N92-17987
p 1220 N92-17988
p 1220 N92-17989
HANSON, K. M. p 1352 N92-17455
HAPSTACK, M. p 1306 N92-17183
HARDING, JEFF W. p 1231 N92-17160
p 1232 N92-17163
HARDING, W. B. p 1238 N92-17967
HARGETT, C. E., JR. p 1326 N92-17269
p 1329 N92-17299
HARLETT, JOHN C. p 1355 N92-17236
HARP, DAVID M. p 1380 N92-17388
HARPER, MARK A. p 1267 N92-17042
HARRINGTON, S. p 1289 N92-17468
HARRIS, BERNARD A. p 1330 N92-17645
HARRIS, MARTHA C. p 1385 N92-17283
HARRIS, T. E. p 1302 N92-17454
HART, G. F. p 1317 N92-16990
HARTJES, FREDERIK GOTTLIEB p 1303 N92-17434
HARTMAN, RICHARD W. p 1383 N92-17401
HASSE, WOLFGANG p 1386 N92-17523
HASTIE, ROBERT L., JR. p 1258 N92-17932
HATHAWAY, K. B. p 1381 N92-17940
HAVANCZAK, K. p 1266 N92-17808
HAVENS, STEPHEN J. p 1272 N92-17693
HAWKES, RICHARD M. p 1381 N92-17669
HAWKINSON, TODD D. p 1237 N92-17442
HAYASHI, YOUICHI p 1257 N92-17869
HAYES, JUDITH C. p 1330 N92-17645
HAZLETT, MICHAEL A. p 1284 N92-17662
HEADLEY, T. J. p 1377 N92-17790
HEARN, DAVID R. p 1281 N92-17241
HEATH, RONALD E. p 1324 N92-17298
HEBERLEIN, J. p 1369 N92-17469
HECKMAN, SCOT T. p 1321 N92-17631
HEDDINGS, CLYDE R. p 1280 N92-17095
HEINDEL, TROY A. p 1249 N92-17421
HELD, T. W. p 1227 N92-17478
HELLDOERFER, RICK p 1352 N92-17223
HEMMENT, PETER L. p 1289 N92-17439
HENDERSON, MADELINE p 1381 N92-17001
HENDERSON, T. J. p 1274 N92-17947
HERCZFELD, P. R. p 1292 N92-17708
HERGET, C. J. p 1349 N92-17965
HERMSEN, P. A. p 1232 N92-17266
HERRERA, A. p 1376 N92-17781
HILL, CHRISTOPHER T. p 1388 N92-17696
HILL, ROBERT W. p 1286 N92-17087
HILLARD, G. BARRY p 1389 N92-17069
HILLS, RICHARD A. p 1285 N92-17829
HINKAMP, J. J. p 1318 N92-17027
HINKLEY, JEFFREY A. p 1267 N92-17032
HOCK, S. M. p 1313 N92-17875
HODGSON, ED p 1276 N92-16989
HOFLER, THOMAS p 1302 N92-17826
HOLLAND, CHARLES W. p 1323 N92-17083
HOLMBERG, GERALD E. p 1367 N92-17828
HOLT, MARK S. p 1336 N92-17720
HONG, YOUNG S. p 1294 N92-16978
HOOD, S. T. p 1340 N92-17296
HOOK, W. RAY p 1244 N92-17108
HOOMAN, JOZEF JOHANNES MARIA p 1341 N92-17521
HOOVER, BRIAN D. p 1355 N92-17506
HOPPLE, GERALD p 1347 N92-17203
HORDIJK, ARIE p 1349 N92-17838
HORIUCHI, SHOUJI p 1236 N92-17855
HOWARD, KRIS R. p 1251 N92-17762
HOWE, CLAYTON P. p 1376 N92-17746
HSIEH, BERNARD B. p 1324 N92-17298
HSIEH, J. H. p 1306 N92-17575
HU, Y. Z. p 1259 N92-17247
p 1290 N92-17596
HUANG, F. H. p 1311 N92-17713
HUANG, H. p 1260 N92-17489
HUBBARD, DAVID C. p 1333 N92-17758
HUBERICH, MARKUS p 1351 N92-17525
HUBLER, GRAHAM K. p 1359 N92-17505
HUCKABY, DALE A. p 1264 N92-17370
HUEBERT, BARRY p 1313 N92-17393
HUGHES, STEVEN A. p 1238 N92-17287
HULLIGAN, DAVID D. p 1235 N92-17061
HULT, A. p 1269 N92-17448
HUNG, CHING-CHEH p 1261 N92-17902
HUNTER, A. T. p 1293 N92-17949
HUNTER, KYLE p 1284 N92-17691
HURLEY, JAMES A. p 1295 N92-17018
HUTCHINSON, JOHN J. p 1226 N92-16986
p 1227 N92-17587
HWANG, J. S. p 1288 N92-17290
HWANG, YONG G. p 1282 N92-17277

I

IANNELLI, THOMAS A. p 1283 N92-17516
IDZOREK, G. C. p 1265 N92-17579
IKEUCHI, KATSUSHI p 1365 N92-17146
ILIN, V. D. p 1354 N92-17811
ILINA, A. N. p 1354 N92-17811
ILIUKHIN, A. G. p 1298 N92-17699
ILLES, Z. p 1266 N92-17808
IMHOF, W. L. p 1317 N92-17405
INTHOUT, K. J. p 1351 N92-17517
IRENE, E. A. p 1259 N92-17246
p 1259 N92-17247
p 1259 N92-17248
p 1365 N92-17249
p 1259 N92-17261
p 1290 N92-17596
p 1260 N92-17613
ISHIBASHI, YOSHITSUGU p 1385 N92-17787
ISHIKAWA, KAZUTOSHI p 1237 N92-17917
ISHIKAWA, TAKASHI p 1257 N92-17869
ITTSTEIN, HANS GEORG p 1290 N92-17540
IURASOVA, V. E. p 1362 N92-17818
IVAN, THOMAS R. p 1384 N92-17633
IVANOV, E. A. p 1353 N92-17318
IWASAKI, AKIHITO p 1238 N92-17756
IYENGAR, S. S. p 1300 N92-16983

J

JACKSON, WADE C. p 1256 N92-17007
JACOBS, PATRICIA A. p 1286 N92-16993
p 1321 N92-17764
JACOBS, TIMOTHY M. p 1384 N92-17482
JACOBSON, NATHAN S. p 1267 N92-17070
JAEGER, H. U. p 1363 N92-17957
JAIN, ABHINANDAN p 1349 N92-17895
JAMES, J. R. p 1349 N92-17965
JANECKY, D. R. p 1261 N92-17727
JANSEN, LEONARD J. p 1285 N92-17763
JANSEN, R. H. p 1339 N92-17185
JANTON, W. M. p 1292 N92-17708
JELSKI, DANIEL A. p 1373 N92-17245
JENKINS, ALAN K. p 1341 N92-17558
JENKINS, IAN p 1241 N92-17342
JENSEN, BRIAN J. p 1267 N92-17032
p 1272 N92-17693
JEWELL, DONNA M. p 1234 N92-17221
JEZIOR, B. p 1334 N92-17143

JOHNSON, BILLY H. p 1324 N92-17298
JOHNSON, CHRISTINE M. p 1317 N92-17009
JOHNSON, G. C. p 1325 N92-17951
JOHNSON, GORDON G. p 1344 N92-17860
JOHNSON, H. p 1269 N92-17448
JOHNSON, R. P. p 1366 N92-17294
JOHNSON, STEVEN A. p 1230 N92-17071
JONES, JACK A. p 1277 N92-17674
JONSSON, H. p 1374 N92-17449
JOSEPH, J. p 1259 N92-17247
p 1290 N92-17596
JOYCE, R. A. p 1366 N92-17294
JURKA, J. p 1385 N92-17856

K

KABACOFF, LAWRENCE T. p 1269 N92-17397
p 1374 N92-17610
p 1270 N92-17612
KAISER, D. L. p 1376 N92-17782
KALCHEV, S. D. p 1363 N92-17955
KALCIC, MARIA T. p 1325 N92-17765
KALETKA, JUERGEN p 1230 N92-17155
p 1231 N92-17161
KALMAN, GABOR J. p 1369 N92-17301
KANG, KEEBOM p 1346 N92-17425
KAPUSTNIKOV, A. A. p 1353 N92-17318
KARMARKAR, SUBHASH D. p 1265 N92-17452
KARNOWSKY, M. M. p 1363 N92-17739
KAUFMAN, D. p 1361 N92-17652
KAWA, S. p 1330 N92-17798
KAZMIERCZAK, MICHAEL p 1220 N92-17987
KEARNEY, JOSEPH K. p 1341 N92-17538
KEEFER, DENNIS p 1304 N92-17475
KEIM, DANIEL A. p 1339 N92-17285
KEKELIDZE, G. P. p 1375 N92-17700
KELLER, PAUL p 1228 N92-17147
KELLEY, PAUL p 1262 N92-17056
KELLIHER, MARGARET p 1341 N92-17487
KELM, ERIC W. p 1343 N92-17733
KENNARD, G. S. p 1389 N92-17048
KENNEALY, J. P. p 1316 N92-17239
KENNELLY, M. A. p 1325 N92-17951
KENNING, D. B. R. p 1380 N92-17879
KERCZEWSKI, ROBERT J. p 1279 N92-17062
KEVORKIAN, A. K. p 1351 N92-17560
KHAN, I. A. p 1327 N92-17815
p 1351 N92-17939
KHUON, TIMOTHY S. p 1352 N92-16998
KIM, J. p 1369 N92-17456
KIM, JINWON p 1315 N92-17063
KIM, K. J. p 1305 N92-17868
KIM, K. W. p 1376 N92-17783
KIM, KEU W. p 1324 N92-17298
KIM, KWANG-JE p 1305 N92-17936
KIM, KYUNG-CHANG p 1383 N92-17402
KIM, S. p 1223 N92-17117
KIMOTO, T. p 1265 N92-17703
KINDL, MARK R. p 1340 N92-17403
KINDLER, A. p 1290 N92-17629
KING, H. T. p 1336 N92-17466
KING, ROGER J. p 1253 N92-17510
KING, RONALD W. p 1288 N92-17268
KINTZ, GREGORY J. p 1305 N92-17923
KIRK, MARK T. p 1262 N92-17057
KIRLIK, ALEX p 1333 N92-17132
KISARA, KATSUTO p 1385 N92-17787
KISELEV, YU. F. p 1293 N92-17825
KISIEL, THOMAS K. p 1296 N92-17275
KISSENER, H. R. p 1363 N92-17957
KLAASEN, J. J. p 1282 N92-17279
KLEISS, JAMES A. p 1333 N92-17758
KLEPACZKO, J. R. p 1310 N92-17256
KLEVENOW, F. T. p 1233 N92-17316
KLINE, PAUL A. p 1221 N92-17992
KNICKERBOCKER, K. p 1336 N92-17592
KNOLL, SUSAN E. p 1329 N92-17190
KO, HANSEOK p 1342 N92-17581
KOBAYASHI, A. S. p 1273 N92-17784
KOBAYASHI, SHIGEO p 1257 N92-17869
KOENIG, H. p 1325 N92-17951
KOIKE, AKIRA p 1225 N92-17755
KOIVU, A. H. p 1256 N92-17053
KOLB, EDWARD W. p 1361 N92-17647
KOLECKI, JOSEPH C. p 1389 N92-17069
KOLINKO, N. I. p 1375 N92-17698
KOMATSU, YUKIO p 1225 N92-17755
KONDRATENKO, P. A. p 1375 N92-17701
KOOLE, GER p 1353 N92-17837
p 1349 N92-17838
KOSCHMIEDER, E. L. p 1373 N92-17375
KOSONOCKY, W. F. p 1301 N92-17140
KRAMER, GERRIT JAKOB p 1358 N92-17433
KRAUS, WERNER p 1233 N92-17313
KRAVETZ, GARY A. p 1342 N92-17566
KRITZ, MARY M. p 1314 N92-17982
KROCHUK, A. C. p 1375 N92-17698
KROHN, DOUGLAS D. p 1264 N92-17376
KRUCZYNSKI, DAVID L. p 1235 N92-17642
KRUETZ, KENNETH K. p 1349 N92-17895
KRULIKOVSKAIA, M. P. p 1375 N92-17700
KUHL, MARK R. p 1281 N92-17244
KUMAR, ASHOK p 1338 N92-17122
KUNZ, STEVEN p 1225 N92-17404
KUO, LYNN p 1353 N92-17643
KURKI-SUONIO, T. K. p 1370 N92-17606
KUTNER, V. B. p 1364 N92-17973
KUUSINEN, T. L. p 1314 N92-17665
KUZNETSOV, YU. V. p 1294 N92-17971
KVATERNIK, RAYMOND G. p 1309 N92-17033
p 1309 N92-17034
KWARCIANY, R. p 1336 N92-17592

L

LABOW, G. J. p 1389 N92-17048
LACEY, DONALD J., JR. p 1237 N92-17748
LAGIN, ALAN R. p 1279 N92-17047
LAGOW, RICHARD J. p 1258 N92-17043
LAIBINIS, PAUL E. p 1260 N92-17389
p 1264 N92-17427
p 1289 N92-17490
p 1359 N92-17491
LAING, JOHN S. p 1332 N92-17500
LANG, ROBERT J. p 1305 N92-17862
p 1305 N92-17899
LANG, V. I. p 1315 N92-17035
LANGHALS, TAMMY J. p 1224 N92-17347
LARBALESTIER, D. C. p 1376 N92-17782
LARKIN, R. J. p 1316 N92-17239
LARKO, JEFFREY M. p 1279 N92-17047
LARSON, T. K. p 1298 N92-17626
LAU, S. S. p 1377 N92-17791
LAUCHLE, G. C. p 1297 N92-17387
LAWLER, D. G. p 1245 N92-17349
LAWN, BRIAN R. p 1269 N92-17282
LAZAR, AUREL p 1381 N92-17952
LEATH, K. p 1248 N92-17413
LEDBETTER, RICHARD H. p 1238 N92-17287
LEDERBERG, JOSHUA p 1314 N92-17982
LEE, ANGELENE M. p 1278 N92-17913
LEE, CHARLES R. p 1238 N92-17287
LEE, JASOPIN p 1235 N92-17644
LEE, KIMYEONG p 1388 N92-17377
p 1388 N92-17697
LEE, WOODROW W. p 1260 N92-17628
p 1276 N92-17830
LEE, WOONG M. p 1358 N92-17462
LEGGETT, DANIEL C. p 1254 N92-17055
LEHNER, PAUL E. p 1348 N92-17438
LEIVENT, JONATHAN I. p 1345 N92-17188
LEONARD, ANTHONY p 1294 N92-16979
LEONARD, JOHN J. p 1229 N92-17878
LEONDES, CORNELIUS T. p 1234 N92-17128
LEONOWICH, J. A. p 1358 N92-17453
LEPERA, MAURICE E. p 1275 N92-17066
LESHER, L. L. p 1334 N92-17143
LEVINE, ROBERT Y. p 1352 N92-16998
LEVY, JAMES J. p 1346 N92-17465
LEWIS, WILLIAM p 1314 N92-17982
LEX, CLAUDIA p 1240 N92-17527
LI, HSIN-YUN p 1354 N92-17548
LI, M. p 1259 N92-17248
LI, X. p 1266 N92-17010
p 1357 N92-17423
LIEBENBERG, D. H. p 1375 N92-17685
LIEBMAN, JON C. p 1314 N92-17982
LILLEY, ROBERT W. p 1220 N92-17990
LIM, SUNGJAE p 1283 N92-17464
LIN, D. L. p 1266 N92-17010
p 1357 N92-17423
LINCOLN, JOHN W. p 1235 N92-17204
LINGSCH, STEVE C. p 1325 N92-17765
LINSE, DENNIS J. p 1222 N92-17998
LITTLEJOHN, M. A. p 1376 N92-17783
LIU, JIA-MING p 1286 N92-17017
LIU, Q. p 1259 N92-17261
LIU, TSUEN-HSI p 1367 N92-17675
LIU, X. p 1259 N92-17246
LIVINGSTONE, S. D. p 1334 N92-17278
LIZZA, GRETCHEN D. p 1331 N92-17115
LOELIGER, HANS R. p 1372 N92-17219
LOFTIN, R. BOWEN p 1246 N92-17352
LOLLAR, LOUIS F. p 1252 N92-17774
LONDON, G. J. p 1257 N92-17611
LOUGHRY, THOMAS A. p 1279 N92-17031
LOWE-MA, C. K. p 1372 N92-17182
p 1365 N92-17284
LOZYKOWSKI, HENRY J. p 1375 N92-17667
LUBCHENCO, JANE p 1314 N92-17982
LUDLOW, TIMOTHY L. p 1257 N92-17836
LUDWIG, F. A. p 1290 N92-17629
LUESSEN, LAWRENCE H. p 1293 N92-17831
LUM, VINCENT Y. p 1339 N92-17285
p 1383 N92-17402
LYLES, KEITH O. p 1282 N92-17441
LYNCH, NANCY p 1277 N92-17263

M

MACKIE, ROBERT R. p 1330 N92-17567
MACKO, JOSEPH A., JR. p 1330 N92-17712
MADARAS, ERIC I. p 1309 N92-17859
MADAY, J. H. p 1314 N92-17665
MADDEN, CRAIG J. p 1262 N92-17056
MAGNUSON, CHARLES p 1352 N92-17223
MAHAJAN, A. p 1378 N92-17916
MAHONY, TIMOTHY P. p 1315 N92-17008
MAIBACH, H. I. p 1330 N92-17714
MANHEIMER, WALLACE M. p 1369 N92-17499
MANN, DIANE K. p 1313 N92-17380
p 1314 N92-17551
p 1314 N92-17598
MAR, MARK H. p 1278 N92-16980
MARABLE, W. p 1303 N92-17127
MARCHELLO, JOSEPH M. p 1266 N92-17004
MARINELLI, W. J. p 1361 N92-17652
MARKER, TIMOTHY p 1226 N92-17149
MARRISON, C. p 1221 N92-17997
MARTIN, C. A. p 1223 N92-17281
MARTIN, PAUL A. p 1374 N92-17553
MARTIN, TIMOTHY p 1276 N92-16989
MARTIN, W. C. p 1369 N92-17456
MARTYNIUK, B. A. p 1291 N92-17702
MARYNICK, DENNIS S. p 1269 N92-17460
MASSMAN, DEAN A. p 1357 N92-17321
MASTERSON, R. J. p 1250 N92-17580
MATHIAS, JOHN P. p 1361 N92-17616
MATSUDA, Y. p 1364 N92-17876
MATSUO, HIDETO p 1257 N92-17816
MATSUSHIMA, MASAMICHI p 1257 N92-17869
MATTES, VICTOR R. p 1265 N92-17467
MATTHIES, LARRY H. p 1368 N92-17864
MAURIZI, SUSAN p 1370 N92-17556
MAX, N. L. p 1385 N92-17845
MAY, LEE R. p 1253 N92-17495
MAYER, J. W. p 1377 N92-17791
MAZZOCCA, AUGUSTUS D. p 1330 N92-17645
MCADIE, C. J. p 1321 N92-17621
MCBRINE, JOHN J. p 1330 N92-17645
MCCAFFREY, R. R. p 1274 N92-17935
MCCAULEY, HUGH W. p 1228 N92-17512
MCCLAY, C. P. p 1291 N92-17671
p 1291 N92-17672
MCCLELLAN, GENE E. p 1329 N92-17476
MCCLELLAND, JAMES L. p 1347 N92-16991
MCCLURE, MARK A. p 1236 N92-17096
MCCOLSKEY, J. D. p 1264 N92-17379
MCGOWAN, S. P. p 1316 N92-17239
MCHARDY, J. p 1290 N92-17629
MCHARG, MATTHEW G. p 1371 N92-17015
MCKEE, E. L. p 1369 N92-17456
MCLEAN, JOAN E. p 1336 N92-17720
MCMILLAN, B. K. p 1312 N92-17292
MCNEAR, ANDREW E. p 1346 N92-17507
MCVEY, B. D. p 1304 N92-17726
MEARS, C. A. p 1377 N92-17799
MECHELAY, JOSEPH E. p 1240 N92-16974
MEESON, REGINALD N. p 1337 N92-17068
MEISS, J. D. p 1378 N92-17324
MEISSNER, P. L. p 1376 N92-17781
MELROY, OWEN R. p 1262 N92-16985
p 1263 N92-17271
MELTON, DAVID W. p 1356 N92-17305
MELTZ, MARTIN L. p 1326 N92-17288
MENDENHALL, MARCUS p 1356 N92-17026
MERAY, G. M. p 1301 N92-17140
MEREDITH, B. D. p 1248 N92-17413
MERKEL, PHILIP A. p 1348 N92-17438
MERKLE, K. L. p 1376 N92-17782
MESSA, NORMAN C. p 1343 N92-17680
MEYRES, WILLIAM G. p 1334 N92-17569
MIHRAN, RICHARD T. p 1326 N92-17474
MILES, WILLIAM L. p 1228 N92-17512
MILLER, R. N. p 1250 N92-17580
MILLER, RICHARD L. p 1282 N92-17293
MINEI, M. K. p 1339 N92-17211
MINSTER, JEAN-BERNARD p 1316 N92-17202
MIRIYALA, SHRAVAN p 1269 N92-17262
MITCHELTREE, R. A. p 1294 N92-17002
MITTERER, K. F. p 1294 N92-17002
MIYANO, K. E. p 1376 N92-17781
MIZIOLEK, ANDRZEJ W. p 1303 N92-17137
MIZUMA, MITSUO p 1331 N92-17802
MOBILIA, J. p 1317 N92-17405

MOERNER, W. E. ..... p 1268 N92-17195
p 1356 N92-17196
p 1356 N92-17197
p 1271 N92-17659
p 1361 N92-17660
p 1271 N92-17661
MOES, TIMOTHY R. ..... p 1234 N92-17128
MOLINARI, R. L. ..... p 1319 N92-17138
MOLLERACH, SILVIA ..... p 1361 N92-17646
MONELL, DONALD W. ..... p 1244 N92-17112
MONTGOMERY, ALBERT G. ..... p 1291 N92-17672
MONTGOMERY, SANDY ..... p 1246 N92-17355
MONTOYA, R. J. ..... p 1234 N92-17221
MOORE, G. ..... p 1336 N92-17592
MOORE, JENNIFER L. ..... p 1250 N92-17430
MORAN, ANGELA L. ..... p 1262 N92-17056
MORENCY, ROGER L. ..... p 1367 N92-17828
MORO, AKIO ..... p 1385 N92-17787
MORRELL, FREDERICK R. ..... p 1219 N92-17984
MORRISON, CLYDE A. ..... p 1371 N92-16995
MORRISON, P. J. ..... p 1378 N92-17324
MORRISSEY, JAMES F. ..... p 1319 N92-17233
MORROW, DARRELL S. ..... p 1297 N92-17337
MOSS, J. E. ..... p 1235 N92-17552
MOULTON, N. E. ..... p 1375 N92-17685
MUELLER, CHRISTOPH ..... p 1224 N92-17311
MUELLER, R. ..... p 1304 N92-17526
MUKUNDA, H. S. ..... p 1223 N92-17131
MULGUND, SANDEEP S. ..... p 1221 N92-17996
MULLICK, SANJOY ..... p 1273 N92-17753
MUNGER, A. C. ..... p 1275 N92-17533
MURATORE, DEBRA ..... p 1249 N92-17419
MURGASH, L. ..... p 1266 N92-17808
MURPHY, MARIAN J. ..... p 1335 N92-17673
MURRAY-SMITH, DAVID J. ..... p 1230 N92-17154
p 1231 N92-17159
MURTHY, T. SREEKANTA ..... p 1309 N92-17033
MURUSIDZE, I. G. ..... p 1371 N92-17805
MUSGRAVE, J. A. ..... p 1261 N92-17727
MYERS, LEARY O. A. ..... p 1288 N92-17317
MYNES, M. S. ..... p 1338 N92-17118

N

NAHORY, R. E. ..... p 1374 N92-17528
NAIR, V. P. ..... p 1388 N92-17377
p 1388 N92-17697
NAKAMURA, SEIGO ..... p 1225 N92-17755
NAKONECHNY, BASIL V. ..... p 1385 N92-17141
NAMDAR, BAHMAN S. ..... p 1224 N92-17347
NAQWI, A. ..... p 1304 N92-17526
NARVAEZ, ADABELLE ..... p 1279 N92-17047
NASSIMBENE, RYAN D. ..... p 1295 N92-17018
NAZAROV, V. M. ..... p 1378 N92-17944
NEGANOV, B. S. ..... p 1293 N92-17825
NEGAST, WILLIAM J. ..... p 1228 N92-17481
NELSON, MICHAEL D. ..... p 1223 N92-17114
NESTEROV, V. ..... p 1292 N92-17801
NEUMANN, CHARLES J. ..... p 1321 N92-17705
NEWLANDER, C. D. ..... p 1256 N92-17053
NEWMASTER, JEFFREY T. ..... p 1302 N92-17826
NEWNAM, B. E. ..... p 1304 N92-17726
NEYER, B. T. ..... p 1276 N92-17624
NG, KAM W. ..... p 1297 N92-17398
NGUYEN, CHARLES C. ..... p 1252 N92-17150
NGUYEN, PHUC N. ..... p 1295 N92-17168
NICHOLSON, LEONARD S. ..... p 1240 N92-16973
p 1240 N92-16974
p 1241 N92-16975
p 1241 N92-17364
p 1242 N92-17534
NICOLAIDES, S. ..... p 1276 N92-17632
NIINO, MASAYUKI ..... p 1385 N92-17787
NIKITYUK, N. M. ..... p 1351 N92-17813
NILSEN, J. ..... p 1304 N92-17649
NINGELGEN, WILLI ..... p 1313 N92-17380
NOLAN, R. W. ..... p 1334 N92-17278
NORDHAUS, WILLIAM D. ..... p 1314 N92-17982
NOVISKEY, MICHAEL J. ..... p 1339 N92-17179
NOVOTNY, M. A. ..... p 1261 N92-17740
NUR, AMOS ..... p 1324 N92-17391

O

OBRIEN, DANIEL L. ..... p 1353 N92-17479
OBUKHOV, S. A. ..... p 1293 N92-17825
OCONNOR, WILLIAM P. ..... p 1324 N92-17539
OHBUCHI, RYUTAROU ..... p 1342 N92-17637
OKEEFE, A. ..... p 1234 N92-17011
OLIVIER, B. J. ..... p 1274 N92-17938
ONEILL, J. M., III ..... p 1301 N92-17140
ONO, TAKATSUGU ..... p 1237 N92-17917
ONSTOTT, R. G. ..... p 1312 N92-17459
ORIANS, GORDON H. ..... p 1314 N92-17982
ORWIG, L. E. ..... p 1389 N92-17048
OSHCHEPKOV, V. P. ..... p 1294 N92-17971
OSOFSKY, M. S. ..... p 1372 N92-17182
OSTDIEK, PAUL H. ..... p 1287 N92-17189
OSTROVSKIJ, A. O. ..... p 1285 N92-17812
OTT, RICHARD H. ..... p 1243 N92-17105
OYAN, CHEN ..... p 1311 N92-17511

P

PADFIELD, GARETH D. ..... p 1230 N92-17154
p 1231 N92-17162
p 1232 N92-17164
PAGE, C. D., JR. ..... p 1338 N92-17122
PALASZEWSKI, BRYAN A. ..... p 1253 N92-17151
PALEKAR, V. M. ..... p 1275 N92-17184
PALOMINOFONSECA, MIGUEL A. ..... p 1345 N92-17135
PAN, HONGJUN ..... p 1372 N92-17219
PANDA, S. ..... p 1379 N92-17807
PANDOLF, KENT B. ..... p 1329 N92-17473
PANTELL, R. H. ..... p 1361 N92-17608
PAO, L. Y. ..... p 1300 N92-17974
PARESCE, FRANCESCO ..... p 1386 N92-17021
PARK, J. C. ..... p 1318 N92-17027
PARK, JUNE S. ..... p 1346 N92-17425
PARKER, BRADFORD H. ..... p 1258 N92-17881
PARKER, L. W. ..... p 1311 N92-17208
PARROTT, ROB W. ..... p 1328 N92-17089
PASALA, KRISHNA M. ..... p 1350 N92-17330
PATRICK, J. ..... p 1336 N92-17592
PATTERSON, JAMES H., JR. ..... p 1326 N92-17269
p 1329 N92-17299
PAULES, GRANVILLE ..... p 1248 N92-17410
PAVLOV, B. IA. ..... p 1362 N92-17820
PAYNE, DAVID G. ..... p 1331 N92-17052
PAYNE, ROCHELLE D. ..... p 1262 N92-17056
PEACH, LEWIS L., JR. ..... p 1243 N92-17103
PEARLE, P. ..... p 1379 N92-17824
PEASE, R. F. ..... p 1286 N92-17087
PECHAN, M. J. ..... p 1263 N92-17319
PECK, ROBERT G. ..... p 1342 N92-17561
PEPIK, N. I. ..... p 1293 N92-17825
PEPIN, GERARD R. ..... p 1250 N92-17585
PERCEC, V. ..... p 1374 N92-17449
PERCEC, VIRGIL ..... p 1269 N92-17448
PEREZ, RAUL M. ..... p 1293 N92-17865
PERL, THOMAS D. ..... p 1279 N92-17062
PERRYMAN, D. C. ..... p 1319 N92-17338
p 1320 N92-17406
p 1320 N92-17492
p 1320 N92-17493
p 1320 N92-17494
PESCE-RODRIGUEZ, ROSE A. ..... p 1275 N92-17562
PETERS, LESLIE J. ..... p 1331 N92-17052
PETERSEN, ROBBIE ..... p 1391 N92-17372
PETETE, PATRICIA A. ..... p 1252 N92-17775
PETTIT, G. D. ..... p 1376 N92-17781
PFEFFER, RICHARD L. ..... p 1296 N92-17309
PFENDER, E. ..... p 1369 N92-17469
PFITZER, K. A. ..... p 1388 N92-17717
PHAM, H. ..... p 1345 N92-17969
PHAM, M. ..... p 1345 N92-17969
PHILBECK, THOMAS E., JR. ..... p 1287 N92-17216
PHILLABAUM, M. R. ..... p 1275 N92-17533
PIERENS, DAVID A. ..... p 1238 N92-17297
PIKE, JAMES F. ..... p 1307 N92-17677
PINELLI, THOMAS E. ..... p 1381 N92-17001
PINSKI, STEVEN D. ..... p 1367 N92-17736
PINTO, J. ..... p 1276 N92-17632
PINTO, JOSEPH F. ..... p 1304 N92-17627
PIPER, R. K. ..... p 1358 N92-17453
PLANTE, L. ..... p 1334 N92-17143
POE, C. C., JR. ..... p 1256 N92-17007
POLITZER, PETER ..... p 1356 N92-17038
POLL, D. I. A. ..... p 1226 N92-17849
p 1300 N92-17850
POMERANTZ, MARTIN ..... p 1269 N92-17460
PONZIO, STEPHEN J. ..... p 1345 N92-16997
POOLE-KOBER, EVELYN M. ..... p 1315 N92-17134
POPKOV, A. N. ..... p 1293 N92-17825
PORCHER, BRYAN ..... p 1245 N92-17350
POTAPCZUK, MARK G. ..... p 1224 N92-17347
POUND, BRUCE G. ..... p 1263 N92-17327
POWERS, LYNN M. ..... p 1267 N92-17060
PRAIRIE, MICHAEL W. ..... p 1375 N92-17618
PRASAD, LAKSHMAN ..... p 1300 N92-16983
PREEN, PHILIP J. ..... p 1287 N92-17216
PRESS, FRANK ..... p 1385 N92-17283
PRIME, KEVIN L. ..... p 1358 N92-17428
PRINS, JAN F. ..... p 1346 N92-17670
PRIOLO, F. J. ..... p 1225 N92-17446
PRITCHARD, DAVID E. ..... p 1357 N92-17374
PROTSENKO, N. A. ..... p 1348 N92-17819
p 1344 N92-17822
PROUDFOOT, PAUL M. ..... p 1286 N92-17076
PSIAKI, MARK L. ..... p 1222 N92-17999
PURSES, JOHN ..... p 1352 N92-17223
PURTSCHER, P. T. ..... p 1264 N92-17379
PUTNUM, SUSAN S. ..... p 1383 N92-17378

Q

QIU, YONG-JIAN ..... p 1269 N92-17461
QUARLES, GREGORY J. ..... p 1304 N92-17627
QUIRK, W. ..... p 1298 N92-17625

R

RABIN, B. H. ..... p 1274 N92-17842
RADEMAKERS, ALPHONSE ALOUIS ..... p 1359 N92-17519
RAJESHWAR, KRISHNAN ..... p 1269 N92-17460
RAMSEY, J. M. ..... p 1276 N92-17963
RAO, B. S. Y. ..... p 1302 N92-17926
p 1344 N92-17927
RAO, R. R. ..... p 1319 N92-17138
RAPP, ROBERT A. ..... p 1267 N92-17042
RAPPAPORT, E. N. ..... p 1321 N92-17621
RAWLINS, W. T. ..... p 1361 N92-17652
RAY, LAURA R. ..... p 1222 N92-18002
REDD, JUSTIN D. ..... p 1365 N92-17088
REED, R. P. ..... p 1264 N92-17379
REEVES, M. E. ..... p 1372 N92-17220
REHN, L. E. ..... p 1265 N92-17703
REID, CARLTON B., JR. ..... p 1357 N92-17306
REIN, D. H. ..... p 1295 N92-17025
REINKE, KIM ..... p 1338 N92-17122
REISER, BRIAN J. ..... p 1340 N92-17463
REJACK, MICHAEL D. ..... p 1315 N92-17094
REMELIUS, D. ..... p 1305 N92-17795
REMO, JOHN L. ..... p 1367 N92-17690
REYNOLDS, JOHN R. ..... p 1266 N92-16976
p 1269 N92-17460
p 1269 N92-17461
p 1271 N92-17679
REYZER, RONALD J. ..... p 1278 N92-16980
RICHARDSON, R. A. ..... p 1384 N92-17470
RICHIE, A. G. ..... p 1287 N92-17186
RICHTER, D. ..... p 1274 N92-17938
RICHTER, O. ..... p 1363 N92-17957
RICHWINE, D. D. ..... p 1284 N92-17689
RIVERA, SALVADOR, JR. ..... p 1234 N92-17240
ROBEY, FRANK C. ..... p 1279 N92-17040
ROBINETT, WARREN ..... p 1333 N92-17634
ROBINS, L. H. ..... p 1372 N92-17238
ROBINS, LAWRENCE H. ..... p 1268 N92-17170
p 1268 N92-17171
p 1271 N92-17615
ROCHOWIAK, DANIEL ..... p 1344 N92-17778
ROCKETT, THOMAS J. ..... p 1269 N92-17262
ROCKWAY, J. W. ..... p 1345 N92-17395
ROD, BERNARD J. ..... p 1288 N92-17326
RODIONOV, K. G. ..... p 1348 N92-17814
RODNEY, GEORGE A. ..... p 1387 N92-17873
RODRIGUEZ, GUILLERMO ..... p 1349 N92-17895
RODRIGUEZ, J. F. ..... p 1264 N92-17426
RODRIGUEZ, J. R. ..... p 1263 N92-17328
RODRIQUIZ, DAGOBERT ..... p 1368 N92-17863
ROESCH, ERIKA ..... p 1224 N92-17315
ROGERS, L. T. ..... p 1282 N92-17383
ROHAN, P. ..... p 1263 N92-17264
ROJAS, R. G. ..... p 1233 N92-17316
ROLLBUHLER, R. JAMES ..... p 1235 N92-17061
ROLLINGS, MARIAN P. ..... p 1238 N92-17287
ROPER, MARY L. ..... p 1330 N92-17645
ROSE, MILLARD F. ..... p 1293 N92-17831
ROSEN, A. ..... p 1292 N92-17708
ROSS, TIMOTHY D. ..... p 1339 N92-17179
ROUEN, M. ..... p 1246 N92-17354
ROUFF, CHRISTOPHER ..... p 1347 N92-16994
ROULET, ESTEBAN ..... p 1361 N92-17646
ROVERE, M. ..... p 1378 N92-17972
ROWE, NEIL C. ..... p 1340 N92-17403
ROWZEE, CHARLES A. ..... p 1302 N92-17918
ROYCE, WALKER ..... p 1337 N92-17064
ROYSTER, T. L., JR. ..... p 1254 N92-17270
RUDOLF, CARSTEN ..... p 1341 N92-17524
RUFENACH, C. L. ..... p 1312 N92-17459
RUIZ, JOSE P. ..... p 1266 N92-16976
RUMBLEY, DENNIS A. ..... p 1340 N92-17407
RUSSELL, L. C. ..... p 1345 N92-17395
RYANG, H. S. ..... p 1268 N92-17191

S

SABOL, BRUCE ..... p 1234 N92-17240
SACI, R. ..... p 1300 N92-17851
SAHA, ABHIJIT ..... p 1387 N92-17650

SAITOH, TAKASHI p 1236 N92-17855
SALANT, RICHARD F. p 1306 N92-17304
SALOMON, MAJ ROY p 1314 N92-17598
SAMANT, M. G. p 1372 N92-17181
SAMANT, MAHESH G. p 1263 N92-17271
SAMPAIR, THOMAS p 1241 N92-17335
SAMUEL, ARTHUR G. p 1332 N92-17503
SANT, ANDREW J. p 1366 N92-17485
SANTILLI, R. M. p 1379 N92-17531
SANVILLE, C. Y. p 1255 N92-17867
SARIKAYA, MEHMET p 1267 N92-17054
SATHER, DUANE P. p 1297 N92-17447
SAUCILLO, R. J. p 1248 N92-17413
SAUER, KEN p 1280 N92-17139
SAUNDERS, K. D. p 1325 N92-17766
SAVELY, ROBERT T. p 1246 N92-17352
SAWADA, HIDEO p 1225 N92-17755
SAWKA, MICHAEL N. p 1329 N92-17473
SCARBOROUGH, W. K. p 1363 N92-17590
SCARZELLO, JOHN F. p 1368 N92-17959
SCHAEFER, D. W. p 1274 N92-17938
SCHALCH, DIRK D. p 1337 N92-17922
SCHARNHORST, KURT P. p 1310 N92-17320
SCHAUB, S. A. p 1330 N92-17714
SCHEICK, J. T. p 1233 N92-17316
SCHERTZ, W. W. p 1255 N92-17867
SCHMID, WALTHER p 1358 N92-17428
SCHMITT, M. J. p 1304 N92-17726
SCHNEIDER, WALTER p 1348 N92-17457
p 1332 N92-17458
SCHOENBERG, JON S. p 1291 N92-17684
SCHOMER, PAUL D. p 1355 N92-17506
SCHUBERT, RUDOLF p 1278 N92-17780
SCHUDLICH, REBECCA R. p 1324 N92-17583
SCHWARTZ, MISCHA p 1381 N92-17952
SCHWARTZ, R. A. p 1389 N92-17048
SCOTT, G. p 1226 N92-17874
SCOTT, J. C. p 1271 N92-17661
SCOTT, ROBERT W. p 1321 N92-17975
p 1322 N92-17977
SEATON, ROBERT L. p 1265 N92-17759
SECAN, JAMES A. p 1316 N92-17209
SEDLACEK, Z. p 1371 N92-17806
SEGALMAN, D. p 1272 N92-17710
SEIDEL, HELMUT p 1261 N92-17841
SEIFERT, A. p 1299 N92-17719
SEIFFERT, STEPHEN p 1278 N92-17780
SELDIN, J. H. p 1366 N92-17550
SEMPLE, J. p 1345 N92-17960
SERAYDARIAN, R. P. p 1369 N92-17456
SEROT, B. D. p 1362 N92-17789
SETO, CHRISTOPHER T. p 1358 N92-17428
p 1359 N92-17491
p 1361 N92-17616
SHACKELFORD, DOUGLAS E. p 1380 N92-17651
SHAFER, B. P. p 1265 N92-17579
SHAFFER, GARY p 1228 N92-17147
SHAHINPOOR, M. p 1272 N92-17710
SHALLCROSS, F. V. p 1301 N92-17140
SHAVER, A. R. p 1389 N92-17048
SHAW, ARNAB K. p 1291 N92-17654
SHAW, D. T. p 1307 N92-17604
SHAW, DORIS S. p 1343 N92-17716
SHAW, FREDERICK J. p 1275 N92-17562
SHCHEGOLEV, V. A. p 1266 N92-17808
SHEALY, JAMES R. p 1371 N92-16984
SHEARER, V. p 1334 N92-17143
SHECHTMAN, D. p 1372 N92-17238
p 1373 N92-17322
SHEDDEN, JUDITH M. p 1348 N92-17457
SHEEN, J. A. p 1302 N92-17926
SHEN, HAO-MING p 1288 N92-17268
SHENDEROVSKII, V. A. p 1291 N92-17702
SHERMAN, JOHN D. p 1302 N92-17918
SHI, WEN F. p 1228 N92-17147
SHIHO, TORU p 1239 N92-17854
SHIMODAIRA, KAZUO p 1236 N92-17855
SHING, MAN-TAK p 1340 N92-17403
SHIPLEY, BUFORD W., JR. p 1239 N92-17730
SHIROUZU, MASAO p 1251 N92-17754
SHOWALTER, RALPH E. p 1350 N92-17445
SHRUBOVICH, E. V. p 1375 N92-17701
SHUCHMAN, R. A. p 1312 N92-17459
SHULGA, S. Z. p 1375 N92-17701
SICONOLFI, STEVEN F. p 1330 N92-17645
SIGMAN, MATTHEW S. p 1273 N92-17751
SILVESTROV, L. V. p 1357 N92-17408
SIMMERS, JEFFREY A. p 1337 N92-17023
SIMMONS, ANNE p 1370 N92-17556
SIMMS, D. p 1226 N92-17874
SIMO, CONSTANCE p 1227 N92-17259
SIMON, N. J. p 1264 N92-17379
SIMONICH, JOHN C. p 1236 N92-17243
SIMPSON, B. M. p 1274 N92-17935
SIMPSON, R. L. p 1223 N92-17117
p 1223 N92-17222
SIMPSON, ROBERT W. p 1219 N92-17985
SIMPSON, THOMAS B. p 1286 N92-17017
SINGH, JAG J. p 1267 N92-17032
SINGH, JASPRIT p 1365 N92-17044
SINGH, SANJIV p 1303 N92-17080
p 1228 N92-17147
SINGPURWALLA, NOZER D. p 1308 N92-17231
SKELTON, E. F. p 1375 N92-17685
SKIDMORE, TRENT A. p 1221 N92-17993
SKLAR, MIKE p 1250 N92-17422
SLIVSARENKO, S. S. p 1377 N92-17821
SMALL, JAMES F. p 1224 N92-17339
SMIT, K. J. p 1275 N92-17058
SMITH, ADRIAN F. p 1352 N92-17178
p 1353 N92-17643
SMITH, ALVIN p 1389 N92-17123
SMITH, BRADLEY J. p 1296 N92-17307
SMITH, JOHN B. p 1380 N92-17651
SMITH, P. M. p 1323 N92-17041
SMITH, RANDY A. p 1310 N92-17230
SNYDER, DAVID p 1252 N92-17772
SNYDER, GREGORY D. p 1334 N92-17617
SOARES, STEVEN p 1291 N92-17671
SOLIMAN, AL-AMRO p 1281 N92-17252
SOLOMON, FREDRIC p 1365 N92-17146
SOLOWAY, DONALD I. p 1347 N92-16987
SON, S. H. p 1342 N92-17636
SORENSEN, L. B. p 1372 N92-17181
SORKIN, ROBERT D. p 1332 N92-17336
SPARKS, J. SCOTT p 1257 N92-17870
SPEAR, GUY B. p 1257 N92-17836
SPENCER, MICHAEL G. p 1288 N92-17317
SPICER, W. E. p 1376 N92-17781
SPINDT, C. J. p 1376 N92-17781
SPIROV, V. S. p 1299 N92-17810
SPREITER, JOHN R. p 1235 N92-17644
SPRINGMEYER, R. R. p 1385 N92-17845
SQUIRES, WILLIAM p 1328 N92-17022
SRIDHARAN, GOVIND p 1293 N92-17907
ST.CLAIR, TERRY L. p 1267 N92-17032
ST.JOHN, RALPH J. p 1338 N92-17093
STABILE, P. J. p 1292 N92-17708
STACHIW, J. D. p 1274 N92-17947
STAHARA, STEPHEN S. p 1235 N92-17644
STALEY, JAMES T. p 1267 N92-17054
STANLEY, DALE A. p 1285 N92-17737
STARLINGER, ALOIS p 1267 N92-17060
STAVINOHA, LEO L. p 1275 N92-17066
STENGEL, ROBERT F. p 1221 N92-17995
p 1222 N92-17999
p 1222 N92-18000
p 1222 N92-18001
p 1222 N92-18002
STEPHENS, M. A. p 1352 N92-17173
STEPHENS, ROBERT L. p 1328 N92-17084
STEPIN, A. I. p 1309 N92-17809
STERLINSKI, SL. p 1378 N92-17944
STERN, S. A. p 1274 N92-17942
STERN, THOMAS E. p 1381 N92-17952
STERNBERG, SAUL p 1384 N92-17785
STERRETT, A. E. p 1339 N92-17211
STEVENS, SALLY B. p 1371 N92-16995
STEVENSON, STEVEN M. p 1249 N92-17416
STEVENSON, T. N. p 1300 N92-17974
STEWART, CAROLINE B. p 1310 N92-17333
STEWART, LYNNE M. p 1308 N92-17005
STILLE, J. K. p 1272 N92-17745
STONE, LEWIS W. p 1328 N92-17084
STONE, M. L. p 1274 N92-17935
STONE, MARK H., JR. p 1381 N92-17687
STOREY, L. R. O. p 1387 N92-17694
STRADLING, G. L. p 1265 N92-17579
STRATER, JAY W. p 1280 N92-17187
STRATTON, SUZANNE R. p 1283 N92-17571
STREED, DANIEL H. p 1320 N92-17515
STRELKOV, A. V. p 1363 N92-17955
STROEKS, ALEXANDER ANTONIUS MARIE p 1273 N92-17840
STUART, THOMAS A. p 1253 N92-17510
STUBENRAUCH, CARL F. p 1282 N92-17429
STURGE, M. D. p 1374 N92-17528
STURM, MATTHEW p 1312 N92-17715
SUAREZ, PEDRO F. p 1280 N92-17090
SUDO, TAKAYUKI p 1385 N92-17787
SUJIWO p 1290 N92-17573
SULLIVAN, DAVID p 1333 N92-17014
p 1334 N92-17331
SUN, XIAOLI p 1303 N92-17152
SUNDERLAND, J. E. p 1313 N92-17577
SUPERFINE, R. p 1360 N92-17530
SURESH, RAMASUBRAMANIAN p 1234 N92-17221
SUZUKI, ANDREW H. p 1348 N92-17767
SUZUKI, KOICHI p 1225 N92-17755
SVEJKOVSKY, PAUL A. p 1307 N92-17872
SWANSON, MAX L. p 1267 N92-17065
SWANSON, THEODORE D. p 1300 N92-17887
SWIFT, GERALD A. p 1306 N92-17024
SWITZER, D. W. p 1373 N92-17375
SWOBODA, C. p 1336 N92-17592
SZE, K. Y. p 1233 N92-17316
SZWEDO, EDWARD J. p 1382 N92-17174

T

TACHAU, R. D. M. p 1311 N92-17937
TAFF, LARRY p 1386 N92-17020
TAI, BETTY P. p 1308 N92-17005
TAIT, C. D. p 1261 N92-17727
TAKHTAMYSHEV, G. G. p 1357 N92-17408
TAMARGO, M. C. p 1374 N92-17528
TAMARU, TAKASHI p 1236 N92-17855
TANABE, YOSHIKAZU p 1278 N92-17757
TANG, C. M. p 1303 N92-17127
TANNER, J. E. p 1358 N92-17453
TARAJI, HOMA p 1343 N92-17640
TARANENKO, L. V. p 1348 N92-17819
p 1344 N92-17822
TATE, RALPH F. p 1362 N92-17663
TAYLOR, D. H. p 1325 N92-17121
TAYLOR, TIMOTHY N. p 1339 N92-17179
TENNYSON, J. p 1378 N92-17324
TERAZAWA, HIDEZUMI p 1379 N92-17817
TEREKHOV, G. I. p 1363 N92-17955
TERENIK, L. V. p 1299 N92-17810
THAYER, F. J. p 1350 N92-17206
THEYE, LONNIE A. p 1278 N92-17780
THIEL, R. D. p 1266 N92-17858
THIELE, G. A. p 1284 N92-17689
THIESSEN, H. A. p 1364 N92-17794
THOMPSON, ANDREW A., III p 1352 N92-17384
THOMPSON, TIM L. p 1259 N92-17091
THORNTON, WILLIAM E. p 1335 N92-17910
THRESHER, R. W. p 1313 N92-17875
TIEDERMAN, WILLIAM G. p 1296 N92-17176
TIERNEY, J. W. p 1275 N92-17184
TISCHLER, MARK B. p 1231 N92-17158
p 1232 N92-17165
p 1232 N92-17166
TKACH, YU. V. p 1285 N92-17812
TOLBERT, A. K. p 1389 N92-17048
TOLK, NORMAN H. p 1356 N92-17026
TOMAZOS, D. p 1374 N92-17449
TONEY, M. F. p 1372 N92-17181
TONEY, MICHAEL F. p 1262 N92-16985
p 1263 N92-17271
TOPLIKAR, EDWARD G. p 1272 N92-17749
p 1272 N92-17750
TOSI, M. P. p 1378 N92-17972
TOUGH, R. J. p 1365 N92-17180
TOVEY, CRAIG A. p 1352 N92-17440
TRACY, DAN E. p 1323 N92-17051
TRAJDOS, M. p 1363 N92-17956
TREFNY, CHARLES J. p 1235 N92-17546
TRETYAKOV, YU. P. p 1364 N92-17973
TRUDINGER, PETER L. p 1288 N92-17295
TRUONG, T. p 1310 N92-17254
TRYK, DONALD A. p 1253 N92-17365
TSAI, TENLIN p 1255 N92-17867
TSINTSADZE, L. N. p 1371 N92-17805
TSUJIMOTO, TADASHI p 1331 N92-17802
TSUKANO, YUKICHI p 1237 N92-17917
TSUNODA, ROLAND T. p 1283 N92-17600
TUCKER, DENNIS S. p 1257 N92-17870
TUCKER, WAYNE C. p 1269 N92-17262
TUNNICLIFFE, PETER A. p 1324 N92-17169
TURNER, JOYCE E. p 1384 N92-17586
TURNER, TIMOTHY L. p 1234 N92-17221
TURRENTINE, GEORGE p 1329 N92-17299
TURRENTINE, GEORGE A. p 1326 N92-17269
TURRO, NICHOLAS J. p 1258 N92-16977
TUTTLE, B. A. p 1377 N92-17790
TYRONE, BOOKER H., JR. p 1286 N92-17116

U

UBEROI, C. p 1371 N92-17806
UDELHOFEN, PETRO MARIA p 1317 N92-17542
UHLMANN, D. R. p 1272 N92-17745
UHM, HAN S. p 1358 N92-17462
p 1260 N92-17628
UNGER, SHAARI M. p 1323 N92-17078
UPSCHULTE, B. L. p 1361 N92-17652

V

VALLEE, DAVID R. p 1319 N92-17363
VANBLARICUM, VICKI L. p 1338 N92-17122
VANDERAH, T. A. p 1372 N92-17182
p 1372 N92-17219
p 1372 N92-17220
p 1365 N92-17284

VANDERAH, TERRELL A. ..... p 1372 N92-17218
VANDERLUGT, A. ..... p 1340 N92-17286
VANDEVELDE, STEVEN LEENDERT
p 1353 N92-17839
VANDIJK, ADRIAAN LOUIS ..... p 1360 N92-17520
VANGRAAS, FRANK ..... p 1221 N92-17992
p 1221 N92-17994
VANGRASS, FRANK ..... p 1281 N92-17244
VANLANGEVELDE, HUIB JAN .... p 1390 N92-18004
VANLARE, CORNELIS ELISABETH JOHANNES
p 1298 N92-17522
VANOLDENBORGH, GEERT JAN p 1359 N92-17518
VANONSELEN, KYRA ..... p 1312 N92-17436
VARDENY, Z. V. ..... p 1274 N92-17966
VARNUM, KENT C. ..... p 1364 N92-16981
VARSHNEY, AMITABH ..... p 1346 N92-17638
VASNETSOV, M. V. ..... p 1377 N92-17821
VAUGHAN, ARTHUR H. ..... p 1368 N92-17892
VAVASIS, STEVEN A. ..... p 1347 N92-17049
VEERASINGAM, R. ..... p 1371 N92-17933
VEKSHINA, V. S. ..... p 1293 N92-17825
VENANZI, CAROL A. ..... p 1255 N92-17329
VIEBROCK, HERBERT J. ..... p 1315 N92-17134
VIG, JOHN R. ..... p 1281 N92-17258
VILLANI, T. S. ..... p 1301 N92-17140
VILLERE, MONTY P. ..... p 1293 N92-17831
VILSMEIER, J. ..... p 1256 N92-17310
VOGEN, GEORGE S. ..... p 1328 N92-17120
VOIGT, G.-H. ..... p 1316 N92-17227
VOSS, H. D. ..... p 1317 N92-17405
VOSS, R. ..... p 1261 N92-17841
VOURAZELIS, DIMITRIOS G. ..... p 1313 N92-17424
VRBANCICH, JULIAN ..... p 1288 N92-17291

W

WACHTEL, HOWARD ..... p 1326 N92-17474
WAGGONER, PAUL E. ..... p 1314 N92-17982
WAGNER, LEE R. ..... p 1355 N92-17506
WALECKA, J. D. ..... p 1362 N92-17789
WALKER, CHARLES G., JR. ..... p 1382 N92-17067
WALKER, D. A. ..... p 1223 N92-17117
WALL, H. G. ..... p 1255 N92-17373
WALLACE, H. B. ..... p 1283 N92-17571
WALSH, C. ..... p 1271 N92-17661
WALSH, C. A. ..... p 1268 N92-17195
WALSH, J. M. ..... p 1265 N92-17579
WALSH, R. P. ..... p 1264 N92-17379
WALTON, JOANNE C. ..... p 1279 N92-17062
WALTON, M. ..... p 1313 N92-17934
WALTON, MARLEI ..... p 1328 N92-17022
WANG, IUI ..... p 1344 N92-17860
WANG, SHYH ..... p 1374 N92-17594
WANG, TE-KANG ..... p 1262 N92-17000
WANG, Z. L. ..... p 1360 N92-17574
WANGLER, T. P. ..... p 1364 N92-17796
WANKE, CRAIG ..... p 1220 N92-17988
p 1220 N92-17989
WARD, REEDER N. ..... p 1340 N92-17286
WARDLAW, A. B., JR. ..... p 1225 N92-17446
WARNER, K. ..... p 1287 N92-17186
WARREN, L. F. ..... p 1268 N92-17191
WARREN, R. W. ..... p 1304 N92-17726
WARREN, RICHARD M. ..... p 1355 N92-17502
WASHBURN, ANTHONY EUGENE
p 1225 N92-17681
WASIELEWSKI, M. R. ..... p 1326 N92-17471
WATKINS, RICHARD ..... p 1388 N92-17696
WEATHERSBY, P. K. ..... p 1328 N92-17124
WEAVER, M. J. ..... p 1358 N92-17472
WEBSTER, JULIE L. ..... p 1343 N92-17716
WEDDENDORF, BRUCE ..... p 1335 N92-17866
WEGRZYN, J. E. ..... p 1307 N92-17604
WEIMER, L. ..... p 1339 N92-17185
WEINBERG, ERICK J. ..... p 1388 N92-17377
p 1388 N92-17697
WEINRACH, JEFFREY ..... p 1278 N92-17780
WEITZMAN, PETER S. ..... p 1291 N92-17671
WELCH, JAMES F. ..... p 1295 N92-17018
WENDER, I. ..... p 1275 N92-17184
WENTZ, WILLIAM H. ..... p 1227 N92-17587
WENZEL, R. ..... p 1305 N92-17795
WEST, JAY ..... p 1303 N92-17080
WHINNERY, JAMES E. ..... p 1334 N92-17432
WHITE, D. H. ..... p 1362 N92-17666
p 1364 N92-17794
WHITE, RICHARD L. ..... p 1386 N92-17497
WHITESIDES, GEORGE M. ..... p 1260 N92-17389
p 1264 N92-17427
p 1289 N92-17490
p 1359 N92-17491
p 1361 N92-17616
WHITMORE, STEPHEN A. ..... p 1234 N92-17128
WHITTEN, W. B. ..... p 1276 N92-17963
WIEGAND, D. A. ..... p 1276 N92-17632
WIELAND, PAUL ..... p 1246 N92-17355
WIESELTHIER, JEFFREY E. ..... p 1286 N92-17931
WIESLER, D. G. ..... p 1372 N92-17181
WIGHTMAN, FREDERIC L. ..... p 1355 N92-17692
WILKERSON, J. F. ..... p 1389 N92-17201
p 1390 N92-17883
WILLHELM, JOSEPH A., JR. ..... p 1287 N92-17205
WILLIAMS, J. G. ..... p 1257 N92-17611
WILLIAMS, ROBERT M. ..... p 1342 N92-17561
WILLIAMS, WYMAN ..... p 1279 N92-17046
WILLIS, DONALD J. ..... p 1338 N92-17077
WILSON, CHUCK ..... p 1313 N92-17393
WINELAND, D. J. ..... p 1360 N92-17549
p 1370 N92-17635
WINSTEAD, CURTIS M. ..... p 1336 N92-17744
WISSLER, JOHN B. ..... p 1367 N92-17658
WITKOWSKI, W. ..... p 1272 N92-17710
WITTMANN, RONALD C. ..... p 1282 N92-17429
WOLF, S. A. ..... p 1372 N92-17220
p 1375 N92-17685
WOLF, STUART A. ..... p 1372 N92-17218
WOLLRATH, ANN M. ..... p 1345 N92-17188
WOOD, RICHARD M. ..... p 1300 N92-17888
p 1300 N92-17909
WOODALL, J. M. ..... p 1376 N92-17781
WOODS, C. M. ..... p 1275 N92-17533
WOODWARD, A. M. ..... p 1361 N92-17652
WOOLF, STANLEY ..... p 1359 N92-17514
WORK, PAUL R. ..... p 1284 N92-17721
WRIGHT, JONATHAN C. ..... p 1387 N92-17920
WRIGHT, MICHAEL E. ..... p 1272 N92-17749
p 1272 N92-17750
p 1273 N92-17751
p 1273 N92-17752
p 1273 N92-17753
WRIGHT, STEVEN R. ..... p 1233 N92-17300
WU, TAI T. ..... p 1288 N92-17268
WU, TAI TSUN ..... p 1364 N92-17964
WUN-FOGLE, M. ..... p 1381 N92-17940
WYGNANSKI, I. ..... p 1299 N92-17719
WYLIE, DENNIS C. ..... p 1330 N92-17567
WYNNE, ELEANOR C. ..... p 1225 N92-17509

X

XIE, MING ..... p 1305 N92-17936
XIONG, JINCHENG ..... p 1354 N92-17823

Y

YAKOVLEV, V. A. ..... p 1259 N92-17248
p 1259 N92-17261
p 1260 N92-17613
YAMADA, HIDESHI ..... p 1236 N92-17855
YAMADA, M. ..... p 1376 N92-17781
YAMAGUCHI, K. ..... p 1220 N92-17987
YANG, DER-SHUNG ..... p 1343 N92-17716
YANG, ZHONGGUO ..... p 1354 N92-17823
YEAGER, E. ..... p 1253 N92-17365
p 1260 N92-17489
YEE, D. ..... p 1372 N92-17181
YETZBACHER, MARILYN R. ..... p 1295 N92-17018
YOST, F. G. ..... p 1363 N92-17739
YOUNG, NOLAN B. ..... p 1229 N92-17639
YOUNGBLUT, CHRISTINE ..... p 1337 N92-17068
YU, JOHN ..... p 1279 N92-17062
YUSHKOV, B. YU. ..... p 1354 N92-17811

Z

ZAJAC, K. ..... p 1363 N92-17956
ZAMORA, R. J. ..... p 1318 N92-17072
ZELLER, EDWARD J. ..... p 1389 N92-17235
ZELLER, P. ..... p 1304 N92-17526
ZELLMER, MILTON ..... p 1391 N92-17079
ZERKOWSKI, JONATHAN A. ..... p 1359 N92-17491
ZERNIC, MICHAEL J. ..... p 1251 N92-17770
p 1251 N92-17771
ZHANG, NA ..... p 1376 N92-17782
ZHANG, YING ..... p 1321 N92-17543
ZHIDKOV, E. P. ..... p 1354 N92-17811
ZHUKOV, V. A. ..... p 1294 N92-17953
ZIMMERMAN, WAYNE ..... p 1247 N92-17359
p 1247 N92-17360

Typical Corporate Source Index Listing

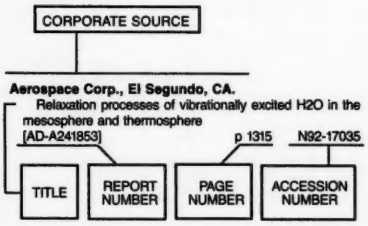

Listings in this index are arranged alphabetically by corporate source. The title of the document provides the user with a brief description of the subject matter. The report number helps to indicate the type of document cited (e.g., NASA report, translation, NASA contractor report). The accession number denotes the number by which the citation is identified. The page number helps you locate the citation in the abstract section. The titles are arranged under each corporate source in ascending accession number order.

A

ACADEMY OF SCIENCES OF THE UKRAINIAN SSR, KHARKOV.

Effects of the high-frequency beam space charge forces on the excitation of electromagnetic waves in relativistic carcinotron
| DE92-610956 | p 1285 N92-17812

ACADEMY OF SCIENCES OF THE UKRAINIAN SSR, KIEV.

An algorithm for calculating the electronic spectrum and function of the charge density distributions of crystals
p 1375 N92-17698

Consistency and integrability of Navier-Stokes and systems of equations for incompressible flow magnetohydrodynamics p 1298 N92-17699

Radiation effects in High Temperature Superconductors (HTSC) oxides p 1375 N92-17700

The EPR of the triplet state of aryl cations in crystals of diazonium salts p 1375 N92-17701

Electrical and thermal conductivity of a variable zone semiconductor in a longitudinal magnetic field
p 1291 N92-17702

Ion sources based on electron cyclotron resonance
p 1362 N92-17743

Ionic physics and technology p 1362 N92-17818

Computer modelling of two-input neural-net learning
p 1348 N92-17819

High frequency sources of ions for ion technology
p 1362 N92-17820

Optical turbulence in second harmonic generation
p 1377 N92-17821

Algorithm and Pascal: A program for neural net learning p 1344 N92-17822

ADVISORY GROUP FOR AEROSPACE RESEARCH AND DEVELOPMENT, NEUILLY-SUR-SEINE (FRANCE).

Rotorcraft System Identification
| AGARD-LS-178 | p 1230 N92-17153

Calendar of selected aeronautical and space meetings, July 1990 onwards
| AGARD-CAL-90/2 | p 1380 N92-17198

Calendar of selected aeronautical and space meetings, January 1992 and onwards
| AGARD-CAL-92/1 | p 1380 N92-17212

Technical evaluation report on the 52nd Symposium on Software for Guidance and Control
| AGARD-AR-302 | p 1341 N92-17498

AEROJET-GENERAL CORP., SACRAMENTO, CA.

Transpiration cooled throat for hydrocarbon rocket engines
| NASA-CR-184272 | p 1253 N92-17495

AEROMET, INC., TULSA, OK.

Radio frequency hazard monitoring-USAKA
| AD-A242873 | p 1283 N92-17563

AERONAUTICAL RESEARCH LABS., MELBOURNE (AUSTRALIA).

Modification of Jindivik air intake duct with an auxiliary intake static aerodynamic tests
| AD-A243002 | p 1232 N92-17234

Determination of symmetric end loads from bulk stresses on a rectangular prism
| AD-A242973 | p 1310 N92-17254

Metallography of aluminide coatings
| AD-A243000 | p 1263 N92-17264

Determination of antisymmetric end loads from bulk stresses on a rectangular prism
| AD-A243001 | p 1310 N92-17265

Wind loads on a mirage III O aircraft mounted above a ground plane
| AD-A243004 | p 1232 N92-17266

The conversion of a FORTRAN data plotting program using DI-3000 graphics to operation on a Macintosh Personal Computer
| AD-A243046 | p 1339 N92-17280

Surface pressure measurements on the wing of a wind tunnel model during steady rotation
| AD-A243047 | p 1223 N92-17281

Stagnation and dynamic pressure limits for the S1 wind tunnel
| AD-A242989 | p 1238 N92-17297

General requirements and techniques for component fatigue life substantiation in Australian service helicopters
| AD-A242881 | p 1233 N92-17565

AEROSPACE CORP., EL SEGUNDO, CA.

Relaxation processes of vibrationally excited H2O in the mesosphere and thermosphere
| AD-A241853 | p 1315 N92-17035

Case bond liner systems for solid rocket motors
| AD-A242297 | p 1253 N92-17085

Contractor software engineering environment evaluations summary report
| AD-A242330 | p 1343 N92-17640

AIR FORCE ACADEMY, CO.

Critical temperature determination in superconductors
| AD-A243537 | p 1371 N92-17015

Comparison of station-keeping algorithms for an interior libration point orbit in the Sun-Earth + Moon elliptic restricted three-body problem
| AD-A241896 | p 1388 N92-17595

AIR FORCE ENVIRONMENTAL TECHNICAL APPLICATIONS CENTER, SCOTT AFB, IL.

Surface observation climatic summaries for Duke Field/Eglin aux no. 3, Florida
| AD-A243310 | p 1318 N92-17073

Surface observation climatic summaries for Castle AFB, California
| AD-A243677 | p 1318 N92-17074

Range reference atmosphere, Fairbanks
| AD-A243314 | p 1318 N92-17113

Surface observation climatic summaries for Hondo Municipal Airport, Texas
| AD-A243311 | p 1319 N92-17144

Surface observation climatic summaries for Boise Air Terminal, ID
| AD-A243012 | p 1319 N92-17257

Surface observation climatic summaries for Fairbanks IAP, Alaska
| AD-A243309 | p 1320 N92-17400

Comparison of two eighth-mesh terrain databases
| AD-A243315 | p 1383 N92-17401

Surface observations climatic summaries for Camp Humphreys, Korea
| AD-A241937 | p 1320 N92-17444

AIR FORCE INST. OF TECH., WRIGHT-PATTERSON AFB, OH.

A topological model for parallel algorithm design
| AD-A241858 | p 1337 N92-17023

Model identification and control system design for the lambda unmanned research vehicle
| AD-A241859 | p 1306 N92-17024

Design and testing of a lightweight, planar microwave lens
| AD-A243685 | p 1286 N92-17076

Feature extraction for pose estimation: A comparison between synthetic and real IR imagery
| AD-A243699 | p 1338 N92-17077

Design of a fiber optic image transmission link
| AD-A243686 | p 1365 N92-17088

Evaluation of scalar value estimation techniques for 3D medical imaging
| AD-A243687 | p 1328 N92-17089

Face recognition with the Karhunen-Loeve transform
| AD-A243688 | p 1280 N92-17090

Vibrational energy transfer in bromine monofluoride
| AD-A243690 | p 1259 N92-17091

A rigorous UTD analysis of electromagnetic scattering from resistive strips and resistive-loaded conducting strips
| AD-A243691 | p 1280 N92-17092

Image analysis using Gabor transforms: Correlated with human saccadic movement data to identify the human visual search strategy
| AD-A243692 | p 1338 N92-17093

Sensing refractive turbulence profiles using wave front slope measurements from two reference sources
| AD-A243696 | p 1315 N92-17094

Determination of bistatic radar clutter power from topographic data
| AD-A243697 | p 1280 N92-17095

Development of high angle of attack control laws for an unstable, non-minimum phase aircraft using variations of the quantitative feedback technique
| AD-A243698 | p 1236 N92-17096

Implementation of an object-oriented flight simulator D.C. electrical system on a hypercube architecture
| AD-A243700 | p 1238 N92-17097

An experimental investigation of leading edge vortical flow about a delta wing during wing rock
| AD-A243363 | p 1223 N92-17114

Neural network classification of mental workload conditions by analysis of spontaneous electroencephalograms
| AD-A243369 | p 1331 N92-17115

The analysis of a stabilized 1.5 Mach-Zehnder interferometric sensor with enhanced sensitivity and common-mode compensation
| AD-A243384 | p 1286 N92-17116

A convergent aspiration based interior point method (CAIN) for Multiple Objective Linear Programming (MOLP)
| AD-A243404 | p 1338 N92-17118

A topographical analysis of the human electroencephalogram for patterns in the development of motion sickness
| AD-A243656 | p 1328 N92-17120

Rapid nonconjugate adaptation of vertical voluntary pursuit eye movements
| AD-A243358 | p 1331 N92-17145

Integration of an anti-parallel pair of planar Schottky barrier diodes for millimeter and submillimeter wavelengths
| AD-A243371 | p 1287 N92-17189

The effects of storage on irradiated red blood cells: An in vitro an in vivo study
| AD-A243387 | p 1329 N92-17190

Influence of knee joint extension on submaximal oxygen consumption and anaerobic power in cyclists
| AD-A243467 | p 1329 N92-17194

Higher-order thickness expansions for cylindrical shells
| AD-A242017 | p 1310 N92-17230
An aerocapture attitude control systems incorporating robustness and vehicle parameter identification
| AD-A243360 | p 1245 N92-17302
Collisional dynamics of the B3Pi(O +) state of bromine of monofluoride
| AD-A241857 | p 1356 N92-17305
Quenching and rotational energy transfer in molecular bromine: Br2(B)
| AD-A241987 | p 1357 N92-17321
Application of silicon micromachining to thermal dissipation issues in wafer scale integrated circuits
| AD-A243744 | p 1288 N92-17332
Design of Style-V: A translator to convert standard VHDL into a stylized form for automated microcode generation
| AD-A243706 | p 1340 N92-17407
A computer solution for multiple satellite-satellite and satellite-ground station visibility determination
| AD-A243490 | p 1250 N92-17430
Incipient fault detection using higher-order statistics
| AD-A243493 | p 1308 N92-17431
Preliminary design of a model to assess the effect of Space Surveillance Network (SSN) sensor upgrades on orbit prediction accuracies relative to the US Anti-Satellite (ASAT) mission
| AD-A243736 | p 1353 N92-17479
Global optimization of digital circuits
| AD-A243740 | p 1289 N92-17480
Incorporation of differential global positioning system measurements using an extended Kalman filter for improved reference system performance
| AD-A243742 | p 1228 N92-17481
An object-oriented database implementation of the Magic VLSI Layout Design System
| AD-A243743 | p 1384 N92-17482
Analysis of visual illusions using multiresolution wavelet decomposition based models
| AD-A243712 | p 1332 N92-17500
Evaluation of an Interdigitated Gate Electrode Field-Effect Transistor (IGEFET) for in situ resin cure monitoring
| AD-A243713 | p 1289 N92-17501
Improved task scheduling for parallel simulations
| AD-A243721 | p 1346 N92-17507
Comparison of AFITPAC versus NOS and a packet radio network design
| AD-A243766 | p 1283 N92-17516
Toward the robust control of high bandwidth high precision flexible optical systems
| AD-A243471 | p 1366 N92-17536
Simulation of finite-precision effects in digital filters
| AD-A243758 | p 1342 N92-17601
Control of a large flexible space structure using multiple model adaptive algorithms
| AD-A243759 | p 1250 N92-17602
Parallel implementation of VHDL simulations on the Intel iPSC/2 hypercube
| AD-A243760 | p 1342 N92-17603
Thermo-mechanical fatigue of a fiber reinforced titanium aluminide composite
| AD-A241988 | p 1256 N92-17607
Visual determination of industrial color-difference tolerances using probit analysis
| AD-A243545 | p 1334 N92-17617
Optical properties of thermally intermixed quantum wells and superlattices
| AD-A243546 | p 1375 N92-17618
Transmission of thin light beams through turbulent mixing layers
| AD-A243470 | p 1367 N92-17658
Gabor segmentation of high resolution synthetic aperture radar imagery
| AD-A243753 | p 1284 N92-17662
Steady-state production and quenching of Br((2)P1/2)
| AD-A243754 | p 1362 N92-17663
Wave propagation in a randomly inhomogeneous medium: A study of the problem
| AD-A243741 | p 1284 N92-17691
A Walsh-domain adaptive filter
| AD-A243701 | p 1292 N92-17718
Parallelizing serial code for a distributed processing environment with an application to high frequency electromagnetic scattering
| AD-A243755 | p 1284 N92-17721
Radar scattering from foamed plastic target supports
| AD-A243756 | p 1284 N92-17722
Control algorithms for aerobraking in the Martian atmosphere
| AD-A243349 | p 1239 N92-17730
The development of military night aviation to 1919
| AD-A243350 | p 1219 N92-17731
An analytic method of propagating a covariance matrix to a maneuver condition for linear covariance analysis during rendezvous
| AD-A243354 | p 1239 N92-17732
Image processing applications for nonlinear decomposition and synthesis
| AD-A243357 | p 1343 N92-17733
A rigorous uniform diffraction analysis of the electromagnetic scattering from impedance edges and junctions
| AD-A243649 | p 1284 N92-17735
Optical image segmentation using wavelet correlation
| AD-A243650 | p 1367 N92-17736
Verification and validation of the simulated radar image (SRIM) code radar cross section predictions
| AD-A243651 | p 1285 N92-17737
A cache design to exploit structural locality
| AD-A243633 | p 1336 N92-17744
Characterizing the sensitivity, selectivity, and reversibility of the metal-doped phthalocyanine thin-films used with the Interdigitated Gate Electrode Field-Effect Transistor (IGEFET) to detect organophosphorous compounds and nitrogen dioxide
| AD-A243635 | p 1376 N92-17746
A robust digital flight control system for an unfanned research vehicle using discrete quantitative feedback theory
| AD-A243638 | p 1237 N92-17748
Electrically erasable programmable integrated circuits for replacement of obsolete TTL logic
| AD-A243652 | p 1292 N92-17760
Verification and validation of the Comprehensive Operational Support Evaluation Model for space
| AD-A243653 | p 1344 N92-17761
Analysis of orbital elements and atmospheric activity to ascertain possible presence of an ion propulsion capability aboard Salyut 7/Cosmos 1686
| AD-A243654 | p 1251 N92-17762
Improving stochastic communication network performance: Reliability vs throughput
| AD-A243655 | p 1285 N92-17763
An investigation of the application of artificial neural networks to adaptive optics imaging systems
| AD-A243780 | p 1348 N92-17767
Evaluation of LOWTRAN and MODTRAN for use over high zenith angle/long path length viewing
| AD-A243599 | p 1387 N92-17920
Effect of spatial locality prefetching on structural locality
| AD-A243632 | p 1337 N92-17922
The effect of physical aging on the creep response of a thermoplastic composite
| AD-A243600 | p 1258 N92-17932

AIR FORCE OCCUPATIONAL MEASUREMENT CENTER, RANDOLPH AFB, TX.
Information management 70XX civilian equivalent
| AD-A242875 | p 1381 N92-17013

AIR FORCE SYSTEMS COMMAND, BROOKS AFB, TX.
Testing and evaluation of the Vanner electrical inverters, models 24-1500 and SP 00112
| AD-A241914 | p 1267 N92-17216
Comparison of experimental US Air Force and Euro-NATO pilot candidate selection test batteries
| AD-A242358 | p 1332 N92-17450

ALABAMA UNIV., HUNTSVILLE.
Knowledge, programming, and programming cultures: LISP, C, and Ada
| NASA-CR-184220 | p 1344 N92-17778

ALLIED-SIGNAL AEROSPACE CO., KANSAS CITY, MO.
Scale-up of recovery process for waste solvents
| KCP-613-4479 | p 1277 N92-17535
Clean room wiping liquids
| DE92-004793 | p 1238 N92-17967
Selective plasma etching
| DE92-004794 | p 1371 N92-17968

AMES LAB., IA.
Structural, electronic, and magnetic properties of La(x)Sr(1-x)VO3 (0 is less than or equal to x is less than or equal to 1.0)
| DE92-003808 | p 1378 N92-17916

APPLIED RESEARCH LAB., STATE COLLEGE, PA.
Basic hydrodynamics
| AD-A243513 | p 1297 N92-17387

ARCON CORP., WALTHAM, MA.
Calculations of electron and photon transport between 1 MeV and 1 eV
| AD-A243725 | p 1359 N92-17514
Gate drain geometry effect on the current voltage characteristics of GaAs MESFETs
| AD-A243430 | p 1291 N92-17684

ARGONNE NATIONAL LAB., IL.
Artificial photosynthesis: Progress toward molecular systems for photoconversion
| DE92-003370 | p 1326 N92-17471
The synergistic effects of solid and liquid lubrication on the tribological behavior of transformation-toughened ZrO2 ceramics
| DE91-018617 | p 1306 N92-17575
Growth rate of dislocation loop in Fe-Ni-Cr alloy under Kr(+) ion and electron irradiation
| DE92-001908 | p 1265 N92-17703
Microstructure and composition of electromagnetically-characterized YBa2Cu3O(7-delta) grain boundaries
| DE92-003520 | p 1376 N92-17782
Process of converting starch to glucose and glucose to lactic acid
| DE92-003840 | p 1255 N92-17867

ARMY AEROMEDICAL RESEARCH LAB., FORT RUCKER, AL.
Effects of the chemical defense antidote atropine sulfate on helicopter pilot performance: An in-flight study
| AD-A241966 | p 1328 N92-17084
The effect of impulse presentation order on hearing trauma in the chinchilla
| AD-A243174 | p 1326 N92-17269
The hazard of exposure to 2.075 kHz center frequency narrow band impulses
| AD-A242997 | p 1329 N92-17299

ARMY ARMAMENT RESEARCH, DEVELOPMENT AND ENGINEERING CENTER, PICATINNY ARSENAL, NJ.
Mechanical and thermomechanical properties of NC base propellants
| AD-A243045 | p 1276 N92-17632

ARMY ARMAMENT RESEARCH, DEVELOPMENT AND ENGINEERING CENTER, WATERVLIET, NY.
Residual stresses in a prestressed steel pressure vessel wrapped with multilayered composites
| AD-A243429 | p 1311 N92-17930

ARMY AVIATION SYSTEMS COMMAND, MOFFETT FIELD, CA.
Identification techniques: Frequency domain methods
p 1231 N92-17158
System identification methods for handling-qualities evaluation p 1232 N92-17165
System identification requirements for high-bandwidth rotorcraft flight control system design
p 1232 N92-17166

ARMY COLD REGIONS RESEARCH AND ENGINEERING LAB., HANOVER, NH.
Role of donor-acceptor interactions in the sorption of TNT and other nitroaromatics from solution
| AD-A243235 | p 1254 N92-17055
The role of thermal convection in heat and mass transport in the subarctic snow cover
| AD-A243674 | p 1312 N92-17715

ARMY COMMUNICATIONS-ELECTRONICS COMMAND, FORT MONMOUTH, NJ.
C3 Systems Technology Symposium on Advance Planning Briefings for Industry
| AD-A243466 | p 1391 N92-17657

ARMY CONSTRUCTION ENGINEERING RESEARCH LAB., CHAMPAIGN, IL.
Cathodic protection diagnostic computer program for sacrificial and impressed current systems: Overview and user's manual
| AD-A243663 | p 1338 N92-17122
Construction equipment for lunar surface operations
| AD-A243665 | p 1389 N92-17123
Worldwide Environmental Compliance Assessment and Management Program (ECAMP): German supplement
| AD-A242967 | p 1313 N92-17380
Human response to helicopter noise: A test of A-weighting
| AD-A243719 | p 1355 N92-17506
Worldwide Environmental Compliance Assessment and Management Program (ECAMP): United Kingdom supplement
| AD-A242928 | p 1314 N92-17551
Worldwide Environmental Compliance Assessment and Management Program (ECAMP)
| AD-A242874 | p 1314 N92-17598
Adaptive on-line help for embedded instructional systems
| AD-A243675 | p 1343 N92-17716

ARMY ENGINEER WATERWAYS EXPERIMENT STATION, VICKSBURG, MS.
Analysis of scene conditions at the light helicopter target acquisition subsystem demonstration/validation, Yuma Proving Ground, Arizona, September 1990
| AD-A243234 | p 1234 N92-17240
Alternate/modified binders for asphalt airfield pavements
| AD-A242829 | p 1238 N92-17260
Large centrifuge: A critical Army capability for the future
| AD-A243287 | p 1238 N92-17287

User's guide for a three-dimensional numerical hydrodynamic, salinity, and temperature model of Chesapeake Bay
|AD-A242993| p 1324 N92-17298

ARMY ENVIRONMENTAL HYGIENE AGENCY, ABERDEEN PROVING GROUND, MD.
Preliminary assessment of the relative toxicity of tetraglycine hydroperiodide, phase 1
|AD-A243334| p 1330 N92-17712

ARMY FIELD ARTILLERY SCHOOL, FORT SILL, OK.
BATTLEKING evaluation, BK 22-91, Meteorological Sensor Package (MSP)
|AD-A241919| p 1317 N92-17009

ARMY LAB. COMMAND, FORT MONMOUTH, NJ.
Low-noise oscillators for airborne radar applications
|AD-A242264| p 1281 N92-17258

ARMY LAB. COMMAND, WATERTOWN, MA.
Novel vacuum bag processing approaches to void reduction in carbon/epoxy composites
|AD-A242396| p 1255 N92-16992
Examining Si3N4 base materials with various rare earth additions
|AD-A243668| p 1372 N92-17082

ARMY MATERIEL SYSTEMS ANALYSIS ACTIVITY, ABERDEEN PROVING GROUND, MD.
The instability of linear heterogeneous Lanchester equations
|AD-A243519| p 1350 N92-17081

ARMY NATICK LABS., MA.
Bibliography of technical publications, papers, and list of patents, October 1988 - September 1989
|AD-A242839| p 1383 N92-17274

ARMY NATICK RESEARCH AND DEVELOPMENT COMMAND, MA.
User evaluation of laser ballistic sun, wind and dust goggle lenses (dye technology)
|AD-A243245| p 1334 N92-17143
Trajectory analysis of the G-11 family of clustered parachutes to determine minimum altitude
|AD-A243375| p 1225 N92-17404

ARMY RESEARCH INST. OF ENVIRONMENTAL MEDICINE, NATICK, MA.
Upper body exercise: Physiology and training application for human presence in space
|AD-A242033| p 1329 N92-17473

ARNOLD ENGINEERING DEVELOPMENT CENTER, ARNOLD AIR FORCE STATION, TN.
Engineering model of unsteady flow in a cavity
|AD-A243636| p 1299 N92-17747

ASPEN CENTER FOR PHYSICS, CO.
Summary of the 1991 ACP Workshop on Coherence and Chaos in Complex Dynamical Systems
|AD-A243226| p 1378 N92-17324

AUBURN UNIV., AL.
Loss terms in free-piston Stirling engine models
|NASA-CR-189840| p 1312 N92-17225
A study of electric transmission lines for use on the lunar surface p 1292 N92-17742

B

BALLISTIC RESEARCH LABS., ABERDEEN PROVING GROUND, MD.
Laser-based ignition of H2/O2 and D2/O2 premixed gases near 243 nm: The first report of a deuterium isotope wavelength effect in laser ignition
|AD-A243180| p 1303 N92-17137
Data fusion for least squares
|AD-A243507| p 1352 N92-17384
Pyrolysis GC-FTIR studies of a LOVA propellant formulation series
|AD-A242844| p 1275 N92-17562
Multipath induced tracking errors at 95 and 140 GHz
|AD-A243111| p 1283 N92-17571
Analysis of ram acceleration for high velocity applications
|AD-A242338| p 1235 N92-17642

BDM INTERNATIONAL, INC., ARLINGTON, VA.
Automated planning with special relevance to associate systems technology and mission planning
|AD-A241924| p 1348 N92-17438

BDM INTERNATIONAL, INC., MCLEAN, VA.
Analog optical neural nets: A noise sensitivity analysis
|AD-A242920| p 1346 N92-17465

BELTRAN, INC., BROOKLYN, NY.
Development of fuel neutralizing agents to prevent flashback on aircraft fires
|AD-A242828| p 1227 N92-17259

BOEING AEROSPACE CO., HUNTSVILLE, AL.
Tandem concentrator photovoltaic array applied to Space Station Freedom evolutionary power requirements
p 1251 N92-17769

BOEING CO., SEATTLE, WA.
Atomic oxygen flux and fluence calculation for Long Duration Exposure Facility (LDEF)
|NASA-CR-187418| p 1245 N92-17215
Systems special investigation group
|NASA-CR-187355| p 1250 N92-17728

BOOZ-ALLEN AND HAMILTON, INC., BETHESDA, MD.
QTCM software documentation. Volume 2: User's manual
|AD-A242744| p 1344 N92-17948

BOSTON COLL., CHESTNUT HILL, MA.
Equation of state and conductivity of hot, dense matter
|AD-A243359| p 1369 N92-17301

BOSTON UNIV., MA.
The cognitive, perceptual, and neural bases of skilled performance
|AD-A243052| p 1332 N92-17554
IRAS and the Boston University Arecibo Galactic H I Survey: A catalog of cloud properties
|NASA-CR-189806| p 1387 N92-17695

BRITISH BROADCASTING CORP., KINGSWOOD (ENGLAND).
Satellite links for television contribution: Reception requirements for links using transportable transmitting earth stations
|BBC-RD-1991/5| p 1285 N92-17885
Image scanning using a fractal curve
|BBC-RD-1991/4| p 1285 N92-17886

BROOKHAVEN NATIONAL LAB., UPTON, NY.
Workshop on Technology Issues of Superconducting MAGLEV Transportation Systems
|DE92-002288| p 1307 N92-17604

BROWN UNIV., PROVIDENCE, RI.
Damage mechanisms in composites
|AD-A242748| p 1258 N92-17950

C

CALIFORNIA INST. OF TECH., PASADENA.
Chemical reactions in turbulent mixing flows
|AD-A243035| p 1294 N92-16979
An experimental investigation of chemically-reacting, gas-phase turbulent jets
|AD-A243036| p 1296 N92-17276

CALIFORNIA UNIV., BERKELEY.
Studies of hetero-epitaxy of GaAs films on Si substrate for effective control of density and internal stress
|AD-A241882| p 1374 N92-17594
Cooperative program to analyze heat transport at high beta in DIII-D
|DE92-003545| p 1370 N92-17606

CALIFORNIA UNIV., BERKELEY. LAWRENCE BERKELEY LAB.
Nonlinear spectroscopic studies of interfacial molecular ordering
|DE92-000864| p 1360 N92-17530
Quantum-limited detection of millimeter waves using superconducting tunnel junctions
|DE92-004757| p 1377 N92-17799
Achromatic and isochronous electron beam transport for tunable free electron lasers
|DE92-003908| p 1305 N92-17868
Performance of hole coupling resonator in the presence of asymmetric modes and FEL gain
|DE92-003907| p 1305 N92-17936

CALIFORNIA UNIV., IRVINE.
Classification of complex sounds
|AD-A243498| p 1355 N92-17381

CALIFORNIA UNIV., LOS ANGELES.
Waveguide four-wave mixing
|AD-A243555| p 1286 N92-17017
UCLA program in reactor studies: The ARIES tokamak reactor study
|DE92-003760| p 1370 N92-17792

CALIFORNIA UNIV., SAN DIEGO, LA JOLLA.
Studies of high-frequency seismic wave propagation
|AD-A241938| p 1316 N92-17202
Ion mixing of semiconductor layered-structures
|DE92-003756| p 1377 N92-17791

CALSPAN FIELD SERVICES, INC., ARNOLD AFS, TN.
Engineering model of unsteady flow in a cavity
|AD-A243636| p 1299 N92-17747

CANADIAN SPACE AGENCY, OTTAWA (ONTARIO).
Canadian Space Station program
p 1243 N92-17102

CARNEGIE-MELLON UNIV., PITTSBURGH, PA.
A computational model of semantic memory impairment: Modality-specificity and emergent category-specificity
|AD-A242377| p 1347 N92-16991
Cyclone: A laser scanner for mobile robot navigation
|AD-A243517| p 1303 N92-17080
Extracting the shape and roughness of specular lobe objects using four light photometric stereo
|AD-A243522| p 1365 N92-17146
A system for fast navigation of autonomous vehicles
|AD-A243523| p 1228 N92-17147
A connectionist simulation of attention and vector comparison: The need for serial processing in parallel hardware
|AD-A242225| p 1348 N92-17457
Attention, automaticity and priority learning
|AD-A242226| p 1332 N92-17458
Program translation tools for systolic arrays
|AD-A242924| p 1336 N92-17466
Optical associative processors and directed graphs
|AD-A242901| p 1366 N92-17630
Serpent: Dialogue editor user's guide. System for user interface development, version 1
|AD-A242331| p 1384 N92-17641

CASE WESTERN RESERVE UNIV., CLEVELAND, OH.
Catalysts for ultrahigh current density oxygen cathodes for space fuel cell applications
|NASA-CR-189787| p 1253 N92-17365
Phase transitions in narrow molecular mass samples of side-chain liquid crystalline polymers: Molecular mass dependence
|AD-A242354| p 1269 N92-17448
Reactions and interactions in liquid crystalline media
|AD-A242355| p 1374 N92-17449
Studies of the adsorption of tetrasulfonated phthalocyanines on graphite substrate
|AD-A243443| p 1260 N92-17489

CATHOLIC UNIV. OF AMERICA, WASHINGTON, DC.
Analysis and experimental evaluation of a Stewart platform-based force/torque sensor
|NASA-CR-189861| p 1252 N92-17150

CENTER FOR MATHEMATICS AND COMPUTER SCIENCE, AMSTERDAM (NETHERLANDS).
A proof theory for a sequential version of POOL
|CWI-CS-R9118| p 1346 N92-17833

CENTRO BRASILEIRO DE PESQUISAS FISICAS, RIO DE JANEIRO.
Y89ONMR study of hyperfine interactions in (R(x)Y(1-x))Fe2
|DE91-641979| p 1376 N92-17779

CHARLES RIVER ANALYTICS, INC., CAMBRIDGE, MA.
An alternative concept for aeroassisted orbit transfers
|AD-A243409| p 1239 N92-17325

CHICAGO UNIV., IL.
The effect of monomer structures and compressibility on the properties of multicomponent polymer blends and solutions
|AD-A242863| p 1273 N92-17777

CHRYSLER CORP., NEW ORLEANS, LA.
Results of the space shuttle vehicle ascent air data system probe calibration test using a 0.07-scale external tank forebody model (68T) in the AEDC 16-foot transonic wind tunnel (IA-310), volume 1
|NASA-CR-167696| p 1241 N92-17167
Results of the space shuttle vehicle ascent air data system probe calibration test using a 0.07-scale external tank forebody model (68T) in the AEDC 16-foot transonic wind tunnel (IA-310), volume 2
|NASA-CR-167697| p 1241 N92-17214

COLOGNE UNIV. (GERMANY, F.R.).
Spatial sampling error of a scanning radiation budget radiometer
|MITT-76| p 1317 N92-17542
Numerical studies of processes in stratiform cirrus
|MITT-78| p 1321 N92-17543

COLORADO STATE UNIV., FORT COLLINS.
Molecular jet studies of vdW clusters and solvation
|AD-A242866| p 1254 N92-17308
Numerical simulation of cirrus clouds: Fire case study and sensitivity analysis
|AD-A242902| p 1321 N92-17631
Molecular composites from high temperature polyquinolines
|AD-A243634| p 1272 N92-17745

COLORADO UNIV., BOULDER.
Pattern selection, wave formation, turbulence, and vortex breakdown in spiral flows
|AD-A242351| p 1297 N92-17447
Temporally-specific modification of myelinated axon excitability in vitro following a single ultrasound pulse
|AD-A242329| p 1326 N92-17474

COLUMBIA UNIV., NEW YORK, NY.
Dynamics and stabilization of materials possessing high energy content
|AD-A243030| p 1258 N92-16977
Topological representation of graph isomorphism types
|AD-A243528| p 1350 N92-17148
Management, control and performance of broadband integrated networks
|AD-A242750| p 1381 N92-17952

CONTEL FEDERAL SYSTEMS, INC., CHANTILLY, VA.
Interim Service ISDN Satellite (ISIS) hardware experiment design for advanced ISDN satellite design and experiments
| NASA-CR-186943 | p 1250 N92-17585
CORNELL UNIV., ITHACA, NY.
Innovative optoelectronic materials and structures using OMVPE
| AD-A243257 | p 1371 N92-16984
Complexity issues in numerical optimization
| AD-A241854 | p 1347 N92-17049
In situ structural studies of the underpotential deposition of copper onto an iodine covered platinum surface using x ray standing waves
| AD-A243475 | p 1263 N92-17328
In situ x ray standing wave study of Cu UPD on an iodine covered platinum surface
| AD-A243474 | p 1264 N92-17426
Development and utilization of new diagnostics for dense-phase pneumatic transport
| DE92-003091 | p 1307 N92-17605
Development and utilization of new diagnostics for dense-phase pneumatic transport
| DE92-000337 | p 1299 N92-17704
Optimal aircraft performance during microburst encounter p 1222 N92-17999
Constraints on cosmic ray propagation in the galaxy
| NASA-CR-189779 | p 1390 N92-18003
Interstellar scattering towards the galactic center as probed by OH/IR stars p 1390 N92-18004
Low frequency interstellar scattering and pulsar observations p 1390 N92-18005
CORPS OF ENGINEERS, SEATTLE, WA.
Aquatic plant management program. Supplement
| AD-A242420 | p 1314 N92-17723
CREE RESEARCH, INC., DURHAM, NC.
Research and development on advanced silicon carbide thin film growth techniques and fabrication of high power and microwave frequency silicon carbide-based device structures
| AD-A243531 | p 1373 N92-17390
CSA ENGINEERING, INC., PALO ALTO, CA.
FEM-X user's guide
| AD-A242374 | p 1383 N92-17396
CYBEROPTICS CORP., MINNEAPOLIS, MN.
Integrated system for missile detection and discrimination
| DE91-018874 | p 1283 N92-17529

D

DARTMOUTH COLL., HANOVER, NH.
Excitons in semiconducting superlattices, quantum wells, and ternary alloys
| DE91-018805 | p 1374 N92-17528
DAVID SARNOFF RESEARCH CENTER, PRINCETON, NJ.
Improved 320x244-element PtSi Schottky-barrier IR-CCD image sensor
| AD-A242026 | p 1301 N92-17140
Innovative switching technology
| DE92-003068 | p 1292 N92-17708
DAVID TAYLOR RESEARCH CENTER, BETHESDA, MD.
Computation of the hydrodynamic forces and moments on a body of revolution with and without appendages
| AD-A243033 | p 1294 N92-16978
An optical roughness sensor for the real time determination of spray formed preform quality
| AD-A243238 | p 1262 N92-17056
The effect of weld metal strength mismatch on the deformation and fracture behavior of steel butt weldments
| AD-A243239 | p 1262 N92-17057
Valuable patents for US businesses: A catalog of DTRC patents available for licensing by the private sector
| AD-A242071 | p 1385 N92-17141
Use of Navier-Stokes analysis in section design
| AD-A242074 | p 1295 N92-17168
A frequency-domain method for estimating the incidence and severity of sliding
| AD-A243077 | p 1334 N92-17569
DAYTON UNIV., OH.
A theory of inverse operators for multiple excitations
| AD-A243484 | p 1350 N92-17330
Explicit finite element method for transparency impact analysis
| AD-A243527 | p 1227 N92-17478
The surface impedance synthesis technique
| AD-A243731 | p 1284 N92-17689
Effect of two types of scene detail on detection of altitude change in a flight simulator
| AD-A242034 | p 1333 N92-17758
DEACON RESEARCH, PALO ALTO, CA.
Laser based, non-intrusive measurement system for analysis of jet engine flows
| AD-A242398 | p 1234 N92-17011
DEFENCE AND CIVIL INST. OF ENVIRONMENTAL MEDICINE, DOWNSVIEW (ONTARIO).
Alleviation of thermal strain in engineering space personnel aboard CF ships with the exotemp personal cooling system
| AD-A242889 | p 1330 N92-17599
DEFENCE RESEARCH ESTABLISHMENT, OTTAWA (ONTARIO).
Heat stress caused by wearing different types of CW protective garment
| AD-A243043 | p 1334 N92-17278
A time-domain incident field extrapolation technique based on the singularity expansion method
| AD-A243044 | p 1282 N92-17279
DEFENSE SYSTEMS, INC., MCLEAN, VA.
Causal schema decision-aiding system
| AD-A242931 | p 1347 N92-17203
DELTA INFORMATION SYSTEMS, INC., HORSHAM, PA.
Comparative analysis of gray scale coding techniques for group 4 facsimile
| AD-A243175 | p 1278 N92-16996
Development of a Federal standard for a video codec operating at P x 64 KBPS
| AD-A243005 | p 1281 N92-17267
DEPARTMENT OF DEFENCE, CANBERRA (AUSTRALIA).
Map maker
| AD-A242980 | p 1312 N92-17292
DEPARTMENT OF DEFENSE, WASHINGTON, DC.
NASA/DoD aerospace knowledge diffusion research project: Chronology of selected literature, reports, policy instruments, and significant events affecting Federal Scientific and Technical Information (STI) in the US
| NASA-TM-101662 | p 1381 N92-17001
DEPARTMENT OF DEFENSE EXPLOSIVES SAFETY BOARD, ALEXANDRIA, VA.
Structures to resist the effects of accidental explosions
| AD-A243272 | p 1277 N92-17272
DEPARTMENT OF ENERGY, UPTON, NY.
Summaries of FY 1991 engineering research
| DE92-004708 | p 1277 N92-17593
DEPARTMENT OF THE NAVY, WASHINGTON, DC.
Method of Kalman filtering for estimating the position and velocity of a tracked object
| AD-D015057 | p 1287 N92-17129
Method of joining diamond structures
| AD-D015066 | p 1269 N92-17397
Method and apparatus for reducing drag and noise associated with fluid flow in a conduit
| AD-D015067 | p 1297 N92-17398
Energetic composites of cyclodextrin nitrate esters and nitrate ester plasticizers
| AD-D015068 | p 1275 N92-17399
Microstructurally toughened articles and casting thereof
| AD-D015065 | p 1265 N92-17452
Steady-state, high dose neutron generation and concentration apparatus and method for deuterium atoms
| AD-D015063 | p 1358 N92-17462
Method of doping single crystal diamond for electronic devices
| AD-D015069 | p 1374 N92-17610
Polymer-reinforced metal matrix composite
| AD-D015070 | p 1257 N92-17611
Consolidation of diamond packed powders
| AD-D015071 | p 1270 N92-17612
A tunable solid state laser with high wavelength selectivity over a preselected wavelength range
| AD-D015055 | p 1304 N92-17627
Concentration of isotopic hydrogen by temperature gradient effect in soluble metal
| AD-D015062 | p 1260 N92-17628
Plasma chemical vapor deposition of halide glasses
| AD-D015060 | p 1370 N92-17706
Method of guiding an in-flight vehicle to a designed flight path
| AD-D015061 | p 1229 N92-17707
Fiber optic angular orientation sensor digital serial encoding
| AD-D015102 | p 1302 N92-17826
Low frequency vibration absorber
| AD-D015103 | p 1307 N92-17827
Precision multi-channel fiber optic interface and method
| AD-D015104 | p 1367 N92-17828
High-speed beam switching processor
| AD-D015108 | p 1285 N92-17829
Launching projectiles with hydrogen gas generated from aluminum fuel powder/water reactions
| AD-D015119 | p 1276 N92-17830
Explosive magnetic field compression generator transformer power supply for high resistive loads
| AD-D015123 | p 1293 N92-17831
High contact blind hole thermocouple plug
| AD-D015105 | p 1302 N92-17835
Thermal insulation chemical composition and method of manufacture
| AD-D015106 | p 1257 N92-17836
Silver-nickel composite cathodes for alkaline secondary batteries
| AD-D015121 | p 1293 N92-17871
Differential pressure sensor
| AD-D015134 | p 1302 N92-17918
Method and apparatus for lasing
| AD-D015154 | p 1305 N92-17923
Magnetic multilayer strain gage
| AD-D015163 | p 1381 N92-17940
Optical fiber magnetometer
| AD-D015133 | p 1368 N92-17959
DEUTSCHE FORSCHUNGSANSTALT FUER LUFT- UND RAUMFAHRT, BRUNSWICK (GERMANY, F.R.).
Instrumentation and data processing p 1230 N92-17155
BO 105 identification results p 1231 N92-17161
DOUGLAS AIRCRAFT CO., INC., LONG BEACH, CA.
Assessment of cockpit interface concepts for data link retrofit
| NASA-CR-187615 | p 1228 N92-17512
DU PONT DE NEMOURS (E. I.) AND CO., AIKEN, SC.
Extendable pipe crawler
| DE91-011570 | p 1306 N92-17183
DYNACS ENGINEERING CO., INC., PALM HARBOR, FL.
Modes of interconnected lattice trusses using continuum models, part 1
| NASA-CR-189568 | p 1242 N92-17045
DYNAMICS TECHNOLOGY, INC., TORRANCE, CA.
Metriwave final report
| NASA-CR-189816 | p 1279 N92-17046

E

EDGERTON, GERMESHAUSEN AND GRIER, INC., IDAHO FALLS, ID.
Experimental measurements of plasma properties for Miller SG-100 torch with Mach I setting
| DE92-003309 | p 1369 N92-17469
Versatile Data Acquisition System Model II user's manual
| DE92-003311 | p 1384 N92-17470
Downflow heat transfer in a heated ribbed vertical annulus with a cosine power profile (results from test series ECS-2c)
| DE92-003259 | p 1298 N92-17626
A method for joining ceramic shapes
| DE92-003815 | p 1274 N92-17842
Phosphazene polymer containing composites and method for making phosphazene polymer containing composites
| DE92-003826 | p 1274 N92-17935
Software reliability models for critical applications
| DE92-004797 | p 1345 N92-17969
EG AND G MOUND APPLIED TECHNOLOGIES, MIAMISBURG, OH.
Sensitivity testing and analysis
| DE92-002033 | p 1276 N92-17624
EG AND G ROCKY FLATS, INC., GOLDEN, CO.
Inductively coupled plasma atomic emission spectroscopy analysis of gold electroplating solutions
| DE92-004798 | p 1266 N92-17858
ELECTRONICS RESEARCH LAB., ADELAIDE (AUSTRALIA).
Constant modulus algorithm techniques for the enhancement of signal quality
| AD-A242986 | p 1288 N92-17295
Decompiling with definite clause grammars
| AD-A242987 | p 1340 N92-17296
ENVIRONMENTAL PROTECTION AGENCY, RESEARCH TRIANGLE PARK, NC.
NOAA Atmospheric Sciences Modeling Division support to the US Environmental Protection Agency
| PB91-235499 | p 1315 N92-17134
ENVIRONMENTAL RESEARCH INST. OF MICHIGAN, ANN ARBOR.
Simultaneous active and passive microwave measurements of the ocean surface
| AD-A242232 | p 1312 N92-17459
High resolution imaging using phase retrieval, volume 2
| AD-A242925 | p 1366 N92-17550
ERG SYSTEMS, INC., SAINT JAMES, NY.
Full surface testing of grazing incidence mirrors
| AD-A243734 | p 1367 N92-17690
ESDU INTERNATIONAL LTD., LONDON (ENGLAND).
Strength of lugs
| ESDU-91008 | p 1311 N92-17834

Example of statistical techniques applied to cruise performance guarantees (Student's t distribution)
| ESDU-91018 | p 1233 N92-17843
Example of statistical techniques applied to autoland touchdown dispersion (confidence intervals for normal and skew distributions)
| ESDU-91019 | p 1229 N92-17844
Variability of standard aircraft performance parameters
| ESDU-91020 | p 1233 N92-17847
Analysis of cam roller followers
| ESDU-91026 | p 1307 N92-17852
Mean wind speeds over hills and other topography
| ESDU-91043 | p 1321 N92-17853

EUROPEAN SPACE AGENCY, PARIS (FRANCE).
Columbus Programme (current status)
p 1243 N92-17100
Theoretical investigation of the injection and evaporation of water in a hydrogen/oxygen steam generator
| ESA-TT-1252 | p 1379 N92-17848

EXECUTIVE OFFICE OF THE PRESIDENT, WASHINGTON, DC.
Publications of the Executive Office of the President, January 20, 1989 to June 30, 1991
| PB91-202762 | p 1382 N92-17228

F

FAIL-SAFE TECHNOLOGY CORP., LOS ANGELES, CA.
Embedded fault-tolerant computer for mission critical applications
| AD-A242886 | p 1342 N92-17566

FEDERAL AVIATION ADMINISTRATION, ATLANTIC CITY, NJ.
Effectiveness of an onboard water spray system during an oxygen enriched cabin fire
| DOT/FAA/CT-TN91/51 | p 1226 N92-17149

FEDERAL AVIATION ADMINISTRATION, CAMBRIDGE, MA.
Multisensor signal processing techniques (hybrid GPS/LORAN-C with RAIM)
| AD-A242323 | p 1281 N92-17244

FERMI NATIONAL ACCELERATOR LAB., BATAVIA, IL.
Black holes in magnetic monopoles
| NASA-CR-189842 | p 1388 N92-17377
Results from a data acquisition system prototype project using a switch-based event builder
| DE92-004638 | p 1336 N92-17592
Axino-induced baryogenesis
| NASA-CR-189858 | p 1361 N92-17646
Fluctuation driven electroweak phase transition
| NASA-CR-189859 | p 1361 N92-17647
Late time cosmological phase transitions 1: Particle physics models and cosmic evolution
| NASA-CR-189857 | p 1388 N92-17696
A classical instability of Reissner-Nordstrom solutions and the fate of magnetically charged black holes
| NASA-CR-189843 | p 1388 N92-17697

FLORIDA STATE UNIV., TALLAHASSEE.
Studies of baroclinic flow
| AD-A243050 | p 1296 N92-17309
Mechanisms of temporal pattern discrimination by human observers
| AD-A243051 | p 1332 N92-17336

G

GALLAGHER ASSOCIATES, INC., WEST LAFAYETTE, IN.
Integrated system for missile detection and discrimination
| DE91-018874 | p 1283 N92-17529

GENERAL ACCOUNTING OFFICE, WASHINGTON, DC.
Early warning satellites: Funding for follow-on system is premature
| AD-A242836 | p 1245 N92-17250
Rocket tests in Mississippi to be heavily restricted
| GAO/NSIAD-92-86 | p 1240 N92-17741

GENERAL ATOMIC CO., SAN DIEGO, CA.
Active heater control and regulation for the Varian VGT-8011 gyrotron
| DE92-003638 | p 1302 N92-17454
The charge exchange recombination diagnostic system on the D3-D tokamak
| DE92-003805 | p 1369 N92-17456

GENERAL ELECTRIC CO., CINCINNATI, OH.
Qualification test report. Fuel pump test stand 3C3965G05
| AD-A242929 | p 1235 N92-17552

GENERAL ELECTRIC CO., SCHENECTADY, NY.
CMS reverse engineering and encore/model integration
| AD-A243438 | p 1341 N92-17487
Local extinction mechanisms in non-premixed turbulent combustion
| AD-A242027 | p 1260 N92-17682

GENERAL ELECTRIC CO., SYRACUSE, NY.
Failure mechanisms in GaAs ICs: The effects of deep traps
| AD-A243013 | p 1374 N92-17553

GEO-CENTERS, INC., NEWTON, MA.
User evaluation of laser ballistic sun, wind and dust goggle lenses (dye technology)
| AD-A243245 | p 1334 N92-17143

GEOLOGICAL SURVEY, DENVER, CO.
Workshop on Geologic Applications of Modern Aeromagnetic Surveys
| PB91-221788 | p 1316 N92-17229

GEORGE WASHINGTON UNIV., WASHINGTON, DC.
Research in some future directions in reliability and quality control
| AD-A242865 | p 1308 N92-17231
The effect of freestream turbulence on the vortical flow over a delta wing p 1225 N92-17681

GEORGIA INST. OF TECH., ATLANTA.
Periodic trim solutions with HP-version finite elements in time
| NASA-CR-189778 | p 1236 N92-17019
Optical content-addressable memories for data/knowledge base processing
| AD-A241866 | p 1382 N92-17037
Acquisition and production of skilled behavior in dynamic decision-making tasks
| NASA-CR-189846 | p 1333 N92-17132
Actively controlled shaft seals for aerospace applications
| NASA-CR-189808 | p 1306 N92-17304

GEORGIA TECH RESEARCH INST., ATLANTA.
Biophysical techniques for examining metabolic, proliferative, and genetic effects of microwave radiation
| AD-A241903 | p 1326 N92-17288

GLASGOW UNIV. (SCOTLAND).
Design of experiments p 1230 N92-17154
Modelling aspects and robustness issues in rotorcraft system identification p 1231 N92-17159

GORDON RESEARCH CONFERENCES, INC., KINGSTON, RI.
Ceramics with superelectrical and supermechanical properties
| AD-A243062 | p 1267 N92-17029

GOSUDARSTVENNYI KOMITET PO ISPOLZOVANIYU ATOMNOI ENERGII, OBNINSK (USSR).
Development of a system for void fraction measuring by electroprobing method
| DE92-610933 | p 1309 N92-17809
Experimental study of amplitude-phase-frequency characteristics of flow when following over a vibrating plate
| DE92-610935 | p 1299 N92-17810

GOSUDARSTVENNYI KOMITET PO ISPOLZOVANIYU ATOMNOI ENERGII, SERPUKHOV (USSR).
Analysis of possible schemes for twisting multiwire superconducting cables and design of twisting equipment
| DE92-609667 | p 1294 N92-17971

GUMBS (R.) ASSOCIATES, EAST BRUNSWICK, NJ.
Ultrafast passive shields for laser and ballistic protection
| AD-A243206 | p 1303 N92-17175

H

HARRY DIAMOND LABS., ADELPHI, MD.
HEMP test on FD-565
| AD-A243099 | p 1278 N92-16980
Theoretical crystal-field calculations for rare-earth ions in 3-5 semiconductor compounds
| AD-A243098 | p 1371 N92-16995
Preparation of ferroelectric samples for electrical and radiation characterization studies
| AD-A243432 | p 1288 N92-17326
A PC program to calculate the one-sided lower tolerance limit for total ionizing dose radiation data
| AD-A242365 | p 1357 N92-17394

HARVARD UNIV., CAMBRIDGE, MA.
Superdirective properties of closed loops of parallel coplanar dipoles
| AD-A243009 | p 1288 N92-17268
Omega-terminated alkanethiolate monolayers on surfaces of copper, silver and gold have similar wettabilities
| AD-A243529 | p 1260 N92-17389
Comparisons of self-assembled monolayers on silver and gold: Mixed monolayers derived from HS(CH2)21X and HS(CH2)10(sup Y) (X,Y-CH3, CH2OH) have similar properties
| AD-A243487 | p 1264 N92-17427
Molecular recognition in gels, monolayers, and solids
| AD-A243488 | p 1358 N92-17428
X ray damage to CF3CO2-Terminated organic monolayers on Si/Au supports is due primarily to x ray induced electrons
| AD-A243446 | p 1289 N92-17490
Designing ordered molecular arrays in two and three dimensions
| AD-A243447 | p 1359 N92-17491
Molecular self-assembly and nanochemistry: A chemical strategy for the synthesis of nanostructures
| AD-A243530 | p 1361 N92-17616
Proton-proton and proton-antiproton elastic scattering at high energies: Theory, phenomenology, and experiment
| DE92-004414 | p 1364 N92-17964

HOUSTON UNIV., TX.
Intelligent Computer-Aided Training (ICAT)
p 1246 N92-17352

HOWARD UNIV., WASHINGTON, DC.
A comparative study of the noise performance of Alluminum Gallium Arsenide/Gallium Arsenide high electron mobility transistors with and without superconducting gate electrodes p 1288 N92-17317

HUGHES AIRCRAFT CO., EL SEGUNDO, CA.
Determination of the tribological fundamentals of solid lubricated ceramics. Volume 3: Appendices P through 2
| AD-A242872 | p 1270 N92-17597
Determination of the tribological fundamentals of solid lubricated ceramics. Volume 2: Appendices A through O
| AD-A242871 | p 1270 N92-17614
Thermally regenerative fuel cells
| AD-A242900 | p 1290 N92-17629
Determination of the tribological fundamentals of solid lubricated ceramics. Volume 1: Summary
| AD-A243219 | p 1272 N92-17683

HUGHES RESEARCH LABS., MALIBU, CA.
High temperature superconductor thin films and Josephson junctions
| AD-A242747 | p 1293 N92-17949

HUMAN ENGINEERING LABS., ABERDEEN PROVING GROUND, MD.
The effects of speech intelligibility level on concurrent visual task performance
| AD-A243015 | p 1331 N92-17052
Automatic recognition of speech in stressful environments
| AD-A242917 | p 1283 N92-17464

I

IIT RESEARCH INST., ROME, NY.
CALS database usage and analysis tool study
| AD-A243205 | p 1382 N92-17174

ILLINOIS INST. OF TECH., CHICAGO.
Determination of cohesive and normal stresses and simulation of fluidization using kinetic theory
| DE92-002905 | p 1299 N92-17709

ILLINOIS STATE WATER SURVEY, CHAMPAIGN.
A variational assimilation method for satellite and conventional data: Development of basic model for diagnosis of cyclone systems
| NASA-CR-188236 | p 1321 N92-17975
A variational assimilation method for satellite and conventional data: Model 2 (version 1)
p 1322 N92-17976
A variational assimilation method for satellite and conventional data: A revised basic model 2B
p 1322 N92-17977
A variational formalism for the radiative transfer equation: Prelude to model 3 p 1322 N92-17978
A variational formalism for the radiative transfer equation and a geostrophic, hydrostatic atmosphere: Prelude to model 3 p 1322 N92-17979
On the concept of varying influence radii for a successive corrections objective analysis p 1322 N92-17980
Modification of a successive corrections objective analysis for improved derivative calculations
p 1322 N92-17981

ILLINOIS UNIV., URBANA.
Thin films under chemical stress
| DE92-004684 | p 1377 N92-17857

IMPERIAL COLL. OF SCIENCE AND TECHNOLOGY, LONDON (ENGLAND).
Workshop for Finite Element Methods for Composites
| AD-A243534 | p 1256 N92-17392
Enhanced backscattering of light from randomly rough diffusers: Appendix
| AD-A243436 | p 1366 N92-17485
Enhanced backscattering from rough surfaces
| AD-A243437 | p 1366 N92-17486

INDIANA UNIV., BLOOMINGTON.
NASA/DoD aerospace knowledge diffusion research project: Chronology of selected literature, reports, policy instruments, and significant events affecting Federal Scientific and Technical Information (STI) in the US
|NASA-TM-101662| p 1381 N92-17001
Relativistic nuclear many-body theory
|DE92-003258| p 1362 N92-17789
INSTITUTE FOR DEFENSE ANALYSES, ALEXANDRIA, VA.
An examination of selected commercial software testing tools
|AD-A243089| p 1337 N92-17068
INSTITUTE FOR NAVAL OCEANOGRAPHY, BAY SAINT LOUIS, MS.
A user's manual for the Princeton Numerical Ocean Model
|AD-A243773| p 1324 N92-17539
INSTITUTO DE FISICA TEORICA, SAO PAULO (BRAZIL).
Inequalities among partial traces of Hermitian operators and partial sums of their Eigenvalues
|DE91-641495| p 1351 N92-17622
INTERNATIONAL BUSINESS MACHINES CORP., SAN JOSE, CA.
In situ surface x ray scattering of metal monolayers adsorbed at solid-liquid interfaces
|AD-A243258| p 1262 N92-16985
Two-beam coupling measurements of grating phase in a photorefractive polymer
|AD-A243746| p 1268 N92-17195
Detection and spectroscopy of single pentacene molecules in a p-terphenyl crystal by means of fluorescence excitation
|AD-A243747| p 1356 N92-17196
Single molecule spectral diffusion in a solid detected via fluorescence spectroscopy
|AD-A243748| p 1356 N92-17197
Optical spectra and kinetics of single impurity molecules in a polymer: Spectral diffusion and persistent spectral hole-burning
|AD-A243749| p 1271 N92-17659
Optical modification of a single impurity molecule in a solid
|AD-A243750| p 1361 N92-17660
Photorefractivity in doped nonlinear organic polymers
|AD-A243751| p 1271 N92-17661
INTERNATIONAL CENTRE FOR THEORETICAL PHYSICS, TRIESTE (ITALY).
Gauge-covariant Wess-Zumino actions for super p-branes in superspace
|DE91-641524| p 1353 N92-17318
Lie-isotopic generalization of the Poincare symmetry: Classical formulation
|DE91-642825| p 1379 N92-17531
A GNS-type theorem for a non-involutive Banach algebra
|DE91-641481| p 1354 N92-17803
Topological duals of Banach spaces as Banach algebras and applications
|DE91-641482| p 1354 N92-17804
On the generation of large-amplitude plasma wakefields with low phase velocities by an intense short laser pulse
|DE92-609543| p 1371 N92-17805
Alfven waves in inhomogeneous magnetic fields: An integro-differential equation formulation
|DE92-609544| p 1371 N92-17806
Temperature dependent anomalous statistics
|DE92-609665| p 1379 N92-17807
Mathematics and biology
|DE92-611247| p 1327 N92-17815
Chaos caused by a topologically mixing map
|DE91-641486| p 1354 N92-17823
State vector reduction. Part 1: Dynamical reduction theories; changing quantum theory so the statevector represents reality
|DE91-641488| p 1379 N92-17824
Evolution as a molecular cooperative phenomenon
|DE92-609575| p 1327 N92-17877
Some results for extended Jacobi polynomials
|DE92-609035| p 1351 N92-17939
Kinetics of a new phase formation in supersaturated solid solutions. 1. Dilute one-component systems
|DE92-610065| p 1262 N92-17943
Global models for the biomechanics of green plants, part 1
|DE91-641478| p 1327 N92-17946
Comments on a novel approach to the role of chirality in the origin of life
|DE92-609034| p 1327 N92-17970
Liquid-solid transition in the bond particle model for elemental semiconductors
|DE92-610441| p 1378 N92-17972

J

JAPAN ATOMIC ENERGY RESEARCH INST., TOKYO.
Effect of thermal annealing on property changes of neutron-irradiated non-graphitized carbon materials and nuclear graphite
|DE92-704180| p 1257 N92-17816
JAYCOR, SAN DIEGO, CA.
Waveguide four-wave mixing
|AD-A243555| p 1286 N92-17017
JET PROPULSION LAB., CALIFORNIA INST. OF TECH., PASADENA.
Operations mission planner beyond the baseline
p 1246 N92-17353
ECLSS predictive monitoring p 1247 N92-17357
JPL space station telerobotic engineering prototype development: Advanced telerobotics system technology
p 1247 N92-17358
JPL space station telerobotic engineering prototype development FY 91 status/achievements
p 1247 N92-17359
Telerobotic ground-remote operations
p 1247 N92-17360
Optical protocols for advanced spacecraft networks
p 1249 N92-17418
Three-stage sorption type cryogenic refrigeration system and method employing heat regeneration
|NASA-CASE-NPO-18366-1-CU| p 1277 N92-17674
Real-time edge-enhanced optical correlator
|NASA-CASE-NPO-18379-1-CU| p 1367 N92-17675
Multiperiod-grating surface-emitting lasers
|NASA-CASE-NPO-17763-1-CU| p 1305 N92-17862
Near real-time stereo vision system
|NASA-CASE-NPO-18593-1-CU| p 1368 N92-17864
Method for non-destructive estimation of waveguide directional coupler dimensions
|NASA-CASE-NPO-18454-1-CU| p 1293 N92-17865
Neural-network dedicated processor for solving competitive assignment problems
|NASA-CASE-NPO-17781-1-CU| p 1337 N92-17884
Wide field strip-imaging optical system
|NASA-CASE-NPO-18146-1-CU| p 1368 N92-17892
High level language-based robotic control system
|NASA-CASE-NPO-17918-2-CU| p 1349 N92-17895
Self-collimated unstable resonator semiconductor laser
|NASA-CASE-NPO-18386-1-CU| p 1305 N92-17899
Transformerless DC-DC voltage amplifier with optically isolated switching devices
|NASA-CASE-NPO-17994-1-CU| p 1293 N92-17907
JOHNS HOPKINS UNIV., BALTIMORE, MD.
Receiver performance of laser ranging measurements between the Lunar Observer and a subsatellite for lunar gravity studies
|NASA-CR-189860| p 1303 N92-17152
JOINT INST. FOR NUCLEAR RESEARCH, DUBNA (USSR).
What experiments say about possibility of the new particle existence with mass less than the kaon mass
|DE91-634551| p 1357 N92-17408
Data acquisition and measurement system for plastic parameters of radiation metal research experiments
|DE92-610350| p 1266 N92-17808
On the nonadiabatic theory of charged particles motion in the magnetic dipole field
|DE92-610951| p 1354 N92-17811
Use of the algebraic coding theory in nuclear electronics
|DE92-611125| p 1351 N92-17813
Microprocessor controller in CAMAC standard for temperature regulation and stabilization
|DE92-611158| p 1348 N92-17814
Cryogenic thermoresistor made from p-InSb(Mn)
|DE92-600473| p 1293 N92-17825
Experimental findings on self-recovery and improvement of representative parameters of some semiconductor devices as irradiated in fast neutron flux
|DE92-611185| p 1378 N92-17944
Comparative study of irreversibility effects in Nb foil and high temperature superconducting ceramics by muon spin rotation
|DE92-600475| p 1294 N92-17953
Investigation of heated ultracold neutrons on copper surface
|DE92-600625| p 1363 N92-17955
Importance of the neutron-proton interactions for the even Ra-Th nuclei
|DE92-600628| p 1363 N92-17956
One nucleon transition densities for 1p shell nuclei
|DE92-600629| p 1363 N92-17957
Pion-nucleus cross sections
|DE92-600631| p 1363 N92-17958
Multiply charged ion sources for cyclotrons
|DE92-610975| p 1364 N92-17973

K

KANSAS UNIV., LAWRENCE.
Evaluation of solar flares and electron precipitation by nitrate distribution in Antarctica
|AD-A243026| p 1389 N92-17235
KINGS COLL., LONDON (ENGLAND).
Permittivity probe modelling
|AD-A243236| p 1260 N92-17572
KYOTO UNIV., KUMATORI (JAPAN).
Summary reports of activities under visiting research program
|DE91-522477| p 1391 N92-17623
Proceedings of the Conference on Health Physics
|DE92-704335| p 1331 N92-17802

L

LAWRENCE LIVERMORE NATIONAL LAB., CA.
Application of linear inverse theory to borehole gravity data
|DE92-002172| p 1317 N92-17578
The effect of detonation curvature on cylindrical wall motion
|DE92-003110| p 1298 N92-17625
X ray laser
|DE91-011705| p 1304 N92-17649
The effect of shower/bath frequency on the health and operational effectiveness of soldiers in a field setting: Recommendation of showering frequencies for reducing performance-degrading nonsystemic microbial skin infections
|AD-A242923| p 1330 N92-17714
Collaborative research on experimental astrophysics
|DE92-003970| p 1388 N92-17832
Developing a broader basis for scientific data analysis interfaces
|DE92-003963| p 1385 N92-17845
Correlator optical wavefront sensor COWS
|DE92-003964| p 1368 N92-17846
Energy production using fission fragment rockets
|DE92-002192| p 1364 N92-17876
Software tools for distributed intelligent control systems
|DE92-004656| p 1349 N92-17965
LEIDEN UNIV. (NETHERLANDS).
A new interpolation procedure for adapting Runge-Kutta methods to delay differential equations
|TW-90-09| p 1351 N92-17517
Marked point processes as limits of Markovian arrival streams
|TW-91-04| p 1353 N92-17837
The micro-c rule is not optimal in the 2nd node of the tandem queue; 2 counterexamples
|TW-91-05| p 1349 N92-17838
LINUS PAULING INST. OF SCIENCE AND MEDICINE, PALO ALTO, CA.
Efficient identification and analysis of low and medium frequency repeats
|DE92-003758| p 1385 N92-17856
LOCKHEED AERONAUTICAL SYSTEMS CO., BURBANK, CA.
Heat flux sensor research and development: The cool film calorimeter
|NASA-CR-189789| p 1301 N92-17006
LOCKHEED MISSILES AND SPACE CO., HUNTSVILLE, AL.
Space Station Freedom solar alpha joint growth capability p 1252 N92-17772
LOCKHEED MISSILES AND SPACE CO., PALO ALTO, CA.
Aries x ray objective grating spectrograph
|NASA-CR-189245| p 1386 N92-17003
Investigation of mechanisms for the source and loss of electrons from the radiation belts using data from SEEP, SCATHA and P78-1 satellites
|AD-A243376| p 1317 N92-17405
LOS ALAMOS NATIONAL LAB., NM.
Solar neutrinos: Probing the sun or neutrinos?
|DE92-003849| p 1389 N92-17201
Performance of the Rayleigh task based on the posterior probability of tomographic reconstructions
|DE92-003785| p 1352 N92-17455
On size scaling in shock hydrodynamics and the stress-strain behavior of copper at exceedingly high strain rates
|DE92-003797| p 1265 N92-17579
Recent developments in neutrino physics
|DE92-003855| p 1360 N92-17589
Beam position monitor multiplexer controller upgrade at the LAMPF proton storage ring
|DE92-003859| p 1363 N92-17590

A distributed design for monitoring, logging, and replaying device readings at LAMPF
| DE92-003860 | p 1240 N92-17591
Medium-energy neutrino physics
| DE92-003790 | p 1362 N92-17666
In situ observations of coronal mass ejections in interplanetary space
| DE92-003857 | p 1389 N92-17725
Development of an XUV-IR free-electron laser user facility for scientific research and industrial applications
| DE92-003862 | p 1304 N92-17726
Direct speciation of metal and metalloid ions by optical spectroscopies
| DE92-003868 | p 1261 N92-17727
Evaluation of environmentally safe cleaning agents for diamond turned optics
| DE92-002524 | p 1278 N92-17780
Au and Al Schottky barrier formation on GaAs (100) surfaces prepared by thermal desorption of a protective arsenic coating
| DE92-002456 | p 1376 N92-17781
PILAC: A Pion Linac facility for 1-GeV pion physics at LAMPF
| DE92-003789 | p 1364 N92-17794
The Los Alamos FEL photoinjector drive laser
| DE92-003791 | p 1305 N92-17795
Emittance growth from space-charge forces
| DE92-003804 | p 1364 N92-17796
Solar neutrino physics in the nineties
| DE92-003848 | p 1390 N92-17883

LOUISIANA STATE UNIV., BATON ROUGE.
A general computational framework for distributed sensing and fault-tolerant sensor integration
| AD-A243256 | p 1300 N92-16983

LOYOLA COLL., BALTIMORE, MD.
X ray lithography in Japan
| AD-A243660 | p 1286 N92-17087

M

MANCHESTER UNIV. (ENGLAND).
Boundary-layer transition and heat transfer on slender delta wings
| AERO-REPT-8904 | p 1226 N92-17849
The effect of isolated roughness elements on transition in attachment-line flows
| AERO-REPT-8905 | p 1300 N92-17850
Flow between two stationary disks and a rotating shroud
| AERO-REPT-9001 | p 1300 N92-17851
Sydney Goldstein FRS Hon FRAeS: An appreciation
| AERO-REPT-8903 | p 1391 N92-17928
Physical and computational modelling of stratified shear flows
| AERO-REPT-8909 | p 1300 N92-17974

MARINE BIOLOGICAL LAB., WOODS HOLE, MA.
The 7th Annual Workshop on Computational Neuroscience
| AD-A243462 | p 1335 N92-17656

MARTIN MARIETTA AEROSPACE, DENVER, CO.
Extravehicular mobility unit subcritical liquid oxygen storage and supply system
| NASA-CR-189831 | p 1276 N92-16989

MARYLAND UNIV., COLLEGE PARK.
Inelastic strain analysis of solder joint in NASA fatigue specimen
| NASA-CR-189882 | p 1311 N92-17511

MASSACHUSETTS INST. OF TECH., CAMBRIDGE.
The real-time cost of timing uncertainty: Consensus and failure detection
| AD-A243176 | p 1345 N92-16997
Gas transport in polybutadiene treated with aqueous bromine
| AD-A241871 | p 1295 N92-17025
Using mappings to prove timing properties
| AD-A242862 | p 1277 N92-17263
Atom wave interferometer
| AD-A243482 | p 1357 N92-17374
Compact free electron lasers for medical applications
| AD-A243497 | p 1304 N92-17582
Upper ocean dynamics during the LOTUS and Tropic Heat Experiments
| AD-A243730 | p 1324 N92-17583
Grain boundaries
| DE92-004420 | p 1378 N92-17941
Radar-satellite studies of the high-latitude ionosphere
| AD-A243275 | p 1317 N92-17961
An investigation of air transportation technology at the Massachusetts Institute of Technology, 1990-1991
p 1219 N92-17985
Experimental investigation of passive infrared ice detection for helicopter applications
p 1220 N92-17986
Deterministic multi-zone ice accretion modeling
p 1220 N92-17987
Alert generation and cockpit presentation for an integrated microburst alerting system
p 1220 N92-17988
Cockpit display of hazardous weather information
p 1220 N92-17989

MASSACHUSETTS INST. OF TECH., LEXINGTON.
Performance measures for adaptive decisioning systems
| AD-A243183 | p 1352 N92-16998
Terminal Doppler weather radar test bed operation, Orlando: January-June 1990
| AD-A242890 | p 1318 N92-17028
A covariance modeling approach to adaptive beamforming and detection
| AD-A241887 | p 1279 N92-17040
Analysis of the terminal Doppler weather radar algorithm for detecting rotation associated with microbursts
| AD-A242840 | p 1318 N92-17050
Performance of ground-based infrared detectors for acquisition of satellites
| AD-A243247 | p 1281 N92-17241

MASSACHUSETTS UNIV., AMHERST.
Preliminary design study of a central solar heating plant with seasonal storage at the University of Massachusetts, Amherst
| DE92-000762 | p 1313 N92-17577

MATERIALS RESEARCH LABS., ASCOT VALE (AUSTRALIA).
A theoretical study of the combustion of magnesium/teflon/viton pyrotechnic compositions
| AD-A243244 | p 1275 N92-17058
Magnetic field distribution and design of Helmholtz coils
| AD-A242978 | p 1288 N92-17291

MAX-PLANCK-INST. FUER STROEMUNGSFORSCHUNG, GOETTINGEN (GERMANY, F.R.).
A short or a long cylinder: What difference does it make to the Karman vortex street?
| MPIS-98/1990 | p 1224 N92-17314
Investigation on the control of a Karman vortex street
| MPIS-99/1990 | p 1224 N92-17315
The influence of cavitation in the breakup of liquid free jets
| MPIS-1/1991 | p 1297 N92-17343
Development of an electronic high speed camera system for the quantitative analysis of unsteady flows
| MPIS-100/1991 | p 1301 N92-17344
Recording of three dimensional trajectories and velocity fields by automatic image processing
| MPIS-101/1991 | p 1301 N92-17345

MCDONNELL AIRCRAFT CO., SAINT LOUIS, MO.
Product Definition Data Interface (PDDI) translator user's manual
| AD-A243463 | p 1352 N92-17223

MCDONNELL-DOUGLAS HELICOPTER CO., MESA, AZ.
Assessment of rotorcraft system identification as applied to the AH-64 p 1231 N92-17160
Industry view on rotorcraft system identification
p 1232 N92-17163

MCDONNELL-DOUGLAS SPACE SYSTEMS CO., HUNTINGTON BEACH, CA.
Mars aerobrake assembly demonstration
p 1247 N92-17362
Magnetospheric response to variations in the interplanetary magnetic field
| AD-A243683 | p 1388 N92-17717

MCDONNELL-DOUGLAS SPACE SYSTEMS CO., WASHINGTON, DC.
STV fueling options p 1249 N92-17415
ISE advanced technology p 1249 N92-17420
Thermal Control System Automation Project (TCSAP)
p 1252 N92-17776

MESSERSCHMITT-BOELKOW-BLOHM G.M.B.H., MUNICH (GERMANY, F.R.).
Comparison of two solution methods for the numerical calculation of hypersonic flows
| MBB-FE211-S-PUB-446 | p 1224 N92-17311
Numerical grid generation using a variational method
| MBB-FE211-S-PUB-447 | p 1297 N92-17312
Aerodynamic development of the X-31 aircraft for the high angle of attack region
| MBB-FE211-S-PUB-452 | p 1233 N92-17313
A managerial approach for reliability verification of mechanical equipment
| MBB-UK-0140-91-PUB | p 1308 N92-17341
Product assurance and safety implementation in Space Shuttle payloads: An industrial perspective
| MBB-UK-0143-91-PUB | p 1241 N92-17342
LDA and PDA systems based on diode-pumped Neodym:YAG lasers
| MBB-Z-0361-91-PUB | p 1304 N92-17526
Integration of RAMS activities during the development phase of Ariane 5-components (example: Vulcain thrust chamber)
| MBB-UK-0144-91-PUB | p 1240 N92-17527
Constraints and difficulties in implementations of RAMS assurance programmes
| MBB-UK-0141-91-PUB | p 1309 N92-17544
The need for active software product assurance management for systems critical software
| MBB-UK-0142-91-PUB | p 1341 N92-17545
Light-controlled, electrochemical, anisotropic etching of silicon
| MBB-Z-0368-91-PUB | p 1261 N92-17841

MESSERSCHMITT-BOELKOW-BLOHM G.M.B.H., OTTOBRUNN (GERMANY, F.R.).
Rapid repair of integrally stiffened carbon fibre composite structures by bolted aluminium elements
| MBB-FE202-S-PUB-0453-A | p 1256 N92-17310

METZ UNIV. (FRANCE).
Experimental investigation of adiabatic shear banding at different impact velocities
| AD-A243011 | p 1310 N92-17256

MIAMI UNIV., FL.
Characterization of the P. brevis polyether neurotoxin binding component in excitable membranes
| AD-A242877 | p 1327 N92-17564

MIAMI UNIV., OXFORD, OH.
Assessment of the behavioral and neurotoxic effects of hexachlorobenzene (HCB) in the developing rat
| AD-A243658 | p 1325 N92-17121
Magnetic muitilayer interface anisotropy
| DE92-000635 | p 1263 N92-17319

MICHIGAN STATE UNIV., EAST LANSING.
Microbial diversity: Course report 1991
| AD-A243464 | p 1326 N92-17224

MICHIGAN UNIV., ANN ARBOR.
Th 3-5 modulation and switching devices for optical system applications
| AD-A243055 | p 1365 N92-17044
Hard-surface contamination detection exercise
| DE92-004750 | p 1330 N92-17798

MIDWEST RESEARCH INST., GOLDEN, CO.
Dynamic stall on wind turbine blades
| DE92-001157 | p 1226 N92-17874
An overview: Challenges in wind technology development
| DE92-001190 | p 1313 N92-17875

MINNESOTA GEOLOGICAL SURVEY, SAINT PAUL.
University of Minnesota Aquifer Thermal Energy Storage (ATES) project report on the first long-term cycle
| DE92-004699 | p 1313 N92-17934

MISSION RESEARCH CORP., COSTA MESA, CA.
Effect of coatings and processing on failure mechanisms of polycarbonate material, phase 1
| AD-A243018 | p 1256 N92-17053

MISSION RESEARCH CORP., NASHUA, NH.
Background Atmosphere Radiance Day (BARD) and Night (BARN)
| AD-A243153 | p 1316 N92-17239

MISSION RESEARCH CORP., SANTA BARBARA, CA.
Investigation of coding techniques for memory and delay efficient interleaving in slow Rayleigh fading
| AD-A243154 | p 1280 N92-17187

MISSOURI UNIV., ROLLA.
Molecular motions of the head group of SHBS in lamellar liquid crystals
| AD-A243499 | p 1373 N92-17382

MITRE CORP., BEDFORD, MA.
Resource allocation in distributed memory multiprocessing
| AD-A243165 | p 1345 N92-17188
IMPS: An Interactive Mathematical Proof System
| AD-A243162 | p 1350 N92-17206
FY92 mathematical research project proposal briefing
| AD-A243163 | p 1350 N92-17207
Groundscreen characterization
| AD-A243164 | p 1311 N92-17208
Summary of professional activities, center for intelligence and special programs, 1990
| AD-A243508 | p 1347 N92-17385
Summary of professional activities, center for Air Force C3 systems
| AD-A243509 | p 1348 N92-17386
Superconducting microwave transmission lines
| AD-A243166 | p 1291 N92-17671
Design and evaluation of a Josephson array oscillator
| AD-A243167 | p 1291 N92-17672
USI rapid prototyping tool evaluations survey
| AD-A243168 | p 1335 N92-17673

MOHAMMED V UNIV., RABAT (MOROCCO).
Determination of diffusion parameters of thermal neutrons for non-moderator media by a pulsed method and a time independent method
| DE92-600624 | p 1362 N92-17954

MOUND LAB., MIAMISBURG, OH.
Evaluation of squib performance variables
| DE92-002034 | p 1275 N92-17533
Chromatographic separation of calcium isotopes
| DE92-004623 | p 1261 N92-17740

MSE, INC., BUTTE, MT.
Magnetohydrodynamic projects at the CDIF
|DE92-002636| p 1370 N92-17664

N

NATIONAL ACADEMY OF SCIENCES - NATIONAL RESEARCH COUNCIL, WASHINGTON, DC.
Scientific and technological relations between the United States and Japan: Issues and recommendations
|PB91-219170| p 1385 N92-17283
Plasma processing of materials: Scientific opportunities and technological challenges
|LC-91-66812| p 1370 N92-17556
Catalysis looks to the future
|LC-91-66333| p 1261 N92-17786
Policy implications of greenhouse warming: Report of the adaptation panel p 1314 N92-17982

NATIONAL ADVISORY COMMITTEE ON SEMICONDUCTORS, ARLINGTON, VA.
Toward a national semiconductor strategy. Regaining markets in high-volume electronics, volume 2
|PB91-201301| p 1290 N92-17559
Toward a national semiconductor strategy, volume 1
|PB91-201293| p 1290 N92-17620

NATIONAL AERO- AND ASTRONAUTICAL RESEARCH INST., AMSTERDAM (NETHERLANDS).
Flight test data quality evaluation
p 1230 N92-17156

NATIONAL AERONAUTICS AND SPACE ADMINISTRATION, WASHINGTON, DC.
NASA total quality management 1989 accomplishments report
|NASA-TM-105467| p 1308 N92-17005
Beyond the Baseline 1991: Proceedings of the Space Station Evolution Symposium. Volume 1: Space Station Freedom, part 1
|NASA-CP-10083-VOL-1-PT-1| p 1242 N92-17098
Space Station Freedom status p 1242 N92-17099
Advanced space transportation systems
p 1242 N92-17104
Space Station Freedom Evolution Symposium
p 1243 N92-17105
Technology development on evolutionary space station p 1243 N92-17106
Space Station Freedom science utilization: 2000 and beyond p 1244 N92-17107
Advanced studies program overview
p 1244 N92-17109
Space Station Freedom engineering prototype development p 1244 N92-17110
Space Station Freedom program. Commercial infrastructure and technology utilization
p 1244 N92-17111
NASA total quality management 1990 accomplishments report
|NASA-TM-105465| p 1308 N92-17199
Beyond the Baseline 1991: Proceedings of the Space Station Evolution Symposium. Volume 2: Space Station Freedom, part 2
|NASA-CP-10083-VOL-2-PT-2| p 1245 N92-17348
Beyond the Baseline 1991: Proceedings of the Space Station Evolution Symposium. Volume 1: Space Station Freedom, part 2
|NASA-CP-10083-VOL-1-PT-2| p 1248 N92-17409
Space Station Freedom baseline operations concept
p 1248 N92-17410
Beyond the Baseline 1991: Proceedings of the Space Station Evolution Symposium. Volume 2: Space Station Freedom, part 1
|NASA-CP-10083-VOL-2-PT-1| p 1251 N92-17768
Hubble Space Telescope: SRM/QA observations and lessons learned
|NASA-TM-105505| p 1387 N92-17873
Microgravity Science and Applications Program tasks, 1990 revision
|NASA-TM-4284| p 1276 N92-17945

NATIONAL AERONAUTICS AND SPACE ADMINISTRATION. AMES RESEARCH CENTER, MOFFETT FIELD, CA.
Facing page test for the astronaut science advisor presentation p 1248 N92-17411
The astronaut science advisor: Ground testing during SLS-1 p 1248 N92-17412
Data management system advanced architectures
p 1249 N92-17417

NATIONAL AERONAUTICS AND SPACE ADMINISTRATION. GODDARD SPACE FLIGHT CENTER, GREENBELT, MD.
The complete hard x ray burst spectrometer event list, 1980-1989
|NASA-TM-4332| p 1389 N92-17048
Collision avoidance sensor skin p 1247 N92-17361
Radio sky mapping from satellites at very low frequencies
|NASA-TM-105452| p 1387 N92-17694
Acoustic emission monitoring of low velocity impact damage in graphite/epoxy laminates during tensile loading
|NASA-TM-4339| p 1258 N92-17881
Numerical simulation of fluid flow and heat transfer in a thin liquid film over a stationary and rotating disk and comparison with experimental data
|NASA-CR-189253| p 1300 N92-17887

NATIONAL AERONAUTICS AND SPACE ADMINISTRATION. HUGH L. DRYDEN FLIGHT RESEARCH FACILITY, EDWARDS, CA.
Aircraft ground test and subscale model results of axial thrust loss caused by thrust vectoring using turning vanes
|NASA-TM-4341| p 1230 N92-17071
Failure detection and fault management techniques for flush airdata sensing systems
|NASA-TM-4335| p 1234 N92-17128
Flight vehicle thermal testing with infrared lamps
|NASA-TM-4336| p 1232 N92-17226

NATIONAL AERONAUTICS AND SPACE ADMINISTRATION. JOHN F. KENNEDY SPACE CENTER, COCOA BEACH, FL.
Computer system evolution requirements for autonomous checkout of exploration vehicles
p 1250 N92-17422

NATIONAL AERONAUTICS AND SPACE ADMINISTRATION. LYNDON B. JOHNSON SPACE CENTER, HOUSTON, TX.
STS-41 Space Shuttle mission report
|NASA-TM-105479| p 1240 N92-16973
STS-36 Space Shuttle mission report
|NASA-TM-105477| p 1240 N92-16974
STS-35 Space Shuttle mission report
|NASA-TM-105476| p 1241 N92-16975
Techniques for determination of impact forces during walking and running in a zero-G environment
|NASA-TP-3159| p 1328 N92-17022
SEI: An update p 1243 N92-17103
Failure Environment Analysis Tool (FEAT)
p 1245 N92-17349
Advanced flight software reconfiguraton
p 1245 N92-17350
Software life cycle methodologies and environments
p 1246 N92-17351
Intelligent Computer-Aided Training (ICAT)
p 1246 N92-17352
EMU evolution p 1246 N92-17354
STS-31 Space Shuttle mission report
|NASA-TM-105475| p 1241 N92-17364
Long-term corrosion evaluation of stainless steels in Space Shuttle iodinated resin and water
|NASA-TM-104743| p 1264 N92-17376
Advanced Crew Personal Support Computer (CPSC) task p 1249 N92-17419
Real Time Data System (RTDS) p 1249 N92-17421
STS-38 Space Shuttle mission report
|NASA-TM-105478| p 1242 N92-17534
Eccentric and concentric muscle performance following 7 days of simulated weightlessness
|NASA-TP-3182| p 1330 N92-17645
Active thermal control system evolution
p 1252 N92-17775
Dynamic pattern matcher using incomplete data
|NASA-CASE-MSC-21415-1-SB| p 1344 N92-17860
Closed-loop motor control using high-speed fiber optics
|NASA-CASE-MSC-21806-1| p 1368 N92-17863
Thruster sealing system and apparatus
|NASA-CASE-MSC-21898-1| p 1307 N92-17872
Treadmill for space flight
|NASA-CASE-MSC-21752-1| p 1335 N92-17910
Sharps container
|NASA-CASE-MSC-21776-1| p 1278 N92-17913

NATIONAL AERONAUTICS AND SPACE ADMINISTRATION. LANGLEY RESEARCH CENTER, HAMPTON, VA.
Neural network modeling of nonlinear systems based on Volterra series extension of a linear model
|NASA-TM-104177| p 1347 N92-16987
NASA/DoD aerospace knowledge diffusion research project: Chronology of selected literature, reports, policy instruments, and significant events affecting Federal Scientific and Technical Information (STI) in the US
|NASA-TM-101662| p 1381 N92-17001
Application of program LAURA to perfect gas shock tube flows: A parametric study
|NASA-TM-104190| p 1294 N92-17002
The use of impact force as a scale parameter for the impact response of composite laminates
|NASA-TM-104189| p 1256 N92-17007
Free volume variation with molecular weight of polymers
|NASA-TM-4326| p 1267 N92-17032
Experiences at Langley Research Center in the application of optimization techniques to helicopter airframes for vibration reduction
|NASA-TM-104193| p 1309 N92-17033
The NASA/industry design analysis methods for vibrations (DAMVIBS) program: Accomplishments and contributions
|NASA-TM-104192| p 1309 N92-17034
A historical perspective on space station
p 1244 N92-17108
Evolution design requirements and design strategy
p 1244 N92-17112
The multi-attribute task battery for human operator workload and strategic behavior research
|NASA-TM-104174| p 1338 N92-17130
Two-dimensional stability of laminar flames
|NASA-TP-3131| p 1223 N92-17131
The computational structural mechanics testbed procedures manual
|NASA-TM-100646| p 1310 N92-17333
Long duration exposure facility post-flight thermal analysis: Orbital/thermal environment data package
|NASA-CR-189872| p 1245 N92-17334
Long duration exposure facility solar illumination data package
|NASA-CR-189873| p 1241 N92-17335
Evolution user requirements for the restructured space station p 1248 N92-17413
SSF growth concepts and configurations
p 1248 N92-17414
Structural dynamics division research and technology accomplishments for F.Y. 1991 and plans for F.Y. 1992
|NASA-TM-104188| p 1225 N92-17509
User guide for WIACX: A transonic wind-tunnel wall interference assessment and correction procedure for the NTF
|NASA-TM-104168| p 1225 N92-17547
Polyimides containing amide and perfluoroisopropyl connecting groups
|NASA-CASE-LAR-14608-1| p 1271 N92-17676
Substantially oxygen-free contact tube
|NASA-CASE-LAR-14169-1| p 1307 N92-17677
Imide/arylene ether copolymers with pendent trifluoromethyl groups
|NASA-TM-104195| p 1272 N92-17693
A method and apparatus for indicating disbonds in joint regions
|NASA-CASE-LAR-14626-1| p 1309 N92-17859
Active control of pressure loads using passive porosity
|NASA-CASE-LAR-14594-1| p 1300 N92-17888
Passive control of pressure loads using porosity
|NASA-CASE-LAR-14547-1| p 1300 N92-17909
Joint University Program for Air Transportation Research, 1990-1991
|NASA-CP-3131| p 1219 N92-17984

NATIONAL AERONAUTICS AND SPACE ADMINISTRATION. LEWIS RESEARCH CENTER, CLEVELAND, OH.
Advanced Communication Technology Satellite (ACTS) multibeam antenna analysis and experiment
|NASA-TM-105420| p 1279 N92-17047
Advanced nozzle and engine components test facility
|NASA-TM-103684| p 1237 N92-17059
Reliability analysis of structural ceramic components using a three-parameter Weibull distribution
|NASA-TM-105370| p 1267 N92-17060
Safety considerations in testing a fuel-rich aeropropulsion gas generator
|NASA-TM-105258| p 1235 N92-17061
Multiple-access phased array antenna simulator for a digital beam forming system investigation
|NASA-TM-105422| p 1279 N92-17062
Environmental interactions in Space Exploration: Announcement of the formation of an Environmental Interactions Working Group
|NASA-TM-105294| p 1389 N92-17069
High-temperature durability considerations for HSCT combustor
|NASA-TP-3162| p 1267 N92-17070
Upper stages using liquid propulsion and metallized propellants
|NASA-TP-3191| p 1253 N92-17151
Viscous three-dimensional calculations of transonic fan performance
|NASA-TM-103800| p 1219 N92-17346
Experimental ice shape and performance characteristics for a multi-element airfoil in the NASA Lewis Icing Research Tunnel
|NASA-TM-105380| p 1224 N92-17347
Space Station Freedom/lunar transfer vehicle propellant operation hazard analysis p 1249 N92-17416

Experiments and analysis concerning the use of external burning to reduce aerospace vehicle transonic drag
|NASA-TM-105397| p 1235 N92-17546
Three point lead screw positioning apparatus
|NASA-CASE-LEW-15216-1| p 1307 N92-17678
Solar dynamic technology status for Space Station Freedom application p 1251 N92-17770
Space Station Freedom electric power system evolution analysis status p 1251 N92-17771
Automated power management and control p 1252 N92-17773
Intercalated hybrid graphite fiber composite
|NASA-CASE-LEW-15241-1| p 1257 N92-17861
Substituted 1,1,1-triaryl-2,2,2-trifluoroethanes and processes for their synthesis
|NASA-CASE-LEW-14345-6| p 1255 N92-17882
Storing fluorine gas in carbon fibers and releasing the same
|NASA-CASE-LEW-15359-1| p 1261 N92-17902

NATIONAL AERONAUTICS AND SPACE ADMINISTRATION. MARSHALL SPACE FLIGHT CENTER, HUNTSVILLE, AL.

Partnership for Continuous Improvement
|NASA-TM-105464| p 1308 N92-16988
Environmental control and life support system evolution analysis p 1246 N92-17355
The environmental control and life support system advanced automation project p 1246 N92-17356
System for testing bearings
|NASA-CASE-MFS-28589-1| p 1306 N92-17584
FY 1991 scientific and technical reports, articles, papers, and presentations
|NASA-TM-103567| p 1384 N92-17586
The SSM/PMAD automated test bed project p 1252 N92-17774
Automatic locking orthotic knee device
|NASA-CASE-MFS-28633-1| p 1335 N92-17866
Production of mullite fibers
|NASA-CASE-MFS-28431-1| p 1257 N92-17870

NATIONAL AERONAUTICS AND SPACE ADMINISTRATION. PASADENA OFFICE, CA.

Three-stage sorption type cryogenic refrigeration system and method employing heat regeneration
|NASA-CASE-NPO-18366-1-CU| p 1277 N92-17674
Real-time edge-enhanced optical correlator
|NASA-CASE-NPO-18379-1-CU| p 1367 N92-17675
Multiperiod-grating surface-emitting lasers
|NASA-CASE-NPO-17763-1-CU| p 1305 N92-17862
Near real-time stereo vision system
|NASA-CASE-NPO-18593-1-CU| p 1368 N92-17864
Method for non-destructive estimation of waveguide directional coupler dimensions
|NASA-CASE-NPO-18454-1-CU| p 1293 N92-17865
Neural-network dedicated processor for solving competitive assignment problems
|NASA-CASE-NPO-17781-1-CU| p 1337 N92-17884
Wide field strip-imaging optical system
|NASA-CASE-NPO-18146-1-CU| p 1368 N92-17892
High level language-based robotic control system
|NASA-CASE-NPO-17918-2-CU| p 1349 N92-17895
Self-collimated unstable resonator semiconductor laser
|NASA-CASE-NPO-18386-1-CU| p 1305 N92-17899
Transformerless DC-DC voltage amplifier with optically isolated switching devices
|NASA-CASE-NPO-17994-1-CU| p 1293 N92-17907

NATIONAL AEROSPACE LAB., TOKYO (JAPAN).

Weight evaluation and sensitivity analysis for space plane. Part 2: TSTO
|NAL-TM-602-PT-2| p 1251 N92-17754
Results of measured temperature distribution on an adiabatic wing model with radiation thermometer
|NAL-TM-610| p 1225 N92-17755
Improvement of data processing system for gust wind tunnel data acquisition part: System conversion from off-line to on-line processing
|NAL-TM-611| p 1238 N92-17756
Discussion for possibility of some aerodynamic ground effect craft
|NAL-TM-619| p 1278 N92-17757
Making of functionally gradient materials data base
|NAL-TM-621| p 1385 N92-17787
Systematic computation algorithm to obtain osculating orbit elements from position and velocity vectors
|NAL-TM-614| p 1239 N92-17854
Hydrogen fueled subsonic-ram-combustor model tests for an air-turbo-ram engine
|NAL-TR-1064T| p 1236 N92-17855
Experimental investigation of interlaminar fracture toughness of carbon fiber/thermoplastic and carbon fiber/thermosetting composites by DCB specimens
|NAL-TR-1096| p 1257 N92-17869
Identification of the stability and control derivatives of a DLC-flap system for VSRA
|NAL-TR-1116| p 1237 N92-17917

NATIONAL CENTER FOR ATMOSPHERIC RESEARCH, BOULDER, CO.

Meeting Review: Airborne Aerosol Inlet Workshop
|NASA-CR-189814| p 1313 N92-17393

NATIONAL GEOPHYSICAL DATA CENTER, BOULDER, CO.

Solar-geophysical data number 562, June 1991. Part 2: (Comprehensive reports). Data for December 1990 and miscellaneous
|PB91-230219| p 1387 N92-17251

NATIONAL HURRICANE CENTER, CORAL GABLES, FL.

Diagnostic report of the National Hurricane Center, August and September 1990, volume 3, number 2
|PB91-226886| p 1321 N92-17621

NATIONAL INST. OF STANDARDS AND TECHNOLOGY, BOULDER, CO.

Unsteady laminar flow in a circular tube: A test of the HERCOL (Hermitian collocation) computer code
|PB91-222679| p 1295 N92-17018
Aluminum alloys for ALS cryogenic tanks: Comparative measurements of cryogenic mechanical properties of Al-Li alloys and alloy 2219
|AD-A242956| p 1264 N92-17379
Spherical near-field scanning: Experimental and theoretical studies
|AD-A243489| p 1282 N92-17429
Cooled ion frequency standard
|AD-A242030| p 1360 N92-17549
Liquid and solid ion plasmas
|AD-A242029| p 1370 N92-17635

NATIONAL INST. OF STANDARDS AND TECHNOLOGY, GAITHERSBURG, MD.

Determination of the optical constants of thin Chemical-Vapor-Deposited diamond windows from 0.5 to 6.5 eV
|AD-A243094| p 1268 N92-17170
Chemical vapor deposited diamond
|AD-A243095| p 1268 N92-17171
Use of diamond as an optical material
|AD-A243097| p 1268 N92-17172
High resolution electron microscopy of diamond film growth defects and their interactions
|AD-A243093| p 1372 N92-17238
Strength and microstructure of ceramics
|AD-A243049| p 1269 N92-17282
Transmission electron microscopy of the CVD diamond film/substrate interface
|AD-A243096| p 1373 N92-17322
Spatially and spectrally resolved cathodoluminescence measurements of CVD-grown diamond particles and films
|AD-A243220| p 1271 N92-17615

NATIONAL OCEANIC AND ATMOSPHERIC ADMINISTRATION, BOULDER, CO.

Recommendations for a wind profiling network to support Space Shuttle launches
|NASA-CR-4421| p 1318 N92-17072

NATIONAL OCEANIC AND ATMOSPHERIC ADMINISTRATION, MIAMI, FL.

Surface meteorological and near surface oceanographic atlas of the tropical Indian Ocean
|PB91-234286| p 1319 N92-17138

NATIONAL RESEARCH COUNCIL OF CANADA, OTTAWA (ONTARIO).

Flight evaluation of curved MLS precision approaches in a twin otter aircraft, phase 2
|AD-A243025| p 1229 N92-17568

NATIONAL SPACE DEVELOPMENT AGENCY, TOKYO (JAPAN).

Status of Japanese Experiment Module (JEM) activities p 1243 N92-17101

NATIONAL TRANSPORTATION SAFETY BOARD, WASHINGTON, DC.

Aircraft accident reports: Brief format. US civil and foreign aviation issue number 4 of 1989 accidents
|PB90-916904| p 1226 N92-17133
Aircraft accident report: Northwest Airlines, Inc., Flights 1482 and 299. Runway incursion and collision, Detroit Metropolitan/Wayne County Airport, Romulus, Michigan, December 3, 1990
|PB91-910405| p 1226 N92-17213

NATIONAL WEATHER SERVICE, BOHEMIA, NY.

The use of ADAP to examine warm and quasi-stationary frontal events in the northeastern United States
|PB91-225037| p 1319 N92-17363

NAVAL AIR DEVELOPMENT CENTER, WARMINSTER, PA.

Aircrew critique of high-G centrifuge training: Part 3: What can we change to better serve you?
|AD-A243496| p 1334 N92-17432
The square root cordic
|AD-A242318| p 1342 N92-17561

NAVAL MEDICAL RESEARCH INST., BETHESDA, MD.

Statistically-based decompression tables. 6: Repeat dives on oxyen/nitrogen mixes
|AD-A243667| p 1328 N92-17124

NAVAL OCEAN SYSTEMS CENTER, SAN DIEGO, CA.

Performance modeling of the Ada rendezvous
|AD-A243392| p 1339 N92-17211
Information Management Engineering (IME) laboratory: A database development facility
|AD-A243191| p 1383 N92-17369
Evaporation duct communication: Test plan, part 2
|AD-A243505| p 1282 N92-17383
Parallel processing applied to computational electromagnetics
|AD-A242372| p 1345 N92-17395
Parallel block methods for sparse symmetric linear systems of equations
|AD-A242315| p 1351 N92-17560
Novel ceramic matrix composites for deep submergence pressure vessel applications
|AD-A242740| p 1274 N92-17947

NAVAL OCEANOGRAPHIC AND ATMOSPHERIC RESEARCH LAB., BAY SAINT LOUIS, MS.

Sea surface environmental conditions in the Gulf of Alaska during April 1990 using SSM/I
|AD-A241909| p 1323 N92-17041
Multispectral software development for the Airborne Bathymetric Survey System
|AD-A243774| p 1325 N92-17765
Ocean simulation model. Version 2: First order frontal simulation
|AD-A243775| p 1325 N92-17766

NAVAL OCEANOGRAPHIC AND ATMOSPHERIC RESEARCH LAB., MONTEREY, CA.

Severe weather guide mediterranean ports. Part 35: Rota
|AD-A243539| p 1319 N92-17338
Severe weather guide Mediterranean ports. Part 38: Alexandria
|AD-A243451| p 1320 N92-17406
Severe weather guide Mediterranean ports. Part 36: Limassol
|AD-A243448| p 1320 N92-17492
Severe weather guide Mediterranean ports. Part 37: Larnaca
|AD-A243449| p 1320 N92-17493
Severe weather guide Mediterranean ports. Part 39: Port Said
|AD-A243450| p 1320 N92-17494

NAVAL POSTGRADUATE SCHOOL, MONTEREY, CA.

Noncoherent detection of coherent optical heterodyne signals corrupted by laser phase noise
|AD-A243103| p 1364 N92-16981
A Kalman filter for a Poisson series with covariates and Laplace approximation integration
|AD-A242960| p 1286 N92-16993
Acoustic impedance of materials from reverberation time
|AD-A243184| p 1354 N92-16999
A powder x ray diffraction study of two aluminum-lithium based alloys
|AD-A243186| p 1262 N92-17000
Water vapor influence on satellite-measured aerosol characteristics
|AD-A241918| p 1315 N92-17008
A CAD model for the axial inductive strip with finite thickness centered in homogeneous finline with w/b = 1
|AD-A243553| p 1278 N92-17016
Exploring plasma sheath solutions for planar and cylindrical anodes
|AD-A243237| p 1369 N92-17030
A ring model for local/mobile radio communications with variable packet length
|AD-A241856| p 1279 N92-17036
Source of cold water in Monterey Bay observed by AVHRR satellite imagery
|AD-A242843| p 1323 N92-17051
Economic analysis of information system
|AD-A243079| p 1382 N92-17067
A study on hydrographic conditions and salt budget calculation for the Gulf of Farallones with the data collected in August 1990
|AD-A243406| p 1324 N92-17119
Benefit analysis of proposed information systems
|AD-A243707| p 1382 N92-17125
Local area network strategies and guidelines for a Peruvian Air Force Computer Center
|AD-A242841| p 1345 N92-17135
Electronic data interchange
|AD-A242959| p 1382 N92-17136
An investigation of cold overflow over the Iceland/Faeroes Ridge
|AD-A243084| p 1324 N92-17169
The effect of titanium inclusions on HY-80 GMA weld deposits
|AD-A243408| p 1239 N92-17192
Computer aided thermal analysis of a microcircuit structure
|AD-A243160| p 1287 N92-17205

Escape strategies for turboprop aircraft in a microburst windshear
| AD-A243090 | p 1227 N92-17217
An overview of cellular telecommunications
| AD-A242951 | p 1281 N92-17232
An analysis of mission critical computer software in Naval aviation
| AD-A243078 | p 1339 N92-17237
Communication network survivability
| AD-A242969 | p 1281 N92-17252
Stellar spectral line synthesis from an individual photon-following simulation
| AD-A242970 | p 1388 N92-17253
The top ten critical MIS issues in the Department of Defense
| AD-A242975 | p 1382 N92-17255
Study of plane wave impingement on a thin plate capable of deformation
| AD-A242947 | p 1296 N92-17275
Optimal configuration of digital communication network
| AD-A243041 | p 1282 N92-17277
A graphical database interface for a multimedia DBMS
| AD-A243283 | p 1339 N92-17285
A discontinuity study in shielded coplanar line
| AD-A242976 | p 1288 N92-17290
Training methodologies for dependent Speech Recognition (SR) systems
| AD-A242983 | p 1282 N92-17293
A wing rock model for the F-14A aircraft
| AD-A243109 | p 1233 N92-17300
Measurement of electron beam emittance using optical transition radiation and development of a diffuse screen electron beam monitor
| AD-A241893 | p 1357 N92-17306
Study of transition phenomena in a straight channel with 40 to 1 aspect ratio with and without imposed pulsations. Part two: Reynolds number surveys
| AD-A241894 | p 1296 N92-17307
Transition phenomena in a straight channel with a 40 to 1 aspect ratio with and without imposed pulsations. Part 1: Near-wall and central region profiles
| AD-A243251 | p 1297 N92-17337
Flow visualization and wake analysis for standard and modified configurations of the AN/ALQ-78 antenna pod
| AD-A243552 | p 1224 N92-17339
Cost models and the Corporate Information Management (CIM) initiative
| AD-A243554 | p 1383 N92-17340
Effect of economic techniques on radio frequency utilization
| AD-A243187 | p 1282 N92-17366
Static analysis of thick composite plates using higher order three dimensional finite elements
| AD-A243188 | p 1256 N92-17367
The development of user interface tools for the computer aided prototyping system
| AD-A243189 | p 1340 N92-17368
A management case analysis of the Department of Defense contractor risk assessment guide program
| AD-A243515 | p 1380 N92-17388
Towards intelligent data retrieval in multimedia databases
| AD-A243323 | p 1383 N92-17402
A stochastic approach to the weighted-region problem: 1. The design of the path annealing algorithm
| AD-A243324 | p 1340 N92-17403
Optimization in solar heating/photovoltaic systems
| AD-A242363 | p 1313 N92-17424
Delay analysis for multidimensional queueing process in CSMA/CD local area networks
| AD-A242364 | p 1346 N92-17425
Some foundations for empirical study in the euclidean spatial model of social choice
| AD-A241928 | p 1352 N92-17440
Natural resonances of slotted cylinder configurations
| AD-A241934 | p 1282 N92-17441
Multiple input sliding mode control for autonomous diving and steering of underwater vehicles
| AD-A241935 | p 1237 N92-17442
Nucleate pool boiling performance of small high flux and turbo-B tube bundles in R-114/oil mixtures
| AD-A241936 | p 1378 N92-17443
Feedback in dynamic decision making: An experiment in software project management
| AD-A242361 | p 1380 N92-17451
Microstructure and mechanical properties of HSLA-100 steel
| AD-A242937 | p 1265 N92-17467
The V-22: Can the nation afford to forgo its production?
| AD-A243158 | p 1219 N92-17477
High-frequency meteorological phenomena observed with the Naval Postgraduate School's UHF Doppler wind profiler
| AD-A243762 | p 1320 N92-17515
A probabilistic derivation of Stirling's formula
| AD-A241899 | p 1354 N92-17548
Modeling convergence zone gain on MS-DOS based personal computers
| AD-A243252 | p 1341 N92-17558
Comparison of alkali ion emitters
| AD-A243105 | p 1290 N92-17570
Suspended substrate resonator design
| AD-A243250 | p 1290 N92-17573
A comparison of data integrity models
| AD-A243770 | p 1384 N92-17633
Using the Global Positioning System (GPS) to fulfill the position/location requirements of the National Training Center (NTC) and other US Army instrumented testing and training ranges
| AD-A242064 | p 1229 N92-17639
Bayesian computations in survival models via the Gibbs sampler
| AD-A242343 | p 1353 N92-17643
Design implementation into field programmable gate arrays
| AD-A242538 | p 1343 N92-17680
Effects of power pulsations on heat transfer from discrete heat sources
| AD-A243434 | p 1379 N92-17686
Development of a knowledge base for use in an Expert System Advisor for Aircraft Maintenance Scheduling (ESAAMS)
| AD-A243435 | p 1381 N92-17687
Heat transfer enhancement due to bubble pumping in FC-72 near the saturation temperature
| AD-A243558 | p 1292 N92-17724
An analysis of the aircraft engine Component Improvement Program (CIP): A life cycle cost approach
| AD-A243346 | p 1236 N92-17729
The influence of temperature and composition on the activation energy for creep in binary aluminum lithium alloys
| AD-A242299 | p 1265 N92-17759
Preliminary results from the analysis of wind component error
| AD-A243772 | p 1321 N92-17764

NAVAL RESEARCH LAB., WASHINGTON, DC.

Effective viscosity in the simulation of spatially evolving shear flows with monotonic FCT models
| AD-A243709 | p 1295 N92-17126
The effects of field errors on low-gain free electron lasers
| AD-A243710 | p 1303 N92-17127
Some aspects of nonneutral plasma physics
| AD-A243711 | p 1369 N92-17499
Evidence for MeV particle emission from Ti charged with low energy deuterium ions
| AD-A243718 | p 1359 N92-17505
A study of channel-access schemes for integrated voice/data radio networks
| AD-A243584 | p 1286 N92-17931

NAVAL SURFACE WARFARE CENTER, DAHLGREN, VA.

Significant digit computation of the ellipsoidal coverage function and its inverse
| AD-A242322 | p 1350 N92-17242
Forth Graphics Toolbox (A user's guide for use with RFF FORTH)
| AD-A242916 | p 1342 N92-17581

NAVAL SURFACE WARFARE CENTER, SILVER SPRING, MD.

Effective dynamic material parameters and localized scattering
| AD-A241957 | p 1310 N92-17320
ZEUS user manual real gas effects
| AD-A242224 | p 1225 N92-17446

NAVAL TRAINING SYSTEMS CENTER, ORLANDO, FL.

Research and development project summaries, October 1991
| AD-A243477 | p 1391 N92-17372

NAVAL UNDERWATER SYSTEMS CENTER, WEST PALM BEACH, FL.

A statistical analysis of Eleuthera Island wind data for the period 27 April 1989 through 30 March 1990
| AD-A241885 | p 1318 N92-17027

NAVAL WEAPONS CENTER, CHINA LAKE, CA.

Growth of near-free-standing YBa2Cu3O7-type crystals using a self-decanting flux method
| AD-A243221 | p 1372 N92-17182
Evidence for strong electron-phonon coupling in thermal conductivity of YBa2Cu3O(7-delta)
| AD-A243192 | p 1372 N92-17218
A reexamination of F-19 NMR in selected solids, the conductor Ag2F and reference insulators for studies of YBa2Cu3O7-type superconductors
| AD-A243194 | p 1372 N92-17219
Determination of the electronic density of states of YBa2Cu3O(7-delta)
| AD-A243223 | p 1372 N92-17220
New optical materials for the long-wave (8-12 microns) region: Design criteria for the solid-state chemist
| AD-A243280 | p 1365 N92-17284
Pressure dependence of Tc in Tl2Ba2CaCu2O8 at hydrostatic pressures to 6 GPa
| AD-A243433 | p 1375 N92-17685

NAVY CLOTHING AND TEXTILE RESEARCH FACILITY, NATICK, MA.

Thermal energy test apparatus
| AD-A243526 | p 1379 N92-17537

NAVY EXPERIMENTAL DIVING UNIT, PANAMA CITY, FL.

Evaluation of BAUER high pressure breathing air P-2 purification system
| AD-A243535 | p 1333 N92-17014
Unmanned evaluation of BAUER high pressure breathing air P-5 purification system
| AD-A243486 | p 1334 N92-17331

NEBRASKA UNIV., LINCOLN.

Study of features of binary images using algebra techniques
| AD-A242010 | p 1351 N92-17609

NETROLOGIC, INC., SAN DIEGO, CA.

Fractal image encoding
| AD-A243620 | p 1344 N92-17921

NEW JERSEY INST. OF TECH., NEWARK.

The shapes and cavities of four cholic acid host systems
| AD-A243483 | p 1255 N92-17329

NEW MEXICO UNIV., ALBUQUERQUE.

Characterization of the thermalness of a fissile system with a 2-group diffusion theory parameter
| AD-A243065 | p 1360 N92-17555

NEW ORLEANS UNIV., LA.

Computational studies of energetic nitramines
| AD-A241870 | p 1356 N92-17038

NORTH CAROLINA STATE UNIV., RALEIGH.

Adaptive presort processing
| AD-A243286 | p 1340 N92-17286
Research and development on advanced silicon carbide thin film growth techniques and fabrication of high power and microwave frequency silicon carbide-based device structures
| AD-A243531 | p 1373 N92-17390
A theoretical search for supervelocity semiconductors
| AD-A241981 | p 1376 N92-17783

NORTH CAROLINA UNIV., CHAPEL HILL.

Materials processing of diamond: Etching, doping by ion implantation and contact formation
| AD-A243060 | p 1267 N92-17065
An oxygen tracer study of InP oxidation
| AD-A242832 | p 1259 N92-17246
An in-situ spectroscopic ellipsometry study of the electron cyclotron resonance plasma oxidation of silicon and interfacial
| AD-A242833 | p 1259 N92-17247
Infrared rotating analyzer ellipsometry: Calibration and data processing
| AD-A242834 | p 1259 N92-17248
A study of nonlinear reflection and optical switching in indium antimonide
| AD-A242835 | p 1365 N92-17249
A spectroscopic immersion ellipsometry study of the mechanism of Si/SiO2 interface annealing
| AD-A242831 | p 1259 N92-17261
A kinetics study of the electron cyclotron resonance plasma oxidation of silicon
| AD-A242868 | p 1290 N92-17596
An interface enhanced spectroscopic ellipsometry technique: Application to Si-SiO2
| AD-A242867 | p 1260 N92-17613
Electronic expansion of human perception
| AD-A242028 | p 1333 N92-17634
Incremental volume rendering algorithm for interactive 3D ultrasound imaging
| AD-A242048 | p 1342 N92-17637
Parallel radiosity techniques for mesh-connected SIMD computers
| AD-A242049 | p 1346 N92-17638
The UNC graph server: A distributed hypermedia data management system
| AD-A242041 | p 1380 N92-17651
Mathematical basis for a system to manage automated protocol analysis
| AD-A242042 | p 1381 N92-17669
Scan directed load balancing for highly-parallel mesh-connected computers
| AD-A242045 | p 1346 N92-17670

NORTHROP CORP., HAWTHORNE, CA.

Finite element analysis of ASTOVL fighter structure
| AD-A243724 | p 1233 N92-17513

NORTHWEST RESEARCH ASSOCIATES, INC., BELLEVUE, WA.
An investigation of methods for updating ionospheric scintillation models using topside in-situ plasma density measurements
| AD-A243378 | p 1316 N92-17209
NOTRE DAME UNIV., IN.
Sub-band/transform compression of video sequences
| NASA-CR-189786 | p 1280 N92-17139
NSI TECHNOLOGY SERVICES CORP., DAYTON, OH.
Assessment of the behavioral and neurotoxic effects of hexachlorobenzene (HCB) in the developing rat
| AD-A243658 | p 1325 N92-17121
Evaluation of the initiation/promotion potential of CTFE trimer acid
| AD-A243479 | p 1255 N92-17373

O

OAK RIDGE ASSOCIATED UNIVERSITIES, INC., TN.
Labor market trends for health physicists
| DE92-004770 | p 1331 N92-17800
OAK RIDGE NATIONAL LAB., TN.
Diffraction and imaging theory of inelastically scattered electrons: A new approach
| DE91-018248 | p 1360 N92-17574
DOE Task Force Meeting on Electrical Breakdown of Insulating Ceramics in a High Radiation Field
| DE92-000459 | p 1270 N92-17576
Detection of explosives material on single microparticles
| DE92-004408 | p 1276 N92-17963
OFFICE OF NAVAL RESEARCH, ARLINGTON, VA.
Workshop on Plasma Experiments in the Laboratory and in Space. Abstracts
| AD-A243645 | p 1370 N92-17734
OFFICE OF TECHNOLOGY ASSESSMENT, WASHINGTON, DC.
Changing by degrees: Steps to reduce greenhouse gases
| PB91-205120 | p 1314 N92-17619
OHIO STATE UNIV., COLUMBUS.
Codeposition of elements in diffusion coatings by the halide-activated pack cementation method
| AD-A242860 | p 1267 N92-17042
Automated composite ellipsoid modelling for high frequency GTD analysis
| NASA-CR-189853 | p 1233 N92-17316
Evaluation of liposome-encapsulated Hemoglobin/LR16 formulations as a potential blood substitute
| AD-A243075 | p 1329 N92-17557
OHIO UNIV., ATHENS.
Luminescence and electroluminescence properties of Nd, Tm, Yb doped GaAs II-VI compounds
| AD-A242039 | p 1375 N92-17667
Investigation of air transportation technology at Ohio University, 1990-1991 p 1220 N92-17990
A hybrid modulation for the dissemination of weather data to aircraft p 1220 N92-17991
Fault detection and isolation for multisensor navigation systems p 1221 N92-17992
Establishing an evoked-potential vision-tracking system p 1221 N92-17993
GPS interferometric attitude and heading determination: Initial flight test results p 1221 N92-17994
OLD DOMINION UNIV., NORFOLK, VA.
Polymer infiltration studies
| NASA-CR-189773 | p 1266 N92-17004
The solution of a singular integral equation arising from a lifting surface theory for rotating blades p 1224 N92-17303
OREGON STATE UNIV., CORVALLIS.
Turbulent and gravity wave transport in the free atmosphere p 1315 N92-17063
OXFORD UNIV. (ENGLAND).
Application of multi-target tracking to sonar-based mobile robot navigation
| OUEL-1819/90 | p 1229 N92-17878
Wall temperature patterns in nucleate boiling
| OUEL-1876/91 | p 1380 N92-17879
Adaptive generalized predictive control
| OUEL-1879/91 | p 1349 N92-17880
A fully decentralized multi-sensor system for tracking and surveillance
| OUEL-1886/91 | p 1302 N92-17926
A decentralized Bayesian algorithm for identification of tracked targets
| OUEL-1892/91 | p 1344 N92-17927

P

PACIFIC MISSILE TEST CENTER, POINT MUGU, CA.
Tidal and lunar data for Point Mugu, San Nicolas Island, and the Barking Sands area during 1992
| AD-A243210 | p 1324 N92-17177
PACIFIC NORTHWEST LAB., RICHLAND, WA.
Verification of an effective dose equivalent model for neutrons
| DE92-002738 | p 1358 N92-17453
Evolution of an environmental audit program
| DE92-002681 | p 1314 N92-17665
University of Minnesota Aquifer Thermal Energy Storage (ATES) project report on the first long-term cycle
| DE92-004699 | p 1313 N92-17934
PACIFIC-SIERRA RESEARCH CORP., LOS ANGELES, CA.
Biological effects of protracted exposure to ionizing radiation: Review, analysis, and model development
| AD-A242981 | p 1329 N92-17476
PENNSYLVANIA STATE UNIV., UNIVERSITY PARK.
Bottom contour influence on ray tracing
| AD-A242411 | p 1323 N92-17078
The effects of sediment porosity on acoustic reflection and transmission at the seafloor
| AD-A241943 | p 1323 N92-17083
The 5th Annual US-Japan Seminar on Dielectric and Piezoelectric Ceramics
| AD-A243465 | p 1268 N92-17193
A one-dimensional plasma and impurity transport model for reversed field pinches
| DE92-004691 | p 1371 N92-17933
PENNSYLVANIA UNIV., PHILADELPHIA.
Computational and neural network models for the analysis of visual texture
| AD-A243717 | p 1327 N92-17504
Programming mechanical simulations
| AD-A243767 | p 1341 N92-17538
The dynamics of visual representation, attention, encoding, and retrieval processes
| AD-A243031 | p 1384 N92-17785
PHILLIPS LAB., HANSCOM AFB, MA.
A proposed improved method of radiosonde humidity sensing
| AD-A242954 | p 1319 N92-17233
PHILLIPS LAB., KIRKLAND AFB, NM.
Frequency stirring: An alternate approach to mechanical mode-stirring for the conduct of electromagnetic susceptibility testing
| AD-A243551 | p 1279 N92-17031
Correlator optical wavefront sensor COWS
| DE92-003964 | p 1368 N92-17846
PHYSICAL SCIENCES, INC., ANDOVER, MA.
Velocity measurements in high temperature gases using laser-induced no fluorescence
| AD-A242399 | p 1295 N92-17012
Rates and mechanisms of metastable deactivation over surfaces
| AD-A243391 | p 1361 N92-17652
PITTSBURGH UNIV., PA.
Catalytic studies on a novel synthesis of methanol
| DE92-002904 | p 1275 N92-17184
Study of turbulence by photon correlation spectroscopy
| AD-A243726 | p 1298 N92-17688
PLESSEY RESEARCH (CASWELL) LTD., TOWCESTER (ENGLAND).
Microstrip discontinuity models to 60 GHz
| AD-A242038 | p 1339 N92-17185
PRATT AND WHITNEY AIRCRAFT, WEST PALM BEACH, FL.
Fatigue in single crystal nickel superalloys
| AD-A243453 | p 1265 N92-17653
PRINCETON UNIV., NJ.
Causal models in the acquisition and instruction of programming skills
| AD-A242899 | p 1340 N92-17463
Surface chemistry at the semiconductor/electrolyte interface
| DE91-018511 | p 1374 N92-17532
Investigation of air transportation technology at Princeton University, 1990-1991 p 1221 N92-17995
Target pitch angle for the microburst escape maneuver p 1221 N92-17996
Stochastic robustness p 1221 N92-17997
Neural networks for aircraft system identification p 1222 N92-17998
Intelligent failure-tolerant control p 1222 N92-18000
Systematic methods for knowledge acquisition and expert system development p 1222 N92-18001
Technical notes and correspondence: Stochastic robustness of linear time-invariant control systems p 1222 N92-18002
PUERTO RICO UNIV., RIO PIEDRAS.
In situ surface x ray scattering of metal monolayers adsorbed at solid-liquid interfaces
| AD-A243258 | p 1262 N92-16985
In situ surface x ray crystallography of electrochemically deposited Bi on Ag(111): Structure, compressibility, and anisotropy
| AD-A243218 | p 1372 N92-17181
An investigation of underpotentially deposited thallium of silver (111) by in-situ surface x ray scattering
| AD-A243270 | p 1263 N92-17271
Estimation of the outer sphere contribution to the activation parameters for homogeneous electron transfer reactions using the mean spherical approximation
| AD-A243217 | p 1259 N92-17323
A model for voltammograms of the underpotential deposition of metals
| AD-A243199 | p 1264 N92-17370
Application of the mean spherical approximation to describe the Gibbs solvation energies of monovalent monoatomic ions in non-aqueous solvents
| AD-A243200 | p 1259 N92-17371
PURDUE UNIV., WEST LAFAYETTE, IN.
Injection of drag reducing additives into turbulent water flows
| AD-A243209 | p 1296 N92-17176
Atomic relaxation at ordered electrochemical surfaces probed by scanning tunneling microscopy: Au(111) in aqueous solution compared with ultrahigh-vacuum environments
| AD-A242031 | p 1358 N92-17472

R

RANGE COMMANDERS COUNCIL, WHITE SANDS MISSILE RANGE, NM.
Laser range safety
| AD-A243606 | p 1305 N92-17962
RESEARCH TRIANGLE INST., RESEARCH TRIANGLE PARK, NC.
AGSSS: The Airborne Graphics Software Support System; an Ada/PHIGS-based display editor for the rapid development of cockpit display software systems
| AD-A243224 | p 1234 N92-17221
RHODE ISLAND UNIV., KINGSTON.
Blistering of graphite/polymer composites galvanically coupled with metals in sea water
| AD-A242861 | p 1269 N92-17262
RICE UNIV., HOUSTON, TX.
A numerical code for a three-dimensional magnetospheric MHD equilibrium model
| NASA-CR-189852 | p 1318 N92-17227
RMA AEROSPACE, INC., MOUNTAIN VIEW, CA.
Preliminary development of a three-dimensional nonlinear approximation procedure for turbomachinery design optimization applications
| AD-A243155 | p 1235 N92-17644
ROCKWELL INTERNATIONAL CORP., DOWNEY, CA.
Results of the space shuttle vehicle ascent air data system probe calibration test using a 0.07-scale external tank forebody model (68T) in the AEDC 16-foot transonic wind tunnel (IA-310), volume 1
| NASA-CR-167696 | p 1241 N92-17167
Results of the space shuttle vehicle ascent air data system probe calibration test using a 0.07-scale external tank forebody model (68T) in the AEDC 16-foot transonic wind tunnel (IA-310), volume 2
| NASA-CR-167697 | p 1241 N92-17214
ROCKWELL INTERNATIONAL SCIENCE CENTER, ANAHEIM, CA.
Dielectric properties of aligned conducting polymers
| AD-A243389 | p 1268 N92-17191
ROME LAB., GRIFFISS AFB, NY.
A performance model of Thermal Imaging System (TISs) which includes the human observer's response to state of the art displays
| AD-A242838 | p 1301 N92-17273
Gate drain geometry effect on the current voltage characteristics of GaAs MESFETs
| AD-A243430 | p 1291 N92-17684
ROYAL AEROSPACE ESTABLISHMENT, BEDFORD (ENGLAND).
SA 330 Puma identification results p 1231 N92-17162
Application areas for rotorcraft system identification: Simulation model validation p 1232 N92-17164
ROYAL AIRCRAFT ESTABLISHMENT, FARNBOROUGH (ENGLAND).
Lithiated Vanadium Oxide (LVO), gamma-lithium vanadium bronze (Gamma-LiV2O5) and vanadium dioxide (VO2) as thermal battery cathode materials
| AD-A242948 | p 1287 N92-17186

ROYAL SIGNALS AND RADAR ESTABLISHMENT, MALVERN (ENGLAND).
The physical optics description of microwave scattering by the sea surface
|AD-A243216| p 1365 N92-17180

S

SANDIA NATIONAL LABS., ALBUQUERQUE, NM.
Performance of battery charge controllers: First year test report
|DE92-002924| p 1289 N92-17468
Electrically-controlled polymeric gels as active materials in adaptive structures
|DE92-002947| p 1272 N92-17710
Solder extrusion pressure bonding process and bonded products produced thereby
|DE92-004603| p 1363 N92-17739
Characterization of PZT thin films: Crystallographic phases
|DE92-003514| p 1377 N92-17790
Collisional energy deposition threshold for extended damage depths in ion-implanted silicates
|DE92-004737| p 1377 N92-17797
An investigation of gouge initiation in high-velocity sliding contact
|DE92-003944| p 1311 N92-17937
Structure and topology of silica aerogels
|DE92-004728| p 1274 N92-17938
SCHAFER (W. J.) ASSOCIATES, INC., ALBUQUERQUE, NM.
Correlator optical wavefront sensor COWS
|DE92-003964| p 1368 N92-17846
SCIENCE APPLICATIONS INTERNATIONAL CORP., LA JOLLA, CA.
The National Hurricane Center Risk Analysis Program (HURISK)
|PB91-236463| p 1321 N92-17705
SCIENCE APPLICATIONS INTERNATIONAL CORP., MCLEAN, VA.
Theoretical studies in tokamaks: Three-dimensional simulation of lower hybrid wave launching in tokamaks
|DE92-003773| p 1371 N92-17793
SCRIPPS INSTITUTION OF OCEANOGRAPHY, LA JOLLA, CA.
Development of real-time image and in situ data analysis at sea
|AD-A243682| p 1242 N92-17075
SONOQUEST/ADVANCED ULTRASONICS RESEARCH, WELLESLEY HILLS, MA.
Ultrasonic studies of transient seismo-acoustic waves in bounded solids and Liquid/Solid interfaces
|AD-A243441| p 1355 N92-17488
SOUTHEASTERN CENTER FOR ELECTRICAL ENGINEERING EDUCATION, INC., SAINT CLOUD, FL.
Electromagnetic pulse-induced current measurement device
|AD-A241946| p 1291 N92-17668
SOUTHWEST RESEARCH INST., SAN ANTONIO, TX.
Evaluation of motor gasoline stability
|AD-A243063| p 1275 N92-17066
SPACE COMPUTER CORP., SANTA MONICA, CA.
Object acquisition and tracking for space-based surveillance
|AD-A243333| p 1367 N92-17711
SPACE TELESCOPE SCIENCE INST., BALTIMORE, MD.
Hubble Space Telescope: Fine guidance sensors instrument handbook. Version 2.1
|NASA-CR-189745| p 1386 N92-17020
Hubble Space Telescope: Faint object camera instrument handbook. Version 2.0
|NASA-CR-189746| p 1386 N92-17021
Hubble Space Telescope: Optical telescope assembly handbook. Version 1.0
|NASA-CR-189751| p 1386 N92-17483
Hubble Space Telescope: Wide field and planetary camera instrument handbook. Version 2.1
|NASA-CR-189753| p 1386 N92-17484
Hubble Space Telescope: High speed photometer instrument handbook. Version 2.0
|NASA-CR-189750| p 1386 N92-17497
Hubble Space Telescope: The GO and GTO Observing Programs. Version 1.0
|NASA-CR-189815| p 1387 N92-17650
SRI INTERNATIONAL CORP., MENLO PARK, CA.
Evaluation of a diffusion/trapping model for hydrogen ingress in high-strength alloys
|AD-A243461| p 1263 N92-17327
Auroral-clutter predictions for Fylingdales, England
|AD-A242957| p 1283 N92-17600
ST SYSTEMS CORP., LEXINGTON, MA.
Front detection with Doppler radar
|AD-A242880| p 1319 N92-17289
STANFORD LINEAR ACCELERATOR CENTER, CA.
High current transistor pulse generator
|DE92-004774| p 1292 N92-17801
STANFORD UNIV., CA.
Tests of fit for the Cauchy distribution based on the empirical distribution function
|AD-A243201| p 1352 N92-17173
Gibbs sampling for marginal posterior expectations
|AD-A243212| p 1352 N92-17178
Acoustical and other physical properties of marine sediments
|AD-A243532| p 1324 N92-17391
A study of gamma ray generation from channeled electrons and positions
|AD-A241993| p 1361 N92-17608
Au and Al Schottky barrier formation on GaAs (100) surfaces prepared by thermal desorption of a protective arsenic coating
|DE92-002456| p 1373 N92-17781
STATE UNIV. OF NEW YORK, BUFFALO.
Ligand redistribution reactions of Me2Ga(C5H5) and MeGa(C5H5)2
|AD-A243264| p 1254 N92-17270
SURREY UNIV., GUILDFORD (ENGLAND).
Total Dielectric Isolation (TDI) of fully depleted device structures
|AD-A241926| p 1289 N92-17439
SYRACUSE UNIV., NY.
Mechanisms of gas permeation through polymer membranes
|DE92-004423| p 1274 N92-17942
SYSTRAN CORP., DAYTON, OH.
Contributive research and development
|AD-A243331| p 1391 N92-17079

T

TECHNISCHE UNIV., BERLIN (GERMANY, F.R.).
Geometrical methods for the analysis of cosmological observations
|ETN-92-90584| p 1386 N92-17523
A knowledge-based approach for configuring computer aided measuring systems
|ETN-92-90585| p 1341 N92-17524
Large ideals and non-regular ultrafilters
|ETN-92-90587| p 1351 N92-17525
Analytical determination of arrest and starting torque of a bipolar DC motor with permanent magnets
|ETN-92-90586| p 1290 N92-17540
Test method for the evaluation of the water treeing behavior of cross-linked polyethylene medium voltage cables
|ETN-92-90588| p 1270 N92-17541
TECHNISCHE UNIV., DELFT (NETHERLANDS).
Spectral error models applied to the geodetic boundary value problem
|ETN-92-90582| p 1312 N92-17436
The calibration process of digital cameras
|ETN-92-90583| p 1301 N92-17437
TECHNISCHE UNIV., EINDHOVEN (NETHERLANDS).
The proton spectral function of Ca-40 and Ca-48 studies with (e, e prime p) reaction: An investigation of ground-state correlations
|ETN-92-90566| p 1358 N92-17433
A diffraction limited nitrogen laser for detector calibration in high energy physics
|ETN-92-90567| p 1303 N92-17434
The ZEUS second level calorimeter trigger: Physics simulation, design and implementation
|ETN-92-90568| p 1358 N92-17435
One-loop calculations with massive particles
|ETN-92-90563| p 1359 N92-17518
The determination of the number of light neutrino species
|ETN-92-90564| p 1359 N92-17519
Muons in UA1; the 2nd level trigger and dimuon results
|ETN-92-90565| p 1360 N92-17520
Specification and compositional verification of real-time systems
|ETN-92-90580| p 1341 N92-17521
Mass transfer in gas fluidized beds: Scaling, modeling, and particle size influence
|ETN-92-90581| p 1298 N92-17522
Machine scheduling and Lagrangian relaxation
|ETN-92-90569| p 1353 N92-17839
Modelling of some equilibrium thermodynamic properties of polymer systems
|ETN-92-90570| p 1273 N92-17840
Propane aromatization over gallium containing HZSM-5 zeolites
|ETN-92-90897| p 1262 N92-17925
TEL-AVIV UNIV. (ISRAEL).
On the origin and control of large coherent structures in turbulent shear flow
|AD-A243727| p 1299 N92-17719
TENNESSEE APPLIED PHYSICAL SCIENCES, INC., FAYETTEVILLE.
Wind profiler signal detection improvements
|NASA-CR-189781| p 1317 N92-16990
TENNESSEE UNIV. SPACE INST., TULLAHOMA.
Picosecond laser breakdown thresholds in gases
|AD-A242941| p 1304 N92-17475
TEXAS A&M UNIV., COLLEGE STATION.
High energy physics program at Texas A and M University
|DE92-004426| p 1363 N92-17738
TEXAS UNIV., ARLINGTON.
Electronic and ionic transport in processable conducting polymers
|AD-A242258| p 1269 N92-17460
Electrochemically initiated chain polymerization of pyrrole in aqueous media
|AD-A242259| p 1269 N92-17461
Separation of neutral-to-polaron and polaron-to-bipolaron redox events in alkoxy substituted di-2-thienylphenylene polymers
|AD-A242423| p 1271 N92-17679
TEXAS UNIV., AUSTIN.
Electronic and ionic transport in processable conducting polymers. Symmetry effects on the physical and electrically conducting, substituted poly(di-2-thienylphenylenes)
|AD-A242328| p 1266 N92-16976
New experimental challenges in elemental fluorine chemistry: An emerging technology
|AD-A243054| p 1258 N92-17043
Hypervelocity impact simulation for micrometeorite and debris shield design
|NASA-CR-189807| p 1244 N92-17200
The wave numbers of supercritical surface tension driven Benard convection
|NASA-CR-189856| p 1373 N92-17375
Regularization and approximation of a class of evolution problems in applied mathematics
|AD-A242223| p 1350 N92-17445
Practical error bounds for a class of quadratic programming problems
|AD-A243249| p 1345 N92-17960
TEXAS UNIV. HEALTH SCIENCE CENTER, SAN ANTONIO.
Biophysical techniques for examining metabolic, proliferative, and genetic effects of microwave radiation
|AD-A241903| p 1326 N92-17288
BrainMap: A database of functional neuroanatomy derived from human brain images
|AD-A243161| p 1333 N92-17648
TOKYO UNIV., TANASHI (JAPAN).
Future prospects of pregeometry
|DE92-704278| p 1379 N92-17817
TOLEDO UNIV., OH.
A study of ignition and simulation circuits for arcjet thrusters, part 1
|NASA-CR-189097| p 1253 N92-17510
TORONTO UNIV. (ONTARIO).
Identification techniques: Model structure and time domain methods p 1231 N92-17157
TRW, INC., CARSON CITY, CA.
A system for specifying and rapidly prototyping user interfaces
|AD-A242963| p 1347 N92-16994
TRW SPACE AND DEFENSE SECTOR, REDONDO BEACH, CA.
Pragmatic quality metrics for evolutionary software development models
|AD-A243022| p 1337 N92-17064
TRW SYSTEMS GROUP, REDONDO BEACH, CA.
Testing of spacecraft in long-term storage
|AD-A242906| p 1250 N92-17580

U

UNITED TECHNOLOGIES RESEARCH CENTER, EAST HARTFORD, CT.
Loading and vibration reduction through active aerodynamic control
|AD-A242321| p 1236 N92-17243
UNIVERSITY OF SOUTHERN CALIFORNIA, LOS ANGELES.
Nitration and nitrocompounds
|AD-A243380| p 1259 N92-17210
Development of processible electroactive oligomers and polymers
|AD-A243723| p 1270 N92-17508
UTAH STATE UNIV., LOGAN.
Environmental containment property estimation using QSARs in an expert system
|AD-A243728| p 1336 N92-17720

New ferrocene complexes and polymers for nonlinear optical applications
| AD-A243640 | p 1272 N92-17749
Organometallic NLO polymers. Linear main-chain NLO polymers of ferrocene
| AD-A243641 | p 1272 N92-17750
Organometallic NLO polymers. Accordian main-chain NLO polymers of ferrocene
| AD-A243642 | p 1273 N92-17751
Aryl bis(triflates) in palladium (0) cross-coupling reactions. Synthesis of polyphenyl-alkynyl, alkenyl, and aryl ethers
| AD-A243643 | p 1273 N92-17752
Organic NLO polymers. Linear and accordian main-chain NLO polymers prepared by a Knoevenagel polycondensation
| AD-A243644 | p 1273 N92-17753

UTAH UNIV., SALT LAKE CITY.
Photomodulation spectroscopy of photocarrier dynamics, electronic defects and morphology of conducting polymers
| DE92-004687 | p 1274 N92-17966

V

VANDERBILT UNIV., NASHVILLE, TN.
Electronic interactions of directed photon beams with surfaces
| AD-A241878 | p 1356 N92-17026

VECTOR RESEARCH, INC., ANN ARBOR, MI.
Fatigue effects on human performance in combat: A literature review, volume 1
| AD-A242887 | p 1330 N92-17567

VIRGINIA POLYTECHNIC INST. AND STATE UNIV., BLACKSBURG.
Observation and measurements of flow structures in the stagnation region of a wing-body junction
| AD-A243403 | p 1223 N92-17117
An experimental study of a turbulent wing-body junction and wake flow
| AD-A243388 | p 1223 N92-17222

VIRGINIA UNIV., CHARLOTTESVILLE.
The StarLite Project prototyping real-time software
| AD-A242032 | p 1342 N92-17636

W

WASHINGTON STATE UNIV., PULLMAN.
Anomalous hole burning in polymers with inhomogeneous broadening
| AD-A242397 | p 1266 N92-17010
Stability and structure of C12B24N24: A hybrid analog of buckminsterfullerene
| AD-A242327 | p 1373 N92-17245
Optical nonlinearity in coupled exciton-phonon systems near metal surfaces
| AD-A242362 | p 1357 N92-17423

WASHINGTON UNIV., SEATTLE.
Eddy breakdown and structure development
| AD-A241886 | p 1295 N92-17039
Processing of ceramics of biopolymers. Ultrastructure-property relationships in biocrystals
| AD-A243061 | p 1267 N92-17054
The applied tomography experiment of 1990
| AD-A243525 | p 1354 N92-17086
Acoustic simulation for acoustics education
| AD-A243027 | p 1355 N92-17236
Neutral network models of primate motor system
| AD-A243460 | p 1343 N92-17655
Dynamic fracture characterization of Al2O3 and SiC(w)/Al2O3
| AD-A242187 | p 1273 N92-17784
Proceedings of the 2nd Gulf of Cadiz Expedition Workshop
| AD-A242749 | p 1325 N92-17951

WEAPONS SYSTEMS RESEARCH LAB., ADELAIDE (AUSTRALIA).
Evaluation of a compact Cassegrain optical system
| AD-A242985 | p 1366 N92-17294

WELLESLEY COLL., MA.
Melatonin action on the circadian pacemaker in Siberian hamsters
| AD-A243057 | p 1325 N92-17142

WEST VIRGINIA UNIV., MORGANTOWN.
Reaction kinetics and transport properties of the CaO-SO2-O2 system in absence of intra-particle diffusion
| DE91-002086 | p 1261 N92-17788

WESTINGHOUSE HANFORD CO., RICHLAND, WA.
Fracture toughness evaluation for N Reactor pressure tubes of Zircaloy-2 using the electric-potential method
| DE92-003631 | p 1311 N92-17713

WESTINGHOUSE SAVANNAH RIVER CO., AIKEN, SC.
Downflow heat transfer in a heated ribbed vertical annulus with a cosine power profile (results from test series ECS-2c)
| DE92-003259 | p 1298 N92-17626

WICHITA STATE UNIV., KS.
Wichita State University 1986 aviation safety research projects
| DOT/FAA/CT-91/4 | p 1226 N92-16986
Program plans: Aviation safety research
| NIAR-91-30 | p 1227 N92-17587
Computation of three-dimensional flows using two stream functions
| NASA-CR-187802 | p 1298 N92-17588

WISCONSIN UNIV., MADISON.
Psychophysical evaluation of three-dimensional auditory displays
| NASA-CR-189848 | p 1355 N92-17692

WISCONSIN UNIV., MILWAUKEE.
Mechanisms mediating the perception of complex acoustic patterns
| AD-A243715 | p 1355 N92-17502

WOODS HOLE OCEANOGRAPHIC INST., MA.
Bibliography of technical reports 1990
| AD-A242376 | p 1383 N92-17378
Upper ocean dynamics during the LOTUS and Tropic Heat Experiments
| AD-A243730 | p 1324 N92-17583

WRIGHT LAB., WRIGHT-PATTERSON AFB, OH.
Dual color and shape coding in the visual periphery: A study of Joint Tactical Information Distribution System (JTIDS) symbology
| AD-A243253 | p 1333 N92-16982
Pattern Theory: An engineering paradigm for algorithm design
| AD-A243214 | p 1339 N92-17179
Proceedings of the USAF Structural Integrity Program Conference
| AD-A242943 | p 1235 N92-17204

WRIGHT STATE UNIV., DAYTON, OH.
New algorithms for broad-band and narrowband source localization and a separable 2-D IIR filter realization
| AD-A243457 | p 1291 N92-17654

Y

YALE UNIV., NEW HAVEN, CT.
Signal- and listener-based factors in complex auditory pattern perception
| AD-A243716 | p 1332 N92-17503

Typical Contract Number Index Listing

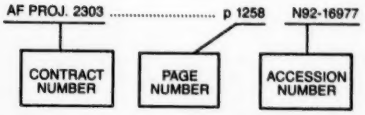

Listings in this index are arranged alphanumerically by contract number. Under each contract number the accession numbers denoting documents that have been produced as a result of research done under that contract are arranged in ascending order. The page number helps to locate the citation in the abstract section. The accession number denotes the number by which the citation is identified.

AF PROJ. 2303 ..... p 1258 N92-16977
p 1267 N92-17054
AF PROJ. 2304 ..... p 1308 N92-17231
p 1291 N92-17654
AF PROJ. 2305 ..... p 1365 N92-17044
p 1366 N92-17630
p 1291 N92-17684
AF PROJ. 2306 ..... p 1267 N92-17029
p 1269 N92-17282
AF PROJ. 2307 ..... p 1298 N92-17688
p 1299 N92-17719
AF PROJ. 2308 ..... p 1294 N92-16979
p 1296 N92-17276
p 1304 N92-17475
AF PROJ. 2310 ..... p 1296 N92-17309
p 1317 N92-17961
AF PROJ. 2311 ..... p 1389 N92-17235
AF PROJ. 2312 ..... p 1325 N92-17142
p 1336 N92-17720
AF PROJ. 2313 ..... p 1332 N92-17336
p 1355 N92-17502
p 1332 N92-17503
p 1327 N92-17504
p 1384 N92-17785
AF PROJ. 2418 ..... p 1235 N92-17204
AF PROJ. 2673 ..... p 1238 N92-17260
AF PROJ. 3484 ..... p 1332 N92-17554
AF PROJ. 4600 ..... p 1301 N92-17273
AF PROJ. 6302 ..... p 1325 N92-17121
AF PROJ. 7629 ..... p 1339 N92-17179
AF-AFOSR-ISSA-90-0003 ..... p 1269 N92-17282
AF-AFOSR-ISSA-91-0002 ..... p 1269 N92-17282
AF-AFOSR-0009-90 ..... p 1296 N92-17309
AF-AFOSR-0015-91 ..... p 1384 N92-17785
AF-AFOSR-0020-91 ..... p 1332 N92-17503
AF-AFOSR-0046-90 ..... p 1351 N92-17609
AF-AFOSR-0049-90 ..... p 1258 N92-16977
AF-AFOSR-0065-88 ..... p 1389 N92-17235
AF-AFOSR-0065-91 ..... p 1332 N92-17336
AF-AFOSR-0067-90 ..... p 1325 N92-17142
AF-AFOSR-0084-88 ..... p 1258 N92-17043
AF-AFOSR-0135-88 ..... p 1267 N92-17054
AF-AFOSR-0143-88 ..... p 1321 N92-17631
AF-AFOSR-0168-88 ..... p 1365 N92-17044
AF-AFOSR-0174-88 ..... p 1374 N92-17594
AF-AFOSR-0175-90 ..... p 1332 N92-17554
AF-AFOSR-0291-89 ..... p 1291 N92-17654
AF-AFOSR-0296-88 ..... p 1327 N92-17504
AF-AFOSR-0304-90 ..... p 1294 N92-16979
p 1296 N92-17276
AF-AFOSR-0307-89 ..... p 1299 N92-17719
AF-AFOSR-0311-91 ..... p 1267 N92-17029
AF-AFOSR-0317-86 ..... p 1304 N92-17475
AF-AFOSR-0320-88 ..... p 1355 N92-17502
AF-AFOSR-0355-90 ..... p 1366 N92-17630
AF-AFOSR-0356-88 ..... p 1289 N92-17439
AF-AFOSR-0381-89 ..... p 1308 N92-17231
AF-AFOSR-0404-89 ..... p 1295 N92-17039
AF-AFOSR-0415-89 ..... p 1298 N92-17688
AF-AFOSR-0454-89 ..... p 1317 N92-17961
AF-AFOSR-0462-89 ..... p 1296 N92-17309
AF-AFOSR-0496-89 ..... p 1267 N92-17054
AF-AFOSR-0509-89 ..... p 1336 N92-17720
AF-AFOSR-0878-91 ..... p 1347 N92-17049
AF-AFOSR-90-0322A ..... p 1375 N92-17667
ARE-2052/70 ..... p 1300 N92-17974
ARPA ORDER 6707 ..... p 1348 N92-17438
ARPA ORDER 7597 ..... p 1365 N92-17146
BARR-10-119 ..... p 1220 N92-17988
p 1220 N92-17989
BMFT-KF-111 ..... p 1321 N92-17543
BMFT-07-KF-1113 ..... p 1317 N92-17542
DA PROJ. 1E4-64804-D-279 ..... p 1225 N92-17404
DA PROJ. 1L1-61102-AH-43 ..... p 1283 N92-17571
DA PROJ. 1L1-61102-B-74-A ..... p 1331 N92-17052
DA PROJ. 1L1-621-OSAH-84 ..... p 1255 N92-16992
DA PROJ. 1L1-62105-AH-84 ..... p 1372 N92-17082
DA PROJ. 1L1-62618-AH-80 ..... p 1352 N92-17384
p 1235 N92-17642
DA PROJ. 1L1-62705-AH-94 ..... p 1281 N92-17258
DA PROJ. 1L2-63001-D-150 ..... p 1275 N92-17066
DA PROJ. 3E1-62777-A-878 ..... p 1326 N92-17269
p 1329 N92-17299
DA PROJ. 3M1-61102-BS-15 ..... p 1326 N92-17269
p 1329 N92-17299
DA PROJ. 3M1-62787-A-871 ..... p 1327 N92-17564
DA PROJ. 4A1-61101-A-91-D ..... p 1312 N92-17715
DAAG29-84-K-0048 ..... p 1222 N92-18001
DAAH01-91-C-R061 ..... p 1239 N92-17325
DAAK60-89-C-0011 ..... p 1256 N92-17053
DAAK70-87-C-0043 ..... p 1275 N92-17066
DAAL03-89-K-0092 ..... p 1222 N92-18000
DAAL04-91-C-0019 ..... p 1303 N92-17175
DAJA45-87-C-0039 ..... p 1366 N92-17485
p 1366 N92-17486
DAJA45-90-C-0052 ..... p 1310 N92-17256
DAJA45-91-M-0227 ..... p 1256 N92-17392
DAMD17-86-C-6139 ..... p 1329 N92-17299
DAMD17-88-C-8148 ..... p 1327 N92-17564
DARPA ORDER 5177 ..... p 1270 N92-17597
p 1270 N92-17614
p 1272 N92-17683
DASG60-91-C-0027 ..... p 1283 N92-17563
DCA100-87-C-0063 ..... p 1344 N92-17948
DCA100-87-C-0078 ..... p 1278 N92-16996
p 1281 N92-17267
DE-AC02-76CH-00016 ..... p 1307 N92-17604
DE-AC02-76CH-03000 ..... p 1336 N92-17592
DE-AC02-83CH-10093 ..... p 1226 N92-17874
p 1313 N92-17875
DE-AC02-83ER-40105 ..... p 1362 N92-17789
DE-AC03-76SF-00098 ..... p 1360 N92-17530
p 1377 N92-17799
p 1305 N92-17868
p 1305 N92-17936
DE-AC03-76SF-00515 ..... p 1292 N92-17801
DE-AC03-87SF-16732 ..... p 1283 N92-17529
DE-AC03-87SF-17127 ..... p 1292 N92-17708
DE-AC03-88ER-53270 ..... p 1371 N92-17793
DE-AC03-89ER-51114 ..... p 1302 N92-17454
p 1369 N92-17456
DE-AC04-76DP-00613 ..... p 1277 N92-17535
p 1238 N92-17967
p 1371 N92-17968
DE-AC04-76DP-00789 ..... p 1289 N92-17468
p 1272 N92-17710
p 1363 N92-17739
p 1377 N92-17790
p 1377 N92-17797
p 1311 N92-17937
p 1274 N92-17938
DE-AC04-88DP-43495 ..... p 1275 N92-17533
p 1276 N92-17624
p 1261 N92-17740
DE-AC05-76OR-00033 ..... p 1330 N92-17798
p 1331 N92-17800
DE-AC05-84OR-21400 ..... p 1360 N92-17574
p 1270 N92-17576
p 1276 N92-17963
DE-AC06-76RL-01830 ..... p 1358 N92-17453
p 1314 N92-17665
p 1313 N92-17934
DE-AC06-87RL-10930 ..... p 1311 N92-17713
DE-AC07-76ID-01570 ..... p 1369 N92-17469
DE-AC07-88ID-12735 ..... p 1384 N92-17470
DE-AC09-76SR-00001 ..... p 1298 N92-17626
DE-AC09-89SR-18035 ..... p 1274 N92-17842
DE-AC22-88PC-88947 ..... p 1274 N92-17935
p 1345 N92-17969
p 1370 N92-17664
p 1306 N92-17183
p 1298 N92-17626
p 1307 N92-17605
p 1299 N92-17704
DE-AC34-90DP-62349 ..... p 1266 N92-17858
DE-AI05-83ER-40017 ..... p 1303 N92-17127
DE-FC21-87MC-24207 ..... p 1261 N92-17788
DE-FG02-84ER-40158 ..... p 1364 N92-17964
DE-FG02-85ER-13438 ..... p 1374 N92-17532
DE-FG02-86ER-45281 ..... p 1263 N92-17319
DE-FG02-87ER-13649 ..... p 1274 N92-17942
DE-FG02-87ER-45310 ..... p 1378 N92-17941
DE-FG02-87ER-45330 ..... p 1374 N92-17528
DE-FG02-87ER-53252 ..... p 1371 N92-17933
DE-FG02-88ER-13949 ..... p 1377 N92-17857
DE-FG02-89ER-45409 ..... p 1274 N92-17966
DE-FG03-84ER-45156 ..... p 1377 N92-17791
DE-FG03-86ER-52126 ..... p 1370 N92-17792
DE-FG03-88SF-17853 ..... p 1313 N92-17577
DE-FG03-89ER-51116 ..... p 1370 N92-17606
DE-FG03-91ER-61152 ..... p 1385 N92-17856
DE-FG05-90ER-14103 ..... p 1261 N92-17786
DE-FG05-91ER-40633 ..... p 1363 N92-17738
DE-FG22-89PC-89769 ..... p 1299 N92-17709
DE-FG22-89PC-89786 ..... p 1275 N92-17184
DNA001-86-C-0307 ..... p 1329 N92-17476
DNA001-87-C-0104 ..... p 1329 N92-17476
DNA001-87-C-0169 ..... p 1280 N92-17187
DNA001-88-C-0029 ..... p 1316 N92-17239
DTFA01-L-83-4-10579 ..... p 1318 N92-17028
DTFA01-89-Z-02033 ..... p 1318 N92-17050
DTFA03-86-C-00041 ..... p 1226 N92-16986
DTFA03-90-C-00050 ..... p 1227 N92-17587
F04701-88-C-0089 ..... p 1315 N92-17035
p 1253 N92-17085
p 1343 N92-17640
F04704-89-C-0044 ..... p 1342 N92-17566
F08635-87-C-0302 ..... p 1227 N92-17259
F19628-86-C-0019 ..... p 1359 N92-17514
F19628-86-C-0111 ..... p 1339 N92-17185
F19628-87-C-0124 ..... p 1319 N92-17289
F19628-88-C-0088 ..... p 1301 N92-17140
F19628-88-K-0024 ..... p 1288 N92-17268
F19628-88-K-0044 ..... p 1316 N92-17202
F19628-90-C-0001 ..... p 1318 N92-17028
F19628-90-C-0002 ..... p 1352 N92-16998
p 1279 N92-17040
p 1281 N92-17241
F19628-90-C-0003 ..... p 1384 N92-17641
F19628-90-C-0072 ..... p 1316 N92-17209
F19628-90-K-0036 ..... p 1283 N92-17600
F29601-88-C-0023 ..... p 1286 N92-17017
F30602-81-C-0185 ..... p 1382 N92-17037
F30602-88-D-0025 ..... p 1340 N92-17286
F30602-88-D-0027 ..... p 1284 N92-17689
F30602-88-F-0021 ..... p 1282 N92-17429
F30602-89-C-0063 ..... p 1374 N92-17553
F33600-88-D-0414 ..... p 1227 N92-17478
F33615-82-C-5036 ..... p 1352 N92-17223
F33615-85-C-0532 ..... p 1325 N92-17121
p 1255 N92-17373
F33615-85-C-2561 ..... p 1361 N92-17652
F33615-85-C-2591 ..... p 1235 N92-17644
F33615-85-C-5087 ..... p 1270 N92-17597
p 1270 N92-17614
p 1272 N92-17683
F33615-87-C-1531 ..... p 1234 N92-17221
F33615-87-D-0609 ..... p 1291 N92-17668
F33615-87-D-0626 ..... p 1326 N92-17288
p 1260 N92-17572
F33615-88-C-3205 ..... p 1233 N92-17513
F33615-88-C-5402 ..... p 1391 N92-17079
F33615-89-C-3205 ..... p 1383 N92-17396
F33615-90-C-0005 ..... p 1333 N92-17758
F33615-90-C-1465 ..... p 1365 N92-17146
F33615-90-C-2069 ..... p 1295 N92-17012
F33615-90-C-2077 ..... p 1234 N92-17011

F33657-84-C-2011 p 1235 N92-17552
F49620-86-C-0102 p 1272 N92-17745
F49620-86-K-0015 p 1361 N92-17608
F49620-88-C-0066 p 1260 N92-17682
F49620-88-C-0071 p 1270 N92-17508
F49620-88-C-0080 p 1356 N92-17026
F49620-89-C-0115 p 1346 N92-17465
MDA072-90-C-0039 p 1348 N92-17438
MDA903-85-C-0191 p 1347 N92-17203
MDA903-86-C-0428 p 1330 N92-17567
MDA903-87-C-0652 p 1340 N92-17463
MDA903-89-C-0003 p 1337 N92-17068
MDA903-89-K-0174 p 1348 N92-17457
p 1332 N92-17458
MDA903-90-D-0022 p 1382 N92-17174
MIPR-N-86-28 p 1238 N92-17260
MIPR-N-87-5 p 1238 N92-17260
MIPR-N-88-15 p 1238 N92-17260
NAGW-1340 p 1361 N92-17647
p 1388 N92-17696
NAGW-1646 p 1390 N92-18003
p 1390 N92-18004
p 1390 N92-18005
NAGW-1781 p 1316 N92-17227
NAGW-2381 p 1388 N92-17377
p 1361 N92-17646
p 1388 N92-17697
NAG1-1027 p 1236 N92-17019
NAG1-1058 p 1233 N92-17316
NAG1-1067 p 1266 N92-17004
NAG1-690 p 1220 N92-17989
NAG1-940 p 1221 N92-17993
NAG2-656 p 1333 N92-17132
NAG3-1102 p 1253 N92-17510
NAG3-1104 p 1373 N92-17375
NAG3-1161 p 1312 N92-17225
NAG3-1186 p 1280 N92-17139
NAG3-666 p 1220 N92-17987
NAG3-694 p 1253 N92-17365
NAG3-927 p 1220 N92-17986
NAG3-974 p 1306 N92-17304
NAG5-1193 p 1387 N92-17695
NAG5-1331 p 1311 N92-17511
NAG5-1521 p 1303 N92-17152
NAG5-780 p 1252 N92-17150
NAG5-956 p 1300 N92-17887
NAG8-59 p 1321 N92-17975
NAG9-444 p 1244 N92-17200
NASA ORDER H-08074-D p 1317 N92-16990
NASA ORDER H-59348-B p 1318 N92-17072
NASW-4520 p 1250 N92-17585
NAS1-18028 p 1228 N92-17512
NAS1-18224 p 1245 N92-17215
p 1245 N92-17334
p 1250 N92-17728
NAS1-18570 p 1301 N92-17006
NAS1-18585 p 1225 N92-17547
NAS1-19158 p 1242 N92-17045
NAS3-25266 p 1224 N92-17347
NAS5-26555 p 1386 N92-17020
p 1386 N92-17021
p 1386 N92-17483
p 1386 N92-17484
p 1386 N92-17497
p 1387 N92-17650
NAS5-27900 p 1386 N92-17003
NAS7-1071 p 1279 N92-17046
NAS7-918 p 1277 N92-17674
p 1367 N92-17675
p 1305 N92-17862
p 1368 N92-17864
p 1293 N92-17865
p 1337 N92-17884
p 1368 N92-17892
p 1349 N92-17895
p 1305 N92-17899
p 1293 N92-17907
NAS8-36952 p 1253 N92-17495
NAS8-36955 p 1344 N92-17778
NAS9-17840 p 1241 N92-17167
p 1241 N92-17214
NAS9-18608 p 1276 N92-16989
NCC2-542 p 1355 N92-17692
NCC3-81 p 1267 N92-17060
NGL-22-009-640 p 1220 N92-17987
p 1220 N92-17988
p 1220 N92-17989
NGL-31-001-252 p 1222 N92-17999
p 1222 N92-18000
p 1222 N92-18001
p 1222 N92-18002
NGR-36-009-017 p 1221 N92-17994
NMRI PROJ. M00-99 p 1328 N92-17124
NOAA-50-DCNC-6-00209 p 1321 N92-17705
NR PROJ. RB2-3-C-22 p 1295 N92-17168
NSF ATM-83-18186 p 1387 N92-17694
NSF CCR-86-09588 p 1346 N92-17638
NSF CCR-86-11442 p 1277 N92-17263
NSF CCR-89-15206 p 1277 N92-17263
NSF CHE-89-21664 p 1261 N92-17786
NSF CTS-89-21829 p 1261 N92-17786
NSF ECS-89-22375 p 1370 N92-17556
NSF IRI-85-19517 p 1381 N92-17669
NSF IRI-88-08896 p 1341 N92-17538
NSF IRI-88-17305 p 1381 N92-17669
NSF IRI-90-06137 p 1341 N92-17538
NSF IRI-90-15443 p 1380 N92-17651
NSF PHY-88-14509 p 1370 N92-17556
NSF SES-87-22504 p 1345 N92-17960
N00014-83-C-3043 p 1260 N92-17489
N00014-83-K-0183 p 1296 N92-17176
N00014-85-K-0168 p 1345 N92-16997
p 1277 N92-17263
N00014-85-K-0217 p 1356 N92-17038
N00014-85-K-0768 p 1350 N92-17148
N00014-86-C-0587 p 1366 N92-17550
N00014-86-K-0125 p 1258 N92-17950
N00014-86-K-0678 p 1348 N92-17457
p 1332 N92-17458
N00014-86-K-0680 p 1333 N92-17634
p 1342 N92-17637
p 1346 N92-17638
p 1380 N92-17651
p 1381 N92-17669
p 1346 N92-17670
N00014-86-K-0756 p 1260 N92-17389
p 1264 N92-17427
p 1358 N92-17428
p 1289 N92-17490
p 1359 N92-17491
p 1361 N92-17616
N00014-87-K-0196 p 1297 N92-17387
N00014-87-K-0243 p 1267 N92-17065
N00014-87-K-0313 p 1326 N92-17474
N00014-87-K-0326 p 1273 N92-17784
N00014-87-K-0385 p 1336 N92-17466
N00014-87-K-0397 p 1348 N92-17457
p 1332 N92-17458
N00014-87-K-0825 p 1277 N92-17263
N00014-88-C-0033 p 1317 N92-17405
N00014-88-C-0667 p 1293 N92-17949
N00014-88-K-0341 p 1373 N92-17390
N00014-88-K-0361 p 1259 N92-17210
N00014-88-K-0472 p 1255 N92-17329
N00014-88-K-0591 p 1341 N92-17538
N00014-88-K-0632 p 1341 N92-17538
N00014-89-C-0015 p 1367 N92-17711
N00014-89-C-0071 p 1290 N92-17629
N00014-89-C-0075 p 1268 N92-17191
N00014-89-C-0117 p 1312 N92-17459
N00014-89-C-0122 p 1388 N92-17717
N00014-89-F-0020 p 1370 N92-17635
N00014-89-J-1002 p 1350 N92-17445
N00014-89-J-1053 p 1324 N92-17583
N00014-89-J-1178 p 1259 N92-17246
p 1259 N92-17247
p 1259 N92-17248
p 1365 N92-17249
p 1259 N92-17261
p 1290 N92-17596
p 1260 N92-17613
N00014-89-J-1207 p 1357 N92-17374
N00014-89-J-1237 p 1254 N92-17308
N00014-89-J-1240 p 1343 N92-17655
N00014-89-J-1275 p 1223 N92-17117
p 1223 N92-17222
N00014-89-J-1311 p 1371 N92-16984
N00014-89-J-1316 p 1324 N92-17391
N00014-89-J-1627 p 1352 N92-17173
p 1352 N92-17178
N00014-89-J-1728 p 1370 N92-17556
N00014-89-J-1828 p 1269 N92-17448
p 1374 N92-17449
N00014-89-J-1946 p 1341 N92-17538
N00014-89-J-1988 p 1277 N92-17263
N00014-89-K-2021 p 1369 N92-17301
N00014-90-C-0072 p 1355 N92-17488
N00014-90-C-0246 p 1367 N92-17690
N00014-90-F-0004 p 1360 N92-17549
N00014-90-F-0011 p 1268 N92-17170
p 1268 N92-17171
p 1268 N92-17172
p 1372 N92-17238
p 1373 N92-17322
p 1271 N92-17615
N00014-90-J-1024 p 1242 N92-17075
N00014-90-J-1046 p 1277 N92-17263
N00014-90-J-1193 p 1266 N92-17010
p 1373 N92-17245
p 1357 N92-17423
N00014-90-J-1212 p 1260 N92-17489
N00014-90-J-1263 p 1262 N92-16985
N00014-90-J-1289 p 1381 N92-17952
N00014-90-J-1320 p 1266 N92-16976
p 1269 N92-17460
p 1269 N92-17461
p 1271 N92-17679
N00014-90-J-1336 p 1297 N92-17447
N00014-90-J-1530 p 1254 N92-17270
N00014-90-J-1553 p 1376 N92-17783
N00014-90-J-1648 p 1329 N92-17557
N00014-90-J-1765 p 1267 N92-17042
N00014-90-J-1853 p 1286 N92-17087
N00014-90-J-1909 p 1223 N92-17117
p 1223 N92-17222
N00014-90-J-1928 p 1268 N92-17193
N00014-90-J-4130 p 1304 N92-17582
N00014-90-J-4146 p 1355 N92-17236
N00014-91-C-0117 p 1344 N92-17921
N00014-91-C-0124 p 1265 N92-17653
N00014-91-C-0148 p 1236 N92-17243
N00014-91-C-0166 p 1268 N92-17195
p 1356 N92-17196
p 1356 N92-17197
p 1271 N92-17659
p 1361 N92-17660
p 1271 N92-17661
N00014-91-C-0240 p 1341 N92-17487
N00014-91-C-0263 p 1263 N92-17327
N00014-91-J-1045 p 1295 N92-17025
N00014-91-J-1046 p 1345 N92-16997
N00014-91-J-1102 p 1342 N92-17636
N00014-91-J-1122 p 1355 N92-17381
N00014-91-J-1274 p 1373 N92-17382
N00014-91-J-1306 p 1300 N92-16983
N00014-91-J-1328 p 1269 N92-17262
N00014-91-J-1409 p 1358 N92-17472
N00014-91-J-1442 p 1273 N92-17777
N00014-91-J-1625 p 1272 N92-17749
p 1272 N92-17750
p 1273 N92-17751
p 1273 N92-17752
p 1273 N92-17753
N00014-91-J-1646 p 1297 N92-17387
N00014-91-J-1706 p 1378 N92-17324
N00014-91-J-1903 p 1333 N92-17648
N00014-91WX-24046 p 1365 N92-17284
N00014-91WX-24155 p 1375 N92-17685
N00039-88-C-0051 p 1323 N92-17083
N00039-88-C-0054 p 1354 N92-17086
N60921-91-M-3233 p 1370 N92-17556
PROJ. RV3-6121 p 1345 N92-17395
SERC-ACME-GRE/42419 p 1229 N92-17878
W-31-109-ENG-38 p 1326 N92-17471
p 1306 N92-17575
p 1265 N92-17703
p 1376 N92-17782
p 1255 N92-17867
W-7405-ENG-36 p 1389 N92-17201
p 1352 N92-17455
p 1265 N92-17579
p 1360 N92-17589
p 1363 N92-17590
p 1240 N92-17591
p 1362 N92-17666
p 1389 N92-17725
p 1304 N92-17726
p 1261 N92-17727
p 1278 N92-17780
p 1376 N92-17781
p 1364 N92-17794
p 1305 N92-17795
p 1364 N92-17796
p 1390 N92-17883
W-7405-ENG-48 p 1317 N92-17578
p 1298 N92-17625
p 1304 N92-17649
p 1388 N92-17832
p 1385 N92-17845
p 1368 N92-17846
p 1364 N92-17876
p 1274 N92-17938
p 1349 N92-17965
W-7405-ENG-82 p 1378 N92-17916
307-50-11-08 p 1347 N92-16987
505-59-53-01 p 1225 N92-17547
505-62-20 p 1219 N92-17346
505-62-84 p 1237 N92-17059
505-63-20 p 1267 N92-17070
505-63-36-01 p 1309 N92-17033
p 1309 N92-17034
505-63-50-04 p 1256 N92-17007
505-63-50-13 p 1225 N92-17509

505-63-50	p 1232	N92-17226
	p 1272	N92-17693
505-63-53-01	p 1310	N92-17333
505-64-13	p 1338	N92-17130
505-64-52-01	p 1219	N92-17984
505-66-41-02	p 1228	N92-17512
505-68-00	p 1230	N92-17071
505-68-10	p 1224	N92-17347
505-68-40	p 1234	N92-17128
505-90-00	p 1381	N92-17001
506-40-91-02	p 1294	N92-17002
506-41-41	p 1389	N92-17069
506-42-72	p 1253	N92-17151
506-43-21-05	p 1267	N92-17032
537-02-20	p 1235	N92-17061
590-14-51-01	p 1242	N92-17045
650-60-23	p 1279	N92-17062
679-40-00	p 1279	N92-17047
763-01-21-16	p 1223	N92-17131
763-01-21	p 1235	N92-17546
778-32-11	p 1267	N92-17060

REPORT NUMBER INDEX

Typical Report Number Index Listing

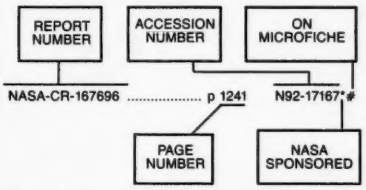

Listings in this index are arranged alphanumerically by report number. The accession number denotes the number by which the citation is identified. The page number helps to locate the citation in the abstract section. An asterisk (*) indicates that the item is a NASA report. A pound sign (#) indicates that the item is available on microfiche.

AAMRL-TR-90-066 ..... p 1255 N92-17373 #
AAMRL-TR-90-076 ..... p 1325 N92-17121 #

AD-A241853 ..... p 1315 N92-17035 #
AD-A241854 ..... p 1347 N92-17049 #
AD-A241856 ..... p 1279 N92-17036 #
AD-A241857 ..... p 1356 N92-17305 #
AD-A241858 ..... p 1337 N92-17023 #
AD-A241859 ..... p 1306 N92-17024 #
AD-A241866 ..... p 1382 N92-17037 #
AD-A241870 ..... p 1356 N92-17038 #
AD-A241871 ..... p 1295 N92-17025 #
AD-A241878 ..... p 1356 N92-17026 #
AD-A241882 ..... p 1374 N92-17594 #
AD-A241885 ..... p 1318 N92-17027 #
AD-A241886 ..... p 1295 N92-17039 #
AD-A241887 ..... p 1279 N92-17040 #
AD-A241893 ..... p 1357 N92-17306 #
AD-A241894 ..... p 1296 N92-17307 #
AD-A241896 ..... p 1388 N92-17595 #
AD-A241899 ..... p 1354 N92-17548 #
AD-A241903 ..... p 1326 N92-17288 #
AD-A241909 ..... p 1323 N92-17041 #
AD-A241914 ..... p 1287 N92-17216 #
AD-A241918 ..... p 1315 N92-17008 #
AD-A241919 ..... p 1317 N92-17009 #
AD-A241924 ..... p 1348 N92-17438 #
AD-A241926 ..... p 1289 N92-17439 #
AD-A241928 ..... p 1352 N92-17440 #
AD-A241934 ..... p 1282 N92-17441 #
AD-A241935 ..... p 1237 N92-17442 #
AD-A241936 ..... p 1378 N92-17443 #
AD-A241937 ..... p 1320 N92-17444 #
AD-A241938 ..... p 1316 N92-17202 #
AD-A241943 ..... p 1323 N92-17083 #
AD-A241946 ..... p 1291 N92-17668 #
AD-A241957 ..... p 1310 N92-17320 #
AD-A241966 ..... p 1328 N92-17084 #
AD-A241981 ..... p 1376 N92-17783 #
AD-A241987 ..... p 1357 N92-17321 #
AD-A241988 ..... p 1256 N92-17607 #
AD-A241993 ..... p 1361 N92-17608 #
AD-A242010 ..... p 1351 N92-17609 #
AD-A242017 ..... p 1310 N92-17230 #
AD-A242026 ..... p 1301 N92-17140 #
AD-A242027 ..... p 1260 N92-17682 #
AD-A242028 ..... p 1333 N92-17634 #
AD-A242029 ..... p 1370 N92-17635 #
AD-A242030 ..... p 1360 N92-17549 #
AD-A242031 ..... p 1358 N92-17472 #
AD-A242032 ..... p 1342 N92-17636 #
AD-A242033 ..... p 1329 N92-17473 #
AD-A242034 ..... p 1333 N92-17758 #
AD-A242038 ..... p 1339 N92-17185 #
AD-A242039 ..... p 1375 N92-17667 #
AD-A242041 ..... p 1380 N92-17651 #
AD-A242042 ..... p 1381 N92-17669 #
AD-A242045 ..... p 1346 N92-17670 #
AD-A242048 ..... p 1342 N92-17637 #
AD-A242049 ..... p 1346 N92-17638 #
AD-A242064 ..... p 1229 N92-17639 #
AD-A242071 ..... p 1385 N92-17141 #
AD-A242074 ..... p 1295 N92-17168 #
AD-A242187 ..... p 1273 N92-17784 #
AD-A242223 ..... p 1350 N92-17445 #
AD-A242224 ..... p 1225 N92-17446 #
AD-A242225 ..... p 1348 N92-17457 #
AD-A242226 ..... p 1332 N92-17458 #
AD-A242232 ..... p 1312 N92-17459 #
AD-A242258 ..... p 1269 N92-17460 #
AD-A242259 ..... p 1269 N92-17461 #
AD-A242264 ..... p 1281 N92-17258 #
AD-A242297 ..... p 1253 N92-17085 #
AD-A242299 ..... p 1265 N92-17759 #
AD-A242315 ..... p 1351 N92-17560 #
AD-A242318 ..... p 1342 N92-17561 #
AD-A242321 ..... p 1236 N92-17243 #
AD-A242322 ..... p 1350 N92-17242 #
AD-A242323 ..... p 1281 N92-17244 #
AD-A242327 ..... p 1373 N92-17245 #
AD-A242328 ..... p 1266 N92-16976 #
AD-A242329 ..... p 1326 N92-17474 #
AD-A242330 ..... p 1343 N92-17640 #
AD-A242331 ..... p 1384 N92-17641 #
AD-A242338 ..... p 1235 N92-17642 #
AD-A242343 ..... p 1353 N92-17643 #
AD-A242351 ..... p 1297 N92-17447 #
AD-A242354 ..... p 1269 N92-17448 #
AD-A242355 ..... p 1374 N92-17449 #
AD-A242358 ..... p 1332 N92-17450 #
AD-A242361 ..... p 1380 N92-17451 #
AD-A242362 ..... p 1357 N92-17423 #
AD-A242363 ..... p 1313 N92-17424 #
AD-A242364 ..... p 1346 N92-17425 #
AD-A242365 ..... p 1357 N92-17394 #
AD-A242372 ..... p 1345 N92-17395 #
AD-A242374 ..... p 1382 N92-17396 #
AD-A242376 ..... p 1383 N92-17378 #
AD-A242377 ..... p 1347 N92-16991 #
AD-A242396 ..... p 1255 N92-16992 #
AD-A242397 ..... p 1266 N92-17010 #
AD-A242398 ..... p 1234 N92-17011 #
AD-A242399 ..... p 1295 N92-17012 #
AD-A242411 ..... p 1323 N92-17078 #
AD-A242420 ..... p 1314 N92-17723 #
AD-A242423 ..... p 1271 N92-17679 #
AD-A242538 ..... p 1343 N92-17680 #
AD-A242740 ..... p 1274 N92-17947 #
AD-A242744 ..... p 1344 N92-17948 #
AD-A242747 ..... p 1293 N92-17949 #
AD-A242748 ..... p 1258 N92-17950 #
AD-A242749 ..... p 1325 N92-17951 #
AD-A242750 ..... p 1381 N92-17952 #
AD-A242828 ..... p 1227 N92-17259 #
AD-A242829 ..... p 1238 N92-17260 #
AD-A242831 ..... p 1259 N92-17261 #
AD-A242832 ..... p 1259 N92-17246 #
AD-A242833 ..... p 1259 N92-17247 #
AD-A242834 ..... p 1259 N92-17248 #
AD-A242835 ..... p 1365 N92-17249 #
AD-A242836 ..... p 1245 N92-17250 #
AD-A242838 ..... p 1301 N92-17273 #
AD-A242839 ..... p 1383 N92-17274 #
AD-A242840 ..... p 1318 N92-17050 #
AD-A242841 ..... p 1345 N92-17135 #
AD-A242843 ..... p 1323 N92-17051 #
AD-A242844 ..... p 1275 N92-17562 #
AD-A242860 ..... p 1267 N92-17042 #
AD-A242861 ..... p 1269 N92-17262 #
AD-A242862 ..... p 1277 N92-17263 #
AD-A242863 ..... p 1273 N92-17777 #
AD-A242865 ..... p 1308 N92-17231 #
AD-A242866 ..... p 1254 N92-17308 #
AD-A242867 ..... p 1260 N92-17613 #
AD-A242868 ..... p 1290 N92-17596 #
AD-A242871 ..... p 1270 N92-17614 #
AD-A242872 ..... p 1270 N92-17597 #
AD-A242873 ..... p 1283 N92-17563 #
AD-A242874 ..... p 1314 N92-17598 #
AD-A242875 ..... p 1381 N92-17013 #
AD-A242877 ..... p 1327 N92-17564 #
AD-A242880 ..... p 1319 N92-17289 #
AD-A242881 ..... p 1233 N92-17565 #
AD-A242886 ..... p 1342 N92-17566 #
AD-A242887 ..... p 1330 N92-17567 #
AD-A242889 ..... p 1330 N92-17599 #
AD-A242890 ..... p 1318 N92-17028 #
AD-A242899 ..... p 1340 N92-17463 #
AD-A242900 ..... p 1290 N92-17629 #
AD-A242901 ..... p 1366 N92-17630 #
AD-A242902 ..... p 1321 N92-17631 #
AD-A242906 ..... p 1250 N92-17580 #
AD-A242916 ..... p 1342 N92-17581 #
AD-A242917 ..... p 1283 N92-17464 #
AD-A242920 ..... p 1346 N92-17465 #
AD-A242923 ..... p 1330 N92-17714 #
AD-A242924 ..... p 1336 N92-17466 #
AD-A242925 ..... p 1366 N92-17550 #
AD-A242928 ..... p 1314 N92-17551 #
AD-A242929 ..... p 1235 N92-17552 #
AD-A242931 ..... p 1347 N92-17203 #
AD-A242937 ..... p 1265 N92-17467 #
AD-A242941 ..... p 1304 N92-17475 #
AD-A242943 ..... p 1235 N92-17204 #
AD-A242947 ..... p 1296 N92-17275 #
AD-A242948 ..... p 1287 N92-17186 #
AD-A242951 ..... p 1281 N92-17232 #
AD-A242954 ..... p 1319 N92-17233 #
AD-A242956 ..... p 1264 N92-17379 #
AD-A242957 ..... p 1283 N92-17600 #
AD-A242959 ..... p 1382 N92-17136 #
AD-A242960 ..... p 1286 N92-16993 #
AD-A242963 ..... p 1347 N92-16994 #
AD-A242967 ..... p 1313 N92-17380 #
AD-A242969 ..... p 1281 N92-17252 #
AD-A242970 ..... p 1388 N92-17253 #
AD-A242973 ..... p 1310 N92-17254 #
AD-A242975 ..... p 1382 N92-17255 #
AD-A242976 ..... p 1288 N92-17290 #
AD-A242978 ..... p 1288 N92-17291 #
AD-A242980 ..... p 1312 N92-17292 #
AD-A242981 ..... p 1329 N92-17476 #
AD-A242983 ..... p 1282 N92-17293 #
AD-A242985 ..... p 1366 N92-17294 #
AD-A242986 ..... p 1288 N92-17295 #
AD-A242987 ..... p 1340 N92-17296 #
AD-A242989 ..... p 1238 N92-17297 #
AD-A242993 ..... p 1324 N92-17298 #
AD-A242997 ..... p 1329 N92-17299 #
AD-A243000 ..... p 1263 N92-17264 #
AD-A243001 ..... p 1310 N92-17265 #
AD-A243002 ..... p 1232 N92-17234 #
AD-A243004 ..... p 1232 N92-17266 #
AD-A243005 ..... p 1281 N92-17267 #
AD-A243009 ..... p 1288 N92-17268 #
AD-A243011 ..... p 1310 N92-17256 #
AD-A243012 ..... p 1319 N92-17257 #
AD-A243013 ..... p 1374 N92-17553 #
AD-A243015 ..... p 1331 N92-17052 #
AD-A243018 ..... p 1256 N92-17053 #
AD-A243022 ..... p 1337 N92-17064 #
AD-A243025 ..... p 1229 N92-17568 #
AD-A243026 ..... p 1389 N92-17235 #
AD-A243027 ..... p 1355 N92-17236 #
AD-A243030 ..... p 1258 N92-16977 #
AD-A243031 ..... p 1384 N92-17785 #
AD-A243033 ..... p 1294 N92-16978 #
AD-A243035 ..... p 1294 N92-16979 #
AD-A243036 ..... p 1296 N92-17276 #
AD-A243041 ..... p 1282 N92-17277 #
AD-A243043 ..... p 1334 N92-17278 #
AD-A243044 ..... p 1282 N92-17279 #
AD-A243045 ..... p 1276 N92-17632 #
AD-A243046 ..... p 1339 N92-17280 #
AD-A243047 ..... p 1223 N92-17281 #
AD-A243049 ..... p 1269 N92-17282 #
AD-A243050 ..... p 1296 N92-17309 #
AD-A243051 ..... p 1332 N92-17336 #
AD-A243052 ..... p 1332 N92-17554 #
AD-A243054 ..... p 1258 N92-17043 #
AD-A243055 ..... p 1365 N92-17044 #

AD-A243057 ..... p 1325 N92-17142 #
AD-A243060 ..... p 1267 N92-17065 #
AD-A243061 ..... p 1267 N92-17054 #
AD-A243062 ..... p 1267 N92-17029 #
AD-A243063 ..... p 1275 N92-17066 #
AD-A243065 ..... p 1360 N92-17555 #
AD-A243075 ..... p 1329 N92-17557 #
AD-A243077 ..... p 1334 N92-17569 #
AD-A243078 ..... p 1339 N92-17237 #
AD-A243079 ..... p 1382 N92-17067 #
AD-A243084 ..... p 1324 N92-17169 #
AD-A243089 ..... p 1337 N92-17068 #
AD-A243090 ..... p 1227 N92-17217 #
AD-A243093 ..... p 1372 N92-17238 #
AD-A243094 ..... p 1268 N92-17170 #
AD-A243095 ..... p 1268 N92-17171 #
AD-A243096 ..... p 1373 N92-17322 #
AD-A243097 ..... p 1268 N92-17172 #
AD-A243098 ..... p 1371 N92-16995 #
AD-A243099 ..... p 1278 N92-16980 #
AD-A243103 ..... p 1364 N92-16981 #
AD-A243105 ..... p 1290 N92-17570 #
AD-A243109 ..... p 1233 N92-17300 #
AD-A243111 ..... p 1283 N92-17571 #
AD-A243153 ..... p 1316 N92-17239 #
AD-A243154 ..... p 1280 N92-17187 #
AD-A243155 ..... p 1235 N92-17644 #
AD-A243158 ..... p 1219 N92-17477 #
AD-A243160 ..... p 1287 N92-17205 #
AD-A243161 ..... p 1333 N92-17648 #
AD-A243162 ..... p 1350 N92-17206 #
AD-A243163 ..... p 1350 N92-17207 #
AD-A243164 ..... p 1311 N92-17208 #
AD-A243165 ..... p 1345 N92-17188 #
AD-A243166 ..... p 1291 N92-17671 #
AD-A243167 ..... p 1291 N92-17672 #
AD-A243168 ..... p 1335 N92-17673 #
AD-A243174 ..... p 1326 N92-17269 #
AD-A243175 ..... p 1278 N92-16996 #
AD-A243176 ..... p 1345 N92-16997 #
AD-A243180 ..... p 1303 N92-17137 #
AD-A243183 ..... p 1352 N92-16998 #
AD-A243184 ..... p 1354 N92-16999 #
AD-A243186 ..... p 1262 N92-17000 #
AD-A243187 ..... p 1282 N92-17366 #
AD-A243188 ..... p 1256 N92-17367 #
AD-A243189 ..... p 1340 N92-17368 #
AD-A243191 ..... p 1383 N92-17369 #
AD-A243192 ..... p 1372 N92-17218 #
AD-A243194 ..... p 1372 N92-17219 #
AD-A243199 ..... p 1264 N92-17370 #
AD-A243200 ..... p 1259 N92-17371 #
AD-A243201 ..... p 1352 N92-17173 #
AD-A243205 ..... p 1382 N92-17174 #
AD-A243206 ..... p 1303 N92-17175 #
AD-A243209 ..... p 1296 N92-17176 #
AD-A243210 ..... p 1324 N92-17177 #
AD-A243212 ..... p 1352 N92-17178 #
AD-A243214 ..... p 1339 N92-17179 #
AD-A243216 ..... p 1365 N92-17180 #
AD-A243217 ..... p 1259 N92-17323 #
AD-A243218 ..... p 1372 N92-17181 #
AD-A243219 ..... p 1272 N92-17683 #
AD-A243220 ..... p 1271 N92-17615 #
AD-A243221 ..... p 1372 N92-17182 #
AD-A243223 ..... p 1372 N92-17220 #
AD-A243224 ..... p 1234 N92-17221 #
AD-A243226 ..... p 1378 N92-17324 #
AD-A243234 ..... p 1234 N92-17240 #
AD-A243235 ..... p 1254 N92-17055 #
AD-A243236 ..... p 1260 N92-17572 #
AD-A243237 ..... p 1369 N92-17030 #
AD-A243238 ..... p 1262 N92-17056 #
AD-A243239 ..... p 1262 N92-17057 #
AD-A243244 ..... p 1275 N92-17058 #
AD-A243245 ..... p 1334 N92-17143 #
AD-A243247 ..... p 1281 N92-17241 #
AD-A243249 ..... p 1345 N92-17960 #
AD-A243250 ..... p 1290 N92-17573 #
AD-A243251 ..... p 1297 N92-17337 #
AD-A243252 ..... p 1341 N92-17558 #
AD-A243253 ..... p 1333 N92-16982 #
AD-A243256 ..... p 1300 N92-16983 #
AD-A243257 ..... p 1371 N92-16984 #
AD-A243258 ..... p 1262 N92-16985 #
AD-A243264 ..... p 1254 N92-17270 #
AD-A243270 ..... p 1263 N92-17271 #
AD-A243272 ..... p 1277 N92-17272 #
AD-A243275 ..... p 1317 N92-17961 #
AD-A243280 ..... p 1365 N92-17284 #
AD-A243283 ..... p 1339 N92-17285 #
AD-A243286 ..... p 1340 N92-17286 #
AD-A243287 ..... p 1238 N92-17287 #
AD-A243309 ..... p 1320 N92-17400 #
AD-A243310 ..... p 1318 N92-17073 #
AD-A243311 ..... p 1319 N92-17144 #
AD-A243314 ..... p 1318 N92-17113 #
AD-A243315 ..... p 1383 N92-17401 #
AD-A243323 ..... p 1383 N92-17402 #
AD-A243324 ..... p 1340 N92-17403 #
AD-A243331 ..... p 1391 N92-17079 #
AD-A243333 ..... p 1367 N92-17711 #
AD-A243334 ..... p 1330 N92-17712 #
AD-A243346 ..... p 1236 N92-17729 #
AD-A243349 ..... p 1239 N92-17730 #
AD-A243350 ..... p 1219 N92-17731 #
AD-A243354 ..... p 1239 N92-17732 #
AD-A243357 ..... p 1343 N92-17733 #
AD-A243358 ..... p 1331 N92-17145 #
AD-A243359 ..... p 1369 N92-17301 #
AD-A243360 ..... p 1245 N92-17302 #
AD-A243363 ..... p 1223 N92-17114 #
AD-A243369 ..... p 1331 N92-17115 #
AD-A243371 ..... p 1287 N92-17189 #
AD-A243375 ..... p 1225 N92-17404 #
AD-A243376 ..... p 1317 N92-17405 #
AD-A243378 ..... p 1316 N92-17209 #
AD-A243380 ..... p 1259 N92-17210 #
AD-A243384 ..... p 1286 N92-17116 #
AD-A243387 ..... p 1329 N92-17190 #
AD-A243388 ..... p 1223 N92-17222 #
AD-A243389 ..... p 1268 N92-17191 #
AD-A243391 ..... p 1361 N92-17652 #
AD-A243392 ..... p 1339 N92-17211 #
AD-A243403 ..... p 1223 N92-17117 #
AD-A243404 ..... p 1338 N92-17118 #
AD-A243406 ..... p 1324 N92-17119 #
AD-A243408 ..... p 1239 N92-17192 #
AD-A243409 ..... p 1239 N92-17325 #
AD-A243429 ..... p 1311 N92-17930 #
AD-A243430 ..... p 1291 N92-17684 #
AD-A243432 ..... p 1288 N92-17326 #
AD-A243433 ..... p 1375 N92-17685 #
AD-A243434 ..... p 1379 N92-17686 #
AD-A243435 ..... p 1381 N92-17687 #
AD-A243436 ..... p 1366 N92-17485 #
AD-A243437 ..... p 1366 N92-17486 #
AD-A243438 ..... p 1341 N92-17487 #
AD-A243441 ..... p 1355 N92-17488 #
AD-A243443 ..... p 1260 N92-17489 #
AD-A243446 ..... p 1289 N92-17490 #
AD-A243447 ..... p 1359 N92-17491 #
AD-A243448 ..... p 1320 N92-17492 #
AD-A243449 ..... p 1320 N92-17493 #
AD-A243450 ..... p 1320 N92-17494 #
AD-A243451 ..... p 1320 N92-17406 #
AD-A243453 ..... p 1265 N92-17653 #
AD-A243457 ..... p 1291 N92-17654 #
AD-A243460 ..... p 1343 N92-17655 #
AD-A243461 ..... p 1263 N92-17327 #
AD-A243462 ..... p 1335 N92-17656 #
AD-A243463 ..... p 1352 N92-17223 #
AD-A243464 ..... p 1326 N92-17224 #
AD-A243465 ..... p 1268 N92-17193 #
AD-A243466 ..... p 1391 N92-17657 #
AD-A243467 ..... p 1329 N92-17194 #
AD-A243470 ..... p 1367 N92-17658 #
AD-A243471 ..... p 1366 N92-17536 #
AD-A243474 ..... p 1264 N92-17426 #
AD-A243475 ..... p 1263 N92-17328 #
AD-A243477 ..... p 1391 N92-17372 #
AD-A243479 ..... p 1255 N92-17373 #
AD-A243482 ..... p 1357 N92-17374 #
AD-A243483 ..... p 1255 N92-17329 #
AD-A243484 ..... p 1350 N92-17330 #
AD-A243486 ..... p 1334 N92-17331 #
AD-A243487 ..... p 1264 N92-17427 #
AD-A243488 ..... p 1358 N92-17428 #
AD-A243489 ..... p 1282 N92-17429 #
AD-A243490 ..... p 1250 N92-17430 #
AD-A243493 ..... p 1308 N92-17431 #
AD-A243496 ..... p 1334 N92-17432 #
AD-A243497 ..... p 1304 N92-17582 #
AD-A243498 ..... p 1355 N92-17381 #
AD-A243499 ..... p 1373 N92-17382 #
AD-A243505 ..... p 1282 N92-17383 #
AD-A243507 ..... p 1352 N92-17384 #
AD-A243508 ..... p 1347 N92-17385 #
AD-A243509 ..... p 1348 N92-17386 #
AD-A243513 ..... p 1297 N92-17387 #
AD-A243515 ..... p 1380 N92-17388 #
AD-A243517 ..... p 1303 N92-17080 #
AD-A243519 ..... p 1350 N92-17081 #
AD-A243522 ..... p 1365 N92-17146 #
AD-A243523 ..... p 1228 N92-17147 #
AD-A243525 ..... p 1354 N92-17086 #
AD-A243526 ..... p 1379 N92-17537 #
AD-A243527 ..... p 1227 N92-17478 #
AD-A243528 ..... p 1350 N92-17148 #
AD-A243529 ..... p 1260 N92-17389 #
AD-A243530 ..... p 1361 N92-17616 #
AD-A243531 ..... p 1373 N92-17390 #
AD-A243532 ..... p 1324 N92-17391 #
AD-A243534 ..... p 1256 N92-17392 #
AD-A243535 ..... p 1333 N92-17014 #
AD-A243537 ..... p 1371 N92-17015 #
AD-A243539 ..... p 1319 N92-17338 #
AD-A243545 ..... p 1334 N92-17617 #
AD-A243546 ..... p 1375 N92-17618 #
AD-A243551 ..... p 1279 N92-17031 #
AD-A243552 ..... p 1224 N92-17339 #
AD-A243553 ..... p 1278 N92-17016 #
AD-A243554 ..... p 1383 N92-17340 #
AD-A243555 ..... p 1286 N92-17017 #
AD-A243558 ..... p 1292 N92-17724 #
AD-A243584 ..... p 1286 N92-17931 #
AD-A243599 ..... p 1387 N92-17920 #
AD-A243600 ..... p 1258 N92-17932 #
AD-A243606 ..... p 1305 N92-17962 #
AD-A243620 ..... p 1344 N92-17921 #
AD-A243632 ..... p 1337 N92-17922 #
AD-A243633 ..... p 1336 N92-17744 #
AD-A243634 ..... p 1272 N92-17745 #
AD-A243635 ..... p 1376 N92-17746 #
AD-A243636 ..... p 1299 N92-17747 #
AD-A243638 ..... p 1237 N92-17748 #
AD-A243640 ..... p 1272 N92-17749 #
AD-A243641 ..... p 1272 N92-17750 #
AD-A243642 ..... p 1273 N92-17751 #
AD-A243643 ..... p 1273 N92-17752 #
AD-A243644 ..... p 1273 N92-17753 #
AD-A243645 ..... p 1370 N92-17734 #
AD-A243649 ..... p 1284 N92-17735 #
AD-A243650 ..... p 1367 N92-17736 #
AD-A243651 ..... p 1285 N92-17737 #
AD-A243652 ..... p 1292 N92-17760 #
AD-A243653 ..... p 1344 N92-17761 #
AD-A243654 ..... p 1251 N92-17762 #
AD-A243655 ..... p 1285 N92-17763 #
AD-A243656 ..... p 1328 N92-17120 #
AD-A243658 ..... p 1325 N92-17121 #
AD-A243660 ..... p 1286 N92-17087 #
AD-A243663 ..... p 1338 N92-17122 #
AD-A243665 ..... p 1389 N92-17123 #
AD-A243667 ..... p 1328 N92-17124 #
AD-A243668 ..... p 1372 N92-17082 #
AD-A243674 ..... p 1312 N92-17715 #
AD-A243675 ..... p 1343 N92-17716 #
AD-A243677 ..... p 1318 N92-17074 #
AD-A243682 ..... p 1242 N92-17075 #
AD-A243683 ..... p 1388 N92-17717 #
AD-A243685 ..... p 1286 N92-17076 #
AD-A243686 ..... p 1365 N92-17088 #
AD-A243687 ..... p 1328 N92-17089 #
AD-A243688 ..... p 1280 N92-17090 #
AD-A243690 ..... p 1259 N92-17091 #
AD-A243691 ..... p 1280 N92-17092 #
AD-A243692 ..... p 1338 N92-17093 #
AD-A243696 ..... p 1315 N92-17094 #
AD-A243697 ..... p 1280 N92-17095 #
AD-A243698 ..... p 1236 N92-17096 #
AD-A243699 ..... p 1338 N92-17077 #
AD-A243700 ..... p 1238 N92-17097 #
AD-A243701 ..... p 1292 N92-17718 #
AD-A243706 ..... p 1340 N92-17407 #
AD-A243707 ..... p 1382 N92-17125 #
AD-A243709 ..... p 1295 N92-17126 #
AD-A243710 ..... p 1303 N92-17127 #
AD-A243711 ..... p 1369 N92-17499 #
AD-A243712 ..... p 1332 N92-17500 #
AD-A243713 ..... p 1289 N92-17501 #
AD-A243715 ..... p 1355 N92-17502 #
AD-A243716 ..... p 1332 N92-17503 #
AD-A243717 ..... p 1327 N92-17504 #
AD-A243718 ..... p 1359 N92-17505 #
AD-A243719 ..... p 1355 N92-17506 #
AD-A243721 ..... p 1346 N92-17507 #
AD-A243723 ..... p 1270 N92-17508 #
AD-A243724 ..... p 1233 N92-17513 #
AD-A243725 ..... p 1359 N92-17514 #
AD-A243726 ..... p 1298 N92-17688 #
AD-A243727 ..... p 1299 N92-17719 #
AD-A243728 ..... p 1336 N92-17720 #
AD-A243730 ..... p 1324 N92-17583 #
AD-A243731 ..... p 1284 N92-17689 #
AD-A243734 ..... p 1367 N92-17690 #
AD-A243736 ..... p 1353 N92-17479 #
AD-A243740 ..... p 1289 N92-17480 #
AD-A243741 ..... p 1284 N92-17691 #
AD-A243742 ..... p 1228 N92-17481 #
AD-A243743 ..... p 1384 N92-17482 #
AD-A243744 ..... p 1288 N92-17332 #
AD-A243746 ..... p 1268 N92-17195 #
AD-A243747 ..... p 1356 N92-17196 #
AD-A243748 ..... p 1356 N92-17197 #
AD-A243749 ..... p 1271 N92-17659 #
AD-A243750 ..... p 1361 N92-17660 #
AD-A243751 ..... p 1271 N92-17661 #

AD-A243753 ..... p 1284 N92-17662 #
AD-A243754 ..... p 1362 N92-17663 #
AD-A243755 ..... p 1284 N92-17721 #
AD-A243756 ..... p 1284 N92-17722 #
AD-A243758 ..... p 1342 N92-17601 #
AD-A243759 ..... p 1250 N92-17602 #
AD-A243760 ..... p 1342 N92-17603 #
AD-A243762 ..... p 1320 N92-17515 #
AD-A243766 ..... p 1283 N92-17516 #
AD-A243767 ..... p 1341 N92-17538 #
AD-A243770 ..... p 1384 N92-17633 #
AD-A243772 ..... p 1321 N92-17764 #
AD-A243773 ..... p 1324 N92-17539 #
AD-A243774 ..... p 1325 N92-17765 #
AD-A243775 ..... p 1325 N92-17766 #
AD-A243780 ..... p 1348 N92-17767 #

AD-D015055 ..... p 1304 N92-17627 #
AD-D015057 ..... p 1287 N92-17129
AD-D015060 ..... p 1370 N92-17706 #
AD-D015061 ..... p 1229 N92-17707 #
AD-D015062 ..... p 1260 N92-17628 #
AD-D015063 ..... p 1358 N92-17462 #
AD-D015065 ..... p 1265 N92-17452 #
AD-D015066 ..... p 1269 N92-17397 #
AD-D015067 ..... p 1297 N92-17398 #
AD-D015068 ..... p 1275 N92-17399 #
AD-D015069 ..... p 1374 N92-17610 #
AD-D015070 ..... p 1257 N92-17611 #
AD-D015071 ..... p 1270 N92-17612 #
AD-D015102 ..... p 1302 N92-17826
AD-D015103 ..... p 1307 N92-17827
AD-D015104 ..... p 1367 N92-17828
AD-D015105 ..... p 1302 N92-17835
AD-D015106 ..... p 1257 N92-17836
AD-D015108 ..... p 1285 N92-17829
AD-D015119 ..... p 1276 N92-17830
AD-D015121 ..... p 1293 N92-17871
AD-D015123 ..... p 1293 N92-17831
AD-D015133 ..... p 1368 N92-17959
AD-D015134 ..... p 1302 N92-17918
AD-D015154 ..... p 1305 N92-17923
AD-D015163 ..... p 1381 N92-17940

AD-E040096 ..... p 1325 N92-17766 #
AD-E040106 ..... p 1325 N92-17765 #
AD-E040128 ..... p 1323 N92-17041 #
AD-E040155 ..... p 1324 N92-17539 #
AD-E200776 ..... p 1319 N92-17233 #
AD-E200781 ..... p 1264 N92-17379 #
AD-E200783 ..... p 1283 N92-17600 #
AD-E200790 ..... p 1279 N92-17031 #

AEDC-TR-91-17 ..... p 1299 N92-17747 #

AEHA-75-51-0742-91 ..... p 1330 N92-17712 #

AERO-REPT-8903 ..... p 1391 N92-17928 #
AERO-REPT-8904 ..... p 1226 N92-17849 #
AERO-REPT-8905 ..... p 1300 N92-17850 #
AERO-REPT-8909 ..... p 1300 N92-17974 #
AERO-REPT-9001 ..... p 1300 N92-17851 #

AEROMET/TUL-9110151 ..... p 1283 N92-17563 #

AF-AFR-88-22 ..... p 1277 N92-17272 #

AFESC/ESL-TR-89-40 ..... p 1238 N92-17260 #
AFESC/ESL-TR-90-60 ..... p 1227 N92-17259 #

AFIT/CI/CIA-91-014D ..... p 1286 N92-17116 #
AFIT/CI/CIA-91-015D ..... p 1367 N92-17658 #
AFIT/CI/CIA-91-017D ..... p 1258 N92-17932 #
AFIT/CI/CIA-91-018D ..... p 1366 N92-17536 #
AFIT/CI/CIA-91-019D ..... p 1287 N92-17189 #
AFIT/CI/CIA-91-020D ..... p 1375 N92-17618 #
AFIT/CI/CIA-91-021D ..... p 1239 N92-17730 #
AFIT/CI/CIA-91-022D ..... p 1331 N92-17145 #
AFIT/CI/CIA-91-023D ..... p 1308 N92-17431 #
AFIT/CI/CIA-91-065 ..... p 1343 N92-17733 #
AFIT/CI/CIA-91-066 ..... p 1223 N92-17114 #
AFIT/CI/CIA-91-068 ..... p 1219 N92-17731 #
AFIT/CI/CIA-91-070 ..... p 1329 N92-17194 #
AFIT/CI/CIA-91-073 ..... p 1329 N92-17190 #
AFIT/CI/CIA-91-074 ..... p 1245 N92-17302 #
AFIT/CI/CIA-91-075 ..... p 1387 N92-17920 #
AFIT/CI/CIA-91-083 ..... p 1334 N92-17617 #
AFIT/CI/CIA-91-084 ..... p 1239 N92-17732 #
AFIT/CI/CIA-91-086 ..... p 1338 N92-17118 #
AFIT/CI/CIA-91-095 ..... p 1331 N92-17115 #
AFIT/CI/CIA-91-098 ..... p 1250 N92-17430 #

AFIT/DS/ENG/91-02 ..... p 1337 N92-17023 #

AFIT/DS/ENP/91-01 ..... p 1356 N92-17305 #

AFIT/DS/ENY/91-1 ..... p 1310 N92-17230 #

AFIT/ENG/GEO/91D-06 ..... p 1338 N92-17077 #

AFIT/GAE/ENY/91S-1 ..... p 1256 N92-17607 #
AFIT/GAE/ENY/91S-4 ..... p 1306 N92-17024 #

AFIT/GCE/ENG/91D-04 ..... p 1289 N92-17480 #

AFIT/GCE/ENS/91D-01 ..... p 1238 N92-17097 #

AFIT/GCS/ENG/91D-03 ..... p 1342 N92-17603 #
AFIT/GCS/ENG/91D-09 ..... p 1384 N92-17482 #
AFIT/GCS/ENG/91D-14 ..... p 1346 N92-17507 #
AFIT/GCS/ENG/91D-19 ..... p 1340 N92-17407 #
AFIT/GCS/ENG/91D-20 ..... p 1337 N92-17922 #
AFIT/GCS/ENG/91D-25 ..... p 1336 N92-17744 #
AFIT/GCS/ENG/91D-26 ..... p 1284 N92-17721 #

AFIT/GE/ENG/91-D-11 ..... p 1342 N92-17601 #
AFIT/GE/ENG/91D-06 ..... p 1292 N92-17760 #
AFIT/GE/ENG/91D-09 ..... p 1280 N92-17092 #
AFIT/GE/ENG/91D-10 ..... p 1284 N92-17722 #
AFIT/GE/ENG/91D-12 ..... p 1288 N92-17332 #
AFIT/GE/ENG/91D-15 ..... p 1292 N92-17718 #
AFIT/GE/ENG/91D-17 ..... p 1328 N92-17089 #
AFIT/GE/ENG/91D-18 ..... p 1284 N92-17735 #
AFIT/GE/ENG/91D-22 ..... p 1250 N92-17602 #
AFIT/GE/ENG/91D-23 ..... p 1284 N92-17662 #
AFIT/GE/ENG/91D-24 ..... p 1280 N92-17095 #
AFIT/GE/ENG/91D-26 ..... p 1376 N92-17746 #
AFIT/GE/ENG/91D-28 ..... p 1284 N92-17691 #
AFIT/GE/ENG/91D-30 ..... p 1283 N92-17516 #
AFIT/GE/ENG/91D-33 ..... p 1237 N92-17748 #
AFIT/GE/ENG/91D-34 ..... p 1332 N92-17500 #
AFIT/GE/ENG/91D-39 ..... p 1236 N92-17096 #
AFIT/GE/ENG/91D-41 ..... p 1228 N92-17481 #
AFIT/GE/ENG/91D-43 ..... p 1286 N92-17076 #
AFIT/GE/ENG/91D-45 ..... p 1365 N92-17088 #
AFIT/GE/ENG/91D-46 ..... p 1315 N92-17094 #
AFIT/GE/ENG/91D-51 ..... p 1285 N92-17737 #
AFIT/GE/ENG/91D-52 ..... p 1338 N92-17093 #
AFIT/GE/ENG/91D-54 ..... p 1280 N92-17090 #
AFIT/GE/ENG/91D-55 ..... p 1289 N92-17501 #

AFIT/GE/ENP/91D-01 ..... p 1362 N92-17663 #

AFIT/GEO/ENG/91D-04 ..... p 1348 N92-17767 #
AFIT/GEO/ENG/91D-3 ..... p 1367 N92-17736 #

AFIT/GEP/ENP/91D-8 ..... p 1259 N92-17091 #
AFIT/GEP/ENP/91J-1 ..... p 1357 N92-17321 #

AFIT/GSO/ENG/91D-17 ..... p 1328 N92-17120 #

AFIT/GSO/ENS/ENY/91D-14 ..... p 1353 N92-17479 #

AFIT/GSO/ENS/91D-05 ..... p 1344 N92-17761 #
AFIT/GSO/ENS/91D-09 ..... p 1251 N92-17762 #
AFIT/GSO/ENS/91D-10 ..... p 1285 N92-17763 #

AFOSR-91-0283TR ..... p 1332 N92-17503 #
AFOSR-91-0776TR ..... p 1321 N92-17631 #
AFOSR-91-0817TR ..... p 1375 N92-17667 #
AFOSR-91-0819TR ..... p 1366 N92-17630 #
AFOSR-91-0827TR ..... p 1351 N92-17609 #
AFOSR-91-0843TR ..... p 1361 N92-17608 #
AFOSR-91-0871TR ..... p 1260 N92-17682 #
AFOSR-91-0874TR ..... p 1295 N92-17039 #
AFOSR-91-0878TR ..... p 1347 N92-17049 #
AFOSR-91-0879TR ..... p 1308 N92-17231 #
AFOSR-91-0883TR ..... p 1374 N92-17594 #
AFOSR-91-0892TR ..... p 1269 N92-17282 #
AFOSR-91-0895TR ..... p 1296 N92-17276 #
AFOSR-91-0905TR ..... p 1384 N92-17785 #
AFOSR-91-0906TR ..... p 1294 N92-16979 #
AFOSR-91-0911TR ..... p 1325 N92-17142 #
AFOSR-91-0912TR ..... p 1389 N92-17235 #
AFOSR-91-0913TR ..... p 1332 N92-17554 #
AFOSR-91-0914TR ..... p 1317 N92-17961 #
AFOSR-91-0915TR ..... p 1332 N92-17336 #
AFOSR-91-0916TR ..... p 1296 N92-17309 #
AFOSR-91-0917TR ..... p 1291 N92-17654 #
AFOSR-91-0918TR ..... p 1267 N92-17054 #
AFOSR-91-0919TR ..... p 1258 N92-16977 #
AFOSR-91-0920TR ..... p 1267 N92-17029 #
AFOSR-91-0926TR ..... p 1258 N92-17043 #
AFOSR-91-0927TR ..... p 1365 N92-17044 #
AFOSR-91-0973TR ..... p 1270 N92-17508 #
AFOSR-91-0986TR ..... p 1327 N92-17504 #
AFOSR-91-0988TR ..... p 1272 N92-17745 #
AFOSR-91-0989TR ..... p 1355 N92-17502 #
AFOSR-91-0992TR ..... p 1336 N92-17720 #
AFOSR-91-0995TR ..... p 1299 N92-17719 #
AFOSR-91-0996TR ..... p 1298 N92-17688 #

AFPT-90-70X-877 ..... p 1381 N92-17013 #

AGARD-AR-302 ..... p 1341 N92-17498 #

AGARD-CAL-90/2 ..... p 1380 N92-17198 #
AGARD-CAL-92/1 ..... p 1380 N92-17212 #

AGARD-LS-178 ..... p 1230 N92-17153 #

AIP-147 ..... p 1347 N92-16991 #

AL-TP-1991-0034 ..... p 1332 N92-17450 #

AL-TR-1991-0004 ..... p 1326 N92-17288 #
AL-TR-1991-0043 ..... p 1333 N92-17758 #
AL-TR-1991-0055 ..... p 1260 N92-17572 #
AL-TR-1991-0058 ..... p 1291 N92-17668 #
AL-TR-1991-0094 ..... p 1287 N92-17216 #

AMSAA-TR-501 ..... p 1350 N92-17081 #

ANL/CP-72505 ..... p 1306 N92-17575 #
ANL/CP-74527 ..... p 1265 N92-17703 #
ANL/CP-74610 ..... p 1326 N92-17471 #
ANL/CP-74697 ..... p 1376 N92-17782 #

APL-UW-TM-6-91 ..... p 1325 N92-17951 #

APL-UW-TR-9106 ..... p 1354 N92-17086 #

ARAED-TR-91023 ..... p 1276 N92-17632 #

ARCCB-TR-91033 ..... p 1311 N92-17930 #

ARI-RN-91-90 ..... p 1330 N92-17567 #
ARI-RN-92-01 ..... p 1347 N92-17203 #
ARI-RN-92-04 ..... p 1340 N92-17463 #

ARL-FLIGHT-MECH-TM-434 ..... p 1232 N92-17266 #
ARL-FLIGHT-MECH-TM-435 ..... p 1238 N92-17297 #
ARL-FLIGHT-MECH-TM-443 ..... p 1223 N92-17281 #
ARL-FLIGHT-MECH-TM-446 ..... p 1339 N92-17280 #

ARL-MAT-TM-404 ..... p 1263 N92-17264 #

ARL-PROP-R-187 ..... p 1233 N92-17565 #

ARL-PROP-TM-460 ..... p 1232 N92-17234 #

ARL-STRUC-TM-536 ..... p 1310 N92-17254 #
ARL-STRUC-TM-539 ..... p 1310 N92-17265 #

ATC-180 ..... p 1318 N92-17028 #
ATC-183 ..... p 1318 N92-17050 #

AVSCOM-TR-92-B-001 ..... p 1256 N92-17007 #

B-247007 ..... p 1240 N92-17741 #

BBC-RD-1991/4 ..... p 1285 N92-17886
BBC-RD-1991/5 ..... p 1285 N92-17885

BDM/MCL-91-0364-TR ..... p 1346 N92-17465 #

BDM/VSQ-91-0742-TR ..... p 1348 N92-17438 #

BFLRF-266 ..... p 1275 N92-17066 #

BK-22-91 ..... p 1317 N92-17009 #

BMO-TR-91-26 ..... p 1342 N92-17566 #

BNL-52302 ..... p 1307 N92-17604 #

BRL-MR-3947 ..... p 1283 N92-17571 #

BRL-TR-3257 ..... p 1235 N92-17642 #
BRL-TR-3288 ..... p 1275 N92-17562 #
BRL-TR-3295 ..... p 1303 N92-17137 #
BRL-TR-3303 ..... p 1352 N92-17384 #

CBPF-NF-004/91 ..... p 1376 N92-17779 #

CCS-663 ..... p 1345 N92-17960 #

CEBAF-PR-91-037 ..... p 1362 N92-17789 #

CERL-ADP-M-91/24 ..... p 1338 N92-17122 #

CERL-SR-N-91/10 ..... p 1314 N92-17598 #
CERL-SR-N-91/11 ..... p 1314 N92-17551 #
CERL-SR-N-91/35 ..... p 1313 N92-17380 #

CERL-TR-M-91/25 ..... p 1389 N92-17123 #

CERL-TR-N-91/13 ..... p 1355 N92-17506 #

CERL-TR-91/52 ..... p 1343 N92-17716 #

CMU-AIP-148 ..... p 1332 N92-17458 #
CMU-AIP-149 ..... p 1348 N92-17457 #

CMU-RI-TR-91-17 ..... p 1365 N92-17146 #
CMU-RI-TR-91-18 ..... p 1303 N92-17080 #
CMU-RI-TR-91-20 ..... p 1228 N92-17147 #

CMU/SEI-91-UG-4 ..... p 1384 N92-17641 #

CONF-9003295 ..... p 1331 N92-17802 #
CONF-9006267-35 ..... p 1390 N92-17883 #
CONF-901145-2 ..... p 1364 N92-17964 #
CONF-910115-1 ..... p 1376 N92-17781 #
CONF-9105133 ..... p 1307 N92-17604 #
CONF-9105176 ..... p 1270 N92-17576 #
CONF-9105221-3 ..... p 1362 N92-17666 #
CONF-9105221-4 ..... p 1364 N92-17794 #
CONF-9105285-2 ..... p 1385 N92-17845 #
CONF-9106187-3 ..... p 1275 N92-17533 #
CONF-9106187-4 ..... p 1276 N92-17624 #
CONF-910626-14 ..... p 1364 N92-17876 #
CONF-9106260-5 ..... p 1364 N92-17796 #
CONF-9107115-59 ..... p 1304 N92-17726 #
CONF-9107182-3 ..... p 1265 N92-17579 #
CONF-9108118-32 ..... p 1305 N92-17795 #
CONF-9108118-33 ..... p 1305 N92-17936 #
CONF-9108118-34 ..... p 1305 N92-17868 #
CONF-9108142-4 ..... p 1362 N92-17789 #
CONF-9108182-1 ..... p 1389 N92-17725 #
CONF-910835-1 ..... p 1360 N92-17589 #
CONF-910852-16 ..... p 1275 N92-17184 #
CONF-910862-6 ..... p 1377 N92-17790 #
CONF-9109112-7 ..... p 1226 N92-17874 #
CONF-9109112-8 ..... p 1313 N92-17875 #
CONF-9109114-5 ..... p 1317 N92-17578 #
CONF-9109256-1 ..... p 1360 N92-17574 #
CONF-9109259-11 ..... p 1278 N92-17780 #
CONF-9109316-2 ..... p 1349 N92-17965 #
CONF-910960-3 ..... p 1274 N92-17938 #
CONF-910968-45 ..... p 1302 N92-17454 #
CONF-910968-47 ..... p 1369 N92-17456 #
CONF-911002-1 ..... p 1306 N92-17575 #
CONF-9110181-1 ..... p 1376 N92-17782 #
CONF-9110275-2 ..... p 1314 N92-17665 #
CONF-911029-2 ..... p 1358 N92-17453 #
CONF-911055-9 ..... p 1289 N92-17468 #
CONF-911106-22 ..... p 1336 N92-17592 #
CONF-911106-27 ..... p 1352 N92-17455 #
CONF-911106-31 ..... p 1292 N92-17801 #
CONF-911111-6 ..... p 1265 N92-17703 #
CONF-9111114-2 ..... p 1261 N92-17727 #
CONF-9111129-4 ..... p 1276 N92-17963 #
CONF-9111130-1 ..... p 1272 N92-17710 #
CONF-9111136-1 ..... p 1389 N92-17201 #
CONF-911116-10 ..... p 1240 N92-17591 #
CONF-911116-11 ..... p 1363 N92-17590 #
CONF-911202-4 ..... p 1377 N92-17797 #
CONF-911264-1 ..... p 1326 N92-17471 #
CONF-920146-1 ..... p 1311 N92-17713 #

CP-503 ..... p 1341 N92-17498 #

CRREL-SR-91-13 ..... p 1254 N92-17055 #

CRREL-91-19 ..... p 1312 N92-17715 #

CSA-91-01-03 ..... p 1383 N92-17396 #

CSB-WP-MAPS1 ..... p 1312 N92-17292 #

CSC-92-0141 ..... p 1276 N92-16989 * #

CSU-ATSP-483 ..... p 1321 N92-17631 #

CU-TP-539 ..... p 1388 N92-17377 * #
CU-TP-540 ..... p 1388 N92-17697 * #

CWI-CS-R9118 ..... p 1346 N92-17833 #

DA-TM-5-1300 ..... p 1277 N92-17272 #

DCIEM-91-62 ..... p 1330 N92-17599 #

DE91-002086 ..... p 1261 N92-17788 #
DE91-011570 ..... p 1306 N92-17183 #
DE91-011705 ..... p 1304 N92-17649 #
DE91-018248 ..... p 1360 N92-17574 #
DE91-018511 ..... p 1374 N92-17532 #
DE91-018617 ..... p 1306 N92-17575 #
DE91-018805 ..... p 1374 N92-17528 #
DE91-018874 ..... p 1283 N92-17529 #
DE91-522477 ..... p 1391 N92-17623 #
DE91-634551 ..... p 1357 N92-17408 #
DE91-641478 ..... p 1327 N92-17946 #
DE91-641481 ..... p 1354 N92-17803 #
DE91-641482 ..... p 1354 N92-17804 #
DE91-641486 ..... p 1354 N92-17823 #
DE91-641488 ..... p 1379 N92-17824 #
DE91-641495 ..... p 1351 N92-17622 #
DE91-641524 ..... p 1353 N92-17318 #
DE91-641979 ..... p 1376 N92-17779 #
DE91-642825 ..... p 1379 N92-17531 #
DE92-000337 ..... p 1299 N92-17704 #
DE92-000459 ..... p 1270 N92-17576 #
DE92-000635 ..... p 1263 N92-17319 #
DE92-000762 ..... p 1313 N92-17577 #
DE92-000864 ..... p 1360 N92-17530 #
DE92-001157 ..... p 1226 N92-17874 #
DE92-001190 ..... p 1313 N92-17875 #
DE92-001908 ..... p 1265 N92-17703 #
DE92-002033 ..... p 1276 N92-17624 #
DE92-002034 ..... p 1275 N92-17533 #
DE92-002172 ..... p 1317 N92-17578 #
DE92-002192 ..... p 1364 N92-17876 #
DE92-002288 ..... p 1307 N92-17604 #
DE92-002456 ..... p 1376 N92-17781 #
DE92-002524 ..... p 1278 N92-17780 #
DE92-002636 ..... p 1370 N92-17664 #
DE92-002681 ..... p 1314 N92-17665 #
DE92-002738 ..... p 1358 N92-17453 #
DE92-002904 ..... p 1275 N92-17184 #
DE92-002905 ..... p 1299 N92-17709 #
DE92-002924 ..... p 1289 N92-17468 #
DE92-002947 ..... p 1272 N92-17710 #
DE92-003068 ..... p 1292 N92-17708 #
DE92-003091 ..... p 1307 N92-17605 #
DE92-003110 ..... p 1298 N92-17625 #
DE92-003258 ..... p 1362 N92-17789 #
DE92-003259 ..... p 1298 N92-17626 #
DE92-003309 ..... p 1369 N92-17469 #
DE92-003311 ..... p 1384 N92-17470 #
DE92-003370 ..... p 1326 N92-17471 #
DE92-003514 ..... p 1377 N92-17790 #
DE92-003520 ..... p 1376 N92-17782 #
DE92-003545 ..... p 1370 N92-17606 #
DE92-003631 ..... p 1311 N92-17713 #
DE92-003638 ..... p 1302 N92-17454 #
DE92-003756 ..... p 1377 N92-17791 #
DE92-003758 ..... p 1385 N92-17856 #
DE92-003760 ..... p 1370 N92-17792 #
DE92-003773 ..... p 1371 N92-17793 #
DE92-003785 ..... p 1352 N92-17455 #
DE92-003789 ..... p 1364 N92-17794 #
DE92-003790 ..... p 1362 N92-17666 #
DE92-003791 ..... p 1305 N92-17795 #
DE92-003797 ..... p 1265 N92-17579 #
DE92-003804 ..... p 1364 N92-17796 #
DE92-003805 ..... p 1369 N92-17456 #
DE92-003808 ..... p 1378 N92-17916 #
DE92-003815 ..... p 1274 N92-17842 #
DE92-003826 ..... p 1274 N92-17935 #
DE92-003840 ..... p 1255 N92-17867 #
DE92-003848 ..... p 1390 N92-17883 #
DE92-003849 ..... p 1389 N92-17201 #
DE92-003855 ..... p 1360 N92-17589 #
DE92-003857 ..... p 1389 N92-17725 #
DE92-003859 ..... p 1363 N92-17590 #
DE92-003860 ..... p 1240 N92-17591 #
DE92-003862 ..... p 1304 N92-17726 #
DE92-003868 ..... p 1261 N92-17727 #
DE92-003907 ..... p 1305 N92-17936 #
DE92-003908 ..... p 1305 N92-17868 #
DE92-003944 ..... p 1311 N92-17937 #
DE92-003963 ..... p 1385 N92-17845 #
DE92-003964 ..... p 1368 N92-17846 #
DE92-003970 ..... p 1388 N92-17832 #
DE92-004408 ..... p 1276 N92-17963 #
DE92-004414 ..... p 1364 N92-17964 #
DE92-004420 ..... p 1378 N92-17941 #
DE92-004423 ..... p 1274 N92-17942 #
DE92-004426 ..... p 1363 N92-17738 #
DE92-004603 ..... p 1363 N92-17739 #
DE92-004623 ..... p 1261 N92-17740 #
DE92-004638 ..... p 1336 N92-17592 #
DE92-004656 ..... p 1349 N92-17965 #
DE92-004684 ..... p 1377 N92-17857 #
DE92-004687 ..... p 1274 N92-17966 #
DE92-004691 ..... p 1371 N92-17933 #
DE92-004699 ..... p 1313 N92-17934 #
DE92-004708 ..... p 1277 N92-17593 #
DE92-004728 ..... p 1274 N92-17938 #
DE92-004737 ..... p 1377 N92-17797 #
DE92-004750 ..... p 1330 N92-17798 #
DE92-004757 ..... p 1377 N92-17799 #
DE92-004770 ..... p 1331 N92-17800 #
DE92-004774 ..... p 1292 N92-17801 #
DE92-004793 ..... p 1238 N92-17967 #
DE92-004794 ..... p 1371 N92-17968 #
DE92-004797 ..... p 1345 N92-17969 #
DE92-004798 ..... p 1266 N92-17858 #
DE92-600473 ..... p 1293 N92-17825 #
DE92-600475 ..... p 1294 N92-17953 #
DE92-600624 ..... p 1362 N92-17954 #
DE92-600625 ..... p 1363 N92-17955 #
DE92-600628 ..... p 1363 N92-17956 #
DE92-600629 ..... p 1363 N92-17957 #
DE92-600631 ..... p 1363 N92-17958 #
DE92-609034 ..... p 1327 N92-17970 #
DE92-609035 ..... p 1351 N92-17939 #
DE92-609543 ..... p 1371 N92-17805 #
DE92-609544 ..... p 1371 N92-17806 #
DE92-609575 ..... p 1327 N92-17877 #
DE92-609665 ..... p 1379 N92-17807 #
DE92-609667 ..... p 1294 N92-17971 #
DE92-610065 ..... p 1262 N92-17943 #
DE92-610350 ..... p 1266 N92-17808 #
DE92-610441 ..... p 1378 N92-17972 #
DE92-610933 ..... p 1309 N92-17809 #
DE92-610935 ..... p 1299 N92-17810 #
DE92-610951 ..... p 1354 N92-17811 #
DE92-610956 ..... p 1285 N92-17812 #
DE92-610975 ..... p 1364 N92-17973 #
DE92-611125 ..... p 1351 N92-17813 #
DE92-611158 ..... p 1348 N92-17814 #
DE92-611185 ..... p 1378 N92-17944 #
DE92-611247 ..... p 1327 N92-17815 #
DE92-704180 ..... p 1257 N92-17816 #
DE92-704278 ..... p 1379 N92-17817 #
DE92-704335 ..... p 1331 N92-17802 #

DLR-FB-90-20 ..... p 1379 N92-17848 #

DMS-DR-2547-VOL-1 ..... p 1241 N92-17167 * #
DMS-DR-2547-VOL-2 ..... p 1241 N92-17214 * #

DNA-TR-90157 ..... p 1329 N92-17476 #
DNA-TR-91-33 ..... p 1280 N92-17187 #
DNA-TR-91-97 ..... p 1316 N92-17239 #

DODA-AR-005-791 ..... p 1312 N92-17292 #
DODA-AR-006-355 ..... p 1288 N92-17291 #
DODA-AR-006-379 ..... p 1275 N92-17058 #
DODA-AR-006-489 ..... p 1366 N92-17294 #
DODA-AR-006-590 ..... p 1232 N92-17266 #
DODA-AR-006-591 ..... p 1238 N92-17297 #
DODA-AR-006-596 ..... p 1310 N92-17254 #
DODA-AR-006-600 ..... p 1232 N92-17234 #
DODA-AR-006-602 ..... p 1263 N92-17264 #
DODA-AR-006-614 ..... p 1223 N92-17281 #
DODA-AR-006-619 ..... p 1233 N92-17565 #
DODA-AR-006-621 ..... p 1310 N92-17265 #
DODA-AR-006-643 ..... p 1339 N92-17280 #
DODA-AR-006-756 ..... p 1288 N92-17295 #
DODA-AR-006-765 ..... p 1340 N92-17296 #

DOE/ER-0529P ..... p 1277 N92-17593 #
DOE/ER-13438/2 ..... p 1374 N92-17532 #
DOE/ER-13649/5 ..... p 1274 N92-17942 #
DOE/ER-13949/3 ..... p 1377 N92-17857 #
DOE/ER-40105/175 ..... p 1362 N92-17789 #
DOE/ER-40633/1 ..... p 1363 N92-17738 #
DOE/ER-45156/T4 ..... p 1377 N92-17791 #
DOE/ER-45281/6 ..... p 1263 N92-17319 #
DOE/ER-45310/35 ..... p 1378 N92-17941 #
DOE/ER-45330/4 ..... p 1374 N92-17528 #
DOE/ER-45409/2 ..... p 1274 N92-17966 #
DOE/ER-51116/1 ..... p 1370 N92-17606 #
DOE/ER-52126/T1 ..... p 1370 N92-17792 #
DOE/ER-53252/28 ..... p 1371 N92-17933 #
DOE/ER-53270/T1 ..... p 1371 N92-17793 #
DOE/ER-61152/T1 ..... p 1385 N92-17856 #

DOE/ID-12735/T19 ..... p 1370 N92-17664 #

DOE/MC-24207/3005 ..... p 1261 N92-17788 #

DOE/OR-00033/T455 ..... p 1330 N92-17798 #
DOE/OR-00033/T462 ..... p 1331 N92-17800 #

DOE/PC-88947/T11 ..... p 1299 N92-17704 #
DOE/PC-88947/T12 ..... p 1307 N92-17605 #
DOE/PC-89769/T6 ..... p 1299 N92-17709 #

DOE/SF-16732/T1 ..... p 1283 N92-17529 #
DOE/SF-17127/T1 ..... p 1292 N92-17708 #
DOE/SF-17853/T1 ..... p 1313 N92-17577 #

DOT/FAA/CT-TN91/51 ..... p 1226 N92-17149 #

DOT/FAA/CT-91/4 ..... p 1226 N92-16986 #

DOT/FAA/NR-91/9 ..... p 1318 N92-17050 #

DOT/FAA/SE-91/4 ..... p 1281 N92-17244 #

DOTVNTSC-FAA-91-13 ..... p 1281 N92-17244 #

DREO-TN-91-14 ..... p 1334 N92-17278 #

DREO-1076 ..... p 1282 N92-17279 #

DRIC-BR-305032 ..... p 1287 N92-17186 #
DRIC-BR-306218 ..... p 1365 N92-17180 #

DTRC-91/CT07 ..... p 1385 N92-17141 #

DTRC/SHD-1003-06 ..... p 1294 N92-16978 #
DTRC/SHD-1262-04 ..... p 1295 N92-17168 #
DTRC/SHD-1361-01 ..... p 1334 N92-17569 #

DTRC/SME-91/06 ..... p 1262 N92-17057 #
DTRC/SME-91/51 ..... p 1262 N92-17056 #

DTW-8944-91003 ..... p 1279 N92-17046 * #

E-5902 ..... p 1237 N92-17059 * #
E-5976 ..... p 1235 N92-17061 * #
E-6088 ..... p 1219 N92-17346 * #
E-6105 ..... p 1253 N92-17151 * #
E-6343 ..... p 1267 N92-17070 * #
E-6633 ..... p 1389 N92-17069 * #
E-6749 ..... p 1267 N92-17060 * #
E-6767 ..... p 1224 N92-17347 * #
E-6789 ..... p 1235 N92-17546 * #
E-6835 ..... p 1279 N92-17047 * #
E-6838 ..... p 1279 N92-17062 * #

EGG-EAST-9348 ..... p 1298 N92-17626 #

EGG-EP-9846 ..... p 1384 N92-17470 #

EGG-SCM-9576 ..... p 1369 N92-17469 #

EGG-2663 ..... p 1345 N92-17969 #

EOARD-TR-91-11 ..... p 1289 N92-17439 #

ER-13065-666 ..... p 1379 N92-17807 #

ERIM-196800-18-F-VOL-2 ..... p 1366 N92-17550 #
ERIM-218600-4-F ..... p 1312 N92-17459 #

ERL-0568-RR ..... p 1288 N92-17295 #
ERL-0571-RR ..... p 1340 N92-17296 #

ERP-1081 ..... p 1319 N92-17233 #

ESA-TT-1252 ..... p 1379 N92-17848 #

ESD-TR-91-056 ..... p 1279 N92-17040 #
ESD-TR-91-080 ..... p 1281 N92-17241 #
ESD-TR-91-094 ..... p 1352 N92-16998 #

ESDU-91008 ..... p 1311 N92-17834
ESDU-91018 ..... p 1233 N92-17843
ESDU-91019 ..... p 1229 N92-17844
ESDU-91020 ..... p 1233 N92-17847
ESDU-91026 ..... p 1307 N92-17852
ESDU-91043 ..... p 1321 N92-17853

ESG-133 ..... p 1305 N92-17868 #

ETN-92-90557 ..... p 1346 N92-17833 #
ETN-92-90560 ..... p 1353 N92-17837 #
ETN-92-90561 ..... p 1349 N92-17838 #
ETN-92-90562 ..... p 1351 N92-17517 #
ETN-92-90563 ..... p 1359 N92-17518 #
ETN-92-90564 ..... p 1359 N92-17519 #
ETN-92-90565 ..... p 1360 N92-17520 #
ETN-92-90566 ..... p 1358 N92-17433 #
ETN-92-90567 ..... p 1303 N92-17434 #
ETN-92-90568 ..... p 1358 N92-17435 #
ETN-92-90569 ..... p 1353 N92-17839 #
ETN-92-90570 ..... p 1273 N92-17840 #
ETN-92-90580 ..... p 1341 N92-17521 #
ETN-92-90581 ..... p 1298 N92-17522 #
ETN-92-90582 ..... p 1312 N92-17436 #
ETN-92-90583 ..... p 1301 N92-17437 #
ETN-92-90584 ..... p 1386 N92-17523 #
ETN-92-90585 ..... p 1341 N92-17524 #
ETN-92-90586 ..... p 1290 N92-17540 #
ETN-92-90587 ..... p 1351 N92-17525 #
ETN-92-90588 ..... p 1270 N92-17541 #
ETN-92-90594 ..... p 1317 N92-17542 #
ETN-92-90595 ..... p 1321 N92-17543 #
ETN-92-90598 ..... p 1304 N92-17526 #
ETN-92-90599 ..... p 1261 N92-17841 #
ETN-92-90601 ..... p 1308 N92-17341 #
ETN-92-90602 ..... p 1309 N92-17544 #
ETN-92-90603 ..... p 1341 N92-17545 #
ETN-92-90604 ..... p 1241 N92-17342 #
ETN-92-90605 ..... p 1240 N92-17527 #
ETN-92-90616 ..... p 1256 N92-17310 #
ETN-92-90617 ..... p 1224 N92-17311 #
ETN-92-90618 ..... p 1297 N92-17312 #
ETN-92-90620 ..... p 1233 N92-17313 #
ETN-92-90621 ..... p 1224 N92-17314 #
ETN-92-90622 ..... p 1224 N92-17315 #
ETN-92-90623 ..... p 1297 N92-17343 #
ETN-92-90624 ..... p 1301 N92-17344 #
ETN-92-90625 ..... p 1301 N92-17345 #
ETN-92-90747 ..... p 1379 N92-17848 #
ETN-92-90897 ..... p 1262 N92-17925 #
ETN-92-90904 ..... p 1229 N92-17878 #
ETN-92-90905 ..... p 1380 N92-17879 #
ETN-92-90906 ..... p 1349 N92-17880 #
ETN-92-90910 ..... p 1302 N92-17926 #
ETN-92-90911 ..... p 1344 N92-17927 #
ETN-92-90912 ..... p 1391 N92-17928 #
ETN-92-90913 ..... p 1226 N92-17849 #
ETN-92-90914 ..... p 1300 N92-17850 #
ETN-92-90917 ..... p 1300 N92-17974 #
ETN-92-90918 ..... p 1300 N92-17851 #

FEI-2119 ..... p 1309 N92-17809 #
FEI-2131 ..... p 1299 N92-17810 #

FERMILAB-PUB-91/305-A ..... p 1361 N92-17647 * #
FERMILAB-PUB-91/312-A/T ..... p 1388 N92-17377 * #
FERMILAB-PUB-91/324-A ..... p 1388 N92-17696 * #
FERMILAB-PUB-91/326-A/T ..... p 1388 N92-17697 * #
FERMILAB-PUB-91/340-A ..... p 1361 N92-17646 * #

FNAL/C-91/303 ..... p 1336 N92-17592 #

FR89-1(R)-VOL-1 ..... p 1330 N92-17567 #

FST91-281-2 ..... p 1342 N92-17566 #

GA-A-20645 ..... p 1302 N92-17454 #
GA-A-20652 ..... p 1369 N92-17456 #

GAO/NSIAD-92-39 ..... p 1245 N92-17250 #
GAO/NSIAD-92-86 ..... p 1240 N92-17741 #

H-1743 ..... p 1230 N92-17071 * #
H-1779 ..... p 1232 N92-17226 * #
H-1780 ..... p 1234 N92-17128 * #

HAC-REF-G4663 ..... p 1293 N92-17949 #

HDL-SR-91-8 ..... p 1278 N92-16980 #

HDL-TM-91-12 ..... p 1357 N92-17394 #
HDL-TM-91-14 ..... p 1288 N92-17326 #
HDL-TM-91-16 ..... p 1371 N92-16995 #

HEL-TM-14-91 ..... p 1283 N92-17464 #
HEL-TM-17-91 ..... p 1331 N92-17052 #

IAR-AN-73 ..... p 1229 N92-17568 #

IBM-RJ8248 ..... p 1356 N92-17196 #
IBM-RJ8287 ..... p 1271 N92-17661 #
IBM-RJ8411 ..... p 1356 N92-17197 #
IBM-RJ8420 ..... p 1361 N92-17660 #
IBM-RJ8469 ..... p 1271 N92-17659 #
IBM-RJ8490 ..... p 1268 N92-17195 #

IC-90/425 ..... p 1353 N92-17318 #
IC-90/473 ..... p 1327 N92-17946 #
IC-91/108 ..... p 1327 N92-17877 #
IC-91/109 ..... p 1371 N92-17805 #
IC-91/115 ..... p 1327 N92-17815 #
IC-91/121 ..... p 1371 N92-17806 #
IC-91/126 ..... p 1327 N92-17970 #
IC-91/132 ..... p 1351 N92-17939 #
IC-91/145 ..... p 1379 N92-17807 #
IC-91/151 ..... p 1262 N92-17943 #
IC-91/153 ..... p 1378 N92-17972 #
IC-91/19 ..... p 1354 N92-17803 #
IC-91/22 ..... p 1379 N92-17824 #
IC-91/2 ..... p 1354 N92-17804 #
IC-91/45 ..... p 1379 N92-17531 #
IC-91/7 ..... p 1354 N92-17823 #

IDA-P-2628 ..... p 1337 N92-17068 #

IDA/HQ-91-39501 ..... p 1337 N92-17068 #

IFT-P-36/90 ..... p 1351 N92-17622 #

IFVE-OEA-91-2 ..... p 1294 N92-17971 #

INIS-MF-12963 ..... p 1362 N92-17954 #

INO-SP-5 ..... p 1324 N92-17539 #

INS-879 ..... p 1379 N92-17817 #

IS-T-1537 ..... p 1378 N92-17916 #

ISBN-0-309-04584-3 ..... p 1261 N92-17786 #
ISBN-0-309-04597-5 ..... p 1370 N92-17556 #
ISBN-0-85679-770-7 ..... p 1311 N92-17834
ISBN-0-85679-780-4 ..... p 1233 N92-17843
ISBN-0-85679-781-2 ..... p 1229 N92-17844
ISBN-0-85679-782-0 ..... p 1233 N92-17847
ISBN-0-85679-788-X ..... p 1307 N92-17852
ISBN-0-85679-805-3 ..... p 1321 N92-17853
ISBN-92-835-0575-1 ..... p 1380 N92-17198 #
ISBN-92-835-0640-5 ..... p 1230 N92-17153 #
ISBN-92-835-0647-2 ..... p 1341 N92-17498 #
ISBN-92-835-0651-O ..... p 1380 N92-17212 #

ISSN-0069-5882 ..... p 1317 N92-17542 #
ISSN-0069-5882 ..... p 1321 N92-17543 #
ISSN-0141-4046 ..... p 1307 N92-17852
ISSN-0141-4054 ..... p 1233 N92-17843
ISSN-0141-4054 ..... p 1229 N92-17844
ISSN-0141-4054 ..... p 1233 N92-17847
ISSN-0141-4097 ..... p 1311 N92-17834
ISSN-0143-2702 ..... p 1321 N92-17853
ISSN-0374-1257 ..... p 1224 N92-17314 #
ISSN-0374-1257 ..... p 1224 N92-17315 #
ISSN-0374-1257 ..... p 1301 N92-17344 #
ISSN-0374-1257 ..... p 1301 N92-17345 #
ISSN-0389-4010 ..... p 1257 N92-17869 #
ISSN-0389-4010 ..... p 1237 N92-17917 #
ISSN-0389-4014 ..... p 1236 N92-17855 #
ISSN-0436-1199 ..... p 1297 N92-17343 #
ISSN-0452-2982 ..... p 1251 N92-17754 #
ISSN-0452-2982 ..... p 1225 N92-17755 #
ISSN-0452-2982 ..... p 1238 N92-17756 #
ISSN-0452-2982 ..... p 1278 N92-17757 #
ISSN-0452-2982 ..... p 1385 N92-17787 #
ISSN-0452-2982 ..... p 1239 N92-17854 #
ISSN-1049-667X ..... p 1308 N92-16988 * #
ISSN-1051-225X ..... p 1308 N92-17005 * #
ISSN-1051-225X ..... p 1308 N92-17199 * #

IU/NTC-91-12 ..... p 1362 N92-17789 #

JAERI-M-91-090 ..... p 1257 N92-17816 #

JINR-E-10-90-184 ..... p 1351 N92-17813 #
JINR-E-14-90-254 ..... p 1294 N92-17953 #
JINR-E-14-90-345 ..... p 1378 N92-17944 #
JINR-E-4-90-249 ..... p 1363 N92-17956 #
JINR-E-4-90-57 ..... p 1363 N92-17957 #

JINR-R-1-89-452 ..... p 1357 N92-17408 #
JINR-R-10-90-299 ..... p 1266 N92-17808 #
JINR-R-10-90-398 ..... p 1348 N92-17814 #
JINR-R-2-90-158 ..... p 1363 N92-17958 #
JINR-R-3-90-120 ..... p 1363 N92-17955 #
JINR-R-8-90-127 ..... p 1293 N92-17825 #
JINR-R-9-90-154 ..... p 1354 N92-17811 #
JINR-R-9-90-37 ..... p 1364 N92-17973 #

JRC-RR-90-04 ..... p 1344 N92-17778 * #

JRC-34-91 ..... p 1355 N92-17488 #

JTN-92-80241 ..... p 1251 N92-17754 #
JTN-92-80246 ..... p 1225 N92-17755 #
JTN-92-80247 ..... p 1238 N92-17756 #
JTN-92-80250 ..... p 1239 N92-17854 #
JTN-92-80290 ..... p 1278 N92-17757 #
JTN-92-80292 ..... p 1385 N92-17787 #
JTN-92-80298 ..... p 1236 N92-17855 #

J200-91-0080/7208 ..... p 1286 N92-17017 #

KCP-613-4479 ..... p 1277 N92-17535 #
KCP-613-4480 ..... p 1371 N92-17968 #
KCP-613-4529 ..... p 1238 N92-17967 #

KEE6-FR ..... p 1253 N92-17495 * #

KFTI-90-2 ..... p 1285 N92-17812 #

KURRI-TR-341 ..... p 1391 N92-17623 #
KURRI-TR-347 ..... p 1331 N92-17802 #

L-16604 ..... p 1223 N92-17131 * #
L-16982 ..... p 1267 N92-17032 * #
L-17017 ..... p 1219 N92-17984 * #

LA-UR-91-3257 ..... p 1376 N92-17781 #
LA-UR-91-3287 ..... p 1364 N92-17796 #
LA-UR-91-3437 ..... p 1278 N92-17780 #
LA-UR-91-3495 ..... p 1265 N92-17579 #
LA-UR-91-3498 ..... p 1261 N92-17727 #
LA-UR-91-3532 ..... p 1304 N92-17726 #
LA-UR-91-3539 ..... p 1240 N92-17591 #

LA-UR-91-3540 ..... p 1363 N92-17590 #
LA-UR-91-3546 ..... p 1389 N92-17725 #
LA-UR-91-3569 ..... p 1360 N92-17589 #
LA-UR-91-3616 ..... p 1389 N92-17201 #
LA-UR-91-3617 ..... p 1390 N92-17883 #
LA-UR-91-3688 ..... p 1352 N92-17455 #
LA-UR-91-3825 ..... p 1305 N92-17795 #
LA-UR-91-3830 ..... p 1362 N92-17666 #
LA-UR-91-3831 ..... p 1364 N92-17794 #

LBL-30672 ..... p 1305 N92-17936 #
LBL-30674 ..... p 1305 N92-17868 #
LBL-31130 ..... p 1360 N92-17530 #
LBL-31391 ..... p 1377 N92-17799 #

LC-91-66333 ..... p 1261 N92-17786 #
LC-91-66812 ..... p 1370 N92-17556 #

LR-31824 ..... p 1301 N92-17006 * #

M-678 ..... p 1318 N92-17072 * #

MBB-FE202-S-PUB-0453-A ..... p 1256 N92-17310 #
MBB-FE211-S-PUB-446 ..... p 1224 N92-17311 #
MBB-FE211-S-PUB-447 ..... p 1297 N92-17312 #
MBB-FE211-S-PUB-452 ..... p 1233 N92-17313 #

MBB-UK-0140-91-PUB ..... p 1308 N92-17341 #
MBB-UK-0141-91-PUB ..... p 1309 N92-17544 #
MBB-UK-0142-91-PUB ..... p 1341 N92-17545 #
MBB-UK-0143-91-PUB ..... p 1241 N92-17342 #
MBB-UK-0144-91-PUB ..... p 1240 N92-17527 #

MBB-Z-0361-91-PUB ..... p 1304 N92-17526 #
MBB-Z-0368-91-PUB ..... p 1261 N92-17841 #

MCR-92-1310 ..... p 1276 N92-16989 * #

MIT-TR-918 ..... p 1279 N92-17040 #
MIT-TR-919 ..... p 1281 N92-17241 #
MIT-TR-927 ..... p 1352 N92-16998 #

MIT/LCS/TM-412-D ..... p 1277 N92-17263 #

MIT/LCS/TR-518 ..... p 1345 N92-16997 #

MITT-76 ..... p 1317 N92-17542 #
MITT-78 ..... p 1321 N92-17543 #

MLM-3700(OP) ..... p 1275 N92-17533 #
MLM-3701(OP) ..... p 1276 N92-17624 #
MLM-3716 ..... p 1261 N92-17740 #

MPIS-1/1991 ..... p 1297 N92-17343 #
MPIS-100/1991 ..... p 1301 N92-17344 #
MPIS-101/1991 ..... p 1301 N92-17345 #
MPIS-98/1990 ..... p 1224 N92-17314 #
MPIS-99/1990 ..... p 1224 N92-17315 #

MRC-R-1335 ..... p 1280 N92-17187 #

MRC/NSH-91-0002 ..... p 1316 N92-17239 #

MRL-TR-91-25 ..... p 1275 N92-17058 #
MRL-TR-91-8 ..... p 1288 N92-17291 #

MTL-TR-91-41 ..... p 1255 N92-16992 #
MTL-TR-91-45 ..... p 1372 N92-17082 #

MTR-11209 ..... p 1345 N92-17188 #
MTR-11230 ..... p 1291 N92-17671 #
MTR-11252 ..... p 1291 N92-17672 #
MTR-11259 ..... p 1335 N92-17673 #

M90-19 ..... p 1350 N92-17206 #
M91-40 ..... p 1350 N92-17207 #
M91-41 ..... p 1347 N92-17385 #
M91-42 ..... p 1348 N92-17386 #
M91-82 ..... p 1311 N92-17208 #

NADC-91067-50 ..... p 1342 N92-17561 #
NADC-91071-90 ..... p 1334 N92-17432 #

NAL-TM-602-PT-2 ..... p 1251 N92-17754 #
NAL-TM-610 ..... p 1225 N92-17755 #
NAL-TM-611 ..... p 1238 N92-17756 #
NAL-TM-614 ..... p 1239 N92-17854 #
NAL-TM-619 ..... p 1278 N92-17757 #
NAL-TM-621 ..... p 1385 N92-17787 #

NAL-TR-1064T ..... p 1236 N92-17855 #
NAL-TR-1096 ..... p 1257 N92-17869 #
NAL-TR-1116 ..... p 1237 N92-17917 #

NAS 1.15:100646 ..... p 1310 N92-17333 * #
NAS 1.15:101662 ..... p 1381 N92-17001 * #
NAS 1.15:103567 ..... p 1384 N92-17586 * #
NAS 1.15:103684 ..... p 1237 N92-17059 * #
NAS 1.15:103800 ..... p 1219 N92-17346 * #
NAS 1.15:104168 ..... p 1225 N92-17547 * #
NAS 1.15:104174 ..... p 1338 N92-17130 * #
NAS 1.15:104177 ..... p 1347 N92-16987 * #
NAS 1.15:104188 ..... p 1225 N92-17509 * #
NAS 1.15:104189 ..... p 1256 N92-17007 * #
NAS 1.15:104190 ..... p 1294 N92-17002 * #
NAS 1.15:104192 ..... p 1309 N92-17034 * #
NAS 1.15:104193 ..... p 1309 N92-17033 * #
NAS 1.15:104195 ..... p 1272 N92-17693 * #
NAS 1.15:104743 ..... p 1264 N92-17376 * #
NAS 1.15:105258 ..... p 1235 N92-17061 * #
NAS 1.15:105294 ..... p 1389 N92-17069 * #
NAS 1.15:105370 ..... p 1267 N92-17060 * #
NAS 1.15:105380 ..... p 1224 N92-17347 * #
NAS 1.15:105397 ..... p 1235 N92-17546 * #
NAS 1.15:105420 ..... p 1279 N92-17047 * #
NAS 1.15:105422 ..... p 1279 N92-17062 * #
NAS 1.15:105452 ..... p 1387 N92-17694 * #
NAS 1.15:105464 ..... p 1308 N92-16988 * #
NAS 1.15:105465 ..... p 1308 N92-17199 * #
NAS 1.15:105467 ..... p 1308 N92-17005 * #
NAS 1.15:105475 ..... p 1241 N92-17364 * #
NAS 1.15:105476 ..... p 1241 N92-16975 * #
NAS 1.15:105477 ..... p 1240 N92-16974 * #
NAS 1.15:105478 ..... p 1242 N92-17534 * #
NAS 1.15:105479 ..... p 1240 N92-16973 * #
NAS 1.15:105505 ..... p 1387 N92-17873 * #
NAS 1.15:4284 ..... p 1276 N92-17945 * #
NAS 1.15:4326 ..... p 1267 N92-17032 * #
NAS 1.15:4332 ..... p 1389 N92-17048 * #
NAS 1.15:4335 ..... p 1234 N92-17128 * #
NAS 1.15:4336 ..... p 1232 N92-17226 * #
NAS 1.15:4339 ..... p 1258 N92-17881 * #
NAS 1.15:4341 ..... p 1230 N92-17071 * #
NAS 1.26:167696 ..... p 1241 N92-17167 * #
NAS 1.26:167697 ..... p 1241 N92-17214 * #
NAS 1.26:184220 ..... p 1344 N92-17778 * #
NAS 1.26:184272 ..... p 1253 N92-17495 * #
NAS 1.26:186943 ..... p 1250 N92-17585 * #
NAS 1.26:187355 ..... p 1250 N92-17728 * #
NAS 1.26:187418 ..... p 1245 N92-17215 * #
NAS 1.26:187615 ..... p 1228 N92-17512 * #
NAS 1.26:187802 ..... p 1298 N92-17588 * #
NAS 1.26:188236 ..... p 1321 N92-17975 * #
NAS 1.26:189097 ..... p 1253 N92-17510 * #
NAS 1.26:189245 ..... p 1386 N92-17003 * #
NAS 1.26:189253 ..... p 1300 N92-17887 * #
NAS 1.26:189568 ..... p 1242 N92-17045 * #
NAS 1.26:189745 ..... p 1386 N92-17020 * #
NAS 1.26:189746 ..... p 1386 N92-17021 * #
NAS 1.26:189750 ..... p 1386 N92-17497 * #
NAS 1.26:189751 ..... p 1386 N92-17483 * #
NAS 1.26:189753 ..... p 1386 N92-17484 * #
NAS 1.26:189773 ..... p 1266 N92-17004 * #
NAS 1.26:189778 ..... p 1236 N92-17019 * #
NAS 1.26:189779 ..... p 1390 N92-18003 * #
NAS 1.26:189781 ..... p 1317 N92-16990 * #
NAS 1.26:189786 ..... p 1280 N92-17139 * #
NAS 1.26:189787 ..... p 1253 N92-17365 * #
NAS 1.26:189789 ..... p 1301 N92-17006 * #
NAS 1.26:189806 ..... p 1387 N92-17695 * #
NAS 1.26:189807 ..... p 1244 N92-17200 * #
NAS 1.26:189808 ..... p 1306 N92-17304 * #
NAS 1.26:189814 ..... p 1313 N92-17393 * #
NAS 1.26:189815 ..... p 1387 N92-17650 * #
NAS 1.26:189816 ..... p 1279 N92-17046 * #
NAS 1.26:189831 ..... p 1276 N92-16989 * #
NAS 1.26:189840 ..... p 1312 N92-17225 * #
NAS 1.26:189842 ..... p 1388 N92-17377 * #
NAS 1.26:189843 ..... p 1388 N92-17697 * #
NAS 1.26:189846 ..... p 1333 N92-17132 * #
NAS 1.26:189848 ..... p 1355 N92-17692 * #
NAS 1.26:189852 ..... p 1316 N92-17227 * #
NAS 1.26:189853 ..... p 1233 N92-17316 * #
NAS 1.26:189856 ..... p 1373 N92-17375 * #
NAS 1.26:189857 ..... p 1388 N92-17696 * #
NAS 1.26:189858 ..... p 1361 N92-17646 * #
NAS 1.26:189859 ..... p 1361 N92-17647 * #
NAS 1.26:189860 ..... p 1303 N92-17152 * #
NAS 1.26:189861 ..... p 1252 N92-17150 * #
NAS 1.26:189872 ..... p 1245 N92-17334 * #
NAS 1.26:189873 ..... p 1241 N92-17335 * #
NAS 1.26:189882 ..... p 1311 N92-17511 * #
NAS 1.26:4421 ..... p 1318 N92-17072 * #
NAS 1.55:10083-VOL-1-PT-1 ..... p 1242 N92-17098 * #
NAS 1.55:10083-VOL-1-PT-2 ..... p 1248 N92-17409 * #
NAS 1.55:10083-VOL-2-PT-1 ..... p 1251 N92-17768 * #
NAS 1.55:10083-VOL-2-PT-2 ..... p 1245 N92-17348 * #
NAS 1.55:3131 ..... p 1219 N92-17984 * #
NAS 1.60:3131 ..... p 1223 N92-17131 * #
NAS 1.60:3159 ..... p 1328 N92-17022 * #
NAS 1.60:3162 ..... p 1267 N92-17070 * #
NAS 1.60:3182 ..... p 1330 N92-17645 * #
NAS 1.60:3191 ..... p 1253 N92-17151 * #
NAS 1.71:LAR-14169-1 ..... p 1307 N92-17677 * #
NAS 1.71:LAR-14547-1 ..... p 1300 N92-17909 * #
NAS 1.71:LAR-14594-1 ..... p 1300 N92-17888 * #
NAS 1.71:LAR-14608-1 ..... p 1271 N92-17676 * #
NAS 1.71:LAR-14626-1 ..... p 1309 N92-17859 * #
NAS 1.71:LEW-14345-6 ..... p 1255 N92-17882 * #
NAS 1.71:LEW-15216-1 ..... p 1307 N92-17678 * #
NAS 1.71:LEW-15241-1 ..... p 1257 N92-17861 * #
NAS 1.71:LEW-15359-1 ..... p 1261 N92-17902 * #
NAS 1.71:MFS-28431-1 ..... p 1257 N92-17870 * #
NAS 1.71:MFS-28589-1 ..... p 1306 N92-17584 * #
NAS 1.71:MFS-28633-1 ..... p 1335 N92-17866 * #
NAS 1.71:MSC-21415-1-SB ..... p 1344 N92-17860 * #
NAS 1.71:MSC-21752-1 ..... p 1335 N92-17910 * #
NAS 1.71:MSC-21776-1 ..... p 1278 N92-17913 * #
NAS 1.71:MSC-21806-1 ..... p 1368 N92-17863 * #
NAS 1.71:MSC-21898-1 ..... p 1307 N92-17872 * #
NAS 1.71:NPO-17763-1-CU ..... p 1305 N92-17862 * #
NAS 1.71:NPO-17781-1-CU ..... p 1337 N92-17884 * #
NAS 1.71:NPO-17918-2-CU ..... p 1349 N92-17895 * #
NAS 1.71:NPO-17994-1-CU ..... p 1293 N92-17907 * #
NAS 1.71:NPO-18146-1-CU ..... p 1368 N92-17892 * #
NAS 1.71:NPO-18366-1-CU ..... p 1277 N92-17674 * #
NAS 1.71:NPO-18379-1-CU ..... p 1367 N92-17675 * #
NAS 1.71:NPO-18386-1-CU ..... p 1305 N92-17899 * #
NAS 1.71:NPO-18454-1-CU ..... p 1293 N92-17865 * #
NAS 1.71:NPO-18593-1-CU ..... p 1368 N92-17864 * #

NASA-CASE-LAR-14169-1 ..... p 1307 N92-17677 * #
NASA-CASE-LAR-14547-1 ..... p 1300 N92-17909 * #
NASA-CASE-LAR-14594-1 ..... p 1300 N92-17888 * #
NASA-CASE-LAR-14608-1 ..... p 1271 N92-17676 * #
NASA-CASE-LAR-14626-1 ..... p 1309 N92-17859 * #

NASA-CASE-LEW-14345-6 ..... p 1255 N92-17882 * #
NASA-CASE-LEW-15216-1 ..... p 1307 N92-17678 * #
NASA-CASE-LEW-15241-1 ..... p 1257 N92-17861 * #
NASA-CASE-LEW-15359-1 ..... p 1261 N92-17902 * #

NASA-CASE-MFS-28431-1 ..... p 1257 N92-17870 * #
NASA-CASE-MFS-28589-1 ..... p 1306 N92-17584 * #
NASA-CASE-MFS-28633-1 ..... p 1335 N92-17866 * #

NASA-CASE-MSC-21415-1-SB .... p 1344 N92-17860 * #
NASA-CASE-MSC-21752-1 ..... p 1335 N92-17910 * #
NASA-CASE-MSC-21776-1 ..... p 1278 N92-17913 * #
NASA-CASE-MSC-21806-1 ..... p 1368 N92-17863 * #
NASA-CASE-MSC-21898-1 ..... p 1307 N92-17872 * #

NASA-CASE-NPO-17763-1-CU .... p 1305 N92-17862 * #
NASA-CASE-NPO-17781-1-CU .... p 1337 N92-17884 * #
NASA-CASE-NPO-17918-2-CU .... p 1349 N92-17895 * #
NASA-CASE-NPO-17994-1-CU .... p 1293 N92-17907 * #
NASA-CASE-NPO-18146-1-CU .... p 1368 N92-17892 * #
NASA-CASE-NPO-18366-1-CU .... p 1277 N92-17674 * #
NASA-CASE-NPO-18379-1-CU .... p 1367 N92-17675 * #
NASA-CASE-NPO-18386-1-CU .... p 1305 N92-17899 * #
NASA-CASE-NPO-18454-1-CU .... p 1293 N92-17865 * #
NASA-CASE-NPO-18593-1-CU .... p 1368 N92-17864 * #

NASA-CP-10083-VOL-1-PT-1 ..... p 1242 N92-17098 * #
NASA-CP-10083-VOL-1-PT-2 ..... p 1248 N92-17409 * #
NASA-CP-10083-VOL-2-PT-1 ..... p 1251 N92-17768 * #
NASA-CP-10083-VOL-2-PT-2 ..... p 1245 N92-17348 * #
NASA-CP-3131 ..... p 1219 N92-17984 * #

NASA-CR-167696 ..... p 1241 N92-17167 * #
NASA-CR-167697 ..... p 1241 N92-17214 * #
NASA-CR-184220 ..... p 1344 N92-17778 * #
NASA-CR-184272 ..... p 1253 N92-17495 * #
NASA-CR-186943 ..... p 1250 N92-17585 * #
NASA-CR-187355 ..... p 1250 N92-17728 * #
NASA-CR-187418 ..... p 1245 N92-17215 * #
NASA-CR-187615 ..... p 1228 N92-17512 * #
NASA-CR-187802 ..... p 1298 N92-17588 * #
NASA-CR-188236 ..... p 1321 N92-17975 * #
NASA-CR-189097 ..... p 1253 N92-17510 * #
NASA-CR-189245 ..... p 1386 N92-17003 * #
NASA-CR-189253 ..... p 1300 N92-17887 * #
NASA-CR-189568 ..... p 1242 N92-17045 * #
NASA-CR-189745 ..... p 1386 N92-17020 * #
NASA-CR-189746 ..... p 1386 N92-17021 * #
NASA-CR-189750 ..... p 1386 N92-17497 * #
NASA-CR-189751 ..... p 1386 N92-17483 * #
NASA-CR-189753 ..... p 1386 N92-17484 * #
NASA-CR-189773 ..... p 1266 N92-17004 * #
NASA-CR-189778 ..... p 1236 N92-17019 * #
NASA-CR-189779 ..... p 1390 N92-18003 * #
NASA-CR-189781 ..... p 1317 N92-16990 * #
NASA-CR-189786 ..... p 1280 N92-17139 * #
NASA-CR-189787 ..... p 1253 N92-17365 * #
NASA-CR-189789 ..... p 1301 N92-17006 * #
NASA-CR-189806 ..... p 1387 N92-17695 * #
NASA-CR-189807 ..... p 1244 N92-17200 * #
NASA-CR-189808 ..... p 1306 N92-17304 * #

NASA-CR-189814 ..... p 1313 N92-17393 * #
NASA-CR-189815 ..... p 1387 N92-17650 * #
NASA-CR-189816 ..... p 1279 N92-17046 * #
NASA-CR-189831 ..... p 1276 N92-16989 * #
NASA-CR-189840 ..... p 1312 N92-17225 * #
NASA-CR-189842 ..... p 1388 N92-17377 * #
NASA-CR-189843 ..... p 1388 N92-17697 * #
NASA-CR-189846 ..... p 1333 N92-17132 * #
NASA-CR-189848 ..... p 1355 N92-17692 * #
NASA-CR-189852 ..... p 1316 N92-17227 * #
NASA-CR-189853 ..... p 1233 N92-17316 * #
NASA-CR-189856 ..... p 1373 N92-17375 * #
NASA-CR-189857 ..... p 1388 N92-17696 * #
NASA-CR-189858 ..... p 1361 N92-17646 * #
NASA-CR-189859 ..... p 1361 N92-17647 * #
NASA-CR-189860 ..... p 1303 N92-17152 * #
NASA-CR-189861 ..... p 1252 N92-17150 * #
NASA-CR-189872 ..... p 1245 N92-17334 * #
NASA-CR-189873 ..... p 1241 N92-17335 * #
NASA-CR-189882 ..... p 1311 N92-17511 * #
NASA-CR-4421 ..... p 1318 N92-17072 * #

NASA-TM-100646 ..... p 1310 N92-17333 * #
NASA-TM-101662 ..... p 1381 N92-17001 * #
NASA-TM-103567 ..... p 1384 N92-17586 * #
NASA-TM-103684 ..... p 1237 N92-17059 * #
NASA-TM-103800 ..... p 1219 N92-17346 * #
NASA-TM-104168 ..... p 1225 N92-17547 * #
NASA-TM-104174 ..... p 1338 N92-17130 * #
NASA-TM-104177 ..... p 1347 N92-16987 * #
NASA-TM-104188 ..... p 1225 N92-17509 * #
NASA-TM-104189 ..... p 1256 N92-17007 * #
NASA-TM-104190 ..... p 1294 N92-17002 * #
NASA-TM-104192 ..... p 1309 N92-17034 * #
NASA-TM-104193 ..... p 1309 N92-17033 * #
NASA-TM-104195 ..... p 1272 N92-17693 * #
NASA-TM-104743 ..... p 1264 N92-17376 * #
NASA-TM-105258 ..... p 1235 N92-17061 * #
NASA-TM-105294 ..... p 1389 N92-17069 * #
NASA-TM-105370 ..... p 1267 N92-17060 * #
NASA-TM-105380 ..... p 1224 N92-17347 * #
NASA-TM-105397 ..... p 1235 N92-17546 * #
NASA-TM-105420 ..... p 1279 N92-17047 * #
NASA-TM-105422 ..... p 1279 N92-17062 * #
NASA-TM-105452 ..... p 1387 N92-17694 * #
NASA-TM-105464 ..... p 1308 N92-16988 * #
NASA-TM-105465 ..... p 1308 N92-17199 * #
NASA-TM-105467 ..... p 1308 N92-17005 * #
NASA-TM-105475 ..... p 1241 N92-17364 * #
NASA-TM-105476 ..... p 1241 N92-16975 * #
NASA-TM-105477 ..... p 1240 N92-16974 * #
NASA-TM-105478 ..... p 1242 N92-17534 * #
NASA-TM-105479 ..... p 1240 N92-16973 * #
NASA-TM-105505 ..... p 1387 N92-17873 * #
NASA-TM-4284 ..... p 1276 N92-17945 * #
NASA-TM-4326 ..... p 1267 N92-17032 * #
NASA-TM-4332 ..... p 1389 N92-17048 * #
NASA-TM-4335 ..... p 1234 N92-17128 * #
NASA-TM-4336 ..... p 1232 N92-17226 * #
NASA-TM-4339 ..... p 1258 N92-17881 * #
NASA-TM-4341 ..... p 1230 N92-17071 * #

NASA-TP-3131 ..... p 1223 N92-17131 * #
NASA-TP-3159 ..... p 1328 N92-17022 * #
NASA-TP-3162 ..... p 1267 N92-17070 * #
NASA-TP-3182 ..... p 1330 N92-17645 * #
NASA-TP-3191 ..... p 1253 N92-17151 * #

NATICK-TR-92/004-PHASE-1 ..... p 1256 N92-17053 #

NATICK/TR-90/001 ..... p 1383 N92-17274 #
NATICK/TR-92/005 ..... p 1225 N92-17404 #
NATICK/TR-92/007 ..... p 1334 N92-17143 #

NAVFAC-P-397 ..... p 1277 N92-17272 #

NAVSWC-MP-91-404 ..... p 1342 N92-17581 #

NAVSWC-TR-91-182 ..... p 1310 N92-17320 #
NAVSWC-TR-91-487 ..... p 1350 N92-17242 #
NAVSWC-TR-91-86 ..... p 1225 N92-17446 #

NAVY-CASE-70998 ..... p 1370 N92-17706 #
NAVY-CASE-71788 ..... p 1257 N92-17611 #
NAVY-CASE-73170 ..... p 1374 N92-17610 #
NAVY-CASE-73171 ..... p 1265 N92-17452 #
NAVY-CASE-73256 ..... p 1229 N92-17707 #
NAVY-CASE-73297 ..... p 1358 N92-17462 #
NAVY-CASE-73376 ..... p 1304 N92-17627 #
NAVY-CASE-73405 ..... p 1297 N92-17398 #
NAVY-CASE-73414 ..... p 1270 N92-17612 #
NAVY-CASE-73415 ..... p 1381 N92-17940
NAVY-CASE-73416 ..... p 1269 N92-17397 #
NAVY-CASE-73550 ..... p 1260 N92-17628 #
NAVY-CASE-73644 ..... p 1275 N92-17399 #

NCAR/TN-362+1A ..... p 1313 N92-17393 * #

NCS-TIB-90-14 ..... p 1344 N92-17948 #
NCS-TIB-90-16 ..... p 1278 N92-16996 #
NCS-TIB-91-3 ..... p 1281 N92-17267 #

NCTRF-187 ..... p 1379 N92-17537 #

NEDU-10-91 ..... p 1333 N92-17014 #
NEDU-12-91 ..... p 1334 N92-17331 #

NIAR-91-27 ..... p 1298 N92-17588 * #
NIAR-91-30 ..... p 1227 N92-17587 #

NIST-TR-10 ..... p 1373 N92-17322 #
NIST-TR-11 ..... p 1268 N92-17171 #
NIST-TR-6 ..... p 1271 N92-17615 #
NIST-TR-7 ..... p 1372 N92-17238 #
NIST-TR-8 ..... p 1268 N92-17170 #
NIST-TR-9 ..... p 1268 N92-17172 #

NISTIR-3963 ..... p 1295 N92-17018 #

NOAA-TM-ERL-AOML-69 ..... p 1319 N92-17138 #

NOAA-TM-ERL-ARL-188 ..... p 1315 N92-17134 #

NOAA-TM-NWS-ER-85 ..... p 1319 N92-17363 #

NOAA-TM-NWS-NHC-38 ..... p 1321 N92-17705 #

NOARL-R-17 ..... p 1325 N92-17765 #

NOARL-TN-111 ..... p 1319 N92-17338 #
NOARL-TN-112 ..... p 1320 N92-17492 #
NOARL-TN-113 ..... p 1320 N92-17493 #
NOARL-TN-114 ..... p 1320 N92-17406 #
NOARL-TN-115 ..... p 1320 N92-17494 #
NOARL-TN-127 ..... p 1325 N92-17766 #
NOARL-TN-136 ..... p 1323 N92-17041 #

NOR-89-101 ..... p 1233 N92-17513 #

NOSC-TD-2174 ..... p 1383 N92-17369 #
NOSC-TD-2222 ..... p 1274 N92-17947 #

NOSC-TR-1399 ..... p 1351 N92-17560 #
NOSC-TR-1460 ..... p 1282 N92-17383 #

NOSC/TD-2194 ..... p 1339 N92-17211 #

NOSC/TR-1450 ..... p 1345 N92-17395 #

NPS-AS-91-016 ..... p 1346 N92-17425 #

NPS-CS-91-009 ..... p 1383 N92-17402 #
NPS-CS-91-013 ..... p 1339 N92-17285 #
NPS-CS-91-014 ..... p 1340 N92-17403 #

NPSOR-91-020 ..... p 1353 N92-17643 #
NPSOR-91-025 ..... p 1352 N92-17440 #
NPSOR-91-029 ..... p 1321 N92-17764 #
NPSOR-91-030 ..... p 1286 N92-16993 #

NRC-32149 ..... p 1229 N92-17568 #

NREL/TP-257-4510 ..... p 1226 N92-17874 #
NREL/TP-257-4518 ..... p 1313 N92-17875 #

NRL-MR-6911 ..... p 1303 N92-17127 #
NRL-MR-6912 ..... p 1369 N92-17499 #
NRL-MR-6926 ..... p 1295 N92-17126 #
NRL-MR-6927 ..... p 1359 N92-17505 #

NRL-9359 ..... p 1286 N92-17931 #

NRMI-91-84 ..... p 1328 N92-17124 #

NSSDC/WDC-A-R/S-91-25 ..... p 1387 N92-17694 * #

NSTS-08194 ..... p 1240 N92-16973 * #
NSTS-08207 ..... p 1241 N92-17364 * #
NSTS-08302 ..... p 1241 N92-16975 * #
NSTS-08308 ..... p 1242 N92-17534 * #
NSTS-08354 ..... p 1240 N92-16974 * #

NTSB/AAB-90/04 ..... p 1226 N92-17133 #

NTSB/AAR-91/05 ..... p 1226 N92-17213 #

NTSC-91-01 ..... p 1391 N92-17372 #

NUSC-TD-7016 ..... p 1318 N92-17027 #

NWRA-CR-91-R072 ..... p 1316 N92-17209 #

OUEL-1819/90 ..... p 1229 N92-17878 #
OUEL-1876/91 ..... p 1380 N92-17879 #
OUEL-1879/91 ..... p 1349 N92-17880 #
OUEL-1886/91 ..... p 1302 N92-17926 #
OUEL-1892/91 ..... p 1344 N92-17927 #

PATENTS-US-A7420433 ..... p 1304 N92-17649 #
PATENTS-US-A7461591 ..... p 1306 N92-17183 #
PATENTS-US-A7504223 ..... p 1255 N92-17867 #
PATENTS-US-A7511684 ..... p 1363 N92-17739 #
PATENTS-US-A7543897 ..... p 1274 N92-17842 #
PATENTS-US-A7559234 ..... p 1274 N92-17935 #

PB90-916904 ..... p 1226 N92-17133 #
PB91-201293 ..... p 1290 N92-17620 #
PB91-201301 ..... p 1290 N92-17559 #
PB91-202762 ..... p 1382 N92-17228 #
PB91-205120 ..... p 1314 N92-17619 #
PB91-219170 ..... p 1385 N92-17283 #
PB91-221788 ..... p 1316 N92-17229 #
PB91-222679 ..... p 1295 N92-17018 #
PB91-225037 ..... p 1319 N92-17363 #
PB91-226886 ..... p 1321 N92-17621 #
PB91-230219 ..... p 1387 N92-17251 #
PB91-233783 ..... p 1313 N92-17393 * #
PB91-234286 ..... p 1319 N92-17138 #
PB91-235499 ..... p 1315 N92-17134 #
PB91-236463 ..... p 1321 N92-17705 #
PB91-910405 ..... p 1226 N92-17213 #

PL-TR-91-1036 ..... p 1279 N92-17031 #
PL-TR-91-1045 ..... p 1286 N92-17017 #
PL-TR-91-2034 ..... p 1319 N92-17289 #
PL-TR-91-2070 ..... p 1316 N92-17202 #
PL-TR-91-2075 ..... p 1319 N92-17233 #
PL-TR-91-2171 ..... p 1316 N92-17209 #
PL-TR-91-2198 ..... p 1283 N92-17600 #
PL-TR-91-3073 ..... p 1264 N92-17379 #

PME-FM-91-2 ..... p 1296 N92-17176 #

PMTC-TP-000060 ..... p 1324 N92-17177 #

PNL-SA-19136 ..... p 1358 N92-17453 #
PNL-SA-20109 ..... p 1314 N92-17665 #

PNL-7817 ..... p 1313 N92-17934 #

PSI-2145/TR-1108 ..... p 1295 N92-17012 #

PSR-2040 ..... p 1329 N92-17476 #

PSU/ARL-TM-91-299 ..... p 1297 N92-17387 #

PSU/ARL-TR-91-011 ..... p 1323 N92-17078 #
PSU/ARL-TR-91-012 ..... p 1323 N92-17083 #

PWA-FR21998-1 ..... p 1265 N92-17653 #

QTR-CDRL-29087 ..... p 1235 N92-17552 #

R/D-6148-MS-01 ..... p 1310 N92-17256 #
R/D-6703-MS-03 ..... p 1256 N92-17392 #

RAE-TR-91044 ..... p 1287 N92-17186 #

RCC-316-91 ..... p 1305 N92-17962 #

RD-5830-EE-01-APP ..... p 1366 N92-17485 #
RD-5830-EE-01 ..... p 1366 N92-17486 #

REPT-11 ..... p 1381 N92-17001 * #
REPT-4-20-630-4183 ..... p 1356 N92-17026 #
REPT-722792-2 ..... p 1233 N92-17316 * #
REPT-92B00009 ..... p 1389 N92-17048 * #
REPT-92B00027 ..... p 1258 N92-17881 * #

RFP-4387 ..... p 1266 N92-17858 #

RL-TR-91-181 ..... p 1291 N92-17684 #
RL-TR-91-192 ..... p 1382 N92-17037 #
RL-TR-91-198 ..... p 1339 N92-17185 #
RL-TR-91-199 ..... p 1301 N92-17140 #
RL-TR-91-221 ..... p 1288 N92-17268 #
RL-TR-91-253 ..... p 1340 N92-17286 #
RL-TR-91-263 ..... p 1374 N92-17553 #
RL-TR-91-278 ..... p 1350 N92-17330 #
RL-TR-91-279 ..... p 1284 N92-17689 #
RL-TR-91-289 ..... p 1359 N92-17514 #
RL-TR-91-307 ..... p 1301 N92-17273 #
RL-TR-91-56 ..... p 1282 N92-17429 #

RMA-TMR-0101 ..... p 1235 N92-17644 #

RPT/F0175.98 ..... p 1253 N92-17495 * #

RSRE-MEMO-4529 ..... p 1365 N92-17180 #

RTI/3966/00-01F ..... p 1234 N92-17221 #

S-651 ..... p 1328 N92-17022 * #
S-653-VOL-1-PT-1 ..... p 1242 N92-17098 * #
S-653-VOL-1-PT-2 ..... p 1248 N92-17409 * #
S-653-VOL-2-PT-1 ..... p 1251 N92-17768 * #
S-653-VOL-2-PT-2 ..... p 1245 N92-17348 * #
S-660 ..... p 1264 N92-17376 * #
S-665 ..... p 1330 N92-17645 * #

SAND-91-0051C ..... p 1377 N92-17790 #
SAND-91-1423C ..... p 1272 N92-17710 #
SAND-91-1635C ..... p 1377 N92-17797 #
SAND-91-1732 ..... p 1311 N92-17937 #
SAND-91-2212C ..... p 1289 N92-17468 #
SAND-91-2509C ..... p 1274 N92-17938 #

SGD-562-PT-2 ..... p 1387 N92-17251 #

SLAC-PUB-5698 ..... p 1292 N92-17801 #

SLCET-TR-91-26 ..... p 1281 N92-17258 #

SR-1 ..... p 1316 N92-17209 #
SR-1 ..... p 1283 N92-17600 #
SR-3 ..... p 1319 N92-17289 #

SSD-TR-91-24 ..... p 1343 N92-17640 #
SSD-TR-91-30 ..... p 1253 N92-17085 #

SU-TR-448 ..... p 1352 N92-17178 #

TAPS-010-1992 ..... p 1317 N92-16990 * #

TOR-0091(6078)-2 ..... p 1315 N92-17035 #

TR-R90222 ..... p 1239 N92-17325 #

TR-0090(5935-02)-1 ..... p 1253 N92-17085 #
TR-10 ..... p 1263 N92-17271 #
TR-112 ..... p 1358 N92-17472 #
TR-11 ..... p 1372 N92-17181 #
TR-12 ..... p 1255 N92-17329 #
TR-12 ..... p 1264 N92-17370 #
TR-13 ..... p 1259 N92-17371 #
TR-14 ..... p 1259 N92-17323 #
TR-1 ..... p 1272 N92-17749 #
TR-2 ..... p 1272 N92-17750 #
TR-31 ..... p 1254 N92-17270 #
TR-31 ..... p 1271 N92-17659 #
TR-32 ..... p 1269 N92-17460 #
TR-32 ..... p 1361 N92-17660 #
TR-33 ..... p 1269 N92-17461 #
TR-33 ..... p 1271 N92-17661 #
TR-34 ..... p 1356 N92-17197 #
TR-35 ..... p 1266 N92-16976 #
TR-35 ..... p 1356 N92-17196 #
TR-35 ..... p 1259 N92-17247 #
TR-36 ..... p 1268 N92-17195 #
TR-36 ..... p 1365 N92-17249 #
TR-36 ..... p 1271 N92-17679 #
TR-37 ..... p 1259 N92-17246 #
TR-38 ..... p 1290 N92-17596 #
TR-39 ..... p 1260 N92-17613 #
TR-3 ..... p 1273 N92-17751 #
TR-40 ..... p 1259 N92-17248 #
TR-40 ..... p 1260 N92-17389 #
TR-41 ..... p 1259 N92-17261 #
TR-41 ..... p 1358 N92-17428 #
TR-42 ..... p 1264 N92-17427 #
TR-43 ..... p 1359 N92-17491 #
TR-44 ..... p 1289 N92-17490 #
TR-45 ..... p 1361 N92-17616 #
TR-4 ..... p 1273 N92-17752 #
TR-51 ..... p 1269 N92-17448 #
TR-55 ..... p 1374 N92-17449 #
TR-5 ..... p 1273 N92-17753 #
TR-6 ..... p 1295 N92-17025 #
TR-6 ..... p 1365 N92-17284 #
TR-6 ..... p 1375 N92-17685 #
TR-86 ..... p 1260 N92-17489 #
TR-9 ..... p 1262 N92-16985 #

TRW-TS-91-01 ..... p 1337 N92-17064 #
TRW-TS-91-02 ..... p 1347 N92-16994 #

TR91-003 ..... p 1342 N92-17637 #
TR91-019 ..... p 1380 N92-17651 #
TR91-024 ..... p 1381 N92-17669 #
TR91-028 ..... p 1346 N92-17638 #

TW-90-09 ..... p 1351 N92-17517 #
TW-91-04 ..... p 1353 N92-17837 #
TW-91-05 ..... p 1349 N92-17838 #

UCRL-CR-107449 ..... p 1330 N92-17714 #
UCRL-CR-108433 ..... p 1388 N92-17832 #
UCRL-CR-108459 ..... p 1368 N92-17846 #

UCRL-ID-107480 ..... p 1298 N92-17625 #

UCRL-JC-106782 ..... p 1317 N92-17578 #
UCRL-JC-107357 ..... p 1364 N92-17876 #
UCRL-JC-108590 ..... p 1349 N92-17965 #
UCRL-JC-108648 ..... p 1385 N92-17845 #

UDR-TR-89-115 ..... p 1350 N92-17330 #
UDR-TR-89-119 ..... p 1284 N92-17689 #
UDR-TR-90-114 ..... p 1227 N92-17478 #

UMR-FDB-22 ..... p 1373 N92-17382 #

UR-1214 ..... p 1379 N92-17807 #

US-PATENT-APPL-SN-230547 ..... p 1302 N92-17826
US-PATENT-APPL-SN-395547 ..... p 1293 N92-17871
US-PATENT-APPL-SN-420433 ..... p 1304 N92-17649 #
US-PATENT-APPL-SN-445329 ..... p 1302 N92-17918
US-PATENT-APPL-SN-461591 ..... p 1306 N92-17183 #
US-PATENT-APPL-SN-488411 ..... p 1305 N92-17923
US-PATENT-APPL-SN-501068 ..... p 1302 N92-17835
US-PATENT-APPL-SN-504223 ..... p 1255 N92-17867 #
US-PATENT-APPL-SN-511684 ..... p 1363 N92-17739 #
US-PATENT-APPL-SN-517354 ..... p 1285 N92-17829
US-PATENT-APPL-SN-531488 ..... p 1270 N92-17612 #
US-PATENT-APPL-SN-543897 ..... p 1274 N92-17842 #
US-PATENT-APPL-SN-544556 ..... p 1367 N92-17828
US-PATENT-APPL-SN-559234 ..... p 1274 N92-17935 #
US-PATENT-APPL-SN-564894 ..... p 1276 N92-17830
US-PATENT-APPL-SN-590183 ..... p 1307 N92-17827
US-PATENT-APPL-SN-621102 ..... p 1257 N92-17836
US-PATENT-APPL-SN-654111 ..... p 1287 N92-17129
US-PATENT-APPL-SN-660364 ..... p 1257 N92-17611 #
US-PATENT-APPL-SN-684091 ..... p 1304 N92-17627 #
US-PATENT-APPL-SN-704563 ..... p 1265 N92-17452 #
US-PATENT-APPL-SN-708991 ..... p 1229 N92-17707 #
US-PATENT-APPL-SN-722447 ..... p 1370 N92-17706 #
US-PATENT-APPL-SN-724083 ..... p 1358 N92-17462 #
US-PATENT-APPL-SN-725709 ..... p 1368 N92-17959
US-PATENT-APPL-SN-726483 ..... p 1269 N92-17397 #
US-PATENT-APPL-SN-726489 ..... p 1374 N92-17610 #
US-PATENT-APPL-SN-728918 ..... p 1275 N92-17399 #
US-PATENT-APPL-SN-729743 ..... p 1297 N92-17398 #
US-PATENT-APPL-SN-744042 ..... p 1337 N92-17884 * #
US-PATENT-APPL-SN-748224 ..... p 1300 N92-17909 * #
US-PATENT-APPL-SN-748225 ..... p 1300 N92-17888 * #
US-PATENT-APPL-SN-749357 ..... p 1260 N92-17628 #
US-PATENT-APPL-SN-749819 ..... p 1344 N92-17860 * #
US-PATENT-APPL-SN-751440 ..... p 1305 N92-17899 * #
US-PATENT-APPL-SN-751489 ..... p 1309 N92-17859 * #
US-PATENT-APPL-SN-752246 ..... p 1271 N92-17676 * #
US-PATENT-APPL-SN-772763 ..... p 1278 N92-17913 * #
US-PATENT-APPL-SN-775404 ..... p 1335 N92-17910 * #
US-PATENT-APPL-SN-780512 ..... p 1307 N92-17872 * #
US-PATENT-APPL-SN-780513 ..... p 1368 N92-17863 * #
US-PATENT-APPL-SN-781520 ..... p 1277 N92-17674 * #
US-PATENT-APPL-SN-781521 ..... p 1293 N92-17865 * #
US-PATENT-APPL-SN-782009 ..... p 1305 N92-17862 * #
US-PATENT-APPL-SN-786499 ..... p 1349 N92-17895 * #
US-PATENT-APPL-SN-786618 ..... p 1368 N92-17892 * #
US-PATENT-APPL-SN-786641 ..... p 1381 N92-17940
US-PATENT-APPL-SN-791728 ..... p 1307 N92-17677 * #
US-PATENT-APPL-SN-791759 ..... p 1293 N92-17907 * #
US-PATENT-APPL-SN-797168 ..... p 1293 N92-17831
US-PATENT-APPL-SN-797484 ..... p 1261 N92-17902 * #
US-PATENT-APPL-SN-797569 ..... p 1367 N92-17675 * #
US-PATENT-APPL-SN-798464 ..... p 1257 N92-17861 * #
US-PATENT-APPL-SN-812084 ..... p 1257 N92-17870 * #
US-PATENT-APPL-SN-812901 ..... p 1368 N92-17864 * #
US-PATENT-APPL-SN-813628 ..... p 1306 N92-17584 * #
US-PATENT-APPL-SN-813629 ..... p 1335 N92-17866 * #
US-PATENT-APPL-SN-822240 ..... p 1255 N92-17882 * #
US-PATENT-APPL-SN-826547 ..... p 1307 N92-17678 * #

US-PATENT-CLASS-102-418 ..... p 1302 N92-17918
US-PATENT-CLASS-136-201 ..... p 1302 N92-17835
US-PATENT-CLASS-248-635 ..... p 1307 N92-17827
US-PATENT-CLASS-252-62 ..... p 1257 N92-17836
US-PATENT-CLASS-310-10 ..... p 1293 N92-17831
US-PATENT-CLASS-324-244 ..... p 1368 N92-17959
US-PATENT-CLASS-33-363-K ..... p 1302 N92-17826
US-PATENT-CLASS-342-107 ..... p 1287 N92-17129
US-PATENT-CLASS-342-374 ..... p 1285 N92-17829
US-PATENT-CLASS-350-96.20 ..... p 1367 N92-17828
US-PATENT-CLASS-372-41 ..... p 1305 N92-17923
US-PATENT-CLASS-427-113 ..... p 1293 N92-17871
US-PATENT-CLASS-89-7 ..... p 1276 N92-17830

US-PATENT-5,021,098 ..... p 1302 N92-17835
US-PATENT-5,023,006 ..... p 1257 N92-17836
US-PATENT-5,028,112 ..... p 1367 N92-17828

US-PATENT-5,038,103 ..... p 1368 N92-17959
US-PATENT-5,038,353 ..... p 1305 N92-17923
US-PATENT-5,040,764 ..... p 1307 N92-17827
US-PATENT-5,042,157 ..... p 1302 N92-17826
US-PATENT-5,045,349 ..... p 1293 N92-17871
US-PATENT-5,045,857 ..... p 1285 N92-17829
US-PATENT-5,046,427 ..... p 1302 N92-17918
US-PATENT-5,051,751 ..... p 1287 N92-17129
US-PATENT-5,052,272 ..... p 1276 N92-17830
US-PATENT-5,059,839 ..... p 1293 N92-17831

USAARL-91-17 ..... p 1328 N92-17084 #
USAARL-91-20 ..... p 1329 N92-17299 #
USAARL-91-21 ..... p 1326 N92-17269 #

USAFA-TR-91-13 ..... p 1388 N92-17595 #
USAFA-TR-91-17 ..... p 1371 N92-17015 #

USAFETAC/DS-91/244 ..... p 1319 N92-17257 #
USAFETAC/DS-91/248 ..... p 1320 N92-17444 #
USAFETAC/DS-91/250 ..... p 1320 N92-17400 #
USAFETAC/DS-91/252 ..... p 1318 N92-17073 #
USAFETAC/DS-91/253 ..... p 1318 N92-17074 #
USAFETAC/DS-91/255 ..... p 1319 N92-17144 #

USAFETAC/PR-91/007 ..... p 1318 N92-17113 #
USAFETAC/PR-91/019 ..... p 1383 N92-17401 #

USGS-BULL-1924 ..... p 1316 N92-17229 #

UT-5473-1 ..... p 1375 N92-17667 #

UTRC-R91-970089-01 ..... p 1236 N92-17243 #

UVA/525449/CS92/101 ..... p 1342 N92-17636 #

UWA/DME/TR-91/7 ..... p 1273 N92-17784 #

VPI-AOE-179 ..... p 1223 N92-17222 #

VPI-E-91-20 ..... p 1223 N92-17117 #

VRI-ARI-9 ..... p 1330 N92-17567 #

WES/MP/GL-91-12 ..... p 1238 N92-17287 #

WES/TR/EL-91-15 ..... p 1234 N92-17240 #

WES/TR/HL-91-20 ..... p 1324 N92-17298 #

WHC-SA-1210 ..... p 1311 N92-17713 #

WHOI-91-16 ..... p 1383 N92-17378 #
WHOI-91-29 ..... p 1324 N92-17583 #

WL-TM-91-315-FIGK ..... p 1333 N92-16982 #

WL-TR-91-1042 ..... p 1234 N92-17221 #
WL-TR-91-1060 ..... p 1339 N92-17179 #
WL-TR-91-2067 ..... p 1361 N92-17652 #
WL-TR-91-2071 ..... p 1235 N92-17204 #
WL-TR-91-2073 ..... p 1235 N92-17644 #
WL-TR-91-2108 ..... p 1234 N92-17011 #
WL-TR-91-2109 ..... p 1295 N92-17012 #
WL-TR-91-3006 ..... p 1227 N92-17478 #
WL-TR-91-3056 ..... p 1383 N92-17396 #
WL-TR-91-3104 ..... p 1233 N92-17513 #
WL-TR-91-4044 ..... p 1391 N92-17079 #
WL-TR-91-8035 ..... p 1352 N92-17223 #

WRDC-TR-90-4096-VOL-1 ..... p 1272 N92-17683 #
WRDC-TR-90-4096-VOL-2 ..... p 1270 N92-17614 #
WRDC-TR-90-4096-VOL-3 ..... p 1270 N92-17597 #

WSRL-TM-5/91 ..... p 1366 N92-17294 #

WSU/DC/91/TR-65 ..... p 1373 N92-17245 #
WSU/DC/91/TR-66 ..... p 1357 N92-17423 #
WSU/DC/91/TR-68 ..... p 1266 N92-17010 #

Typical Accession Number Index Listing

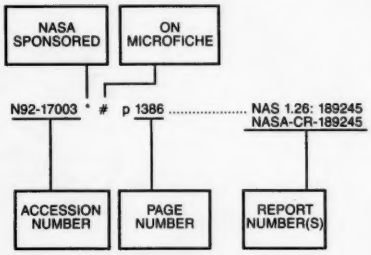

Listings in this index are arranged alphanumerically by accession number. The page number helps to locate the citation in the abstract section. An asterisk (*) indicates that the item is a NASA report. A pound sign (#) indicates that the item is available on microfiche.

N92-16973* # p 1240 ..... NAS 1.15:105479
N92-16973* # p 1240 ..... NASA-TM-105479
NSTS-08194
N92-16974* # p 1240 ..... NAS 1.15:105477
NASA-TM-105477
NSTS-08354
N92-16975* # p 1241 ..... NAS 1.15:105476
NASA-TM-105476
NSTS-08302
N92-16976 # p 1266 ..... AD-A242328
TR-35
N92-16977 # p 1258 ..... AD-A243030
AFOSR-91-0919TR
N92-16978 # p 1294 ..... AD-A243033
DTRC/SHD-1003-06
N92-16979 # p 1294 ..... AD-A243035
AFOSR-91-0906TR
N92-16980 # p 1278 ..... AD-A243099
HDL-SR-91-8
N92-16981 # p 1364 ..... AD-A243103
N92-16982 # p 1333 ..... AD-A243253
WL-TM-91-315-FIGK
N92-16983 # p 1300 ..... AD-A243256
N92-16984 # p 1371 ..... AD-A243257
N92-16985 # p 1262 ..... AD-A243258
TR-9
N92-16986 # p 1226 ..... DOT/FAA/CT-91/4
N92-16987* # p 1347 ..... NAS 1.15:104177
NASA-TM-104177
N92-16988* # p 1308 ..... ISSN-1049-667X
NAS 1.15:105464
NASA-TM-105464
N92-16989* # p 1276 ..... CSC-92-0141
MCR-92-1310
NAS 1.26:189831
NASA-CR-189831
N92-16990* # p 1317 ..... NAS 1.26:189781
NASA-CR-189781
TAPS-010-1992
N92-16991 # p 1347 ..... AD-A242377
AIP-147
N92-16992 # p 1255 ..... AD-A242396
MTL-TR-91-41
N92-16993 # p 1286 ..... AD-A242960
NPSOR-91-030
N92-16994 # p 1347 ..... AD-A242963
TRW-TS-91-02
N92-16995 # p 1371 ..... AD-A243098
HDL-TM-91-16
N92-16996 # p 1278 ..... AD-A243175
NCS-TIB-90-16
N92-16997 # p 1345 ..... AD-A243176
MIT/LCS/TR-518
N92-16998 # p 1352 ..... AD-A243183
ESD-TR-91-094
MIT-TR-927
N92-16999 # p 1354 ..... AD-A243184
N92-17000 # p 1262 ..... AD-A243186
N92-17001* # p 1381 ..... NAS 1.15:101662
NASA-TM-101662
REPT-11
N92-17002* # p 1294 ..... NAS 1.15:104190
NASA-TM-104190
N92-17003* # p 1386 ..... NAS 1.26:189245
NASA-CR-189245
N92-17004* # p 1266 ..... NAS 1.26:189773
NASA-CR-189773
N92-17005* # p 1308 ..... ISSN-1051-225X
NAS 1.15:105467
NASA-TM-105467
N92-17006* # p 1301 ..... LR-31824
NAS 1.26:189789
NASA-CR-189789
N92-17007* # p 1256 ..... AVSCOM-TR-92-B-001
NAS 1.15:104189
NASA-TM-104189
N92-17008 # p 1315 ..... AD-A241918
N92-17009 # p 1317 ..... AD-A241919
BK-22-91
N92-17010 # p 1266 ..... AD-A242397
WSU/DC/91/TR-68
N92-17011 # p 1234 ..... AD-A242398
WL-TR-91-2108
N92-17012 # p 1295 ..... AD-A242399
PSI-2145/TR-1108
WL-TR-91-2109
N92-17013 # p 1381 ..... AD-A242875
AFPT-90-70X-877
N92-17014 # p 1333 ..... AD-A243535
NEDU-10-91
N92-17015 # p 1371 ..... AD-A243537
USAFA-TR-91-17
N92-17016 # p 1278 ..... AD-A243553
N92-17017 # p 1286 ..... AD-A243555
J200-91-0080/7208
PL-TR-91-1045
N92-17018 # p 1295 ..... NISTIR-3963
PB91-222679
N92-17019* # p 1236 ..... NAS 1.26:189778
NASA-CR-189778
N92-17020* # p 1386 ..... NAS 1.26:189745
NASA-CR-189745
N92-17021* # p 1386 ..... NAS 1.26:189746
NASA-CR-189746
N92-17022* # p 1328 ..... NAS 1.60:3159
NASA-TP-3159
S-651
N92-17023 # p 1337 ..... AD-A241858
AFIT/DS/ENG/91-02
N92-17024 # p 1306 ..... AD-A241859
AFIT/GAE/ENY/91S-4
N92-17025 # p 1295 ..... AD-A241871
TR-6
N92-17026 # p 1356 ..... AD-A241878
REPT-4-20-630-4183
N92-17027 # p 1318 ..... AD-A241885
NUSC-TD-7016
N92-17028 # p 1318 ..... AD-A242890
ATC-180
N92-17029 # p 1267 ..... AD-A243062
AFOSR-91-0920TR
N92-17030 # p 1369 ..... AD-A243237
N92-17031 # p 1279 ..... AD-A243551
AD-E200790
PL-TR-91-1036
N92-17032* # p 1267 ..... L-16982
NAS 1.15:4326
NASA-TM-4326
N92-17033* # p 1309 ..... NAS 1.15:104193
NASA-TM-104193
N92-17034* # p 1309 ..... NAS 1.15:104192
NASA-TM-104192
N92-17035 # p 1315 ..... AD-A241853
TOR-0091(6078)-2
N92-17036 # p 1279 ..... AD-A241856
N92-17037 # p 1382 ..... AD-A241866
RL-TR-91-192
N92-17038 # p 1356 ..... AD-A241870
N92-17039 # p 1295 ..... AD-A241886
AFOSR-91-0874TR
N92-17040 # p 1279 ..... AD-A241887
ESD-TR-91-056
MIT-TR-918
N92-17041 # p 1323 ..... AD-A241909
AD-E040128
NOARL-TN-136
N92-17042 # p 1267 ..... AD-A242860
N92-17043 # p 1258 ..... AD-A243054
AFOSR-91-0926TR
N92-17044 # p 1365 ..... AD-A243055
AFOSR-91-0927TR
N92-17045* # p 1242 ..... NAS 1.26:189568
NASA-CR-189568
N92-17046* # p 1279 ..... DTW-8944-91003
NAS 1.26:189816
NASA-CR-189816
N92-17047* # p 1279 ..... E-6835
NAS 1.15:105420
NASA-TM-105420
N92-17048* # p 1389 ..... NAS 1.15:4332
NASA-TM-4332
REPT-92B00009
N92-17049 # p 1347 ..... AD-A241854
AFOSR-91-0878TR
N92-17050 # p 1318 ..... AD-A242840
ATC-183
DOT/FAA/NR-91/9
N92-17051 # p 1323 ..... AD-A242843
N92-17052 # p 1331 ..... AD-A243015
HEL-TM-17-91
N92-17053 # p 1256 ..... AD-A243018
NATICK-TR-92/004-PHASE-1
N92-17054 # p 1267 ..... AD-A243061
AFOSR-91-0918TR
N92-17055 # p 1254 ..... AD-A243235
CRREL-SR-91-13
N92-17056 # p 1262 ..... AD-A243238
DTRC/SME-91/51
N92-17057 # p 1262 ..... AD-A243239
DTRC/SME-91/06
N92-17058 # p 1275 ..... AD-A243244
DODA-AR-006-379
MRL-TR-91-25
N92-17059* # p 1237 ..... E-5902
NAS 1.15:103684
NASA-TM-103684
N92-17060* # p 1267 ..... E-6749
NAS 1.15:105370
NASA-TM-105370
N92-17061* # p 1235 ..... E-5976
NAS 1.15:105258
NASA-TM-105258
N92-17062* # p 1279 ..... E-6838
NAS 1.15:105422
NASA-TM-105422
N92-17063 p 1315 ..... NO REPORT NUMBER
N92-17064 # p 1337 ..... AD-A243022
TRW-TS-91-01
N92-17065 # p 1267 ..... AD-A243060
N92-17066 # p 1275 ..... AD-A243063
BFLRF-266
N92-17067 # p 1382 ..... AD-A243079
N92-17068 # p 1337 ..... AD-A243089
IDA-P-2628
IDA/HQ-91-39501
N92-17069* # p 1389 ..... E-6633
NAS 1.15:105294
NASA-TM-105294
N92-17070* # p 1267 ..... E-6343
NAS 1.60:3162
NASA-TP-3162
N92-17071* # p 1230 ..... H-1743
NAS 1.15:4341
NASA-TM-4341
N92-17072* # p 1318 ..... M-678
NAS 1.26:4421
NASA-CR-4421
N92-17073 # p 1318 ..... AD-A243310
USAFETAC/DS-91/252
N92-17074 # p 1318 ..... AD-A243677
USAFETAC/DS-91/253

N92-17075 # p 1242 ..... AD-A243682
N92-17076 # p 1286 ..... AD-A243685
AFIT/GE/ENG/91D-43
N92-17077 # p 1338 ..... AD-A243699
AFIT/ENG/GEO/91D-06
N92-17078 # p 1323 ..... AD-A242411
PSU/ARL-TR-91-011
N92-17079 # p 1391 ..... AD-A243331
WL-TR-91-4044
N92-17080 # p 1303 ..... AD-A243517
CMU-RI-TR-91-18
N92-17081 # p 1350 ..... AD-A243519
AMSAA-TR-501
N92-17082 # p 1372 ..... AD-A243668
MTL-TR-91-45
N92-17083 # p 1323 ..... AD-A241943
PSU/ARL-TR-91-012
N92-17084 # p 1328 ..... AD-A241966
USAARL-91-17
N92-17085 # p 1253 ..... AD-A242297
SSD-TR-91-30
TR-0090(5935-02)-1
N92-17086 # p 1354 ..... AD-A243525
APL-UW-TR-9106
N92-17087 # p 1286 ..... AD-A243660
N92-17088 # p 1365 ..... AD-A243686
AFIT/GE/ENG/91D-45
N92-17089 # p 1328 ..... AD-A243687
AFIT/GE/ENG/91D-17
N92-17090 # p 1280 ..... AD-A243688
AFIT/GE/ENG/91D-54
N92-17091 # p 1259 ..... AD-A243690
AFIT/GEP/ENP/91D-8
N92-17092 # p 1280 ..... AD-A243691
AFIT/GE/ENG/91D-09
N92-17093 # p 1338 ..... AD-A243692
AFIT/GE/ENG/91D-52
N92-17094 # p 1315 ..... AD-A243696
AFIT/GE/ENG/91D-46
N92-17095 # p 1280 ..... AD-A243697
AFIT/GE/ENG/91D-24
N92-17096 # p 1236 ..... AD-A243698
AFIT/GE/ENG/91D-39
N92-17097 # p 1238 ..... AD-A243700
AFIT/GCE/ENS/91D-01
N92-17098* # p 1242 ..... NAS 1.55:10083-VOL-1-PT-1
NASA-CP-10083-VOL-1-PT-1
S-653-VOL-1-PT-1
N92-17099* # p 1242 ..... NO REPORT NUMBER
N92-17100* # p 1243 ..... NO REPORT NUMBER
N92-17101* # p 1243 ..... NO REPORT NUMBER
N92-17102* # p 1243 ..... NO REPORT NUMBER
N92-17103* # p 1243 ..... NO REPORT NUMBER
N92-17104* # p 1243 ..... NO REPORT NUMBER
N92-17105* # p 1243 ..... NO REPORT NUMBER
N92-17106* # p 1243 ..... NO REPORT NUMBER
N92-17107* # p 1244 ..... NO REPORT NUMBER
N92-17108* # p 1244 ..... NO REPORT NUMBER
N92-17109* # p 1244 ..... NO REPORT NUMBER
N92-17110* # p 1244 ..... NO REPORT NUMBER
N92-17111* # p 1244 ..... NO REPORT NUMBER
N92-17112* # p 1244 ..... NO REPORT NUMBER
N92-17113 # p 1318 ..... AD-A243314
USAFETAC/PR-91/007
N92-17114 # p 1223 ..... AD-A243363
AFIT/CI/CIA-91-066
N92-17115 # p 1331 ..... AD-A243369
AFIT/CI/CIA-91-095
N92-17116 # p 1286 ..... AD-A243384
AFIT/CI/CIA-91-014D
N92-17117 # p 1223 ..... AD-A243403
VPI-E-91-20
N92-17118 # p 1338 ..... AD-A243404
AFIT/CI/CIA-91-086
N92-17119 # p 1324 ..... AD-A243406
N92-17120 # p 1328 ..... AD-A243656
AFIT/GSO/ENG/91D-17
N92-17121 # p 1325 ..... AAMRL-TR-90-076
AD-A243658
N92-17122 # p 1338 ..... AD-A243663
CERL-ADP-M-91/24
N92-17123 # p 1389 ..... AD-A243665
CERL-TR-M-91/25
N92-17124 # p 1328 ..... AD-A243667
NRMI-91-84
N92-17125 # p 1382 ..... AD-A243707
N92-17126 # p 1295 ..... AD-A243709
NRL-MR-6926
N92-17127 # p 1303 ..... AD-A243710
NRL-MR-6911
N92-17128* # p 1234 ..... H-1780
NAS 1.15:4335
NASA-TM-4335
N92-17129 p 1287 ..... AD-D015057
US-PATENT-APPL-SN-654111
US-PATENT-CLASS-342-107
US-PATENT-5,051,751
N92-17130* # p 1338 ..... NAS 1.15:104174
NASA-TM-104174
N92-17131* # p 1223 ..... L-16604
NAS 1.60:3131
NASA-TP-3131
N92-17132* # p 1333 ..... NAS 1.26:189846
NASA-CR-189846
N92-17133 # p 1226 ..... NTSB/AAB-90/04
PB90-916904
N92-17134 # p 1315 ..... NOAA-TM-ERL-ARL-188
PB91-235499
N92-17135 # p 1345 ..... AD-A242841
N92-17136 # p 1382 ..... AD-A242959
N92-17137 # p 1303 ..... AD-A243180
BRL-TR-3295
N92-17138 # p 1319 ..... NOAA-TM-ERL-AOML-69
PB91-234286
N92-17139* # p 1280 ..... NAS 1.26:189786
NASA-CR-189786
N92-17140 # p 1301 ..... AD-A242026
RL-TR-91-199
N92-17141 # p 1385 ..... AD-A242071
DTRC-91/CT07
N92-17142 # p 1325 ..... AD-A243057
AFOSR-91-0911TR
N92-17143 # p 1334 ..... AD-A243245
NATICK/TR-92/007
N92-17144 # p 1319 ..... AD-A243311
USAFETAC/DS-91/255
N92-17145 # p 1331 ..... AD-A243358
AFIT/CI/CIA-91-022D
N92-17146 # p 1365 ..... AD-A243522
CMU-RI-TR-91-17
N92-17147 # p 1228 ..... AD-A243523
CMU-RI-TR-91-20
N92-17148 # p 1350 ..... AD-A243528
N92-17149 # p 1226 ..... DOT/FAA/CT-TN91/51
N92-17150* # p 1252 ..... NAS 1.26:189861
NASA-CR-189861
N92-17151* # p 1253 ..... E-6105
NAS 1.60:3191
NASA-TP-3191
N92-17152* # p 1303 ..... NAS 1.26:189860
NASA-CR-189860
N92-17153 # p 1230 ..... AGARD-LS-178
ISBN-92-835-0640-5
N92-17154 # p 1230 ..... NO REPORT NUMBER
N92-17155 # p 1230 ..... NO REPORT NUMBER
N92-17156 # p 1230 ..... NO REPORT NUMBER
N92-17157 # p 1231 ..... NO REPORT NUMBER
N92-17158 # p 1231 ..... NO REPORT NUMBER
N92-17159 # p 1231 ..... NO REPORT NUMBER
N92-17160 # p 1231 ..... NO REPORT NUMBER
N92-17161 # p 1231 ..... NO REPORT NUMBER
N92-17162 # p 1231 ..... NO REPORT NUMBER
N92-17163 # p 1232 ..... NO REPORT NUMBER
N92-17164 # p 1232 ..... NO REPORT NUMBER
N92-17165 # p 1232 ..... NO REPORT NUMBER
N92-17166 # p 1232 ..... NO REPORT NUMBER
N92-17167* # p 1241 ..... DMS-DR-2547-VOL-1
NAS 1.26:167696
NASA-CR-167696
N92-17168 # p 1295 ..... AD-A242074
DTRC/SHD-1262-04
N92-17169 # p 1324 ..... AD-A243084
N92-17170 # p 1268 ..... AD-A243094
NIST-TR-8
N92-17171 # p 1268 ..... AD-A243095
NIST-TR-11
N92-17172 # p 1268 ..... AD-A243097
NIST-TR-9
N92-17173 # p 1352 ..... AD-A243201
N92-17174 # p 1382 ..... AD-A243205
N92-17175 # p 1303 ..... AD-A243206
N92-17176 # p 1296 ..... AD-A243209
PME-FM-91-2
N92-17177 # p 1324 ..... AD-A243210
PMTC-TP-000060
N92-17178 # p 1352 ..... AD-A243212
SU-TR-448
N92-17179 # p 1339 ..... AD-A243214
WL-TR-91-1060
N92-17180 # p 1365 ..... AD-A243216
DRIC-BR-306218
RSRE-MEMO-4529
N92-17181 # p 1372 ..... AD-A243218
TR-11
N92-17182 # p 1372 ..... AD-A243221
N92-17183 # p 1306 ..... DE91-011570
PATENTS-US-A7461591
US-PATENT-APPL-SN-461591
N92-17184 # p 1275 ..... CONF-910852-16
DE92-002904
N92-17185 # p 1339 ..... AD-A242038
RL-TR-91-198
N92-17186 # p 1287 ..... AD-A242948
DRIC-BR-305032
RAE-TR-91044
N92-17187 # p 1280 ..... AD-A243154
DNA-TR-91-33
MRC-R-1335
N92-17188 # p 1345 ..... AD-A243165
MTR-11209
N92-17189 # p 1287 ..... AD-A243371
AFIT/CI/CIA-91-019D
N92-17190 # p 1329 ..... AD-A243387
AFIT/CI/CIA-91-073
N92-17191 # p 1268 ..... AD-A243389
N92-17192 # p 1239 ..... AD-A243408
N92-17193 # p 1268 ..... AD-A243465
N92-17194 # p 1329 ..... AD-A243467
AFIT/CI/CIA-91-070
N92-17195 # p 1268 ..... AD-A243746
IBM-RJ8490
TR-36
N92-17196 # p 1356 ..... AD-A243747
IBM-RJ8248
TR-35
N92-17197 # p 1356 ..... AD-A243748
IBM-RJ8411
TR-34
N92-17198 # p 1380 ..... AGARD-CAL-90/2
ISBN-92-835-0575-1
N92-17199* # p 1308 ..... ISSN-1051-225X
NAS 1.15:105465
NASA-TM-105465
N92-17200* # p 1244 ..... NAS 1.26:189807
NASA-CR-189807
N92-17201 # p 1389 ..... CONF-9111136-1
DE92-003849
LA-UR-91-3616
N92-17202 # p 1316 ..... AD-A241938
PL-TR-91-2070
N92-17203 # p 1347 ..... AD-A242931
ARI-RN-92-01
N92-17204 # p 1235 ..... AD-A242943
WL-TR-91-2071
N92-17205 # p 1287 ..... AD-A243160
N92-17206 # p 1350 ..... AD-A243162
M90-19
N92-17207 # p 1350 ..... AD-A243163
M91-40
N92-17208 # p 1311 ..... AD-A243164
M91-82
N92-17209 # p 1316 ..... AD-A243378
NWRA-CR-91-R072
PL-TR-91-2171
SR-1
N92-17210 # p 1259 ..... AD-A243380
N92-17211 # p 1339 ..... AD-A243392
NOSC/TD-2194
N92-17212 # p 1380 ..... AGARD-CAL-92/1
ISBN-92-835-0651-O
N92-17213 # p 1226 ..... NTSB/AAR-91/05
PB91-910405
N92-17214* # p 1241 ..... DMS-DR-2547-VOL-2
NAS 1.26:167697
NASA-CR-167697
N92-17215* # p 1245 ..... NAS 1.26:187418
NASA-CR-187418
N92-17216 # p 1287 ..... AD-A241914
AL-TR-1991-0094
N92-17217 # p 1227 ..... AD-A243090
N92-17218 # p 1372 ..... AD-A243192
N92-17219 # p 1372 ..... AD-A243194
N92-17220 # p 1372 ..... AD-A243223
N92-17221 # p 1234 ..... AD-A243224
RTI/3966/00-01F
WL-TR-91-1042
N92-17222 # p 1223 ..... AD-A243388
VPI-AOE-179
N92-17223 # p 1352 ..... AD-A243463
WL-TR-91-8035
N92-17224 # p 1326 ..... AD-A243464
N92-17225* # p 1312 ..... NAS 1.26:189840
NASA-CR-189840
N92-17226* # p 1232 ..... H-1779
NAS 1.15:4336
NASA-TM-4336
N92-17227* # p 1316 ..... NAS 1.26:189852
NASA-CR-189852
N92-17228 # p 1382 ..... PB91-202762
N92-17229 # p 1316 ..... PB91-221788
USGS-BULL-1924
N92-17230 # p 1310 ..... AD-A242017
AFIT/DS/ENY/91-1
N92-17231 # p 1308 ..... AD-A242865
AFOSR-91-0879TR
N92-17232 # p 1281 ..... AD-A242951
N92-17233 # p 1319 ..... AD-A242954
AD-E200776

ERP-1081
PL-TR-91-2075
N92-17234 # p 1232 ..... AD-A243002
ARL-PROP-TM-460
DODA-AR-006-600
N92-17235 # p 1389 ..... AD-A243026
AFOSR-91-0912TR
N92-17236 # p 1355 ..... AD-A243027
N92-17237 # p 1339 ..... AD-A243078
N92-17238 # p 1372 ..... AD-A243093
NIST-TR-7
N92-17239 # p 1316 ..... AD-A243153
DNA-TR-91-97
MRC/NSH-91-0002
N92-17240 # p 1234 ..... AD-A243234
WES/TR/EL-91-15
N92-17241 # p 1281 ..... AD-A243247
ESD-TR-91-080
MIT-TR-919
N92-17242 # p 1350 ..... AD-A242322
NAVSWC-TR-91-487
N92-17243 # p 1236 ..... AD-A242321
UTRC-R91-970089-01
N92-17244 # p 1281 ..... AD-A242323
DOT/FAA/SE-91/4
DOTVNTSC-FAA-91-13
N92-17245 # p 1373 ..... AD-A242327
WSU/DC/91/TR-65
N92-17246 # p 1259 ..... AD-A242832
TR-37
N92-17247 # p 1259 ..... AD-A242833
TR-35
N92-17248 # p 1259 ..... AD-A242834
TR-40
N92-17249 # p 1365 ..... AD-A242835
TR-36
N92-17250 # p 1245 ..... AD-A242836
GAO/NSIAD-92-39
N92-17251 # p 1387 ..... PB91-230219
SGD-562-PT-2
N92-17252 # p 1281 ..... AD-A242969
N92-17253 # p 1388 ..... AD-A242970
N92-17254 # p 1310 ..... AD-A242973
ARL-STRUC-TM-536
DODA-AR-006-596
N92-17255 # p 1382 ..... AD-A242975
N92-17256 # p 1310 ..... AD-A243011
R/D-6148-MS-01
N92-17257 # p 1319 ..... AD-A243012
USAFETAC/DS-91/244
N92-17258 # p 1281 ..... AD-A242264
SLCET-TR-91-26
N92-17259 # p 1227 ..... AD-A242828
AFESC/ESL-TR-90-60
N92-17260 # p 1238 ..... AD-A242829
AFESC/ESL-TR-89-40
N92-17261 # p 1259 ..... AD-A242831
TR-41
N92-17262 # p 1269 ..... AD-A242861
N92-17263 # p 1277 ..... AD-A242862
MIT/LCS/TM-412-D
N92-17264 # p 1263 ..... AD-A243000
ARL-MAT-TM-404
DODA-AR-006-602
N92-17265 # p 1310 ..... AD-A243001
ARL-STRUC-TM-539
DODA-AR-006-621
N92-17266 # p 1232 ..... AD-A243004
ARL-FLIGHT-MECH-TM-434
DODA-AR-006-590
N92-17267 # p 1281 ..... AD-A243005
NCS-TIB-91-3
N92-17268 # p 1288 ..... AD-A243009
RL-TR-91-221
N92-17269 # p 1326 ..... AD-A243174
USAARL-91-21
N92-17270 # p 1254 ..... AD-A243264
TR-31
N92-17271 # p 1263 ..... AD-A243270
TR-10
N92-17272 # p 1277 ..... AD-A243272
AF-AFR-88-22
DA-TM-5-1300
NAVFAC-P-397
N92-17273 # p 1301 ..... AD-A242838
RL-TR-91-307
N92-17274 # p 1383 ..... AD-A242839
NATICK/TR-90/001
N92-17275 # p 1296 ..... AD-A242947
N92-17276 # p 1296 ..... AD-A243036
AFOSR-91-0895TR
N92-17277 # p 1282 ..... AD-A243041
N92-17278 # p 1334 ..... AD-A243043
DREO-TN-91-14
N92-17279 # p 1282 ..... AD-A243044
DREO-1076
N92-17280 # p 1339 ..... AD-A243046
ARL-FLIGHT-MECH-TM-446
DODA-AR-006-643
N92-17281 # p 1223 ..... AD-A243047
ARL-FLIGHT-MECH-TM-443
DODA-AR-006-614
N92-17282 # p 1269 ..... AD-A243049
AFOSR-91-0892TR
N92-17283 # p 1385 ..... PB91-219170
N92-17284 # p 1365 ..... AD-A243280
TR-6
N92-17285 # p 1339 ..... AD-A243283
NPS-CS-91-013
N92-17286 # p 1340 ..... AD-A243286
RL-TR-91-253
N92-17287 # p 1238 ..... AD-A243287
WES/MP/GL-91-12
N92-17288 # p 1326 ..... AD-A241903
AL-TR-1991-0004
N92-17289 # p 1319 ..... AD-A242880
PL-TR-91-2034
SR-3
N92-17290 # p 1288 ..... AD-A242976
N92-17291 # p 1288 ..... AD-A242978
DODA-AR-006-355
MRL-TR-91-8
N92-17292 # p 1312 ..... AD-A242980
CSB-WP-MAPS1
DODA-AR-005-791
N92-17293 # p 1282 ..... AD-A242983
N92-17294 # p 1366 ..... AD-A242985
DODA-AR-006-489
WSRL-TM-5/91
N92-17295 # p 1288 ..... AD-A242986
DODA-AR-006-756
ERL-0568-RR
N92-17296 # p 1340 ..... AD-A242987
DODA-AR-006-765
ERL-0571-RR
N92-17297 # p 1238 ..... AD-A242989
ARL-FLIGHT-MECH-TM-435
DODA-AR-006-591
N92-17298 # p 1324 ..... AD-A242993
WES/TR/HL-91-20
N92-17299 # p 1329 ..... AD-A242997
USAARL-91-20
N92-17300 # p 1233 ..... AD-A243109
N92-17301 # p 1369 ..... AD-A243359
N92-17302 # p 1245 ..... AD-A243360
AFIT/CI/CIA-91-074
N92-17303 # p 1224 ..... NO REPORT NUMBER
N92-17304* # p 1306 ..... NAS 1.26:189808
NASA-CR-189808
N92-17305 # p 1356 ..... AD-A241857
AFIT/DS/ENP/91-01
N92-17306 # p 1357 ..... AD-A241893
N92-17307 # p 1296 ..... AD-A241894
N92-17308 # p 1254 ..... AD-A242866
N92-17309 # p 1296 ..... AD-A243050
AFOSR-91-0916TR
N92-17310 # p 1256 ..... ETN-92-90616
MBB-FE202-S-PUB-0453-A
N92-17311 # p 1224 ..... ETN-92-90617
MBB-FE211-S-PUB-446
N92-17312 # p 1297 ..... ETN-92-90618
MBB-FE211-S-PUB-447
N92-17313 # p 1233 ..... ETN-92-90620
MBB-FE211-S-PUB-452
N92-17314 # p 1224 ..... ETN-92-90621
ISSN-0374-1257
MPIS-98/1990
N92-17315 # p 1224 ..... ETN-92-90622
ISSN-0374-1257
MPIS-99/1990
N92-17316* # p 1233 ..... NAS 1.26:189853
NASA-CR-189853
REPT-722792-2
N92-17317 # p 1288 ..... NO REPORT NUMBER
N92-17318 # p 1353 ..... DE91-641524
IC-90/425
N92-17319 # p 1263 ..... DE92-000635
DOE/ER-45281/6
N92-17320 # p 1310 ..... AD-A241957
NAVSWC-TR-91-182
N92-17321 # p 1357 ..... AD-A241987
AFIT/GEP/ENP/91J-1
N92-17322 # p 1373 ..... AD-A243096
NIST-TR-10
N92-17323 # p 1259 ..... AD-A243217
TR-14
N92-17324 # p 1378 ..... AD-A243226
N92-17325 # p 1239 ..... AD-A243409
TR-R90222
N92-17326 # p 1288 ..... AD-A243432
HDL-TM-91-14
N92-17327 # p 1263 ..... AD-A243461
N92-17328 # p 1263 ..... AD-A243475
N92-17329 # p 1255 ..... AD-A243483
TR-12
N92-17330 # p 1350 ..... AD-A243484
RL-TR-91-278
UDR-TR-89-115
N92-17331 # p 1334 ..... AD-A243486
NEDU-12-91
N92-17332 # p 1288 ..... AD-A243744
AFIT/GE/ENG/91D-12
N92-17333* # p 1310 ..... NAS 1.15:100646
NASA-TM-100646
N92-17334* # p 1245 ..... NAS 1.26:189872
NASA-CR-189872
N92-17335* # p 1241 ..... NAS 1.26:189873
NASA-CR-189873
N92-17336 # p 1332 ..... AD-A243051
AFOSR-91-0915TR
N92-17337 # p 1297 ..... AD-A243251
N92-17338 # p 1319 ..... AD-A243539
NOARL-TN-111
N92-17339 # p 1224 ..... AD-A243552
N92-17340 # p 1383 ..... AD-A243554
N92-17341 # p 1308 ..... ETN-92-90601
MBB-UK-0140-91-PUB
N92-17342 # p 1241 ..... ETN-92-90604
MBB-UK-0143-91-PUB
N92-17343 # p 1297 ..... ETN-92-90623
ISSN-0436-1199
MPIS-1/1991
N92-17344 # p 1301 ..... ETN-92-90624
ISSN-0374-1257
MPIS-100/1991
N92-17345 # p 1301 ..... ETN-92-90625
ISSN-0374-1257
MPIS-101/1991
N92-17346* # p 1219 ..... E-6088
NAS 1.15:103800
NASA-TM-103800
N92-17347* # p 1224 ..... E-6767
NAS 1.15:105380
NASA-TM-105380
N92-17348* # p 1245 ..... NAS 1.55:10083-VOL-2-PT-2
NASA-CP-10083-VOL-2-PT-2
S-653-VOL-2-PT-2
N92-17349* # p 1245 ..... NO REPORT NUMBER
N92-17350* # p 1245 ..... NO REPORT NUMBER
N92-17351* # p 1246 ..... NO REPORT NUMBER
N92-17352* # p 1246 ..... NO REPORT NUMBER
N92-17353* # p 1246 ..... NO REPORT NUMBER
N92-17354* # p 1246 ..... NO REPORT NUMBER
N92-17355* # p 1246 ..... NO REPORT NUMBER
N92-17356* # p 1246 ..... NO REPORT NUMBER
N92-17357* # p 1247 ..... NO REPORT NUMBER
N92-17358* # p 1247 ..... NO REPORT NUMBER
N92-17359* # p 1247 ..... NO REPORT NUMBER
N92-17360* # p 1247 ..... NO REPORT NUMBER
N92-17361* # p 1247 ..... NO REPORT NUMBER
N92-17362* # p 1247 ..... NO REPORT NUMBER
N92-17363 # p 1319 ..... NOAA-TM-NWS-ER-85
PB91-225037
N92-17364* # p 1241 ..... NAS 1.15:105475
NASA-TM-105475
NSTS-08207
N92-17365* # p 1253 ..... NAS 1.26:189787
NASA-CR-189787
N92-17366 # p 1282 ..... AD-A243187
N92-17367 # p 1256 ..... AD-A243188
N92-17368 # p 1340 ..... AD-A243189
N92-17369 # p 1383 ..... AD-A243191
NOSC-TD-2174
N92-17370 # p 1264 ..... AD-A243199
TR-12
N92-17371 # p 1259 ..... AD-A243200
TR-13
N92-17372 # p 1391 ..... AD-A243477
NTSC-91-01
N92-17373 # p 1255 ..... AAMRL-TR-90-066
AD-A243479
N92-17374 # p 1357 ..... AD-A243482
N92-17375* # p 1373 ..... NAS 1.26:189856
NASA-CR-189856
N92-17376* # p 1264 ..... NAS 1.15:104743
NASA-TM-104743
S-660
N92-17377* # p 1388 ..... CU-TP-539
FERMILAB-PUB-91/312-A/T
NAS 1.26:189842
NASA-CR-189842
N92-17378 # p 1383 ..... AD-A242376
WHOI-91-16
N92-17379 # p 1264 ..... AD-A242956
AD-E200781
PL-TR-91-3073
N92-17380 # p 1313 ..... AD-A242967
CERL-SR-N-91/35

N92-17381 # p 1355 ..... AD-A243498
N92-17382 # p 1373 ..... AD-A243499
UMR-FDB-22
N92-17383 # p 1282 ..... AD-A243505
NOSC-TR-1460
N92-17384 # p 1352 ..... AD-A243507
BRL-TR-3303
N92-17385 # p 1347 ..... AD-A243508
M91-41
N92-17386 # p 1348 ..... AD-A243509
M91-42
N92-17387 # p 1297 ..... AD-A243513
PSU/ARL-TM-91-299
N92-17388 # p 1380 ..... AD-A243515
N92-17389 # p 1260 ..... AD-A243529
TR-40
N92-17390 # p 1373 ..... AD-A243531
N92-17391 # p 1324 ..... AD-A243532
N92-17392 # p 1256 ..... AD-A243534
R/D-6703-MS-03
N92-17393* # p 1313 ..... NAS 1.26:189814
NASA-CR-189814
NCAR/TN-362+1A
PB91-233783
N92-17394 # p 1357 ..... AD-A242365
HDL-TM-91-12
N92-17395 # p 1345 ..... AD-A242372
NOSC/TR-1450
N92-17396 # p 1383 ..... AD-A242374
CSA-91-01-03
WL-TR-91-3056
N92-17397 # p 1269 ..... AD-D015066
NAVY-CASE-73416
US-PATENT-APPL-SN-726483
N92-17398 # p 1297 ..... AD-D015067
NAVY-CASE-73405
US-PATENT-APPL-SN-729743
N92-17399 # p 1275 ..... AD-D015068
NAVY-CASE-73644
US-PATENT-APPL-SN-726918
N92-17400 # p 1320 ..... AD-A243309
USAFETAC/DS-91/250
N92-17401 # p 1383 ..... AD-A243315
USAFETAC/PR-91/019
N92-17402 # p 1383 ..... AD-A243323
NPS-CS-91-009
N92-17403 # p 1340 ..... AD-A243324
NPS-CS-91-014
N92-17404 # p 1225 ..... AD-A243375
NATICK/TR-92/005
N92-17405 # p 1317 ..... AD-A243376
N92-17406 # p 1320 ..... AD-A243451
NOARL-TN-114
N92-17407 # p 1340 ..... AD-A243706
AFIT/GCS/ENG/91D-19
N92-17408 # p 1357 ..... DE91-634551
JINR-R-1-89-452
N92-17409* # p 1248 ..... NAS 1.55:10083-VOL-1-PT-2
NASA-CP-10083-VOL-1-PT-2
S-653-VOL-1-PT-2
N92-17410* # p 1248 ..... NO REPORT NUMBER
N92-17411* # p 1248 ..... NO REPORT NUMBER
N92-17412* # p 1248 ..... NO REPORT NUMBER
N92-17413* # p 1248 ..... NO REPORT NUMBER
N92-17414* # p 1248 ..... NO REPORT NUMBER
N92-17415* # p 1249 ..... NO REPORT NUMBER
N92-17416* # p 1249 ..... NO REPORT NUMBER
N92-17417* # p 1249 ..... NO REPORT NUMBER
N92-17418* # p 1249 ..... NO REPORT NUMBER
N92-17419* # p 1249 ..... NO REPORT NUMBER
N92-17420* # p 1249 ..... NO REPORT NUMBER
N92-17421* # p 1249 ..... NO REPORT NUMBER
N92-17422* # p 1250 ..... NO REPORT NUMBER
N92-17423 # p 1357 ..... AD-A242362
WSU/DC/91/TR-66
N92-17424 # p 1313 ..... AD-A242363
N92-17425 # p 1346 ..... AD-A242364
NPS-AS-91-016
N92-17426 # p 1264 ..... AD-A243474
N92-17427 # p 1264 ..... AD-A243487
TR-42
N92-17428 # p 1358 ..... AD-A243488
TR-41
N92-17429 # p 1282 ..... AD-A243489
RL-TR-91-56
N92-17430 # p 1250 ..... AD-A243490
AFIT/CI/CIA-91-098
N92-17431 # p 1308 ..... AD-A243493
AFIT/CI/CIA-91-023D
N92-17432 # p 1334 ..... AD-A243496
NADC-91071-90
N92-17433 # p 1358 ..... ETN-92-90566
N92-17434 # p 1303 ..... ETN-92-90567
N92-17435 # p 1358 ..... ETN-92-90568
N92-17436 # p 1312 ..... ETN-92-90582
N92-17437 # p 1301 ..... ETN-92-90583
N92-17438 # p 1348 ..... AD-A241924
BDM/VSQ-91-0742-TR
N92-17439 # p 1289 ..... AD-A241926
EOARD-TR-91-11
N92-17440 # p 1352 ..... AD-A241928
NPSOR-91-025
N92-17441 # p 1282 ..... AD-A241934
N92-17442 # p 1237 ..... AD-A241935
N92-17443 # p 1378 ..... AD-A241936
N92-17444 # p 1320 ..... AD-A241937
USAFETAC/DS-91/248
N92-17445 # p 1350 ..... AD-A242223
N92-17446 # p 1225 ..... AD-A242224
NAVSWC-TR-91-86
N92-17447 # p 1297 ..... AD-A242351
N92-17448 # p 1269 ..... AD-A242354
TR-51
N92-17449 # p 1374 ..... AD-A242355
TR-55
N92-17450 # p 1332 ..... AD-A242358
AL-TP-1991-0034
N92-17451 # p 1380 ..... AD-A242361
N92-17452 # p 1265 ..... AD-D015065
NAVY-CASE-73171
US-PATENT-APPL-SN-704563
N92-17453 # p 1358 ..... CONF-911029-2
DE92-002738
PNL-SA-19136
N92-17454 # p 1302 ..... CONF-910968-45
DE92-003638
GA-A-20645
N92-17455 # p 1352 ..... CONF-911106-27
DE92-003785
LA-UR-91-3688
N92-17456 # p 1369 ..... CONF-910968-47
DE92-003805
GA-A-20652
N92-17457 # p 1348 ..... AD-A242225
CMU-AIP-149
N92-17458 # p 1332 ..... AD-A242226
CMU-AIP-148
N92-17459 # p 1312 ..... AD-A242232
ERIM-218600-4-F
N92-17460 # p 1269 ..... AD-A242258
TR-32
N92-17461 # p 1269 ..... AD-A242259
TR-33
N92-17462 # p 1358 ..... AD-D015063
NAVY-CASE-73297
US-PATENT-APPL-SN-724083
N92-17463 # p 1340 ..... AD-A242899
ARI-RN-92-04
N92-17464 # p 1283 ..... AD-A242917
HEL-TM-14-91
N92-17465 # p 1346 ..... AD-A242920
BDM/MCL-91-0364-TR
N92-17466 # p 1336 ..... AD-A242924
N92-17467 # p 1265 ..... AD-A242937
N92-17468 # p 1289 ..... CONF-911055-9
DE92-002924
SAND-91-2212C
N92-17469 # p 1369 ..... DE92-003309
EGG-SCM-9576
N92-17470 # p 1384 ..... DE92-003311
EGG-EP-9846
N92-17471 # p 1326 ..... ANL/CP-74610
CONF-911264-1
DE92-003370
N92-17472 # p 1358 ..... AD-A242031
TR-112
N92-17473 # p 1329 ..... AD-A242033
N92-17474 # p 1326 ..... AD-A242329
N92-17475 # p 1304 ..... AD-A242941
N92-17476 # p 1329 ..... AD-A242981
DNA-TR-90157
PSR-2040
N92-17477 # p 1219 ..... AD-A243158
N92-17478 # p 1227 ..... AD-A243527
UDR-TR-90-114
WL-TR-91-3006
N92-17479 # p 1353 ..... AD-A243736
AFIT/GSO/ENS/ENY/91D-14
N92-17480 # p 1289 ..... AD-A243740
AFIT/GCE/ENG/91D-04
N92-17481 # p 1228 ..... AD-A243742
AFIT/GE/ENG/91D-41
N92-17482 # p 1384 ..... AD-A243743
AFIT/GCS/ENG/91D-09
N92-17483* # p 1386 ..... NAS 1.26:189751
NASA-CR-189751
N92-17484* # p 1386 ..... NAS 1.26:189753
NASA-CR-189753
N92-17485 # p 1366 ..... AD-A243436
RD-5830-EE-01-APP
N92-17486 # p 1366 ..... AD-A243437
RD-5830-EE-01
N92-17487 # p 1341 ..... AD-A243438
N92-17488 # p 1355 ..... AD-A243441
JRC-34-91
N92-17489 # p 1260 ..... AD-A243443
TR-86
N92-17490 # p 1289 ..... AD-A243446
TR-44
N92-17491 # p 1359 ..... AD-A243447
TR-43
N92-17492 # p 1320 ..... AD-A243448
NOARL-TN-112
N92-17493 # p 1320 ..... AD-A243449
NOARL-TN-113
N92-17494 # p 1320 ..... AD-A243450
NOARL-TN-115
N92-17495* # p 1253 ..... KEE6-FR
NAS 1.26:184272
NASA-CR-184272
RPT/F0175.98
N92-17497* # p 1386 ..... NAS 1.26:189750
NASA-CR-189750
N92-17498 # p 1341 ..... AGARD-AR-302
CP-503
ISBN-92-835-0647-2
N92-17499 # p 1369 ..... AD-A243711
NRL-MR-6912
N92-17500 # p 1332 ..... AD-A243712
AFIT/GE/ENG/91D-34
N92-17501 # p 1289 ..... AD-A243713
AFIT/GE/ENG/91D-55
N92-17502 # p 1355 ..... AD-A243715
AFOSR-91-0989TR
N92-17503 # p 1332 ..... AD-A243716
AFOSR-91-0283TR
N92-17504 # p 1327 ..... AD-A243717
AFOSR-91-0986TR
N92-17505 # p 1359 ..... AD-A243718
NRL-MR-6927
N92-17506 # p 1355 ..... AD-A243719
CERL-TR-N-91/13
N92-17507 # p 1346 ..... AD-A243721
AFIT/GCS/ENG/91D-14
N92-17508 # p 1270 ..... AD-A243723
AFOSR-91-0973TR
N92-17509* # p 1225 ..... NAS 1.15:104188
NASA-TM-104188
N92-17510* # p 1253 ..... NAS 1.26:189097
NASA-CR-189097
N92-17511* # p 1311 ..... NAS 1.26:189882
NASA-CR-189882
N92-17512* # p 1228 ..... NAS 1.26:187615
NASA-CR-187615
N92-17513 # p 1233 ..... AD-A243724
NOR-89-101
WL-TR-91-3104
N92-17514 # p 1359 ..... AD-A243725
RL-TR-91-289
N92-17515 # p 1320 ..... AD-A243762
N92-17516 # p 1283 ..... AD-A243766
AFIT/GE/ENG/91D-30
N92-17517 # p 1351 ..... ETN-92-90562
TW-90-09
N92-17518 # p 1359 ..... ETN-92-90563
N92-17519 # p 1359 ..... ETN-92-90564
N92-17520 # p 1360 ..... ETN-92-90565
N92-17521 # p 1341 ..... ETN-92-90580
N92-17522 # p 1298 ..... ETN-92-90581
N92-17523 # p 1386 ..... ETN-92-90584
N92-17524 # p 1341 ..... ETN-92-90585
N92-17525 # p 1351 ..... ETN-92-90587
N92-17526 # p 1304 ..... ETN-92-90598
MBB-Z-0361-91-PUB
N92-17527 # p 1240 ..... ETN-92-90605
MBB-UK-0144-91-PUB
N92-17528 # p 1374 ..... DE91-018805
DOE/ER-45330/4
N92-17529 # p 1283 ..... DE91-018874
DOE/SF-16732/T1
N92-17530 # p 1360 ..... DE92-000864
LBL-31130
N92-17531 # p 1379 ..... DE91-642825
IC-91/45
N92-17532 # p 1374 ..... DE91-018511
DOE/ER-13438/2
N92-17533 # p 1275 ..... CONF-9106187-3
DE92-002034
MLM-3700(OP)
N92-17534* # p 1242 ..... NAS 1.15:105478
NASA-TM-105478
NSTS-08308
N92-17535 # p 1277 ..... KCP-613-4479
N92-17536 # p 1366 ..... AD-A243471
AFIT/CI/CIA-91-018D
N92-17537 # p 1379 ..... AD-A243526
NCTRF-187
N92-17538 # p 1341 ..... AD-A243767

N92-17539 # p 1324 AD-A243773
AD-E040155
INO-SP-5
N92-17540 # p 1290 ETN-92-90586
N92-17541 # p 1270 ETN-92-90588
N92-17542 # p 1317 ETN-92-90594
ISSN-0069-5882
MITT-76
N92-17543 # p 1321 ETN-92-90595
ISSN-0069-5882
MITT-78
N92-17544 # p 1309 ETN-92-90602
MBB-UK-0141-91-PUB
N92-17545 # p 1341 ETN-92-90603
MBB-UK-0142-91-PUB
N92-17546* # p 1235 E-6789
NAS 1.15:105397
NASA-TM-105397
N92-17547* # p 1225 NAS 1.15:104168
NASA-TM-104168
N92-17548 # p 1354 AD-A241899
N92-17549 # p 1360 AD-A242030
N92-17550 # p 1366 AD-A242925
ERIM-196800-18-F-VOL-2
N92-17551 # p 1314 AD-A242928
CERL-SR-N-91/11
N92-17552 # p 1235 AD-A242929
QTR-CDRL-29087
N92-17553 # p 1374 AD-A243013
RL-TR-91-263
N92-17554 # p 1332 AD-A243052
AFOSR-91-0913TR
N92-17555 # p 1360 AD-A243065
N92-17556 # p 1370 ISBN-0-309-04597-5
LC-91-66812
N92-17557 # p 1329 AD-A243075
N92-17558 # p 1341 AD-A243252
N92-17559 # p 1290 PB91-201301
N92-17560 # p 1351 AD-A242315
NOSC-TR-1399
N92-17561 # p 1342 AD-A242318
NADC-91067-50
N92-17562 # p 1275 AD-A242844
BRL-TR-3288
N92-17563 # p 1283 AD-A242873
AEROMET/TUL-9110151
N92-17564 # p 1327 AD-A242877
N92-17565 # p 1233 AD-A242881
ARL-PROP-R-187
DODA-AR-006-619
N92-17566 # p 1342 AD-A242886
BMO-TR-91-26
FST91-281-2
N92-17567 # p 1330 AD-A242887
ARI-RN-91-90
FR89-1(R)-VOL-1
VRI-ARI-9
N92-17568 # p 1229 AD-A243025
IAR-AN-73
NRC-32149
N92-17569 # p 1334 AD-A243077
DTRC/SHD-1361-01
N92-17570 # p 1290 AD-A243105
N92-17571 # p 1283 AD-A243111
BRL-MR-3947
N92-17572 # p 1260 AD-A243236
AL-TR-1991-0055
N92-17573 # p 1290 AD-A243250
N92-17574 # p 1360 CONF-9109256-1
DE91-018248
N92-17575 # p 1306 ANL/CP-72505
CONF-911002-1
DE91-018617
N92-17576 # p 1270 CONF-9105176
DE92-000459
N92-17577 # p 1313 DE92-000762
DOE/SF-17853/T1
N92-17578 # p 1317 CONF-9109114-5
DE92-002172
UCRL-JC-106782
N92-17579 # p 1265 CONF-9107182-3
DE92-003797
LA-UR-91-3495
N92-17580 # p 1250 AD-A242906
N92-17581 # p 1342 AD-A242916
NAVSWC-MP-91-404
N92-17582 # p 1304 AD-A243497
N92-17583 # p 1324 AD-A243730
WHOI-91-29
N92-17584* # p 1306 NAS 1.71:MFS-28589-1
NASA-CASE-MFS-28589-1
US-PATENT-APPL-SN-813628
N92-17585* # p 1250 NAS 1.26:186943
NASA-CR-186943
N92-17586* # p 1384 NAS 1.15:103567
NASA-TM-103567
N92-17587 # p 1227 NIAR-91-30
N92-17588* # p 1298 NAS 1.26:187802
NASA-CR-187802
NIAR-91-27
N92-17589 # p 1360 CONF-910835-1
DE92-003855
LA-UR-91-3569
N92-17590 # p 1363 CONF-911116-11
DE92-003859
LA-UR-91-3540
N92-17591 # p 1240 CONF-911116-10
DE92-003860
LA-UR-91-3539
N92-17592 # p 1336 CONF-911106-22
DE92-004638
FNAL/C-91/303
N92-17593 # p 1277 DE92-004708
DOE/ER-0529P
N92-17594 # p 1374 AD-A241882
AFOSR-91-0883TR
N92-17595 # p 1388 AD-A241896
USAFA-TR-91-13
N92-17596 # p 1290 AD-A242868
TR-38
N92-17597 # p 1270 AD-A242872
WRDC-TR-90-4096-VOL-3
N92-17598 # p 1314 AD-A242874
CERL-SR-N-91/10
N92-17599 # p 1330 AD-A242889
DCIEM-91-62
N92-17600 # p 1283 AD-A242957
AD-E200783
PL-TR-91-2198
SR-1
N92-17601 # p 1342 AD-A243758
AFIT/GE/ENG/91-D-11
N92-17602 # p 1250 AD-A243759
AFIT/GE/ENG/91D-22
N92-17603 # p 1342 AD-A243760
AFIT/GCS/ENG/91D-03
N92-17604 # p 1307 BNL-52302
CONF-9105133
DE92-002288
N92-17605 # p 1307 DE92-003091
DOE/PC-88947/T12
N92-17606 # p 1370 DE92-003545
DOE/ER-51116/1
N92-17607 # p 1256 AD-A241988
AFIT/GAE/ENY/91S-1
N92-17608 # p 1361 AD-A241993
AFOSR-91-0843TR
N92-17609 # p 1351 AD-A242010
AFOSR-91-0827TR
N92-17610 # p 1374 AD-D015069
NAVY-CASE-73170
US-PATENT-APPL-SN-726489
N92-17611 # p 1257 AD-D015070
NAVY-CASE-71788
US-PATENT-APPL-SN-660364
N92-17612 # p 1270 AD-D015071
NAVY-CASE-73414
US-PATENT-APPL-SN-531488
N92-17613 # p 1260 AD-A242867
TR-39
N92-17614 # p 1270 AD-A242871
WRDC-TR-90-4096-VOL-2
N92-17615 # p 1271 AD-A243220
NIST-TR-6
N92-17616 # p 1361 AD-A243530
TR-45
N92-17617 # p 1334 AD-A243545
AFIT/CI/CIA-91-083
N92-17618 # p 1375 AD-A243546
AFIT/CI/CIA-91-020D
N92-17619 # p 1314 PB91-205120
N92-17620 # p 1290 PB91-201293
N92-17621 # p 1321 PB91-226886
N92-17622 # p 1351 DE91-641495
IFT-P-36/90
N92-17623 # p 1391 DE91-522477
KURRI-TR-341
N92-17624 # p 1276 CONF-9106187-4
DE92-002033
MLM-3701(OP)
N92-17625 # p 1298 DE92-003110
UCRL-ID-107480
N92-17626 # p 1298 DE92-003259
EGG-EAST-9348
N92-17627 # p 1304 AD-D015055
NAVY-CASE-73376
US-PATENT-APPL-SN-684091
N92-17628 # p 1260 AD-D015062
NAVY-CASE-73550
US-PATENT-APPL-SN-749357
N92-17629 # p 1290 AD-A242900
N92-17630 # p 1366 AD-A242901
AFOSR-91-0819TR
N92-17631 # p 1321 AD-A242902
AFOSR-91-0776TR
CSU-ATSP-483
N92-17632 # p 1276 AD-A243045
ARAED-TR-91023
N92-17633 # p 1384 AD-A243770
N92-17634 # p 1333 AD-A242028
N92-17635 # p 1370 AD-A242029
N92-17636 # p 1342 AD-A242032
UVA/525449/CS92/101
N92-17637 # p 1342 AD-A242048
TR91-003
N92-17638 # p 1346 AD-A242049
TR91-028
N92-17639 # p 1229 AD-A242064
N92-17640 # p 1343 AD-A242330
SSD-TR-91-24
N92-17641 # p 1384 AD-A242331
CMU/SEI-91-UG-4
N92-17642 # p 1235 AD-A242338
BRL-TR-3257
N92-17643 # p 1353 AD-A242343
NPSOR-91-020
N92-17644 # p 1235 AD-A243155
RMA-TMR-0101
WL-TR-91-2073
N92-17645* # p 1330 NAS 1.60:3182
NASA-TP-3182
S-665
N92-17646* # p 1361 FERMILAB-PUB-91/340-A
NAS 1.26:189858
NASA-CR-189858
N92-17647* # p 1361 FERMILAB-PUB-91/305-A
NAS 1.26:189859
NASA-CR-189859
N92-17648 # p 1333 AD-A243161
N92-17649 # p 1304 DE91-011705
PATENTS-US-A7420433
US-PATENT-APPL-SN-420433
N92-17650* # p 1387 NAS 1.26:189815
NASA-CR-189815
N92-17651 # p 1380 AD-A242041
TR91-019
N92-17652 # p 1361 AD-A243391
WL-TR-91-2067
N92-17653 # p 1265 AD-A243453
PWA-FR21998-1
N92-17654 # p 1291 AD-A243457
AFOSR-91-0917TR
N92-17655 # p 1343 AD-A243460
N92-17656 # p 1335 AD-A243462
N92-17657 # p 1391 AD-A243466
N92-17658 # p 1367 AD-A243470
AFIT/CI/CIA-91-015D
N92-17659 # p 1271 AD-A243749
IBM-RJ8469
TR-31
N92-17660 # p 1361 AD-A243750
IBM-RJ8420
TR-32
N92-17661 # p 1271 AD-A243751
IBM-RJ8287
TR-33
N92-17662 # p 1284 AD-A243753
AFIT/GE/ENG/91D-23
N92-17663 # p 1362 AD-A243754
AFIT/GE/ENP/91D-01
N92-17664 # p 1370 DE92-002636
DOE/ID-12735/T19
N92-17665 # p 1314 CONF-9110275-2
DE92-002681
PNL-SA-20109
N92-17666 # p 1362 CONF-9105221-3
DE92-003790
LA-UR-91-3830
N92-17667 # p 1375 AD-A242039
AFOSR-91-0817TR
UT-5473-1
N92-17668 # p 1291 AD-A241946
AL-TR-1991-0058
N92-17669 # p 1381 AD-A242042
TR91-024
N92-17670 # p 1346 AD-A242045
N92-17671 # p 1291 AD-A243166
MTR-11230
N92-17672 # p 1291 AD-A243167
MTR-11252
N92-17673 # p 1335 AD-A243168
MTR-11259
N92-17674* # p 1277 NAS 1.71:NPO-18366-1-CU
NASA-CASE-NPO-18366-1-CU
US-PATENT-APPL-SN-781520
N92-17675* # p 1367 NAS 1.71:NPO-18379-1-CU
NASA-CASE-NPO-18379-1-CU
US-PATENT-APPL-SN-797569

N92-17676* # p 1271 ..... NAS 1.71:LAR-14608-1
NASA-CASE-LAR-14608-1
US-PATENT-APPL-SN-752246
N92-17677* # p 1307 ..... NAS 1.71:LAR-14169-1
NASA-CASE-LAR-14169-1
US-PATENT-APPL-SN-791728
N92-17678* # p 1307 ..... NAS 1.71:LEW-15216-1
NASA-CASE-LEW-15216-1
US-PATENT-APPL-SN-826547
N92-17679 # p 1271 ..... AD-A242423
TR-36
N92-17680 # p 1343 ..... AD-A242538
N92-17681 # p 1225 ..... NO REPORT NUMBER
N92-17682 # p 1260 ..... AD-A242027
AFOSR-91-0871TR
N92-17683 # p 1272 ..... AD-A243219
WRDC-TR-90-4096-VOL-1
N92-17684 # p 1291 ..... AD-A243430
RL-TR-91-181
N92-17685 # p 1375 ..... AD-A243433
TR-6
N92-17686 # p 1379 ..... AD-A243434
N92-17687 # p 1381 ..... AD-A243435
N92-17688 # p 1298 ..... AD-A243726
AFOSR-91-0996TR
N92-17689 # p 1284 ..... AD-A243731
RL-TR-91-279
UDR-TR-89-119
N92-17690 # p 1367 ..... AD-A243734
N92-17691 # p 1284 ..... AD-A243741
AFIT/GE/ENG/91D-28
N92-17692* # p 1355 ..... NAS 1.26:189848
NASA-CR-189848
N92-17693* # p 1272 ..... NAS 1.15:104195
NASA-TM-104195
N92-17694* # p 1387 ..... NAS 1.15:105452
NASA-TM-105452
NSSDC/WDC-A-R/S-91-25
N92-17695* # p 1387 ..... NAS 1.26:189806
NASA-CR-189806
N92-17696* # p 1388 ..... FERMILAB-PUB-91/324-A
NAS 1.26:189857
NASA-CR-189857
N92-17697* # p 1388 ..... CU-TP-540
FERMILAB-PUB-91/326-A/T
NAS 1.26:189843
NASA-CR-189843
N92-17698 p 1375 ..... NO REPORT NUMBER
N92-17699 p 1298 ..... NO REPORT NUMBER
N92-17700 p 1375 ..... NO REPORT NUMBER
N92-17701 p 1375 ..... NO REPORT NUMBER
N92-17702 p 1291 ..... NO REPORT NUMBER
N92-17703 # p 1265 ..... ANL/CP-74527
CONF-911111-6
DE92-001908
N92-17704 # p 1299 ..... DE92-000337
DOE/PC-88947/T11
N92-17705 # p 1321 ..... NOAA-TM-NWS-NHC-38
PB91-236463
N92-17706 # p 1370 ..... AD-D015060
NAVY-CASE-70998
US-PATENT-APPL-SN-722447
N92-17707 # p 1229 ..... AD-D015061
NAVY-CASE-73256
US-PATENT-APPL-SN-708991
N92-17708 # p 1292 ..... DE92-003068
DOE/SF-17127/T1
N92-17709 # p 1299 ..... DE92-002905
DOE/PC-89769/T6
N92-17710 # p 1272 ..... CONF-9111130-1
DE92-002947
SAND-91-1423C
N92-17711 # p 1367 ..... AD-A243333
N92-17712 # p 1330 ..... AD-A243334
AEHA-75-51-0742-91
N92-17713 # p 1311 ..... CONF-920146-1
DE92-003631
WHC-SA-1210
N92-17714 # p 1330 ..... AD-A242923
UCRL-CR-107449
N92-17715 # p 1312 ..... AD-A243674
CRREL-91-19
N92-17716 # p 1343 ..... AD-A243675
CERL-TR-91/52
N92-17717 # p 1388 ..... AD-A243683
N92-17718 # p 1292 ..... AD-A243701
AFIT/GE/ENG/91D-15
N92-17719 # p 1299 ..... AD-A243727
AFOSR-91-0995TR
N92-17720 # p 1336 ..... AD-A243728
AFOSR-91-0992TR
N92-17721 # p 1284 ..... AD-A243755
AFIT/GCS/ENG/91D-26
N92-17722 # p 1284 ..... AD-A243756
AFIT/GE/ENG/91D-10
N92-17723 # p 1314 ..... AD-A242420
N92-17724 # p 1292 ..... AD-A243558
N92-17725 # p 1389 ..... CONF-9108182-1
DE92-003857
LA-UR-91-3546
N92-17726 # p 1304 ..... CONF-9107115-59
DE92-003862
LA-UR-91-3532
N92-17727 # p 1261 ..... CONF-9111114-2
DE92-003868
LA-UR-91-3498
N92-17728* # p 1250 ..... NAS 1.26:187355
NASA-CR-187355
N92-17729 # p 1236 ..... AD-A243346
N92-17730 # p 1239 ..... AD-A243349
AFIT/CI/CIA-91-021D
N92-17731 # p 1219 ..... AD-A243350
AFIT/CI/CIA-91-068
N92-17732 # p 1239 ..... AD-A243354
AFIT/CI/CIA-91-084
N92-17733 # p 1343 ..... AD-A243357
AFIT/CI/CIA-91-065
N92-17734 # p 1370 ..... AD-A243645
N92-17735 # p 1284 ..... AD-A243649
AFIT/GE/ENG/91D-18
N92-17736 # p 1367 ..... AD-A243650
AFIT/GEO/ENG/91D-3
N92-17737 # p 1285 ..... AD-A243651
AFIT/GE/ENG/91D-51
N92-17738 # p 1363 ..... DE92-004426
DOE/ER-40633/1
N92-17739 # p 1363 ..... DE92-004603
PATENTS-US-A7511684
US-PATENT-APPL-SN-511684
N92-17740 # p 1261 ..... DE92-004623
MLM-3716
N92-17741 # p 1240 ..... B-247007
GAO/NSIAD-92-86
N92-17742 # p 1292 ..... NO REPORT NUMBER
N92-17743 p 1362 ..... NO REPORT NUMBER
N92-17744 # p 1336 ..... AD-A243633
AFIT/GCS/ENG/91D-25
N92-17745 # p 1272 ..... AD-A243634
AFOSR-91-0988TR
N92-17746 # p 1376 ..... AD-A243635
AFIT/GE/ENG/91D-26
N92-17747 # p 1299 ..... AD-A243636
AEDC-TR-91-17
N92-17748 # p 1237 ..... AD-A243638
AFIT/GE/ENG/91D-33
N92-17749 # p 1272 ..... AD-A243640
TR-1
N92-17750 # p 1272 ..... AD-A243641
TR-2
N92-17751 # p 1273 ..... AD-A243642
TR-3
N92-17752 # p 1273 ..... AD-A243643
TR-4
N92-17753 # p 1273 ..... AD-A243644
TR-5
N92-17754 # p 1251 ..... ISSN-0452-2982
JTN-92-80241
NAL-TM-602-PT-2
N92-17755 # p 1225 ..... ISSN-0452-2982
JTN-92-80246
NAL-TM-610
N92-17756 # p 1238 ..... ISSN-0452-2982
JTN-92-80247
NAL-TM-611
N92-17757 # p 1278 ..... ISSN-0452-2982
JTN-92-80290
NAL-TM-619
N92-17758 # p 1333 ..... AD-A242034
AL-TR-1991-0043
N92-17759 # p 1265 ..... AD-A242299
N92-17760 # p 1292 ..... AD-A243652
AFIT/GE/ENG/91D-06
N92-17761 # p 1344 ..... AD-A243653
AFIT/GSO/ENS/91D-05
N92-17762 # p 1251 ..... AD-A243654
AFIT/GSO/ENS/91D-09
N92-17763 # p 1285 ..... AD-A243655
AFIT/GSO/ENS/91D-10
N92-17764 # p 1321 ..... AD-A243772
NPSOR-91-029
N92-17765 # p 1325 ..... AD-A243774
AD-E040106
NOARL-R-17
N92-17766 # p 1325 ..... AD-A243775
AD-E040096
NOARL-TN-127
N92-17767 # p 1348 ..... AD-A243780
AFIT/GEO/ENG/91D-04
N92-17768* # p 1251 ..... NAS 1.55:10083-VOL-2-PT-1
NASA-CP-10083-VOL-2-PT-1
S-653-VOL-2-PT-1
N92-17769* # p 1251 ..... NO REPORT NUMBER
N92-17770* # p 1251 ..... NO REPORT NUMBER
N92-17771* # p 1251 ..... NO REPORT NUMBER
N92-17772* # p 1252 ..... NO REPORT NUMBER
N92-17773* # p 1252 ..... NO REPORT NUMBER
N92-17774* # p 1252 ..... NO REPORT NUMBER
N92-17775* # p 1252 ..... NO REPORT NUMBER
N92-17776* # p 1252 ..... NO REPORT NUMBER
N92-17777 # p 1273 ..... AD-A242863
N92-17778* # p 1344 ..... JRC-RR-90-04
NAS 1.26:184220
NASA-CR-184220
N92-17779 # p 1376 ..... CBPF-NF-004/91
DE91-641979
N92-17780 # p 1278 ..... CONF-9109259-11
DE92-002524
LA-UR-91-3437
N92-17781 # p 1376 ..... CONF-910115-1
DE92-002456
LA-UR-91-3257
N92-17782 # p 1376 ..... ANL/CP-74697
CONF-9110181-1
DE92-003520
N92-17783 # p 1376 ..... AD-A241981
N92-17784 # p 1273 ..... AD-A242187
UWA/DME/TR-91/7
N92-17785 # p 1384 ..... AD-A243031
AFOSR-91-0905TR
N92-17786 # p 1261 ..... ISBN-0-309-04584-3
LC-91-66333
N92-17787 # p 1385 ..... ISSN-0452-2982
JTN-92-80292
NAL-TM-621
N92-17788 # p 1261 ..... DE91-002086
DOE/MC-24207/3005
N92-17789 # p 1362 ..... CEBAF-PR-91-037
CONF-9108142-4
DE92-003258
DOE/ER-40105/175
IU/NTC-91-12
N92-17790 # p 1377 ..... CONF-910862-6
DE92-003514
SAND-91-0051C
N92-17791 # p 1377 ..... DE92-003756
DOE/ER-45156/T4
N92-17792 # p 1370 ..... DE92-003760
DOE/ER-52126/T1
N92-17793 # p 1371 ..... DE92-003773
DOE/ER-53270/T1
N92-17794 # p 1364 ..... CONF-9105221-4
DE92-003789
LA-UR-91-3831
N92-17795 # p 1305 ..... CONF-9108118-32
DE92-003791
LA-UR-91-3825
N92-17796 # p 1364 ..... CONF-9106260-5
DE92-003804
LA-UR-91-3287
N92-17797 # p 1377 ..... CONF-911202-4
DE92-004737
SAND-91-1635C
N92-17798 # p 1330 ..... DE92-004750
DOE/OR-00033/T455
N92-17799 # p 1377 ..... DE92-004757
LBL-31391
N92-17800 # p 1331 ..... DE92-004770
DOE/OR-00033/T462
N92-17801 # p 1292 ..... CONF-911106-31
DE92-004774
SLAC-PUB-5698
N92-17802 # p 1331 ..... CONF-9003295
DE92-704335
KURRI-TR-347
N92-17803 # p 1354 ..... DE91-641481
IC-91/19
N92-17804 # p 1354 ..... DE91-641482
IC-91/2
N92-17805 # p 1371 ..... DE92-609543
IC-91/109
N92-17806 # p 1371 ..... DE92-609544
IC-91/121
N92-17807 # p 1379 ..... DE92-609665
ER-13065-666
IC-91/145
UR-1214
N92-17808 # p 1266 ..... DE92-610350
JINR-R-10-90-299
N92-17809 # p 1309 ..... DE92-610933
FEI-2119
N92-17810 # p 1299 ..... DE92-610935
FEI-2131
N92-17811 # p 1354 ..... DE92-610951
JINR-R-9-90-154
N92-17812 # p 1285 ..... DE92-610956
KFTI-90-2
N92-17813 # p 1351 ..... DE92-611125
JINR-E-10-90-184

N92-17814 # p 1348 ..... DE92-611158
JINR-R-10-90-398
N92-17815 # p 1327 ..... DE92-611247
IC-91/115
N92-17816 # p 1257 ..... DE92-704180
JAERI-M-91-090
N92-17817 # p 1379 ..... DE92-704278
INS-879
N92-17818 p 1362 ..... NO REPORT NUMBER
N92-17819 p 1348 ..... NO REPORT NUMBER
N92-17820 p 1362 ..... NO REPORT NUMBER
N92-17821 p 1377 ..... NO REPORT NUMBER
N92-17822 p 1344 ..... NO REPORT NUMBER
N92-17823 # p 1354 ..... DE91-641486
IC-91/7
N92-17824 # p 1379 ..... DE91-641488
IC-91/22
N92-17825 # p 1293 ..... DE92-600473
JINR-R-8-90-127
N92-17826 p 1302 ..... AD-D015102
US-PATENT-APPL-SN-230547
US-PATENT-CLASS-33-363-K
US-PATENT-5,042,157
N92-17827 p 1307 ..... AD-D015103
US-PATENT-APPL-SN-590183
US-PATENT-CLASS-248-635
US-PATENT-5,040,764
N92-17828 p 1367 ..... AD-D015104
US-PATENT-APPL-SN-544556
US-PATENT-CLASS-350-96.20
US-PATENT-5,028,112
N92-17829 p 1285 ..... AD-D015108
US-PATENT-APPL-SN-517354
US-PATENT-CLASS-342-374
US-PATENT-5,045,857
N92-17830 p 1276 ..... AD-D015119
US-PATENT-APPL-SN-564894
US-PATENT-CLASS-89-7
US-PATENT-5,052,272
N92-17831 p 1293 ..... AD-D015123
US-PATENT-APPL-SN-797168
US-PATENT-CLASS-310-10
US-PATENT-5,059,839
N92-17832 # p 1388 ..... DE92-003970
UCRL-CR-108433
N92-17833 # p 1346 ..... CWI-CS-R9118
ETN-92-90557
N92-17834 p 1311 ..... ESDU-91008
ISBN-0-85679-770-7
ISSN-0141-4097
N92-17835 p 1302 ..... AD-D015105
US-PATENT-APPL-SN-501068
US-PATENT-CLASS-136-201
US-PATENT-5,021,098
N92-17836 p 1257 ..... AD-D015106
US-PATENT-APPL-SN-621102
US-PATENT-CLASS-252-62
US-PATENT-5,023,006
N92-17837 # p 1353 ..... ETN-92-90560
TW-91-04
N92-17838 # p 1349 ..... ETN-92-90561
TW-91-05
N92-17839 # p 1353 ..... ETN-92-90569
N92-17840 # p 1273 ..... ETN-92-90570
N92-17841 # p 1261 ..... ETN-92-90599
MBB-Z-0368-91-PUB
N92-17842 # p 1274 ..... DE92-003815
PATENTS-US-A7543897
US-PATENT-APPL-SN-543897
N92-17843 p 1233 ..... ESDU-91018
ISBN-0-85679-780-4
ISSN-0141-4054
N92-17844 p 1229 ..... ESDU-91019
ISBN-0-85679-781-2
ISSN-0141-4054
N92-17845 # p 1385 ..... CONF-9105285-2
DE92-003963
UCRL-JC-108648
N92-17846 # p 1368 ..... DE92-003964
UCRL-CR-108459
N92-17847 p 1233 ..... ESDU-91020
ISBN-0-85679-782-0
ISSN-0141-4054
N92-17848 # p 1379 ..... DLR-FB-90-20
ESA-TT-1252
ETN-92-90747
N92-17849 # p 1226 ..... AERO-REPT-8904
ETN-92-90913
N92-17850 # p 1300 ..... AERO-REPT-8905
ETN-92-90914
N92-17851 # p 1300 ..... AERO-REPT-9001
ETN-92-90918
N92-17852 p 1307 ..... ESDU-91026
ISBN-0-85679-788-X
ISSN-0141-4046
N92-17853 p 1321 ..... ESDU-91043
ISBN-0-85679-805-3
ISSN-0143-2702
N92-17854 # p 1239 ..... ISSN-0452-2982
JTN-92-80250
NAL-TM-614
N92-17855 # p 1236 ..... ISSN-0389-4014
JTN-92-80298
NAL-TR-1064T
N92-17856 # p 1385 ..... DE92-003758
DOE/ER-61152/T1
N92-17857 # p 1377 ..... DE92-004684
DOE/ER-13949/3
N92-17858 # p 1266 ..... DE92-004798
RFP-4387
N92-17859* # p 1309 ..... NAS 1.71:LAR-14626-1
NASA-CASE-LAR-14626-1
US-PATENT-APPL-SN-751489
N92-17860* # p 1344 ..... NAS 1.71:MSC-21415-1-SB
NASA-CASE-MSC-21415-1-SB
US-PATENT-APPL-SN-749819
N92-17861* # p 1257 ..... NAS 1.71:LEW-15241-1
NASA-CASE-LEW-15241-1
US-PATENT-APPL-SN-798464
N92-17862* # p 1305 ..... NAS 1.71:NPO-17763-1-CU
NASA-CASE-NPO-17763-1-CU
US-PATENT-APPL-SN-782009
N92-17863* # p 1368 ..... NAS 1.71:MSC-21806-1
NASA-CASE-MSC-21806-1
US-PATENT-APPL-SN-780513
N92-17864* # p 1368 ..... NAS 1.71:NPO-18593-1-CU
NASA-CASE-NPO-18593-1-CU
US-PATENT-APPL-SN-812901
N92-17865* # p 1293 ..... NAS 1.71:NPO-18454-1-CU
NASA-CASE-NPO-18454-1-CU
US-PATENT-APPL-SN-781521
N92-17866* # p 1335 ..... NAS 1.71:MFS-28633-1
NASA-CASE-MFS-28633-1
US-PATENT-APPL-SN-813629
N92-17867 # p 1255 ..... DE92-003840
PATENTS-US-A7504223
US-PATENT-APPL-SN-504223
N92-17868 # p 1305 ..... CONF-9108118-34
DE92-003908
ESG-133
LBL-30674
N92-17869 # p 1257 ..... ISSN-0389-4010
NAL-TR-1096
N92-17870* # p 1257 ..... NAS 1.71:MFS-28431-1
NASA-CASE-MFS-28431-1
US-PATENT-APPL-SN-812084
N92-17871 p 1293 ..... AD-D015121
US-PATENT-APPL-SN-395547
US-PATENT-CLASS-427-113
US-PATENT-5,045,349
N92-17872* # p 1307 ..... NAS 1.71:MSC-21898-1
NASA-CASE-MSC-21898-1
US-PATENT-APPL-SN-780512
N92-17873* # p 1387 ..... NAS 1.15:105505
NASA-TM-105505
N92-17874 # p 1226 ..... CONF-9109112-7
DE92-001157
NREL/TP-257-4510
N92-17875 # p 1313 ..... CONF-9109112-8
DE92-001190
NREL/TP-257-4518
N92-17876 # p 1364 ..... CONF-910626-14
DE92-002192
UCRL-JC-107357
N92-17877 # p 1327 ..... DE92-609575
IC-91/108
N92-17878 # p 1229 ..... ETN-92-90904
OUEL-1819/90
N92-17879 # p 1380 ..... ETN-92-90905
OUEL-1876/91
N92-17880 # p 1349 ..... ETN-92-90906
OUEL-1879/91
N92-17881* # p 1258 ..... NAS 1.15:4339
NASA-TM-4339
REPT-92B00027
N92-17882* # p 1255 ..... NAS 1.71:LEW-14345-6
NASA-CASE-LEW-14345-6
US-PATENT-APPL-SN-822240
N92-17883 # p 1390 ..... CONF-9006267-35
DE92-003848
LA-UR-91-3617
N92-17884* # p 1337 ..... NAS 1.71:NPO-17781-1-CU
NASA-CASE-NPO-17781-1-CU
US-PATENT-APPL-SN-744042
N92-17885 p 1285 ..... BBC-RD-1991/5
N92-17886 p 1285 ..... BBC-RD-1991/4
N92-17887* # p 1300 ..... NAS 1.26:189253
NASA-CR-189253
N92-17888* # p 1300 ..... NAS 1.71:LAR-14594-1
NASA-CASE-LAR-14594-1
US-PATENT-APPL-SN-748225
N92-17892* # p 1368 ..... NAS 1.71:NPO-18146-1-CU
NASA-CASE-NPO-18146-1-CU
US-PATENT-APPL-SN-786618
N92-17895* # p 1349 ..... NAS 1.71:NPO-17918-2-CU
NASA-CASE-NPO-17918-2-CU
US-PATENT-APPL-SN-786499
N92-17899* # p 1305 ..... NAS 1.71:NPO-18386-1-CU
NASA-CASE-NPO-18386-1-CU
US-PATENT-APPL-SN-751440
N92-17902* # p 1261 ..... NAS 1.71:LEW-15359-1
NASA-CASE-LEW-15359-1
US-PATENT-APPL-SN-797484
N92-17907* # p 1293 ..... NAS 1.71:NPO-17994-1-CU
NASA-CASE-NPO-17994-1-CU
US-PATENT-APPL-SN-791759
N92-17909* # p 1300 ..... NAS 1.71:LAR-14547-1
NASA-CASE-LAR-14547-1
US-PATENT-APPL-SN-748224
N92-17910* # p 1335 ..... NAS 1.71:MSC-21752-1
NASA-CASE-MSC-21752-1
US-PATENT-APPL-SN-775404
N92-17913* # p 1278 ..... NAS 1.71:MSC-21776-1
NASA-CASE-MSC-21776-1
US-PATENT-APPL-SN-772763
N92-17916 # p 1378 ..... DE92-003808
IS-T-1537
N92-17917 # p 1237 ..... ISSN-0389-4010
NAL-TR-1116
N92-17918 p 1302 ..... AD-D015134
US-PATENT-APPL-SN-445329
US-PATENT-CLASS-102-418
US-PATENT-5,046,427
N92-17920 # p 1387 ..... AD-A243599
AFIT/CI/CIA-91-075
N92-17921 # p 1344 ..... AD-A243620
N92-17922 # p 1337 ..... AD-A243632
AFIT/GCS/ENG/91D-20
N92-17923 p 1305 ..... AD-D015154
US-PATENT-APPL-SN-488411
US-PATENT-CLASS-372-41
US-PATENT-5,038,353
N92-17925 # p 1262 ..... ETN-92-90897
N92-17926 # p 1302 ..... ETN-92-90910
OUEL-1886/91
N92-17927 # p 1344 ..... ETN-92-90911
OUEL-1892/91
N92-17928 # p 1391 ..... AERO-REPT-8903
ETN-92-90912
N92-17930 # p 1311 ..... AD-A243429
ARCCB-TR-91033
N92-17931 # p 1286 ..... AD-A243584
NRL-9359
N92-17932 # p 1258 ..... AD-A243600
AFIT/CI/CIA-91-017D
N92-17933 # p 1371 ..... DE92-004691
DOE/ER-53252/28
N92-17934 # p 1313 ..... DE92-004699
PNL-7817
N92-17935 # p 1274 ..... DE92-003826
PATENTS-US-A7559234
US-PATENT-APPL-SN-559234
N92-17936 # p 1305 ..... CONF-9108118-33
DE92-003907
LBL-30672
N92-17937 # p 1311 ..... DE92-003944
SAND-91-1732
N92-17938 # p 1274 ..... CONF-910960-3
DE92-004728
SAND-91-2509C
N92-17939 # p 1351 ..... DE92-609035
IC-91/132
N92-17940 p 1381 ..... AD-D015163
NAVY-CASE-73415
US-PATENT-APPL-SN-786641
N92-17941 # p 1378 ..... DE92-004420
DOE/ER-45310/35
N92-17942 # p 1274 ..... DE92-004423
DOE/ER-13649/5
N92-17943 # p 1262 ..... DE92-610065
IC-91/151
N92-17944 # p 1378 ..... DE92-611185
JINR-E-14-90-345
N92-17945* # p 1276 ..... NAS 1.15:4284
NASA-TM-4284
N92-17946 # p 1327 ..... DE91-641478
IC-90/473
N92-17947 # p 1274 ..... AD-A242740
NOSC-TD-2222
N92-17948 # p 1344 ..... AD-A242744
NCS-TIB-90-14
N92-17949 # p 1293 ..... AD-A242747
HAC-REF-G4663
N92-17950 # p 1258 ..... AD-A242748
N92-17951 # p 1325 ..... AD-A242749
APL-UW-TM-6-91
N92-17952 # p 1381 ..... AD-A242750
N92-17953 # p 1294 ..... DE92-600475

JINR-E-14-90-254
N92-17954 # p 1362 ..... DE92-600624
INIS-MF-12963
N92-17955 # p 1363 ..... DE92-600625
JINR-R-3-90-120
N92-17956 # p 1363 ..... DE92-600628
JINR-E-4-90-249
N92-17957 # p 1363 ..... DE92-600629
JINR-E-4-90-57
N92-17958 # p 1363 ..... DE92-600631
JINR-R-2-90-158
N92-17959 p 1368 ..... AD-D015133
US-PATENT-APPL-SN-725709
US-PATENT-CLASS-324-244
US-PATENT-5,038,103
N92-17960 # p 1345 ..... AD-A243249
CCS-663
N92-17961 # p 1317 ..... AD-A243275
AFOSR-91-0914TR
N92-17962 # p 1305 ..... AD-A243606
RCC-316-91
N92-17963 # p 1276 ..... CONF-9111129-4
DE92-004408
N92-17964 # p 1364 ..... CONF-901145-2
DE92-004414
N92-17965 # p 1349 ..... CONF-9109316-2
DE92-004656
UCRL-JC-108590
N92-17966 # p 1274 ..... DE92-004687
DOE/ER-45409/2
N92-17967 # p 1238 ..... DE92-004793
KCP-613-4529
N92-17968 # p 1371 ..... DE92-004794
KCP-613-4480
N92-17969 # p 1345 ..... DE92-004797
EGG-2663
N92-17970 # p 1327 ..... DE92-609034
IC-91/126
N92-17971 # p 1294 ..... DE92-609667
IFVE-OEA-91-2
N92-17972 # p 1378 ..... DE92-610441
IC-91/153
N92-17973 # p 1364 ..... DE92-610975
JINR-R-9-90-37
N92-17974 # p 1300 ..... AERO-REPT-8909
ETN-92-90917
N92-17975* # p 1321 ..... NAS 1.26:188236
NASA-CR-188236
N92-17976* # p 1322 ..... NO REPORT NUMBER
N92-17977* # p 1322 ..... NO REPORT NUMBER
N92-17978* # p 1322 ..... NO REPORT NUMBER
N92-17979* # p 1322 ..... NO REPORT NUMBER
N92-17980* # p 1322 ..... NO REPORT NUMBER
N92-17981* # p 1322 ..... NO REPORT NUMBER
N92-17982 # p 1314 ..... NO REPORT NUMBER
N92-17984* # p 1219 ..... L-17017
NAS 1.55:3131
NASA-CP-3131
N92-17985* # p 1219 ..... NO REPORT NUMBER
N92-17986* # p 1220 ..... NO REPORT NUMBER
N92-17987* # p 1220 ..... NO REPORT NUMBER
N92-17988* # p 1220 ..... NO REPORT NUMBER
N92-17989* # p 1220 ..... NO REPORT NUMBER
N92-17990* # p 1220 ..... NO REPORT NUMBER
N92-17991* # p 1220 ..... NO REPORT NUMBER
N92-17992* # p 1221 ..... NO REPORT NUMBER
N92-17993* # p 1221 ..... NO REPORT NUMBER
N92-17994* # p 1221 ..... NO REPORT NUMBER
N92-17995* # p 1221 ..... NO REPORT NUMBER
N92-17996* # p 1221 ..... NO REPORT NUMBER
N92-17997* # p 1221 ..... NO REPORT NUMBER
N92-17998* # p 1222 ..... NO REPORT NUMBER
N92-17999* # p 1222 ..... NO REPORT NUMBER
N92-18000* # p 1222 ..... NO REPORT NUMBER
N92-18001* # p 1222 ..... NO REPORT NUMBER
N92-18002* # p 1222 ..... NO REPORT NUMBER
N92-18003* # p 1390 ..... NAS 1.26:189779
NASA-CR-189779
N92-18004* # p 1390 ..... NO REPORT NUMBER
N92-18005* # p 1390 ..... NO REPORT NUMBER

Appendix

NASA SCIENTIFIC AND TECHNICAL INFORMATION PROGRAM PRODUCTS AND SERVICES

The NASA Scientific and Technical Information (STI) Program provides for the collection and announcement of aerospace-related reports and literature obtained worldwide through agreements and exchanges. The result of the collection is the comprehensive NASA STI Database that covers aeronautics, space, and supporting disciplines.

The STI Database, documents generated or obtained by NASA, and products and services derived from or supporting the database are made available to the NASA research community and to the public. Descriptions and sources of these items are presented in the following pages.

Scientific and Technical Aerospace Reports (*STAR*) is an abstract journal, listing citations with abstracts for aerospace-related reports obtained from worldwide sources. *STAR* is issued on the 8th and 23rd of each month and announces current documents that have been entered into the NASA STI Database during the previous two weeks. The reports are of the following types:

- NASA, NASA contractor, and NASA grantee reports;
- Reports issued by other U.S. Government agencies, domestic and foreign institutions, universities, and private firms;
- Translations in report form;
- NASA-owned patents and patent applications;
- Other U.S. Government agency and foreign patents and patent applications;
- Domestic and foreign dissertations and theses.

Journal, book, and conference literature, journal translations, and certain foreign dissertations having the same subject scope as *STAR* are announced in a companion journal, *International Aerospace Abstracts* (*IAA*). *IAA* is issued on the 1st and 15th of each month and is available from the American Institute of Aeronautics and Astronautics, Technical Information Service, 555 West 57th Street, 12th Floor, New York, NY 10019.

ELIGIBILITY AND REGISTRATION FOR NASA STI PRODUCTS AND SERVICES

Organizations of the type listed below that have registered with NASA can receive products and services.

- NASA offices and installations, contractors, subcontractors, grantees, and consultants;
- Other U.S. Government agencies and their contractors;
- Libraries in the United States that have arrangements with NASA to maintain collections of NASA documents for public reference;
- Other organizations in the United States having a need for NASA documents in work related to aeronautics and space research;
- Organizations abroad that have established reciprocal documents exchange arrangements with NASA.

Only the central service points or central points of document acquisition and control within qualified organizations are eligible to register for NASA STI products and services. Domestic organizations that may be eligible to receive various classes of NASA publications and services should address their requests for registration or further information to:

NASA Center for AeroSpace Information
ATTN: Registration Services
P.O. Box 8757
Baltimore, MD 21240-0757
301-621-0153

Organizations abroad should direct requests to:

National Aeronautics and Space Administration
Director, Scientific and Technical Information Program
Code JTT
Washington, DC 20546
USA
703-271-5640

SUBJECT SCOPE

The subject scope of *STAR* and *IAA* includes all aspects of aeronautics and space research and development, supporting basic and applied research, and applications. Aerospace aspects of Earth resources, energy development, conservation, oceanography, environmental protection, urban transportation, and other topics of high national priority are also covered.

HOW TO USE *STAR* SUBJECT CATEGORIES

Abstracts in *STAR* are categorized by 10 major subject divisions that are divided further into 76 specific subject categories. The subject divisions and categories are listed in the Table of Contents together with a note for each that defines its scope and provides any cross-references. For example:

16 SPACE TRANSPORTATION
Includes passenger and cargo space transportation, e.g., shuttle operations; and space rescue techniques. For related information see also *03 Air Transportation and Safety* and *18 Spacecraft Design, Testing and Performance.* For space suits see *54 Man/System Technology and Life Support.*

CROSS-REFERENCES

Individual *STAR* abstracts are not ordinarily cross-referenced, except for certain conference reports or book translations that have had separate abstracts written for their component papers or chapters. Citations and abstracts of the components follow immediately after those of the parent document. When the subject content of a component differs sufficiently from the general content of the parent, a cross-reference citation also is printed at the end of the category to which it normally would have been assigned if it were independent.

DOCUMENTS ON MICROFICHE

Documents available on microfiche are designated by a pound sign (#) following the accession number.

LIMITED REPRODUCIBILITY

A note of limited reproducibility appears in the citation, if there are factors affecting the reproducibility of more than 20% of the document. These factors include faint or broken type, color photographs, black and white photographs, foldouts, dot matrix print, or some other factor that limits the reproducibility of the document. This notation also appears on the microfiche header with the specific factor checked off on a list visible in the second frame.

COLOR COPIES

An increasing number of NASA scientific and technical reports are being produced with color graphs, charts, illustrations, and photographs. An indication that a document has color pages follows the source and pricing (SAP) information in the *STAR* citation.

Registered users of the NASA Scientific and Technical Information Program will receive ordered documents with color at no additional cost, as long as stock copies of the document are available. Otherwise, an additional fee of $2.00 per color page will be charged. The NASA Center for AeroSpace Information staff will contact registered users to determine individual user's needs.

NASA PATENTS AND PATENT APPLICATIONS

Patents and patent applications owned by NASA are announced in *STAR* under appropriate subject categories and are referenced in the *STAR* indexes. In the Report/Accession Number Index, patents are indexed by the NASA Case Number, and the U.S. Patent Class. Patent applications are indexed by the NASA Case Number and the U.S. Patent Application Serial Number.

Printed copies of patents (which are not microfiched) are available for purchase from the U.S. Patent and Trademark Office.

NASA patent application specifications are sold in both paper copy and microfiche by the National Technical Information Service (NTIS). The US-Patent-Appl-SN-number should be used in ordering either paper copy or microfiche from NTIS.

When ordering patents, the U.S. Patent Number should be used, and payment must be remitted in advance, by money order or check payable to the Commissioner of Patents and Trademarks. Prepaid purchase coupons for ordering are also available from the U.S. Patent and Trademark Office.

The patents and patent applications announced in *STAR* are owned by NASA and are available for royalty-free licensing. Requests for licensing terms and further information should be addressed to:

National Aeronautics and Space Administration
Associate General Counsel for Intellectual Property
Code GP
Washington, DC 20546

SOURCES FOR DOCUMENTS

One or more sources from which a document announced in *STAR* is available to the public is given in each citation. The most commonly indicated sources and their acronyms or abbreviations are listed on page A-6. If the publication is available from a source other than those listed, the publisher and address will be displayed on the availability line or in combination with the corporate source line.

Avail: NTIS. Sold by the National Technical Information Service. Prices for hard copy (HC) and microfiche (MF) are indicated by a price code following the letters HC or MF in the *STAR* citation. Current values for the price codes are given in the tables on page A-7.

Initially distributed microfiche under the NTIS SRIM (Selected Research in Microfiche) is available at greatly reduced unit prices. For this service and for information concerning subscription to NASA printed reports, consult the NTIS Subscription Section, Springfield, VA 22161.

NOTE ON ORDERING DOCUMENTS: When ordering NASA publications (those followed by the * symbol), use the N accession number. NASA patent applications (only the specifications are offered) should be ordered by the US-Patent-Appl-SN number. Non-NASA publications (no asterisk) should be ordered by the AD, PB, or other *report number* shown on the last line of the citation, not by the N accession number. It is also advisable to cite the title and other bibliographic identification.

Avail: SOD (or GPO). Sold by the Superintendent of Documents, U.S. Government Printing Office, in hard copy. The current price and order number are given following the availability line. (NTIS will fill microfiche requests, as indicated above, for those documents identified by a # symbol.)

Avail: BLL (formerly NLL): British Library Lending Division, Boston Spa, Wetherby, Yorkshire, England. Photocopies available from this organization at the price shown. (If none is given, address inquiry to the BLL.)

Avail: DOE Depository Libraries. Organizations in U.S. cities and abroad that maintain collections of Department of Energy reports, usually in microfiche form, are listed in *Energy Research Abstracts.* Services available from the DOE and its depositories are described in a booklet, *DOE Technical Information Center - Its Functions and Services* (TID-4660), which may be obtained without charge from the DOE Technical Information Center.

Avail: ESDU. Pricing information on specific data, computer programs, and details on Engineering Sciences Data Unit (ESDU) topic categories can be obtained from ESDU International Ltd. Requesters in North America should use the Virginia address while all other requesters should use the London address, both of which are on page A-6.

Avail: Fachinformationszentrum, Karlsruhe. Sold by the Fachinformationszentrum Energie, Physik, Mathematik GMBH, Eggenstein Leopoldshafen, Federal Republic of Germany, at the price shown in deutschmarks (DM).

Avail: HMSO. Publications of Her Majesty's Stationery Office are sold in the U.S. by Pendragon House, Inc. (PHI), Redwood City, CA. The U.S. price (including a service and mailing charge) is given, or a conversion table may be obtained from PHI.

Avail: NASA Public Document Rooms. Documents so indicated may be examined at or purchased from the National Aeronautics and Space Administration, Public Documents Room (Room 126), 600 Independence Ave., S.W., Washington, DC 20546, or public document rooms located at NASA installations, and the NASA Pasadena Office at the Jet Propulsion Laboratory.

Avail: Univ. Microfilms. Documents so indicated are dissertations selected from *Dissertation Abstracts* and are sold by University Microfilms as xerographic copy (HC) and microfilm. All requests should cite the author and the Order Number as they appear in the citation.

Avail: US Patent and Trademark Office. Sold by Commissioner of Patents and Trademarks, U.S. Patent and Trademark Office, at the standard price of $1.50 each, postage free. (See discussion of NASA patents and patent applications below.)

Avail: (US Sales Only). These foreign documents are available to users within the United States from the National Technical Information Service (NTIS). They are available to users outside the United States through the International Nuclear Information Service (INIS) representative in their country, or by applying directly to the issuing organization.

Avail: USGS. Originals of many reports from the U.S. Geological Survey, which may contain color illustrations, or otherwise may not have the quality of illustrations preserved in the microfiche or facsimile reproduction, may be examined by the public at the libraries of the USGS field offices whose addresses are listed on page A-6. The libraries may be queried concerning the availability of specific documents and the possible utilization of local copying services, such as color reproduction.

Avail: Issuing Activity, or Corporate Author, or no indication of availability. Inquiries as to the availability of these documents should be addressed to the organization shown in the citation as the corporate author of the document.

FEDERAL DEPOSITORY LIBRARIES: To provide the general public with greater access to U.S. Government publications, Congress established the Federal Depository Library Program under the Government Printing Office (GPO), with 52 regional depositories responsible for permanent retention of material, inter-library loan, and reference services. (These libraries are not sales outlets.) At least one copy of nearly every NASA and NASA-sponsored publication, either in printed or microfiche format, is received and retained by the 52 regional depositories. A list of the regional GPO libraries, appears on page A-8. A local library can contact a regional depository library to help locate specific reports, or direct contact may be made by an individual.

PUBLIC COLLECTION OF NASA DOCUMENTS

An extensive collection of NASA and NASA-sponsored publications is maintianed by the British Library Lending Divison, Boston Spa, Wetherby, Yorkshire, England, for public access. The British Library Lending Division also has available many of the non-NASA publications cited in *STAR.*

European requesters may purchase facsimile copy or microfiche of NASA and NASA-sponsored documents, those identified by both the symbols # and * from ESA—Information Retrieval Service, European Space Agency, 8-10 rue Mario-Nikis, 75738 Paris CEDEX 15, France.

SUBMITTING DOCUMENTS

All users of this abstract service are urged to forward reports to be considered for announcement in *STAR.* This will aid NASA in its efforts to provide the fullest possible coverage of all scientific and technical publications that might support aeronautics and space research and development. If you have prepared relevant reports (other than those you will transmit to NASA, DOD, or DOE through the usual contract- or grant-reporting channels), please send them for consideration to the NASA Center for AeroSpace Information, P.O. Box 8757, Baltimore, MD 21240-0757.

Reprints of journal articles, book chapters, and conference papers are also welcome. These will be considered for announcement in *STAR*'s companion journal, *IAA.*

You may specify a particular source to be included in a report announcement if you wish; otherwise the report will be placed on a public sale at the National Technical Information Service. Copyrighted publications will be announced but not distributed or sold.

PURCHASE OF *STAR*

STAR is publicly available on annual subscription from the Superintendent of Documents, U.S. Government Printing Office, Washington, DC 20402.

STAR is available to registered users on annual subscription from the NASA Center for AeroSpace Information, ATTN: Registration Services, P.O. Box 8757, Baltimore, MD 21240-0757.

Microfiche of the abstract sections of *STAR* are available, on annual subscription only, from NTIS as PB92-911300, Attn: Subscriptions, 5285 Port Royal Road, Springfield, VA 22161. Annual subscription rates are $100.00 North America; $200.00 foreign. Abstract sections for previous years retroactive to 1964 are available at the current rates.

ADDRESSES OF ORGANIZATIONS

American Institute of Aeronautics and Astronautics
Technical Information Service
555 West 57th Street, 12th Floor
New York, New York 10019

British Library Lending Division,
Boston Spa, Wetherby, Yorkshire,
England

Commissioner of Patents and Trademarks
U.S. Patent and Trademark Office
Washington, DC 20231

Department of Energy
Technical Information Center
P.O. Box 62
Oak Ridge, Tennessee 37830

European Space Agency-Information Retrieval Service
ESRIN
Via Galileo Galilei
00044 Frascati (Rome) Italy

Engineering Sciences Data Unit International
P.O. Box 1633
Manassas, Virginia 22110

Engineering Sciences Data Unit International, Ltd.
251-259 Regent Street
London, W1R 7AD, England

Fachinformationszentrum Energie, Physik, Mathematik
GMBH
7514 Eggenstein Leopoldshafen
Federal Republic of Germany

Her Majesty's Stationery Office
P.O. Box 569, S.E. 1
London, England

NASA Center for AeroSpace Information
P.O. Box 8757
Baltimore, Maryland 21240-0757

National Aeronautics and Space Administration
Scientific and Technical Information Program (JTT)
Washington, DC 20546-0001

National Technical Information Service
5285 Port Royal Road
Springfield, Virginia 22161

Pendragon House, Inc.
899 Broadway Avenue
Redwood City, California 94063

Superintendent of Documents
U.S. Government Printing Office
Washington, DC 20402

University Microfilms
A Xerox Company
300 North Zeeb Road
Ann Arbor, Michigan 48106

University Microfilms, Ltd.
Tylers Green
London, England

U.S. Geological Survey Library National Center
MS 950
12201 Sunrise Valley Drive
Reston, Virginia 22092

U.S. Geological Survey Library
2255 North Gemini Drive
Flagstaff, Arizona 86001

U.S. Geological Survey
345 Middlefield Road
Menlo Park, California 94025

U.S. Geological Survey Library
Box 25046
Denver Federal Center, MS914
Denver, Colorado 80225

NTIS PRICE SCHEDULES

(Effective October 1, 1991)

Schedule A
STANDARD PRICE DOCUMENTS AND MICROFICHE**

PRICE CODE	NORTH AMERICAN PRICE	FOREIGN PRICE
A01	$ 9.00	$ 18.00
A02	12.50	25.00
A03	17.00	34.00
A04-A05	19.00	38.00
A06-A09	26.00	52.00
A10-A13	35.00	70.00
A14-A17	43.00	86.00
A18-A21	50.00	100.00
A22-A25	59.00	118.00
A99	*	*
N01	60.00	120.00
N02	59.00	118.00
N03	20.00	40.00

Schedule E
EXCEPTION PRICE DOCUMENTS AND MICROFICHE**

PRICE CODE	NORTH AMERICAN PRICE	FOREIGN PRICE
E01	$11.00	$ 22.00
E02	14.00	28.00
E03	16.00	32.00
E04	19.00	38.00
E05	21.00	42.00
E06	24.00	48.00
E07	27.00	54.00
E08	30.00	60.00
E09	33.00	66.00
E10	36.00	72.00
E11	39.00	78.00
E12	43.00	86.00
E13	46.00	92.00
E14	50.00	100.00
E15	54.00	108.00
E16	59.00	118.00
E17	64.00	128.00
E18	69.00	138.00
E19	76.00	152.00
E20	88.00	176.00
E99	*	*

* Contact NTIS for price quote.

** Effective January 1, 1991, the microfiche copy of any new document entering the NTIS collection will be priced the same as the paper copy of the document.

IMPORTANT NOTICE

NTIS Shipping and Handling Charges

U.S., Canada, Mexico — ADD $3.00 per TOTAL ORDER

All Other Countries — ADD $4.00 per TOTAL ORDER

Exceptions — Does NOT apply to:

ORDERS REQUESTING NTIS RUSH HANDLING

ORDERS FOR SUBSCRIPTION OR STANDING ORDER PRODUCTS *ONLY*

NOTE: Each additional delivery address on an order requires a separate shipping and handling charge.

FEDERAL REGIONAL DEPOSITORY LIBRARIES

ALABAMA

AUBURN UNIV. AT MONTGOMERY LIBRARY
Documents Dept.
7300 University Drive
Montgomery, AL 36117-3596
(205) 244-3650 FAX: (205) 244-0678

UNIV. OF ALABAMA
Amelia Gayle Gorgas Library
Govt. Documents
Box 870266
Tuscaloosa, AL 35487-0266
(205) 348-6046 FAX: (205) 348-8833

ARIZONA

DEPT. OF LIBRARY, ARCHIVES, AND PUBLIC RECORDS
Federal Documents
Third Floor State Capitol
1700 West Washington
Phoenix, AZ 85007
(602) 542-4121 FAX: (602) 542-4400; 542-4500

ARKANSAS

ARKANSAS STATE LIBRARY
State Library Services
One Capitol Mall
Little Rock, AR 72201
(501) 682-2869

CALIFORNIA

CALIFORNIA STATE LIBRARY
Govt. Publications Section
914 Capitol Mall - P.O. Box 942837
Sacramento, CA 94237-0001
(916) 322-4572 FAX: (916) 324-8120

COLORADO

UNIV. OF COLORADO - BOULDER
Norlin Library
Govt. Publications
Campus Box 184
Boulder, CO 80309-0184
(303) 492-8834 FAX: (303) 492-2185

DENVER PUBLIC LIBRARY
Govt. Publications Dept. BS/GPD
1357 Broadway
Denver, CO 80203
(303) 571-2135

CONNECTICUT

CONNECTICUT STATE LIBRARY
231 Capitol Avenue
Hartford, CT 06106
(203) 566-4971 FAX: (203) 566-3322

FLORIDA

UNIV. OF FLORIDA LIBRARIES
Documents Dept.
Library West
Gainesville, FL 32611-2048
(904) 392-0366 FAX: (904) 392-7251

GEORGIA

UNIV. OF GEORGIA LIBRARIES
Govt. Documents Dept.
Jackson Street
Athens, GA 30602
(404) 542-8949 FAX: (404) 542-6522

HAWAII

UNIV. OF HAWAII
Hamilton Library
Govt. Documents Collection
2550 The Mall
Honolulu, HI 96822
(808) 948-8230 FAX: (808) 956-5968

IDAHO

UNIV. OF IDAHO LIBRARY
Documents Section
Moscow, ID 83843
(208) 885-6344 FAX: (208) 885-6817

ILLINOIS

ILLINOIS STATE LIBRARY
Reference Dept.
300 South Second
Springfield, IL 62701-1796
(217) 782-7596 FAX: (217) 524-0041

INDIANA

INDIANA STATE LIBRARY
Serials/Documents Section
140 North Senate Avenue
Indianapolis, IN 46204
(317) 232-3678 FAX: (317) 232-3728

IOWA

UNIV. OF IOWA LIBRARIES
Govt. Publications Dept.
Washington & Madison Streets
Iowa City, IA 52242
(319) 335-5926 FAX: (319) 335-5830

KANSAS

UNIV. OF KANSAS
Govt. Documents & Map Library
6001 Malatt Hall
Lawrence, KS 66045-2800
(913) 864-4660 FAX: (913) 864-5380

KENTUCKY

UNIV. OF KENTUCKY LIBRARIES
Govt. Publications/Maps Dept.
Lexington, KY 40506-0039
(606) 257-3139 FAX: (606) 257-1563; 257-8379

LOUISIANA

LOUISIANA STATE UNIV.
Middleton Library
Govt. Documents Dept.
Baton Rouge, LA 70803
(504) 388-2570 FAX: (504) 388-6992

LOUISIANA TECHNICAL UNIV.
Prescott Memorial Library
Govt. Documents Dept.
305 Wisteria Street
Ruston, LA 71270-9985
(318) 257-4962 FAX: (318) 257-2447

MAINE

TRI-STATE DOCUMENTS DEPOSITORY
Raymond H. Fogler Library
Govt. Documents & Microforms Dept.
Univ. of Maine
Orono, ME 04469
(207) 581-1680

MARYLAND

UNIV. OF MARYLAND
Hornbake Library
Govt. Documents/Maps Unit
College Park, MD 20742
(301) 454-3034 FAX: (301) 454-4985

MASSACHUSETTS

BOSTON PUBLIC LIBRARY
Govt. Documents Dept.
666 Boylston Street
Boston, MA 02117
(617) 536-5400 ext. 226
FAX: (617) 267-8273; 267-8248

MICHIGAN

DETROIT PUBLIC LIBRARY
5201 Woodward Avenue
Detroit, MI 48202-4093
(313) 833-1440; 833-1409
FAX: (313) 833-5039

LIBRARY OF MICHIGAN
Govt. Documents Unit
P.O. Box 30007
Lansing, MI 48909
(517) 373-0640 FAX: (517) 373-3381

MINNESOTA

UNIV. OF MINNESOTA
Wilson Library
Govt. Publications Library
309 19th Avenue South
Minneapolis, MN 55455
(612) 624-5073 FAX: (612) 626-9353

MISSISSIPPI

UNIV. OF MISSISSIPPI
J.D. Williams Library
Federal Documents Dept.
106 Old Gym Bldg.
University, MS 38677
(601) 232-5857 FAX: (601) 232-5453

MISSOURI

UNIV. OF MISSOURI - COLUMBIA
Ellis Library
Govt. Documents
Columbia, MO 65201
(314) 882-6733 FAX: (314) 882-8044

MONTANA

UNIV. OF MONTANA
Maureen & Mike Mansfield Library
Documents Div.
Missoula, MT 59812-1195
(406) 243-6700 FAX: (406) 243-2060

NEBRASKA

UNIV. OF NEBRASKA - LINCOLN
D.L. Love Memorial Library
Documents Dept.
Lincoln, NE 68588
(402) 472-2562

NEVADA

UNIV. OF NEVADA
Reno Library
Govt. Publications Dept.
Reno, NV 89557
(702) 784-6579 FAX: (702) 784-1751

NEW JERSEY

NEWARK PUBLIC LIBRARY
U.S. Documents Div.
5 Washington Street - P.O. Box 630
Newark, NJ 07101-0630
(201) 733-7812 FAX: (201) 733-5648

NEW MEXICO

UNIV. OF NEW MEXICO
General Library
Govt. Publications Dept.
Albuquerque, NM 87131-1466
(505) 277-5441 FAX: (505) 277-6019

NEW MEXICO STATE LIBRARY
325 Don Gaspar Avenue
Santa Fe, NM 87503
(505) 827-3826 FAX: (505) 827-3820

NEW YORK

NEW YORK STATE LIBRARY
Documents/Gift & Exchange Section
Federal Depository Program
Cultural Education Center
Albany, NY 12230
(518) 474-5563 FAX: (518) 474-5786

NORTH CAROLINA

UNIV. OF NORTH CAROLINA - CHAPEL HILL
CB#3912, Davis Library
BA/SS Dept.—Documents
Chapel Hill, NC 27599
(919) 962-1151 FAX: (919) 962-0484

NORTH DAKOTA

NORTH DAKOTA STATE UNIV. LIBRARY
Documents Office
Fargo, ND 58105
(701) 237-8886 FAX: (701) 237-7138
In cooperation with Univ. of North Dakota, Chester Fritz Library
Grand Forks

OHIO

STATE LIBRARY OF OHIO
Documents Dept.
65 South Front Street
Columbus, OH 43266
(614) 644-7051 FAX: (614) 752-9178

OKLAHOMA

OKLAHOMA DEPT. OF LIBRARIES
U.S. Govt. Information Div.
200 NE 18th Street
Oklahoma City, OK 73105-3298
(405) 521-2502, ext. 252, 253
FAX: (405) 525-7804

OKLAHOMA STATE UNIV.
Edmon Low Library
Documents Dept.
Stillwater, OK 74078
(405) 744-6546 FAX: (405) 744-5183

OREGON

PORTLAND STATE UNIV.
Millar Library
934 SW Harrison - P.O. Box 1151
Portland, OR 97207
(503) 725-3673 FAX: (503) 725-4527

PENNSYLVANIA

STATE LIBRARY OF PENN.
Govt. Publications Section
Walnut St. & Commonwealth Ave. - P.O. Box 1601
Harrisburg, PA 17105
(717) 787-3752

SOUTH CAROLINA

CLEMSON UNIV.
Cooper Library
Public Documents Unit
Clemson, SC 29634-3001
(803) 656-5174 FAX: (803) 656-3025
In cooperation with Univ. of South Carolina, Thomas Cooper Library, Columbia

TENNESSEE

MEMPHIS STATE UNIV. LIBRARIES
Govt. Documents
Memphis, TN 38152
(901) 678-2586 FAX: (901) 678-2511

TEXAS

TEXAS STATE LIBRARY
United States Documents
P.O. Box 12927 - 1201 Brazos
Austin, TX 78711
(512) 463-5455 FAX: (512) 463-5436

TEXAS TECH. UNIV. LIBRARY
Documents Dept.
Lubbock, TX 79409
(806) 742-2268 FAX: (806) 742-1920

UTAH

UTAH STATE UNIV.
Merrill Library & Learning Resources Center, UMC-3000
Documents Dept.
Logan, UT 84322-3000
(801) 750-2684 FAX: (801) 750-2677

VIRGINIA

UNIV. OF VIRGINIA
Alderman Library
Govt. Documents
Charlottesville, VA 22903-2498
(804) 924-3133 FAX: (804) 924-4337

WASHINGTON

WASHINGTON STATE LIBRARY
Document Section
MS AJ-11
Olympia, WA 98504-0111
(206) 753-4027 FAX: (206) 753-3546

WEST VIRGINIA

WEST VIRGINIA UNIV. LIBRARY
Govt. Documents Section
P.O. Box 6069
Morgantown, WV 26506
(304) 293-3640

WISCONSIN

ST. HIST. SOC. OF WISCONSIN LIBRARY
Govt. Publications Section
816 State Street
Madison, WI 53706
(608) 262-2781 FAX: (608) 262-4711
In cooperation with Univ. of Wisconsin-Madison, Memorial Library

MILWAUKEE PUBLIC LIBRARY
Documents Div.
814 West Wisconsin Avenue
Milwaukee, WI 53233
(414) 278-2167 FAX: (414) 278-2137

WYOMING

WYOMING STATE LIBRARY
Supreme Court & Library Bldg.
Govt. Publications
Cheyenne, WY 82002
(307) 777-5920 FAX: (307) 777-6289

* U.S. G.P.O.:1992-313-125:60008

National Aeronautics and
Space Administration
Code JTT
Washington, D.C.
20546-0001

Official Business
Penalty for Private Use, $300

SPECIAL FOURTH-CLASS RATE
POSTAGE & FEES PAID
NASA
PERMIT No. G27

POSTMASTER: If Undeliverable (Section 158
Postal Manual) Do Not Return